

NAT'L INST OF STAND & TECH R.I.C.



A11104 060507

NATIONAL INSTITUTE OF STANDARDS &
TECHNOLOGY
Research Information Center
Gaithersburg, MD 20899 /

NBSIR 82-2587

Physical Properties Data for Basalt

U.S. DEPARTMENT OF COMMERCE
National Bureau of Standards
National Measurement Laboratory
Office of Standard Reference Data
Washington, DC 20234

September 1982

Final

Prepared for
Office of Nuclear Waste Isolation
Carnegie Memorial Institute

QC
100 King Avenue
Columbus, OH 43201

.U56
82-2587
1982
C.2

NBSIR 82-2587

OCT 8 1982

Notated - etc
QC 100
u56
82-2587
1982
C 2

PHYSICAL PROPERTIES DATA FOR BASALT

L. H. Gevantman, Editor

U.S. DEPARTMENT OF COMMERCE
National Bureau of Standards
National Measurement Laboratory
Office of Standard Reference Data
Washington, DC 20234

September 1982

Final

Prepared for
Office of Nuclear Waste Isolation
Battelle Memorial Institute
505 King Avenue
Columbus, OH 43201



U.S. DEPARTMENT OF COMMERCE, Malcolm Baldrige, *Secretary*
NATIONAL BUREAU OF STANDARDS, Ernest Ambler, *Director*

ABSTRACT

This work provides compiled experimental data and associated information on the thermodynamic, mechanical, thermophysical, and electrical properties of basalts from various locations in the United States and abroad. The thermodynamic properties include the chemical characterization of basalts, heat capacity, relative enthalpy, entropy, Gibbs energy, and molar volume. A summing procedure for obtaining values of heat capacity and calorimetric entropy above 298K is introduced.

KEY WORDS: Basalt; chemical characterization; data compilation; dielectric properties; electrical properties; mechanical properties; thermal properties; thermodynamic properties; thermophysical properties.

FOREWORD

This report was assembled by the Office of Standard Reference Data, National Bureau of Standards in collaboration with the National Center for Thermodynamic Data of Minerals, U.S. Geological Survey and the Center for Information and Numerical Data Analysis and Synthesis (CINDAS), Purdue University. It is in response to a request and funding support by the Office of National Waste Isolation (ONWI), Battelle Memorial Institute to compile and evaluate the physical and mechanical properties data of basalt. Because of changes in the management structure of ONWI the work on this project had to be terminated. The present report represents the effort to date in which the data on thermodynamic, mechanical, thermophysical and electrical properties have been compiled. Some attempt at evaluation has been made. In most instances, recommended values for the assembled data as a function of the given variables cannot be specified. Therefore, the data in this report must be viewed as an attempt to bring the property values being examined within narrower limits.

L. H. Gevantman

Introduction

The data contained in this report are being issued as a continuation of a project established under the sponsorship of the Office of Nuclear Waste Isolation, Battelle Memorial Institute with the N.B.S. Office of Standard Reference Data (OSRD) to compile and evaluate data on candidate minerals in which high level nuclear waste is to be emplaced. To date, the OSRD has issued property data on rock salt [1] and a feasibility report on the availability of data currently in the literature on the properties of basalt, granite, tuff, and shale [2]. This report consists of data on the chemical, thermodynamic, thermophysical, mechanical and electrical properties of generic basalts. A serious attempt has been made to review these data in a critical fashion with a view toward recommending specific values as a function of temperature, pressure and other variables. While some success has been achieved, it must be noted that due to the degree of variability in the physical makeup of the basalt and the inadequacy of reporting in the literature on the chemical makeup of the material under examination, experimental method, etc., only a few of the data can be accepted as rigorous.

Newer work and more refined methods for dealing with such chemically heterogeneous materials are starting to appear in the literature. These may help confirm or narrow the limitations which must accompany the present data. A very cursory comparison between these and unpublished site-specific data reveals a degree of agreement within broad error limits. It is recommended that many of these data be used with an awareness of their limitations.

The data are reported in four chapters. There is a degree of repetitiveness in two chapters dealing with thermophysical properties where heat capacity values are employed (Chapter 1 and 3). However, this overlap is considered useful and reinforcing. Each chapter contains a brief introduction to the subject area, a review of experimental method used to achieve the recorded values and the data. In some of the chapters error limits have been discussed and values recorded. As a result of this work, a method for extending heat capacity values beyond 298K has been refined and used as a tool for evaluating and extrapolating the thermodynamic data. This method is fully documented in an appendix to Chapter 1. References to the subject matter discussed in each chapter are to be found at the end of each chapter.

References

1. Gevantman, L.H., Editor, Physical Properties Data for Rock Salt, NBS Monograph 167, January 1981.
2. Gevantman, L.H., Feasibility Study: Compilation and Evaluation of Properties Data for Basalt, Granite, Tuff, and Shale, NBSIR 81-2217, January 1981.

ACKNOWLEDGEMENT

In completing this project, I wish to acknowledge the sponsorship of ONWI and Dr. G. E. Raines, the project manager. Special thanks go to Drs. C. Y. Ho and J. L. Haas, Jr., for their cooperation and perserverence in completing a difficult and demanding data effort.

PHYSICAL PROPERTIES DATA FOR BASALT

Lewis H. Gevantman

- CHAPTER 1 - THERMODYNAMIC AND THERMOPHYSICAL
PROPERTIES OF MINERAL COMPONENTS
OF BASALTS

- CHAPTER 2 - MECHANICAL PROPERTIES

- CHAPTER 3 - THERMOPHYSICAL PROPERTIES

- CHAPTER 4 - ELECTRICAL PROPERTIES

CHAPTER 1

THERMODYNAMIC AND THERMOPHYSICAL PROPERTIES OF MINERAL COMPONENTS OF BASALTS

Gilpin R. Robinson, Jr., John L. Haas, Jr.,
Constance M. Schafer, and H. T. Haselton, Jr.*

	<u>Page</u>
1.1. Introduction	1
1.2. Physical, Chemical, and Mineralogical Characteristics of Flood Basalt.	3
1.2.1. Introduction	3
1.2.2. Major Constituents	3
1.2.3. Alteration Products.	5
1.3. Thermodynamic and Thermophysical Properties.	8
1.3.1. Introduction	8
1.3.1.1. Definitions, notation, and nomenclature.	8
1.3.1.2. Types of data used in study.	8
1.3.1.2.1. Low-temperature calorimetry.	11
1.3.1.2.2. Differential-scanning calorimetry.	12
1.3.1.2.3. Drop calorimetry	13
1.3.1.2.4. X-ray crystallography.	14
1.3.1.2.5. Relative-volume measurements	15
1.3.1.2.6. Enthalpy-of-reaction measurements	16
1.3.1.2.7. Phase-equilibria experiments	18
1.3.1.2.8. Electromotive-force measure- ments.	20
1.3.2. Calculation of Estimated Thermophysical Properties of Rocks and Minerals: Heat Capacity, Relative	

*U.S. Geological Survey, National Center for the Thermodynamic Data
of Minerals, Branch of Experimental Geochemistry and Mineralogy,
National Center, Stop 959, Reston, VA 22092

Enthalpy, and Calorimetric Entropy of Silicate	
Minerals and Specific Heat of Silicate Rocks	21
1.3.2.1. Introduction	21
1.3.2.2. Evaluation of fictive molar properties . .	23
1.3.2.2.1. Introduction	23
1.3.2.2.2. Fitting procedure.	23
1.3.2.2.3. Results.	29
1.3.2.3. Procedures to calculate estimated molar heat capacities, relative enthalpies and calorimetric molar entropies for minerals.	43
1.3.2.3.1. Heat capacity.	43
1.3.2.3.2. Relative enthalpy.	50
1.3.2.3.3. Entropy.	52
1.3.2.4. Procedure to calculate estimated specific heats for rocks.	56
1.3.3. Evaluated Thermodynamic and Thermophysical Properties of Selected Mineral Phases in the MgO-SiO ₂ -H ₂ O-CO ₂ , CaO-Al ₂ O ₃ -SiO ₂ -H ₂ O-CO ₂ , and Fe-FeO-Fe ₂ O ₃ -SiO ₂ -H ₂ O Chemical Systems	60
1.3.3.1. Introduction	60
1.3.3.2. Fitting procedure.	60
1.3.3.2.1. Introduction	60
1.3.3.3. Data entry	63
1.3.3.4. Weighting of experimental data	65
1.3.3.5. Data rejection	67

	<u>Page</u>
1.3.3.6. Preparation of tables and summaries.	72
1.3.3.7. Confidence limits.	73
1.3.3.8. Results.	74
1.4. References	76
1.5. Appendix - Thermodynamic Tables and Summaries.	118
1.5.1. Chemical Index to Tables and Summaries	118
1.5.2. Mineral Index to Tables and Summaries.	118
1.5.3. Functions Describing Thermophysical Properties as a Function of Pressure and Temperature	125
1.5.4. Tables of Mineral Thermodynamic and Thermophysical Properties at 101.325 kPa (1 atm).	127
1.5.5. Summaries of Data Sources, Standard State Pro- perties, and Fitted Functions Describing Mineral Thermodynamic and Thermophysical Properties.	287
1.5.5.1. Al, aluminum	287
1.5.5.2. Al ₁₀₀ H.	287
1.5.5.2.1. Boehmite	287
1.5.5.2.2. Diaspore	290
1.5.5.3. Al(OH) ₃ , gibbsite.	293
1.5.5.4. Al ₂ O ₃ , corundum.	296
1.5.5.5. Al ₂ SiO ₅	296
1.5.5.5.1. Andalusite	296
1.5.5.5.2. Kyanite.	300
1.5.5.5.3. Sillimanite.	303

	<u>Page</u>
1.5.5.6. $\text{Al}_2\text{Si}_2\text{O}_5(\text{OH})_4$	303
1.5.5.6.1. Kaolinite	306
1.5.5.6.2. Dickite	306
1.5.5.6.3. Halloysite	306
1.5.5.7. $\text{Al}_2\text{Si}_4\text{O}_{10}(\text{OH})_2$, pyrophyllite	313
1.5.5.8. C, graphite	313
1.5.5.9. CO, carbon monoxide	313
1.5.5.10. CO ₂ , carbon dioxide	313
1.5.5.11. Ca, calcium	316
1.5.5.12. $\text{CaAl}_2\text{SiO}_6$, Ca-Al clinopyroxene	316
1.5.5.13. $\text{CaAl}_2\text{Si}_2\text{O}_8$, anorthite	316
1.5.5.14. $\text{CaAl}_4\text{Si}_2\text{O}_{10}(\text{OH})_2$, margarite	323
1.5.5.15. CaCO ₃	323
1.5.5.15.1. Calcite	323
1.5.5.15.2. Aragonite	328
1.5.5.16. CaO, lime	328
1.5.5.17. CaSiO ₃	328
1.5.5.17.1. Wollastonite	332
1.5.5.17.2. Cyclo wollastonite (= "pseudo- wollastonite")	332
1.5.5.18. $\text{Ca}_2\text{Al}_2\text{SiO}_6(\text{OH})_2$, bicchulite	338
1.5.5.19. $\text{Ca}_2\text{Al}_2\text{SiO}_6$, gehlenite	338
1.5.5.20. $\text{Ca}_2\text{Al}_2\text{Si}_3\text{O}_{10}(\text{OH})_2$, prehnite	343
1.5.5.21. $\text{Ca}_2\text{Al}_3\text{Si}_3\text{O}_{12}(\text{OH})$, zoisite	343

	<u>Page</u>
1.5.5.22. Ca_2SiO_4	343
1.5.5.22.1. Alpha- Ca_2SiO_4	354
1.5.5.22.2. Bredigite.	354
1.5.5.22.3. Ca olivine	354
1.5.5.22.4. Larnite.	354
1.5.5.23. $\text{Ca}_3\text{Al}_2\text{Si}_3\text{O}_{12}$, grossular	356
1.5.5.24. Ca_3SiO_5 , hatrurite.	356
1.5.5.25. $\text{Ca}_3\text{Si}_2\text{O}_7$, rankinite	362
1.5.5.26. $\text{Ca}_4\text{Al}_6\text{Si}_6\text{O}_{24}(\text{CO}_3)$, meionite	362
1.5.5.27. Fe, iron.	362
1.5.5.28. $\text{Fe}_{.947}\text{O}$, wustite.	367
1.5.5.29. FeSiO_3 , ferrosilite	367
1.5.5.30. Fe_2O_3 , hematite	373
1.5.5.31. Fe_2SiO_4 , fayalite	376
1.5.5.32. Fe_3O_4 , magnetite.	379
1.5.5.33. H_2 , hydrogen.	379
1.5.5.34. H_2O , water and the ideal and real gases .	382
1.5.5.35. H_4SiO_4 , silicic acid.	382
1.5.5.36. Mg, magnesium	383
1.5.5.37. MgCO_3 , magnesite.	383
1.5.5.38. MgO , periclase.	386
1.5.5.39. $\text{Mg}(\text{OH})_2$, brucite.	386
1.5.5.40. MgSiO_3 , clinoenstatite, enstatite, and protoenstatite.	386
1.5.5.41. Mg_2SiO_4 , forsterite	396

	<u>Page</u>
1.5.5.42. $Mg_3Si_2O_5(OH)_4$, chrysotile	396
1.5.5.43. $Mg_3Si_4O_{10}(OH)_2$, talc.	396
1.5.5.44. $Mg_7Si_8O_{22}(OH)_2$, anthophyllite	396
1.5.5.45. $Mg_{48}Si_{34}O_{85}(OH)_{62}$, antigorite	407
1.5.5.46. O_2 , oxygen.	407
1.5.5.47. Si, silicon	407
1.5.5.48. SiO_2	407
1.5.5.48.1. Quartz	410
1.5.5.48.2. Cristobalite	410
1.5.5.49. Constants	410
1.6. Symbols and Units.	414
1.7. Fundamental Constants, Defined Constants, and Conversion	
Factors from Non-SI Units to SI Units.	416

List of tables

	<u>Page</u>
Table 1. Representative flood basalt composition, norm, and mode.	4
Table 2. Experimental (and evaluated) data used to develop the functions for the fictive components	30
Table 3. Structural factors for common silicate minerals.	38
Table 4. Component coefficients to estimate mineral heat capacity and entropy (joules/mol.-kelvin)	40
Table 5.a. Conversion of the illite analysis to the number of moles of each oxide.	45
Table 5.b. Calculation of the constants a_1 , a_2 , a_3 , a_6 , and a_7 for use in equations 10 and 11 to calculate the relative heat capacity of illite of the composition given in part a of this table.	46
Table 6. Calculation of the constants a_1 , a_2 , a_3 , a_6 , and a_7 for use in equations 10 and 11 to calculate the relative heat content of acmite ($\text{NaFe}^{+3}\text{Si}_2\text{O}_6$).	51
Table 7.a. Calculation of the constants a_1 , a_2 , a_3 , a_4 , a_6 , and a_7 for use in equations 13 and 14 to calculate the calorimetric entropy of illite ($\text{K}_3\text{Al}_7\text{Mg}(\text{Si}_{14}\text{Al}_2)\text{O}_{40}(\text{OH})_8$) at 298.15 K	54
Table 7.b. Comparison of the observed calorimetric molar entropy of illite($\text{K}_3\text{Al}_7\text{Mg}(\text{Si}_{14}\text{Al}_2)\text{O}_{40}(\text{OH})_8$) with estimated values calculated from 1) the technique described	

	<u>Page</u>
here, 2) the technique described by Helgeson and others, 1978, and 3) the sum of oxide entropies. . . .	55
Table 8. Component coefficients to calculate rock specific heat (joules/gm-kelvin)	57
Table 9.a. Representative composition of terrestrial flood basalt (weight fraction).	58
Table 9.b. Estimated specific heats of selected basalts using the compositions given in part a of this table. Measured specific heats of basalt at Dreser, Wisconsin (data from Hanley and others, 1977).	59
Table 10. Chemical index to tables and summaries.	119
Table 11. Mineral index to tables and summaries	122
Table 12. Thermophysical values for stable phases of the element aluminum (Al) at 1.01325 bars (1 atm)	128
Table 13. Thermochemical properties of stable phases of the element aluminum (Al) at 1.01325 bars (1 atm)	129
Table 14. Thermophysical values for stable phases with the composition Al ₁₀₀ H at 1.01325 bars (1 atm)	130
Table 15. Thermochemical properties of stable phases with the composition Al ₁₀₀ H at 1.01325 bars (1 atm)	131
Table 16. Thermophysical values for boehmite, Al ₁₀₀ H, at 1.01325 bars (1 atm).	132
Table 17. Thermochemical properties of boehmite, Al ₁₀₀ H, at 1.01325 bars (1 atm).	133

	<u>Page</u>
Table 18. Thermophysical values for diaspore, AlOOH, at 1.01325 bars (1 atm).	134
Table 19. Thermochemical properties of diaspore, AlOOH, at 1.01325 bars (1 atm).	135
Table 20. Thermophysical values for gibbsite, Al(OH) ₃ , at 1.01325 bars (1 atm).	136
Table 21. Thermochemical properties of gibbsite, Al(OH) ₃ , at 1.01325 bars (1 atm).	137
Table 22. Thermophysical values for corundum, Al ₂ O ₃ , at 1.01325 bars (1 atm).	138
Table 23. Thermochemical properties of corundum, Al ₂ O ₃ , at 1.01325 bars (1 atm).	139
Table 24. Thermophysical values for stable phases with the composition Al ₂ SiO ₅ at 1.01325 bars (1 atm)	140
Table 25. Thermochemical properties of stable phases with the composition Al ₂ SiO ₅ at 1.01325 bars (1 atm)	141
Table 26. Thermophysical values for andalusite, Al ₂ SiO ₅ , at 1.01325 bars (1 atm).	142
Table 27. Thermochemical properties of andalusite, Al ₂ SiO ₅ , at 1.01325 bars (1 atm).	143
Table 28. Thermophysical values for kyanite, Al ₂ SiO ₅ , at 1.01325 bars (1 atm).	144
Table 29. Thermochemical properties of kyanite, Al ₂ SiO ₅ , at 1.01325 bars (1 atm).	145

Table 30.	Thermophysical values for sillimanite, Al_2SiO_5 , at 1.01325 bars (1 atm).	146
Table 31.	Thermochemical properties of sillimanite, Al_2SiO_5 , at 1.01325 bars (1 atm).	147
Table 32.	Thermophysical values for kaolinite, $\text{Al}_2\text{Si}_2\text{O}_5(\text{OH})_4$, at 1.01325 bars (1 atm).	148
Table 33.	Thermochemical properties of kaolinite, $\text{Al}_2\text{Si}_2\text{O}_5(\text{OH})_4$, at 1.01325 bars (1 atm)	149
Table 34.	Thermophysical values for dickite, $\text{Al}_2\text{Si}_2\text{O}_5(\text{OH})_4$, at 1.01325 bars (1 atm).	150
Table 35.	Thermochemical properties of dickite, $\text{Al}_2\text{Si}_2\text{O}_5(\text{OH})_4$, at 1.01325 bars (1 atm).	151
Table 36.	Thermophysical values for halloysite, $\text{Al}_2\text{Si}_2\text{O}_5(\text{OH})_4$, at 1.01325 bars (1 atm).	152
Table 37.	Thermochemical properties of halloysite, $\text{Al}_2\text{Si}_2\text{O}_5(\text{OH})_4$, at 1.01325 bars (1 atm)	153
Table 38.	Thermophysical values for pyrophyllite, $\text{Al}_2\text{Si}_4\text{O}_{10}(\text{OH})_2$, at 1.01325 bars (1 atm)	154
Table 39.	Thermochemical properties of pyrophyllite, $\text{Al}_2\text{Si}_4\text{O}_{10}(\text{OH})_2$, at 1.01325 bars (1 atm)	155
Table 40.	Thermophysical values for the elemental phase graphite (C) at 1.01325 bars (1 atm)	156
Table 41.	Thermochemical properties of the elemental phase graphite (C) at 1.01325 bars (1 atm).	157

Table 42.	Thermophysical values for carbon monoxide (CO, ideal gas) at 1.01325 bars (1 atm).	158
Table 43.	Thermochemical properties of carbon monoxide (CO, ideal gas) at 1.01325 bars (1 atm).	159
Table 44.	Thermophysical values for carbon dioxide (CO ₂ , ideal gas) at 1.01325 bars (1 atm).	160
Table 45.	Thermochemical properties of carbon dioxide (CO ₂ , ideal gas) at 1.01325 bars (1 atm).	161
Table 46.	Thermophysical values for stable phases of the element calcium (Ca) at 1.01325 bars (1 atm).	162
Table 47.	Thermochemical properties of stable phases of the element calcium (Ca) at 1.01325 bars (1 atm).	163
Table 48.	Thermophysical values for Ca-Al clinopyroxene, CaAl ₂ SiO ₆ , at 1.01325 bars (1 atm).	164
Table 49.	Thermochemical properties of Ca-Al clinopyroxene, CaAl ₂ SiO ₆ , at 1.01325 bars (1 atm).	165
Table 50.	Thermophysical values for anorthite, CaAl ₂ Si ₂ O ₈ , at 1.01325 bars (1 atm).	166
Table 51.	Thermochemical properties of anorthite, CaAl ₂ Si ₂ O ₈ , at 1.01325 bars (1 atm).	167
Table 52.	Thermophysical values for margarite, CaAl ₄ Si ₂ O ₁₀ (OH) ₂ , at 1.01325 bars (1 atm)	168
Table 53.	Thermochemical properties of margarite, CaAl ₄ Si ₂ O ₁₀ (OH) ₂ , at 1.01325 bars (1 atm)	169

	<u>Page</u>
Table 54. Thermophysical values for calcite, CaCO_3 , at 1.01325 bars (1 atm).	170
Table 55. Thermochemical properties of calcite, CaCO_3 , at 1.01325 bars (1 atm).	171
Table 56. Thermophysical values for aragonite, CaCO_3 , at 1.01325 bars (1 atm).	172
Table 57. Thermochemical properties of aragonite, CaCO_3 , at 1.01325 bars (1 atm).	173
Table 58. Thermophysical values for lime, CaO , at 1.01325 bars (1 atm).	174
Table 59. Thermochemical properties of lime, CaO , at 1.01325 bars (1 atm)	175
Table 60. Thermophysical values for stable phases with the composition CaSiO_3 at 1.01325 bars (1 atm).	176
Table 61. Thermochemical properties of stable phases with the composition CaSiO_3 at 1.01325 bars (1 atm).	177
Table 62. Thermophysical values for wollastonite, CaSiO_3 , at 1.01325 bars (1 atm).	178
Table 63. Thermochemical properties of wollastonite, CaSiO_3 , at 1.01325 bars (1 atm).	179
Table 64. Thermophysical values for cyclo wollastonite (= "pseudowollastonite"), CaSiO_3 , at 1.01325 bars (1 atm).	180
Table 65. Thermochemical properties of cyclo wollastonite (= "pseudowollastonite"), CaSiO_3 , at 1.01325 bars (1 atm).	181

	<u>Page</u>
Table 66. Thermophysical values for bicchulite, $\text{Ca}_2\text{Al}_2\text{SiO}_6(\text{OH})_2$, at 1.01325 bars (1 atm)	182
Table 67. Thermochemical properties of bicchulite, $\text{Ca}_2\text{Al}_2\text{SiO}_6(\text{OH})_2$, at 1.01325 bars (1 atm).	183
Table 68. Thermophysical values for gehlenite, $\text{Ca}_2\text{Al}_2\text{SiO}_7$, at 1.01325 bars (1 atm).	184
Table 69. Thermochemical properties of gehlenite, $\text{Ca}_2\text{Al}_2\text{SiO}_7$, at 1.01325 bars (1 atm).	185
Table 70. Thermophysical values for prehnite, $\text{Ca}_2\text{Al}_2\text{Si}_3\text{O}_{10}(\text{OH})_2$, at 1.01325 bars (1 atm)	186
Table 71. Thermochemical properties of prehnite, $\text{Ca}_2\text{Al}_2\text{Si}_3\text{O}_{10}(\text{OH})_2$, at 1.01325 bars (1 atm).	187
Table 72. Thermophysical values for zoisite, $\text{Ca}_2\text{Al}_3\text{Si}_3\text{O}_{12}(\text{OH})$, at 1.01325 bars (1 atm).	188
Table 73. Thermochemical properties of zoisite, $\text{Ca}_2\text{Al}_3\text{Si}_3\text{O}_{12}(\text{OH})$, at 1.01325 bars (1 atm)	189
Table 74. Thermophysical values for stable phases with the composition Ca_2SiO_4 at 1.01325 bars (1 atm)	190
Table 75. Thermochemical properties of stable phases with the composition Ca_2SiO_4 at 1.01325 bars (1 atm)	191
Table 76. Thermophysical values for alpha- Ca_2SiO_4 at 1.01325 bars (1 atm)	192
Table 77. Thermochemical properties of alpha- Ca_2SiO_4 at 1.01325 bars (1 atm).	193

	<u>Page</u>
Table 78. Thermophysical values for bredigite, Ca_2SiO_4 , at 1.01325 bars (1 atm)	194
Table 79. Thermochemical properties of bredigite, Ca_2SiO_4 , at 1.01325 bars (1 atm)	195
Table 80. Thermophysical values for Ca-olivine, Ca_2SiO_4 , at 1.01325 bars (1 atm)	196
Table 81. Thermochemical properties of Ca-olivine, Ca_2SiO_4 , at 1.01325 bars (1 atm)	197
Table 82. Thermophysical values for larnite, Ca_2SiO_4 , at 1.01325 bars (1 atm)	198
Table 83. Thermochemical properties of larnite, Ca_2SiO_4 , at 1.01325 bars (1 atm)	199
Table 84. Thermophysical values for grossular, $\text{Ca}_3\text{Al}_2\text{Si}_3\text{O}_{12}$, at 1.01325 bars (1 atm)	200
Table 85. Thermochemical properties of grossular, $\text{Ca}_3\text{Al}_2\text{Si}_3\text{O}_{12}$, at 1.01325 bars (1 atm)	201
Table 86. Thermophysical values for hatrurite, Ca_3SiO_5 , at 1.01325 bars (1 atm)	202
Table 87. Thermochemical properties of hatrurite, Ca_3SiO_5 , at 1.01325 bars (1 atm)	203
Table 88. Thermophysical values for rankinite, $\text{Ca}_3\text{Si}_2\text{O}_7$, at 1.01325 bars (1 atm)	204
Table 89. Thermochemical properties of rankinite, $\text{Ca}_3\text{Si}_2\text{O}_7$, at 1.01325 bars (1 atm)	205

	<u>Page</u>
Table 90. Thermophysical values for meionite, $\text{Ca}_4\text{Al}_6\text{Si}_6\text{O}_{24}(\text{CO}_3)$, at 1.01325 bars (1 atm)	206
Table 91. Thermochemical properties of meionite, $\text{Ca}_4\text{Al}_6\text{Si}_6\text{O}_{24}(\text{CO}_3)$, at 1.01325 bars (1 atm).	207
Table 92. Thermophysical values for stable phases of the element iron (Fe) at 1.01325 bars (1 atm)	208
Table 93. Thermochemical properties of stable phases of the element iron (Fe) at 1.01325 bars (1 atm)	209
Table 94. Thermophysical values for wustite, $\text{Fe}_{.947}\text{O}$, at 1.01325 bars (1 atm).	210
Table 95. Thermochemical properties of wustite, $\text{Fe}_{.947}\text{O}$, at 1.01325 bars (1 atm).	211
Table 96. Thermophysical values for ferrosilite, FeSiO_3 , at 1.01325 bars (1 atm).	212
Table 97. Thermochemical properties of ferrosilite, FeSiO_3 , at 1.01325 bars (1 atm).	213
Table 98. Thermophysical values for hematite, Fe_2O_3 , at 1.01325 bars (1 atm).	214
Table 99. Thermochemical properties of hematite, Fe_2O_3 , at 1.01325 bars (1 atm).	215
Table 100. Thermophysical values for fayalite, Fe_2SiO_4 , at 1.01325 bars (1 atm)	216
Table 101. Thermochemical properties of fayalite, Fe_2SiO_4 , at 1.01325 bars (1 atm)	217

	<u>Page</u>
Table 102. Thermophysical values for magnetite, Fe_3O_4 , at 1.01325 bars (1 atm)	218
Table 103. Thermochemical properties of magnetite, Fe_3O_4 , at 1.01325 bars (1 atm)	219
Table 104. Thermophysical values for the element hydrogen (H_2) at 1.01325 bars (1 atm).	220
Table 105. Thermochemical properties of the element hydrogen (H_2) at 1.01325 bars (1 atm).	221
Table 106. Thermophysical values for stable phases with the composition H_2O at 1.01325 bars (1 atm).	222
Table 107. Thermochemical properties of stable phases with the composition H_2O at 1.01325 bars (1 atm).	223
Table 108. Thermophysical values for water, H_2O , at 1.01325 bars (1 atm).	224
Table 109. Thermochemical properties of water, H_2O , at 1.01325 bars (1 atm)	225
Table 110. Thermophysical values for H_2O (ideal gas), at 1.01325 bars (1 atm)	226
Table 111. Thermochemical properties of H_2O (ideal gas), at 1.01325 bars (1 atm)	227
Table 112. Thermophysical values for stable phases of the element magnesium (Mg) at 1.01325 bars (1 atm)	228
Table 113. Thermochemical properties of stable phases of the element magnesium (Mg) at 1.01325 bars (1 atm)	229

	<u>Page</u>
Table 114. Thermophysical values for magnesite, $MgCO_3$, at 1.01325 bars (1 atm)	230
Table 115. Thermochemical properties of magnesite, $MgCO_3$, at 1.01325 bars (1 atm)	231
Table 116. Thermophysical values for periclase, MgO , at 1.01325 bars (1 atm)	232
Table 117. Thermochemical properties of periclase, MgO , at 1.01325 bars (1 atm)	233
Table 118. Thermophysical values for brucite, $Mg(OH)_2$, at 1.01325 bars (1 atm)	234
Table 119. Thermochemical properties of brucite, $Mg(OH)_2$, at 1.01325 bars (1 atm)	235
Table 120. Thermophysical values for Mg pyroxene, $MgSiO_3$, at 1.01325 bars (1 atm)	236
Table 121. Thermochemical properties of Mg pyroxene, $MgSiO_3$, at 1.01325 bars (1 atm)	237
Table 122. Thermophysical values for clinoenstatite, $MgSiO_3$, at 1.01325 bars (1 atm)	238
Table 123. Thermochemical properties of clinoenstatite, $MgSiO_3$, at 1.01325 bars (1 atm).	239
Table 124. Thermophysical values for enstatite, $MgSiO_3$, at 1.01325 bars (1 atm)	240
Table 125. Thermochemical properties of enstatite, $MgSiO_3$, at 1.01325 bars (1 atm)	241

	<u>Page</u>
Table 126. Thermophysical values for protoenstatite, MgSiO_3 , at 1.01325 bars (1 atm)	242
Table 127. Thermochemical properties of protoenstatite, MgSiO_3 , at 1.01325 bars (1 atm).	243
Table 128. Thermophysical values for forsterite, Mg_2SiO_4 , at 1.01325 bars (1 atm)	244
Table 129. Thermochemical properties of forsterite, Mg_2SiO_4 , at 1.01325 bars (1 atm)	245
Table 130. Thermophysical values for chrysotile, $\text{Mg}_3\text{Si}_2\text{O}_5(\text{OH})_4$, at 1.01325 bars (1 atm).	246
Table 131. Thermochemical properties of chrysotile, $\text{Mg}_3\text{Si}_2\text{O}_5(\text{OH})_4$, at 1.01325 bars (1 atm)	247
Table 132. Thermophysical values for talc, $\text{Mg}_3\text{Si}_4\text{O}_{10}(\text{OH})_2$, at 1.01325 bars (1 atm)	248
Table 133. Thermochemical properties of talc, $\text{Mg}_3\text{Si}_4\text{O}_{10}(\text{OH})_2$, at 1.01325 bars (1 atm)	249
Table 134. Thermophysical values for anthophyllite, $\text{Mg}_7\text{Si}_8\text{O}_{22}(\text{OH})_2$, at 1.01325 bars (1 atm).	250
Table 135. Thermochemical properties of anthophyllite, $\text{Mg}_7\text{Si}_8\text{O}_{22}(\text{OH})_2$, at 1.01325 bars (1 atm).	251
Table 136. Thermophysical values for antigorite, $\text{Mg}_{48}\text{Si}_{34}\text{O}_{85}(\text{OH})_{62}$, at 1.01325 bars (1 atm)	252
Table 137. Thermochemical properties of antigorite, $\text{Mg}_{48}\text{Si}_{34}\text{O}_{85}(\text{OH})_{62}$, at 1.01325 bars (1 atm)	253

	<u>Page</u>
Table 138. Thermophysical values for the element oxygen (O_2) at 1.01325 bars (1 atm)	254
Table 139. Thermochemical properties of the element oxygen (O_2) at 1.01325 bars (1 atm).	255
Table 140. Thermophysical values for stable phases of the element silicon (Si) at 1.01325 bars (1 atm)	256
Table 141. Thermochemical properties of stable phases of the element silicon (Si) at 1.01325 bars (1 atm)	257
Table 142. Thermophysical values for quartz, SiO_2 , at 1.01325 bars (1 atm)	258
Table 143. Thermochemical properties of quartz, SiO_2 , at 1.01325 bars (1 atm)	259
Table 144. Thermophysical values for cristobalite, SiO_2 , at 1.01325 bars (1 atm)	260
Table 145. Thermochemical properties of cristobalite, SiO_2 , at 1.01325 bars (1 atm)	261
Table 146. Molar volume in cm^3/g of boehmite, $AlOOH$, to 1000 K and 10,000 bars.	262
Table 147. Molar volume in cm^3/g of diaspore, $AlOOH$, to 1800 K and 10,000 bars.	262
Table 148. Molar volume in cm^3/g of gibbsite, $Al(OH)_3$, to 1000 K and 10,000 bars.	263
Table 149. Molar volume in cm^3/g of corundum, Al_2O_3 , to 1800 K and 10,000 bars.	263

	<u>Page</u>
Table 150. Molar volume in cm ³ /g of andalusite, Al ₂ SiO ₅ , to 1800 K and 10,000 bars.	264
Table 151. Molar volume in cm ³ /g of kyanite, Al ₂ SiO ₅ , to 1800 K and 10,000 bars.	264
Table 152. Molar volume in cm ³ /g of sillimanite, Al ₂ SiO ₅ , to 1800 K and 10,000 bars.	265
Table 153. Molar volume in cm ³ /g of kaolinite, Al ₂ Si ₂ O ₅ (OH) ₄ , to 1000 K and 10,000 bars	265
Table 154. Molar volume in cm ³ /g of dickite, Al ₂ Si ₂ O ₅ (OH) ₄ , to 1000 K and 10,000 bars	266
Table 155. Molar volume in cm ³ /g of halloysite, Al ₂ Si ₂ O ₅ (OH) ₄ , to 1000 K and 10,000 bars	266
Table 156. Molar volume in cm ³ /g of pyrophyllite, Al ₂ Si ₄ O ₁₀ (OH) ₂ , to 1000 K and 10,000 bars.	267
Table 157. Molar volume in cm ³ /g of Ca-Al clinopyroxene, CaAl ₂ SiO ₆ , to 1800 K and 10,000 bars	267
Table 158. Molar volume in cm ³ /g of anorthite, CaAl ₂ Si ₂ O ₈ , to 1800 K and 10,000 bars	268
Table 159. Molar volume in cm ³ /g of margarite, CaAl ₄ Si ₂ O ₁₀ (OH) ₂ , to 1000 K and 10,000 bars.	268
Table 160. Molar volume in cm ³ /g of calcite, CaCO ₃ , to 1800 K and 10,000 bars.	269
Table 161. Molar volume in cm ³ /g of aragonite, CaCO ₃ , to 1800 K and 10,000 bars.	269

Table 162.	Molar volume in cm^3/g of lime, CaO , to 1800 K and 10,000 bars.	270
Table 163.	Molar volume in cm^3/g of wollastonite, CaSiO_3 , to 1800 K and 10,000 bars.	270
Table 164.	Molar volume in cm^3/g of cyclo wollastonite, CaSiO_3 , to 1800 K and 10,000 bars	271
Table 165.	Molar volume in cm^3/g of bicchulite, $\text{Ca}_2\text{Al}_2\text{SiO}_6(\text{OH})_2$, to 1000 K and 10,000 bars.	271
Table 166.	Molar volume in cm^3/g of gehlenite, $\text{Ca}_2\text{Al}_2\text{SiO}_7$, to 1800 K and 10,000 bars	272
Table 167.	Molar volume in cm^3/g of prehnite, $\text{Ca}_2\text{Al}_2\text{Si}_3\text{O}_{10}(\text{OH})_2$, to 1000 K and 10,000 bars.	272
Table 168.	Molar volume in cm^3/g of zoisite, $\text{Ca}_2\text{Al}_3\text{Si}_3\text{O}_{12}(\text{OH})$, to 1000 K and 10,000 bars	273
Table 169.	Molar volume in cm^3/g of alpha, Ca_2SiO_4 , to 1800 K and 10,000 bars.	273
Table 170.	Molar volume in cm^3/g of bredigite, Ca_2SiO_4 , to 1800 K and 10,000 bars.	274
Table 171.	Molar volume in cm^3/g of ca-olivine, Ca_2SiO_4 , to 1800 K and 10,000 bars.	274
Table 172.	Molar volume in cm^3/g of larnite, Ca_2SiO_4 , to 1800 K and 10,000 bars.	275
Table 173.	Molar volume in cm^3/g of grossular, $\text{Ca}_3\text{Al}_2\text{Si}_3\text{O}_{12}$, to 1800 K and 10,000 bars	275

	<u>Page</u>
Table 174. Molar volume in cm^3/g of hatrurite, Ca_3SiO_5 , to 1800 K and 10,000 bars.	276
Table 175. Molar volume in cm^3/g of rankinite, $\text{Ca}_3\text{Si}_2\text{O}_7$, to 1800 K and 10,000 bars.	276
Table 176. Molar volume in cm^3/g of meionite, $\text{Ca}_4\text{Al}_6\text{Si}_6\text{O}_{24}(\text{CO}_3)$, to 1800 K and 10,000 bars.	277
Table 177. Molar volume in cm^3/g of wustite, $\text{Fe}_{.947}\text{O}$, to 1800 K and 10,000 bars.	277
Table 178. Molar volume in cm^3/g of ferrosilite, FeSiO_3 , to 1800 K and 10,000 bars.	278
Table 179. Molar volume in cm^3/g of hematite, Fe_2O_3 , to 1800 K and 10,000 bars.	278
Table 180. Molar volume in cm^3/g of fayalite, Fe_2SiO_4 , to 1800 K and 10,000 bars.	279
Table 181. Molar volume in cm^3/g of magnetite, Fe_3O_4 , to 1800 K and 10,000 bars.	279
Table 182. Molar volume in cm^3/g of water and H_2O (real gas) to 1800 K and 10,000 bars	280
Table 183. Molar volume in cm^3/g of magnesite, MgCO_3 , to 1800 K and 10,000 bars.	280
Table 184. Molar volume in cm^3/g of periclase, MgO , to 1800 K and 10,000 bars.	281
Table 185. Molar volume in cm^3/g of brucite, $\text{Mg}(\text{OH})_2$, to 1000 K and 10,000 bars.	281

	<u>Page</u>
Table 186. Molar volume in cm^3/g of clinoenstatite, MgSiO_3 , to 1800 K and 10,000 bars	282
Table 187. Molar volume in cm^3/g of enstatite, MgSiO_3 , to 1800 K and 10,000 bars.	282
Table 188. Molar volume in cm^3/g of protoenstatite, MgSiO_3 , to 1800 K and 10,000 bars	283
Table 189. Molar volume in cm^3/g of forsterite, Mg_2SiO_4 , to 1800 K and 10,000 bars.	283
Table 190. Molar volume in cm^3/g of chrysotile, $\text{Mg}_3\text{Si}_2\text{O}_5(\text{OH})_4$, to 1000 K and 10,000 bars	284
Table 191. Molar volume in cm^3/g of talc, $\text{Mg}_3\text{Si}_4\text{O}_{10}(\text{OH})_2$, to 1000 K and 10,000 bars.	284
Table 192. Molar volume in cm^3/g of anthophyllite, $\text{Mg}_7\text{Si}_8\text{O}_{22}(\text{OH})_2$, to 1000 K and 10,000 bars.	285
Table 193. Molar volume in cm^3/g of antigorite, $\text{Mg}_{48}\text{Si}_{34}\text{O}_{85}(\text{OH})_{62}$, to 1000 K and 10,000 bars	285
Table 194. Molar volume in cm^3/g of quartz, SiO_2 , to 1800 K and 10,000 bars.	286
Table 195. Molar volume in cm^3/g of cristobalite, SiO_2 , to 1800 K and 10,000 bars.	286
Table 196. Sources of thermophysical data for boehmite, $\text{Al}(\text{OH})_3$. .	288
Table 197. Sources of thermochemical data for boehmite, $\text{Al}(\text{OH})_3$. .	289
Table 198. Sources of thermophysical data for diaspore, $\text{Al}(\text{OH})_3$. .	291
Table 199. Sources of thermochemical data for diaspore, $\text{Al}(\text{OH})_3$. .	292

	<u>Page</u>
Table 200. Sources of thermophysical data for gibbsite, $\text{Al}(\text{OH})_3$.	294
Table 201. Sources of thermochemical data for gibbsite, $\text{Al}(\text{OH})_3$.	295
Table 202. Sources of volumetric data for corundum, Al_2O_3	297
Table 203. Sources of thermophysical data for andalusite, Al_2SiO_5	298
Table 204. Sources of thermochemical data for andalusite, Al_2SiO_5	299
Table 205. Sources of thermophysical data for kyanite, Al_2SiO_5 .	301
Table 206. Sources of thermochemical data for kyanite, Al_2SiO_5 .	302
Table 207. Sources of thermophysical data for sillimanite, Al_2SiO_5	304
Table 208. Sources of thermochemical data for sillimanite, Al_2SiO_5	305
Table 209. Sources of thermophysical data for kaolinite, $\text{Al}_2\text{Si}_2\text{O}_5(\text{OH})_4$	307
Table 210. Sources of thermochemical data for kaolinite, $\text{Al}_2\text{Si}_2\text{O}_5(\text{OH})_4$	308
Table 211. Sources of thermophysical data for dickite, $\text{Al}_2\text{Si}_2\text{O}_5(\text{OH})_4$	309
Table 212. Sources of thermochemical data for dickite, $\text{Al}_2\text{Si}_2\text{O}_5(\text{OH})_4$	310
Table 213. Sources of thermophysical data for halloysite, $\text{Al}_2\text{Si}_2\text{O}_5(\text{OH})_4$	311
Table 214. Sources of thermochemical data for halloysite, $\text{Al}_2\text{Si}_2\text{O}_5(\text{OH})_4$	312

Table 215.	Sources of thermophysical data for pyrophyllite, $\text{Al}_2\text{Si}_4\text{O}_{10}(\text{OH})_2$	314
Table 216.	Sources of thermochemical data for pyrophyllite, $\text{Al}_2\text{Si}_4\text{O}_{10}(\text{OH})_2$	315
Table 217.	Sources of thermophysical data for Ca-Al clinopyroxene, $\text{CaAl}_2\text{SiO}_6$	317
Table 218.	Sources of thermochemical data for Ca-Al clinopyroxene, $\text{CaAl}_2\text{SiO}_6$	318
Table 219.	Sources of thermophysical data for anorthite, $\text{CaAl}_2\text{Si}_2\text{O}_8$	319
Table 220.	Sources of thermochemical data for anorthite, $\text{CaAl}_2\text{Si}_2\text{O}_8$	320
Table 221.	Sources of thermophysical data for margarite, $\text{CaAl}_4\text{Si}_2\text{O}_{10}(\text{OH})_2$	324
Table 222.	Sources of thermochemical data for margarite, $\text{CaAl}_4\text{Si}_2\text{O}_{10}(\text{OH})_2$	325
Table 223.	Sources of thermophysical data for calcite, CaCO_3 . . .	326
Table 224.	Sources of thermochemical data for calcite, CaCO_3 . . .	327
Table 225.	Sources of thermophysical data for aragonite, CaCO_3 . . .	329
Table 226.	Sources of thermochemical data for aragonite, CaCO_3 . . .	330
Table 227.	Sources of volumetric data for lime, CaO	331
Table 228.	Sources of thermophysical data for wollastonite, CaSiO_3	333
Table 229.	Sources of thermochemical data for wollastonite,	

	<u>Page</u>
CaSiO ₃	334
Table 230. Sources of thermophysical data for cyclo wollastonite, CaSiO ₃	336
Table 231. Sources of thermochemical data for cyclo wollastonite (= "pseudowollastonite"), CaSiO ₃	337
Table 232. Sources of thermophysical data for bicchulite, Ca ₂ Al ₂ SiO ₆ (OH) ₂	339
Table 233. Sources of thermochemical data for bicchulite, Ca ₂ Al ₂ SiO ₆ (OH) ₂	340
Table 234. Sources of thermophysical data for gehlenite, Ca ₂ Al ₂ SiO ₇	341
Table 235. Sources of thermochemical data for gehlenite, Ca ₂ Al ₂ SiO ₇	342
Table 236. Sources of thermophysical data for prehnite, Ca ₂ Al ₂ Si ₃ O ₁₀ (OH) ₂	344
Table 237. Sources of thermochemical data for prehnite, Ca ₂ Al ₂ Si ₃ O ₁₀ (OH) ₂	345
Table 238. Sources of thermophysical data for zoisite, Ca ₂ Al ₃ Si ₃ O ₁₂ (OH)	346
Table 239. Sources of thermochemical data for zoisite, Ca ₂ Al ₃ Si ₃ O ₁₂ (OH)	347
Table 240. Sources of thermophysical data for alpha-Ca ₂ SiO ₄ . . .	348
Table 241. Sources of thermophysical data for bredigite, Ca ₂ SiO ₄ .	349
Table 242. Sources of thermochemical data for bredigite, Ca ₂ SiO ₄ .	350

	<u>Page</u>
Table 243. Sources of thermophysical data for Ca-olivine, Ca ₂ SiO ₄	351
Table 244. Sources of thermophysical data for larnite, Ca ₂ SiO ₄	352
Table 245. Sources of thermochemical data for larnite, Ca ₂ SiO ₄	353
Table 246. Sources of thermophysical data for grossular, Ca ₃ Al ₂ Si ₃ O ₁₂	357
Table 247. Sources of thermochemical data for grossular, Ca ₃ Al ₂ Si ₃ O ₁₂	358
Table 248. Sources of thermophysical data for hatrurite, Ca ₃ SiO ₅	360
Table 249. Sources of thermochemical data for hatrurite, Ca ₃ SiO ₅	361
Table 250. Sources of thermophysical data for rankinite, Ca ₃ Si ₂ O ₇	363
Table 251. Sources of thermochemical data for rankinite, Ca ₃ Si ₂ O ₇	364
Table 252. Sources of thermophysical data for meionite, Ca ₄ Al ₆ Si ₆ O ₂₄ (CO ₃)	365
Table 253. Sources of thermochemical data for meionite, Ca ₄ Al ₆ Si ₆ O ₂₄ (CO ₃)	366
Table 254. Sources of thermophysical data for wustite, Fe _{.947} O	368
Table 255. Sources of thermochemical data for wustite, Fe _{.947} O	369
Table 256. Sources of thermophysical data for ferrosillite, FeSiO ₃	371
Table 257. Sources of thermochemical data for ferrosillite, FeSiO ₃	372

	<u>Page</u>
Table 258. Sources of thermophysical data for hematite, Fe_2O_3 . .	374
Table 259. Sources of thermochemical data for hematite, Fe_2O_3 . .	375
Table 260. Sources of thermophysical data for fayalite, Fe_2SiO_4 .	377
Table 261. Sources of thermochemical data for fayalite, Fe_2SiO_4 .	378
Table 262. Sources of thermophysical data for magnetite, Fe_3O_4 .	380
Table 263. Sources of thermochemical data for magnetite, Fe_3O_4 .	381
Table 264. Sources of thermophysical data for magnesite, MgCO_3 .	384
Table 265. Sources of thermochemical data for magnesite, MgCO_3 .	385
Table 266. Sources of thermophysical data for periclase, MgO . . .	387
Table 267. Sources of thermophysical data for brucite, $\text{Mg}(\text{OH})_2$.	388
Table 268. Sources of thermochemical data for brucite, $\text{Mg}(\text{OH})_2$.	389
Table 269. Sources of thermophysical data for clinoenstatite, MgSiO_3	390
Table 270. Sources of thermochemical data for clinoenstatite, MgSiO_3	391
Table 271. Sources of thermophysical data for orthoenstatite, MgSiO_3	392
Table 272. Sources of thermochemical data for enstatite, MgSiO_3 .	393
Table 273. Sources of thermophysical data for protoenstatite, MgSiO_3	394
Table 274. Sources of thermochemical data for protoenstatite, MgSiO_3	395
Table 275. Sources of thermophysical data for forsterite, Mg_2SiO_4	397

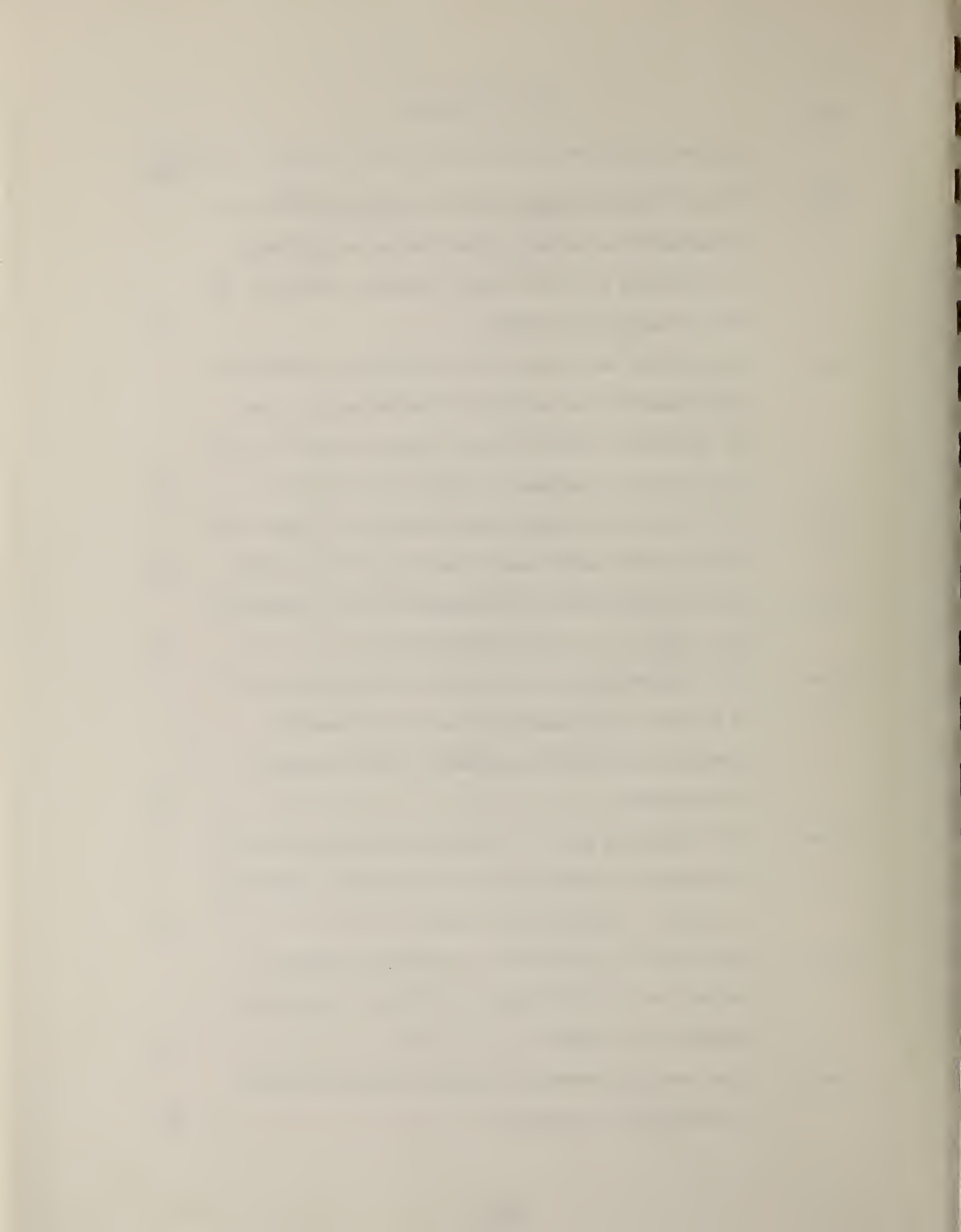
	<u>Page</u>
Table 276. Sources of thermochemical data for forsterite, Mg_2SiO_4	398
Table 277. Sources of thermophysical data for chrysotile, $Mg_3Si_2O_5(OH)_4$	400
Table 278. Sources of thermochemical data for chrysotile, $Mg_3Si_2O_5(OH)_4$	401
Table 279. Sources of thermophysical data for talc, $Mg_3Si_4O_{10}(OH)_2$	402
Table 280. Sources of thermochemical data for talc, $Mg_3Si_4O_{10}(OH)_2$	403
Table 281. Sources of thermophysical data for anthophyllite, $Mg_7Si_8O_{22}(OH)_2$	405
Table 282. Sources of thermochemical data for anthophyllite, $Mg_7Si_8O_{22}(OH)_2$	406
Table 283. Sources of thermophysical data for antigorite, $Mg_3Si_2O_5(OH)_4$	408
Table 284. Sources of thermochemical data for antigorite, $Mg_{48}Si_{34}O_{85}(OH)_{62}$	409
Table 285. Sources of volumetric data for quartz, SiO_2	411
Table 286. Sources of data on the alpha - beta transition in quartz, SiO_2	412
Table 287. Sources of thermophysical data for cristobalite, SiO_2	413
Table 288. Constants for energy-related functions in section 1.5.3.	414

Table 289. Constants for volume-related functions in section

1.5.3. 419

List of Figures

	<u>Page</u>
Figure 1. Plots of the percentage errors for estimates from the oxide-summation method against the percentage errors for estimates from the fictive component method for 85 sets of heat-capacity data.	42
Figure 2. Plots of the percentage errors for estimates from the oxide summation method against the percentage errors for estimates from the fictive component method for 45 sets of molar calorimetric entropy data at 298.15 K	44
Figure 3. Plot of the experimental and estimated heat capacities for an illite sample used by Robie and others (1976).	49
Figure 4. Plot of experimental and estimated relative enthalpies ($H_T - H_{298.15}$) for acmite ($\text{NaFe}^{+3}\text{Si}_2\text{O}_6$)	53
Figure 5. Error (observed value - calculated value)/precision as a function of temperature for the differential scanning calorimeter measurements of heat capacity for anorthite	68
Figure 6. Error (observed value - calculated value)/precision as a function of temperature for the reaction: Kaolinite + 2 Quartz = Pyrophyllite + Steam	70
Figure 7. Gibbs energy of reaction as a function of absolute temperature for the reaction: Kaolinite + 2 Quartz = Pyrophyllite + Steam.	71
Figure 8. Gibbs energy difference of phases indicated relative to bredigite at 1.01 bars	355



OUTLINE:

CHAPTER 1: THERMODYNAMIC AND THERMOPHYSICAL PROPERTIES
OF MINERAL COMPONENTS OF BASALTS

by

Gilpin R. Robinson, Jr., John L. Haas, Jr.,
Constance M. Schafer, and H. T. Haselton, Jr.

- 1.1. Introduction
- 1.2. Physical, Chemical, and Mineralogical Characteristics of Flood Basalt
 - 1.2.1. Introduction
 - 1.2.2. Major Constituents
 - 1.2.3. Alteration Products
- 1.3. Thermodynamic and Thermophysical Properties
 - 1.3.1. Introduction
 - 1.3.1.1. Definitions, notation, and nomenclature
 - 1.3.1.2. Types of data used in study
 - 1.3.1.2.1. Low-temperature calorimetry
 - 1.3.1.2.2. Differential-scanning calorimetry
 - 1.3.1.2.3. Drop calorimetry
 - 1.3.1.2.4. X-ray crystallography
 - 1.3.1.2.5. Relative-volume measurements
 - 1.3.1.2.6. Enthalpy-of-reaction measurements
 - 1.3.1.2.7. Phase-equilibria experiments
 - 1.3.1.2.8. Electromotive-force measurements
 - 1.3.2. Calculation of Estimated Thermophysical Properties of Rocks and Minerals: Heat Capacity, Relative Enthalpy, and Calorimetric Entropy of Silicate Minerals and Specific Heat of Silicate Rocks

- 1.3.2.1. Introduction
- 1.3.2.2. Evaluation of fictive molar properties
 - 1.3.2.2.1. Introduction
 - 1.3.2.2.2. Fitting procedure
 - 1.3.2.2.3. Results
- 1.3.2.3. Procedures to calculate estimated molar heat capacities, relative enthalpies and calorimetric molar entropies for minerals
 - 1.3.2.3.1. Heat capacity
 - 1.3.2.3.2. Relative enthalpy
 - 1.3.2.3.3. Entropy
- 1.3.2.4. Procedure to calculate estimated specific heats for rocks
- 1.3.3. Evaluated Thermodynamic and Thermophysical Properties of Selected Mineral Phases in the MgO-SiO₂-H₂O-CO₂, CaO-Al₂O₃-SiO₂-H₂O-CO₂, and Fe-FeO-Fe₂O₃-SiO₂-H₂O Chemical Systems
 - 1.3.3.1. Introduction
 - 1.3.3.2. Fitting procedure
 - 1.3.3.3. Data entry
 - 1.3.3.4. Weighting of experimental data
 - 1.3.3.5. Data rejection
 - 1.3.3.6. Preparation of tables and summaries
 - 1.3.3.7. Confidence limits
- 1.4. References

- 1.5. Appendix - Thermodynamic Tables and Summaries
 - 1.5.1. Chemical Index to Tables and Summaries
 - 1.5.2. Mineral Index to Tables and Summaries
 - 1.5.3. Functions Describing Thermophysical Properties as a Function of Pressure and Temperature
 - 1.5.4. Tables of Mineral Thermodynamic and Thermophysical Properties at 101.325 kPa (1 atm)
 - 1.5.5. Summaries of Data Sources, Standard State Properties, and Fitted Functions Describing Mineral Thermodynamic and Thermophysical Properties
 - 1.5.5.1. Al, aluminum
 - 1.5.5.2. Al₂O₃
 - 1.5.5.2.1. Boehmite
 - 1.5.5.2.2. Diaspore
 - 1.5.5.3. Al(OH)₃, gibbsite
 - 1.5.5.4. Al₂O₃, corundum
 - 1.5.5.5. Al₂SiO₅
 - 1.5.5.5.1. Andalusite
 - 1.5.5.5.2. Kyanite
 - 1.5.5.5.3. Sillimanite
 - 1.5.5.6. Al₂Si₂O₅(OH)₄
 - 1.5.5.6.1. Kaolinite
 - 1.5.5.6.2. Dickite
 - 1.5.5.6.3. Halloysite
 - 1.5.5.7. Al₂Si₄O₁₀(OH)₂, pyrophyllite
 - 1.5.5.8. C, graphite

- 1.5.5.9. CO, carbon monoxide
- 1.5.5.10. CO₂, carbon dioxide
- 1.5.5.11. Ca, calcium
- 1.5.5.12. CaAl₂SiO₆, Ca-Al clinopyroxene
- 1.5.5.13. CaAl₂Si₂O₈, anorthite
- 1.5.5.14. CaAl₄Si₂O₁₀(OH)₂, margarite
- 1.5.5.15. CaCO₃
 - 1.5.5.15.1. Calcite
 - 1.5.5.15.2. Aragonite
- 1.5.5.16. CaO, lime
- 1.5.5.17. CaSiO₃
 - 1.5.5.17.1. Wollastonite
 - 1.5.5.17.2. Cyclo wollastonite (= "pseudo-wollastonite")
- 1.5.5.18. Ca₂Al₂SiO₆(OH)₂, bicchulite
- 1.5.5.19. Ca₂Al₂SiO₆, gehlenite
- 1.5.5.20. Ca₂Al₂Si₃O₁₀(OH)₂, prehnite
- 1.5.5.21. Ca₂Al₃Si₃O₁₂(OH), zoisite
- 1.5.5.22. Ca₂SiO₄
 - 1.5.5.22.1. Alpha-Ca₂SiO₄
 - 1.5.5.22.2. Bredigite
 - 1.5.5.22.3. Ca olivine
 - 1.5.5.22.4. Larnite
- 1.5.5.23. Ca₃Al₂Si₃O₁₂, grossular
- 1.5.5.24. Ca₃SiO₅, hatrurite
- 1.5.5.25. Ca₃Si₂O₇, rankinite

- 1.5.5.26. $\text{Ca}_4\text{Al}_6\text{Si}_6\text{O}_{24}(\text{CO}_3)$, meionite
- 1.5.5.27. Fe, iron
- 1.5.5.28. $\text{Fe}_{.947}\text{O}$, wustite
- 1.5.5.29. FeSiO_3 , ferrosilite
- 1.5.5.30. Fe_2O_3 , hematite
- 1.5.5.31. Fe_2SiO_4 , fayalite
- 1.5.5.32. Fe_3O_4 , magnetite
- 1.5.5.33. H_2 , hydrogen
- 1.5.5.34. H_2O , water and the ideal and real gases
- 1.5.5.35. H_4SiO_4 , silicic acid
- 1.5.5.36. Mg, magnesium
- 1.5.5.37. MgCO_3 , magnesite
- 1.5.5.38. MgO , periclase
- 1.5.5.39. $\text{Mg}(\text{OH})_2$, brucite
- 1.5.5.40. MgSiO_3 , clinoenstatite, enstatite, and proto-enstatite
- 1.5.5.41. Mg_2SiO_4 , forsterite
- 1.5.5.42. $\text{Mg}_3\text{Si}_2\text{O}_5(\text{OH})_4$, chrysotile
- 1.5.5.43. $\text{Mg}_3\text{Si}_4\text{O}_{10}(\text{OH})_2$, talc
- 1.5.5.44. $\text{Mg}_7\text{Si}_8\text{O}_{22}(\text{OH})_2$, anthophyllite
- 1.5.5.45. $\text{Mg}_{48}\text{Si}_{34}\text{O}_{85}(\text{OH})_{62}$, antigorite
- 1.5.5.46. O_2 , oxygen
- 1.5.5.47. Si, silicon
- 1.5.5.48. SiO_2
 - 1.5.5.48.1. Quartz
 - 1.5.5.48.2. Cristobalite

1.6. Symbols and Units

1.7. Fundamental Constants, Defined Constants, and Conversion
Factors from Non-SI Units to SI Units

CHAPTER 1

THERMODYNAMIC AND THERMOPHYSICAL PROPERTIES OF MINERAL COMPONENTS OF BASALTS

Gilpin R. Robinson, Jr., and John L. Haas, Jr.
Constance M. Schafer and H. T. Haselton, Jr.

National Center for the Thermodynamic Data of Minerals,
U.S. Geological Survey, Reston, VA 22091

1.1. Introduction

The thermal and chemical environment of a potential nuclear waste repository must be known and understood before an intelligent decision can be made regarding radioactive waste storage. A properly evaluated set of thermodynamic data can provide some of the needed information. This report contains a tabulation of thermodynamic and thermophysical properties for selected phases in the $MgO-SiO_2-H_2O-CO_2$, $Fe-FeO-Fe_2O_3-SiO_2$, and $CaO-Al_2O_3-SiO_2-H_2O-CO_2$ chemical systems and presents the procedure used to evaluate the internally consistent set of thermodynamic data for minerals.

The chapter is divided into five sections. The first section is a brief introduction. The second section summarizes the chemical and physical character of basalt rock and identifies:

1. a generalized chemical system describing the rock type,
2. major mineral constituents,
3. minor mineral constituents, and
4. common alteration phases.

The third section describes the procedure used to evaluate the inter-

nally consistent set of thermodynamic and thermophysical properties for mineral phases presented as tables in the Appendix. A procedure to estimate thermophysical properties of minerals and rocks is described. Section 4 contains reference citations to the sources of data used in the evaluation, and section 5 (Appendix) contains tables of thermodynamic and thermophysical properties for selected phases and critiques the specific sources of information used in the evaluation of these properties.

1.2. Physical, Chemical, and Mineralogical Characteristics of Flood Basalt

1.2.1. Introduction

Flood basalt occurs as sheets of rapidly cooled basaltic lava erupted from a volcanic center in continental basement. Individual sheets typically have great areal extent and range between less than 1 meter to 100 meters in thickness.

The model chemical system is $\text{CaO}-(\text{Na}_2\text{O})-\text{FeO}-(\text{Fe}_2\text{O}_3)-\text{MgO}-\text{Al}_2\text{O}_3-\text{SiO}_2-(\text{H}_2\text{O},\text{CO}_2)$. A typical analysis, norm, and mode is given in table 1.

1.2.2. Major Constituents

The major constituents consist of phenocrysts and matrix phases. Phenocrysts typically account for 0 to 10 percent of the rock volume with matrix comprising the remainder. Gas bubbles (vesicles) occur in some basalt units, usually near the top surface of the flow.

1. Phenocrysts usually are:

Olivine	- typically For 90:Fay 10
Forsterite	- Mg_2SiO_4
Fayalite	- Fe_2SiO_4
Plagioclase	- typically Ano 60:Alb 40
Anorthite	- $\text{CaAl}_2\text{Si}_2\text{O}_8$
Albite	- $\text{NaAlSi}_3\text{O}_8$

2. Matrix, which typically is a microcrystalline intergrowth of:

Clinopyroxene	- typically pigeonite - approximately Cen 46:Cfs 38:Dio 9:Hed 7
---------------	---

Table 1. Representative flood basalt composition, norm, and mode

Oxide wt. %	Basalt ^a	Norm (wt. %) (calculated from chemical composition)	
<u>Chemical composition</u>		Quartz	3.9
SiO ₂	53.8	K-feldspar	8.9
TiO ₂	2.0	Albite	25.2
Al ₂ O ₃	13.9	Anorthite	20.0
Fe ₂ O ₃	2.6	Diopside	13.9
FeO	9.3	Hypersthene	15.3
MnO	0.2	Ilmenite	3.8
MgO	4.1	Magnetite	3.7
CaO	7.9	Apatite	<u>0.9</u>
Na ₂ O	3.0	TOTAL	98.6
K ₂ O	1.5		
H ₂ O	1.2	Mode (measured) (volume %)	
P ₂ O ₅	0.4	Plagioclase	<1
TOTAL	99.9	Orthopyroxene	<5
		Clinopyroxene	<5
		Olivine	<5
		Matrix	>90 ^b
		An content of Plagioclase (mole %)	<u>63</u>
		TOTAL	100.0

^aAverage Yakima basalt (analysis b, p. 593), Columbia River Plateau, Washington-Oregon, Waters, 1961.

^bMatrix comprises: intergrown microcrystalline clinopyroxene (pigeonite), orthopyroxene, and plagioclase with minor cristobalite (listed in order of decreasing abundance).

Diopside	-	$\text{CaMg}(\text{SiO}_3)_2$
Hedenbergite	-	$\text{CaFe}(\text{SiO}_3)_2$
Clinoenstatite	-	MgSiO_3
Clinoferrosilite	-	FeSiO_3
Hypersthene	-	approximately Ens 60:Fes 40
Enstatite	-	MgSiO_3
Ferrosilite	-	FeSiO_3
Plagioclase		
Anorthite	-	$\text{CaAl}_2\text{Si}_2\text{O}_8$
Albite	-	$\text{NaAlSi}_3\text{O}_8$

1.2.3. Alteration Products

Alteration products typically occur in vesicles or along fractures and flow-unit contacts in basalts. The low- and intermediate-temperature alterations are temperature-induced responses to heated fluids moving through the rock, and most of the alteration phases require the addition of either water or carbon dioxide to the rock. The intermediate- and high-temperature alterations are a result of thermal metamorphism of the rock body. Basalts which have experienced thermal metamorphism may show pervasive alteration.

1. Low temperature ($T < 250^\circ\text{C}$) reactions typically produce the following minerals:

Calcite	-	CaCO_3
Dolomite	-	$\text{CaMg}(\text{CO}_3)_2$
Epidote - Zoisite	-	$\text{Ca}_2\text{FeAl}_2\text{Si}_3\text{O}_{12}(\text{OH})$ - $\text{Ca}_2\text{Al}_3\text{Si}_3\text{O}_{12}(\text{OH})$
Prehnite	-	$\text{Ca}_2\text{Al}_2\text{Si}_3\text{O}_{10}(\text{OH})_2$

Lawsonite - $\text{CaAl}_2\text{Si}_2\text{O}_7(\text{OH})_2 \cdot \text{H}_2\text{O}$

Zeolites

Laumontite - $\text{CaAl}_2\text{Si}_4\text{O}_{12} \cdot \text{H}_2\text{O}$

Heulandite - $\text{CaAl}_2\text{Si}_7\text{O}_{18} \cdot 6\text{H}_2\text{O}$

Analcite - $\text{NaAlSi}_2\text{O}_6 \cdot \text{H}_2\text{O}$

Wairakite - $\text{CaAl}_2\text{Si}_4\text{O}_{12} \cdot 2\text{H}_2\text{O}$

2. Intermediate temperature ($T < 375^\circ\text{C}$) reactions typically produce the following minerals:

Calcite - CaCO_3

Dolomite - $\text{CaMg}(\text{CO}_3)_2$

Albite - $\text{NaAlSi}_3\text{O}_8$

Zoisite - $\text{Ca}_2\text{Al}_3\text{Si}_3\text{O}_{12}(\text{OH})$

Chlorite (Clinochlore) - $\text{Mg}_5\text{Al}_2\text{Si}_3\text{O}_{10}(\text{OH})_4$

Amphibole

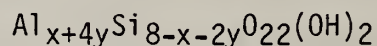
Tremolite - $\text{Ca}_2\text{Mg}_5\text{Si}_8\text{O}_{22}(\text{OH})_2$

Actinolite - $\text{Ca}_2\text{Fe}_5\text{Si}_8\text{O}_{22}(\text{OH})_2$

Anthophyllite - $\text{Mg}_7\text{Si}_8\text{O}_{22}(\text{OH})_2$

3. High temperature ($T > 350^\circ\text{C}$) reactions typically produce the following minerals:

Amphibole - commonly Hornblende - $\text{Na}_x\text{Ca}_2(\text{Mg,Fe})_{5-2y}$



$$x \approx 0-1, y \approx 0.5$$

Garnet - typically Almandine or Grossular

Grossular - $\text{Ca}_3\text{Al}_2\text{Si}_3\text{O}_{12}$

Almandine - $\text{Fe}_3\text{Al}_2\text{Si}_3\text{O}_{12}$

Pyrope - $\text{Mg}_3\text{Al}_2\text{Si}_3\text{O}_{12}$

Clinopyroxene

Hedenbergite - $\text{CaFe}(\text{SiO}_3)_2$

Diopside - $\text{CaMg}(\text{SiO}_3)_2$

Ca-Al Clino-

pyroxene - $\text{CaAl}_2\text{SiO}_6$

Wollastonite - CaSiO_3

Othopyroxene

Enstatite - MgSiO_3

Ferrosilite - FeSiO_3

Olivine

Forsterite - Mg_2SiO_4

Fayalite - Fe_2SiO_4

Spinel

Magnetite - Fe_3O_4

1.3. Thermodynamic and Thermophysical Properties

1.3.1. Introduction

1.3.1.1. Definitions and notation

Heat capacity is defined as the quantity of heat required to raise the temperature of a unit quantity of a substance one degree kelvin at constant pressure. The heat capacity is generally normalized per unit mass or per unit volume of the substance. "Specific heat" is defined as the heat capacity per gram of the substance. "Molar heat capacity" is defined as the heat capacity per gram formula weight of the substance. "Thermal capacity" is defined as the heat capacity per unit volume of the substance.

Thermodynamic properties of an extensive nature, such as volume, heat capacity, entropy, enthalpy, and Gibbs energy, will be presented in units normalized per molar quantity of each phase. This choice is convenient since the thermodynamic properties describing reactions among minerals are easily expressed and calculated in "molar" units. "Specific heat" will be used to describe the thermal properties of rocks and mineral aggregates.

Relative enthalpy is defined as the quantity of heat required to change the temperature of a unit quantity of substance from a reference temperature (T_r) to a measurement temperature (T). Relative enthalpy is related to heat capacity by the following thermodynamic identity.

$$H_T - H_{T_r} = \int_{T_r}^T C_p dT \quad (1)$$

Calorimetric entropy is defined as

$$S_T - S_0 = \int_0^T \frac{C_p}{T} dT \quad (2)$$

and is determined from experimental low-temperature heat-capacity data.

Thermodynamic entropy, S_T , is defined as the sum of calorimetric entropy and residual entropy, S_0 . Non-zero values for residual entropy can arise from configurational entropies related either to disorder among crystallographic sites or molecular disorder, or to the lack of significant magnetic ordering at those temperatures reached by the heat capacity measurements.

Molar volume, V , is defined as the volume occupied by one mole of a phase and is a function of pressure and temperature. Enthalpy, as a function of temperature and pressure, is related to heat capacity and molar volume by the thermodynamic identity

$$H_{T,P} = H_0 + \int_0^T C_p dT + \int_{P_{ref}}^P (V_T - T(\frac{\partial V}{\partial T})_P) dP \quad (3)$$

where H_0 is the zero point contribution to enthalpy at the reference state pressure. Entropy, as a function of pressure is related to molar volume by the thermodynamic identity

$$S_{T,P} = S_{T,P_{ref}} - \int_{P_{ref}}^P (\frac{\partial V}{\partial T})_P dP. \quad (4)$$

Gibbs energy is related to enthalpy and entropy by the thermodynamic identity

$$G_{T,P} = H_{T,P} - T S_{T,P}. \quad (5)$$

The isobaric coefficient of thermal expansion, α_p , and the isothermal coefficient of compressibility, β_T , are related to molar volume by the following identities

$$\alpha_p = \frac{1}{V} \left(\frac{\partial V}{\partial T} \right)_p \quad (6)$$

$$\beta_T = - \frac{1}{V} \left(\frac{\partial V}{\partial T} \right)_T. \quad (7)$$

1.3.1.2. Types of data used in study

Data from three general categories of experimental techniques have been used in the evaluation of the heat capacity, relative enthalpy, and calorimetric entropy. Data from low-temperature calorimetry was used in the evaluation to supply accurate values of heat capacity, at temperatures generally 200-300 K, and calorimetric entropy at 298 K. Data from differential scanning calorimetry was used to supply values of heat capacity at temperatures 300-800 K. Data from drop calorimetry was used to evaluate mineral heat capacities and relative enthalpies at temperatures generally 300-1800 K.

Volume as a function of temperature and pressure may be measured directly, as in x-ray crystallography, or determined as a change in volume under changing pressure and temperature conditions from a reference state (relative volume measurements).

Data from enthalpy-of-reaction measurements, including solution calorimetry and combustion calorimetry, measure the enthalpy of a phase relative to other phases.

Data from phase-equilibrium experiments and EMF measurements supply measurements of the Gibbs energy of a phase relative to other phases.

The simultaneous evaluation procedure followed in this study and the relationships among thermodynamic properties shown in equations 1 to 7 allow the direct measurement of individual thermodynamic properties to supply indirect constraints on the permissible values of the other thermodynamic properties.

1.3.1.2.1. Low-temperature calorimetry

Low-temperature calorimetry is used to obtain accurate heat capacities and calorimetric entropies for substances at temperatures generally below 300 K. McCullough and Scott (1968, Ch. 4-5) provide an excellent description of the design and operation of low-temperature calorimeters. The heat capacity of an unknown sample is determined by accurately measuring the heat energy (electrical) added to a sample in a calorimeter to change its temperature by a measured amount. The calorimeter is cooled to its initial low temperature by a liquified gas, often helium. The calorimeter is shielded to minimize heat exchange between the calorimeter and its surroundings. The heat capacity of the sample is determined at closely spaced temperature intervals, using the formula:

$$\frac{dE}{dT} - \left(\frac{dE}{dT}\right)_{cal} \frac{dT}{dt} = MC_p \frac{dT}{dt}$$

where E is heat energy

$\left(\frac{dE}{dT}\right)_{cal}$ is the heat effect of the calorimeter as temperature is changed

t is time

T is temperature (kelvin)

M is mass of sample/molar weight of sample

C_p is heat capacity of sample

The temperature range of operation is generally between 5 and 300 K, with a precision better than 0.1 percent for heat capacity. The calorimetric entropy ($S_T - S_0$) is determined using the formula:

$$S_T - S_0 = \int_0^T C_p/T \, dT.$$

The precision of measurement is generally better than 0.2 percent.

Data from low-temperature calorimetry was used to constrain the evaluation for entropy and for heat capacity of structural components above 200 K.

1.3.1.2.2 Differential Scanning Calorimetry

McNaughton and Mortimer (1975) provide an excellent description of the operation and use of a differential scanning calorimeter to measure heat capacity. Differential Scanning Calorimetry (DSC) is used to determine the heat capacity of a substance by measuring the differential heat flow required to maintain the sample and an inert reference material at the same temperature, when both are heated. The sample and reference are subjected to a programmed linear temperature change, and the rates of heat flow into the sample and reference are proportional to their instantaneous specific heat. Heat capacity as

a function of temperature can be obtained by evaluating the differential rate of heat flow between the sample and reference, as a function of temperature, using the formula:

$$C_p(s) = \frac{M(r)}{M(s)} \frac{(dT/dt)(r)}{(dT/dt)(s)} \frac{(dE/dt)(s)}{(dE/dt)(r)}$$

where E is heat energy

t is time

T is temperature (kelvin)

M is mass of sample/mol wt. of sample

C_p is molar heat capacity of the respective materials

Subscript s refers to sample material

Subscript r refers to reference material.

The heat capacity of the reference material is known.

The temperature range of operation is generally between 300 and 800 K (27-527°C), with a precision of measurement estimated to be better than 1.0 percent and often as low as 0.3%.

1.3.1.2.3. Drop calorimetry

The enthalpy change of a substance is determined by measuring the heat flow from a sample as it is dropped from a known temperature into a calorimeter held at a constant reference temperature. McCullough and Scott (1968, Ch. 8) provide an excellent description of drop calorimetry. The heat capacity of the sample can be determined from a series of drop calorimetry measurements with differing initial temperatures by evaluating the differential enthalpy changes as a function of temperature using the formula:

$$\frac{d(H_T - H_{T_r})}{dT} = MC_p$$

where $H_T - H_{T_r}$ is the measured enthalpy change between the sample at the initial temperature and reference temperature, corrected for the heat effects of the sample container

T is temperature (kelvin)

M is mass of sample/molecular weight of sample

C_p is molar heat capacity of sample

The temperature range of operation is generally between 273 and 1600 K (0 to 1327°C), with a precision of measurement, on modern equipment, estimated to be 0.2 percent. The precision of measurement from older literature sources is estimated to be approximately 0.5 percent.

1.3.1.2.4. X-ray crystallography

The measurement of molar volume by x-ray crystallography is based upon the determination of crystallographic lattice dimensions from the diffraction of a collimated beam of monochromatic x-rays that is scattered by atoms in the crystal lattice. A general description of measurement techniques is provided by Krishnan and others (1979) and Hazen (1976a). Volume measurements at temperatures above room temperature are generally produced using a heating mechanism and a calibrated thermocouple to measure sample temperature. The temperature range of measurement is generally between 298 and 1400 K (24-1127°C) depending upon the stability of the sample and equipment design. Volume measurement at pressures greater than 1 atmosphere are generally produced

using a miniature diamond pressure cell (Merrill and Bassett, 1975). Pressures are generated by squeezing the sample and an internal standard between two diamond plates, and sample pressures are determined by measuring the lattice parameters of the internal standard whose volume properties as a function of pressure are known. The pressure range of measurement is generally between 10,000 and 100,000 bars, depending, again on sample stability and equipment design. The measurement of lattice dimensions using the x-ray technique has a precision of measurement generally between 0.02 and 0.5 percent of the measured value, and typically is approximately 0.1 percent of the observed value. The precision of temperature determination is generally better than 10°C , and the precision of pressure measurement is generally between 1000 and 2000 bars.

1.3.1.2.5. Relative-volume measurements

The measurement of molar volume by relative-volume techniques is based upon the determination of a change in volume or linear dimensions of a sample and container as pressure or temperature is changed from reference conditions. A general description of techniques for relative-volume measurements as a function of temperature is given by Krishnan and others (1979). The sample is heated from a reference temperature to a measurement temperature, and sample temperature is generally determined from a calibrated thermocouple attached to the sample. The volume change is determined by accurately measuring the change in linear dimensions of the sample. The change in linear dimensions can frequently be measured with a precision better than 1 percent (depending upon calibration and equipment design), with a precision of

temperature measurement better than $\pm 10^{\circ}\text{C}$. The range of measurement is generally between 298 and 1400 K (24-1127 $^{\circ}\text{C}$).

A general description of techniques to measure relative volume as a function of pressure is given by Vaidya and Kennedy (1970). The sample is packed in a container and placed in a pressure bomb of known volume filled with a hydrostatic pressure medium (a fluid or solid with low-yield strength). Pressure is increased from a reference pressure by displacement of a piston into the pressure bomb chamber, and pressures are measured by gauge. The volume change is determined from the displacement of the piston after correcting for the volume compressibility of the pressure medium and sample container. The range of measurement is generally between 1000 bars and 50,000 bars, with a precision of pressure measurement generally between 100 and 1000 bars. The precision of relative volume measurement is approximately 1 percent.

1.3.1.2.6. Enthalpy-of-reaction measurements

The enthalpy of reaction between phases is determined by measuring the heat effects of a reaction or a step-wise series of reactions in a calorimeter of similar design to those described in sections 1.3.1.2.1 and 1.3.1.2.3. Combustion calorimetry directly measures the enthalpy of reaction between a known quantity of a phase (usually an element) and a known quantity of gas during sustained combustion. Solution calorimetry indirectly measures the enthalpy of reaction among phases by measuring the heat effects of dissolution of a known quantity of "product" phases of the reaction in a solvent versus the heat effects

of dissolution of a known quantity of "reactant phases" in the solvent. Since the solution formed from the dissolution of product and reactant phases are identical, the enthalpy of reaction between reactant and product phases is equal to the difference of the heat effects of the dissolution reactions. Low-temperature (generally between 298 and 370 K) solution calorimetry generally utilizes HF as the solvent for silicate minerals. Problems with use are the slow dissolution rates of some phases and the non-equilibrium precipitation of fluoride phases during the dissolution process. High-temperature (generally between 900 and 1100 K) solution calorimetry generally utilizes molten salts (often borates) as the solvent.

In borate-melt solution calorimetry, the volume ratio of solvent to reactant phase is very large. Since the solvent melts remain essentially "isochemical" during the dissolution process, it has been assumed that the heat of mixing effects between the "reactant" components in the solvent will be negligably small. This simplifies the determination of the enthalpy of reaction among phases since the enthalpy of reaction can be computed from the sum of the heat effects of dissolution of each of the reactant phases in pure solvent minus the sum of the heat effects of dissolution of each of the product phases. The precision of measurement varies between 0.3 and 2 percent of the observed value, depending upon the kinetics of the dissolution process and equipment design.

1.3.1.2.7. Phase equilibria experiments

Phase equilibria experiments measure the Gibbs energy of a phase by reference to the Gibbs energy of other phases, which together define a reaction monitored by experiment. Edgar (1973) and Ulmer (1971) provide descriptions of equipment and techniques used in phase equilibria experiments. Two types of experiments are typically performed to measure phase equilibria.

1. In the reaction-reversal technique, pressure, temperature, and the direction of a univariant reaction is measured. By determining two closely spaced pressure-temperature points between which the reaction reverses direction, a narrow interval bracketing a point where the free energy of reaction among the assembled phases is zero has been determined. The direction of reaction is frequently determined by starting the experiment with a mixture of product and reactant phases and using some technique on the result of the experiment to determine the increase or decrease in abundance of each of the assembled phases (often x-ray analysis, or weight loss-weight gain studies of individual phases). If x-ray analysis is used, the minimum amount of change in abundance of a phase that can be measured is approximately five percent, by volume.

2. In the activity-measurement technique, pressure, temperature, and the composition (activity) of a phase (or phases) of variable composition is measured in a divariant assemblage of phases. If the composition-activity relationship is known for the phase of variable composition, and the assemblage of phases has reached equilibrium, then the free energy of reaction among an idealized assemblage of phases of fixed

composition can be calculated for the measured pressure and temperature conditions. Examples of this technique are the silicic acid experiments of Hemley and others (1977a, 1977b, 1980), the vapor pressure measurements of H₂O equilibrated with periclase and brucite (Kennedy, 1956; Fyfe, 1958; Barnes and Ernst, 1963), and the vapor pressure measurements of CO₂ equilibrated with periclase and magnesite (Marc and Simek, 1913). An essential feature of this technique is the demonstration that equilibrium among phases has been achieved during the experiment. This can be done by setting up duplicate experiments at a pressure-temperature condition using initial compositions of the variable phase which bracket the equilibrium composition (eq. Hemley and others, 1977b). Equilibrium among phases can be inferred from experiments which monitor the composition of the variable phase as a function of time. At times greater than the time in which no or little change can be observed in the composition of the variable phase, equilibrium can be presumed.

The precision of measurement in phase-equilibrium experiments is controlled by the diligence of the experimentalist, kinetics of reactions, and measurement uncertainties of temperature, pressure, phase composition, and abundance of phases. The precision of measurement of temperature and pressure is approximately ± 1 to 10°C , and ± 100 to 500 bars for pressures less than 8000 bars, and ± 500 to 1000 bars for pressures greater than 8000 bars. The precision of measurement of composition or change in abundance of phases depends upon the design of the equipment, but typically is a few percent of the variable measured. The temperature-pressure window bracketing a reaction reversal is commonly measured with a precision of ± 5 - 20°C and ± 100 - 1000 bars.

1.3.1.2.8. Electromotive-force measurements

In electromotive force (EMF) measurements, the Gibbs energy of a reaction is determined by measuring the electrochemical potential for ion migration through an electrolyte (which is an impervious barrier to everything else) separating assemblages of phases which are either 1) unstable with respect to each other, or 2) both define an activity of the mobile ion. The book, *Electromotive Force Measurements in High-Temperature Systems* (Alcock (ed.), 1968), supplies a description of equipment and techniques frequently used in the measurement of EMF.

A high impedance potentiometer is used to measure the potential energy. The electromotive potential is related to free energy by the relationship

$$E = - \frac{1}{n\mathcal{F}} \sum_{i=1}^k N_i G_i$$

where N_i is the stoichiometric coefficient for the i th phase and is positive for products and negative for reactants.

G_i is the Gibbs energy of the i th phase,

E is electromotive potential,

\mathcal{F} is the Faraday constant,

k is the number of phases in the reaction, and

n is the number of electrons transferred during the reaction.

The precision of measurement of electrochemical potential is generally ± 1 millivolt but, under special conditions, can be as small as ± 0.1 millivolt. The precision of measurement is related to the

kinetics of the reaction, with kinetically fast reactions having better precision. Failure to accurately determine free energy of reaction from EMF measurements usually results from the following problems:

1. electrical conductivity of the electrolyte (varies with temperature and electrical potential),
2. slow kinetics of reaction (varies with temperature), and
3. junction potentials, or poor electrical contacts.

Problem 3 usually generates a systematic error in all measurements, but the errors should be different for different electrochemical cells or equipment designs.

1.3.2. Calculation of Estimated Thermophysical Properties of Rocks and Minerals: Heat Capacity, Relative Enthalpy, and Calorimetric Entropy of Silicate Minerals and Specific Heat of Silicate Rocks

1.3.2.1. Introduction

The heat capacity of rocks and minerals must be known to evaluate data on both thermochemical and thermophysical properties. The heat capacity of minerals is needed to describe their entropy, enthalpy, and Gibbs energy properties as a function of temperature. The specific heats of minerals and rocks are needed to evaluate data on thermal diffusivity and to calculate thermal diffusivity as a function of temperature.

The experimental heat capacity measurements are lacking, inadequate, or unreliable for many minerals and for most rocks. In these cases, the heat capacity and calorimetric entropy must be estimated.

The standard molal heat capacity and calorimetric entropy of minerals at temperatures greater than 298 K have often been approximated by summing, in appropriate proportions, the standard molal heat capacity and calorimetric entropy of their constituent oxide formula groups. The realization that the heat capacity of most substances is approximately equal to the sum of the heat capacities of its constituent oxides or elements is quite old and can be traced back to Kopp's Law. More accurate estimates often can be obtained by a mineral summation technique, in which the standard molar heat capacity or entropy of reaction among oxides and silicates of similar structural class is assumed to be zero or a function of atomic mass, ionic size and charge, and/or molar volume (Helgeson and others, 1978).

The general validity of these approaches indicates that the standard molar heat capacity and calorimetric entropy of minerals can be accurately estimated by summing, in appropriate proportions, fictive molar heat capacities and calorimetric entropies for the constituent structural groups in minerals. This approach offers several advantages over other estimation techniques. The following problems with the other estimation techniques are eliminated:

1. The mineral summation techniques are path dependent. Results differ depending upon the specific minerals in structural classes which are used to derive estimates.

2. The mineral summation technique produces discontinuities in the estimated heat capacity whenever phases in the summation have a lambda transition or phase inversion in the temperature interval of interest.

The following improvements are offered:

1. improved accuracy relative to oxide-summation or mineral-summation techniques because the coordination of the cation is accounted for,
2. the ability to estimate heat capacity and calorimetric entropy even through data on representative minerals in similar structural classes is not available, and
3. anomalies in the properties of reference phases or in the oxides have been removed through averaging over a large body of data.

1.3.2.2. Evaluation of fictive molar properties

1.3.2.2.1. Introduction

Fictive molar heat capacities and fictive molar entropies are the average molar heat capacities and molar entropies of an oxide component in a given coordination within the oxygen framework of the phase. Under this definition, Mg in 4-fold, 6-fold, and 8-fold coordination are listed as MgO-4, MgO-6, and MgO-8, respectively. They are assumed to have different contributions to the heat capacity or entropy of the phases in which they are found. The values for each were found by least-squares evaluation as will be described below.

1.3.2.2.2. Fitting procedure

The heat capacity and entropy properties of the fictive structural components of mineral phases have been evaluated following the procedure described by Haas and Fisher (1976) and Haas (1974). The approach and procedure given there have been followed closely and will

not be described here in detail. The following description summarizes the evaluation procedure:

1. Literature search
 - a. Review of literature for data that define the heat capacity and calorimetric entropy properties of a phase or a group of phases.
 - b. Close scrutiny of each citation to determine:
 - (1) what was physically observed, and
 - (2) with what precision was it observed.
2. Refinement cycle
 - a. Comparison of data with related data (heat capacity, relative enthalpy) for mineral phases described in terms of structural components using weighted, simultaneous, multiple, least-squares regression.
 - b. Review of the pertinent literature where data are found not to be in agreement.
 - c. Removal of assumed or apparently erroneous data from the set of data being fit by the regression.
 - d. Repeat of steps a through c until all discordant data have been identified and removed.

The mathematical model used in the regression in step 2a is based on equation 8 for the heat capacity of mineral phases at constant pressure.

$$C_p(\text{phase a}) = \sum_i N_i C_{p,i}^{\circ} \quad (8)$$

where: N_i represents the stoichiometric coefficient of the i th fictive structural component in mineral phase a; and $C_{p,i}^{\circ}$ represents the heat capacity function for the i th fictive structural component (the superscript $^{\circ}$ is used here to denote properties of the fictive components);

$$C_{p,i}^{\circ} = a_i + 2b_i T + \frac{c_i}{T^2} + f_i T^2 + \frac{g_i}{T^{1/2}} \quad (9)$$

where: a_i , b_i , c_i , f_i , and g_i are fitted coefficients for the fictive structural component and T is temperature in kelvins.

Equation 9 is a restatement of equation 6 in Haas and Fisher (1976).

The mathematical model used in regression step 2a to fit relative enthalpy is based on the thermodynamic identity

$$H_T(\text{phase b}) - H_{T_r}(\text{phase a}) = \int_0^T C_p(\text{phase b}) dT - \int_0^{T_r} C_p(\text{phase a}) dT$$

In the case where phases a and b are identical, the mathematical model used to fit relative enthalpy is

$$(H_T - H_{T_r})(\text{phase a}) = \sum_i N_i (H_{i,T}^{\circ} - H_{i,T_r}^{\circ}) \quad (10)$$

where: N_i represents the stoichiometric coefficient of the i th structural component in mineral phase a, and $(H_{i,T}^{\circ} - H_{i,T_r}^{\circ})$ represents the relative enthalpy contribution of the i th fictive structural component.

$$\begin{aligned}
 (H_{i,T}^{\circ} - H_{i,T_r}^{\circ}) &= a_i(T - T_r) + b_i(T^2 - T_r^2) - \\
 &c_i\left(\frac{1}{T} - \frac{1}{T_r}\right) + \frac{1}{3} f_i(T^3 - T_r^3) + 2g_i(T^{1/2} - T_r^{1/2}) \quad (11)
 \end{aligned}$$

where: T_r represents the reference temperature of the relative enthalpy measurement.

In the case where phases a and b are not identical (a phase inversion occurs during the measurement process), the mathematical model used to fit relative enthalpy is

$$(H_T(\text{phase a}) - H_{T_r}(\text{phase b})) = \Delta H_r + \sum_i N_i (H_{i,T}^{\circ} - H_{i,T_r}^{\circ}) \quad (12)$$

where: H_r is the enthalpy of reaction of phase b to phase a, and the other terms are the same as in equations 10 and 11.

Equation 12 is valid because, for all phases studied to date, phase inversions rapid enough to occur during a drop calorimetry measurement do not involve a change in structural components.

The mathematical model used in the regression step 2a to fit calorimetric entropy (at 298.15 K) is

$$(S_T - S_0)(\text{phase a}) = \sum_i N_i S_i^{\circ} \quad (13)$$

where: N_i represents the stoichiometric coefficient of the i th fictive structural component in mineral phase a, and S_i° represents the calorimetric entropy contribution of the i th fictive structural component.

$$S_i^o = a_i \ln T + 2b_i T - \frac{c_i}{T^2} + e_i + \frac{f_i T^2}{2} - \frac{2g_i}{T^{1/2}} \quad (14)$$

Equations 9, 11 and 14 are smoothing functions and have no theoretical basis beyond the thermodynamic identities shown in equations 1 and 2. In our work, data at temperatures below 200 K were not considered. Above 200 K, the functions readily describe most data. In order to avoid overfitting of the data, nonsignificant constants have been eliminated from the general equation wherever they were not needed to describe the properties of a phase or fictive component. This is particularly common for the $f_i T^2$ term in equation 9. Removal of this term eliminated any rapid excursions of the calculated values in the temperature region around and above the highest experimental temperature. Equations 9, 11, and 14 have been fit within the temperature range represented for each fictive structural component and should not be extended indiscriminately to higher or lower temperatures.

Haas (1974) described the mechanics used to fit the model to discrete experimental observations in detail. The typical problem includes the following information:

1. Title for problem.
2. Control codes to identify the options used.
3. Number and labels for the phases (structural components) in the problem.
4. Sets of data being fit.
 - a. Name of the set and reference.

b. Control codes related to the observation and to data editing.

c. Label(s) for the phase(s), the stoichiometric coefficient(s) and any pertinent data on polymorphs.

d. Data as given in the reference.

(1) Temperature (and correction factor if needed to convert to kelvins).

(2) Observed value (and correction factor if needed to convert to joules, etc.).

(3) Precision.

(4) Second independent variable (if needed).

5. Constants of equation 8 above for each of the reference phases as well as the trial constants for the structural components for which the properties are being refined.

6. Control parameters for the error plots.

The input format is designed to reduce manual conversions before entry into the computer for fitting.

Data were weighted by the reciprocal of the precision; the higher (smaller in magnitude) the precision, the higher (larger in magnitude) the weight. The use of weighting served two purposes. First, it allowed the simultaneous fitting of different properties that have large variations in magnitude. An example is the simultaneous fitting of relative enthalpy data that could exceed 7 Megajoules and heat capacity data that are generally less than 1 Kilojoule. Second, weighting constrained the solution towards the more precise observations. This was particularly desirable where precise data from

low-temperature, adiabatic calorimetry were being matched with the less precise data from differential scanning calorimetry or from drop calorimetry.

The author's stated precision was used in the first fitting of a data set from a particular reference. In subsequent cycles this would be modified if logic or other data showed the author's estimate to be abnormally small.

1.3.2.2.3. Results

The data used in the evaluation of the fictive component properties is summarized in table 2. Table 3 lists the structural components for common silicate minerals. Table 4 gives the coefficients for the heat-capacity function, equation 9, and for the entropy function, equation 14. They are given for the 20 different fictive components allowed in this study. Figure 1a and b contrast the standard errors of estimate for 86 data sets using the fictive molar heat-capacity summation and the oxide heat-capacity summation, respectively. The dashed lines represent a 2-percent error of estimate for the data sets. On figure 1a, only 15 sets, a little more than 17 percent, lie outside the 2-percent brackets. On figure 1b, 35 sets, a little less than 41 percent, lie outside the 2-percent bracket. Clearly, an estimate using the summation of the fictive component heat capacities is a significant improvement over a summation using the oxide heat capacities. Because the mineral-summation technique of Helgeson and others (1978) is pathdependent, a similar analysis is not available.

Table 2. Experimental (and evaluated) data used to develop the functions for the fictive components

Phase	Property	No. of observations	Temperature range (K)	Reference
Akermanite	relative enthalpy entropy	27	357-1605	Pankratz and Kelley, 1964a
		1	298	Robie and others, 1979
Albite	apparent specific heats relative enthalpy entropy	14	373-1373	White, 1919
		5	472-1270	Kelley and others, 1953
		1	298	Robie and others, 1979
Analbite	apparent specific heats relative enthalpy heat capacity heat capacity	14	373-1373	White, 1919
		5	472-1270	Kelley and others, 1953
		75	339-997	Hemingway and others, 1981
		20	200-370	Openshaw and others, 1976
Analcite	heat capacity entropy	11	206-298	King, 1955
		1	298	Robie and others, 1979
Andalusite	heat capacity relative enthalpy entropy	10	206-296	Todd, 1950
		13	397-1601	Pankratz and Kelley, 1964b
		1	298	Robie and others, 1979
Anorthite	heat capacity heat capacity apparent specific heats relative enthalpy entropy	95	349-986	Krupka and others, 1979
		49	202-381	Robie and others, 1978
		17	373-1673	White, 1919
		15	400-1800	Ferrier, 1969
		1	298	Robie and others, 1979
Anthophyllite	heat capacity entropy	36	200-700	K.M. Krupka, 1982, unpub. data
		1	298	K.M. Krupka, 1982, unpub. data

Table 2. Continued

Phase	Property	No. of observations	Temperature range (K)	Reference
Antigorite	heat capacity relative enthalpy	10	206-296	King and others, 1967
		11	405-847	King and others, 1967
Bredigite	relative enthalpy	12	974-1690	Coughlin and O'Brien, 1957
Brucite	heat capacity entropy relative enthalpy	21	216-320	Giauque and Archibald, 1937
		1	298	Robie and others, 1979
		12	350-699	King and others, 1975
Ca-Olivine	heat capacity relative enthalpy entropy	10	206-296	King, 1957
		18	405-1112	Coughlin and O'Brien, 1957
		1	298	Robie and others, 1979
Ca-Al Clinopyroxene	heat capacity heat capacity entropy	16	298-1000	Thompson and others, 1978
		50	199-379	H.T. Haselton, unpublished data
		1	298	Robie and others, 1979
Ca ₂ SiO ₄ , alpha	relative enthalpy	5	1714-1816	Coughlin and O'Brien, 1957
Ca ₃ SiO ₅	heat capacity relative enthalpy	9	206-296	Todd, 1951
		7	573-1773	Gronow and Schweite, 1933
Chrysothile	heat capacity	10	206-296	King and others, 1967
Clinoenstatite	heat capacity heat capacity relative enthalpy entropy	14	298-1600	Robie and others, 1979
		9	215-295	Kelley, 1943
		13	580-1570	Wagner, 1932
		1	298	Robie and others, 1979

Table 2. Continued

Phase	Property	No. of observations	Temperature range (K)	Reference
Cristobalite, alpha	heat capacity	6	200-700	Robie and others, 1979
	entropy	1	298	Robie and others, 1979
Cristobalite, beta	heat capacity	17	400-2000	Robie and others, 1979
Cyclowollastonite	heat capacity	7	201-295	Wagner, 1932
	relative enthalpy	12	576-1558	Wagner, 1932
	apparent specific heats	28	373-1673	White, 1919
	specific heat	6	194-298	Parks and Kelley, 1926
Analcite (dehydrated)	heat capacity	10	206-296	King and Weller, 1961b
	relative enthalpy	9	407-997	Pankratz, 1968
	entropy	1	298	Robie and others, 1979
Diaspore	heat capacity	19	340-509	K.M. Krupka, 1982, unpub. data
	heat capacity	10	206-295	King and Weller, 1961a
	heat capacity	215	203-345	Perkins and others, 1979
	heat capacity	15	312-585	Mukaibo and others, 1969
	entropy	1	298	Robie and others, 1979
Dickite	heat capacity	10	206-296	King and Weller, 1961a
Diopside	heat capacity	14	298-1600	Robie and others, 1979
	heat capacity	29	298-1000	Krupka and others, 1980
	relative enthalpy	15	599-1576	Wagner, 1932
	entropy	1	29	Robie and others, 1979
Epidote	relative enthalpy	10	335-1100	Kiseleva and others, 1974

Table 2. Continued

Phase	Property	No. of observations	Temperature range (K)	Reference
Fayalite	heat capacity relative enthalpy entropy	31	208-381	Robie and others, in press
		13	395-1370	Orr, 1953
		1	298	Robie and others, 1979
Fluorophlogopite	heat capacity relative enthalpy entropy	10	206-296	Kelley and others, 1959
		12	400-1499	Kelley and others, 1959
		1	298	Robie and others, 1979
Forsterite	heat capacity relative enthalpy entropy	9	206-295	Kelley, 1943
		16	398-1807	Orr, 1953
		1	298	Robie and others, 1979
Gehlenite	heat capacity relative enthalpy entropy	10	206-296	Weller and Kelley, 1963
		15	402-1801	Pankratz and Kelley, 1964a
		1	298	Robie and others, 1979
Gibbsite	heat capacity heat capacity relative enthalpy	23	200-479	Hemingway and others, 1977
		10	205-296	Shomate and Cook, 1946
		5	322-423	Shomate and Cook, 1946
Grossular	heat capacity heat capacity heat capacity entropy	1	298	Haselton and Westrum, 1979
		50	350-978	Krupka and others, 1979
		57	200-596	Westrum and others, 1979
		1	298	Haselton and Westrum, 1979
Halloysite	heat capacity	10	206-296	King and Weller, 1961a
High Sanidine	apparent specific heats	14	373-1373	White, 1919

Table 2. Continued

Phase	Property	No. of observations	Temperature range (K)	Reference
High Sanidine (continued)	heat capacity	69	339-997	Hemingway and others, 1981
	heat capacity	20	200-370	Openshaw and others, 1976
Jadeite	heat capacity	10	206-296	Kelley and others, 1953
	heat capacity	11	298-1300	Robie and others, 1979
	entropy	1	298	Robie and others, 1979
Kaliophilite	heat capacity	10	206-296	Kelley and others, 1953
	relative enthalpy	23	409-1799	Pankratz, 1968
Kaolinite	heat capacity	27	340-800	Hemingway and others, 1978
	heat capacity	10	206-296	King and Weller, 1961a
	entropy	1	298	Robie and others, 1979
Kyanite	heat capacity	10	206-296	Todd, 1950
	relative enthalpy	12	390-1503	Pankratz and Kelley, 1964b
	entropy	1	298	Robie and others, 1979
Larnite	heat capacity	10	206-296	Todd, 1951
	relative enthalpy	10	406-964	Coughlin and O'Brien, 1957
	entropy	1	298	Robie and others, 1979
Lawsonite	heat capacity	16	206-296	King and Weller, 1961b
	heat capacity	8	298-600	Perkins and others, 1980
	entropy	1	298	Robie and others, 1979
Leonhardite	heat capacity	10	206-296	King and Weller, 1961b
	entropy	1	298	Robie and others, 1979

Table 2. Continued

Phase	Property	No. of observations	Temperature range (K)	Reference
Leucite	heat capacity	10	206-296	Kelley and others, 1953
	relative enthalpy	21	409-1798	Pankratz, 1968
	entropy	1	298	Kelley and others, 1953
Low Albite	heat capacity	75	339-997	Hemingway and others, 1981
	heat capacity	20	200-370	Openshaw and others, 1976
	entropy	1	298	Robie and others, 1979
Margarite	heat capacity	24	200-1000	Perkins and others, 1980
	entropy	1	298	Haas and others, 1980
Merwinite	relative enthalpy	17	397-1601	Pankratz and Kelley, 1964a
	entropy	1	298	Robie and others, 1979
Microcline	heat capacity	69	339-997	Hemingway and others, 1981
	heat capacity	20	200-370	Openshaw and others, 1976
	apparent specific heats	14	373-1373	White, 1919
	entropy	1	298	Robie and others, 1979
	heat capacity	62	332-967	Krupka and others, 1979
Muscovite	heat capacity	30	202-385	Robie and others, 1976
	entropy	1	298	Robie and others, 1979
	relative enthalpy	20	367-1164	Naylor, 1945
$\text{Na}_2\text{Si}_2\text{O}_5$	heat capacity	10	206-296	Kelley and others, 1953
Nepheline	entropy	1	298	Kelley and others, 1953

Table 2. Continued

Phase	Property	No. of observations	Temperature range (K)	Reference
Orthoenstatite	heat capacity entropy	151	318-999	Krupka and others, 1980
		1	298	Krupka and others, 1980
Paragonite	heat capacity entropy	82	200-759	Robie and Hemingway, in review
		1	298	Robie and Hemingway, in review
Phlogopite	entropy	1	298	Robie and others, 1979
Prehnite	heat capacity	8	200-298	Perkins and others, 1980
	heat capacity entropy	12	298-800	Perkins and others, 1980
	entropy	1	298	Haas and others, 1980
Pyrope	heat capacity	9	264-345	Haselton and Westrum, 1980
	heat capacity entropy	8	298-1000	Robie and others, 1979
	entropy	1	298	Haselton and Westrum, 1980
Pyrophyllite	heat capacity	20	200-370	Robie and others, 1976
	heat capacity entropy	48	335-679	Krupka and others, 1979
	entropy	1	298	Robie and others, 1979
Quartz, alpha	heat capacity entropy	5	200-600	Robie and others, 1979
	entropy	1	298	Robie and others, 1979
Quartz, beta	heat capacity	4	900-1200	Robie and others, 1979
Rankinite	heat capacity	10	206-296	King, 1957

Table 2. Continued

Phase	Property	No. of observations	Temperature range (K)	Reference
Sillimanite	heat capacity	10	206-296	Todd, 1950
	relative enthalpy	13	401-1496	Pankratz and Kelley, 1964b
	entropy	1	298	Robie and others, 1979
Talc	heat capacity	13	200-300	Robie and Stout, 1963
	heat capacity	6	298-800	Robie and others, 1979
	heat capacity	26	298-650	Krupka and others, 1977
	entropy	1	298	Robie and others, 1979
Tremolite	heat capacity	9	298-1100	Robie and others, 1979
	heat capacity	21	298-800	Krupka and others, 1977
	entropy	1	298	Robie and others, 1979
Wollastonite	heat capacity	2	200-210	Cristescu and Simon, 1934
	heat capacity	7	199-303	Christescu, 1981
	heat capacity	137	205-999	Krupka and others, 1980
	relative enthalpy	5	573-1373	Gronow and Schweite, 1933
	relative enthalpy	13	484-1294	Southard, 1941
	relative enthalpy	7	323-1157	Roth and Bertram, 1929
	apparent specific heat	18	373-1573	White, 1919
	relative enthalpy	11	566-1383	Wagner, 1932
	entropy	1	298	Robie and others, 1979
	Zoisite	heat capacity	8	200-300
heat capacity		11	298-730	Perkins and others, 1980
entropy		1	298	Haas and others, 1980

Table 3. Structural factors for common silicate minerals

Mineral group/components	Coordination number	Discussion
1. Olivine group - A_2SiO_4		
A site - $Mg^{+2}, Fe^{+2}, Ni^{+2}, Ca^{+2}, Mn^{+2}$	6	
SiO ₂ site	4	
2. Garnet group - $A_3B_2Si_3O_{12}$		
A site - $Ca^{+2}, Fe^{+2}, Mg^{+2}, Mn^{+2}$	8	
B site - $Al^{+3}, Fe^{+3}, Mn^{+3}$	6	
SiO ₂ site	4	
3. Mica group - $M_0-1Y_2-3(Z_4O_{10})(OH)_2$		
W site - $K^{+1}, Na^{+1}, Ca^{+2}, H_3O^{+1}$	8-12*	*Coordination number of 8 used for Na and Ca, 8 used for K in muscovite, and 6 used for K in phlogopite in evaluation of component properties.
Y site - $Al^{+3}, Fe^{+2}, Mg^{+2}, Fe^{+3}$	6	
Z site - Si^{+4}, Al^{+3}	4	
OH site - hydroxyl	-	
4. Silica polymorphs - SiO ₂ , quartz, tridymite, cristobalite		
SiO ₂	4	
5. Feldspar group - XZ_4O_8		
X site - K^{+1}, Na^{+1}, Ca^{+2}	6-9*	*7 used.
Z site - Si^{+4}, Al^{+3}	4	
6. Pyroxenoid group - $A_2Z_2O_5$		
A site - $Ca^{+2}, Fe^{+2}, Mg^{+2}$	6	
Z site - Si^{+4}	4	

Table 3. Continued

Mineral group/components	Coordination number	Discussion
7. Pyroxene group - ABZ_2O_6 (C2/C symmetry)		
A site - Ca^{+2} , Na^{+1}	8	
A site - Mg^{+2} , Fe^{+2}	6	
B site - Mg^{+2} , Fe^{+2} , Al^{+3}	6	
Z site - Si^{+4} , Al^{+3}	4	
8. Kaolinite group - $M_2-3Z_2O_5(OH)_4$		
M site - Al^{+3} , Mg^{+2} , Fe^{+2} , Fe^{+3}	6	
Z site - Si^{+4} , Al^{+3}	4	
OH site - hydroxyl	-	
9. Aluminosilicate minerals - $ABSi_2O_5$ (andalusite, kyanite, sillimanite)		
A site - Al^{+3}	4, 5, 6*	*Coordination numbers of 4, 5, and 6 used for sillimanite, andalusite, and kyanite, respectively.
B site - Al^{+3}	6	
SiO_2 site	4	

Table 4. Component coefficients to estimate mineral heat capacity and entropy (joules/mol.-kelvin)

Component	a	b	c	e	f	g
Al ₂ O ₃ -4*1	1.56985D+02	6.34774D-03	0.00000D+00	-9.92000D+02	0.00000D+00	-1.37221D+03
Al ₂ O ₃ -5	2.05756D+02	-7.82311D-03	0.00000D+00	-1.34963D+03	0.00000D+00	-2.08406D+03
Al ₂ O ₃ -6	2.22740D+02	-8.20451D-03	0.00000D+00	-1.50724D+03	0.00000D+00	-2.46456D+03
Ca0-6	7.88255D+01	-1.91875D-03	0.00000D+00	-4.80538D+02	0.00000D+00	-6.22865D+02
Ca0-7	7.88255D+01	-1.91875D-03	0.00000D+00	-4.71709D+02	0.00000D+00	-6.22865D+02
Ca0-8	8.36079D+01	-2.97891D-03	1.96615D+04	-5.15167D+02	0.00000D+00	-7.16401D+02
Fe ₂ O ₃ -4/6	3.18412D+02	-4.89380D-02	4.17088D+05	***** ^{*2}	2.57115D-05	-3.30795D+03
Fe0-6	8.11612D+01	0.00000D+00	0.00000D+00	-4.85209D+02	0.00000D+00	-6.51941D+02
fluorine	1.39627D+01	1.28265D-02	0.00000D+00	-5.22387D+01	0.00000D+00	0.00000D+00
hydrate	5.69125D+01	0.00000D+00	0.00000D+00	-3.00702D+02	0.00000D+00	-2.63847D+02
hydroxyl	1.29124D+02	-6.01221D-03	6.32070D+05	-8.86693D+02	0.00000D+00	-1.64532D+03
K ₂ O-8	7.71711D+00	5.27163D-02	0.00000D+00	1.08368D+02	0.00000D+00	6.56875D+02
K ₂ O-6	4.24609D+01	1.70942D-02	0.00000D+00	-1.25937D+02	0.00000D+00	1.71435D+02
Mg0-4	4.30846D+01	7.44796D-04	0.00000D+00	-2.06902D+02	0.00000D+00	0.00000D+00
Mg0-6	8.99331D+01	-3.19321D-03	0.00000D+00	-5.88796D+02	0.00000D+00	-8.72529D+02

Table 4. Continued

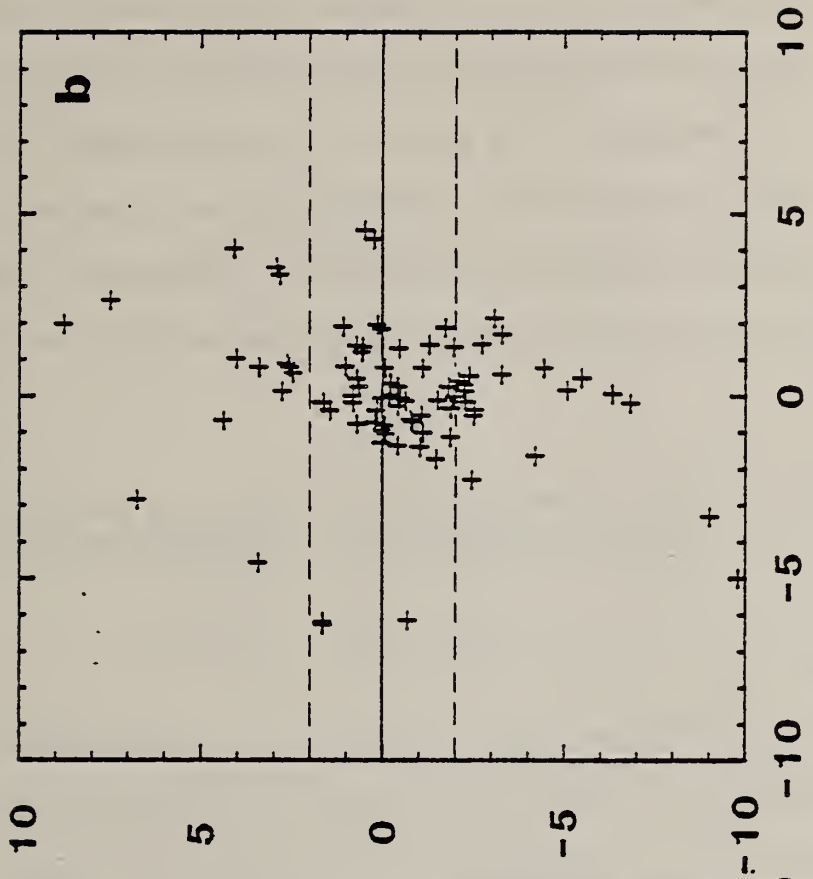
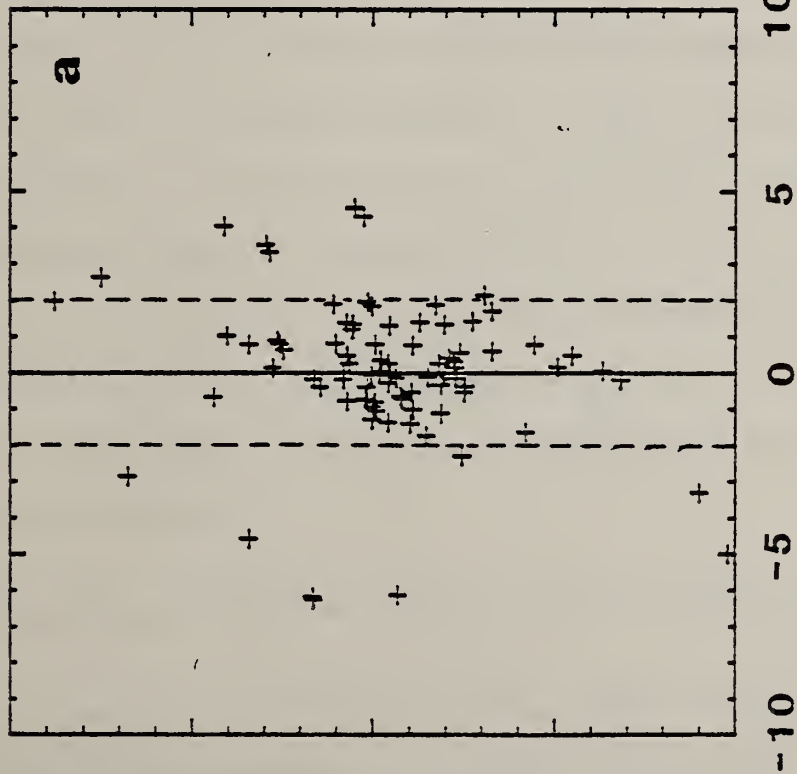
Component	a	b	c	e	f	g
MgO-8	4.78300D+01	0.00000D+00	-8.10599D+05	-2.45321D+02	0.00000D+00	0.00000D+00
Na ₂ O-6	5.80738D+01	1.24598D-02	0.00000D+00	-2.26355D+02	0.00000D+00	-4.58234D+01
Na ₂ O-7	5.80738D+01	1.24598D-02	0.00000D+00	-2.51172D+02	0.00000D+00	-4.58234D+01
Na ₂ O-8	5.80738D+01	1.24598D-02	0.00000D+00	-2.59204D+02	0.00000D+00	-4.58234D+01
SiO ₂ -4	1.09383D+02	-2.77591D-03	0.00000D+00	-7.04147D+02	0.00000D+00	-1.08305D+03

*1 The number after the "-" in each component name indicates the coordination number of the component.

*2 Stars indicate coefficient value has not been determined.

Figure 1. Plots of the percentage errors for estimates from the oxide-summation method against the percentage errors for estimates from the fictive component method for 85 sets of heat-capacity data. Each (+) symbol represents the percentage standard error of estimate for each data set over the temperature range of each set. The dashed lines on figure a emphasize 2-percent error for estimates using the fictive component method. The dashed lines on figure b emphasize 2-percent error of estimates using the oxide summation method. Less than half as many sets lie outside of the 2-percent envelope for the fictive component method than do for the oxide summation method.

ERRORS, OXIDE METHOD (percent)



ERRORS, FICTIVE COMPONENT METHOD (percent)

Main body of faint text, appearing to be a list or series of entries. The text is illegible due to blurriness.

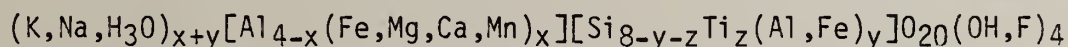
Figure 2a and b contrast the standard errors of estimate for 45 data sets using the fictive molar-entropy summation and the oxide-entropy summation, respectively. The dashed lines represent a 5-percent error of estimate for the data sets. On figure 2a, only 7 sets, approximately 16 percent, lie outside the 5-percent brackets. On figure 2b, 20 sets, approximately 44 percent, lie outside the 5-percent bracket.

1.3.2.3. Procedures to calculate estimated molar heat capacities, relative enthalpies, and calorimetric molar entropies for minerals

1.3.2.3.1. Heat capacity

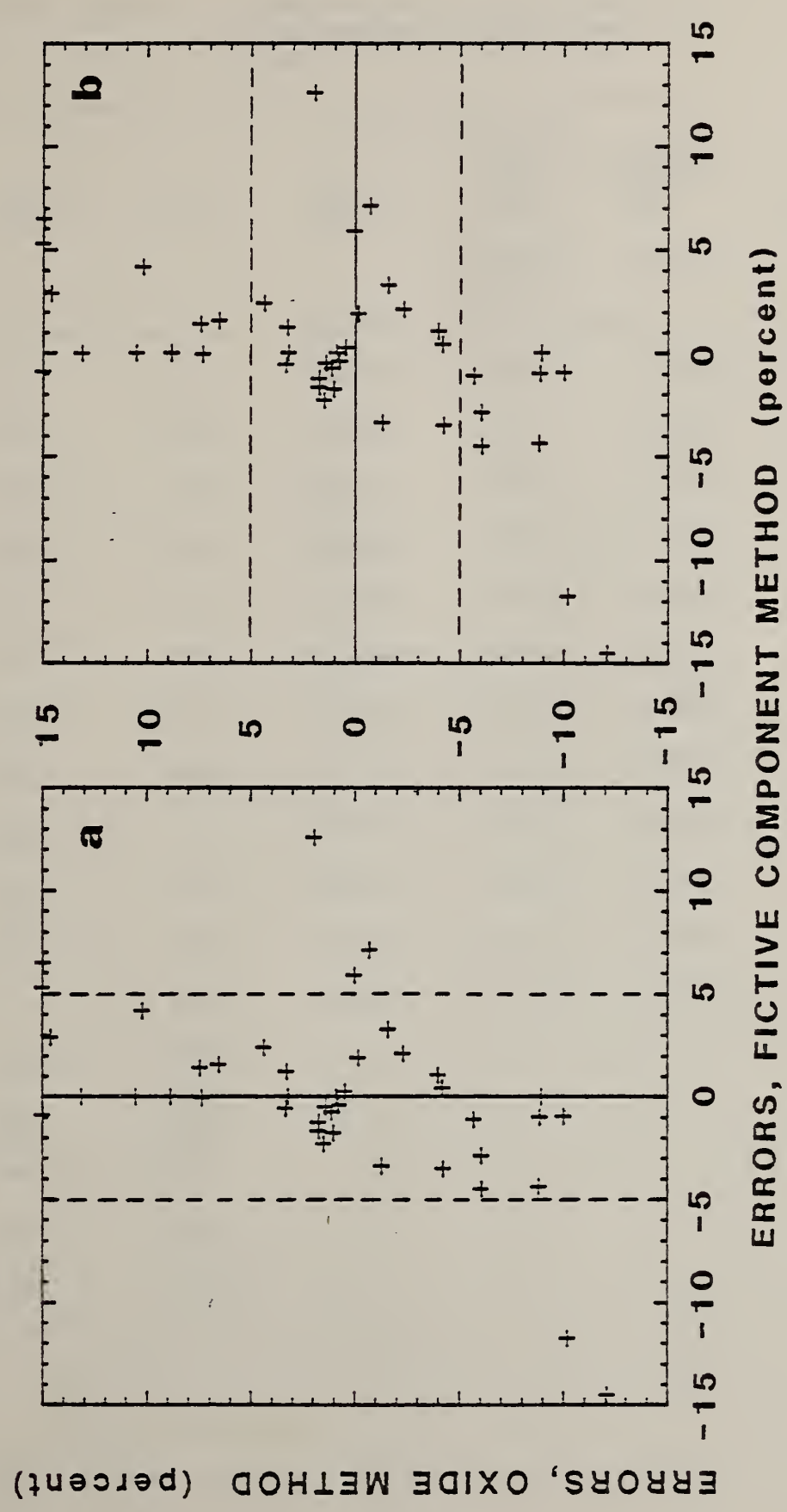
The molar heat capacity of silicate minerals as a function of temperature can be estimated using equations 8 and 9. The coefficients a_i , b_i , c_i , f_i , and g_i for each structural component i can be found in table 4. Table 3 contains a list of common silicate minerals defined in terms of their structural components. Other information regarding the structure of silicate minerals can be found in Papike and Cameron (1976) and Ulbrich and Waldbaum (1976).

As an example, table 5a shows the calculation procedure for estimating the heat capacity of illite of the composition given in column 2. Part a of the table shows the steps to get the moles of each oxide using the generalized formula:



The procedure will work for any other acceptable generalized formula. Part b of the table shows the procedure for getting the constants for

Figure 2. Plots of the percentage errors for estimates from the oxide summation method against the percentage errors for estimates from the fictive component method for 45 sets of molar calorimetric entropy data at 298.15 K. The dashed lines on figure a emphasize 5-percent error of estimates using the fictive component method. The dashed lines on figure b emphasize 5-percent error of estimates using the oxide summation method. Less than half as many sets lie outside of the 5-percent envelope for the fictive component method than do for the oxide summation method.



1. Introduction

2. Methodology

3. Results

4. Discussion

5. Conclusion

6. References

7. Appendix

8. Acknowledgements

9. Contact Information

10. Summary

11. Bibliography

12. Index

13. Glossary

14. Appendix A

15. Appendix B

Table 5, part a. Conversion of the illite analysis to the number of moles of each oxide

Oxide	Wt %	Mol wt	Mols in 100 g sample $\left(\frac{\text{wt \%}}{\text{mol wt}}\right)$	Adjusted mols (n)
SiO ₂	51.62	60.0843	0.8591	7.0202
TiO ₂	0.92	79.899	0.0115	0.0939
Fe ₂ O ₃	1.63	159.692	0.0102	0.0834
Al ₂ O ₃	23.96	101.9613	0.2350	1.9203
FeO	0.29	71.8764	0.0040	0.0327
MgO	3.83	40.3044	0.0950	0.7763
CaO	0.47	56.0794	0.0084	0.0686
MnO	0.01	70.9374	0.0001	0.0008
Na ₂ O	0.14	61.975	0.0023	0.0188
K ₂ O	8.12	94.195	0.0862	0.7044
H ₂ O ⁺	5.00	18.0152	0.2775	2.2676
F	0.74	18.9984	0.0390	0.3187
H ₂ O ⁻	2.90	-		
P ₂ O ₅	<u>0.09</u>	-		
Subtotal	99.72			
Less 0	<u>0.31</u>			
Total	99.41			

Table 5, part b. Calculation of the constants a_1 , a_2 , a_3 , a_6 , and a_7 for use in equations 8 and 9 to calculate the heat capacity of illite of the composition given in part a of this table

Structural Component	n'	$n' \cdot a_j$	$n' \cdot b_j$ $\times 10^3$	$n' \cdot c_j$ $\times 10^{-5}$	$n' \cdot f_j$ $\times 10^5$	$n' \cdot g_j$ $\times 10^{-3}$
SiO ₂ -4	7.1141	778.16	-19.7481	0.0	0.0	-7.70493
TiO ₂ included in SiO ₂ -4						
Fe ₂ O ₃ -4	0.0834	26.56	-4.0814	0.34785	21.4434	-0.27588
Al ₂ O ₃ -4	0.3596	56.45	2.2826	0.0	0.0	-0.49345
Al ₂ O ₃ -6	1.5607	347.63	-12.8048	0.0	0.0	-3.84644
FeO-6	0.0328	2.66	0.0	0.0	0.0	-0.02138
MgO-6	0.7763	69.82	-2.4789	0.0	0.0	-0.67734
CaO-8	0.0686	5.74	-0.2044	0.01349	0.0	-0.04915
MnO included in FeO-6						
Na ₂ O-8	0.0188	1.09	0.2342	0.0	0.0	-0.00086
K ₂ O-12	0.7044	5.44	37.1334	0.0	0.0	0.46270
H ₂ O hydrate	0.4269	24.30	0.0	0.0	0.0	-0.11264
H ₂ O hydroxyl	1.8407	237.68	-11.0667	11.63451	0.0	-3.02854
F	0.3187	4.45	4.0878	0.0	0.0	0.0
H ₂ O ⁻ corrected by Robie and others to remove effect.						
P ₂ O ₅ neglected in these calculations.						
		<u>a</u>	<u>b</u>	<u>c</u>	<u>f</u>	<u>g</u>
Constants for equation 2		1559.98	-6.6463 $\times 10^{-3}$	11.99585 $\times 10^5$	21.4434 $\times 10^{-5}$	-15.74791 $\times 10^3$

illite of the cited composition for use in equations 8 and 9, above. The analysis was chosen because 1) Robie and others (1976) used this sample to measure the heat capacity between 15 and 380 K and 2) these data were not used to evaluate the estimation functions given on table 4. The detailed steps for the calculation are as follows:

1. Divide the weight percent (table 5a, column 2) of the oxide in the analysis by the molecular weight of that oxide (table 5a, column 3) to get the number of moles (table 5a, column 4) in a 100-gram sample.

2. If we neglect the alkalis K, Na, and H₃O, the number of cation sites total 12. Again, neglecting the alkalis, the sum of moles of cations in column 4 for the 100 grams of illite is 1.4685. In order to adjust the 100 grams up to be equivalent to the above formula, multiply all values in column 3 by (12/1.4685) or 8.17160. These results are shown in column 5. The amount of P₂O₅ and "H₂O-" in the analysis was neglected because the P₂O₅ content was low and because the heat capacities for the illite as given by Robie and others in their table 6 had already been adjusted for the adsorbed water. Part b of table 5 continues the calculation.

3. Column 1 gives the structural components for which there are functions. Column 2 gives the adjusted moles for each of these structural components. Note that there are no structural components for TiO₂ and MnO. These have been approximated by adjusting the moles of SiO₂-4 and FeO-6. In this analysis, these corrections are minor. Had the TiO₂ or MnO contents of the mineral been a major part, such proxies would not necessarily work.

4. The breakdown between Al₂O₃-4 and Al₂O₃-6 was made such that, after the moles of TiO₂ and twice the moles of Fe₂O₃ were added to the

moles of SiO_2 , the balance to make up 8 moles was made up by Al_2O_3 -4. The remaining aluminum oxide was calculated as Al_2O_3 -6.

5. The breakdown between hydroxyl water and hydronium water was done in a similar fashion. Fluorine will be found in the hydroxyl sites both because of size and of charge. Therefore, the balance to make up 4 moles was accomplished with $n(\text{H}_2\text{O})/2$ moles of water. The remaining H_2O was considered to be the hydronium ion H_3O^+ needed to balance the charge.

6. The calculations are rechecked for this mineral by the following. In theory, the sum of moles of the alkali cations should be equal to the number of moles y of Al and Fe in Si sites plus the number of moles x of Fe, Mg, Ca, and Mn in the Al site. In this analysis, $x = 0.886$ moles and $y = 0.8777$ moles. They sum to 1.7637 moles. However, the moles of alkalis sum to $[(0.088 + 0.7044) \times 2 + 0.4269 \times 2/3]$ or 1.731 moles. There is an alkali deficiency of 0.0327 moles. This is consistent with a chemical analysis for a mineral such as illite. It is not a perfect world. Column 2 of part b contains the adjusted moles n' that are used in further calculations.

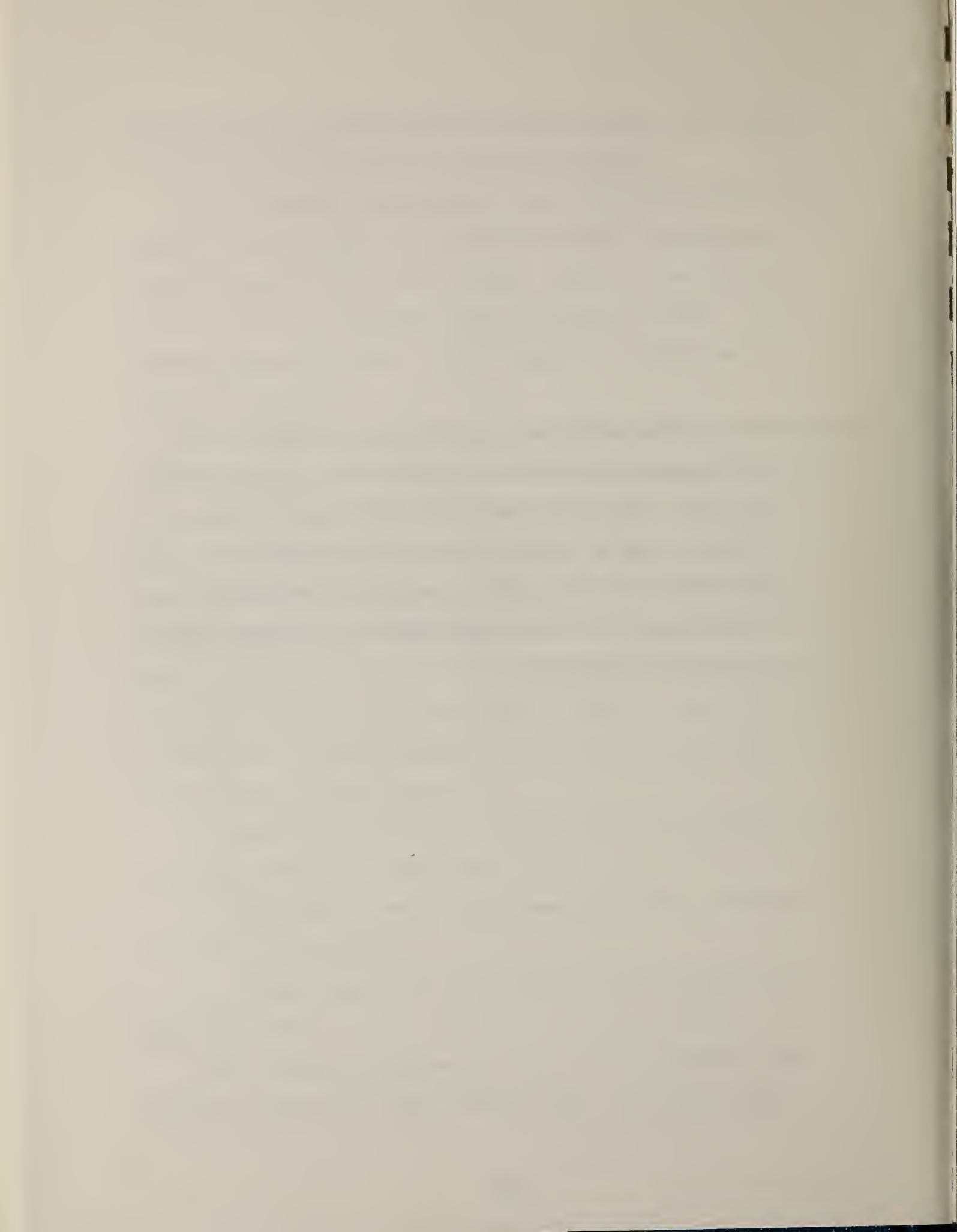
7. Columns 3 through 7 of part b were obtained by multiplying the constants a through f of table 3 by n' .

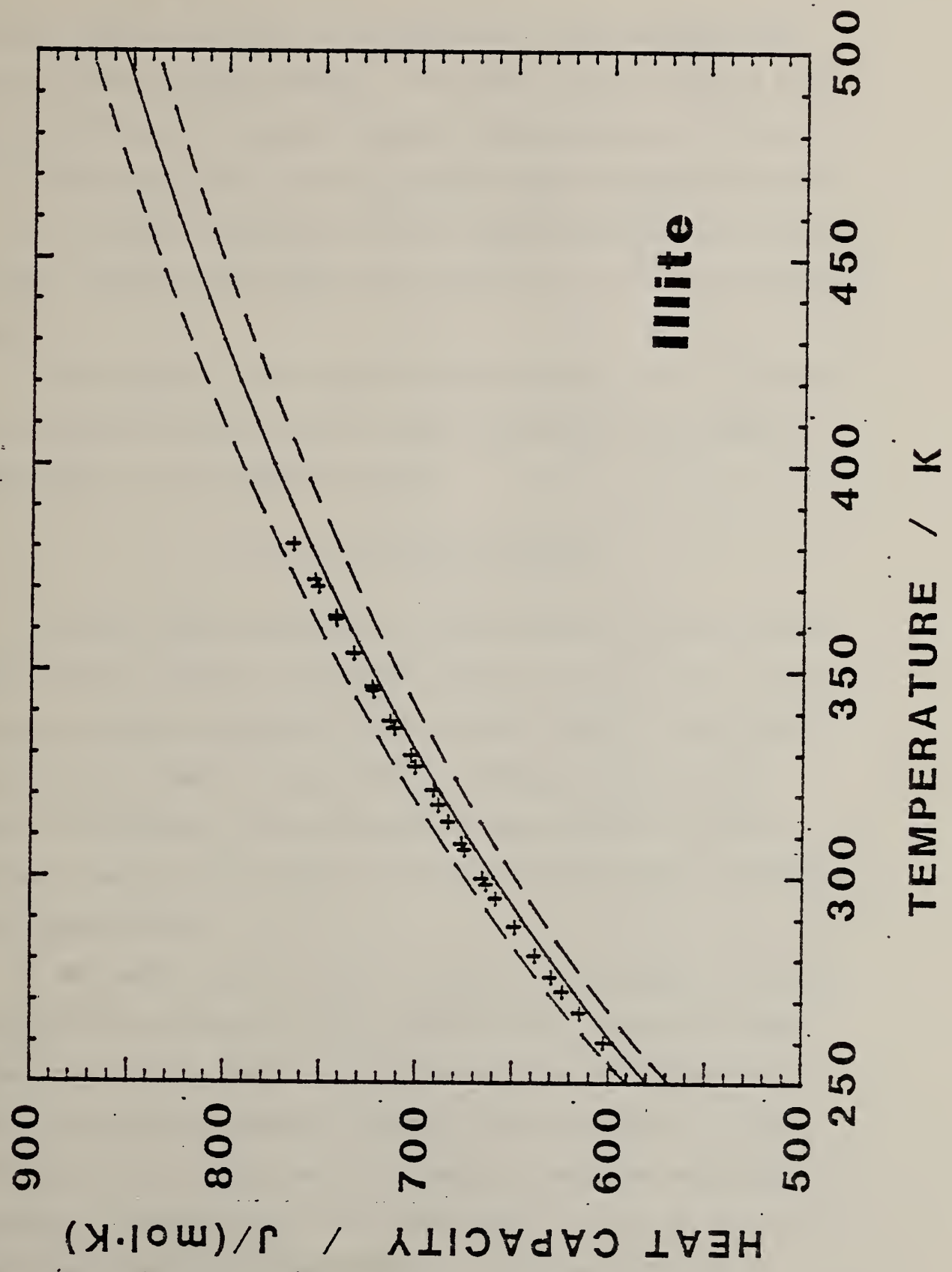
8. The columns 3 through 7 were summed to get the constants for illite for use in equation 2.

9. The heat capacity of illite at any desired temperature was then calculated.

Figure 3 shows the experimental data of Robie and others (1976) adjusted to the formula weight of 790.39 grams, the formula weight

Figure 3. Plot of the experimental and estimated heat capacities for an illite sample used by Robie and others (1976). They are shown by + and a solid line, respectively. The analysis of the illite is given on table 4a, column 2. The dashed lines represent an error of 2 percent about the estimated heat-capacity function. The function departs from the experimental data by about 0.9 percent.







derived from this analysis. The solid line is the estimated value derived from the above constants. The dashed lines in figure 3 represent a deviation of 2 percent from the calculated curve. The departure of the estimated values from the observed values is about 0.9 percent. This is a marked improvement over other methods where similar data for phases, especially those that have hydroxyl ions, can be estimated only poorly.

The estimation of the molar calorimetric entropy of an illite of this composition would follow the same approach and the procedure described in in the entropy section.

1.3.2.3.2. Relative enthalpy

The molar relative enthalpy of silicate minerals can be estimated using equations 10 and 11. The coefficients a_1 , a_2 , a_3 , a_4 , a_6 , and a_7 for each structural component i can be found in table 4. Table 3 contains a list of common silicate minerals defined in terms of their structural components. Other information regarding the structure of silicate minerals can be found in Papike and Cameron (1976) and Ulbrich and Waldbaum (1976).

As an example, table 6 shows the calculation procedure for estimating the relative enthalpy of acmite ($\text{NaFe}^{+3}\text{Si}_2\text{O}_6$). Acmite was chosen because experimental data on the relative enthalpy of acmite were not used to evaluate the estimation functions given on table 4. As the calculation is for a stoichiometric end-member phase, the computational procedure is straightforward. The coefficients, a_1 , a_2 , a_3 , a_6 , and a_7 used to describe the relative enthalpy of acmite are calculated by

[The text on this page is extremely faint and illegible. It appears to be a multi-paragraph document, possibly a letter or a report, but the specific content cannot be discerned.]

Table 6. Calculation of the constants a_1 , a_2 , a_3 , a_6 , and a_7 for use in equations 10 and 11 to calculate the relative heat content of acmite ($\text{NaFe}^{+3}\text{Si}_2\text{O}_6$)

Structural Component	Moles (n_i)	$n_i \cdot a_i$ $\times 10^{-2}$	$n_i \cdot b_i$ $\times 10^{+3}$	$n_i \cdot c_i$ $\times 10^{-5}$	$n_i \cdot f_i$ $\times 10^{+5}$	$n_i \cdot g_i$ $\times 10^{-3}$
$\text{Na}_2\text{O}-8$	0.5	0.29037	6.22990	0.0	0.0	-0.02291
Fe_2O_3-6	0.5	1.59206	2.44690	2.08544	1.28558	-1.65398
SiO_2-4	2.0	2.18766	-5.55182	0.0	0.0	-2.16610
		<u>a</u>	<u>b</u>	<u>c</u>	<u>f</u>	<u>g</u>
Constants for equation 5		4.07009 $\times 10^2$	3.12498 $\times 10^{-3}$	2.08544 $\times 10^{+5}$	1.28558 $\times 10^{-5}$	-3.84299 $\times 10^{+3}$

summing the products of the moles of each component i in one mole of acmite and the coefficients, $a_i \dots g_i$, for each component i . Figure 4 compares the calculated relative enthalpies with measured relative enthalpies (Ko and others, 1977) for acmite. The dashed lines in figure 4 represent a deviation of 2 percent from the calculated curve. Note that the measured relative enthalpy values lie well within this 2-percent window.

1.3.2.3.3. Entropy

The calorimetric molar entropy of silicate minerals can be estimated using equations 13 and 14. The coefficients a_i , b_i , c_i , d_i , f_i , and g_i for each structural component i can be found in table 4. Table 3 contains a list of common silicate minerals defined in terms of their structural components. Other information regarding the structure of silicate minerals can be found in Papike and Cameron (1976) and Ulbrich and Waldbaum (1976). In addition, Ulbrich and Waldbaum (1976) present structural information on silicate minerals needed to correct calorimetric entropy to third-law entropy.

The general procedure for the estimation of the molar calorimetric entropy for a phase would follow the same approach described in the calculation of estimated heat capacity of illite and relative enthalpy of acmite.

As an example, table 7a shows the calculation procedure to estimate the calorimetric molar entropy of an ideal illite ($K_3Al_7Mg(Si_{14}Al_2)O_{40}(OH)_8$). Measured data on the calorimetric molar entropy of illite was excluded from the evaluation. Table 7b compares the

Figure 4. Plot of experimental and estimated relative enthalpies ($H_T - H_{298.15}$) for acmite ($\text{NaFe}^{+3}\text{Si}_2\text{O}_6$). The estimated values were calculated using equations 5 and 6 and the coefficients listed in table 5 and are shown by a solid line. The dashed lines represent an error of 2 percent about the estimated relative enthalpy function. The experimental measurements of Ko and others, 1977, on a synthetic acmite are shown by x. The function departs from the experimental data by about 0.4 percent.

[The text on this page is extremely faint and illegible. It appears to be a list or a series of entries, possibly a table of contents or a list of references, but the specific details cannot be discerned.]

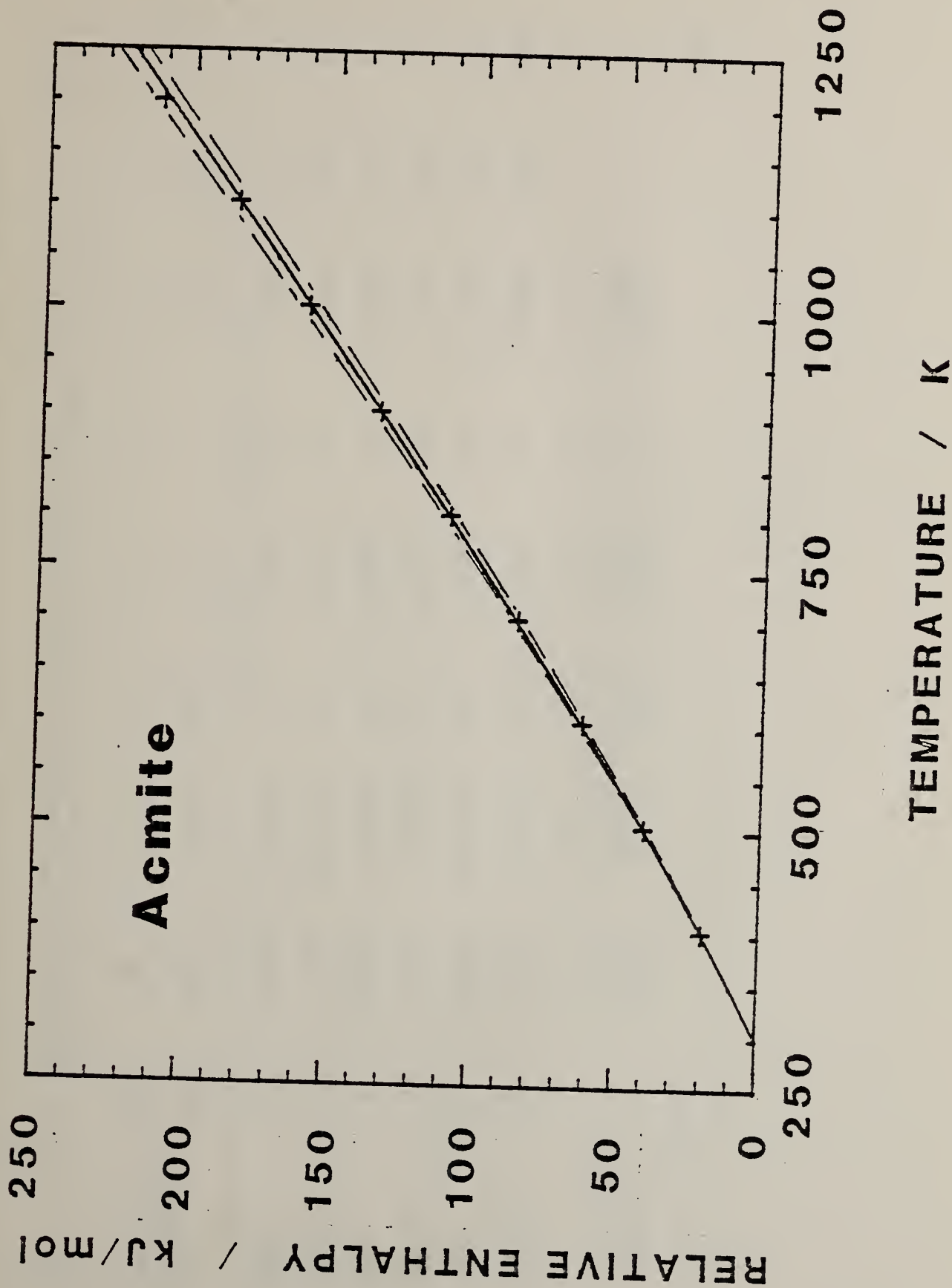




Table 7, part a. Calculation of the constants $a_1, a_2, a_3, a_4, a_6,$ and a_7 for use in equations 13 and 14 to calculate the calorimetric entropy of illite ($K_3Al_7Mg(Si_{14}Al_2)O_{40}(OH)_8$) at 298.15 K.

Structural Component	Moles (n_j)	$n_j \cdot a_j$ $\times 10^{-2}$	$n_j \cdot b_j$ $\times 10^{+3}$	$n_j \cdot c_j$ $\times 10^{-6}$	$n_j \cdot e_j$ $\times 10^{-3}$	$n_j \cdot f_j$	$n_j \cdot g_j$ $\times 10^{-3}$	S_{298} $J/mol \cdot K$	$n_j \cdot S_{298}$ $J/mol \cdot K$
K ₂ O-8	1.5	0.11576	79.07445	0.0	0.16255	0.0	0.98531	107.687	161.53
Al ₂ O ₃ -6	3.5	7.79590	-28.71579	0.0	-5.27534	0.0	-8.26596	42.411	148.44
MgO-6	1	0.89933	-3.13921	0.0	-0.58880	0.0	-0.87253	22.766	22.77
Al ₂ O ₃ -4	1	1.56985	6.34474	0.0	-0.99200	0.0	-1.37221	65.162	65.16
SiO ₂ -4	14	15.31362	-38.86274	0.0	-9.85806	0.0	-15.16270	42.865	600.11
Hydroxyl	4	5.16496	-24.04884	2.52828	-3.54677	0.0	-6.58128	32.437	129.75
Constants for equation 9		$\frac{a}{\times 10^{+3}}$	$\frac{b}{\times 10^{-3}}$	$\frac{c}{\times 10^{+6}}$	$\frac{e}{\times 10^{+4}}$	$\frac{f}{0.0}$	$\frac{g}{\times 10^{+4}}$		
Entropy at 298.15 K		3.08594	-9.39839	2.52828	-2.00984	0.0	-3.16294		1127.8

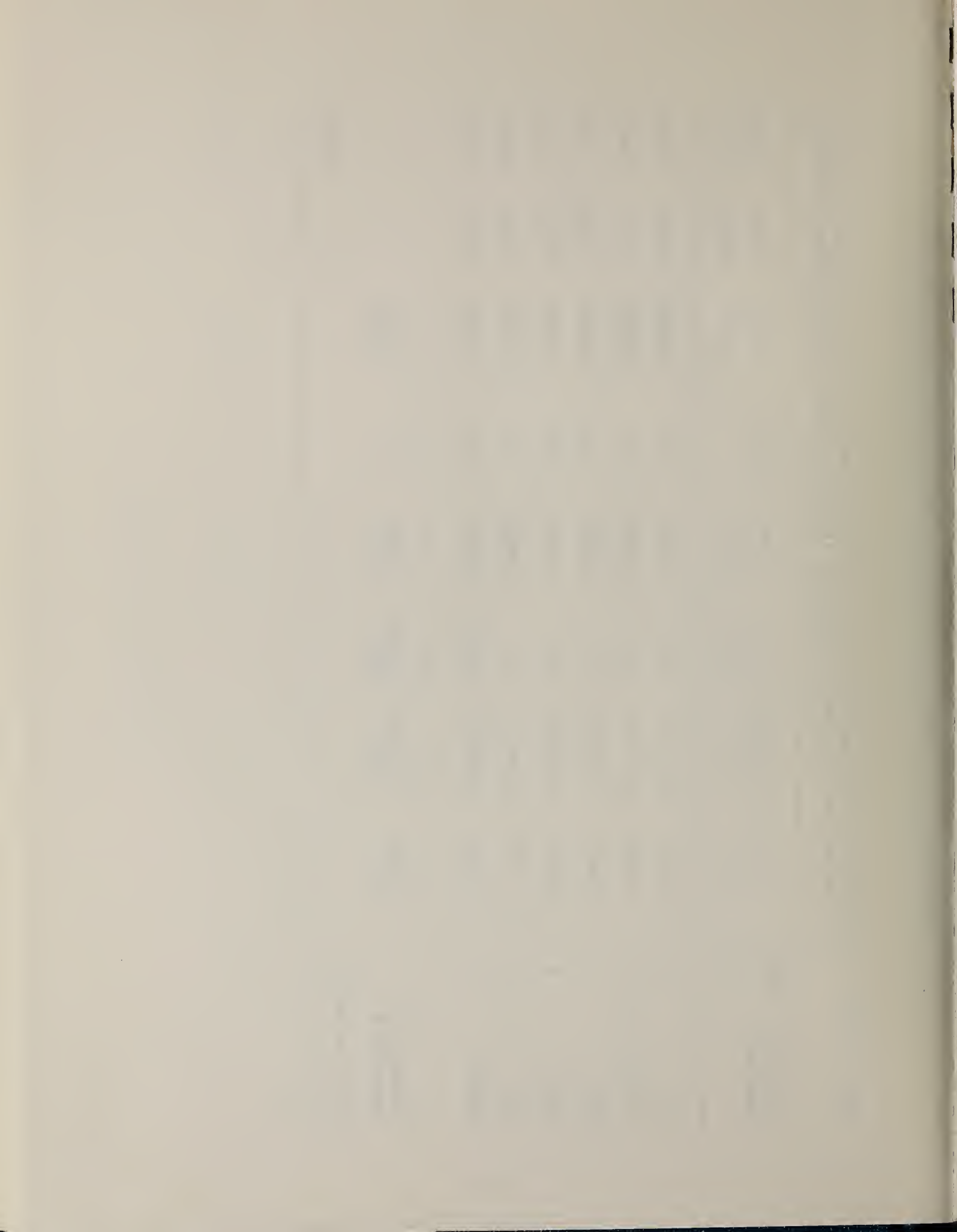


Table 7, part b. Comparison of the observed calorimetric molar entropy of illite ($K_3Al_7Mg(Si_{14}Al_2)O_{40}(OH)_8$) with estimated values calculated from 1) the technique described here, 2) the technique described by Helgeson and others, 1978, and 3) the sum of oxide entropies

	Observed ^a	Estimated (This paper)	Estimated ^b (Helgeson technique)	Estimated ^c (Oxide sum)
Calorimetric entropy (at 298.15 K) J/mol·K	1104.2 6.0	1127.8	1131.7	1125.3
Estimated value- observed value		23.6	27.5	21.1
Percent error		2.14	2.49	1.91

^aData from Robie and others, 1979.

^bCalculated using the method of Helgeson and others (1978), volume and entropy data from Robie and others (1979), molar volume for illite of $558.3 \pm 0.3 \text{ cm}^3/\text{mol}$ from Guven (1972), and the reaction illite = 3 muscovite + brucite + 5 quartz.

^cData from Robie and others, 1979. An estimated value of $(S_{298} - S_0)$ for crystalline H_2O of $35 \text{ J/mol}\cdot\text{K}$ was used in the calculation.

observed value for the calorimetric molar entropy of illite (Robie and others, 1976) with estimated values using 1) the estimation technique described here, 2) the estimation technique described by Helgeson and others, 1978, and 3) estimation based on sum of oxide entropies. The estimated molar entropy of illite at 298.15 K (1127.8 J/mol·K) differs by 2.1 percent from the measured molar entropy (1104.2 ± 6.0 J/mol·K, Robie and others, 1976).

1.3.2.4. Procedure to calculate estimated specific heats for rocks

The specific heat of silicate rocks as a function of temperature can be estimated using the following procedure.

$$\text{rock specific heat (J/gm K)} = \frac{\sum_i X_i C_i}{\sum_i X_i}$$

where X_i = (gm. of component i in rock)/(gm rock)

$$C_i = a_i + 2b_i T + \frac{c_i}{T^2} + f_i T^2 + \frac{g_i}{T^{1/2}} \quad (15)$$

The coefficients a_i , b_i , c_i , f_i , and g_i for each component i can be found in table 8. An example of calculations of estimated specific heat for basalt is shown in table 9, part b, based upon the basalt chemistry shown in table 9, part a. A comparison of the estimated specific heats for basalt and measured specific heats for a basalt from Dresser, Wisconsin (Hanley and others, 1977) is shown in table 9, part b.

Table 8. Component coefficients to calculate rock specific heat (Joules/gm-kelvin)

	a	b	c	f	g
SiO ₂	1.82029D+00	-4.61871D-05	0.00000D+00	0.00000D+00	-1.80210D+01
TiO ₂	1.62105D+00	-1.41404D-04	0.00000D+00	6.59702D-08	-1.47083D+01
Al ₂ O ₃	1.53910D+00	6.23640D-05	0.00000D+00	0.00000D+00	-1.34537D+01
Fe ₂ O ₃	1.99391D+00	-3.06452D-04	2.61183D+03	1.61007D-07	-2.07146D+01
FeO	1.12971D+00	0.00000D+00	0.00000D+00	0.00000D+00	-9.07581D+00
MnO	5.60685D-01	1.44421D-04	0.00000D+00	-8.04267D-08	0.00000D+00
MgO	2.23223D+00	-7.94663D-05	0.00000D+00	0.00000D+00	-2.16622D+01
CaO	1.40329D+00	-3.35115D-05	0.00000D+00	0.00000D+00	-1.10740D+01
Na ₂ O	9.10305D-01	2.14390D-04	0.00000D+00	0.00000D+00	-4.80940D-01
K ₂ O	4.51022D-01	1.81504D-04	0.00000D+00	0.00000D+00	1.81573D+00
P ₂ O ₅	5.64294D-01	8.30332D-04	0.00000D+00	-5.20355D-07	-4.61346D+00
hydroxyl	7.18335D+00	-3.34688D-04	3.55918D+04	0.00000D+00	-9.17058D+01
Fluorine	3.68074D-01	3.36682D-04	0.00000D+00	0.00000D+00	0.00000D+00

Table 9, part a. Representative composition of terrestrial flood basalt (weight fraction)

	Avg. Yakima basalt Waters, 1961	Grande Ronde basalt (museum flow) rho-bwi-st-4	Grande Ronde basalt (flow e) rho-bwi-st-4	Grande Ronde basalt (Umtanum unit) rho-bwi-st-4
SiO ₂	0.5380	0.5420	0.5358	0.5459
TiO ₂	0.0200	0.0169	0.0191	0.0215
Al ₂ O ₃	0.1390	0.1505	0.1480	0.1459
Fe ₂ O ₃	0.0260	not determined	not determined	not determined
FeO	0.0930	0.0955	0.1056	0.1115
MnO	0.0020	not determined	not determined	not determined
MgO	0.0410	0.0479	0.0464	0.0345
CaO	0.0790	0.0859	0.0853	0.0721
Na ₂ O	0.0300	not determined	not determined	not determined
K ₂ O	0.0150	0.0115	0.0107	0.0165
P ₂ O ₅	0.0040	0.0029	0.0028	0.0035
hydroxyl	0.0120	not determined	not determined	not determined
Total	0.9990	0.9531	0.9537	0.9514

Table 9, part b. Estimated specific heats of selected basalts using the compositions given in part a of this table. Measured specific heats of basalt at Dreser, Wisconsin (data from Hanley and others, 1977)

T/C	Estimated specific heat Joules/gm-K				Measured specific heat ^e
	(1) ^a	(2) ^b	(3) ^c	(4) ^d	
50	0.8027	0.7832	0.7810	0.7769	0.8090
100	0.8614	0.8414	0.8389	0.8345	0.8689
150	0.9092	0.8885	0.8858	0.8811	0.9200
200	0.9490	0.9276	0.9247	0.9199	0.9617
250	0.9826	0.9606	0.9575	0.9526	0.9932
300	1.0116	0.9890	0.9857	0.9807	1.0110
350	1.0367	1.0135	1.0101	1.0051	
400	1.0588	1.0351	1.0316	1.0265	
450	1.0783	1.0541	1.0505	1.0455	
500	1.0957	1.0711	1.0673	1.0623	

^aAverage Yakima basalt, Waters, 1961 (table 8, part a, column 1)

^bGrande Rhonde basalt (Museum flow), rho-bwi-st-4 (table 8, part a, column 2)

^cGrande Rhonde basalt (flow e), rho-bwi-st-4 (table 8, part a, column 3)

^dGrande Rhonde basalt (Umtanum unit), rho-bwi-st-4 (table 8, part a, column 4)

^eData from Hanley and others, 1977

1.3.3. Evaluated Thermodynamic and Thermophysical Properties of Selected Mineral Phases in the $\text{MgO-SiO}_2\text{-H}_2\text{O-CO}_2$, $\text{Fe-FeO-Fe}_2\text{O}_3\text{-SiO}_2$, and $\text{CaO-Al}_2\text{O}_3\text{-SiO}_2\text{-H}_2\text{O-CO}_2$ Chemical Systems

1.3.3.1. Introduction

The experimental data on the selected phases (Appendix section 1.5.1) in the $\text{MgO-SiO}_2\text{-H}_2\text{O-CO}_2$, $\text{Fe-FeO-Fe}_2\text{O}_3\text{-SiO}_2$, and $\text{CaO-Al}_2\text{O}_3\text{-SiO}_2\text{-H}_2\text{O-CO}_2$ chemical systems were evaluated using the method of Haas and Fisher (1976). The goal was to produce a set of thermodynamic properties for each phase at a standard state of 1 atm (101.325 kPa) that is consistent with thermodynamic theory, the observed properties of each phase, and the observed phase relations among the phases. The experimental data used in the study came from a literature search through March 1982.

1.3.3.2. Fitting procedure

1.3.3.2.1. Introduction

The details of the approach and the procedure are described by Haas and Fisher (1976) and by Haas (1974). The approach and procedure given there have been followed closely and will not be described here in detail. The following description summarizes the evaluation procedure:

1. Literature search
 - a. Review of literature for data that define thermodynamic properties of a phase or a group of phases.
 - b. Close scrutiny of each citation to determine:
 - (1) What was physically observed.
 - (2) With what precision was it observed.

2. Refinement cycle

a. Comparison of related data (heat capacity, relative enthalpy, enthalpies of formation, enthalpies of reaction, Gibbs energy of reaction, entropies, molar volumes, expansivities, compressibilities) for phases in a chemical system using weighted, simultaneous, multiple, least-squares regression.

b. Review of the pertinent literature where data are found not to be in agreement.

c. Removal of assumed or apparently erroneous data from the set of data being fit by the regression.

d. Repeat of steps a through c until all discordant data have been identified and removed.

3. Preparation of tables using the smoothing functions and the variance-covariance matrix from the last execution of step 2a.

The mathematical model used in the regression in step 2a is based on equation 15 for the heat capacity at constant pressure, equation 16 for molar volume as a function of pressure and temperature, and the known relations among heat capacity, enthalpy, entropy, Gibbs energy and volume for the i th phase in a group of chemically related phases. The constants $a_{2,i}$ and $a_{4,i}$ were reserved for the constants of integration to describe the enthalpy and entropy of the i th phase respectively. Equation 15 is a restatement of Haas and Fisher's equation 6:

$$C_{p,i}^{\circ} = \frac{a_{1,i}}{T^2} + \frac{a_{3,i}}{T^{1/2}} + a_{5,i} + 2 a_{6,i} T + a_{7,i} T^2 \quad (15)$$

$$V_i^0 = b_{1,i} + b_{2,i}T + b_{3,i} \exp(-T/300) + b_{4,i}P + b_{5,i} \exp(-P/35000) \quad (16)$$

Equations 15 and 16 have no theoretical basis. They are smoothing functions only and must be so considered! At the absolute zero of temperature equation 15 is indeterminate. In our work, data at temperatures below 200 K were not considered. Above 200 K, the functions readily describe most data. In order to avoid overfitting of the data, nonsignificant constants have been eliminated from the general equation wherever they were not needed to describe the properties of a phase. This is particularly common for the last term, $a_{7,i}T^2$, in equation 15. Removal of this term eliminated any rapid excursions of the calculated values in the temperature region around and above the highest experimental temperature. Equation 15 has been fit within the temperature range presented for each phase in the appendix and should not be extended indiscriminately to higher or lower temperatures.

For grossular, the experimental heat capacities were measured at or below 978 K. The estimated values used in the fitting for the heat capacity above 1000 K joined smoothly with the experimental data below 1000 K and did not contain a maximum. Therefore, the maximum in the fitted function was a result of the constraints imposed on the thermal data by the phase equilibria that included observations up to 1523 K. In this case, no action was taken. The presence of the maximum emphasizes the need for measured high-temperature heat capacities. Until this has been accomplished, the tabulations are considered the best available.

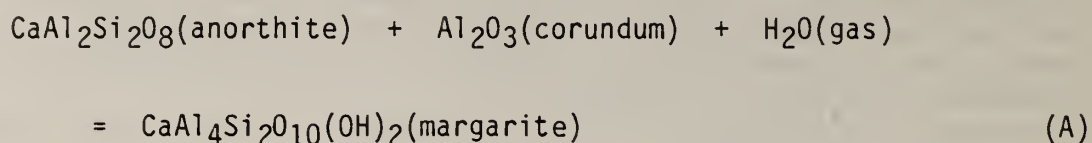
1.3.3.3. Data entry

Haas (1974) described the mechanics used to fit the model to discrete experimental observations in detail. The typical problem includes the following information:

1. Title for problem.
2. Control codes to identify the options used.
3. Number and labels for the phases in the problem.
4. Sets of data being fit.
 - a. Name of the set and reference.
 - b. Control codes related to the observation and to data editing.
 - c. Label(s) for the phase(s), the stoichiometric coefficient(s) and any pertinent data on polymorphs.
 - d. Data as given in the reference.
 - (1) Temperature (and correction factor if needed to convert to kelvins).
 - (2) Observed value (and correction factor if needed to convert to joules, volts, moles, etc.).
 - (3) Precision.
 - (4) Second independent variable (if needed).
5. Constants of Equation 15 above for each of the reference phases as well as the trial constants for the phases for which the properties are being refined.
6. Control parameters for the error plots.

The input format is designed to reduce manual conversions before entry into the computer for fitting.

The class of data that is not discussed by Haas consists of bracketed observations like those typical of phase equilibria studies. As an example, let us consider reaction A, below.



Chatterjee (1974) determined that the equilibrium at 100 MPa was located between 743.15 and 773.15 K. If we consider no additional information, there is an equal probability of equilibrium occurring at any temperature between these two bracketing temperatures at 100 MPa. Therefore, if we neglect the errors associated with the measurement of temperature and pressure, the probability curve is a square wave whose bounds are at 743.15 K and 773.15 K. To consider the reaction to occur at the midpoint of the bracket, 758.15 K, is unwarranted; this would cause the fitting algorithms to give too much weight to the midpoints of bracketed data. We evaluated the phase equilibrium data by calculating the Gibbs energy of reaction for each two experimentally measured bracketing pressures and temperatures as if each bracketing pressure and temperature represented equilibrium. This procedure does not define a square probability curve between the bracketing values but does define a nearly uniform probability between the bracketing values and allows a sufficient probability of occurrence outside the bracketing values to compensate for errors in measurement of pressure and temperature. The Gibbs energy for the reaction for both bracketing reaction points is calculated using equation 17:

$$\Delta G_{r,P,T} = \sum n_i H_{i,T,P,\text{solids}} - T \sum n_i S_{i,T,P,\text{solids}} + n_{\text{gas}} G_{P_{\text{ref}},T}^{\text{gas}} + \int_{P_{\text{ref}}}^P \frac{n_{\text{gas}}}{1000} V(\text{gas}) dP_T \quad (17)$$

where n_i is the stoichiometric coefficient for each phase, i , and V is the volume of the gas phase. The factor 1000 is the conversion factor for cm^3/mol to $\text{J}/(\text{kPa}\cdot\text{mol})$. The integral represents the Gibbs energy difference of the gas between the pressure of observation and the reference pressure, 101.325 kPa. The Gibbs energy difference for H_2O at constant temperature was calculated from data on the P - V - T function proposed by Haar and others (1979).

1.3.3.4. Weighting of experimental data

Data were weighted by the reciprocal of the precision; the higher (smaller in magnitude) the precision, the higher (larger in magnitude) the weight. The use of weighting served two purposes. First, it allowed the simultaneous fitting of different properties that have large variations in magnitude. An example is the simultaneous fitting of enthalpy data that could exceed 7 MJ and electrochemical potentials that are more like 1.0 millivolt. Second, weighting constrained the solution towards the more precise observations. This was particularly desirable where precise data from low-temperature, adiabatic calorimetry were being matched with the less precise data from differential scanning calorimetry or from drop calorimetry.

In the first fitting of a data set from a particular reference, the author's stated precision was used. In subsequent cycles this would be modified if logic or other data showed the author's estimate to be abnormally small.

Weighting of data within the above guideline was straightforward with two exceptions. The first exception is when the author makes many observations of a phenomenon but only reports an average value and the standard deviation. To enter one value, the average value, would underweight the work that went into the determination relative to the significance of discrete measurements on the same or other properties. We arbitrarily overcame this by making three entries: (1) the average value, (2) the average value less the deviation, and (3) the average value plus the deviation. All three entries had a weight equal to the stated standard deviation.

The second exception is related to the treatment of brackets in phase equilibria. As stated in the preceding section, the Gibbs energy at the experimental pressure for both temperature limits (or at both pressure limits or the combination that defines the bracket) was entered. The weight was calculated from the arbitrary decision that the precision for each bracket was the difference in Gibbs energy for the bracket with the constraint that the magnitude of the assigned precision was equal to or greater than the precision associated with the determination of the temperature (or pressure) of the limit of the bracket. In this fashion, we reduced the tendency of the regression to settle on the midpoint of a bracket. We will return to this point again when we consider the topic of data rejection.

1.3.3.5. Data rejection

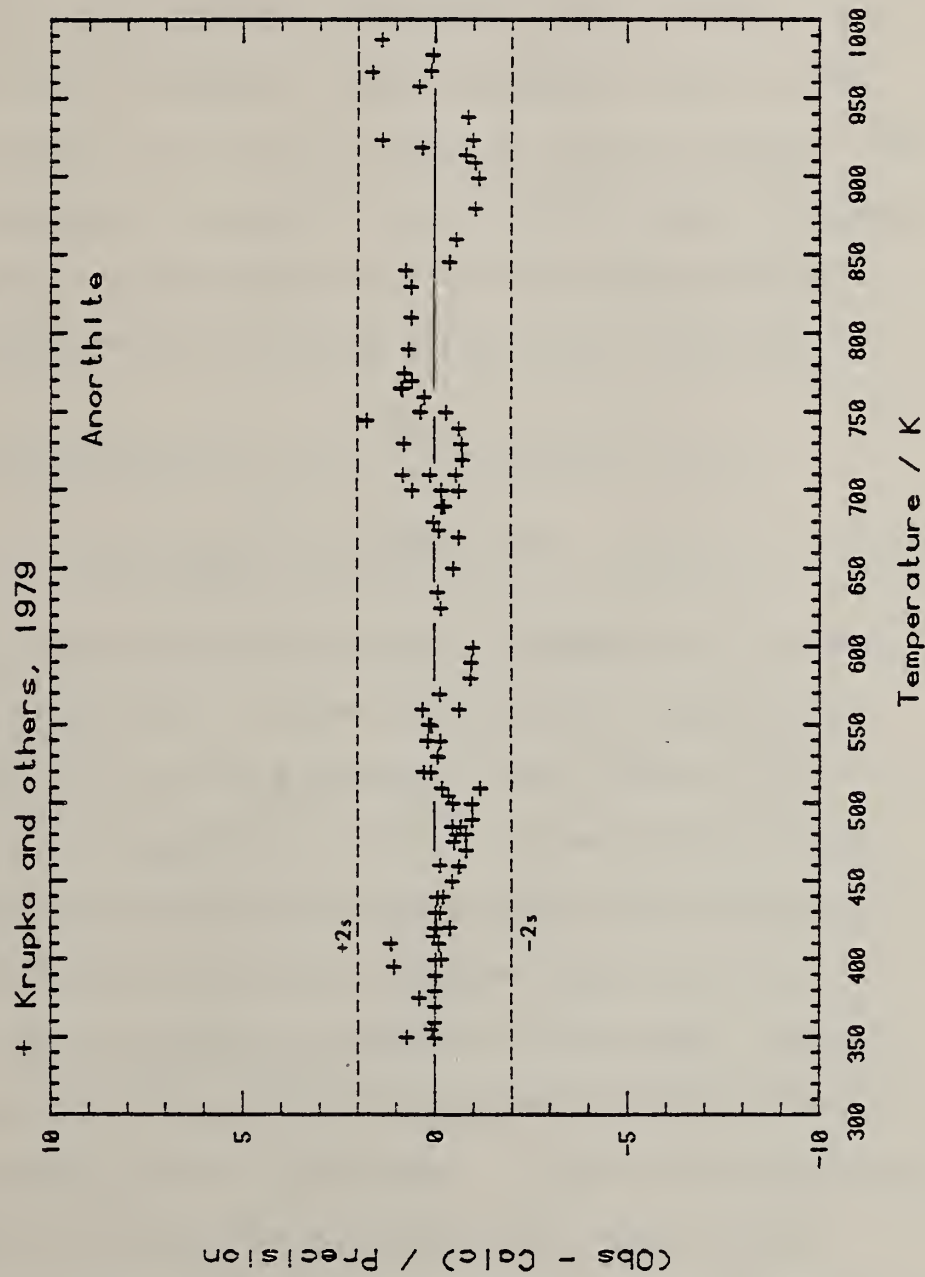
Data were rejected during the literature search and during the refinement cycles. Data were rejected during the literature search if there was a clear error in the measurement technique or if there was ambiguity in the identification of the reactants or products.

During the refinement cycle, where all data for all phases in the chemical system are simultaneously fit by the model, the model returns the weighted average of all the data. Error plots such as figure 5 are part of the printed output. On the error plots for each source and type of data, the weighted difference, calculated as (observed-calculated)/precision, is plotted as a function of temperature. These plots give a quick visual picture of the quality of the agreement between the function in the model, the other data in the refinement, and the specific data set. Ideally, the errors should be centered about the zero axis and should not exceed ± 2 units ($\pm 2s$). Not attaining such an ideal plot can be the result of one or more of the following:

1. The function does not adequately describe the data.
2. Some set (or sets) of data is not consistent with the balance of the data considered.
3. The magnitude of the experimental precision is larger than that which the author stated. As a rule of thumb, if more than one third of the data plots outside the bounds of +1 to -1 (equal to $\pm 1s$), this leads to overweighting of the data set. More realistic precisions were entered in this situation.

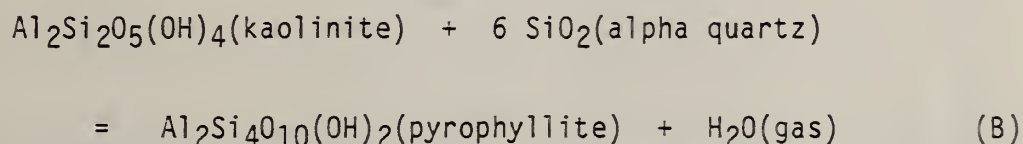
Figure 5. Error (observed value - calculated value)/precision as a function of temperature for the differential scanning calorimeter measurements of heat capacity for anorthite. Plus signs (+) indicate the data of Krupka and others, 1979.

Error Plot





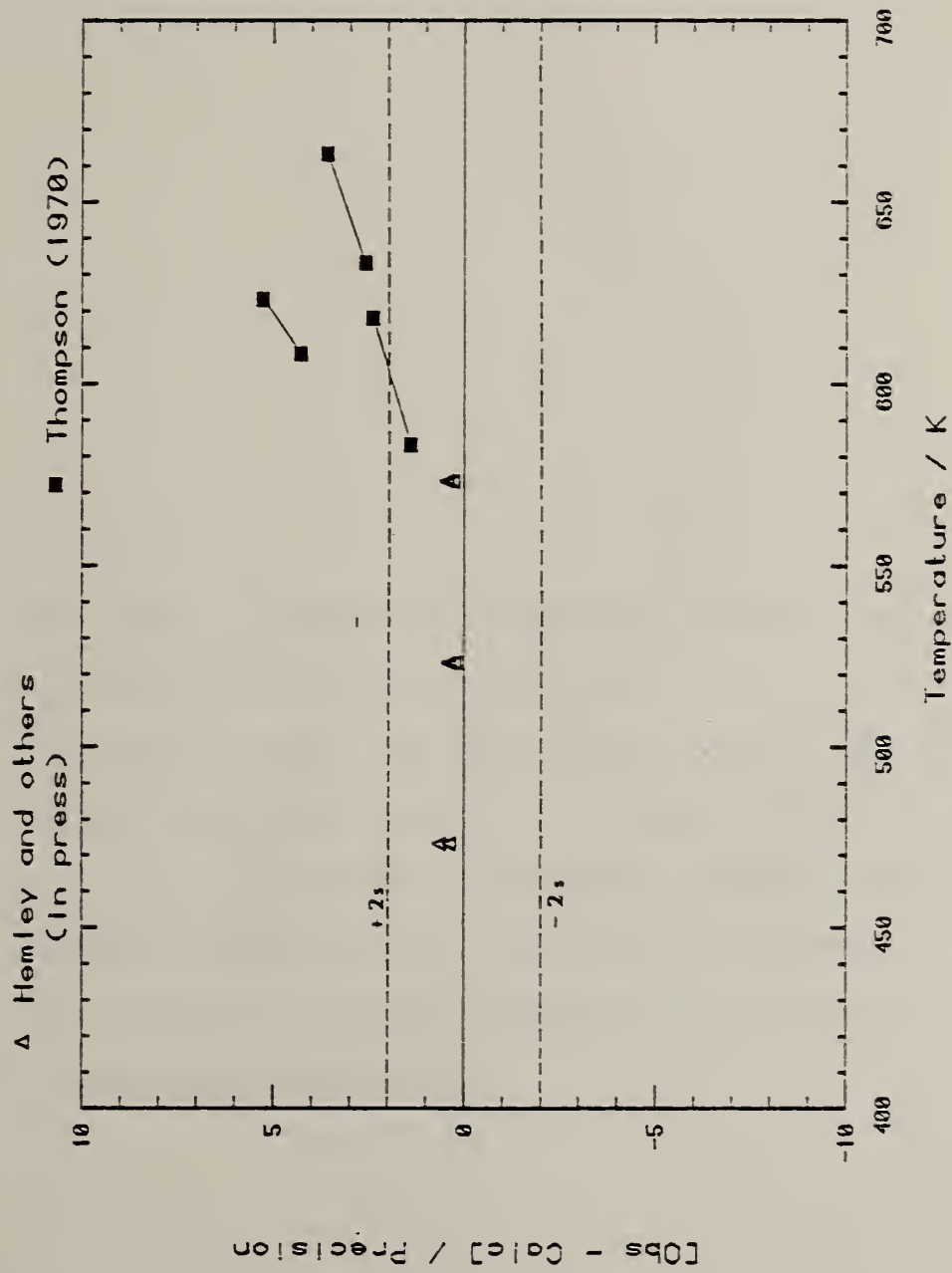
Error plots alert the evaluator to the existence of a conflict in the data sets. The evaluator must determine the source for the conflict and make the appropriate correction to the data. As an example, figure 6 is a combination of the error plots for reaction B. The relative errors for the silicic acid solubilities of Hemley and others (1980) and the reversed brackets of Thompson (1970) are shown. The data of Hemley and his coworkers plot systematically high for this reaction, but they are well within 1 sigma of the zero abscissa. The systematic discrepancy is caused by a minor misfit between these data and one or more of the enthalpies of solution and Gibbs energies of reaction in which either kaolinite or pyrophyllite is involved.



However, the reversed observations of Thompson (1970) lie well outside the 2 sigma limits. Figure 7 shows the calculated Gibbs energy for reaction B and the experimental data cited on figure 6. As expected, the data of Hemley and coworkers lie near the calculated values. Because the calculated line also reflects the other data in the problem, particularly entropies and other phase equilibria, we conclude that data of Hemley and coworkers are consistent. However, both the magnitude and the slope of the reversed brackets of Thompson are not in agreement with the other data. A review of the experimental method suggests that the error may be due to the finely ground kaolinite and pyrophyllite ("less than 300 mesh," p. 454) that was

Figure 6. Error (observed value - calculated value)/precision as a function of temperature for the reaction: Kaolinite + 2 Quartz = Pyrophyllite + Steam. The open triangles were calculated from the silicic acid solubilities of Hemley and others (in press). The connected solid squares represent the brackets of Thompson (1970). The dashed lines represent two times the precision stated by the authors or two times the width of the Gibbs energy bracket, whichever is appropriate.

Kaolinite + 2 Quartz = Pyrophyllite + Steam



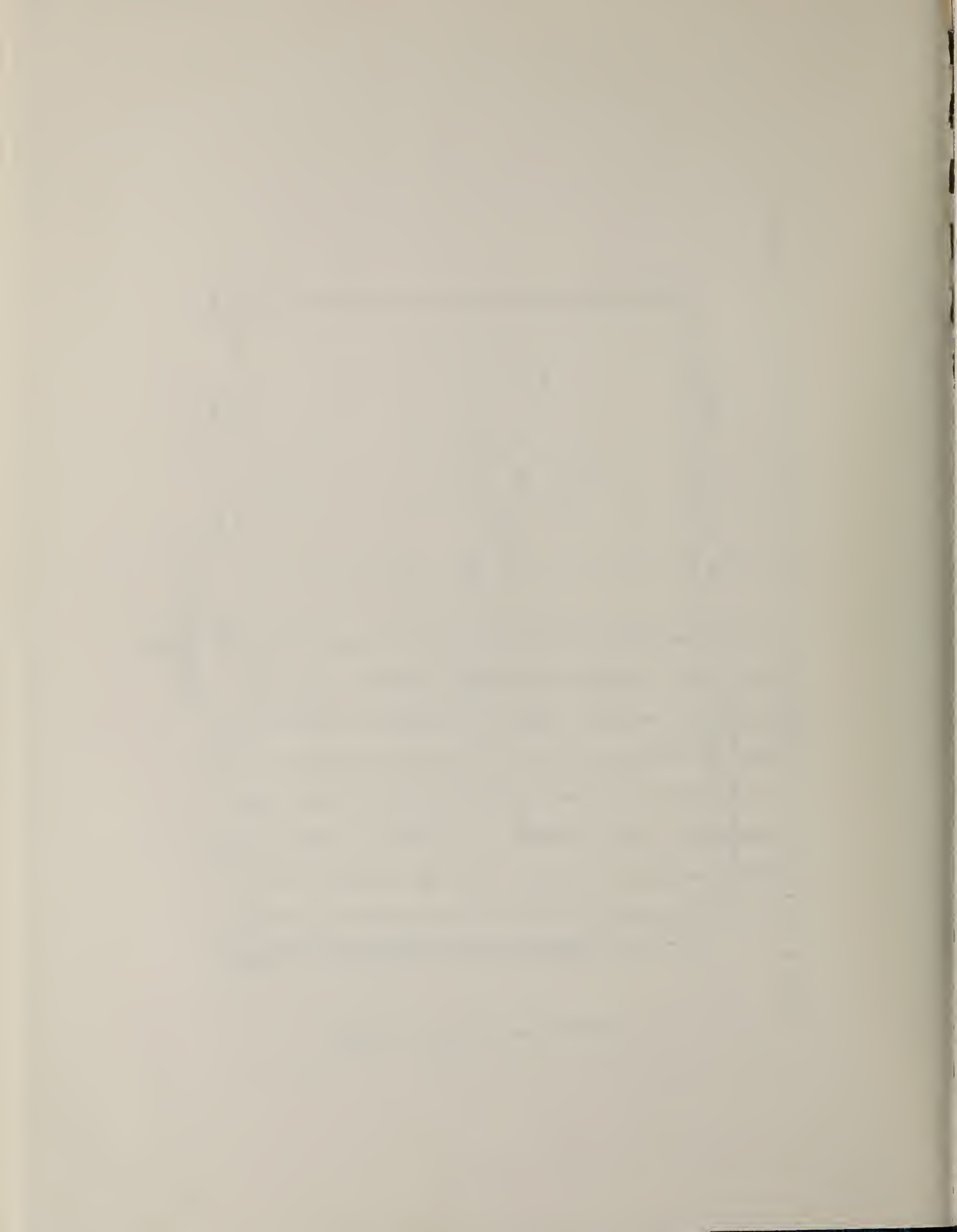
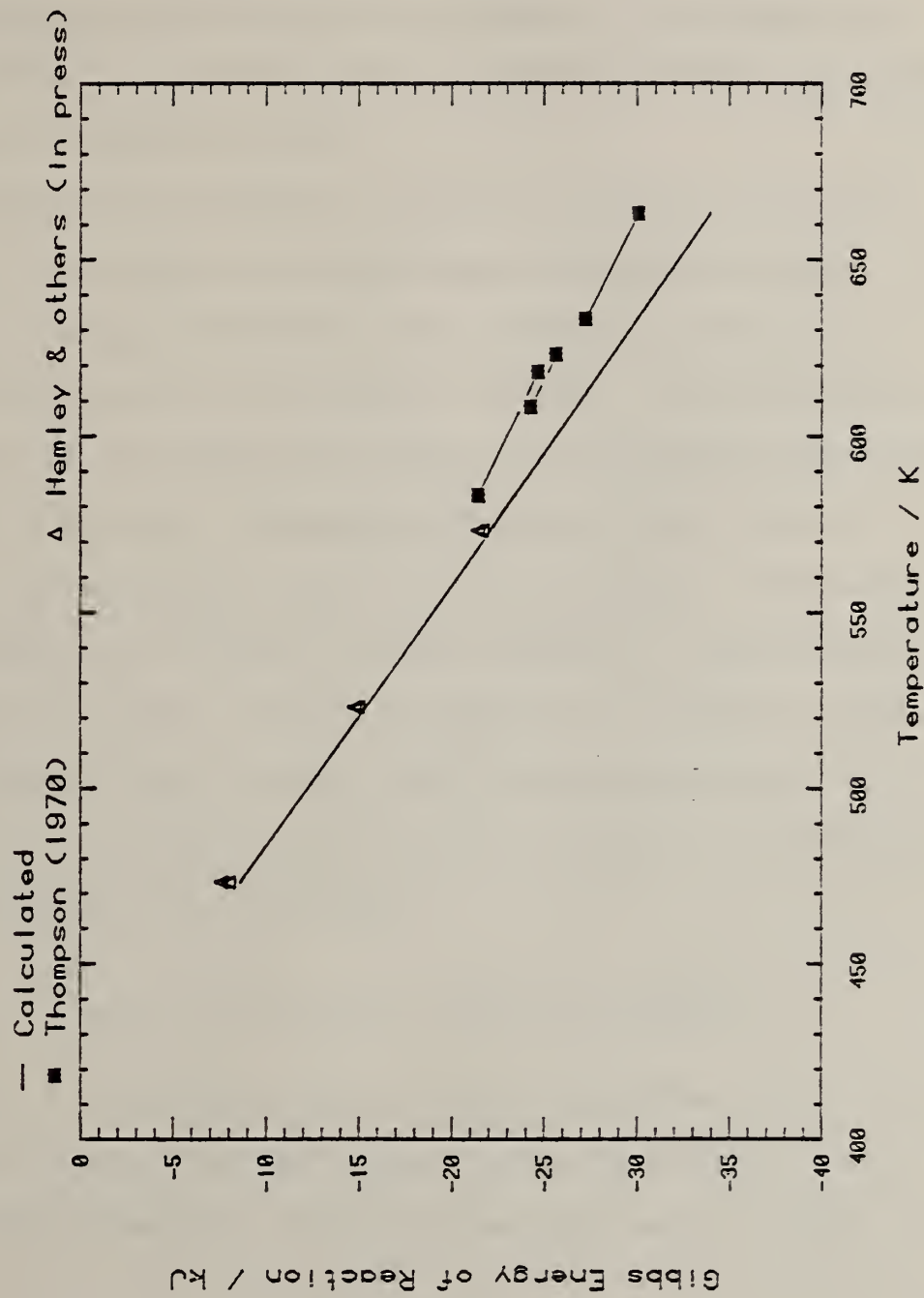


Figure 7. Gibbs energy of reaction as a function of absolute temperature for the reaction: Kaolinite + 2 Quartz = Pyrophyllite + Steam. The open triangles were calculated from the silicic acid solubilities of Hemley and others (in press). The connected solid squares represent the brackets of Thompson (1970). The solid line was calculated from the least-squares solution to the entire set of experimental observations.

Kaolinite + 2 Quartz = Pyrophyllite + Steam





used in the study and to the relatively short duration of the experiments ("usually 28 days" at 100 MPa, "for 1 week" at 200 and 400 MPa, p. 455-456). These data were not included in the evaluation. The above conjecture on the part of the evaluators is not proven; only detailed discussions with the authors or repetition of the experiments could prove the data are in error.

Discordant data are readily identified. The cause of the disagreement is not always as straightforward as the identification. Fortunately, because sufficient related data were available for the phases in question, the right decision was made. In the discussions associated with the thermodynamic tables, all data used to produce the final results are given. Because of manpower and time, however, we have not included the much larger set of excluded data. The reference section contains all literature sources considered in the evaluation. References which contain indirect or supporting information on thermodynamic properties and references containing experimental data considered, but excluded from the evaluation, are marked with an asterisk (*) at the beginning of the citation.

1.3.3.6. Preparation of tables and summaries

Tables of thermodynamic data at 101.325 kPa between 273.15 K and 1800 K were prepared from the functions in the fitted model. The commonly used thermodynamic functions given below were tabulated:

C_p	heat capacity
S	entropy



$[G_T - H_{T_r}]/T$	Gibb's function
$H_T - H_{T_r}$	relative enthalpy
V	molar volume
$\Delta H_{f,e}^\circ$	enthalpy of formation from the elements
$\Delta G_{f,e}^\circ$	Gibbs energy of formation from the elements
$\log K_{f,e}^\circ$	equilibrium constant for formation from the elements
$\Delta H_{f,ox}^\circ$	enthalpy of formation from the oxides
$\Delta G_{f,ox}^\circ$	Gibbs energy of formation from the oxides
$\log K_{f,ox}^\circ$	equilibrium constant for formation from the oxides

The summaries associated with each table contain functions for heat capacity, entropy, relative enthalpy, and molar volume as obtained in fitting the model to the data. The summaries also cite those data used in the final evaluation that were directly pertinent to determine the properties of the phase in question. In the interest of saving manpower for more evaluations, data that were considered and rejected and not tabulated.

1.3.3.7. Confidence limits

All evaluations must start with some base that is accepted without question. In this effort, the properties of the elements and the oxides cited in Appendix section 1.5.4 were used without question. The properties for the evaluated phases are determined relative to those

reference values. In the course of the evaluation, we found no inconsistency of sufficient magnitude that would require us to consider reevaluating any of that reference base. This does not mean that the tabulated values are without error. For example, the uncertainty for the entropy at 298.15 K for Ca or CaO is about 1 percent (CODATA Task Group, 1978).

In preparing the tabulations, the 2-sigma confidence limits were given for the 298.15 K isotherm and for every isotherm that is a multiple of 250 K. These limits reflect only the variation in the final set of data on the chemical system. They do not include confidence limits on the reference data in Appendix section 1.5.4. For this reason the confidence limits for formation from the elements is omitted. If such a time arises when manpower is abundant or when other data centers adopt similar evaluation procedures, the imprecision in the reference base will be included in the tables.

1.3.3.8. Results

The Appendix, section 1.5, contains the thermochemical properties of phases of interest in exploring possible chemical reactions in basalt systems. These data, as tabulated, are consistent with the recommendations of the CODATA Task Group (1978). In general, we used the same reference base as Robie and others (1979) and as used in preparing the JANAF Thermochemical Tables (Stull and Prophet, 1971) and the JANAF thermochemical data^a.

^aJANAF Thermochemical Tables, looseleaf pages for 1979 issued by Dow Chemical Company, 1707 Building, Midland, Michigan.

The arrangement of the compounds is alphabetical using the commonly accepted chemical formula for the phase. Sections 1.5.1 and 1.5.2 contain the index arranged by chemical formula and by mineral name, respectively.

1.4. References

- Ackermann, Raymond J., and Sanford, R.W., Jr., 1966, Thermodynamic study of the wustite phase: U.S. Atomic Energy Commission, ANL-7250, 46 p.
- Adams, L.H., and Gibson, R.E., 1929, The elastic properties of certain basic rocks and of their constituent minerals: Proceedings of the National Academy of Science, v. 15, p. 713-724.
- Adams, Leason H., Williamson, Erskine D., and Johnston, John, 1919, The determination of the compressibility of solids at high pressures: Journal of the American Chemical Society, v. 41, p. 12-42.
- Alcock, C.B., ed., 1968, Electromotive Force Measurements in High-temperature Systems: American Elsevier Publishing Company, Inc., New York, 227 p.
- *Althaus, Egon, 1966, Die bildung von pyrophyllit und andalusit zwischen 2000 und 7000 bar H_2O -druck: Naturwissenschaften, v. 53, p. 105-106.
- *Althaus, Egon, 1969, Das system $Al_2O_3-SiO_2-H_2O$. Experimentelle untersuchungen und folgerungen fur die petrogenese der metamorphen gesteine: Neues Jahrbuch fur Mineralogie, Abhandlungen, v. 111, p. 74-110.
- Anderson, C. Travis, 1934, The heat capacities of magnesium, zinc, lead, manganese and iron carbonates at low temperatures: Journal of the American Chemical Society, v. 56, p. 849-851.
- Anderson, P.A.M, and Kleppa, U.J., 1969, The thermochemistry of the

- kyanite - sillimanite equilibrium: American Journal of Science, v. 267, p. 285 -290.
- Anderson, P.A.M., Newton, R.C., and Kleppa, O.J., 1977, The enthalpy change of the andalusite-sillimanite reaction and the Al_2SiO_5 diagram: American Journal of Science, v. 277, p. 585-593.
- Atlas, Leon, 1952, The polymorphism of $MgSiO_3$ and solid-state equilibria in the system $MgSiO_3$ - $CaMgSi_2O_6$: Journal of Geology, v. 60, p. 125-147.
- Baker, E.H., 1962, The calcium oxide-carbon dioxide system in the pressure range 1-300 atmospheres: Journal of the Chemical Society, London, Part I, p. 464-470.
- Barany, Ronald, 1963, Heats of formation of gehlenite and talc: U.S. Bureau of Mines, Report of Investigations 6251, 9 p.
- Barany, Ronald, 1966, Glass-crystal transformation of nepheline and wollastonite and heat of formation of nepheline: U.S. Bureau of Mines, Report of Investigations 6784, 8 p.
- Barany, Ronald, and Kelley, K.K., 1961, Heats and free energies of formation of gibbsite, kaolinite, halloysite, and dickite: U.S. Bureau of Mines, Report of Investigations 5825, 13 p.
- Barnes, H.L., and Ernst, W.G., 1963, Ideality and ionization in hydrothermal fluids: the system MgO - H_2O - $NaOH$: American Journal of Science, v. 261, p. 129-150.
- *Bell, Peter M., 1963, Aluminum silicate system: experimental determination of the triple point: Science, v. 139, p. 1055-1056.
- Bennington, K.O., Ferrante, M.J., and Stuve, J.M., 1978, Thermodynamic

- data on the amphibole asbestos minerals amosite and crocidolite:
U.S. Bureau of Mines, Report of Investigations 8265, 30 p.
- Benz, Robert, and Wagner, Carl, 1961, Thermodynamics of the solid system CaO-SiO₂ from electromotive force data: Journal of Physical Chemistry, v. 65, p. 1308-1311.
- *Best, N.F., and Graham, C.M., 1978, Redetermination of the reaction 2 zoisite + quartz + kyanite = 4 anorthite + H₂O: Progress in Experimental Petrology, p. 153-154.
- Birch, Francis, 1966, Compressibility; elastic constants: Handbook of Physical Constants - Revised Edition, GSA Memoir 97, p. 97-173.
- Birks, N., 1966, Some problems in the use of solid-state galvanic cells at low temperatures: the determination of the eutectoid temperature of the iron-oxygen system: Nature, v. 210, p. 407-408.
- Boettcher, A.L., 1970, The system CaO-Al₂O₃-SiO₂-H₂O at high pressures and temperatures: Journal of Petrology, v. 11(2), p. 337-379.
- Boettcher, A.L., and Wyllie, P.J., 1968, The calcite-aragonite transition measured in the system CaO-CO₂-H₂O: Journal of Geology, v. 76, p. 314-330.
- Bohlen, Steven R., Essene, Eric J., and Boettcher, A.L., 1980, Reinvestigation and application of olivine-quartz-orthopyroxene barometry: Earth and Planetary Science Letters, v. 47, p. 1-10.
- Boyd, F.R., and England, L.J., 1965, The rhombic enstatite-clinoenstatite inversion: Year Book - Carnegie Institution

- of Washington, v. 64, p. 117-123.
- Boyd, F.R., England, J.L., and Davis, Brian T.C., 1964, Effects of pressure on the melting and polymorphism of enstatite, $MgSiO_3$: Journal of Geophysical Research, v. 69, p. 2101-2109.
- Brace, W.F., Scholz, C.H., and La Mori, P.N., 1969, Isothermal compressibility of kyanite, andalusite, and sillimanite from synthetic aggregates: Journal of Geophysical Research, v. 74, p. 2089-2098.
- Bransky, I., and Hed, A.Z., 1968, Thermogravimetric determination of the composition-oxygen partial pressure diagram of wustite ($Fe_{1-y}O$): Journal of the American Ceramic Society, v. 51, p. 231-232.
- *Brown, G.C., and Fyfe, W.S., 1971, Kyanite-andalusite equilibrium: Contributions to Mineralogy and Petrology, v. 33, p. 227-231.
- Brunauer, Stephen, Kantro, D.L., and Weise, C.H., 1956, The heat of decomposition of tricalcium silicate into beta-dicalcium silicate and calcium oxide: Journal of Physical Chemistry, v. 60, p. 771-774.
- Burnham, Charles W., 1966, Ferrosilite: Year Book - Carnegie Institute of Washington, v. 65, p. 285-290.
- *Byker, H., and Howald, R.A., 1978, Discussion of standard free energy of formation of alumina by D. Ghosh and D.A.R. Kay: Journal of the Electrochemical Society, v. 125, p. 889-890.
- Carlson, E.T., 1931, Decomposition of tricalcium silicate in temperature range 1000° to 1300°C: U.S. Bureau of Standards

- Journal of Research, v. 7(5), p. 893-902.
- Cnang, Byong-Tae, 1981, Determination of thermodynamic properties of boenmite from its solubility data in NaOH solutions: Bulletin of the Chemical Society of Japan, v. 54, p. 2579-2582.
- Charlu, T.V., Newton, R.C., and Kleppa, O.J., 1975, Enthalpies of formation at 970 K of compounds in the system MgO-Al₂O₃-SiO₂ from high temperature solution calorimetry: Geochimica et Cosmochimica Acta, v. 39, p. 1487-1497.
- Charlu, T.V., Newton, R.C., and Kleppa, O.J., 1978, Enthalpy of formation of some lime silicates by high-temperature solution calorimetry, with discussion of high pressure phase equilibria: Geochimica et Cosmochimica Acta, v. 42, p. 367-375.
- Chase, Malcolm W., Jr., Curnutt, J.L., McDonald, R.A., Syverud, A.N., 1978, JANAF Thermochemical Tables, 1978 Supplement: Journal of Physical and Chemical Reference Data, v. 7, p. 793-940 (data for 1977, 1978, and 1979 issued separately in looseleaf format by Dow Chemical Company, 1707 Building, Midland, Michigan).
- Chatterjee, N.D., 1971, Preliminary results on the synthesis and upper stability limit of margarite: Naturwissenschaften, v. 58, p. 147.
- Chatterjee, N.D., 1974, Synthesis and upper thermal stability limit of 2M-margarite, CaAl₂[Al₂Si₂O₁₀/(OH)₂]: Schweizerische Mineralogische und Petrographische Mitteilungen, v. 54(2/3), p. 753-767.
- Chernosky, Joseph V., Jr., 1976, The stability of anthophyllite--A

- reevaluation based on new experimental data: *American Mineralogist*, v. 61, p. 1145-1155.
- Chernosky, Joseph V., Jr., 1982, The stability of clinochrysotile: *American Mineralogist* (in press).
- Chernosky, Joseph V., Jr., unpublished data.
- Chernosky, Joseph V., Jr., and Autio, Laurie Knapp, 1979, The stability of anthophyllite in the presence of quartz: *American Mineralogist*, v. 64, p. 294-303.
- *Chou, I-Ming, 1978, Calibration of oxygen buffers at elevated P and T using the hydrogen fugacity sensor: *American Mineralogist*, v. 63, p. 690-703.
- Christescu, S., 1931, Diss. Berlin: in Wagner, Hubert, 1932, Zur thermochemie der metasilikate des calciums und magnesiums und des diopsids: *Zeitschrift fur Anorganische und Allgemeine Chemie*, Band 208, Heft 1, p. 1-22.
- *Clark, Sydney P., Jr., Robertson, Eugene C., and Birch, Francis, 1957, Experimental determination of kyanite-sillimanite equilibrium relations at high temperatures and pressures: *American Journal of Science*, v. 25b, p. 628-640.
- CODATA Task Group on Key Values for Thermodynamics, 1978, CODATA recommended key values for thermodynamics 1977: *CODATA Bull.*, v. 28, p. 1-16.
- Cohen, L.H., and Klement, W., Jr., 1967, High-low quartz inversion: determination to 35 kilobars: *Journal of Geophysical Research*, v. 72, p. 4245.

- Comite International des Poids et Measures, (1969), The international practical temperature scale of 1968: *Metrologia*, v. 5, p. 35-44.
- Commission on Atomic Weights, International Union of Pure and Applied Chemistry, 1976, Atomic weights of the elements 1975: *Pure and Applied Chemistry*, v. 47, p. 75-95.
- Coughlin, J.P., King, E.G., and Bonnicksen, K.R., 1951, High-temperature heat contents of ferrous oxide, magnetite and ferric oxide: *Journal of the American Chemical Society*, v. 73, p. 3891-3893.
- Coughlin, J.P., and O'Brien, C.J., 1957, High temperature heat contents of calcium orthosilicate: *Journal of Physical Chemistry*, v. 61, p. 767-769.
- Cristescu, Silvia, and Simon, Franz, 1934, Die spezifischen wärmen von beryllium, germanium und hafnium bei tiefen temperaturen: *Zeitschrift für Physikalische Chemie*, v. 25, p. 273-282.
- d'Amour, H., Schiferl, D., Denner, W., Schulz, Heinz, and Holzappel, W.B., 1978, High-pressure single-crystal structure determinations for ruby up to 90 kbar using an automatic diffractometer: *Journal of Applied Physics*, v. 49, p. 4411-4416.
- Darken, L.S., and Gurry, R.W., 1945, The system iron-oxygen. I. The wüstite field and related equilibria: *Journal of the American Chemical Society*, v. 67, p. 1398-1412.
- Darken, L.S., and Gurry, R.W., 1946, The system iron-oxygen. II. Equilibrium and thermodynamics of liquid oxide and other phases: *Journal of the American Chemical Society*, v. 68, p. 798-816.

- *Devereux, O.F., 1978, Discussion of standard free energy of formation of alumina by D. Ghosh and D.A.R. Kay: *Journal of the Electrochemical Society*, v. 125, p. 890-891.
- Douglas, Audrey M.B., 1952, X-ray investigation of bredigite: *Mineralogical Magazine*, v. 29, p. 875-884.
- Edgar, Alan D., 1973, *Experimental Petrology - Basic Principles and Techniques*: Oxford University Press, New York, 217 p.
- Emmett, P.H., and Shultz, J.F., 1933, Gaseous thermal diffusion - the principal cause of discrepancies among equilibrium measurements on the systems $\text{Fe}_3\text{O}_4\text{-H}_2\text{-Fe-H}_2\text{O}$, $\text{Fe}_3\text{O}_4\text{-H}_2\text{-FeO-H}_2\text{O}$ and $\text{FeO-H}_2\text{-Fe-H}_2\text{O}$: *Journal of the American Chemical Society*, v. 55, p. 1376-1389.
- Essene, Eric, 1974, High-pressure transformations in CaSiO_3 : *Contributions to Mineralogy and Petrology*, v. 45, p. 247-250.
- Evans, Bernard W., Johannes, W., and Trommsdorff, Volkmar, 1976, Stability of chrysotile and antigorite in the serpentinite multisystem: *Schweizerische Mineralogische und Petrographische Mitteilungen*, v. 56, p. 79-93.
- Evans, Howard, 1977, unpublished data.
- Ferrier, A., 1969, Enthalpy of synthetic anorthite between 298 and 1950 K: *Comptes Rendus de l'Academie des Sciences (Paris)*, v. 269C, p. 951-954.
- *Ferrier, A., 1971, Etude experimentale de l'enthalpie de cristallisation du diopside et de l'anorthite synthetiques: *Revue Internationale des Hautes Temperatures et des Refractaires*, v. 8, p.

31-36.

- Finger, Larry W., and Hazen, Robert M., 1978, Crystal structure and compression of ruby to 46 kbar: *Journal of Applied Physics*, v. 49, p. 5823-5826.
- Fisher, J.R., and Zen, E-an, 1971, Thermochemical calculations from hydrothermal phase equilibrium data and the free energy of H₂O: *American Journal of Science*, v. 270, p. 297-314.
- Fyfe, W.S., 1958, A further attempt to determine the vapor pressure of brucite: *American Journal of Science*, v. 256, p. 729-732.
- Fyfe, W.S., and Godwin, L.H., 1962, Further studies on the approach to equilibrium in the simple hydrate systems, MgO-H₂O and Al₂O₃-H₂O: *American Journal of Science*, v. 260, p. 289-293.
- Gasparik, T., 1981, Mixing properties of the binary Jd-CaTe: EOS, *Transactions of the American Geophysical Union*, v. 62, p. 412.
- *Ghosh, D., and Kay, D.A.R., 1977, Standard free energy of formation of alumina: *Journal of the Electrochemical Society*, v. 124, p. 1836-1845.
- *Ghosh, D., and Kay, D.A.R., 1978, Reply to Discussion by H. Byker and R.A. Howald of Standard free energy of formation of alumina: *Journal of the Electrochemical Society*, v. 125, p. 890.
- *Ghosh, D., and Kay, D.A.R., 1978, Reply to Discussion by O.F. Devereux of Standard free energy of formation of alumina: *Journal of the Electrochemical Society*, v. 125, p. 891.
- Giauque, W.F., and Archibald, R.C., 1937, The entropy of water from the Third Law of Thermodynamics. The dissociation pressure and

- calorimetric heat of the reaction $\text{Mg(OH)}_2 = \text{MgO} + \text{H}_2\text{O}$. The heat capacities of Mg(OH)_2 and MgO from 20 to 300 K: *Journal of the American Chemical Society*, v. 59, p. 561-569.
- Giddings, Robert Arthur, 1972, Effect of electronic conductivity on coulometric titration in solid oxide galvanic cells: Ph.D. thesis, University of Utah, 184 p.
- *Goldsmith, Julian R., 1980, The melting and breakdown reactions of anorthite at high pressures and temperatures: *American Mineralogist*, v. 65, p. 272-284.
- Goldsmith, Julian R., and Newton, Robert C., 1969, P-T-X relations in the system $\text{CaCO}_3\text{-MgCO}_3$ at high temperatures and pressures: *American Journal of Science*, v. 267-A, p. 160-190.
- Goldsmith, Julian R., and Newton, Robert C., 1977, Scapolite-plagioclase stability relations at high pressures and temperatures in the system $\text{NaAlSi}_3\text{O}_8\text{-CaAl}_2\text{Si}_2\text{O}_8\text{-CaCO}_3\text{-CaSO}_4$: *American Mineralogist*, v. 62, p. 1063-1081.
- *Good, W.D., Lacina, J.L., DePrater, B.L., and McCullough, J.P., 1964, A new approach to the combustion calorimetry of silicon and organosilicon compounds. Heats of formation of quartz, fluorosilicic acid, and hexamethyldisiloxane: *Journal of Physical Chemistry*, v. 68, p. 579-586.
- Grain, Clark F., and Campbell, William J., 1962, Thermal expansion and phase inversion of six refractory oxides: Bureau of Mines, Report of Investigations 5982, 21 p.
- Greenwood, H.J., 1963, The synthesis and stability of anthophyllite:

- Journal of Petrology, v. 4, p. 317-351.
- Gronow, H.E., and Schwiete, H.E., 1933, Die spezifischen warmen CaO, Al₂O₃, CaO·Al₂O₃, 3CaO·Al₂O₃, 2CaO·Al₂O₃·SiO₂ von 20° bis 1500°C: Zeitschrift für Anorganische und Allgemeine Chemie, v. 216, p. 185-195.
- 216, p. 185-195.
- Grønvold, Fredrik, and Samuelsen, E.J., 1975, Heat capacity and thermodynamic properties of alpha-Fe₂O₃ in the region 300-1050 K. Antiferromagnetic transition: Journal of Journal of Physics and Chemistry of Solids, v. 36, p. 249-256.
- Grønvold, Fredrik, and Sveen, Arvid, 1974, Heat capacity and thermodynamic properties of synthetic magnetite (Fe₃O₄) from 300 to 1050 K. Ferrimagnetic transition and zero-point entropy: Journal of Chemical Thermodynamics, v. 6, p. 859-872.
- Grønvold, Fredrik, and Westrum, Edgar F., Jr., 1959, Alpha-ferric oxide: low temperature heat capacity and thermodynamic functions: Journal of Physical Chemistry, v. 81, p. 1780-1783.
- Grundy, H.D., and Brown, W.L., 1974, High-temperature x-ray study of low and high plagioclase feldspars: Feldspars, Proceedings of the NATO Advanced Study Institute, 2nd, 1972, p. 162-173.
- Gupta, Alok K., and Chatterjee, Niranjana D., 1978, Synthesis, composition, thermal stability, and thermodynamic properties of bicchulite, Ca₂[Al₂SiO₆](OH)₂: American Mineralogist, v. 63, p. 58-65.

- Guven, N., 1972, Electron optical observations on Marblehead illite: *Clays and Clay Minerals*, v. 20(2), p. 83-88.
- Haar, Lester, Gallagher, John, and Kell, G.S., 1979, Thermodynamic properties for fluid water: *Water and Steam - Their Properties and Current Industrial Applications*, Proceedings of the 9th International Conference on the Properties of Steam, p. 69-82.
- Haar, Lester, Gallagher, John, and Kell, G.S., 1981, The anatomy of the thermodynamic surface of water: the formulation and comparisons with data: *Proceedings of the 8th Symposium on Thermophysical Properties*, p. 298.
- Haas, Herbert, 1972, Diaspore-corundum equilibrium determined by epitaxis of diaspore on corundum: *American Mineralogist*, v. 57, p. 1375-1385.
- Haas, Herbert, and Holdaway, M.J., 1973, Equilibria in the system $Al_2O_3-SiO_2-H_2O$ involving the stability limits of pyrophyllite, and thermodynamic data of pyrophyllite: *American Journal of Science*, v. 273, p. 449-464.
- Haas, J.L., Jr., 1974, PHAS20, A program for simultaneous multiple regression of a mathematical model to thermochemical data: U.S. Dept. Commerce, National Technical Information Service, AD-780 301, 162 p.
- Haas, J.L., Jr., and Fisher, J.R., 1976, Simultaneous evaluation and correlation of thermodynamic data: *American Journal of Science*, v. 276, p. 525-545.
- Haas, J.L., Robinson, G.R., and Hemingway, B.S., 1980, Thermodynamic

- tabulations for selected phases in the system CaO-Al₂O₃-SiO₂-H₂O:
U.S. Geological Survey, Open-File Report 80-908, 135 p.
- Haas, John L., Jr., Robinson, Gilpin R., Jr., and Hemingway, Bruce S.,
1981, Thermodynamic tabulations for selected phases in the system
CaO-Al₂O₃-SiO₂-H₂O at 101.325 kPa (1 atm) between 273.15 and
1800 K: Journal of Physical and Chemical Reference Data, v. 10,
p. 575-669.
- Hanley, E.J., DeWitt, D.P., and Taylor, R.E., 1977, The thermal
transport properties at normal and elevated temperature of eight
representative rocks: Proceedings of the 7th Symposium on
Thermophysical Properties, American Society of Mechanical
Engineers, p. 386-391.
- *Hariya, Yu, and Arima, Makoto, 1975, Kyanite-sillimanite transition
with excess quartz and corundum: Journal of the Faculty of Science,
Hokkaido University, Series IV, v. 16, p. 357-365.
- Harker, R.I., and Tuttle, O.F., 1955, Studies in the system CaO-MgO-
CO₂, Part I. The thermal dissociation of calcite, dolomite, and
magnesite: American Journal of Science, v. 253, p. 209-224.
- Haselton, H.T., 1982, unpublished data.
- *Haselton, H.T., Jr., Sharp, W.E., and Newton, R.C., 1978, CO₂
fugacity at high temperatures and pressures from experimental
decarbonation reactions: Geophysical Research Letters, v. 5, p.
753-756.
- Haselton, H.T., Jr., and Westrum, E.F., Jr., 1979, Heat capacities
(5-350 K) of synthetic pyrope, grossular, and pyrope₆₀grossular₄₀:

- EOS, Transactions of the American Geophysical Union, v. 60, p. 405.
- Haselton, H.T., Jr., and Westrum, E.F., Jr., 1980, Low-temperature heat capacities of synthetic pyrope, grossular, and pyrope₆₀grossular₄₀: *Geochimica et Cosmochimica Acta*, v. 44, p. 701-709.
- Hays, James Fred, 1966, Lime-alumina-silica: Year Book - Carnegie Institution of Washington, v. 65, p. 234-239.
- Hazen, Robert M., 1976a, Effects of temperature and pressure on the cell dimension and x-ray temperature factors of periclase: *American Mineralogist*, v. 61, p. 260-271.
- Hazen, Robert M., 1976b, Effects of temperature and pressure on the crystal structure of forsterite: *American Mineralogist*, v. 61, p. 1280-1293.
- Hazen, Robert M., 1977, Effects of temperature and pressure on the crystal structure of ferromagnesian olivine: *American Mineralogist*, v. 62, p. 286-295.
- Hazen, Robert M., and Finger, Larry W., 1978, Crystal structures and compressibilities of pyrope and grossular to 60 kbar: *American Mineralogist*, v. 63, p. 297-303.
- Hazen, R.M., and Finger, L.W., 1980, Crystal structure of forsterite at 40 kbar: Year Book - Carnegie Institute of Washington, v. 1979, p. 364-367.
- Hazen, R.M., Mao, H.K., Finger, L.W., and Bell, P.M., 1981, Irreversible unit-cell volume changes of wüstite single crystals quenched from high pressure: Year Book - Carnegie Institute of Washington, v. 1980, p. 274-277.

- Helgeson, H.C., Delany, J.M., Nesbitt, H.W., and Bird, D.K., 1978, Summary and critique of the thermodynamic properties of rock-forming minerals: *American Journal of Science*, v. 278-A, p. 1-229.
- Hemingway, B.S., Krupka, K.M., and Robie, R.A., 1981, Heat capacities of the alkali feldspars between 350 and 1000 K from differential scanning calorimetry, the thermodynamic functions of the alkali feldspars from 298 to 1400 K, and the reaction of quartz + jadeite = analbite: *American Mineralogist*, v. 66, p. 1202-1245.
- Hemingway, B.S., and Robie, R.A., 1977, Enthalpies of formation of low albite ($\text{NaAlSi}_3\text{O}_8$), gibbsite ($\text{Al}(\text{OH})_3$), and NaAlO_2 ; revised values for $\Delta H^\circ_{f,298}$ and $\Delta G^\circ_{f,298}$ of some aluminosilicate minerals: *U.S. Geological Survey Journal of Research*, v. 5(4), p. 413-429.
- Hemingway, Bruce S., and Robie, Richard A., 1978, Revised values for the Gibbs free energy of formation of $[\text{Al}(\text{OH})_4(-)](\text{aq})$, diaspore, boehmite and bayerite at 298.15 K and 1 bar, the thermodynamic properties of kaolinite to 800 K and 1 bar, and the heats of solution of several gibbsite samples: *Geochimica et Cosmochimica Acta*, v. 42, p. 1533-1543.
- Hemingway, B.S., Robie, R.A., Fisher, J.R., and Wilson, W.H., 1977, The heat capacities of gibbsite, $\text{Al}(\text{OH})_3$, between 13 and 480 K and magnesite, MgCO_3 , between 13 and 380 and their standard entropies at 298.15 K: *U.S. Geological Survey Journal of Research*, v. 5, p. 797-806.

Hemingway, B.S., Robie, R.A., and Kittrick, J.A., 1978, Revised values for the Gibbs free energy of formation of $[Al(OH)_4]_{aq}$, diaspore, boehmite, and bayerite at 298.15 K and 1 bar, the thermodynamic properties of kaolinite to 800 K and 1 bar, and the heats of solution of several gibbsite samples: *Geochimica et Cosmochimica Acta*, v. 42, p. 1533-1543.

Hemley, J.J., Montoya, J.W., Christ, C.L., and Hostetler, P.B., 1977a, Mineral equilibria in the $MgO-SiO_2-H_2O$ system: I. Talc-chrysotile-forsterite-brucite stability relations: *American Journal of Science*, v. 277, p. 322-351.

Hemley, J.J., Montoya, J.W., Marinenko, J.W., and Luce, R.W., 1977b, Mineral equilibria in the system $Al_2O_3-SiO_2-H_2O$: II. Talc-antigorite-forsterite-anthophyllite-enstatite stability relations and some geologic implications in the system: *American Journal of Science*, v. 277, p. 353-383.

Hemley, J.J., Montoya, J.W., Marinenko, J.W., and Luce, R.W., 1980, Equilibria in the system $Al_2O_3-SiO_2-H_2O$ and some general implications for alteration/mineralization processes: *Economic Geology*, v. 75, p. 210-228.

Hewitt, David A., 1978, A redetermination of the fayalite-magnetite-quartz equilibrium between 650° and 850°C: *American Journal of Science*, v. 278, p. 715-724.

Holdaway, M.J., 1971, Stability of andalusite and the aluminum silicate phase diagram: *American Journal of Science*, v. 271, p. 97-131.

- *Holm, J.L., and Kleppa, O.J., 1966, The thermodynamic properties of the aluminum silicates: *American Mineralogist*, v. 51, p. 1608-1622.
- Huang, Wu-Liang, and Wyllie, Peter J., 1975, Melting and subsolidus phase relationships for CaSiO_3 to 35 kilobars pressure: *American Mineralogist*, v. 60, p. 213-217.
- *Huber, Elmer J., Jr., and Holley, Charles E., Jr., 1956, The heat of combustion of calcium: *Journal of Physical Chemistry*, v. 60, p. 498-499.
- Huckenholz, Hans Gerald, 1974, The grossularite relations in the $\text{CaO-Al}_2\text{O}_3\text{-SiO}_2\text{-H}_2\text{O}$ system: *Year Book - Carnegie Institution of Washington*, v. 73, p. 411-426.
- Huckenholz, H.G., 1977, Gehlenite stability relations in the join $\text{Ca}_2\text{Al}_2\text{SiO}_7\text{-H}_2\text{O}$ up to 10 kbar: *Neues Jahrbuch fur Mineralogie, Abhandlungen*, v. 130, p. 169-186.
- Hultgren, Ralph; Desai, Pramod D.; Hawkins, Donald T.; Gleiser, Molly; Kelley, Kenneth K., and Wagman, Donald D., 1973, Selected values of the thermodynamic properties for the elements: *Metals Park, Ohio, American Society for Metals*, 636 p.
- *Humphrey, G.L., King, E.G., and Kelley, K.K., 1952, Some thermodynamic values for ferrous oxide: *Bureau of Mines, Report of Investigations 4870*, 16 p.
- Irving, Anthony J., and Wyllie, Peter J., 1975, Subsolidus and melting relationships for calcite, magnesite and the join $\text{CaCO}_3\text{-MgCO}_3$ to 36 kb: *Geochimica et Cosmochimica Acta*, v. 39, p. 35-53.
- Jacobs, Gary K., and Kerrick, Derrill M., 1981, APL and Fortran

- programs for a new equation of state for H_2O , CO_2 and their mixtures at supercritical conditions: Computers and Geosciences, v. 7, p. 131-143.
- Jacobs, Gary K., Kerrick, Derrill M., and Krupka, Kenneth M., 1981, The high-temperature heat capacity of natural calcite ($CaCO_3$): Physics and Chemistry of Minerals, v. 7, p. 55-59.
- Jay, A.H., 1933, The thermal expansion of quartz by x-ray measurements: Proceedings of the Royal Society of London, Series A, v. 142, p. 237-247.
- Johannes, W., 1968, Experimental investigation of the reaction forsterite + H_2O = serpentine + brucite: Contributions to Mineralogy and Petrology, v. 19, p. 309-315.
- Johannes, W., 1969, An experimental investigation of the system $MgO-SiO_2-H_2O-CO_2$: American Journal of Science, v. 267, p. 1083-1104.
- Jonannes, W., and Metz, P., 1968, Experimentelle bestimmungen von gleichgewichtsbeziehungen im system $MgO-CO_2-H_2O$: Neues Jahrbuch fur Mineralogie, Monatshefte, p. 15-26.
- Johannes, W., and Puhon, D., 1971, The calcite-aragonite transition, reinvestigated: Contributions to Mineralogy and Petrology, v. 31, p. 28-38.
- *Johannson, O.K., and Thorvaldson, T., 1934, Studies of the thermochemistry of the compounds occurring in the system $CaO-Al_2O_3-SiO_2$. V. The heats of formation of tricalcium silicate and dicalcium silicate: Journal of the American Chemical Society, v. 56, p. 2327-2330.

- Johnson, W., and Andrews, K.W., 1956, An x-ray study of the inversion and thermal expansion of cristobalite: Transactions of the British Ceramic Society, v. 55, p. 227-236.
- *Juan, Veichow C., Youh, Chang-Ching, and Lo, Huann-Jih, 1967, The stability field of prehnite: Proceedings of the Geological Society of China, no. 10, p. 53-63.
- *Juan, Veichow C., and Lo, Huann-Jih, 1975, Syntheses of boehmite and margarite and their bearing on the formation of some aluminous deposits: Acta Geologica Taiwanica, no. 13, p. 1-8.
- Kay, D.A.R., and Taylor, J., 1960, Activities of silica in the lime + alumina + silica system: Faraday Society Transactions, v. 56, p. 1372-1386.
- Kelley, K.K., 1943, Specific heats at low temperature of magnesium orthosilicate and magnesium metasilicate: Journal of the American Chemical Society, v. 65, p. 339-341.
- Kelley, K.K., 1960, Contributions to the data on theoretical metallurgy. XIII. High-temperature heat-content, heat-capacity, and entropy data for the elements and inorganic compounds: U.S. Bureau of Mines Bulletin 584, 232 p.
- Kelley, K.K., Barany, R., King, E.G., and Christensen, A.V., 1959, Some thermodynamic properties of fluorphlogopite mica: U.S. Bureau of Mines, Report of Investigations 5436, 16 p.
- Kelley, K.K.; Todd, S.S.; Orr, R.L.; King, E.G.; and Bonnicksen, K.R., 1953, Thermodynamic properties of sodium-aluminum and potassium-aluminum silicates: U.S. Bureau of Mines, Report of Investiga-

tions 4955, 21 p.

Kennedy, George C., 1956, The brucite-periclase equilibrium: *American Journal of Science*, v. 254, p. 567-573.

*Kerrick, Derrill M., 1968, Experiments on the upper stability limit of pyrophyllite at 1.8 kilobars and 3.9 kilobars water pressure: *American Journal of Science*, v. 266, p. 204-214.

*Khitarov, N.I., Putin, V.A., Chao, Pin, and Slutskii, A.B., 1963, Relations between andalusite, kyanite, and sillimanite at moderate temperatures and pressures; *Geochemistry International*, no. 3, p. 235-238.

*Kilday, Marthada V., and Prosen, Edward J., 1973, The enthalpy of solution of low quartz (alpha-quartz) in aqueous hydrofluoric acid: *Journal of Research of the National Bureau of Standards*, v. 77A, p. 205-215.

King, E.G., 1951, Heats of formation of crystalline calcium orthosilicate, tricalcium silicate and zinc orthosilicate: *Journal of the American Chemical Society*, v. 73, p. 656-658.

King, E.G., 1955, Low-temperature heat capacity and entropy at 298.16 K of analcite: *Journal of the American Chemical Society*, v. 77, p. 2192-2193.

King, E.G., 1957, Low temperature heat capacities and entropies at 298.15°K of some crystalline silicates containing calcium: *Journal of the American Chemical Society*, v. 79, p. 5437-5438.

King, E.G., Barany, R., Weller, W.A., and Pankratz, L.B., 1967, The thermodynamic properties of forsterite and serpentine: U.S.

- Bureau of Mines, Report of Investigations 6962, 19 p.
- King, E.G., Ferrante, M.J., and Pankratz, L.B., 1975, Thermodynamic data for $Mg(OH)_2$ (brucite): U.S. Bureau of Mines, Report of Investigations 8041, 13 p.
- King, E.G., and Weller, W.W., 1961a, Low-temperature heat capacities and entropies at 298.15°K of diaspore, kaolinite, dickite, and halloysite: U.S. Bureau of Mines, Report of Investigations 5810, 6 p.
- King, E.G., and Weller, W.W., 1961b, Low-temperature heat capacities and entropies at 298.15°K of some sodium- and calcium-aluminum silicates: U.S. Bureau of Mines, Report of Investigation 5855, 8 p.
- Kiseleva, I.A.; Ogorodova, L.P.; Topor, N.D., and Chigareva, O.G., 1979, A thermochemical study of the CaO-MgO-SiO₂ system: *Geochemistry International*, v. 16, p. 122-134.
- Kiseleva, I.A.; Ogorodova, L.P.; Topor, N.D.; and Chigareva, O.G., 1981, Experimental determination of the heats of formation of forsterite and clinoenstatite: *Moscow University Geology Bulletin*, v. 36, p. 28-36.
- *Kiseleva, I.A., and Topor, N.D., 1973, On the thermodynamic properties of zoisite: *Geokhimiia*, no. 10, p. 1547-1555.
- Kiseleva, I.A., Topor, N.D., and Andreyenko, E.D., 1974, Thermodynamic parameters of minerals of the epidote group: *Geochemistry International*, v. 11(2), p. 389-398 (Russian original is: *Geokhimiia*, v. 4, p. 543-553).

- *Kitayama, Kenzo, and Katsura, Takashi, 1968, Composition of fayalite and its standard free energy of formation: Bulletin of the Chemical Society of Japan, v. 41, p. 525-528.
- *Kittrick, J.A., 1966, Free energy of formation of kaolinite from solubility measurements: American Mineralogist, v. 51, p. 1457-1466.
- *Ko, H.C., Ahmad, N., and Chang, Y.A., 1982, Thermodynamics of calcination of calcite: U.S. Bureau of Mines, Report of Investigations 8647, 9 p.
- Ko, H.C., Ferrante, M.J., and Stuve, J.M., 1977, Thermophysical properties of acmite: Proceedings of the 7th Symposium on Thermophysical Properties, American Society of Mechanical Engineers, p. 392-395.
- *Koehler, M.F., Barany, Ronald, and Kelley, K.K., 1961, Heats and free energies of formation of ferrites and aluminates of calcium, magnesium, sodium, and lithium: U.S. Bureau of Mines, Report of Investigations 5711, 14 p.
- Komarov, V.F., Uleinikov, N.N., and Tret-yakov, Yu. D., 1967, Thermodynamic properties of solid solutions based on hematite in an iron-oxygen system: Izvestiia Akademii Nauk SSSR, Neorganicheskie Materialy, v. 3, p. 1064-1072.
- Koster van Groos, A.F., and ter Heege, J.P., 1973, The high-low quartz transition up to 10 kilobars pressure: Journal of Geology, v. 81, p. 717-724.
- Kozu, Shikusuke, and Kani, Ko-ichi, 1934, Thermal expansion of

- aragonite and its atomic displacements by transformation into calcite between 450°C and 490°C in air, I: Proceedings of the Imperial Academy, v. 10, p. 222-225.
- Kozu, Shukusuke, and Ueda, Junichi, 1933, Thermal expansion of plagioclase: Proceedings of the Imperial Academy of Japan, v. 9, p. 262-264.
- Kracek, F.C., and Neuvonen, K.J., 1952, Thermochemistry of plagioclase and alkali feldspars: American Journal of Science, Bowen Volume, p. 293-318.
- Kracek, F.C., Neuvonen, K.J., and Burley, Gordon, 1953, Thermochemical properties of minerals: Carnegie Institution of Washington, Year Book No. 52, p. 69-75.
- Krishnan, R.S., Srinivasan, R., and Devanarayanan, S., 1979, Thermal Expansion of Crystals: Pergamon Press, New York, 305 p.
- Krupka, Kenneth M., 1982, Ph.D. Thesis, The Pennsylvania State University, unpublished data.
- Krupka, Kenneth M., Kerrick, Derrill M., and Robie, Richard A., 1977, High-temperature heat capacities of dolomite, talc, and tremolite, and implications to equilibrium in the siliceous dolomite system: Geological Society of America, Abstracts with Programs, p. 1060.
- Krupka, K.M., Kerrick, D.M., and Robie, R.A., 1980, Heat capacities from 5 to 1000 K for natural diopside, wollastonite, and orthoenstatite: EOS, Transactions of the American Geophysical Union, v. 61, p. 407.

- Krupka, K.M., Robie, R.A., and Hemingway, B.S., 1979, High-temperature heat capacities of corundum, periclase, anorthite, $\text{CaAl}_2\text{Si}_2\text{O}_8$ glass, muscovite, pyrophyllite, KAlSi_3O_8 grossular, and $\text{NaAlSi}_3\text{O}_8$ glass: *American Mineralogist*, v. 64, p. 86-101.
- Kunze, Gunther, 1961, Antigorit, strukturtheoretische grundlager und ihre praktische bedeutung fur die weitere serpentinforschung: *Fortschritte der Mineralogie*, v. 39, p. 206-324.
- Kurepin, V.A., 1975, Activity of components, thermodynamical characteristics of reactions, and phase equilibriums in the iron-oxygen system at high temperatures and pressures: *Geokhimiia*, no. 10, p. 1475-1483.
- *Kuskov, O.L., 1973, The thermodynamic constants of pyrophyllite and the anomalous specific heats of metapyrophyllite and metakaolin: *Geochemistry International*, v. 10, p. 406-412.
- *Kuskov, O.L., and Khitarov, N.I., 1969, Thermodynamic constants of kaolinite and kinetic parameters of kaolinite dehydration: *Geochemistry International*, v. 6, p. 1147-1151.
- Lebedev, B.G., and Levitskii, V.A., 1962, Equilibrium of the reaction of iron orthosilicate with carbon monoxide at 850-1150°: *Zhurnal Fizicheskoi Khimii*, v. 36, p. 630-632.
- *Leonidov, V. Ya., Barskii, Yu. P., and Khitarov, N.I., 1964, Determination of the heat capacity of kaynite and quartz at high temperatures by the method of thermal analysis: *Geokhimiia*, no. 5, p. 414-419.
- *Leonidov, V. Ya., Barskii, Yu. P., and Khitarov, N.I., 1966, Deter-

- mination of specific heats of quartz, kyanite, and granite at high temperatures: *Issledovanie Prirodnogo i Tekhnicheskogo Mineralo-obrazovaniia, po Materialam Soveshchaniia po Eksperimental'noi i Tekhnicheskoi Mineralogii i Petrografii*, 7th, Lvov 1964, p. 301-306.
- Lewis, G.K., Jr., and Drickamer, H.G., 1966, Effect of high pressure on the lattice parameters of Cr_2O_3 and $\alpha\text{-Fe}_2\text{O}_3$: *The Journal of Chemical Physics*, v. 45, p. 224-226.
- Liou, J.G., 1971, Synthesis and stability relations of prehnite, $\text{Ca}_2\text{Al}_2\text{Si}_3\text{O}_{10}(\text{OH})_2$: *American Mineralogist*, v. 56, p. 507-531.
- Lohberg, Karl, and Stannek, W., 1975, Thermodynamic description of the wustite phase within its range of existence: *Berichte der Bunsengesellschaft fur Physikalische Chemie*, v. 79, p. 244-255.
- *Lyon, D.N., and Giauque, W.F., 1949, Magnetism and third law of thermodynamics. Magnetic properties of ferrous sulfate heptohydrate from 1 to 20 K. Heat capacity from 1 to 310 K: *American Chemical Society Journal*, v. 71, p. 1647-1656.
- *Mah, Alla D., 1957, Heats of formation of alumina, molybdenum trioxide and molybdenum dioxide: *Journal of Physical Chemistry*, v. 61, p. 1572-1573.
- Marc, R., and Simek, A., 1913, Über die thermische dissoziation des magnesiumkarbonats: *Zeitschrift fur Anorganische Chemie*, v. 82, p. 17-49.
- *Matsushima, Shoyo, Kennedy, George C., Akella, Jagannadham, and Haygarth, John, 1967, A study of equilibrium relations in the systems $\text{Al}_2\text{O}_3\text{-SiO}_2\text{-H}_2\text{O}$ and $\text{Al}_2\text{O}_3\text{-H}_2\text{O}$: *American Journal of Science*,

v. 265, p. 28-44.

McCullough, J.P., and Scott, D.W., 1968, *Experimental Thermodynamics*, Vol. 1, *Calorimetry of Non-Reacting Systems*: Plenum Press, New York, 606 p.

McNaughton, J.L., and Mortimer, C.T., 1975, *Differential scanning calorimetry*: *International Review of Science, Physical Chemistry Series 2*, v. 10, p. 176-195.

Meagher, E.P., 1975, The crystal structures of pyrope and grossularite at elevated temperatures: *American Mineralogist*, v. 60, p. 218-228.

Megaw, Helen D., 1933, The thermal expansions of certain crystals with layer lattices: *Proceedings of the Royal Society of London*, v. A142, p. 198-214.

Merrill, Leo, and Bassett, W.A., 1975, Crystal structure of calcium carbonate(II), a high-pressure metastable phase of calcium carbonate: *Acta Crystallography, Section B*, v. B31, p. 343-349.

Meyer, J., 1981, unpublished data.

Mirwald, P.W., 1979, Determination of a high-temperature transition of calcite at 800°C and one bar CO₂ pressure: *Neues Jahrbuch für Mineralogie, Monatshefte*, no. 7, p. 309-315.

Mukaibo, T., Takahashi, Y., and Yamada, K., 1969, The heat capacity and the heat of dehydration of the hydrated aluminas: *Proceedings of the First International Conference on Calorimetry and Thermodynamics*, Warsaw, p. 375-380.

Myers, C.W., Price, S.M., Caggiano, J.A., Cochran, M.P., et al., 1979,

- Geologic studies of the Columbia Plateau, a status report: U.S. Department of Commerce, National Technical Information Service, RHO-BWI-ST-4.
- Nacken, R., 1930, Ueber die bestimmung der bildungswarmen von silikaten aus ihren oxyden: Zement, v. 19, p. 818-825 and p. 847-849.
- *Navrotsky, A., Newton, R.C., and Kleppa, O.J., 1973, Sillimanite - disordering enthalpy by calorimetry: Geochimica et Cosmochimica Acta, v. 37, p. 2497-2508.
- Navrotsky, Alexandra, Pintchovski, Faivel S., and Akimoto, Syun-iti, 1979, Calorimetric study of the stability of high pressure phases in the systems CoO-SiO_2 and " FeO "- SiO_2 , and calculation of phase diagrams in MO-SiO_2 systems: Physics of the Earth and Planetary Interiors, v. 19, p. 275-292.
- Naylor, B.F., 1945, High-temperature heat contents of sodium metasilicate and sodium disilicate: Journal of the American Chemical Society, v. 67, p. 466.
- *Neuvonen, K.J., 1952, Thermochemical investigation of the akermanite-gehlenite series: Bulletin de la Commission Geologique de Finlande, v. 158, 57 p.
- *Newman, Edwin S., 1959, Heat of formation of potassium calcium silicate: Journal of Research of the National Bureau of Standards, Research Paper 2955, v. 62, p. 207-211.
- Newton, R.C., 1965, The thermal stability of zoisite: Journal of Geology, v. 73(3), p. 431-441.

- Newton, R.C., 1966a, Kyanite-andalusite equilibrium from 700° to 800°C: *Science*, v. 153, p. 170-172.
- Newton, R.C., 1966b, Some calc-silicate equilibrium relations: *American Journal of Science*, v. 264, p. 204-222.
- *Newton, R.C., Charlu, T.V., and Kleppa, O.J., 1977, Thermochemistry of high pressure garnets and clinopyroxenes in the system CaO-MgO-Al₂O₃-SiO₂: *Geochimica et Cosmochimica Acta*, v. 41, p. 369-377.
- *Newton, R.C., Charlu, T.V., and Kleppa, O.J., 1980, Thermochemistry of the high structural state plagioclases: *Geochimica et Cosmochimica Acta*, v. 44, p. 933-941.
- *Newton, Robert C., and Kennedy, G.C., 1963, Some equilibrium reactions in the join CaAl₂Si₂O-H₂O: *Journal of Geophysical Research*, v. 68, p. 2967-2983.
- *Nitsch, K.-H., and Winkler, H.G.F., 1965, Bildungsbedingungen von epidot und orthozoisit: *Contributions to Mineralogy and Petrology*, v. 11, p. 470-486.
- Norton, F.J., 1955, Dissociation pressures of iron and copper oxides: General Electric Research Laboratory, Report 55-RL-1248, Schenectady, N.Y., 16 p.
- Olinger, Bart, and Halleck, P.M., 1974, Redetermination of the relative compressions of the cell edges of olivine: *Journal of Geophysical Research*, v. 79, p. 5535-5536.
- Olinger, Bart, and Halleck, P.M., 1976, The compression of alpha quartz: *Journal of Geophysical Research*, v. 81, p. 5711-5714.
- Openshaw, R.E., Hemingway, B.S., Robie, R.A., Waldbaum, D.R., and

- Krupka, K.M., 1976, The heat capacities at low temperatures and entropies at 298.15 K of low albite, analbite, microcline, and high sanidine: U.S. Geological Survey Journal of Research, v. 4(2), p. 195-204.
- Orr, R.L., 1953, High temperature heat contents of magnesium ortho-silicate and ferrous orthosilicate: Journal of the American Chemical Society, v. 75, p. 528-529.
- Osborn, E.F., and Schairer, J.R., 1941, The ternary system pseudo-wollastonite-akermanite-gehlenite: American Journal of Science, v. 239, p. 715-763.
- *Ostapenko, G.T., Timoshkova, L.P., and Tsymbol, S.N., 1977, The Gibbs energy of sillimanite from data on its solubility in water at 530°C and 1300 bars: Zapiski Vsesoyuznogo Mineralogicheskogo Obshchestva, v. 106, p. 243-244.
- Pankratz, L.B., 1964, High-temperature heat contents and entropies of muscovite and dehydrated muscovite: U.S. Bureau of Mines, Report of Investigations 6371, 6 p.
- Pankratz, L.B., 1968, High-temperature heat contents and entropies of dehydrated analcite, kaliophilite, and leucite: U.S. Bureau of Mines, Report of Investigations 7073, 8 p.
- Pankratz, L.B., and Kelley, K.K., 1964a, High-temperature heat contents and entropies of akermanite, cordierite, gehlenite, and merwinite: U.S. Bureau of Mines, Report of Investigations 6555, 7 p.
- Pankratz, L.B., and Kelley, K.K., 1964b, High-temperature heat con-

- tents and entropies of andalusite, kyanite, and sillimanite:
U.S. Bureau of Mines, Report of Investigations 6370, 7 p.
- Papike, J.J., and Cameron, M., 1976, Crystal chemistry of silicate minerals of geophysical interest: *Reviews in Geophysics and Space Physics*, v. 14, p. 37-80.
- Parks, G.S., and Kelley, K.K., 1926, The heat capacity of calcium silicate: *Journal of Physical Chemistry*, v. 30, p. 1175-1178.
- Perkins, Dexter, III; Essene, Eric J.; Westrum, Edgar F., Jr.; and Wall, Victor J., 1979, New thermodynamic data for diaspore and their application to the system $\text{Al}_2\text{O}_3\text{-SiO}_2\text{-H}_2\text{O}$: *American Mineralogist*, v. 64, p. 1080-1090.
- Perkins, Dexter, III; Westrum, Edgar F., Jr.; and Essene, Eric J., 1980, The thermodynamic properties and phase relations of some minerals in the system $\text{CaO-Al}_2\text{O}_3\text{-SiO}_2\text{-H}_2\text{O}$: *Geochimica et Cosmochimica Acta*, v. 44, p. 61-84.
- *Pistorius, Carl W.F.T., Kennedy, George C., and Sourirajan, S., 1962, Some relations between the phases anorthite, zoisite and lawsonite at high temperatures and pressures: *American Journal of Science*, v. 260, p. 44-56.
- *Pugin, V.A., and Khitarov, N.I., 1968, The $\text{Al}_2\text{O}_3\text{-SiO}_2$ system at high temperatures and pressures: *Geochemistry International*, v. 5, p. 120-128.
- Ralph, R.L., and Ghose, Subrata, 1980, Enstatite, $\text{Mg}_2\text{Si}_2\text{O}_6$: compressibility and crystal structure at 21 kbar: *EOS, Transactions of the American Geophysical Union*, v. 61, p. 409.

- Ralph, R.L., Hazen, R.M., and Finger, L.W., 1981, Cell parameters of orthoenstatite at high temperature and pressure: Year Book - Carnegie Institute of Washington, v. 1980, p. 376-379.
- Rau, H., 1972, Thermodynamics of the reduction of iron oxide powders with hydrogen: Journal of Chemical Thermodynamics, v. 4, p. 57-64.
- *Reesman, A.L., and Keller, W.D., 1968, Aqueous solubility studies of high-alumina and clay minerals: American Mineralogist, v. 53, p. 929-942.
- *Reznitskii, L.A., and Filippova, S.E., 1972, True heat capacity of alpha-hematite and natural hematite at 298-1000°K: Izvestiia Akademii Nauk SSSR, Neorganicheskie Materialy, v. 3, p. 1064-1072.
- *Richardson, S.W., Bell, P.M., and Gilbert, M.C., 1967, The aluminum silicates: Year Book - Carnegie Institute of Washington, v. 66, p. 392-397.
- *Richardson, S.W., Bell, P.M., and Gilbert, M.C., 1968, Kyanite-sillimanite equilibrium between 700° and 1500°C: American Journal of Science, v. 266, p. 513-541.
- Rigby, G.R., and Green, A.T., 1942, The thermal expansion characteristics of some calcareous and magnesian minerals: Transactions of the British Ceramic Society, v. 41, p. 123-143.
- *Rigby, G.R., Lovell, G.H.B., and Green, A.T., 1946, The reversible thermal expansion and other properties of some magnesian ferrous silicates: Transactions of the British Ceramic Society, v. 45,

p. 237-250.

Robie, Richard A., Bethke, Philip M., and Beardsley, K.M., 1967, Selected x-ray crystallographic data, molar volumes, and densities of minerals and related substances: U.S. Geological Survey Bulletin 1248, 87 p.

Robie, R.A., Finch, C.B., and Hemingway, B.S., 1982, Heat capacity and entropy of fayalite (Fe_2SiO_4) between 5.1 and 383 K. Comparison of calorimetric and equilibrium values for the QFM buffer reaction: *American Mineralogist*, v. 67 (in press).

Robie, R.A., and Hemingway, B.S., (in review), Heat capacities and entropies of phlogopite, $(\text{KMg}_2[\text{AlSi}_3\text{O}_{10}](\text{OH})_2)$ and paragonite, $(\text{NaAl}_2[\text{AlSi}_3\text{O}_{10}](\text{OH})_2)$ between 5 and 900 K and estimates of the enthalpy and free energy of formation at 298.15 K and 1 bar.

Robie, Richard A., and Hemingway, Bruce S., 1982, unpublished data.

Robie, Richard A., Hemingway, Bruce S., and Fisher, James R., 1979, Thermodynamic properties of minerals and related substances at 298.15 K and 1 bar (10^5 pascals) pressure and at higher temperatures (revised edition): U.S. Geological Survey Bulletin 1452, 456 p.

Robie, R.A., Hemingway, B.S., and Wilson, W.H., 1976, The heat capacities of calorimetry conference copper and of muscovite $\text{KAl}_2(\text{AlSi}_3)\text{O}_{10}(\text{OH})_2$, pyrophyllite $\text{Al}_2\text{Si}_4\text{O}_{10}(\text{OH})_2$, and illite $\text{K}_3(\text{Al}_7\text{Mg})(\text{Si}_{14}\text{Al}_2)\text{O}_{40}(\text{OH})_8$ between 15 and 375 K and their standard entropies at 298.15 K: U.S. Geological Survey Journal of Research, v. 4(6), p. 631-644.

- Robie, R.A., Hemingway, B.W., and Wilson, W.H., 1978, Low-temperature heat capacities and entropies of feldspar glasses and of anorthite: *American Mineralogist*, v. 63, p. 109-123.
- Robie, R.A., and Stout, J.W., 1963, Heat capacity from 12 to 305 K and entropy of talc and tremolite: *Journal of Physical Chemistry*, v. 67, p. 2252-2256.
- *Rog, G., Langanke, B., Borchardt, G., and Schmalzried, H., 1974, Determination of the standard Gibbs free energies of formation of the silicates of cobalt, magnesium, and strontium by e.m.f. measurements: *Journal of Chemical Thermodynamics*, v. 6, p. 1113-1119.
- Rosenholtz, Joseph L., and Smith, Dudley T., 1949, Linear thermal expansion of calcite, var. Iceland spar, and Yule marble: *American Mineralogist*, v. 34, p. 846-854.
- Roth, W.A., and Bertram, W., 1929, Messung der spezifischen warmen von metallurgisch wichtigen stoffen in einem grosseren temperaturintervall mit hilfe von zwei neuen calorimetertypen: *Zeitschrift fur Elektrochemie und Angewandte Physikalische Chemie*, Bd. 35, Nr. 6, p. 297-384.
- *Roy, Della M., 1958, Studies in the system $\text{CaO-Al}_2\text{O}_3\text{-SiO}_2\text{-H}_2\text{O}$: III, New data on the polymorphism of Ca_2SiO_4 and its stability in the system $\text{CaO-SiO}_2\text{-H}_2\text{O}$: *Journal of The American Ceramic Society*, v. 41, p. 293-299.
- Saburi, Shinsuke; Kusachi, Isao; Henmi, Chiyoko; Kawahara, Akira; Henmi, Kitinosuke, and Kawada, Isao, 1976, Refinement of the structure of rankinite: *Mineralogical Journal (Tokyo)*, v. 8(4),

p. 240-246.

Salmon, Oliver N., 1961, High temperature thermodynamics of the iron oxide system: *Journal of Physical Chemistry*, v. 65, p. 550-556.

Schauer, Alois, 1965, Thermal expansion, Grueneisen parameter, and temperature dependence of lattice vibration frequencies of aluminum oxide: *Canadian Journal of Physics*, v. 43, p. 523-531.

Schmahl, N.G., 1941, Die beziehungen zwischen sauerstoffdruck, temperatur und zusammensetzung im system $Fe_2O_3-Fe_3O_4$: *Zeitschrift fur Elektrochemie*, Bd. 47, p. 821-843.

*Schmid, Rolf, 1978, Experimental determination of univariant equilibria using divariant solid-solution assemblages: *American Mineralogist*, v. 63, p. 511-515.

*Schneider, A., and Gattow, G., 1954, Zur bildungswarme des aluminiumoxyds: *Zeitschrift fur anorganische und allgemeine Chemie*, v. 277, p. 41-48.

Schneider, Hartmut, 1979, Thermal expansion of andalusite: *Journal of the American Ceramic Society*, v. 62, p. 307.

Schramke, Janet A., Kerrick, Derrill M., and Blencoe, James G., 1982, Experimental determination of the brucite = periclase + water equilibrium with a new volumetric technique: *American Mineralogist*, v. 67, p. 269-276.

Schwerdtfeger, Klaus, and Muan, Arnulf, 1966, Activities in olivine and pyroxenoid solid solutions of the system Fe-Mn-Si-O at 1150°C: *Transactions of the Metallurgical Society of AIME*, v. 236, p. 201-211.

- *Shearer, J.A., and Kleppa, O.J., 1973, The enthalpies of formation of $MgAl_2O_4$, $MgSiO_3$, Mg_2SiO_4 , and Al_2SiO_5 by oxide melt solution calorimetry: *Geochimica et Cosmochimica Acta*, v. 35, p. 1073-1078.
- *Shibanov, E.V., and Chukhlantsev, V.G., 1972, Heats of solution of calcium orthosilicate and chloro-orthosilicate in hydrochloric acid solution: *Russian Journal of Physical Chemistry*, v. 46, p. 617.
- *Shibanov, E.V., Chukhlantsev, V.G., and Alyamovskaya, K.V., 1972, Enthalpies of solution and formation of the sodium zirconosilicates $Na_6Zr_2Si_4O_{15}$ and $Na_{14}Zr_2Si_{10}O_{31}$: *Russian Journal of Physical Chemistry*, v. 46, p. 617.
- Shmulovich, K.I., 1974, Phase equilibria in the $CaO-Al_2O_3-SiO_2-CO_2$ system: *Geochemistry International*, v. 11(4), p. 883-887.
- Shomate, C.H., and Cook, O.A., 1946, Low-temperature heat capacities and high-temperature heat contents of $Al_2O_3 \cdot 3H_2O$ and $Al_2O_3 \cdot H_2O$: *Journal of the American Chemical Society*, v. 68, p. 2140-2142.
- Skinner, Brian J., 1956, Physical properties of end-members of the garnet group: *American Mineralogist*, v. 41, p. 428-436.
- Skinner, Brian J., 1957, The thermal expansions of thoria, periclase and diamond: *American Mineralogist*, v. 42, p. 39-55.
- Skinner, Brian J., 1962, Thermal expansion of ten minerals: U.S. Geological Survey, Professional Paper No. 450-D, p. D109-D112.
- Skinner, Brian J., 1966, Thermal expansion: *Handbook of Physical Constants - Revised Edition*, GSA Memoir 97, p. 75-96.
- Skinner, Brian J., Clark, Sydney P., Jr., and Appleman, Daniel E.,

- 1961, Molar volume and thermal expansion of andalusite, kyanite, and sillimanite: *American Journal of Science*, v. 259, p. 651-668.
- Smiltens, J., 1957, Standard free energy of oxidation of magnetite to hematite at temperatures above 1000°: *Journal of the American Chemical Society*, v. 79, p. 4877-4880.
- Smith, J.V., 1959, The crystal structure of proto-enstatite, $MgSiO_3$: *Acta Crystallographica*, v. 12, p. 515-519.
- Smyth, F. Hastings, and Adams, Leason H., 1923, The system, calcium oxide-carbon dioxide: *Journal of the American Chemical Society*, v. 45, p. 1167-1184.
- Smyth, Joseph R., 1975, High temperature crystal chemistry of fayalite: *American Mineralogist*, v. 60, p. 1092-1097.
- *Snyder, Paul E., and Seltz, Harry, 1945, The heat of formation of aluminum oxide: *Journal of the American Chemical Society*, v. 67, p. 683-685.
- Southard, J.C., 1941, A modified calorimeter for high temperatures. The heat content of silica, wollastonite, and thorium dioxide above 25°: *Journal of the American Chemical Society*, v. 63, p. 3142-3146.
- Staveley, L.A.K., and Linford, R.G., 1969, The heat capacity and entropy of calcite and aragonite, and their interpretation: *Journal of Chemical Thermodynamics*, v. 1, p. 1-11.
- Stephenson, D.A., Sclar, C.B., and Smith, J.V., 1966, Unit cell volumes of synthetic orthoenstatite and low clinoenstatite: *Mineralogical Magazine*, v. 35, p. 838-846.

- Storre, Bernhard, and Nitsch, K.-H., 1974, Zur stabilitat von margarit im system $\text{CaO-Al}_2\text{O}_3\text{-SiO}_2\text{-H}_2\text{O}$: Contributions to Mineralogy and Petrology, v. 43, p. 1-24.
- Strens, R.G.J., 1968, Reconnaissance of the prehnite stability field: Mineralogical Magazine, v. 36, p. 864-867.
- Stull, D.R., and Prophet, H., 1971, JANAF thermochemical tables: U.S. National Bureau of Standards NSRDS-NBS 37.
- Sueno, Shigeho, Cameron, Maryellen, and Prewitt, C.T., 1976, Orthoferrosilite: high temperature crystal chemistry: American Mineralogist, v. 61, p. 38-53.
- Swanson, H.E., and Tatge, E., 1953, Standard x-ray diffraction powder patterns: National Bureau of Standards Circular 539, v. 1, 93 p.
- Swaroop, B., and Wagner, J.B., Jr., 1967, On the vacancy concentrations of wüstite (FeO_x) near the p to n transition: Transactions of the Metallurgical Society of AIME, v. 239, p. 1215-1218.
- Taylor, L.A., and Bell, P.M., 1970, Thermal expansion of pyrophyllite: Carnegie Institution Year Book, v. 69, p. 193-194.
- *Taylor, R.W., and Schmalzried, H., 1964, The free energy of formation of some titanates, silicates, and magnesium aluminate from measurements made with galvanic cells involving solid electrolytes: Journal of Physical Chemistry, v. 68, p. 2444-2449.
- Thompson, A.B., 1970, A note on the kaolinite-pyrophyllite equilibrium: American Journal of Science, v. 268, p. 454-458.
- Thompson, A.B., Perkins, D., Sonderegger, U., and Newton, R.C., 1978, Heat capacities of synthetic $\text{CaAl}_2\text{SiO}_6\text{-CaMgSi}_2\text{O}_6\text{-Mg}_2\text{Si}_2\text{O}_6$

- pyroxenes: EOS, Transactions of the American Geophysical Union, v. 59, p. 395.
- Todd, S.S., 1950, Heat capacities at low temperatures and entropies at 298.16°K of andalusite, kyanite, and sillimanite: Journal of the American Chemical Society, v. 72, p. 4742-4743.
- Todd, S.S., 1951, Low-temperature heat capacities and entropies at 298.16°K of crystalline calcium orthosilicate, zinc orthosilicate and tricalcium silicate: Journal of the American Chemical Society, v. 73, p. 3277-3278.
- Todd, S.S., and Bonnicksen, K.R., 1951, Low temperature heat capacities and entropies at 298.16°K of ferrous oxide, manganous oxide and vanadium monoxide: Journal of the American Chemical Society, v. 73, p. 3894-3895.
- Tombs, N.C., and Rooksby, H.P., 1951, Structure transition and anti-ferromagnetism in magnetite: Acta Crystallography, v. 4, p. 474-475.
- *Topor, N.D., Kiseleva, I.A., and Mel'chakova, L.V., 1972, Measurement of enthalpies of minerals by high temperature microcalorimetry: Geokhimiia, no. 3, p. 335-343.
- *Torgeson, D.R., and Sahama, Th. G., 1948, A hydrofluoric acid solution calorimeter and the determination of the heats of formation of Mg_2SiO_4 , $MgSiO_3$, and $CaSiO_3$: Journal of the American Chemical Society, v. 70, p. 2156-2160.
- Tret'yakov, Yu. D., and Khomyakov, K.G., 1962, Apparatus for measuring dissociation pressure of ferrites and oxides at high temperatures:

- Russian Journal of Inorganic Chemistry, v. 7, p. 628-631.
- Ulbrich, Horst H., and Waldbaum, David R., 1976, Structural and other contributions to the third-law entropies of silicates: *Geochimica et Cosmochimica Acta*, v. 40, p. 1-24.
- Ulmer, Gene C., ed., 1971, *Research Techniques for High Pressure and High Temperature*: Springer-Verlag, New York, 367 p.
- Vaidya, S.N., and Kennedy, George C., 1970, Compressibility of 18 metals to 45 kilobars: *Journal of Physics and Chemistry of Solids*, v. 31, p. 2329-2345.
- Vaidya, S.N., Bailey, S., Pasternack, T., and Kennedy, G.C., 1973, Compressibility of fifteen minerals to 45 kilobars: *Journal of Geophysical Research*, v. 78, p. 6893-6898.
- Vallet, Pierre, and Raccah, Paul, 1965, Thermodynamic properties of solid iron(II) oxide: *Memoires Scientifiques de la Revue de Metallurgie*, v. 62, p. 1-29.
- *Velde, Bruce, 1971, The stability and natural occurrence of margarite: *Mineralogical Magazine*, v. 38, p. 317-323.
- Wagner, Hubert, 1932, Zur thermochemie der metasilikate des calciums und magnesiums und des diopsids: *Zeitschrift fur Anorganische und Allgemeine Chemie*, Band 208, Heft 1, p. 1-22.
- Waters, A.C., 1961, Stratigraphic and lithologic variations in the Columbia River basalt: *American Journal of Science*, v. 259, p. 583-611.
- Weill, D.F., 1966, Stability relations in the $Al_2O_3-SiO_2$ system calculated from solubilities in the $Al_2O_3-SiO_2-Na_3AlF_6$ system:

- Geochimica et Cosmochimica Acta, v. 30, p. 223-237.
- Weir, C.E., 1956, Isothermal compressibilities of alkaline Earth oxides at 21°C: Journal of Research of the National Bureau of Standards, v. 56, p. 187-189.
- *Welch, J.H., and Gutt, W., 1959, Tricalcium silicate and its stability within the system CaO-SiO₂: Journal of The American Ceramic Society, v. 42, p. 11-15.
- Weller, W.W., and Kelley, K.K., 1963, Low-temperature heat capacities and entropies at 298.15°K of akermanite, cordierite, genlente, and merwinite: U.S. Bureau of Mines, Report of Investigations 6343, 7 p.
- *West, E.D., and Ginnings, D.C., 1957, The heat capacity of aluminum oxide in the range 300 to 700°K: Journal of Physical Chemistry, v. 61, p. 1573-1574.
- Westrum, Edgar F., Jr.; Essene, Eric J.; and Perkins, Dexter, III, 1979, Thermophysical properties of the garnet, grossular: Ca₃Al₂Si₃O₁₂: Journal of Chemical Thermodynamics, v. 11, p. 47-66.
- Westrum, Edgar F., Jr., and Grønvoold, Fredrik, 1965, Magnetite (Fe₃O₄) heat capacity and thermodynamic properties from 5 to 350 K, low-temperature transition: Journal of Chemical Thermodynamics, v. 1, p. 543-557.
- White, W.P., 1919, Silicate specific heats: American Journal of Science, 2d series, v. 47(277), p. 1-59.
- Wilburn, David R., and Bassett, William A., 1977, Isothermal com-

- pression of magnetite (Fe_3O_4) up to 70 kbar under hydrostatic conditions: High Temperature - High Pressure, v. 9, p. 3539.
- Wilburn, David R., Bassett, William A., Sato, Y., and Akimoto, S., 1978, X-ray diffraction compression studies of hematite under hydrostatic, isothermal conditions: Journal of Geophysical Research, v. 83, p. 3509-3512.
- Willis, B.T.M., and Rooksby, H.P., 1952, Crystal structure and anti-ferromagnetism in haematite: Proceedings of the Physical Society of London, Section B, v. 65, p. 950-954.
- *Windom, Kenneth Earl, 1976, The effect of reduced activity of anorthite on the reaction grossular + quartz = anorthite + wollastonite: a model for plagioclase in the earth's lower crust and upper mantle: Ph.D. Thesis, The Pennsylvania State University.
- *Windom, K.E., and Boettcher, A.L., 1976, The effect of reduced activity of anorthite on the reaction grossular + quartz = anorthite + wollastonite: a model for plagioclase in the earth's lower crust and upper mantle: American Mineralogist, v. 61, p. 889-896.
- *Winkler, Helmut G.F., and Nitsch, K.H., 1962, Zoisitbildung bei der experimentellen metamorphose: Naturwissenschaften, v. 24, p. 605.
- Winter, John K., and Ghose, Subrata, 1979, Thermal expansion and high-temperature crystal chemistry of the Al_2SiO_5 polymorphs: American Mineralogist, v. 64, p. 573-586.
- *Wones, David R., 1967, A low pressure investigation of the stability of phlogopite: Geochimica et Cosmochimica Acta, v. 31, p.

2248-2253.

- *Wones, David R., and Dodge, Franklin C.W., 1977, The stability of phlogopite in the presence of quartz and diopside: NATO Advanced Study Institute Series, Series C: Mathematical and Physical Sciences, v. C30 (Thermodynamics in Geology), p. 229-247.
- *Wones, David R., and Gilbert, M. Charles, 1969, The fayalite-magnetite-quartz assemblage between 600° and 800°C: American Journal of Science, v. 267-A, p. 480-488.
- Wood, B.J., and Kleppa, O.J., 1981, Thermochemistry of forsterite-fayalite olivine solutions: *Geochimica et Cosmochimica Acta*, v. 45, p. 529-534.
- *Yagi, Takehiko, Mao, Ho-Kwang, and Bell, Peter M., 1978, Structure and crystal chemistry of perovskite-type $MgSiO_3$: *Physics and Chemistry of Minerals*, v. 3, p. 97-110.
- Yamaguchi, Goro, and Miyabe, Hisako, 1960, Precise determination of the $3CaO-SiO_2$ cells and interpretation of their x-ray diffraction patterns: *American Ceramic Society Journal*, v. 43, p. 219-224.
- Yoder, Hatten S., Jr., 1950, High-low quartz inversion up to 10,000 bars: *Transactions of the American Geophysical Union*, v. 31, p. 827-835.

1.5. Appendix - Thermodynamic Tables and Summaries

The refined thermodynamic properties (thermophysical, thermochemical, and volumetric) for the chemical compounds considered in this study are given in sections 1.5.4 below. Sections 1.5.1 and 1.5.2 give the arrangement by chemical formula and the cross index for the minerals respectively.

Section 1.5.3 gives algebraic and thermodynamic functions that were followed in this study. The summaries of data that were considered in this study, special comments appropriate for each phase, and the constants as would be used in equations in section 1.5.3 are given in section 1.5.5.

1.5.1. Chemical Index to Tables and Summaries

The compounds for which data are given in sections 1.5.4 and 1.5.5 are arranged alphabetically by the commonly accepted formula. The data in table 10 give the table numbers and pages on which the reader will find the needed properties.

1.5.2. Mineral Index to Tables and Summaries

The data, in table 11, are supplied as a convenient cross-index of mineral names, formulas, and property tables.

Table 10. Chemical index to tables and summaries.

Chemical formula (In order of arrangement.)	Properties				
	Mineral name	Thermophysical (Table number)	Thermochemical (Table number)	Volumetric	Summaries (page number)
Al (crystal, liquid)	---	12	13	-	287
Al ₂ O ₃	boehmite	14, 16	15, 17	146	287
Al ₂ SiO ₅	diaspore	14, 18	15, 19	147	290
Al(OH) ₃	gibbsite	20	21	148	293
Al ₂ O ₃	corundum	22	23	149	296
Al ₂ SiO ₅	andalusite	24, 26	25, 27	150	296
Al ₂ SiO ₅	kyanite	24, 28	25, 29	151	300
Al ₂ SiO ₅	sillimanite	24, 30	25, 31	152	303
Al ₂ Si ₂ O ₅ (OH) ₄	kaolinite	32	33	153	306
Al ₂ Si ₂ O ₅ (OH) ₄	dickite	34	35	154	306
Al ₂ Si ₂ O ₅ (OH) ₄	halloysite	36	37	155	306
Al ₂ Si ₄ O ₁₀ (OH) ₂	pyrophyllite	38	39	156	313
C	graphite	40	41	-	313
CO (ideal gas)	---	42	43	-	313
CO ₂ (ideal gas)	---	44	45	-	313
Ca (crystal, liquid, ideal gas)	---	46	47	-	316
CaAl ₂ SiO ₆	Ca-Al clinopyroxene	48	49	157	316
CaAl ₂ Si ₂ O ₈	anorthite	50	51	158	316
CaAl ₄ Si ₂ O ₁₀ (OH) ₂	margarite	52	53	159	323
CaCO ₃	calcite	54	55	160	323
CaCO ₃	aragonite	56	57	161	328
CaO	lime	58	59	162	328
CaSiO ₃	wollastonite	60, 62	61, 63	163	332
Ca ₂ SiO ₃	cyclo wollastonite	60, 64	61, 65	164	332

Table 10. Continued

Chemical formula (in order of arrangement)	Mineral name	Properties				Summaries Constants (page number)
		Thermophysical (table number)	Thermochemical (table number)	Volumetric		
$\text{Ca}_2\text{Al}_2\text{SiO}_6(\text{OH})_2$	bicchulite	66	67	165	338	415,420
$\text{Ca}_2\text{Al}_2\text{SiO}_7$	gehlenite	68	69	166	338	415,420
$\text{Ca}_2\text{Al}_2\text{Si}_3\text{O}_{10}(\text{OH})_2$	prehnite	70	71	167	343	416,421
$\text{Ca}_2\text{Al}_3\text{Si}_3\text{O}_{12}(\text{OH})$	zoisite	72	73	168	343	416,421
Ca_2SiO_4 (alpha)	---	74,76	75,77	169	354	416,421
Ca_2SiO_4 (alpha-prime)	breddigite	74,78	75,79	170	354	416,421
Ca_2SiO_4 (gamma)	Ca olivine	74,80	75,81	171	354	416,421
Ca_2SiO_4 (beta)	larnite	74,82	75,83	172	354	416,421
$\text{Ca}_3\text{Al}_2\text{Si}_3\text{O}_{12}$	grossular	84	85	173	356	416,421
Ca_3SiO_5	hattrurite	86	87	174	356	416,421
$\text{Ca}_3\text{Si}_2\text{O}_7$	rankinite	88	89	175	362	416,421
$\text{Ca}_4\text{Al}_6\text{Si}_6\text{O}_{24}(\text{CO}_3)$	metonite	90	91	176	362	416,421
Fe (alpha, alpha-prime, gamma)	---	92	93	-	362	416,421
Fe_9O_{10}	wustite	94	95	177	367	416,421
FeSiO_3	ferrosillite	96	97	178	367	416,421
Fe_2O_3	hematite	98	99	179	373	417,422
Fe_2SiO_4	fayalite	100	101	180	376	417,422
Fe_3O_4	magnetite	102	103	181	379	417,422
H_2 (ideal gas)	---	104	105	-	379	417,422
H_2O (liquid)	water	106,108	107,109	182	382	417,422
H_2O (ideal gas)	---	106,110	107,111	-	382	417,422
H_2O (real gas)	---	-	-	182	382	417,422
H_4SiO_4 , silicic acid	---	-	-	-	382	---

Table 10. Continued

Chemical formula (in order of arrangement)	Mineral name	Properties			
		Thermophysical (table number)	Thermochemical (table number)	Volumetric	Summaries (page number)
Mg	---	112	113	-	383
Mg ₂ O ₃	magnesite	114	115	183	383
MgO	periclase	116	117	184	386
Mg(OH) ₂	brucite	118	119	185	386
MgSiO ₃	clinoenstatite	120, 122	121, 123	186	386
MgSiO ₃	enstatite	120, 124	121, 125	187	386
MgSiO ₃	protoenstatite	120, 126	121, 127	188	386
Mg ₂ SiO ₄	forsterite	128	129	189	396
Mg ₃ Si ₂ O ₅ (OH) ₄	chrysotile	130	131	190	396
Mg ₃ Si ₄ O ₁₀ (OH) ₂	talc	132	133	191	396
Mg ₇ Si ₈ O ₂₂ (OH) ₂	anthophyllite	134	135	192	396
Mg ₄ Si ₃ O ₈ (OH) ₆	antigorite	136	137	193	407
O ₂ (ideal gas)	---	138	139	-	407
Si (crystal, liquid)	---	140	141	-	407
SiO ₂	quartz	142	143	194	410
SiO ₂	cristobalite	144	145	195	410

Table 11. Mineral index to tables and summaries.

Mineral name	Chemical formula	Properties				Summaries (page number)	Constants (page number)
		Thermophysical	Thermochemical (table number)	Volumetric			
andalusite	Al_2SiO_5	24, 26	25, 27	150	296	414, 419	
anorthite	$CaAl_2Si_2O_8$	50	51	158	316	415, 420	
anthophyllite	$Mg_7Si_8O_{22}(OH)_2$	134	135	192	396	418, 423	
antigorite	$Mg_{48}Si_{34}O_{85}(OH)_{62}$	136	137	193	407	418, 423	
aragonite	$CaCO_3$	56	57	161	328	415, 420	
blechulite	$Ca_2Al_2SiO_6(OH)_2$	66	67	165	338	415, 420	
boehmite	$Al(OH)_3$	14, 16	15, 17	146	287	414, 419	
broedigeite	Ca_2SiO_4 (alpha-prime)	74, 78	75, 79	170	354	416, 421	
brucite	$Mg(OH)_2$	118	119	185	386	417, 422	
Ca olivine	Ca_2SiO_4 (gamma)	74, 80	75, 81	171	354	416, 421	
Ca-Al clinopyroxene	$CaAl_2SiO_6$	48	49	157	316	415, 420	
calcite	$CaCO_3$	54	55	160	323	415, 420	
chrysotile	$Mg_3Si_2O_5(OH)_4$	130	131	190	396	418, 423	
clay minerals	See dickite, halloysite, kaolinite, pyrophyllite.						
clinochlore	$MgSiO_3$	120, 122	121, 123	186	386	417, 422	
corundum	Al_2O_3	22	23	149	296	414, 419	
crystalite	SiO_2	144	145	195	410	418, 423	
cycloallastone	$CaSiO_3$	60, 64	61, 65	164	332	415, 420	
diaspore	$Al(OH)_3$	14, 18	15, 19	147	290	414, 419	
dickite	$Al_2Si_2O_5(OH)_4$	34	35	154	306	414, 419	
ensatite	$MgSiO_3$	120, 124	121, 125	187	386	418, 423	
epidote group	See zoisite						
fayalite	Fe_2SiO_4	100	101	180	387	417, 422	

Table 11. Continued

Mineral name	Chemical formula	Properties			
		Thermophysical (table number)	Thermochemical (table number)	Volumetric	Summaries (page number)
feldspar group	See anorthite				
ferrosilite	FeSiO ₃	96	97	178	367 416, 421
forsterite	Mg ₂ SiO ₄	128	129	189	396 418, 423
garnet group	See grossular				
gehlenite	Ca ₂ Al ₂ SiO ₇	68	69	166	338 415, 420
gibbsite	Al(OH) ₃	20	21	148	293 414, 419
graphite	C	40	41	-	313 414, 419
grossular	Ca ₃ Al ₂ Si ₃ O ₁₂	84	85	173	356 416, 421
halloysite	Al ₂ Si ₂ O ₅ (OH) ₄	36	37	155	306 414, 419
hasturite	Ca ₃ SiO ₆	86	87	174	356 416, 421
hematite	Fe ₂ O ₃	98	99	179	373 417, 422
kaolinite	Al ₂ Si ₂ O ₅ (OH) ₄	32	33	153	306 414, 419
kyanite	Al ₂ SiO ₅	24, 28	25, 29	151	300 414, 419
larnite	Ca ₂ SiO ₄ (beta)	74, 82	75, 83	172	354 416, 421
lime	CaO	58	59	162	328 415, 420
magnesite	MgCO ₃	114	115	183	383 417, 422
magnetite	Fe ₃ O ₄	102	103	181	379 417, 422
margarite	CaAl ₃ Si ₂ O ₁₀ (OH) ₂	52	53	159	323 415, 420
metonite	Ca ₄ Al ₆ Si ₆ O ₂₄ (CO ₃)	90	91	176	362 416, 421
metilite group	See gehlenite, rankinite				
olivine group	See Ca olivine, fayalite, forsterite				
periclase	MgO	116	117	184	386 417, 422

Table 11. Continued

Mineral name	Chemical formula	Properties				
		Thermophysical	Thermochemical (table number)	Volumetric	Summaries (page number)	Constants (page number)
prehnite	$\text{Ca}_2\text{Al}_2\text{Si}_3\text{O}_{10}(\text{OH})_2$	70	71	167	343	416, 421
protoenstatite	MgSiO_3	120, 126	121, 127	188	386	418, 423
"pseudowollastonite"	See cyclo wollastonite					
pyrophyllite	$\text{Al}_2\text{Si}_4\text{O}_{10}(\text{OH})_2$	38	39	156	313	414, 419
pyroxene group	See Ca-Al clinopyroxene, clinoenstatite, enstatite, protoenstatite, ferrosillite, pyroxenoids					
pyroxenoids	See wollastonite, cyclo wollastonite					
quartz	SiO_2	142	143	194	410	418, 423
rankinite	$\text{Ca}_3\text{Si}_2\text{O}_7$	88	89	175	362	416, 421
serpentine group	See antigorite, chrysotile					
sillimanite	Al_2SiO_5	24, 30	25, 31	152	303	414, 419
talc	$\text{Mg}_3\text{Si}_4\text{O}_{10}(\text{OH})_2$	132	133	191	396	418, 423
water	H_2O (liquid)	106, 108	107, 109	182	382	417, 422
wollastonite	CaSiO_3	60, 62	61, 63	163	332	415, 420
wustite	Fe_{94}O	94	95	177	367	416, 421
zoisite	$\text{Ca}_2\text{Al}_3\text{Si}_3\text{O}_{12}(\text{OH})$	72	73	168	343	416, 421

1.5.3. Functions Describing Thermophysical Properties as a Function of Pressure and Temperature

General Thermodynamic Relationships

Thermodynamic theory provides the following exact functional relations among heat capacity (C_p) at a reference pressure P_r , volume (V), entropy (S), enthalpy (H), free energy (G), equilibrium constant (K), and electrochemical potential (E):

$$C_{p,i} - C_{p_r,i} = - \int_{P_r}^P T (\partial^2 V_i / \partial T^2) dP \quad (16)$$

$$S_i = S_0 + \int_0^T \frac{C_{p_r,i}}{T} dT - \int_{P_r}^P \left(\frac{\partial V_i}{\partial T} \right)_P dP \quad (17)$$

$$H_i = H_0 + \int_0^T C_{p_r,i} dT + \int_{P_r}^P \left(V_i - T \left(\frac{\partial V_i}{\partial T} \right)_P \right) dP \quad (18)$$

$$G_i = H_i - T S_i \quad (19)$$

$$-RT \ln K = \sum_{i=1}^k s_i G_i \quad (20)$$

$$-nFE = \sum_{i=1}^k s_i G_i \quad (21)$$

where T is thermodynamic temperature, R and F are the ideal gas constant and Faraday constant, respectively. The term k is the number of species in the reaction, and s is the stoichiometric coefficient, positive for products and negative for reactants. The term n is the

number of electrons involved in the reaction. From these, it follows that an empirical relation which describes $C_{p_r,i}$ as a function of temperature and V_i as a function of temperature and pressure will generate the mathematical description of the other thermodynamic properties.

Formulae Describing Thermodynamic Properties

$$C_{p_r,i} = \frac{a_{1,i}}{T^2} + \frac{a_{3,i}}{T^{1/2}} + a_{5,i} + 2a_{6,i} T + a_{7,i} T^2 \quad (22)$$

$$V_i = b_{1,i} + b_{2,i} T + b_{3,i} \exp(-T/300) + b_{4,i} P + b_{5,i} \exp(-P/35000) \quad (23)$$

$$C_{p,i} - C_{p_r,i} = \frac{-b_{3,i}}{90000} T \exp(-T/300)(P - P_r) \quad (24)$$

$$H_i = \frac{-a_{1,i}}{T} + a_{2,i} + 2 a_{3,i} \sqrt{T} + a_{5,i} T + a_{6,i} T^2 + a_{7,i} \frac{T^3}{3} +$$

$$b_{1,i} (P - P_r) + b_{3,i} \left(1 + \frac{T}{300}\right) (\exp(-T/300)) (P - P_r) +$$

$$\frac{b_{4,i}}{2} (p^2 - p_r^2) - (35000) b_{5,i} \{ \exp(-P/35000) -$$

$$\exp(-P_r/35000) \} \quad (25)$$

$$S_i = \frac{-a_{1,i}}{2T^2} - \frac{2a_{3,i}}{\sqrt{T}} + a_{4,i} + a_{5,i} \ln T + 2 a_{6,i} T + a_{7,i} \frac{T^2}{T} -$$

$$b_{2,i} (P - P_r) + \left(\frac{b_{3,i}}{300}\right) (P - P_r) \exp(-T/300) \quad (26)$$

$$\begin{aligned}
G_i = & -\frac{a_{1,i}}{2T} + a_{2,i} - 4 a_{3,i} \sqrt{T} - a_{4,i} T + a_{5,i} (T - T \ln T) - \\
& a_{6,i} T^2 - a_{7,i} \frac{T^3}{6} + b_{1,i} (P - P_r) + b_{2,i} T (P - P_r) + \\
& b_{3,i} (P - P_r) \exp(-T/300) + \frac{b_{4,i}}{2} (P^2 - P_r^2) - \\
& (35000) b_{5,i} \{ \exp(-P/35000) - \exp(-P_r/35000) \} \quad (27)
\end{aligned}$$

1.5.4. Tables of Mineral Thermodynamic and Thermophysical Properties at 101.325 kPa (1 atm)

TABLES 12 THROUGH 195 FOLLOW IN SEQUENCE.

TABLES 12 THROUGH 145 ARE DESIGNED TO BE

ON FACING PAGES.

Table 12. Thermophysical values for stable phases of the element aluminum (Al) at 1.01325 bars (1 atm). The sources of data are given in section 1.5.5.

T K	C _p J/(mol K)	S J/(mol K)	H-H(298) J/mol	[G-H(298)]/T J/(mol K)	V ³ cm ³ /mol
aluminum (crystal)					
200.	21.513	19.138	-2273.	-30.505	---
250.	23.308	24.153	-1148.	-28.745	---
(2 sigma)	---	---	---	---	---
273.15	23.844	26.241	-602.	-28.445	---
298.15	24.307	28.350	0.	-28.350	---
(2 sigma)	---	---	---	---	---
300.	24.338	28.500	45.	-28.351	---
350.	25.049	32.308	1281.	-28.650	---
400.	25.625	35.691	2548.	-29.322	---
450.	26.157	38.741	3842.	-30.202	---
500.	26.692	41.524	5163.	-31.197	---
(2 sigma)	---	---	---	---	---
550.	27.255	44.094	6512.	-32.254	---
600.	27.863	46.491	7890.	-33.342	---
650.	28.525	48.747	9299.	-34.441	---
700.	29.249	50.887	10743.	-35.540	---
750.	30.039	52.932	12225.	-36.632	---
(2 sigma)	---	---	---	---	---
800.	30.898	54.898	13748.	-37.712	---
850.	31.828	56.798	15316.	-38.779	---
900.	32.831	58.645	16932.	-39.832	---
933.25	33.539	59.849	18036.	-40.524	---
aluminum (liquid)					
933.25	31.756	71.413	28828.	-40.524	---
950.	31.756	71.978	29360.	-41.073	---
1000.	31.756	73.607	30948.	-42.660	---
(2 sigma)	---	---	---	---	---
1050.	31.756	75.157	32535.	-44.170	---
1100.	31.756	76.634	34123.	-45.613	---
1150.	31.756	78.045	35711.	-46.992	---
1200.	31.756	79.397	37299.	-48.315	---
1250.	31.756	80.693	38887.	-49.584	---
(2 sigma)	---	---	---	---	---
1300.	31.756	81.939	40474.	-50.805	---
1350.	31.756	83.137	42062.	-51.980	---
1400.	31.756	84.292	43650.	-53.114	---
1450.	31.756	85.407	45238.	-54.208	---
1500.	31.756	86.483	46826.	-55.266	---
(2 sigma)	---	---	---	---	---
1550.	31.756	87.525	48414.	-56.290	---
1600.	31.756	88.533	50001.	-57.282	---
1650.	31.756	89.510	51589.	-58.244	---
1700.	31.756	90.458	53177.	-59.177	---
1750.	31.756	91.379	54765.	-60.084	---
(2 sigma)	---	---	---	---	---
1800.	31.756	92.273	56353.	-60.966	---
(2 sigma)	---	---	---	---	---

Table 13. Thermochemical properties of stable phases of the element aluminum (Al) at 1.01325 bars (1 atm). Columns 2 through 4 give the thermochemical values relative to the elements; columns 5 through 7 give the values relative to the oxides.

T K	Formation from the Elements			Formation from the Oxides		
	H J/mol	G J/mol	log K	H J/mol	G J/mol	log K
aluminum (crystal)						
200.	0.	0.	0.	---	---	---
250.	0.	0.	0.	---	---	---
(2 sigma)	0.	0.	0.	---	---	---
273.15	0.	0.	0.	---	---	---
298.15	0.	0.	0.	---	---	---
(2 sigma)	0.	0.	0.	---	---	---
300.	0.	0.	0.	---	---	---
350.	0.	0.	0.	---	---	---
400.	0.	0.	0.	---	---	---
450.	0.	0.	0.	---	---	---
500.	0.	0.	0.	---	---	---
(2 sigma)	0.	0.	0.	---	---	---
550.	0.	0.	0.	---	---	---
600.	0.	0.	0.	---	---	---
650.	0.	0.	0.	---	---	---
700.	0.	0.	0.	---	---	---
750.	0.	0.	0.	---	---	---
(2 sigma)	0.	0.	0.	---	---	---
800.	0.	0.	0.	---	---	---
850.	0.	0.	0.	---	---	---
900.	0.	0.	0.	---	---	---
933.25	0.	0.	0.	---	---	---
aluminum (liquid)						
933.25	0.	0.	0.	---	---	---
950.	0.	0.	0.	---	---	---
1000.	0.	0.	0.	---	---	---
(2 sigma)	0.	0.	0.	---	---	---
1050.	0.	0.	0.	---	---	---
1100.	0.	0.	0.	---	---	---
1150.	0.	0.	0.	---	---	---
1200.	0.	0.	0.	---	---	---
1250.	0.	0.	0.	---	---	---
(2 sigma)	0.	0.	0.	---	---	---
1300.	0.	0.	0.	---	---	---
1350.	0.	0.	0.	---	---	---
1400.	0.	0.	0.	---	---	---
1450.	0.	0.	0.	---	---	---
1500.	0.	0.	0.	---	---	---
(2 sigma)	0.	0.	0.	---	---	---
1550.	0.	0.	0.	---	---	---
1600.	0.	0.	0.	---	---	---
1650.	0.	0.	0.	---	---	---
1700.	0.	0.	0.	---	---	---
1750.	0.	0.	0.	---	---	---
(2 sigma)	0.	0.	0.	---	---	---
1800.	0.	0.	0.	---	---	---
(2 sigma)	0.	0.	0.	---	---	---

Table 14. Thermophysical values for stable phases with the composition Al₁₀₀H at 1.01325 bars (1 atm). The tabulations are based on a fit of the thermophysical and thermochemical data given in Section 1.5.5.

T K	C _p J/(mol K)	S J/(mol K)	H-H(298) J/mol	[G-H(298)]/T J/(mol K)	V cm ³ /mol
diaspore					
200.	34.372	17.801	-4373.	-39.664	17.6435
250.	45.103	26.675	-2374.	-36.172	17.7030
(2 sigma)	0.108	0.099	5.	0.097	0.1664
273.150	49.230	30.852	-1281.	-35.544	17.7305
298.150	53.214	35.339	0.	-35.339	17.7602
(2 sigma)	0.114	0.097	0.	0.097	0.1333
300.	53.491	35.669	99.	-35.340	17.7624
350.	60.222	44.438	2947.	-36.017	17.8219
400.	65.750	52.852	6101.	-37.600	17.8813
450.	70.379	60.871	9507.	-39.744	17.9407
500.	74.319	68.496	13127.	-42.241	18.0002
(2 sigma)	0.442	0.155	51.	0.099	0.3905
550.	77.718	75.742	16930.	-44.960	18.0596
583.550	79.751	80.405	19572.	-46.864	18.0995
boehmite					
583.550	101.938	104.866	33847.	-46.864	20.3931
600.	103.357	107.720	35536.	-48.494	20.4426
650.	107.403	116.155	40806.	-53.376	20.5929
700.	111.098	124.251	46270.	-58.152	20.7432
750.	114.498	132.034	51911.	-62.819	20.8936
(2 sigma)	1.176	0.880	1083.	1.303	1.1698
800.	117.645	139.525	57716.	-67.381	21.0439
850.	120.576	146.746	63672.	-71.838	21.1942
900.	123.320	153.717	69770.	-76.195	21.3446
950.	125.900	160.454	76001.	-80.453	21.4949
1000.	128.336	166.975	82358.	-84.617	21.6452
(2 sigma)	1.496	1.127	1209.	1.048	1.8101

Table 15. Thermochemical properties of stable phases with the composition Al₂O₃H at 1.01325 bars (1 atm). Columns 2 through 4 give the thermochemical values relative to the elements; columns 5 through 7 give the values relative to the oxides.

T K	Formation from the Elements			Formation from the Oxides		
	H J/mol	G J/mol	log K	H J/mol	G J/mol	log K
diaspore						
200.	-997816.	-946920.	247.310	-16465.	-13671.	3.570
250.	-999077.	-934042.	195.157	-17947.	-12795.	2.673
(2 sigma)	---	---	---	406.	403.	0.084
273.150	-999533.	-927998.	177.462	-18555.	-12290.	2.350
298.150	-999944.	-921432.	161.431	-19171.	-11689.	2.048
(2 sigma)	---	---	---	406.	403.	0.071
300.	-999971.	-920945.	160.351	-19215.	-11643.	2.027
350.	-1000563.	-907723.	135.470	-20351.	-10289.	1.536
400.	-1000910.	-894434.	116.801	-41263.	-7330.	0.957
450.	-1001058.	-881114.	102.277	-41179.	-3092.	0.359
500.	-1001042.	-867786.	90.657	-41019.	1132.	-0.118
(2 sigma)	---	---	---	414.	401.	0.042
550.	-1000894.	-854467.	81.150	-40791.	5336.	-0.507
583.550	-1000733.	-845540.	75.686	-40604.	8145.	-0.729
boehmite						
583.550	-986459.	-845540.	75.686	-26330.	8145.	-0.729
600.	-985995.	-841574.	73.265	-25860.	9110.	-0.793
650.	-984484.	-829599.	66.667	-24349.	11964.	-0.961
700.	-982836.	-817745.	61.021	-22720.	14697.	-1.097
750.	-981063.	-806014.	56.136	-20980.	17309.	-1.206
(2 sigma)	---	---	---	1085.	979.	0.068
800.	-979198.	-794404.	51.869	-19137.	19802.	-1.293
850.	-977240.	-782914.	48.112	-17195.	22177.	-1.363
900.	-975207.	-771542.	44.779	-15160.	24435.	-1.418
950.	-983740.	-759960.	41.786	-13038.	26577.	-1.461
1000.	-981455.	-748241.	39.084	-10831.	28605.	-1.494
(2 sigma)	---	---	---	1210.	1049.	0.055

Table 16. Thermophysical values for boehmite, AlOOH, at 1.01325 bars (1 atm). The tabulations are based on a fit of the thermophysical and thermochemical data given in Section 1.5.5.

T K	C _p J/(mol K)	S J/(mol K)	H-H(298) J/mol	[G-H(298)]/T J/(mol K)	cm ³ /mol
200.	42.915	26.848	-5383.	-53.761	19.2399
250.	55.388	37.806	-2916.	-49.469	19.3902
(2 sigma)	0.160	0.541	9.	0.540	0.1823
273.150	60.436	42.934	-1574.	-48.698	19.4598
298.150	65.427	48.446	0.	-48.446	19.5350
(2 sigma)	0.234	0.540	0.	0.540	0.1338
300.	65.779	48.852	121.	-48.447	19.5406
350.	74.488	59.664	3634.	-49.281	19.6909
400.	81.897	70.107	7549.	-51.236	19.8412
450.	88.300	80.132	11807.	-53.893	19.9916
500.	93.911	89.731	16365.	-57.001	20.1419
(2 sigma)	0.910	0.608	116.	0.542	0.5361
550.	98.890	98.920	21188.	-60.397	20.2922
600.	103.357	107.720	26246.	-63.977	20.4426
650.	107.403	116.155	31516.	-67.668	20.5929
700.	111.098	124.251	36980.	-71.422	20.7432
750.	114.498	132.034	42621.	-75.206	20.8936
(2 sigma)	1.176	0.880	377.	0.575	1.1698
800.	117.645	139.525	48426.	-78.993	21.0439
850.	120.576	146.746	54382.	-82.767	21.1942
900.	123.320	153.717	60480.	-86.516	21.3446
950.	125.900	160.454	66712.	-90.232	21.4949
1000.	128.336	166.975	73068.	-93.907	21.6452
(2 sigma)	1.496	1.127	647.	0.647	1.8101

Table 17. Thermochemical properties of boehmite, AlOOH, at 1.01325 bars (1 atm). Columns 2 through 4 give the thermochemical values relative to the elements; columns 5 through 7 give the values relative to the oxides.

T K	Formation from the Elements			Formation from the Oxides		
	H J/mol	G J/mol	log K	H J/mol	G J/mol	log K
200.	-989536.	-940450.	245.620	-8185.	-7201.	1.881
250.	-990329.	-928076.	193.911	-9199.	-6829.	1.427
(2 sigma)	---	---	---	1006.	976.	0.204
273.150	-990536.	-922302.	176.372	-9558.	-6593.	1.261
298.150	-990654.	-916050.	160.488	-9881.	-6307.	1.105
(2 sigma)	---	---	---	1006.	973.	0.170
300.	-990659.	-915587.	159.418	-9902.	-6285.	1.094
350.	-990587.	-903076.	134.777	-10374.	-5642.	0.842
400.	-990173.	-890599.	116.300	-30526.	-3494.	0.456
450.	-989468.	-878192.	101.938	-29590.	-170.	0.020
500.	-988514.	-865877.	90.457	-28491.	3042.	-0.318
(2 sigma)	---	---	---	1016.	965.	0.101
550.	-987347.	-853668.	81.075	-27244.	6136.	-0.583
600.	-985995.	-841574.	73.265	-25860.	9110.	-0.793
650.	-984484.	-829599.	66.667	-24349.	11964.	-0.961
700.	-982836.	-817745.	61.021	-22720.	14697.	-1.097
750.	-981068.	-806014.	56.136	-20980.	17309.	-1.206
(2 sigma)	---	---	---	1085.	979.	0.068
800.	-979198.	-794404.	51.869	-19137.	19802.	-1.293
850.	-977240.	-782914.	48.112	-17195.	22177.	-1.363
900.	-975207.	-771542.	44.779	-15160.	24435.	-1.418
950.	-983740.	-759960.	41.786	-13038.	26577.	-1.461
1000.	-981455.	-748241.	39.084	-10831.	28605.	-1.494
(2 sigma)	---	---	---	1210.	1049.	0.055

Table 18. Thermophysical values for diaspor, AlOOH, at 1.01325 bars (1 atm). The tabulations are based on a fit of the thermophysical and thermochemical data given in Section 1.5.5.

T K	C _p J/(mol K)	S J/(mol K)	H-H(298) J/mol	[G-H(298)]/T J/(mol K)	cm ³ /mol
200.	34.372	17.801	-4373.	-39.664	17.6435
250.	45.103	26.675	-2374.	-36.172	17.7030
(2 sigma)	0.108	0.099	5.	0.097	0.1664
273.150	49.230	30.852	-1281.	-35.544	17.7305
298.150	53.214	35.339	0.	-35.339	17.7602
(2 sigma)	0.114	0.097	0.	0.097	0.1333
300.	53.491	35.669	99.	-35.340	17.7624
350.	60.222	44.438	2947.	-36.017	17.8219
400.	65.750	52.852	6101.	-37.600	17.8813
450.	70.379	60.871	9507.	-39.744	17.9407
500.	74.319	68.496	13127.	-42.241	18.0002
(2 sigma)	0.442	0.155	51.	0.099	0.3905
500.	77.718	75.742	16930.	-44.960	18.0596
600.	80.684	82.635	20892.	-47.815	18.1191
650.	83.297	89.198	24993.	-50.747	18.1785
700.	85.618	95.458	29217.	-53.719	18.2380
750.	87.693	101.437	33551.	-56.703	18.2974
(2 sigma)	0.722	0.355	191.	0.132	0.8449
800.	89.562	107.157	37983.	-59.679	18.3569
850.	91.253	112.638	42504.	-62.634	18.4163
900.	92.791	117.898	47106.	-65.559	18.4758
950.	94.195	122.954	51781.	-68.447	18.5352
1000.	95.483	127.818	56523.	-71.295	18.5946
(2 sigma)	1.105	0.561	386.	0.201	1.3083

Table 19. Thermochemical properties of diaspore, AlOOH, at 1.01325 bars (1 atm). Columns 2 through 4 give the thermochemical values relative to the elements; columns 5 through 7 give the values relative to the oxides.

T K	Formation from the Elements			Formation from the Oxides		
	H J/mol	G J/mol	log K	H J/mol	G J/mol	log K
200.	-997816.	-946920.	247.310	-16465.	-13671.	3.570
250.	-999077.	-934042.	195.157	-17947.	-12795.	2.673
(2 sigma)	---	---	---	406.	403.	0.084
273.150	-999533.	-927998.	177.462	-18555.	-12290.	2.350
298.150	-999944.	-921432.	161.431	-19171.	-11689.	2.048
(2 sigma)	---	---	---	406.	403.	0.071
300.	-999971.	-920945.	160.351	-19215.	-11643.	2.027
350.	-1000563.	-907723.	135.470	-20351.	-10289.	1.536
400.	-1000910.	-894434.	116.801	-41263.	-7330.	0.957
450.	-1001058.	-881114.	102.277	-41179.	-3092.	0.359
500.	-1001042.	-867786.	90.657	-41019.	1132.	-0.118
(2 sigma)	---	---	---	414.	401.	0.042
550.	-1000894.	-854467.	81.150	-40791.	5336.	-0.507
600.	-1000639.	-841166.	73.230	-40503.	9518.	-0.829
650.	-1000298.	-827890.	66.530	-40162.	13673.	-1.099
700.	-999889.	-814643.	60.789	-39773.	17799.	-1.328
750.	-999429.	-801427.	55.816	-39341.	21897.	-1.525
(2 sigma)	---	---	---	463.	401.	0.028
800.	-998931.	-788243.	51.467	-38869.	25964.	-1.695
850.	-998408.	-775091.	47.631	-38363.	30001.	-1.844
900.	-997871.	-761970.	44.224	-37825.	34007.	-1.974
950.	-1007960.	-748555.	41.158	-37258.	37982.	-2.088
1000.	-1007290.	-734919.	38.388	-36665.	41927.	-2.190
(2 sigma)	---	---	---	579.	426.	0.022

Table 20. Thermophysical values for gibbsite, $\text{Al}(\text{OH})_3$, at 1.01325 bars (1 atm). The tabulations are based on a fit of the thermophysical and thermochemical data given in Section 1.5.5.

T K	C_p J/(mol K)	S J/(mol K)	H-H(298) J/mol	[G-H(298)]/T J/(mol K)	v cm^3/mol
200.	60.817	38.082	-7564.	-75.900	31.9033
250.	77.745	53.518	-4089.	-69.874	31.9301
(2 sigma)	0.091	0.361	5.	0.360	0.0774
273.150	84.744	60.712	-2207.	-68.793	31.9426
298.150	91.756	68.440	0.	-68.440	31.9560
(2 sigma)	0.151	0.360	0.	0.360	0.0772
300.	92.254	69.009	170.	-68.442	31.9570
350.	104.736	84.190	5102.	-69.612	31.9839
400.	115.626	98.903	10617.	-72.359	32.0107
450.	125.273	113.089	16644.	-76.102	32.0376
500.	133.936	126.744	23128.	-80.487	32.0645
(2 sigma)	0.837	0.435	102.	0.363	0.0814
550.	141.813	139.884	30025.	-85.294	32.0913
600.	149.049	152.538	37299.	-90.373	32.1182
650.	155.758	164.737	44921.	-95.627	32.1450
700.	162.026	176.511	52867.	-100.987	32.1719
750.	167.923	187.893	61117.	-106.403	32.1988
(2 sigma)	1.419	0.759	370.	0.402	0.0966
800.	173.504	198.910	69654.	-111.842	32.2256
850.	178.812	209.589	78463.	-117.280	32.2525
900.	183.884	219.955	87532.	-122.697	32.2794
950.	188.750	230.028	96848.	-128.082	32.3062
1000.	193.434	239.829	106404.	-133.426	32.3331
(2 sigma)	2.308	1.161	774.	0.501	0.1188

Table 21. Thermochemical properties of gibbsite, $\text{Al}(\text{OH})_3$, at 1.01325 bars (1 atm). Columns 2 through 4 give the thermochemical values relative to the elements, columns 5 through 7 give the values relative to the oxides.

T K	Formation from the Elements			Formation from the Oxides		
	H J/mol	G J/mol	log K	H J/mol	G J/mol	log K
200.	-1291535.	-1201456.	313.788	-20890.	-14411.	3.764
250.	-1293406.	-1178707.	246.277	-24886.	-12310.	2.572
(2 sigma)	---	---	---	620.	627.	0.131
273.150	-1294065.	-1168055.	223.368	-26474.	-11074.	2.118
298.150	-1294633.	-1156496.	202.613	-28052.	-9593.	1.681
(2 sigma)	---	---	---	620.	630.	0.110
300.	-1294669.	-1155639.	201.214	-28164.	-9478.	1.650
350.	-1295369.	-1132404.	169.002	-30977.	-6136.	0.916
400.	-1295566.	-1109104.	144.834	-93054.	1936.	-0.253
450.	-1295318.	-1085807.	126.037	-92071.	13754.	-1.597
500.	-1294677.	-1062559.	111.005	-90793.	25447.	-2.658
(2 sigma)	---	---	---	629.	646.	0.068
550.	-1293685.	-1039393.	98.713	-89242.	36998.	-3.514
600.	-1292380.	-1016331.	88.479	-87440.	48396.	-4.213
650.	-1290792.	-993389.	79.830	-85405.	59635.	-4.792
700.	-1288949.	-970580.	72.425	-83151.	70709.	-5.276
750.	-1286872.	-947910.	66.018	-80691.	81614.	-5.684
(2 sigma)	---	---	---	722.	690.	0.048
800.	-1284584.	-925386.	60.421	-78035.	92349.	-6.030
850.	-1282102.	-903011.	55.492	-75192.	102912.	-6.324
900.	-1279441.	-880788.	51.120	-72171.	113302.	-6.576
950.	-1287246.	-858393.	47.198	-68978.	123520.	-6.792
1000.	-1284135.	-835901.	43.663	-65619.	133565.	-6.977
(2 sigma)	---	---	---	992.	798.	0.042

Table 22. Thermophysical values for corundum, Al_2O_3 , at 1.01325 bars (1 atm). The tabulations are based on a fit of the thermophysical and thermochemical data given in Section 1.5.5.

T K	Cp J/(mol K)	S. J/(mol K)	H-H(298) J/mol	[G-H(298)]/T J/(mol K)	v^3 cm ³ /mol
200.	50.491	24.844	-6509.	-57.386	25.5339
250.	67.336	38.033	-3538.	-52.183	25.5667
(2 sigma)	---	---	---	---	---
273.150	73.389	44.267	-1907.	-51.248	25.5819
298.150	79.030	50.943	0.	-50.943	25.5983
(2 sigma)	---	---	---	---	---
300.	79.416	51.433	147.	-50.945	25.5995
350.	88.490	64.388	4354.	-51.947	25.6323
400.	95.532	76.682	8962.	-54.278	25.6650
450.	101.132	88.270	13884.	-57.417	25.6978
500.	105.668	99.168	19057.	-61.053	25.7306
(2 sigma)	---	---	---	---	---
550.	109.397	109.420	24437.	-64.989	25.7634
600.	112.500	119.075	29987.	-69.098	25.7961
650.	115.108	128.186	35679.	-73.296	25.8289
700.	117.319	136.800	41491.	-77.527	25.8617
750.	119.209	144.960	47405.	-81.753	25.8945
(2 sigma)	---	---	---	---	---
800.	120.835	152.707	53407.	-85.948	25.9273
850.	122.244	160.076	59485.	-90.093	25.9600
900.	123.473	167.098	65629.	-94.178	25.9928
950.	124.552	173.804	71830.	-98.193	26.0256
1000.	125.506	180.217	78082.	-102.135	26.0584
(2 sigma)	---	---	---	---	---
1050.	126.356	186.362	84379.	-106.001	26.0911
1100.	127.118	192.258	90716.	-109.789	26.1239
1150.	127.809	197.924	97089.	-113.498	26.1567
1200.	128.439	203.377	103496.	-117.130	26.1895
1250.	129.021	208.632	109933.	-120.686	26.2222
(2 sigma)	---	---	---	---	---
1300.	129.563	213.703	116397.	-124.166	26.2550
1350.	130.073	218.602	122888.	-127.574	26.2878
1400.	130.559	223.341	129404.	-130.910	26.3206
1450.	131.026	227.931	135944.	-134.177	26.3533
1500.	131.481	232.381	142507.	-137.376	26.3861
(2 sigma)	---	---	---	---	---
1550.	131.928	236.699	149092.	-140.511	26.4189
1600.	132.372	240.895	155699.	-143.583	26.4517
1650.	132.815	244.975	162329.	-146.594	26.4844
1700.	133.262	248.947	168981.	-149.546	26.5172
1750.	133.717	252.816	175655.	-152.442	26.5500
(2 sigma)	---	---	---	---	---
1800.	134.180	256.589	182353.	-155.282	26.5828
(2 sigma)	---	---	---	---	---

Table 23. Thermochemical properties of corundum, Al_2O_3 , at 1.01325 bars (1 atm). Columns 2 through 4 give the thermochemical values relative to the elements; columns 5 through 7 give the values relative to the oxides.

T K	Formation from the Elements			Formation from the Oxides		
	H J/mol	G J/mol	log K	H J/mol	G J/mol	log K
200.	-1673409.	-1612703.	421.195	0.0	0.0	0.0
250.	-1674870.	-1597344.	333.746	0.0	0.0	0.0
(2 sigma)	---	---	---	0.0	0.0	0.0
273.150	-1675343.	-1590143.	304.084	0.0	0.0	0.0
298.150	-1675738.	-1582326.	277.217	0.0	0.0	0.0
(2 sigma)	---	---	---	0.0	0.0	0.0
300.	-1675763.	-1581747.	275.406	0.0	0.0	0.0
350.	-1676247.	-1566034.	233.718	0.0	0.0	0.0
400.	-1676430.	-1550274.	202.445	0.0	0.0	0.0
450.	-1676390.	-1534505.	178.121	0.0	0.0	0.0
500.	-1676186.	-1518749.	158.663	0.0	0.0	0.0
(2 sigma)	---	---	---	0.0	0.0	0.0
550.	-1675866.	-1503020.	142.745	0.0	0.0	0.0
600.	-1675467.	-1487324.	129.483	0.0	0.0	0.0
650.	-1675020.	-1471664.	118.264	0.0	0.0	0.0
700.	-1674551.	-1456038.	108.651	0.0	0.0	0.0
750.	-1674083.	-1440447.	100.322	0.0	0.0	0.0
(2 sigma)	---	---	---	0.0	0.0	0.0
800.	-1673635.	-1424886.	93.035	0.0	0.0	0.0
850.	-1673225.	-1409352.	86.608	0.0	0.0	0.0
900.	-1672869.	-1393840.	80.896	0.0	0.0	0.0
950.	-1693839.	-1377699.	75.751	0.0	0.0	0.0
1000.	-1693359.	-1361073.	71.095	0.0	0.0	0.0
(2 sigma)	---	---	---	0.0	0.0	0.0
1050.	-1692852.	-1344471.	66.884	0.0	0.0	0.0
1100.	-1692323.	-1327894.	63.056	0.0	0.0	0.0
1150.	-1691774.	-1311341.	59.563	0.0	0.0	0.0
1200.	-1691207.	-1294812.	56.362	0.0	0.0	0.0
1250.	-1690624.	-1278308.	53.418	0.0	0.0	0.0
(2 sigma)	---	---	---	0.0	0.0	0.0
1300.	-1690026.	-1261827.	50.701	0.0	0.0	0.0
1350.	-1689413.	-1245369.	48.186	0.0	0.0	0.0
1400.	-1688787.	-1228935.	45.852	0.0	0.0	0.0
1450.	-1688146.	-1212523.	43.680	0.0	0.0	0.0
1500.	-1687492.	-1196133.	41.653	0.0	0.0	0.0
(2 sigma)	---	---	---	0.0	0.0	0.0
1550.	-1686823.	-1179765.	39.758	0.0	0.0	0.0
1600.	-1686139.	-1163420.	37.982	0.0	0.0	0.0
1650.	-1685439.	-1147095.	36.314	0.0	0.0	0.0
1700.	-1684723.	-1130793.	34.745	0.0	0.0	0.0
1750.	-1683988.	-1114511.	33.266	0.0	0.0	0.0
(2 sigma)	---	---	---	0.0	0.0	0.0
1800.	-1683234.	-1098251.	31.870	0.0	0.0	0.0
(2 sigma)	---	---	---	0.0	0.0	0.0

Table 24. Thermophysical values for stable phases with the composition Al_2SiO_5 at 1.01325 bars (1 atm). The tabulations are based on a fit of the thermophysical and thermochemical data given in Section 1.5.5.

T K	Cp J/(mol K)	S J/(mol K)	H-H(298) J/mol	[G-H(298)]/T J/(mol K)	cm^3V /mol
kyanite					
200.	80.961	41.807	-10116.	-92.388	44.1175
250.	104.208	62.455	-5468.	-84.326	44.1618
(2 sigma)	0.145	0.303	6.	0.303	0.0306
273.150	113.385	72.091	-2947.	-82.881	44.1833
298.150	122.219	82.410	0.	-82.410	44.2071
(2 sigma)	0.121	0.302	0.	0.302	0.0229
300.	122.831	83.168	227.	-82.413	44.2089
350.	137.448	103.246	6748.	-83.965	44.2584
400.	148.930	122.380	13919.	-87.581	44.3098
408.450	150.616	125.511	15185.	-88.334	44.3187
andalusite					
408.450	150.075	134.690	18934.	-88.334	51.6899
450.	156.958	149.568	25317.	-93.307	51.7443
500.	163.667	166.465	33339.	-99.787	51.8128
(2 sigma)	0.294	0.353	421.	0.653	0.0222
550.	169.038	182.326	41662.	-106.577	51.8841
600.	173.382	197.227	50226.	-113.517	51.9578
650.	176.937	211.250	58987.	-120.500	52.0335
700.	179.886	224.473	67910.	-127.459	52.1109
750.	182.375	236.971	76968.	-134.347	52.1898
(2 sigma)	0.313	0.377	433.	0.408	0.0230
800.	184.520	248.811	86141.	-141.135	52.2699
850.	186.413	260.056	95416.	-147.802	52.3511
900.	188.131	270.760	104780.	-154.338	52.4331
942.450	189.500	279.462	112795.	-159.779	52.5033
sillimanite					
942.450	189.991	283.311	116423.	-159.779	50.4826
950.	190.273	284.828	117858.	-160.767	50.4892
1000.	192.164	294.636	127419.	-167.217	50.5332
(2 sigma)	0.452	0.368	391.	0.372	0.0109
1050.	194.126	304.059	137076.	-173.510	50.5777
1100.	196.204	313.137	146834.	-179.652	50.6225
1150.	198.433	321.907	156699.	-185.647	50.6676
1200.	200.847	330.403	166680.	-191.503	50.7130
1250.	203.472	338.654	176787.	-197.225	50.7586
(2 sigma)	0.892	0.380	409.	0.337	0.0170
1300.	206.334	346.689	187031.	-202.819	50.8044
1350.	209.453	354.534	197425.	-208.294	50.8503
1400.	212.848	362.212	207981.	-213.654	50.8964
1450.	216.535	369.745	218714.	-218.907	50.9425
1500.	220.529	377.152	229640.	-224.059	50.9888
(2 sigma)	2.830	0.474	609.	0.320	0.0303
1550.	224.842	384.452	240773.	-229.115	51.0351
1600.	229.488	391.663	252129.	-234.082	51.0816
1650.	234.475	398.800	263727.	-238.966	51.1280
1700.	239.813	405.879	275583.	-243.771	51.1746
1750.	245.511	412.912	287714.	-248.503	51.2211
(2 sigma)	6.160	1.001	1568.	0.321	0.0456
1800.	251.576	419.912	300140.	-253.168	51.2677
(2 sigma)	6.994	1.171	1882.	0.327	0.0488

Table 25. Thermochemical properties of stable phases with the composition Al_2SiO_5 at 1.01325 bars (1 atm). Columns 2 through 4 give the thermochemical values relative to the elements; columns 5 through 7 give the values relative to the oxides.

T K	Formation from the Elements			Formation from the Oxides		
	H J/mol	G J/mol	log K	H J/mol	G J/mol	log K
kyanite						
200.	-2592988.	-2494666.	651.539	-9699.	-7887.	2.060
250.	-2595078.	-2469826.	516.041	-9834.	-7419.	1.550
(2 sigma)	---	---	---	520.	491.	0.103
273.150	-2595769.	-2458195.	470.082	-9891.	-7193.	1.375
298.150	-2596346.	-2445577.	428.455	-9937.	-6944.	1.217
(2 sigma)	---	---	---	520.	487.	0.085
300.	-2596382.	-2444641.	425.650	-9940.	-6925.	1.206
350.	-2597064.	-2419289.	361.059	-9986.	-6418.	0.958
400.	-2597272.	-2393874.	312.608	-9987.	-5908.	0.772
408.450	-2597269.	-2389577.	305.591	-9985.	-5822.	0.745
andalusite						
408.450	-2593520.	-2389577.	305.591	-6236.	-5822.	0.745
450.	-2593410.	-2368835.	274.967	-6252.	-5779.	0.671
500.	-2593070.	-2343898.	244.865	-6303.	-5724.	0.598
(2 sigma)	---	---	---	504.	438.	0.046
550.	-2592568.	-2319004.	220.241	-6401.	-5662.	0.538
600.	-2591961.	-2294161.	199.724	-6558.	-5589.	0.487
650.	-2591291.	-2269371.	182.369	-6781.	-5499.	0.442
700.	-2590596.	-2244634.	167.497	-7077.	-5390.	0.402
750.	-2589901.	-2219947.	154.611	-7447.	-5257.	0.366
(2 sigma)	---	---	---	512.	429.	0.030
800.	-2589230.	-2195306.	143.339	-7892.	-5097.	0.333
850.	-2588602.	-2170705.	133.395	-9121.	-4902.	0.301
900.	-2588029.	-2146140.	124.559	-9286.	-4649.	0.270
942.450	-2608884.	-2124834.	117.767	-9425.	-4427.	0.245
sillimanite						
942.450	-2605257.	-2124834.	117.767	-5798.	-4427.	0.245
950.	-2605150.	-2120986.	116.620	-5818.	-4416.	0.243
1000.	-2604413.	-2095523.	109.459	-5945.	-4339.	0.227
(2 sigma)	---	---	---	550.	489.	0.026
1050.	-2603620.	-2070097.	102.982	-6045.	-4256.	0.212
1100.	-2602765.	-2044711.	97.095	-6110.	-4169.	0.198
1150.	-2601836.	-2019366.	91.722	-6128.	-4080.	0.185
1200.	-2600825.	-1994062.	86.799	-6089.	-3992.	0.174
1250.	-2599718.	-1968803.	82.272	-5979.	-3906.	0.163
(2 sigma)	---	---	---	562.	516.	0.022
1300.	-2598503.	-1943590.	78.094	-5785.	-3827.	0.154
1350.	-2597165.	-1918426.	74.228	-5494.	-3757.	0.145
1400.	-2595688.	-1893314.	70.640	-5089.	-3699.	0.138
1450.	-2594057.	-1868258.	67.302	-4556.	-3659.	0.132
1500.	-2592254.	-1843260.	64.188	-3880.	-3639.	0.127
(2 sigma)	---	---	---	711.	556.	0.019
1550.	-2590263.	-1818326.	61.277	-3043.	-3644.	0.123
1600.	-2588065.	-1793459.	58.550	-2030.	-3679.	0.120
1650.	-2585642.	-1768665.	55.991	-824.	-3749.	0.119
1700.	-2533484.	-1743497.	53.571	594.	-3858.	0.119
1750.	-2630411.	-1717365.	51.261	2239.	-4013.	0.120
(2 sigma)	---	---	---	1601.	621.	0.019
1800.	-2627049.	-1691325.	49.081	4131.	-4218.	0.122
(2 sigma)	---	---	---	1907.	645.	0.019

Table 26. Thermophysical values for andalusite, Al_2SiO_5 , at 1.01325 bars (1 atm). The tabulations are based on a fit of the thermophysical and thermochemical data given in Section 1.5.5.

T K	Cp J/(mol K)	S J/(mol K)	H-H(298) J/mol	[G-H(298)]/T J/(mol K)	V cm ³ /mol
200.	83.694	50.069	-10312.	-101.630	51.4657
250.	106.213	71.256	-5544.	-93.432	51.5103
(2 sigma)	0.149	0.346	6.	0.345	0.0226
273.150	114.981	81.052	-2982.	-91.968	51.5332
298.150	123.374	91.492	0.	-91.492	51.5593
(2 sigma)	0.129	0.345	0.	0.345	0.0155
300.	123.954	92.257	229.	-91.494	51.5613
350.	137.744	112.444	6786.	-93.057	51.6179
400.	148.501	131.569	13953.	-96.687	51.6791
450.	156.958	149.568	21598.	-101.573	51.7443
500.	163.667	166.465	29620.	-107.226	51.8128
(2 sigma)	0.294	0.353	35.	0.345	0.0222
550.	169.038	182.326	37942.	-113.340	51.8841
600.	173.382	197.227	46506.	-119.716	51.9578
650.	176.937	211.250	55267.	-126.223	52.0335
700.	179.886	224.473	64190.	-132.773	52.1109
750.	182.375	236.971	73248.	-139.307	52.1898
(2 sigma)	0.313	0.377	88.	0.348	0.0230
800.	184.520	248.811	82422.	-145.784	52.2699
850.	186.413	260.056	91696.	-152.178	52.3511
900.	188.131	270.760	101060.	-158.471	52.4331
950.	189.737	280.975	110507.	-164.652	52.5158
1000.	191.283	290.747	120033.	-170.714	52.5992
(2 sigma)	0.517	0.387	133.	0.351	0.0189
1050.	192.814	300.117	129635.	-176.655	52.6831
1100.	194.366	309.122	139314.	-182.473	52.7675
1150.	195.972	317.797	149073.	-188.169	52.8523
1200.	197.659	326.173	158913.	-193.746	52.9374
1250.	199.450	334.278	168840.	-199.206	53.0227
(2 sigma)	0.603	0.399	195.	0.354	0.0312
1300.	201.366	342.137	178860.	-204.553	53.1083
1350.	203.425	349.775	188979.	-209.790	53.1941
1400.	205.643	357.213	199205.	-214.923	53.2800
1450.	208.034	364.470	209546.	-219.955	53.3661
1500.	210.609	371.566	220012.	-224.891	53.4523
(2 sigma)	1.993	0.420	300.	0.357	0.0538
1550.	213.381	378.516	230611.	-229.735	53.5386
1600.	216.358	385.337	241353.	-234.491	53.6250
1650.	219.549	392.043	252250.	-239.164	53.7115
1700.	222.962	398.647	263312.	-243.758	53.7980
1750.	226.605	405.163	274550.	-248.277	53.8846
(2 sigma)	4.807	0.723	1013.	0.361	0.0796
1800.	230.484	411.600	285976.	-252.724	53.9712
(2 sigma)	5.534	0.845	1259.	0.364	0.0849

Table 27. Thermochemical properties of andalusite, Al_2SiO_5 , at 1.01325 bars (1 atm). Columns 2 through 4 give the thermochemical values relative to the elements; columns 5 through 7 give the values relative to the oxides.

T K	Formation from the Elements			Formation from the Oxides		
	H J/mol	G J/mol	log K	H J/mol	G J/mol	log K
200.	-2589464.	-2492795.	651.051	-6176.	-6016.	1.571
250.	-2591434.	-2468382.	515.740	-6190.	-5976.	1.249
(2 sigma)	---	---	---	500.	462.	0.097
273.150	-2592084.	-2456957.	469.845	-6205.	-5955.	1.139
298.150	-2592626.	-2444564.	428.277	-6217.	-5932.	1.039
(2 sigma)	---	---	---	500.	456.	0.080
300.	-2592660.	-2443645.	425.476	-6218.	-5930.	1.032
350.	-2593307.	-2418752.	360.979	-6229.	-5881.	0.878
400.	-2593519.	-2393796.	312.598	-6234.	-5831.	0.761
450.	-2593410.	-2368835.	274.967	-6252.	-5779.	0.671
500.	-2593070.	-2343898.	244.865	-6303.	-5724.	0.598
(2 sigma)	---	---	---	504.	438.	0.046
550.	-2592568.	-2319004.	220.241	-6401.	-5662.	0.538
600.	-2591961.	-2294161.	199.724	-6558.	-5589.	0.487
650.	-2591291.	-2269371.	182.369	-6781.	-5499.	0.442
700.	-2590596.	-2244634.	167.497	-7077.	-5390.	0.402
750.	-2589901.	-2219947.	154.611	-7447.	-5257.	0.366
(2 sigma)	---	---	---	512.	429.	0.030
800.	-2589230.	-2195306.	143.339	-7892.	-5097.	0.333
850.	-2588602.	-2170705.	133.395	-9121.	-4902.	0.301
900.	-2588029.	-2146140.	124.559	-9286.	-4649.	0.270
950.	-2608781.	-2120957.	116.618	-9450.	-4387.	0.241
1000.	-2608080.	-2095300.	109.447	-9611.	-4116.	0.215
(2 sigma)	---	---	---	518.	440.	0.023
1050.	-2607341.	-2069679.	102.961	-9766.	-3837.	0.191
1100.	-2606564.	-2044094.	97.066	-9909.	-3552.	0.169
1150.	-2605743.	-2018546.	91.685	-10034.	-3260.	0.148
1200.	-2604872.	-1993034.	86.754	-10136.	-2963.	0.129
1250.	-2603945.	-1967559.	82.220	-10206.	-2663.	0.111
(2 sigma)	---	---	---	533.	470.	0.020
1300.	-2602954.	-1942123.	78.035	-10237.	-2360.	0.095
1350.	-2601890.	-1916727.	74.163	-10219.	-2057.	0.080
1400.	-2600744.	-1891371.	70.568	-10145.	-1756.	0.066
1450.	-2599505.	-1866058.	67.223	-10004.	-1459.	0.053
1500.	-2598162.	-1840789.	64.102	-9788.	-1168.	0.041
(2 sigma)	---	---	---	583.	517.	0.018
1550.	-2596705.	-1815567.	61.184	-9485.	-885.	0.030
1600.	-2595121.	-1790394.	58.450	-9086.	-614.	0.020
1650.	-2593399.	-1765272.	55.884	-8581.	-357.	0.011
1700.	-2642035.	-1739755.	53.456	-7957.	-116.	0.004
1750.	-2639855.	-1713249.	51.138	-7205.	104.	-0.003
(2 sigma)	---	---	---	1139.	578.	0.017
1800.	-2637493.	-1686808.	48.950	-6313.	300.	-0.009
(2 sigma)	---	---	---	1367.	595.	0.017

Table 23. Thermophysical values for kyanite, Al_2SiO_5 , at 1.01325 bars (1 atm). The tabulations are based on a fit of the thermophysical and thermochemical data given in Section 1.5.5.

T K	Cp J/(mol K)	S J/(mol K)	H-H(298) J/mol	[G-H(298)]/T J/(mol K)	V cm ³ /mol
200.	80.961	41.807	-10116.	-92.388	44.1175
250.	104.208	62.455	-5468.	-84.326	44.1618
(2 sigma)	0.145	0.303	6.	0.303	0.0306
273.150	113.385	72.091	-2947.	-82.681	44.1833
298.150	122.219	82.410	0.	-82.410	44.2071
(2 sigma)	0.121	0.302	0.	0.302	0.0229
300.	122.831	83.168	227.	-82.413	44.2089
350.	137.448	103.246	6748.	-83.965	44.2584
400.	148.930	122.380	13919.	-87.581	44.3098
450.	158.009	140.466	21602.	-92.462	44.3630
500.	165.247	157.503	29690.	-98.123	44.4175
(2 sigma)	0.307	0.311	38.	0.302	0.0173
550.	171.070	173.535	38103.	-104.257	44.4733
600.	175.801	188.630	46779.	-110.666	44.5301
650.	179.689	202.860	55669.	-117.216	44.5878
700.	182.926	216.299	64737.	-123.818	44.6461
750.	185.667	229.015	73953.	-130.411	44.7052
(2 sigma)	0.351	0.332	89.	0.304	0.0158
800.	188.032	241.075	83297.	-136.954	44.7647
850.	190.121	252.538	92752.	-143.418	44.8247
900.	192.015	263.460	102306.	-149.786	44.8850
950.	193.780	273.889	111951.	-156.046	44.9457
1000.	195.471	283.872	121683.	-162.189	45.0067
(2 sigma)	0.534	0.339	140.	0.305	0.0144
1050.	197.137	293.449	131498.	-168.213	45.0679
1100.	198.816	302.659	141397.	-174.116	45.1292
1150.	200.543	311.534	151380.	-179.899	45.1908
1200.	202.346	320.107	161452.	-185.564	45.2524
1250.	204.251	328.406	171617.	-191.112	45.3142
(2 sigma)	0.875	0.350	194.	0.306	0.0288
1300.	206.280	336.455	181879.	-196.548	45.3761
1350.	208.451	344.281	192247.	-201.876	45.4381
1400.	210.782	351.903	202727.	-207.098	45.5001
1450.	213.297	359.343	213328.	-212.220	45.5622
1500.	215.979	366.619	224059.	-217.246	45.6244
(2 sigma)	2.969	0.452	453.	0.309	0.0500
1550.	218.871	373.747	234929.	-222.180	45.6866
1600.	221.972	380.744	245949.	-227.026	45.7488
1650.	225.293	387.625	257130.	-231.789	45.8111
1700.	228.840	394.403	268483.	-236.472	45.8734
1750.	232.623	401.090	280018.	-241.080	45.9357
(2 sigma)	6.734	1.039	1557.	0.325	0.0731
1800.	236.647	407.699	291749.	-245.517	45.9980
(2 sigma)	7.687	1.223	1908.	0.335	0.0778

Table 29. Thermochemical properties of kyanite, Al_2SiO_5 , at 1.01325 bars (1 atm). Columns 2 through 4 give the thermochemical values relative to the elements; columns 5 through 7 give the values relative to the oxides.

T K	Formation from the Elements			Formation from the Oxides		
	H J/mol	G J/mol	log K	H J/mol	G J/mol	log K
200.	-2592988.	-2494666.	651.539	-9699.	-7887.	2.060
250.	-2595078.	-2469826.	516.041	-9834.	-7419.	1.550
(2 sigma)	---	---	---	520.	491.	0.103
273.150	-2595769.	-2458195.	470.082	-9891.	-7193.	1.375
298.150	-2596346.	-2445577.	428.455	-9937.	-6944.	1.217
(2 sigma)	---	---	---	520.	487.	0.085
300.	-2596382.	-2444641.	425.650	-9940.	-6925.	1.206
350.	-2597064.	-2419289.	361.059	-9986.	-6418.	0.958
400.	-2597272.	-2393874.	312.608	-9987.	-5908.	0.772
450.	-2597126.	-2368455.	274.923	-9968.	-5399.	0.527
500.	-2596719.	-2343067.	244.778	-9953.	-4893.	0.511
(2 sigma)	---	---	---	524.	472.	0.049
550.	-2596127.	-2317729.	220.119	-9960.	-4387.	0.417
600.	-2595408.	-2292451.	199.575	-10005.	-3878.	0.338
650.	-2594609.	-2267236.	182.197	-10099.	-3364.	0.270
700.	-2593769.	-2242085.	167.306	-10250.	-2841.	0.212
750.	-2592916.	-2216995.	154.405	-10462.	-2305.	0.161
(2 sigma)	---	---	---	531.	463.	0.032
800.	-2592075.	-2191961.	143.120	-10736.	-1752.	0.114
850.	-2591265.	-2166979.	133.166	-11785.	-1176.	0.072
900.	-2590503.	-2142043.	124.321	-11759.	-652.	0.032
950.	-2611057.	-2116501.	116.373	-11725.	70.	-0.004
1000.	-2610149.	-2090495.	109.196	-11681.	689.	-0.036
(2 sigma)	---	---	---	534.	469.	0.025
1050.	-2609198.	-2064535.	102.705	-11623.	1306.	-0.066
1100.	-2608201.	-2038622.	96.806	-11547.	1920.	-0.091
1150.	-2607155.	-2012755.	91.422	-11447.	2530.	-0.116
1200.	-2606053.	-1986935.	86.489	-11317.	3135.	-0.136
1250.	-2604889.	-1961152.	81.952	-11149.	3734.	-0.156
(2 sigma)	---	---	---	546.	490.	0.020
1300.	-2603655.	-1935437.	77.767	-10937.	4326.	-0.174
1350.	-2602342.	-1909751.	73.893	-10671.	4908.	-0.190
1400.	-2600942.	-1884136.	70.298	-10343.	5479.	-0.204
1450.	-2599443.	-1858562.	66.953	-9943.	6037.	-0.217
1500.	-2597835.	-1833041.	63.832	-9461.	6580.	-0.229
(2 sigma)	---	---	---	596.	522.	0.013
1550.	-2596106.	-1807576.	60.915	-8887.	7106.	-0.239
1600.	-2594245.	-1782109.	58.182	-8210.	7611.	-0.248
1650.	-2592239.	-1756822.	55.616	-7420.	8094.	-0.256
1700.	-2640584.	-1731089.	53.190	-6506.	8550.	-0.263
1750.	-2638107.	-1704374.	50.873	-5457.	8978.	-0.268
(2 sigma)	---	---	---	1665.	585.	0.017
1800.	-2635440.	-1677734.	48.687	-4260.	9374.	-0.272
(2 sigma)	---	---	---	2003.	610.	0.013

Table 30. Thermophysical values for sillimanite, Al_2SiO_5 , at 1.01325 bars (1 atm). The tabulations are based on a fit of the thermophysical and thermochemical data given in Section 1.5.5.

T K	C_p J/(mol K)	S J/(mol K)	H-H(298) J/mol	[G-H(298)]/T J/(mol K)	V cm^3/mol
200.	86.686	53.855	-10377.	-105.738	49.9871
250.	106.536	75.362	-5539.	-97.518	50.0005
(2 sigma)	0.133	0.334	6.	0.333	0.0219
273.150	114.855	85.165	-2975.	-96.057	50.0085
298.150	123.013	95.581	0.	-95.581	50.0183
(2 sigma)	0.116	0.333	0.	0.333	0.0165
300.	123.583	96.344	228.	-95.584	50.0190
350.	137.289	116.464	6763.	-97.141	50.0419
400.	148.127	135.533	13909.	-100.760	50.0684
450.	156.678	153.493	21538.	-105.632	50.0980
500.	163.450	170.365	29547.	-111.270	50.1303
(2 sigma)	0.230	0.338	28.	0.333	0.0144
550.	168.852	186.206	37860.	-117.370	50.1648
600.	173.204	201.091	46415.	-123.733	50.2012
650.	176.760	215.100	55167.	-130.228	50.2391
700.	179.721	228.311	64081.	-136.766	50.2785
750.	182.248	240.799	73132.	-143.289	50.3190
(2 sigma)	0.345	0.351	74.	0.334	0.0143
800.	184.470	252.633	82301.	-149.757	50.3604
850.	186.492	263.878	91576.	-156.142	50.4027
900.	188.403	274.592	100948.	-162.427	50.4456
950.	190.273	284.828	110415.	-168.602	50.4892
1000.	192.164	294.636	119976.	-174.660	50.5332
(2 sigma)	0.452	0.368	139.	0.335	0.0109
1050.	194.126	304.059	129633.	-180.599	50.5777
1100.	196.204	313.137	139390.	-186.418	50.6225
1150.	198.433	321.907	149256.	-192.120	50.6676
1200.	200.847	330.403	159237.	-197.705	50.7130
1250.	203.472	338.654	169344.	-203.179	50.7586
(2 sigma)	0.892	0.380	188.	0.337	0.0170
1300.	206.334	346.689	179588.	-208.545	50.8044
1350.	209.453	354.534	189982.	-213.807	50.8503
1400.	212.848	362.212	200538.	-218.971	50.8964
1450.	216.535	369.745	211271.	-224.040	50.9425
1500.	220.529	377.152	222197.	-229.021	50.9888
(2 sigma)	2.830	0.474	458.	0.340	0.0303
1550.	224.842	384.452	233329.	-233.917	51.0351
1600.	229.488	391.663	244686.	-238.734	51.0816
1650.	234.475	398.800	256284.	-243.477	51.1280
1700.	239.813	405.879	268140.	-248.149	51.1746
1750.	245.511	412.912	280271.	-252.757	51.2211
(2 sigma)	6.160	1.001	1488.	0.353	0.0456
1800.	251.576	419.912	292697.	-257.303	51.2677
(2 sigma)	6.994	1.171	1809.	0.360	0.0488

Table 31. Thermochemical properties of sillimanite, Al_2SiO_5 , at 1.01325 bars (1 atm). Columns 2 through 4 give the thermochemical values relative to the elements; columns 5 through 7 give the values relative to the oxides.

T K	Formation from the Elements			Formation from the Oxides		
	H J/mol	G J/mol	log K	H J/mol	G J/mol	log K
200.	-2585805.	-2489893.	650.293	-2517.	-3114.	0.813
250.	-2587706.	-2465680.	515.175	-2462.	-3274.	0.684
(2 sigma)	---	---	---	537.	505.	0.106
273.150	-2588354.	-2454351.	469.347	-2475.	-3349.	0.640
298.150	-2588902.	-2442060.	427.839	-2494.	-3428.	0.601
(2 sigma)	---	---	---	537.	500.	0.088
300.	-2588937.	-2441149.	425.042	-2496.	-3433.	0.598
350.	-2589606.	-2416458.	360.636	-2528.	-3587.	0.535
400.	-2589839.	-2391702.	312.324	-2554.	-3737.	0.488
450.	-2589747.	-2366938.	274.747	-2589.	-3882.	0.451
500.	-2589418.	-2342197.	244.687	-2652.	-4023.	0.420
(2 sigma)	---	---	---	539.	485.	0.051
550.	-2588927.	-2317498.	220.097	-2760.	-4155.	0.395
600.	-2588328.	-2292848.	199.610	-2925.	-4276.	0.372
650.	-2587668.	-2268251.	182.279	-3158.	-4379.	0.352
700.	-2586981.	-2243706.	167.427	-3462.	-4462.	0.333
750.	-2586294.	-2219211.	154.559	-3840.	-4521.	0.315
(2 sigma)	---	---	---	543.	479.	0.033
800.	-2585628.	-2194760.	143.303	-4289.	-4552.	0.297
850.	-2584999.	-2170351.	133.373	-5518.	-4548.	0.279
900.	-2584417.	-2145977.	124.549	-5674.	-4486.	0.260
950.	-2605150.	-2120986.	116.620	-5818.	-4416.	0.243
1000.	-2604413.	-2095523.	109.459	-5945.	-4339.	0.227
(2 sigma)	---	---	---	550.	489.	0.026
1050.	-2603620.	-2070097.	102.982	-6045.	-4256.	0.212
1100.	-2602765.	-2044711.	97.095	-6110.	-4169.	0.198
1150.	-2601836.	-2019366.	91.722	-6128.	-4080.	0.185
1200.	-2600825.	-1994062.	86.799	-6089.	-3992.	0.174
1250.	-2599718.	-1968803.	82.272	-5979.	-3906.	0.163
(2 sigma)	---	---	---	562.	516.	0.022
1300.	-2598503.	-1943590.	78.094	-5785.	-3827.	0.154
1350.	-2597165.	-1918426.	74.228	-5494.	-3757.	0.145
1400.	-2595688.	-1893314.	70.640	-5089.	-3699.	0.138
1450.	-2594057.	-1868258.	67.302	-4556.	-3659.	0.132
1500.	-2592254.	-1843260.	64.188	-3880.	-3639.	0.127
(2 sigma)	---	---	---	711.	556.	0.019
1550.	-2590263.	-1818326.	61.277	-3043.	-3644.	0.123
1600.	-2588065.	-1793459.	58.550	-2030.	-3679.	0.120
1650.	-2585642.	-1768665.	55.991	-824.	-3749.	0.119
1700.	-2633484.	-1743497.	53.571	594.	-3858.	0.119
1750.	-2630411.	-1717365.	51.261	2239.	-4013.	0.120
(2 sigma)	---	---	---	1601.	621.	0.019
1800.	-2627049.	-1691325.	49.081	4131.	-4218.	0.122
(2 sigma)	---	---	---	1907.	645.	0.019

Table 32. Thermophysical values for kaolinite, $\text{Al}_2\text{Si}_2\text{O}_5(\text{OH})_4$, at 1.01325 bars (1 atm). The tabulations are based on a fit of the thermophysical and thermochemical data given in Section 1.5.5.

T K	Cp J/(mol K)	S J/(mol K)	H-H(298) J/mol	[G-H(298)]/T J/(mol K)	cm^3/mol
200.	174.249	120.780	-20937.	-225.465	99.1332
250.	215.518	164.291	-11149.	-208.887	99.3116
(2 sigma)	0.726	1.073	34.	1.064	0.6797
273.150	231.285	184.079	-5974.	-205.949	99.3943
298.150	246.285	204.995	0.	-204.995	99.4835
(2 sigma)	1.064	1.064	0.	1.064	0.6682
300.	247.318	206.522	457.	-205.000	99.4901
350.	271.802	246.566	13461.	-208.106	99.6686
400.	290.742	284.150	27545.	-215.289	99.8471
450.	305.433	319.280	42465.	-224.914	100.0256
500.	316.809	352.075	58033.	-236.009	100.2041
(2 sigma)	3.746	1.335	331.	1.076	0.8451
550.	325.552	382.699	74102.	-247.968	100.3826
600.	332.168	411.323	90553.	-260.402	100.5611
650.	337.039	438.114	107289.	-273.053	100.7396
700.	340.459	463.224	124232.	-285.749	100.9181
750.	342.658	486.795	141315.	-298.375	101.0965
(2 sigma)	27.539	5.362	3480.	1.275	1.3386
800.	343.819	508.952	158481.	-310.850	101.2750
850.	344.089	529.808	175682.	-323.123	101.4535
900.	343.588	549.465	192877.	-335.157	101.6320
950.	342.413	568.013	210030.	-346.929	101.8105
1000.	340.648	585.534	227108.	-358.425	101.9890
(2 sigma)	64.234	17.834	14682.	3.346	1.9222
1050.	338.360	602.101	244086.	-369.638	102.1675
1100.	335.608	617.779	260937.	-380.564	102.3460
1150.	332.441	632.629	277640.	-391.204	102.5245
1200.	328.902	646.704	294175.	-401.559	102.7029
1250.	325.026	660.053	310524.	-411.634	102.8814
(2 sigma)	107.558	36.620	36001.	7.920	2.5344

Table 33. Thermochemical properties of kaolinite, $\text{Al}_2\text{Si}_2\text{O}_5(\text{OH})_4$, at 1.01325 bars (1 atm). Columns 2 through 4 give the thermochemical values relative to the elements; columns 5 through 7 give the values relative to the oxides.

T K	Formation from the Elements			Formation from the Oxides		
	H J/mol	G J/mol	log K	H J/mol	G J/mol	log K
200.	-4124570.	-3909897.	1021.160	-45149.	-38446.	10.041
250.	-4129704.	-3855611.	805.585	-49937.	-36192.	7.562
(2 sigma)	---	---	---	1048.	964.	0.201
273.150	-4131701.	-3830138.	732.439	-51824.	-34833.	6.661
298.150	-4133616.	-3802451.	666.173	-53707.	-33194.	5.815
(2 sigma)	---	---	---	1049.	955.	0.167
300.	-4133748.	-3800396.	661.707	-53842.	-33066.	5.757
350.	-4136906.	-3744577.	558.847	-57287.	-29327.	4.377
400.	-4139383.	-3688353.	481.649	-139990.	-19309.	2.521
450.	-4141357.	-3631852.	421.574	-138920.	-4287.	0.498
500.	-4142976.	-3575151.	373.493	-137814.	10613.	-1.109
(2 sigma)	---	---	---	1124.	944.	0.099
550.	-4144363.	-3518300.	334.140	-136748.	25403.	-2.413
600.	-4145618.	-3461329.	301.335	-135786.	40101.	-3.491
650.	-4146828.	-3404255.	273.569	-134981.	54724.	-4.398
700.	-4148064.	-3347088.	249.763	-134378.	69293.	-5.171
750.	-4149389.	-3289830.	229.124	-134014.	83826.	-5.838
(2 sigma)	---	---	---	3614.	1123.	0.078
800.	-4150856.	-3232480.	211.059	-133922.	98345.	-6.421
850.	-4152512.	-3175031.	195.114	-135554.	112876.	-6.937
900.	-4154400.	-3117479.	180.934	-135240.	127480.	-7.399
950.	-4135095.	-3104120.	170.676	-135139.	142072.	-7.812
1000.	-4134636.	-3049871.	159.309	-135276.	156664.	-8.183
(2 sigma)	---	---	---	14683.	3385.	0.177
1050.	-4134371.	-2995640.	149.025	-135673.	171270.	-8.520
1100.	-4134319.	-2941417.	139.676	-136348.	185901.	-8.828
1150.	-4134500.	-2887191.	131.140	-137319.	200569.	-9.110
1200.	-4134928.	-2832952.	123.315	-138601.	215286.	-9.371
1250.	-4135619.	-2778690.	116.115	-140208.	230063.	-9.614
(2 sigma)	---	---	---	35975.	9926.	0.415

Table 34. Thermophysical values for dickite, $\text{Al}_2\text{Si}_2\text{O}_5(\text{OH})_4$, at 1.01325 bars (1 atm). The tabulations are based on a fit of the thermophysical and thermochemical data given in Section 1.5.5.

T K	Cp J/(mol K)	S J/(mol K)	H-H(298) J/mol	[G-H(298)]/T J/(mol K)	cm^3/mol
200.	168.792	115.478	-20284.	-216.900	98.9368
250.	208.625	157.588	-10812.	-200.835	99.1218
(2 sigma)	0.584	3.231	32.	3.229	0.2185
273.150	224.230	176.756	-5798.	-197.984	99.2075
298.150	239.361	197.058	0.	-197.058	99.3000
(2 sigma)	0.764	3.229	0.	3.229	0.1801
300.	240.416	198.542	444.	-197.063	99.3068
350.	265.995	237.593	13126.	-200.088	99.4918
400.	286.869	274.519	26965.	-207.107	99.6768
450.	304.136	309.336	41753.	-216.550	99.8618
500.	318.591	342.150	57332.	-227.486	100.0468
(2 sigma)	2.151	3.297	276.	3.231	0.5495
550.	330.811	373.104	73575.	-239.330	100.2318
600.	341.226	402.346	90383.	-251.708	100.4168
650.	350.159	430.021	107673.	-264.369	100.6018
700.	357.862	456.259	125379.	-277.147	100.7868
750.	364.529	481.182	143442.	-289.925	100.9718
(2 sigma)	2.820	3.621	891.	3.262	1.1761
800.	370.315	504.897	161817.	-302.626	101.1568
850.	375.344	527.502	180461.	-315.194	101.3418
900.	379.720	549.083	199340.	-327.593	101.5268
950.	383.524	569.717	218424.	-339.798	101.7118
1000.	386.827	589.475	237684.	-351.791	101.8968
(2 sigma)	3.397	3.984	1529.	3.336	1.8143
1050.	389.686	608.420	257099.	-363.564	102.0818
1100.	392.152	626.606	276646.	-375.109	102.2668
1150.	394.265	644.086	296308.	-386.427	102.4518
1200.	396.063	660.905	316068.	-397.515	102.6368
1250.	397.575	677.104	335910.	-408.377	102.8218
(2 sigma)	5.430	4.305	2252.	3.434	2.4550

Table 35. Thermochemical properties of dickite, $\text{Al}_2\text{Si}_2\text{O}_5(\text{OH})_4$, at 1.01325 bars (1 atm). Columns 2 through 4 give the thermochemical values relative to the elements; columns 5 through 7 give the values relative to the oxides.

T K	Formation from the Elements			Formation from the Oxides		
	H J/mol	G J/mol	log K	H J/mol	G J/mol	log K
200.	-4122604.	-3906870.	1020.369	-43183.	-35419.	9.251
250.	-4128053.	-3852284.	804.890	-48286.	-32865.	6.867
(2 sigma)	---	---	---	1240.	1479.	0.309
273.150	-4130211.	-3826649.	731.772	-50335.	-31344.	5.994
298.150	-4132302.	-3798770.	665.528	-52393.	-29513.	5.171
(2 sigma)	---	---	---	1239.	1569.	0.275
300.	-4132447.	-3796700.	661.064	-52540.	-29371.	5.114
350.	-4135926.	-3740456.	558.232	-56308.	-25206.	3.762
400.	-4138648.	-3683767.	481.050	-139256.	-14722.	1.922
450.	-4140754.	-3626774.	420.985	-138317.	791.	-0.092
500.	-4142363.	-3569575.	372.911	-137200.	16189.	-1.691
(2 sigma)	---	---	---	1270.	2036.	0.213
550.	-4143575.	-3512234.	333.564	-135960.	31468.	-2.989
600.	-4144474.	-3454798.	300.767	-134641.	46631.	-4.060
650.	-4145130.	-3397297.	273.010	-133283.	61682.	-4.957
700.	-4145604.	-3339753.	249.215	-131917.	76629.	-5.718
750.	-4145947.	-3282179.	228.591	-130572.	91478.	-6.371
(2 sigma)	---	---	---	1526.	2742.	0.191
800.	-4146206.	-3224586.	210.544	-129272.	106238.	-6.937
850.	-4146419.	-3166978.	194.619	-129461.	120930.	-7.431
900.	-4146622.	-3109358.	180.462	-127462.	135601.	-7.870
950.	-4125387.	-3096031.	170.232	-125431.	150161.	-8.256
1000.	-4122746.	-3041923.	158.894	-123386.	164612.	-8.598
(2 sigma)	---	---	---	1968.	3559.	0.186
1050.	-4120044.	-2987948.	148.642	-121345.	178962.	-8.903
1100.	-4117296.	-2934103.	139.329	-119324.	193215.	-9.175
1150.	-4114517.	-2880384.	130.831	-117336.	207377.	-9.419
1200.	-4111721.	-2826785.	123.047	-115394.	221453.	-9.640
1250.	-4108919.	-2773304.	115.890	-113509.	235449.	-9.839
(2 sigma)	---	---	---	2571.	4467.	0.187

Table 36. Thermophysical values for halloysite, $\text{Al}_2\text{Si}_2\text{O}_5(\text{OH})_4$, at 1.01325 bars (1 atm). The tabulations are based on a fit of the thermophysical and thermochemical data given in Section 1.5.5.

T K	Cp J/(mol K)	S J/(mol K)	H-H(298) J/mol	[G-H(298)]/T J/(mol K)	cm^3/mol ^V
200.	173.879	119.323	-20883.	-223.736	99.0368
250.	215.076	162.787	-11105.	-207.209	99.2218
(2 sigma)	0.609	3.231	33.	3.229	1.2921
273.150	230.388	182.517	-5945.	-204.283	99.3075
298.150	244.925	203.334	0.	-203.334	99.4000
(2 sigma)	0.787	3.229	0.	3.229	1.2861
300.	245.929	204.852	454.	-203.339	99.4068
350.	269.953	244.639	13374.	-206.426	99.5918
400.	289.211	281.988	27370.	-213.562	99.7768
450.	304.997	316.993	42238.	-223.130	99.9618
500.	318.165	349.829	57827.	-234.176	100.1468
(2 sigma)	2.342	3.308	297.	3.231	1.3869
550.	329.303	380.690	74021.	-246.107	100.3318
600.	338.828	409.762	90730.	-258.545	100.5168
650.	347.050	437.215	107882.	-271.243	100.7018
700.	354.200	463.202	125417.	-284.034	100.8868
750.	360.456	487.857	143287.	-296.808	101.0718
(2 sigma)	3.333	3.689	975.	3.267	1.7335
800.	365.957	511.300	161450.	-309.487	101.2568
850.	370.813	533.635	179872.	-322.020	101.4418
900.	375.115	554.954	198522.	-334.373	101.6268
950.	378.935	575.340	217375.	-346.523	101.8118
1000.	382.333	594.865	236409.	-358.456	101.9968
(2 sigma)	5.036	4.180	1799.	3.356	2.2166
1050.	385.360	613.593	255603.	-370.162	102.1818
1100.	388.057	631.584	274939.	-381.639	102.3668
1150.	390.461	648.888	294403.	-392.885	102.5518
1200.	392.602	665.552	313981.	-403.901	102.7368
1250.	394.507	681.618	333660.	-414.690	102.9218
(2 sigma)	8.439	4.825	3071.	3.484	2.7656

Table 37. Thermochemical properties of halloysite, $\text{Al}_2\text{Si}_2\text{O}_5(\text{OH})_4$, at 1.01325 bars (1 atm). Columns 2 through 4 give the thermochemical values relative to the elements; columns 5 through 7 give the values relative to the oxides.

T K	Formation from the Elements			Formation from the Oxides		
	H J/mol	G J/mol	log K	H J/mol	G J/mol	log K
200.	-4105755.	-3890790.	1016.169	-26334.	-19339.	5.051
250.	-4110899.	-3836430.	801.578	-31132.	-17011.	3.554
(2 sigma)	---	---	---	1199.	1445.	0.302
273.150	-4112911.	-3810922.	728.764	-33035.	-15617.	2.986
298.150	-4114854.	-3783194.	662.799	-34946.	-13937.	2.442
(2 sigma)	---	---	---	1198.	1537.	0.269
300.	-4114989.	-3781136.	658.354	-35083.	-13806.	2.404
350.	-4118231.	-3725227.	555.959	-38613.	-9977.	1.489
400.	-4120796.	-3668901.	479.109	-121403.	143.	-0.019
450.	-4122822.	-3612288.	419.303	-120385.	15277.	-1.773
500.	-4124421.	-3555473.	371.437	-119259.	30291.	-3.164
(2 sigma)	---	---	---	1234.	2011.	0.210
550.	-4125682.	-3498514.	332.261	-118067.	45189.	-4.292
600.	-4126680.	-3441453.	299.605	-116847.	59976.	-5.221
650.	-4127474.	-3384318.	271.967	-115627.	74662.	-6.000
700.	-4128118.	-3327127.	248.273	-114431.	89254.	-6.660
750.	-4128655.	-3269894.	227.735	-113280.	103763.	-7.227
(2 sigma)	---	---	---	1545.	2728.	0.190
800.	-4129125.	-3212627.	209.763	-112191.	118197.	-7.717
850.	-4129561.	-3155333.	193.903	-112603.	132575.	-8.147
900.	-4129993.	-3098013.	179.804	-110833.	146946.	-8.529
950.	-4108988.	-3084974.	169.624	-109032.	161218.	-8.864
1000.	-4106575.	-3031140.	158.330	-107214.	175395.	-9.162
(2 sigma)	---	---	---	2162.	3563.	0.186
1050.	-4104093.	-2977429.	148.119	-105395.	189481.	-9.426
1100.	-4101556.	-2923838.	138.841	-103584.	203480.	-9.662
1150.	-4098975.	-2870363.	130.376	-101794.	217397.	-9.874
1200.	-4096361.	-2817001.	122.621	-100034.	231237.	-10.065
1250.	-4093722.	-2763749.	115.491	-98312.	245005.	-10.238
(2 sigma)	---	---	---	3296.	4517.	0.189

Table 38. Thermophysical values for pyrophyllite, $\text{Al}_2\text{Si}_4\text{O}_{10}(\text{OH})_2$, at 1.01325 bars (1 atm). The tabulations are based on a fit of the thermophysical and thermochemical data given in Section 1.5.5.

T K	Cp J/(mol K)	S J/(mol K)	H-H(298) J/mol	[G-H(298)]/T J/(mol K)	cm^3V
200.	208.741	138.995	-24944.	-263.715	127.5344
250.	250.332	190.835	-13284.	-243.970	127.6066
(2 sigma)	0.355	1.023	15.	1.022	0.2819
273.150	275.484	214.385	-7124.	-240.467	127.6204
298.150	294.131	239.330	0.	-239.330	127.6374
(2 sigma)	0.304	1.022	0.	1.022	0.1460
300.	295.431	241.154	545.	-239.336	127.6387
350.	326.835	289.142	16131.	-243.054	127.6792
400.	352.103	334.494	33127.	-251.677	127.7268
450.	372.607	377.190	51262.	-263.275	127.7803
500.	389.424	417.347	70326.	-276.695	127.8389
(2 sigma)	1.036	1.053	109.	1.023	0.1633
550.	403.375	455.138	90157.	-291.216	127.9018
600.	415.089	490.752	110626.	-306.375	127.9683
650.	425.051	524.381	131636.	-321.863	128.0379
700.	433.642	556.202	153109.	-337.476	128.1101
750.	441.160	586.382	174983.	-353.072	128.1845
(2 sigma)	3.253	1.383	569.	1.040	0.5781
800.	447.846	615.072	197211.	-368.558	128.2608
850.	453.895	642.406	219757.	-383.869	128.3386
900.	459.466	668.510	242592.	-398.963	128.4178
950.	464.692	693.493	265698.	-413.812	128.4981
1000.	469.681	717.456	289058.	-428.399	128.5794
(2 sigma)	4.928	2.252	1549.	1.132	1.5153
1050.	474.528	740.490	312663.	-442.715	128.6614
1100.	479.310	762.675	336509.	-456.758	128.7442
1150.	484.095	784.087	360594.	-470.527	128.8275
1200.	488.940	804.792	384920.	-484.026	128.9114
1250.	493.895	824.852	409490.	-497.259	128.9956
(2 sigma)	6.925	3.199	2763.	1.346	2.6320

Table 39. Thermochemical properties of pyrophyllite, $\text{Al}_2\text{Si}_4\text{O}_{10}(\text{OH})_2$, at 1.01325 bars (1 atm). Columns 2 through 4 give the thermochemical values relative to the elements; columns 5 through 7 give the values relative to the oxides.

T K	Formation from the Elements			Formation from the Oxides		
	H J/mol	G J/mol	log K	H J/mol	G J/mol	log K
200.	-5635721.	-5390571.	1407.872	-33500.	-27770.	7.253
250.	-5639805.	-5328777.	1113.386	-36049.	-26033.	5.439
(2 sigma)	---	---	---	983.	831.	0.174
273.150	-5641174.	-5299912.	1013.505	-37075.	-25059.	4.792
298.150	-5642319.	-5268625.	923.041	-38094.	-23913.	4.189
(2 sigma)	---	---	---	983.	807.	0.141
300.	-5642391.	-5266306.	916.945	-38166.	-23825.	4.148
350.	-5643738.	-5203504.	776.580	-39990.	-21287.	3.177
400.	-5644099.	-5140578.	671.290	-81384.	-15600.	2.037
450.	-5643689.	-5077655.	589.398	-80859.	-7408.	0.860
500.	-5642678.	-5014812.	523.893	-80309.	723.	-0.076
(2 sigma)	---	---	---	998.	735.	0.077
550.	-5641202.	-4952094.	470.310	-79792.	8801.	-0.836
600.	-5639370.	-4889526.	425.671	-79355.	16835.	-1.466
650.	-5637267.	-4827122.	387.912	-79035.	24837.	-1.996
700.	-5634960.	-4764889.	355.560	-78857.	32819.	-2.449
750.	-5632502.	-4702826.	327.534	-78841.	40795.	-2.841
(2 sigma)	---	---	---	1167.	724.	0.050
800.	-5629937.	-4640931.	303.021	-78999.	48775.	-3.185
850.	-5627297.	-4579199.	281.403	-82188.	56791.	-3.490
900.	-5624608.	-4517623.	262.196	-81019.	64933.	-3.769
950.	-5643146.	-4455551.	244.983	-79770.	73007.	-4.014
1000.	-5640138.	-4393123.	229.473	-78449.	81014.	-4.232
(2 sigma)	---	---	---	1869.	903.	0.047
1050.	-5637004.	-4330849.	215.448	-77059.	88954.	-4.425
1100.	-5633743.	-4268727.	202.705	-75601.	96825.	-4.598
1150.	-5630350.	-4206756.	191.077	-74071.	104629.	-4.752
1200.	-5626817.	-4144936.	180.424	-72463.	112364.	-4.891
1250.	-5623134.	-4083266.	170.630	-70771.	120031.	-5.016
(2 sigma)	---	---	---	2960.	1403.	0.059

Table 40. Thermophysical values for the elemental phase graphite (C) at 1.01325 bars (1 atm). The sources of data are given in Section 1.5.5.

T K	Cp J/(mol K)	S J/(mol K)	H-H(298) J/mol	[G-H(298)]/T J/(mol K)	V cm ³ /mol
200.000	6.646	2.872	-710.	-6.420	---
250.000	7.087	4.366	-374.	-5.863	---
(2 sigma)	---	---	---	---	---
273.150	7.728	5.021	-203.	-5.764	---
298.150	8.532	5.732	0.	-5.732	---
(2 sigma)	---	---	---	---	---
300.000	8.594	5.785	16.	-5.732	---
350.000	10.296	7.237	488.	-5.843	---
400.000	11.923	8.720	1044.	-6.109	---
450.000	13.397	10.211	1678.	-6.482	---
500.000	14.704	11.691	2381.	-6.929	---
(2 sigma)	---	---	---	---	---
550.000	15.855	13.148	3146.	-7.429	---
600.000	16.865	14.572	3964.	-7.965	---
650.000	17.750	15.957	4830.	-8.527	---
700.000	18.528	17.302	5737.	-9.106	---
750.000	19.212	18.604	6681.	-9.696	---
(2 sigma)	---	---	---	---	---
800.000	19.814	19.863	7657.	-10.292	---
850.000	20.346	21.081	8661.	-10.891	---
900.000	20.817	22.257	9691.	-11.490	---
950.000	21.234	23.394	10742.	-12.087	---
1000.000	21.604	24.493	11813.	-12.680	---
(2 sigma)	---	---	---	---	---
1050.000	21.933	25.555	12902.	-13.268	---
1100.000	22.226	26.583	14006.	-13.850	---
1150.000	22.488	27.576	15124.	-14.425	---
1200.000	22.721	28.538	16254.	-14.993	---
1250.000	22.931	29.470	17396.	-15.554	---
(2 sigma)	---	---	---	---	---
1300.000	23.119	30.373	18547.	-16.106	---
1350.000	23.288	31.249	19707.	-16.651	---
1400.000	23.441	32.099	20876.	-17.188	---
1450.000	23.579	32.924	22051.	-17.716	---
1500.000	23.704	33.725	23233.	-18.237	---
(2 sigma)	---	---	---	---	---
1550.000	23.819	34.505	24421.	-18.749	---
1600.000	23.924	35.262	25615.	-19.253	---
1650.000	24.021	36.000	26814.	-19.749	---
1700.000	24.111	36.719	28017.	-20.238	---
1750.000	24.195	37.419	29225.	-20.719	---
(2 sigma)	---	---	---	---	---
1800.000	24.275	38.101	30436.	-21.192	---
(2 sigma)	---	---	---	---	---

Table 41. Thermochemical properties of the elemental phase graphite (C) at 1.01325 bars (1 atm). Columns 2 through 4 give the thermochemical values relative to the elements; columns 5 through 7 give the values relative to the oxides.

T K	Formation from the Elements			Formation from the Oxides		
	H J/mol	G J/mol	log K	H J/mol	G J/mol	log K
200.	0.	0.	0.	---	---	---
250.	0.	0.	0.	---	---	---
(2 sigma)	0.	0.	0.	---	---	---
273.15	0.	0.	0.	---	---	---
298.15	0.	0.	0.	---	---	---
(2 sigma)	0.	0.	0.	---	---	---
300.	0.	0.	0.	---	---	---
350.	0.	0.	0.	---	---	---
400.	0.	0.	0.	---	---	---
450.	0.	0.	0.	---	---	---
500.	0.	0.	0.	---	---	---
(2 sigma)	0.	0.	0.	---	---	---
550.	0.	0.	0.	---	---	---
600.	0.	0.	0.	---	---	---
650.	0.	0.	0.	---	---	---
700.	0.	0.	0.	---	---	---
750.	0.	0.	0.	---	---	---
(2 sigma)	0.	0.	0.	---	---	---
800.	0.	0.	0.	---	---	---
850.	0.	0.	0.	---	---	---
900.	0.	0.	0.	---	---	---
950.	0.	0.	0.	---	---	---
1000.	0.	0.	0.	---	---	---
(2 sigma)	0.	0.	0.	---	---	---
1050.	0.	0.	0.	---	---	---
1100.	0.	0.	0.	---	---	---
1150.	0.	0.	0.	---	---	---
1200.	0.	0.	0.	---	---	---
1250.	0.	0.	0.	---	---	---
(2 sigma)	0.	0.	0.	---	---	---
1300.	0.	0.	0.	---	---	---
1350.	0.	0.	0.	---	---	---
1400.	0.	0.	0.	---	---	---
1450.	0.	0.	0.	---	---	---
1500.	0.	0.	0.	---	---	---
(2 sigma)	0.	0.	0.	---	---	---
1550.	0.	0.	0.	---	---	---
1600.	0.	0.	0.	---	---	---
1650.	0.	0.	0.	---	---	---
1700.	0.	0.	0.	---	---	---
1750.	0.	0.	0.	---	---	---
(2 sigma)	0.	0.	0.	---	---	---
1800.	0.	0.	0.	---	---	---
(2 sigma)	0.	0.	0.	---	---	---

Table 42. Thermophysical values for carbon monoxide (CO, ideal gas) at 1.01325 bars (1 atm). The tabulations are based on a fit of the thermophysical and thermochemical data given in Section 1.5.5.

T K	Cp J/(mol K)	S J/(mol K)	H-H(298) J/mol	[G-H(298)]/T J/(mol K)	cm ³ /mol
200.000	29.751	185.853	-2872.	-200.211	---
250.000	29.181	192.417	-1401.	-198.022	---
(2 sigma)	---	---	---	---	---
273.150	29.093	194.997	-727.	-197.658	---
298.150	29.069	197.544	0.	-197.544	---
(2 sigma)	---	---	---	---	---
300.000	29.070	197.723	54.	-197.544	---
350.000	29.171	202.210	1509.	-197.898	---
400.000	29.378	206.118	2973.	-198.687	---
450.000	29.644	209.593	4448.	-199.709	---
500.000	29.941	212.732	5937.	-200.857	---
(2 sigma)	---	---	---	---	---
550.000	30.254	215.600	7442.	-202.069	---
600.000	30.575	218.246	8963.	-203.308	---
650.000	30.899	220.706	10500.	-204.553	---
700.000	31.221	223.008	12053.	-205.790	---
750.000	31.538	225.173	13622.	-207.010	---
(2 sigma)	---	---	---	---	---
800.000	31.850	227.218	15207.	-208.210	---
850.000	32.155	229.158	16807.	-209.386	---
900.000	32.452	231.005	18422.	-210.536	---
950.000	32.740	232.767	20052.	-211.660	---
1000.000	33.019	234.453	21696.	-212.758	---
(2 sigma)	---	---	---	---	---
1050.000	33.288	236.071	23354.	-213.830	---
1100.000	33.548	237.626	25024.	-214.876	---
1150.000	33.797	239.122	26708.	-215.898	---
1200.000	34.037	240.566	28404.	-216.896	---
1250.000	34.265	241.960	30112.	-217.871	---
(2 sigma)	---	---	---	---	---
1300.000	34.483	243.308	31830.	-218.823	---
1350.000	34.691	244.614	33560.	-219.754	---
1400.000	34.887	245.879	35299.	-220.665	---
1450.000	35.073	247.106	37048.	-221.556	---
1500.000	35.248	248.298	38806.	-222.427	---
(2 sigma)	---	---	---	---	---
1550.000	35.412	249.457	40573.	-223.281	---
1600.000	35.564	250.583	42347.	-224.116	---
1650.000	35.706	251.680	44129.	-224.935	---
1700.000	35.837	252.748	45918.	-225.738	---
1750.000	35.957	253.789	47713.	-226.524	---
(2 sigma)	---	---	---	---	---
1800.000	36.065	254.803	49513.	-227.296	---
(2 sigma)	---	---	---	---	---

Table 43. Thermochemical properties of carbon monoxide (CO, ideal gas) at 1.01325 bars (1 atm). Columns 2 through 4 give the thermochemical values relative to the elements; columns 5 through 7 give the values relative to the oxides.

T K	Formation from the Elements			Formation from the Oxides		
	H J/mol	G J/mol	log K	H J/mol	G J/mol	log K
200.000	-111296.	-128552.	33.574	0.	0.	0.
250.000	-110888.	-132915.	27.771	0.	0.	0.
(2 sigma)	---	---	---	0.	0.	0.
273.150	-110722.	-134962.	25.809	0.	0.	0.
298.150	-110564.	-137188.	24.035	0.	0.	0.
(2 sigma)	---	---	---	0.	0.	0.
300.000	-110553.	-137353.	23.915	0.	0.	0.
350.000	-110310.	-141840.	21.168	0.	0.	0.
400.000	-110155.	-146356.	19.112	0.	0.	0.
450.000	-110077.	-150886.	17.514	0.	0.	0.
500.000	-110067.	-155422.	16.237	0.	0.	0.
(2 sigma)	---	---	---	0.	0.	0.
550.000	-110114.	-159955.	15.191	0.	0.	0.
600.000	-110211.	-164482.	14.319	0.	0.	0.
650.000	-110348.	-169000.	13.581	0.	0.	0.
700.000	-110521.	-173505.	12.947	0.	0.	0.
750.000	-110723.	-177997.	12.397	0.	0.	0.
(2 sigma)	---	---	---	0.	0.	0.
800.000	-110951.	-182475.	11.914	0.	0.	0.
850.000	-111199.	-186938.	11.488	0.	0.	0.
900.000	-111465.	-191385.	11.108	0.	0.	0.
950.000	-111745.	-195818.	10.767	0.	0.	0.
1000.000	-112038.	-200235.	10.459	0.	0.	0.
(2 sigma)	---	---	---	0.	0.	0.
1050.000	-112340.	-204637.	10.180	0.	0.	0.
1100.000	-112651.	-209025.	9.926	0.	0.	0.
1150.000	-112968.	-213399.	9.693	0.	0.	0.
1200.000	-113290.	-217759.	9.479	0.	0.	0.
1250.000	-113617.	-222105.	9.281	0.	0.	0.
(2 sigma)	---	---	---	0.	0.	0.
1300.000	-113946.	-226438.	9.098	0.	0.	0.
1350.000	-114278.	-230758.	8.929	0.	0.	0.
1400.000	-114611.	-235066.	8.770	0.	0.	0.
1450.000	-114946.	-239362.	8.623	0.	0.	0.
1500.000	-115281.	-243647.	8.485	0.	0.	0.
(2 sigma)	---	---	---	0.	0.	0.
1550.000	-115616.	-247920.	8.355	0.	0.	0.
1600.000	-115951.	-252182.	8.233	0.	0.	0.
1650.000	-116286.	-256435.	8.118	0.	0.	0.
1700.000	-116620.	-260676.	8.010	0.	0.	0.
1750.000	-116955.	-264909.	7.907	0.	0.	0.
(2 sigma)	---	---	---	0.	0.	0.
1800.000	-117288.	-269131.	7.810	0.	0.	0.
(2 sigma)	---	---	---	0.	0.	0.

Table 44. Thermophysical values for carbon dioxide (CO₂, ideal gas) at 1.01325 bars (1 atm). The tabulations are based on a fit of the thermophysical and thermochemical data given in Section 1.5.5.

T K	Cp J/(mol K)	S J/(mol K)	H-H(298) J/mol	[G-H(298)]/T J/(mol K)	cm ³ /mol
200.000	33.619	199.689	-3452.	-216.950	---
250.000	35.115	207.329	-1739.	-214.284	---
(2 sigma)	---	---	---	---	---
273.150	36.066	210.480	-915.	-213.830	---
298.150	37.138	213.685	0.	-213.685	---
(2 sigma)	---	---	---	---	---
300.000	37.218	213.915	69.	-213.685	---
350.000	39.334	219.812	1983.	-214.146	---
400.000	41.298	225.195	4000.	-215.196	---
450.000	43.075	230.163	6110.	-216.586	---
500.000	44.670	234.786	8304.	-218.178	---
(2 sigma)	---	---	---	---	---
550.000	46.100	239.111	10574.	-219.886	---
600.000	47.386	243.179	12912.	-221.659	---
650.000	48.545	247.018	15310.	-223.464	---
700.000	49.595	250.655	17764.	-225.277	---
750.000	50.548	254.110	20268.	-227.085	---
(2 sigma)	---	---	---	---	---
800.000	51.417	257.400	22818.	-228.878	---
850.000	52.211	260.541	25409.	-230.649	---
900.000	52.940	263.547	28038.	-232.394	---
950.000	53.610	266.427	30702.	-234.110	---
1000.000	54.228	269.193	33398.	-235.795	---
(2 sigma)	---	---	---	---	---
1050.000	54.798	271.853	36124.	-237.449	---
1100.000	55.326	274.414	38877.	-239.071	---
1150.000	55.816	276.884	41656.	-240.662	---
1200.000	56.270	279.270	44458.	-242.221	---
1250.000	56.692	281.575	47282.	-243.750	---
(2 sigma)	---	---	---	---	---
1300.000	57.085	283.807	50127.	-245.248	---
1350.000	57.450	285.968	52990.	-246.716	---
1400.000	57.791	288.064	55871.	-248.155	---
1450.000	58.108	290.097	58769.	-249.567	---
1500.000	58.403	292.072	61682.	-250.951	---
(2 sigma)	---	---	---	---	---
1550.000	58.578	293.992	64609.	-252.309	---
1600.000	58.934	295.859	67549.	-253.640	---
1650.000	59.173	297.676	70502.	-254.947	---
1700.000	59.394	299.446	73466.	-256.230	---
1750.000	59.600	301.170	76441.	-257.490	---
(2 sigma)	---	---	---	---	---
1800.000	59.791	302.852	79426.	-258.727	---
(2 sigma)	---	---	---	---	---

Table 45. Thermochemical properties of carbon dioxide (CO₂, ideal gas) at 1.01325 bars (1 atm). Columns 2 through 4 give the thermochemical values relative to the elements; columns 5 through 7 give the values relative to the oxides.

T K	Formation from the Elements			Formation from the Oxides		
	H J/mol	G J/mol	log K	H J/mol	G J/mol	log K
200.000	-393507.	-394191.	102.952	0.	0.	0.
250.000	-393583.	-394352.	82.395	0.	0.	0.
(2 sigma)	---	---	---	0.	0.	0.
273.150	-393605.	-394422.	75.426	0.	0.	0.
298.150	-393626.	-394496.	69.114	0.	0.	0.
(2 sigma)	---	---	---	0.	0.	0.
300.000	-393627.	-394502.	68.689	0.	0.	0.
350.000	-393665.	-394644.	58.897	0.	0.	0.
400.000	-393709.	-394781.	51.553	0.	0.	0.
450.000	-393760.	-394912.	45.840	0.	0.	0.
500.000	-393821.	-395037.	41.269	0.	0.	0.
(2 sigma)	---	---	---	0.	0.	0.
550.000	-393891.	-395156.	37.529	0.	0.	0.
600.000	-393969.	-395267.	34.411	0.	0.	0.
650.000	-394053.	-395372.	31.772	0.	0.	0.
700.000	-394143.	-395470.	29.510	0.	0.	0.
750.000	-394238.	-395562.	27.549	0.	0.	0.
(2 sigma)	---	---	---	0.	0.	0.
800.000	-394337.	-395647.	25.833	0.	0.	0.
850.000	-394438.	-395725.	24.318	0.	0.	0.
900.000	-394542.	-395798.	22.972	0.	0.	0.
950.000	-394647.	-395865.	21.766	0.	0.	0.
1000.000	-394753.	-395927.	20.681	0.	0.	0.
(2 sigma)	---	---	---	0.	0.	0.
1050.000	-394859.	-395983.	19.699	0.	0.	0.
1100.000	-394965.	-396034.	18.806	0.	0.	0.
1150.000	-395070.	-396080.	17.991	0.	0.	0.
1200.000	-395173.	-396122.	17.243	0.	0.	0.
1250.000	-395276.	-396159.	16.555	0.	0.	0.
(2 sigma)	---	---	---	0.	0.	0.
1300.000	-395377.	-396192.	15.919	0.	0.	0.
1350.000	-395475.	-396222.	15.331	0.	0.	0.
1400.000	-395571.	-396248.	14.784	0.	0.	0.
1450.000	-395665.	-396270.	14.275	0.	0.	0.
1500.000	-395756.	-396290.	13.800	0.	0.	0.
(2 sigma)	---	---	---	0.	0.	0.
1550.000	-395845.	-396306.	13.355	0.	0.	0.
1600.000	-395930.	-396319.	12.938	0.	0.	0.
1650.000	-396012.	-396330.	12.547	0.	0.	0.
1700.000	-396091.	-396339.	12.178	0.	0.	0.
1750.000	-396166.	-396345.	11.830	0.	0.	0.
(2 sigma)	---	---	---	0.	0.	0.
1800.000	-396238.	-396349.	11.502	0.	0.	0.
(2 sigma)	---	---	---	0.	0.	0.

Table 46. Thermophysical values for stable phases of the element calcium (Ca) at 1.01325 bars (1 atm). The sources of data are given in Section 1.5.5.

T K	Cp J/(mol K)	S J/(mol K)	H-H(298) J/mol	[G-H(298)]/T J/(mol K)	V cm ³ /mol
calcium (crystal, face centered cubic)					
200.	24.567	31.642	-2454.	-43.913	---
250.	25.033	37.181	-1213.	-42.032	---
(2 sigma)	---	---	---	---	---
273.15	25.180	39.404	-631.	-41.716	---
298.15	25.341	41.616	0.	-41.616	---
(2 sigma)	---	---	---	---	---
300.	25.354	41.773	47.	-41.617	---
350.	25.743	45.709	1324.	-41.927	---
400.	26.255	49.178	2623.	-42.620	---
450.	26.900	52.307	3952.	-43.525	---
500.	27.671	55.180	5315.	-44.549	---
(2 sigma)	---	---	---	---	---
550.	28.560	57.858	6721.	-45.639	---
600.	29.558	60.385	8173.	-46.763	---
650.	30.657	62.794	9678.	-47.904	---
700.	31.849	65.109	11240.	-49.051	---
720.	32.351	66.013	11882.	-49.510	---
calcium (crystal, body centered cubic)					
720.	29.341	67.289	12801.	-49.510	---
750.	30.581	68.512	13700.	-50.245	---
(2 sigma)	---	---	---	---	---
800.	32.647	70.552	15281.	-51.451	---
850.	34.712	72.593	16965.	-52.634	---
900.	36.776	74.635	18752.	-53.800	---
950.	38.840	76.679	20642.	-54.950	---
1000.	40.903	78.724	22636.	-56.088	---
(2 sigma)	---	---	---	---	---
1050.	42.966	80.769	24733.	-57.214	---
1100.	45.029	82.816	26933.	-58.331	---
1112.	45.524	83.307	27476.	-58.598	---
calcium (liquid)					
1112.	29.275	90.968	35995.	-58.598	---
1150.	29.275	91.952	37108.	-59.684	---
1200.	29.275	93.198	38571.	-61.055	---
1250.	29.275	94.393	40035.	-62.365	---
(2 sigma)	---	---	---	---	---
1300.	29.275	95.541	41499.	-63.619	---
1350.	29.275	96.646	42963.	-64.822	---
1400.	29.275	97.711	44427.	-65.977	---
1450.	29.275	98.738	45890.	-67.089	---
1500.	29.275	99.730	47354.	-68.161	---
(2 sigma)	---	---	---	---	---
1550.	29.275	100.690	48818.	-69.195	---
1600.	29.275	101.620	50282.	-70.194	---
1650.	29.275	102.521	51745.	-71.160	---
1700.	29.275	103.395	53209.	-72.095	---
1750.	29.275	104.243	54673.	-73.002	---
(2 sigma)	---	---	---	---	---
1755.	29.275	104.327	54819.	-73.091	---
calcium (ideal monatomic gas)					
1755.	20.351	191.628	208032.	-73.091	---
1800.	20.862	192.156	208971.	-76.061	---
(2 sigma)	---	---	---	---	---

Table 47. Thermochemical properties of stable phases of the element calcium (Ca) at 1.01325 bars (1 atm). Columns 2 through 4 give the thermochemical values relative to the elements; columns 5 through 7 give the values relative to the oxides.

T K	Formation from the Elements			Formation from the Oxides		
	H J/mol	G J/mol	log K	H J/mol	G J/mol	log K
calcium (crystal, face centered cubic)						
200.	0.	0.	0.	---	---	---
250.	0.	0.	0.	---	---	---
(2 sigma)	0.	0.	0.	---	---	---
273.15	0.	0.	0.	---	---	---
298.15	0.	0.	0.	---	---	---
(2 sigma)	0.	0.	0.	---	---	---
300.	0.	0.	0.	---	---	---
350.	0.	0.	0.	---	---	---
400.	0.	0.	0.	---	---	---
450.	0.	0.	0.	---	---	---
500.	0.	0.	0.	---	---	---
(2 sigma)	0.	0.	0.	---	---	---
550.	0.	0.	0.	---	---	---
600.	0.	0.	0.	---	---	---
650.	0.	0.	0.	---	---	---
700.	0.	0.	0.	---	---	---
720.	0.	0.	0.	---	---	---
calcium (crystal, body centered cubic)						
720.	0.	0.	0.	---	---	---
750.	0.	0.	0.	---	---	---
(2 sigma)	0.	0.	0.	---	---	---
800.	0.	0.	0.	---	---	---
850.	0.	0.	0.	---	---	---
900.	0.	0.	0.	---	---	---
950.	0.	0.	0.	---	---	---
1000.	0.	0.	0.	---	---	---
(2 sigma)	0.	0.	0.	---	---	---
1050.	0.	0.	0.	---	---	---
1100.	0.	0.	0.	---	---	---
1112.	0.	0.	0.	---	---	---
calcium (liquid)						
1112.	0.	0.	0.	---	---	---
1150.	0.	0.	0.	---	---	---
1200.	0.	0.	0.	---	---	---
1250.	0.	0.	0.	---	---	---
(2 sigma)	0.	0.	0.	---	---	---
1300.	0.	0.	0.	---	---	---
1350.	0.	0.	0.	---	---	---
1400.	0.	0.	0.	---	---	---
1450.	0.	0.	0.	---	---	---
1500.	0.	0.	0.	---	---	---
(2 sigma)	0.	0.	0.	---	---	---
1550.	0.	0.	0.	---	---	---
1600.	0.	0.	0.	---	---	---
1650.	0.	0.	0.	---	---	---
1700.	0.	0.	0.	---	---	---
1750.	0.	0.	0.	---	---	---
(2 sigma)	0.	0.	0.	---	---	---
1755.	0.	0.	0.	---	---	---
calcium (ideal diatomic gas)						
1755.	0.	0.	0.	---	---	---
1800.	0.	0.	0.	---	---	---
(2 sigma)	0.	0.	0.	---	---	---

Table 48. Thermophysical values for Ca-Al clinopyroxene, $\text{CaAl}_2\text{SiO}_6$, at 1.01325 bars (1 atm). The tabulations are based on a fit of the thermophysical and thermochemical data given in Section 1.5.5.

T K	Cp J/(mol K)	S J/(mol K)	H-H(298) J/mol	[G-H(298)]/T J/(mol K)	cm^3V mol
200.	99.917	88.557	-13535.	-156.232	63.4567
250.	140.960	115.672	-7421.	-145.357	63.5153
(2 sigma)	6.530	4.185	210.	4.100	0.0948
273.150	154.072	128.747	-4001.	-143.395	63.5443
298.150	165.638	142.756	0.	-142.756	63.5770
(2 sigma)	2.880	4.102	0.	4.102	0.0725
300.	166.408	143.783	307.	-142.759	63.5794
350.	183.831	170.819	9088.	-144.854	63.6483
400.	196.596	196.240	18613.	-149.706	63.7212
450.	206.414	219.986	28699.	-156.211	63.7974
500.	214.247	242.153	39222.	-163.709	63.8765
(2 sigma)	2.171	3.913	381.	4.050	0.0431
550.	220.673	262.884	50100.	-171.793	63.9581
600.	226.063	282.323	61272.	-180.203	64.0417
650.	230.668	300.604	72693.	-188.768	64.1270
700.	234.659	317.848	84329.	-197.378	64.2138
750.	238.162	334.159	96151.	-205.958	64.3018
(2 sigma)	1.777	3.784	763.	3.946	0.0461
800.	241.268	349.631	108138.	-214.458	64.3909
850.	244.047	364.343	120272.	-222.846	64.4808
900.	246.553	378.364	132538.	-231.099	64.5716
950.	248.828	391.757	144924.	-239.205	64.6629
1000.	250.906	404.573	157418.	-247.156	64.7548
(2 sigma)	2.782	3.678	1051.	3.858	0.0379
1050.	252.814	416.862	170012.	-254.946	64.8472
1100.	254.573	428.664	182697.	-262.576	64.9399
1150.	256.203	440.017	195467.	-270.046	65.0330
1200.	257.718	450.953	208315.	-277.357	65.1264
1250.	259.131	461.502	221237.	-284.513	65.2200
(2 sigma)	4.066	3.675	1592.	3.786	0.0404
1300.	260.454	471.692	234227.	-291.517	65.3138
1350.	261.696	481.545	247281.	-298.374	65.4077
1400.	262.865	491.084	260395.	-305.087	65.5018
1450.	263.967	500.327	273566.	-311.661	65.5960
1500.	265.009	509.294	286791.	-318.100	65.6904
(2 sigma)	5.196	3.849	2536.	3.731	0.0652
1550.	265.996	518.000	300066.	-324.409	65.7848
1600.	266.933	526.460	313390.	-330.591	65.8792
1650.	267.825	534.687	326759.	-336.652	65.9738
1700.	268.673	542.695	340171.	-342.595	66.0684
1750.	269.483	550.495	353625.	-348.424	66.1630
(2 sigma)	5.149	4.201	3821.	3.700	0.0997
1800.	270.257	558.098	367119.	-354.143	66.2577
(2 sigma)	6.321	4.290	4112.	3.698	0.1071

Table 49. Thermochemical properties of Ca-Al clinopyroxene, $\text{CaAl}_2\text{SiO}_6$, at 1.01325 bars (1 atm). Columns 2 through 4 give the thermochemical values relative to the elements; columns 5 through 7 give the values relative to the oxides.

T K	Formation from the Elements			Formation from the Oxides		
	H J/mol	G J/mol	log K	H J/mol	G J/mol	log K
200.	-3294801.	-3180161.	830.572	-76525.	-79495.	20.762
250.	-3297395.	-3151165.	658.399	-77018.	-80168.	16.750
(2 sigma)	---	---	---	5449.	4502.	0.941
273.150	-3298105.	-3137591.	600.003	-77095.	-80456.	15.386
298.150	-3298625.	-3122875.	547.114	-77123.	-80762.	14.149
(2 sigma)	---	---	---	5447.	4324.	0.758
300.	-3298655.	-3121784.	543.551	-77123.	-80785.	14.066
350.	-3299095.	-3092262.	461.495	-77086.	-81397.	12.148
400.	-3299000.	-3062716.	399.949	-77009.	-82018.	10.710
450.	-3298543.	-3033205.	352.085	-76942.	-82648.	9.594
500.	-3297841.	-3003758.	313.800	-76906.	-83284.	8.701
(2 sigma)	---	---	---	5418.	3601.	0.376
550.	-3296977.	-2974391.	282.484	-76912.	-83922.	7.970
600.	-3296012.	-2945107.	256.394	-76965.	-84558.	7.361
650.	-3294996.	-2915906.	234.325	-77067.	-85186.	6.846
700.	-3293969.	-2886783.	215.414	-77218.	-85806.	6.403
750.	-3293797.	-2857698.	199.028	-77416.	-86412.	6.018
(2 sigma)	---	---	---	5377.	2764.	0.192
800.	-3292730.	-2828660.	184.692	-77663.	-87004.	5.681
850.	-3291769.	-2799685.	172.048	-78668.	-87574.	5.382
900.	-3290933.	-2770764.	160.811	-78584.	-88101.	5.113
950.	-3311497.	-2741238.	150.724	-78479.	-88632.	4.873
1000.	-3310685.	-2711246.	141.621	-78357.	-89170.	4.658
(2 sigma)	---	---	---	5342.	2021.	0.106
1050.	-3309924.	-2681292.	133.387	-78219.	-89713.	4.463
1100.	-3309218.	-2651374.	125.903	-78069.	-90264.	4.286
1150.	-3316443.	-2621207.	119.059	-77908.	-90822.	4.125
1200.	-3314916.	-2591012.	112.784	-77738.	-91387.	3.978
1250.	-3313351.	-2560881.	107.013	-77563.	-91960.	3.843
(2 sigma)	---	---	---	5393.	1461.	0.061
1300.	-3311751.	-2530814.	101.689	-77384.	-92539.	3.718
1350.	-3310117.	-2500809.	96.762	-77203.	-93125.	3.603
1400.	-3308450.	-2470865.	92.189	-77023.	-93718.	3.497
1450.	-3306753.	-2440981.	87.934	-76847.	-94318.	3.398
1500.	-3305026.	-2411156.	83.964	-76676.	-94923.	3.306
(2 sigma)	---	---	---	5669.	1333.	0.046
1550.	-3303270.	-2381389.	80.252	-76513.	-95534.	3.219
1600.	-3301485.	-2351679.	76.774	-76360.	-96150.	3.139
1650.	-3299672.	-2322026.	73.509	-76220.	-96771.	3.064
1700.	-3348341.	-2291978.	70.424	-76096.	-97395.	2.993
1750.	-3346330.	-2260938.	67.485	-75989.	-98023.	2.926
(2 sigma)	---	---	---	6284.	1804.	0.054
1800.	-3497121.	-2226032.	64.598	-75902.	-98654.	2.863
(2 sigma)	---	---	---	6453.	1952.	0.057

Table 50. Thermophysical values for anorthite, $\text{CaAl}_2\text{Si}_2\text{O}_8$, at 1.01325 bars (1 atm). The tabulations are based on a fit of the thermophysical and thermochemical data given in Section 1.5.5.

T K	Cp J/(mol K)	S J/(mol K)	H-H(298) J/mol	[G-H(298)]/T J/(mol K)	cm^3V mol
200.	158.036	125.573	-18292.	-217.033	100.6014
250.	187.683	164.097	-9632.	-202.626	100.6655
(2 sigma)	0.200	0.155	9.	0.152	0.0812
273.150	199.792	181.255	-5145.	-200.091	100.6951
298.150	211.605	199.271	0.	-199.271	100.7272
(2 sigma)	0.154	0.152	0.	0.152	0.0763
300.	212.428	200.582	392.	-199.275	100.7296
350.	232.271	234.876	11528.	-201.938	100.7936
400.	248.088	266.964	23552.	-208.083	100.8577
450.	260.749	296.943	36285.	-216.310	100.9218
500.	270.967	324.963	49587.	-225.790	100.9859
(2 sigma)	0.427	0.188	47.	0.153	0.0613
550.	279.295	351.193	63350.	-236.011	101.0500
600.	286.166	375.798	77492.	-246.645	101.1141
650.	291.914	398.937	91948.	-257.479	101.1782
700.	296.803	420.754	106669.	-268.370	101.2423
750.	301.042	441.379	121617.	-279.222	101.3064
(2 sigma)	0.750	0.340	175.	0.170	0.0615
800.	304.801	460.930	136765.	-289.973	101.3704
850.	308.215	479.512	152092.	-300.581	101.4345
900.	311.397	497.220	167583.	-311.017	101.4986
950.	314.440	514.139	183229.	-321.266	101.5627
1000.	317.423	530.343	199026.	-331.317	101.6268
(2 sigma)	1.217	0.491	339.	0.212	0.0815
1050.	320.409	545.902	214971.	-341.168	101.6909
1100.	323.456	560.878	231068.	-350.816	101.7550
1150.	326.611	575.325	247319.	-360.265	101.8191
1200.	329.914	589.295	263731.	-369.519	101.8831
1250.	333.402	602.833	280313.	-378.582	101.9472
(2 sigma)	3.451	0.698	676.	0.260	0.1112
1300.	337.105	615.980	297075.	-387.461	102.0113
1350.	341.050	628.776	314028.	-396.163	102.0754
1400.	345.260	641.254	331185.	-404.694	102.1395
1450.	349.757	653.448	348559.	-413.062	102.2036
1500.	354.560	665.385	366165.	-421.275	102.2677
(2 sigma)	7.990	1.450	1881.	0.328	0.1446
1550.	359.684	677.094	384020.	-429.339	102.3318
1600.	365.145	688.598	402139.	-437.261	102.3958
1650.	370.956	699.923	420540.	-445.050	102.4599
1700.	377.128	711.087	439241.	-452.710	102.5240
1750.	383.673	722.113	458259.	-460.250	102.5881
(2 sigma)	14.878	3.035	4581.	0.517	0.1798
1800.	390.600	733.018	477615.	-467.676	102.6522
(2 sigma)	16.544	3.458	5349.	0.580	0.1869

Table 51. Thermochemical properties of anorthite, $\text{CaAl}_2\text{Si}_2\text{O}_8$, at 1.01325 bars (1 atm). Columns 2 through 4 give the thermochemical values relative to the elements; columns 5 through 7 give the values relative to the oxides.

T K	Formation from the Elements			Formation from the Oxides		
	H J/mol	G J/mol	log K	H J/mol	G J/mol	log K
200.	-4226995.	-4078749.	1065.259	-98839.	-104007.	27.164
250.	-4229349.	-4041394.	844.402	-98598.	-105334.	22.008
(2 sigma)	---	---	---	1167.	1166.	0.244
273.15U	-4230100.	-4023954.	769.503	-98554.	-105960.	20.263
298.15U	-4230697.	-4005058.	701.669	-98525.	-106639.	18.683
(2 sigma)	---	---	---	1167.	1165.	0.204
300.	-4230733.	-4003658.	697.098	-98524.	-106689.	18.576
350.	-4231330.	-3965755.	591.856	-98490.	-108053.	16.126
400.	-4231326.	-3927810.	512.919	-98480.	-109420.	14.289
450.	-4230876.	-3889894.	451.527	-98507.	-110787.	12.860
500.	-4230107.	-3852046.	402.420	-98591.	-112147.	11.716
(2 sigma)	---	---	---	1168.	1165.	0.122
550.	-4229118.	-3814286.	362.250	-98753.	-113496.	10.779
600.	-4227990.	-3776623.	328.784	-99007.	-114825.	9.996
650.	-4226786.	-3739057.	300.474	-99367.	-116130.	9.332
700.	-4225557.	-3701586.	276.216	-99838.	-117402.	8.761
750.	-4225177.	-3664166.	255.195	-100425.	-118637.	8.263
(2 sigma)	---	---	---	1174.	1168.	0.081
800.	-4223897.	-3626807.	236.806	-101126.	-119829.	7.824
850.	-4222721.	-3589526.	220.585	-103365.	-120963.	7.433
900.	-4221665.	-3552310.	206.171	-103441.	-121996.	7.080
950.	-4241996.	-3514502.	193.241	-103485.	-123025.	6.764
1000.	-4240934.	-3476241.	181.580	-103496.	-124053.	6.480
(2 sigma)	---	---	---	1208.	1181.	0.062
1050.	-4239895.	-3438032.	171.033	-103466.	-125082.	6.222
1100.	-4238871.	-3399872.	161.446	-103390.	-126113.	5.989
1150.	-4245728.	-3361478.	152.683	-103258.	-127148.	5.775
1200.	-4243767.	-3323074.	144.650	-103060.	-128191.	5.580
1250.	-4241688.	-3284754.	137.262	-102785.	-129244.	5.401
(2 sigma)	---	---	---	1372.	1204.	0.050
1300.	-4239479.	-3246519.	130.447	-102420.	-130309.	5.236
1350.	-4237123.	-3208373.	124.139	-101951.	-131390.	5.084
1400.	-4234604.	-3170317.	118.286	-101365.	-132491.	4.943
1450.	-4231907.	-3132353.	112.839	-100646.	-133615.	4.813
1500.	-4229012.	-3094487.	107.760	-99779.	-134766.	4.693
(2 sigma)	---	---	---	2285.	1245.	0.043
1550.	-4225902.	-3056720.	103.011	-98748.	-135948.	4.581
1600.	-4222556.	-3019057.	98.562	-97536.	-137167.	4.478
1650.	-4218956.	-2981503.	94.386	-96125.	-138427.	4.382
1700.	-4316099.	-2943162.	90.432	-94499.	-139733.	4.293
1750.	-4311643.	-2902845.	86.645	-92639.	-141090.	4.211
(2 sigma)	---	---	---	4817.	1424.	0.043
1800.	-4459694.	-2858737.	82.958	-90528.	-142503.	4.135
(2 sigma)	---	---	---	5565.	1505.	0.044

Table 52. Thermophysical values for margarite, $\text{CaAl}_4\text{Si}_2\text{O}_{10}(\text{OH})_2$, at 1.01325 bars (1 atm). The tabulations are based on a fit of the thermophysical and thermochemical data given in Section 1.5.5.

T K	Cp J/(mol K)	S J/(mol K)	H-H(298) J/mol	[G-H(298)]/T J/(mol K)	cm^3/mol
200.	233.508	150.974	-28011.	-291.027	133.4726
250.	288.597	209.347	-14880.	-268.866	133.6249
(2 sigma)	0.520	0.686	28.	0.678	0.2834
273.150	308.720	235.803	-7961.	-264.947	133.6954
298.150	327.702	263.677	0.	-263.677	133.7715
(2 sigma)	0.727	0.678	0.	0.678	0.2567
300.	329.009	265.708	607.	-263.684	133.7772
350.	360.200	318.863	17869.	-267.810	133.9295
400.	385.154	368.648	36524.	-277.338	134.0818
450.	405.658	415.234	56310.	-290.100	134.2341
500.	422.853	458.889	77035.	-304.819	134.3864
(2 sigma)	1.435	0.883	228.	0.687	0.5331
550.	437.512	499.897	98553.	-320.709	134.5387
600.	450.173	538.521	120753.	-337.266	134.6910
650.	461.230	575.000	143544.	-354.163	134.8433
700.	470.973	609.545	166854.	-371.182	134.9956
750.	479.627	642.339	190623.	-388.175	135.1479
(2 sigma)	2.107	1.370	626.	0.770	1.0854
800.	487.363	673.545	214802.	-405.044	135.3002
850.	494.320	703.304	239347.	-421.720	135.4525
900.	500.606	731.739	264222.	-438.159	135.6048
950.	506.312	758.961	289398.	-454.332	135.7571
1000.	511.510	785.066	314845.	-470.221	135.9094
(2 sigma)	3.359	1.914	1201.	0.928	1.6620
1050.	516.262	810.139	340541.	-485.814	136.0617
1100.	520.620	834.258	366465.	-501.108	136.2140
1150.	524.626	857.490	392597.	-516.101	136.3663
1200.	528.317	879.897	418922.	-530.795	136.5186
1250.	531.726	901.534	445424.	-545.194	136.6709
(2 sigma)	5.013	2.597	2115.	1.134	2.2442

Table 53. Thermochemical properties of margarite, $\text{CaAl}_4\text{Si}_2\text{O}_{10}(\text{OH})_2$, at 1.01325 bars (1 atm). Columns 2 through 4 give the thermochemical values relative to the elements; columns 5 through 7 give the values relative to the oxides.

T K	Formation from the Elements			Formation from the Oxides		
	H J/mol	G J/mol	log K	H J/mol	G J/mol	log K
200.	-6235930.	-5983852.	1562.821	-145072.	-142612.	37.246
250.	-6240331.	-5920281.	1236.974	-147321.	-141727.	29.612
(2 sigma)	---	---	---	1688.	1643.	0.343
273.150	-6241747.	-5890578.	1126.458	-148246.	-141167.	26.995
298.150	-6242914.	-5858382.	1026.364	-149196.	-140477.	24.611
(2 sigma)	---	---	---	1692.	1636.	0.287
300.	-6242987.	-5855996.	1019.619	-149265.	-140423.	24.450
350.	-6244341.	-5791375.	864.315	-151076.	-138805.	20.715
400.	-6244706.	-5726630.	747.821	-192566.	-134031.	17.503
450.	-6244310.	-5661888.	657.214	-192183.	-126736.	14.711
500.	-6243327.	-5597222.	584.737	-191764.	-119487.	12.483
(2 sigma)	---	---	---	1757.	1599.	0.167
550.	-6241893.	-5532678.	525.450	-191321.	-112280.	10.663
600.	-6240120.	-5468280.	476.056	-190866.	-105115.	9.151
650.	-6238101.	-5404040.	434.274	-190410.	-97987.	7.874
700.	-6235913.	-5339963.	398.473	-189962.	-90895.	6.783
750.	-6234459.	-5276009.	367.454	-189531.	-83834.	5.839
(2 sigma)	---	---	---	1929.	1553.	0.108
800.	-6232018.	-5212192.	340.321	-189124.	-76801.	5.015
850.	-6229620.	-5148527.	316.390	-190174.	-69782.	4.288
900.	-6227308.	-5085001.	295.126	-188992.	-62733.	3.641
950.	-6267639.	-5020305.	276.035	-187724.	-55753.	3.066
1000.	-6265070.	-4954722.	258.808	-186382.	-48842.	2.551
(2 sigma)	---	---	---	2249.	1574.	0.082
1050.	-6262458.	-4889269.	243.228	-184978.	-41999.	2.089
1100.	-6259817.	-4823940.	229.070	-183521.	-35224.	1.673
1150.	-6265034.	-4758452.	216.136	-182021.	-28517.	1.295
1200.	-6261432.	-4693026.	204.282	-180487.	-21876.	0.952
1250.	-6257733.	-4627751.	193.383	-178928.	-15299.	0.639
(2 sigma)	---	---	---	2885.	1760.	0.074

Table 34. Thermophysical values for calcite, CaCO_3 , at 1.01325 bars (1 atm). The tabulations are based on a fit of the thermophysical and thermochemical data given in Section 1.5.5.

T K	Cp J/(mol K)	S J/(mol K)	H-H(298) J/mol	[G-H(298)]/T J/(mol K)	cm^3V /mol
200.	65.922	61.997	-7378.	-98.884	36.7652
250.	75.672	77.806	-3826.	-93.110	36.7709
(2 sigma)	0.251	0.446	10.	0.444	0.1402
273.150	79.387	84.673	-2031.	-92.106	36.7739
298.150	82.991	91.783	0.	-91.783	36.7775
(2 sigma)	0.163	0.444	0.	0.444	0.1407
300.	83.244	92.297	154.	-91.785	36.7777
350.	89.447	105.609	4476.	-92.822	36.7854
400.	94.725	117.907	9083.	-95.199	36.7939
450.	99.342	129.336	13937.	-98.364	36.8029
500.	103.469	140.020	19009.	-102.001	36.8126
(2 sigma)	0.123	0.448	25.	0.444	0.1487
550.	107.218	150.060	24278.	-105.918	36.8226
600.	110.672	159.539	29726.	-109.995	36.8331
650.	113.887	168.526	35341.	-114.155	36.8439
700.	116.908	177.077	41112.	-118.347	36.8550
750.	119.767	185.242	47029.	-122.536	36.8663
(2 sigma)	0.203	0.451	43.	0.445	0.1416
800.	122.489	193.059	53086.	-126.701	36.8778
850.	125.096	200.563	59276.	-130.827	36.8894
900.	127.603	207.785	65594.	-134.903	36.9013
950.	130.025	214.749	72035.	-138.923	36.9132
1000.	132.371	221.479	78595.	-142.884	36.9252
(2 sigma)	0.545	0.461	103.	0.446	0.1517
1050.	134.650	227.993	85271.	-146.782	36.9374
1100.	136.872	234.308	92059.	-150.618	36.9496
1150.	139.041	240.440	98957.	-154.390	36.9618
1200.	141.163	246.403	105963.	-158.101	36.9741
1250.	143.243	252.208	113073.	-161.749	36.9865
(2 sigma)	0.969	0.517	279.	0.448	0.2026
1300.	145.286	257.866	120286.	-165.338	36.9989
1350.	147.294	263.387	127601.	-168.867	37.0113
1400.	149.271	268.779	135015.	-172.340	37.0238
1450.	151.219	274.051	142527.	-175.756	37.0362
1500.	153.142	279.210	150137.	-179.119	37.0487
(2 sigma)	1.434	0.647	573.	0.455	0.2805
1550.	155.040	284.263	157841.	-182.430	37.0612
1600.	156.916	289.215	165640.	-185.690	37.0738
1650.	158.772	294.072	173533.	-188.901	37.0863
1700.	160.609	298.839	181517.	-192.064	37.0989
1750.	162.428	303.521	189593.	-195.182	37.1114
(2 sigma)	1.923	0.848	989.	0.474	0.3705
1800.	164.231	308.122	197760.	-198.255	37.1240
(2 sigma)	2.023	0.895	1087.	0.480	0.3893

Table 55. Thermochemical properties of calcite, CaCO_3 , at 1.01325 bars (1 atm). Columns 2 through 4 give the thermochemical values relative to the elements; columns 5 through 7 give the values relative to the oxides.

T K	Formation from the Elements			Formation from the Oxides		
	H J/mol	G J/mol	log K	H J/mol	G J/mol	log K
200.	-1208980.	-1156457.	302.035	-180485.	-148379.	38.752
250.	-1209187.	-1143294.	238.878	-180470.	-140351.	29.325
(2 sigma)	---	---	---	894.	826.	0.173
273.150	-1209155.	-1137193.	217.466	-180419.	-136638.	26.129
298.150	-1209058.	-1130610.	198.078	-180338.	-132634.	23.237
(2 sigma)	---	---	---	894.	814.	0.143
300.	-1209048.	-1130124.	196.772	-180332.	-132338.	23.042
350.	-1208696.	-1116995.	166.702	-180099.	-124356.	18.559
400.	-1208200.	-1103927.	144.158	-179785.	-116413.	15.202
450.	-1207600.	-1090928.	126.632	-179396.	-108515.	12.596
500.	-1206923.	-1078000.	112.618	-178933.	-100663.	10.516
(2 sigma)	---	---	---	895.	768.	0.080
550.	-1206187.	-1065143.	101.159	-178398.	-92861.	8.819
600.	-1205405.	-1052355.	91.616	-177792.	-85112.	7.410
650.	-1204587.	-1039634.	83.546	-177114.	-77415.	6.221
700.	-1203741.	-1026977.	76.634	-176365.	-69774.	5.207
750.	-1203709.	-1014345.	70.645	-175545.	-62188.	4.331
(2 sigma)	---	---	---	898.	722.	0.050
800.	-1202717.	-1001753.	65.408	-174652.	-54660.	3.569
850.	-1201748.	-989223.	60.790	-173689.	-47189.	2.900
900.	-1200801.	-976749.	56.689	-172653.	-39778.	2.309
950.	-1199879.	-964327.	53.022	-171546.	-32426.	1.783
1000.	-1198979.	-951952.	49.725	-170367.	-25134.	1.313
(2 sigma)	---	---	---	910.	589.	0.036
1050.	-1198104.	-939623.	46.744	-169116.	-17903.	0.891
1100.	-1197252.	-927334.	44.035	-167793.	-10733.	0.510
1150.	-1204295.	-914803.	41.552	-166399.	-3625.	0.165
1200.	-1202548.	-902254.	39.274	-164933.	3421.	-0.149
1250.	-1200721.	-889779.	37.182	-163396.	10405.	-0.435
(2 sigma)	---	---	---	958.	673.	0.028
1300.	-1198813.	-877379.	35.253	-161787.	17325.	-0.696
1350.	-1196826.	-865053.	33.471	-160108.	24183.	-0.936
1400.	-1194757.	-852803.	31.818	-158358.	30976.	-1.156
1450.	-1192608.	-840628.	30.283	-156537.	37706.	-1.358
1500.	-1190377.	-828529.	28.852	-154645.	44372.	-1.545
(2 sigma)	---	---	---	1096.	680.	0.024
1550.	-1188065.	-816505.	27.516	-152684.	50974.	-1.718
1600.	-1185672.	-804557.	26.266	-150652.	57512.	-1.878
1650.	-1183196.	-792685.	25.094	-148551.	63984.	-2.026
1700.	-1180638.	-780890.	23.994	-146380.	70392.	-2.163
1750.	-1177997.	-769171.	22.958	-144140.	76736.	-2.290
(2 sigma)	---	---	---	1376.	731.	0.022
1800.	-1328108.	-753605.	21.869	-141831.	83014.	-2.409
(2 sigma)	---	---	---	1452.	749.	0.022

Table 56. Thermophysical values for aragonite, CaCO_3 , at 1.01325 bars (1 atm). The tabulations are based on a fit of the thermophysical and thermochemical data given in Section 1.5.5.

T K	C_p J/(mol K)	S J/(mol K)	H-H(298) J/mol	$[G-H(298)]/T$ J/(mol K)	v^3 cm^3/mol
200.	66.274	58.305	-7338.	-94.993	34.1417
250.	75.230	74.104	-3789.	-89.261	34.1420
(2 sigma)	0.249	0.429	13.	0.430	0.0876
273.150	78.628	80.917	-2008.	-88.267	34.1423
298.150	81.915	87.948	0.	-87.948	34.1426
(2 sigma)	0.325	0.430	0.	0.430	0.0876
300.	82.145	88.455	152.	-87.949	34.1426
350.	87.777	101.554	4404.	-88.971	34.1434
400.	92.542	113.594	8915.	-91.306	34.1443
450.	96.688	124.739	13648.	-94.410	34.1454
500.	100.373	135.120	18576.	-97.967	34.1466
(2 sigma)	0.678	0.440	80.	0.428	0.0876
550.	103.706	144.845	23680.	-101.792	34.1478
600.	106.761	154.002	28942.	-105.765	34.1492
650.	109.593	162.660	34352.	-109.811	34.1506
700.	112.242	170.880	39898.	-113.882	34.1521
750.	114.740	178.710	45574.	-117.945	34.1536
(2 sigma)	2.367	0.654	396.	0.413	0.0877
800.	117.110	186.191	51370.	-121.978	34.1552
850.	119.371	193.359	57283.	-125.968	34.1568
900.	121.540	200.244	63306.	-129.904	34.1585
950.	123.627	206.872	69435.	-133.782	34.1602
1000.	125.644	213.265	75667.	-137.597	34.1619
(2 sigma)	4.607	1.495	1235.	0.461	0.0884
1050.	127.599	219.442	81999.	-141.348	34.1636
1100.	129.499	225.422	88426.	-145.035	34.1653
1150.	131.350	231.220	94948.	-148.656	34.1670
1200.	133.158	236.848	101561.	-152.214	34.1688
1250.	134.926	242.320	108263.	-155.710	34.1706
(2 sigma)	7.075	2.733	2676.	0.702	0.0897
1300.	136.658	247.646	115053.	-159.144	34.1723
1350.	138.359	252.835	121928.	-162.518	34.1741
1400.	140.030	257.897	128888.	-165.834	34.1759
1450.	141.674	262.840	135931.	-169.095	34.1777
1500.	143.294	267.670	143055.	-172.300	34.1795
(2 sigma)	9.667	4.222	4755.	1.120	0.0917
1550.	144.892	272.395	150260.	-175.453	34.1813
1600.	146.469	277.020	157544.	-178.555	34.1831
1650.	148.026	281.551	164906.	-181.608	34.1849
1700.	149.566	285.993	172346.	-184.613	34.1867
1750.	151.089	290.351	179863.	-187.572	34.1885
(2 sigma)	12.336	5.893	7494.	1.659	0.0945
1800.	152.598	294.628	187455.	-190.486	34.1903
(2 sigma)	12.876	6.245	8123.	1.778	0.0951

Table 57. Thermochemical properties of aragonite, CaCO₃, at 1.01325 bars (1 atm). Columns 2 through 4 give the thermochemical values relative to the elements; columns 5 through 7 give the values relative to the oxides.

T K	Formation from the Elements			Formation from the Oxides		
	H J/mol	G J/mol	log K	H J/mol	G J/mol	log K
200.	-1209543.	-1156283.	301.990	-181049.	-148204.	38.707
250.	-1209753.	-1142935.	238.803	-181037.	-139992.	29.250
(2 sigma)	---	---	---	827.	797.	0.166
273.150	-1209736.	-1136748.	217.381	-180999.	-136192.	26.044
298.150	-1209661.	-1130070.	197.983	-180942.	-132094.	23.142
(2 sigma)	---	---	---	827.	792.	0.139
300.	-1209654.	-1129576.	196.677	-180937.	-131791.	22.947
350.	-1209371.	-1116251.	166.591	-180774.	-123612.	18.448
400.	-1208971.	-1102974.	144.034	-180557.	-115460.	15.078
450.	-1208492.	-1089752.	126.495	-180288.	-107339.	12.460
500.	-1207959.	-1076587.	112.470	-179969.	-99250.	10.369
(2 sigma)	---	---	---	837.	778.	0.081
550.	-1207388.	-1063477.	101.001	-179600.	-91195.	8.661
600.	-1206792.	-1050420.	91.447	-179179.	-83177.	7.241
650.	-1206179.	-1037414.	83.368	-178707.	-75195.	6.043
700.	-1205557.	-1024456.	76.446	-178182.	-67252.	5.018
750.	-1205768.	-1011505.	70.447	-177604.	-59348.	4.133
(2 sigma)	---	---	---	939.	763.	0.053
800.	-1205036.	-998578.	65.200	-176972.	-51485.	3.362
850.	-1204345.	-985696.	60.573	-176285.	-43663.	2.683
900.	-1203693.	-972853.	56.463	-175545.	-35883.	2.083
950.	-1203082.	-960046.	52.787	-174749.	-28145.	1.548
1000.	-1202511.	-947269.	49.480	-173898.	-20451.	1.068
(2 sigma)	---	---	---	1519.	783.	0.041
1050.	-1201980.	-934521.	46.490	-172991.	-12801.	0.637
1100.	-1201488.	-921796.	43.772	-172029.	-5195.	0.247
1150.	-1208908.	-908813.	41.280	-171012.	2366.	-0.107
1200.	-1207553.	-895794.	38.993	-169938.	9881.	-0.430
1250.	-1206134.	-882833.	36.892	-168809.	17351.	-0.725
(2 sigma)	---	---	---	2832.	1033.	0.043
1300.	-1204650.	-869930.	34.954	-167624.	24774.	-0.995
1350.	-1203102.	-857085.	33.163	-166384.	32151.	-1.244
1400.	-1201488.	-844299.	31.501	-165088.	39480.	-1.473
1450.	-1199808.	-831572.	29.956	-163737.	46763.	-1.685
1500.	-1198062.	-818904.	28.517	-162330.	53997.	-1.880
(2 sigma)	---	---	---	4855.	1731.	0.060
1550.	-1196250.	-806295.	27.172	-160868.	61184.	-2.062
1600.	-1194371.	-793745.	25.913	-159352.	68323.	-2.231
1650.	-1192426.	-781256.	24.732	-157780.	75414.	-2.387
1700.	-1190412.	-768826.	23.623	-156154.	82456.	-2.534
1750.	-1188331.	-756457.	22.579	-154474.	89450.	-2.670
(2 sigma)	---	---	---	7567.	2908.	0.087
1800.	-1339017.	-740224.	21.481	-152740.	96395.	-2.797
(2 sigma)	---	---	---	8192.	3200.	0.093

Table 58. Thermophysical values for lime, CaO, at 1.01325 bars (1 atm). The tabulations are based on a fit of the thermophysical and thermochemical data given in Section 1.5.5.

T K	Cp J/(mol K)	S J/(mol K)	H-H(298) J/mol	[G-H(298)]/T J/(mol K)	V cm^3/mol
200.	33.606	22.842	-3778.	-41.734	16.6616
250.	38.873	30.955	-1956.	-38.777	16.6978
(2 sigma)	---	---	---	---	---
273.150	40.605	34.475	-1035.	-38.265	16.7145
298.150	42.153	38.100	0.	-38.100	16.7326
(2 sigma)	---	---	---	---	---
300.	42.256	38.361	78.	-38.101	16.7339
350.	44.624	45.063	2253.	-38.625	16.7701
400.	46.380	51.142	4530.	-39.815	16.8062
450.	47.738	56.686	6885.	-41.387	16.8424
500.	48.821	61.774	9300.	-43.174	16.8785
(2 sigma)	---	---	---	---	---
550.	49.707	66.470	11764.	-45.081	16.9147
600.	50.446	70.827	14268.	-47.048	16.9508
650.	51.075	74.891	16806.	-49.035	16.9870
700.	51.617	78.696	19374.	-51.019	17.0231
750.	52.092	82.274	21967.	-52.985	17.0593
(2 sigma)	---	---	---	---	---
800.	52.513	85.649	24582.	-54.922	17.0954
850.	52.891	88.845	27218.	-56.824	17.1316
900.	53.235	91.878	29871.	-58.688	17.1677
950.	53.550	94.764	32541.	-60.511	17.2039
1000.	53.842	97.519	35225.	-62.293	17.2400
(2 sigma)	---	---	---	---	---
1050.	54.117	100.152	37924.	-64.034	17.2762
1100.	54.376	102.676	40637.	-65.733	17.3123
1150.	54.624	105.099	43362.	-67.393	17.3485
1200.	54.863	107.428	46099.	-69.012	17.3846
1250.	55.095	109.673	48848.	-70.594	17.4208
(2 sigma)	---	---	---	---	---
1300.	55.321	111.838	51608.	-72.139	17.4569
1350.	55.545	113.930	54380.	-73.648	17.4931
1400.	55.766	115.954	57163.	-75.123	17.5293
1450.	55.986	117.915	59957.	-76.565	17.5654
1500.	56.207	119.817	62762.	-77.976	17.6016
(2 sigma)	---	---	---	---	---
1550.	56.429	121.663	65577.	-79.355	17.6377
1600.	56.652	123.458	68404.	-80.705	17.6739
1650.	56.879	125.205	71243.	-82.028	17.7100
1700.	57.109	126.906	74092.	-83.323	17.7462
1750.	57.342	128.565	76954.	-84.592	17.7823
(2 sigma)	---	---	---	---	---
1800.	57.580	130.184	79827.	-85.836	17.8185
(2 sigma)	---	---	---	---	---

Table 59. Thermochemical properties of lime, CaO, at 1.01325 bars (1 atm). Columns 2 through 4 give the thermochemical values relative to the elements; columns 5 through 7 give the values relative to the oxides.

T K	Formation from the Elements			Formation from the Oxides		
	H J/mol	G J/mol	log K	H J/mol	G J/mol	log K
200.	-634987.	-613888.	160.331	0.0	0.0	0.0
250.	-635133.	-608591.	127.158	0.0	0.0	0.0
(2 sigma)	---	---	---	0.0	0.0	0.0
273.150	-635131.	-606133.	115.911	0.0	0.0	0.0
298.150	-635094.	-603480.	105.727	0.0	0.0	0.0
(2 sigma)	---	---	---	0.0	0.0	0.0
300.	-635090.	-603284.	105.041	0.0	0.0	0.0
350.	-634931.	-597994.	89.246	0.0	0.0	0.0
400.	-634706.	-592732.	77.403	0.0	0.0	0.0
450.	-634444.	-587501.	68.195	0.0	0.0	0.0
500.	-634169.	-582300.	60.832	0.0	0.0	0.0
(2 sigma)	---	---	---	0.0	0.0	0.0
550.	-633898.	-577126.	54.811	0.0	0.0	0.0
600.	-633644.	-571977.	49.795	0.0	0.0	0.0
650.	-633419.	-566847.	45.552	0.0	0.0	0.0
700.	-633232.	-561733.	41.917	0.0	0.0	0.0
750.	-633927.	-556595.	38.765	0.0	0.0	0.0
(2 sigma)	---	---	---	0.0	0.0	0.0
800.	-633728.	-551447.	36.006	0.0	0.0	0.0
850.	-633621.	-546308.	33.572	0.0	0.0	0.0
900.	-633606.	-541173.	31.409	0.0	0.0	0.0
950.	-633686.	-536036.	29.473	0.0	0.0	0.0
1000.	-633860.	-530892.	27.731	0.0	0.0	0.0
(2 sigma)	---	---	---	0.0	0.0	0.0
1050.	-634129.	-525737.	26.154	0.0	0.0	0.0
1100.	-634494.	-520568.	24.720	0.0	0.0	0.0
1150.	-642827.	-515099.	23.397	0.0	0.0	0.0
1200.	-642442.	-509554.	22.180	0.0	0.0	0.0
1250.	-642049.	-504025.	21.062	0.0	0.0	0.0
(2 sigma)	---	---	---	0.0	0.0	0.0
1300.	-641649.	-498512.	20.030	0.0	0.0	0.0
1350.	-641242.	-493014.	19.076	0.0	0.0	0.0
1400.	-640828.	-487532.	18.190	0.0	0.0	0.0
1450.	-640406.	-482064.	17.366	0.0	0.0	0.0
1500.	-639976.	-476612.	16.597	0.0	0.0	0.0
(2 sigma)	---	---	---	0.0	0.0	0.0
1550.	-639537.	-471173.	15.878	0.0	0.0	0.0
1600.	-639090.	-465749.	15.205	0.0	0.0	0.0
1650.	-638633.	-460339.	14.573	0.0	0.0	0.0
1700.	-638167.	-454944.	13.979	0.0	0.0	0.0
1750.	-637691.	-449562.	13.419	0.0	0.0	0.0
(2 sigma)	---	---	---	0.0	0.0	0.0
1800.	-790039.	-440270.	12.776	0.0	0.0	0.0
(2 sigma)	---	---	---	0.0	0.0	0.0

Table 60. Thermophysical values for stable phases with the composition CaSiO_3 at 1.01325 bars (1 atm). The tabulations are based on a fit of the thermophysical and thermochemical data given in Section 1.5.5.

T K	C_p J/(mol K)	S J/(mol K)	H-H(298) J/mol	[G-H(298)]/T J/(mol K)	V cm^3/mol
wollastonite					
200.	65.696	50.950	-7572.	-88.810	39.5612
250.	77.862	66.995	-3965.	-82.857	39.6874
(2 sigma)	0.075	0.689	3.	0.689	0.1482
273.150	82.290	74.088	-2111.	-81.815	39.7403
298.150	86.456	81.479	0.	-81.479	39.7940
(2 sigma)	0.076	0.689	0.	0.689	0.0986
300.	86.742	82.015	160.	-81.481	39.7978
350.	93.556	95.919	4675.	-82.563	39.8948
400.	98.972	108.778	9493.	-85.047	39.9804
450.	103.389	120.699	14555.	-88.354	40.0564
500.	107.062	131.788	19819.	-92.149	40.1243
(2 sigma)	0.118	0.688	17.	0.688	0.0807
550.	110.165	142.141	25252.	-96.229	40.1854
600.	112.818	151.844	30828.	-100.463	40.2406
650.	115.108	160.967	36528.	-104.770	40.2909
700.	117.102	169.572	42334.	-109.094	40.3370
750.	118.849	177.712	48234.	-113.400	40.3795
(2 sigma)	0.180	0.690	50.	0.688	0.0745
800.	120.387	185.432	54216.	-117.663	40.4191
850.	121.748	192.772	60270.	-121.867	40.4562
900.	122.955	199.766	66388.	-126.002	40.4911
950.	124.029	206.443	72563.	-130.061	40.5242
1000.	124.987	212.830	78789.	-134.041	40.5558
(2 sigma)	0.260	0.693	80.	0.688	0.1827
1050.	125.842	218.949	85060.	-137.940	40.5860
1100.	126.605	224.821	91371.	-141.756	40.6152
1150.	127.286	230.464	97719.	-145.491	40.6434
1200.	127.894	235.895	104099.	-149.146	40.6709
1250.	128.435	241.127	110507.	-152.721	40.6977
(2 sigma)	0.837	0.696	145.	0.688	0.3695
1300.	128.917	246.174	116941.	-156.219	40.7239
1350.	129.343	251.047	123398.	-159.641	40.7496
1398.150	129.706	255.586	129635.	-162.868	40.7740
cyclo wollastonite (= "pseudowollastonite")					
1398.150	124.159	256.828	131371.	-162.868	40.9142
1400.	124.176	256.992	131600.	-162.992	40.9157
1450.	124.633	261.358	137821.	-166.309	40.9564
1500.	125.066	265.590	144063.	-169.548	40.9972
(2 sigma)	2.315	0.968	1032.	0.685	0.5886
1550.	125.478	269.698	150327.	-172.713	41.0381
1600.	125.869	273.688	156611.	-175.806	41.0791
1650.	126.241	277.567	162913.	-178.831	41.1201
1700.	126.597	281.341	169234.	-181.791	41.1612
1750.	126.936	285.015	175573.	-184.688	41.2023
(2 sigma)	2.652	1.220	1478.	0.699	0.8142
1800.	127.261	288.596	181928.	-187.525	41.2434
(2 sigma)	2.712	1.277	1589.	0.706	0.8601

Table 61. Thermochemical properties of stable phases with the composition CaSiO_3 at 1.01325 bars (1 atm). Columns 2 through 4 give the thermochemical values relative to the elements; columns 5 through 7 give the values relative to the oxides.

T K	Formation from the Elements			Formation from the Oxides		
	H J/mol	G J/mol	log K	H J/mol	G J/mol	log K
wollastonite						
200.	-1633703.	-1577216.	411.926	-88836.	-89253.	23.310
250.	-1634371.	-1563007.	326.572	-88864.	-89354.	18.669
(2 sigma)	---	---	---	741.	657.	0.137
273.150	-1634543.	-1556391.	297.629	-88876.	-89399.	17.096
298.150	-1634651.	-1549232.	271.419	-88888.	-89446.	15.671
(2 sigma)	---	---	---	741.	644.	0.113
300.	-1634656.	-1548702.	269.653	-88889.	-89449.	15.574
350.	-1634672.	-1534372.	228.992	-88910.	-89541.	13.363
400.	-1634494.	-1520054.	198.499	-88933.	-89630.	11.700
450.	-1634178.	-1505767.	174.785	-88966.	-89715.	10.414
500.	-1633765.	-1491520.	155.818	-89016.	-89796.	9.381
(2 sigma)	---	---	---	741.	610.	0.064
550.	-1633286.	-1477319.	140.304	-89088.	-89870.	8.535
600.	-1632767.	-1463162.	127.380	-89187.	-89937.	7.830
650.	-1632228.	-1449050.	116.447	-89319.	-89995.	7.232
700.	-1631686.	-1434980.	107.079	-89486.	-90041.	6.719
750.	-1631991.	-1420912.	98.961	-89693.	-90073.	6.273
(2 sigma)	---	---	---	743.	611.	0.043
800.	-1631375.	-1406860.	91.858	-89943.	-90091.	5.882
850.	-1630826.	-1392845.	85.594	-90950.	-90086.	5.536
900.	-1630351.	-1378861.	80.027	-90870.	-90037.	5.226
950.	-1629954.	-1364900.	75.047	-90775.	-89994.	4.948
1000.	-1629639.	-1350958.	70.567	-90669.	-89955.	4.699
(2 sigma)	---	---	---	745.	657.	0.034
1050.	-1629410.	-1337030.	66.514	-90557.	-89922.	4.473
1100.	-1629269.	-1323111.	62.829	-90443.	-89895.	4.269
1150.	-1637092.	-1308916.	59.453	-90331.	-89872.	4.082
1200.	-1636194.	-1294667.	56.355	-90224.	-89855.	3.911
1250.	-1635289.	-1280455.	53.507	-90125.	-89842.	3.754
(2 sigma)	---	---	---	752.	742.	0.031
1300.	-1634378.	-1266280.	50.880	-90037.	-89832.	3.609
1350.	-1633463.	-1252139.	48.448	-89963.	-89826.	3.476
1398.150	-1632579.	-1238554.	46.272	-89906.	-89822.	3.356
cyclo wollastonite (= "pseudowollastonite")						
1398.150	-1630843.	-1238554.	46.272	-88171.	-89822.	3.356
1400.	-1630819.	-1238035.	46.192	-88179.	-89824.	3.351
1450.	-1630174.	-1224019.	44.094	-88413.	-89879.	3.238
1500.	-1629520.	-1210025.	42.137	-88662.	-89925.	3.131
(2 sigma)	---	---	---	1222.	855.	0.030
1550.	-1628859.	-1196052.	40.307	-88925.	-89963.	3.032
1600.	-1628190.	-1182101.	38.592	-89205.	-89992.	2.938
1650.	-1627514.	-1168172.	36.981	-89501.	-90012.	2.850
1700.	-1677339.	-1153812.	35.452	-89817.	-90023.	2.766
1750.	-1676504.	-1138427.	33.980	-90151.	-90024.	2.687
(2 sigma)	---	---	---	1650.	1020.	0.030
1800.	-1828491.	-1119141.	32.477	-90506.	-90015.	2.512
(2 sigma)	---	---	---	1757.	1062.	0.031

Table 62. Thermophysical values for wollastonite, CaSiO_3 , at 1.01325 bars (1 atm). The tabulations are based on a fit of the thermophysical and thermochemical data given in Section 1.5.5.

T K	Cp J/(mol K)	S J/(mol K)	H-H(298) J/mol	[G-H(298)]/T J/(mol K)	cm^3/mol
200.	65.696	50.950	-7572.	-88.810	39.5612
250.	77.862	66.995	-3965.	-82.857	39.6874
(2 sigma)	0.075	0.689	3.	0.689	0.1482
273.150	82.290	74.088	-2111.	-81.815	39.7403
298.150	86.456	81.479	0.	-81.479	39.7940
(2 sigma)	0.076	0.689	0.	0.689	0.0986
300.	86.742	82.015	160.	-81.481	39.7978
350.	93.556	95.919	4675.	-82.563	39.8948
400.	98.972	108.778	9493.	-85.047	39.9804
450.	103.389	120.699	14555.	-88.354	40.0564
500.	107.062	131.788	19819.	-92.149	40.1243
(2 sigma)	0.118	0.688	17.	0.688	0.0807
550.	110.165	142.141	25252.	-96.229	40.1854
600.	112.818	151.844	30328.	-100.463	40.2406
650.	115.108	160.967	36528.	-104.770	40.2909
700.	117.102	169.572	42334.	-109.094	40.3370
750.	118.849	177.712	48234.	-113.400	40.3795
(2 sigma)	0.180	0.690	50.	0.688	0.0745
800.	120.387	185.432	54216.	-117.663	40.4191
850.	121.748	192.772	60270.	-121.867	40.4562
900.	122.955	199.766	66388.	-126.002	40.4911
950.	124.029	206.443	72563.	-130.061	40.5242
1000.	124.987	212.830	78789.	-134.041	40.5558
(2 sigma)	0.260	0.693	80.	0.688	0.1827
1050.	125.842	218.949	85060.	-137.940	40.5860
1100.	126.605	224.821	91371.	-141.756	40.6152
1150.	127.286	230.464	97719.	-145.491	40.6434
1200.	127.894	235.895	104099.	-149.146	40.6709
1250.	128.435	241.127	110507.	-152.721	40.6977
(2 sigma)	0.837	0.696	145.	0.688	0.3695
1300.	128.917	246.174	116941.	-156.219	40.7239
1350.	129.343	251.047	123398.	-159.641	40.7496
1398.150	129.706	255.586	129635.	-162.868	40.7740
1400.	129.719	255.758	129875.	-162.990	40.7750
1450.	130.048	260.316	136369.	-166.268	40.8000
1500.	130.335	264.730	142879.	-169.477	40.8247
(2 sigma)	1.868	0.753	438.	0.688	0.5803
1550.	130.583	269.007	149402.	-172.619	40.8491
1600.	130.794	273.157	155937.	-175.696	40.8734
1650.	130.972	277.184	162481.	-178.711	40.8974
1700.	131.117	281.096	169033.	-181.665	40.9214
1750.	131.233	284.899	175592.	-184.561	40.9452
(2 sigma)	3.333	0.970	1062.	0.692	0.8008
1800.	131.321	288.597	182156.	-187.399	40.9689
(2 sigma)	3.678	1.041	1235.	0.695	0.3456

Table 63. Thermochemical properties of wollastonite, CaSiO_3 , at 1.01325 bars (1 atm). Columns 2 through 4 give the thermochemical values relative to the elements; columns 5 through 7 give the values relative to the oxides.

T K	Formation from the Elements			Formation from the Oxides		
	H J/mol	G J/mol	log K	H J/mol	G J/mol	log K
200.	-1633703.	-1577216.	411.926	-88836.	-89253.	23.310
250.	-1634371.	-1563007.	326.572	-88864.	-89354.	18.669
(2 sigma)	---	---	---	741.	657.	0.137
273.150	-1634543.	-1556391.	297.629	-88876.	-89399.	17.096
298.150	-1634651.	-1549232.	271.419	-88888.	-89446.	15.671
(2 sigma)	---	---	---	741.	644.	0.113
300.	-1634656.	-1548702.	269.653	-88889.	-89449.	15.574
350.	-1634672.	-1534372.	228.992	-88910.	-89541.	13.363
400.	-1634494.	-1520054.	198.499	-88933.	-89630.	11.704
450.	-1634178.	-1505767.	174.785	-88966.	-89715.	10.414
500.	-1633765.	-1491520.	155.818	-89016.	-89796.	9.381
(2 sigma)	---	---	---	741.	610.	0.064
550.	-1633286.	-1477319.	140.304	-89088.	-89870.	8.535
600.	-1632767.	-1463162.	127.380	-89187.	-89937.	7.830
650.	-1632228.	-1449050.	116.447	-89319.	-89995.	7.232
700.	-1631686.	-1434980.	107.079	-89486.	-90041.	6.719
750.	-1631991.	-1420912.	98.961	-89693.	-90073.	6.273
(2 sigma)	---	---	---	743.	611.	0.043
800.	-1631375.	-1406860.	91.858	-89943.	-90091.	5.882
850.	-1630826.	-1392845.	85.594	-90950.	-90086.	5.536
900.	-1630351.	-1378861.	80.027	-90870.	-90037.	5.226
950.	-1629954.	-1364900.	75.047	-90775.	-89994.	4.948
1000.	-1629639.	-1350958.	70.567	-90669.	-89955.	4.699
(2 sigma)	---	---	---	745.	557.	0.034
1050.	-1629410.	-1337030.	66.514	-90557.	-89922.	4.473
1100.	-1629269.	-1323111.	62.829	-90443.	-89895.	4.269
1150.	-1637092.	-1308916.	59.453	-90331.	-89872.	4.082
1200.	-1636194.	-1294667.	56.355	-90224.	-89855.	3.911
1250.	-1635289.	-1280455.	53.507	-90125.	-89842.	3.754
(2 sigma)	---	---	---	752.	742.	0.031
1300.	-1634378.	-1266280.	50.880	-90037.	-89832.	3.609
1350.	-1633463.	-1252139.	48.448	-89963.	-89826.	3.476
1398.150	-1632579.	-1238554.	46.272	-89906.	-89822.	3.356
1400.	-1632545.	-1238033.	46.192	-89905.	-89822.	3.351
1450.	-1631625.	-1223960.	44.092	-89865.	-89819.	3.236
1500.	-1630704.	-1209918.	42.133	-89846.	-89818.	3.128
(2 sigma)	---	---	---	850.	855.	0.030
1550.	-1629784.	-1195907.	40.302	-89850.	-39817.	3.027
1600.	-1628864.	-1181925.	38.586	-89879.	-39816.	2.932
1650.	-1627946.	-1167973.	36.975	-89934.	-39813.	2.843
1700.	-1677540.	-1153598.	35.446	-90018.	-39808.	2.759
1750.	-1676485.	-1138203.	33.973	-90132.	-39800.	2.580
(2 sigma)	---	---	---	1279.	996.	0.030
1800.	-1828263.	-1118915.	32.470	-90277.	-39789.	2.606
(2 sigma)	---	---	---	1423.	1029.	0.030

Table 64. Thermophysical values for cyclowollastonite (= "pseudo-wollastonite"), CaSiO_3 , at 1.01325 bars (1 atm). The tabulations are based on a fit of the thermophysical and thermochemical data given in Section 1.5.5.

T K	Cp J/(mol K)	S J/(mol K)	H-H(298) J/mol	[G-H(298)]/T J/(mol K)	cm^3/mol
200.	69.327	55.409	-7897.	-94.893	40.1374
250.	81.283	72.268	-4108.	-88.700	40.1453
(2 sigma)	1.149	0.975	59.	0.899	0.1800
273.150	85.285	79.646	-2179.	-87.622	40.1508
298.150	88.906	87.276	0.	-87.276	40.1578
(2 sigma)	1.290	0.904	0.	0.904	0.1244
300.	89.150	87.826	165.	-87.277	40.1584
350.	94.798	102.015	4770.	-88.385	40.1758
400.	99.098	114.966	9622.	-90.910	40.1968
450.	102.511	126.842	14666.	-94.252	40.2210
500.	105.304	137.792	19863.	-98.066	40.2478
(2 sigma)	0.958	0.884	236.	0.867	0.0994
550.	107.646	147.941	25188.	-102.144	40.2769
600.	109.646	157.396	30622.	-106.359	40.3078
650.	111.380	166.242	36149.	-110.629	40.3403
700.	112.903	174.553	41756.	-114.901	40.3742
750.	114.255	182.390	47436.	-119.142	40.4092
(2 sigma)	0.884	0.872	389.	0.822	0.1000
800.	115.466	189.803	53180.	-123.328	40.4452
850.	116.559	196.836	58981.	-127.447	40.4820
900.	117.551	203.527	64834.	-131.490	40.5195
950.	118.459	209.907	70734.	-135.450	40.5576
1000.	119.292	216.005	76678.	-139.327	40.5962
(2 sigma)	1.406	0.798	519.	0.785	0.1913
1050.	120.061	221.844	82663.	-143.118	40.6352
1100.	120.774	227.446	88684.	-146.825	40.6746
1150.	121.438	232.830	94739.	-150.448	40.7142
1200.	122.057	238.011	100827.	-153.989	40.7542
1250.	122.636	243.006	106944.	-157.450	40.7943
(2 sigma)	1.905	0.812	794.	0.744	0.3748
1300.	123.180	247.826	113090.	-160.834	40.8346
1350.	123.693	252.485	119262.	-164.143	40.8751
1398.150	124.159	256.828	125229.	-167.260	40.9142
1400.	124.176	256.992	125459.	-167.379	40.9157
1450.	124.633	261.358	131679.	-170.545	40.9564
1500.	125.066	265.590	137921.	-173.643	40.9972
(2 sigma)	2.315	0.968	1236.	0.709	0.5886
1550.	125.478	269.698	144185.	-176.675	41.0381
1600.	125.869	273.688	150469.	-179.645	41.0791
1650.	126.241	277.567	156772.	-182.554	41.1201
1700.	126.597	281.341	163093.	-185.404	41.1612
1750.	126.936	285.015	169431.	-188.198	41.2023
(2 sigma)	2.652	1.220	1804.	0.691	0.8142
1800.	127.261	288.596	175786.	-190.937	41.2434
(2 sigma)	2.712	1.277	1930.	0.690	0.8601

Table 65. Thermochemical properties of cyclowollastonite (= "pseudowollastonite"), CaSiO_3 , at 1.01325 bars (1 atm). Columns 2 through 4 give the thermochemical values relative to the elements, columns 5 through 7 give the values relative to the oxides.

T K	Formation from the Elements			Formation from the Oxides		
	H J/mol	G J/mol	log K	H J/mol	G J/mol	log K
200.	-1627886.	-1572291.	410.640	-83019.	-84328.	22.024
250.	-1628372.	-1558326.	325.594	-82865.	-84673.	17.691
(2 sigma)	---	---	---	1012.	896.	0.187
273.150	-1628470.	-1551835.	296.758	-82803.	-84843.	16.225
298.150	-1628510.	-1544819.	270.646	-82746.	-85032.	14.897
(2 sigma)	---	---	---	1021.	879.	0.154
300.	-1628510.	-1544300.	268.886	-82743.	-85047.	14.808
350.	-1628434.	-1530268.	228.380	-82672.	-85437.	12.751
400.	-1628223.	-1516258.	198.003	-82662.	-85834.	11.209
450.	-1627926.	-1502279.	174.380	-82714.	-86227.	10.009
500.	-1627579.	-1488337.	155.485	-82830.	-86612.	9.048
(2 sigma)	---	---	---	1073.	796.	0.083
550.	-1627208.	-1474430.	140.030	-83010.	-86982.	8.261
600.	-1626832.	-1460558.	127.153	-83252.	-87333.	7.603
650.	-1626466.	-1446717.	116.260	-83556.	-87661.	7.045
700.	-1626122.	-1432903.	106.924	-83922.	-87964.	6.564
750.	-1626047.	-1419076.	98.833	-84349.	-88238.	6.145
(2 sigma)	---	---	---	1072.	717.	0.050
800.	-1626269.	-1405251.	91.753	-84837.	-88482.	5.777
850.	-1625973.	-1391447.	85.508	-86097.	-88688.	5.450
900.	-1625763.	-1377658.	79.957	-86282.	-88835.	5.156
950.	-1625640.	-1363878.	74.991	-86462.	-88972.	4.892
1000.	-1625607.	-1350102.	70.522	-86638.	-89099.	4.654
(2 sigma)	---	---	---	1010.	704.	0.037
1050.	-1625665.	-1336326.	66.479	-86813.	-89218.	4.438
1100.	-1625815.	-1322545.	62.802	-86989.	-89328.	4.242
1150.	-1633930.	-1308474.	59.433	-87169.	-89431.	4.062
1200.	-1633325.	-1294337.	56.341	-87354.	-89525.	3.897
1250.	-1632711.	-1280225.	53.498	-87546.	-89612.	3.745
(2 sigma)	---	---	---	1014.	752.	0.031
1300.	-1632088.	-1266138.	50.874	-87747.	-89690.	3.604
1350.	-1631458.	-1252075.	48.446	-87957.	-89761.	3.473
1398.150	-1630843.	-1238554.	46.272	-88171.	-89822.	3.356
1400.	-1630819.	-1238035.	46.192	-88179.	-89824.	3.351
1450.	-1630174.	-1224019.	44.094	-88413.	-89879.	3.238
1500.	-1629520.	-1210025.	42.137	-88662.	-89925.	3.131
(2 sigma)	---	---	---	1222.	855.	0.030
1550.	-1628859.	-1196052.	40.307	-88925.	-89963.	3.032
1600.	-1628190.	-1182101.	38.592	-89205.	-89992.	2.938
1650.	-1627514.	-1168172.	36.981	-89501.	-90012.	2.850
1700.	-1677339.	-1153812.	35.452	-89817.	-90023.	2.766
1750.	-1676504.	-1138427.	33.980	-90151.	-90024.	2.687
(2 sigma)	---	---	---	1650.	1020.	0.030
1800.	-1828491.	-1119141.	32.477	-90506.	-90015.	2.612
(2 sigma)	---	---	---	1757.	1062.	0.031

Table 60. Thermophysical values for bicchulite, $\text{Ca}_2\text{Al}_2\text{SiO}_6(\text{OH})_2$, at 1.01325 bars (1 atm). The tabulations are based on a fit of the thermophysical and thermochemical data given in Section 1.5.5.

T K	Cp J/(mol K)	S J/(mol K)	H-H(298) J/mol	[G-H(298)]/T J/(mol K)	cm^3/mol
200.	178.990	132.525	-21044.	-237.746	103.1788
250.	216.623	176.750	-11100.	-221.149	103.3668
(2 sigma)	---	19.874	---	19.874	1.5404
273.150	230.317	196.546	-5923.	-218.228	103.4538
298.150	243.200	217.285	0.	-217.285	103.5478
(2 sigma)	---	19.874	---	19.874	1.5335
300.	244.086	218.792	451.	-217.289	103.5548
350.	265.161	258.066	13203.	-220.343	103.7427
400.	281.913	294.607	26895.	-227.369	103.9307
450.	295.582	328.627	41344.	-236.752	104.1187
500.	306.959	360.376	56415.	-247.545	104.3066
(2 sigma)	---	19.874	---	19.874	1.6092
550.	316.578	390.096	72010.	-259.168	104.4946
600.	324.813	418.004	88050.	-271.253	104.6826
650.	331.936	444.290	104473.	-283.563	104.8705
700.	338.150	469.122	121229.	-295.938	105.0585
750.	343.608	492.642	138275.	-308.275	105.2465
(2 sigma)	---	19.874	---	19.874	1.9015
800.	348.430	514.975	155579.	-320.502	105.4344
850.	352.713	536.229	173109.	-332.571	105.6224
900.	356.531	556.500	190842.	-344.453	105.8104
950.	359.946	575.870	208756.	-356.127	105.9983
1000.	363.010	594.412	226831.	-367.581	106.1863
(2 sigma)	---	19.874	---	19.874	2.3348
1050.	365.765	612.191	245052.	-378.809	106.3743
1100.	368.246	629.265	263403.	-389.808	106.5622
1150.	370.484	645.684	281872.	-400.578	106.7502
1200.	372.504	661.495	300448.	-411.122	106.9381
1250.	374.329	676.739	319119.	-421.444	107.1261
(2 sigma)	---	19.874	---	19.874	2.8454

Table 67. Thermochemical properties of bicchulite, $\text{Ca}_2\text{Al}_2\text{SiO}_6(\text{OH})_2$, at 1.01325 bars (1 atm). Columns 2 through 4 give the thermochemical values relative to the elements; columns 5 through 7 give the values relative to the oxides.

T K	Formation from the Elements			Formation from the Oxides		
	H J/mol	G J/mol	log K	H J/mol	G J/mol	log K
200.	-4332877.	-4158124.	1085.990	-190320.	-189775.	49.564
250.	-4335695.	-4114080.	859.589	-192795.	-189342.	39.561
(2 sigma)	---	---	---	18768.	13855.	2.895
273.150	-4336559.	-4093517.	782.805	-193805.	-188976.	36.138
298.150	-4337238.	-4071241.	713.264	-194835.	-188488.	33.022
(2 sigma)	---	---	---	18768.	12913.	2.262
300.	-4337279.	-4069590.	708.578	-194909.	-188449.	32.812
350.	-4337955.	-4024911.	600.685	-196836.	-187218.	27.941
400.	-4337956.	-3980184.	519.758	-238395.	-182818.	23.874
450.	-4337454.	-3935488.	456.819	-238041.	-175891.	20.417
500.	-4336582.	-3890869.	406.476	-237617.	-169007.	17.656
(2 sigma)	---	---	---	18768.	9002.	0.940
550.	-4335444.	-3846351.	365.296	-237141.	-162169.	15.402
600.	-4334125.	-3801945.	330.988	-236629.	-155376.	13.527
650.	-4332695.	-3757654.	301.969	-236095.	-148626.	11.944
700.	-4331215.	-3713476.	277.103	-235551.	-141918.	10.590
750.	-4331407.	-3669330.	255.555	-235007.	-135249.	9.420
(2 sigma)	---	---	---	18768.	4416.	0.308
800.	-4329755.	-3625246.	236.704	-234472.	-128616.	8.398
850.	-4328254.	-3581261.	220.077	-234667.	-122011.	7.498
900.	-4326933.	-3537359.	205.303	-233753.	-115410.	6.698
950.	-4347075.	-3492878.	192.052	-232806.	-108862.	5.986
1000.	-4345914.	-3447951.	180.102	-231834.	-102363.	5.347
(2 sigma)	---	---	---	18768.	2708.	0.141
1050.	-4344881.	-3403079.	169.294	-230847.	-95914.	4.771
1100.	-4343988.	-3358253.	159.470	-229852.	-89512.	4.251
1150.	-4358989.	-3312903.	150.477	-228857.	-83155.	3.777
1200.	-4356518.	-3267474.	142.229	-227867.	-76841.	3.345
1250.	-4354006.	-3222149.	134.646	-226890.	-70569.	2.949
(2 sigma)	---	---	---	18768.	6674.	0.279

Table 68. Thermophysical values for gehlenite, $\text{Ca}_2\text{Al}_2\text{SiO}_7$, at 1.01325 bars (1 atm). The tabulations are based on a fit of the thermophysical and thermochemical data given in Section 1.5.5.

T K	Cp J/(mol K)	S J/(mol K)	H-H(298) J/mol	[G-H(298)]/T J/(mol K)	V^0 cm ³ /mol
200.	157.139	137.516	-17976.	-227.398	90.0044
250.	184.553	175.645	-9407.	-213.274	90.1287
(2 sigma)	0.533	1.024	27.	1.019	0.2395
273.150	195.180	192.461	-5010.	-210.802	90.1863
298.150	205.390	210.004	0.	-210.004	90.2485
(2 sigma)	0.601	1.019	0.	1.019	0.2312
300.	206.098	211.276	381.	-210.008	90.2531
350.	223.067	244.372	11126.	-212.582	90.3774
400.	236.587	275.074	22630.	-218.499	90.5017
450.	247.494	303.592	34742.	-226.388	90.6260
500.	256.399	330.144	47346.	-235.452	90.7503
(2 sigma)	1.099	1.100	169.	1.022	0.3329
550.	263.749	354.937	60356.	-245.200	90.8747
600.	269.877	378.157	73701.	-255.323	90.9990
650.	275.035	399.968	87327.	-265.619	91.1233
700.	279.418	420.515	101191.	-275.956	91.2476
750.	283.178	439.924	115259.	-286.246	91.3719
(2 sigma)	1.196	1.235	359.	1.047	0.5892
800.	286.438	458.307	129501.	-296.431	91.4963
850.	289.294	475.760	143896.	-306.471	91.6206
900.	291.826	492.368	158425.	-316.341	91.7449
950.	294.099	508.208	173074.	-326.025	91.8692
1000.	296.169	523.347	187831.	-335.516	91.9935
(2 sigma)	1.981	1.284	538.	1.075	0.8753
1050.	298.080	537.844	202688.	-344.808	92.1179
1100.	299.871	551.752	217637.	-353.900	92.2422
1150.	301.576	565.120	232674.	-362.795	92.3665
1200.	303.222	577.990	247794.	-371.495	92.4908
1250.	304.834	590.401	262995.	-380.004	92.6151
(2 sigma)	1.933	1.360	839.	1.096	1.1696
1300.	306.433	602.388	278277.	-388.328	92.7395
1350.	308.038	613.983	293639.	-396.472	92.8638
1400.	309.665	625.215	309081.	-404.442	92.9881
1450.	311.328	636.110	324606.	-412.244	93.1124
1500.	313.040	646.693	340215.	-419.883	93.2367
(2 sigma)	4.049	1.373	1006.	1.112	1.4672
1550.	314.812	656.987	355911.	-427.367	93.3611
1600.	316.654	667.010	371697.	-434.699	93.4854
1650.	318.575	676.783	387578.	-441.888	93.6097
1700.	320.584	686.323	403556.	-448.937	93.7340
1750.	322.687	695.647	419638.	-455.854	93.8583
(2 sigma)	10.352	1.659	1970.	1.125	1.7664
1800.	324.891	704.768	435827.	-462.642	93.9827
(2 sigma)	12.039	1.841	2434.	1.128	1.8263

Table 69. Thermochemical properties of gehlenite, $\text{Ca}_2\text{Al}_2\text{SiO}_7$, at 1.01325 bars (1 atm). Columns 2 through 4 give the thermochemical values relative to the elements; columns 5 through 7 give the values relative to the oxides.

T K	Formation from the Elements			Formation from the Oxides		
	H J/mol	G J/mol	log K	H J/mol	G J/mol	log K
200.	-3980020.	-3849503.	1005.386	-722656.	-735417.	192.071
250.	-3982126.	-3816609.	797.436	-720692.	-738836.	154.371
(2 sigma)	---	---	---	2537.	2422.	0.506
273.150	-3982778.	-3801252.	726.915	-719792.	-740557.	141.617
298.150	-3983286.	-3784613.	663.048	-718812.	-742501.	130.083
(2 sigma)	---	---	---	2538.	2403.	0.421
300.	-3983317.	-3783380.	658.745	-718739.	-742648.	129.306
350.	-3983810.	-3750010.	559.658	-716736.	-746790.	111.452
400.	-3983787.	-3716607.	485.339	-714681.	-751223.	98.100
450.	-3983397.	-3683230.	427.538	-712587.	-755916.	87.744
500.	-3982753.	-3649910.	381.303	-710470.	-760844.	79.485
(2 sigma)	---	---	---	2568.	2324.	0.243
550.	-3981950.	-3616664.	343.482	-708345.	-765984.	72.747
600.	-3981064.	-3583495.	311.971	-706225.	-771318.	67.149
650.	-3980156.	-3550401.	285.314	-704122.	-776828.	62.427
700.	-3979280.	-3517376.	262.470	-702044.	-782499.	58.391
750.	-3980151.	-3484338.	242.671	-699997.	-788317.	54.903
(2 sigma)	---	---	---	2627.	2236.	0.156
800.	-3979245.	-3451315.	225.348	-697989.	-794271.	51.861
850.	-3978552.	-3418342.	210.066	-131830.	-159923.	9.828
900.	-3978092.	-3385403.	196.484	-132136.	-161567.	9.377
950.	-3999141.	-3351835.	184.297	-132438.	-163194.	8.973
1000.	-3998926.	-3317773.	173.303	-132737.	-164805.	8.608
(2 sigma)	---	---	---	2671.	2174.	0.114
1050.	-3998870.	-3283717.	163.356	-133035.	-166401.	8.278
1100.	-3998977.	-3249660.	154.313	-133333.	-167982.	7.977
1150.	-4014993.	-3215034.	146.031	-133631.	-169551.	7.701
1200.	-4013546.	-3180284.	138.434	-133927.	-171106.	7.448
1250.	-4012058.	-3145595.	131.447	-134221.	-172649.	7.215
(2 sigma)	---	---	---	2730.	2152.	0.090
1300.	-4010527.	-3110967.	125.000	-134510.	-174181.	6.999
1350.	-4008949.	-3076398.	119.033	-134793.	-175701.	6.798
1400.	-4007323.	-3041889.	113.494	-135068.	-177211.	6.612
1450.	-4005644.	-3007439.	108.340	-135332.	-178711.	6.438
1500.	-4003907.	-2973047.	103.531	-135581.	-180203.	6.275
(2 sigma)	---	---	---	2753.	2182.	0.076
1550.	-4002108.	-2938715.	99.034	-135814.	-181686.	6.123
1600.	-4000240.	-2904441.	94.820	-136025.	-183163.	5.980
1650.	-3998298.	-2870227.	90.864	-136212.	-184633.	5.845
1700.	-4046784.	-2835624.	87.128	-136371.	-186098.	5.718
1750.	-4044531.	-2800034.	83.576	-136498.	-187558.	5.598
(2 sigma)	---	---	---	3209.	2259.	0.067
1800.	-4347847.	-2756663.	79.996	-136589.	-189016.	5.485
(2 sigma)	---	---	---	3511.	2231.	0.066

Table 70. Thermophysical values for prehnite, $\text{Ca}_2\text{Al}_2\text{Si}_3\text{O}_{10}(\text{OH})_2$, at 1.01325 bars (1 atm). The tabulations are based on a fit of the thermophysical and thermochemical data given in Section 1.5.5.

T K	Cp J/(mol K)	S J/(mol K)	H-H(298) J/mol	[G-H(298)]/T J/(mol K)	cm^3/mol
200.	244.310	177.684	-28569.	-320.529	139.9306
250.	293.554	237.707	-15074.	-298.002	140.1868
(2 sigma)	0.346	0.755	16.	0.753	1.6079
273.150	312.686	264.555	-8053.	-294.035	140.3054
298.150	331.165	292.751	0.	-292.751	140.4334
(2 sigma)	0.414	0.753	0.	0.753	1.5934
300.	332.451	294.804	614.	-292.757	140.4429
350.	363.534	348.472	18041.	-296.925	140.6991
400.	388.759	398.718	36870.	-306.543	140.9553
450.	409.525	445.744	56843.	-319.426	141.2114
500.	426.825	489.814	77765.	-334.285	141.4676
(2 sigma)	2.111	0.975	259.	0.760	1.6296
550.	441.379	531.197	99480.	-350.324	141.7238
600.	453.721	570.146	121866.	-367.036	141.9799
650.	464.249	606.890	144822.	-384.086	142.2361
700.	473.272	641.633	168266.	-401.253	142.4923
750.	481.029	674.556	192128.	-418.386	142.7484
(2 sigma)	2.968	1.793	892.	0.874	1.8704
800.	487.712	705.820	216351.	-435.381	143.0046
850.	493.472	735.564	240884.	-452.172	143.2608
900.	498.434	763.915	265685.	-468.709	143.5170
950.	502.701	790.981	290716.	-484.964	143.7731
1000.	506.356	816.861	315945.	-500.917	144.0293
(2 sigma)	3.975	2.544	1627.	1.125	2.2614
1050.	509.472	841.644	341342.	-516.556	144.2855
1100.	512.109	865.407	366884.	-531.876	144.5416
1150.	514.316	888.222	392546.	-546.877	144.7978
1200.	516.140	910.151	418309.	-561.560	145.0540
1250.	517.616	931.251	444154.	-575.928	145.3101
(2 sigma)	6.144	3.246	2584.	1.419	2.7389

Table 71. Thermochemical properties of prehnite, $\text{Ca}_2\text{Al}_2\text{Si}_3\text{O}_{10}(\text{OH})_2$, at 1.01325 bars (1 atm). Columns 2 through 4 give the thermochemical values relative to the elements; columns 5 through 7 give the values relative to the oxides.

T K	Formation from the Elements			Formation from the Oxides		
	H J/mol	G J/mol	log K	H J/mol	G J/mol	log K
200.	-6190713.	-5942974.	1552.144	-228397.	-226474.	59.149
250.	-6194593.	-5880553.	1228.673	-230945.	-225690.	47.155
(2 sigma)	---	---	---	1882.	1834.	0.383
273.15U	-6195829.	-5851415.	1118.969	-232004.	-225155.	43.057
298.15U	-6196820.	-5819846.	1019.612	-233078.	-224480.	39.328
(2 sigma)	---	---	---	1882.	1827.	0.320
300.	-6196881.	-5817507.	1012.917	-233154.	-224427.	39.076
350.	-6197907.	-5754181.	858.764	-235126.	-222814.	33.253
400.	-6197949.	-5690779.	743.139	-276678.	-218029.	28.472
450.	-6197231.	-5627419.	653.213	-276282.	-210720.	24.460
500.	-6195931.	-5564171.	581.285	-275805.	-203461.	21.255
(2 sigma)	---	---	---	1945.	1796.	0.188
550.	-6194195.	-5501076.	522.448	-275291.	-196251.	18.638
600.	-6192143.	-5438154.	473.433	-274776.	-189088.	16.462
650.	-6189874.	-5375412.	431.973	-274293.	-181968.	14.623
700.	-6187473.	-5312851.	396.450	-273873.	-174882.	13.050
750.	-6186684.	-5250391.	365.669	-273541.	-167823.	11.688
(2 sigma)	---	---	---	2220.	1763.	0.123
800.	-6184010.	-5188059.	338.745	-273319.	-160783.	10.498
850.	-6181461.	-5125891.	314.999	-275365.	-153738.	9.448
900.	-6179080.	-5063868.	293.899	-274152.	-146618.	8.509
950.	-6198162.	-5001325.	274.992	-272907.	-139566.	7.674
1000.	-6195951.	-4938391.	257.955	-271652.	-132581.	6.925
(2 sigma)	---	---	---	2675.	1843.	0.096
1050.	-6193889.	-4875565.	242.546	-270408.	-125658.	6.251
1100.	-6191993.	-4812833.	228.542	-269194.	-118794.	5.641
1150.	-6206026.	-4749622.	215.734	-268026.	-111984.	5.086
1200.	-6202629.	-4686373.	203.992	-266920.	-105223.	4.580
1250.	-6199237.	-4623265.	193.196	-265891.	-98507.	4.116
(2 sigma)	---	---	---	3369.	2159.	0.090

Table 72. Thermophysical values for zoisite, $\text{Ca}_2\text{Al}_3\text{Si}_3\text{O}_{12}(\text{OH})$, at 1.01325 bars (1 atm). The tabulations are based on a fit of the thermophysical and thermochemical data given in Section 1.5.5.

T K	Cp J/(mol K)	S J/(mol K)	H-H(298) J/mol	[G-H(298)]/T J/(mol K)	V cm^3/mol
200.	253.187	175.254	-29971.	-325.110	136.2311
250.	308.188	237.915	-15879.	-301.433	136.4800
(2 sigma)	0.367	0.760	17.	0.757	1.0162
273.150	329.369	266.151	-8495.	-297.251	136.5953
298.150	349.800	295.896	0.	-295.896	136.7198
(2 sigma)	0.439	0.757	0.	0.757	0.9945
300.	351.219	298.064	648.	-295.902	136.7290
350.	385.421	354.870	19096.	-300.310	136.9779
400.	413.084	408.204	39082.	-310.499	137.2268
450.	435.800	458.212	60322.	-324.163	137.4757
500.	454.690	505.136	82598.	-339.939	137.7246
(2 sigma)	2.227	0.989	275.	0.762	1.0239
550.	470.559	549.238	105741.	-356.982	137.9736
600.	483.996	590.774	129614.	-374.751	138.2225
650.	495.447	629.978	154107.	-392.890	138.4714
700.	505.249	667.063	179131.	-411.161	138.7203
750.	513.668	702.216	204609.	-429.404	138.9692
(2 sigma)	3.189	1.846	936.	0.878	1.2899
800.	520.912	735.604	230478.	-447.506	139.2182
850.	527.149	767.376	256684.	-465.395	139.4671
900.	532.515	797.663	283179.	-483.020	139.7160
950.	537.123	826.581	309923.	-500.347	139.9649
1000.	541.065	854.235	336880.	-517.355	140.2138
(2 sigma)	4.767	2.657	1743.	1.139	1.6967
1050.	544.419	880.717	364019.	-534.032	140.4628
1100.	547.251	906.111	391313.	-550.372	140.7117
1150.	549.616	930.491	418737.	-566.372	140.9606
1200.	551.562	953.925	446268.	-582.035	141.2095
1250.	553.131	976.474	473886.	-597.364	141.4584
(2 sigma)	7.762	3.538	2956.	1.455	2.1664

Table 73. Thermochemical properties of zoisite, $\text{Ca}_2\text{Al}_2\text{Si}_2\text{O}_{12}(\text{OH})$, at 1.01325 bars (1 atm). Columns 2 through 4 give the thermochemical values relative to the elements; columns 5 through 7 give the values relative to the oxides.

T K	Formation from the Elements			Formation from the Oxides		
	H J/mol	G J/mol	log K	H J/mol	G J/mol	log K
200.	-6887201.	-6627758.	1730.992	-232827.	-231804.	60.541
250.	-6891657.	-6562340.	1371.125	-234269.	-231379.	48.344
(2 sigma)	---	---	---	2249.	2201.	0.460
273.150	-6893086.	-6531778.	1249.075	-234896.	-231083.	44.190
298.150	-6894244.	-6498655.	1138.537	-235536.	-230706.	40.419
(2 sigma)	---	---	---	2250.	2193.	0.384
300.	-6894316.	-6496200.	1131.088	-235582.	-230676.	40.164
350.	-6895573.	-6429731.	959.584	-236758.	-229763.	34.290
400.	-6895747.	-6363159.	830.943	-257693.	-227240.	29.674
450.	-6895090.	-6296617.	730.892	-257630.	-223436.	25.936
500.	-6893801.	-6230185.	650.862	-257513.	-219643.	22.946
(2 sigma)	---	---	---	2343.	2152.	0.225
550.	-6892043.	-6163905.	585.398	-257375.	-215863.	20.501
600.	-6889947.	-6097801.	530.860	-257249.	-212094.	18.464
650.	-6887626.	-6031881.	484.728	-257161.	-208336.	16.742
700.	-6885173.	-5966146.	445.199	-257139.	-204581.	15.266
750.	-6884341.	-5900516.	410.948	-257204.	-200825.	13.987
(2 sigma)	---	---	---	2577.	2067.	0.144
800.	-6881641.	-5835016.	380.987	-257377.	-197062.	12.867
850.	-6879089.	-5769681.	354.561	-259813.	-193268.	11.877
900.	-6876737.	-5704491.	331.080	-258986.	-189377.	10.991
950.	-6906513.	-5638454.	310.024	-258121.	-185533.	10.201
1000.	-6904273.	-5571772.	291.039	-257240.	-181736.	9.493
(2 sigma)	---	---	---	3187.	2046.	0.107
1050.	-6902171.	-5505200.	273.869	-256364.	-177982.	8.854
1100.	-6900226.	-5438724.	258.263	-255511.	-174270.	8.275
1150.	-6914201.	-5371771.	243.993	-254699.	-170595.	7.749
1200.	-6910739.	-5304783.	230.911	-253943.	-166955.	7.267
1250.	-6907277.	-5237940.	218.881	-253259.	-163345.	6.826
(2 sigma)	---	---	---	4036.	2253.	0.094

Table 74. Thermophysical values for stable phases with the composition Ca_2SiO_4 at 1.01325 bars (1 atm). The tabulations are based on a fit of the thermophysical and thermochemical data given in Section 1.5.5.

T K	C_p J/(mol K)	S J/(mol K)	H-H(298) J/mol	$[G-H(298)]/T$ J/(mol K)	v^V cm^3/mol
Ca-olivine					
200.	97.496	75.402	-11176.	-131.282	58.9137
250.	115.197	99.254	-5815.	-122.515	59.0137
(2 sigma)	0.307	2.153	17.	2.152	0.9342
273.150	120.737	109.706	-3082.	-120.989	59.0600
298.150	125.690	120.499	0.	-120.499	59.1100
(2 sigma)	0.407	2.152	0.	2.152	0.9260
300.	126.025	121.278	233.	-120.502	59.1137
350.	133.898	141.321	6739.	-122.067	59.2137
400.	140.297	159.630	13598.	-125.634	59.3137
450.	145.851	176.482	20755.	-130.360	59.4137
500.	150.846	192.112	28174.	-135.763	59.5137
(2 sigma)	0.526	2.162	82.	2.153	1.0616
550.	155.417	206.706	35833.	-141.556	59.6137
600.	159.629	220.413	43710.	-147.562	59.7137
650.	163.510	233.345	51790.	-153.668	59.8137
700.	167.074	245.595	60056.	-159.801	59.9137
750.	170.322	257.234	68492.	-165.912	60.0137
(2 sigma)	0.433	2.182	185.	2.156	1.4860
800.	173.251	268.322	77083.	-171.968	60.1137
850.	175.859	278.905	85812.	-177.950	60.2137
900.	178.138	289.023	94663.	-183.842	60.3137
950.	180.084	298.708	103620.	-189.634	60.4137
970.	180.767	302.467	107229.	-191.922	60.4537
1000.	181.690	307.987	112666.	-195.322	60.5137
(2 sigma)	1.428	2.172	158.	2.159	2.0289
1050.	182.952	316.884	121783.	-200.900	60.6137
1100.	183.864	325.417	130955.	-206.367	60.7137
1120.	184.130	328.733	134635.	-208.523	60.7537
bredigite					
1120.	185.297	341.377	148797.	-208.523	53.5615
1150.	186.587	346.292	154375.	-212.053	53.6185
1200.	188.814	354.280	163759.	-217.813	53.7135
1250.	191.135	362.034	173258.	-223.428	53.8085
(2 sigma)	2.241	1.488	2941.	1.941	2.8942
1300.	193.551	369.577	182875.	-228.905	53.9035
1350.	196.062	376.929	192614.	-234.251	53.9985
1400.	198.668	384.106	202482.	-239.476	54.0935
1450.	201.368	391.124	212483.	-244.584	54.1885
1500.	204.163	397.998	222621.	-249.584	54.2835
(2 sigma)	6.096	1.486	2960.	1.655	3.4552
1550.	207.053	404.739	232901.	-254.481	54.3785
1600.	210.037	411.360	243328.	-259.280	54.4735
1650.	213.117	417.870	253906.	-263.987	54.5685
1700.	216.291	424.279	264641.	-268.608	54.6635
1710.	216.937	425.549	266807.	-269.522	54.6825
alpha- Ca_2SiO_4					
1710.	199.600	433.962	281193.	-269.522	54.9805
1750.	199.600	438.577	289177.	-273.333	55.0565
(2 sigma)	35.790	1.506	3100.	1.474	3.7697
1800.	199.600	444.200	299157.	-278.002	55.1515
(2 sigma)	35.790	1.735	3471.	1.446	3.8972

Table 75. Thermochemical properties of stable phases with the composition Ca_2SiO_4 at 1.01325 bars (1 atm). Columns 2 through 4 give the thermochemical values relative to the elements; columns 5 through 7 give the values relative to the oxides.

T K	Formation from the Elements			Formation from the Oxides		
	H J/mol	G J/mol	log K	H J/mol	G J/mol	log K
Ca-olivine						
200.	-2316298.	-2239033.	584.775	-136444.	-137183.	35.828
250.	-2317181.	-2219600.	463.760	-136541.	-137356.	28.699
(2 sigma)	---	---	---	2563.	2065.	0.432
273.150	-2317393.	-2210554.	422.725	-136595.	-137429.	26.281
298.150	-2317527.	-2200769.	385.565	-136670.	-137502.	24.090
(2 sigma)	---	---	---	2563.	1972.	0.345
300.	-2317534.	-2200044.	383.062	-136676.	-137508.	23.942
350.	-2317574.	-2180456.	325.415	-136880.	-137631.	20.540
400.	-2317406.	-2160877.	282.181	-137140.	-137721.	17.984
450.	-2317089.	-2141329.	248.559	-137433.	-137776.	15.993
500.	-2316660.	-2121822.	221.665	-137743.	-137798.	14.396
(2 sigma)	---	---	---	2570.	1592.	0.166
550.	-2316149.	-2102363.	199.666	-138053.	-137788.	13.086
600.	-2315580.	-2082952.	181.337	-138355.	-137751.	11.992
650.	-2314974.	-2063591.	165.832	-138645.	-137688.	11.065
700.	-2314353.	-2044277.	152.546	-138921.	-137604.	10.268
750.	-2315409.	-2024934.	141.029	-139184.	-137501.	9.576
(2 sigma)	---	---	---	2583.	1169.	0.081
800.	-2314600.	-2005597.	130.952	-139440.	-137380.	8.970
850.	-2313904.	-1986306.	122.063	-140408.	-137239.	8.434
900.	-2313335.	-1967052.	114.165	-140248.	-137057.	7.955
950.	-2312905.	-1947827.	107.099	-140040.	-136885.	7.526
970.	-2312776.	-1940142.	104.477	-139947.	-136819.	7.368
1000.	-2312629.	-1928620.	100.741	-139800.	-136725.	7.142
(2 sigma)	---	---	---	2576.	888.	0.046
1050.	-2312522.	-1909423.	94.989	-139540.	-136577.	6.794
1100.	-2312599.	-1890227.	89.759	-139278.	-136442.	6.479
1120.	-2329460.	-1882425.	87.793	-139177.	-136392.	6.361
bredigite						
1120.	-2315299.	-1882425.	87.793	-125015.	-136392.	6.361
1150.	-2314408.	-1870842.	84.976	-124819.	-136699.	6.209
1200.	-2312857.	-1851589.	80.598	-124444.	-137223.	5.973
1250.	-2311218.	-1832403.	76.572	-124005.	-137765.	5.757
(2 sigma)	---	---	---	1590.	933.	0.039
1300.	-2309485.	-1813284.	72.859	-123494.	-138325.	5.558
1350.	-2307651.	-1794234.	69.423	-122909.	-138906.	5.375
1400.	-2305710.	-1775254.	66.235	-122242.	-139511.	5.205
1450.	-2303656.	-1756345.	63.270	-121490.	-140140.	5.048
1500.	-2301482.	-1737509.	60.505	-120648.	-140798.	4.903
(2 sigma)	---	---	---	1633.	1168.	0.041
1550.	-2299182.	-1718747.	57.921	-119711.	-141484.	4.768
1600.	-2296750.	-1700062.	55.501	-118674.	-142203.	4.642
1650.	-2294180.	-1681455.	53.230	-117534.	-142956.	4.526
1700.	-2341975.	-1662478.	51.082	-116285.	-143744.	4.417
1710.	-2341386.	-1658483.	50.561	-116022.	-143907.	4.396
alpha- Ca_2SiO_4						
1710.	-2327000.	-1658483.	50.561	-101635.	-143907.	4.396
1750.	-2325327.	-1642864.	49.037	-101283.	-144900.	4.325
(2 sigma)	---	---	---	1877.	1440.	0.043
1800.	-2628909.	-1615547.	46.882	-100885.	-146152.	4.241
(2 sigma)	---	---	---	2441.	1495.	0.043

Table 76. Thermophysical values for $\alpha\text{-Ca}_2\text{SiO}_4$ at 1.01325 bars (1 atm). The tabulations are based on a fit of the thermophysical and thermochemical data given in Section 1.5.5.

T K	Cp J/(mol K)	S J/(mol K)	H-H(298) J/mol	[G-H(298)]/T J/(mol K)	cm^3/mol
200.000	199.600	5.634	-20203.	-106.649	52.1115
250.000	199.600	50.174	-10223.	-91.065	52.2065
(2 sigma)	35.790	69.796	53989.	146.275	0.5291
273.150	199.600	67.850	-5602.	-88.360	52.2505
298.150	199.600	85.331	-612.	-87.384	52.2980
(2 sigma)	35.790	63.493	52268.	111.933	0.5144
300.000	199.600	86.565	-243.	-87.375	52.3015
350.000	199.600	117.334	9737.	-89.513	52.3965
400.000	199.600	143.987	19717.	-94.694	52.4915
450.000	199.600	167.496	29697.	-101.502	52.5865
500.000	199.600	188.526	39677.	-109.172	52.6815
(2 sigma)	35.790	44.997	45059.	45.258	0.7309
550.000	199.600	207.550	49657.	-117.264	52.7765
600.000	199.600	224.917	59637.	-125.522	52.8715
650.000	199.600	240.894	69617.	-133.791	52.9665
700.000	199.600	255.686	79597.	-141.976	53.0615
750.000	199.600	269.457	89577.	-150.021	53.1565
(2 sigma)	35.790	30.497	36138.	17.879	1.2710
800.000	199.600	282.339	99557.	-157.892	53.2515
850.000	199.600	294.439	109537.	-165.572	53.3465
900.000	199.600	305.848	119517.	-173.051	53.4415
950.000	199.600	316.640	129497.	-180.327	53.5365
970.000	199.600	320.799	133489.	-183.181	53.5745
1000.000	199.600	326.878	139477.	-187.401	53.6315
(2 sigma)	35.790	20.220	27234.	7.330	1.8772
1050.000	199.600	336.617	149457.	-194.277	53.7265
1100.000	199.600	345.902	159437.	-200.959	53.8215
1120.000	199.600	349.499	163429.	-203.580	53.8595
1150.000	199.600	354.775	169417.	-207.455	53.9165
1200.000	199.600	363.270	179397.	-213.772	54.0115
1250.000	199.600	371.418	189377.	-219.916	54.1065
(2 sigma)	35.790	12.270	18372.	3.038	2.5018
1300.000	199.600	379.246	199357.	-225.894	54.2015
1350.000	199.600	386.779	209337.	-231.715	54.2965
1400.000	199.600	394.038	219317.	-237.383	54.3915
1450.000	199.600	401.042	229297.	-242.906	54.4865
1500.000	199.600	407.809	239277.	-248.291	54.5815
(2 sigma)	35.790	5.848	9670.	1.725	3.1339
1550.000	199.600	414.354	249257.	-253.543	54.6765
1600.000	199.600	420.691	259237.	-258.668	54.7715
1650.000	199.600	426.833	269217.	-263.671	54.8665
1700.000	199.600	432.792	279197.	-268.558	54.9615
1710.000	199.600	433.962	281193.	-269.522	54.9805
1750.000	199.600	438.577	289177.	-273.333	55.0565
(2 sigma)	35.790	1.506	3100.	1.474	3.7697
1800.000	199.600	444.200	299157.	-278.002	55.1515
(2 sigma)	35.790	1.735	3471.	1.446	3.8972

Table 77. Thermochemical properties of $\alpha\text{-Ca}_2\text{SiO}_4$ at 1.01325 bars (1 atm). Columns 2 through 4 give the thermochemical values relative to the elements; columns 5 through 7 give the values relative to the oxides.

T K	Formation from the Elements			Formation from the Oxides		
	H J/mol	G J/mol	log K	H J/mol	G J/mol	log K
1500.	-2284826.	-1735569.	60.438	-103992.	-138858.	4.835
(2 sigma)	---	---	---	9350.	1378.	0.048
1550.	-2282826.	-1717294.	57.872	-103355.	-140031.	4.719
1600.	-2280840.	-1699082.	55.469	-102765.	-141223.	4.610
1650.	-2278869.	-1680933.	53.214	-102223.	-142434.	4.509
1700.	-2327418.	-1662393.	51.079	-101729.	-143660.	4.414
1710.	-2327000.	-1658483.	50.661	-101635.	-143907.	4.396
1750.	-2325327.	-1642864.	49.037	-101283.	-144900.	4.325
(2 sigma)	---	---	---	1877.	1440.	0.043
1800.	-2628909.	-1615547.	46.882	-100885.	-146152.	4.241
(2 sigma)	---	---	---	2441.	1495.	0.043

Table 78. Thermophysical values for bredigite, Ca_2SiO_4 , at 1.01325 bars (1 atm). The tabulations are based on a fit of the thermophysical and thermochemical data given in Section 1.5.5.

T K	Cp J/(mol K)	S J/(mol K)	H-H(298) J/mol	[G-H(298)]/T J/(mol K)	cm^3V /mol
200.	162.284	51.598	-15971.	-131.452	51.8135
250.	162.711	87.855	-7846.	-119.240	51.9085
(2 sigma)	14.480	16.855	692.	14.102	1.5483
273.150	162.940	102.275	-4077.	-117.200	51.9525
298.150	163.211	116.556	0.	-116.556	52.0000
(2 sigma)	14.242	14.336	0.	14.336	1.5433
300.	163.232	117.565	302.	-116.559	52.0035
350.	163.848	142.773	8479.	-118.548	52.0985
400.	164.558	164.697	16688.	-122.976	52.1935
450.	165.364	184.125	24936.	-128.711	52.2885
500.	166.264	201.593	33226.	-135.141	52.3835
(2 sigma)	12.786	7.359	2740.	12.776	1.6283
550.	167.259	217.486	41564.	-141.915	52.4785
600.	168.348	232.085	49954.	-148.829	52.5735
650.	169.533	245.606	58400.	-155.760	52.6685
700.	170.812	258.216	66909.	-162.633	52.7635
750.	172.186	270.047	75483.	-169.403	52.8585
(2 sigma)	9.979	2.893	5608.	10.105	1.9320
800.	173.654	281.206	84129.	-176.046	52.9535
850.	175.218	291.781	92850.	-182.545	53.0485
900.	176.876	301.842	101652.	-188.896	53.1435
950.	178.628	311.452	110539.	-195.095	53.2385
970.	179.356	315.181	114119.	-197.533	53.2765
1000.	180.476	320.661	119516.	-201.145	53.3335
(2 sigma)	6.132	1.363	7633.	7.929	2.3751
1050.	182.418	329.513	128588.	-207.048	53.4285
1100.	184.455	338.046	137760.	-212.810	53.5235
1120.	185.297	341.377	141457.	-215.076	53.5615
1150.	186.587	346.292	147036.	-218.435	53.6185
1200.	188.814	354.280	156420.	-223.929	53.7135
1250.	191.135	362.034	165918.	-229.299	53.8085
(2 sigma)	2.241	1.488	8547.	6.327	2.8942
1300.	193.551	369.577	175535.	-234.550	53.9035
1350.	196.062	376.929	185275.	-239.688	53.9985
1400.	198.668	384.106	195143.	-244.718	54.0935
1450.	201.368	391.124	205144.	-249.646	54.1885
1500.	204.163	397.998	215281.	-254.477	54.2835
(2 sigma)	6.096	1.486	8109.	5.231	3.4552
1550.	207.053	404.739	225561.	-259.216	54.3785
1600.	210.037	411.360	235988.	-263.867	54.4735
1650.	213.117	417.870	246567.	-268.435	54.5685
1700.	216.291	424.279	257301.	-272.925	54.6635
1710.	216.937	425.549	259468.	-273.814	54.6825
1750.	219.559	430.595	268197.	-277.340	54.7585
(2 sigma)	13.312	2.059	6203.	4.574	4.0408
1800.	222.923	436.828	279259.	-281.684	54.8535
(2 sigma)	14.917	2.342	5674.	4.490	4.1599

Table 79. Thermochemical properties of bredigite, Ca_2SiO_4 , at 1.01325 bars (1 atm). Columns 2 through 4 give the thermochemical values relative to the elements; columns 5 through 7 give the values relative to the oxides.

T K	Formation from the Elements			Formation from the Oxides		
	H J/mol	G J/mol	log K	H J/mol	G J/mol	log K
200.	-2313753.	-2231728.	582.867	-133899.	-129877.	33.920
250.	-2311873.	-2211442.	462.055	-131232.	-129198.	26.994
(2 sigma)	---	---	---	8611.	4447.	0.929
273.150	-2311048.	-2202180.	421.124	-130251.	-129055.	24.679
298.150	-2310188.	-2192254.	384.074	-129331.	-128987.	22.598
(2 sigma)	---	---	---	7931.	3718.	0.651
300.	-2310125.	-2191522.	381.578	-129268.	-128985.	22.458
350.	-2308495.	-2171886.	324.136	-127802.	-129060.	19.261
400.	-2306977.	-2152475.	281.084	-126711.	-129318.	16.887
450.	-2305569.	-2133248.	247.621	-125913.	-129695.	15.055
500.	-2304269.	-2114172.	220.866	-125351.	-130147.	13.596
(2 sigma)	---	---	---	5266.	1729.	0.181
550.	-2303078.	-2095221.	198.987	-124982.	-130646.	12.408
600.	-2301997.	-2076373.	180.764	-124773.	-131171.	11.419
650.	-2301024.	-2057611.	165.352	-124695.	-131708.	10.584
700.	-2300161.	-2038920.	152.146	-124729.	-132247.	9.868
750.	-2301078.	-2020214.	140.700	-124854.	-132781.	9.248
(2 sigma)	---	---	---	2631.	854.	0.059
800.	-2300215.	-2001519.	130.686	-125055.	-133303.	8.704
850.	-2299527.	-1982872.	121.852	-126030.	-133805.	8.223
900.	-2299007.	-1964261.	114.003	-125920.	-134266.	7.793
950.	-2298647.	-1945675.	106.981	-125782.	-134733.	7.408
970.	-2298546.	-1938245.	104.375	-125718.	-134922.	7.266
1000.	-2298439.	-1927104.	100.661	-125610.	-135208.	7.063
(2 sigma)	---	---	---	1428.	800.	0.042
1050.	-2298378.	-1908539.	94.945	-125396.	-135693.	6.750
1100.	-2298455.	-1889974.	89.747	-125134.	-136190.	6.467
1120.	-2315299.	-1882425.	87.793	-125015.	-136392.	6.361
1150.	-2314408.	-1870842.	84.976	-124819.	-136699.	6.209
1200.	-2312857.	-1851589.	80.598	-124444.	-137223.	5.973
1250.	-2311218.	-1832403.	76.572	-124005.	-137765.	5.757
(2 sigma)	---	---	---	1590.	933.	0.039
1300.	-2309485.	-1813284.	72.859	-123494.	-138325.	5.558
1350.	-2307651.	-1794234.	69.423	-122909.	-138906.	5.375
1400.	-2305710.	-1775254.	66.235	-122242.	-139511.	5.205
1450.	-2303656.	-1756345.	63.270	-121490.	-140140.	5.048
1500.	-2301482.	-1737509.	60.505	-120648.	-140798.	4.903
(2 sigma)	---	---	---	1633.	1168.	0.041
1550.	-2299182.	-1718747.	57.921	-119711.	-141484.	4.768
1600.	-2296750.	-1700062.	55.501	-118674.	-142203.	4.642
1650.	-2294180.	-1681455.	53.230	-117534.	-142956.	4.526
1700.	-2341975.	-1662478.	51.082	-116285.	-143744.	4.417
1710.	-2341386.	-1658483.	50.661	-116022.	-143907.	4.396
1750.	-2338968.	-1642536.	49.027	-114923.	-144572.	4.315
(2 sigma)	---	---	---	2989.	1444.	0.043
1800.	-2541468.	-1614835.	46.861	-113444.	-145439.	4.221
(2 sigma)	---	---	---	3588.	1507.	0.044

Table 80. Thermophysical values for Ca-olivine, Ca_2SiO_4 , at 1.01325 bars (1 atm). The tabulations are based on a fit of the thermophysical and thermochemical data given in Section 1.5.5.

T K	C_p J/(mol K)	S J/(mol K)	H-H(298) J/mol	$[G-H(298)]/T$ J/(mol K)	cm^3/mol
200.	97.496	75.402	-11176.	-131.282	58.9137
250.	115.197	99.254	-5815.	-122.515	59.0137
(2 sigma)	0.307	2.153	17.	2.152	0.9342
273.150	120.737	109.706	-3082.	-120.989	59.0600
298.150	125.690	120.499	0.	-120.499	59.1100
(2 sigma)	0.407	2.152	0.	2.152	0.9260
300.	126.025	121.278	233.	-120.502	59.1137
350.	133.898	141.321	6739.	-122.067	59.2137
400.	140.297	159.630	13598.	-125.634	59.3137
450.	145.851	176.482	20755.	-130.360	59.4137
500.	150.846	192.112	28174.	-135.763	59.5137
(2 sigma)	0.526	2.162	82.	2.153	1.0616
550.	155.417	206.706	35833.	-141.556	59.6137
600.	159.629	220.413	43710.	-147.562	59.7137
650.	163.510	233.345	51790.	-153.668	59.8137
700.	167.074	245.595	60056.	-159.801	59.9137
750.	170.322	257.234	68492.	-165.912	60.0137
(2 sigma)	0.433	2.182	185.	2.156	1.4860
800.	173.251	268.322	77083.	-171.968	60.1137
850.	175.859	278.905	85812.	-177.950	60.2137
900.	178.138	289.023	94663.	-183.842	60.3137
950.	180.084	298.708	103620.	-189.634	60.4137
970.	180.767	302.467	107229.	-191.922	60.4537
1000.	181.690	307.987	112666.	-195.322	60.5137
(2 sigma)	1.428	2.172	158.	2.159	2.0289
1050.	182.952	316.884	121783.	-200.900	60.6137
1100.	183.864	325.417	130955.	-206.367	60.7137
1120.	184.130	328.733	134635.	-208.523	60.7537
1150.	184.422	333.604	140164.	-211.723	60.8137
1200.	184.622	341.459	149391.	-216.966	60.9137
1250.	184.459	348.993	158620.	-222.097	61.0137
(2 sigma)	4.401	2.214	680.	2.159	2.6176

Table 81. Thermochemical properties of Ca-olivine, Ca_2SiO_4 , at 1.01325 bars (1 atm). Columns 2 through 4 give the thermochemical values relative to the elements; columns 5 through 7 give the values relative to the oxides.

T K	Formation from the Elements			Formation from the Oxides		
	H J/mol	G J/mol	log K	H J/mol	G J/mol	log K
200.	-2316298.	-2239033.	584.775	-136444.	-137183.	35.828
250.	-2317181.	-2219600.	463.760	-136541.	-137356.	28.699
(2 sigma)	---	---	---	2563.	2065.	0.432
273.150	-2317393.	-2210564.	422.725	-136595.	-137429.	26.281
298.150	-2317527.	-2200769.	385.565	-136670.	-137502.	24.090
(2 sigma)	---	---	---	2563.	1972.	0.345
300.	-2317534.	-2200044.	383.062	-136676.	-137508.	23.942
350.	-2317574.	-2180456.	325.415	-136880.	-137631.	20.540
400.	-2317406.	-2160877.	282.181	-137140.	-137721.	17.984
450.	-2317089.	-2141329.	248.559	-137433.	-137776.	15.993
500.	-2316660.	-2121822.	221.665	-137743.	-137798.	14.396
(2 sigma)	---	---	---	2570.	1592.	0.166
550.	-2316149.	-2102363.	199.666	-138053.	-137788.	13.086
600.	-2315580.	-2082952.	181.337	-138355.	-137751.	11.992
650.	-2314974.	-2063591.	165.832	-138645.	-137688.	11.065
700.	-2314353.	-2044277.	152.546	-138921.	-137604.	10.268
750.	-2315409.	-2024934.	141.029	-139184.	-137501.	9.576
(2 sigma)	---	---	---	2583.	1169.	0.081
800.	-2314600.	-2005597.	130.952	-139440.	-137380.	8.970
850.	-2313904.	-1986306.	122.063	-140408.	-137239.	8.434
900.	-2313335.	-1967052.	114.165	-140248.	-137057.	7.955
950.	-2312905.	-1947827.	107.099	-140040.	-136885.	7.526
970.	-2312776.	-1940142.	104.477	-139947.	-136819.	7.368
1000.	-2312629.	-1928620.	100.741	-139800.	-136725.	7.142
(2 sigma)	---	---	---	2576.	888.	0.046
1050.	-2312522.	-1909423.	94.989	-139540.	-136577.	6.794
1100.	-2312599.	-1890227.	89.759	-139278.	-136442.	6.479
1120.	-2329460.	-1882425.	87.793	-139177.	-136392.	6.361
1150.	-2328619.	-1870462.	84.959	-139030.	-136319.	6.192
1200.	-2327225.	-1850572.	80.553	-138812.	-136206.	5.929
1250.	-2325856.	-1830740.	76.502	-138642.	-136101.	5.687
(2 sigma)	---	---	---	2627.	895.	0.037

Table 82. Thermophysical values for larnite, Ca_2SiO_4 , at 1.01325 bars (1 atm). The tabulations are based on a fit of the thermophysical and thermochemical data given in Section 1.5.5.

T K	C _p J/(mol K)	S J/(mol K)	H-H(298) J/mol	[G-H(298)]/T J/(mol K)	cm ³ /mol
200.	101.598	81.036	-11418.	-138.127	51.5499
250.	117.236	105.484	-5926.	-129.186	51.5742
(2 sigma)	0.269	1.289	12.	1.286	1.3890
273.150	122.974	116.122	-3144.	-127.632	51.5863
298.150	128.404	127.131	0.	-127.131	51.6000
(2 sigma)	0.250	1.286	0.	1.286	1.3890
300.	128.779	127.927	238.	-127.134	51.6010
350.	137.750	148.479	6910.	-128.736	51.6301
400.	144.982	167.361	13984.	-132.401	51.6610
450.	150.972	184.793	21387.	-137.266	51.6934
500.	156.039	200.969	29066.	-142.837	51.7272
(2 sigma)	0.488	1.281	72.	1.283	1.3893
550.	160.399	216.051	36980.	-148.815	51.7621
600.	164.202	230.174	45097.	-155.013	51.7980
650.	167.557	243.452	53392.	-161.310	51.8346
700.	170.545	255.981	61846.	-167.629	51.8720
750.	173.230	267.841	70442.	-173.918	51.9099
(2 sigma)	0.700	1.311	220.	1.279	1.3894
800.	175.659	279.099	79165.	-180.143	51.9483
850.	177.870	289.816	88004.	-186.282	51.9871
900.	179.895	300.041	96949.	-192.320	52.0262
950.	181.757	309.818	105991.	-198.249	52.0657
970.	182.461	313.612	109633.	-200.588	52.0815
1000.	183.478	319.185	115122.	-204.063	52.1054
(2 sigma)	0.832	1.374	410.	1.283	1.3895
1050.	185.074	328.176	124337.	-209.760	52.1453
1100.	186.561	336.821	133628.	-215.341	52.1854
1150.	187.949	345.144	142991.	-220.805	52.2256
1200.	189.249	353.171	152421.	-226.154	52.2660
1250.	190.471	360.922	161915.	-231.390	52.3065
(2 sigma)	0.923	1.456	628.	1.294	1.3904

Table 83. Thermochemical properties of larnite, Ca_2SiO_4 , at 1.01325 bars (1 atm). Columns 2 through 4 give the thermochemical values relative to the elements; columns 5 through 7 give the values relative to the oxides.

T K	Formation from the Elements			Formation from the Oxides		
	H J/mol	G J/mol	log K	H J/mol	G J/mol	log K
200.	-2306237.	-2230099.	582.442	-126383.	-128248.	33.495
250.	-2306988.	-2210965.	461.955	-126348.	-128721.	26.895
(2 sigma)	---	---	---	1348.	1105.	0.231
273.150	-2307151.	-2202065.	421.102	-126353.	-128940.	24.657
298.150	-2307224.	-2192443.	384.107	-126367.	-129176.	22.631
(2 sigma)	---	---	---	1348.	1064.	0.186
300.	-2307225.	-2191731.	381.614	-126368.	-129194.	22.495
350.	-2307100.	-2172487.	324.226	-126406.	-129662.	19.351
400.	-2306717.	-2153281.	281.189	-126451.	-130124.	16.992
450.	-2306153.	-2134133.	247.724	-126498.	-130580.	15.157
500.	-2305465.	-2115056.	220.958	-126548.	-131031.	13.689
(2 sigma)	---	---	---	1353.	911.	0.095
550.	-2304699.	-2096052.	199.066	-126603.	-131477.	12.487
600.	-2303890.	-2077119.	180.829	-126666.	-131918.	11.484
650.	-2303068.	-2058255.	165.403	-126739.	-132352.	10.636
700.	-2302259.	-2039454.	152.186	-126827.	-132781.	9.908
750.	-2303155.	-2020636.	140.730	-126931.	-133203.	9.277
(2 sigma)	---	---	---	1376.	795.	0.055
800.	-2302214.	-2001833.	130.706	-127055.	-133617.	8.724
850.	-2301409.	-1983084.	121.865	-127912.	-134017.	8.236
900.	-2300746.	-1964379.	114.010	-127659.	-134384.	7.799
950.	-2300231.	-1945707.	106.982	-127366.	-134765.	7.410
970.	-2300068.	-1938245.	104.375	-127239.	-134922.	7.266
1000.	-2299870.	-1927058.	100.659	-127040.	-135163.	7.060
(2 sigma)	---	---	---	1428.	800.	0.042
1050.	-2299666.	-1908423.	94.939	-126684.	-135578.	6.745
1100.	-2299623.	-1889794.	89.739	-126302.	-136010.	6.459
1150.	-2315488.	-1870603.	84.965	-125900.	-136460.	6.198
1200.	-2313892.	-1851294.	80.585	-125479.	-136928.	5.960
1250.	-2312258.	-1832052.	76.557	-125044.	-137414.	5.742
(2 sigma)	---	---	---	1515.	943.	0.039

Table 84. Thermophysical values for grossular, $\text{Ca}_3\text{Al}_2\text{Si}_3\text{O}_{12}$, at 1.01325 bars (1 atm). The tabulations are based on a fit of the thermophysical and thermochemical data given in Section 1.5.5.

T K	Cp J/(mol K)	S J/(mol K)	H-H(298) J/mol	[G-H(298)]/T J/(mol K)	cm^3/mol
200.	235.117	142.930	-28191.	-283.887	124.9446
250.	290.295	201.622	-14989.	-261.577	125.0676
(2 sigma)	0.191	3.744	9.	3.743	0.0727
273.150	310.963	228.252	-8024.	-257.628	125.1270
298.150	330.541	256.348	0.	-256.348	125.1926
(2 sigma)	0.160	3.743	0.	3.743	0.0462
300.	331.890	258.397	613.	-256.355	125.1975
350.	363.910	312.066	18041.	-260.520	125.3333
400.	389.041	362.365	36889.	-270.142	125.4740
450.	409.085	409.388	56861.	-283.030	125.6189
500.	425.281	453.357	77734.	-297.889	125.7673
(2 sigma)	0.168	3.745	26.	3.743	0.0589
550.	438.509	494.532	99340.	-313.914	125.9187
600.	449.408	533.169	121546.	-330.592	126.0727
650.	458.454	569.509	144250.	-347.587	126.2288
700.	466.010	603.769	167367.	-364.674	126.3867
750.	472.357	636.143	190830.	-381.703	126.5462
(2 sigma)	0.762	3.733	96.	3.742	0.0524
800.	477.718	666.804	214586.	-398.572	126.7070
850.	482.270	695.906	238589.	-415.213	126.8688
900.	486.157	723.585	262802.	-431.583	127.0316
950.	489.498	749.962	287195.	-447.651	127.1952
1000.	492.389	775.145	311744.	-463.401	127.3595
(2 sigma)	1.770	3.716	379.	3.735	0.1130
1050.	494.913	799.231	336428.	-478.823	127.5243
1100.	497.138	822.307	361231.	-493.915	127.6896
1150.	499.124	844.450	386138.	-508.678	127.8553
1200.	500.920	865.731	411140.	-523.115	128.0214
1250.	502.570	886.213	436228.	-537.231	128.1877
(2 sigma)	3.710	3.748	975.	3.724	0.2297
1300.	504.112	905.955	461395.	-551.036	128.3543
1350.	505.577	925.008	486637.	-564.536	128.5211
1400.	506.996	943.420	511952.	-577.740	128.6881
1450.	508.392	961.236	537337.	-590.659	128.8552
1500.	509.788	978.495	562791.	-603.301	129.0224
(2 sigma)	7.278	3.970	2193.	3.715	0.3627
1550.	511.205	995.234	588316.	-615.675	129.1898
1600.	512.659	1011.487	613912.	-627.791	129.3572
1650.	514.167	1027.285	639583.	-639.659	129.5248
1700.	515.743	1042.657	665330.	-651.287	129.6924
1750.	517.399	1057.531	691158.	-662.684	129.8600
(2 sigma)	12.727	4.675	4510.	3.723	0.5021
1800.	519.147	1072.231	717072.	-673.858	130.0277
(2 sigma)	14.052	4.903	5149.	3.730	0.5304

Table 85. Thermochemical properties of grossular, $\text{Ca}_3\text{Al}_2\text{Si}_3\text{O}_{12}$, at 1.01325 bars (1 atm). Columns 2 through 4 give the thermochemical values relative to the elements; columns 5 through 7 give the values relative to the oxides.

T K	Formation from the Elements			Formation from the Oxides		
	H J/mol	G J/mol	log K	H J/mol	G J/mol	log K
200.	-6632735.	-6395616.	1670.362	-324725.	-319023.	83.320
250.	-6636790.	-6335822.	1323.797	-325399.	-317518.	66.342
(2 sigma)	---	---	---	4071.	3313.	0.692
273.150	-6638009.	-6307895.	1206.262	-325666.	-316776.	60.577
298.150	-6638943.	-6277637.	1099.815	-325915.	-315951.	55.353
(2 sigma)	---	---	---	4071.	3178.	0.557
300.	-6638998.	-6275395.	1092.643	-325931.	-315889.	55.001
350.	-6639850.	-6214711.	927.494	-326316.	-314183.	46.889
400.	-6639713.	-6153976.	803.626	-326600.	-312430.	40.799
450.	-6638863.	-6093304.	707.292	-326838.	-310644.	36.059
500.	-6637513.	-6032755.	630.237	-327080.	-308832.	32.263
(2 sigma)	---	---	---	4072.	2570.	0.279
550.	-6635829.	-5972359.	567.207	-327368.	-306994.	29.156
600.	-6633945.	-5912125.	514.696	-327738.	-305126.	26.564
650.	-6631968.	-5852053.	470.276	-328219.	-303223.	24.367
700.	-6629987.	-5792135.	432.214	-328836.	-301278.	22.482
750.	-6630583.	-5732246.	399.229	-329607.	-299284.	20.844
(2 sigma)	---	---	---	4066.	2244.	0.156
800.	-6628478.	-5672427.	370.371	-330548.	-297232.	19.407
850.	-6626660.	-5612731.	344.916	-333807.	-295101.	18.135
900.	-6625162.	-5553133.	322.295	-333852.	-292823.	16.995
950.	-6645274.	-5492961.	302.024	-333899.	-290542.	15.975
1000.	-6644230.	-5432341.	283.756	-333962.	-288259.	15.057
(2 sigma)	---	---	---	4055.	2164.	0.113
1050.	-6643463.	-5371767.	267.231	-334052.	-285972.	14.226
1100.	-6642982.	-5311222.	252.209	-334180.	-283679.	13.471
1150.	-6666410.	-5249852.	238.456	-334352.	-281380.	12.781
1200.	-6663694.	-5188321.	225.842	-334575.	-279072.	12.148
1250.	-6660969.	-5126903.	214.241	-334852.	-276754.	11.565
(2 sigma)	---	---	---	4097.	2462.	0.103
1300.	-6658238.	-5065594.	203.538	-335188.	-274424.	11.026
1350.	-6655498.	-5004391.	193.631	-335584.	-272080.	10.527
1400.	-6652749.	-4943289.	184.436	-336041.	-269719.	10.063
1450.	-6649987.	-4882285.	175.879	-336560.	-267342.	9.631
1500.	-6647208.	-4821377.	167.895	-337141.	-264945.	9.226
(2 sigma)	---	---	---	4461.	3036.	0.106
1550.	-6644408.	-4760562.	160.430	-337783.	-262528.	8.847
1600.	-6641580.	-4699838.	153.434	-338484.	-260090.	8.491
1650.	-6638719.	-4639203.	146.365	-339242.	-257628.	8.156
1700.	-6787344.	-4577306.	140.543	-340055.	-255143.	7.840
1750.	-6783967.	-4512353.	134.686	-340919.	-252633.	7.541
(2 sigma)	---	---	---	5862.	3814.	0.114
1800.	-7239023.	-4435728.	128.721	-341833.	-250098.	7.258
(2 sigma)	---	---	---	6347.	3996.	0.116

Table 86. Thermophysical values for hatrurite, Ca_3SiO_6 , at 1.01325 bars (1 atm). The tabulations are based on a fit of the thermophysical and thermochemical data given in Section 1.5.5.

T K	Cp J/(mol K)	S J/(mol K)	H-H(298) J/mol	[G-H(298)]/T J/(mol K)	cm^3V cm ³ /mol
200.	135.792	106.976	-15266.	-183.305	72.7052
250.	156.756	139.601	-7923.	-171.352	72.7213
(2 sigma)	0.547	0.345	33.	0.321	0.5146
273.150	164.422	153.885	-4203.	-169.273	72.7306
298.150	171.658	168.604	0.	-168.604	72.7420
(2 sigma)	0.880	0.321	0.	0.321	0.5144
300.	172.157	169.667	318.	-168.607	72.7429
350.	184.064	197.136	9235.	-170.749	72.7692
400.	193.607	222.359	18685.	-175.646	72.7994
450.	201.463	245.630	28568.	-182.146	72.8331
500.	208.066	267.208	38811.	-189.586	72.8695
(2 sigma)	1.547	0.706	261.	0.340	0.5153
550.	213.707	287.310	49359.	-197.567	72.9084
600.	218.592	306.119	60169.	-205.838	72.9493
650.	222.868	323.788	71208.	-214.238	72.9919
700.	226.647	340.446	82447.	-222.664	73.0360
750.	230.012	356.200	93865.	-231.046	73.0813
(2 sigma)	2.608	1.271	667.	0.493	0.5157
800.	233.030	371.142	105443.	-239.339	73.1276
850.	235.753	385.353	117164.	-247.513	73.1749
900.	238.221	398.899	129014.	-255.550	73.2229
950.	240.469	411.840	140982.	-263.438	73.2715
1000.	242.525	424.228	153058.	-271.170	73.3206
(2 sigma)	4.951	1.969	1416.	0.710	0.5164
1050.	244.412	436.107	165232.	-278.743	73.3703
1100.	246.150	447.518	177496.	-286.157	73.4203
1150.	247.754	458.495	189844.	-293.413	73.4706
1200.	249.239	469.071	202270.	-300.513	73.5212
1250.	250.617	479.274	214767.	-307.461	73.5720
(2 sigma)	7.861	3.076	2855.	0.991	0.5197
1300.	251.898	489.129	227330.	-314.260	73.6230
1350.	253.092	498.658	239955.	-320.914	73.6742
1400.	254.206	507.883	252638.	-327.427	73.7256
1450.	255.247	516.822	265374.	-333.805	73.7770
1500.	256.221	525.491	278161.	-340.051	73.8286
(2 sigma)	11.041	4.574	5100.	1.380	0.5256
1550.	257.134	533.908	290995.	-346.169	73.8802
1600.	257.991	542.085	303874.	-352.164	73.9319
1650.	258.795	550.037	316794.	-358.040	73.9837
1700.	259.551	557.774	329752.	-363.802	74.0356
1750.	260.263	565.308	342748.	-369.452	74.0874
(2 sigma)	14.375	6.375	8188.	1.892	0.5374
1800.	260.932	572.649	355778.	-374.995	74.1393
(2 sigma)	15.055	6.764	8909.	2.009	0.5399

Table 87. Thermochemical properties of hatrurite, Ca_3SiO_5 , at 1.01325 bars (1 atm). Columns 2 through 4 give the thermochemical values relative to the elements; columns 5 through 7 give the values relative to the oxides.

T K	Formation from the Elements			Formation from the Oxides		
	H J/mol	G J/mol	log K	H J/mol	G J/mol	log K
200.	-2932681.	-2836063.	740.703	-117839.	-120324.	31.425
250.	-2933550.	-2811790.	587.491	-117776.	-120955.	25.272
(2 sigma)	---	---	---	1689.	1689.	0.353
273.150	-2933694.	-2800507.	535.542	-117765.	-121250.	23.187
298.150	-2933704.	-2788316.	488.501	-117754.	-121569.	21.298
(2 sigma)	---	---	---	1692.	1690.	0.296
300.	-2933700.	-2787414.	485.331	-117753.	-121593.	21.171
350.	-2933347.	-2763055.	412.363	-117721.	-122235.	18.243
400.	-2932640.	-2738772.	357.647	-117667.	-122883.	16.047
450.	-2931688.	-2714594.	315.102	-117589.	-123540.	14.340
500.	-2930576.	-2690531.	281.078	-117490.	-124206.	12.976
(2 sigma)	---	---	---	1810.	1672.	0.175
550.	-2929368.	-2666584.	253.251	-117374.	-124883.	11.860
600.	-2928117.	-2642749.	230.072	-117248.	-125571.	10.932
650.	-2926866.	-2619020.	210.467	-117117.	-126270.	10.147
700.	-2925651.	-2595385.	193.670	-116987.	-126979.	9.475
750.	-2927013.	-2571726.	179.111	-116862.	-127697.	8.694
(2 sigma)	---	---	---	2211.	1566.	0.109
800.	-2925634.	-2548086.	166.373	-116746.	-128423.	8.385
850.	-2924475.	-2524526.	155.138	-117357.	-129151.	7.937
900.	-2923545.	-2501027.	145.156	-116852.	-129859.	7.537
950.	-2922854.	-2477574.	136.226	-116303.	-130597.	7.181
1000.	-2922407.	-2454151.	128.192	-115717.	-131364.	6.862
(2 sigma)	---	---	---	2945.	1344.	0.070
1050.	-2922212.	-2430744.	120.923	-115100.	-132161.	6.575
1100.	-2922273.	-2407341.	114.315	-114458.	-132989.	6.315
1150.	-2946211.	-2383087.	108.243	-113795.	-133846.	6.079
1200.	-2943971.	-2358651.	102.669	-113117.	-134732.	5.865
1250.	-2941690.	-2334310.	97.545	-112428.	-135647.	5.668
(2 sigma)	---	---	---	4251.	1067.	0.045
1300.	-2939372.	-2310060.	92.819	-111731.	-136589.	5.488
1350.	-2937017.	-2285901.	88.447	-111032.	-137559.	5.322
1400.	-2934630.	-2261829.	84.390	-110333.	-138554.	5.170
1450.	-2932211.	-2237843.	80.616	-109639.	-139574.	5.028
1500.	-2929763.	-2213941.	77.096	-108953.	-140618.	4.897
(2 sigma)	---	---	---	6344.	1199.	0.042
1550.	-2927286.	-2190121.	73.807	-108278.	-141685.	4.775
1600.	-2924782.	-2166381.	70.725	-107617.	-142773.	4.661
1650.	-2922252.	-2142720.	67.833	-106973.	-143881.	4.555
1700.	-2970207.	-2118686.	65.099	-106349.	-145009.	4.456
1750.	-2967485.	-2093681.	62.493	-105749.	-146155.	4.362
(2 sigma)	---	---	---	9310.	2204.	0.066
1800.	-3423238.	-2056983.	59.692	-105175.	-147318.	4.275
(2 sigma)	---	---	---	10010.	2494.	0.072

Table 88. Thermophysical values for rankinite, $\text{Ca}_3\text{Si}_2\text{O}_7$, at 1.01325 bars (1 atm). The tabulations are based on a fit of the thermophysical and thermochemical data given in Section 1.5.5.

T K	C_p J/(mol K)	S J/(mol K)	H-H(298) J/mol	[G-H(298)]/T J/(mol K)	V cm^3/mol
200.	167.933	133.933	-18983.	-228.847	96.4050
250.	194.970	174.476	-9873.	-213.969	96.4535
(2 sigma)	0.522	3.095	30.	3.091	0.2582
273.150	204.896	192.186	-5242.	-211.377	96.4770
298.150	214.259	210.543	0.	-210.543	96.5030
(2 sigma)	0.758	3.092	0.	3.092	0.2572
300.	214.903	211.870	397.	-210.547	96.5050
350.	230.239	246.198	11541.	-213.223	96.5590
400.	242.407	277.766	23368.	-219.345	96.6151
450.	252.284	306.906	35744.	-227.476	96.6731
500.	260.443	333.923	48568.	-236.786	96.7326
(2 sigma)	1.511	3.122	225.	3.090	0.2619
550.	267.276	359.075	61766.	-246.773	96.7934
600.	273.060	382.586	75278.	-257.122	96.8553
650.	277.996	404.643	89058.	-267.630	96.9181
700.	282.238	425.403	103066.	-278.166	96.9817
750.	285.901	445.004	117272.	-288.641	97.0460
(2 sigma)	1.707	3.259	611.	3.099	0.2636
800.	289.076	463.559	131648.	-298.999	97.1109
850.	291.835	481.169	146173.	-309.201	97.1762
900.	294.230	497.919	160826.	-319.224	97.2420
950.	296.327	513.885	175591.	-329.052	97.3081
1000.	298.146	529.132	190454.	-338.678	97.3745
(2 sigma)	2.046	3.390	957.	3.126	0.2659
1050.	299.726	543.718	205402.	-348.097	97.4411
1100.	301.095	557.694	220423.	-357.309	97.5079
1150.	302.275	571.105	235508.	-366.315	97.5750
1200.	303.285	583.991	250648.	-375.118	97.6421
1250.	304.144	596.390	265834.	-383.722	97.7094
(2 sigma)	3.560	3.495	1343.	3.160	0.2784
1300.	304.866	608.333	281060.	-392.133	97.7768
1350.	305.463	619.850	296319.	-400.355	97.8443
1400.	305.946	630.968	311604.	-408.394	97.9119
1450.	306.326	641.711	326912.	-416.255	97.9795
1500.	306.612	652.101	342235.	-423.944	98.0472
(2 sigma)	5.811	3.683	2143.	3.193	0.3043
1550.	306.810	662.158	357571.	-431.467	98.1149
1600.	306.927	671.901	372915.	-438.829	98.1827
1650.	306.971	681.347	388263.	-446.036	98.2505
1700.	306.945	690.511	403611.	-453.092	98.3183
1750.	306.856	699.407	418956.	-460.003	98.3862
(2 sigma)	3.440	4.104	3647.	3.232	0.3418
1800.	306.708	708.049	434296.	-466.774	98.4540
(2 sigma)	6.997	4.226	4040.	3.242	0.3504

Table 89. Thermochemical properties of rankinite, $\text{Ca}_3\text{Si}_2\text{O}_7$, at 1.01325 bars (1 atm). Columns 2 through 4 give the thermochemical values relative to the elements; columns 5 through 7 give the values relative to the oxides.

T K	Formation from the Elements			Formation from the Oxides		
	H J/mol	G J/mol	log K	H J/mol	G J/mol	log K
200.	-3973107.	-3840871.	1003.132	-248386.	-251058.	65.570
250.	-3974516.	-3807628.	795.560	-248369.	-251730.	52.596
(2 sigma)	---	---	---	3366.	2715.	0.567
273.150	-3974857.	-3792158.	725.176	-248392.	-252041.	48.198
298.150	-3975050.	-3775426.	661.439	-248429.	-252373.	44.215
(2 sigma)	---	---	---	3368.	2597.	0.455
300.	-3975057.	-3774188.	657.144	-248432.	-252398.	43.946
350.	-3974990.	-3740708.	558.270	-248534.	-253051.	37.766
400.	-3974494.	-3707268.	484.119	-248667.	-253687.	33.128
450.	-3973705.	-3673910.	426.456	-248837.	-254305.	29.519
500.	-3972722.	-3640651.	380.336	-249055.	-254902.	26.629
(2 sigma)	---	---	---	3404.	2133.	0.223
550.	-3971625.	-3607496.	342.611	-249331.	-255473.	24.263
600.	-3970478.	-3574444.	311.183	-249674.	-256017.	22.288
650.	-3969333.	-3541488.	284.597	-250095.	-256529.	20.615
700.	-3968234.	-3508618.	261.816	-250602.	-257006.	19.178
750.	-3969725.	-3475715.	242.070	-251202.	-257443.	17.930
(2 sigma)	---	---	---	3497.	1675.	0.117
800.	-3968496.	-3442822.	224.793	-251904.	-257837.	16.835
850.	-3967510.	-3409999.	209.553	-254138.	-258173.	15.865
900.	-3966782.	-3377227.	196.009	-254214.	-258408.	14.998
950.	-3966322.	-3344487.	183.893	-254278.	-258639.	14.221
1000.	-3966140.	-3311765.	172.989	-254340.	-258867.	13.522
(2 sigma)	---	---	---	3602.	1523.	0.080
1050.	-3966245.	-3279045.	163.123	-254410.	-259092.	12.889
1100.	-3966643.	-3246313.	154.154	-254496.	-259313.	12.314
1150.	-3990957.	-3212715.	145.926	-254607.	-259529.	11.788
1200.	-3989133.	-3178918.	138.375	-254750.	-259740.	11.306
1250.	-3987309.	-3145196.	131.430	-254932.	-259944.	10.862
(2 sigma)	---	---	---	3716.	1808.	0.076
1300.	-3985491.	-3111548.	125.023	-255158.	-260141.	10.453
1350.	-3983679.	-3077969.	119.094	-255436.	-260327.	10.073
1400.	-3981879.	-3044457.	113.590	-255771.	-260502.	9.719
1450.	-3980093.	-3011009.	108.468	-256167.	-260665.	9.390
1500.	-3978322.	-2977623.	103.690	-256630.	-260812.	9.082
(2 sigma)	---	---	---	4028.	2404.	0.084
1550.	-3976509.	-2944295.	99.222	-257164.	-260943.	8.794
1600.	-3974835.	-2911024.	95.035	-257773.	-261055.	8.523
1650.	-3973122.	-2877806.	91.104	-258463.	-261147.	8.267
1700.	-4072449.	-2843741.	87.377	-259237.	-261217.	8.026
1750.	-4070497.	-2807631.	83.803	-260099.	-261263.	7.798
(2 sigma)	---	---	---	4919.	3175.	0.095
1800.	-4527061.	-2759805.	80.087	-261052.	-261283.	7.582
(2 sigma)	---	---	---	5199.	3347.	0.097

Table 90. Thermophysical values for meionite, $\text{Ca}_4\text{Al}_8\text{Si}_6\text{O}_{24}(\text{CO}_3)$, at 1.01325 bars (1 atm). The tabulations are based on a fit of the thermophysical and thermochemical data given in Section 1.5.5.

T K	Cp J/(mol K)	S J/(mol K)	H-H(298) J/mol	[G-H(298)]/T J/(mol K)	cm^3V /mol
200.	466.964	450.253	-60109.	-750.796	337.0425
250.	623.750	572.781	-32508.	-702.815	337.3241
(2 sigma)	20.017	12.267	684.	11.982	2.1893
273.150	674.831	630.323	-17458.	-694.236	337.4544
298.150	720.385	691.450	0.	-691.450	337.5952
(2 sigma)	10.808	12.002	0.	12.002	2.0810
300.	723.434	695.915	1336.	-691.463	337.6056
350.	793.116	812.953	39342.	-700.546	337.8872
400.	845.051	922.404	80354.	-721.518	338.1687
450.	885.571	1024.367	123659.	-749.570	338.4503
500.	918.281	1119.421	168782.	-781.857	338.7319
(2 sigma)	11.223	8.118	1997.	11.184	1.6348
550.	945.390	1208.252	215394.	-816.627	339.0134
600.	968.325	1291.521	263252.	-852.768	339.2950
650.	988.058	1369.827	312173.	-889.560	339.5766
700.	1005.271	1443.693	362016.	-926.528	339.8581
750.	1020.460	1513.578	412666.	-963.356	340.1397
(2 sigma)	8.890	5.199	4377.	9.411	1.1179
800.	1033.994	1579.877	464034.	-999.835	340.4212
850.	1046.155	1642.934	516043.	-1035.825	340.7028
900.	1057.161	1703.047	568630.	-1071.236	340.9844
950.	1067.186	1760.478	621743.	-1106.012	341.2659
1000.	1076.368	1815.454	675335.	-1140.119	341.5475
(2 sigma)	7.320	4.229	6072.	7.917	0.7244
1050.	1084.819	1868.177	729367.	-1173.542	341.8291
1100.	1092.533	1918.826	783806.	-1206.275	342.1106
1150.	1099.886	1967.557	838621.	-1238.321	342.3922
1200.	1106.643	2014.513	893787.	-1269.690	342.6737
1250.	1112.958	2059.817	949278.	-1300.395	342.9553
(2 sigma)	7.837	4.162	7284.	6.816	0.7055
1300.	1118.878	2103.585	1005076.	-1330.450	343.2369
1350.	1124.443	2145.917	1061160.	-1359.873	343.5184
1400.	1129.686	2186.906	1117515.	-1388.681	343.8000
1450.	1134.639	2226.636	1174124.	-1416.895	344.0816
1500.	1139.327	2265.181	1230974.	-1444.532	344.3631
(2 sigma)	9.390	4.658	8386.	6.041	1.0810
1550.	1143.772	2302.613	1288053.	-1471.611	344.6447
1600.	1147.996	2338.993	1345348.	-1498.151	344.9263
1650.	1152.017	2374.381	1402849.	-1524.170	345.2078
1700.	1155.849	2408.830	1460546.	-1549.685	345.4894
1750.	1159.508	2442.388	1518431.	-1574.713	345.7709
(2 sigma)	11.140	5.545	9724.	5.528	1.5929
1800.	1163.007	2475.102	1576495.	-1599.272	346.0525
(2 sigma)	11.483	5.756	10042.	5.453	1.7014

Table 91. Thermochemical properties of meionite, $\text{Ca}_4\text{Al}_5\text{Si}_6\text{O}_{24}(\text{CO}_3)$, at 1.01325 bars (1 atm). Columns 2 through 4 give the thermochemical values relative to the elements; columns 5 through 7 give the values relative to the oxides.

T K	Formation from the Elements			Formation from the Oxides		
	H J/mol	G J/mol	log K	H J/mol	G J/mol	log K
200.	-13884220.	-13389268.	3496.916	-471259.	-456964.	119.347
250.	-13893419.	-13264332.	2771.429	-472450.	-453209.	94.693
(2 sigma)	---	---	---	8922.	6463.	1.350
273.150	-13895848.	-13205962.	2525.382	-472475.	-451425.	86.326
298.150	-13897549.	-13142738.	2302.552	-472316.	-449504.	78.751
(2 sigma)	---	---	---	8939.	6043.	1.059
300.	-13897643.	-13138055.	2287.537	-472298.	-449363.	78.241
350.	-13898807.	-13011331.	1941.833	-471690.	-445585.	66.500
400.	-13897964.	-12884587.	1682.553	-471012.	-441903.	57.707
450.	-13895762.	-12758035.	1480.913	-470449.	-438300.	50.876
500.	-13892631.	-12631782.	1319.632	-470093.	-434749.	45.418
(2 sigma)	---	---	---	7793.	4725.	0.494
550.	-13888876.	-12505874.	1187.708	-469991.	-431222.	40.954
600.	-13884727.	-12380328.	1077.803	-470165.	-427692.	37.234
650.	-13880359.	-12255137.	984.834	-470628.	-424135.	34.084
700.	-13875914.	-12130287.	905.172	-471384.	-420533.	31.380
750.	-13874855.	-12005607.	836.144	-472434.	-416865.	29.033
(2 sigma)	---	---	---	6494.	3949.	0.275
800.	-13870157.	-11881146.	775.759	-473780.	-413119.	26.974
850.	-13865821.	-11756968.	722.495	-479694.	-409247.	25.149
900.	-13861908.	-11633033.	675.163	-479089.	-405120.	23.513
950.	-13922247.	-11507360.	632.718	-478382.	-401030.	22.050
1000.	-13918520.	-11380358.	594.449	-477592.	-396978.	20.736
(2 sigma)	---	---	---	5882.	3665.	0.191
1050.	-13915006.	-11253538.	559.832	-476734.	-392969.	19.549
1100.	-13911723.	-11126879.	528.371	-475821.	-389001.	18.472
1150.	-13940172.	-10999243.	499.601	-474867.	-385076.	17.491
1200.	-13933620.	-10871516.	473.224	-473885.	-381193.	16.593
1250.	-13926922.	-10744066.	448.970	-472886.	-377351.	15.769
(2 sigma)	---	---	---	5838.	3702.	0.155
1300.	-13920086.	-10616886.	426.591	-471883.	-373550.	15.009
1350.	-13913118.	-10489972.	405.881	-470887.	-369787.	14.308
1400.	-13906024.	-10363318.	386.660	-469907.	-366060.	13.658
1450.	-13898808.	-10236920.	368.773	-468955.	-362368.	13.054
1500.	-13891473.	-10110772.	352.088	-468042.	-358708.	12.491
(2 sigma)	---	---	---	6472.	4029.	0.140
1550.	-13884020.	-9984871.	336.488	-467177.	-355078.	11.966
1600.	-13876452.	-9859213.	321.870	-466370.	-351475.	11.474
1650.	-13868770.	-9733793.	308.146	-465632.	-347897.	11.013
1700.	-14164029.	-9605908.	295.153	-464972.	-344339.	10.580
1750.	-14155267.	-9471973.	282.723	-464400.	-340799.	10.172
(2 sigma)	---	---	---	7913.	4673.	0.139
1800.	-14757700.	-9322595.	270.534	-463925.	-337275.	9.787
(2 sigma)	---	---	---	8297.	4844.	0.141

Table 92. Thermophysical values for stable phases of the element iron (Fe) at 1.01325 bars (1 atm). The sources of data are given in Section 1.5.5.

T K	C _p J/(mol K)	S J/(mol K)	H-H(298) J/mol	[G-H(298)]/T J/(mol K)	V^3 cm ³ /mol
iron (crystal, body centered cubic)					
200.	34.683	16.270	-2677.	-29.652	---
250.	26.027	22.838	-1213.	-27.688	---
(2 sigma)	---	---	---	---	---
273.15	25.059	25.093	-623.	-27.375	---
298.15	24.925	27.276	-0.	-27.276	---
(2 sigma)	---	---	---	---	---
300.	24.939	27.431	46.	-27.277	---
350.	25.946	31.339	1314.	-27.583	---
400.	27.366	34.896	2647.	-28.278	---
450.	28.704	38.198	4050.	-29.199	---
500.	29.872	41.284	5515.	-30.255	---
(2 sigma)	---	---	---	---	---
550.	30.926	44.181	7035.	-31.391	---
600.	31.966	46.916	8607.	-32.571	---
650.	33.097	49.519	10233.	-33.776	---
700.	34.419	52.018	11920.	-34.990	---
750.	36.021	54.446	13679.	-36.206	---
(2 sigma)	---	---	---	---	---
800.	37.980	56.831	15528.	-37.421	---
850.	40.362	59.203	17485.	-38.633	---
900.	43.225	61.588	19572.	-39.842	---
950.	46.617	64.014	21816.	-41.050	---
1000.	50.581	66.503	24243.	-42.260	---
(2 sigma)	---	---	---	---	---
1042.	54.378	68.660	26446.	-43.280	---
1042.	52.347	69.309	27122.	-43.280	---
1050.	51.421	69.700	27537.	-43.480	---
1100.	46.636	71.981	29982.	-44.725	---
1150.	43.281	73.976	32225.	-45.954	---
1184.	41.640	75.212	33667.	-46.777	---
iron (crystal, face centered cubic)					
1184.	33.882	75.975	34570.	-46.777	---
1200.	34.016	76.430	35113.	-47.169	---
1250.	34.434	77.827	36824.	-48.368	---
(2 sigma)	---	---	---	---	---
1300.	34.853	79.186	38557.	-49.527	---
1350.	35.271	80.509	40310.	-50.650	---
1400.	35.690	81.799	42084.	-51.740	---
1450.	36.108	83.059	43879.	-52.798	---
1500.	36.526	84.290	45694.	-53.827	---
(2 sigma)	---	---	---	---	---
1550.	36.945	85.495	47531.	-54.830	---
1600.	37.363	86.674	49389.	-55.806	---
1650.	37.782	87.831	51268.	-56.759	---
1665.	37.907	88.173	51835.	-57.041	---
iron (crystal, body centered cubic)					
1665.	41.138	88.666	52656.	-57.040	---
1700.	41.620	89.527	54105.	-57.700	---
1750.	42.204	90.742	56201.	-58.627	---
(2 sigma)	---	---	---	---	---
1800.	42.732	91.939	58325.	-59.536	---
(2 sigma)	---	---	---	---	---

Table 93. Thermochemical properties of stable phases of the element iron (Fe) at 1.01325 bars (1 atm). Columns 2 through 4 give the thermochemical values relative to the elements; columns 5 through 7 give the values relative to the oxides.

T K	Formation from the Elements			Formation from the Oxides		
	H J/mol	G J/mol	log K	H J/mol	G J/mol	log K
iron (crystal, body centered cubic)						
200.	0.	0.	0.	---	---	---
250.	0.	0.	0.	---	---	---
(2 sigma)	0.	0.	0.	---	---	---
273.15	0.	0.	0.	---	---	---
298.15	0.	0.	0.	---	---	---
(2 sigma)	0.	0.	0.	---	---	---
300.	0.	0.	0.	---	---	---
350.	0.	0.	0.	---	---	---
400.	0.	0.	0.	---	---	---
450.	0.	0.	0.	---	---	---
500.	0.	0.	0.	---	---	---
(2 sigma)	0.	0.	0.	---	---	---
550.	0.	0.	0.	---	---	---
600.	0.	0.	0.	---	---	---
650.	0.	0.	0.	---	---	---
700.	0.	0.	0.	---	---	---
750.	0.	0.	0.	---	---	---
(2 sigma)	0.	0.	0.	---	---	---
800.	0.	0.	0.	---	---	---
850.	0.	0.	0.	---	---	---
900.	0.	0.	0.	---	---	---
950.	0.	0.	0.	---	---	---
1000.	0.	0.	0.	---	---	---
(2 sigma)	0.	0.	0.	---	---	---
1042.	0.	0.	0.	---	---	---
1042.	0.	0.	0.	---	---	---
1050.	0.	0.	0.	---	---	---
1100.	0.	0.	0.	---	---	---
1150.	0.	0.	0.	---	---	---
1184.	0.	0.	0.	---	---	---
iron (crystal, face centered cubic)						
1184.	0.	0.	0.	---	---	---
1200.	0.	0.	0.	---	---	---
1250.	0.	0.	0.	---	---	---
(2 sigma)	0.	0.	0.	---	---	---
1300.	0.	0.	0.	---	---	---
1350.	0.	0.	0.	---	---	---
1400.	0.	0.	0.	---	---	---
1450.	0.	0.	0.	---	---	---
1500.	0.	0.	0.	---	---	---
(2 sigma)	0.	0.	0.	---	---	---
1550.	0.	0.	0.	---	---	---
1600.	0.	0.	0.	---	---	---
1650.	0.	0.	0.	---	---	---
1665.	0.	0.	0.	---	---	---
iron (crystal, body centered cubic)						
1665.	0.	0.	0.	---	---	---
1700.	0.	0.	0.	---	---	---
1750.	0.	0.	0.	---	---	---
(2 sigma)	0.	0.	0.	---	---	---
1800.	0.	0.	0.	---	---	---
(2 sigma)	0.	0.	0.	---	---	---

Table 94. Thermophysical values for wustite, Fe_{947}O , at 1.01325 bars (1 atm). The tabulations are based on a fit of the thermophysical and thermochemical data given in Section 1.5.5.

T K	Cp J/(mol K)	S J/(mol K)	H-H(298) J/mol	[G-H(298)]/T J/(mol K)	V cm^3/mol
200.	44.634	39.849	-4587.	-62.785	12.0395
250.	46.879	50.066	-2296.	-59.249	12.0395
(2 sigma)	0.244	0.565	10.	0.563	0.0053
273.150	47.671	54.253	-1201.	-58.550	12.0395
298.150	48.402	58.460	0.	-58.460	12.0395
(2 sigma)	0.207	0.563	0.	0.563	0.0053
300.	48.452	58.760	90.	-58.461	12.0395
350.	49.619	66.320	2543.	-59.056	12.0395
400.	50.524	73.008	5047.	-60.390	12.0395
450.	51.256	79.002	7592.	-62.130	12.0395
500.	51.870	84.435	10171.	-64.093	12.0395
(2 sigma)	0.208	0.560	42.	0.561	0.0053
550.	52.403	89.404	12778.	-66.172	12.0395
600.	52.883	93.985	15410.	-68.301	12.0395
650.	53.327	98.235	18066.	-70.442	12.0395
700.	53.750	102.203	20743.	-72.571	12.0395
750.	54.164	105.926	23440.	-74.672	12.0395
(2 sigma)	0.311	0.548	79.	0.556	0.0053
800.	54.576	109.434	26159.	-76.736	12.0395
850.	54.994	112.756	28898.	-78.758	12.0395
900.	55.422	115.911	31659.	-80.735	12.0395
950.	55.865	118.919	34441.	-82.666	12.0395
1000.	56.327	121.796	37245.	-84.551	12.0395
(2 sigma)	0.320	0.541	128.	0.550	0.0053
1050.	56.810	124.556	40074.	-86.391	12.0395
1100.	57.317	127.211	42927.	-88.186	12.0395
1150.	57.851	129.770	45806.	-89.939	12.0395
1200.	58.412	132.244	48712.	-91.650	12.0395
1250.	59.003	134.640	51648.	-93.322	12.0395
(2 sigma)	0.615	0.539	151.	0.545	0.0053
1300.	59.625	136.967	54613.	-94.956	12.0395
1350.	60.279	139.229	57611.	-96.554	12.0395
1400.	60.965	141.433	60641.	-98.118	12.0395
1450.	61.686	143.585	63708.	-99.549	12.0395
1500.	62.442	145.689	66811.	-101.149	12.0395
(2 sigma)	1.702	0.571	293.	0.543	0.0053
1550.	63.233	147.749	69952.	-102.619	12.0395
1600.	64.060	149.770	73135.	-104.061	12.0395
1650.	64.923	151.754	76359.	-105.476	12.0395
1700.	65.824	153.706	79627.	-106.866	12.0395
1750.	66.762	155.627	82942.	-108.232	12.0395
(2 sigma)	3.433	0.780	869.	0.545	0.0053
1800.	67.738	157.522	86304.	-109.575	12.0395
(2 sigma)	3.854	0.550	1045.	0.547	0.0053

Table 95. Thermochemical properties of wustite, $\text{Fe}_{0.947}\text{O}$, at 1.01325 bars (1 atm). Columns 2 through 4 give the thermochemical values relative to the elements. The properties relative to the oxides were unavailable. Refer to Section 1.5.5 for details.

T K	Formation from the Elements			Formation from the Oxides		
	H J/mol	G J/mol	log K	H J/mol	G J/mol	log K
200.	-266038.	-251586.	65.708	---	---	---
250.	-265860.	-247984.	51.813	---	---	---
(2 sigma)	621.	492.	0.103	---	---	---
273.150	-265661.	-246337.	47.107	---	---	---
298.150	-265416.	-244579.	42.849	---	---	---
(2 sigma)	621.	468.	0.082	---	---	---
300.	-265397.	-244450.	42.562	---	---	---
350.	-264885.	-240999.	35.967	---	---	---
400.	-264395.	-237621.	31.030	---	---	---
450.	-263942.	-234301.	27.197	---	---	---
500.	-263527.	-231031.	24.136	---	---	---
(2 sigma)	622.	371.	0.039	---	---	---
550.	-263147.	-227800.	21.635	---	---	---
600.	-262802.	-224602.	19.553	---	---	---
650.	-262495.	-221431.	17.794	---	---	---
700.	-262234.	-218283.	16.288	---	---	---
750.	-262030.	-215151.	14.984	---	---	---
(2 sigma)	618.	267.	0.019	---	---	---
800.	-261898.	-212030.	13.844	---	---	---
850.	-261855.	-208915.	12.838	---	---	---
900.	-261924.	-205800.	11.944	---	---	---
950.	-262125.	-202677.	11.144	---	---	---
1000.	-262485.	-199540.	10.423	---	---	---
(2 sigma)	614.	208.	0.011	---	---	---
1050.	-263647.	-196375.	9.769	---	---	---
1100.	-263987.	-193163.	9.173	---	---	---
1150.	-264114.	-189940.	8.627	---	---	---
1200.	-264831.	-186704.	8.127	---	---	---
1250.	-264409.	-183458.	7.666	---	---	---
(2 sigma)	613.	226.	0.009	---	---	---
1300.	-263981.	-180228.	7.242	---	---	---
1350.	-263545.	-177015.	6.849	---	---	---
1400.	-263098.	-173818.	6.485	---	---	---
1450.	-262640.	-170638.	6.147	---	---	---
1500.	-262167.	-167473.	5.832	---	---	---
(2 sigma)	673.	308.	0.011	---	---	---
1550.	-261679.	-164325.	5.538	---	---	---
1600.	-261172.	-161192.	5.262	---	---	---
1650.	-260644.	-158076.	5.004	---	---	---
1700.	-260983.	-154959.	4.761	---	---	---
1750.	-260575.	-151847.	4.532	---	---	---
(2 sigma)	1084.	429.	0.013	---	---	---
1800.	-260146.	-148746.	4.317	---	---	---
(2 sigma)	1236.	459.	0.013	---	---	---

Table 96. Thermophysical values for ferrosilite, FeSiO_3 , at 1.01325 bars (1 atm). The tabulations are based on a fit of the thermophysical and thermochemical data given in Section 1.5.5.

T K	Cp J/(mol K)	S J/(mol K)	H-H(298) J/mol	[G-H(298)]/T J/(mol K)	V cm ³ /mol
200.	41.873	69.753	-6577.	-102.635	32.8694
250.	69.252	82.360	-3726.	-97.265	32.9300
(2 sigma)	5.802	2.358	201.	2.232	0.0376
273.150	77.404	88.863	-2025.	-96.276	32.9580
298.150	84.327	95.952	0.	-95.952	32.9883
(2 sigma)	3.005	2.235	0.	2.235	0.0352
300.	84.778	96.475	156.	-95.954	32.9906
350.	94.685	110.339	4659.	-97.026	33.0511
400.	101.577	123.457	9575.	-99.518	33.1117
450.	106.696	135.730	14788.	-102.868	33.1722
500.	110.699	147.187	20226.	-106.734	33.2328
(2 sigma)	2.137	1.667	381.	2.105	0.0310
550.	113.956	157.895	25845.	-110.903	33.2933
600.	116.691	167.931	31613.	-115.242	33.3539
650.	119.046	177.366	37508.	-119.661	33.4145
700.	121.114	186.266	43513.	-124.104	33.4750
750.	122.955	194.686	49616.	-128.531	33.5356
(2 sigma)	1.681	1.316	791.	1.832	0.0405
800.	124.616	202.675	55806.	-132.918	33.5961
850.	126.126	210.276	62075.	-137.246	33.6567
900.	127.509	217.525	68416.	-141.506	33.7173
950.	128.782	224.453	74824.	-145.691	33.7778
1000.	129.957	231.089	81293.	-149.796	33.8384
(2 sigma)	1.651	1.291	1064.	1.627	0.0588
1050.	131.045	237.456	87818.	-153.820	33.8989
1100.	132.053	243.576	94396.	-157.762	33.9595
1150.	132.987	249.467	101022.	-161.622	34.0200
1200.	133.853	255.146	107694.	-165.401	34.0806
1250.	134.653	260.626	114407.	-169.101	34.1412
(2 sigma)	1.842	1.401	1282.	1.503	0.0800
1300.	135.391	265.922	121158.	-172.723	34.2017
1350.	136.070	271.044	127945.	-176.271	34.2623
1400.	136.692	276.004	134764.	-179.744	34.3228
1450.	137.258	280.811	141613.	-183.147	34.3834
1500.	137.770	285.473	148489.	-186.481	34.4440
(2 sigma)	1.750	1.556	1511.	1.440	0.1024
1550.	138.230	289.998	155389.	-189.747	34.5045
1600.	138.637	294.394	162311.	-192.949	34.5651
1650.	138.994	298.665	169252.	-196.088	34.6256
1700.	139.301	302.819	176210.	-199.167	34.6862
1750.	139.558	306.861	183181.	-202.186	34.7467
(2 sigma)	1.912	1.675	1716.	1.418	0.1253
1800.	139.767	310.796	190165.	-205.149	34.8073
(2 sigma)	2.095	1.691	1752.	1.417	0.1299

Table 97. Thermochemical properties of ferrosilite, FeSiO_3 , at 1.01325 bars (1 atm). Columns 2 through 4 give the thermochemical values relative to the elements. The properties relative to the oxides were unavailable. Refer to Section 1.5.5 for details.

T K	Formation from the Elements			Formation from the Oxides		
	H J/mol	G J/mol	log K	H J/mol	G J/mol	log K
200.000	-1192120.	-1142467.	298.382	---	---	---
250.000	-1193767.	-1129829.	236.065	---	---	---
(2 sigma)	1457.	961.	0.201	---	---	---
273.150	-1194100.	-1123892.	214.922	---	---	---
298.150	-1194286.	-1117457.	195.774	---	---	---
(2 sigma)	1460.	875.	0.153	---	---	---
300.000	-1194294.	-1116981.	194.483	---	---	---
350.000	-1194312.	-1104089.	164.776	---	---	---
400.000	-1194069.	-1091214.	142.498	---	---	---
450.000	-1193678.	-1078379.	125.175	---	---	---
500.000	-1193191.	-1065594.	111.322	---	---	---
(2 sigma)	1283.	585.	0.061	---	---	---
550.000	-1192641.	-1052860.	99.992	---	---	---
600.000	-1192050.	-1040179.	90.556	---	---	---
650.000	-1191437.	-1027548.	82.575	---	---	---
700.000	-1190821.	-1014964.	75.737	---	---	---
750.000	-1190223.	-1002424.	69.815	---	---	---
(2 sigma)	1077.	458.	0.032	---	---	---
800.000	-1189666.	-989922.	64.635	---	---	---
850.000	-1189175.	-977454.	60.067	---	---	---
900.000	-1188777.	-965012.	56.008	---	---	---
950.000	-1188500.	-952588.	52.377	---	---	---
1000.000	-1188376.	-940176.	49.110	---	---	---
(2 sigma)	1014.	579.	0.030	---	---	---
1050.000	-1189090.	-927760.	46.154	---	---	---
1100.000	-1188928.	-915319.	43.465	---	---	---
1150.000	-1188540.	-902890.	41.011	---	---	---
1200.000	-1188776.	-890470.	38.761	---	---	---
1250.000	-1187813.	-878061.	36.692	---	---	---
(2 sigma)	1118.	840.	0.035	---	---	---
1300.000	-1186853.	-865689.	34.784	---	---	---
1350.000	-1185898.	-853355.	33.018	---	---	---
1400.000	-1184947.	-841056.	31.380	---	---	---
1450.000	-1184004.	-828791.	29.856	---	---	---
1500.000	-1183069.	-816558.	28.435	---	---	---
(2 sigma)	1358.	1169.	0.041	---	---	---
1550.000	-1182145.	-804356.	27.107	---	---	---
1600.000	-1181232.	-792184.	25.862	---	---	---
1650.000	-1180332.	-780041.	24.694	---	---	---
1700.000	-1230894.	-767456.	23.581	---	---	---
1750.000	-1230058.	-753838.	22.501	---	---	---
(2 sigma)	1603.	1542.	0.046	---	---	---
1800.000	-1229242.	-740243.	21.481	---	---	---
(2 sigma)	1646.	1620.	0.047	---	---	---

Table 98. Thermophysical values for hematite, Fe₂O₃, at 1.01325 bars (1 atm). The tabulations are based on a fit of the thermophysical and thermochemical data given in Section 1.5.5.

T K	C _p J/(mol K)	S J/(mol K)	H-H(298) J/mol	[G-H(298)]/T J/(mol K)	V cm ³ /mol
200.	76.761	51.370	-3965.	-96.193	30.1601
250.	92.138	70.206	-4730.	-89.125	30.2187
(2 sigma)	0.116	0.320	5.	0.319	0.0208
273.150	98.132	78.633	-2526.	-37.880	30.2458
298.150	103.801	87.477	0.	-37.477	30.2751
(2 sigma)	0.109	0.319	0.	0.319	0.0181
300.	104.190	88.121	192.	-37.479	30.2772
350.	113.284	104.897	5640.	-88.783	30.3358
400.	120.215	120.497	11485.	-91.785	30.3944
450.	125.694	134.983	17637.	-95.789	30.4530
500.	130.279	148.470	24039.	-100.391	30.5115
(2 sigma)	0.276	0.332	39.	0.320	0.0346
550.	134.398	161.082	30657.	-105.341	30.5702
600.	138.380	172.947	37477.	-110.485	30.6287
650.	142.478	184.184	44497.	-115.725	30.6873
700.	146.389	194.901	51730.	-121.001	30.7459
750.	151.771	205.199	59194.	-126.273	30.8045
(2 sigma)	0.374	0.370	104.	0.324	0.0719
800.	157.250	215.166	66917.	-131.519	30.8631
850.	163.427	224.880	74931.	-136.726	30.9217
900.	170.385	234.415	83273.	-141.889	30.9802
950.	178.195	243.832	91984.	-147.007	31.0388
955.500	179.108	244.863	92966.	-147.568	31.0453
955.500	159.010	246.970	94979.	-147.568	31.0388
1000.	150.364	254.002	101851.	-152.150	31.0974
(2 sigma)	0.824	1.247	1179.	0.330	0.1111
1050.	143.691	261.165	109191.	-157.173	31.1560
1100.	139.445	267.743	116261.	-162.052	31.2146
1150.	137.000	273.882	123166.	-166.782	31.2732
1200.	135.880	279.685	129983.	-171.366	31.3317
1250.	135.720	285.225	136770.	-175.811	31.3903
(2 sigma)	2.386	1.254	1201.	0.417	0.1508
1300.	136.238	290.558	143566.	-180.122	31.4489
1350.	137.217	295.716	150401.	-184.308	31.5075
1400.	138.487	300.729	157293.	-188.377	31.5661
1450.	139.919	305.613	164252.	-192.336	31.6247
1500.	141.408	310.382	171286.	-196.192	31.6832
(2 sigma)	2.464	1.368	1420.	0.530	0.1906
1550.	142.876	315.043	178393.	-199.951	31.7418
1600.	144.251	319.501	185572.	-203.619	31.8004
1650.	145.516	324.060	192817.	-207.201	31.8590
1700.	146.603	328.420	200121.	-210.702	31.9176
1750.	147.496	332.684	207474.	-214.127	31.9762
(2 sigma)	2.380	1.509	1731.	0.535	0.2206
1800.	148.173	336.849	214867.	-217.478	32.0347
(2 sigma)	2.297	1.534	1792.	0.655	0.2386

Table 99. Thermochemical properties of hematite, Fe₂O₃, at 1.01325 bars (1 atm). Columns 2 through 4 give the thermochemical values relative to the elements. The properties relative to the oxides were unavailable. Refer to Section 1.5.5 for details.

T K	Formation from the Elements			Formation from the Oxides		
	H J/mol	G J/mol	log K	H J/mol	G J/mol	log K
200.	-826468.	-772215.	201.682	---	---	---
250.	-827343.	-758517.	158.483	---	---	---
(2 sigma)	1071.	1043.	0.218	---	---	---
273.150	-827329.	-752143.	143.833	---	---	---
298.150	-827148.	-745259.	130.568	---	---	---
(2 sigma)	1071.	1038.	0.182	---	---	---
300.	-827130.	-744761.	129.674	---	---	---
350.	-825439.	-731083.	109.108	---	---	---
400.	-825515.	-717522.	93.699	---	---	---
450.	-824460.	-704085.	81.728	---	---	---
500.	-823316.	-690770.	72.164	---	---	---
(2 sigma)	1075.	1019.	0.106	---	---	---
550.	-822101.	-677574.	64.351	---	---	---
600.	-820821.	-664491.	57.849	---	---	---
650.	-819478.	-651518.	52.357	---	---	---
700.	-818075.	-638650.	47.657	---	---	---
750.	-816612.	-625884.	43.590	---	---	---
(2 sigma)	1086.	999.	0.070	---	---	---
800.	-815094.	-613218.	40.039	---	---	---
850.	-813526.	-600649.	36.911	---	---	---
900.	-811915.	-588173.	34.137	---	---	---
950.	-810268.	-575788.	31.659	---	---	---
955.500	-810085.	-574431.	31.403	---	---	---
955.	-808079.	-574553.	31.426	---	---	---
1000.	-807851.	-563557.	29.437	---	---	---
1050.	-809714.	-551322.	27.427	---	---	---
1100.	-810166.	-539006.	25.595	---	---	---
1150.	-810395.	-526675.	23.922	---	---	---
1200.	-812019.	-514315.	22.388	---	---	---
1250.	-811332.	-501925.	20.974	---	---	---
(2 sigma)	2035.	778.	0.032	---	---	---
1300.	-810691.	-489561.	19.671	---	---	---
1350.	-810065.	-477222.	18.465	---	---	---
1400.	-809435.	-464906.	17.346	---	---	---
1450.	-808789.	-452513.	16.305	---	---	---
1500.	-808120.	-440342.	15.334	---	---	---
(2 sigma)	2195.	594.	0.024	---	---	---
1550.	-807427.	-428094.	14.427	---	---	---
1600.	-806712.	-415869.	13.577	---	---	---
1650.	-805978.	-403666.	12.779	---	---	---
1700.	-807109.	-391450.	12.028	---	---	---
1750.	-806712.	-379231.	11.319	---	---	---
(2 sigma)	2419.	766.	0.023	---	---	---
1800.	-806334.	-367023.	10.651	---	---	---
(2 sigma)	2465.	801.	0.023	---	---	---
(2 sigma)	---	---	---	---	---	---

Table 100. Thermophysical values for fayalite, Fe_2SiO_4 , at 1.01325 bars (1 atm). The tabulations are based on a fit of the thermophysical and thermochemical data given in Section 1.5.5.

T K	Cp J/(mol K)	S J/(mol K)	H-H(298) J/mol	[G-H(298)]/T J/(mol K)	V cm ³ /mol
200.	102.407	104.772	-11594.	-162.740	46.0018
250.	118.884	129.437	-6051.	-153.643	46.0761
(2 sigma)	0.193	1.072	9.	1.072	0.0331
273.150	125.550	140.262	-3221.	-152.053	46.1105
298.150	131.991	151.540	0.	-151.540	46.1477
(2 sigma)	0.167	1.072	0.	1.072	0.0309
300.	132.437	152.358	245.	-151.543	46.1505
350.	143.065	173.606	7143.	-153.196	46.2248
400.	151.318	193.271	14512.	-156.993	46.2991
450.	157.747	211.481	22245.	-162.048	46.3734
500.	162.797	228.373	30263.	-167.846	46.4477
(2 sigma)	0.470	1.079	54.	1.072	0.0224
550.	166.821	244.085	38507.	-174.071	46.5220
600.	170.088	258.745	46933.	-180.524	46.5964
650.	172.811	272.470	55507.	-187.074	46.6707
700.	175.155	285.364	64208.	-193.639	46.7450
750.	177.253	297.521	73019.	-200.163	46.8193
(2 sigma)	0.929	1.121	202.	1.074	0.0171
800.	179.210	309.024	81931.	-206.611	46.8936
850.	181.113	319.945	90939.	-212.959	46.9679
900.	183.033	330.352	100042.	-219.194	47.0423
950.	185.028	340.301	109243.	-225.308	47.1166
1000.	187.147	349.845	118547.	-231.298	47.1909
(2 sigma)	0.990	1.174	360.	1.082	0.0216
1050.	189.431	359.030	127961.	-237.163	47.2652
1100.	191.917	367.899	137493.	-242.905	47.3395
1150.	194.633	376.489	147156.	-248.527	47.4138
1200.	197.605	384.834	156961.	-254.034	47.4882
1250.	200.857	392.966	166921.	-259.429	47.5625
(2 sigma)	4.041	1.176	521.	1.088	0.0321
1300.	204.406	400.912	177052.	-254.718	47.6368
1350.	208.271	408.698	187367.	-259.907	47.7111
1400.	212.466	416.347	197884.	-275.001	47.7854
1450.	217.005	423.881	208620.	-280.005	47.8597
1500.	221.898	431.319	219591.	-284.925	47.9341
(2 sigma)	10.553	1.796	2066.	1.090	0.0445
1550.	227.157	438.680	230815.	-289.766	48.0084
1600.	232.791	445.980	242313.	-294.534	48.0827
1650.	238.808	453.234	254101.	-299.233	48.1570
1700.	245.216	460.457	266200.	-303.869	48.2313
1750.	252.021	467.663	278629.	-308.446	48.3056
(2 sigma)	20.446	3.837	5795.	1.153	0.0576
1800.	259.230	474.863	291409.	-312.969	48.3800
(2 sigma)	22.841	4.415	6865.	1.189	0.0602

Table 101. Thermochemical properties of fayalite, Fe_2SiO_4 , at 1.01325 bars (1 atm). Columns 2 through 4 give the thermochemical values relative to the elements. The properties relative to the oxides were not available. Refer to Section 1.5.5 for details.

T K	Formation from the Elements			Formation from the Oxides		
	H J/mol	G J/mol	log K	H J/mol	G J/mol	log K
200.000	-1477912.	-1412670.	368.951	---	---	---
250.000	-1479058.	-1396195.	291.719	---	---	---
(2 sigma)	1381.	1147.	0.240	---	---	---
273.150	-1479189.	-1388515.	265.526	---	---	---
298.150	-1479168.	-1380216.	241.808	---	---	---
(2 sigma)	1380.	1104.	0.193	---	---	---
300.000	-1479161.	-1379602.	240.210	---	---	---
350.000	-1478792.	-1363033.	203.421	---	---	---
400.000	-1478182.	-1346536.	175.839	---	---	---
450.000	-1477436.	-1330123.	154.397	---	---	---
500.000	-1476611.	-1313799.	137.252	---	---	---
(2 sigma)	1387.	931.	0.097	---	---	---
550.000	-1475744.	-1297560.	123.232	---	---	---
600.000	-1474866.	-1281400.	111.556	---	---	---
650.000	-1474007.	-1265313.	101.682	---	---	---
700.000	-1473201.	-1249290.	93.223	---	---	---
750.000	-1472482.	-1233322.	85.896	---	---	---
(2 sigma)	1423.	739.	0.051	---	---	---
800.000	-1471887.	-1217398.	79.488	---	---	---
850.000	-1471458.	-1201507.	73.836	---	---	---
900.000	-1471237.	-1185635.	68.812	---	---	---
950.000	-1471270.	-1169769.	64.318	---	---	---
1000.000	-1471604.	-1153893.	60.273	---	---	---
(2 sigma)	1469.	602.	0.031	---	---	---
1050.000	-1473595.	-1137982.	56.611	---	---	---
1100.000	-1473800.	-1121993.	53.279	---	---	---
1150.000	-1473501.	-1106007.	50.236	---	---	---
1200.000	-1474380.	-1090020.	57.447	---	---	---
1250.000	-1472774.	-1074038.	44.882	---	---	---
(2 sigma)	1483.	484.	0.024	---	---	---
1300.000	-1471064.	-1058121.	42.516	---	---	---
1350.000	-1469233.	-1042273.	40.328	---	---	---
1400.000	-1467264.	-1026496.	38.299	---	---	---
1450.000	-1465137.	-1010791.	36.413	---	---	---
1500.000	-1462834.	-995163.	34.655	---	---	---
(2 sigma)	2408.	713.	0.025	---	---	---
1550.000	-1460335.	-979614.	33.013	---	---	---
1600.000	-1457621.	-964150.	31.476	---	---	---
1650.000	-1454670.	-948774.	30.036	---	---	---
1700.000	-1503849.	-933005.	28.668	---	---	---
1750.000	-1500572.	-916263.	27.349	---	---	---
(2 sigma)	5853.	1162.	0.035	---	---	---
1800.000	-1497006.	-899618.	26.106	---	---	---
(2 sigma)	6897.	1328.	0.039	---	---	---

Table 102. Thermophysical values for magnetite, Fe₃O₄, at 1.01325 bars (1 atm). The tabulations are based on a fit of the thermophysical and thermochemical data given in Section 1.5.5.

T K	C _p J/(mol K)	S J/(mol K)	H-H(298) J/mol	[G-H(298)]/T J/(mol K)	V cm ³ /mol
200.	117.048	92.578	-13247.	-158.815	44.4806
250.	135.804	120.733	-6921.	-148.417	44.5025
(2 sigma)	0.196	0.504	3.	0.503	0.0149
273.150	143.597	133.106	-3685.	-146.598	44.5127
298.150	151.081	146.011	0.	-146.011	44.5236
(2 sigma)	0.174	0.503	0.	0.503	0.0159
300.	151.598	146.947	280.	-146.014	44.5244
350.	163.830	171.275	8179.	-147.907	44.5463
400.	173.572	193.808	16621.	-152.254	44.5683
450.	182.011	214.747	25514.	-158.048	44.5902
500.	190.153	234.344	34818.	-164.708	44.6121
(2 sigma)	0.646	0.522	67.	0.503	0.0615
550.	198.796	252.866	44538.	-171.888	44.6340
600.	208.567	270.572	54716.	-179.378	44.6559
650.	219.955	287.704	65422.	-187.055	44.6778
700.	233.348	304.481	76745.	-194.845	44.6998
750.	249.053	321.102	88795.	-202.708	44.7217
(2 sigma)	1.054	0.638	235.	0.510	0.1256
800.	267.320	337.744	101693.	-210.628	44.7436
848.500	287.678	354.058	115141.	-218.359	44.7648
848.500	248.927	354.718	115701.	-218.359	44.5420
850.	248.205	355.157	116074.	-218.600	44.5420
900.	229.055	368.760	127968.	-226.573	44.5420
950.	217.256	380.801	139101.	-234.379	44.5420
1000.	210.378	391.753	149775.	-241.977	44.5420
(2 sigma)	1.254	2.788	2346.	0.650	---
1050.	206.725	401.918	160192.	-249.354	44.5420
1100.	205.108	411.492	170482.	-256.509	44.5420
1150.	204.704	420.597	180723.	-263.446	44.5420
1200.	204.944	429.313	190963.	-270.177	44.5420
1250.	205.442	437.689	201222.	-276.711	44.5420
(2 sigma)	5.143	2.924	2536.	1.012	---
1300.	205.948	445.756	211507.	-283.059	44.5420
1350.	206.306	453.536	221814.	-289.230	44.5420
1400.	206.429	461.042	232134.	-295.232	44.5420
1450.	206.282	468.284	242453.	-301.076	44.5420
1500.	205.867	475.271	252757.	-306.766	44.5420
(2 sigma)	5.169	3.314	3246.	1.321	---
1550.	205.208	482.011	263035.	-312.311	44.5420
1600.	204.353	488.514	273275.	-317.717	44.5420
1650.	203.358	494.787	283468.	-322.988	44.5420
1700.	202.299	500.842	293609.	-328.130	44.5420
1750.	201.220	506.690	303697.	-333.149	44.5420
(2 sigma)	3.702	3.631	3897.	1.593	---
1800.	200.223	512.345	313733.	-338.049	44.5420
(2 sigma)	3.685	3.663	3970.	1.643	---

Table 103. Thermochemical properties of magnetite, Fe_3O_4 , at 1.01325 bars (1 atm). Columns 2 through 4 give the thermochemical values relative to the elements. The properties relative to the oxides were not available. Refer to Section 1.5.5 for details.

T K	Formation from the Elements			Formation from the Oxides		
	H J/mol	G J/mol	log K	H J/mol	G J/mol	log K
200.	-1116758.	-1048153.	273.749	---	---	---
250.	-1117732.	-1030843.	215.383	---	---	---
(2 sigma)	888.	828.	0.173	---	---	---
273.150	-1117613.	-1022800.	195.591	---	---	---
298.150	-1117262.	-1014137.	177.672	---	---	---
(2 sigma)	887.	818.	0.143	---	---	---
300.	-1117229.	-1013497.	176.465	---	---	---
350.	-1116096.	-996292.	148.688	---	---	---
400.	-1114659.	-979273.	127.880	---	---	---
450.	-1113030.	-962446.	111.718	---	---	---
500.	-1111226.	-945809.	98.808	---	---	---
(2 sigma)	897.	783.	0.082	---	---	---
550.	-1109216.	-929363.	88.263	---	---	---
600.	-1106948.	-913110.	79.493	---	---	---
650.	-1104355.	-897060.	72.089	---	---	---
700.	-1101366.	-881224.	65.758	---	---	---
750.	-1097905.	-865617.	60.287	---	---	---
(2 sigma)	944.	750.	0.052	---	---	---
800.	-1093896.	-850258.	55.516	---	---	---
848.500	-1089411.	-835618.	51.442	---	---	---
848.	-1088882.	-835767.	51.481	---	---	---
850.	-1088762.	-835170.	51.323	---	---	---
900.	-1086537.	-820324.	47.610	---	---	---
950.	-1085570.	-805566.	44.293	---	---	---
1000.	-1085640.	-790832.	41.309	---	---	---
(2 sigma)	2508.	841.	0.044	---	---	---
1050.	-1088591.	-776055.	38.507	---	---	---
1100.	-1089146.	-761157.	36.144	---	---	---
1150.	-1089164.	-746247.	33.896	---	---	---
1200.	-1091142.	-731310.	31.833	---	---	---
1250.	-1089587.	-716349.	29.935	---	---	---
(2 sigma)	2694.	1325.	0.055	---	---	---
1300.	-1088086.	-701449.	28.185	---	---	---
1350.	-1086642.	-686606.	26.566	---	---	---
1400.	-1085263.	-671816.	25.066	---	---	---
1450.	-1083960.	-657073.	23.670	---	---	---
1500.	-1082747.	-642373.	22.369	---	---	---
(2 sigma)	3380.	1985.	0.069	---	---	---
1550.	-1081634.	-627713.	21.154	---	---	---
1600.	-1080631.	-613087.	20.015	---	---	---
1650.	-1079746.	-598490.	18.947	---	---	---
1700.	-1081797.	-583864.	17.940	---	---	---
1750.	-1081682.	-569221.	16.990	---	---	---
(2 sigma)	4013.	2763.	0.082	---	---	---
1800.	-1081708.	-554520.	16.093	---	---	---
(2 sigma)	4084.	2929.	0.085	---	---	---

Table 104. Thermophysical values for the element hydrogen (H_2) at 1.01325 bars (1 atm). The sources of data are given in Section 1.5.5.

T K	Cp J/(mol K)	S J/(mol K)	H-H(298) J/mol	[G-H(298)]/T J/(mol K)	V cm ³ /mol
200.	25.971	119.495	-2731.	-133.152	---
250.	28.057	125.552	-1372.	-131.041	---
(2 sigma)	---	---	---	---	---
273.15	28.513	128.058	-717.	-130.683	---
298.15	28.822	130.570	-0.	-130.570	---
(2 sigma)	---	---	---	---	---
300.	28.839	130.748	53.	-130.570	---
350.	29.127	135.219	1504.	-130.923	---
400.	29.221	139.116	2963.	-131.709	---
450.	29.244	142.559	4425.	-132.727	---
500.	29.250	145.641	5887.	-133.867	---
(2 sigma)	---	---	---	---	---
550.	29.263	148.429	7350.	-135.066	---
600.	29.293	150.977	8814.	-136.287	---
650.	29.345	153.323	10280.	-137.509	---
700.	29.417	155.500	11748.	-138.717	---
750.	29.511	157.533	13222.	-139.904	---
(2 sigma)	---	---	---	---	---
800.	29.623	159.441	14700.	-141.066	---
850.	29.751	161.241	16184.	-142.201	---
900.	29.895	162.945	17575.	-143.306	---
950.	30.052	164.566	19174.	-144.383	---
1000.	30.220	166.112	20681.	-145.431	---
(2 sigma)	---	---	---	---	---
1050.	30.397	167.590	22196.	-146.451	---
1100.	30.584	169.009	23720.	-147.445	---
1150.	30.777	170.372	25254.	-148.412	---
1200.	30.975	171.686	26798.	-149.354	---
1250.	31.179	172.955	28352.	-150.273	---
(2 sigma)	---	---	---	---	---
1300.	31.387	174.182	29916.	-151.169	---
1350.	31.597	175.370	31491.	-152.044	---
1400.	31.810	176.523	33076.	-152.898	---
1450.	32.024	177.643	34672.	-153.732	---
1500.	32.239	178.733	36278.	-154.547	---
(2 sigma)	---	---	---	---	---
1550.	32.455	179.793	37896.	-155.344	---
1600.	32.670	180.827	39524.	-156.125	---
1650.	32.885	181.836	41163.	-156.888	---
1700.	33.099	182.820	42812.	-157.637	---
1750.	33.311	183.783	44473.	-158.370	---
(2 sigma)	---	---	---	---	---
1800.	33.522	184.724	46143.	-159.089	---
(2 sigma)	---	---	---	---	---

Table 105. Thermochemical properties of the element hydrogen (H_2) at 1.01325 bars (1 atm). Columns 2 through 4 give the thermochemical values relative to the elements; columns 5 through 7 give the values relative to the oxides.

T K	Formation from the Elements			Formation from the Oxides		
	H J/mol	G J/mol	log K	H J/mol	G J/mol	log K
200.	0.	0.	0.	---	---	---
250.	0.	0.	0.	---	---	---
(2 sigma)	0.	0.	0.	---	---	---
273.15	0.	0.	0.	---	---	---
298.15	0.	0.	0.	---	---	---
(2 sigma)	0.	0.	0.	---	---	---
300.	0.	0.	0.	---	---	---
350.	0.	0.	0.	---	---	---
400.	0.	0.	0.	---	---	---
450.	0.	0.	0.	---	---	---
500.	0.	0.	0.	---	---	---
(2 sigma)	0.	0.	0.	---	---	---
550.	0.	0.	0.	---	---	---
600.	0.	0.	0.	---	---	---
650.	0.	0.	0.	---	---	---
700.	0.	0.	0.	---	---	---
750.	0.	0.	0.	---	---	---
(2 sigma)	0.	0.	0.	---	---	---
800.	0.	0.	0.	---	---	---
850.	0.	0.	0.	---	---	---
900.	0.	0.	0.	---	---	---
950.	0.	0.	0.	---	---	---
1000.	0.	0.	0.	---	---	---
(2 sigma)	0.	0.	0.	---	---	---
1050.	0.	0.	0.	---	---	---
1100.	0.	0.	0.	---	---	---
1150.	0.	0.	0.	---	---	---
1200.	0.	0.	0.	---	---	---
1250.	0.	0.	0.	---	---	---
(2 sigma)	0.	0.	0.	---	---	---
1300.	0.	0.	0.	---	---	---
1350.	0.	0.	0.	---	---	---
1400.	0.	0.	0.	---	---	---
1450.	0.	0.	0.	---	---	---
1500.	0.	0.	0.	---	---	---
(2 sigma)	0.	0.	0.	---	---	---
1550.	0.	0.	0.	---	---	---
1600.	0.	0.	0.	---	---	---
1650.	0.	0.	0.	---	---	---
1700.	0.	0.	0.	---	---	---
1750.	0.	0.	0.	---	---	---
(2 sigma)	0.	0.	0.	---	---	---
1800.	0.	0.	0.	---	---	---
(2 sigma)	0.	0.	0.	---	---	---

Table 106. Thermophysical values for stable phases with the composition H₂O at 1.01325 bars (1 atm). The tabulations are based on a fit of the thermophysical and thermochemical data given in Section 1.5.5.

T K	C _p J/(mol K)	S J/(mol K)	H-H(298) J/mol	[G-H(298)]/T J/(mol K)	V cm ³ /mol
H ₂ O [liquid] = water					
273.150	75.884	63.307	-1888.	-70.218	0.0000
298.150	75.254	69.921	0.	-69.921	0.0000
(2 sigma)	---	---	---	---	---
300.	75.230	70.386	139.	-69.922	0.0000
350.	75.469	81.981	3900.	-70.837	0.0000
373.150	76.003	86.831	5653.	-71.681	0.0000
H ₂ O [gas]					
373.150	34.048	196.318	46509.	-71.681	0.0000
400.	34.245	198.691	47425.	-80.127	0.0000
450.	34.669	202.748	49148.	-93.530	0.0000
500.	35.154	206.426	50893.	-104.639	0.0000
(2 sigma)	---	---	---	---	---
550.	35.686	209.801	52664.	-114.048	0.0000
600.	36.253	212.930	54463.	-122.159	0.0000
650.	36.846	215.855	56290.	-129.255	0.0000
700.	37.458	218.608	58147.	-135.540	0.0000
750.	38.082	221.213	60036.	-141.165	0.0000
(2 sigma)	---	---	---	---	---
800.	38.715	223.691	61956.	-146.247	0.0000
850.	39.352	226.057	63907.	-150.872	0.0000
900.	39.989	228.325	65891.	-155.113	0.0000
950.	40.624	230.504	67906.	-159.024	0.0000
1000.	41.254	232.604	69953.	-162.650	0.0000
(2 sigma)	---	---	---	---	---
1050.	41.878	234.632	72032.	-166.030	0.0000
1100.	42.494	236.594	74141.	-169.193	0.0000
1150.	43.100	238.496	76281.	-172.165	0.0000
1200.	43.695	240.343	78451.	-174.968	0.0000
1250.	44.278	242.139	80650.	-177.619	0.0000
(2 sigma)	---	---	---	---	---
1300.	44.848	243.887	82878.	-180.134	0.0000
1350.	45.404	245.590	85135.	-182.527	0.0000
1400.	45.945	247.251	87418.	-184.809	0.0000
1450.	46.472	248.872	89729.	-186.990	0.0000
1500.	46.982	250.456	92065.	-189.079	0.0000
(2 sigma)	---	---	---	---	---
1550.	47.477	252.005	94427.	-191.084	0.0000
1600.	47.954	253.520	96813.	-193.012	0.0000
1650.	48.415	255.003	99222.	-194.868	0.0000
1700.	48.858	256.455	101654.	-196.658	0.0000
1750.	49.283	257.877	104108.	-198.387	0.0000
(2 sigma)	---	---	---	---	---
1800.	49.689	259.271	106582.	-200.059	0.0000
(2 sigma)	---	---	---	---	---

Table 107. Thermochemical properties of stable phases with the composition H_2O at 1.01325 bars (1 atm). Columns 2 through 4 give the thermochemical values relative to the elements; columns 5 through 7 give the values relative to the oxides.

T K	Formation from the Elements			Formation from the Oxides		
	H J/mol	G J/mol	log K	H J/mol	G J/mol	log K
		H_2O [liquid] = water				
273.150	-286613.	-241274.	46.139	0.0	0.0	0.0
298.150	-285808.	-237160.	41.549	0.0	0.0	0.0
(2 sigma)	---	---	---	0.0	0.0	0.0
300.	-285749.	-236858.	41.241	0.0	0.0	0.0
350.	-284178.	-228834.	34.152	0.0	0.0	0.0
373.150	-283447.	-225197.	31.524	0.0	0.0	0.0
		H_2O [gas]				
373.150	-242592.	-225197.	31.524	0.0	0.0	0.0
400.	-242865.	-223936.	29.243	0.0	0.0	0.0
450.	-243368.	-221539.	25.716	0.0	0.0	0.0
500.	-243861.	-219088.	22.888	0.0	0.0	0.0
(2 sigma)	---	---	---	0.0	0.0	0.0
550.	-244340.	-216587.	20.570	0.0	0.0	0.0
600.	-244804.	-214043.	18.634	0.0	0.0	0.0
650.	-245251.	-211462.	16.993	0.0	0.0	0.0
700.	-245681.	-208846.	15.584	0.0	0.0	0.0
750.	-246093.	-206201.	14.361	0.0	0.0	0.0
(2 sigma)	---	---	---	0.0	0.0	0.0
800.	-246488.	-203528.	13.289	0.0	0.0	0.0
850.	-246864.	-200832.	12.342	0.0	0.0	0.0
900.	-247224.	-198113.	11.498	0.0	0.0	0.0
950.	-247566.	-195375.	10.742	0.0	0.0	0.0
1000.	-247891.	-192620.	10.061	0.0	0.0	0.0
(2 sigma)	---	---	---	0.0	0.0	0.0
1050.	-248200.	-189849.	9.444	0.0	0.0	0.0
1100.	-248492.	-187063.	8.883	0.0	0.0	0.0
1150.	-248769.	-184265.	8.370	0.0	0.0	0.0
1200.	-249031.	-181455.	7.899	0.0	0.0	0.0
1250.	-249278.	-178634.	7.465	0.0	0.0	0.0
(2 sigma)	---	---	---	0.0	0.0	0.0
1300.	-249511.	-175803.	7.064	0.0	0.0	0.0
1350.	-249730.	-172964.	6.692	0.0	0.0	0.0
1400.	-249936.	-170117.	6.347	0.0	0.0	0.0
1450.	-250129.	-167263.	6.025	0.0	0.0	0.0
1500.	-250310.	-164403.	5.725	0.0	0.0	0.0
(2 sigma)	---	---	---	0.0	0.0	0.0
1550.	-250480.	-161536.	5.444	0.0	0.0	0.0
1600.	-250638.	-158655.	5.180	0.0	0.0	0.0
1650.	-250786.	-155788.	4.932	0.0	0.0	0.0
1700.	-250923.	-152907.	4.698	0.0	0.0	0.0
1750.	-251051.	-150023.	4.478	0.0	0.0	0.0
(2 sigma)	---	---	---	0.0	0.0	0.0
1800.	-251170.	-147134.	4.270	0.0	0.0	0.0
(2 sigma)	---	---	---	0.0	0.0	0.0

Table 108. Thermophysical values for water, H₂O, at 1.01325 bars (1 atm). The tabulations are based on a fit² of the thermophysical and thermochemical data given in Section 1.5.5.

T K	C _p J/(mol K)	S J/(mol K)	H-H(298) J/mol	[G-H(298)]/T J/(mol K)	V cm ³ /mol
273.150	75.884	63.307	-1888.	-70.218	0.0000
298.150	75.254	69.921	0.	-69.921	0.0000
(2 sigma)	---	---	---	---	---
300.	75.230	70.386	139.	-69.922	0.0000
350.	75.469	81.981	3900.	-70.837	0.0000
373.150	76.003	86.831	5653.	-71.681	0.0000
400.	76.849	92.140	7705.	-72.877	0.0000
(2 sigma)	---	---	---	---	---

Table 109. Thermochemical properties of water, H₂O, at 1.01325 bars (1 atm). Columns 2 through 4 give the thermochemical values relative to the elements; columns 5 through 7 give the values relative to the oxides.

T K	Formation from the Elements			Formation from the Oxides		
	H J/mol	G J/mol	log K	H J/mol	G J/mol	log K
200.	-289294.	-253795.	66.284	0.0	0.0	0.0
250.	-287390.	-245150.	51.221	0.0	0.0	0.0
(2 sigma)	---	---	---	0.0	0.0	0.0
273.150	-286613.	-241274.	46.139	0.0	0.0	0.0
298.150	-285808.	-237160.	41.549	0.0	0.0	0.0
(2 sigma)	---	---	---	0.0	0.0	0.0
300.	-285749.	-236858.	41.241	0.0	0.0	0.0
350.	-284178.	-228834.	34.152	0.0	0.0	0.0
373.150	-283447.	-225197.	31.524	0.0	0.0	0.0
400.	-282585.	-221036.	28.864	0.0	0.0	0.0

Table 110. Thermophysical values for H₂O (ideal gas), at 1.01325 bars (1 atm). The tabulations are based on a fit of the thermophysical and thermochemical data given in Section 1.5.5.

T K	C _p J/(mol K)	S J/(mol K)	H-H(298) J/mol	[G-H(298)]/T J/(mol K)	V cm ³ /mol
200.	33.329	175.369	-3286.	-191.797	0.0000
250.	33.473	182.823	-1615.	-189.284	0.0000
(2 sigma)	---	---	---	---	---
273.150	33.540	185.790	-840.	-188.864	0.0000
298.150	33.632	188.731	0.	-188.731	0.0000
(2 sigma)	---	---	---	---	---
300.	33.640	188.939	62.	-188.732	0.0000
350.	33.897	194.143	1750.	-189.142	0.0000
373.150	34.048	196.318	2537.	-189.520	0.0000
400.	34.245	198.691	3453.	-190.057	0.0000
450.	34.669	202.748	5176.	-191.246	0.0000
500.	35.154	206.426	6921.	-192.583	0.0000
(2 sigma)	---	---	---	---	---
550.	35.686	209.801	8692.	-193.997	0.0000
600.	36.253	212.930	10491.	-195.446	0.0000
650.	36.846	215.855	12318.	-196.904	0.0000
700.	37.458	218.608	14175.	-198.357	0.0000
750.	38.082	221.213	16064.	-199.795	0.0000
(2 sigma)	---	---	---	---	---
800.	38.715	223.691	17984.	-201.211	0.0000
850.	39.352	226.057	19935.	-202.604	0.0000
900.	39.989	228.325	21919.	-203.970	0.0000
950.	40.624	230.504	23934.	-205.310	0.0000
1000.	41.254	232.604	25981.	-206.622	0.0000
(2 sigma)	---	---	---	---	---
1050.	41.878	234.632	28060.	-207.908	0.0000
1100.	42.494	236.594	30169.	-209.168	0.0000
1150.	43.100	238.496	32309.	-210.402	0.0000
1200.	43.695	240.343	34479.	-211.611	0.0000
1250.	44.278	242.139	36678.	-212.796	0.0000
(2 sigma)	---	---	---	---	---
1300.	44.848	243.887	38906.	-213.959	0.0000
1350.	45.404	245.590	41163.	-215.099	0.0000
1400.	45.945	247.251	43446.	-216.217	0.0000
1450.	46.472	248.872	45757.	-217.316	0.0000
1500.	46.982	250.456	48093.	-218.394	0.0000
(2 sigma)	---	---	---	---	---
1550.	47.477	252.005	50455.	-219.453	0.0000
1600.	47.954	253.520	52841.	-220.494	0.0000
1650.	48.415	255.003	55250.	-221.518	0.0000
1700.	48.858	256.455	57682.	-222.524	0.0000
1750.	49.283	257.377	60136.	-223.514	0.0000
(2 sigma)	---	---	---	---	---
1800.	49.689	259.271	62610.	-224.488	0.0000
(2 sigma)	---	---	---	---	---

Table 111. Thermochemical properties of H₂O (ideal gas), at 1.01325 bars (1 atm). Columns 2 through 4 give the thermochemical values relative to the elements; columns 5 through 7 give the values relative to the oxides.

T K	Formation from the Elements			Formation from the Oxides		
	H J/mol	G J/mol	log K	H J/mol	G J/mol	log K
200.	-240959.	-232795.	60.800	0.0	0.0	0.0
250.	-241376.	-230707.	48.204	0.0	0.0	0.0
(2 sigma)	---	---	---	0.0	0.0	0.0
273.150	-241592.	-229710.	43.927	0.0	0.0	0.0
298.150	-241836.	-228611.	40.052	0.0	0.0	0.0
(2 sigma)	---	---	---	0.0	0.0	0.0
300.	-241854.	-228529.	39.790	0.0	0.0	0.0
350.	-242357.	-226269.	33.769	0.0	0.0	0.0
373.150	-242592.	-225197.	31.524	0.0	0.0	0.0
400.	-242865.	-223936.	29.243	0.0	0.0	0.0
450.	-243368.	-221539.	25.716	0.0	0.0	0.0
500.	-243861.	-219088.	22.888	0.0	0.0	0.0
(2 sigma)	---	---	---	0.0	0.0	0.0
550.	-244340.	-216587.	20.570	0.0	0.0	0.0
600.	-244804.	-214043.	18.634	0.0	0.0	0.0
650.	-245251.	-211462.	16.993	0.0	0.0	0.0
700.	-245681.	-208846.	15.584	0.0	0.0	0.0
750.	-246093.	-206201.	14.361	0.0	0.0	0.0
(2 sigma)	---	---	---	0.0	0.0	0.0
800.	-246488.	-203528.	13.289	0.0	0.0	0.0
850.	-246864.	-200832.	12.342	0.0	0.0	0.0
900.	-247224.	-198113.	11.498	0.0	0.0	0.0
950.	-247566.	-195375.	10.742	0.0	0.0	0.0
1000.	-247891.	-192620.	10.061	0.0	0.0	0.0
(2 sigma)	---	---	---	0.0	0.0	0.0
1050.	-248200.	-189849.	9.444	0.0	0.0	0.0
1100.	-248492.	-187063.	8.883	0.0	0.0	0.0
1150.	-248769.	-184265.	8.370	0.0	0.0	0.0
1200.	-249031.	-181455.	7.899	0.0	0.0	0.0
1250.	-249278.	-178634.	7.465	0.0	0.0	0.0
(2 sigma)	---	---	---	0.0	0.0	0.0
1300.	-249511.	-175803.	7.064	0.0	0.0	0.0
1350.	-249730.	-172964.	6.692	0.0	0.0	0.0
1400.	-249936.	-170117.	6.347	0.0	0.0	0.0
1450.	-250129.	-167263.	6.025	0.0	0.0	0.0
1500.	-250310.	-164403.	5.725	0.0	0.0	0.0
(2 sigma)	---	---	---	0.0	0.0	0.0
1550.	-250480.	-161536.	5.444	0.0	0.0	0.0
1600.	-250638.	-158665.	5.180	0.0	0.0	0.0
1650.	-250786.	-155788.	4.932	0.0	0.0	0.0
1700.	-250923.	-152907.	4.698	0.0	0.0	0.0
1750.	-251051.	-150023.	4.478	0.0	0.0	0.0
(2 sigma)	---	---	---	0.0	0.0	0.0
1800.	-251170.	-147134.	4.270	0.0	0.0	0.0
(2 sigma)	---	---	---	0.0	0.0	0.0

Table 112. Thermophysical values for stable phases of the element magnesium (Mg) at 1.01325 bars (1 atm). The sources of data are given in Section 1.5.5.

T K	C _p J/(mol K)	S J/(mol K)	H-H(298) J/mol	[G-H(298)]/T J/(mol K)	V cm ³ /mol
magnesium (crystal)					
200.	22.761	23.170	-2347.	-34.908	---
250.	23.980	28.386	-1178.	-33.097	---
(2 sigma)	---	---	---	---	---
273.15	24.452	30.530	-617.	-32.789	---
298.15	24.905	32.692	-0.	-32.692	---
(2 sigma)	---	---	---	---	---
300.	24.937	32.846	46.	-32.692	---
350.	25.699	36.749	1313.	-32.999	---
400.	26.335	40.223	2614.	-33.688	---
450.	26.895	43.358	3945.	-34.592	---
500.	27.420	46.219	5303.	-35.613	---
(2 sigma)	---	---	---	---	---
550.	27.937	48.857	6687.	-36.699	---
600.	28.470	51.310	8097.	-37.815	---
650.	29.033	53.611	9534.	-38.943	---
700.	29.640	55.784	11001.	-40.069	---
750.	30.302	57.852	12499.	-41.186	---
(2 sigma)	---	---	---	---	---
800.	31.025	59.830	14032.	-42.290	---
850.	31.817	61.734	15603.	-43.378	---
900.	32.683	63.577	17215.	-44.449	---
922.	33.089	64.371	17939.	-44.915	---
magnesium (liquid)					
922.	32.122	74.086	26895.	-44.915	---
950.	32.426	75.051	27799.	-45.789	---
1000.	32.970	76.728	29434.	-47.294	---
(2 sigma)	---	---	---	---	---
1050.	33.514	78.350	31096.	-48.735	---
1100.	34.058	79.922	32785.	-50.117	---
1150.	34.602	81.448	34502.	-51.446	---
1200.	35.146	82.932	36245.	-52.727	---
1250.	35.690	84.378	38016.	-53.964	---
(2 sigma)	---	---	---	---	---
1300.	36.234	85.788	39814.	-55.161	---
1350.	36.777	87.166	41640.	-56.321	---
1378.	37.082	87.924	42674.	-56.956	---
magnesium (ideal monatomic gas)					
1378.	20.786	180.368	170062.	-56.956	---
1400.	20.786	180.697	170519.	-58.898	---
1450.	20.786	181.426	171558.	-63.110	---
1500.	20.786	182.131	172597.	-67.066	---
(2 sigma)	---	---	---	---	---
1550.	20.786	182.813	173637.	-70.789	---
1600.	20.786	183.473	174676.	-74.300	---
1650.	20.786	184.112	175715.	-77.618	---
1700.	20.786	184.733	176755.	-80.759	---
1750.	20.786	185.335	177794.	-83.739	---
(2 sigma)	---	---	---	---	---
1800.	20.786	185.921	178833.	-86.569	---
(2 sigma)	---	---	---	---	---

Table 113. Thermochemical properties of stable phases of the element magnesium (Mg) at 1.01325 bars (1 atm). Columns 2 through 4 give the thermochemical values relative to the elements; columns 5 through 7 give the values relative to the oxides.

T K	Formation from the Elements			Formation from the Oxides		
	H J/mol	G J/mol	log K	H J/mol	G J/mol	log K
magnesium (crystal)						
200.	0.	0.	0.	---	---	---
250.	0.	0.	0.	---	---	---
(2 sigma)	0.	0.	0.	---	---	---
273.15	0.	0.	0.	---	---	---
298.15	0.	0.	0.	---	---	---
(2 sigma)	0.	0.	0.	---	---	---
300.	0.	0.	0.	---	---	---
350.	0.	0.	0.	---	---	---
400.	0.	0.	0.	---	---	---
450.	0.	0.	0.	---	---	---
500.	0.	0.	0.	---	---	---
(2 sigma)	0.	0.	0.	---	---	---
550.	0.	0.	0.	---	---	---
600.	0.	0.	0.	---	---	---
650.	0.	0.	0.	---	---	---
700.	0.	0.	0.	---	---	---
750.	0.	0.	0.	---	---	---
(2 sigma)	0.	0.	0.	---	---	---
800.	0.	0.	0.	---	---	---
850.	0.	0.	0.	---	---	---
900.	0.	0.	0.	---	---	---
922.	0.	0.	0.	---	---	---
magnesium (liquid)						
922.	0.	0.	0.	---	---	---
950.	0.	0.	0.	---	---	---
1000.	0.	0.	0.	---	---	---
(2 sigma)	0.	0.	0.	---	---	---
1050.	0.	0.	0.	---	---	---
1100.	0.	0.	0.	---	---	---
1150.	0.	0.	0.	---	---	---
1200.	0.	0.	0.	---	---	---
1250.	0.	0.	0.	---	---	---
(2 sigma)	0.	0.	0.	---	---	---
1300.	0.	0.	0.	---	---	---
1350.	0.	0.	0.	---	---	---
1378.	0.	0.	0.	---	---	---
magnesium (ideal monatomic gas)						
1378.	0.	0.	0.	---	---	---
1400.	0.	0.	0.	---	---	---
1450.	0.	0.	0.	---	---	---
1500.	0.	0.	0.	---	---	---
(2 sigma)	0.	0.	0.	---	---	---
1550.	0.	0.	0.	---	---	---
1600.	0.	0.	0.	---	---	---
1650.	0.	0.	0.	---	---	---
1700.	0.	0.	0.	---	---	---
1750.	0.	0.	0.	---	---	---
(2 sigma)	0.	0.	0.	---	---	---
1800.	0.	0.	0.	---	---	---
(2 sigma)	0.	0.	0.	---	---	---

Table 114. Thermophysical values for magnesite, $MgCO_3$, at 1.01325 bars (1 atm). The tabulations are based on a fit of the thermophysical and thermochemical data given in Section 1.5.5.

T K	Cp J/(mol K)	S J/(mol K)	H-H(298) J/mol	[G-H(298)]/T J/(mol K)	V cm ³ /mol
200.	57.411	38.410	-6618.	-71.498	27.9626
250.	67.903	52.385	-3476.	-66.291	27.9909
(2 sigma)	0.253	0.713	12.	0.712	0.0674
273.150	72.105	58.585	-1355.	-65.376	28.0040
298.150	76.233	65.081	0.	-65.081	28.0181
(2 sigma)	0.258	0.712	0.	0.712	0.0663
300.	76.523	65.553	141.	-65.082	28.0192
350.	83.648	77.901	4151.	-66.041	28.0474
400.	89.621	89.472	8487.	-68.254	28.0757
450.	94.706	100.329	13098.	-71.221	28.1040
500.	99.092	110.540	17946.	-74.648	28.1323
(2 sigma)	0.788	0.737	81.	0.713	0.0839
550.	102.923	120.168	22998.	-78.352	28.1606
600.	106.303	129.271	28231.	-82.220	28.1889
650.	109.312	137.901	33622.	-86.174	28.2172
700.	112.012	146.102	39157.	-90.164	28.2455
750.	114.453	153.915	44819.	-94.156	28.2738
(2 sigma)	1.690	0.968	384.	0.728	0.1328
800.	116.673	161.374	50598.	-98.125	28.3021
850.	118.702	168.509	56483.	-102.057	28.3304
900.	120.567	175.347	62466.	-105.940	28.3587
950.	122.288	181.912	68538.	-109.767	28.3870
1000.	123.883	188.226	74693.	-113.533	28.4153
(2 sigma)	2.347	1.415	886.	0.790	0.1906
1050.	125.366	194.307	80924.	-117.236	28.4436
1100.	126.750	200.171	87228.	-120.873	28.4719
1150.	128.045	205.834	93598.	-124.445	28.5001
1200.	129.260	211.309	100031.	-127.951	28.5284
1250.	130.403	216.610	106523.	-131.392	28.5567
(2 sigma)	2.831	1.928	1532.	0.914	0.2513
1300.	131.481	221.745	113070.	-134.768	28.5850
1350.	132.501	226.727	119670.	-138.082	28.6133
1400.	133.466	231.563	126319.	-141.335	28.6416
1450.	134.381	236.263	133015.	-144.528	28.6699
1500.	135.251	240.833	139756.	-147.662	28.6982
(2 sigma)	3.204	2.442	2285.	1.086	0.3132
1550.	136.080	245.282	146540.	-150.740	28.7265
1600.	136.870	249.615	153364.	-153.762	28.7548
1650.	137.624	253.838	160226.	-156.731	28.7831
1700.	138.346	257.957	167126.	-159.648	28.8114
1750.	139.036	261.978	174060.	-162.514	28.8397
(2 sigma)	3.500	2.936	3122.	1.286	0.3757
1800.	139.698	265.904	181029.	-165.332	28.8680
(2 sigma)	3.553	3.032	3297.	1.329	0.3882

Table 115. Thermochemical properties of magnesite, $MgCO_3$, at 1.01325 bars (1 atm). Columns 2 through 4 give the thermochemical values relative to the elements, columns 5 through 7 give the values relative to the oxides.

T K	Formation from the Elements			Formation from the Oxides		
	H J/mol	G J/mol	log K	H J/mol	G J/mol	log K
200.	-1112494.	-1056948.	276.046	-118309.	-83252.	21.743
250.	-1113039.	-1042989.	217.921	-118392.	-74476.	15.561
(2 sigma)	---	---	---	1786.	1735.	0.362
273.150	-1113161.	-1036497.	198.210	-118390.	-70409.	13.464
298.150	-1113225.	-1029477.	180.360	-118360.	-66019.	11.566
(2 sigma)	---	---	---	1785.	1727.	0.303
300.	-1113227.	-1028957.	179.157	-118357.	-65694.	11.438
350.	-1113176.	-1014913.	151.467	-118212.	-56927.	8.496
400.	-1112953.	-1000889.	130.703	-117968.	-48188.	6.293
450.	-1112599.	-986901.	114.556	-117634.	-39484.	4.583
500.	-1112141.	-972959.	101.644	-117222.	-30823.	3.220
(2 sigma)	---	---	---	1796.	1700.	0.178
550.	-1111599.	-959066.	91.084	-116739.	-22205.	2.109
600.	-1110991.	-945226.	82.289	-116192.	-13635.	1.187
650.	-1110328.	-931438.	74.851	-115587.	-5113.	0.411
700.	-1109623.	-917704.	68.480	-114928.	3361.	-0.251
750.	-1108885.	-904021.	62.962	-114221.	11786.	-0.821
(2 sigma)	---	---	---	1867.	1677.	0.117
800.	-1108123.	-890388.	58.136	-113468.	20162.	-1.316
850.	-1107345.	-876803.	53.882	-112673.	28489.	-1.751
900.	-1106559.	-863265.	50.103	-111840.	36769.	-2.134
950.	-1114699.	-849498.	46.709	-110970.	45002.	-2.474
1000.	-1113847.	-835562.	43.645	-110067.	53188.	-2.778
(2 sigma)	---	---	---	2075.	1684.	0.088
1050.	-1112981.	-821669.	40.876	-109131.	61327.	-3.051
1100.	-1112103.	-807818.	38.360	-108166.	69422.	-3.297
1150.	-1111216.	-794007.	36.065	-107173.	77472.	-3.519
1200.	-1110321.	-780234.	33.963	-106153.	85478.	-3.721
1250.	-1109419.	-766499.	32.030	-105108.	93442.	-3.905
(2 sigma)	---	---	---	2470.	1779.	0.074
1300.	-1108512.	-752800.	30.248	-104039.	101363.	-4.073
1350.	-1107600.	-739136.	28.599	-102948.	109242.	-4.227
1400.	-1232139.	-721902.	26.934	-101837.	117081.	-4.368
1450.	-1230381.	-703710.	25.350	-100705.	124879.	-4.499
1500.	-1228594.	-685579.	23.874	-99554.	132638.	-4.619
(2 sigma)	---	---	---	3039.	2027.	0.071
1550.	-1226779.	-667509.	22.495	-98386.	140359.	-4.730
1600.	-1224936.	-649497.	21.204	-97200.	148041.	-4.833
1650.	-1223066.	-631543.	19.993	-95999.	155687.	-4.929
1700.	-1221169.	-613647.	18.855	-94783.	163295.	-5.017
1750.	-1219245.	-595807.	17.784	-93552.	170868.	-5.100
(2 sigma)	---	---	---	3749.	2465.	0.074
1800.	-1217295.	-578022.	16.774	-92308.	178405.	-5.177
(2 sigma)	---	---	---	3904.	2575.	0.075

Table 115. Thermophysical values for periclase, MgO, at 1.01325 bars (1 atm). The tabulations are based on a fit of the thermophysical and thermochemical data given in Section 1.5.5.

T K	Cp J/(mol K)	S J/(mol K)	H-H(298) J/mol	[G-H(298)]/T J/(mol K)	V cm ³ /mol
200.	26.590	14.005	-3217.	-30.089	11.2031
250.	33.261	20.719	-1706.	-27.544	11.2240
(2 sigma)	---	---	---	---	0.0090
273.150	35.424	23.762	-910.	-27.095	11.2336
298.150	37.344	26.950	0.	-26.950	11.2441
(2 sigma)	---	---	---	---	0.0083
300.	37.472	27.181	69.	-26.950	11.2449
350.	40.380	33.188	2020.	-27.418	11.2657
400.	42.514	38.726	4094.	-28.490	11.2866
450.	44.151	43.832	6263.	-29.915	11.3075
500.	45.446	48.554	8504.	-31.546	11.3284
(2 sigma)	---	---	---	---	0.0064
550.	46.499	52.936	10803.	-33.294	11.3493
600.	47.373	57.021	13151.	-35.103	11.3702
650.	48.111	60.842	15538.	-36.937	11.3911
700.	48.743	64.432	17960.	-38.774	11.4120
750.	49.292	67.814	20411.	-40.599	11.4329
(2 sigma)	---	---	---	---	0.0074
800.	49.774	71.011	22888.	-42.400	11.4538
850.	50.203	74.041	25388.	-44.173	11.4747
900.	50.588	76.922	27908.	-45.913	11.4956
950.	50.938	79.666	30446.	-47.618	11.5165
1000.	51.258	82.288	33001.	-49.286	11.5374
(2 sigma)	---	---	---	---	0.0110
1050.	51.554	84.796	35571.	-50.918	11.5583
1100.	51.831	87.200	38156.	-52.513	11.5792
1150.	52.090	89.510	40754.	-54.072	11.6001
1200.	52.337	91.732	43365.	-55.595	11.6209
1250.	52.572	93.874	45988.	-57.083	11.6418
(2 sigma)	---	---	---	---	0.0154
1300.	52.799	95.940	48622.	-58.538	11.6627
1350.	53.019	97.937	51268.	-59.961	11.6836
1400.	53.234	99.869	53924.	-61.352	11.7045
1450.	53.445	101.741	56591.	-62.712	11.7254
1500.	53.653	103.556	59268.	-64.044	11.7463
(2 sigma)	---	---	---	---	0.0202
1550.	53.860	105.319	61956.	-65.347	11.7672
1600.	54.066	107.032	64654.	-66.623	11.7881
1650.	54.273	108.699	67363.	-67.873	11.8090
1700.	54.480	110.322	70082.	-69.098	11.8299
1750.	54.689	111.904	72811.	-70.298	11.8508
(2 sigma)	---	---	---	---	0.0252
1800.	54.900	113.448	75551.	-71.475	11.8717
(2 sigma)	---	---	---	---	0.0262

Table 117. Thermochemical properties of periclase, MgO, at 1.01325 bars (1 atm). Columns 2 through 4 give the thermochemical values relative to the elements; columns 5 through 7 give the values relative to the oxides.

T K	Formation from the Elements			Formation from the Oxides		
	H J/mol	G J/mol	log K	H J/mol	G J/mol	log K
200.	-600677.	-579505.	151.351	0.0	0.0	0.0
250.	-601064.	-574161.	119.964	0.0	0.0	0.0
(2 sigma)	---	---	---	0.0	0.0	0.0
273.150	-601166.	-571665.	109.320	0.0	0.0	0.0
298.150	-601239.	-568961.	99.680	0.0	0.0	0.0
(2 sigma)	---	---	---	0.0	0.0	0.0
300.	-601243.	-568761.	99.030	0.0	0.0	0.0
350.	-601299.	-563342.	84.074	0.0	0.0	0.0
400.	-601277.	-557920.	72.857	0.0	0.0	0.0
450.	-601204.	-552504.	64.133	0.0	0.0	0.0
500.	-601097.	-547099.	57.155	0.0	0.0	0.0
(2 sigma)	---	---	---	0.0	0.0	0.0
550.	-600969.	-541705.	51.447	0.0	0.0	0.0
600.	-600830.	-536323.	46.691	0.0	0.0	0.0
650.	-600688.	-530954.	42.668	0.0	0.0	0.0
700.	-600552.	-525594.	39.220	0.0	0.0	0.0
750.	-600426.	-520245.	36.233	0.0	0.0	0.0
(2 sigma)	---	---	---	0.0	0.0	0.0
800.	-600318.	-514903.	33.620	0.0	0.0	0.0
850.	-600234.	-509567.	31.314	0.0	0.0	0.0
900.	-600178.	-504236.	29.265	0.0	0.0	0.0
950.	-609082.	-498635.	27.417	0.0	0.0	0.0
1000.	-609027.	-492823.	25.742	0.0	0.0	0.0
(2 sigma)	---	---	---	0.0	0.0	0.0
1050.	-608990.	-487014.	24.228	0.0	0.0	0.0
1100.	-608973.	-481206.	22.851	0.0	0.0	0.0
1150.	-608974.	-475399.	21.593	0.0	0.0	0.0
1200.	-608995.	-469591.	20.441	0.0	0.0	0.0
1250.	-609035.	-463782.	19.380	0.0	0.0	0.0
(2 sigma)	---	---	---	0.0	0.0	0.0
1300.	-609096.	-457970.	18.401	0.0	0.0	0.0
1350.	-609177.	-452156.	17.495	0.0	0.0	0.0
1400.	-734731.	-442735.	16.519	0.0	0.0	0.0
1450.	-734011.	-432319.	15.574	0.0	0.0	0.0
1500.	-733284.	-421928.	14.693	0.0	0.0	0.0
(2 sigma)	---	---	---	0.0	0.0	0.0
1550.	-732549.	-411562.	13.870	0.0	0.0	0.0
1600.	-731806.	-401219.	13.098	0.0	0.0	0.0
1650.	-731055.	-390900.	12.375	0.0	0.0	0.0
1700.	-730295.	-380604.	11.695	0.0	0.0	0.0
1750.	-729527.	-370330.	11.054	0.0	0.0	0.0
(2 sigma)	---	---	---	0.0	0.0	0.0
1800.	-728749.	-360078.	10.449	0.0	0.0	0.0
(2 sigma)	---	---	---	0.0	0.0	0.0

Table 118. Thermophysical values for brucite, $\text{Mg}(\text{OH})_2$, at 1.01325 bars (1 atm). The tabulations are based on a fit² of the thermophysical and thermochemical data given in Section 1.5.5.

T K	C_p J/(mol K)	S J/(mol K)	H-H(298) J/mol	$[\text{G}-\text{H}(298)]/T$ J/(mol K)	V cm ³ /mol
200.	55.856	36.369	-6661.	-69.673	24.5785
250.	68.611	50.285	-3531.	-64.408	24.6052
(2 sigma)	0.152	0.662	0.	0.662	0.3555
273.150	73.261	56.568	-1888.	-63.479	24.6176
298.150	77.641	63.178	0.	-63.178	24.6309
(2 sigma)	0.099	0.662	0.	0.662	0.3552
300.	77.942	63.659	144.	-63.179	24.6319
350.	85.123	76.235	4228.	-64.156	24.6586
400.	90.849	87.989	8632.	-66.409	24.6853
450.	95.538	98.969	13295.	-69.423	24.7120
500.	99.455	109.244	18173.	-72.897	24.7387
(2 sigma)	0.092	0.662	14.	0.662	0.3587
550.	102.780	118.883	23231.	-76.644	24.7654
600.	105.639	127.951	28443.	-80.546	24.7921
650.	108.125	136.507	33789.	-84.524	24.8188
700.	110.304	144.602	39251.	-88.529	24.8455
750.	112.228	152.279	44815.	-92.526	24.8722
(2 sigma)	0.164	0.665	39.	0.662	0.3729
800.	113.939	159.578	50470.	-96.490	24.8989
850.	115.468	166.532	56206.	-100.407	24.9256
900.	116.841	173.171	62014.	-104.267	24.9523
950.	118.078	179.522	67888.	-108.062	24.9790
1000.	119.197	185.608	73820.	-111.788	25.0057
(2 sigma)	0.281	0.672	86.	0.663	0.3969
1050.	120.212	191.448	79806.	-115.443	25.0324
1100.	121.135	197.062	85840.	-119.026	25.0591
1150.	121.975	202.466	91918.	-122.537	25.0858
1200.	122.743	207.673	98036.	-125.977	25.1125
1250.	123.445	212.698	104191.	-129.346	25.1391
(2 sigma)	0.430	0.686	166.	0.664	0.4290

Table 119. Thermochemical properties of brucite, $Mg(OH)_2$, at 1.01325 bars (1 atm). Columns 2 through 4 give the thermochemical values relative to the elements; columns 5 through 7 give the values relative to the oxides.

T K	Formation from the Elements			Formation from the Oxides		
	H J/mol	G J/mol	log K	H J/mol	G J/mol	log K
200.	-924028.	-864090.	225.677	-34057.	-30790.	8.041
250.	-924881.	-848996.	177.388	-36428.	-29685.	6.202
(2 sigma)	---	---	---	1258.	1187.	0.248
273.150	-925129.	-841958.	161.008	-37350.	-29019.	5.549
298.150	-925307.	-834337.	146.172	-38261.	-28215.	4.943
(2 sigma)	---	---	---	1258.	1175.	0.206
300.	-925317.	-833772.	145.173	-38325.	-28153.	4.902
350.	-925431.	-818502.	122.155	-39953.	-26326.	3.929
400.	-925290.	-803233.	104.891	-81149.	-21377.	2.792
450.	-924948.	-787995.	91.468	-80376.	-13951.	1.619
500.	-924443.	-772803.	80.734	-79485.	-6617.	0.691
(2 sigma)	---	---	---	1258.	1135.	0.119
550.	-923806.	-757669.	71.957	-78497.	622.	-0.059
600.	-923065.	-742598.	64.649	-77431.	7769.	-0.676
650.	-922240.	-727592.	58.470	-76300.	14823.	-1.191
700.	-921351.	-712652.	53.179	-75118.	21789.	-1.626
750.	-920413.	-697777.	48.598	-73893.	28668.	-1.997
(2 sigma)	---	---	---	1259.	1106.	0.077
800.	-919441.	-682967.	44.593	-72635.	35465.	-2.316
850.	-918448.	-668217.	41.064	-71350.	42182.	-2.592
900.	-917447.	-653527.	37.930	-70045.	48822.	-2.834
950.	-925373.	-638620.	35.114	-68726.	55390.	-3.046
1000.	-924313.	-623555.	32.571	-67395.	61888.	-3.233
(2 sigma)	---	---	---	1262.	1102.	0.058
1050.	-923248.	-608544.	30.273	-66058.	68319.	-3.399
1100.	-922183.	-593583.	28.187	-64718.	74687.	-3.547
1150.	-921121.	-578670.	26.284	-63378.	80994.	-3.679
1200.	-920066.	-563804.	24.542	-62041.	87242.	-3.798
1250.	-919021.	-548981.	22.941	-60708.	93435.	-3.904
(2 sigma)	---	---	---	1271.	1123.	0.047

Table 120. Thermophysical values for Mg pyroxene, MgSiO_3 , at 1.01325 bars (1 atm). The tabulations are based on a fit of the thermophysical and thermochemical data given in Section 1.5.5.

T K	Cp J/(mol K)	S J/(mol K)	H-H(298) J/mol	[G-H(298)]/T J/(mol K)	V cm ³ /mol
clinoenstatite					
200.	58.831	39.463	-7030.	-74.611	31.1757
250.	72.520	54.170	-3721.	-69.056	31.2256
(2 sigma)	0.117	1.811	6.	1.810	0.0282
273.150	77.237	60.804	-1987.	-68.077	31.2487
298.150	81.569	67.760	0.	-67.760	31.2736
(2 sigma)	0.145	1.810	0.	1.810	0.0238
300.	81.864	68.266	151.	-67.762	31.2755
350.	88.756	81.427	4425.	-68.785	31.3254
400.	94.112	93.642	9001.	-71.139	31.3752
450.	98.429	104.985	13819.	-74.277	31.4251
500.	102.007	115.546	18832.	-77.882	31.4750
(2 sigma)	0.183	1.810	36.	1.810	0.0466
550.	105.036	125.414	24010.	-81.759	31.5248
600.	107.644	134.668	29329.	-85.787	31.5747
650.	109.922	143.376	34769.	-89.885	31.6246
700.	111.934	151.597	40316.	-94.002	31.6744
750.	113.728	159.382	45959.	-98.104	31.7243
(2 sigma)	0.159	1.812	75.	1.810	0.0997
900.	115.341	166.774	51686.	-102.167	31.7742
950.	116.802	173.811	57490.	-106.176	31.8241
900.	118.134	180.526	63364.	-110.121	31.8739
950.	119.354	186.946	69302.	-113.997	31.9238
968.500	119.780	189.252	71514.	-115.412	31.9423
enstatite					
968.500	125.855	192.652	74659.	-115.565	31.9376
1000.	126.493	196.690	78633.	-118.057	31.9692
(2 sigma)	0.099	0.342	37.	0.338	0.1073
1050.	127.405	202.884	84981.	-121.950	32.0197
1100.	128.207	208.830	91372.	-125.765	32.0704
1150.	128.913	214.545	97800.	-129.501	32.1214
1200.	129.530	220.045	104262.	-133.160	32.1727
1250.	130.069	225.344	110752.	-136.742	32.2241
(2 sigma)	0.189	0.345	58.	0.339	0.2139
1257.400	130.143	226.112	111715.	-137.266	32.2317
protoenstatite					
1257.400	120.006	229.007	102545.	-147.454	33.2299
1300.	120.634	233.016	107671.	-150.192	33.2695
1350.	121.332	237.582	113720.	-153.345	33.3159
1400.	121.992	242.007	119804.	-156.433	33.3624
1450.	122.619	246.298	125919.	-159.458	33.4089
1500.	123.213	250.466	132065.	-162.422	33.4554
(2 sigma)	3.716	1.272	3278.	2.578	0.1137
1550.	123.778	254.515	138240.	-165.328	33.5019
1600.	124.317	258.453	144442.	-168.177	33.5484
1650.	124.831	262.287	150671.	-170.971	33.5949
1700.	125.322	266.021	156925.	-173.712	33.6414
1750.	125.792	259.660	163203.	-176.401	33.6879
(2 sigma)	4.048	1.368	4042.	2.284	0.1479
1800.	126.243	273.210	169504.	-179.041	33.7343
(2 sigma)	4.108	1.415	4208.	2.231	0.1550

Table 121. Thermochemical properties of Mg pyroxene, $MgSiO_3$, at 1.01325 bars (1 atm). Columns 2 through 4 give the thermochemical values relative to the elements; columns 5 through 7 give the values relative to the oxides.

T K	Formation from the Elements			Formation from the Oxides		
	H J/mol	G J/mol	log K	H J/mol	G J/mol	log K
clinoenstatite						
200.	-1543460.	-1486369.	388.200	-32903.	-32789.	8.564
250.	-1544355.	-1471983.	307.554	-32917.	-32759.	6.845
(2 sigma)	---	---	---	4087.	4021.	0.840
273.150	-1544626.	-1465269.	280.204	-32924.	-32744.	6.262
298.150	-1544844.	-1457995.	255.435	-32935.	-32727.	5.734
(2 sigma)	---	---	---	4087.	4014.	0.703
300.	-1544857.	-1457456.	253.766	-32936.	-32726.	5.698
350.	-1545103.	-1442867.	215.336	-32973.	-32689.	4.879
400.	-1545168.	-1428256.	186.511	-33036.	-32644.	4.263
450.	-1545100.	-1413645.	164.091	-33128.	-32590.	3.783
500.	-1544932.	-1399047.	146.157	-33255.	-32524.	3.398
(2 sigma)	---	---	---	4087.	4005.	0.418
550.	-1544687.	-1384470.	131.486	-33417.	-32443.	3.081
600.	-1544383.	-1369917.	119.262	-33617.	-32346.	2.816
650.	-1544035.	-1355392.	108.921	-33857.	-32230.	2.590
700.	-1543657.	-1340896.	100.059	-34137.	-32095.	2.395
750.	-1543258.	-1326426.	92.380	-34460.	-31938.	2.224
(2 sigma)	---	---	---	4087.	4040.	0.281
800.	-1542848.	-1311984.	85.664	-34826.	-31758.	2.074
850.	-1542436.	-1297568.	79.739	-35947.	-31549.	1.939
900.	-1542030.	-1283176.	74.474	-35978.	-31289.	1.816
950.	-1550564.	-1268534.	69.749	-35989.	-31029.	1.706
968.500	-1550399.	-1263044.	68.120	-35988.	-30932.	1.668
enstatite						
968.500	-1547107.	-1263044.	68.120	-32696.	-30932.	1.668
1000.	-1546637.	-1253812.	65.492	-32500.	-30878.	1.613
(2 sigma)	---	---	---	4108.	4099.	0.214
1050.	-1545896.	-1239189.	61.646	-32183.	-30804.	1.532
1100.	-1545166.	-1224601.	58.151	-31862.	-30746.	1.460
1150.	-1544450.	-1210046.	54.962	-31542.	-30703.	1.395
1200.	-1543750.	-1195522.	52.040	-31227.	-30673.	1.335
1250.	-1543070.	-1181027.	49.352	-30920.	-30656.	1.281
(2 sigma)	---	---	---	4108.	4101.	0.171
1257.400	-1542972.	-1178884.	48.973	-30875.	-30655.	1.273
protoenstatite						
1257.400	-1539329.	-1178882.	48.973	-27233.	-30654.	1.273
1300.	-1539197.	-1166673.	46.877	-27409.	-30767.	1.236
1350.	-1539051.	-1152348.	44.587	-27616.	-30892.	1.195
1400.	-1664368.	-1134424.	42.326	-27825.	-31009.	1.157
1450.	-1663403.	-1115514.	40.185	-28037.	-31119.	1.121
1500.	-1662422.	-1096638.	38.188	-28255.	-31222.	1.087
(2 sigma)	---	---	---	4409.	4117.	0.143
1550.	-1661425.	-1077795.	36.321	-28479.	-31317.	1.055
1600.	-1660413.	-1058985.	34.572	-28711.	-31405.	1.025
1650.	-1659386.	-1040206.	32.930	-28952.	-31486.	0.997
1700.	-1708854.	-1021008.	31.372	-29203.	-31559.	0.970
1750.	-1707655.	-1000795.	29.872	-29466.	-31624.	0.944
(2 sigma)	---	---	---	4507.	4151.	0.124
1800.	-1706437.	-980616.	28.457	-29742.	-31682.	0.919
(2 sigma)	---	---	---	4554.	4160.	0.121

Table 122. Thermophysical values for clinoenstatite, MgSiO_3 , at 1.01325 bars (1 atm). The tabulations are based on a fit of the thermophysical and thermochemical data given in Section 1.5.5.

T K	C_p J/(mol K)	S J/(mol K)	H-H(298) J/mol	$[G-H(298)]/T$ J/(mol K)	v cm ³ /mol
200.	58.831	39.463	-7030.	-74.611	31.1757
250.	72.520	54.170	-3721.	-59.056	31.2256
(2 sigma)	0.117	1.811	5.	1.810	0.0292
273.150	77.237	60.804	-1987.	-68.077	31.2487
298.150	81.569	67.760	0.	-67.760	31.2736
(2 sigma)	0.145	1.810	0.	1.810	0.0238
300.	81.864	68.266	151.	-67.762	31.2755
350.	88.756	81.427	4425.	-68.785	31.3254
400.	94.112	93.642	9001.	-71.139	31.3752
450.	98.429	104.985	13819.	-74.277	31.4251
500.	102.007	115.546	18832.	-77.882	31.4750
(2 sigma)	0.183	1.810	36.	1.810	0.0466
550.	105.036	125.414	24010.	-81.759	31.5248
600.	107.644	134.668	29329.	-85.787	31.5747
650.	109.922	143.376	34769.	-89.885	31.6246
700.	111.934	151.597	40316.	-94.002	31.6744
750.	113.728	159.382	45959.	-98.104	31.7243
(2 sigma)	0.159	1.812	75.	1.810	0.0997
800.	115.341	166.774	51686.	-102.167	31.7742
850.	116.802	173.811	57490.	-106.176	31.8241
900.	118.134	180.526	63364.	-110.121	31.8739
950.	119.354	186.945	69302.	-113.997	31.9238
968.500	119.780	189.252	71514.	-115.412	31.9423
1000.	120.478	193.097	75298.	-117.799	31.9737
(2 sigma)	0.177	1.814	107.	1.810	0.1552
1050.	121.517	199.001	81348.	-121.525	32.0235
1100.	122.482	204.676	87448.	-125.178	32.0734
1150.	123.381	210.141	93595.	-128.754	32.1233
1200.	124.222	215.410	99786.	-132.255	32.1732
1250.	125.010	220.497	106017.	-135.684	32.2230
(2 sigma)	0.214	1.816	141.	1.810	0.2112
1300.	125.751	225.415	112286.	-139.041	32.2729
1350.	126.449	230.174	118591.	-142.328	32.3228
1400.	127.108	234.784	124930.	-145.549	32.3726
1450.	127.733	239.256	131301.	-148.703	32.4225
1500.	128.325	243.596	137703.	-151.794	32.4724
(2 sigma)	0.251	1.819	184.	1.811	0.2574
1550.	128.887	247.813	144133.	-154.824	32.5222
1600.	129.423	251.914	150591.	-157.794	32.5721
1650.	129.933	255.904	157075.	-160.707	32.6220
1700.	130.421	259.790	163584.	-163.564	32.6719
1750.	130.887	263.578	170117.	-166.368	32.7217
(2 sigma)	0.285	1.822	238.	1.812	0.3237
1800.	131.333	267.271	176672.	-169.120	32.7716
(2 sigma)	0.291	1.822	250.	1.812	0.3350

Table 123. Thermochemical properties of clinoenstatite, $MgSiO_3$, at 1.01325 bars (1 atm). Columns 2 through 4 give the thermochemical values relative to the elements; columns 5 through 7 give the values relative to the oxides.

T K	Formation from the Elements			Formation from the Oxides		
	H J/mol	G J/mol	log K	H J/mol	G J/mol	log K
200.	-1543460.	-1486369.	388.200	-32903.	-32739.	8.564
250.	-1544355.	-1471983.	307.554	-32917.	-32759.	6.345
(2 sigma)	---	---	---	4087.	4021.	0.840
273.150	-1544626.	-1465269.	280.204	-32924.	-32744.	6.262
298.150	-1544844.	-1457995.	255.435	-32935.	-32727.	5.734
(2 sigma)	---	---	---	4087.	4014.	0.703
300.	-1544857.	-1457456.	253.766	-32936.	-32726.	5.698
350.	-1545103.	-1442867.	215.336	-32973.	-32689.	4.879
400.	-1545168.	-1428256.	186.511	-33036.	-32644.	4.263
450.	-1545100.	-1413645.	164.091	-33128.	-32590.	3.783
500.	-1544932.	-1399047.	146.157	-33255.	-32524.	3.398
(2 sigma)	---	---	---	4087.	4005.	0.418
550.	-1544687.	-1384470.	131.486	-33417.	-32443.	3.081
600.	-1544383.	-1369917.	119.262	-33617.	-32346.	2.816
650.	-1544035.	-1355392.	108.921	-33857.	-32230.	2.590
700.	-1543657.	-1340896.	100.059	-34137.	-32095.	2.395
750.	-1543258.	-1326426.	92.380	-34460.	-31938.	2.224
(2 sigma)	---	---	---	4087.	4040.	0.231
800.	-1542848.	-1311984.	85.664	-34826.	-31758.	2.074
850.	-1542436.	-1297568.	79.739	-35947.	-31549.	1.939
900.	-1542030.	-1283176.	74.474	-35978.	-31239.	1.815
950.	-1550564.	-1268534.	69.749	-35989.	-31029.	1.706
968.500	-1550399.	-1263044.	68.120	-35988.	-30932.	1.668
1000.	-1550120.	-1253702.	65.487	-35983.	-30758.	1.607
(2 sigma)	---	---	---	4087.	4125.	0.215
1050.	-1549677.	-1238892.	61.631	-35963.	-30507.	1.518
1100.	-1549237.	-1224103.	58.128	-35933.	-30248.	1.436
1150.	-1548802.	-1209334.	54.930	-35894.	-29991.	1.362
1200.	-1548374.	-1194584.	51.999	-35850.	-29735.	1.294
1250.	-1547953.	-1179851.	49.303	-35803.	-29481.	1.232
(2 sigma)	---	---	---	4088.	4258.	0.178
1300.	-1547541.	-1165135.	46.816	-35753.	-29229.	1.174
1350.	-1547139.	-1150435.	44.513	-35704.	-28979.	1.121
1400.	-1572201.	-1132145.	42.241	-35658.	-28731.	1.072
1450.	-1670980.	-1112879.	40.090	-35614.	-28484.	1.025
1500.	-1669743.	-1093655.	38.084	-35576.	-28239.	0.983
(2 sigma)	---	---	---	4089.	4433.	0.154
1550.	-1668491.	-1074473.	36.209	-35545.	-27995.	0.943
1600.	-1667223.	-1055331.	34.453	-35521.	-27752.	0.906
1650.	-1665941.	-1036229.	32.804	-35507.	-27509.	0.871
1700.	-1715154.	-1016717.	31.240	-35504.	-27267.	0.838
1750.	-1713700.	-996196.	29.735	-35512.	-27025.	0.807
(2 sigma)	---	---	---	4091.	4646.	0.139
1800.	-1712228.	-975716.	28.315	-35532.	-26782.	0.777
(2 sigma)	---	---	---	4092.	4693.	0.136

Table 124. Thermophysical values for enstatite, MgSiO_3 , at 1.01325 bars (1 atm). The tabulations are based on a fit of the thermophysical and thermochemical data given in Section 1.5.5.

T K	C_p J/(mol K)	S J/(mol K)	H-H(298) J/mol	$[G-H(298)]/T$ J/(mol K)	V cm ³ /mol
200.	58.925	37.989	-7034.	-73.158	31.2970
250.	72.421	52.665	-3733.	-57.596	31.3221
(2 sigma)	0.067	0.338	3.	0.337	0.0658
275.150	77.440	59.303	-1997.	-66.613	31.3351
298.150	82.203	66.294	0.	-66.294	31.3501
(2 sigma)	0.065	0.337	0.	0.337	0.0355
300.	82.532	66.804	152.	-66.296	31.3513
350.	90.396	80.141	4483.	-67.331	31.3841
400.	96.688	92.637	9166.	-69.722	31.4198
450.	101.832	104.332	14133.	-72.925	31.4582
500.	106.110	115.289	19335.	-76.619	31.4986
(2 sigma)	0.060	0.339	11.	0.337	0.0895
550.	109.714	125.576	24733.	-80.507	31.5410
600.	112.785	135.257	30297.	-84.762	31.5848
650.	115.423	144.392	36004.	-89.001	31.6300
700.	117.705	153.031	41834.	-93.269	31.6762
750.	119.690	161.221	47770.	-97.528	31.7234
(2 sigma)	0.072	0.341	24.	0.338	0.0858
800.	121.425	169.002	53798.	-101.754	31.7714
850.	122.945	176.410	59909.	-105.930	31.8201
900.	124.281	183.476	66090.	-110.043	31.8694
950.	125.457	190.228	72334.	-114.087	31.9191
968.500	125.855	192.652	74659.	-115.565	31.9376
1000.	126.493	196.690	78633.	-118.057	31.9692
(2 sigma)	0.099	0.342	37.	0.338	0.1073
1050.	127.405	202.884	84981.	-121.950	32.0197
1100.	128.207	208.830	91372.	-125.765	32.0704
1150.	128.913	214.545	97800.	-129.501	32.1214
1200.	129.530	220.045	104252.	-133.160	32.1727
1250.	130.069	225.344	110752.	-136.742	32.2241
(2 sigma)	0.189	0.345	56.	0.339	0.2139
1257.400	130.143	226.112	111715.	-137.266	32.2317
1300.	130.537	230.454	117267.	-140.249	32.2756
1350.	130.940	235.389	123805.	-143.681	32.3273
1400.	131.285	240.157	130360.	-147.042	32.3791
1450.	131.576	244.769	136932.	-150.333	32.4309
1500.	131.818	249.234	143517.	-153.556	32.4829
(2 sigma)	0.320	0.351	108.	0.339	0.3497
1550.	132.014	253.560	150113.	-156.712	32.5349
1600.	132.169	257.753	156718.	-159.805	32.5870
1650.	132.285	261.822	163329.	-162.835	32.6391
1700.	132.365	265.773	169946.	-165.805	32.6912
1750.	132.413	269.610	176565.	-168.716	32.7434
(2 sigma)	0.472	0.367	198.	0.340	0.4953
1800.	132.429	273.341	183187.	-171.571	32.7956
(2 sigma)	0.504	0.372	221.	0.341	0.5250

Table 125. Thermochemical properties of enstatite, $MgSiO_3$, at 1.01325 bars (1 atm). Columns 2 through 4 give the thermochemical values relative to the elements; columns 5 through 7 give the values relative to the oxides.

T K	Formation from the Elements			Formation from the Oxides		
	H J/mol	G J/mol	log K	H J/mol	G J/mol	log K
200.	-1543316.	-1485931.	388.085	-32759.	-32351.	8.449
250.	-1544219.	-1471471.	307.447	-32781.	-32247.	6.738
(2 sigma)	---	---	---	4108.	4103.	0.857
273.150	-1544489.	-1464721.	280.099	-32787.	-32197.	6.157
298.150	-1544696.	-1457411.	255.332	-32788.	-32143.	5.631
(2 sigma)	---	---	---	4108.	4102.	0.719
300.	-1544708.	-1456869.	253.663	-32788.	-32139.	5.596
350.	-1544897.	-1442211.	215.238	-32767.	-32032.	4.781
400.	-1544856.	-1427542.	186.418	-32724.	-31930.	4.170
450.	-1544639.	-1412889.	164.004	-32666.	-31834.	3.695
500.	-1544282.	-1398268.	146.076	-32605.	-31745.	3.316
(2 sigma)	---	---	---	4108.	4100.	0.428
550.	-1543817.	-1383689.	131.412	-32547.	-31662.	3.007
600.	-1543267.	-1369155.	119.195	-32501.	-31584.	2.750
650.	-1542653.	-1354670.	108.863	-32474.	-31508.	2.532
700.	-1541992.	-1340235.	100.009	-32473.	-31434.	2.346
750.	-1541299.	-1325847.	92.340	-32502.	-31359.	2.184
(2 sigma)	---	---	---	4108.	4098.	0.285
800.	-1540588.	-1311507.	85.633	-32566.	-31281.	2.042
850.	-1539870.	-1297212.	79.717	-33382.	-31193.	1.917
900.	-1539157.	-1282958.	74.461	-33105.	-31072.	1.803
950.	-1547384.	-1268473.	69.745	-32809.	-30967.	1.703
968.500	-1547107.	-1263044.	68.120	-32696.	-30932.	1.668
1000.	-1546637.	-1253812.	65.492	-32500.	-30878.	1.613
(2 sigma)	---	---	---	4108.	4099.	0.214
1050.	-1545896.	-1239189.	61.646	-32183.	-30804.	1.532
1100.	-1545166.	-1224601.	58.151	-31862.	-30746.	1.460
1150.	-1544450.	-1210046.	54.962	-31542.	-30703.	1.395
1200.	-1543750.	-1195522.	52.040	-31227.	-30673.	1.335
1250.	-1543070.	-1181027.	49.352	-30920.	-30656.	1.281
(2 sigma)	---	---	---	4108.	4101.	0.171
1257.400	-1542972.	-1178884.	48.973	-30875.	-30655.	1.273
1300.	-1542412.	-1166558.	46.873	-30624.	-30652.	1.232
1350.	-1541778.	-1152114.	44.578	-30343.	-30658.	1.186
1400.	-1666623.	-1134089.	42.313	-30080.	-30675.	1.144
1450.	-1665201.	-1115095.	40.170	-29836.	-30700.	1.106
1500.	-1663781.	-1096150.	38.171	-29614.	-30734.	1.070
(2 sigma)	---	---	---	4109.	4105.	0.143
1550.	-1662363.	-1077253.	36.303	-29417.	-30775.	1.037
1600.	-1660949.	-1058401.	34.553	-29247.	-30821.	1.006
1650.	-1659540.	-1039593.	32.911	-29105.	-30873.	0.977
1700.	-1708645.	-1020378.	31.352	-28994.	-30928.	0.950
1750.	-1707104.	-1000157.	29.853	-28915.	-30986.	0.925
(2 sigma)	---	---	---	4113.	4111.	0.123
1800.	-1705566.	-979980.	28.438	-28871.	-31046.	0.901
(2 sigma)	---	---	---	4114.	4112.	0.119

Table 12b. Thermophysical values for protoenstatite, MgSiO_3 , at 1.01325 bars (1 atm). The tabulations are based on a fit of the thermophysical and thermochemical data given in Section 1.5.5.

T K	C_p J/(mol K)	S J/(mol K)	H-H(298) J/mol	$[G-H(298)]/T$ J/(mol K)	V cm ³ /mol
200.	62.755	53.053	-7089.	-88.500	32.2467
250.	72.809	68.199	-3586.	-82.944	32.2932
(2 sigma)	7.141	5.625	314.	4.755	0.1218
273.150	76.499	74.812	-1957.	-81.977	32.3147
298.150	79.990	81.665	0.	-81.665	32.3380
(2 sigma)	5.960	4.822	0.	4.822	0.1154
300.	80.231	82.161	148.	-81.667	32.3397
350.	85.998	94.979	4309.	-82.666	32.3862
400.	90.648	106.776	8730.	-84.952	32.4327
450.	94.499	117.682	13361.	-87.991	32.4792
500.	97.757	127.812	18170.	-91.472	32.5257
(2 sigma)	3.430	3.347	893.	4.424	0.0908
550.	100.560	137.263	23129.	-95.210	32.5721
600.	103.005	146.120	28220.	-99.088	32.6186
650.	105.162	154.452	33425.	-103.029	32.6651
700.	107.083	162.317	38732.	-106.986	32.7116
750.	108.809	169.765	44130.	-110.925	32.7581
(2 sigma)	2.725	2.515	1555.	3.815	0.0689
800.	110.371	176.838	49610.	-114.825	32.8046
850.	111.793	183.573	55185.	-118.673	32.8511
900.	113.094	190.000	60787.	-122.458	32.8976
950.	114.291	196.147	66472.	-126.176	32.9440
1000.	115.398	202.038	72215.	-129.823	32.9905
(2 sigma)	2.943	1.903	2077.	3.324	0.0661
1050.	116.424	207.693	78011.	-133.397	33.0370
1100.	117.380	213.132	83856.	-136.899	33.0835
1150.	118.272	218.369	89748.	-140.328	33.1300
1200.	119.109	223.421	95682.	-143.685	33.1765
1250.	119.894	228.299	101658.	-146.973	33.2230
(2 sigma)	3.336	1.463	2528.	2.920	0.0843
1257.400	120.006	229.007	102545.	-147.454	33.2299
1300.	120.634	233.016	107571.	-150.192	33.2695
1350.	121.332	237.582	113720.	-153.345	33.3159
1400.	121.992	242.007	119804.	-156.433	33.3624
1450.	122.619	246.298	125919.	-159.458	33.4089
1500.	123.213	250.466	132065.	-162.422	33.4554
(2 sigma)	3.716	1.272	3278.	2.578	0.1137
1550.	123.778	254.515	138240.	-165.328	33.5019
1600.	124.317	258.453	144442.	-168.177	33.5484
1650.	124.831	262.287	150671.	-170.971	33.5949
1700.	125.322	266.021	156925.	-173.712	33.6414
1750.	125.792	269.660	163203.	-176.401	33.6879
(2 sigma)	4.048	1.368	4042.	2.284	0.1479
1800.	126.243	273.210	169504.	-179.041	33.7343
(2 sigma)	4.108	1.415	4208.	2.231	0.1550

Table 127. Thermochemical properties of protoenstatite, MgSiO_3 , at 1.01325 bars (1 atm). Columns 2 through 4 give the thermochemical values relative to the elements; columns 5 through 7 give the values relative to the oxides.

T K	Formation from the Elements			Formation from the Oxides		
	H J/mol	G J/mol	log K	H J/mol	G J/mol	log K
200.	-1530560.	-1476188.	385.541	-20003.	-22608.	5.905
250.	-1531361.	-1462496.	305.572	-19923.	-23272.	4.863
(2 sigma)	---	---	---	5580.	4850.	1.013
273.150	-1531637.	-1456106.	278.452	-19936.	-23582.	4.510
298.150	-1531885.	-1449182.	253.891	-19976.	-23914.	4.190
(2 sigma)	---	---	---	5502.	4746.	0.832
300.	-1531901.	-1448669.	252.235	-19980.	-23939.	4.168
350.	-1532259.	-1434766.	214.127	-20129.	-24588.	3.670
400.	-1532481.	-1420822.	185.540	-20349.	-25211.	3.292
450.	-1532599.	-1406857.	163.304	-20627.	-25802.	2.995
500.	-1532636.	-1392883.	145.513	-20958.	-26360.	2.754
(2 sigma)	---	---	---	5263.	4432.	0.463
550.	-1532609.	-1378909.	130.958	-21339.	-26882.	2.553
600.	-1532533.	-1364939.	118.828	-21767.	-27367.	2.383
650.	-1532421.	-1350977.	108.566	-22242.	-27815.	2.235
700.	-1532282.	-1337025.	99.770	-22763.	-28225.	2.106
750.	-1532127.	-1323083.	92.148	-23330.	-28595.	1.992
(2 sigma)	---	---	---	4993.	4219.	0.294
800.	-1531965.	-1309152.	85.479	-23943.	-28926.	1.889
850.	-1531802.	-1295232.	79.595	-25314.	-29213.	1.795
900.	-1531648.	-1281320.	74.366	-25596.	-29434.	1.708
950.	-1540434.	-1267146.	69.672	-25859.	-29640.	1.630
1000.	-1540244.	-1252767.	65.438	-26107.	-29832.	1.558
(2 sigma)	---	---	---	4722.	4128.	0.216
1050.	-1540055.	-1238398.	61.607	-26341.	-30013.	1.493
1100.	-1539870.	-1224037.	58.125	-26566.	-30182.	1.433
1150.	-1539691.	-1209685.	54.946	-26783.	-30342.	1.378
1200.	-1539518.	-1195341.	52.032	-26994.	-30492.	1.327
1250.	-1539353.	-1181004.	49.351	-27202.	-30634.	1.280
(2 sigma)	---	---	---	4503.	4105.	0.172
1257.400	-1539329.	-1178882.	48.973	-27233.	-30654.	1.273
1300.	-1539197.	-1166673.	46.877	-27409.	-30767.	1.236
1350.	-1539051.	-1152348.	44.587	-27616.	-30892.	1.195
1400.	-1664368.	-1134424.	42.326	-27825.	-31009.	1.157
1450.	-1663403.	-1115514.	40.185	-28037.	-31119.	1.121
1500.	-1662422.	-1096638.	38.188	-28255.	-31222.	1.087
(2 sigma)	---	---	---	4409.	4117.	0.143
1550.	-1661425.	-1077795.	36.321	-28479.	-31317.	1.055
1600.	-1660413.	-1058985.	34.572	-28711.	-31405.	1.025
1650.	-1659386.	-1040206.	32.930	-28952.	-31486.	0.997
1700.	-1708854.	-1021008.	31.372	-29203.	-31559.	0.970
1750.	-1707655.	-1000795.	29.872	-29466.	-31624.	0.944
(2 sigma)	---	---	---	4507.	4151.	0.124
1800.	-1706437.	-980616.	28.457	-29742.	-31682.	0.919
(2 sigma)	---	---	---	4554.	4160.	0.121

Table 123. Thermophysical values for forsterite, Mg_2SiO_4 , at 1.01325 bars (1 atm). The tabulations are based on a fit of the thermophysical and thermochemical data given in Section 1.5.5.

T K	Cp J/(mol K)	S J/(mol K)	H-H(298) J/mol	[G-H(298)]/T J/(mol K)	V cm ³ /mol
200.	84.941	54.595	-10165.	-105.421	43.5534
250.	104.867	75.847	-5385.	-97.386	43.6002
(2 sigma)	0.185	3.633	11.	3.632	0.0406
273.150	111.759	85.443	-2375.	-95.969	43.6246
298.150	118.099	95.511	0.	-95.511	43.6527
(2 sigma)	0.297	3.632	0.	3.632	0.0203
300.	118.530	96.243	219.	-95.513	43.6548
350.	128.641	115.309	6410.	-96.996	43.7162
400.	136.515	133.020	13046.	-100.405	43.7832
450.	142.875	149.479	20036.	-104.955	43.8550
500.	148.153	164.814	27316.	-110.133	43.9308
(2 sigma)	0.568	3.629	85.	3.631	0.0751
550.	152.625	179.150	34838.	-115.808	44.0101
600.	156.482	192.599	42568.	-121.652	44.0923
650.	159.851	205.250	50478.	-127.602	44.1759
700.	162.328	217.218	58546.	-133.580	44.2537
750.	165.485	228.544	66755.	-139.536	44.3521
(2 sigma)	0.960	3.637	259.	3.628	0.0848
800.	167.875	239.301	75090.	-145.438	44.4421
850.	170.040	249.545	83539.	-151.253	44.5324
900.	172.014	259.321	92091.	-156.997	44.6257
950.	173.324	268.670	100738.	-162.630	44.7189
1000.	175.490	277.629	109471.	-168.158	44.8129
(2 sigma)	1.294	3.669	525.	3.627	0.0869
1050.	177.032	286.229	118285.	-173.577	44.9075
1100.	178.464	294.498	127173.	-178.887	45.0027
1150.	179.799	302.461	136130.	-184.087	45.0983
1200.	181.047	310.140	145151.	-189.181	45.1943
1250.	182.217	317.554	154233.	-194.168	45.2907
(2 sigma)	1.552	3.725	870.	3.630	0.1331
1300.	183.317	324.723	163372.	-199.052	45.3874
1350.	184.354	331.661	172564.	-203.836	45.4842
1400.	185.333	338.383	181806.	-208.522	45.5813
1450.	186.261	344.903	191096.	-213.113	45.6786
1500.	187.140	351.233	200431.	-217.612	45.7760
(2 sigma)	1.755	3.802	1274.	3.639	0.2080
1550.	187.975	357.383	209809.	-222.022	45.8735
1600.	188.771	363.363	219228.	-225.346	45.9712
1650.	189.530	369.184	228686.	-230.586	46.0689
1700.	190.254	374.853	238181.	-234.746	46.1667
1750.	190.946	380.378	247711.	-238.829	46.2645
(2 sigma)	1.919	3.893	1725.	3.653	0.2935
1800.	191.609	385.766	257275.	-242.836	46.3624
(2 sigma)	1.948	3.912	1821.	3.656	0.3114

Table 129. Thermochemical properties of forsterite, Mg_2SiO_4 , at 1.01325 bars (1 atm). Columns 2 through 4 give the thermochemical values relative to the elements; columns 5 through 7 give the values relative to the oxides.

T K	Formation from the Elements			Formation from the Oxides		
	H J/mol	G J/mol	log K	H J/mol	G J/mol	log K
200.	-2170703.	-2092666.	546.548	-59469.	-59581.	15.561
250.	-2172023.	-2072988.	433.127	-59522.	-59603.	12.453
(2 sigma)	---	---	---	7703.	7434.	1.553
273.150	-2172417.	-2063799.	394.661	-59550.	-59610.	11.399
298.150	-2172729.	-2053843.	359.824	-59583.	-59614.	10.444
(2 sigma)	---	---	---	7703.	7394.	1.295
300.	-2172748.	-2053105.	357.477	-59585.	-59614.	10.380
350.	-2173084.	-2033133.	303.428	-59655.	-59613.	8.897
400.	-2173143.	-2013134.	262.888	-59733.	-59602.	7.783
450.	-2172997.	-1993140.	231.357	-59821.	-59580.	6.916
500.	-2172697.	-1973170.	206.136	-59922.	-59548.	6.221
(2 sigma)	---	---	---	7703.	7268.	0.759
550.	-2172278.	-1953237.	185.503	-60040.	-59505.	5.651
600.	-2171772.	-1933346.	168.313	-60176.	-59451.	5.176
650.	-2171200.	-1913500.	153.771	-60334.	-59384.	4.772
700.	-2170586.	-1893700.	141.309	-60515.	-59305.	4.425
750.	-2169946.	-1873944.	130.513	-60722.	-59211.	4.124
(2 sigma)	---	---	---	7706.	7214.	0.502
800.	-2169297.	-1854232.	121.069	-60957.	-59103.	3.859
850.	-2168656.	-1834560.	112.738	-61933.	-58974.	3.624
900.	-2168035.	-1814925.	105.335	-61806.	-58803.	3.413
950.	-2185303.	-1794781.	98.684	-61646.	-58641.	3.224
1000.	-2184622.	-1774245.	92.677	-61458.	-58487.	3.055
(2 sigma)	---	---	---	7716.	7274.	0.380
1050.	-2183949.	-1753743.	87.244	-61245.	-58344.	2.902
1100.	-2183289.	-1733272.	82.306	-61012.	-58211.	2.764
1150.	-2182643.	-1712832.	77.799	-60762.	-58089.	2.638
1200.	-2182015.	-1692419.	73.669	-60497.	-57979.	2.524
1250.	-2181407.	-1672031.	69.870	-60221.	-57879.	2.419
(2 sigma)	---	---	---	7744.	7448.	0.311
1300.	-2180821.	-1651668.	66.365	-59937.	-57791.	2.322
1350.	-2180258.	-1631327.	63.120	-59647.	-57714.	2.233
1400.	-2430627.	-1603797.	59.838	-59353.	-57648.	2.151
1450.	-2428435.	-1574306.	56.713	-59058.	-57592.	2.075
1500.	-2426214.	-1544891.	53.798	-58764.	-57547.	2.004
(2 sigma)	---	---	---	7795.	7734.	0.269
1550.	-2423967.	-1515551.	51.074	-58472.	-57511.	1.938
1600.	-2421694.	-1486283.	48.522	-58186.	-57485.	1.877
1650.	-2419396.	-1457087.	46.128	-57907.	-57467.	1.819
1700.	-2467582.	-1427511.	43.862	-57636.	-57458.	1.765
1750.	-2465092.	-1396957.	41.697	-57376.	-57457.	1.715
(2 sigma)	---	---	---	7877.	8126.	0.243
1800.	-2462573.	-1366475.	39.654	-57123.	-57462.	1.668
(2 sigma)	---	---	---	7897.	8217.	0.238

Table 130. Thermophysical values for chrysotile, $Mg_3Si_2O_5(OH)_4$, at 1.01325 bars (1 atm). The tabulations are based on a fit of the thermophysical and thermochemical data given in Section 1.5.5.

T K	Cp J/(mol K)	S J/(mol K)	H-H(298) J/mol	[G-H(298)]/T J/(mol K)	V cm ³ /mol
200.	196.745	127.091	-23420.	-244.190	107.0710
250.	240.970	175.972	-12426.	-225.676	107.1752
(2 sigma)	0.499	1.131	25.	1.127	1.2252
273.150	257.763	198.060	-6649.	-222.403	107.2234
298.150	273.853	221.342	0.	-221.342	107.2755
(2 sigma)	0.770	1.127	0.	1.127	1.2170
300.	274.975	223.039	508.	-221.347	107.2794
350.	301.883	267.524	14954.	-224.799	107.3836
400.	323.696	309.307	30611.	-232.779	107.4878
450.	341.730	348.506	47261.	-243.483	107.5921
500.	356.878	385.317	64736.	-255.844	107.6963
(2 sigma)	4.820	1.769	570.	1.149	1.3111
550.	369.766	419.952	82911.	-269.205	107.8005
600.	380.849	452.613	101683.	-283.141	107.9047
650.	390.464	483.485	120971.	-297.376	108.0089
700.	398.866	512.736	140709.	-311.723	108.1131
750.	406.253	540.512	160841.	-326.058	108.2174
(2 sigma)	7.360	3.987	2114.	1.515	1.6534
800.	412.782	566.944	181320.	-340.294	108.3216
850.	418.575	592.146	202107.	-354.373	108.4258
900.	423.734	616.220	223167.	-368.256	108.5300
950.	428.342	639.256	244471.	-381.918	108.6342
1000.	432.466	661.334	265993.	-395.340	108.7384
(2 sigma)	8.644	6.056	4000.	2.279	2.1321
1050.	436.163	682.525	287711.	-408.515	108.8427
1100.	439.482	702.893	309603.	-421.436	108.9469
1150.	442.463	722.496	331653.	-434.102	109.0511
1200.	445.142	741.385	353845.	-446.514	109.1553
1250.	447.548	759.606	376163.	-458.675	109.2595
(2 sigma)	10.842	7.777	6086.	3.141	2.6749

Table 131. Thermochemical properties of chrysotile, $Mg_3Si_2O_5(OH)_4$, at 1.01325 bars (1 atm). Columns 2 through 4 give the thermochemical values relative to the elements; columns 5 through 7 give the values relative to the oxides.

T K	Formation from the Elements			Formation from the Oxides		
	H J/mol	G J/mol	log K	H J/mol	G J/mol	log K
200.	-4470806.	-4178448.	1091.298	-153888.	-145013.	37.873
250.	-4477197.	-4104587.	857.606	-159030.	-142175.	29.706
(2 sigma)	---	---	---	11722.	11705.	2.446
273.15u	-4479664.	-4069970.	778.302	-161073.	-140521.	26.872
298.15u	-4482037.	-4032365.	706.453	-163105.	-138548.	24.273
(2 sigma)	---	---	---	11723.	11703.	2.050
300.	-4482201.	-4029575.	701.611	-163249.	-138396.	24.097
350.	-4486142.	-3953812.	590.074	-166897.	-133959.	19.992
400.	-4489252.	-3877544.	506.355	-249642.	-123225.	16.092
450.	-4491704.	-3800927.	441.200	-248426.	-107493.	12.477
500.	-4493634.	-3724067.	389.050	-246962.	-91910.	9.602
(2 sigma)	---	---	---	11775.	11688.	1.221
550.	-4495147.	-3647034.	346.366	-245309.	-76484.	7.264
600.	-4496331.	-3569878.	310.785	-243519.	-61214.	5.329
650.	-4497258.	-3492634.	280.671	-241633.	-46098.	3.704
700.	-4497991.	-3415327.	254.855	-239688.	-31129.	2.323
750.	-4498582.	-3337973.	232.477	-237714.	-16301.	1.135
(2 sigma)	---	---	---	12050.	11665.	0.812
800.	-4499080.	-3260582.	212.894	-235737.	-1605.	0.105
850.	-4499526.	-3183162.	195.613	-235205.	12979.	-0.798
900.	-4499957.	-3105717.	180.251	-232442.	27499.	-1.596
950.	-4527189.	-3027432.	166.460	-229603.	41863.	-2.302
1000.	-4527477.	-2948490.	154.013	-226710.	56076.	-2.929
(2 sigma)	---	---	---	12626.	11729.	0.613
1050.	-4527769.	-2869533.	142.751	-223781.	70143.	-3.489
1100.	-4528078.	-2790562.	132.513	-220832.	84070.	-3.992
1150.	-4528417.	-2711577.	123.164	-217876.	97863.	-4.445
1200.	-4528796.	-2632576.	114.593	-214928.	111528.	-4.855
1250.	-4529225.	-2553558.	106.707	-211998.	125070.	-5.226
(2 sigma)	---	---	---	13515.	12032.	0.503

Table 132. Thermophysical values for talc, $Mg_3Si_4O_{10}(OH)_2$, at 1.01325 bars (1 atm). The tabulations are based on a fit of the thermophysical and thermochemical data given in Section 1.5.5.

T K	Cp J/(mol K)	S J/(mol K)	H-H(298) J/mol	[G-H(298)]/T J/(mol K)	V cm ³ /mol
200.	219.745	151.735	-27144.	-287.456	135.6673
250.	280.133	207.648	-14560.	-265.887	135.8134
(2 sigma)	1.203	1.339	45.	1.328	0.8281
273.150	302.061	233.436	-7815.	-262.046	135.8810
298.150	322.661	260.799	0.	-260.799	135.9541
(2 sigma)	0.739	1.328	0.	1.328	0.7568
300.	324.076	262.799	598.	-260.805	135.9595
350.	357.691	315.387	17677.	-264.881	136.1055
400.	384.318	364.953	36252.	-274.324	136.2516
450.	405.959	411.510	56026.	-287.007	136.3977
500.	423.895	455.239	76786.	-301.667	136.5437
(2 sigma)	0.792	1.356	109.	1.329	0.6206
550.	438.988	496.368	98368.	-317.516	136.5898
600.	451.844	535.131	120648.	-334.051	136.8358
650.	462.901	571.745	143523.	-350.940	136.9819
700.	472.489	606.409	166913.	-367.961	137.1290
750.	480.854	639.299	190751.	-384.963	137.2740
(2 sigma)	1.084	1.457	327.	1.340	0.8906
800.	488.193	670.572	214992.	-401.845	137.4201
850.	494.657	700.366	239556.	-418.535	137.5661
900.	500.371	728.805	264435.	-434.988	137.7122
950.	505.434	755.997	289582.	-451.173	137.8583
1000.	509.929	782.039	314969.	-467.070	138.0043
(2 sigma)	1.160	1.594	587.	1.364	1.3819
1050.	513.924	807.017	340567.	-482.667	138.1504
1100.	517.477	831.008	366354.	-497.959	138.2965
1150.	520.636	854.082	392308.	-512.945	138.4425
1200.	523.443	876.301	418412.	-527.625	138.5886
1250.	525.934	897.720	444647.	-542.003	138.7346
(2 sigma)	1.328	1.722	848.	1.400	1.9326

Table 133. Thermochemical properties of talc, $Mg_3Si_4O_{10}(OH)_2$, at 1.01325 bars (1 atm). Columns 2 through 4 give the thermochemical values relative to the elements; columns 5 through 7 give the values relative to the oxides.

T K	Formation from the Elements			Formation from the Oxides		
	H J/mol	G J/mol	log K	H J/mol	G J/mol	log K
200.	-6179020.	-5736774.	1498.291	-156827.	-150212.	39.231
250.	-6190709.	-5624813.	1175.239	-160013.	-148170.	30.958
(2 sigma)	---	---	---	13081.	13048.	2.726
273.150	-6195456.	-5572195.	1065.573	-161211.	-147018.	28.114
298.150	-6200218.	-5514937.	966.193	-162363.	-145667.	25.520
(2 sigma)	---	---	---	13080.	13043.	2.285
300.	-6200558.	-5510684.	959.495	-162444.	-145563.	25.345
350.	-6209141.	-5395011.	805.161	-164417.	-142589.	21.280
400.	-6216812.	-5278174.	689.258	-205850.	-135451.	17.819
450.	-6223807.	-5160418.	599.005	-205269.	-127810.	14.836
500.	-6230292.	-5041912.	526.725	-204572.	-119240.	12.457
(2 sigma)	---	---	---	13084.	13024.	1.361
550.	-6236395.	-4922776.	467.526	-203823.	-110743.	10.517
600.	-6242212.	-4803098.	418.146	-203069.	-102314.	8.907
650.	-6247823.	-4682943.	376.326	-202354.	-93947.	7.550
700.	-6253294.	-4562361.	340.447	-201712.	-85633.	6.390
750.	-6258678.	-4441392.	309.326	-201171.	-77361.	5.388
(2 sigma)	---	---	---	13094.	13006.	0.906
800.	-6264024.	-4320065.	282.071	-200755.	-69121.	4.513
850.	-6269373.	-4198404.	258.002	-203336.	-60882.	3.741
900.	-6274762.	-4076427.	236.590	-201540.	-52554.	3.050
950.	-6307002.	-3953334.	217.369	-199663.	-44328.	2.437
1000.	-6312351.	-3829319.	200.023	-197729.	-36202.	1.891
(2 sigma)	---	---	---	13109.	12997.	0.679
1050.	-6317752.	-3705035.	184.315	-195760.	-28174.	1.402
1100.	-6323217.	-3580492.	170.023	-193778.	-20241.	0.961
1150.	-6328757.	-3455698.	156.963	-191799.	-12397.	0.563
1200.	-6334381.	-3330663.	144.980	-189840.	-4639.	0.202
1250.	-6340096.	-3205391.	133.946	-187914.	3038.	-0.127
(2 sigma)	---	---	---	13129.	13000.	0.543

Table 134. Thermophysical values for anthophyllite, $Mg_7Si_8O_{22}(OH)_2$, at 1.01325 bars (1 atm). The tabulations are based on a fit of the thermophysical and thermochemical data given in Section 1.5.5.

T K	Cp J/(mol K)	S J/(mol K)	H-H(298) J/mol	[G-H(298)]/T J/(mol K)	V cm ³ /mol
200.	476.042	309.014	-56657.	-592.298	263.7887
250.	582.722	427.172	-30082.	-547.499	263.8268
(2 sigma)	0.895	1.032	42.	1.021	2.5885
273.150	623.991	480.613	-16105.	-539.573	263.8445
298.150	663.615	537.004	0.	-537.004	263.8636
(2 sigma)	0.838	1.021	0.	1.021	2.5884
300.	666.361	541.118	1230.	-537.017	263.8650
350.	732.181	643.978	36258.	-545.384	263.9031
400.	784.583	750.297	74225.	-564.734	263.9412
450.	826.807	845.233	114547.	-590.684	263.9794
500.	861.200	934.186	156776.	-620.634	264.0175
(2 sigma)	1.212	1.116	181.	1.025	2.5883
550.	889.479	1017.636	200565.	-652.972	264.0556
600.	912.918	1096.067	245643.	-686.662	264.0938
650.	932.483	1169.935	291793.	-721.023	264.1319
700.	948.917	1239.659	338840.	-755.602	264.1700
750.	962.802	1305.614	386642.	-790.091	264.2081
(2 sigma)	2.474	1.324	461.	1.055	2.5897
800.	974.600	1368.138	435085.	-824.282	264.2463
850.	984.683	1427.533	484073.	-858.035	264.2844
900.	993.354	1484.068	533530.	-891.257	264.3225
950.	1000.863	1537.982	583390.	-923.887	264.3607
1000.	1007.416	1589.489	633600.	-955.889	264.3988
(2 sigma)	4.894	1.840	1202.	1.111	2.5927
1050.	1013.188	1538.784	684118.	-987.243	264.4369
1100.	1018.326	1686.038	734908.	-1017.940	264.4751
1150.	1022.955	1731.408	785942.	-1047.980	264.5132
1200.	1027.183	1775.036	837197.	-1077.371	264.5513
1250.	1031.102	1817.048	888655.	-1106.123	264.5895
(2 sigma)	6.230	2.782	2508.	1.236	2.5972

Table 135. Thermochemical properties of anthophyllite, $\text{Mg}_7\text{Si}_8\text{O}_{22}(\text{OH})_2$, at 1.01325 bars (1 atm). Columns 2 through 4 give the thermochemical values relative to the elements; columns 5 through 7 give the values relative to the oxides.

T K	Formation from the Elements			Formation from the Oxides		
	H J/mol	G J/mol	log K	H J/mol	G J/mol	log K
200.	-12047331.	-11570007.	3021.774	-274258.	-267075.	69.753
250.	-12054571.	-11449759.	2392.294	-276745.	-264980.	55.365
(2 sigma)	---	---	---	29301.	29292.	6.120
273.150	-12056737.	-11393651.	2178.813	-277679.	-263848.	50.456
298.150	-12058366.	-11332884.	1985.473	-278531.	-262543.	45.996
(2 sigma)	---	---	---	29301.	29291.	5.132
300.	-12058460.	-11328382.	1972.445	-278588.	-262443.	45.695
350.	-12059770.	-11206568.	1672.488	-279854.	-259646.	38.750
400.	-12059098.	-11084707.	1447.513	-320451.	-253796.	33.142
450.	-12056902.	-10963025.	1272.534	-318962.	-245551.	28.503
500.	-12053539.	-10841655.	1132.619	-317355.	-237480.	24.809
(2 sigma)	---	---	---	29303.	29285.	3.059
550.	-12049290.	-10720666.	1018.163	-315760.	-229571.	21.803
600.	-12044384.	-10600095.	922.820	-314283.	-221802.	19.310
650.	-12039005.	-10479953.	842.179	-313015.	-214148.	17.209
700.	-12033310.	-10360237.	773.090	-312027.	-206582.	15.415
750.	-12027429.	-10240937.	713.242	-311382.	-199075.	13.865
(2 sigma)	---	---	---	29313.	29279.	2.039
800.	-12021471.	-10122031.	660.900	-311125.	-191598.	12.510
850.	-12015534.	-10003498.	614.740	-316995.	-184083.	11.312
900.	-12009700.	-9885312.	573.728	-314241.	-176344.	10.235
950.	-12066526.	-9765545.	536.947	-311444.	-168759.	9.279
1000.	-12060606.	-9644595.	503.782	-308646.	-161322.	8.427
(2 sigma)	---	---	---	29344.	29274.	1.529
1050.	-12054800.	-9523937.	473.790	-305381.	-154024.	7.562
1100.	-12049129.	-9403554.	446.537	-303175.	-146856.	6.974
1150.	-12043609.	-9283424.	421.666	-300550.	-139810.	6.350
1200.	-12038250.	-9163532.	398.878	-298024.	-132876.	5.784
1250.	-12033058.	-9043859.	377.922	-295609.	-126045.	5.267
(2 sigma)	---	---	---	29436.	29277.	1.223

Table 136. Thermophysical values for antigorite, $Mg_4Si_3O_{10}(OH)_2$, at 1.01325 bars (1 atm). The tabulations are based on a fit of the thermophysical and thermochemical data given in Section 1.5.5.

T K	Cp J/(mol K)	S J/(mol K)	H-H(298) J/mol	[G-H(298)]/T J/(mol K)	V cm ³ /mol
200.	3187.253	2079.151	-379417.	-3976.237	1745.6268
250.	3903.932	2871.061	-201307.	-3676.290	1747.4221
(2 sigma)	8.082	18.445	406.	18.387	12.7897
273.150	4175.912	3228.897	-107721.	-3623.263	1748.2533
298.150	4436.520	3606.080	0.	-3606.080	1749.1510
(2 sigma)	12.488	18.387	0.	18.387	12.7276
300.	4454.596	3633.579	8224.	-3606.164	1749.2174
350.	4890.106	4354.200	242243.	-3662.077	1751.0127
400.	5242.994	5031.003	495864.	-3791.343	1752.8080
450.	5534.599	5665.895	765525.	-3964.729	1754.6033
500.	5779.416	6262.055	1048546.	-4164.962	1756.3986
(2 sigma)	78.216	28.792	9257.	18.748	13.7113
550.	5987.621	6822.914	1342858.	-4381.355	1758.1939
600.	6166.575	7351.768	1646822.	-4607.065	1759.9892
650.	6321.739	7851.628	1959119.	-4837.598	1761.7845
700.	6457.258	8325.190	2278669.	-5069.948	1763.5798
750.	6576.337	8774.842	2604572.	-5302.080	1765.3751
(2 sigma)	118.420	64.752	34310.	24.672	17.1262
800.	6681.498	9202.695	2936071.	-5532.606	1767.1704
850.	6774.756	9610.612	3272523.	-5760.585	1768.9657
900.	6857.741	10000.241	3613376.	-5985.379	1770.7610
950.	6931.789	10373.041	3958149.	-6206.569	1772.5563
1000.	6998.004	10730.311	4306424.	-6423.887	1774.3517
(2 sigma)	140.061	98.307	64900.	37.059	21.8975
1050.	7057.311	11073.206	4657834.	-6637.174	1776.1470
1100.	7110.487	11402.762	5012053.	-6846.350	1777.9423
1150.	7158.194	11719.907	5368792.	-7051.393	1779.7376
1200.	7200.998	12025.478	5727791.	-7252.319	1781.5329
1250.	7239.385	12320.230	6088818.	-7449.175	1783.3282
(2 sigma)	175.420	126.177	98673.	51.027	27.3236

Table 137. Thermochemical properties of antigorite, $Mg_{48}Si_{34}O_{85}(OH)_{62}$, at 1.01325 bars (1 atm). Columns 2 through 4 give the thermochemical values relative to the elements; columns 5 through 7 give the values relative to the oxides.

T K	Formation from the Elements			Formation from the Oxides		
	H J/mol	G J/mol	log K	H J/mol	G J/mol	log K
200.	-71308557.	-67838940.	17717.701	-2572031.	-2436498.	636.348
250.	-71364590.	-66964522.	13991.461	-2651734.	-2393018.	499.993
(2 sigma)	---	---	---	224225.	223949.	46.792
273.150	-71382546.	-66556233.	12727.580	-2683386.	-2367618.	452.761
298.150	-71397109.	-66113823.	11582.859	-2714846.	-2337300.	409.485
(2 sigma)	---	---	---	224232.	223907.	39.228
300.	-71398003.	-66081038.	11505.723	-2717079.	-2334951.	406.551
350.	-71413640.	-65193422.	9729.579	-2773515.	-2266706.	338.287
400.	-71415142.	-64304567.	8397.309	-4055953.	-2100871.	274.345
450.	-71405292.	-63416230.	7361.159	-4036981.	-1857579.	215.622
500.	-71386271.	-62529500.	6532.407	-4014194.	-1616614.	168.886
(2 sigma)	---	---	---	225291.	223600.	23.359
550.	-71359831.	-61645048.	5854.554	-3988543.	-1378078.	130.879
600.	-71327414.	-60763276.	5289.909	-3960830.	-1141973.	99.418
650.	-71290230.	-59884410.	4812.367	-3931732.	-908241.	72.987
700.	-71249313.	-59008553.	4403.269	-3901821.	-676783.	50.502
750.	-71205561.	-58135725.	4048.929	-3871584.	-447478.	31.165
(2 sigma)	---	---	---	230028.	222836.	15.520
800.	-71159767.	-57265887.	3739.076	-3841439.	-220189.	14.377
850.	-71112638.	-56398958.	3465.856	-3835959.	5405.	-0.332
900.	-71064814.	-55534825.	3223.155	-3792639.	230124.	-13.356
950.	-71445345.	-54660321.	3005.432	-3748118.	452402.	-24.875
1000.	-71394390.	-53778214.	2809.084	-3702733.	672311.	-35.118
(2 sigma)	---	---	---	239070.	222927.	11.644
1050.	-71343099.	-52898666.	2631.563	-3656777.	889934.	-44.272
1100.	-71291734.	-52021564.	2470.296	-3610512.	1105361.	-52.489
1150.	-71240518.	-51146795.	2323.159	-3564170.	1318681.	-59.896
1200.	-71189651.	-50274247.	2188.379	-3517959.	1529988.	-66.599
1250.	-71139306.	-49403808.	2064.471	-3472064.	1739374.	-72.684
(2 sigma)	---	---	---	252396.	226079.	9.447

Table 138. Thermophysical values for the element oxygen (O₂) at 1.01325 bars (1 atm). The sources of data are given in Section 1.5.5.

T K	C _p J/(mol K)	S J/(mol K)	H-H(298) J/mol	[G-H(298)]/T J/(mol K)	V cm ³ /mol
200.	29.198	193.397	-2861.	-207.702	---
250.	29.087	199.898	-1407.	-205.514	---
(2 sigma)	---	---	---	---	---
273.15	29.199	202.468	-732.	-205.148	---
298.15	29.377	205.033	-0.	-205.033	---
(2 sigma)	---	---	---	---	---
300.	29.391	205.214	54.	-205.033	---
350.	29.836	209.778	1535.	-205.393	---
400.	30.320	213.793	3039.	-206.197	---
450.	30.805	217.392	4567.	-207.244	---
500.	31.274	220.662	6119.	-208.425	---
(2 sigma)	---	---	---	---	---
550.	31.722	223.664	7694.	-209.676	---
600.	32.145	226.443	9291.	-210.959	---
650.	32.545	229.032	10908.	-212.250	---
700.	32.921	231.457	12545.	-213.537	---
750.	33.275	233.741	14200.	-214.808	---
(2 sigma)	---	---	---	---	---
800.	33.607	235.899	15872.	-216.059	---
850.	33.919	237.946	17560.	-217.287	---
900.	34.212	239.893	19263.	-218.489	---
950.	34.487	241.750	20981.	-219.665	---
1000.	34.744	243.526	22712.	-220.814	---
(2 sigma)	---	---	---	---	---
1050.	34.985	245.227	24455.	-221.936	---
1100.	35.209	246.860	26210.	-223.032	---
1150.	35.419	248.429	27976.	-224.103	---
1200.	35.613	249.941	29752.	-225.148	---
1250.	35.793	251.399	31537.	-226.169	---
(2 sigma)	---	---	---	---	---
1300.	35.960	252.806	33331.	-227.167	---
1350.	36.112	254.166	35133.	-228.142	---
1400.	36.252	255.482	36942.	-229.095	---
1450.	36.378	256.756	38757.	-230.027	---
1500.	36.492	257.991	40579.	-230.938	---
(2 sigma)	---	---	---	---	---
1550.	36.594	259.189	42406.	-231.830	---
1600.	36.683	260.353	44238.	-232.704	---
1650.	36.760	261.483	46075.	-233.559	---
1700.	36.826	262.581	47914.	-234.396	---
1750.	36.880	263.649	49757.	-235.217	---
(2 sigma)	---	---	---	---	---
1800.	36.922	264.689	51602.	-236.021	---
(2 sigma)	---	---	---	---	---

Table 139. Thermochemical properties of the element oxygen (O_2) at 1.01325 bars (1 atm). Columns 2 through 4 give the thermochemical values relative to the elements; columns 5 through 7 give the values relative to the oxides.

T K	Formation from the Elements			Formation from the Oxides		
	H J/mol	G J/mol	log K	H J/mol	G J/mol	log K
200.	0.	0.	0.	---	---	---
250.	0.	0.	0.	---	---	---
(2 sigma)	0.	0.	0.	---	---	---
273.15	0.	0.	0.	---	---	---
298.15	0.	0.	0.	---	---	---
(2 sigma)	0.	0.	0.	---	---	---
300.	0.	0.	0.	---	---	---
350.	0.	0.	0.	---	---	---
400.	0.	0.	0.	---	---	---
450.	0.	0.	0.	---	---	---
500.	0.	0.	0.	---	---	---
(2 sigma)	0.	0.	0.	---	---	---
550.	0.	0.	0.	---	---	---
600.	0.	0.	0.	---	---	---
650.	0.	0.	0.	---	---	---
700.	0.	0.	0.	---	---	---
750.	0.	0.	0.	---	---	---
(2 sigma)	0.	0.	0.	---	---	---
800.	0.	0.	0.	---	---	---
850.	0.	0.	0.	---	---	---
900.	0.	0.	0.	---	---	---
950.	0.	0.	0.	---	---	---
1000.	0.	0.	0.	---	---	---
(2 sigma)	0.	0.	0.	---	---	---
1050.	0.	0.	0.	---	---	---
1100.	0.	0.	0.	---	---	---
1150.	0.	0.	0.	---	---	---
1200.	0.	0.	0.	---	---	---
1250.	0.	0.	0.	---	---	---
(2 sigma)	0.	0.	0.	---	---	---
1300.	0.	0.	0.	---	---	---
1350.	0.	0.	0.	---	---	---
1400.	0.	0.	0.	---	---	---
1450.	0.	0.	0.	---	---	---
1500.	0.	0.	0.	---	---	---
(2 sigma)	0.	0.	0.	---	---	---
1550.	0.	0.	0.	---	---	---
1600.	0.	0.	0.	---	---	---
1650.	0.	0.	0.	---	---	---
1700.	0.	0.	0.	---	---	---
1750.	0.	0.	0.	---	---	---
(2 sigma)	0.	0.	0.	---	---	---
1800.	0.	0.	0.	---	---	---
(2 sigma)	0.	0.	0.	---	---	---

Table 140. Thermophysical values for stable phases of the element silicon (Si) at 1.01325 bars (1 atm). The sources of data are given in Section 1.5.5.

T K	C _p J/(mol K)	S J/(mol K)	H-H(298) J/mol	[G-H(298)]/T J/(mol K)	V cm ³ /mol
silicon (crystal)					
200.	15.588	11.648	-1775.	-20.521	---
250.	18.271	15.440	-923.	-19.130	---
(2 sigma)	---	---	---	---	---
273.15	19.154	17.097	-489.	-18.888	---
298.15	19.946	18.810	0.	-18.810	---
(2 sigma)	---	---	---	---	---
300.	19.999	18.934	37.	-18.810	---
350.	21.222	22.113	1069.	-19.059	---
400.	22.146	25.010	2154.	-19.624	---
450.	22.875	27.662	3280.	-20.372	---
500.	23.470	30.104	4439.	-21.225	---
(2 sigma)	---	---	---	---	---
550.	23.970	32.365	5626.	-22.136	---
600.	24.398	34.469	6835.	-23.077	---
650.	24.771	36.437	8065.	-24.030	---
700.	25.100	38.285	9312.	-24.983	---
750.	25.394	40.027	10574.	-25.928	---
(2 sigma)	---	---	---	---	---
800.	25.659	41.675	11851.	-26.861	---
850.	25.901	43.238	13140.	-27.779	---
900.	26.122	44.724	14440.	-28.680	---
950.	26.327	46.142	15752.	-29.562	---
1000.	26.517	47.498	17073.	-30.425	---
(2 sigma)	---	---	---	---	---
1050.	26.693	48.796	18403.	-31.269	---
1100.	26.859	50.041	19742.	-32.094	---
1150.	27.015	51.239	21089.	-32.901	---
1200.	27.162	52.392	22443.	-33.689	---
1250.	27.302	53.503	23805.	-34.459	---
(2 sigma)	---	---	---	---	---
1300.	27.435	54.577	25173.	-35.213	---
1350.	27.561	55.614	26548.	-35.949	---
1400.	27.682	56.619	27929.	-36.669	---
1450.	27.797	57.592	29316.	-37.374	---
1500.	27.908	58.537	30709.	-38.064	---
(2 sigma)	---	---	---	---	---
1550.	28.015	59.454	32107.	-38.739	---
1600.	28.118	60.345	33510.	-39.401	---
1650.	28.217	61.211	34919.	-40.048	---
1685.	28.285	61.804	35908.	-40.494	---
silicon (liquid)					
1685.	25.522	91.805	86459.	-40.494	---
1700.	25.522	92.031	86841.	-40.948	---
1750.	25.522	92.771	88117.	-42.418	---
(2 sigma)	---	---	---	---	---
1800.	25.522	93.490	89394.	-43.827	---
(2 sigma)	---	---	---	---	---

Table 141. Thermochemical properties of stable phases of the element silicon (Si) at 1.01325 bars (1 atm). Columns 2 through 4 give the thermochemical values relative to the elements; columns 5 through 7 give the values relative to the oxides.

T K	Formation from the Elements			Formation from the Oxides		
	H J/mol	G J/mol	log K	H J/mol	G J/mol	log K
silicon (crystal)						
200.	0.	0.	0.	---	---	---
250.	0.	0.	0.	---	---	---
(2 sigma)	0.	0.	0.	---	---	---
273.15	0.	0.	0.	---	---	---
298.15	0.	0.	0.	---	---	---
(2 sigma)	0.	0.	0.	---	---	---
300.	0.	0.	0.	---	---	---
350.	0.	0.	0.	---	---	---
400.	0.	0.	0.	---	---	---
450.	0.	0.	0.	---	---	---
500.	0.	0.	0.	---	---	---
(2 sigma)	0.	0.	0.	---	---	---
550.	0.	0.	0.	---	---	---
600.	0.	0.	0.	---	---	---
650.	0.	0.	0.	---	---	---
700.	0.	0.	0.	---	---	---
750.	0.	0.	0.	---	---	---
(2 sigma)	0.	0.	0.	---	---	---
800.	0.	0.	0.	---	---	---
850.	0.	0.	0.	---	---	---
900.	0.	0.	0.	---	---	---
950.	0.	0.	0.	---	---	---
1000.	0.	0.	0.	---	---	---
(2 sigma)	0.	0.	0.	---	---	---
1050.	0.	0.	0.	---	---	---
1100.	0.	0.	0.	---	---	---
1150.	0.	0.	0.	---	---	---
1200.	0.	0.	0.	---	---	---
1250.	0.	0.	0.	---	---	---
(2 sigma)	0.	0.	0.	---	---	---
1300.	0.	0.	0.	---	---	---
1350.	0.	0.	0.	---	---	---
1400.	0.	0.	0.	---	---	---
1450.	0.	0.	0.	---	---	---
1500.	0.	0.	0.	---	---	---
(2 sigma)	0.	0.	0.	---	---	---
1550.	0.	0.	0.	---	---	---
1600.	0.	0.	0.	---	---	---
1650.	0.	0.	0.	---	---	---
1685.	0.	0.	0.	---	---	---
silicon (liquid)						
1685.	0.	0.	0.	---	---	---
1700.	0.	0.	0.	---	---	---
1750.	0.	0.	0.	---	---	---
(2 sigma)	0.	0.	0.	---	---	---
1800.	0.	0.	0.	---	---	---
(2 sigma)	0.	0.	0.	---	---	---

Table 142. Thermophysical values for quartz, SiO₂, at 1.01325 bars (1 atm). The tabulations are based on a fit of the thermophysical and thermochemical data given in Section 1.5.5.

T K	C _p J/(mol K)	S J/(mol K)	H-H(298) J/mol	[G-H(298)]/T J/(mol K)	V cm ³ /mol
200.	32.629	26.024	-3846.	-45.251	22.4533
250.	39.535	34.083	-2033.	-42.216	22.5212
(2 sigma)	---	---	---	---	---
273.150	42.175	37.701	-1087.	-41.681	22.5526
298.150	44.741	41.507	0.	-41.507	22.5865
(2 sigma)	---	---	---	---	---
300.	44.921	41.785	83.	-41.508	22.5890
350.	49.351	49.052	2443.	-42.072	22.6569
400.	53.136	55.895	5007.	-43.376	22.7248
450.	56.459	62.349	7749.	-45.129	22.7926
500.	59.439	68.454	10648.	-47.159	22.8605
(2 sigma)	---	---	---	---	---
550.	62.156	74.249	13688.	-49.361	22.9283
600.	64.667	79.766	16860.	-51.667	22.9962
650.	67.011	85.036	20152.	-54.032	23.0641
700.	69.219	90.083	23559.	-56.428	23.1319
750.	71.314	94.931	27072.	-58.835	23.1998
(2 sigma)	---	---	---	---	---
800.	73.314	99.598	30688.	-61.237	23.2677
844.	75.007	103.568	33952.	-63.341	23.3274
844.	67.386	104.467	35287.	-62.657	23.5794
850.	67.446	104.944	35692.	-62.954	23.5794
900.	67.948	108.814	39076.	-65.395	23.5794
950.	68.450	112.501	42486.	-67.778	23.5794
1000.	68.952	116.025	45921.	-70.103	23.5794
(2 sigma)	---	---	---	---	---
1050.	69.454	119.401	49382.	-72.371	23.5794
1100.	69.956	122.644	52867.	-74.583	23.5794
1150.	70.458	125.764	56377.	-76.741	23.5794
1200.	70.960	128.774	59913.	-78.846	23.5794
1250.	71.462	131.681	63473.	-80.902	23.5794
(2 sigma)	---	---	---	---	---
1300.	71.964	134.493	67059.	-82.909	23.5794
1350.	72.466	137.219	70670.	-84.871	23.5794
1400.	72.968	139.863	74306.	-86.788	23.5794
1450.	73.470	142.432	77967.	-88.662	23.5794
1500.	73.972	144.932	81653.	-90.497	23.5794
(2 sigma)	---	---	---	---	---
1550.	74.474	147.365	85364.	-92.292	23.5794
1600.	74.976	149.738	89100.	-94.050	23.5794
1650.	75.478	152.052	92861.	-95.773	23.5794
1700.	75.980	154.313	96648.	-97.462	23.5794
1750.	76.482	156.523	100459.	-99.118	23.5794
(2 sigma)	---	---	---	---	---
1800.	76.984	158.684	104296.	-100.742	23.5794
(2 sigma)	---	---	---	---	---

Table 143. Thermochemical properties of quartz, SiO₂, at 1.01325 bars (1 atm). Columns 2 through 4 give the thermochemical values relative to the elements; columns 5 through 7 give the values relative to the oxides.

T K	Formation from the Elements			Formation from the Oxides		
	H J/mol	G J/mol	log K	H J/mol	G J/mol	log K
200.	-909880.	-874075.	228.285	0.0	0.0	0.0
250.	-910374.	-865063.	180.745	0.0	0.0	0.0
(2 sigma)	---	---	---	0.0	0.0	0.0
273.150	-910536.	-860859.	164.623	0.0	0.0	0.0
298.150	-910670.	-856306.	150.021	0.0	0.0	0.0
(2 sigma)	---	---	---	0.0	0.0	0.0
300.	-910678.	-855969.	149.037	0.0	0.0	0.0
350.	-910831.	-846837.	126.383	0.0	0.0	0.0
400.	-910855.	-837692.	109.391	0.0	0.0	0.0
450.	-910768.	-828551.	96.176	0.0	0.0	0.0
500.	-910581.	-819425.	85.605	0.0	0.0	0.0
(2 sigma)	---	---	---	0.0	0.0	0.0
500.	-910301.	-810322.	76.958	0.0	0.0	0.0
600.	-909936.	-801248.	69.755	0.0	0.0	0.0
650.	-909490.	-792209.	63.663	0.0	0.0	0.0
700.	-908968.	-783206.	58.444	0.0	0.0	0.0
750.	-908371.	-774243.	53.923	0.0	0.0	0.0
(2 sigma)	---	---	---	0.0	0.0	0.0
800.	-907704.	-765323.	49.970	0.0	0.0	0.0
844.	-907059.	-757509.	46.882	0.0	0.0	0.0
844.	-906301.	-757509.	46.882	0.0	0.0	0.0
850.	-906255.	-756452.	46.486	0.0	0.0	0.0
900.	-905874.	-747651.	43.392	0.0	0.0	0.0
950.	-905493.	-738871.	40.626	0.0	0.0	0.0
1000.	-905110.	-730111.	38.137	0.0	0.0	0.0
(2 sigma)	---	---	---	0.0	0.0	0.0
1050.	-904723.	-721371.	35.886	0.0	0.0	0.0
1100.	-904332.	-712649.	33.841	0.0	0.0	0.0
1150.	-903934.	-703945.	31.974	0.0	0.0	0.0
1200.	-903529.	-695258.	30.264	0.0	0.0	0.0
1250.	-903115.	-686589.	28.591	0.0	0.0	0.0
(2 sigma)	---	---	---	0.0	0.0	0.0
1300.	-902692.	-677936.	27.240	0.0	0.0	0.0
1350.	-902258.	-669300.	25.897	0.0	0.0	0.0
1400.	-901812.	-660680.	24.650	0.0	0.0	0.0
1450.	-901354.	-652076.	23.490	0.0	0.0	0.0
1500.	-900883.	-643488.	22.408	0.0	0.0	0.0
(2 sigma)	---	---	---	0.0	0.0	0.0
1550.	-900397.	-634916.	21.397	0.0	0.0	0.0
1600.	-899896.	-626360.	20.449	0.0	0.0	0.0
1650.	-899379.	-617820.	19.559	0.0	0.0	0.0
1700.	-949355.	-608846.	18.708	0.0	0.0	0.0
1750.	-948662.	-598841.	17.874	0.0	0.0	0.0
(2 sigma)	---	---	---	0.0	0.0	0.0
1800.	-947947.	-588857.	17.088	0.0	0.0	0.0
(2 sigma)	---	---	---	0.0	0.0	0.0

Table 144. Thermophysical values for cristobalite, SiO₂, at 1.01325 bars (1 atm). The tabulations are based on a fit of the thermophysical and thermochemical data given in Section 1.5.5.

T K	C _p J/(mol K)	S J/(mol K)	H-H(298) J/mol	[G-H(298)]/T J/(mol K)	V cm ³ /mol
alpha cristobalite					
200.000	32.999	29.306	-3873.	-48.671	25.5527
250.000	39.806	37.435	-2045.	-45.616	25.6816
(2 sigma)	---	---	---	---	0.0790
273.150	42.421	41.077	-1093.	-45.077	25.7412
298.150	44.961	44.903	0.	-44.903	25.8057
(2 sigma)	---	---	---	---	0.0574
300.000	45.139	45.182	83.	-44.904	25.8104
350.000	49.484	52.477	2452.	-45.470	25.9393
400.000	53.110	59.328	5020.	-46.779	25.0682
450.000	56.174	65.766	7754.	-48.534	26.1970
500.000	58.779	71.823	10630.	-50.563	26.3259
(2 sigma)	---	---	---	---	0.0694
523.000	59.844	74.490	11994.	-51.557	26.3851
beta cristobalite					
523.000	58.312	77.016	13315.	-51.557	27.3414
550.000	59.797	79.989	14910.	-52.880	27.3471
600.000	62.048	85.292	17958.	-55.362	27.3577
650.000	63.813	90.331	21106.	-57.860	27.3683
700.000	65.228	95.114	24334.	-60.352	27.3789
750.000	66.381	99.655	27625.	-62.822	27.3895
(2 sigma)	---	---	---	---	0.0573
800.000	67.337	103.970	30968.	-65.260	27.4001
850.000	68.140	108.078	34356.	-67.659	27.4107
900.000	68.824	111.992	37781.	-70.014	27.4213
950.000	69.412	115.729	41237.	-72.322	27.4319
1000.000	69.924	119.303	44720.	-74.583	27.4425
(2 sigma)	---	---	---	---	0.0604
1050.000	70.373	122.726	48228.	-76.794	27.4531
1100.000	70.771	126.009	51757.	-78.957	27.4637
1150.000	71.126	129.163	55304.	-81.072	27.4743
1200.000	71.446	132.197	58869.	-83.139	27.4849
1250.000	71.736	135.119	62449.	-85.160	27.4955
(2 sigma)	---	---	---	---	0.0884
1300.000	72.000	137.938	66042.	-87.136	27.5061
1350.000	72.243	140.660	69648.	-89.069	27.5167
1400.000	72.466	143.291	73266.	-90.959	27.5273
1450.000	72.674	145.838	76895.	-92.807	27.5378
1500.000	72.867	148.305	80533.	-94.616	27.5484
(2 sigma)	---	---	---	---	0.1255
1550.000	73.048	150.697	84181.	-96.387	27.5590
1600.000	73.219	153.019	87838.	-98.121	27.5696
1650.000	73.380	155.275	91503.	-99.819	27.5802
1700.000	73.532	157.468	95176.	-101.482	27.5908
1750.000	73.677	159.601	98856.	-103.112	27.6014
(2 sigma)	---	---	---	---	0.1658
1800.000	73.816	161.679	102543.	-104.710	27.6120
(2 sigma)	---	---	---	---	0.1740

Table 145. Thermochemical properties of cristobalite, SiO₂, at 1.01325 bars (1 atm). Columns 2 through 4 give the thermochemical values relative to the elements; columns 5 through 7 give the values relative to the oxides.

T K	Formation from the Elements			Formation from the Oxides		
	H J/mol	G J/mol	log K	H J/mol	G J/mol	log K
alpha cristobalite						
200.000	-907133.	-871985.	227.739	0.	0.	0.
250.000	-907611.	-863138.	180.343	0.	0.	0.
(2 sigma)	---	---	---	0.	0.	0.
273.150	-907767.	-859013.	164.269	0.	0.	0.
298.150	-907895.	-854545.	149.713	0.	0.	0.
(2 sigma)	---	---	---	0.	0.	0.
300.000	-907903.	-854213.	148.732	0.	0.	0.
350.000	-908047.	-845252.	126.147	0.	0.	0.
400.000	-908068.	-836278.	109.207	0.	0.	0.
450.000	-907988.	-827309.	96.031	0.	0.	0.
500.000	-907824.	-818352.	85.493	0.	0.	0.
(2 sigma)	---	---	---	0.	0.	0.
523.000	-907724.	-814239.	81.322	0.	0.	0.
beta cristobalite						
523.000	-906403.	-814239.	81.322	0.	0.	0.
550.000	-906305.	-809483.	76.878	0.	0.	0.
600.000	-906063.	-800691.	69.706	0.	0.	0.
650.000	-905762.	-791922.	63.640	0.	0.	0.
700.000	-905418.	-783178.	58.441	0.	0.	0.
750.000	-905044.	-774459.	53.938	0.	0.	0.
(2 sigma)	---	---	---	0.	0.	0.
800.000	-904649.	-765767.	49.999	0.	0.	0.
850.000	-904239.	-757099.	46.526	0.	0.	0.
900.000	-903818.	-748456.	43.439	0.	0.	0.
950.000	-903391.	-739836.	40.679	0.	0.	0.
1000.000	-902959.	-731239.	38.196	0.	0.	0.
(2 sigma)	---	---	---	0.	0.	0.
1050.000	-902525.	-722664.	35.951	0.	0.	0.
1100.000	-902090.	-714109.	33.910	0.	0.	0.
1150.000	-901655.	-705574.	32.048	0.	0.	0.
1200.000	-901221.	-697058.	30.342	0.	0.	0.
1250.000	-900788.	-688560.	28.773	0.	0.	0.
(2 sigma)	---	---	---	0.	0.	0.
1300.000	-900357.	-680080.	27.326	0.	0.	0.
1350.000	-899928.	-671616.	25.986	0.	0.	0.
1400.000	-899500.	-663167.	24.743	0.	0.	0.
1450.000	-899075.	-654735.	23.586	0.	0.	0.
1500.000	-898650.	-646316.	22.507	0.	0.	0.
(2 sigma)	---	---	---	0.	0.	0.
1550.000	-898228.	-637912.	21.497	0.	0.	0.
1600.000	-897806.	-629522.	20.552	0.	0.	0.
1650.000	-897386.	-621144.	19.664	0.	0.	0.
1700.000	-947475.	-612330.	18.815	0.	0.	0.
1750.000	-946914.	-602481.	17.983	0.	0.	0.
(2 sigma)	---	---	---	0.	0.	0.
1800.000	-946348.	-592648.	17.198	0.	0.	0.
(2 sigma)	---	---	---	0.	0.	0.

Table 146. Molar volume in cm^3/g of boehmite, AlOOH , to 1000 K and 10,000 bars. The tabulations are based on a fit of the thermophysical and thermochemical data given in Section 1.5.5.

Pressure (bars)	Temperature (K)							
	298.15	400.	500.	600.	800.	1000.	1400.	1800.
1.	19.54	19.84	20.14	20.44	21.04	21.65	---	---
500.	19.52	19.83	20.13	20.43	21.03	21.63	---	---
1000.	19.51	19.81	20.11	20.41	21.01	21.62	---	---
2000.	19.48	19.78	20.08	20.38	20.98	21.59	---	---
4000.	19.42	19.72	20.02	20.32	20.92	21.53	---	---
6000.	19.36	19.66	19.96	20.26	20.86	21.47	---	---
8000.	19.30	19.60	19.90	20.20	20.80	21.41	---	---
10000.	19.24	19.54	19.84	20.14	20.74	21.35	---	---

Table 147. Molar volume in cm^3/g of diaspore, AlOOH , to 1800 K and 10,000 bars. The tabulations are based on a fit of the thermophysical and thermochemical data given in Section 1.5.5.

Pressure (bars)	Temperature (K)							
	298.15	400.	500.	600.	800.	1000.	1400.	1800.
1.	17.76	17.88	18.00	18.12	18.36	18.59	19.07	19.55
500.	17.74	17.86	17.98	18.10	18.34	18.58	19.05	19.53
1000.	17.72	17.84	17.96	18.08	18.32	18.56	19.03	19.51
2000.	17.69	17.81	17.93	18.05	18.28	18.52	19.00	19.47
4000.	17.61	17.73	17.85	17.97	18.21	18.45	18.92	19.40
6000.	17.54	17.66	17.78	17.90	18.14	18.37	18.85	19.33
8000.	17.47	17.59	17.71	17.83	18.06	18.30	18.78	19.25
10000.	17.39	17.51	17.63	17.75	17.99	18.23	18.70	19.18

Table 148. Molar volume in cm^3/g of gibbsite, $\text{Al}(\text{OH})_3$, to 1000 K and 10,000 bars. The tabulations are based on a fit of the thermophysical and thermochemical data given in Section 1.5.5.

Pressure (bars)	Temperature (K)							
	298.15	400.	500.	600.	800.	1000.	1400.	1800.
1.	31.96	32.01	32.06	32.12	32.23	32.33	---	---
500.	31.96	32.01	32.06	32.12	32.23	32.33	---	---
1000.	31.96	32.01	32.06	32.12	32.23	32.33	---	---
2000.	31.95	32.01	32.06	32.12	32.22	32.33	---	---
4000.	31.95	32.01	32.06	32.12	32.22	32.33	---	---
6000.	31.95	32.01	32.06	32.11	32.22	32.33	---	---
8000.	31.95	32.01	32.06	32.11	32.22	32.33	---	---
10000.	31.95	32.00	32.06	32.11	32.22	32.33	---	---

Table 149. Molar volume in cm^3/g of corundum, Al_2O_3 , to 1800 K and 10,000 bars. The tabulations are based on a fit of the thermophysical and thermochemical data given in Section 1.5.5.

Pressure (bars)	Temperature (K)							
	298.15	400.	500.	600.	800.	1000.	1400.	1800.
1.	25.60	25.67	25.73	25.80	25.93	26.06	26.32	26.58
500.	25.59	25.66	25.72	25.79	25.92	26.05	26.31	26.58
1000.	25.59	25.65	25.72	25.78	25.92	26.05	26.31	26.57
2000.	25.58	25.64	25.71	25.77	25.90	26.04	26.30	26.56
4000.	25.55	25.62	25.68	25.75	25.88	26.01	26.27	26.54
6000.	25.53	25.60	25.66	25.73	25.86	25.99	26.25	26.51
8000.	25.51	25.58	25.64	25.71	25.84	25.97	26.23	26.49
10000.	25.49	25.55	25.62	25.69	25.82	25.95	26.21	26.47

Table 150. Molar volume in cm^3/g of andalusite, Al_2SiO_5 , to 1800 K and 10,000 bars. The tabulations are based on a fit of the thermophysical and thermochemical data given in Section 1.5.5.

Pressure (bars)	Temperature (K)							
	298.15	400.	500.	600.	800.	1000.	1400.	1800.
1.	51.56	51.68	51.81	51.96	52.27	52.60	53.28	53.97
500.	51.54	51.66	51.79	51.94	52.25	52.58	53.26	53.95
1000.	51.52	51.64	51.77	51.91	52.23	52.56	53.24	53.93
2000.	51.47	51.59	51.73	51.87	52.18	52.51	53.19	53.89
4000.	51.39	51.51	51.64	51.79	52.10	52.43	53.11	53.80
6000.	51.31	51.43	51.56	51.71	52.02	52.35	53.03	53.72
8000.	51.23	51.35	51.48	51.63	51.94	52.27	52.95	53.64
10000.	51.15	51.27	51.40	51.55	51.86	52.19	52.87	53.56

Table 151. Molar volume in cm^3/g of kyanite, Al_2SiO_5 , to 1800 K and 10,000 bars. The tabulations are based on a fit of the thermophysical and thermochemical data given in Section 1.5.5.

Pressure (bars)	Temperature (K)							
	298.15	400.	500.	600.	800.	1000.	1400.	1800.
1.	44.21	44.31	44.42	44.53	44.76	45.01	45.50	46.00
500.	44.19	44.29	44.40	44.51	44.75	44.99	45.48	45.98
1000.	44.17	44.28	44.39	44.50	44.73	44.97	45.47	45.97
2000.	44.14	44.25	44.35	44.47	44.70	44.94	45.44	45.93
4000.	44.08	44.19	44.30	44.41	44.64	44.88	45.38	45.88
6000.	44.03	44.13	44.24	44.35	44.59	44.83	45.32	45.82
8000.	43.98	44.08	44.19	44.30	44.54	44.78	45.27	45.77
10000.	43.93	44.03	44.14	44.25	44.49	44.73	45.22	45.72

Table 152. Molar volume in cm^3/g of sillimanite, Al_2SiO_5 , to 1800 K and 10,000 bars. The tabulations are based on a fit of the thermophysical and thermochemical data given in Section 1.5.5.

Pressure (bars)	Temperature (K)							
	298.15	400.	500.	600.	800.	1000.	1400.	1800.
1.	50.02	50.07	50.13	50.20	50.36	50.53	50.90	51.27
500.	50.00	50.05	50.11	50.18	50.34	50.51	50.88	51.25
1000.	49.98	50.03	50.09	50.16	50.32	50.49	50.86	51.23
2000.	49.94	49.99	50.05	50.12	50.28	50.46	50.82	51.19
4000.	49.87	49.92	49.98	50.05	50.21	50.38	50.74	51.11
6000.	49.79	49.84	49.90	49.97	50.13	50.31	50.67	51.04
8000.	49.72	49.77	49.83	49.90	50.06	50.23	50.60	50.97
10000.	49.65	49.70	49.76	49.83	49.99	50.16	50.52	50.89

Table 153. Molar volume in cm^3/g of kaolinite, $\text{Al}_2\text{Si}_2\text{O}_5(\text{OH})_4$, to 1000 K and 10,000 bars. The tabulations are based on a fit of the thermophysical and thermochemical data given in Section 1.5.5.

Pressure (bars)	Temperature (K)							
	298.15	400.	500.	600.	800.	1000.	1400.	1800.
1.	99.48	99.85	100.20	100.56	101.28	101.99	---	---
500.	99.28	99.65	100.00	100.36	101.07	101.79	---	---
1000.	99.08	99.44	99.80	100.16	100.87	101.58	---	---
2000.	98.68	99.04	99.40	99.75	100.47	101.18	---	---
4000.	97.87	98.23	98.59	98.94	99.66	100.37	---	---
6000.	97.06	97.42	97.78	98.13	98.85	99.56	---	---
8000.	96.25	96.61	96.97	97.33	98.04	98.75	---	---
10000.	95.44	95.80	96.16	96.52	97.23	97.95	---	---

Table 154. Molar volume in cm^3/g of dickite, $\text{Al}_2\text{Si}_2\text{O}_5(\text{OH})_4$, to 1000 K and 10,000 bars. The tabulations are based on a fit of the thermophysical and thermochemical data given in Section 1.5.5.

Pressure (bars)	Temperature (K)							
	298.15	400.	500.	600.	800.	1000.	1400.	1800.
1.	99.30	99.68	100.05	100.42	101.16	101.90	---	---
500.	99.10	99.48	99.85	100.22	100.96	101.70	---	---
1000.	98.90	99.28	99.65	100.02	100.76	101.50	---	---
2000.	98.50	98.88	99.25	99.62	100.36	101.10	---	---
4000.	97.70	98.08	98.45	98.82	99.56	100.30	---	---
6000.	96.90	97.28	97.65	98.02	98.76	99.50	---	---
8000.	96.10	96.48	96.85	97.22	97.96	98.70	---	---
10000.	95.30	95.68	96.05	96.42	97.16	97.90	---	---

Table 155. Molar volume in cm^3/g of halloysite, $\text{Al}_2\text{Si}_2\text{O}_5(\text{OH})_4$, to 1000 K and 10,000 bars. The tabulations are based on a fit of the thermophysical and thermochemical data given in Section 1.5.5.

Pressure (bars)	Temperature (K)							
	298.15	400.	500.	600.	800.	1000.	1400.	1800.
1.	99.40	99.78	100.15	100.52	101.26	102.00	---	---
500.	99.20	99.58	99.95	100.32	101.06	101.80	---	---
1000.	99.00	99.38	99.75	100.12	100.86	101.60	---	---
2000.	98.60	98.98	99.35	99.72	100.46	101.20	---	---
4000.	97.80	98.18	98.55	98.92	99.66	100.40	---	---
6000.	97.00	97.38	97.75	98.12	98.86	99.60	---	---
8000.	96.20	96.58	96.95	97.32	98.06	98.80	---	---
10000.	95.40	95.78	96.15	96.52	97.26	98.00	---	---

Table 156. Molar volume in cm^3/g of pyrophyllite, $\text{Al}_2\text{Si}_4\text{O}_{10}(\text{OH})_2$, to 1000 K and 10,000 bars. The tabulations are based on a fit of the thermophysical and thermochemical data given in Section 1.5.5.

Pressure (bars)	Temperature (K)							
	298.15	400.	500.	600.	800.	1000.	1400.	1800.
1.	127.64	127.73	127.84	127.97	128.26	128.58	---	---
500.	127.63	127.72	127.83	127.96	128.25	128.58	---	---
1000.	127.63	127.72	127.83	127.96	128.25	128.57	---	---
2000.	127.62	127.71	127.82	127.95	128.25	128.56	---	---
4000.	127.61	127.70	127.81	127.94	128.23	128.55	---	---
6000.	127.59	127.68	127.80	127.92	128.22	128.54	---	---
8000.	127.58	127.67	127.78	127.91	128.20	128.52	---	---
10000.	127.56	127.65	127.77	127.90	128.19	128.51	---	---

Table 157. Molar volume in cm^3/g of Ca-Al clinopyroxene, $\text{CaAl}_2\text{SiO}_6$, to 1800 K and 10,000 bars. The tabulations are based on a fit of the thermophysical and thermochemical data given in Section 1.5.5.

Pressure (bars)	Temperature (K)							
	298.15	400.	500.	600.	800.	1000.	1400.	1800.
1.	63.58	63.72	63.88	64.04	64.39	64.75	65.50	66.25
500.	63.55	63.70	63.85	64.02	64.37	64.73	65.48	66.23
1000.	63.53	63.67	63.83	63.99	64.34	64.71	65.45	66.21
2000.	63.48	63.62	63.78	63.94	64.29	64.66	65.40	66.16
4000.	63.38	63.53	63.68	63.85	64.20	64.56	65.31	66.06
6000.	63.28	63.43	63.58	63.75	64.10	64.46	65.21	65.96
8000.	63.19	63.33	63.49	63.65	64.00	64.36	65.11	65.87
10000.	63.09	63.23	63.39	63.55	63.90	64.27	65.01	65.77

Table 158. molar volume in cm^3/g of anorthite, $\text{CaAl}_2\text{Si}_2\text{O}_8$, to 1800 K and 10,000 bars. The tabulations are based on a fit of the thermophysical and thermochemical data given in Section 1.5.5.

Pressure (bars)	Temperature (K)							
	298.15	400.	500.	600.	800.	1000.	1400.	1800.
1.	100.73	100.86	100.99	101.11	101.37	101.63	102.14	102.65
500.	100.66	100.79	100.92	101.05	101.30	101.56	102.07	102.59
1000.	100.60	100.73	100.85	100.98	101.24	101.50	102.01	102.52
2000.	100.46	100.59	100.72	100.85	101.11	101.36	101.88	102.39
4000.	100.20	100.33	100.46	100.59	100.85	101.10	101.62	102.13
6000.	99.95	100.08	100.20	100.33	100.59	100.84	101.36	101.87
8000.	99.69	99.82	99.95	100.08	100.33	100.59	101.10	101.61
10000.	99.43	99.57	99.69	99.82	100.08	100.33	100.85	101.36

Table 159. Molar volume in cm^3/g of margarite, $\text{CaAl}_4\text{Si}_2\text{O}_{10}(\text{OH})_2$, to 1000 K and 10,000 bars. The tabulations are based on a fit of the thermophysical and thermochemical data given in Section 1.5.5.

Pressure (bars)	Temperature (K)							
	298.15	400.	500.	600.	800.	1000.	1400.	1800.
1.	133.77	134.08	134.39	134.69	135.30	135.91	---	---
500.	133.59	133.90	134.20	134.51	135.12	135.73	---	---
1000.	133.40	133.71	134.02	134.32	134.93	135.54	---	---
2000.	133.04	133.35	133.65	133.96	134.57	135.17	---	---
4000.	132.30	132.61	132.92	133.22	133.83	134.44	---	---
6000.	131.57	131.88	132.18	132.49	133.10	133.70	---	---
8000.	130.83	131.14	131.45	131.75	132.36	132.97	---	---
10000.	130.10	130.41	130.71	131.02	131.62	132.23	---	---

Table 160. Molar volume in cm^3/g of calcite, CaCO_3 , to 1800 K and 10,000 bars. The tabulations are based on a fit of the thermophysical and thermochemical data given in Section 1.5.5.

Pressure (bars)	Temperature (K)							
	298.15	400.	500.	600.	800.	1000.	1400.	1800.
1.	36.78	36.79	36.81	36.83	36.88	36.93	37.02	37.12
500.	36.75	36.77	36.79	36.81	36.85	36.90	37.00	37.10
1000.	36.72	36.74	36.76	36.78	36.82	36.87	36.97	37.07
2000.	36.67	36.69	36.70	36.72	36.77	36.82	36.92	37.02
4000.	36.56	36.58	36.60	36.62	36.66	36.71	36.81	36.91
6000.	36.46	36.47	36.49	36.51	36.56	36.61	36.70	36.80
8000.	36.35	36.37	36.39	36.41	36.45	36.50	36.60	36.70
10000.	36.25	36.27	36.29	36.31	36.35	36.40	36.50	36.50

Table 161. Molar volume in cm^3/g of aragonite, CaCO_3 , to 1800 K and 10,000 bars. The tabulations are based on a fit of the thermophysical and thermochemical data given in Section 1.5.5.

Pressure (bars)	Temperature (K)							
	298.15	400.	500.	600.	800.	1000.	1400.	1800.
1.	34.14	34.14	34.15	34.15	34.16	34.16	34.18	34.19
500.	34.14	34.14	34.15	34.15	34.16	34.16	34.18	34.19
1000.	34.14	34.14	34.14	34.15	34.15	34.16	34.17	34.19
2000.	34.13	34.13	34.14	34.14	34.14	34.15	34.16	34.18
4000.	34.09	34.10	34.10	34.10	34.11	34.11	34.13	34.14
6000.	34.03	34.03	34.03	34.04	34.04	34.05	34.06	34.08
8000.	33.94	33.94	33.95	33.95	33.96	33.96	33.98	33.99
10000.	33.83	33.83	33.84	33.84	33.84	33.85	33.87	33.88

Table 162. Molar volume in cm^3/g of lime, CaO , to 1800 K and 10,000 bars. The tabulations are based on a fit of the thermophysical and thermochemical data given in Section 1.5.5.

Pressure (bars)	Temperature (K)							
	298.15	400.	500.	600.	800.	1000.	1400.	1800.
1.	16.76	16.81	16.87	16.94	17.08	17.23	17.53	17.84
500.	16.75	16.81	16.86	16.93	17.07	17.22	17.52	17.83
1000.	16.74	16.80	16.86	16.92	17.06	17.21	17.51	17.82
2000.	16.73	16.78	16.84	16.90	17.04	17.19	17.49	17.81
4000.	16.69	16.74	16.80	16.87	17.01	17.16	17.46	17.77
6000.	16.66	16.71	16.77	16.84	16.98	17.12	17.43	17.74
8000.	16.63	16.68	16.74	16.81	16.95	17.09	17.40	17.71
10000.	16.60	16.65	16.71	16.78	16.92	17.06	17.37	17.68

Table 163. Molar volume in cm^3/g of wollastonite, CaSiO_3 , to 1800 K and 10,000 bars. The tabulations are based on a fit of the thermophysical and thermochemical data given in Section 1.5.5.

Pressure (bars)	Temperature (K)							
	298.15	400.	500.	600.	800.	1000.	1400.	1800.
1.	39.79	39.98	40.12	40.24	40.42	40.56	40.77	40.97
500.	39.77	39.95	40.10	40.21	40.39	40.53	40.75	40.94
1000.	39.74	39.93	40.07	40.19	40.36	40.50	40.72	40.91
2000.	39.69	39.87	40.02	40.13	40.31	40.45	40.67	40.86
4000.	39.58	39.77	39.91	40.03	40.21	40.34	40.56	40.76
6000.	39.48	39.67	39.81	39.93	40.11	40.24	40.46	40.66
8000.	39.38	39.57	39.71	39.83	40.01	40.15	40.37	40.56
10000.	39.29	39.48	39.62	39.74	39.92	40.05	40.27	40.47

Table 164. Molar volume in cm^3/g of cyclowollastonite, CaSiO_3 , to 1800 K and 10,000 bars. The tabulations are based on a fit of the thermophysical and thermochemical data given in Section 1.5.5.

Pressure (bars)	Temperature (K)							
	298.15	400.	500.	600.	800.	1000.	1400.	1800.
1.	40.16	40.20	40.25	40.31	40.45	40.60	40.92	41.24
500.	40.12	40.16	40.21	40.27	40.40	40.56	40.88	41.20
1000.	40.08	40.12	40.17	40.23	40.36	40.52	40.84	41.16
2000.	40.00	40.04	40.09	40.15	40.29	40.44	40.76	41.09
4000.	39.85	39.89	39.94	40.00	40.14	40.29	40.61	40.94
6000.	39.71	39.75	39.80	39.86	40.00	40.15	40.47	40.80
8000.	39.58	39.62	39.67	39.73	39.87	40.02	40.34	40.67
10000.	39.46	39.50	39.55	39.61	39.75	39.90	40.22	40.55

Table 165. molar volume in cm^3/g of bicchulite, $\text{Ca}_2\text{Al}_2\text{SiO}_6(\text{OH})_2$, to 1000 K and 10,000 bars. The tabulations are based on a fit of the thermophysical and thermochemical data given in Section 1.5.5.

Pressure (bars)	Temperature (K)							
	298.15	400.	500.	600.	800.	1000.	1400.	1800.
1.	103.55	103.93	104.31	104.68	105.43	106.19	---	---
500.	103.48	103.86	104.24	104.62	105.37	106.12	---	---
1000.	103.41	103.80	104.17	104.55	105.30	106.05	---	---
2000.	103.28	103.66	104.04	104.42	105.17	105.92	---	---
4000.	103.02	103.40	103.77	104.15	104.90	105.65	---	---
6000.	102.75	103.13	103.51	103.88	104.64	105.39	---	---
8000.	102.48	102.87	103.24	103.62	104.37	105.12	---	---
10000.	102.22	102.60	102.98	103.35	104.10	104.86	---	---

Table 166. Molar volume in cm^3/g of gehlenite, $\text{Ca}_2\text{Al}_2\text{SiO}_7$, to 1800 K and 10,000 bars. The tabulations are based on a fit of the thermophysical and thermochemical data given in Section 1.5.5.

Pressure (bars)	Temperature (K)							
	298.15	400.	500.	600.	800.	1000.	1400.	1800.
1.	90.25	90.50	90.75	91.00	91.50	91.99	92.99	93.98
500.	90.23	90.48	90.73	90.98	91.48	91.97	92.97	93.96
1000.	90.21	90.46	90.71	90.96	91.46	91.95	92.95	93.94
2000.	90.17	90.42	90.67	90.92	91.41	91.91	92.91	93.90
4000.	90.08	90.34	90.59	90.84	91.33	91.83	92.82	93.82
6000.	90.00	90.26	90.50	90.75	91.25	91.75	92.74	93.74
8000.	89.92	90.17	90.42	90.67	91.17	91.67	92.66	93.66
10000.	89.84	90.09	90.34	90.59	91.09	91.58	92.58	93.57

Table 167. Molar volume in cm^3/g of prehnite, $\text{Ca}_2\text{Al}_2\text{Si}_3\text{O}_{10}(\text{OH})_2$, to 1000 K and 10,000 bars. The tabulations are based on a fit of the thermophysical and thermochemical data given in Section 1.5.5.

Pressure (bars)	Temperature (K)							
	298.15	400.	500.	600.	800.	1000.	1400.	1800.
1.	140.43	140.96	141.47	141.98	143.00	144.03	---	---
500.	140.32	140.84	141.36	141.87	142.89	143.92	---	---
1000.	140.21	140.73	141.24	141.76	142.78	143.81	---	---
2000.	139.99	140.51	141.02	141.53	142.56	143.58	---	---
4000.	139.54	140.06	140.57	141.08	142.11	143.13	---	---
6000.	139.09	139.61	140.12	140.64	141.66	142.69	---	---
8000.	138.64	139.16	139.68	140.19	141.21	142.24	---	---
10000.	138.19	138.72	139.23	139.74	140.77	141.79	---	---

Table 168. Molar volume in cm^3/g of zoisite, $\text{Ca}_2\text{Al}_3\text{Si}_3\text{O}_{12}(\text{OH})$, to 1000 K and 10,000 bars. The tabulations are based on a fit of the thermophysical and thermochemical data given in Section 1.5.5.

Pressure (bars)	Temperature (K)							
	298.15	400.	500.	600.	800.	1000.	1400.	1800.
1.	136.72	137.23	137.73	138.22	139.22	140.21	---	---
500.	136.64	137.14	137.64	138.14	139.14	140.13	---	---
1000.	136.55	137.06	137.56	138.06	139.05	140.05	---	---
2000.	136.39	136.90	137.39	137.89	138.89	139.88	---	---
4000.	136.06	136.57	137.06	137.56	138.56	139.55	---	---
6000.	135.73	136.23	136.73	137.23	138.23	139.22	---	---
8000.	135.40	135.90	136.40	136.90	137.89	138.89	---	---
10000.	135.06	135.57	136.07	136.57	137.56	138.56	---	---

Table 169. Molar volume in cm^3/g of alpha- Ca_2SiO_4 to 1800 K and 10,000 bars. The tabulations are based on a fit of the thermophysical and thermochemical data given in Section 1.5.5.

Pressure (bars)	Temperature (K)							
	298.15	400.	500.	600.	800.	1000.	1400.	1800.
1.	52.30	52.49	52.68	52.87	53.25	53.63	54.39	55.16
500.	52.28	52.48	52.67	52.86	53.24	53.62	54.38	55.14
1000.	52.27	52.46	52.65	52.84	53.22	53.60	54.36	55.12
2000.	52.23	52.43	52.62	52.81	53.19	53.57	54.33	55.09
4000.	52.17	52.36	52.55	52.74	53.12	53.50	54.26	55.02
6000.	52.10	52.29	52.48	52.67	53.05	53.43	54.19	54.96
8000.	52.04	52.23	52.42	52.61	52.99	53.37	54.13	54.89
10000.	51.97	52.16	52.35	52.54	52.92	53.30	54.06	54.82

Table 170. Molar volume in cm^3/g of bredigite, Ca_2SiO_4 , to 1800 K and 10,000 bars. The tabulations are based on a fit of the thermophysical and thermochemical data given in Section 1.5.5.

Pressure (bars)	Temperature (K)							
	298.15	400.	500.	600.	800.	1000.	1400.	1800.
1.	52.00	52.19	52.38	52.57	52.95	53.33	54.09	54.85
500.	51.98	52.18	52.37	52.56	52.94	53.32	54.08	54.84
1000.	51.97	52.16	52.35	52.54	52.92	53.30	54.06	54.82
2000.	51.93	52.13	52.32	52.51	52.89	53.27	54.03	54.79
4000.	51.87	52.06	52.25	52.44	52.82	53.20	53.96	54.72
6000.	51.80	52.00	52.19	52.38	52.76	53.14	53.90	54.66
8000.	51.74	51.93	52.12	52.31	52.69	53.07	53.83	54.59
10000.	51.67	51.86	52.05	52.24	52.62	53.00	53.76	54.52

Table 171. Molar volume in cm^3/g of Ca-olivine, Ca_2SiO_4 , to 1800 K and 10,000 bars. The tabulations are based on a fit of the thermophysical and thermochemical data given in Section 1.5.5.

Pressure (bars)	Temperature (K)							
	298.15	400.	500.	600.	800.	1000.	1400.	1800.
1.	59.11	59.31	59.51	59.71	60.11	60.51	61.31	62.11
500.	59.09	59.30	59.50	59.70	60.10	60.50	61.30	62.10
1000.	59.07	59.28	59.48	59.68	60.08	60.48	61.28	62.08
2000.	59.04	59.24	59.44	59.64	60.04	60.44	61.24	62.04
4000.	58.97	59.17	59.37	59.57	59.97	60.37	61.17	61.97
6000.	58.90	59.10	59.30	59.50	59.90	60.30	61.10	61.90
8000.	58.83	59.03	59.23	59.43	59.83	60.23	61.03	61.83
10000.	58.76	58.96	59.16	59.36	59.76	60.16	60.96	61.76

Table 172. Molar volume in cm^3/g of larnite, Ca_2SiO_4 , to 1800 K and 10,000 bars. The tabulations are based on a fit of the thermophysical and thermochemical data given in Section 1.5.5.

Pressure (bars)	Temperature (K)							
	298.15	400.	500.	600.	800.	1000.	1400.	1800.
1.	51.60	51.66	51.73	51.80	51.95	52.11	52.43	52.76
500.	51.58	51.64	51.71	51.78	51.93	52.09	52.41	52.74
1000.	51.57	51.63	51.69	51.77	51.92	52.07	52.40	52.72
2000.	51.54	51.60	51.66	51.73	51.88	52.04	52.36	52.69
4000.	51.47	51.53	51.60	51.67	51.82	51.98	52.30	52.63
6000.	51.41	51.47	51.53	51.60	51.75	51.91	52.23	52.56
8000.	51.34	51.40	51.47	51.54	51.69	51.85	52.17	52.50
10000.	51.28	51.34	51.40	51.47	51.62	51.78	52.10	52.43

Table 173. Molar volume in cm^3/g of grossular, $\text{Ca}_3\text{Al}_2\text{Si}_3\text{O}_{12}$, to 1800 K and 10,000 bars. The tabulations are based on a fit of the thermophysical and thermochemical data given in Section 1.5.5.

Pressure (bars)	Temperature (K)							
	298.15	400.	500.	600.	800.	1000.	1400.	1800.
1.	125.19	125.47	125.77	126.07	126.71	127.36	128.69	130.03
500.	125.15	125.43	125.72	126.03	126.66	127.32	128.64	129.98
1000.	125.11	125.39	125.68	125.99	126.62	127.27	128.60	129.94
2000.	125.02	125.30	125.59	125.90	126.53	127.19	128.51	129.85
4000.	124.85	125.13	125.42	125.73	126.36	127.01	128.34	129.68
6000.	124.68	124.96	125.25	125.56	126.19	126.84	128.17	129.51
8000.	124.51	124.79	125.08	125.39	126.02	126.68	128.00	129.34
10000.	124.34	124.62	124.92	125.22	125.86	126.51	127.84	129.18

Table 174. Molar volume in cm^3/g of hatrurite, Ca_3SiO_5 , to 1800 K and 10,000 bars. The tabulations are based on a fit of the thermophysical and thermochemical data given in Section 1.5.5.

Pressure (bars)	Temperature (K)							
	298.15	400.	500.	600.	800.	1000.	1400.	1800.
1.	72.74	72.80	72.87	72.95	73.13	73.32	73.73	74.14
500.	72.72	72.78	72.85	72.93	73.11	73.30	73.71	74.12
1000.	72.70	72.76	72.83	72.91	73.09	73.28	73.69	74.10
2000.	72.66	72.72	72.79	72.87	73.05	73.24	73.65	74.06
4000.	72.58	72.64	72.71	72.79	72.97	73.16	73.57	73.98
6000.	72.50	72.56	72.63	72.71	72.89	73.08	73.49	73.90
8000.	72.42	72.48	72.55	72.63	72.81	73.00	73.41	73.82
10000.	72.34	72.40	72.47	72.55	72.73	72.92	73.33	73.74

Table 175. Molar volume in cm^3/g of rankinite, $\text{Ca}_3\text{Si}_2\text{O}_7$, to 1800 K and 10,000 bars. The tabulations are based on a fit of the thermophysical and thermochemical data given in Section 1.5.5.

Pressure (bars)	Temperature (K)							
	298.15	400.	500.	600.	800.	1000.	1400.	1800.
1.	96.50	96.62	96.73	96.86	97.11	97.37	97.91	98.45
500.	96.46	96.58	96.69	96.82	97.07	97.33	97.87	98.41
1000.	96.42	96.54	96.65	96.78	97.03	97.29	97.83	98.37
2000.	96.34	96.46	96.57	96.70	96.95	97.21	97.75	98.29
4000.	96.18	96.30	96.41	96.54	96.79	97.05	97.59	98.13
6000.	96.02	96.14	96.25	96.38	96.63	96.89	97.43	97.97
8000.	95.86	95.98	96.09	96.22	96.47	96.73	97.27	97.81
10000.	95.70	95.82	95.93	96.06	96.31	96.57	97.11	97.65

Table 176. Molar volume in cm^3/g of meionite, $\text{Ca}_4\text{Al}_6\text{Si}_6\text{O}_{24}(\text{CO}_3)$, to 1800 K and 10,000 bars. The tabulations are based on a fit of the thermophysical and thermochemical data given in Section 1.5.5.

Pressure (bars)	Temperature (K)							
	298.15	400.	500.	600.	800.	1000.	1400.	1800.
1.	337.60	338.17	338.73	339.30	340.42	341.55	343.80	346.05
500.	337.38	337.95	338.51	339.08	340.20	341.33	343.58	345.84
1000.	337.16	337.73	338.30	338.86	339.99	341.11	343.36	345.62
2000.	336.72	337.30	337.86	338.42	339.55	340.68	342.93	345.18
4000.	335.85	336.42	336.99	337.55	338.68	339.80	342.05	344.31
6000.	334.98	335.55	336.11	336.68	337.80	338.93	341.18	343.43
8000.	334.10	334.68	335.24	335.80	336.93	338.06	340.31	342.56
10000.	333.23	333.80	334.37	334.93	336.06	337.18	339.44	341.69

Table 177. Molar volume in cm^3/g of wustite, Fe_{947}O , to 1800 K and 10,000 bars. The tabulations are based on a fit of the thermophysical and thermochemical data given in Section 1.5.5.

Pressure (bars)	Temperature (K)							
	298.15	400.	500.	600.	800.	1000.	1400.	1800.
1.	12.04	12.04	12.04	12.04	12.04	12.04	12.04	12.04
500.	12.04	12.04	12.04	12.04	12.04	12.04	12.04	12.04
1000.	12.03	12.03	12.03	12.03	12.03	12.03	12.03	12.03
2000.	12.02	12.02	12.02	12.02	12.02	12.02	12.02	12.02
4000.	12.01	12.01	12.01	12.01	12.01	12.01	12.01	12.01
6000.	11.99	11.99	11.99	11.99	11.99	11.99	11.99	11.99
8000.	11.97	11.97	11.97	11.97	11.97	11.97	11.97	11.97
10000.	11.96	11.96	11.96	11.96	11.96	11.96	11.96	11.96

Table 178. Molar volume in cm^3/g of ferrosilite, FeSiO_3 , to 1800 K and 10,000 bars. The tabulations are based on a fit of the thermophysical and thermochemical data given in Section 1.5.5.

Pressure (bars)	Temperature (K)							
	298.15	400.	500.	600.	800.	1000.	1400.	1800.
1.	32.99	33.11	33.23	33.35	33.60	33.84	34.32	34.81
500.	32.95	33.08	33.20	33.32	33.56	33.80	34.29	34.77
1000.	32.92	33.04	33.16	33.28	33.53	33.77	34.25	34.74
2000.	32.85	32.97	33.09	33.21	33.45	33.70	34.18	34.67
4000.	32.70	32.83	32.95	33.07	33.31	33.55	34.04	34.52
6000.	32.56	32.68	32.81	32.93	33.17	33.41	33.90	34.38
8000.	32.42	32.54	32.66	32.78	33.03	33.27	33.75	34.24
10000.	32.28	32.40	32.52	32.64	32.88	33.13	33.61	34.10

Table 179. Molar volume in cm^3/g of hematite, Fe_2O_3 , to 1800 K and 10,000 bars. The tabulations are based on a fit of the thermophysical and thermochemical data given in Section 1.5.5.

Pressure (bars)	Temperature (K)							
	298.15	400.	500.	600.	800.	1000.	1400.	1800.
1.	30.28	30.39	30.51	30.63	30.86	31.10	31.57	32.03
500.	30.27	30.39	30.50	30.62	30.85	31.09	31.56	32.03
1000.	30.26	30.38	30.49	30.61	30.85	31.08	31.55	32.02
2000.	30.24	30.36	30.48	30.59	30.83	31.06	31.53	32.00
4000.	30.21	30.33	30.44	30.56	30.79	31.03	31.50	31.97
6000.	30.17	30.29	30.41	30.53	30.76	31.00	31.46	31.93
8000.	30.14	30.26	30.38	30.49	30.73	30.96	31.43	31.90
10000.	30.11	30.23	30.35	30.46	30.70	30.93	31.40	31.87

Table 180. Molar volume in cm^3/g of fayalite, Fe_2SiO_4 , to 1800 K and 10,000 bars. The tabulations are based on a fit of the thermophysical and thermochemical data given in Section 1.5.5.

Pressure (bars)	Temperature (K)							
	298.15	400.	500.	600.	800.	1000.	1400.	1800.
1.	46.15	46.30	46.45	46.60	46.89	47.19	47.79	48.38
500.	46.13	46.28	46.43	46.58	46.88	47.17	47.77	48.36
1000.	46.11	46.26	46.41	46.56	46.86	47.16	47.75	48.35
2000.	46.08	46.23	46.38	46.53	46.82	47.12	47.72	48.31
4000.	46.01	46.16	46.31	46.46	46.75	47.05	47.65	48.24
6000.	45.94	46.09	46.24	46.39	46.68	46.98	47.58	48.17
8000.	45.87	46.02	46.17	46.32	46.61	46.91	47.51	48.10
10000.	45.80	45.95	46.10	46.25	46.54	46.84	47.44	48.03

Table 181. Molar volume in cm^3/g of magnetite, Fe_3O_4 , to 1800 K and 10,000 bars. The tabulations are based on a fit of the thermophysical and thermochemical data given in Section 1.5.5.

Pressure (bars)	Temperature (K)							
	298.15	400.	500.	600.	800.	1000.	1400.	1800.
1.	44.52	44.57	44.61	44.66	44.74	44.54	44.54	44.54
500.	44.51	44.56	44.60	44.64	44.73	44.54	44.54	44.54
1000.	44.50	44.54	44.59	44.63	44.72	44.54	44.54	44.54
2000.	44.47	44.52	44.56	44.60	44.69	44.54	44.54	44.54
4000.	44.42	44.46	44.51	44.55	44.64	44.54	44.54	44.54
6000.	44.37	44.41	44.46	44.50	44.59	44.54	44.54	44.54
8000.	44.32	44.36	44.41	44.45	44.54	44.54	44.54	44.54
10000.	44.27	44.31	44.35	44.40	44.49	44.54	44.54	44.54

Table 182. Molar volume in cm^3/g of water and H_2O (real gas) to 1400 K and 10,000 bars. The tabulation is based on data cited in Section 1.5.5.

Pressure (bars)	Temperature (K)							
	298.15	400.	500.	600.	800.	1000.	1200.	1400.
1.	18.068	32460.	40854.	49132.	65601.	82035.	98458.	114876.
500.	17.690	18.744	20.732	24.520	82.569	145.900	191.664	231.875
1000.	17.358	18.350	20.034	22.762	37.363	67.766	94.032	116.557
2000.	16.809	17.714	19.044	20.904	27.152	37.597	49.725	61.299
4000.	----	16.786	17.767	18.970	22.194	26.499	31.477	36.668
6000.	----	16.114	16.906	17.813	20.035	22.782	25.863	29.086
8000.	----	15.592	16.255	16.986	18.681	20.690	22.913	25.235
10000.	----	15.170	15.732	16.342	17.704	19.274	20.997	22.802

Table 183. Molar volume in cm^3/g of magnesite, MgCO_3 , to 1800 K and 10,000 bars. The tabulations are based on a fit of the thermophysical and thermochemical data given in Section 1.5.5.

Pressure (bars)	Temperature (K)							
	298.15	400.	500.	600.	800.	1000.	1400.	1800.
1.	28.02	28.08	28.13	28.19	28.30	28.42	28.64	28.87
500.	28.00	28.06	28.11	28.17	28.28	28.40	28.62	28.85
1000.	27.98	28.04	28.10	28.15	28.27	28.38	28.61	28.83
2000.	27.95	28.00	28.06	28.12	28.23	28.34	28.57	28.80
4000.	27.87	27.93	27.99	28.04	28.16	28.27	28.50	28.72
6000.	27.80	27.86	27.92	27.97	28.09	28.20	28.43	28.65
8000.	27.73	27.79	27.84	27.90	28.01	28.13	28.35	28.58
10000.	27.66	27.72	27.77	27.83	27.94	28.06	28.28	28.51

Table 184. Molar volume in cm^3/g of periclase, MgO , to 1800 K and 10,000 bars. The tabulations are based on a fit of the thermophysical and thermochemical data given in Section 1.5.5.

Pressure (bars)	Temperature (K)							
	298.15	400.	500.	600.	800.	1000.	1400.	1800.
1.	11.24	11.29	11.33	11.37	11.45	11.54	11.70	11.87
500.	11.24	11.28	11.33	11.37	11.45	11.53	11.70	11.87
1000.	11.24	11.28	11.32	11.36	11.45	11.53	11.70	11.87
2000.	11.23	11.27	11.32	11.36	11.44	11.53	11.69	11.86
4000.	11.22	11.26	11.30	11.35	11.43	11.51	11.68	11.85
6000.	11.21	11.25	11.29	11.33	11.42	11.50	11.67	11.84
8000.	11.20	11.24	11.28	11.32	11.41	11.49	11.66	11.82
10000.	11.18	11.23	11.27	11.31	11.39	11.48	11.64	11.81

Table 185. Molar volume in cm^3/g of brucite, $\text{Mg}(\text{OH})_2$, to 1000 K and 10,000 bars. The tabulations are based on a fit of the thermophysical and thermochemical data given in Section 1.5.5.

Pressure (bars)	Temperature (K)							
	298.15	400.	500.	600.	800.	1000.	1400.	1800.
1.	24.63	24.69	24.74	24.79	24.90	25.01	---	---
500.	24.63	24.68	24.74	24.79	24.90	25.00	---	---
1000.	24.62	24.68	24.73	24.79	24.89	25.00	---	---
2000.	24.62	24.67	24.73	24.78	24.89	24.99	---	---
4000.	24.61	24.66	24.71	24.77	24.87	24.98	---	---
6000.	24.59	24.65	24.70	24.76	24.86	24.97	---	---
8000.	24.58	24.64	24.69	24.74	24.85	24.96	---	---
10000.	24.57	24.63	24.68	24.73	24.84	24.95	---	---

Table 186. Molar volume in cm^3/g of clinoenstatite, MgSiO_3 , to 1800 K and 10,000 bars. The tabulations are based on a fit of the thermophysical and thermochemical data given in Section 1.5.5.

Pressure (bars)	Temperature (K)							
	298.15	400.	500.	600.	800.	1000.	1400.	1800.
1.	31.27	31.38	31.47	31.57	31.77	31.97	32.37	32.77
500.	31.26	31.36	31.46	31.56	31.76	31.96	32.36	32.76
1000.	31.25	31.35	31.45	31.55	31.75	31.95	32.35	32.74
2000.	31.22	31.32	31.42	31.52	31.72	31.92	32.32	32.72
4000.	31.16	31.27	31.37	31.47	31.66	31.86	32.26	32.66
6000.	31.11	31.21	31.31	31.41	31.61	31.81	32.21	32.61
8000.	31.05	31.16	31.26	31.36	31.56	31.75	32.15	32.55
10000.	31.00	31.10	31.20	31.30	31.50	31.70	32.10	32.50

Table 187. Molar volume in cm^3/g of enstatite, MgSiO_3 , to 1800 K and 10,000 bars. The tabulations are based on a fit of the thermophysical and thermochemical data given in Section 1.5.5.

Pressure (bars)	Temperature (K)							
	298.15	400.	500.	600.	800.	1000.	1400.	1800.
1.	31.35	31.42	31.50	31.58	31.77	31.97	32.38	32.80
500.	31.34	31.41	31.48	31.57	31.76	31.95	32.36	32.78
1000.	31.32	31.39	31.47	31.56	31.74	31.94	32.35	32.77
2000.	31.29	31.36	31.44	31.53	31.71	31.91	32.32	32.74
4000.	31.24	31.31	31.39	31.47	31.66	31.86	32.27	32.68
6000.	31.18	31.25	31.33	31.42	31.61	31.80	32.21	32.63
8000.	31.13	31.20	31.28	31.37	31.55	31.75	32.16	32.58
10000.	31.08	31.15	31.23	31.31	31.50	31.70	32.11	32.52

Table 188. Molar volume in cm^3/g of protoenstatite, MgSiO_3 , to 1800 K and 10,000 bars. The tabulations are based on a fit of the thermophysical and thermochemical data given in Section 1.5.5.

Pressure (bars)	Temperature (K)							
	298.15	400.	500.	600.	800.	1000.	1400.	1800.
1.	32.34	32.43	32.53	32.62	32.80	32.99	33.36	33.73
500.	32.33	32.42	32.51	32.61	32.79	32.98	33.35	33.72
1000.	32.31	32.41	32.50	32.59	32.78	32.96	33.34	33.71
2000.	32.29	32.38	32.47	32.57	32.75	32.94	33.31	33.68
4000.	32.23	32.33	32.42	32.52	32.70	32.89	33.26	33.63
6000.	32.18	32.28	32.37	32.46	32.65	32.84	33.21	33.58
8000.	32.13	32.23	32.32	32.41	32.60	32.78	33.16	33.53
10000.	32.08	32.17	32.27	32.36	32.55	32.73	33.10	33.48

Table 189. Molar volume in cm^3/g of forsterite, Mg_2SiO_4 , to 1800 K and 10,000 bars. The tabulations are based on a fit of the thermophysical and thermochemical data given in Section 1.5.5.

Pressure (bars)	Temperature (K)							
	298.15	400.	500.	600.	800.	1000.	1400.	1800.
1.	43.65	43.78	43.93	44.09	44.44	44.81	45.58	46.36
500.	43.63	43.76	43.91	44.07	44.42	44.79	45.56	46.34
1000.	43.62	43.75	43.89	44.05	44.40	44.78	45.54	46.32
2000.	43.58	43.71	43.86	44.02	44.37	44.74	45.51	46.29
4000.	43.51	43.64	43.78	43.94	44.29	44.67	45.43	46.21
6000.	43.43	43.56	43.71	43.87	44.22	44.59	45.36	46.14
8000.	43.36	43.49	43.64	43.80	44.15	44.52	45.29	46.07
10000.	43.30	43.43	43.57	43.74	44.08	44.46	45.22	46.01

Table 190. Molar volume in cm^3/g of chrysotile, $\text{Mg}_3\text{Si}_2\text{O}_5(\text{OH})_4$, to 1000 K and 10,000 bars. The tabulations are based on a fit of the thermophysical and thermochemical data given in Section 1.5.5.

Pressure (bars)	Temperature (K)							
	298.15	400.	500.	600.	800.	1000.	1400.	1800.
1.	107.28	107.49	107.70	107.90	108.32	108.74	---	---
500.	107.15	107.37	107.57	107.78	108.20	108.62	---	---
1000.	107.03	107.25	107.45	107.66	108.08	108.50	---	---
2000.	106.80	107.01	107.22	107.43	107.84	108.26	---	---
4000.	106.35	106.56	106.77	106.97	107.39	107.81	---	---
6000.	105.92	106.13	106.34	106.55	106.96	107.38	---	---
8000.	105.52	105.73	105.94	106.14	106.56	106.98	---	---
10000.	105.13	105.35	105.56	105.76	106.18	106.60	---	---

Table 191. Molar volume in cm^3/g of talc, $\text{Mg}_3\text{Si}_4\text{O}_{10}(\text{OH})_2$, to 1000 K and 10,000 bars. The tabulations are based on a fit of the thermophysical and thermochemical data given in Section 1.5.5.

Pressure (bars)	Temperature (K)							
	298.15	400.	500.	600.	800.	1000.	1400.	1800.
1.	135.95	136.25	136.54	136.84	137.42	138.00	---	---
500.	135.80	136.10	136.39	136.68	137.27	137.85	---	---
1000.	135.65	135.95	136.24	136.53	137.12	137.70	---	---
2000.	135.36	135.66	135.95	136.24	136.83	137.41	---	---
4000.	134.80	135.09	135.39	135.68	136.26	136.85	---	---
6000.	134.27	134.56	134.85	135.15	135.73	136.32	---	---
8000.	133.76	134.06	134.35	134.65	135.23	135.81	---	---
10000.	133.29	133.59	133.88	134.17	134.76	135.34	---	---

Table 192. Molar volume in cm^3/g of anthophyllite, $\text{Mg}_7\text{Si}_8\text{O}_{22}(\text{OH})_2$, to 1000 K and 10,000 bars. The tabulations are based on a fit of the thermophysical and thermochemical data given in Section 1.5.5.

Pressure (bars)	Temperature (K)							
	298.15	400.	500.	600.	800.	1000.	1400.	1800.
1.	263.86	263.94	264.02	264.09	264.25	264.40	---	---
500.	263.85	263.92	264.00	264.08	264.23	264.38	---	---
1000.	263.83	263.91	263.98	264.06	264.21	264.36	---	---
2000.	263.80	263.87	263.95	264.03	264.18	264.33	---	---
4000.	263.73	263.80	263.88	263.96	264.11	264.26	---	---
6000.	263.66	263.74	263.81	263.89	264.04	264.19	---	---
8000.	263.59	263.67	263.75	263.82	263.97	264.13	---	---
10000.	263.52	263.60	263.68	263.75	263.91	264.06	---	---

Table 193. Molar volume in cm^3/g of antigorite, $\text{Mg}_{48}\text{Si}_{34}\text{O}_{85}(\text{OH})_{62}$, to 1000 K and 10,000 bars. The tabulations are based on a fit of the thermophysical and thermochemical data given in Section 1.5.5.

Pressure (bars)	Temperature (K)							
	298.15	400.	500.	600.	800.	1000.	1400.	1800.
1.	1749.15	1752.81	1756.40	1759.99	1767.17	1774.35	---	---
500.	1747.23	1750.89	1754.48	1758.07	1765.25	1772.43	---	---
1000.	1745.33	1748.99	1752.58	1756.17	1763.35	1770.53	---	---
2000.	1741.61	1745.26	1748.85	1752.44	1759.63	1766.81	---	---
4000.	1734.47	1738.13	1741.72	1745.31	1752.49	1759.68	---	---
6000.	1727.74	1731.40	1734.99	1738.58	1745.76	1752.94	---	---
8000.	1721.38	1725.04	1728.63	1732.22	1739.40	1746.58	---	---
10000.	1715.37	1719.03	1722.62	1726.21	1733.39	1740.57	---	---

Table 194. Molar volume in cm^3/g of quartz, SiO_2 , to 1800 K and 10,000 bars. The tabulations are based on a fit of the thermophysical and thermochemical data given in Section 1.5.5.

Pressure (bars)	Temperature (K)							
	298.15	400.	500.	600.	800.	1000.	1400.	1800.
1.	22.59	22.72	22.86	23.00	23.27	23.58	23.58	23.58
500.	22.57	22.70	22.84	22.97	23.25	23.56	23.56	23.56
1000.	22.54	22.68	22.82	22.95	23.22	23.53	23.53	23.53
2000.	22.50	22.64	22.78	22.91	23.18	23.48	23.48	23.48
4000.	22.42	22.55	22.69	22.83	23.10	23.39	23.39	23.39
6000.	22.33	22.47	22.60	22.74	23.01	23.28	23.30	23.30
8000.	22.24	22.38	22.52	22.65	22.93	23.20	23.20	23.20
10000.	22.16	22.30	22.43	22.57	22.84	23.11	23.11	23.11

Table 195. Molar volume in cm^3/g of cristobalite, SiO_2 , to 1000 K and 10,000 bars. The tabulations are based on a fit of the thermophysical and thermochemical data given in Section 1.5.5.

Pressure (bars)	Temperature (K)							
	298.15	400.	500.	600.	800.	1000.	1400.	1800.
1.	25.81	26.07	26.33	27.36	27.40	27.44	27.53	27.61
500.	25.77	26.04	26.29	27.33	27.37	27.41	27.50	27.58
1000.	25.74	26.00	26.26	27.29	27.34	27.38	27.46	27.55
2000.	25.68	25.94	26.20	27.23	27.27	27.31	27.40	27.48
4000.	25.55	25.81	26.07	27.10	27.14	27.18	27.27	27.35
6000.	25.42	25.68	25.94	26.97	27.01	27.05	27.14	27.22
8000.	25.29	25.55	25.81	26.84	26.88	26.93	27.01	27.10
10000.	25.16	25.42	25.68	26.71	26.75	26.80	26.88	26.97

1.5.5. Summaries of Data Sources, Standard State Properties, and Fitted Functions Describing Mineral Thermodynamics and Thermophysical Properties

The sources of data used for the evaluation of the properties, both thermophysical and thermochemical, are given in this section. They are arranged by chemical formula in the same order as they appear in the previous section containing the data tables.

The constants that are to be used in the algebraic functions given in section 1.5.3 are given below in section 1.5.49.

1.5.5.1. Al, aluminum (formula weight = 28.892 g/mol)

The properties of aluminum were taken from the JANAF thermochemical data^a. The molar volume of aluminum was not needed in this study and therefore was not evaluated.

1.5.5.2. Al₂O₃H (formula weight = 59.989 g/mol)

1.5.5.2.1. Boehmite

Tables 196 and 197 contain the data used in the final evaluation. All other data, though cited in the reference list, were dropped before the final evaluation.

Shomate and Cook (1946) measured the heat content of a boehmite sample between 298 and 520 K. However, the data do not smoothly connect with the low-temperature data and appear to be too low. It is probable that there was loss of H₂O from the sample without

^aJANAF Thermochemical Tables, looseleaf pages for 1979 issued by Dow Chemical Company, 1707 Building, Midland, Michigan.

Table 196. Sources of thermophysical data for boehmite, AlOOH.

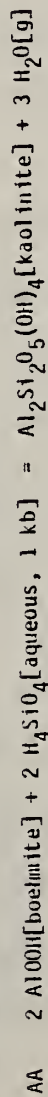
Source	Data type	Method	Number of points	Range		Percent error ^a
				Temperature (K)	Pressure (bars)	
Robie and others, 1979	volume	compilation	1	298	1.01	0.00
Shomate and Cook, 1946	heat capacity	isotherm. cal.	10	206-296	1.01	0.01±0.20
Haas and others, 1981	heat capacity	estimate	7	298-600	1.01	0.10±0.16
Robie and others, 1979	entropy	compilation	1	298	1.01	0.01

^aThe tabulated numbers represent the unweighted, average standard error of estimate for data in the set from the calculated value and the 1-sigma deviation of the errors about the average. Refer to text for details.

Table 197. Sources of thermochemical data for boehmite, Al(OH)₃.

Reaction	Source	Method	No. of Points	Temperature (K)	Range Pressure (kb)	H _f ^o (298.15 K) Third Law, kJ	H _f ^o (298.15 K) kJ/mol
AA	Hemley and others, 1980	H ₄ SiO ₄ concentration	3	473-523	1.0	71.058±1.042	-990.230
AV	Chang, 1981 This Study	Differential Solubility in Water	1	333	0.001	16.758±0.359	-992.066 -990.654

Reactions:



correction for the change in weight and phase content. Mukaibo and others (1969) measured the heat capacity of an impure boehmite between 3.2 and 585 K. The sample contained about 1 percent excess H₂O and had a heat capacity about 1.3 percent lower than the estimated values of Haas and others (1981). The excess H₂O was probably present as admixed gibbsite. The lower heat capacity is consistent with such a hypothesis.

Hemley and others (1980) measured the concentration of silicic acid coexisting with the mineral pair boehmite + kaolinite. During the previous effort (Haas and others, 1981), it was recognized that the experiments lead to a possible inversion of diaspore to boehmite about 570 to 600 K. Discussions at that time and since then with J.J. Hemley indicate that the inversion may exist. Acting upon the suggestion of Hemley, in this evaluation we have used the data that would make boehmite the least stable, that is, we used the three points that had the lowest silicic acid concentration for the temperature of observation. The inversion as derived from this evaluation is calculated to be 583.55 K at 1.01 bars.

1.5.5.2.2. Diaspore

Tables 198 and 199 contain the data used in the final evaluation of the properties of diaspore. Other data, though cited in the reference list, were dropped before the final evaluation.

The heat capacity of diaspore is based on the recent work of Perkins and others (1979). The earlier work by King and Weller (1961a) is in reasonable agreement though it averages slightly lower.

Table 19b. Sources of thermophysical data for diaspore, Al₂O₃.

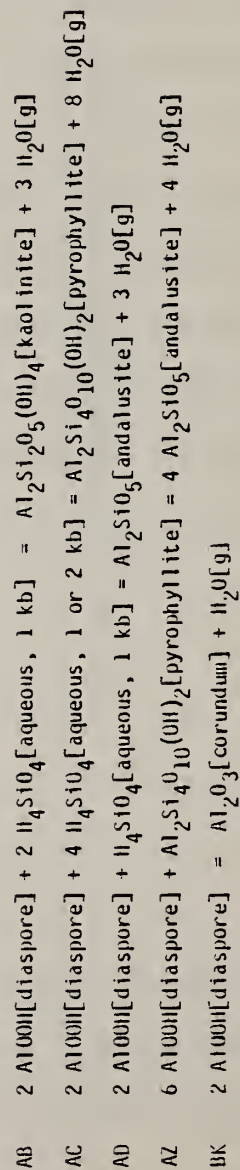
Source	Data type	Method	Number of points	Range		Percent error ^a
				Temperature (K)	Pressure (bars)	
Robie and others, 1979	volume	compilation	1	298	1.01	0.00
King and Weller, 1961a	heat capacity	isotherm. cal.	10	206-296	1.01	-0.68±0.22
Perkins and others, 1979	heat capacity	adiab. cal.	15	204-345	1.01	0.23±0.22
Perkins and others, 1979	heat capacity	d.s.c.	19	340-509	1.01	-0.61±1.03
Perkins and others, 1979	entropy	adiab. cal.	1	298	1.01	-0.003

^aThe tabulated numbers represent the unweighted, average standard error of estimate for data in the set from the calculated value and the 1-sigma deviation of the errors about the average. Refer to text for details.

Table 199. Sources of thermochemical data for diaspore, AlOOH.

Reaction	Source	Method	No. of Points	Temperature (K)	Range (K)	Pressure (kb)	$H_f^\circ(298.15 \text{ K})$ Third Law, kJ	$H_f^\circ(298.15 \text{ K})$ kJ/mol
AB	Hemley and others, 1980	H_4SiO_4 concentration	6	473-573	1.0	88.372±0.414	-1000.151	
AC	Hemley and others, 1980	H_4SiO_4 concentration	3	523-573	2.0	239.616±1.809	-1001.264	
AC	Hemley and others, 1980	H_4SiO_4 concentration	1	598	1.0	295.910	-999.650	
AD	Hemley and others, 1980	H_4SiO_4 concentration	2	623-663	1.0	151.551±0.163	-999.248	
AZ	Ilaas and Holdaway, 1973	Gas-medium Pressure Apparatus	4 pr	618-722	2.4-7.0	306.234±3.143	-999.594	
BK	Ilaas, 1972 This Study	Gas-medium Pressure Apparatus	5 pr	662-741	1.75-7.0	81.731±0.686	-1000.235 -999.944	

Reactions:



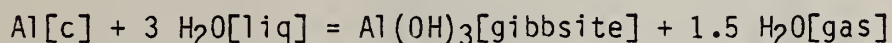
The heat capacity was also measured by Mukaibo and others (1969) on an impure, H₂O-deficient sample to near 600 K. These data are slightly higher than those of Perkins and others. Mukaibo and others did not make composition corrections on their data, and this departure would be expected if a less-hydrous phase such as corundum were present.

The phase equilibria studies of Hemley and others (1980), Haas (1972), and Haas and Holdaway (1973) are in good agreement. Depending upon the work by J.J. Hemley currently in progress, the decomposition reaction of diaspore to corundum and H₂O[*gas*] may be metastable.

1.5.5.3. Al(OH)₃, gibbsite (formula weight = 78.004 g/mol)

The data used to evaluate the properties of gibbsite are given in tables 200 and 201.

In addition to these data, Hemingway and others (1977) measured the enthalpy of the reaction:



They obtained an enthalpy, when reduced to 298.15 K, of -435.957 ± 3.173 kJ/mol as compared to -437.209 kJ/mol calculated from the tabulated properties. The departure is 1.252 kJ/mol. These results are an independent check on the enthalpy of formation recommended by the CODATA Task Group on Key Values for Thermodynamics (1978) and used in preparing the JANAF Thermochemical Tables^a.

^aJANAF Thermochemical Tables, looseleaf pages for 1979 issued by Dow Chemical Company, 1707 Building, Midland, Michigan.

Table 200. Sources of thermophysical data for gibbsite, $\text{Al}(\text{OH})_3$.

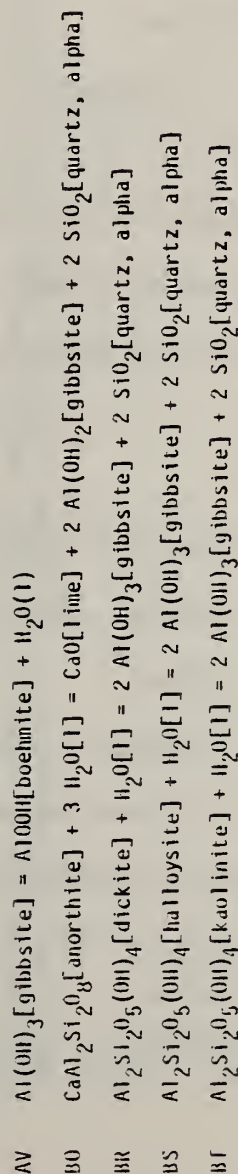
Source	Data type	Method	Number of points	Range		Percent errors ^a
				Temperature (K)	Pressure (bars)	
Kobie and others, 1979	volume expansivity	compilation dilatometry	1	298	1.01	0.0
Meyaw, 1933	heat capacity	adiab. cal.	1	298	1.01	0.0
Hemingway and others, 1977	entropy	adiab. cal. and d.s.c.	23	200-479	1.01	-0.03±0.29
Hemingway and others, 1977	entropy	adiab. cal.	1	298	1.01	0.0

^aThe tabulated numbers represent the unweighted, average standard error of estimate for data in the set from the calculated value and the 1-sigma deviation of the errors about the average. Refer to text for details.

Table 201. Sources of thermochemical data for gibbsite, Al(OH)₃.

Reaction	Source	Method	No. of Points	Temperature (K)	Range (K)	Pressure (kb)	H _r ^o (298.15 K) Third Law, kJ	H _f ^o (298.15 K) kJ/mol
AV	Chang, 1981	Differential Solubility in Water	1	333	0.001	0.001	16.758±0.359	-1296.045
BU	Kracek and Neuvonen, 1952	Solution calorimetry, HF acid	1	347	0.001	0.001	43.470±0.581	-1293.584
BC	Barany and Kelley, 1961	Solution calorimetry, HF acid	6	347	0.001	0.001	7.570±0.383	-1294.567
BS	Barany and Kelley, 1961	Solution calorimetry, HF acid	6	347	0.001	0.001	-9.873±0.342	-1294.567
BT	Barany and Kelley, 1961	Solution calorimetry, HF acid	15	347	0.001	0.001	8.830±0.355	-1294.621
	This Study							-1294.633

Reactions:



1.5.5.4. Al_2O_3 , corundum (formula weight = 101.962 g/mol)

The properties of corundum, with the exception of molar volume, were taken from the JANAF Thermochemical Tables^a. Table 202 contains the sources of data for the molar volume as a function of temperature and pressure.

1.5.5.5. Al_2SiO_5 (formula weight = 162.047 g/mol)

The stable polymorphs of Al_2SiO_5 have calculated inversions at 1.01 bars as follows:

<u>Inversion</u>	<u>Temperature</u>
kyanite = andalusite	408.45 K
andalusite = sillimanite	942.45 K

The data used to establish these reactions as well as the phase equilibria with other minerals are cited below.

1.5.5.5.1. Andalusite

Tables 203 and 204 contain the data used in the final evaluation. All other data, though cited in the reference list, were dropped before the final evaluation.

The molar volumes as measured by Winter and Ghose (1979) are smaller than those measured earlier by Skinner and others (1961). The recent data of Schneider (1979) are intermediate between the two data sets. Because of the scatter, all sets are included in the

^aJANAF Thermochemical Tables, looseleaf pages for 1979 issued by Dow Chemical Company, 1707 Building, Midland, Michigan.

Table 202. Sources of volumetric data for corundum, Al₂O₃.

Source	Data type	Method	Number of points	Range		Percent error ^a
				Temperature (K)	Pressure (bars)	
Schauer, 1965	volume	X-ray	13	300-1470	1.01	-0.01±0.13
Skinner, 1966	volume	X-ray	8	298-1473	1.01	-0.03±0.06
d'Amour and others, 1978	volume	X-ray	7	298	1.01-90000	0.17±0.19
Finger and Hazen, 1978	volume	X-ray	7	296	1.01-80000	-0.11±0.29

^aThe tabulated numbers represent the unweighted, average standard error of estimate for data in the set from the calculated value and the 1-sigma deviation of the errors about the average. Refer to text for details.

Table 203. Sources of thermophysical data for andalusite, Al_2SiO_5 .

Source	Data type	Method	Number of points	Range		Percent error ^d
				Temperature (K)	Pressure (bars)	
Robie and Hemingway, 1982 (unpub.)	compressibility	estimate	4	298	1.01	36.56
Ralph and others, 1981	volume	X-ray	2	298	1.01-37000	-0.02±0.07
Schneider, 1979	volume	X-ray	11	473-1273	1.01	0.04±0.05
Skinner and others, 1961	volume	X-ray	5	290-1281	1.01	0.15±0.23
Winter and Ghose, 1979	volume	X-ray	10	298-1273	1.01	-0.20±0.18
Brace and others, 1969	compressibility	dilatometry	29	298	1000-40000	3.64±3.86
Robie and Hemingway, 1982 (unpub.)	heat capacity	adiab. cal.	13	220-377	1.01	0.02±0.16
Pankratz and Kelley, 1964b	heat content	drop cal.	1	397-1601	1.01	-0.14±0.31
Robie and Hemingway, 1982 (unpub.)	entropy	adiab. cal.	1	298	1.01	-0.11

^dThe tabulated numbers represent the unweighted, average standard error of estimate for data in the set from the calculated value and the 1-sigma deviation of the errors about the average. Refer to text for details.

Table 204. Sources of thermochemical data for andalusite, Al_2SiO_5 .

Reaction	Source	Method	No. of Points	Temperature Range (K)	Pressure (kb)	$H_f^\circ(298.15 \text{ K})$ Third Law, kJ	$H_f^\circ(298.15 \text{ K})$ kJ/mol
AD	Hemley and others, 1980	H_4SiO_4 concentration	2	623-663	1.0	151.551±0.163	-2591.234
AK	Hemley and others, 1980	H_4SiO_4 concentration	3	623-633	2.0	105.020±2.107	-2593.264
AL	Hemley and others, 1980	H_4SiO_4 concentration	8	613-673	1.0	143.886±0.594	-2595.079
AL	Holdaway, 1971	Gas-medium Pressure Apparatus	2 pr	764-917	1.8-3.6	3.833±0.102	-2592.516
AL	Weil, 1966	Differential Solubility In Melt	2	1073-1283	0.001	4.466±0.333	-2593.369
AM	Storre and Nitsch, 1974	Gas- and Solid-medium Pressure Apparatus	2 pr	788-833	4.0-5.0	-88.085±1.706	-2592.287
AX	Holdaway, 1971	Gas-medium Pressure Apparatus	3 pr	650-858	2.4-4.8	3.994±0.205	-2592.352
AX	Newton, 1966a	Gas-medium Pressure Apparatus	7	973-1123	6.1-7.4	3.637±0.226	-2592.707
AZ	Hads and Holdaway, 1973	Gas-medium Pressure Apparatus	4 pr	618-722	2.4-7.0	306.234±3.143	-2592.105
BA	Hads and Holdaway, 1973	Gas-medium Pressure Apparatus	4 pr	643-737	2.4-7.0	75.319±0.620	-2593.155
BM	Hemley and others, 1980	H_4SiO_4 concentration	4 pr	723-773	2.0	53.445±0.276	-2593.465
BM	Hemley and others, 1980	H_4SiO_4 concentration	6	723-753	1.0	67.312±0.156	-2593.158
AX	Anderson and others, 1977 This Study	Solution calorimetry, borate salt	1	970	0.001	5.720±0.685	-2591.474 -2592.626

Reactions:

- AD $2 Al_2O_3[\text{diaspore}] + H_4SiO_4[\text{aqueous, 1 kb}] = Al_2SiO_5[\text{andalusite}] + 3 H_2O[g]$
- AK $Al_2SiO_5[\text{andalusite}] + 3 H_4SiO_4[\text{aqueous, 1 or 2 kb}] + H_2O[g] = Al_2Si_4O_{10}(OH)_2[\text{pyrophyllite}] + 5 H_2O[g]$
- AL $Al_2SiO_5[\text{andalusite}] = Al_2SiO_5[\text{sillimanite}]$
- AM $Al_2SiO_5[\text{andalusite}] + CaAl_2Si_2O_8[\text{lanorthite}] + H_2O[g] = CaAl_4Si_2O_{10}(OH)_2[\text{margarite}] + SiO_2[\text{quartz, alpha}]$
- AX $Al_2SiO_5[\text{kyanite}] = Al_2SiO_5[\text{andalusite}]$
- AZ $6 Al_2O_3[\text{diaspore}] + Al_2Si_4O_{10}(OH)_2[\text{pyrophyllite}] = 4 Al_2SiO_5[\text{andalusite}] + 4 H_2O[g]$
- BA $Al_2Si_4O_{10}(OH)_2[\text{pyrophyllite}] = Al_2SiO_5[\text{andalusite}] + 3 SiO_2[\text{quartz, alpha}] + H_2O[g]$
- BM $Al_2SiO_5[\text{andalusite}] + 2 H_2O[g] = Al_2O_3[\text{corundum}] + H_4SiO_4[\text{aqueous, 1 or 2 kb}]$

evaluated data set and the results are most consistent with Schneider's data, as would be expected.

There is disagreement between the changes in the molar volumes as measured by Ralph and others (1981) and the compressibility as calculated from the elastic constants by Robie and Hemingway (1982, unpub.). However, the mechanically measured compressibilities obtained by Brace and others (1969) are in reasonable agreement with the measured volumes. All three sets were included. The evaluation rejected the calculated compressibility and favored the other sets.

The earlier low-temperature heat capacities of Todd (1950) have been replaced by new measurements of better samples by Robie and Hemingway (in press). The high-temperature heat capacities were obtained from the work of Pankratz and Kelley (1964b).

The data relating the stability of andalusite to other minerals as given in table 204 are reasonably consistent. The major exception is the experiments of Hemley and others (1980) for the concentration of aqueous silicic acid coexisting with pyrophyllite and andalusite at 1 kb. The results for the same mineral pair at 2 kb are in good agreement with the results of Haas and Holdaway (1973) for the breakdown of pyrophyllite.

1.5.5.5.2. Kyanite

The data used in the final evaluation are given on tables 205 and 206. Other data, though cited in the reference list, were dropped before the final evaluation.

Table 205. Sources of thermophysical data for kyanite, Al_2SiO_5 .

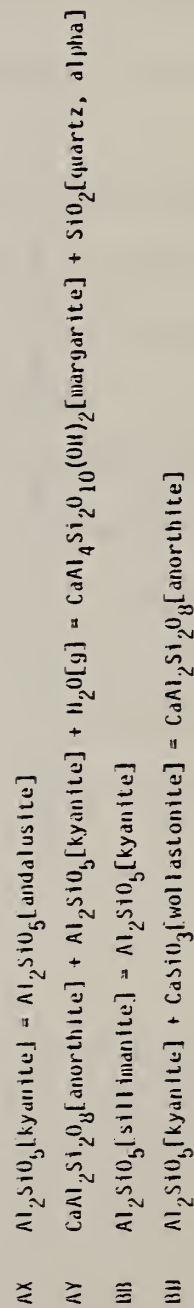
Source	Data type	Method	Number of points	Range		Percent error ^a
				Temperature (K)	Pressure (bars)	
Skinner and others, 1961	volume	X-ray	8	298-1328	1.01	-0.05±0.05
Winter and Ghose, 1979	volume	X-ray	4	298-1073	1.01	0.02±0.04
Bruce and others, 1969	volume diff.	dilatometry	10	298	1000-40000	-0.27±4.55
Robie and Hemingway, 1982 (unpub.)	heat capacity	adiab. cal.	31	225-370	1.01	0.00±0.11
Pankratz and Kelley, 1964b	heat content	drop cal.	12	390-1503	1.01	0.12±0.25
Robie and Hemingway, 1982 (unpub.)	entropy	adiab. cal.	1	298	1.01	-0.13

^aThe tabulated numbers represent the unweighted, average standard error of estimate for data in the set from the calculated value and the 1-sigma deviation of the errors about the average. Refer to text for details.

Table 206. Sources of thermochemical data for kyanite, Al_2SiO_5 .

Reaction	Source	Method	No. of Points	Temperature (K)	Range (K)	Pressure (kb)	$H_f^\circ(298.15 \text{ K})$ Third Law, kJ	$H_f^\circ(298.15 \text{ K})$ kJ/mol
AX	Holdaway, 1971	Gas-medium Pressure Apparatus	3	650-858	2.4-4.8		3.994±0.205	-2598.072
AX	Newton, 1966a	Gas-medium Pressure Apparatus	7	973-1123	6.1-7.4		3.637±0.226	-2598.427
AY	Storre and Mitsch, 1974	Gas- and Solid-medium Pressure Apparatus	3	803-933	5.0-9.0		-86.359±0.132	-2600.000
BB	Weill, 1966	Differential Solubility in Melt	1	1073	0.001		-7.830	-2598.733
AX	Anderson and others, 1977	Solution calorimetry, borate salt	1	970	0.001		5.720±0.685	-2597.194
BB	Anderson and Kleppa, 1969	Solution calorimetry, borate salt	1	970	0.001		8.839±0.312	-2598.951
BU	Anderson and Kleppa, 1969 Ints Study	Solution calorimetry, borate salt	1	970	0.001		3.793±1.296	-2596.853 -2598.346

Reactions:



The thermochemical data are based primarily on the reversed equilibria among the polymorphs kyanite, sillimanite, and andalusite, by Newton (1966a), Holdaway (1971), and Weill (1966).

There remains an inconsistency between the studies of the molar volume by Winter and Ghose (1979) and by Skinner and others (1961). As stated in the discussion for andalusite, the data necessary to discriminate between the sets are not available.

1.5.5.5.3. Sillimanite

Tables 207 and 208 contain the sources of data used in the final evaluation. As with kyanite and andalusite, there is a disagreement between the molar volume studies of Skinner and others (1961) and of Winter and Ghose (1979) and between the compressibility calculated from elastic constants (Robie and Hemingway, 1982, unpub.) and the compressibility derived from dilatometry (Brace and others, 1969). As with the andalusite, all data were used in the final evaluation.

The results of the evaluation of the thermochemical data agree best with the andalusite-sillimanite equilibrium study by Holdaway (1971). The departures from the other studies are within the precision of the observations.

1.5.5.6. $\text{Al}_2\text{Si}_2\text{O}_5(\text{OH})_4$ (formula weight = 258.162 g/mol)

Kaolinite is the stable polymorph in this system at 1.01 bars. The phases dickite and halloysite are metastable to kaolinite. Tables for kaolinite are given in lieu of a reference table for the system.

Table 207. Sources of thermophysical data for sillimanite, Al_2SiO_5 .

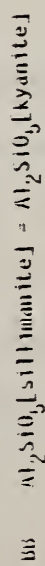
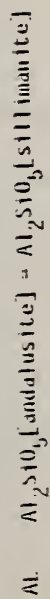
Source	Data type	Method	Number of points	Range		Percent error ^a
				Temperature (K)	Pressure (bars)	
Kobie and Hemingway, 1982 (unpub.)	compressibility	calc. from elas. const.	1	298	1.01	34.32
Skinner and others, 1961	volume	X-ray	11	293-1328	1.01	-0.16±0.16
Brace and others, 1969	volume diff.	dilatometry	10	298	1000-40000	-0.42±1.05
Winter and Chose, 1979	volume	X-ray	5	298-1273	1.01	0.04±0.05
Kobie and Hemingway, 1982 (unpub.)	heat capacity	adiab. cal.	34	217-378	1.01	-0.06±0.15
Pankratz and Kelley, 1964b	heat content	drop cal.	13	401-1496	1.01	0.04±1.18
Kobie and Hemingway, 1982 (unpub.)	entropy	adiab. cal.	1	298	1.01	0.22

^aThe tabulated numbers represent the unweighted, average standard error of estimate for data in the set from the calculated value and the 1-sigma deviation of the errors about the average. Refer to text for details.

Table 208. Sources of thermochemical data for sillimanite, Al_2SiO_5 .

Reaction	Source	Method	No. of Points	Temperature (K)	Range	Pressure (kb)	$H_f^\circ(298.15 \text{ K})$ Third Law, kJ	$H_f^\circ(298.15 \text{ K})$ kJ/mol
Al	Holdaway, 1971	Gas-medium Pressure Apparatus	2 pr	764-917	1.8-3.6	3.833±0.102	-2588.792	
Al	Wells, 1966	Differential Solubility in Melt	2	1073-1283	0.001	4.466±0.333	-2589.645	
BB	Wells, 1966	Differential Solubility in Melt	1	1073	0.001	-7.830	-2589.289	
BB	Anderson and Kleppa, 1969 This Study	Solution calorimetry, borate salt	1	970	0.001	8.839±0.312	-2589.507 -2588.902	

Reactions:



1.5.5.6.1. Kaolinite

The data used in the final evaluation are given in tables 209 and 210. All other data, though cited in the reference list, were deleted prior to the final evaluation. All the data in table 210 are in reasonable agreement. However, as cited in the text, the phase equilibrium study of Thompson (1970) was not used in the final evaluation because it is believed that equilibrium of stable phases was not observed.

1.5.5.6.2. Dickite

Tables 211 and 212 contain the data for dickite used in the final evaluation. The thermochemical properties are based on the measured heats of solution of six dickite samples in HF acid as compared with the stoichiometrically equivalent solution of gibbsite (Barany and Kelley, 1961), water (Barany, 1963), and quartz (Bennington and others, 1978) also in HF acid.

1.5.5.6.3. Halloysite

Tables 213 and 214 contain the data for halloysite used in the final evaluation. The thermochemical properties are based on the heat of solution of six halloysite samples in HF acid as compared with the stoichiometrically equivalent solution of quartz (Bennington and others, 1978), gibbsite (Barany and Kelley, 1961), and water (Barany, 1963) also in HF acid.

Table 209. Sources of thermophysical data for kaolinite, $\text{Al}_2\text{Si}_2\text{O}_5(\text{OH})_4$.

Source	Data type	Method	Number of points	Range		Percent errors
				Temperature (K)	Pressure (bars)	
Robie and others, 1979	volume	compilation	1	298	1.01	0.04
Hemingway and others, 1978	heat capacity	d.s.c.	14	345-500	1.01	0.38±0.45
King and Weller, 1961a	heat capacity	isotherm. cal.	10	206-296	1.01	0.03±0.20
King and Weller, 1961a	entropy	isotherm. cal.	1	298	1.01	-0.17

^dThe tabulated numbers represent the unweighted, average standard error of estimate for data in the set from the calculated value and the 1-sigma deviation of the errors about the average. Refer to text for details.

Table 210. Sources of thermochemical data for kaolinite, $\text{Al}_2\text{Si}_2\text{O}_5(\text{OH})_4$.

Reaction	Source	Method	No. of Points	Temperature Range (K)	Pressure (kb)	$H_f^\circ(298.15 \text{ K})$ Third Law, kJ	$H_f^\circ(298.15 \text{ K})$ kJ/mol
AA	Hemley and others, 1980	H_4SiO_4 concentration	3	473-523	1.0	71.058±1.042	-4132.767
AB	Hemley and others, 1980	H_4SiO_4 concentration	6	473-573	1.0	88.372±0.414	-4134.030
AW	Hemley and others, 1980	H_4SiO_4 concentration	3	523-573	2.0	181.898±1.307	-4132.309
AW	Hemley and others, 1980	H_4SiO_4 concentration	7	473-573	1.0	207.739±0.178	-4133.588
BI	Barany and Kelley, 1961 This Study	Solution calorimetry, HF acid	15	347	0.001	8.830±0.355	-4133.604 -4133.616

Reactions:

- AA $2 \text{Al}(\text{OH})_3[\text{boehmite}] + 2 \text{H}_4\text{SiO}_4[\text{aqueous}, 1 \text{ kb}] = \text{Al}_2\text{Si}_2\text{O}_5(\text{OH})_4[\text{kaolinite}] + 3 \text{H}_2\text{O}[\text{g}]$
- AB $2 \text{Al}(\text{OH})_3[\text{diaspore}] + 2 \text{H}_4\text{SiO}_4[\text{aqueous}, 1 \text{ kb}] = \text{Al}_2\text{Si}_2\text{O}_5(\text{OH})_4[\text{kaolinite}] + 3 \text{H}_2\text{O}[\text{g}]$
- AW $\text{Al}_2\text{Si}_2\text{O}_5(\text{OH})_4[\text{kaolinite}] + 2 \text{H}_4\text{SiO}_4[\text{aqueous}, 1 \text{ or } 2 \text{ kb}] = \text{Al}_2\text{Si}_4\text{O}_{10}(\text{OH})_2[\text{pyrophyllite}] + 5 \text{H}_2\text{O}[\text{g}]$
- BI $\text{Al}_2\text{Si}_2\text{O}_5(\text{OH})_4[\text{kaolinite}] + \text{H}_2\text{O}[\text{l}] = 2 \text{Al}(\text{OH})_3[\text{gibbsite}] + 2 \text{SiO}_2[\text{quartz}, \text{alpha}]$

Table 211. Sources of thermophysical data for diickite, $\text{Al}_2\text{Si}_2\text{O}_5(\text{OH})_4$.

Source	Data type	Method	Number of points	Range		Percent error ^a
				Temperature (K)	Pressure (bars)	
Robie and others, 1979	volume	compilation	1	298	1.01	0.0
Haas and others, 1981	heat capacity	estimate	14	340-500	1.01	0.38±0.45
King and Meller, 1961a	heat capacity	isotherm. cal.	10	206-296	1.01	-0.02±0.11
King and Meller, 1961a	entropy	isotherm. cal.	1	298	1.01	0.0

^aThe tabulated numbers represent the unweighted, average standard error of estimate for data in the set from the calculated value and the 1-sigma deviation of the errors about the average. Refer to text for details.

Table 212. Sources of thermochemical data for dickite, $\text{Al}_2\text{Si}_2\text{O}_5(\text{OH})_4$.

Reaction	Source	Method	No. of Points	Temperature (K)	Range	Pressure (kb)	$H_f^\circ(298.15 \text{ K})$ Third Law, kJ	$H_f^\circ(298.15 \text{ K})$ kJ/mol
BR	Barany and Kelley, 1961 This study	Solution calorimetry, HF acid	6	347	0.001	7.570±0.383	-4132.236 -4132.302	

Reactions:

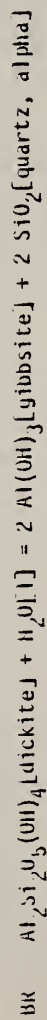


Table 213. Sources of thermophysical data for halloysite, $\text{Al}_2\text{Si}_2\text{O}_5(\text{OH})_4$.

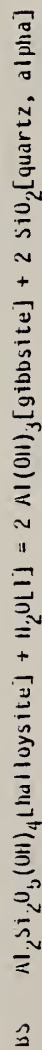
Source	Data type	Method	Range		Pressure (bars)	Percent error ^a
			Number of points	Temperature (K)		
Robie and others, 1979	volume	compilation	1	298	1.01	0.0
Haas and others, 1981	heat capacity	estimate	14	340-500	1.01	-0.10±0.37
King and Møller, 1961a	heat capacity	isotherm. cal.	10	207-296	1.01	0.02±0.21
King and Møller, 1961a	entropy	isotherm. cal.	1	298	1.01	0.0

^aThe tabulated numbers represent the unweighted, average standard error of estimate for data in the set from the calculated value and the 1-sigma deviation of the errors about the average. Refer to text for details.

Table 214. Sources of thermochemical data for halloysite, $\text{Al}_2\text{Si}_2\text{O}_5(\text{OH})_4$.

Reaction	Source	Method	No. of Points	Temperature (K)	Range	Pressure (kb)	$H_f^\circ(298.15 \text{ K})$ Third Law, kJ	$H_f^\circ(298.15 \text{ K})$ kJ/mol
BS	Barany and Kelley, 1961 This study	Solution calorimetry, HF acid	6	347		0.001	-9.873 ± 0.342	-4114.793 -4114.854

Reactions:



1.5.5.7. $\text{Al}_2\text{Si}_4\text{O}_{10}(\text{OH})_2$, pyrophyllite (formula weight =
360.317 g/mol)

Tables 215 and 216 contain the sources of data used in the final evaluation of the properties of pyrophyllite. Other data, though cited in the reference list, were deleted prior to the final evaluation. All the data used in the final evaluation are in acceptable internal agreement.

1.5.5.8. C, graphite (formula weight = 12.011 g/mol)

The properties of graphite were taken from the JANAF Thermochemical Tables^a. The molar volume of graphite was not needed in this study and therefore not evaluated.

1.5.5.9. CO, carbon monoxide (ideal gas, formula weight =
28.010 g/mol)

The properties of carbon monoxide ideal gas was taken from the JANAF Thermochemical Tables (Stull and Prophet, 1971). The molar volume was not needed for this study and therefore not evaluated.

1.5.5.10. CO_2 , carbon dioxide (ideal gas, formula weight =
44.010 g/mol)

The thermodynamic properties of the ideal gas at 1.01 bars were taken from the JANAF Thermochemical Tables (Stull and Prophet, 1971). The corrections for the real gas as a function of pressure at constant temperature were taken from the work of Jacobs and Kerrick (1981).

^aJANAF Thermochemical Tables, looseleaf pages for 1978 issued by Dow Chemical Company, 1707 Building, Midland, Michigan.

Table 215. Sources of thermophysical data for pyrophyllite, $\text{Al}_2\text{Si}_4\text{O}_{10}(\text{OH})_2$.

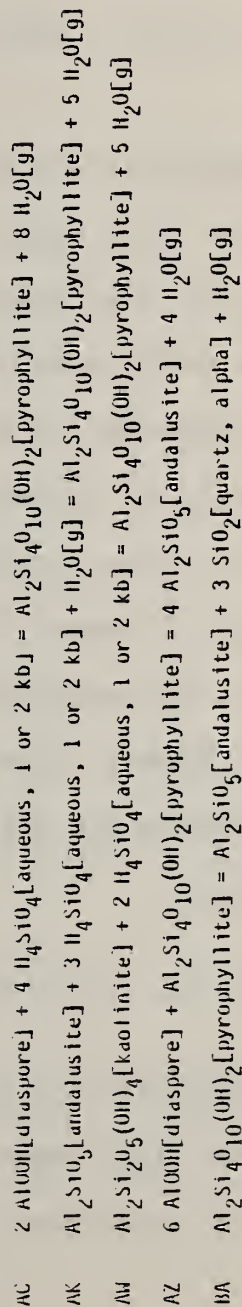
Source	Data type	Method	Number of points	Range			Percent error ^a
				Temperature (K)	Pressure (bars)		
Taylor and Bell, 1970	volume	X-ray	7	295-675	1.01	-0.02±0.04	
Robie and others, 1976	heat capacity	adiab. cal.	20	200-370	1.01	0.03±0.10	
Krupka and others, 1979	heat capacity	d.s.c.	48	335-679	1.01	-0.30±0.51	
Robie and others, 1976	entropy	adiab. cal.	1	298	1.01	0.029	

^aThe tabulated numbers represent the unweighted, average standard error of estimate for data in the set from the calculated value and the 1-sigma deviation of the errors about the average. Refer to text for details.

Table 216. Sources of thermochemical data for pyrophyllite, $\text{Al}_2\text{Si}_4\text{O}_{10}(\text{OH})_2$.

Reaction	Source	Method	No. of Points	Temperature Range (K)	Pressure (kb)	$\Delta_r H^\circ$ (298.15 K) Third Law, kJ	$\Delta_f H^\circ$ (298.15 K) kJ/mol
AC	Hemley and others, 1980	H_4SiO_4 concentration	3	523-573	2.0	239.616±1.809	-5644.960
AC	Hemley and others, 1980	H_4SiO_4 concentration	1	598	1.0	295.910	-5641.731
AK	Hemley and others, 1980	H_4SiO_4 concentration	3	623-633	2.0	105.020±2.107	-5642.957
AK	Hemley and others, 1980	H_4SiO_4 concentration	8	613-673	1.0	143.886±0.594	-5644.772
AW	Hemley and others, 1980	H_4SiO_4 concentration	3	523-573	2.0	181.898±1.307	-5641.012
AW	Hemley and others, 1980	H_4SiO_4 concentration	7	473-573	1.0	207.739±0.178	-5642.291
AZ	Haas and Holdaway, 1973	Gas-medium Pressure Apparatus	4 pr	618-722	2.4-7.0	306.234±3.143	-5640.221
BA	Haas and Holdaway, 1973 This Study	Gas-medium Pressure Apparatus	4 pr	643-737	2.4-7.0	75.319±0.620	-5642.848 -5642.319

Reactions:



1.5.5.11. Ca, calcium (formula weight = 40.08 g/mol)

The heat capacity, heat content, and inversion-related data were taken from the compilation of Hultgren and others (1973). The entropy at 298.15 K for calcium was taken from the CODATA Task Group (1978). The volumetric data for calcium were not needed in this study and, therefore, were not evaluated.

1.5.5.12. $\text{CaAl}_2\text{SiO}_6$, Ca-Al clinopyroxene (formula weight = 218.085 g/mol)

Tables 217 and 218 contain the data used in the final evaluation. All other data, though cited in the reference list, were dropped before the final evaluation.

In addition to the thermochemical data cited on table 218, Hays (1966) observed four reversals for reaction AI. His results lead to an enthalpy of formation from the elements at 298.15 K of -3297.035 kJ/mol, a value 1.6 kJ/mol less stable than obtained through the weighted refinement. Hays used a solid-medium piston cylinder apparatus in his experiments without a pressure correction. The recent work by Gasparik (1981) used a salt medium. The pressure correction is negligible and the data are consistent with the other data in the evaluation.

1.5.5.13. $\text{CaAl}_2\text{Si}_2\text{O}_8$, anorthite (formula weight = 278.209 g/mol)

Tables 219 and 220 contain the data used in the final evaluation. All other data, though cited in the reference list, were dropped before the final evaluation.

Table 217. Sources of thermophysical data for Ca-Al clinopyroxene, $\text{CaAl}_2\text{SiO}_6$.

Source	Data type	Method	Number of points	Range		Percent error ^a
				Temperature (K)	Pressure (bars)	
Hasselton, H. I., Jr., 1982 (unpub.) Thompson and others, 1978	volume heat capacity	X-Ray d.s.c.	7 16	298-1473	1.01	0.00±0.09
				298-1000	1.01	-0.01±0.13

^aThe tabulated numbers represent the unweighted, average standard error of estimate for data in the set from the calculated value and the 1-sigma deviation of the errors about the average. Refer to text for details.

Table 218. Sources of thermochemical data for Ca-Al clinopyroxene, $\text{CaAl}_2\text{SiO}_6$.

Reaction	Source	Method	No. of Points	Temperature (K)	Range (K)	Pressure (kb)	$H_f^\circ(298.15 \text{ K})$ Third Law, kJ	$H_f^\circ(298.15 \text{ K})$ kJ/mol
Al	Gasparik, 1981	Solid-medium Pressure Apparatus	3 pr	1463-1673	10.7b-23.5		-94.622±2.588	-3298.650
AU	Hays, 1966	Solid-medium Pressure Apparatus	4 pr	1473-1673	11.0-14.6		-6.335±1.964	-3298.564
BP	Charlu and others, 1978 This study	Solution calorimetry, borate salt	1	970	0.001		67.438±1.972	-3302.204 -3298.625

Reactions:

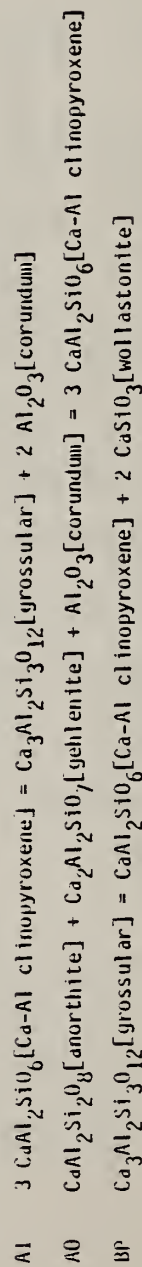


Table 219. Sources of thermophysical data for anorthite, $\text{CaAl}_2\text{Si}_2\text{O}_8$.

Source	Data type	Method	Number of points	Range		Percent errors ^a
				Temperature (K)	Pressure (bars)	
Kozu and Ueda, 1933	volume diff.	dilatometry	24	323-1273	1.01	8.56±10.28
Birch, 1966	volume	compilation	5	298	1.01-40000	0.01±0.03
Grundy and Brown, 1974	volume	X-ray	8	298-1123	1.01	0.00±0.10
Flemingway and others, 1981	heat capacity	d.s.c.	95	349-986	1.01	-0.09±0.46
Kobte and others, 1978	heat capacity	adiab. cal.	49	202-381	1.01	0.01±0.18
White, 1919	heat content	drop cal.	9	1173-1673	1.01	-0.02±0.24
Ferrier, 1969	heat content	drop cal.	6	1300-1800	1.01	-0.08±0.23
Kobte and others, 1978	entropy	adiab. cal.	1	298	1.01	0.01

^aThe tabulated numbers represent the unweighted, average standard error of estimate for data in the set from the calculated value and the 1-sigma deviation of the errors about the average. Refer to text for details.

Table 220. Sources of thermochemical data for anorthite, $\text{CaAl}_2\text{Si}_2\text{O}_8$.

Reaction	Source	Method	No. of Points	Temperature Range (K)	Pressure (kb)	$H_f^\circ(298.15 \text{ K})$ Third Law, kJ	$H_f^\circ(298.15 \text{ K})$ kJ/mol
AL	Newton, 1965	Gas- and Solid-medium Pressure Apparatus	6 pr	843-1113	2.0-6.8	-304.09912, 670	-4231.021
AL	Boettcher, 1970	Gas-medium Pressure Apparatus	1 pr	898-928	3.0	-305.30413, 803	-4231.222
AF	Hays, 1966	Solid-medium Pressure Apparatus	2 pr	1473-1523	7.5-11.0	-157.99416, 068	-4228.743
AF	Huckenthalz, 1974	Unspecified	6 pr	1125-1423	0.2-7.5	-158.84011, 799	-4229.589
AF	Shmulovich, 1974	Gas-medium Pressure Apparatus	1 pr	1133-1153	0.506	-159.47411, 420	-4231.171
AG	Boettcher, 1970	Gas-medium Pressure Apparatus	2 pr	893-1053	3.0-5.9	-50.20411, 453	-4230.713
AG	Newton, 1966b	Gas-medium Pressure Apparatus	2 pr	803-923	1.1-2.0	-51.46713, 013	-4232.951
AG	Newton, 1966b	Gas-medium Pressure Apparatus	2 pr	973-1023	4.7-5.7	-48.97111, 851	-4229.401
AG	Huckenthalz, 1974	Unspecified	1 pr	848-858	2.0	-49.45510, 327	-4230.540
AG	Huckenthalz, 1974	Unspecified	2 pr	888-958	3.0-4.0	-49.93210, 500	-4230.442
AG	Goldsmith and Newton, 1977	Solid-medium Pressure Apparatus	5 pr	1123-1173	1.0-15.0	3.59810, 015	-4230.696
AJ	Boettcher, 1970	Gas-medium Pressure Apparatus	2 pr	853-933	4.0-5.3	-212.73212, 710	-4230.933
AJ	Strens, 1968	Gas-medium Pressure Apparatus	1 pr	770-823	2.0	-219.35815, 645	-4232.259
AJ	Newton, 1966b	Gas-medium Pressure Apparatus	8 pr	758-1042	2.0-8.0	-209.38714, 619	-4230.267
AM	Storre and Mitsch, 1974	Gas- and Solid-medium Pressure Apparatus	2 pr	788-833	4.0-5.0	-88.08511, 706	-4230.358
AN	Chatterjee, 1971	Gas-medium Pressure Apparatus	3 pr	763-973	2.0-6.0	-94.22911, 257	-4230.284
AN	Chatterjee, 1974	Gas-medium Pressure Apparatus	5 pr	743-913	1.0-7.0	-94.01010, 933	-4230.065
AN	Storre and Mitsch, 1974	Gas- and Solid-medium Pressure Apparatus	3 pr	783-933	3.0-7.0	-93.72211, 703	-4229.778
AO	Hays, 1966	Solid-medium Pressure Apparatus	4 pr	1473-1673	11.0-14.0	-6.33511, 964	-4230.879
AP	Boettcher, 1970	Gas-medium Pressure Apparatus	1 pr	1033-1053	1.0	-101.52410, 981	-4231.523
AP	Huckenthalz, 1974	Unspecified	3 pr	1028-1263	1.0-6.0	-102.14611, 163	-4232.145
AQ	Liu, 1971	Gas-medium Pressure Apparatus	5 pr	708-828	1.0-5.0	-89.62910, 446	-4230.690
AY	Storre and Mitsch, 1974	Gas- and Solid-medium Pressure Apparatus	3 pr	803-933	5.0-9.0	-86.35910, 132	-4232.351
BB	Kay and Taylor, 1960	log K	1	1653	0.001	84.43012, 584	-4228.036
bb	Kay and Taylor, 1960	log K	1	1543	0.001	61.01112, 412	-4225.974
BB	Kracek and Newton, 1952	Solution calorimetry, H ⁺ acid	1	347	0.001	43.47010, 581	-4229.648
BB	Anderson and Kleppa, 1969	Solution calorimetry, H ⁺ acid	1	970	0.001	3.79311, 296	-4229.204
	H ⁺ Study						-4230.697

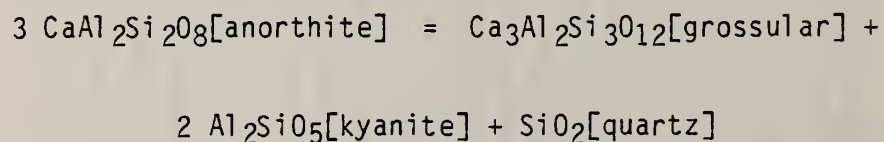
Table 220. Continued

Reaction	Source	Method	No. of Points	Temperature (K)	Range Pressure (kb)	H_f° (298.15 K) Third Law, kJ	H_f° (298.15 K) kJ/mol
Reactions:							
AE	$2 \text{Ca}_3\text{Al}_2\text{Si}_3\text{O}_{12}$ [grossular] + $6 \text{CaAl}_2\text{Si}_2\text{O}_8$ [anorthite] + Al_2O_3 [corundum] + $3 \text{H}_2\text{O}$ [g] = $6 \text{Ca}_2\text{Al}_3\text{Si}_3\text{O}_{12}$ (OH) [zoisite]						
AF	$2 \text{Ca}_3\text{Al}_2\text{Si}_3\text{O}_{12}$ [grossular] = $\text{CaAl}_2\text{Si}_2\text{O}_8$ [anorthite] + $\text{Ca}_2\text{Al}_2\text{Si}_7\text{O}_{17}$ [gehlenite] + 3CaSiO_3 [wollastonite]						
AG	2CaSiO_3 [wollastonite] + $\text{CaAl}_2\text{Si}_2\text{O}_8$ [anorthite] = $\text{Ca}_3\text{Al}_2\text{Si}_3\text{O}_{12}$ [grossular] + SiO_2 [quartz, alpha]						
AG	2CaSiO_3 [wollastonite] + $\text{CaAl}_2\text{Si}_2\text{O}_8$ [anorthite] = $\text{Ca}_3\text{Al}_2\text{Si}_3\text{O}_{12}$ [grossular] + SiO_2 [quartz, beta]						
AH	$3 \text{CaAl}_2\text{Si}_2\text{O}_8$ [anorthite] + CaCO_3 [calcite] = $\text{Ca}_4\text{Al}_6\text{Si}_6\text{O}_{24}$ [meionite]						
AJ	$5 \text{CaAl}_2\text{Si}_2\text{O}_8$ [anorthite] + $\text{Ca}_3\text{Al}_2\text{Si}_3\text{O}_{12}$ [grossular] + $2 \text{H}_2\text{O}$ [g] = $4 \text{Ca}_2\text{Al}_3\text{Si}_3\text{O}_{12}$ (OH) [zoisite] + SiO_2 [quartz, alpha]						
AK	Al_2SiO_5 [andalusite] + $\text{CaAl}_2\text{Si}_2\text{O}_8$ [anorthite] + H_2O [g] = $\text{CaAl}_4\text{Si}_2\text{O}_{10}$ (OH) [margarite] + SiO_2 [quartz, alpha]						
AM	$\text{CaAl}_2\text{Si}_2\text{O}_8$ [anorthite] + Al_2O_3 [corundum] + H_2O [g] = $\text{CaAl}_4\text{Si}_2\text{O}_{10}$ (OH) [margarite]						
AO	$\text{CaAl}_2\text{Si}_2\text{O}_8$ [anorthite] + $\text{Ca}_2\text{Al}_2\text{Si}_7\text{O}_{17}$ [gehlenite] + Al_2O_3 [corundum] = $3 \text{CaAl}_2\text{Si}_6\text{O}_{16}$ [Ca-Al clinopyroxene]						
AP	$\text{CaAl}_2\text{Si}_2\text{O}_8$ [anorthite] + $\text{Ca}_2\text{Al}_2\text{Si}_7\text{O}_{17}$ [gehlenite] = $\text{Ca}_3\text{Al}_2\text{Si}_3\text{O}_{12}$ [grossular] + Al_2O_3 [corundum]						
AQ	$\text{CaAl}_2\text{Si}_2\text{O}_8$ [anorthite] + CaSiO_3 [wollastonite] + H_2O [g] = $\text{Ca}_2\text{Al}_2\text{Si}_3\text{O}_{10}$ (OH) [prehnite]						
AY	$\text{CaAl}_2\text{Si}_2\text{O}_8$ [anorthite] + Al_2SiO_5 [kyanite] + H_2O [g] = $\text{CaAl}_4\text{Si}_2\text{O}_{10}$ (OH) [margarite] + SiO_2 [quartz, alpha]						
BD	$2 \text{CaAl}_2\text{Si}_2\text{O}_8$ [anorthite] = $\text{Ca}_2\text{Al}_2\text{Si}_7\text{O}_{17}$ [gehlenite] + Al_2O_3 [corundum] + 3SiO_2 [cristobalite, beta]						
BF	CaSiO_3 [cyclo wollastonite] + $\text{CaAl}_2\text{Si}_2\text{O}_8$ [anorthite] = $\text{Ca}_2\text{Al}_2\text{Si}_7\text{O}_{17}$ [gehlenite] + 2SiO_2 [cristobalite, beta]						
BO	$\text{CaAl}_2\text{Si}_2\text{O}_8$ [anorthite] + $3 \text{H}_2\text{O}$ [l] = CaO [lime] + 2Al (OH) [g] [gibbsite] + 2SiO_2 [quartz, alpha]						
BU	Al_2SiO_5 [kyanite] + CaSiO_3 [wollastonite] = $\text{CaAl}_2\text{Si}_2\text{O}_8$ [anorthite]						

The relation between volumes and temperature as measured by high-temperature x-ray techniques differs considerably from the results using dilatometry. The weights were set such that the x-ray results were favored because the x-ray results are more precise and less subject to mechanical errors.

The heat capacities as measured by Robie and others (1973) and by Hemingway and others (1981) were used to determine the heat capacities, heat contents, and entropies below 1000 K. The experimental data of White (1919) and the smoothed results of Ferrier (1969) were used to obtain the same properties above 1000 K.

Several studies of the phase equilibria between anorthite and other minerals in the presence of quartz at pressures at and above 10 kb were not used in the evaluation. Goldsmith (1980) discusses the stoichiometry of anorthite and reports that stoichiometric anorthite will partially decompose to an alumina-deficient anorthite and corundum. Hays (1966) and Goldsmith (1980) studied the reaction



between 22 and 32.3 kb. The enthalpies of reaction at 298.15 K and 1.01 bars are -43.619 and -43.399 kJ, respectively. These lead to enthalpies of formation of -4223.529 and -4223.884 kJ/mol. These enthalpies of formation are very anomalous when compared to other data at lower pressure or data where corundum was a reactant or product.

1.5.5.14. $\text{CaAl}_4\text{Si}_2\text{O}_{10}(\text{OH})_2$, margarite (formula weight = 398.186 g/mol)

Tables 221 and 222 contain the sources of data used in the final evaluation of the properties of margarite. In evaluating the heat capacity of margarite, the smoothed, composition-corrected data of Perkins and others (1980) were used.

The data used to evaluate the thermochemical properties are in good agreement. Only the reversal at 9 kb in the study by Storre and Nitsch (1974) is found to be in serious disagreement with the fitted properties.

1.5.5.15. CaCO_3 (formula weight = 100.089 g/mol)

The phase calcite is the stable phase at 1.01 bars. Therefore, the tables for calcite are used as the reference tables.

1.5.5.15.1. Calcite

Tables 223 and 224 contain the data used in the final evaluation. All other data, though cited in the reference list, were dropped before the final evaluation.

The volumetric properties were derived from the studies given in tables 223 and are in reasonable internal consistency. The heat capacities, heat contents, and the entropy of calcite are based primarily on the experimental data of Staveley and Linford (1969) and of Jacobs and others (1981). The compilation of Kelley (1960) was used to fix the properties above 800 K. Calcite has a number of polymorphs that have small differences in the crystal structure. Insuffi-

Table 221. Sources of thermophysical data for margarite, $\text{CaAl}_4\text{Si}_2\text{O}_{10}(\text{OH})_2$.

Source	Data Type	Method	Range		Percent error ^d
			Number of points	Temperature (K)	
Robie and others, 1979	volume	compilation	1	298	0.02
Perkins and others, 1980	heat capacity	adlab. cal.	8	200-298	0.0010.33
Perkins and others, 1980	heat capacity	d.s.c.	16	298-1000	-0.0510.64
Perkins and others, 1980	entropy	adlab. cal.	1	298	-0.02

^dThe tabulated numbers represent the unweighted, average standard error of estimate for data in the set from the calculated value and the 1-sigma deviation of the errors about the average. Refer to text for details.

Table 222. Sources of thermochemical data for margarite, $\text{CaAl}_4\text{Si}_2\text{O}_{10}(\text{OH})_2$.

Reaction	Source	Method	No. of Points	Temperature (K)	Range Pressure (kb)	$H_f^\circ(298.15 \text{ K})$ Third Law, kJ	$H_f^\circ(298.15 \text{ K})$ kJ/mol
AM	Storre and Nitsch, 1974	Gas- and Solid-medium Pressure Apparatus	2 pr	788-833	4.0-5.0	-88.085±1.706	-6242.575
AN	Chatterjee, 1971	Gas-medium Pressure Apparatus	3 pr	763-973	2.0-6.0	-94.229±1.257	-6242.501
AN	Chatterjee, 1974	Gas-medium Pressure Apparatus	5 pr	743-913	1.0-7.0	-94.010±0.933	-6242.282
AN	Storre and Nitsch, 1974	Gas- and Solid-medium Pressure Apparatus	3 pr	783-933	3.0-7.0	-93.722±1.703	-6241.995
AY	Storre and Nitsch, 1974 This Study	Gas- and Solid-medium Pressure Apparatus	3 pr	803-933	5.0-9.0	-86.359±0.132	-6244.568 -6242.914

Reactions:

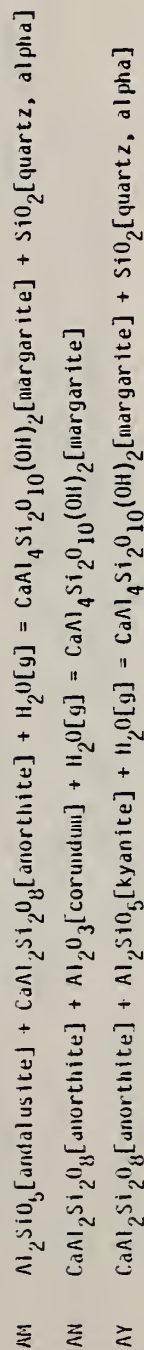


Table 223. Sources of thermophysical data for calcite, CaCO_3 .

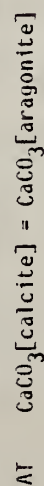
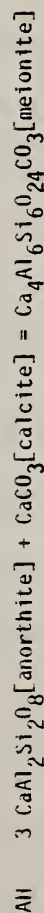
Source	Data type	Method	Number of points	Range		Percent error ^a
				Temperature (K)	Pressure (bars)	
Adams and others, 1919	compressibility	dilatometry	17	298	1900-12000	-2.19±5.45
Rosenholtz and Smith, 1949	expansivity	dilatometry	7	373-973	1.01	6.87±41.38
Vaidya and others, 1973	volume	dilatometry	6	298	1.01-15000	0.13±0.37
Mirwald, 1979	volume	X-ray	3	903-1148	1.01	1.74±0.43
Kelley, 1960	heat content	compilation	9	400-1200	1.01	-0.38±1.81
Jacobs and others, 1981	heat capacity	d.s.c.	122	345-780	1.01	0.03±0.46
Staveley and Linford, 1969	heat capacity	adiab. cal.	10	222-303	1.01	0.22±0.25
Staveley and Linford, 1969	entropy	adiab. cal.	1	298	1.01	-0.08

^aThe tabulated numbers represent the unweighted, average standard error of estimate for data in the set from the calculated value and the 1-sigma deviation of the errors about the average. Refer to text for details.

Table 224. Sources of thermochemical data for calcite, CaCO₃.

Reaction	Source	Method	No. of Points	Temperature (K)	Range Pressure (kb)	H _f ^o (298.15 K) Third Law, kJ	H _f ^o (298.15 K) kJ/mol
AU	Goldsmith and Newton, 1977	Solid-medium Pressure Apparatus	5 pr	1123-1173	1.0-15.0	3.598±0.015	-1209.056
AT	Boettcher and Yllie, 1968	Solid-medium Pressure Apparatus	2 pr	673	8.2-8.6	-0.822±0.049	-1209.277
AT	Boettcher and Yllie, 1968	Solid-medium Pressure Apparatus	5 pr	753-1073	9.0-20.1	-0.730±0.336	-1209.185
AT	Goldsmith and Newton, 1969	Gas- and Solid-medium Pressure Apparatus	3 pr	673-723	8.5-10.5	-0.687±0.111	-1209.141
AT	Goldsmith and Newton, 1969	Gas- and Solid-medium Pressure Apparatus	10 pr	773-973	10.0-11.5	-0.755±0.134	-1209.209
AT	Johannes and Puhai, 1971	Gas-medium Pressure Apparatus	10	403-643	4.0-8.5	-0.591±0.116	-1209.046
AT	Johannes and Puhai, 1971	Gas-medium Pressure Apparatus	34	633-873	8.4-15.5	-0.547±0.138	-1209.002
AU	Baker, 1962	Vapor Pressure	21	1171-1458	0.001-0.025	180.525±0.552	-1209.871
AU	Smyth and Adams, 1923	Vapor Pressure, D.T.A.	12	1115-1355	0.00045-0.0089	180.010±1.076	-1209.385
AU	This Study						-1209.058

Reactions:



cient data exists to evaluate the properties of the individual polymorphs. Therefore, the tabulated data in tables 54, 55, and 160 represent the average properties of all the polymorphs of the calcite-related structural type.

The enthalpy of formation from the oxides is based on the decomposition data of Smyth and Adams (1923) and Baker (1962). These sets are in good agreement. However, the experiments of Harker and Tuttle (1955) lead to an enthalpy of reaction at 298.15 K of 170.564 ± 4.531 kJ/mol, a departure from the evaluated result of -9.773 kJ/mol.

1.5.5.15.2. Aragonite

Tables 225 and 226 contain the data used in the final evaluation. All other data, though cited in the reference list, were dropped before the final evaluation.

The calcite-aragonite reaction has been studied extensively. The data used (table 226) cover a large range in both temperature and pressure and are internally consistent.

1.5.5.16. CaO, lime (formula weight = 56.079 g/mol)

Except for the volumetric data, the properties of lime were taken from the JANAF Thermochemical Tables (Stull and Prophet, 1971). Table 227 gives the sources of data for the volumetric properties that were used in this study.

1.5.5.17. CaSiO₃ (formula weight = 116.164 g/mol)

The two polymorphs included in this study are wollastonite and cyclo-wollastonite (or "pseudowollastonite").

Table 225. Sources of thermophysical data for aragonite, CaCO_3 .

Source	Data type	Method	Number of points	Range		Percent error ^a
				Temperature (K)	Pressure (bars)	
Kozu and Kuni, 1934	volume	dilatometry	13	323-723	1.01	-1934±3.36
Vaidya and others, 1973	volume	dilatometry	6	298	1.01-15000	-0.64±0.41
Kelley, 1960	heat content	compilation	6	350-600	1.01	-0.13±0.10
Staveley and Lingford, 1969	heat capacity	adiab. cal.	9	206-291	1.01	0.06±0.37
Staveley and Lingford, 1969	entropy	adiab. cal.	1	298	1.01	-0.05±0.00

^aThe tabulated numbers represent the unweighted, average standard error of estimate for data in the set from the calculated value and the 1-sigma deviation of the errors about the average. Refer to text for details.

Table 226. Sources of thermochemical data for aragonite, CaCO₃.

Reaction	Source	Method	No. of Points	Temperature (K)	Range Pressure (kb)	H _f ^o (298.15 K) Third Law, kJ	H _f ^o (298.15 K) kJ/mol
AI	Boettcher and Wyllie, 1968	Solid-medium Pressure Apparatus	2 pr	673	8.2-8.6	-0.822±0.049	-1209.880
AI	Boettcher and Wyllie, 1968	Solid-medium Pressure Apparatus	5 pr	753-1073	9.0-20.1	-0.730±0.336	-1209.788
AI	Goldsmith and Newton, 1969	Gas- and Solid-medium Pressure Apparatus	3 pr	673-723	8.5-10.5	-0.687±0.111	-1209.744
AI	Goldsmith and Newton, 1969	Gas- and Solid-medium Pressure Apparatus	10 pr	773-973	10.0-11.5	-0.755±0.134	-1209.812
AI	Johannes and Puhar, 1971	Gas-medium Pressure Apparatus	10	403-643	4.0-8.5	-0.591±0.116	-1209.649
AI	Johannes and Puhar, 1971	Gas-medium Pressure Apparatus	34	633-873	8.4-15.5	-0.547±0.138	-1209.605
	This Study						-1209.660

Reactions:

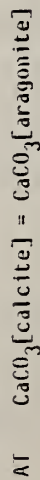


Table 227. Sources of volumetric data for lime, CaO.

Source	Data type	Method	Number of points	Range		Percent errors
				Temperature (K)	Pressure (bars)	
Weir, 1956	V-V(2000 kb)	X-ray	9	294	2000-10000	2.35±6.23
Grain and Campbell, 1962	volume	X-ray	5	528-1398	1.01	0.00±0.03
Roble and others, 1967	volume	compilation	1	298	1.01	0.017
Swanson and Tatge, 1953	volume	X-ray	1	300	1.01	-0.011

^dThe tabulated numbers represent the unweighted, average standard error of estimate for data in the set from the calculated value and the 1-sigma deviation of the errors about the average. Refer to text for details.

1.5.5.17.1. Wollastonite

Tables 228 and 229 contain the sources of data used in the final evaluation of the properties of wollastonite. All other data, though given in the reference list, were dropped before the final evaluation.

The heat capacity data that were given the highest weight in the evaluation were the data from adiabatic calorimetry and differential scanning calorimetry (d.s.c.) by Krupka and others (1980) and the data above 1000 K from the drop calorimetry of Southard (1941).

The thermochemical data used are in good internal agreement. The most divergent data seem to be from the borate-salt solution calorimetry. However, even here the departure in enthalpy of formation from the elements is only 2 kJ/mol. The thermochemical properties of wollastonite were also controlled by the evaluation of the data for cyclo wollastonite and the forcing of an inversion temperature of 1398.15 K (Osborn and Schairer, 1941) where the Gibbs energy difference between the two polymorphs is forced to be zero.

1.5.5.17.2. Cyclo wollastonite (= "pseudowollastonite")

Tables 230 and 231 contain the data in the final evaluation. Other data, though cited in the reference list, were dropped prior to the final evaluation.

The reported inversion temperature at 1.01 bars is 1398.15 ± 10 K (Osborn and Schairer, 1941). The thermochemical properties were determined from the tabulated data relating to cyclo wollastonite and wollastonite using the inversion temperature as a fixed point where the Gibbs energies of the polymorphs are equal.

Table 228. Sources of thermophysical data for wollastonite, CaSiO₃.

Source	Data type	Method	Number of points	Range		Percent error ^a
				Temperature (K)	Pressure (bars)	
Vaidya and others, 1973	volume diff.	dilatometry	9	298	3000-45000	0.00±0.05
Evans, Howard, 1977 (unpub.)	volume	X-ray	7	303-873	1.01	-0.04±0.09
Cristescu and Simon, 1934	heat capacity	isotherm. cal.	2	200-210	1.01	1.93±0.06
Christescu, 1931	heat capacity	isotherm. cal.	7	199-303	1.01	1.46±1.40
Krupka and others, 1980	heat capacity	adiab. cal.	39	200-386	1.01	-0.10±0.29
Gronow and Schweite, 1933	heat content	drop cal.	5	573-1373	1.01	-0.19±0.82
Southard, 1941	heat content	drop cal.	13	484-1418	1.01	0.07±0.40
Koth and Vertram, 1929	heat content	drop cal.	7	323-1157	1.01	-0.98±0.52
White, 1919	heat content	drop cal.	8	973-1573	1.01	-0.45±0.46
White, 1919	heat content	drop cal.	10	373-973	1.01	1.31±1.01
Wagner, 1932	heat content	drop cal.	11	566-1369	1.01	-0.18±0.82
Krupka and others, 1980	heat capacity	d.s.c.	99	349-999	1.01	0.16±0.66
Hemingway and Robie, 1977	entropy	compilation	1	298	1.01	0.64

^aThe tabulated numbers represent the unweighted, average standard error of estimate for data in the set from the calculated value and the 1-sigma deviation of the errors about the average. Refer to text for details.

Table 229. Sources of thermochemical data for wollastonite, CaSiO₃.

Reaction	Source	Method	No. of Points	Temperature Range (K)	Pressure (kb)	$H_f^\circ(298.15 \text{ K})$ Third Law, kJ	$H_f^\circ(298.15 \text{ K})$ kJ/mol
AI	Hayes, 1966	Solid-medium Pressure Apparatus	2 pr	1473-1523	7.5-11.0	-157,994.16,068	-1634,000
AI	Huckenthalz, 1974	Unspec'd	6 pr	1125-1423	0.2-7.5	-158,840.11,799	-1634,282
AI	Shmulovitch, 1974	Gas-medium Pressure Apparatus	1 pr	1133-1153	0.506	-159,474.1,470	-1634,809
AG	Boettcher, 1970	Gas-medium Pressure Apparatus	2 pr	893-1053	3.0-5.9	-50,204.11,453	-1634,643
AG	Newton, 1966b	Gas-medium Pressure Apparatus	2 pr	803-923	1.1-2.0	-51,867.13,013	-1635,778
AG	Newton, 1966b	Gas-medium Pressure Apparatus	2 pr	973-1023	4.7-5.7	-48,971.11,851	-1634,043
AG	Huckenthalz, 1974	Unspec'd	1 pr	648-858	2.0	-49,455.10,327	-1634,572
AG	Huckenthalz, 1974	Unspec'd	2 pr	888-958	3.0-4.0	-49,932.10,500	-1634,523
AG	Huckenthalz, 1974	Gas-medium Pressure Apparatus	5 pr	708-828	1.0-5.0	-49,629.10,446	-1634,644
AQ	L'hou, 1971	L.M.F.	12	898-1148	0.001	-43,707.10,175	-1634,208
BI	Benz and Wagner, 1961	Solid-medium Pressure Apparatus	3 pr	1723-1833	13.0-20.0	6,183.10,044	-1634,610
BI	Essene, 1974	Solid-medium Pressure Apparatus	1 pr	1823	21.0-22.0	6,150.10,043	-1634,642
BI	Huang and Wyllie, 1975	Solid-medium Pressure Apparatus	1 pr	970	0.001	8,215.10,779	-1632,577
BI	Charlu and others, 1978	Solution calorimetry, borate salt	1	1070	0.001	8,245	-1632,547
BI	Kiseleva and others, 1979	Solution calorimetry, borate salt	1	298	0.001	6,525	-1633,774
BI	Kracke and others, 1953	Solution calorimetry, HF acid	5	314	0.001	8,128.11,098	-1632,664
BI	Nacken, 1930	Solution calorimetry, HF acid	1	970	0.001	67,438.11,972	-1636,440
BI	Charlu and others, 1978	Solution calorimetry, borate salt	1	970	0.001	3,793.11,296	-1633,158
BI	Anderson and Kleppa, 1969	Solution calorimetry, borate salt	1	970	0.001	89,764.10,237	-1633,774
BX	Barany, 1966	Solution calorimetry, HF acid	5	347	0.001		-1634,651
BX	This Study						

Table 229. Continued

Reaction	Source	Method	No. of Points	Temperature Range (K)	Pressure (kb)	$H_f^\circ(298.15 \text{ K})$ Third Law, kJ	$H_f^\circ(298.15 \text{ K})$ kJ/mol
Reactions:							
AF	$2 \text{ Ca}_3\text{Al}_2\text{Si}_3\text{O}_{12}$ [grossular] = $\text{CaAl}_2\text{Si}_2\text{O}_8$ [anorthite] + $\text{Ca}_2\text{Al}_2\text{SiO}_7$ [gehlenite] + 3 CaSiO_3 [wollastonite]						
AG	2 CaSiO_3 [wollastonite] + $\text{CaAl}_2\text{Si}_2\text{O}_8$ [anorthite] = $\text{Ca}_3\text{Al}_2\text{Si}_3\text{O}_{12}$ [grossular] + SiO_2 [quartz, alpha]						
AG	2 CaSiO_3 [wollastonite] + $\text{CaAl}_2\text{Si}_2\text{O}_8$ [anorthite] = $\text{Ca}_3\text{Al}_2\text{Si}_3\text{O}_{12}$ [grossular] + SiO_2 [quartz, beta]						
AQ	$\text{CaAl}_2\text{Si}_2\text{O}_8$ [anorthite] + CaSiO_3 [wollastonite] + H_2O [g] = $\text{Ca}_7\text{Al}_2\text{Si}_3\text{O}_{10}$ (OH) ₂ [prehnite]						
BH	CaO [lime] + SiO_2 [quartz, beta] = CaSiO_3 [wollastonite]						
BN	CaSiO_3 [wollastonite] = CaSiO_3 [cyclo wollastonite]						
BP	$\text{Ca}_7\text{Al}_2\text{Si}_3\text{O}_{10}$ [grossular] = $\text{CaAl}_2\text{Si}_2\text{O}_8$ [Ca-Al clinopyroxene] + 2 CaSiO_3 [wollastonite]						
BU	Al_2SiO_5 [kyanite] + CaSiO_3 [wollastonite] = $\text{CaAl}_2\text{Si}_2\text{O}_8$ [anorthite]						
BX	CaSiO_3 [wollastonite] = CaO [lime] + SiO_2 [quartz, alpha]						

Table 230. Sources of thermophysical data for cyclowollastonite, CaSiO₃.

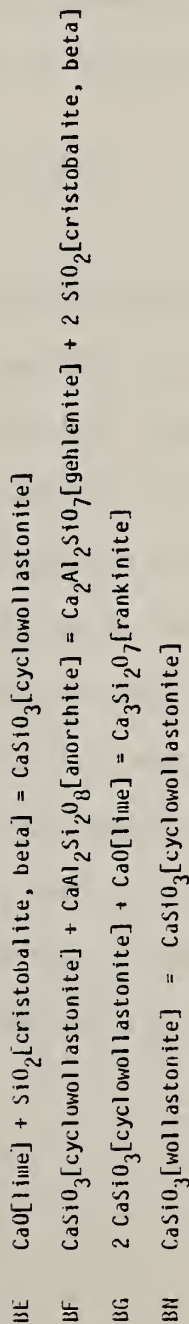
Source	Data type	Method	Range			Percent error ^d
			Number of points	Temperature (K)	Pressure (bars)	
Evans, Howard, 1977 (unpub.)	volume	X-ray dilatometry	7	303-873	1.01	-0.08±0.21
Vaidya and others, 1973	volume	compilation	9	298	5000-45000	0.05±0.10
Robie and others, 1979	volume	drop cal.	1	298	1.01	-0.19
Wagner, 1932	heat content	isotherm. cal.	12	576-1558	1.01	1.93±0.67
Wagner, 1932	heat capacity	drop cal.	7	201-295	1.01	-0.68±1.77
White, 1919	heat content	drop cal.	28	373-1673	1.01	1.54±1.44
Parks and Kelley, 1926	heat capacity	isotherm. cal.	6	194-298	1.01	-0.38±0.70
Hemingway and Robie, 1977	entropy	compilation	1	298	1.01	0.199

^dThe tabulated numbers represent the unweighted, average standard error of estimate for data in the set from the calculated value and the 1-sigma deviation of the errors about the average. Refer to text for details.

Table 231. Sources of thermochemical data for cyclo wollastonite (= "pseudowollastonite"), CaSiO_3 .

Reaction	Source	Method	No. of Points	Temperature Range (K)	Pressure (kb)	$H_f^\circ(298.15 \text{ K})$ Third Law, kJ	$H_f^\circ(298.15 \text{ K})$ kJ/mol
BE	Kay and Taylor, 1960	log K	1	1773	0.001	-87.895±2.771	-1628.937
BF	Kay and Taylor, 1960	log K	1	1543	0.001	61.011±2.412	-1623.787
BG	Benz and Wagner, 1961	E.M.F.	10	943-1003	0.001	-41.476±0.186	-1628.505
BN	Essene, 1974	Solid-medium Pressure Apparatus	3 pr	1723-1833	13.0-20.0	6.183±0.044	-1628.469
BN	Iluang and Yllie, 1975	Solid-medium Pressure Apparatus	1 pr	1823	21.0-22.0	6.150±0.043	-1628.501
BN	Charlu and others, 1978	Solution calorimetry, borate salt	1	970	0.001	8.215±0.779	-1626.436
BN	Kiseleva and others, 1979	Solution calorimetry, borate salt	1	1070	0.001	8.245	-1626.406
BN	Kracek and others, 1953	Solution calorimetry, HF acid	1	298	0.001	6.525	-1628.894
BN	Hacken, 1930	Solution calorimetry, HF acid	5	314	0.001	8.128±1.098	-1626.523
	This Study						-1628.510

Reactions:



1.5.5.18. $\text{Ca}_2\text{Al}_2\text{SiO}_6(\text{OH})_2$, bicchulite (formula weight =
292.220 g/mol)

Tables 232 and 233 contain the data used in the final evaluation. Only the molar volume of bicchulite was available. The other properties were derived from the fictive-component method of estimation as cited in section 1.3.2 or by the slope of the univariant reaction in pressure-temperature space. The large 2-sigma confidence limits given on the tables reflect this lack of available data.

1.5.5.19. $\text{Ca}_2\text{Al}_2\text{SiO}_6$, gehlenite (formula weight =
274.204 g/mol)

Tables 234 and 235 contain the data used in the final evaluation of the properties of gehlenite. All other data, though cited in the reference list, were dropped before the final evaluation.

The enthalpy of solution of gehlenite in HF acid solutions as measured by Barany (1963) was probably obtained from a sample that, at the time of measurement, was not gehlenite even though it had been so identified before grinding and sizing by siltation in water. Gehlenite, being one of the cement phases, may have reacted with the water during the siltation and not converted back to gehlenite during drying at 973 K. In any event, the results Barany achieved were what would be expected if one were working with a metastable or reacted material. They are discordant with the entropy and phase equilibria for gehlenite.

Table 232. Sources of thermophysical data for bicchulite, $\text{Ca}_2\text{Al}_2\text{SiO}_6(\text{OH})_2$.

Source	Data type	Method	Number of points	Range		Percent error ^a
				Temperature (K)	Pressure (bars)	
Gupta and Chatterjee, 1978	volume	X-ray	1	290	1.01	-0.05

^aThe tabulated numbers represent the unweighted, average standard error of estimate for data in the set from the calculated value and the 1- σ deviation of the errors about the average. Refer to text for details.

Table 233. Sources of thermochemical data for bicchulite, $\text{Ca}_2\text{Al}_2\text{SiO}_6(\text{OH})_2$.

Reaction	Source	Method	No. of Points	Temperature (K)	Range (K)	Pressure (kb)	$H_f^\circ(298.15 \text{ K})$ Third Law, kJ	$H_f^\circ(298.15 \text{ K})$ kJ/mol
AS	Gupta and Chatterjee, 1978	Gas-medium Pressure Apparatus	7 pr	890-1033	0.5-7.05	112.694 ± 0.646	-4336.660	
AS	Huckenholz, 1977 This Study	Unspecified	8 pr	884-1023	0.5-7.0	111.563 ± 0.725	-4337.790 -4337.238	

Reactions:

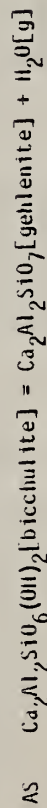


Table 234. Sources of thermophysical data for gehlenite, $\text{Ca}_2\text{Al}_2\text{SiO}_7$.

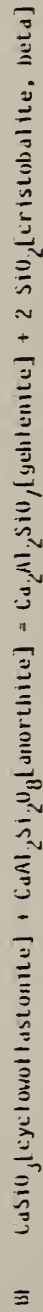
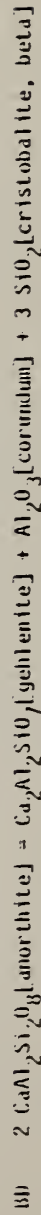
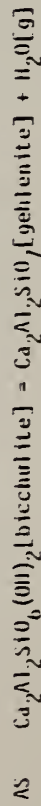
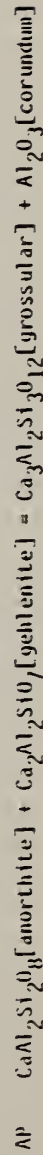
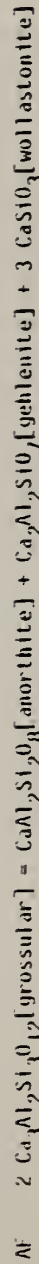
Source	Data type	Method	Range			Percent error ^a
			Number of points	Temperature (K)	Pressure (bars)	
Robie and others, 1979	volume	compilation	1	298	1.01	-0.01
Meller and Kelley, 1963	heat capacity	isotherm. cal.	10	206-296	1.01	-0.03±0.07
Pankratz and Kelley, 1964a	heat content	drop cal.	15	402-1801	1.01	0.01±0.17
Hemingway and Robie, 1977	entropy	compilation	1	978	1.01	-0.097

^aThe tabulated numbers represent the unweighted, average standard error of estimate for data in the set from the calculated value and the 1-sigma deviation of the errors about the average. Refer to text for details.

Table 235. Sources of thermochemical data for gehlenite, $\text{Ca}_2\text{Al}_2\text{SiO}_7$.

Reaction	Source	Method	No. of Points	Temperature (K)	Range Pressure (kb)	$H_f^\circ(298.15 \text{ K})$ Third Law, kJ	$H_f^\circ(298.15 \text{ K})$ kJ/mol
AW	Ilays, 1966	Solid-medium Pressure Apparatus	2 pr	1473-1523	7.5-11.0	-157.99416.068	-3981.332
AW	Iluckenholz, 1974	Unspecified	6 pr	1125-1423	0.2-7.5	-158.84011.799	-3982.178
AW	Shmulovitch, 1974	Gas-medium Pressure Apparatus	1 pr	1133-1153	0.506	-159.47411.420	-3983.760
AW	Ilays, 1966	Solid-medium Pressure Apparatus	4 pr	1473-1673	11.0-14.6	-6.33511.964	-3983.468
AP	Boettcher, 1970	Gas-medium Pressure Apparatus	1 pr	1033-1053	1.0	-101.52410.981	-3984.112
AP	Iluckenholz, 1974	Unspecified	3 pr	1028-1263	1.0-6.0	-102.14611.163	-3984.723
AS	Gupta and Chatterjee, 1978	Gas-medium Pressure Apparatus	7 pr	890-1033	0.5-7.05	112.69410.646	-3982.708
AS	Iluckenholz, 1977	Unspecified	6 pr	884-1023	0.5-7.0	111.56310.725	-3983.838
BB	Kay and Taylor, 1960	log K	1	1653	0.001	84.43012.584	-3980.625
BF	Kay and Taylor, 1960	log K	1	1543	0.001	61.01112.412	-3978.563
	This Study						-3983.286

Reactions:



1.5.5.20. $\text{Ca}_2\text{Al}_2\text{Si}_3\text{O}_{10}(\text{OH})_2$, prehnite (formula weight = 412.388 g/mol)

Tables 236 and 237 contain the sources of data used to evaluate the properties of prehnite. The smoothed, composition-corrected heat capacities of Perkins and others (1980) were used in the evaluation.

Only the study by Liou (1971) on the equilibria among anorthite, wollastonite, prehnite, and $\text{H}_2\text{O}[\text{gas}]$ had a slope that was consistent with the entropy and molar volume. All other studies were therefore discarded.

1.5.5.21. $\text{Ca}_2\text{Al}_3\text{Si}_3\text{O}_{12}(\text{OH})$, zoisite (formula weight = 454.361 g/mol)

Tables 238 and 239 contain the sources of data used in the final evaluation. All other data, though cited in the reference list, were deleted prior to the final evaluation. The smoothed, composition-corrected heat capacities measured by Perkins and others (1980) were used for the final evaluation.

The thermochemical data are in good agreement. The apparently discordant study by Strens (1968) on table 239 is due to the wide temperature bracket for the phase equilibrium reversal of about 53 kelvins. The refined properties lie within the reversal bracket at 2 kb and are consistent with it.

1.5.5.22. Ca_2SiO_4 (formula weight = 172.243 g/mol)

Tables 240 through 245 contain the data used in the final evaluation for the Ca_2SiO_4 polymorphs Ca olivine, bredigite, larnite, and

Table 236. Sources of thermophysical data for prehnite, $\text{Ca}_2\text{Al}_2\text{Si}_3\text{O}_{10}(\text{OH})_2$.

Source	Data type	Method	Number of points	Range		Percent error ^a
				Temperature (K)	Pressure (bars)	
Robie and others, 1979	volume	compilation	1	298	1.01	-0.08
Perkins and others, 1980	heat capacity	adiab. cal.	8	200-298	1.01	0.00±0.05
Perkins and others, 1980	heat capacity	d.s.c.	12	298-800	1.01	-0.08±0.23
Perkins and others, 1980	entropy	adiab. cal.	1	298	1.01	0.001

^aThe tabulated numbers represent the unweighted, average standard error of estimate for data in the set from the calculated value and the 1-sigma deviation of the errors about the average. Refer to text for details.

Table 237. Sources of thermochemical data for prehnite, $\text{Ca}_2\text{Al}_2\text{Si}_3\text{O}_{10}(\text{OH})_2$.

Reaction	Source	Method	No. of Points	Temperature (K)	Range	Pressure (kb)	$H_r^\circ(298.15 \text{ K})$ Third Law, kJ	$H_f^\circ(298.15 \text{ K})$ kJ/mol
AQ	Liou, 1971 This Study	Gas-medium Pressure Apparatus	5 pr	708-828	1.0-5.0		-89.629 ± 0.446	-6196.813 -6196.820

Reactions:



Table 238. Sources of thermophysical data for zoisite, $\text{Ca}_2\text{Al}_3\text{Si}_3\text{O}_{12}(\text{OH})$.

Source	Data type	Method	Range			Percent errors
			Number of points	Temperature (K)	Pressure (bars)	
Robie and others, 1979	volume	compilation	1	298	1.01	-0.15
Perkins and others, 1980	heat capacity	adiab. cal.	8	200-298	1.01	0.01 ± 0.17
Perkins and others, 1980	heat capacity	d.s.c.	11	298-750	1.01	-0.72 ± 0.71
Perkins and others, 1980	entropy	adiab. cal.	1	298	1.01	-0.015

^dThe tabulated numbers represent the unweighted, average standard error of estimate for data in the set from the calculated value and the 1-sigma deviation of the errors about the average. Refer to text for details.

Table 239. Sources of thermochemical data for zoisite, $\text{Ca}_2\text{Al}_3\text{Si}_3\text{O}_{12}(\text{OH})$.

Reaction	Source	Method	No. of Points	Temperature Range (K)	Pressure (kb)	$H_f^\circ(298.15 \text{ K})$ Third Law, kJ	$H_f^\circ(298.15 \text{ K})$ kJ/mol
AE	Newton, 1965	Gas- and Solid-medium Pressure Apparatus	6 pr	843-1113	2.0-6.8	-304.099±2.670	-6894.569
AL	Boettcher, 1970	Gas-medium Pressure Apparatus	1 pr	898-928	3.0	-305.304±3.803	-6894.769
AJ	Boettcher, 1970	Gas-medium Pressure Apparatus	2 pr	853-933	4.0-5.3	-212.732±2.710	-6894.540
AJ	Sirens, 1968	Gas-medium Pressure Apparatus	1 pr	770-823	2.0	-219.358±5.645	-6896.197
AJ	Newton, 1966b This Study	Gas-medium Pressure Apparatus	8 pr	758-1042	2.0-8.0	-209.387±4.619	-6893.704 -6894.244

Reactions:

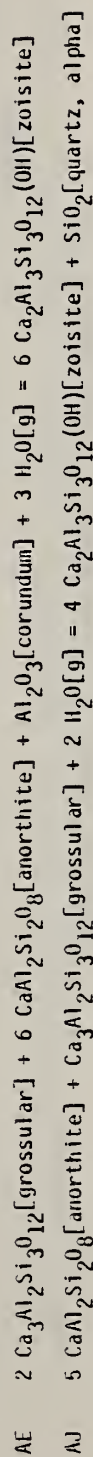


Table 240. Sources of thermophysical data for $\alpha\text{-Ca}_2\text{SiO}_4$.

Source	Data type	Method	Range		Percent error ^a
			Temperature (K)	Pressure (bars)	
Douglas, 1952	volume	X-ray	298	1.01	0.0
Coughlin and O'Brien, 1957	heat content	drop cal.	1714-1816	1.01	0.0±0.10

^aThe tabulated numbers represent the unweighted, average standard error of estimate for data in the set from the calculated value and the 1-sigma deviation of the errors about the average. Refer to text for details.

Table 241. Sources of thermophysical data for bredigite, Ca_2SiO_4 .

Source	Data type	Method	Number of points	Range		Percent error ^a
				Temperature (K)	Pressure (bars)	
Robie and others, 1979	volume	compilation	1	298	1.01	0.0
Coughlin and O'Brien, 1957	heat content	drop cal.	12	974-1690	1.01	0.02±0.14

^aThe tabulated numbers represent the unweighted, average standard error of estimate for data in the set from the calculated value and the 1-sigma deviation of the errors about the average. Refer to text for details.

Table 242. Sources of thermochemical data for bredigite, Ca_2SiO_4 .

Reaction Source	Method	No. of Points	Temperature (K)	Range Pressure (kb)	$H_r^\circ(298.15 \text{ K})$ Third Law, kJ	$H_f^\circ(298.15 \text{ K})$ kJ/mol
AR BI Carlson, 1931 Benz and Wagner, 1961 This Study	Phase Equilibria, Rapid Quench E.M.F.	1 10	1523 971-1143	0.001 0.001	11.573±0.155 -5.080±0.376	-2310.191 -2310.149 -2310.188

Reactions:



Table 243. Sources of thermophysical data for Ca-olivine, Ca_2SiO_4 .

Source	Data type	Method	Range			Percent errors ^a
			Number of points	Temperature (K)	Pressure (bars)	
Robie and others, 1979 King, 1957 Coughlin and O'Brien, 1957 King, 1957	volume	compilation	1	298	1.01	0.0
	heat capacity	isotherm. cal.	10	206-296	1.01	0.05±0.47
	heat content	drop cal.	18	405-1112	1.01	-0.25±0.91
	entropy	isotherm. cal.	1	298	1.01	0.0

^aThe tabulated numbers represent the unweighted, average standard error of estimate for data in the set from the calculated value and the 1-sigma deviation of the errors about the average. Refer to text for details.

Table 244. Sources of thermophysical data for larnite, Ca_2SiO_4 .

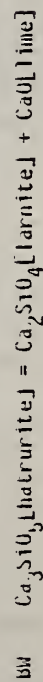
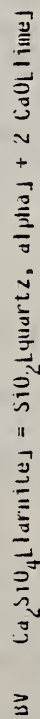
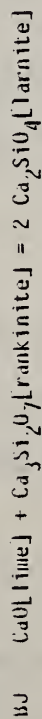
Source	Data type	Method	Number of points	Range		Percent errors
				Temperature (K)	Pressure (bars)	
Rigby and Green, 1942	volume diff.	dilatometry	11	473-1473	1.01	-0.03±2.00
Robie and others, 1979	volume	compilation	1	298	1.01	0.0
Todd, 1951	heat capacity	adiab. cal.	10	206-296	1.01	0.02±0.11
Coughlin and O'Brien, 1957	heat content	drop cal.	10	406-965	1.01	-0.02±0.16
Hemingway and Robie, 1977	entropy	compilation	1	298	1.01	0.37

^aThe tabulated numbers represent the unweighted, average standard error of estimate for data in the set from the calculated value and the 1-sigma deviation of the errors about the average. Refer to text for details.

Table 245. Sources of thermochemical data for larnite, Ca_2SiO_4 .

Reaction	Source	Method	No. of Points	Temperature (K)	Range (K)	Pressure (kb)	$H_r^\circ(298.15 \text{ K})$ Third Law, kJ	$H_f^\circ(298.15 \text{ K})$ kJ/mol
BJ	Benz and Magner, 1961	E.M.F.	3	943-963		0.001	-2.298±0.087	-2307.152
BV	King, 1951	Solution calorimetry, HF acid	1	347		0.001	126.660±1.093	-2306.930
BW	Brunauer and others, 1956 This Study	Solution calorimetry, HF-HNO ₃ acid	1	296		0.001	-8.676±0.926	-2307.286 -2307.224

Reactions:



a high-temperature phase often referred to as α - Ca_2SiO_4 . The inversion temperatures are as follows:

Ca olivine = bredigite	1120 K
bredigite = α - Ca_2SiO_4	1710 K
larnite = bredigite	970 K

The stability relations are best shown by the Gibbs energy - temperature plot (figure 8) where it is readily recognized that larnite is metastable at 1.01 bars at all temperatures between 200 and 1800 K.

1.5.5.22.1. α - Ca_2SiO_4

For α - Ca_2SiO_4 , the thermochemical properties were derived from the thermophysical properties, the inversion temperatures, and the phase equilibria with the other polymorphs.

1.5.5.22.2. Bredigite

For bredigite, the thermochemical properties were derived from the thermophysical properties, the inversion temperatures, and the phase equilibria with the other polymorphs, and with rankinite and hatrurite.

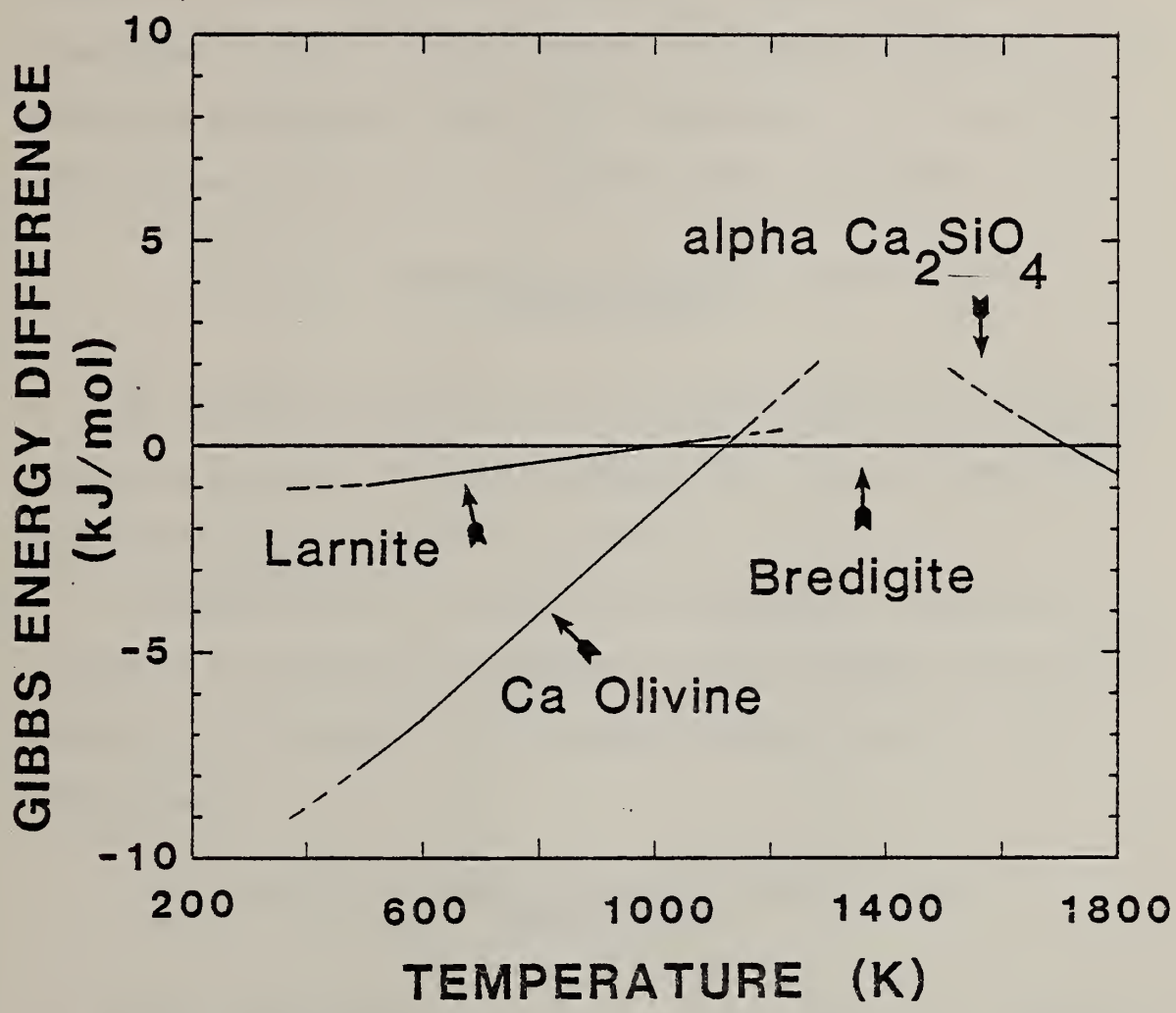
1.5.5.22.3. Ca olivine

For Ca olivine, the thermochemical properties were derived from the thermophysical properties, the inversion temperatures, and the phase equilibria for the other polymorphs.

1.5.5.22.4. Larnite

For larnite, the thermochemical properties were derived from the thermophysical properties, the inversion temperatures, the phase

Figure 8. Gibbs energy difference of phases indicated relative to bredigite at 1.01 bars. Ca olivine is the stable phase up to 1120 K. Bredigite is stable between 1120 and 1710 K. Above 1710, alpha-Ca₂SiO₄ is stable. Larnite is more stable than bredigite below 970 K but less stable than Ca olivine.



equilibria with other calcium silicates, and solution calorimetry. Concerning the latter data, King (1951) measured the heat of solution of larnite in HF acid. These data were combined with the heats of solution of quartz (Bennington and others, 1978) and of 2 moles of lime (Barany, 1963) to get the heat of reaction BV on table 245. In making the combination of data, the stoichiometry of the reactions were observed so that the final solutions were equivalent.

1.5.5.23. $\text{Ca}_3\text{Al}_2\text{Si}_3\text{O}_{12}$, grossular (formula weight = 450.452 g/mol)

The properties of grossular were derived from the data cited in tables 246 and 247. Other data, though cited in the reference list, were deleted prior to the final evaluation.

The thermochemical data are in good agreement. Though there is scatter in the enthalpies of formation from the elements (table 247, column 8), such scatter is to be expected because grossular has a large formula.

1.5.5.24. Ca_3SiO_5 , hatrurite (formula weight = 228.323 g/mol)

Tables 248 and 249 contain the data used in the final evaluation. The heat-capacity and heat-content data are too widely spaced to evaluate the properties of the individual polymorphs. The tabulated data in tables 86, 87, and 174, therefore, represent the average properties of all the polymorphs.

The heat of solution of hatrurite relative to a mechanical mixture of larnite and lime is in excellent agreement with the heat content

Faint, illegible text at the top of the page, possibly a header or introductory paragraph.

Second block of faint, illegible text in the middle of the page.

Third block of faint, illegible text at the bottom of the page.

Table 246. Sources of thermophysical data for grossular, $\text{Ca}_3\text{Al}_2\text{Si}_3\text{O}_{12}$.

Source	Data type	Method	Range			Percent errors ^a
			Number of points	Temperature (K)	Pressure (bars)	
Adams and Gibson, 1929	volume diff.	dilatometry	27	298	3000-12000	4.64±7.23
Vaidya and others, 1973	volume	dilatometry	9	298	5000-45000	-0.01±0.05
Hazen and Finger, 1978	volume	X-ray	4	296	1.01-61000	-0.04±0.03
Meagher, 1975	volume	X-ray	3	298-940	1.01	0.04±0.09
Skinner, 1956	volume	X-ray	13	292-981	1.01	0.01±0.05
Krupka and others, 1979	heat capacity	d.s.c.	50	350-978	1.01	0.71±1.23
Westrum and others, 1979	heat capacity	d.s.c. and adiab. cal.	57	200-596	1.01	-0.01±0.20
Westrum and others, 1979	entropy	adiab. cal.	1	298	1.01	0.554

^aThe tabulated numbers represent the unweighted, average standard error of estimate for data in the set from the calculated value and the 1-sigma deviation of the errors about the average. Refer to text for details.

Table 24/. Sources of thermochemical data for grossular, $\text{Ca}_3\text{Al}_2\text{Si}_3\text{O}_{12}$.

Reaction	Source	Method	No. of Points	Range Temperature (K)	Pressure (kb)	$H_f^\circ(298.15 \text{ K})$ Third Law, kJ	$H_f^\circ(298.15 \text{ K})$ kJ/mol
AE	Newton, 1965	Gas- and Solid-medium Pressure Apparatus	6 pr	843-1113	2.0-6.8	-304.099±2.670	-6639.916
AE	Boettcher, 1970	Gas-medium Pressure Apparatus	1 pr	898-928	3.0	-305.304±3.803	-6640.519
AF	Hays, 1966	Solid-medium Pressure Apparatus	2 pr	1473-1523	7.5-11.0	-157.994±6.068	-6637.966
AF	Huckenholz, 1974	Unspecified	6 pr	1125-1423	0.2-7.5	-158.840±1.799	-6638.389
AF	Shmulovich, 1974	Gas-medium Pressure Apparatus	1 pr	1133-1153	0.506	-159.474±1.420	-6639.180
AG	Boettcher, 1970	Gas-medium Pressure Apparatus	2 pr	893-1053	3.0-5.9	-50.204±1.453	-6638.959
AG	Newton, 1966b	Gas-medium Pressure Apparatus	2 pr	803-923	1.1-2.0	-51.867±3.013	-6641.197
AG	Newton, 1966b	Gas-medium Pressure Apparatus	2 pr	973-1023	4.7-5.7	-48.971±1.851	-6637.727
AG	Huckenholz, 1974	Unspecified	1 pr	848-858	2.0	-49.455±0.327	-6638.786
AG	Huckenholz, 1974	Unspecified	2 pr	888-958	3.0-4.0	-49.932±0.500	-6638.688
AI	Gasparrik, 1981	Solid-medium Pressure Apparatus	3 pr	1463-1673	10.75-23.5	-94.622±2.588	-6639.020
AJ	Boettcher, 1970	Gas-medium Pressure Apparatus	2 pr	853-933	4.0-5.3	-212.732±2.710	-6640.127
AJ	Strens, 1969	Gas-medium Pressure Apparatus	1 pr	770-823	2.0	-219.358±5.645	-6646.753
AJ	Newton, 1966b	Gas-medium Pressure Apparatus	8 pr	758-1042	2.0-8.0	-209.387±4.619	-6636.783
AP	Boettcher, 1970	Gas-medium Pressure Apparatus	1 pr	1033-1053	1.0	-101.524±0.981	-6639.769
AP	Huckenholz, 1974	Unspecified	3 pr	1028-1263	1.0-6.0	-102.146±1.163	-6640.391
BP	Charlu and others, 1978 This Study	Solution calorimetry, borate salt	1	970	0.001	67.438±1.972	-6642.531 -6638.943

Table 247. Continued

Reaction	Source	Method	No. of Points	Temperature Range (K)	Pressure (kb)	$H_f^{\circ}(298.15 \text{ K})$ Third Law, kJ	$H_f^{\circ}(298.15 \text{ K})$ kJ/mol
Reactions:							
AL	$2 \text{ Ca}_3\text{Al}_2\text{Si}_3\text{O}_{12}[\text{grossular}] + 6 \text{ CaAl}_2\text{Si}_2\text{O}_8[\text{anorthite}] + \text{Al}_2\text{O}_3[\text{corundum}] + 3 \text{ H}_2\text{O}[\text{g}] = 6 \text{ Ca}_2\text{Al}_3\text{Si}_3\text{O}_{12}(\text{OH})[\text{zoisite}]$						
AF	$2 \text{ Ca}_3\text{Al}_2\text{Si}_3\text{O}_{12}[\text{grossular}] = \text{CaAl}_2\text{Si}_2\text{O}_8[\text{anorthite}] + \text{Ca}_2\text{Al}_2\text{Si}_2\text{O}_7[\text{gehlenite}] + 3 \text{ CaSiO}_3[\text{wollastonite}]$						
AG	$2 \text{ CaSiO}_3[\text{wollastonite}] + \text{CaAl}_2\text{Si}_2\text{O}_8[\text{anorthite}] = \text{Ca}_3\text{Al}_2\text{Si}_3\text{O}_{12}[\text{grossular}] + \text{SiO}_2[\text{quartz, alpha}]$						
AG	$2 \text{ CaSiO}_3[\text{wollastonite}] + \text{CaAl}_2\text{Si}_2\text{O}_8[\text{anorthite}] = \text{Ca}_3\text{Al}_2\text{Si}_3\text{O}_{12}[\text{grossular}] + \text{SiO}_2[\text{quartz, beta}]$						
AI	$3 \text{ CaAl}_2\text{SiO}_6[\text{Ca-Al clinopyroxene}] = \text{Ca}_3\text{Al}_2\text{Si}_3\text{O}_{12}[\text{grossular}] + 2 \text{ Al}_2\text{O}_3[\text{corundum}]$						
AJ	$5 \text{ CaAl}_2\text{Si}_2\text{O}_8[\text{anorthite}] + \text{Ca}_3\text{Al}_2\text{Si}_3\text{O}_{12}[\text{grossular}] + 2 \text{ H}_2\text{O}[\text{g}] = 4 \text{ Ca}_2\text{Al}_3\text{Si}_3\text{O}_{12}(\text{OH})[\text{zoisite}] + \text{SiO}_2[\text{quartz, alpha}]$						
AP	$\text{CaAl}_2\text{Si}_2\text{O}_8[\text{anorthite}] + \text{Ca}_2\text{Al}_2\text{SiO}_7[\text{gehlenite}] = \text{Ca}_3\text{Al}_2\text{Si}_3\text{O}_{12}[\text{grossular}] + \text{Al}_2\text{O}_3[\text{corundum}]$						
BP	$\text{Ca}_3\text{Al}_2\text{Si}_3\text{O}_{12}[\text{grossular}] = \text{CaAl}_2\text{SiO}_6[\text{Ca-Al clinopyroxene}] + 2 \text{ CaSiO}_3[\text{wollastonite}]$						

Table 248. Sources of thermophysical data for hattrurite, $\text{Ca}_3\text{Si}_2\text{O}_7$.

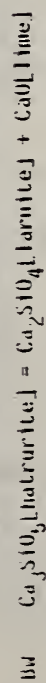
Source	Data Type	Method	Range			Percent error ^a
			Number of points	Temperature (K)	Pressure (bars)	
Rigby and Green, 1942	expansivity	dilatometry	11	473-1473	1.01	0.00±3.13
Yamaguchi and Miyabe, 1960	volume	X-ray	1	298	1.01	0.0
Fodd, 1951	heat capacity	isotherm. cal.	9	206-296	1.01	0.00±0.11
Gronow and Schweitte, 1933	heat content	drop cal.	7	573-1173	1.01	0.44±0.54
Fodd, 1951	entropy	isotherm. cal.	1	298	1.01	0.001

^aThe tabulated numbers represent the unweighted, average standard error of estimate for data in the set from the calculated value and the 1-sigma deviation of the errors about the average. Refer to text for details.

Table 249. Sources of thermochemical data for hatrurite, Ca_3SiO_5 .

Reaction	Source	Method	No. of Points	Temperature (K)	Range	Pressure (kb)	$H_f^\circ(298.15 \text{ K})$ Third Law, kJ	$H_f^\circ(298.15 \text{ K})$ kJ/mol
AR	Carlson, 1931	Phase Equilibria, Rapid Quench	1	1523		0.001	11.573±0.155	-2933.707
BW	Brunauer and others, 1956 This Study	Solution calorimetry, H-HNO ₃ acid	1	296		0.001	-8.676±0.926	-2933.766 -2933.704

Reactions:



data for the three phases and the breakdown temperature of 1523 ± 25 K observed by Carlson (1931). The departure is 0.35 kelvins for a calculated breakdown temperature of 1523.5 K.

1.5.5.25. $\text{Ca}_3\text{Si}_2\text{O}_7$, rankinite (formula weight = 288.407 g/mol)

Tables 250 and 251 contain the data used in the final evaluation. It should be pointed out that the data used for adjusting the thermochemical properties of rankinite are limited to e.m.f. studies. However, other data provided by this source for larnite, bredigite, and wollastonite are in good agreement with data from other sources. It is assumed that these data are also of high quality.

1.5.5.26. $\text{Ca}_4\text{Al}_6\text{Si}_6\text{O}_{24}(\text{CO}_3)$, meionite (formula weight = 931.717 g/mol)

Tables 252 and 253 contain the sources of data for the evaluation of properties of meionite. The errors on the property tables reflect the lack of detailed experimental data that are necessary to provide a more accurate evaluation. Especially needed are data on the entropy and heat capacity.

1.5.5.27. Fe, iron (formula weight = 55.847 g/mol)

The thermodynamic properties of iron were taken from the JANAF Thermochemical Tables^a. The molar volume was not needed in this study and therefore not evaluated.

^aJANAF Thermochemical Tables, looseleaf pages for 1978 issued by Dow Chemical Company, 1707 Building, Midland, Michigan.

Table 250. Sources of thermophysical data for rankinite, $\text{Ca}_3\text{Si}_2\text{O}_7$.

Source	Data type	Method	Number of points	Range		Percent error ^a
				Temperature (K)	Pressure (bars)	
Rigby and Green, 1942	volume diff.	dilatometry	11	473-1473	1.01	-0.17±2.68
Saburi and others, 1976	volume	X-ray	1	298	1.01	0.0
King, 1957	heat capacity	isotherm. cal.	10	206-296	1.01	0.00±0.15
King, 1957	entropy	isotherm. cal.	1	298	1.01	-0.441

^aThe tabulated numbers represent the unweighted, average standard error of estimate for data in the set from the calculated value and the 1-sigma deviation of the errors about the average. Refer to text for details.

Table 251. Sources of thermochemical data for rankinite, $\text{Ca}_3\text{Si}_2\text{O}_7$.

Reaction	Source	Method	No. of Points	Temperature (K)	Range (K)	Pressure (kb)	$H_f^\circ(298.15 \text{ K})$ Third Law, kJ	$H_f^\circ(298.15 \text{ K})$ kJ/mol
BG	Benz and Wagner, 1961	E.M.F.	10	943-1003		0.001	-41.476±0.186	-3975.040
BI	Benz and Wagner, 1961	E.M.F.	10	971-1143		0.001	-5.080±0.376	-3974.972
BJ	Benz and Wagner, 1961 This Study	E.M.F.	3	943-963		0.001	-2.298±0.087	-3974.906 -3975.050

Reactions:

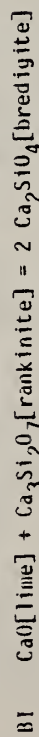
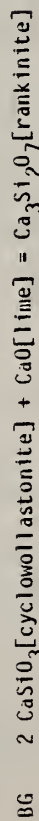


Table 252. Sources of thermophysical data for melonite, $\text{Ca}_4\text{Al}_6\text{Si}_6\text{O}_{24}\text{CO}_3$.

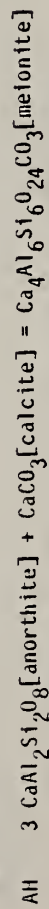
Source	Data type	Method	Number of points	Range		Percent error ^a
				Temperature (K)	Pressure (bars)	
Goldsmith and Newton, 1977	volume	X-ray	1	298	1.01	0.85

^aThe tabulated numbers represent the unweighted, average standard error of estimate for data in the set from the calculated value and the 1-sigma deviation of the errors about the average. Refer to text for details.

Table 253. Sources of thermochemical data for meionite, $\text{Ca}_4\text{Al}_6\text{Si}_6\text{O}_{24}\text{CO}_3$.

Reaction	Source	Method	No. of Points	Temperature Range (K)	Pressure (kb)	$H_f^\circ(298.15 \text{ K})$ Third Law, kJ	$H_f^\circ(298.15 \text{ K})$ kJ/mol
AI	Goldsmith and Newton, 1977 This Study	Solid-medium Pressure Apparatus	5 pr	1123-1173	1.0-15.0	3.598 ± 0.015	-13897.547 -13897.549

Reactions:



1.5.5.28. $\text{Fe}_{0.947}\text{O}$, wustite (formula weight = 68.887 g/mol)

Tables 254 and 255 contain the sources of data used to evaluate the properties of wustite. All other data, though cited in the reference list, were deleted prior to the final evaluation.

The two composite sets of data for wustite-iron and wustite-magnetite equilibria were developed from the compositions of wustite that coexisted with iron or magnetite, respectively, as measured by Darken and Gurry (1945) and from the $\log f(\text{O}_2)$ -composition experiments of Vallet and Raccach (1965), Bransky and Hed (1968), and Lohberg and Stanek (1975).

The breakdown temperature determined by Rau (1972) by $\text{H}_2/\text{H}_2\text{O}$ gas equilibria is 843 ± 10 K. Birks (1966) determined the temperature to be 838 ± 10 K by measuring the potential difference between the wustite-iron and the wustite-magnetite buffers. These are in excellent agreement with the other experiments. The final calculated breakdown temperature is 840.2 K.

During the evaluation, the $\log f(\text{O}_2)$ -composition data were used to derive the properties of the defect phase with an iron/oxygen ration of 0.947. Because the properties of the hypothetical end-member "FeO" remain unevaluated, only the thermochemical data for formation from the elements are tabulated.

1.5.5.29. FeSiO_3 , ferrosilite (formula weight = 131.931 g/mol)

Tables 256 and 257 contain the sources of data used in the final evaluation of the properties of ferrosilite. Other sources, though cited in the reference list, were deleted in preliminary evaluations.

Table 254. Sources of thermophysical data for wustite, Fe₉₄₇₀.

Source	Data type	Method	Number of points	Range		Percent error ^d
				Temperature (K)	Pressure (bars)	
Robie and others, 1979	volume	compilation	1	298	1.01	0.0
Hazen and others, 1981	molar volume	X-ray	11	298	1.01-54700	0.00±0.03
Coughlin and others, 1951	heat content	drop cal.	25	341-1614	1.01	0.05±0.47
Todd and Bonnicksen, 1951	heat capacity	low-temp. cal.	11	202-296	1.01	-0.08±0.79
Todd and Bonnicksen, 1951	entropy	low-temp. cal.	1	298	1.01	1.64

^dThe tabulated numbers represent the unweighted, average standard error of estimate for data in the set from the calculated value and the 1-sigma deviation of the errors about the average. Refer to text for details.

Table 255. Sources of thermochemical data for wustite, Fe_{.947}O.

Reaction	Source	Method	No. of Points	Temperature (K)	Range (K)	Pressure (kb)	H _r ^o (298.15 K) Third Law, kJ	H _f ^o (298.15 K) kJ/mol
CA	Birks, 1966	Electrochemistry	1	838		0.001	-55.492	-265.390
CA	Rau, 1972	Gas reduction	1	843		0.001	-55.747	-265.453
CD	Composite set	Gas reduction	14	1323-1573		0.001	-272.551±0.118	-265.127
CD	Darken and Gurry, 1945	Gas reduction	3	1373-1573		0.001	-272.492±0.137	-265.068
CE	Ackermann & Sanford, 1966	Gas reduction	5	972-1277		0.001	-905.281±0.544	-265.405
CE	Composite set	Gas reduction	12	1373-1573		0.001	-904.952±0.196	-265.295
CE	Darken and Gurry, 1945	Gas reduction	4	1373-1673		0.001	-904.944±0.163	-265.292
CL	Giddings, 1972	Electrochemistry	7	973-1573		0.001	-904.479±0.088	-265.137
CF	Ackermann & Sanford, 1966	Gas reduction	1	1277		0.001	11.462	-264.176
CF	Darken and Gurry, 1945	Gas reduction	8	1311-1638		0.001	10.670±0.219	-264.968
CF	Swaroop and Wagner, 1967	Gas reduction	7	1223-1523		0.001	10.439±0.127	-265.199
CG	Emmett and Schultz, 1933	Gas reduction	19	860-972		0.001	-23.563±0.233	-265.399
CU	Rau, 1972	Gas reduction	11	860-978		0.001	-23.192±0.074	-265.028
CI	Emmett and Schultz, 1933	Gas reduction	17	1080-1172		0.001	275.743±0.202	-265.209
CI	Emmett and Schultz, 1933	Gas reduction	7	1190-1288		0.001	-30.574±0.123	-265.571
CJ	Ackermann & Sanford, 1966	Gas reduction	2	972-1023		0.001	17.265±0.276	-265.797
CK	Ackermann & Sanford, 1966	Gas reduction	2	1075-1182		0.001	317.131±0.499	-265.047
	This Study							-265.416

Reactions:

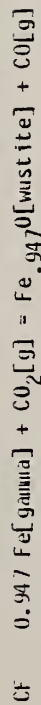
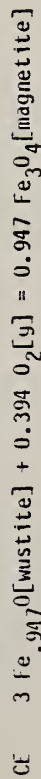
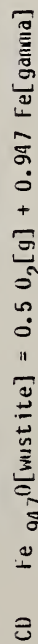
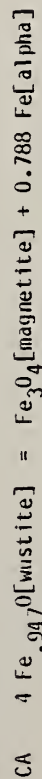


Table 255. Continued

Reaction	Source	Method	No. of Points	Range Temperature (K)	Pressure (kb)	$H_f^\circ(298.15 \text{ K})$ Third Law, kJ	$H_f^\circ(298.15 \text{ K})$ kJ/mol
Reactions (continued):							
CH	0.947 Fe[alpha-delta]	$+ H_2O[g] = Fe_{.947}O[wustite] + H_2[g]$					
CI	0.947 Fe[gamma]	$+ H_2O[g] = Fe_{.947}O[wustite] + H_2[g]$					
CJ	0.947 Fe[alpha]	$+ CO_2[g] = Fe_{.947}O[wustite] + CO[g]$					
CK	0.947 Fe[alpha-delta]	$+ CO_2[g] = Fe_{.947}O[wustite] + CO[g]$					

Table 256. Sources of thermophysical data for ferrosilite, FeSiO₃.

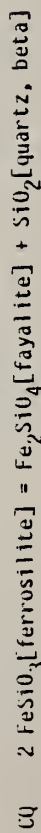
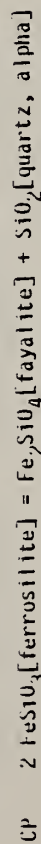
Source	Data type	Method	Number of points	Range		Percent error ^a
				Temperature (K)	Pressure (bars)	
Burnham, 1966 Sueno and others, 1976	volume	X-ray	1	298	1.01	0.01
	volume	X-ray	6	297-1253	1.01	-0.04±0.10

^aThe tabulated numbers represent the unweighted, average standard error of estimate for data in the set from the calculated value and the 1-sigma deviation of the errors about the average. Refer to text for details.

Table 257. Sources of thermochemical data for ferrosillite, FeSiO₃.

Reaction	Source	Method	No. of Points	Temperature (K)	Range	Pressure (kb)	H _f ^o (298.15 K) Third Law, kJ	H _f ^o (298.15 K) kJ/mol
CP	Bohlen and others, 1980	Solid-medium pressure apparatus	8	973-1123	10.5-12.3		-1.253±0.062	-1194.280
CQ	Bohlen and others, 1980	Solid-medium pressure apparatus	8	1173-1323	12.5-15.0		-1.845±0.063	-1194.287
CQ	Navrotsky and others, 1979	Solution calorimetry, borate salt	1	970	0.001		-2.645	-1194.687
CQ	Wood and Kleppa, 1981	Solution calorimetry, borate salt	1	970	0.001		-4.026	-1195.378
	This Study							-1194.286

Reactions:



The heat capacity of ferrosilites was estimated using the method described in section 1.3.2, above. The thermochemical properties of ferrosilite were constrained to fit the tightly reversed equilibria between ferrosilite, fayalite, and quartz (Bohlen and others, 1980). These experiments were supported by the borate-salt solution calorimetry.

1.5.5.30. Fe₂O₃, hematite (formula weight = 159.692 g/mol)

Tables 258 and 259 contain the sources of experimental data used to constrain the final evaluation. Below 1000 K the heat capacity experiments of Grønvold and Westrum (1959) and Grønvold and Samuelson (1975) constrained the heat capacity and heat content of hematite. The drop calorimetry of Coughlin and others (1951) were used to constrain the evaluation above 1000 K.

The thermochemical data available in the chemical system Fe-O are all studies on the equilibrium between magnetite and hematite at controlled oxygen fugacities. At the temperature of the experiments, the magnetite phase has a significant solid solution. Activity corrections were made using the formula of Salmon (1961):

$$a_{\text{Fe}_3\text{O}_4}^{\text{M}} = \frac{N_{\text{Fe}_3\text{O}_4}^{\text{M}}}{0.25 N_{\text{Fe}_2\text{O}_3}^{\text{M}} + N_{\text{Fe}_3\text{O}_4}^{\text{M}}}$$

where the chemical formula denotes the chemical component and the superscript M denotes the phase magnetite. This relationship is in agreement (± 0.01) with the experimental measurements of Darken and Gurry (1946).

Table 258. Sources of thermophysical data for hematite, Fe₂O₃.

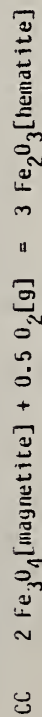
Source	Data type	Method	Number of points	Range		Percent error ^a
				Temperature (K)	Pressure (bars)	
Kobie and others, 1979	volume	compilation	1	298	1.01	0.0
Willis and Rooksby, 1952	volume	X-ray	2	293-1023	1.01	0.03±0.03
Wilburn and others, 1978	volume	dilatometry	37	293	5300-114000	-0.01±0.17
Lewis and Brickner, 1966	volume	dilatometry	10	298	1.01-230000	0.78±0.64
Grönvold and Samuelson, 1975	heat capacity	high-temp. cal.	7	973-1054	1.01	-0.07±0.90
Stull and Prophet, 1971	heat capacity	compilation	8	1500-2200	1.01	-0.20±1.34
Grönvold and Samuelson, 1975	heat capacity	high-temp. cal.	63	301-943	1.01	0.09±0.91
Grönvold and Westrum, 1959	heat capacity	low-temp. cal.	19	202-354	1.01	-0.02±0.27
Coughlin and others, 1951	rel. heat content	drop cal.	21	1002-1730	1.01	4.71±11.3
Grönvold and Westrum, 1959	entropy	low-temp. cal.	1	298	1.01	-0.09

^aThe tabulated numbers represent the unweighted, average standard error of estimate for data in the set from the calculated value and the 1-sigma deviation of the errors about the average. Refer to text for details.

Table 259. Sources of thermochemical data for hematite, Fe₂O₃.

Reaction	Source	Method	No. of Points	Temperature Range (K)	Pressure (kb)	H _r ^o (298.15 K) Third Law, kJ	H _f ^o (298.15 K) kJ/mol
CC	Darken and Gurry, 1946	Gas reduction	3	1586-1730	0.001	-167.299±1.011	-827.553
CC	Komarov and others, 1967	Electrochemistry	21	1526-1731	0.001	-166.849±1.078	-827.403
CC	Kurepin, 1975	Electrochemistry	2	1473-1573	0.001	-165.448±0.008	-826.936
CC	Norton, 1955	Mass spectrometry	8	1051-1342	0.001	-161.138±1.124	-825.500
CC	Schmidt, 1941	Gas equilibria	6	1583-1683	0.001	-167.177±0.438	-827.512
CC	Smitlens, 1957	Gas equilibria	4	1452-1731	0.001	-166.769±1.768	-827.377
	This Study						-827.148

Reactions:



Darken and Gurry (1946), Salmon (1961), and Komarov and others (1967) have shown that the solid solution of Fe_3O_4 in hematite is minor and can be neglected.

Rau (1972) studied the equilibria between hematite and magnetite at 1.01 bars between 767 and 840 K using the gas equilibria between H_2 and H_2O to control the chemical activity of oxygen. The mixture of magnetite + hematite was synthesized from an $\alpha\text{-FeOOH}$ precipitate by hydrogen reduction near 600 K. The magnetite in the mixture probably contained a significant Fe_2O_3 component and was metastable. The departure of these data from the refinement is consistent with such a hypothesis.

1.5.5.31. Fe_2SiO_4 , fayalite (formula weight = 203.777 g/mol)

Tables 260 and 261 contain the sources of data used in the final evaluation of the properties of fayalite. Other data, though cited in the reference list, were deleted in preliminary evaluations.

The thermochemical data of Hewitt (1978) and of Meyer (1981, unpub.) constrain the properties of fayalite. The experimental investigations on the equilibria between fayalite, iron, oxygen (controlled by CO/CO_2 or $\text{H}_2/\text{H}_2\text{O}$ gas equilibria) and an undefined polymorph in the SiO_2 system were given minor weighting because of the lack of positive identification of the SiO_2 polymorph present during the experiment. Where used, the analyses were completed assuming that beta cristobalite was the phase present. This was chosen because of the high temperature and because it readily forms. It is recognized that some interpretations of the data on the stability of the SiO_2

Table 260. Sources of thermophysical data for fayalite, Fe₂SiO₄.

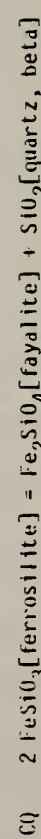
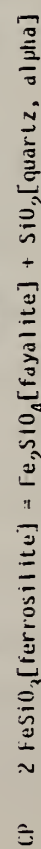
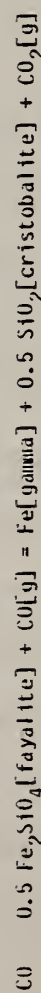
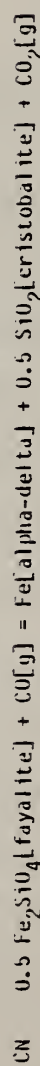
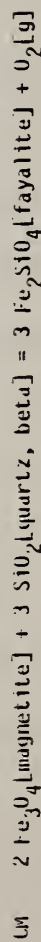
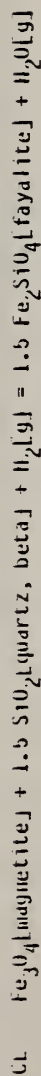
Source	Data type	Method	Range			Percent errors
			Number of points	Temperature (K)	Pressure (bars)	
Hazen, 1977	volume	X-ray	3	296	1.01-42000	0.03±0.09
Hazen, 1977	volume	X-ray	3	77-296	1.01	0.26±0.11
Smyth, 1975	volume	X-ray	6	293-1173	1.01	-0.01±0.14
Robie and Hemingway, 1982 (unpub.)	heat capacity	low-temp. cal.	31	208-381	1.01	0.01±0.09
Orr, 1953	heat content	drop cal.	13	395-1370	1.01	-0.23±0.50
Robie and Hemingway, 1982 (unpub.)	entropy	low-temp. cal.	1	298	1.01	-0.36

^aThe tabulated numbers represent the unweighted, average standard error of estimate for data in the set from the calculated value and the 1-sigma deviation of the errors about the average. Refer to text for details.

Table 261. Sources of thermochemical data for fayalite, Fe₂SiO₄.

Reaction	Source	Method	No. of Points	Temperature Range (K)	Pressure (kb)	H _f ^o (298.15 K) Third Law, kJ	H _f ^o (298.15 K) kJ/mol
CL	Hewitt, 1978	Gas reduction	8	923-1128	1.0	704.020±0.808	-1478.538
CM	Meyer, J., 1981 (unpub.)	Gas-medium pressure apparatus	7	922-1046	0.001	1888.729±1.693	-1479.897
CN	Lebedev & Lefitskii, 1962	Gas reduction	4	1123-1173	0.001	-311.995±0.171	-1479.394
CO	Lebedev & Lefitskii, 1962	Gas reduction	13	1223-1423	0.001	12.555±0.352	-1477.688
CO	Schwerdtfeger & Muan, 1966	Gas reduction	3	1273-1473	0.001	12.050±0.184	-1478.698
CP	Bohlen and others, 1980	Solid-medium pressure apparatus	8	973-1123	10.5-12.3	-1.253±0.062	-1479.155
CQ	Bohlen and others, 1980	Solid-medium pressure apparatus	8	1173-1323	12.5-15.0	-1.845±0.063	-1479.170
CQ	Navrotsky and others, 1979	Solution calorimetry, borate salt	1	970	0.001	-2.645	-1479.970
CQ	Wood and Kleppa, 1981	Solution calorimetry, borate salt	1	970	0.001	-4.026	-1481.351
	This Study						-1479.168

Reactions:



polymorphs would make tridymite the stable phase under the experimental environment.

1.5.5.32. Fe_3O_4 , magnetite (formula weight = 231.539 g/mol)

The sources of data used in the final evaluation are given on tables 262 and 263. Other data, though cited in the reference list, were deleted prior to the final evaluation.

The heat capacity at temperatures below 1000 K were dependent primarily on the experimentally measured heat capacities by Westrum and Grønvoold (1965) and by Grønvoold and Sveen (1974). The drop calorimetry of Coughlin and others (1951) were so weighted as to constrain the fit above 1000 K only. The thermochemical properties observed over the range 583 to 1731 K are consistent with $S^\circ = \text{zero}$. No allowance of an additional contribution due to disorder of any type is needed. With the exception of the relatively inaccurate data of Norton (1955), the final solution of the properties is consistent with the tabulated sources.

1.5.5.33. H_2 , hydrogen (ideal gas, formula weight = 2.016 g/mol)

The properties of the ideal diatomic gas were taken from the JANAF Thermochemical Tables^a. The volumetric properties were not needed in this study and therefore not evaluated.

^aJANAF Thermochemical Tables, looseleaf pages for 1977 issued by Dow Chemical Company, 1707 Building, Midland, Michigan.

Table 262. Sources of thermophysical data for magnetite, Fe₃O₄.

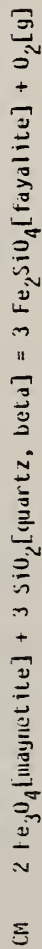
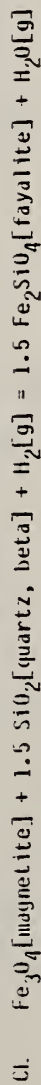
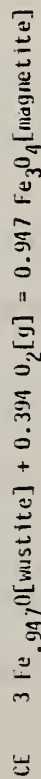
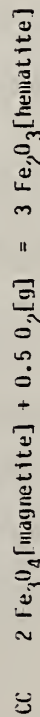
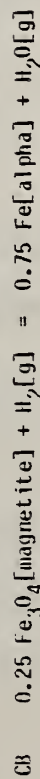
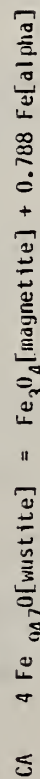
Source	Data type	Method	Number of points	Range		Percent error ^d
				Temperature (K)	Pressure (bars)	
Robie and others, 1979	volume	compilation	1	298	1.01	0.0
Tombs and Rooksby, 1951	volume	X-ray	2	165-295	1.01	0.0±0.0
Wilburn and Bassett, 1977	volume	dilatometry	10	293	1.01-65000	0.02±0.17
Stull and Prophet, 1971	heat capacity	compilation	6	1700-2200	1.01	0.11±0.95
Grönvold and Sveen, 1974	heat capacity	high-temp. cal.	17	861-1044	1.01	0.20±1.76
Grönvold and Sveen, 1974	heat capacity	high-temp. cal.	59	299-837	1.01	0.44±1.48
Westrum and Grönvold, 1965	heat capacity	low-temp. cal.	16	202-347	1.01	-0.05±0.21
Coughlin and others, 1951	heat content	drop cal.	19	874-1825	1.01	-2.8±6.0
Westrum and Grönvold, 1965	entropy	low-temp. cal.	1	298	1.01	0.09

^dThe tabulated numbers represent the unweighted, average standard error of estimate for data in the set from the calculated value and the 1-sigma deviation of the errors about the average. Refer to text for details.

Table 263. Sources of thermochemical data for magnetite, Fe₃O₄.

Reaction	Source	Method	No. of Points	Range Temperature (K)	Pressure (kb)	H _f ^o (298.15 K) Third Law, kJ	H _f ^o (298.15 K) kJ/mol
CA	Birks, 1966	Electrochemistry	1	838	0.001	-55.492	-1117.156
CA	Rau, 1972	Gas reduction	1	843	0.001	-55.747	-1117.411
CB	Emmett and Schultz, 1933	Gas reduction	35	674-823	0.001	37.696±0.165	-1116.398
CB	Rau, 1972	Gas reduction	17	583-810	0.001	37.051±0.244	-1118.978
CC	Darken and Gurry, 1946	Gas reduction	3	1586-1730	0.001	-167.299±1.011	-1117.870
CC	Konarov and others, 1967	Electrochemistry	21	1526-1731	0.001	-166.849±1.078	-1117.645
CC	Kurepin, 1975	Electrochemistry	2	1473-1573	0.001	-165.448±0.008	-1116.945
CC	Norton, 1955	Mass spectrometry	8	1051-1342	0.001	-161.138±1.124	-1114.790
CC	Schmidt, 1941	Gas equilibrium	6	1583-1683	0.001	-167.177±0.438	-1117.809
CC	Smitlens, 1957	Gas equilibrium	4	1452-1731	0.001	-166.769±1.768	-1117.605
CL	Ackermann & Sanford, 1960	Gas reduction	5	972-1277	0.001	-905.281±0.544	-1117.226
CL	Composite set	Gas reduction	12	1373-1573	0.001	-904.952±0.196	-1116.879
CL	Darken and Gurry, 1945	Gas reduction	4	1373-1673	0.001	-904.944±0.163	-1116.870
CE	Giddings, 1972	Electrochemistry	7	973-1573	0.001	-904.479±0.088	-1116.379
CL	Hewitt, 1978	Gas reduction	8	923-1128	1.0	704.020±0.808	-1116.318
CM	Meyer, J., 1981 (unpub.)	Gas-medium pressure apparatus	7	922-1046	0.001	1888.729±1.693	-1117.809
	This Study						-1117.262

Reactions:



1.5.5.34. H₂O, water and the ideal and real gases
(formula weight = 18.0152 g/mol)

The entropy and Gibbs energy of formation at 298.15 K were taken from the CODATA Task Group (1978). The other properties for the ideal gas and for water and the real gas were taken from the work of Haar and others (1979, 1981).

1.5.5.35. H₄SiO₄, silicic acid (formula weight = 96.115 g/mol)

Hemley and others (1977a, 1980) measured the silica concentration in the aqueous fluid coexisting with quartz at 1 and 2 kb. From these data we obtained the following expression for the "Gibbs energy" for the reaction SiO₂(quartz,T,1.01b) + H₂O(gas,T,1.01b) = H₄SiO₄(aqueous, T,P_j):

$$\Delta[P_j] = -\frac{a_{1,j}}{2T} + 4 a_{2,j} \sqrt{T} + a_{3,j} (T - T \ln T) - a_{4,j} T + a_{5,j} - a_{6,j} T^2 + a_{7,j} \frac{T^3}{6}$$

In the above equation, T is the absolute temperature in kelvins and the constants a_{i,j} are as follows:

i	(i,j=1 kb)	(i,j=2 kb)
1	2.62154x10 ⁵	2.62154x10 ₅
2	5.48272x10 ³	4.97309x10 ³
3	-1.04134x10 ²	-1.04134x10 ²
4	9.79088x 10 ²	9.39015x10 ²

i	(i,j=1 kb)	(i,j=2 kb)
5	-2.28273×10^5	-1.97113×10^5
6	-3.69344×10^{-2}	-3.69344×10^{-2}
7	8.93770×10^{-6}	8.93770×10^{-6}

In deriving this relation, it is assumed that the activity coefficient of the silicic acid species is constant in the dilute aqueous solutions and can be neglected.

In the experiments in the magnesia-silica-water system (Hemley and others, 1977a) and in the alumina-silica-water system (Hemley and others, 1980), the concentrations of aqueous silicic acid coexisting with mineral pairs were measured at 1 and 2 kb. These data were evaluated by using the above relations for the formation of aqueous silicic acid from 1-atm quartz and 1-atm $H_2O[g]$.

1.5.5.36. Mg, magnesium (formula weight = 24.305 g/mol)

The properties of magnesium polymorphs were taken from the compilation of Hultgren and others (1973). The volumetric properties were not needed in this study and were not evaluated.

1.5.5.37. $MgCO_3$, magnesite (formula weight = 84.314 g/mol)

Tables 264 and 265 contain the sources of data used in the final evaluation. There exists a large body of information in which the gas phase contained both $H_2O[g]$ and $CO_2[g]$. Those data could not be used to identify the properties of magnesite and the magnesium silicates better because the mixing properties of the two gaseous species would

Table 264. Sources of thermophysical data for magnesite, $MgCO_3$.

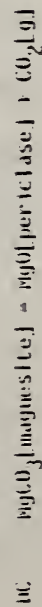
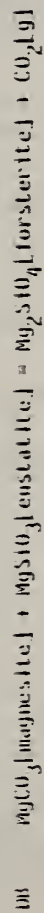
Source	Data type	Method	Number of points	Range		Percent error ^d
				Temperature (K)	Pressure (bars)	
Robie and others, 1979	volume	compilation	1	298	1.01	0.047±0.182
Hemingway and others, 1977	heat capacity	low-l. cal.	29	207-384	1.01	0.413±0.531
Anderson, 1934	heat capacity	low-l. cal.	5	201-292	1.01	0.845±0.471
Kelley, 1960	rel. enthalpy	drop cal.	4	400-700	1.01	0.728±0.423
Robie and others, 1979	heat capacity	compilation	6	298-600	1.01	0.014
Robie and others, 1979	entropy	compilation	1	298	1.01	

^dThe tabulated numbers represent the unweighted, average standard error of estimate for data in the set from the calculated value and the 1-sigma deviation of the errors about the average. Refer to text for details.

Table 265. Sources of thermochemical data for magnesite, $MgCO_3$.

Reaction	Source	Method	No. of Points	Temperature (K)	Range Temperature (K)	Pressure (kb)	$H_f^\circ(298.15 \text{ K})$ Thrd Law, kJ	$H_f^\circ(298.15 \text{ K})$ kJ/mol
DB	Johannes, 1969	Gas-medium pressure apparatus	1 pr	828-833	2.0		90.97240.242	-1113.810
DC	Barker and Tuttle, 1955	Decomposition pressure	5	872-1123	0.06-2.1		119.60141.191	-1112.894
DC	Irvine and Wyllie, 1975	Solid-medium pressure apparatus	4	1623-1743	17.0-20.0		116.34741.769	-1115.237
DC	Johannes and Metz, 1968	Gas-medium pressure apparatus	2 pr	973-1043	0.5-1.0		117.47940.537	-1114.105
DC	Marc and Stueck, 1913 This Study	Decomposition pressure	24	671-782	0.0008-0.011		118.75141.082	-1112.834 -1113.225

Reactions:



only introduce larger uncertainties. The accepted data are in good agreement.

1.5.5.38. MgO, periclase (formula weight = 40.304 g/mol)

The thermodynamic properties for periclase were taken from the JANAF Thermochemical Tables^a. The volumetric properties were evaluated from the sources cited on table 266.

1.5.5.39. Mg(OH)₂, brucite (formula weight = 58.320 g/mol)

The tables 267 and 268 contain the sources of data used in this evaluation. Other data, though cited in the reference list, were deleted prior to the final evaluation.

1.5.5.40. MgSiO₃, clinoenstatite, enstatite, and protoenstatite (formula weight = 100.389 g/mol)

The sources of data used to evaluate the properties of the pyroxene polymorphs clinoenstatite, enstatite, and protoenstatite are contained in tables 269 through 274. Other data, though cited in the reference list, were deleted prior to the final evaluation.

The fitted inversions at 1.01 bars are as follows:

<u>Equilibrium</u>	<u>Temperature</u>
clinoenstatite = enstatite	968.5 K
enstatite = protoenstatite	1257.4 K

The phase equilibria cited on tables 270, 272 and 274 are very consistent with the final results of the evaluation.

^aJANAF Thermochemical Tables, looseleaf pages for 1978 issued by Dow Chemical Company, 1707 Building, Midland, Michigan.

Table 266. Sources of thermophysical data for periclase, MgO.

Source	Data type	Method	Number of points	Range		Percent error ^a
				Temperature (K)	Pressure (bars)	
Hazen, 1976a	volume	X-ray	15	77-1315	1-24000	0.002±0.090
Skinner, 1957	volume	X-ray	12	284-976	1.01	0.007±0.057
Robie and others, 1979	volume	compilation	1	298	1.01	0.035

^aThe tabulated numbers represent the unweighted, average standard error of estimate for data in the set from the calculated value and the 1-sigma deviation of the errors about the average. Refer to text for details.

Table 267. Sources of thermophysical data for brucite, $Mg(OH)_2$.

Source	Data type	Method	Number of points	Range		Percent error ^a
				Temperature (K)	Pressure (bars)	
Robie and others, 1979	volume	compilation	1	298		0.219±0.631
Giauque and Archibald, 1937	heat capacity	low-T. cal.	21	217-321	1.01	0.219±0.332
King and others, 1975	rel. enthalpy	drop cal.	12	350-699	1.01	
Giauque and Archibald, 1937	entropy	low-T. cal.	1	298	1.01	0.0037

^aThe tabulated numbers represent the unweighted, average standard error of estimate for data in the set from the calculated value and the 1-sigma deviation of the errors about the average. Refer to text for details.

Table 268. Sources of thermochemical data for brucite, Mg(OH)₂.

Reaction	Source	Method	No. of Points	Temperature Range (K)	Pressure (kb)	H _f ^o (298.15 K) Third Law, kJ	H _f ^o (298.15 K) kJ/mol
DA	Barnes and Ernst, 1963	Gas-medium pressure apparatus	16	817-937	0.2-2.0	82.940±0.758	-924.600
DA	Fyfe and Godwin, 1962	Gas-medium pressure apparatus	1 pr	864-893	1.0	82.324±0.893	-925.215
DA	Fyfe, 1958	Decomposition pressure	10 pr	803-843	0.2-0.7	82.045±0.913	-925.494
DA	Kennedy, 1956	Decomposition pressure	10 pr	773-873	0.1-1.1	81.663±1.438	-925.877
DA	Schramke and others, 1982	Gas-medium pressure apparatus	4 pr	963-1079	3.9-8.1	82.125±0.592	-925.415
DI	Johannes, 1968 This Study	Gas-medium pressure apparatus	7 pr	603-713	0.5-7.0	216.829±2.644	-922.584 -925.307

Reactions:

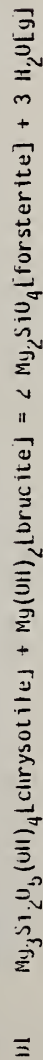


Table 269. Sources of thermophysical data for clinoenstatite, $MgSiO_3$.

Source	Data type	Method	Number of points	Range		Percent error ^d
				Temperature (K)	Pressure (bars)	
Evans, Howard, 1977 (unpub.)	volume	X-ray	7	298-973	1.01	0.041±0.148
Stephenson and others, 1966	volume	X-ray	3	298	1.01	0.006±0.012
Kelley, 1943	heat capacity	low-T. cal.	9	216-295	1.01	0.035±0.311
Wagner, 1932	rel. enthalpy	drop cal.	4	580-767	1.01	0.362±0.631
Wagner, 1932	rel. enthalpy	drop cal.	5	966-1177	1.01	0.518±0.345
Robie and others, 1979	heat capacity	compilation	14	298-1600	1.01	0.018±0.638
Robie and others, 1979	entropy	compilation	1	298	1.01	0.147

^dThe tabulated numbers represent the unweighted, average standard error of estimate for data in the set from the calculated value and the 1-sigma deviation of the errors about the average. Refer to text for details.

Table 270. Sources of thermochemical data for clinoenstatite, MgSiO₃.

Reaction	Source	Method	No. of Points	Temperature (K)	Range Pressure (kb)	H _r ^o (298.15 K) Third Law, kJ	H _f ^o (298.15 K) kJ/mol
DJ	Boyd and England, 1965	Solid-medium pressure apparatus	4 pr	893-1033	5.0-40.0	-0.142±0.120	-1544.834
DL	Greenwood, 1963	Gas-medium pressure apparatus	1 pr	935-985	2.0-2.6	102.495±1.674	-1544.746
DQ	Charlu and others, 1975	Solution calorimetry, borate salt	1	970	0.001	32.720	-1153.906
DQ	Kiseleva and others, 1981 This Study	Solution calorimetry, borate salt	1	1170	0.001	30.672	-1155.954 -1544.844

Reactions:

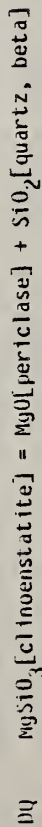
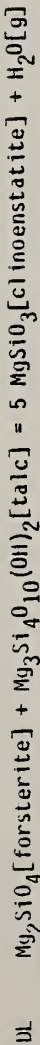


Table 271. Sources of thermophysical data for orthoenstatite, MgSiO_3 .

Source	Data type	Method	Range			Percent error ^d
			Number of points	Temperature (K)	Pressure (bars)	
Ralph and others, 1981	volume	X-ray	23	296-773	1-40200	0.016±0.181
Ralph and Ghose, 1980	volume	X-ray	2	298	1-21000	0.044±0.056
Evans, Howard, 1977 (unpub.)	volume	X-ray	6	298-1073	1.01	0.032±0.054
Charlu and others, 1975	volume	X-ray	2	298	1.01	0.077±0.077
Chernosky and Autio, 1979	volume	X-ray	1	298	1.01	0.009
Krupka and others, 1980	heat capacity	d.s.c.	151	200-1000	1.01	0.012±0.472
Krupka and others, 1980	entropy	low-T. cal.	1	298	1.01	0.008

^dThe tabulated numbers represent the unweighted, average standard error of estimate for data in the set from the calculated value and the 1-sigma deviation of the errors about the average. Refer to text for details.

Table 2/2. Sources of thermochemical data for enstatite, MgSiO₃.

Reaction	Source	Method	No. of Points	Temperature Range (K)	Pressure (kb)	H _f ^o (298.15 K) Third Law, kJ	H _f ^o (298.15 K) kJ/mol
DB	Johannes, 1969	Gas-medium pressure apparatus	1 pr	828-833	2.0	90.972±0.242	-1545.281
DF	Greenwood, 1963	Gas-medium pressure apparatus	1 pr	968-984	2.0	87.806±0.471	-1544.610
DF	Hemley and others, 1977b	H ₄ SiO ₄ concentration	1 pr	936-950	1.0	87.967±0.475	-1544.592
DG	Chernosky and Aulio, 1979	Gas-medium pressure apparatus	4 pr	937-1048	0.5-3.0	93.681±1.030	-1544.519
DG	Greenwood, 1963	Gas-medium pressure apparatus	2 pr	1023-1048	2.0-2.6	92.088±0.854	-1544.746
DG	Hemley and others, 1977b	H ₄ SiO ₄ concentration	1 pr	992-1012	1.0	93.708±0.699	-1544.514
DJ	Boyd and England, 1965	Solid-medium pressure apparatus	4 pr	893-1033	5.0-40.0	-0.142±0.120	-1544.686
DK	Atlas, 1952	Rapid quench	1 pr	1248-1268	0.001	12.811±0.189	-1544.690
DK	Boyd and others, 1964	Solid-medium pressure apparatus	1 pr	1823	6.1-7.4	12.805±0.061	-1544.696
DM	Chernosky, 1976	Gas-medium pressure apparatus	3 pr	921-1017	0.5-2.0	107.174±2.117	-1544.774
DM	Chernosky, 1976	Gas-medium pressure apparatus	8 pr	928-1073	0.5-10.0	107.313±1.824	-1544.728
DM	Greenwood, 1963	Gas-medium pressure apparatus	1 pr	976-1048	2.0-2.6	107.717±2.378	-1544.593
DM	Hemley and others, 1977b	H ₄ SiO ₄ concentration	1 pr	955-971	1.0	106.956±0.726	-1544.847
DO	Chernosky, 1976	Gas-medium pressure apparatus	1 pr	873-894	0.5	101.268±0.892	-1544.839
	This Study						-1544.696

Reactions:

- DB MgCO₃[magnesite] + MgSiO₃[enstatite] = Mg₂SiO₄[forsterite] + CO₂[g]
- DF Mg₇Si₈O₂₂(OH)₂[lanthophyllite] + 4 MgSiO₃[forsterite] = 9 MgSiO₃[enstatite] + H₂O[g]
- DU Mg₇Si₈O₂₂(OH)₂[lanthophyllite] = 7 MgSiO₃[enstatite] + SiO₂[quartz] + H₂O[g]
- DJ MgSiO₃[enstatite] = MgSiO₃[clinoenstatite]
- DK MgSiO₃[enstatite] = MgSiO₃[protoenstatite]
- DM Mg₃Si₄O₁₀(OH)₂[talca] = 3 MgSiO₃[enstatite] + SiO₂[quartz] + H₂O[g]
- DO Mg₂SiO₄[forsterite] + Mg₃Si₄O₁₀(OH)₂[talca] = 5 MgSiO₃[enstatite] + H₂O[g]

Table 273. Sources of thermophysical data for protoenstatite, MgSiO₃.

Source	Data type	Method	Range			Percent errors ^a
			Number of points	Temperature (K)	Pressure (bars)	
Evans, Howard, 1977 (unpub.) Smith, 1959 Wagner, 1932	volume	X-ray	9	373-1473	1.01	0.013±0.083
	volume	X-ray	1	298	1.01	0.117
	rel. enthalpy	drop cal.	4	1364-1570	1.01	-5.2±0.5

^aThe tabulated numbers represent the unweighted, average standard error of estimate for data in the set from the calculated value and the 1-sigma deviation of the errors about the average. Refer to text for details.

Table 274. Sources of thermochemical data for protoenstatite, MgSiO_3 .

Reaction	Source	Method	No. of Points	Range Temperature (K)	Pressure (kb)	$H_r^\circ(298.15 \text{ K})$ Third Law, kJ	$H_f^\circ(298.15 \text{ K})$ kJ/mol
DK	Atlas, 1952	Rapid quench	1 pr	1248-1268	0.001	12.811±0.189	-1531.879
DK	Boyd and others, 1964 This Study	Solid-medium pressure apparatus	1 pr	1823	6.1-7.4	12.805±0.061	-1531.885 -1531.885

Reactions:



1.5.5.41. Mg_2SiO_4 , forsterite (formula weight = 140.693 g/mol)

The sources of data used in the final evaluation are contained on tables 275 and 276. Other data listed in the reference list were deleted prior to the final evaluation. The data used are in satisfactory agreement.

1.5.5.42. $\text{Mg}_3\text{Si}_2\text{O}_5(\text{OH})_4$, chrysotile (formula weight = 277.112 g/mol)

Tables 277 and 278 contain the sources of data used to evaluate the properties of the serpentine mineral, chrysotile. On table 278 the enthalpy of formation from the elements appears to be incorrect, that is, more negative than any of the "averages" shown. The final solution was assymmetrically to one side of the measured brackets. The weighted solution is consistent with the experimental data.

1.5.5.43. $\text{Mg}_3\text{Si}_4\text{O}_{10}(\text{OH})_2$, talc (formula weight = 379.266 g/mol)

Tables 279 and 280 contain the sources of data used in the final evaluation. All other data, though cited in the reference list, were dropped prior to the final fitting.

1.5.5.44. $\text{Mg}_7\text{Si}_8\text{O}_{22}(\text{OH})_2$, anthophyllite (formula weight = 780.820 g/mol)

Tables 281 and 282 contain the sources of data used in the evaluation. All other data, though cited in the reference list, were deleted prior to the final evaluation. The collected data are in good internal agreement.

Table 275. Sources of thermophysical data for forsterite, Mg_2SiO_4 .

Source	Data type	Method	Number of points	Range		Percent error ^a
				Temperature (K)	Pressure (bars)	
Olinger and Halleck, 1974	volume ratio	X-ray	7	298	1-108500	0.079±0.186
Hazen, 1976b	volume	X-ray	4	273	1-50000	0.004±0.095
Hazen, 1976b	volume	X-ray	14	77-1293	1.01	0.176±0.115
Skinner, 1962	volume	X-ray	15	298-1400	1.01	0.270±0.047
Charlu and others, 1975	volume	X-ray	1	298	1.01	0.024
Kelley, 1943	heat capacity	low-T. cal.	9	216-295	1.01	0.005±0.243
Orr, 1953	rel. enthalpy	drop cal.	16	398-1808	1.01	0.142±0.344
Robie and others, 1979	entropy	compilation	1	298	1.01	0.337

^aThe tabulated numbers represent the unweighted, average standard error of estimate for data in the set from the calculated value and the 1-sigma deviation of the errors about the average. Refer to text for details.

Table 276. Sources of thermochemical data for forsterite, Mg₂SiO₄.

Reaction	Source	Method	No. of Points	Range Temperature (K)	Pressure (kb)	H _f ^o (298.15 K) Third Law, kJ	H _f ^o (298.15 K) kJ/mol
DB	Johannes, 1969	Gas-medium pressure apparatus	1 pr	828-833	2.0	90.972±0.242	-2173.314
DU	Greenwood, 1963	Gas-medium pressure apparatus	3 pr	936-965	1.0-4.0	486.883±3.170	-2171.724
DU	Hemley and others, 1977b	H ₄ SiO ₄ concentration	1 pr	902-916	1.0	475.780±3.247	-2174.500
UF	Greenwood, 1963	Gas-medium pressure apparatus	1 pr	968-984	2.0	87.806±0.471	-2171.956
UF	Hemley and others, 1977b	H ₄ SiO ₄ concentration	1 pr	936-950	1.0	87.967±0.475	-2171.795
DH	Evans and others, 1976	Gas- & solid-medium pressure apparatus	5 pr	753-933	2.0-15.0	2168.159±30.183	-2173.394
DH	Hemley and others, 1977b	H ₄ SiO ₄ concentration	1 pr	775-799	1.0	2201.949±21.067	-2171.517
DI	Johannes, 1968	Gas-medium pressure apparatus	7 pr	603-713	0.5-7.0	216.829±2.644	-2171.367
DL	Chernosky, 1976	Gas-medium pressure apparatus	5 pr	923-979	1.0-6.0	101.574±0.869	-2173.157
DL	Greenwood, 1963	Gas-medium pressure apparatus	1 pr	935-985	2.0-2.6	102.495±1.674	-2172.237
DL	Hemley and others, 1977b	H ₄ SiO ₄ concentration	1 pr	908-924	1.0	101.086±0.710	-2173.646
DN	Chernosky, 1982 (in press)	Gas-medium pressure apparatus	5 pr	672-809	0.5-6.9	695.118±9.175	-2172.105
DN	Hemley and others, 1977a	H ₄ SiO ₄ concentration	1 pr	708-720	1.0	698.480±3.379	-2171.544
DU	Chernosky, 1976	Gas-medium pressure apparatus	1 pr	873-894	0.5	101.268±0.892	-2172.706
DU	Charlu and others, 1975	Solution calorimetry, borate salt	1	970	0.001	59.502	-2171.655
DU	Kiseleva and others, 1981	Solution calorimetry, borate salt	1	1170	0.001	57.179	-2173.978
DU	This Study						-2172.729

Reactions:

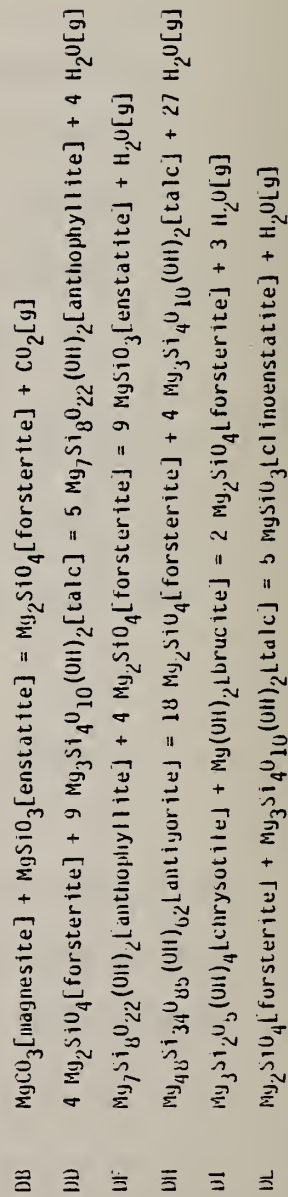


Table 27b. Continued

Reaction	Source	Method	No. of Points	Temperature (K)	Range Pressure (kb)	$H_r^\circ(298.15\text{ K})$ Third Law, kJ	$H_f^\circ(298.15\text{ K})$ kJ/mol
Reactions (continued):							
DN							
DO							
DP							

Reactions (continued):

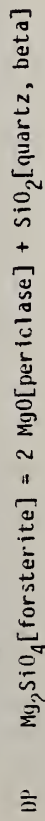
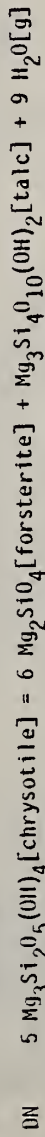


Table 277. Sources of thermophysical data for chrysothle, $\text{Mg}_3\text{Si}_2\text{O}_5(\text{OH})_4$.

Source	Data type	Method	Range			Percent error ^a
			Number of points	Temperature (K)	Pressure (bars)	
Hemley and others, 1977a	volume	X-ray	1	298	1.01	0.053
King and others, 1967	heat capacity	low-T. cal.	10	206-296	1.01	0.002±0.072
King and others, 1967	entropy	low-T. cal.	1	298	1.01	0.004

^aThe tabulated numbers represent the unweighted, average standard error of estimate for data in the set from the calculated value and the 1-sigma deviation of the errors about the average. Refer to text for details.

Table 278. Sources of thermochemical data for chrysotile, $Mg_3Si_2O_5(OH)_4$.

Reaction	Source	Method	No. of Points	Temperature (K)	Range	Pressure (kb)	$H_f^\circ(298.15 \text{ K})$ Third Law, kJ	$H_f^\circ(298.15 \text{ K})$ kJ/mol
DI	Johannes, 1968	Gas-medium pressure apparatus	7 pr	603-713	0.5-7.0		216.829±2.644	-4479.314
DN	Chernosky, 1982 (in press)	Gas-medium pressure apparatus	5 pr	672-809	0.5-6.9		695.118±9.175	-4481.287
DN	Hemley and others, 1977a This Study	H_4SiO_4 concentration	1 pr	708-720	1.0		698.480±3.379	-4480.615 -4482.037

Reactions:

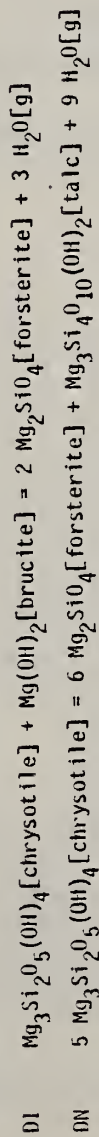


Table 279. Sources of thermophysical data for talc, $\text{Mg}_3\text{Si}_4\text{O}_{10}(\text{OH})_2$.

Source	Data type	Method	Number of points	Range		Percent errors
				Temperature (K)	Pressure (bars)	
Vaidya and others, 1973	volume ratio	rel. volume	9	298	5000-45000	0.020±0.062
Hendley and others, 1977a	volume	X-ray	1	298	1.01	0.707
Robie and Stout, 1963	heat capacity	low-T. cal.	9	240-298	1.01	0.323±0.481
Robie and others, 1979	heat capacity	compilation	3	298-500	1.01	0.487±1.018
Krupka and others, 1977	heat capacity	d.s.c.	15	298-650	1.01	0.582±0.772
Krupka and others, 1977	entropy	low-T. cal.	1	298	1.01	0.0005

^aThe tabulated numbers represent the unweighted, average standard error of estimate for data in the set from the calculated value and the 1-sigma deviation of the errors about the average. Refer to text for details.

Table 280. Sources of thermochemical data for talc, $Mg_3Si_4O_{10}(OH)_2$.

Reaction	Source	Method	No. of Points	Temperature (K)	Range	Pressure (kb)	$H_f^\circ(298.15\text{ K})$ Third Law, kJ	$H_f^\circ(298.15\text{ K})$ kJ/mol
DD	Greenwood, 1963	Gas-medium pressure apparatus	3 pr	936-965	1.0-4.0		486.883±3.170	-6199.771
DE	Hemley and others, 1977b	H_4SiO_4 concentration	1 pr	902-916	1.0		475.780±3.247	-6201.005
DE	Chernosky and Autio, 1979	Gas-medium pressure apparatus	5 pr	920-1015	0.5-3.0		473.811±5.074	-6200.323
DE	Greenwood, 1963	Gas-medium pressure apparatus	1 pr	967-984	2.0		470.118±3.337	-6200.851
DE	Hemley and others, 1977b	H_4SiO_4 concentration	1 pr	941-955	1.0		469.296±2.991	-6200.968
DH	Evans and others, 1976	Gas- & solid-medium pressure apparatus	5 pr	753-933	2.0-15.0		2168.159±30.183	-6203.210
DH	Hemley and others, 1977b	H_4SiO_4 concentration	1 pr	775-799	1.0		2201.949±21.067	-6194.763
DL	Chernosky, 1976	Gas-medium pressure apparatus	5 pr	923-979	1.0-6.0		101.574±0.869	-6200.646
DL	Greenwood, 1963	Gas-medium pressure apparatus	1 pr	935-985	2.0-2.6		102.495±1.674	-6199.726
DM	Hemley and others, 1977b	H_4SiO_4 concentration	1 pr	908-924	1.0		101.086±0.710	-6201.135
DM	Chernosky, 1976	Gas-medium pressure apparatus	3 pr	921-1017	0.5-2.0		107.174±2.117	-6200.452
DM	Chernosky, 1976	Gas-medium pressure apparatus	8 pr	928-1073	0.5-10.0		107.313±1.824	-6200.313
DM	Greenwood, 1963	Gas-medium pressure apparatus	1 pr	976-1048	2.0-2.6		107.717±2.378	-6199.911
DM	Hemley and others, 1977b	H_4SiO_4 concentration	1 pr	955-971	1.0		106.956±0.726	-6200.670
DM	Chernosky, 1982 (in press)	Gas-medium pressure apparatus	5 pr	672-809	0.5-6.9		695.118±9.175	-6196.472
DM	Hemley and others, 1977a	H_4SiO_4 concentration	1 pr	708-720	1.0		698.480±3.379	-6193.109
DU	Chernosky, 1976	Gas-medium pressure apparatus	1 pr	873-894	0.5		101.268±0.892	-6200.195
	This Study							-6200.218

Reactions:

- DD $4 Mg_2SiO_4[\text{forsterite}] + 9 Mg_3Si_4O_{10}(OH)_2[\text{talc}] = 5 Mg_7Si_8O_{22}(OH)_2[\text{anthophyllite}] + 4 H_2O[\text{g}]$
- DE $7 Mg_3Si_4O_{10}(OH)_2[\text{talc}] = 3 Mg_7Si_8O_{22}(OH)_2[\text{anthophyllite}] + 4 SiO_2[\text{quartz}] + 4 H_2O[\text{g}]$
- DH $Mg_48Si_{34}O_{85}(OH)_{62}[\text{antigorite}] = 18 Mg_2SiO_4[\text{forsterite}] + 4 Mg_3Si_4O_{10}(OH)_2[\text{talc}] + 27 H_2O[\text{g}]$
- DL $Mg_2SiO_4[\text{forsterite}] + Mg_3Si_4O_{10}(OH)_2[\text{talc}] = 5 MgSiO_3[\text{clinoenstatite}] + H_2O[\text{g}]$
- DM $Mg_3Si_4O_{10}(OH)_2[\text{talc}] = 3 MgSiO_3[\text{enstatite}] + SiO_2[\text{quartz}] + H_2O[\text{g}]$

Table 280. Continued

Reaction	Source	Method	No. of Points	Range Temperature (K)	Pressure (kb)	$H_f^\circ(298.15 \text{ K})$ Third Law, kJ	$H_f^\circ(298.15 \text{ K})$ kJ/mol
Reactions (continued):							
DN	$5 \text{ Mg}_3\text{Si}_2\text{O}_5(\text{OH})_4[\text{chrysotile}] = 6 \text{ Mg}_2\text{SiO}_4[\text{forsterite}] + \text{Mg}_3\text{Si}_4\text{O}_{10}(\text{OH})_2[\text{talc}] + 9 \text{ H}_2\text{O}[\text{g}]$						
DX	$\text{Mg}_2\text{SiO}_4[\text{forsterite}] + \text{Mg}_3\text{Si}_4\text{O}_{10}(\text{OH})_2[\text{talc}] = 5 \text{ MgSiO}_3[\text{enstatite}] + \text{H}_2\text{O}[\text{g}]$						

Table 281. Sources of thermophysical data for anthophyllite, $\text{Mg}_7\text{Si}_8\text{O}_{22}(\text{OH})_2$.

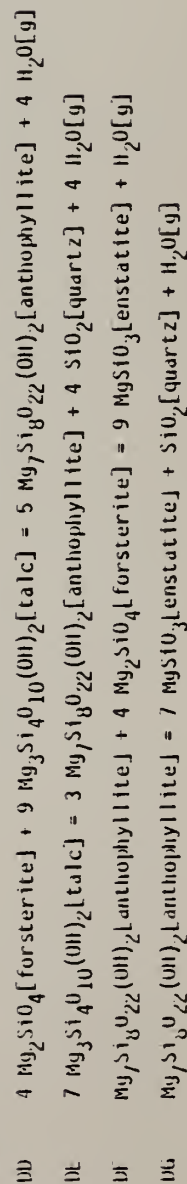
Source	Data type	Method	Number of points	Range		Percent error ^a
				Temperature (K)	Pressure (bars)	
Chernosky and Autio, 1979 Krupka, Kenneth M., 1982 (unpub.) Krupka, Kenneth M., 1982 (unpub.)	volume	X-ray	1	298	1.01	0.266
	heat capacity	d.s.c.	36	200-700	1.01	0.008±0.135
	entropy	low-T. cal.	1	298	1.01	0.008

^aThe tabulated numbers represent the unweighted, average standard error of estimate for data in the set from the calculated value and the 1-sigma deviation of the errors about the average. Refer to text for details.

Table 282. Sources of thermochemical data for anthophyllite, $Mg_7Si_8O_{22}(OH)_2$.

Reaction	Source	Method	No. of Points	Range Temperature (K)	Pressure (kb)	$H_f^\circ(298.15 \text{ K})$ Third Law, kJ	$H_f^\circ(298.15 \text{ K})$ kJ/mol
DD	Greenwood, 1963	Gas-medium pressure apparatus	3 pr	936-965	1.0-4.0	486.883±3.170	-12057.562
DK	Hemley and others, 1977b	H_4SiO_4 concentration	1 pr	902-916	1.0	475.780±3.247	-12059.783
DE	Chernosky and Autio, 1979	Gas-medium pressure apparatus	5 pr	920-1015	0.5-3.0	473.811±5.074	-12058.612
DE	Greenwood, 1963	Gas-medium pressure apparatus	1 pr	967-984	2.0	470.118±3.337	-12059.843
DE	Hemley and others, 1977b	H_4SiO_4 concentration	1 pr	941-955	1.0	469.296±2.991	-12060.117
DF	Greenwood, 1963	Gas-medium pressure apparatus	1 pr	968-984	2.0	87.806±0.471	-12057.593
DF	Hemley and others, 1977b	H_4SiO_4 concentration	1 pr	936-950	1.0	87.967±0.475	-12057.432
DG	Chernosky and Autio, 1979	Gas-medium pressure apparatus	4 pr	937-1048	0.5-3.0	93.681±1.030	-12057.124
DG	Greenwood, 1963	Gas-medium pressure apparatus	2 pr	1023-1048	2.0-2.6	92.088±0.854	-12058.717
DG	Hemley and others, 1977b	H_4SiO_4 concentration	1 pr	992-1012	1.0	93.708±0.699	-12057.097
	This Study						-12058.366

Reactions:



1.5.5.45. $\text{Mg}_{48}\text{Si}_{34}\text{O}_{85}(\text{OH})_{62}$, antigorite (formula weight = 4535.949 g/mol)

Tables 283 and 284 contain the sources of data used in the final evaluation. Other data that were considered but not used are given in the reference list. The thermochemical data, cited in table 284, appear to be inconsistent. However, when the size of the chemical formula for one mole is considered, the two sets are acceptably consistent.

1.5.5.46. O_2 , oxygen (ideal gas, formula weight = 31.999 g/mol)

The properties of the diatomic ideal gas were taken from the JANAF Thermochemical Tables^a. The volumetric properties of the real gas were not needed and were not evaluated.

1.5.5.47. Si, silicon (formula weight = 28.086 g/mol)

The properties of silicon were taken from the compilation of Hultgren and others (1973). The volumetric properties were not needed and, therefore, were not evaluated.

1.5.5.48. SiO_2 (formula weight = 60.084 g/mol)

The data evaluated in this study required a knowledge of two polymorphs of SiO_2 : quartz and cristobalite.

^aJANAF Thermochemical Tables, looseleaf pages for 1977 issued by Dow Chemical Company, 1707 Building, Midland, Michigan.

Table 283. Sources of thermophysical data for antigorite, $Mg_48Si_{34}O_{85}(OH)_6$.

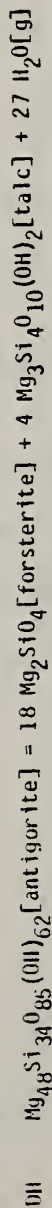
Source	Data type	Method	Number of points	Range		Percent errors
				Temperature (K)	Pressure (bars)	
Kunze, 1961	volume	X-ray	1	298	1.01	0.001
King and others, 1967	heat capacity	low-T. cal.	10	206-296	1.01	0.002±0.073
King and others, 1967	rel. enthalpy	drop cal.	11	406-848	1.01	0.289±0.251
King and others, 1967	entropy	low-T. cal.	1	298	1.01	0.0

^aThe tabulated numbers represent the unweighted, average standard error of estimate for data in the set from the calculated value and the 1-sigma deviation of the errors about the average. Refer to text for details.

Table 284. Sources of thermochemical data for antigorite, $Mg_{48}Si_{34}O_{85}(OH)_{62}$.

Reaction	Source	Method	No. of Points	Temperature (K)	Range	Pressure (kb)	$H_f^\circ(298.15 \text{ K})$ Third Law, kJ	$H_f^\circ(298.15 \text{ K})$ kJ/mol
DIH	Evans and others, 1976	Gas- & solid-medium pressure apparatus	5 pr	753-933	2.0-15.0	2.0-15.0	2168.159±30.183	-71409.070
DII	Hemley and others, 1977b	H_4SiO_4 concentration	1 pr	775-799	1.0	1.0	2201.949±21.067	-71375.289
	This Study							-71397.109

Reactions:



1.5.5.48.1. Quartz

The thermodynamic properties of quartz were taken from the compilation of Robie and others (1978) after adjustment to 1.01 bars. The sources for the volumetric data are given in table 285. In addition, the volumetric data were constrained to conform to the alpha-beta transition for quartz. Table 286 contains the sources for the experimental data on the transition. The data are in good agreement.

1.5.5.48.2. Cristobalite

The thermodynamic data for cristobalite were taken from the JANAF Thermochemical Tables (Stull and Prophet, 1971). The volumetric data are cited by source on table 287.

1.5.5.49. Constants

Tables 288 and 289 contain the constants for the energy- and volume-related functions as given in section 1.5.3. The range is given in parentheses after the formula and name (if applicable). The precision of the functions is given on Tables 12 through 145.

Table 285. Sources of volumetric data for quartz, SiO₂.

Source	Data type	Method	Number of points	Range		Percent errors ^a
				Temperature (K)	Pressure (bars)	
Adams and others, 1919	(V-V°)/V°	dilatometry	18	298	2000-12000	0.05±0.17
Olinger and Hilleck, 1976	V/V°	dilatometry	15	293	33000-120000	3.19±2.25
Vaidya and others, 1973	V/V°	dilatometry	9	298	5000-45000	-0.25±0.22
Jay, 1933	volume	dilatometry	9	291-1003	1.01	0.11±0.17

^aThe tabulated numbers represent the unweighted, average standard error of estimate for data in the set from the calculated value and the 1-sigma deviation of the errors about the average. Refer to text for details.

Table 286. Sources of data on the alpha - beta transition in quartz, SiO₂.

Source	Method	No. of Points	Temperature (K)	Range Pressure (kb)	H°(298.15 K) Third Law, kJ
Koster van Groos and ter Heege, 1973	e.m.f.	48	845-1033	0.001-10.0	-0.577±0.003
Yoder, 1950	Solid-medium pressure apparatus	11	845-1088	0.001-10.0	-0.574±0.003
Colten and Klement, 1967	Solid-medium pressure apparatus	48	961-1641	4.4-35.1	-0.578±0.027
This Study					-0.577

Table 287. Sources of thermophysical data for cristobalite, SiO₂.

Source	Data type	Method	Number of points	Range		Percent error ^a
				Temperature (K)	Pressure (bars)	
Johnson and Andrews, 1956	volume(alpha)		5	296-481	1.01	0.0±0.10
Johnson and Andrews, 1956	volume(beta)		8	492-1411	1.01	0.0±0.11

^aThe tabulated numbers represent the unweighted, average standard error of estimate for data in the set from the calculated value and the 1-sigma deviation of the errors about the average. Refer to text for details.

Table 288. Constants for energy-related functions in section 1.5.3.

Formula, (temperature range in kelvins)	a_1	a_2	a_3	a_4	a_5	a_6	a_7
Al (c), (200-933.25)	-2.05250×10^5	-2.54841×10^2	0.0	-1.28573×10^2	2.76424×10^1	-4.07067×10^{-3}	1.57641×10^{-5}
Al (l), (933.25-1800)	0.0	7.64359×10^3	0.0	-1.45759×10^2	3.17765×10^1	0.0	0.0
Al(OH) Boehmite, (200-1250)	5.82075×10^5	-8.77120×10^5	-2.28992×10^3	-1.29729×10^3	1.87814×10^2	6.17670×10^{-3}	0.0
Al(OH) Diaspore, (200-1250)	2.92012×10^5	-8.93662×10^5	-1.81222×10^3	-1.06013×10^3	1.55894×10^2	-1.69804×10^{-3}	0.0
Al(OH) ₃ Gibbsite, (200-1250)	7.91422×10^5	-1.10591×10^6	-2.90212×10^3	-1.62610×10^3	2.36699×10^2	2.38585×10^{-2}	0.0
Al ₂ O ₃ Corundum, (200-1800)	4.72841×10^4	-1.54782×10^6	-2.56161×10^3	-1.59146×10^3	2.38320×10^2	-2.06378×10^{-2}	9.41963×10^{-6}
Al ₂ SiO ₅ Andalusite, (200-1800)	1.66755×10^6	-2.34464×10^6	-6.11720×10^3	-3.46104×10^3	5.10336×10^2	-9.59010×10^{-2}	6.45249×10^{-5}
Al ₂ SiO ₅ Kyanite, (200-1800)	1.91390×10^6	-2.33903×10^6	-6.56191×10^3	-3.65555×10^3	5.34515×10^2	-1.00205×10^{-1}	6.69583×10^{-5}
Al ₂ SiO ₅ Sillimanite, (200-1800)	2.73570×10^6	-2.31359×10^6	-7.42977×10^3	-4.05054×10^3	5.92346×10^2	-1.31153×10^{-1}	9.43392×10^{-5}
Al ₂ Si ₂ O ₅ (OH) ₄ Kaolinite, (200-1250)	2.13572×10^6	-3.04741×10^6	-9.33595×10^3	-5.46910×10^3	8.17824×10^2	-9.20418×10^{-2}	0.0
Al ₂ Si ₂ O ₅ (OH) ₄ Dickite, (200-1250)	1.80999×10^6	-3.66515×10^6	-7.92102×10^3	-4.65599×10^3	6.95678×10^2	-3.00884×10^{-2}	0.0
Al ₂ Si ₂ O ₅ (OH) ₄ Halloysite, (200-1250)	5.20215×10^5	-3.68344×10^6	-6.38570×10^3	-4.05280×10^3	6.19577×10^2	-1.79153×10^{-2}	0.0
Al ₂ Si ₄ O ₁₀ (OH) ₂ Pyrophyllite, (200-1250)	4.01105×10^6	-5.04493×10^6	-1.30750×10^4	-7.39476×10^3	1.09440×10^3	-1.64948×10^{-1}	1.14631×10^{-4}
C Graphite, (200-1800)	7.48070×10^5	2.15300×10^4	-1.03230×10^3	-4.66151×10^2	6.31600×10^1	-5.73400×10^{-3}	1.80790×10^{-6}
CO (g), (200-1800)	1.14564×10^5	-8.57737×10^4	0.0	5.31939×10^1	2.49304×10^1	5.11676×10^{-3}	-2.25949×10^{-6}

Table 288. Continued

Formula, (temperature range in kelvins)	a_1	a_2	a_3	a_4	a_5	a_6	a_7
CO_2 (g), (200-1800)	5.72343×10^5	-3.22626×10^5	-8.92065×10^2	-3.55944×10^2	8.24113×10^1	0.0	-5.46484×10^{-7}
Ca (c), (200-720)	-2.20152×10^5	-1.86563×10^4	3.64127×10^2	7.62562×10^1	0.0	9.83620×10^{-3}	9.72458×10^{-6}
Ca (c), (720-1112)	0.0	1.49497×10^4	-7.53816	3.71052×10^1	0.0	2.05709×10^{-2}	0.0
Ca (l), (1112-1755)	0.0	1.58488×10^4	0.0	-1.14367×10^2	2.92754×10^1	0.0	0.0
Ca (g), (1755-1800)	0.0	1.84078×10^5	-8.35017	3.19488×10^1	2.14177×10^1	-3.02477×10^{-4}	2.25282×10^{-7}
$\text{CaAl}_2\text{SiO}_6$ Ca-Al Clinopyroxene, (200-1800)	-2.76402×10^6	-3.11084×10^6	-2.16570×10^3	-1.95915×10^3	3.22156×10^2	0.0	0.0
$\text{CaAl}_2\text{Si}_2\text{O}_8$ Anorthite, (200-1800)	3.14402×10^6	-3.83663×10^6	-9.38321×10^3	-5.32656×10^3	7.96492×10^2	-1.44198×10^{-1}	1.02906×10^{-4}
$\text{CaAl}_4\text{Si}_2\text{O}_{10}(\text{OH})_2$ Margarite, (200-1250)	0.0	-5.74866×10^6	-7.50967×10^3	-4.97842×10^3	7.68405×10^2	-9.70931×10^{-3}	0.0
CaCO_3 Calcite, (200-1800)	0.0	-1.10747×10^6	-1.11449×10^3	-8.37835×10^2	1.39006×10^2	1.43039×10^{-2}	0.0
CaCO_3 Aragonite, (200-1800)	0.0	-1.10921×10^6	-1.04452×10^3	-8.11951×10^2	1.35497×10^2	1.15890×10^{-2}	0.0
CaO Lime, (200-1800)	-2.55577×10^5	-5.99178×10^5	-4.31990×10^2	-4.20068×10^2	7.16851×10^1	-3.08248×10^{-3}	2.23862×10^{-6}
CaSiO_3 Wollastonite, (200-1396.15)	0.0	-1.52204×10^6	-1.68000×10^3	-1.17043×10^3	1.85955×10^2	-3.60167×10^{-3}	-6.39008×10^{-7}
CaSiO_3 Cyclowollastonite, (200-1800)	-5.46489×10^5	-1.52204×10^6	-9.42731×10^2	-8.77640×10^2	1.49650×10^2	0.0	0.0
$\text{CaAl}_2\text{Si}_4\text{O}_{16}(\text{OH})_2$ Biechulite, (200-1250)	0.0	-3.99020×10^6	-5.20338×10^3	-3.52194×10^3	5.51767×10^2	-1.21058×10^{-2}	0.0
$\text{CaAl}_2\text{Si}_2\text{O}_7$ Gehlenite, (200-1800)	1.49598×10^6	-3.67055×10^6	-6.24654×10^3	-3.80818×10^3	5.86351×10^2	-6.60911×10^{-2}	3.80365×10^{-5}

Table 288. Continued

Formula, (temperature range in kelvins)	a ₁	a ₂	a ₃	a ₄	a ₅	a ₆	a ₇
Ca ₂ Al ₂ Si ₃ O ₁₀ (OH) ₂ Prehnite, (200-1250)	2.05022x10 ⁶	-5.65525x10 ⁶	-9.60611x10 ³	-5.84599x10 ³	8.88366x10 ²	-4.01441x10 ⁻²	0.0
Ca ₂ Al ₃ Si ₃ O ₁₂ (OH) Zoisite, (200-1250)	2.04129x10 ⁶	-6.32506x10 ⁶	-1.04175x10 ⁴	-6.32203x10 ³	9.56365x10 ²	-4.39555x10 ⁻²	0.0
Ca ₂ SiO ₄ Alpha, (1710-1800)	0.0	-2.22496x10 ⁶	0.0	-1.05191x10 ³	1.99600x10 ²	0.0	0.0
Ca ₂ SiO ₄ Bredigite, (200-1710)	0.0	-2.20583x10 ⁶	0.0	-8.04599x10 ²	1.61526x10 ²	0.0	1.89495x10 ⁻⁵
Ca ₂ SiO ₄ Ca Olivine, (200-1120)	-2.36007x10 ⁶	-2.23871x10 ⁶	1.65638x10 ³	2.39144x10 ²	0.0	1.06586x10 ⁻¹	-8.15012x10 ⁻⁵
Ca ₂ SiO ₄ Larnite, (200-970)	0.0	-2.15665x10 ⁶	-2.09476x10 ³	-1.53830x10 ³	2.49720x10 ²	0.0	0.0
Ca ₃ Al ₂ Si ₃ O ₁₂ grossularite, (200-1800)	1.76828x10 ⁶	-6.11005x10 ⁶	-1.07953x10 ⁴	-6.59048x10 ³	9.94708x10 ²	-1.06084x10 ⁻¹	4.94577x10 ⁻⁵
Ca ₃ SiO ₅ Hatturite, (200-1800)	0.0	-2.74033x10 ⁶	-2.84600x10 ³	-2.08607x10 ³	3.38162x10 ²	-2.81920x10 ⁻³	0.0
Ca ₃ Si ₂ O ₇ Rankinite, (200-1800)	2.11044x10 ⁵	-3.70604x10 ⁶	-4.07831x10 ³	-2.85586x10 ³	4.57070x10 ²	-1.50836x10 ⁻²	0.0
Ca ₄ Al ₆ Si ₆ O ₂₄ (CO ₃) Melonite, (200-1800)	-9.14788x10 ⁶	-1.30405x10 ⁷	-9.97360x10 ³	-8.49709x10 ³	1.40091x10 ³	0.0	0.0
Fe (c), (200-1042)	4.67900x10 ⁶	1.29860x10 ⁵	-6.43900x10 ³	-3.09983x10 ³	4.40747x10 ²	-1.87588x10 ⁻¹	1.83975x10 ⁻⁴
Fe (c), (1042-1184 and 1685-1800)	3.11294x10 ⁸	1.72901x10 ⁶	-3.78574x10 ⁴	-9.46728x10 ³	1.07515x10 ³	-6.56081x10 ⁻²	0.0
Fe (c), (1184-1665)	0.0	8.45146x10 ³	0.0	-1.03591x10 ²	2.39743x10 ¹	4.18400x10 ⁻³	0.0
Fe ₉₄ O Wustite, (200-1800)	0.0	-2.35710x10 ⁵	-3.66286x10 ²	-3.95757x10 ²	7.29225x10 ¹	-6.83700x10 ⁻³	8.66116x10 ⁻⁶
FeSiO ₃ Ferrosillite, (200-1800)	-2.87221x10 ⁶	-1.13188x10 ⁶	0.0	-5.40441x10 ²	1.07120x10 ²	1.72796x10 ⁻²	-8.84986x10 ⁻⁶

Table 288. Continued

Formula, (temperature range in kelvins)	a_1	a_2	a_3	a_4	a_5	a_6	a_7
Fe_2O_3 Hematite, (200-955.5)	2.12782×10^6	-6.32880×10^5	-6.85832×10^3	-3.92482×10^3	5.88529×10^2	-2.26663×10^{-1}	2.66461×10^{-4}
Fe_2O_3 Hematite, (955.5-1800)	4.82281×10^8	2.19790×10^6	-6.74698×10^4	-1.77835×10^4	2.06675×10^3	-1.32541×10^{-1}	0.0
Fe_2SiO_4 Fayalite, (200-1800)	1.98186×10^6	-1.26795×10^6	-5.91318×10^3	-3.39012×10^3	5.15172×10^2	-1.20206×10^{-1}	9.73963×10^{-5}
Fe_3O_4 Magnetite, (200-848.5)	4.99456×10^6	-7.77610×10^5	-1.40898×10^4	-7.94562×10^3	1.19402×10^3	-5.96710×10^{-1}	8.08724×10^{-4}
Fe_3O_4 Magnetite, (848.5-1800)	1.13548×10^9	8.60687×10^6	-2.71125×10^5	-8.39335×10^4	1.02102×10^4	-1.50333	4.45065×10^{-4}
H_2 (g), (200-1800)	-5.10406×10^5	2.03250×10^4	4.10165×10^2	1.29375×10^2	7.44240	5.85357×10^{-3}	-1.38995×10^{-6}
H_2O (water), (273.15-373.15)	1.10338×10^6	-2.28245×10^5	0.0	-1.84121×10^2	4.20228×10^1	3.49132×10^{-2}	0.0
H_2O (g), (200-1800)	-1.31077×10^5	-1.87339×10^5	2.99188×10^2	1.55636×10^2	1.04381×10^1	1.29775×10^{-2}	-4.46885×10^{-6}
Mg (c), (200-922)	1.09922×10^5	9.43865×10^3	-4.20253×10^2	-3.18568×10^2	5.45289×10^1	-1.41605×10^{-2}	2.16245×10^{-5}
Mg (l), (922-1378)	0.0	1.16498×10^4	0.0	-8.67553×10^1	2.20919×10^1	5.43908×10^{-3}	0.0
Mg (g), (200-1800)	0.0	1.51165×10^5	0.0	3.01177×10^1	2.07861×10^1	0.0	0.0
mgCO_3 Magnesite, (200-1800)	4.98826×10^5	-9.94803×10^5	-2.00686×10^3	-1.22914×10^3	1.86847×10^2	0.0	0.0
mgO Periclase, (200-1800)	-3.73496×10^5	-5.66544×10^5	-4.78258×10^2	-4.32701×10^2	7.08871×10^1	-3.05096×10^{-3}	1.97050×10^{-6}
mg(OH)_2 Brucite, (200-1250)	0.0	-8.08692×10^5	-1.75140×10^3	-1.16892×10^3	1.80978×10^2	-3.19863×10^{-3}	0.0
MgSiO_3 Clinoenstatite, (200-968.5)	-4.33797×10^5	-1.44239×10^6	-1.31078×10^3	-1.01158×10^3	1.62362×10^2	0.0	0.0

Table 288. Continued

Formula, (temperature range in kelvins)	a_1	a_2	a_3	a_4	a_5	a_6	a_7
MgSiO ₃ Enstatite, (200-1257.4)	1.87801x10 ⁵	-1.42478x10 ⁶	-2.12685x10 ³	-1.35648x10 ³	2.07387x10 ²	-6.91249x10 ⁻³	0.0
MgSiO ₃ Protoenstatite, (1257.4-1800)	0.0	-1.42543x10 ⁶	-1.34677x10 ³	-9.74472x10 ²	1.57987x10 ²	0.0	0.0
Mg ₂ SiO ₄ Forsterite, (200-1800)	-5.96175x10 ⁵	-2.03090x10 ⁶	-1.95051x10 ³	-1.48847x10 ³	2.37767x10 ²	0.0	0.0
Mg ₃ Si ₂ O ₅ (OH) ₄ Chrysotile, (200-1250)	1.05526x10 ⁶	-3.91400x10 ⁶	-7.44838x10 ³	-4.63858x10 ³	7.04568x10 ²	-1.88092x10 ⁻²	0.0
Mg ₃ Si ₄ O ₁₀ (OH) ₂ Talc, (200-1250)	0.0	-5.39026x10 ⁶	-8.41302x10 ³	-5.39579x10 ³	8.24301x10 ²	-2.41645x10 ⁻²	0.0
Mg ₇ Si ₈ O ₂₂ (OH) ₂ Anthrophyllite, (200-1250)	5.53225x10 ⁶	-1.09427x10 ⁷	-2.37023x10 ⁴	-1.40164x10 ⁴	2.10106x10 ³	-2.29152x10 ⁻¹	1.00662x10 ⁻⁴
Mg ₄ Si ₃₄ O ₈₅ (OH) ₆₂ Antigorite, (200-1250)	1.69609x10 ⁷	-6.41927x10 ⁷	-1.20609x10 ⁵	-7.51253x10 ⁴	1.14157x10 ⁴	-3.10333x10 ⁻¹	0.0
O ₂ (g), (200-1800)	1.84663x10 ⁵	5.68075x10 ⁴	-1.70675x10 ²	-1.75052x10 ¹	3.54525x10 ¹	3.17977x10 ⁻³	-1.85549x10 ⁻⁶
Si (c), (200-1665)	-1.48020x10 ⁵	1.75295x10 ³	-1.77189x10 ²	-1.83356x10 ²	3.17050x10 ¹	2.81373x10 ⁻⁴	0.0
Si (l), (1665-1800)	0.0	4.84612x10 ⁴	0.0	-9.78143x10 ¹	2.55224x10 ¹	0.0	0.0
SiO ₂ Quartz (alpha), (200-844)	0.0	-8.42859x10 ⁵	-7.78110x10 ²	-5.29534x10 ²	8.32575x10 ¹	1.09794x10 ⁻²	0.0
SiO ₂ Quartz (beta), (844-1800)	0.0	-8.62517x10 ⁵	0.0	-3.00970x10 ²	5.89128x10 ¹	5.01976x10 ⁻³	0.0
SiO ₂ Cristobalite, (200-523)	0.0	-8.41305x10 ⁵	-6.70636x10 ²	-4.54294x10 ²	7.15824x10 ¹	2.53644x10 ⁻²	-3.27023x10 ⁻⁵
SiO ₂ Cristobalite, (523-1800)	-4.14084x10 ⁶	-8.73998x10 ⁵	0.0	-3.86787x10 ²	7.27781x10 ¹	6.43199x10 ⁻⁴	0.0

Table 289. Constants for volume-related functions in section 1.5.3. The dashes (---) indicate the parameters were not determined.

Formula, (temperature range in kelvins)	b_1	b_2	b_3	b_4	b_5
Al (c), (200-933.25)	---	---	---	---	---
Al (l), (933.25-1800)	---	---	---	---	---
AlOOH boehmite, (200-1250)	1.86386×10^1	3.00666×10^{-3}	0.0	-3.00000×10^{-5}	0.0
AlOOH diaspore, (200-1250)	1.74058×10^1	1.18889×10^{-3}	0.0	-3.67156×10^{-5}	0.0
Al(OH) ₃ gibbsite, (200-1250)	3.17958×10^1	5.37300×10^{-4}	0.0	-6.29400×10^{-7}	0.0
Al ₂ O ₃ corundum, (200-1800)	2.52017×10^1	6.55518×10^{-4}	0.0	-6.02751×10^{-6}	2.01149×10^{-1}
Al ₂ SiO ₅ andalusite, (200-1800)	5.00729×10^1	1.73719×10^{-3}	5.36253×10^{-1}	-2.16986×10^{-5}	7.70038×10^{-1}
Al ₂ SiO ₅ kyanite, (200-1800)	4.23174×10^1	1.24871×10^{-3}	2.29753×10^{-1}	8.04308×10^{-6}	1.43243
Al ₂ SiO ₅ sillimanite, (200-1800)	4.91338×10^1	9.35712×10^{-4}	4.23863×10^{-1}	-2.61363×10^{-5}	4.48630×10^{-1}
Al ₂ Si ₂ O ₅ (OH) ₄ kaolinite, (200-1250)	9.84196×10^1	3.56979×10^{-3}	0.0	-4.04420×10^{-4}	0.0
Al ₂ Si ₂ O ₅ (OH) ₄ dickite, (200-1250)	9.81973×10^1	3.70000×10^{-3}	0.0	-4.00000×10^{-4}	0.0
Al ₂ Si ₂ O ₅ (OH) ₄ halloysite, (200-1250)	9.82973×10^1	3.70000×10^{-3}	0.0	-4.00000×10^{-4}	0.0
Al ₂ Si ₄ O ₁₀ (OH) ₂ pyrophyllite, (200-1250)	1.26819×10^2	1.73097×10^{-3}	8.15952×10^{-1}	-7.24744×10^{-6}	0.0
C graphite, (200-1800)	---	---	---	---	---
CO (g), (200-1800)	---	---	---	---	---

Table 289. Continued

Formula, (temperature range in kelvins)	b ₁	b ₂	b ₃	b ₄	b ₅
CO ₂ (g), (200-1800)	---	---	---	---	---
Ca (c), (200-720)	---	---	---	---	---
Ca (c), (720-1112)	---	---	---	---	---
Ca (l), (1112-1755)	---	---	---	---	---
Ca (g), (1755-1800)	---	---	---	---	---
CaAl ₂ Si ₆ O ₆ Clinopyroxene, (200-1800)	6.28408x10 ¹	1.89768x10 ⁻³	4.60438x10 ⁻¹	-4.88417x10 ⁻⁵	0.0
CaAl ₂ Si ₂ O ₈ Anorthite, (200-1800)	9.95773x10 ¹	1.28176x10 ⁻³	0.0	-1.10185x10 ⁻⁴	7.67851x10 ⁻¹
CaAl ₄ Si ₂ O ₁₀ (OH) ₂ Margarite, (200-1250)	1.32864x10 ²	3.04606x10 ⁻³	0.0	-3.67641x10 ⁻⁴	0.0
CaCO ₃ Calcite, (200-1800)	3.60246x10 ¹	2.52024x10 ⁻⁴	8.69853x10 ⁻²	-3.63779x10 ⁻⁵	6.45538x10 ⁻¹
CaCO ₃ Aragonite, (200-1800)	4.28575x10 ¹	3.63164x10 ⁻⁵	1.85897x10 ⁻²	-2.48053x10 ⁻⁴	-8.73263
CaO Lime, (200-1800)	1.57869x10 ¹	7.79428x10 ⁻⁴	2.46416x10 ⁻¹	0.0	6.50708x10 ⁻¹
CaSiO ₃ Wollastonite, (200-1398.15)	3.88495x10 ¹	4.62101x10 ⁻⁴	-1.30789	-1.82503x10 ⁻⁵	1.29086
CaSiO ₃ Cyclo wollastonite, (200-1800)	3.65365x10 ¹	8.26635x10 ⁻⁴	4.23913x10 ⁻¹	1.01459x10 ⁻⁵	3.21801
CaAl ₂ Si ₂ O ₆ (OH) ₂ Bicchulite, (200-1250)	1.02427x10 ²	3.75930x10 ⁻³	0.0	-1.32974x10 ⁻⁴	0.0
CaAl ₂ Si ₂ O ₇ Gehlenite, (200-1800)	8.95072x10 ¹	2.48640x10 ⁻³	0.0	-4.09381x10 ⁻⁵	0.0

Table 289. Continued

Formula, (temperature range in kelvins)	b_1	b_2	b_3	b_4	b_5
$\text{Ca}_2\text{Al}_2\text{Si}_3\text{O}_{10}(\text{OH})_2$ Prehnite, (200-1250)	1.38906×10^2	5.12338×10^{-3}	0.0	-2.23955×10^{-4}	0.0
$\text{Ca}_2\text{Al}_3\text{Si}_3\text{O}_{12}$ Zoisite, (200-1250)	1.35236×10^2	4.97840×10^{-3}	0.0	-1.65560×10^{-4}	0.0
$\text{Ca}_2\text{Si}_4\text{O}_4$ Alpha, (1710-1800)	5.17315×10^1	1.90000×10^{-3}	0.0	-3.28000×10^{-5}	0.0
$\text{Ca}_2\text{Si}_4\text{O}_4$ Bredigite, (200-1710)	5.14335×10^1	1.90000×10^{-3}	0.0	-3.30000×10^{-5}	0.0
$\text{Ca}_2\text{Si}_4\text{O}_4$ Ca Olivine, (200-1120)	5.85137×10^1	2.00000×10^{-3}	0.0	-3.50000×10^{-5}	0.0
$\text{Ca}_2\text{Si}_4\text{O}_4$ Larnite, (200-970)	5.12763×10^1	8.21518×10^{-4}	2.12884×10^{-1}	-3.24000×10^{-5}	0.0
$\text{Ca}_3\text{Al}_2\text{Si}_3\text{O}_{12}$ Grossularite, (200-1800)	1.23151×10^2	3.35891×10^{-3}	5.69824×10^{-1}	-6.43965×10^{-5}	8.29661×10^{-1}
$\text{Ca}_3\text{Si}_5\text{O}_8$ Haurerite, (200-1800)	7.22620×10^1	1.04235×10^{-3}	4.57211×10^{-1}	-4.00000×10^{-5}	0.0
$\text{Ca}_3\text{Si}_2\text{O}_7$ Rankinite, (200-1800)	9.60000×10^1	1.35971×10^{-3}	2.47665×10^{-1}	-8.00000×10^{-5}	0.0
$\text{Ca}_4\text{Al}_6\text{Si}_6\text{O}_{24}(\text{CO}_3)$ Melionite, (200-1800)	3.35917×10^2	5.63126×10^{-3}	0.0	-4.36470×10^{-4}	0.0
Fe (c), (200-1042)	7.01063	2.79272×10^{-4}	0.0	-4.08527×10^{-6}	0.0
Fe (c), (1042-1184 and 1685-1800)	7.09200	0.0	0.0	0.0	0.0
Fe (c), (1184-1665)	7.09200	0.0	0.0	0.0	0.0
$\text{Fe}_{.947}\text{O}$ Wustite, (200-1800)	1.19646×10^1	0.0	0.0	-6.20724×10^{-6}	7.49475×10^{-2}
FeSiO_3 Ferrosillite, (200-1800)	3.26273×10^1	1.21117×10^{-3}	0.0	-7.11674×10^{-5}	0.0

Table 289. Continued

Formula, (temperature range in kelvins)	b_1	b_2	b_3	b_4	b_5
Fe_2O_3 Hematite, (200-955.5)	2.96670×10^1	1.17167×10^{-3}	0.0	-1.01344×10^{-5}	2.58748×10^{-1}
Fe_2O_3 Hematite, (955.5-1800)	2.96670×10^1	1.17167×10^{-3}	0.0	-1.01344×10^{-5}	2.58748×10^{-1}
Fe_2SiO_4 Fayalite, (200-1800)	4.57046×10^1	1.48633×10^{-3}	0.0	-3.48762×10^{-5}	0.0
Fe_3O_4 Magnetite, (200-848.5)	4.43930×10^1	4.38323×10^{-4}	0.0	-2.58503×10^{-5}	0.0
Fe_3O_4 Magnetite, (848.5-1800)	4.45420×10^1	0.0	0.0	0.0	0.0
H_2 (g), (200-1800)	---	---	---	---	---
H_2O (water), (273.15-373.15)	---	---	---	---	---
H_2O (g), (200-1800)	---	---	---	---	---
Mg (c), (200-922)	---	---	---	---	---
Mg (l), (922-1376)	---	---	---	---	---
Mg (g), (200-1800)	---	---	---	---	---
MgCu_3 Magnetite, (200-1800)	2.78494×10^1	5.65880×10^{-4}	0.0	-3.60075×10^{-5}	0.0
MgO Periclase, (200-1800)	1.11195×10^1	4.17881×10^{-4}	0.0	-6.09873×10^{-6}	0.0
$\text{Mg}(\text{OH})_2$ Brucite, (200-1250)	2.42379×10^1	5.33947×10^{-4}	0.0	0.0	2.33794×10^{-1}
MgSiO_3 Clinoenstatite, (200-968.5)	3.09763×10^1	9.97411×10^{-4}	0.0	-2.73873×10^{-5}	0.0

Table 289. Continued

Formula, (temperature range in kelvins)	b_1	b_2	b_3	b_4	b_5
Mg_3SiO_3 Enstatite, (200-1257.4)	3.05149×10^1	1.04744×10^{-3}	3.47023×10^{-1}	-1.73729×10^{-5}	3.94505×10^{-1}
Mg_3SiO_3 Protoenstatite, (1257.4-1800)	3.20608×10^1	9.29762×10^{-4}	0.0	-2.58376×10^{-5}	0.0
Mg_2SiO_4 Forsterite, (200-1800)	4.22835×10^1	1.96402×10^{-3}	6.52600×10^{-1}	-2.22563×10^{-5}	5.42082×10^{-1}
$Mg_3Si_2O_5(OH)_4$ Chrysotile, (200-1250)	9.80393×10^1	2.08435×10^{-3}	0.0	0.0	8.61502
$Mg_3Si_4O_{10}(OH)_2$ Talc, (200-1250)	1.24360×10^2	2.92124×10^{-3}	0.0	0.0	1.07237×10^1
$Mg_7Si_8O_{22}(OH)_2$ Anthophyllite, (200-1250)	2.63636×10^2	7.62631×10^{-4}	0.0	-3.40187×10^{-5}	0.0
$Mg_{48}Si_{34}O_{85}(OH)_{62}$ Antigorite, (200-1250)	1.60250×10^3	3.59060×10^{-2}	0.0	0.0	1.35952×10^2
O_2 (g), (200-1800)	---	---	---	---	---
Si (c), (200-1665)	---	---	---	---	---
Si (l), (1665-1800)	---	---	---	---	---
SiO_2 Quartz (alpha), (200-844)	2.21819×10^1	1.35725×10^{-3}	0.0	-4.27012×10^{-5}	0.0
SiO_2 Quartz (beta), (844-1800)	2.35794×10^1	0.0	0.0	-4.73106×10^{-5}	0.0
SiO_2 Cristobalite, (200-523)	2.50374×10^1	2.57716×10^{-3}	0.0	-6.46000×10^{-5}	0.0
SiO_2 Cristobalite, (523-1800)	2.72307×10^1	2.11894×10^{-4}	0.0	-6.46000×10^{-5}	0.0

1.6. Symbols and Units

The following symbols were used in the text, tables, and data summaries.

<u>Symbol</u>	<u>Units</u>	<u>Meaning</u>
C_p	J/(mol·K)	standard molar heat capacity
$C_{p,i}^\circ$	J/(mol·K)	standard molar heat capacity of mineral structural component i
E	volts	standard electrochemical potential in volts
G	J/mol	standard molar Gibbs energy
$[G(T)-H(T_r)]/T$	J/(mol·K)	Gibbs energy function
$G_{f,e}^\circ$	J/mol	standard molar Gibbs energy of formation from the elements
$G_{f,ox}^\circ$	J/mol	standard molar Gibbs energy of formation from the oxides
H	J/mol	standard molar enthalpy
$H(T)-H(298),$ $H(T)-H(T_r),$ or $H_T-H_{T_r}$	J/mol	relative standard molar enthalpy, base is H° at (T_r 298.15 K), 101.325 kPa
$H_{i,T}^\circ-H_{i,T_r}^\circ$	J/mol	relative standard molar enthalpy of mineral structural component i, base is H° at (T_r 298.15 K), 101.325 kPa
$H_{f,e}^\circ$	J/mol	standard molar enthalpy of formation from the elements
$H_{f,ox}^\circ$	J/mol	standard molar enthalpy of formation from the oxides
H_r°	J	standard enthalpy of reaction
$\log K_{f,e}^\circ$		\log_{10} of the standard equilibrium constant for formation from the elements

<u>Symbol</u>	<u>Units</u>	<u>Meaning</u>
$\log K_{f,ox}^{\circ}$		\log_{10} of the standard equilibrium constant for formation from the oxides
P	Pa	absolute pressure in pascals
P_r	Pa	reference pressure (101.325 pascals)
S	J/(mol·K)	standard molar entropy
S_i°	J/(mol·K)	standard molar entropy of mineral structural component i
T	K	absolute temperature in kelvins
T_r	K	reference temperature, absolute scale, equals 298.15 K
V	cm ³ /mol	standard molar volume

Fundamental constants used in this evaluation are given in section 1.7.

Where possible, the data have been corrected to the International Practical Temperature Scale of 1968 (Comite International des Poids et Mesures, 1969). For most phase equilibria, however, this was not possible because the necessary temperature calibration data were not supplied by the authors.

The "formula weights" have been calculated to be consistent with the 1975 relative atomic masses for the elements (Commission on Atomic Weights, 1976).

1.7. Fundamental Constants, Defined Constants, and Conversion Factors from Non-SI Units to SI Units

<u>Name</u>	<u>Symbol</u>	<u>Value and units</u>
<u>Fundamental constants</u>		
Avagadro constant	N	$6.022094 \times 10^{23} \text{ mol}^{-1}$
Faraday constant	\mathcal{F}	96,487.0 J/(volts·mol)
Gas constant	R	8.3143 J/(mol·K)
Absolute temperature of the "ice point," 0°C		273.15 K
<u>Defined units</u>		
Standard atmosphere	atm	101.325 kPa
Standard bar	b	100.000 kPa
Thermochemical calorie	cal	4.1840 J

Conversion factors from non-SI

units to SI units

0°C	=	273.15 K
1 Å	=	10^{-10} m
1 bar	=	10^5 Pa
1 atm	=	101325 Pa
1 cal	=	4.184 J
1 g cm^{-3}	=	$1 \times 10^3 \text{ Kg m}^{-3}$

CHAPTER 2

MECHANICAL PROPERTIES

H. R. Hume and P. D. Desai*

CONTENTS

	<u>Page</u>
2.1. INTRODUCTION -----	2
2.2. DENSITY -----	4
2.3. ELASTIC PROPERTIES - STATIC AND DYNAMIC -----	5
2.3.1. Modulus of Elasticity -----	9
2.3.2. Modulus of Rigidity -----	9
2.3.3. Poisson's Ratio -----	9
2.3.4. Bulk Modulus -----	9
2.3.5. Compressibility -----	17
2.3.6. Wave Velocities (Compression and Shear Velocities) -----	30
2.4. STRENGTH AND CREEP -----	36
2.4.1. Compressive Strength -----	36
2.4.2. Tensile Strength -----	51
2.4.3. Shear Strength -----	51
2.4.4. Creep -----	52
2.4.4.1. Creep of Rock In-Situ -----	59
2.4.4.2. Time Dependent 'Strength' -----	61
2.4.4.3. Summary of Empirical and Phenomenological Creep Models -----	61
2.5. HARDNESS -----	65
2.6. POROSITY AND PERMEABILITY -----	66
2.6.1. Porosity -----	66
2.6.2. Permeability -----	67
2.7. REFERENCES -----	70
2.8. SYMBOLS AND UNITS, AND CONVERSION FACTORS -----	75

*Center for Information and Numerical Data Analysis and Synthesis (CINDAS),
Purdue University, 2595 Yeager Road, West Lafayette, Indiana 47906.

2.1. INTRODUCTION

The mechanical properties of basalt presented here represent a compilation of the data available with a view toward its application in the design of a nuclear waste disposal depository in hard rock.

A knowledge of material behavior under applied forces is essential. This information falls under the category of mechanical properties. Whereas the properties of most structural materials such as steel, wood, or concrete are fairly uniform and easily predictable, those of rock are not. Rock composition is highly variable even over short distances and is susceptible to chemical change under the influences of weathering or chemical environment. For these reasons rocks can rarely be termed homogeneous. For these and structural reasons, e.g., the development of layering and the occurrence of jointing, isotropism is also difficult to claim.

To overcome these difficulties large scale field tests are resorted to, since an aggregate of these effects tends to stabilize any generalizations made about a rock mass. Unfortunately, large scale tests are expensive and, hence, rare. The only alternative in many cases has been to conduct small scale laboratory tests. The drawback of laboratory tests such as these is that they are conducted on small, relatively uniform samples which lack the aggregate properties of the rock mass.

Testing can be divided generally into static and dynamic categories. Both these basic categories provide similar information albeit using different methods. Elastic properties are the properties which are the most commonly measured because the theory of elasticity is one of the most widely used tools in rock mechanics. Although some of the assumptions of elasticity are often violated to some extent, e.g., homogeneity and isotropism, it is possible these violations may not be considered sufficiently extreme enough to invalidate the elastic assumption. In other instances the theory of elasticity may be the only tool available in a given design situation and so it is utilized just to obtain an estimate of the solution.

Commonly used elastic parameters are the elastic constants, modulus of elasticity (Young's modulus), modulus of rigidity (Shear modulus), bulk modulus, and Poisson's ratio. Density is intimately related to these parameters and so it is considered too. These parameters can be obtained

statically or dynamically. Dynamic determinations are experimentally simpler since they can be determined using wave velocities. Additionally, the parameters are all related to one another which also simplifies experimental work (this is providing once more that elastic assumptions hold true).

Mechanics of materials considerations dictate the most common strength measures, i.e., compressive strength, tensile strength, and shear strength. These measures are common to nearly all structural analyses and little needs to be said about their use. Since these tests are generally accomplished at low strain rates, these tests are regarded as static determinations.

Time dependent behavior of rock is represented by creep which is stress-strain behavior over an extended period of time under constant load. This is important input for the design of structures which are meant to retain their structural integrity over very long periods of time, i.e., hundreds or even thousands of years. This is especially important to structures that are to be subjected to higher than normal temperatures for extended periods. Nuclear waste depositories have both of these characteristics: long life spans and abnormal temperatures.

Hardness dictates the relative ease with which a rock can be excavated with a mechanical excavator, such as a tunnel boring machine. This is important from a designer's viewpoint in order to enable the feasibility of construction to be assessed.

Porosity and permeability are significant concerns. These parameters indicate the ability of a rock to support fluid flow. The degree of fluid flow is directly related to the amount of pollution which might be expected in any given situation. Furthermore, the amount of fluid flow is an indication of the efficacy of a nuclear waste depository design. Such a depository should be as impermeable as is possible to prevent contamination of the surrounding rock mass and groundwater.

2.2. DENSITY

This property is defined as the mass per unit volume. The volume, however, varied depending on what phase of the naturally occurring rock is considered. The solid phase obviously has a different volume than the solid phase + gas phase, for example. If one takes into account the three possible phases that coexist in natural rock, i.e., solid, liquid, and gas, it becomes apparent that several definitions of density are possible and, in fact, do exist. These are divided into 'true,' 'apparent,' and 'bulk' determinations.

'True' determinations take into account the volume of only the solid phase of the rock with respect to the mass of the rock.

'Apparent' determinations use the dry (solid+gas) mass of a unit volume of solids.

'Bulk' determinations use the prevailing conditions (solid+liquid+gas) of the rock to determine the mass of a unit volume of rock.

'Specific gravity' is, for practical purposes, a relative density with respect to water.

'Grain density,' as the name implies, is a density determination in which the mass of the grains of the rock and the volume of these grains are utilized.

A problem with published literature at present is that most often the type of density is not stated - the value is merely quoted. Generally, it appears wise to presume that densities given are 'apparent' values. The same applied to specific gravities.

The various densities can be obtained using the 'pycnometric,' 'buoyancy,' or 'direct measurement' techniques. In the case of the first two, both use pycnometers and are applications of Archimedes principle. Of these methods, the 'buoyancy' method is the most accurate.

In general, densities of rocks are a function of many variable factors. The inhomogeneity of chemical composition and physical structure, even between samples of the same rock type, make a 'universal' density of a given rock type impossible to obtain. The degree of vesiculation, proportions of and types of minerals, porosity, degree of saturation, and type and amount of trapped fluids all give rise to the observed variance in density determinations.

The densities of various types of basalt from various locations are presented in the 'Remarks' column of Tables 2.1, 2.2, and 2.3. Since density is a volume dependent property, a plot of volumetric strain versus confining pressure for Nevada Test Site (NTS) basalt from ref. [1] is presented in Figure 2.1. The basalt sample was jacketed in lead to simulate hydrostatic compression while undergoing compression. Tests were accomplished using a high pressure die and sample assembly. Numerous corrections were necessary to obtain compression values, e.g., contraction of pistons, stretching of the die. In order to calibrate the die apparatus, gold was used as a standard. Data were taken using a pressure range up to 4.66 Pa at a temperature of 298 K. As is expected, the strain decreases with decreasing confining pressure. The results obtained were in good agreement with dynamic values previously obtained by Lombard [2].

2.3. ELASTIC PROPERTIES - STATIC AND DYNAMIC

The elastic properties considered here are:

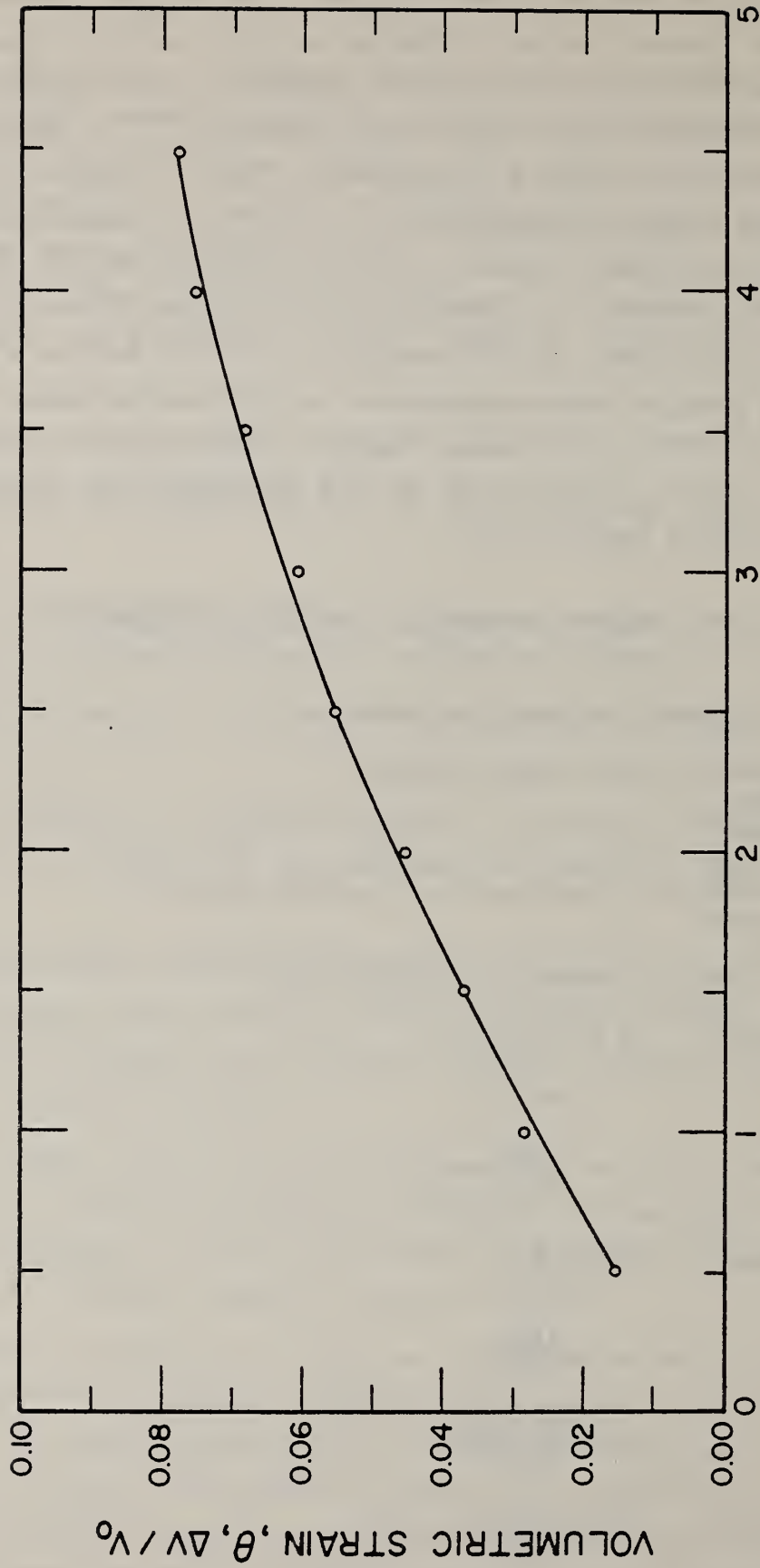
Young's modulus (secant and/or tangent)
 Bulk modulus
 Shear modulus
 Poisson's ratio
 Compressibility (the reciprocal of the bulk modulus)
 Wave velocities

Formulae for elastic properties are given below:

$$\begin{aligned} \text{Young's Modulus} \quad E &= 2G(1+\nu) \\ &= 3K(1-2\nu) \\ &= \frac{9KG}{(3K+G)} \end{aligned}$$

$$\begin{aligned} \text{Shear Modulus} \quad G &= \frac{E}{2(1+\nu)} \\ &= \frac{3EK}{(9K-E)} \\ &= \frac{3K(1-2\nu)}{2(1+\nu)} \end{aligned}$$

$$\text{Bulk Modulus} \quad K = \frac{E}{3(1-2\nu)}$$



CONFINING PRESSURE , P , GPa

FIGURE 2.1.1. VARIATION OF VOLUMETRIC STRAIN WITH CONFINING PRESSURE FOR BASALT [1].

$$\begin{aligned}
 &= \frac{EG}{3(3G-E)} \\
 &= \frac{2G(1+\nu)}{3(1-2\nu)} \\
 \text{Poisson's Ratio } \mu &= \frac{E-2G}{2G} \\
 &= \frac{3K-E}{6K} \\
 &= \frac{(3K-2G)}{2(3K+G)}
 \end{aligned}$$

The determination of the above properties can be static (with the exception of wave velocities) or dynamic, and made either in laboratory or in-situ. Overall, in both in-situ and laboratory tests it is important to be able to measure load stresses and deformation accurately and be able to minimize or remove factors which lead to erroneous or distorted values.

Dynamically obtained elastic constants tend to be higher than those obtained statically; however, they are of importance when one needs to know the behavior of rock subjected to shock loading.

Basically, elastic constants measured by static methods are indicative of large strains, e.g., 10^{-3} , which occur in mining. Dynamic methods investigate lower strains of the order of 10^{-5} . Static methods give rise to larger scatter of results, while dynamic methods give rise to less.

Static Constants

In-situ values are generally obtained by one of the following methods:

- Plate bearing tests
- Pressure tunnel tests
- Borehole tests

These are all 'large scale' tests and are expensive to perform. The specifics of such tests vary depending on the conditions encountered.

Laboratory values are obtained by several methods. Some of the commonly used methods are given below. It is important to note that if any two constants are known, the other two can be easily calculated.

Simple Direct Compression or Tension Test: Young's modulus and Poisson's ratio are possible to determine from tests on prismatic specimens loaded in compression or tension.

Bending Tests: Young's modulus can be determined using 3 or 4 point loading of a beam.

Brazilian Test: Poisson's ratio and Young's modulus can be obtained by measuring the strains at the center of a loaded disk in both vertical and horizontal directions.

Triaxial Test: Solid and hollow specimens can be loaded triaxially and deformations can be measured. These stresses and deformations can then be utilized to find Young's modulus.

All the elastic constants are related to one another provided one assumes a perfectly elastic, isotropic, homogeneous material. Rock seldom fulfills these conditions; however, in certain instances, it may be close enough to allow approximate fulfillment of these assumptions.

Moduli in tension and compression are not the same and may vary from 1 to 10 times or more. Variations of moduli with stress are due to changes occurring in the structure of rocks during loading and unloading. Comparison of in-situ and laboratory values indicate a good deal of difference in many cases, and this discrepancy is a function of discontinuities present in the in-situ condition.

Dynamic Constants

These constants are calculated from elastic wave velocities and density. In-situ seismic reflection or refraction can be used with refraction being the more popular. Laboratory values are determined using either the ultrasonic or resonance techniques.

For the purposes of this work, two kinds of waves are considered; namely: P or compressional waves and S or shear waves. Both of these are body waves, i.e., transmitted through (rather than along the surface) the body. Compressional waves cause longitudinal particle oscillation, while shear waves cause transverse oscillation.

In the case of the laboratory methods mentioned, the basic difference between the two is the frequency at which the velocities are determined. The excitation frequency, however, has been shown to have no effect on the wave velocities, but a significant effect on the calculation of Poisson's ratio.

Wave velocities, like other properties, are affected by various factors.

Briefly, these factors are:

- 1) Rock type
- 2) Texture (grain size is important)
- 3) Density (density and average atomic weight dictate velocity of longitudinal waves)
- 4) Porosity (velocity decreases with increasing porosity)
- 5) Anisotropy (velocity parallel to layers greater than velocity perpendicular to layers)
- 6) Water content (generally water saturation increases velocity in hard rocks)
- 7) Temperature (velocity of longitudinal waves decreases with increase in temperature)

2.3.1. Modulus of Elasticity

Values for the modulus of elasticity of basalt are given in Table 2.1.

2.3.2. Modulus of Rigidity

Table 2.1 contains modulus of rigidity values for basalt.

2.3.3. Poisson's Ratio

Poisson's ratio values for basalt are given in Table 2.1.

2.3.4. Bulk Modulus

Figures 2.2 through 2.6 show the variation of bulk modulus with confining pressure for saturated basalt core samples obtained from Deep Sea Drilling Project (DSDP) Legs 16, 19, 34, 35, and 39, respectively. It should be noted that these curves have been smoothed. The data corresponding to these curves are given in Table 2.2.

Bulk modulus values in a few cases were calculated from velocity measurements made at room temperature on water saturated core samples. The pulse transmission technique was employed to obtain the velocities.

The velocity values obtained for Leg 16 (Fig. 2.2) were uncorrected for length changes at elevated temperatures, which lower the 1000 MPa confining pressure velocities and raise the bulk density very slightly. Sample 163-29-4 (67-74 cm) is a massive fresh basalt, while sample 155-11-1 (143-150 cm) is an

TABLE 2.1. ROOM-TEMPERATURE MODULUS OF ELASTICITY, MODULUS OF RIGIDITY AND POISSON'S RATIO OF BASALT

Data Set No.	Basalt Type & Location	Confining Pressure, P (MPa)	Modulus of Elasticity, E (GPa)	Modulus of Rigidity, G (GPa)	Poisson's Ratio, μ	Remarks	Ref. No.
Andesite Basalt -							
1	Bakuriani Georgia, USSR	21.86	23.54		0.24		3
Olivine Basalt -							
2	Eniwetok, Atoll		68.5		0.20	Density 2.86 g cm ⁻³ .	4
3	Eniwetok, Atoll		67.36		0.19	Perpendicular secant modulus; stress 194 MPa.	4
4	Eniwetok, Atoll		69.29		0.18	Perpendicular secant modulus; stress 0 MPa.	4
5	Genbudo, Japan		55.0				5
6	Nevada Test Site (NTS)		57.0		0.23		6
Basalts -							
7	Black, Canyon Dam, ID		32.41			Density 2.62 g cm ⁻³ .	7
8	Blairden, CA	773	58.80			Differential stress 588 MPa; secant modulus.	8
9	Blairden, CA	773	47.00			Differential stress 960 MPa; secant modulus.	8
10	Blairden, CA	773	27.60			Differential stress 1380 MPa; secant modulus.	8
11	Blairden, CA	778	61.70			Differential stress 617 MPa; secant modulus.	8
12	Blairden, CA	778	20.40			Differential stress 1020 MPa; secant modulus.	8
13	Blairden, CA	778	10.30			Differential stress 1030 MPa; secant modulus.	8
14	Barini Dam, Brazil		21.8-46.4	8.3-21.1	0.31-10	Density 2.97 g cm ⁻³ .	9
15	Bara Bonita Dam, Brazil		29.0-60.6	10.7-23.2	0.31-0.35	Density 2.91 g cm ⁻³ .	9
16	Bara Bonita Dam, Brazil		57.2-62.2		0.19	Compact; porosity 1.4%; density 2.829 cm ⁻³ .	10
17	Bara Bonita Dam, Brazil		61.0		0.19		10
18	Brooklyn Vic., Australia		22.8				11
19	Brooklyn Vic., Australia		23.5				11
20	Brooklyn Vic., Australia		15.9				11
21	Champion Mine, MI		61	27		Density 2.85 g cm ⁻³ .	12
22	Champion Mine, MI		85	34		Density 2.97 g cm ⁻³ .	12
23	Champion Mine, MI		70.0	30.0		Density 2.91 g cm ⁻³ .	12
24	Cochoeira Dam, Brazil		76.5-100.3	33.7-41.5	0.14-0.21	Density 2.94 g cm ⁻³ .	9
25	Dresser, WI		86.10			Horneblende biotite.	14
26	Dresser, WI		100.7		0.24	Density 2.97 g cm ⁻³ .	8
27	Dresser, WI		100.7		0.25	Density 2.9 g cm ⁻³ .	15

TABLE 2.1. ROOM-TEMPERATURE MODULUS OF ELASTICITY, MODULUS OF RIGIDITY AND POISSON'S RATIO OF BASALT (continued)

Data Set No.	Basalt Type & Location	Confining Pressure, P (MPa)	Modulus of Elasticity, E (GPa)	Modulus of Rigidity, G (GPa)	Poisson's Ratio, ν	Remarks	Ref. No.
Basalts (cont.)-							
28	Guadalupe Drill Site (EMT)	2.06	48.5		0.384	Density 2.82 g cm ⁻³ .	16
29	Green Peters Dam		35.0		0.21	Amygdaloidal porosity or phyrritic; density 2.58 g cm ⁻³ .	17
30	Howard Prairie Dam, OR	0-7	63		0.25	Density 2.74 g cm ⁻³ .	12
31	Howard Prairie Dam, OR	0-35	61		0.22	Density 2.74 g cm ⁻³ .	12
32	Howard Prairie Dam, OR	0.10	76.4	31.5	0.22	Density 2.82 g cm ⁻³ .	18
33	Howard Prairie Dam, OR	100	82.5	33.0	0.25	Density 2.82 g cm ⁻³ .	18
34	Howard Prairie Dam, OR		28.27		0.25	Stress 6.98 MPa.	19
35	Howard Prairie Dam, OR		31.72		0.24	Stress 20.7 MPa.	19
36	Howard Prairie Dam, OR		35.85		0.22	Stress 41.4 MPa.	19
37	Howard Prairie Dam, OR		61.8		0.23	Density 2.73 g cm ⁻³ .	20
38	Ibitinga Dam, Brazil		10.7-30.6	3.8-11.7	0.31-0.41	Density 2.79 g cm ⁻³ .	9
39	John Day		83.8		0.27	At 50% of failure.	21
40	Jupia Dam, Brazil		73.0		0.21	Density 3.0 g cm ⁻³ .	10
41	Jupia Dam, Brazil		69.9-74.4		0.21	Compact; porosity 2.1%; density 2.92 g cm ⁻³ .	10
42	Jupia Dam, Brazil		24.1-66.2	10.5-30.4	0.14-0.04	Density 2.77 g cm ⁻³ .	9
43	Jurimirim Dam, Brazil		56.7-43.6		0.16	Porosity 4.2%; density 2.52 g cm ⁻³ .	10
44	Jurimirim Dam, Brazil		42.8		0.16	Density 2.7 g cm ⁻³ .	10
45	Koyna Dam, India		36.20		0.13	Altered vesicular; density 2.54 g cm ⁻³ .	7
46	Little Goose		77.5		0.27	At 50% of failure.	21
47	Lower Granite		50.2		0.24	At 50% of failure.	21
48	Medford, OR	0-41.6	60		0.22	Density 2.72 g cm ⁻³ .	22
49	Medford, OR	0-41.6				Density 2.74 g cm ⁻³ .	22
50	Melhurb Quarry, Brazil		39.3			Porosity 11.6%; density 2.44 g cm ⁻³ .	10
51	Michigan		96	38	0.281	Altered; density 2.85 g cm ⁻³ .	22
52	Michigan		41	18	0.09	Altered amygdaloidal; density 2.70 g cm ⁻³ .	22
53	Michigan		60.0		0.15	Heavily altered amygdaloidal; density 2.80 g cm ⁻³ .	22
54	Michigan		46.19		0.16	Amygdaloidal heavily altered; secant modulus; stress 0 MPa (perpendicular).	23

TABLE 2.1. ROOM-TEMPERATURE MODULUS OF ELASTICITY, MODULUS OF RIGIDITY AND POISSON'S RATIO OF BASALT (continued)

Data Set No.	Basalt Type & Location	Confining Pressure, P (MPa)	Modulus of Elasticity, E (GPa)	Modulus of Rigidity, G (GPa)	Poisson's Ratio, μ	Remarks	Ref. No.
Basalts (cont.) -							
55	Michigan		46.88		0.20	Same as above except stress 59.6 MPa (perpendicular).	23
56	Michigan		42.75		0.26	Same as above except stress 119 MPa (perpendicular).	23
57	Michigan		59.98			Same as above except stress 0 MPa (perpendicular).	23
58	Michigan		57.23		0.15	Same as above except stress 172 MPa (perpendicular).	23
59	Michigan		55.16		0.16	Same as above except stress 342 MPa (perpendicular).	23
60	Mussa Quarry, Brazil		41.6-44.9		0.19	Porosity 2.50%; density 2.50 g cm ⁻³ .	10
61	Mussa Quarry, Brazil		44.0		0.19	Density 2.68 g cm ⁻³ .	10
62	Nevada Test Site (NTS)		29.5		0.37		24
63	Nevada Test Site (NTS)		57.0				6
64	Nevada Test Site (NTS)		33.9		0.32	At 50% of failure; density 2.83 g cm ⁻³ .	25
65	Ostrich, Germany	10-90	11.2				26
66	South Coulee Dam, WA		1.115			Stress 10-90 MPa.	26
67	South Coulee Dam, WA		50.50		0.18	Density 2.81 g cm ⁻³ .	7
68	South Coulee Dam, WA		59.29		0.21	Vesicular; density 2.62 g cm ⁻³ .	7
69	South Coulee Dam, WA		38.61		0.13	Density 2.58 g cm ⁻³ .	7
70	South Coulee Dam, WA		42.06		0.19	Vesicular; density 2.47 g cm ⁻³ .	7
71	Washington		59.29		0.21	Highly vesicular.	7
72	Xavantes Dam, Brazil		24.0-51.8	11.2-23.1	0.07-0.12	Density 2.44 g cm ⁻³ .	9
73	Xavantes Dam, Brazil		44.8-66.19			Density 2.72 g cm ⁻³ .	27
74	Xavantes Dam, Brazil		28.48			Density 2.91 g cm ⁻³ .	28
75	DSDP Leg 16; 155-11-1, 143-150 cm.	40 100 200 600 1000	93.0 95.0 96.0 98.0 99.0	36.0 37.0 37.0 38.0 38.0	0.28 0.28 0.28 0.28 0.29	Deep Sea Drilling Project (DSDP) Leg 16; plagioclase 45%, pyroxene 40%, olivine 4%, opaque and others 11%; value calculated from mean velocities and densities and for water saturated samples; density 2.448 g cm ⁻³ .	29
76	DSDP Leg 16; 163-29-4, 67-74 cm.	40 100 200 600 1000	10.0 11.0 11.0 12.0 12.0	27.0 28.0 29.0 32.0 32.0	0.35 0.35 0.35 0.35 0.36	Same as above except plagioclase 58%, pyroxene 9%, opaques and other 33%; density 2.935 g cm ⁻³ .	29

TABLE 2.1. ROOM-TEMPERATURE MODULUS OF ELASTICITY, MODULUS OF RIGIDITY AND POISSON'S RATIO OF BASALT (continued)

Data Set No.	Basalt Type & Location	Confining Pressure, P (MPa)	Modulus of Elasticity, E (GPa)	Modulus of Rigidity, G (GPa)	Poisson's Ratio, μ	Remarks	Ref. No.
Basalts (cont.) -							
77	DSDP Leg 19; 19-183-39-1, 148-150 cm.	40	72.0	27.0	0.33	Density 2.84 g cm ⁻³ ; values calculated from mean velocities and densities corrected for dimensions.	30
		100	74.0	28.0	0.33		
		200	76.0	29.0	0.33		
		600	80.0	30.0	0.33		
		1000	81.0	31.0	0.33		
78	DSDP Leg 19; 19-191-16-1, 21-25 cm.	40	66.0	25.0	0.29	Same as above except density 2.794 g cm ⁻³ .	30
		100	67.0	26.0	0.29		
		200	68.0	26.0	0.29		
		600	70.0	27.0	0.29		
		1000	71.0	27.0	0.30		
79	DSDP Leg 19; 19-191-16-1, 21-25 cm.	40	41.0	16.0	0.32	Same as above except density 2.563 g cm ⁻³ .	30
		100	43.0	16.0	0.33		
		200	45.0	17.0	0.33		
		600	50.0	19.0	0.33		
		1000	52.0	20.0	0.34		
80	DSDP Leg 34; 319A-1-1, 32-35 cm.	40	83.0	32.0	0.29	Leg 34 of Deep Sea Drilling Project (DSDP); Nazca plate; values calculated from measured densities and velocities; density 2.915 g cm ⁻³ .	31
		100	85.0	33.0	0.29		
		200	87.0	34.0	0.29		
		600	91.0	35.0	0.29		
81	DSDP Leg 34; 319A-2-3, 46-48 cm.	40	76.0	29.0	0.30	Same as above except density 2.864 g cm ⁻³ .	31
		100	80.0	30.0	0.29		
		200	80.0	31.0	0.29		
		600	84.0	32.0	0.30		
82	DSDP Leg 34; 319A-3-2, 114-117 cm.	40	82.0	32.0	0.29	Same as above except density 2.923 g cm ⁻³ .	31
		100	85.0	33.0	0.29		
		200	87.0	34.0	0.29		
		600	91.0	35.0	0.30		
83	DSDP Leg 34; 319A-3-4, 85-88 cm.	40	86.0	33.0	0.29	Same as above except density 2.939 g cm ⁻³ .	31
		100	87.0	34.0	0.29		
		200	89.0	34.0	0.30		
		600	92.0	35.0	0.30		
84	DSDP Leg 34; 319A-4-1, 137-140 cm.	40	82.0	32.0	0.28	Same as above except density 2.911 g cm ⁻³ .	31
		100	83.0	32.0	0.29		
		200	85.0	33.0	0.29		
		600	87.0	34.0	0.30		
85	DSDP Leg 34; 319A-5-1, 80-83 cm.	40	92.0	36.0	0.28	Same as above except density 2.948 g cm ⁻³ .	31
		100	93.0	36.0	0.28		
		200	94.0	36.0	0.28		
		600	95.0	37.0	0.29		
86	DSDP Leg 34; 319A-6-1, 145-148 cm.	40	81.0	31.0	0.30	Same as above except density 2.882 g cm ⁻³ .	31
		100	83.0	32.0	0.29		
		200	84.0	32.0	0.29		
		600	85.0	33.0	0.30		
87	DSDP Leg 34; 319A-7-1, 65-68 cm.	40	78.0	30.0	0.29	Same as above except density 2.851 g cm ⁻³ .	31
		100	79.0	31.0	0.29		
		200	80.0	31.0	0.29		
		600	83.0	32.0	0.29		
88	DSDP Leg 34; 319A-13-1, 52-55 cm.	40	82.0	32.0	0.30	Same as above except density 2.920 g cm ⁻³ .	31
		100	85.0	33.0	0.30		
		200	88.0	34.0	0.29		
		600	91.0	35.0	0.30		
89	DSDP Leg 34; 320B-3-1, 64-67 cm.	40	58.0	22.0	0.29	Same as above except density 2.725 g cm ⁻³ .	31
		100	59.0	23.0	0.29		
		200	60.0	23.0	0.29		
		600	64.0	25.0	0.30		

TABLE 2.1. ROOM-TEMPERATURE MODULUS OF ELASTICITY, MODULUS OF RIGIDITY AND POISSON'S RATIO OF BASALT (continued)

Data Set No.	Basalt Type & Location	Confining Pressure, P (MPa)	Modulus of Elasticity, E (GPa)	Modulus of Rigidity, G (GPa)	Poisson's Ratio, μ	Remarks	Ref. No.
Basalts (cont.) -							
90	DSDP Leg 34; 320B-4-1, 144-147 cm.	40	68.0	26.0	0.30	Same as above except density 2.837 g cm ⁻³ .	31
		100	71.0	27.0	0.30		
		200	74.0	28.0	0.30		
		600	78.0	30.0	0.31		
91	DSDP Leg 34; 320B,5,CC	40	78.0	30.0	0.29	Same as above except density 2.832 g cm ⁻³ .	31
		100	80.0	31.0	0.29		
		200	83.0	32.0	0.28		
		600	87.0	34.0	0.27		
92	DSDP Leg 34; 321-13-4, 104-107 cm.	40	59.0	23.0	0.29	Same as above except density 2.822 g cm ⁻³ .	31
		100	62.0	24.0	0.29		
		200	64.0	25.0	0.29		
		600	68.0	26.0	0.30		
93	DSDP Leg 34; 321-14-1, 76-79 cm.	40	81.0	32.0	0.29	Same as above except density 2.900 g cm ⁻³ .	31
		100	83.0	32.0	0.28		
		200	85.0	33.0	0.28		
		600	89.0	35.0	0.28		
94	DSDP Leg 34; 321-14-4, 51-54 cm.	40	73.0	28.0	0.29	Same as above except density 2.915 g cm ⁻³ .	31
		100	75.0	29.0	0.29		
		200	77.0	30.0	0.28		
		600	82.0	32.0	0.28		
95	DSDP Leg 39; 354-19-3, 131-134 cm.	40	65.0	25.0	0.29	Leg 39 of Deep Sea Drilling Pro- ject (DSDP); values calculated from velocities and densities corrected for dimension changes and for water saturated samples; density 2.733 g cm ⁻³ .	32
		100	66.0	26.0	0.29		
		200	67.0	26.0	0.29		
		600	69.0	27.0	0.30		
96	DSDP Leg 39; 354-19-5, 93-96 cm.	40	68.0	26.0	0.29	Same as above except density 2.753 g cm ⁻³ .	32
		100	69.0	26.0	0.29		
		200	69.0	26.0	0.29		
		600	71.0	27.0	0.30		
97	DSDP Leg 39; 355-21-1, 147-150 cm.	40	65.0	25.0	0.32	Same as above except density 2.808 g cm ⁻³ .	32
		100	65.0	25.0	0.32		
		200	66.0	25.0	0.32		
		600	69.0	27.0	0.31		
98	DSDP Leg 39; 355-22-1, 57-60 cm.	40	75.0	28.0	0.32	Same as above except density 2.884 g cm ⁻³ .	32
		100	76.0	29.0	0.31		
		200	77.0	29.0	0.31		
		600	81.0	31.0	0.31		
99	DSDP Leg 39; 355-22-2, 44-47 cm.	40	75.0	29.0	0.28	Same as above except density 2.838 g cm ⁻³ .	32
		100	76.0	30.0	0.28		
		200	78.0	30.0	0.29		
		600	79.0	30.0	0.30		
100	DSDP Leg 39; 355-22-4, 69-72 cm.	40	62.0	24.0	0.29	Same as above except density 2.757 g cm ⁻³ .	32
		100	63.0	24.0	0.30		
		200	63.0	24.0	0.30		
		600	66.0	26.0	0.30		
101	DSDP Leg 39; 355-22-5, 119-122 cm.	40	68.0	27.0	0.28	Same as above except density 2.798 g cm ⁻³ .	32
		100	69.0	27.0	0.28		
		200	70.0	27.0	0.28		
		600	73.0	28.0	0.29		
102	DSDP Leg 39; 359-4-2, 80-83 cm.	40	26.0	10.0	0.36	Same as above except density 2.258 g cm ⁻³ .	32
		100	28.0	10.0	0.35		
		200	29.0	11.0	0.35		
		600	31.0	11.0	0.35		
103	DSDP Leg 39; 359-4-3, 143-146 cm.	40	27.0	10.0	0.35	Same as above except density 2.308 g cm ⁻³ .	32
		100	29.0	11.0	0.35		
		200	30.0	11.0	0.35		
		600	32.0	12.0	0.36		

TABLE 2.1. ROOM-TEMPERATURE MODULUS OF ELASTICITY, MODULUS OF RIGIDITY AND POISSON'S RATIO OF BASALT (continued)

Data Set No.	Basalt Type & Location	Confining Pressure, P (MPa)	Modulus of Elasticity, E (GPa)	Modulus of Rigidity, G (GPa)	Poisson's Ratio, μ	Remarks	Ref. No.
Basalts (cont.) -							
104	DSDP Leg 39; 359-5-1, 26-29 cm.	40	40.0	15.0	0.35	Same as above except density 2.449 g cm ⁻³ .	32
		100	41.0	15.0	0.35		
		200	42.0	16.0	0.34		
		600	43.0	16.0	0.35		
105	DSDP Leg 35; 322-12-1, Piece 7	40	63.0	24.0	0.29	Deep Sea Drilling Project (DSDP); values calculated from measured densities and velocities and for water saturated samples; density 2.73 g cm ⁻³ .	33
		100	64.0	25.0	0.29		
		200	65.0	25.0	0.29		
		600	68.0	26.0	0.30		
106	DSDP Leg 35; 322-13-2, 56-62 cm.	40	45.0	17.0	0.30	Same as above except density 2.553 g cm ⁻³ .	33
		100	46.0	18.0	0.30		
		200	48.0	19.0	0.30		
		600	51.0	20.0	0.30		
107	DSDP Leg 35; 323-18-6, 110-120 cm.	40	58.0	22.0	0.31	Same as above except density 2.727 g cm ⁻³ .	33
		100	59.0	23.0	0.31		
		200	61.0	23.0	0.31		
		600	33.0	24.0	0.31		
108	DSDP Leg 35; 323-20, CC, 104-114 cm.	40	59.0	23.0	0.29	Same as above except density 2.723 g cm ⁻³ .	33
		100	60.0	23.0	0.29		
		200	61.0	24.0	0.29		
		600	63.0	24.0	0.30		

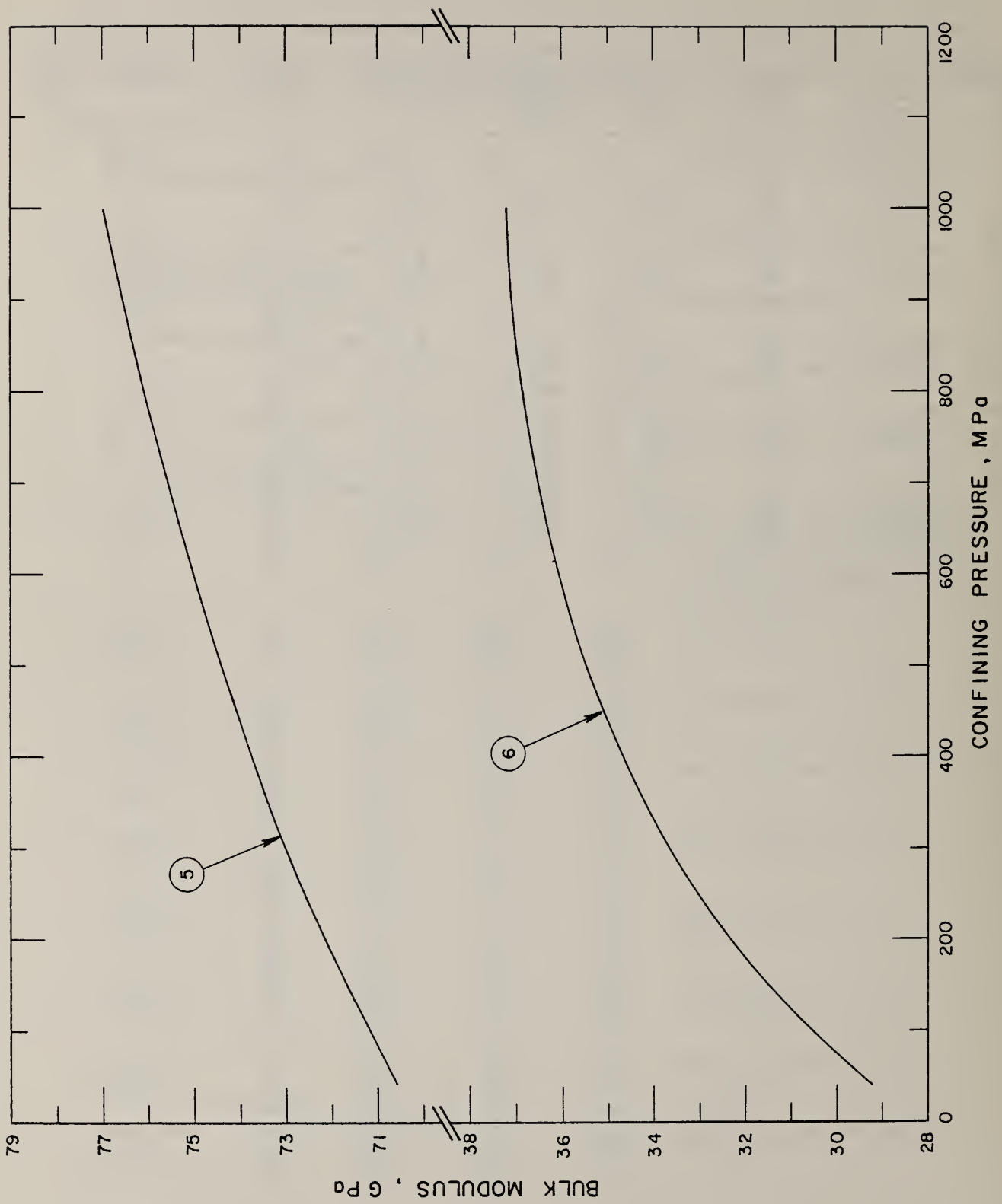


FIGURE 2.2. BULK MODULUS OF SATURATED BASALT CORE SAMPLES FROM DSDP LEG 16 [29].

altered vesicular basalt. The increase in bulk modulus with confining pressure is as expected.

Leg 19 (Fig. 2.3) values were obtained essentially in the same manner as previously described. It is noteworthy, however, that the general rapid increase in velocities up to 200 MPa confining pressure is due to the closure of cracks in the specimen. This obviously, therefore, will affect the variation of the modulus with increasing confining pressure. Again, the modulus behavior with respect to pressure is predictable.

Leg 34 (Fig. 2.4) varies in age and degree of alteration. In general, however, these basalts are young (less than 40 million years old) and are commonly fine- to medium-grained with a minor amount of alteration. The bulk moduli obtained are somewhat higher than those obtained on older basalts which can be explained when alteration of the rock due to weathering with age is taken into account (the more weathered the basalt, the lower is the seismic velocity). Other than this observation, the behavior of the bulk modulus is normal.

Samples used for Leg 35 (Fig. 2.5) determinations were fine-grained and slightly altered. The low bulk modulus obtained for sample 322-13-2 (56-62 cm) is due to the low bulk density due in part to open vesicles present. Behavior with increasing confining pressure is typical.

Leg 39 (Fig. 2.6) samples can be broken into two groups: 354 samples are coarse-grained basalts, whilst 355 samples are much finer. A feature of the 354 samples is that they contain large amounts of calcite which tends to give higher seismic velocities than are usual for basalts of similar density that contain very little calcite.

2.3.5. Compressibility

Compressibility is the reciprocal of the bulk modulus, and Figures 2.7 through 2.11 show variation with confining pressure. It is calculated directly from the bulk modulus and, therefore, is a function of the wave velocities. Once again, curves have been smoothed and the data for these curves are given in Table 2.2.

Since this property is purely a reciprocal of the bulk modulus, the comments which apply to the bulk modulus apply equally to it. For this reason

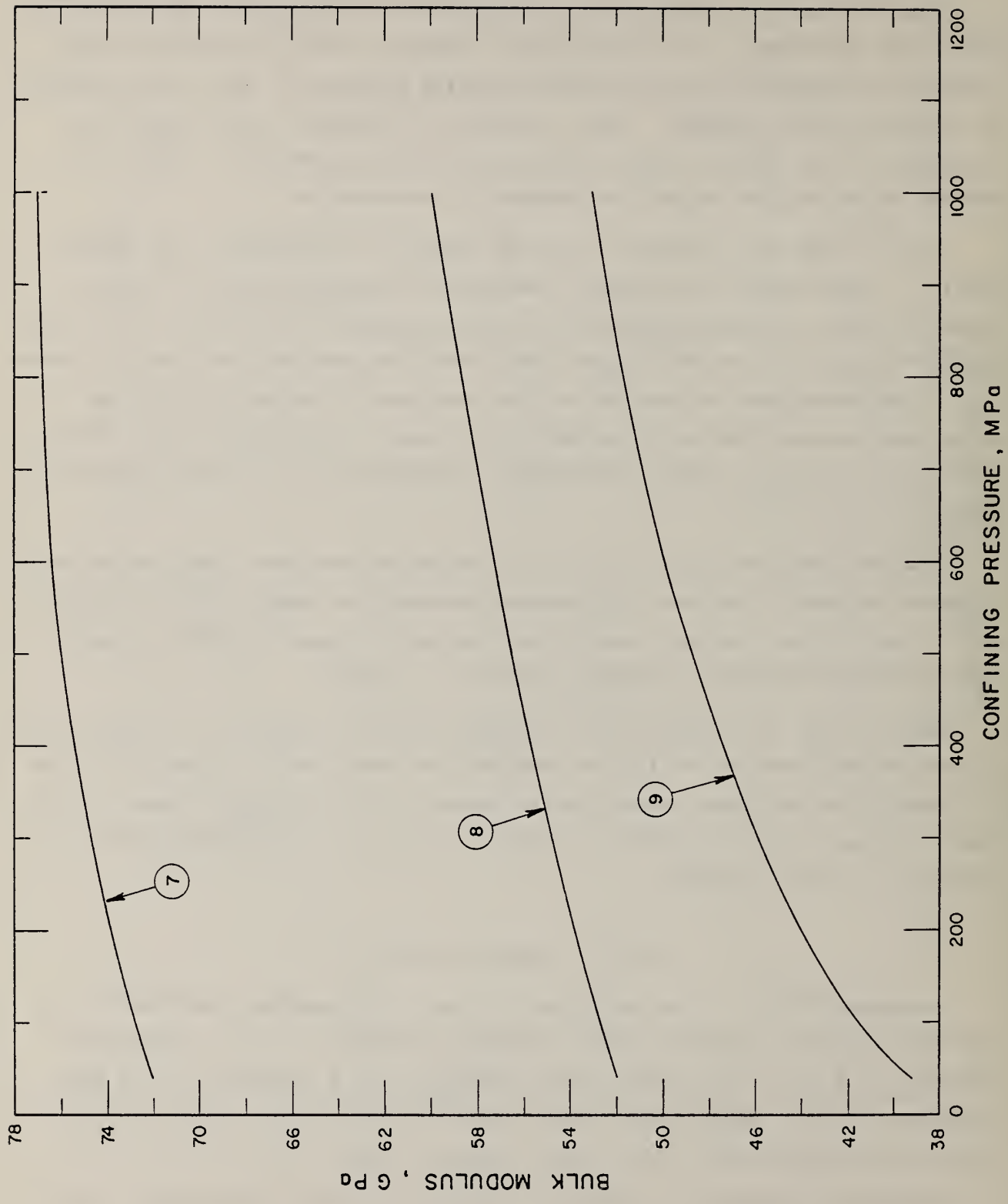


FIGURE 2.3. BULK MODULUS OF SATURATED BASALT CORE SAMPLES FROM DSDP LEG 19 [30].

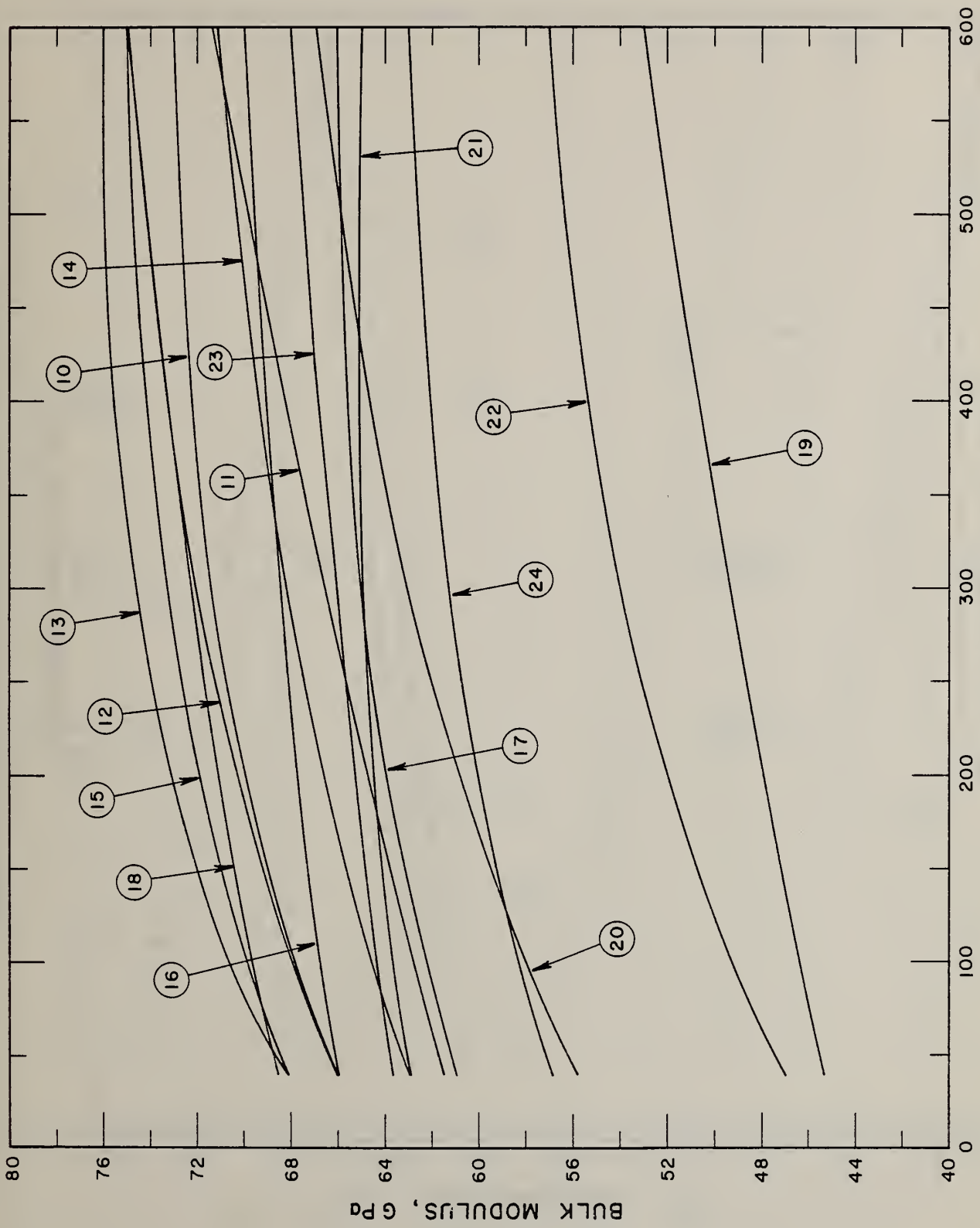


FIGURE 2.4. BULK MODULUS OF SATURATED BASALT CORE SAMPLES FROM DSDP LEG 34 [31].

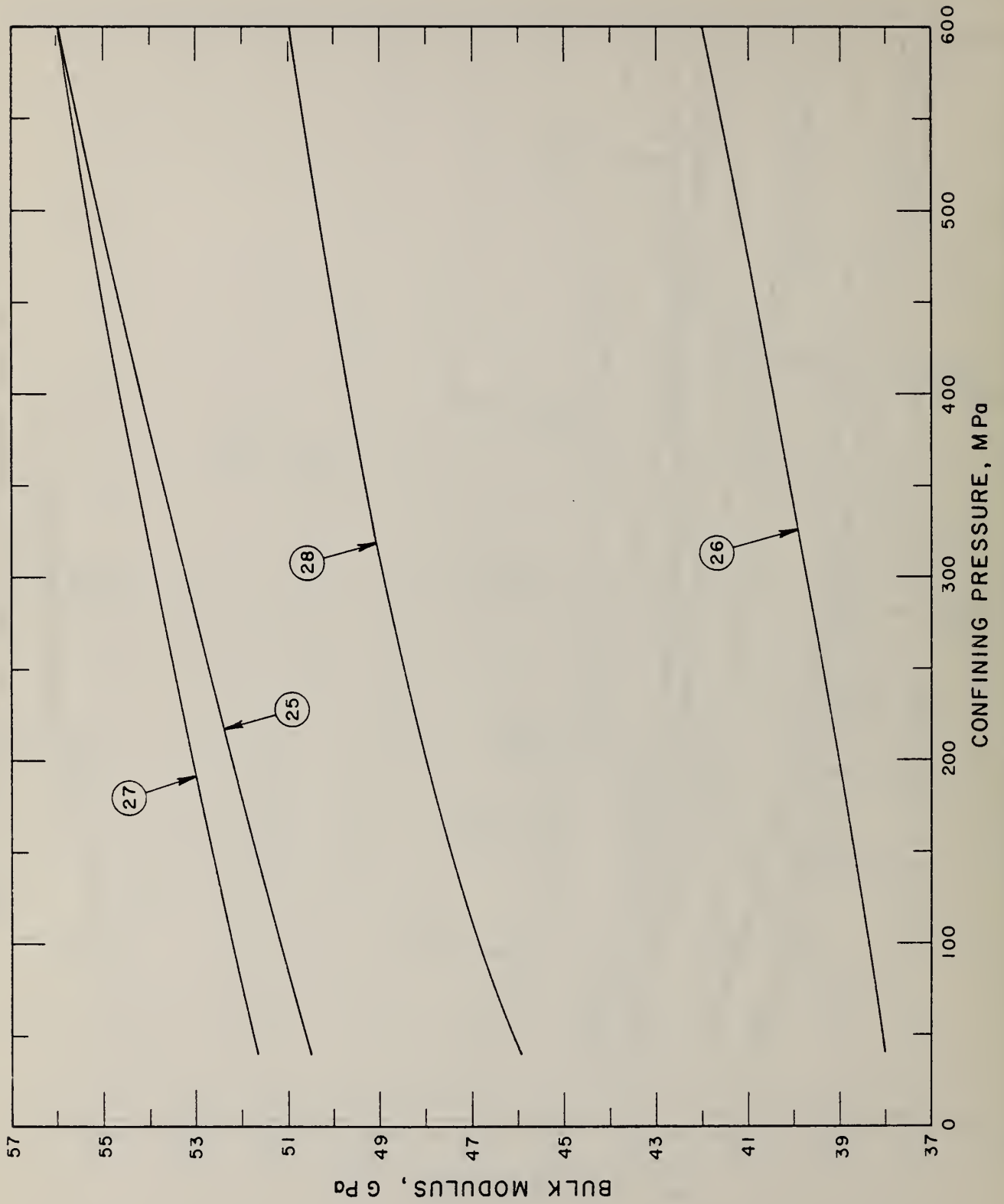


FIGURE 2.5. BULK MODULUS OF SATURATED BASALT CORE SAMPLES FROM DSIP LEG 35 [33].

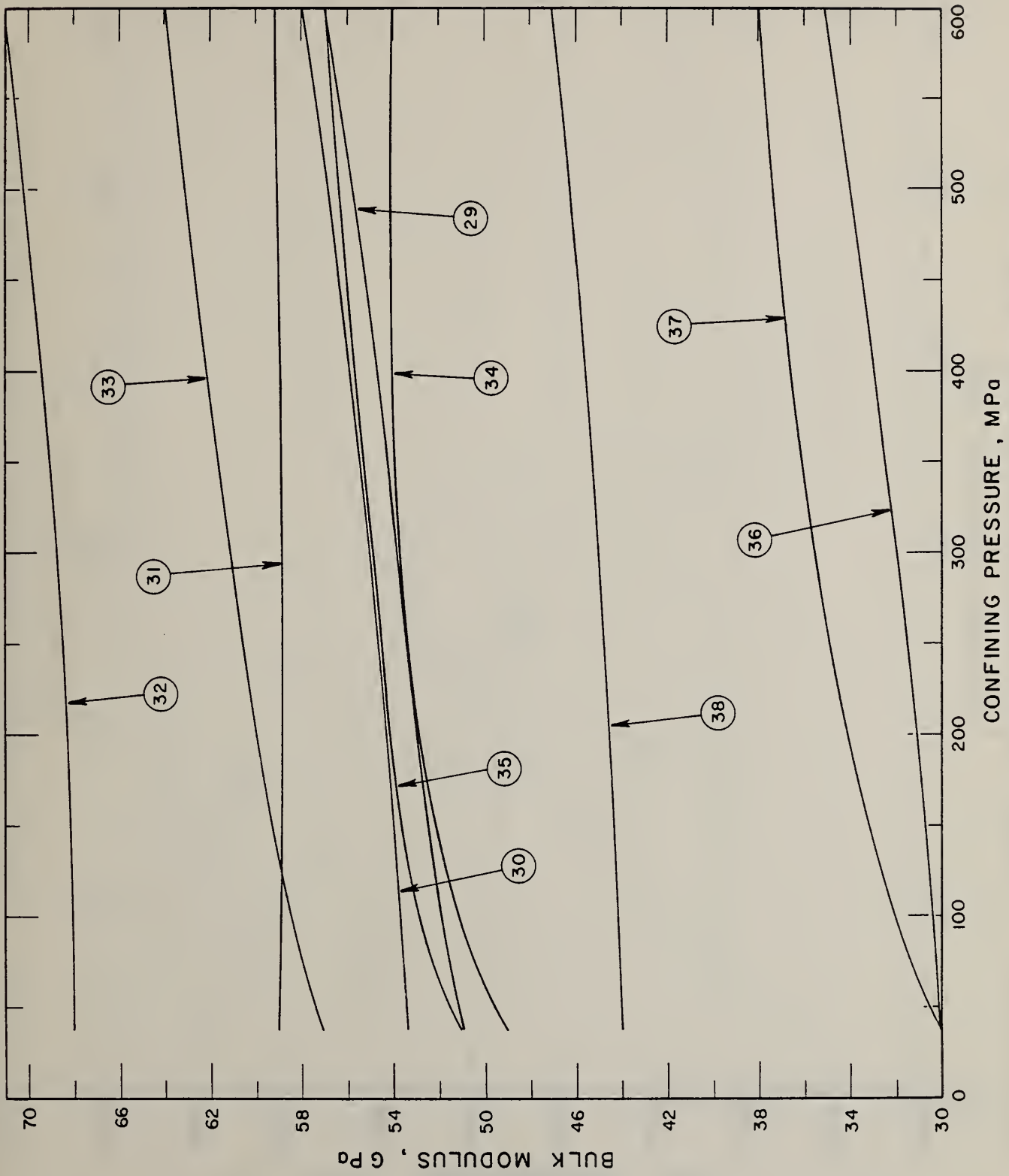


FIGURE 2.6. BULK MODULUS OF SATURATED BASALT CORE SAMPLES FROM DSDP LEG 39 [32].

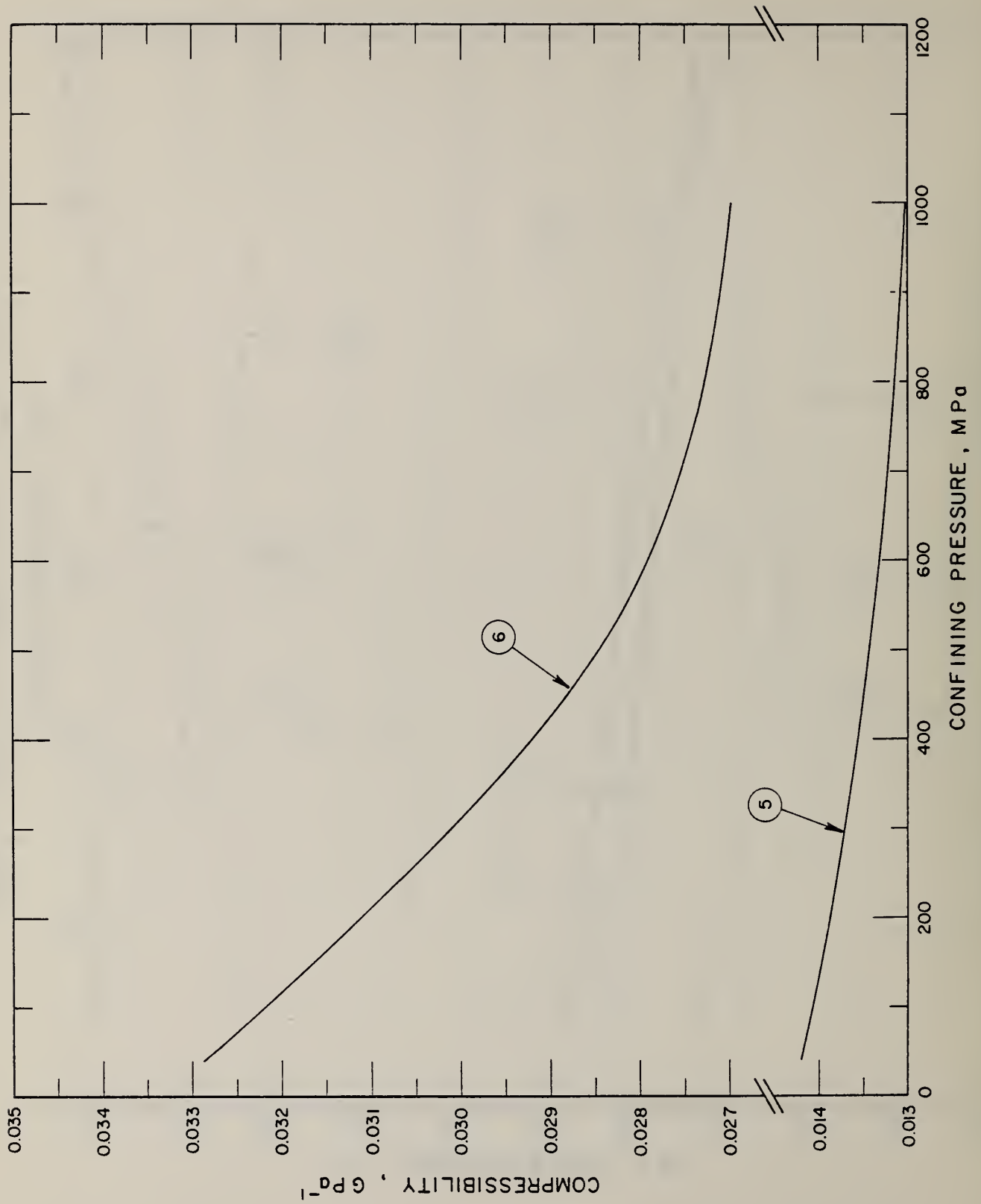


FIGURE 2.7. COMPRESSIBILITY OF SATURATED BASALT CORE SAMPLES FROM DSDP LEG 16 [29].

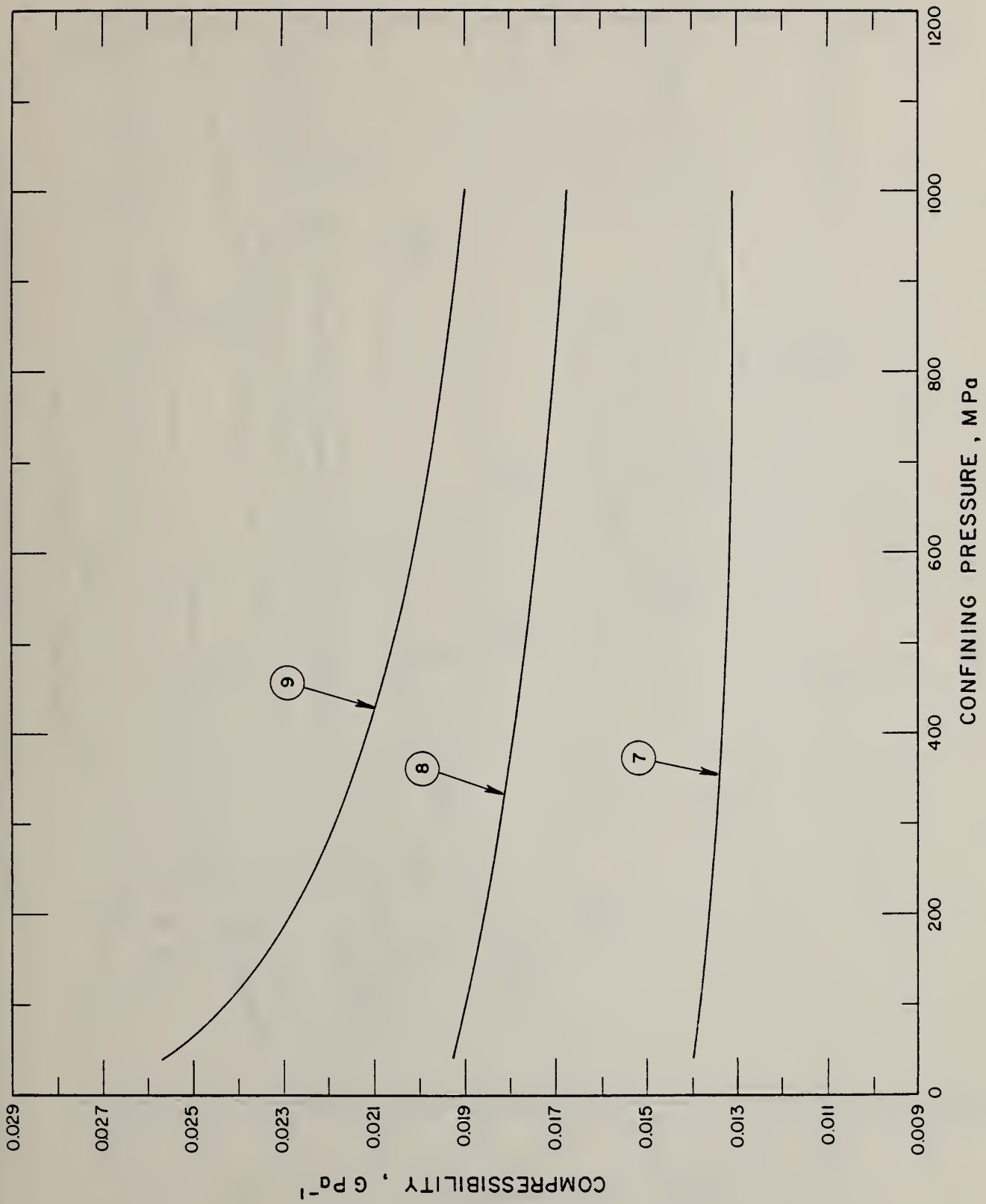


FIGURE 2.8. COMPRESSIBILITY OF SATURATED BASALT CORE SAMPLES FROM DSDP LEG 19 [30].

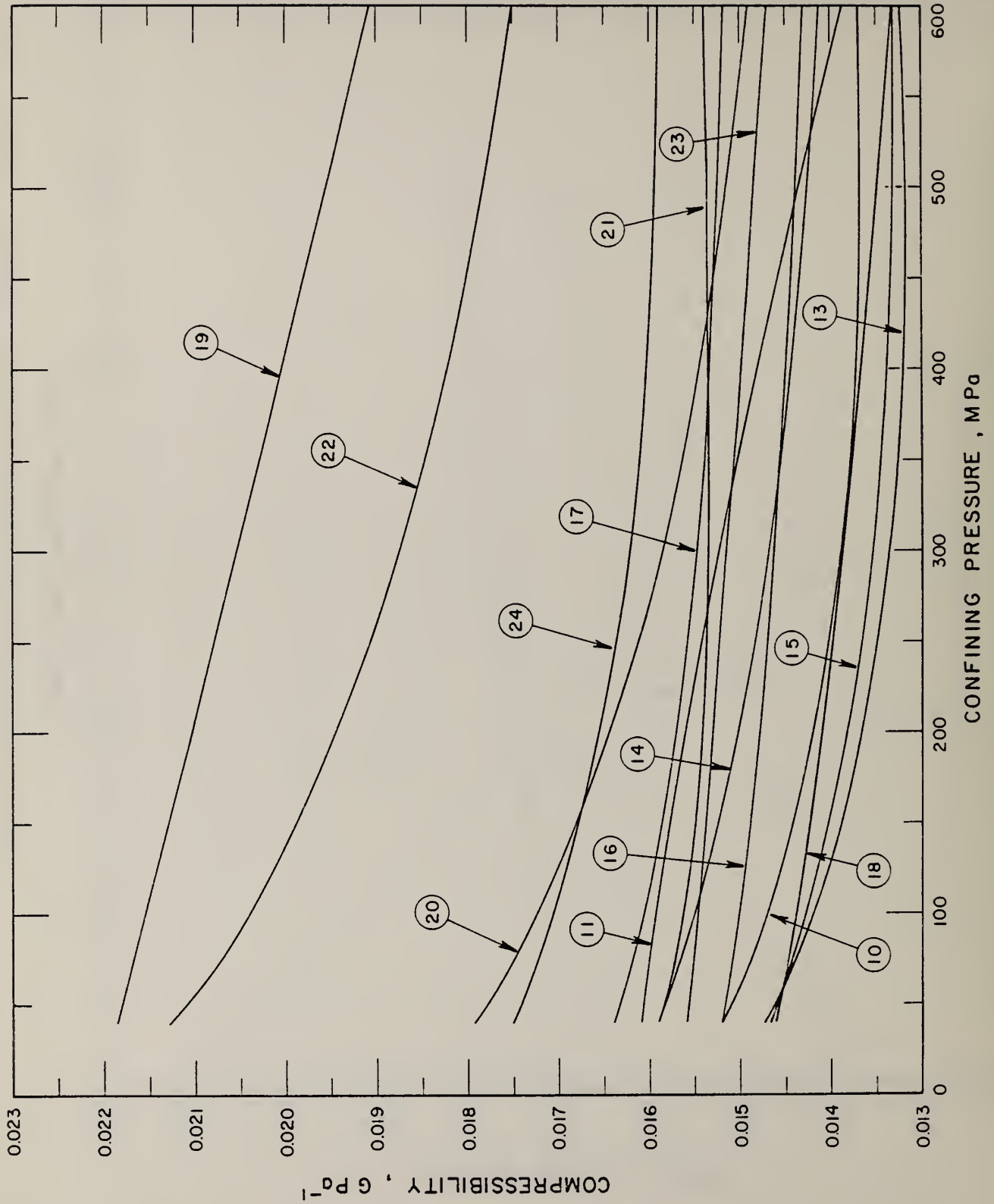


FIGURE 2.9. COMPRESSIBILITY OF SATURATED BASALT CORE SAMPLES FROM DSDP LEG 34 [31].

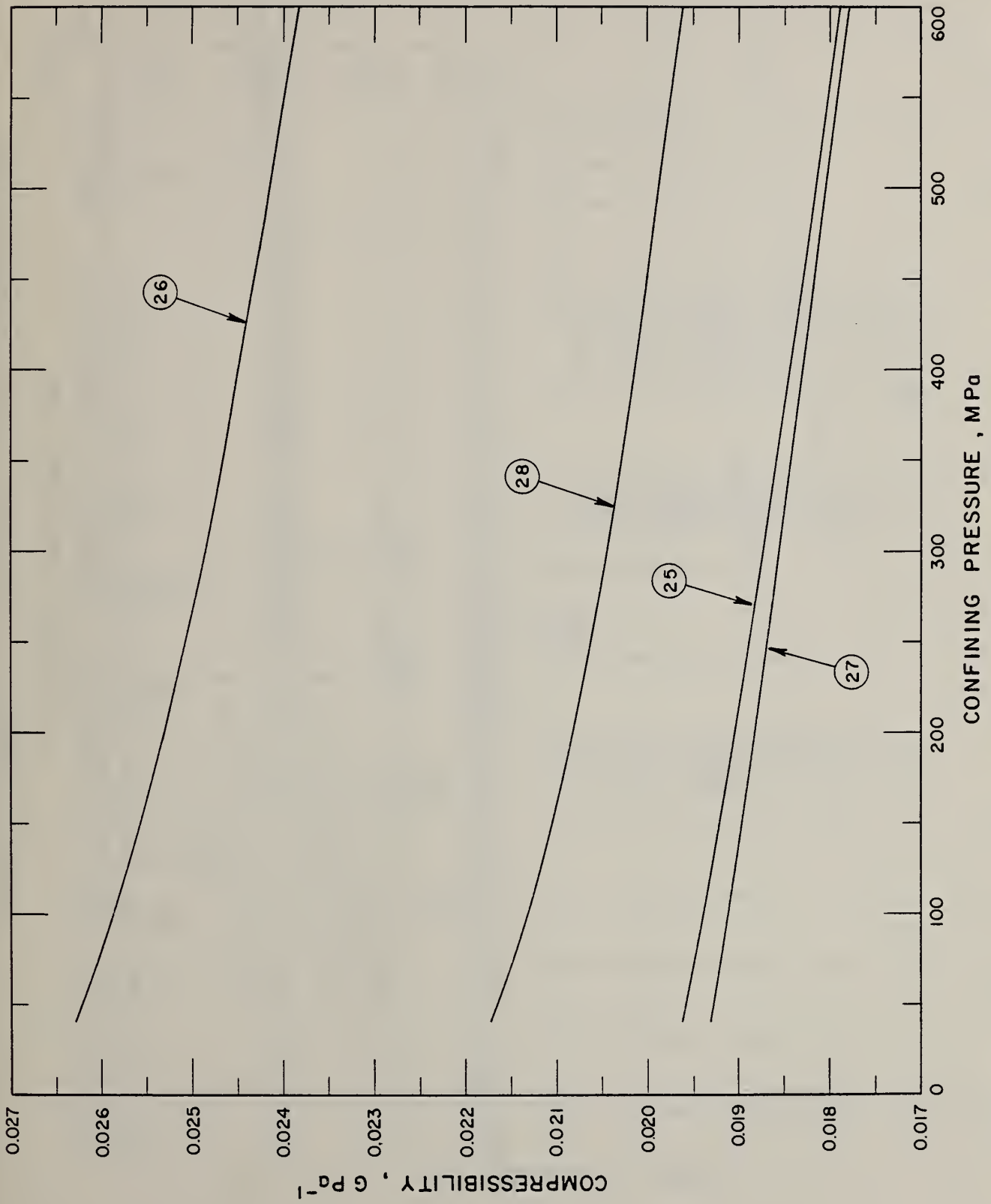


FIGURE 2.10. COMPRESSIBILITY OF SATURATED BASALT CORE SAMPLES FROM DSDP LEG 35 [33].

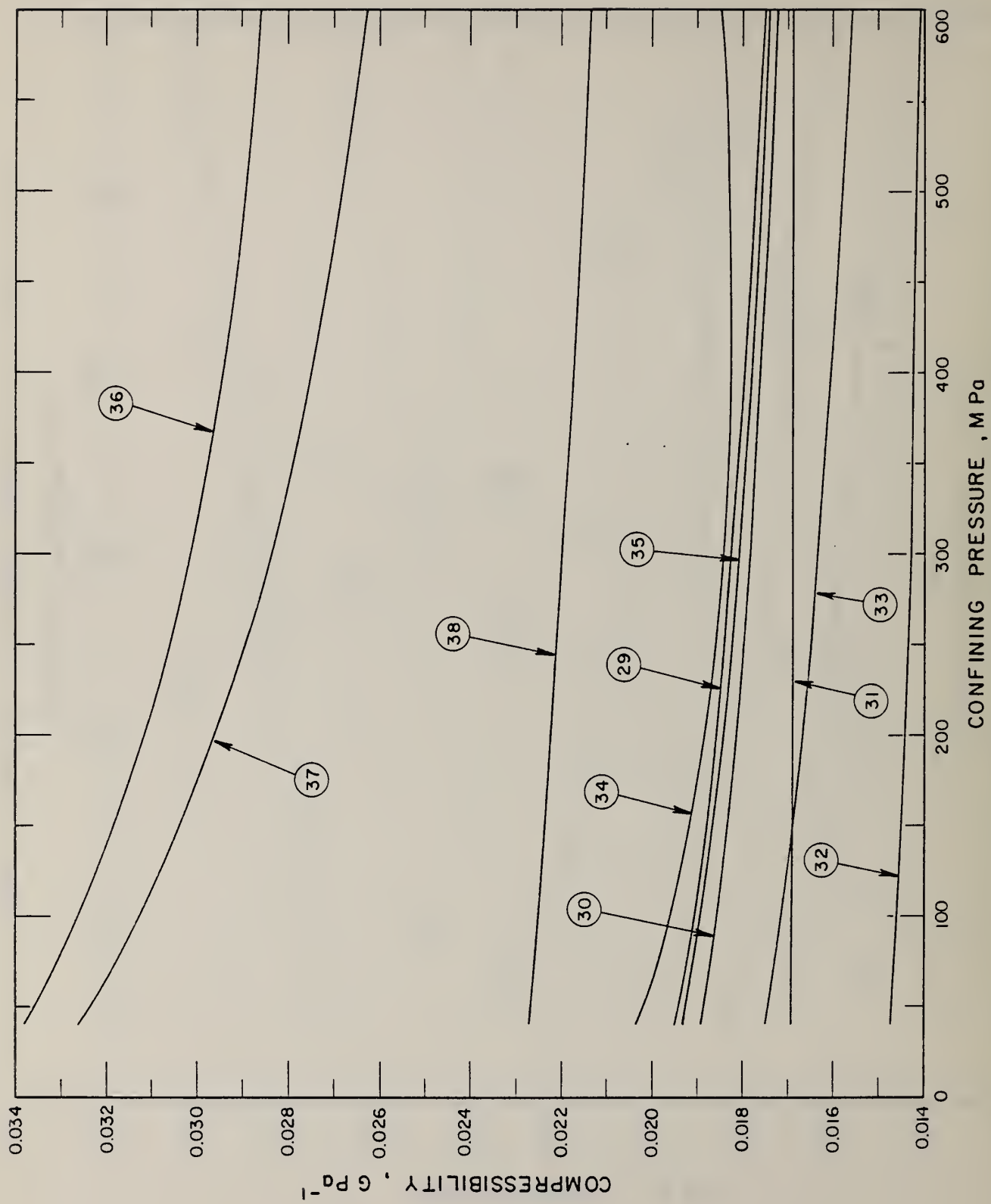


FIGURE 2.11. COMPRESSIBILITY OF SATURATED BASALT CORE SAMPLES FROM DSDP LEG 39 [32].

TABLE 2.2. ROOM-TEMPERATURE PRESSURE DEPENDENCE OF BULK MODULUS AND COMPRESSIBILITY OF BASALT

Data Set No.	Basalt Type & Location	Confining Pressure, P (MPa)	Bulk Modulus, K (GPa)	Compressibility, 1/K (GPa)	Remarks	Ref. No.
1	Basalt, Chaffee, CO	50	43.0	0.0232	Density 2.586 g cm ⁻³ .	34
		500	50.0	0.0200		
2	Basalt, Scotch Plains, NJ	200	42.0	0.0258	Enclosed; density 2.911 g cm ⁻³ .	35
		1000	59.0	0.0169		
3	Basalt	0.1	45.0	0.0222	Enclosed; density 2.901 g cm ⁻³ .	36
		50	67.0	0.0149		
		500	77.0	0.0130		
4	Basalt	0.1	62.0	0.0161	Altered, enclosed, diabasic; density 2.924 g cm ⁻³ .	37
		1000	77.0	0.0130		
5	Basalt, DSDP Leg 16; 155-11-1, 143-150 cm.	40	71.0	0.0141	Deep Sea Drilling Project (DSDP); plagioclase 45%, pyroxene 40%, olivine 4%, opaques and others 11%; values calculated from mean velocities and densities and are for water saturated specimens; density 2.448 g cm ⁻³ .	29
		100	71.0	0.0141		
		200	72.0	0.0139		
		600	75.0	0.0133		
6	Basalt, DSDP Leg 16; 163-29-4, 67-74 cm.	40	29.0	0.0345	Same as above except density 2.936 g cm ⁻³ .	29
		100	31.0	0.0322		
		200	32.0	0.0312		
		600	36.0	0.0278		
7	Basalt, DSDP Leg 19; 19-183-39-1, 148-150 cm.	40	72.0	0.0139	Deep Sea Drilling Project (DSDP); values are calculated from mean velocities and densities corrected for dimension changes and are for water saturated samples; density 2.840 g cm ⁻³ .	30
		100	73.0	0.0137		
		200	74.0	0.0135		
		600	76.0	0.0132		
8	Basalt, DSDP Leg 19; 19-191-16-1, 21-25 cm.	40	52.0	0.0192	Same as above except density 2.794 g cm ⁻³ .	30
		100	53.0	0.0187		
		200	54.0	0.0185		
		600	57.0	0.0175		
9	Basalt, DSDP Leg 19; 19-183-39-1, 148-150 cm.	40	39.0	0.0256	Same as above except density 2.840 g cm ⁻³ .	30
		100	41.0	0.0244		
		200	44.0	0.0227		
		600	50.0	0.0200		
10	Basalt, DSDP Leg 34; 319A-1-1, 32-35 cm.	40	66.0	0.0152	Deep Sea Drilling Project (DSDP); values calculated from densities and velocities are for water saturated samples; density 2.915 g cm ⁻³ .	31
		100	68.0	0.0147		
		200	70.0	0.0143		
		600	73.0	0.0137		
11	Basalt, DSDP Leg 34; 319A-2-3, 46-48 cm.	40	62.0	0.0161	Same as above except density 2.864 g cm ⁻³ .	31
		100	63.0	0.0159		
		200	64.0	0.0156		
		600	72.0	0.0139		
12	Basalt, DSDP Leg 34; 319A-3-2, 114-117 cm	40	66.0	0.0152	Same as above except density 2.923 g cm ⁻³ .	31
		100	68.0	0.0147		
		200	70.0	0.0143		
		600	75.0	0.0133		
13	Basalt, DSDP Leg 34; 319-A-3-4, 85-88 cm.	40	68.0	0.0147	Same as above except density 2.939 g cm ⁻³ .	31
		100	71.0	0.0141		
		200	73.0	0.0137		
		600	76.0	0.0132		
14	Basalt, DSDP Leg 34; 319A-4-1, 137-140 cm.	40	63.0	0.0159	Same as above except density 2.911 g cm ⁻³ .	31
		100	65.0	0.0154		
		200	66.0	0.0152		
		600	71.0	0.0141		
15	Basalt, DSDP Leg 34; 319A-5-1, 80-83 cm.	40	68.0	0.0147	Same as above except density 2.948 g cm ⁻³ .	31
		100	70.0	0.0143		
		200	72.0	0.0139		
		600	75.0	0.0133		

TABLE 2.2. ROOM-TEMPERATURE PRESSURE DEPENDENCE OF BULK MODULUS AND COMPRESSIBILITY OF BASALT (continued)

Data Set No.	Basalt Type & Location	Confining Pressure, P (MPa)	Bulk Modulus, K (GPa)	Compressibility, 1/K (GPa)	Remarks	Ref. No.
16	Basalt, DSDP Leg 34; 319A-6-1, 145-148 cm.	40	66.0	0.0152	Same as above except density 2.882 g cm ⁻³ .	31
		100	67.0	0.0149		
		200	67.0	0.0149		
		600	70.0	0.0143		
17	Basalt, DSDP Leg 34; 319A-7-1, 65-68 cm.	40	61.0	0.0164	Same as above except density 2.851 g cm ⁻³ .	31
		100	63.0	0.0159		
		200	64.0	0.0156		
		600	66.0	0.0152		
18	Basalt, DSDP Leg 34; 319-13-1, 52-55 cm.	40	69.0	0.0145	Same as above except density 2.920 g cm ⁻³ .	31
		100	69.0	0.0145		
		200	71.0	0.0141		
		600	75.0	0.0133		
19	Basalt, DSDP Leg 34; 320B-3-1, 64-67 cm.	40	46.0	0.0217	Same as above except density 2.725 g cm ⁻³ .	31
		100	46.0	0.0217		
		200	47.0	0.0213		
		600	53.0	0.0189		
20	Basalt, DSDP Leg 34; 320B-4-1, 144-147 cm.	40	56.0	0.0179	Same as above except density 2.837 g cm ⁻³ .	31
		100	58.0	0.0172		
		200	61.0	0.0164		
		600	67.0	0.0149		
21	Basalt, DSDP Leg 34; 320B-5,CC	40	63.0	0.0159	Same as above except density 2.832 g cm ⁻³ .	31
		100	64.0	0.0156		
		200	64.0	0.0156		
		600	65.0	0.0154		
22	Basalt, DSDP Leg 34; 321-13-14, 104-107 cm.	40	47.0	0.0213	Same as above except density 2.822 g cm ⁻³ .	31
		100	50.0	0.0200		
		200	51.0	0.196		
		600	57.0	0.175		
23	Basalt, DSDP Leg 34; 321-14-1, 76-79 cm.	40	64.0	0.0156	Same as above except density 2.900 g cm ⁻³ .	31
		100	64.0	0.0156		
		200	65.0	0.0154		
		600	68.0	0.0147		
24	Basalt, DSDP Leg 34; 321-14-4, 51-54 cm.	40	57.0	0.0175	Same as above except density 2.915 g cm ⁻³ .	31
		100	59.0	0.0169		
		200	60.0	0.0167		
		600	63.0	0.0159		
25	Basalt, DSDP Leg 35; 322-12-1, Piece 7.	40	51.0	0.0196	Deep Sea Drilling Project (DSDP); contains plagioclase microphenocrystals in fine grained variolitic ground mass; values calculated from measured densities and velocities and are for water saturated sample; density 2.730 g cm ⁻³ .	33
		100	51.0	0.0196		
		200	52.0	0.0192		
		600	56.0	0.0179		
26	Basalt, DSDP Leg 35; 322-13-2, 56-62 cm.	40	38.0	0.0263	Same as above except density 2.553 g cm ⁻³ .	33
		100	39.0	0.0256		
		200	39.0	0.0256		
		600	42.0	0.0238		
27	Basalt, DSDP Leg 35; 323-18-6, 110-120 cm.	40	52.0	0.0192	Same as above except density 2.727 g cm ⁻³ .	33
		100	52.0	0.0192		
		200	53.0	0.0189		
		600	56.0	0.0178		
28	Basalt, DSDP Leg 35; 323-20,CC, 104-114 cm.	40	46.0	0.0217	Same as above except density 2.723 g cm ⁻³ .	33
		100	47.0	0.0213		
		200	48.0	0.0208		
		600	51.0	0.0196		

TABLE 2.2. ROOM-TEMPERATURE PRESSURE DEPENDENCE OF BULK MODULUS AND COMPRESSIBILITY OF BASALT (continued)

Data Set No.	Basalt Type & Location	Confining Pressure, P (MPa)	Bulk Modulus, K (GPa)	Compressibility, 1/K (GPa)	Remarks	Ref. No.
29	Basalt, DSDP Leg 39; 354-19-3, 131-134 cm.	40	51.0	0.0196	Deep Sea Drilling Project (DSDP); values calculated from velocities and densities corrected for dimension changes and are water saturated samples; density 2.733 g cm ⁻³ .	32
		100	52.0	0.0192		
		200	53.0	0.0189		
		600	57.0	0.0175		
30	Basalt, DSDP Leg 39; 354-19-5, 93-96 cm.	40	53.0	0.0189	Same as above except density 2.753 g cm ⁻³ .	32
		100	54.0	0.0185		
		200	55.0	0.0182		
		600	58.0	0.0172		
31	Basalt, DSDP Leg 39; 355-21-1, 147-150 cm.	40	59.0	0.0169	Same as above except density 2.808 g cm ⁻³ .	32
		100	59.0	0.0169		
		200	59.0	0.0169		
		600	59.0	0.0169		
32	Basalt, DSDP Leg 39; 355-22-1, 57-60 cm.	40	68.0	0.0147	Same as above except density 2.884 g cm ⁻³ .	32
		100	68.0	0.0147		
		200	68.0	0.0147		
		600	71.0	0.0141		
33	Basalt, DSDP Leg 39; 355-22-2, 44-47 cm.	40	57.0	0.0175	Same as above except density 2.838 g cm ⁻³ .	32
		100	59.0	0.0169		
		200	60.0	0.0167		
		600	64.0	0.0156		
34	Basalt, DSDP Leg 39; 355-22-4, 69-72 cm.	40	49.0	0.0204	Same as above except density 2.757 g cm ⁻³ .	32
		100	51.0	0.0196		
		200	53.0	0.0189		
		600	54.0	0.0185		
35	Basalt, DSDP Leg 39; 355-22-5, 119-122 cm.	40	51.0	0.0196	Same as above except density 2.798 g cm ⁻³ .	32
		100	53.0	0.0189		
		200	54.0	0.0185		
		600	57.0	0.0175		
36	Basalt, DSDP Leg 39; 359-4-2, 80-83 cm.	40	30.0	0.0333	Same as above except density 2.258 g cm ⁻³ .	32
		100	30.0	0.0333		
		200	32.0	0.0312		
		600	35.0	0.0286		
37	Basalt, DSDP Leg 39; 359-4-3, 143-146 cm.	40	30.0	0.0333	Same as above except density 2.308 g cm ⁻³ .	32
		100	32.0	0.0312		
		200	34.0	0.0294		
		600	38.0	0.0263		
38	Basalt, DSDP Leg 39; 359-5-1, 26-29 cm.	40	44.0	0.0227	Same as above except density 2.449 g cm ⁻³ .	32
		100	44.4	0.0227		
		200	45.0	0.0222		
		600	47.0	0.0213		

the discussion applicable to each Leg in the preceding section can be taken as applicable in general to the same Legs in this section. No further discussion is, therefore, considered.

2.3.6. Wave Velocities (Compression and Shear Velocities)

Compression wave velocities versus confining pressure obtained from saturated basalt core samples from Deep Sea Drilling Project Legs 16, 19, 26, 34, 35, and 39 are given in Figures 2.12, 2.14, 2.16, 2.17, 2.19, and 2.21. The corresponding shear wave velocities appear in Figures 2.13, 2.15, 2.17, 2.20, and 2.22. The data for these curves can be found in Table 2.3. Curves have been smoothed in most cases.

Velocity measurements were made on saturated basalt core specimens using the pulse transmission method. Bulk densities were obtained from the weight and measurement of the dimensions of the samples. At low confining pressures the rate of increase of velocity is high due to closure of grain boundary cracks. This rate usually decreases around 200 MPa. Saturation tends to affect compression wave velocities (any values are about 10% lower than saturated values), but seems to change shear wave velocities very little. High amounts of filling material like calcite on occasion gave somewhat higher velocities than might be anticipated for basalts of a given density.

Leg 16 (Figs. 2.12 and 2.13) values were obtained on a fresh massive basalt (163-29-4) and an altered vesicular basalt (155-1-1). Velocity measurements were made parallel and perpendicular to core axes. Velocity increased with confining pressure as anticipated. Lower density basalts gave lower velocities, also as expected.

Values obtained from Leg 19 (Figs. 2.14 and 2.15) show a systematic trend with the lower density basalts giving lower velocities. The rapid increase in velocity up to 200-300 MPa due to crack closure can be easily seen.

Leg 26 (Fig. 2.16) determinations are somewhat different from the other legs given in that the maximum confining pressure is only 200 MPa. The effect of grain boundary crack closure and the closure of other possible small cracks is well depicted. It should be noted that samples showing very large rates of increase, for example 251A-31-4 (48 cm) and 254-31-1 (111 cm), are probably extensively fractured.

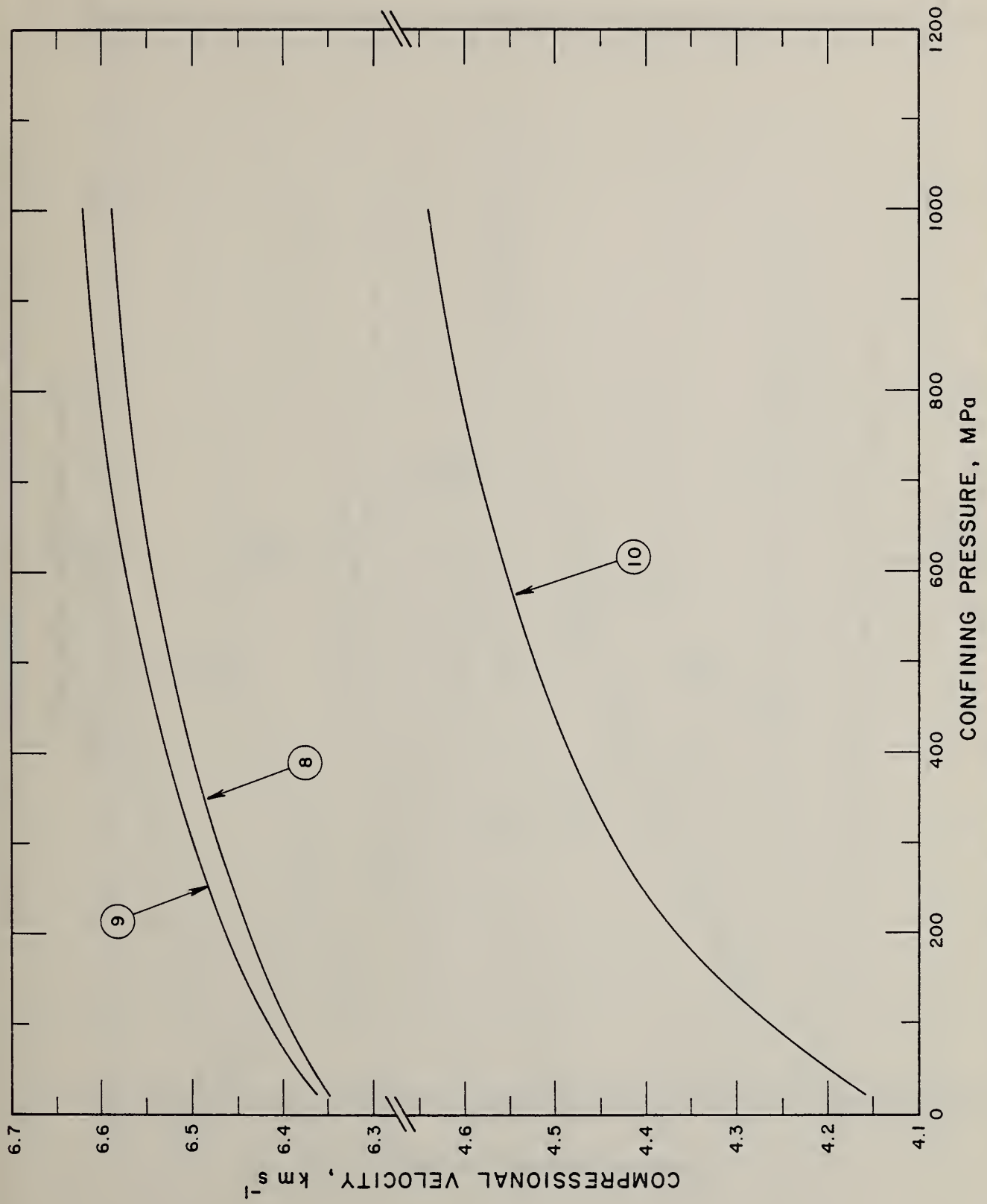


FIGURE 2.12. COMPRESSIONAL WAVE VELOCITY FOR SATURATED BASALT CORE SAMPLES FROM DSDP LEG 16 [29].

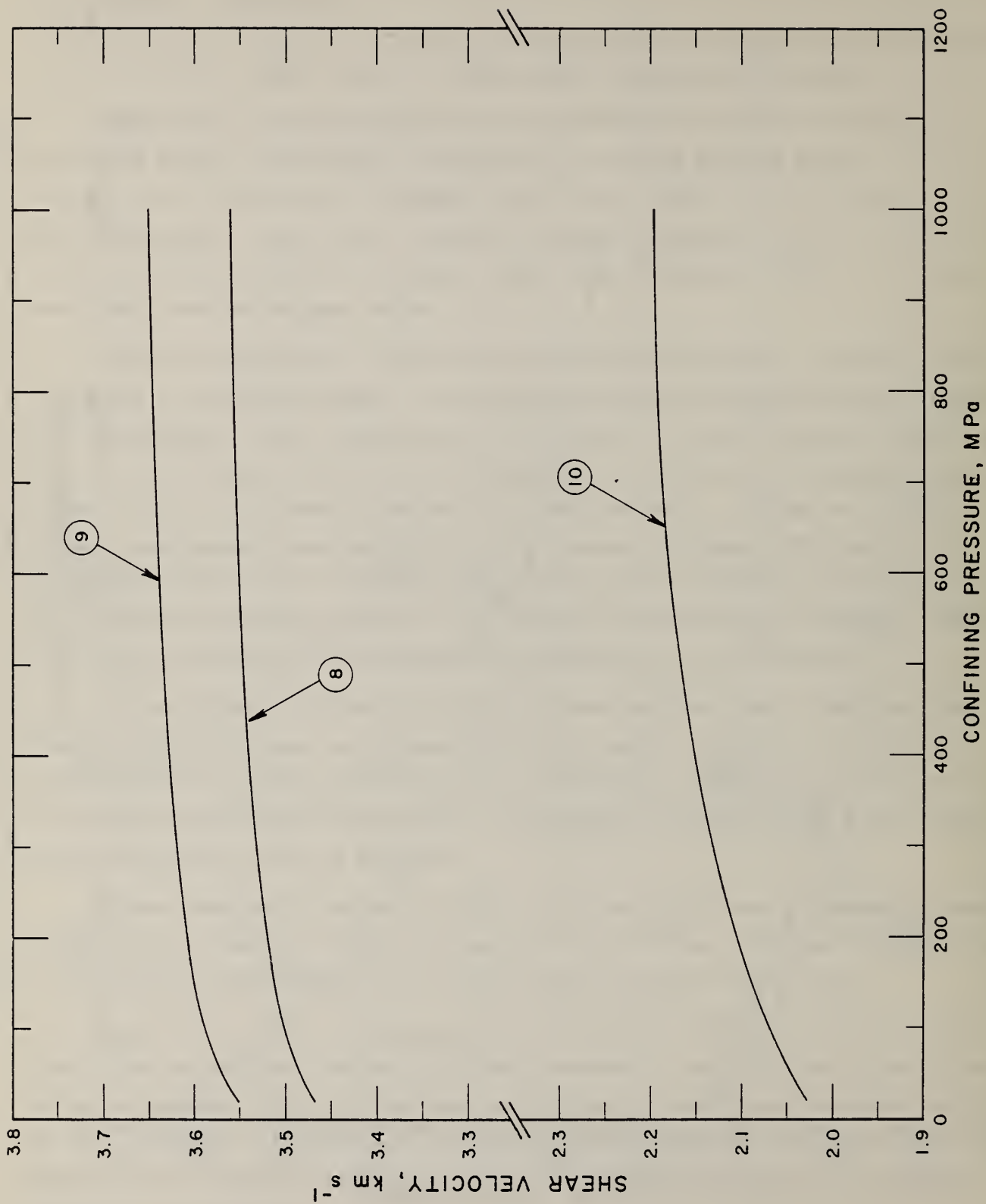


FIGURE 2.13. SHEAR WAVE VELOCITY FOR SATURATED BASALT CORE SAMPLES FROM DSDP LEG 16 [29].

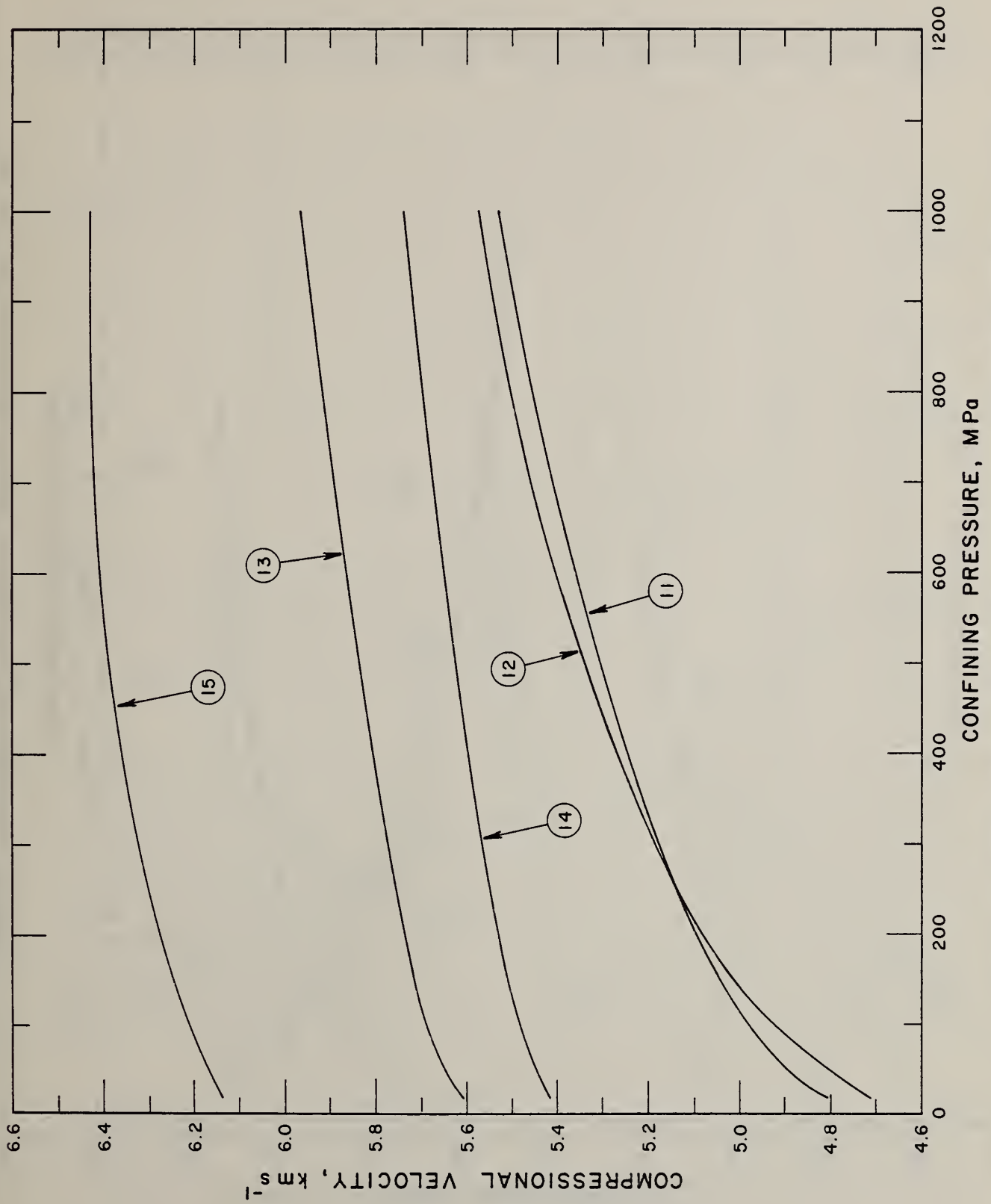


FIGURE 2.14. COMPRESSIONAL WAVE VELOCITY FOR SATURATED BASALT CORE SAMPLES FROM DSDP LEG 19 [30].

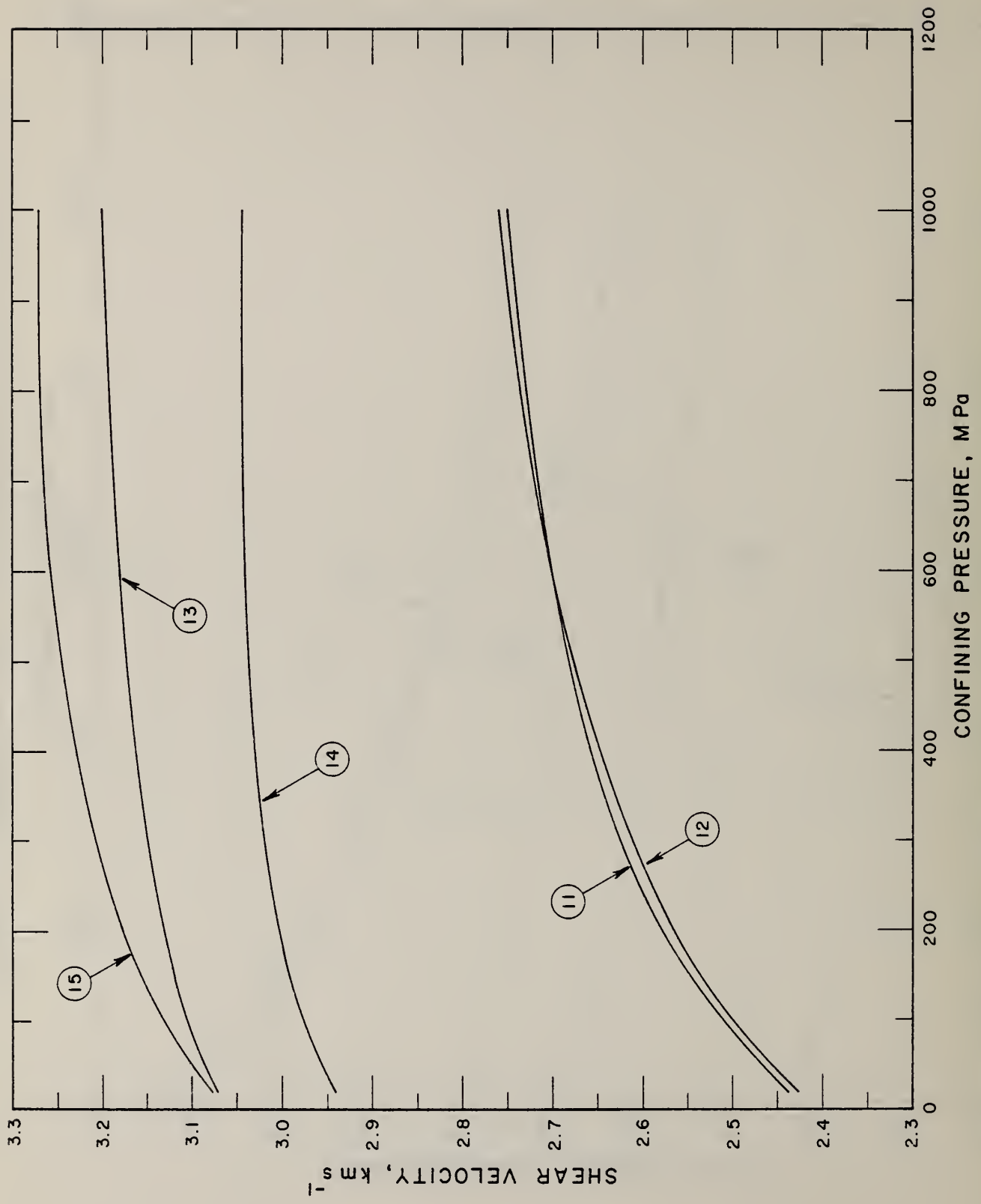


FIGURE 2.15. SHEAR WAVE VELOCITY FOR SATURATED BASALT CORE SAMPLES FROM DSDP LEG 19 [30].

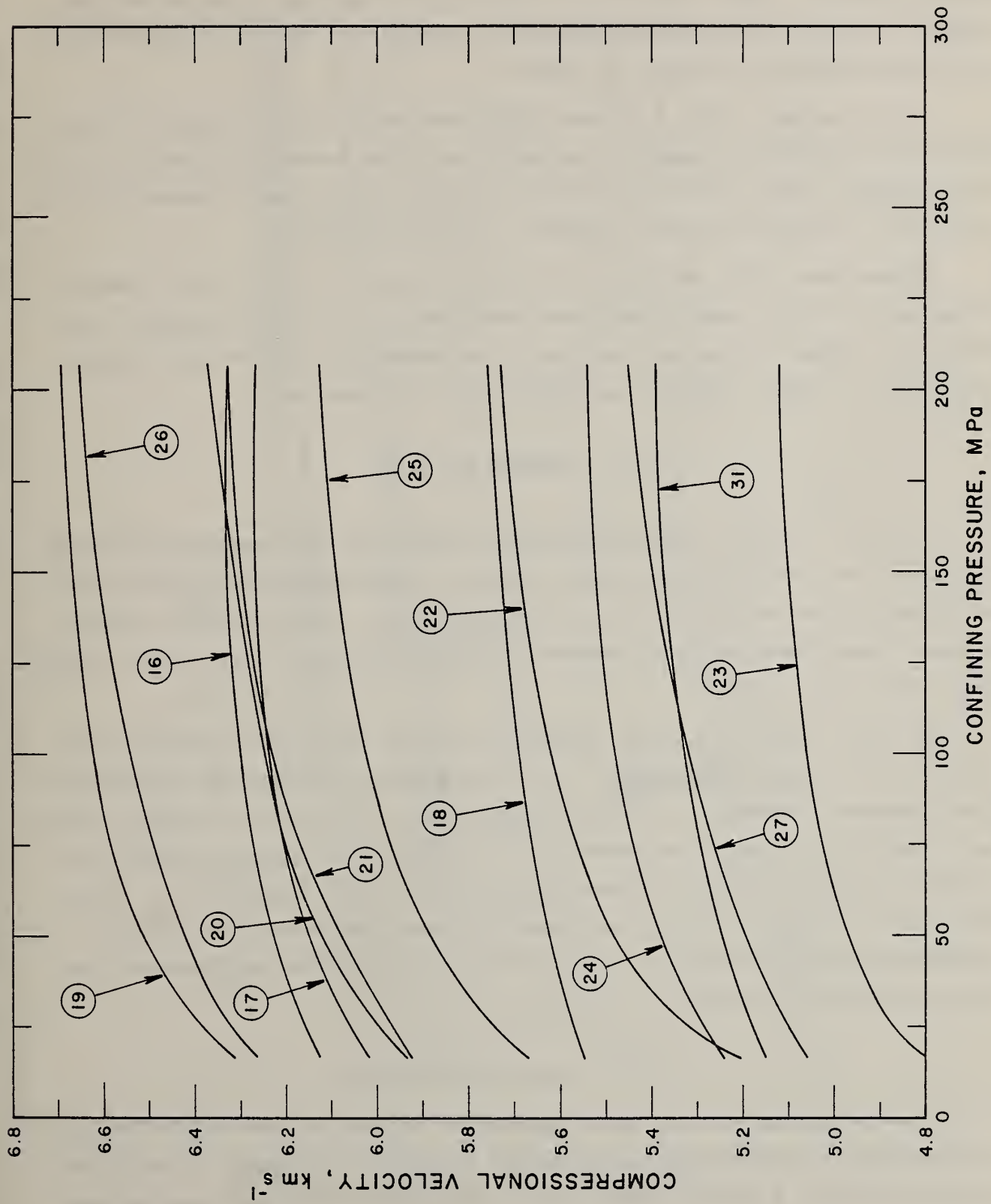


FIGURE 2.16. COMPRESSIONAL WAVE VELOCITY FOR SATURATED BASALT CORE SAMPLES FROM DSDP LEG 26 [42].

Basalt samples for Leg 34 (Figs. 2.17 and 2.18) were obtained from roughly two groups of basalts: one fine-grained, the other medium- to coarse-grained. These basalts are relatively young (less than 40 million years) and show only minor alteration. Behavior of the velocities with increasing confining pressure is normal.

Leg 35 values (Figs. 2.19 and 2.20) were obtained on slightly altered, relatively low-density samples. In addition to the decrease in density caused by alteration, open vesicles were also present in the case of sample 322-13-2 (56-62 cm). Behavior of these samples is once more normal.

Higher than usual velocities for Leg 39 (Figs. 2.21 and 2.22) samples, compared to values usually obtained from basalts of similar density, are reported. These values are ascribed to an unusually high calcite content (10-20%). In other contexts their behavior is as expected.

2.4. STRENGTH AND CREEP

The true relation between stress and strain for rock undergoing loading can often only be described using a curve. Many factors can affect this relationship and so there is no one unique curve. Some of these factors include temperature, moisture content, confining pressure, stress path loading rate, and strain rate.

In this section the term 'strength' has the conventional implication; that is, it is time independent, i.e., time-dependent effects are disregarded. Time-dependent 'strength' is treated in the section dealing with creep. There are three basic strength parameters to be considered: namely, compressive strength ($\sigma_1 - \sigma_3$), tensile strength ($\sigma_1 - \sigma_3$), and shear strength (τ). These terms are generally defined for tests of short duration where neither temperatures nor pressures are so extreme as to make the rock behave other than in a brittle fashion.

2.4.1. Compressive Strength

This is defined as the force applied at failure divided by the initial cross-sectional area perpendicular to the direction of loading. Usually this is obtained from a uniaxial test, but it can also be obtained from triaxial

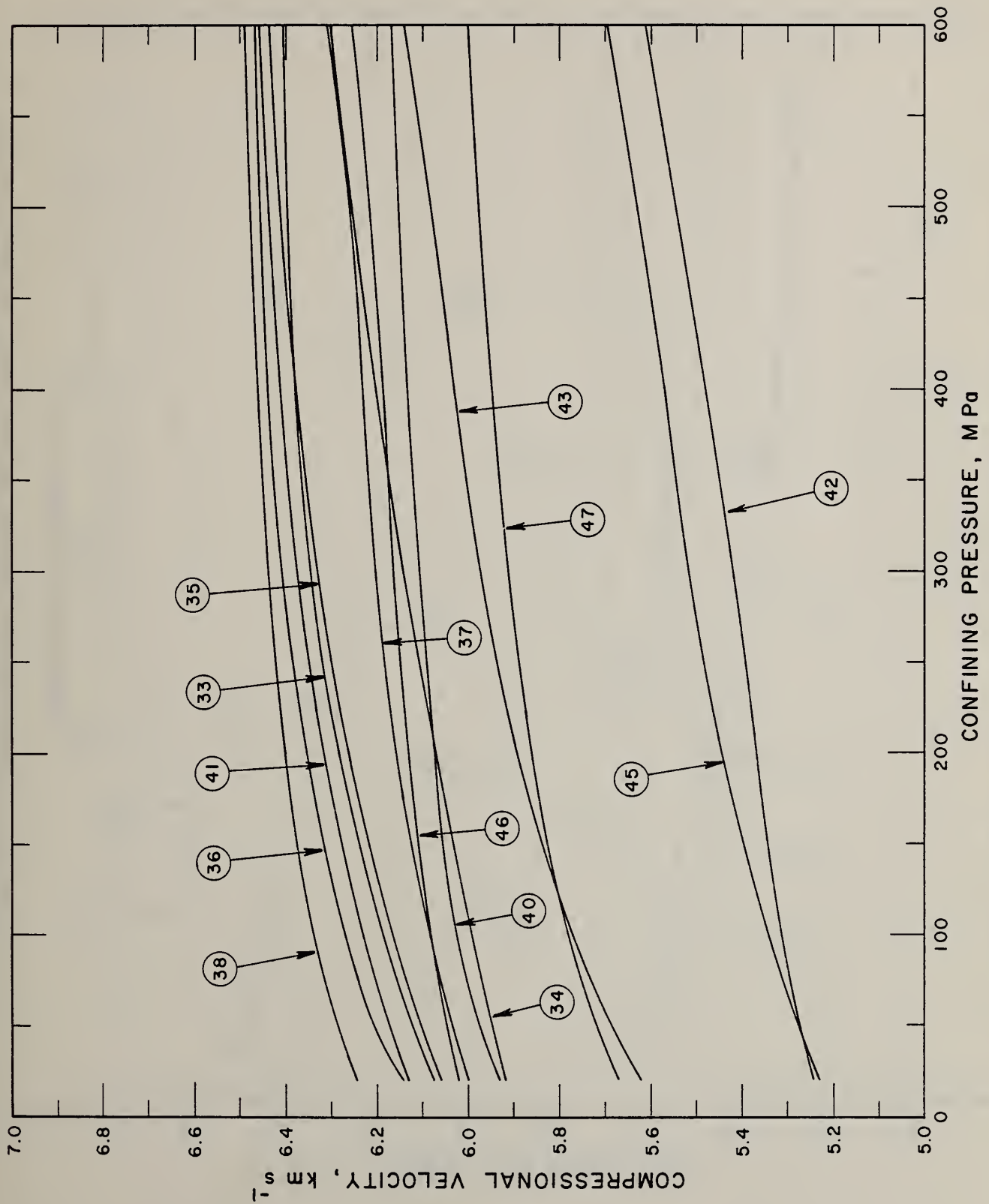


FIGURE 2.17. COMPRESSIONAL WAVE VELOCITY FOR SATURATED BASALT CORE SAMPLES FROM DSDP LEG 34 [31].

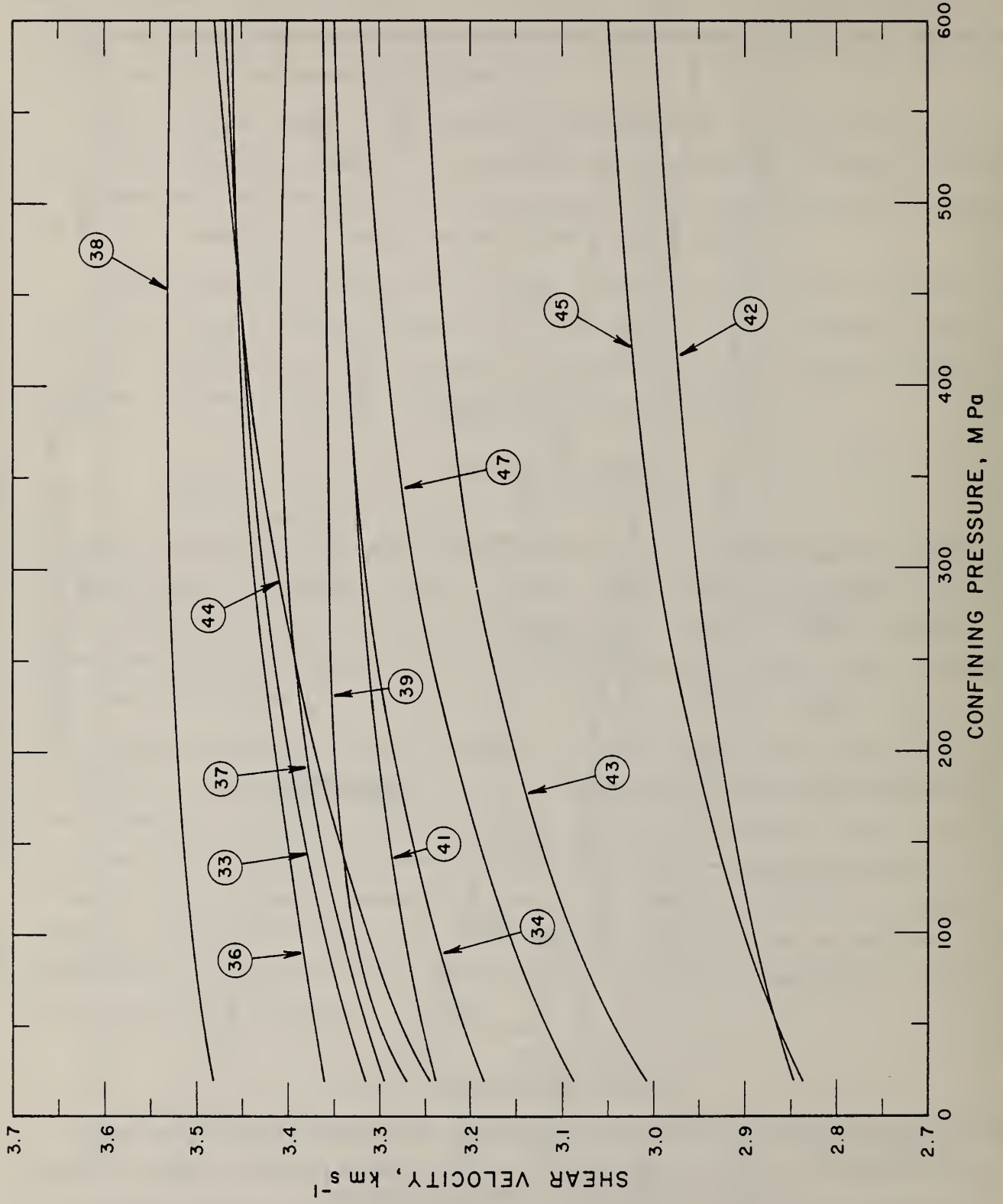


FIGURE 2.18. SHEAR WAVE VELOCITY FOR SATURATED BASALT CORE SAMPLES FROM DSDP LEG 34 [31].

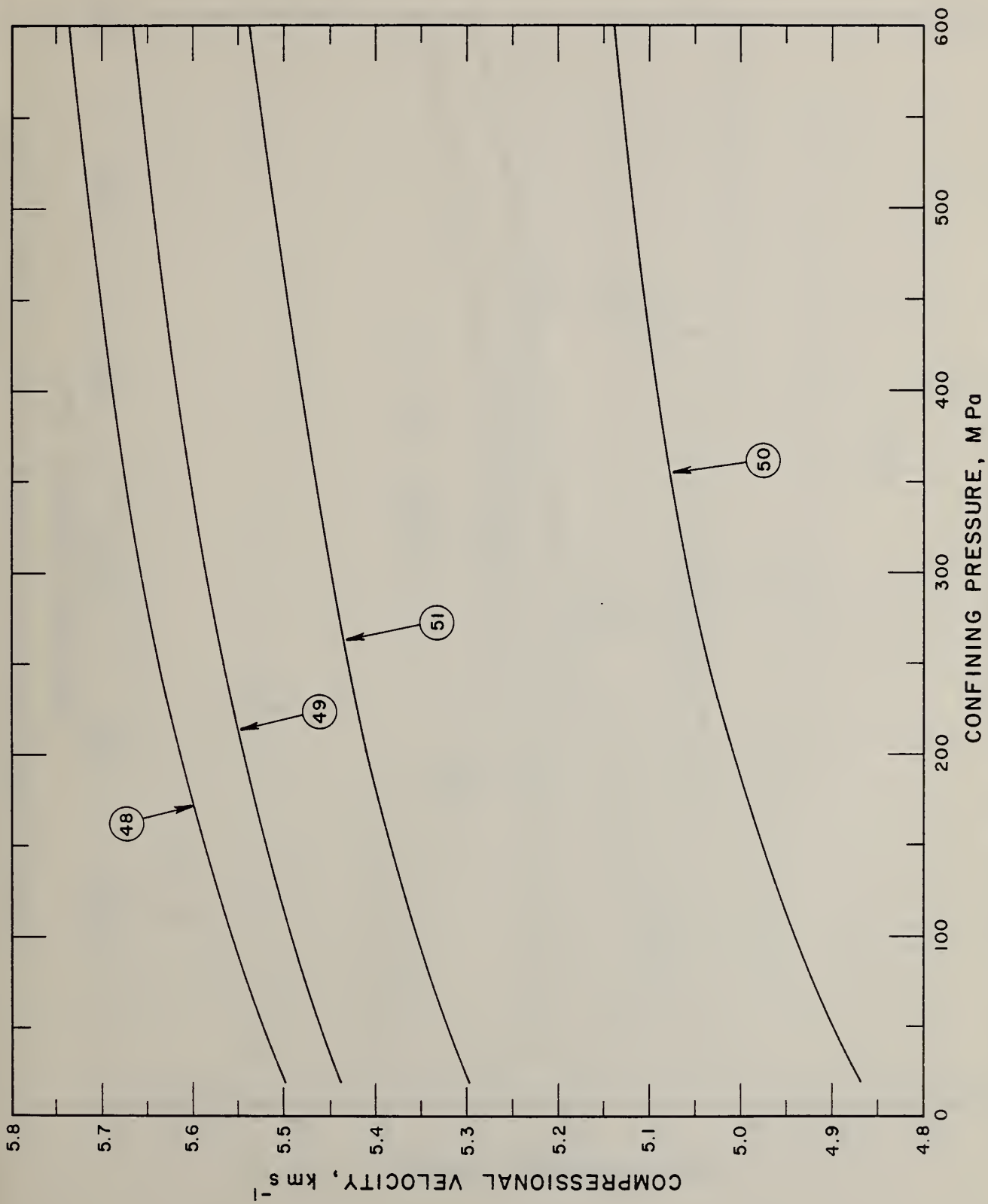


FIGURE 2.19. COMPRESSONAL WAVE VELOCITY FOR SATURATED BASALT CORE SAMPLES FROM DSDP LEG 35 [33].

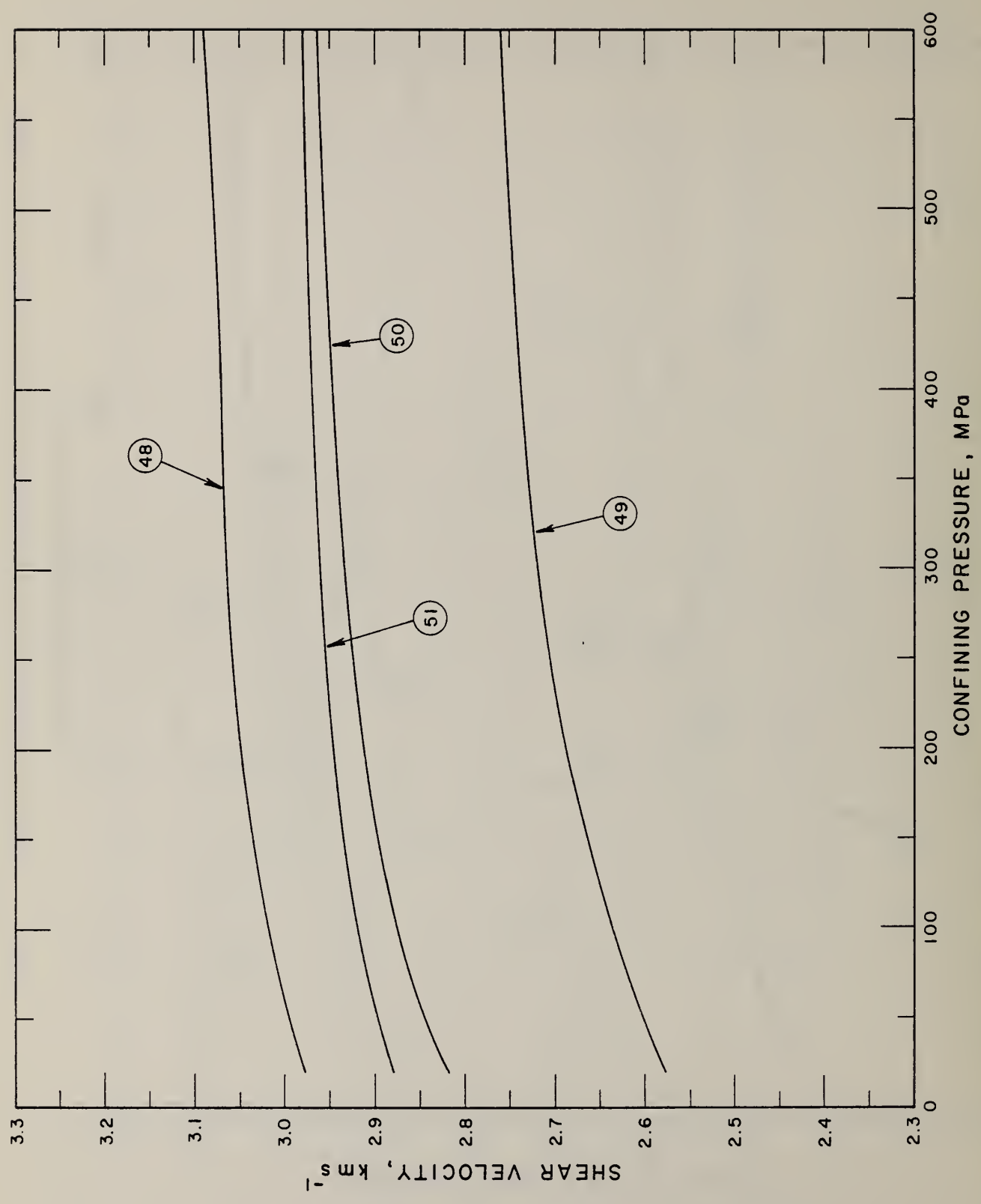


FIGURE 2.20. SHEAR WAVE VELOCITY FOR SATURATED BASALT CORE SAMPLES FROM DSDP LEG 35 [33].

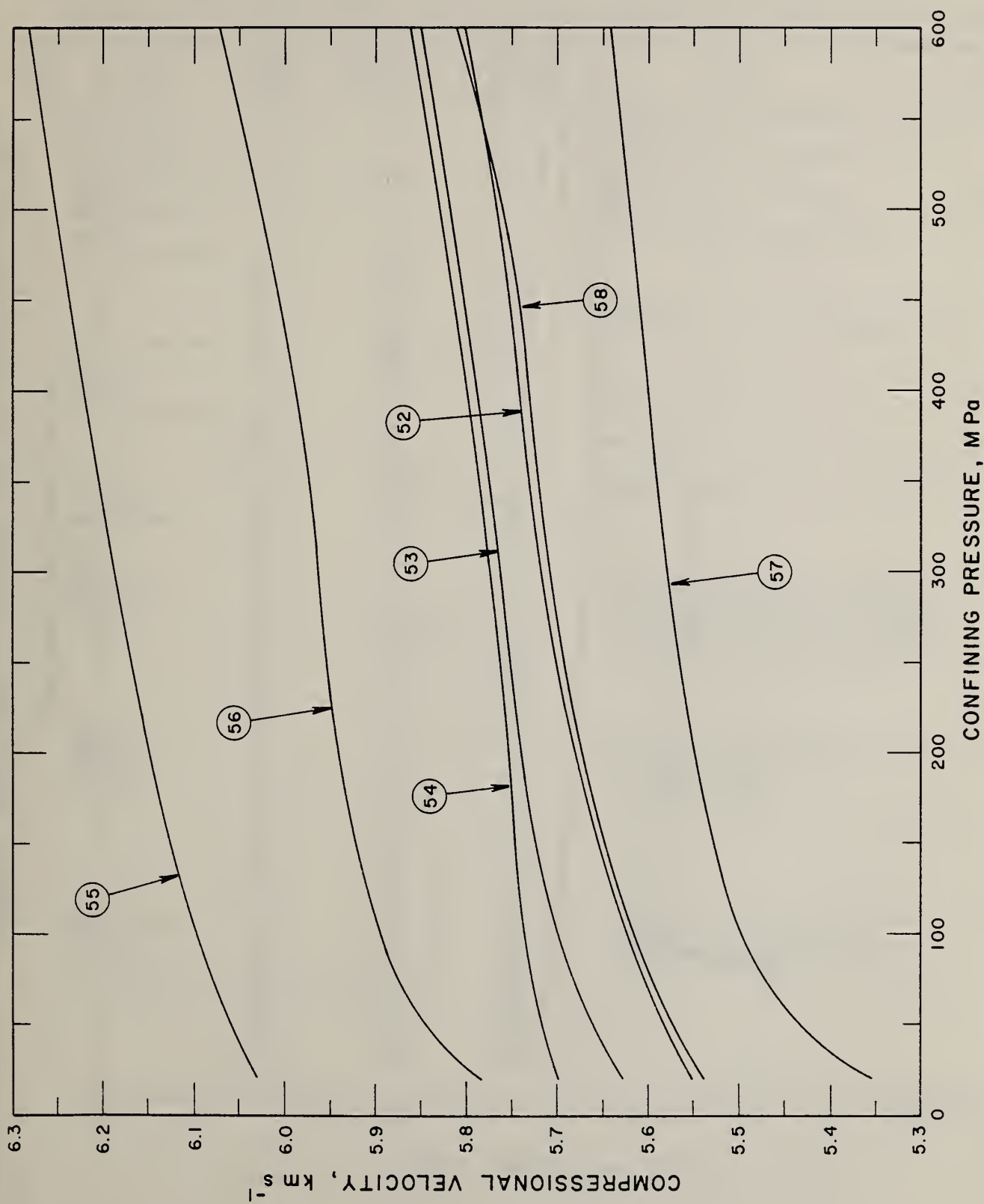


FIGURE 2.21. COMPRESSONAL WAVE VELOCITY FOR SATURATED BASALT CORE SAMPLES FROM DSDP LEG 39 [32].

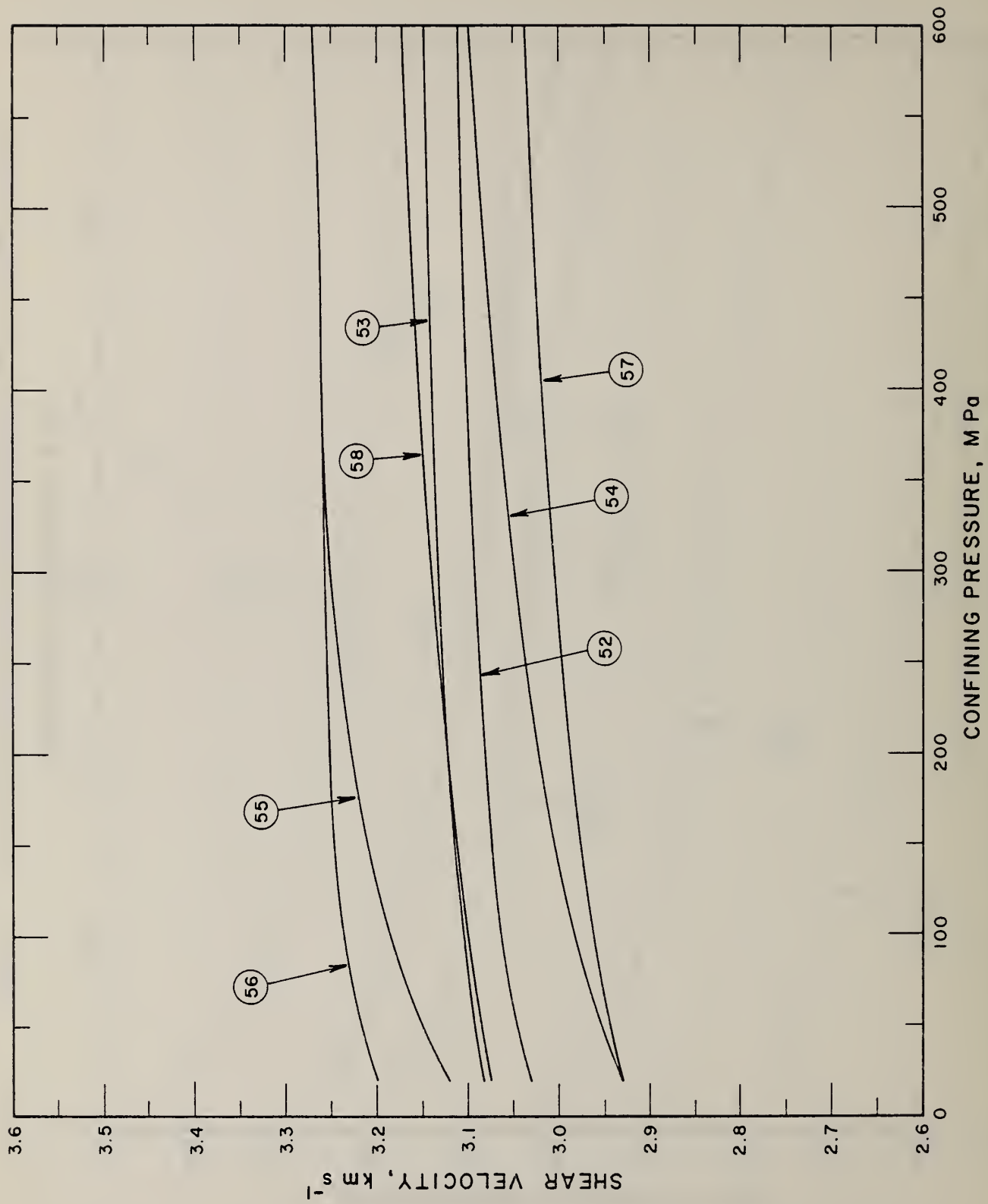


FIGURE 2.22. SHEAR WAVE VELOCITY FOR SATURATED BASALT CORE SAMPLES FROM DSDP LEG 39 [32].

TABLE 2.3. ROOM-TEMPERATURE PRESSURE DEPENDENCE OF COMPRESSIONAL AND SHEAR WAVE VELOCITIES OF BASALT

Data Set No.	Basalt Type & Location	Confining Pressure, P (MPa)	Compressional Wave Velocity, V_p (km s ⁻¹)	Shear Wave Velocity, V_s (km s ⁻¹)	Remarks	Ref. No.
1	Basalt, Armenia, USSR	0.1	5.15	2.92	Density 2.65 g cm ⁻³ ; porosity 5%; dry specimen.	38
2	Basalt, Armenia, USSR	0.1	4.64	2.78	Density 2.66 g cm ⁻³ ; porosity 4%; dry specimen.	38
3	Basalt, Armenia, USSR	0.1	3.94	-	Density 2.46 g cm ⁻³ ; porosity 6%; dry specimen.	38
4	Basalt, Pacific Ocean Floor	20 60 200 600	3.75 3.80 3.89 4.13	1.83 1.89 2.05 2.27	Density 2.15 g cm ⁻³ ; water saturated.	39
5	Basalt, Pacific Ocean Floor	20 60 200 600	6.03 6.09 6.19 6.31	3.28 3.30 3.32 3.35	Density 2.87 g cm ⁻³ ; water saturated.	39
6	Basalt, Atlantic Ocean Floor	20 60 100 400 1000	5.80 5.87 5.90 6.04 6.15	3.11 3.14 3.15 3.21 3.29	Density 2.82 g cm ⁻³ .	40
7	Basalt, Monolith, Voronezh, USSR	0.1 100 200 600 1000	5.53 6.04 6.20 6.42 6.57	- 3.62 3.66 3.70 3.72	Density 2.87 g cm ⁻³ .	41
8	Basalt, DSDP Leg 16; 163-29-4, 67-74 cm.	20 40 60 80 100 200 400 600 800 1000	6.35 6.36 6.37 6.39 6.40 6.44 6.50 6.52 6.57 6.59	3.47 3.48 3.49 3.50 3.50 3.52 3.54 3.55 3.56 3.56	Plagioclase 58%, Pyroxene 9%, opaques and others 33%; density 2.935 g cm ⁻³ ; measurement parallel to axis of core sample at 293-298 K; pulse transmission through water saturated core samples (pore pressure less than confining pressure).	29
9	Basalt, DSDP Leg 16; 163-29-4, 67-74 cm.	20 40 60 80 100 200 400 600 800 1000	6.36 6.38 6.39 6.41 6.42 6.46 6.52 6.57 6.60 6.62	3.55 3.56 3.58 3.59 3.59 3.61 3.63 3.64 3.64 3.65	Same as above except measurement perpendicular to core sample; density 2.937 g cm ⁻³ .	29
10	Basalt, DSDP Leg 16; 155-1-1, 143-150 cm.	20 40 60 80 100 200 400 600 800 1000	4.16 4.19 4.22 4.24 4.27 4.36 4.48 4.56 4.61 4.64	2.03 2.04 2.05 2.06 2.07 2.11 2.15 2.18 2.19 2.20	Same as above except measurement parallel to core of axis; plagioclase 45%, pyroxene 40%, olivine 4%, opaque and other 11%; density 2.448 g cm ⁻³ .	29

TABLE 2.3. ROOM-TEMPERATURE PRESSURE DEPENDENCE OF COMPRESSIONAL AND SHEAR WAVE VELOCITIES OF BASALT (continued)

Data Set No.	Basalt Type & Location	Confining Pressure, P (MPa)	Compressional Wave Velocity, V_p (km s ⁻¹)	Shear Wave Velocity, V_s (km s ⁻¹)	Remarks	Ref. No.
11	Basalt, DSDP Leg 19; 19-192A-5-4, 133-142 cm.	20	4.81	2.44	Leg 19 of Deep Sea Drilling Project (DSDP); density 2.570 g cm ⁻³ ; values calculated from weights and dimensions; room temp measurements from water saturated cylindrical specimens 1.3 cm dia. and 3-4 cm long. [Note: Densities are bulk densities for all DSDP results.]	30
		40	4.87	2.44		
		60	4.92	2.48		
		80	4.95	2.49		
		100	4.98	2.51		
		200	5.10	2.58		
		400	5.25	2.66		
		600	5.36	2.70		
		800	5.45	2.73		
1000	5.53	2.75				
12	Basalt, DSDP Leg 19; 19-192A-5-4, 133-142 cm.	20	4.72	2.43	Same as above except density 2.555 g cm ⁻³ .	30
		40	4.77	2.45		
		60	4.83	2.47		
		80	4.88	2.48		
		100	4.92	2.50		
		200	5.08	2.57		
		400	5.28	2.65		
		600	5.41	2.70		
		800	5.51	2.74		
1000	5.58	2.76				
13	Basalt, DSDP Leg 19; 19-191-16-1, 21-25 cm.	20	5.61	3.07	Same as above except density 2.825 g cm ⁻³ .	30
		40	5.64	3.08		
		60	5.66	3.09		
		80	5.68	3.10		
		100	5.69	3.11		
		200	5.74	3.14		
		400	5.81	3.16		
		600	5.87	3.18		
		800	5.92	3.19		
1000	5.97	3.20				
14	Basalt, DSDP Leg 19; 19-191-16-1, 21-25 cm.	20	5.42	2.94	Same as above except density 2.762 g cm ⁻³ .	30
		40	5.44	2.95		
		60	5.46	2.96		
		80	5.47	2.97		
		100	5.48	2.98		
		200	5.53	3.01		
		400	5.60	3.03		
		600	5.65	3.04		
		800	5.70	3.04		
1000	5.74	3.05				
15	Basalt, DSDP Leg 19; 19-183-39-1, 148-150 cm.	20	6.14	3.08	Same as above except density 2.84 g cm ⁻³ .	30
		40	6.16	3.09		
		60	6.18	3.11		
		80	6.20	3.12		
		100	6.22	3.13		
		200	6.28	3.18		
		400	6.36	3.24		
		600	6.41	3.26		
		800	6.43	3.27		
1000	6.43	3.27				
16	Basalt, DSDP Leg 26; 250A-26-2, 140 cm.	17.2	6.13	-	Leg 26 of Deep Sea Drilling Project (DSDP); samples at 293-298 K were water saturated; density 2.85 g cm ⁻³ .	42
		34.5	6.17	-		
		51.7	6.22	-		
		69.0	6.22	-		
		103.4	6.32	-		
		137.9	6.32	-		
		206.8	6.32	-		
17	Basalt, DSDP Leg 26; 250A-26-6, 58 cm.	17.2	6.02	-	Same as above except density 2.82 g cm ⁻³ .	42
		34.5	6.09	-		
		51.7	6.17	-		
		69.0	6.17	-		
		103.4	6.24	-		
		137.9	6.24	-		
		206.8	6.24	-		

TABLE 2.3. ROOM-TEMPERATURE PRESSURE DEPENDENCE OF COMPRESSIONAL AND SHEAR WAVE VELOCITIES OF BASALT (continued)

Data Set No.	Basalt Type & Location	Confining Pressure, P (MPa)	Compressional Wave Velocity, V_p (km s ⁻¹)	Shear Wave Velocity, V_s (km s ⁻¹)	Remarks	Ref. No.
18	Basalt, DSDP Leg 26; 251A-31-2, 84 cm.	17.2	5.55	-	Same as above except density 2.82 g cm ⁻³ .	42
		34.5	5.61	-		
		51.7	5.61	-		
		69.0	5.68	-		
		103.4	5.68	-		
		137.9	5.68	-		
206.8	5.76	-				
19	Basalt, DSDP Leg 26; 251A-31-3, 50 cm.	17.2	6.31	-	Same as above except density 2.86 g cm ⁻³ .	42
		34.5	6.49	-		
		51.7	6.49	-		
		69.0	6.58	-		
		103.4	6.62	-		
		137.9	6.62	-		
206.8	6.77	-				
20	Basalt, DSDP Leg 26; 251A-31-4, 48 cm.	17.2	5.94	-	Same as above except density 2.93 g cm ⁻³ .	42
		34.5	6.05	-		
		51.7	6.13	-		
		69.0	6.17	-		
		103.4	6.25	-		
		137.9	6.29	-		
206.8	6.37	-				
21	Basalt, DSDP Leg 26; 251A-31-5, 105 cm.	17.2	5.93	-	Same as above except density 2.94 g cm ⁻³ .	42
		34.5	6.01	-		
		51.7	6.06	-		
		69.0	6.15	-		
		103.4	6.24	-		
		137.9	6.33	-		
206.8	6.33	-				
22	Basalt, DSDP Leg 26; 254-31-1, 111 cm.	17.2	5.20	-	Same as above except density 2.74 g cm ⁻³ .	42
		34.5	5.40	-		
		51.7	5.52	-		
		69.0	5.56	-		
		103.4	5.65	-		
		137.9	5.65	-		
206.8	5.73	-				
23	Basalt, DSDP Leg 26; 254-35-1, 107 cm.	17.2	4.79	-	Same as above except density 2.75 g cm ⁻³ .	42
		34.5	4.92	-		
		51.7	4.97	-		
		69.0	5.02	-		
		103.4	5.07	-		
		137.9	5.07	-		
206.8	5.13	-				
24	Basalt, DSDP Leg 26; 254-36-3, 105 cm.	17.2	5.24	-	Same as above except density 2.82 g cm ⁻³ .	42
		34.5	5.30	-		
		51.7	5.36	-		
		69.0	5.42	-		
		103.4	5.48	-		
		137.9	5.48	-		
206.8	5.55	-				
25	Basalt, DSDP Leg 26; 256-10-2, 68 cm.	17.2	5.67	-	Same as above except density 2.96 g cm ⁻³ .	42
		34.5	5.84	-		
		51.7	5.88	-		
		69.0	5.96	-		
		103.4	6.04	-		
		137.9	6.04	-		
206.8	6.12	-				
26	Basalt, DSDP Leg 26; 256-10-3, 85 cm.	17.2	6.23	-	Same as above.	42
		34.5	6.38	-		
		51.7	6.47	-		
		69.0	6.47	-		
		103.4	6.56	-		
		137.9	6.56	-		
206.8	6.65	-				

TABLE 2.3. ROOM-TEMPERATURE PRESSURE DEPENDENCE OF COMPRESSIONAL AND SHEAR WAVE VELOCITIES OF BASALT (continued)

Data Set No.	Basalt Type & Location	Confining Pressure, P (MPa)	Compressional Wave Velocity, V_p (km s ⁻¹)	Shear Wave Velocity, V_s (km s ⁻¹)	Remarks	Ref. No.
27	Basalt, DSDP Leg 26; 257-11-2, 74 cm.	17.2	5.06	-	Same as above except density 2.74 g cm ⁻³ .	42
		34.5	5.18	-		
		51.7	5.21	-		
		69.0	5.24	-		
		103.4	5.31	-		
		137.9	5.38	-		
206.8	5.45	-				
28	Basalt, DSDP Leg 26; 257-12-1, 130 cm.	17.2	5.97	-	Same as above except density 2.73 g cm ⁻³ .	42
		34.5	6.06	-		
		51.7	6.11	-		
		69.0	6.11	-		
		103.4	6.25	-		
		137.9	6.35	-		
206.8	6.35	-				
29	Basalt, DSDP Leg 26; 257-12-3, 35 cm.	17.2	5.88	-	Same as above.	42
		34.5	6.02	-		
		51.7	6.13	-		
		69.0	6.20	-		
		103.4	6.28	-		
		137.9	6.35	-		
206.8	6.43	-				
30	Basalt, DSDP Leg 26; 257-13-3, 15 cm.	17.2	5.46	-	Same as above except density 2.82 g cm ⁻³ .	42
		34.5	5.53	-		
		51.7	5.60	-		
		69.0	5.60	-		
		103.4	5.67	-		
		137.9	5.67	-		
206.8	5.73	-				
31	Basalt, DSDP Leg 26; 257-14-2, 95 cm.	17.2	5.15	-	Same as above except density 2.75 g cm ⁻³ .	42
		34.5	5.21	-		
		51.7	5.27	-		
		69.0	5.27	-		
		103.4	5.33	-		
		137.9	5.33	-		
206.8	5.39	-				
32	Basalt, DSDP Leg 26; 257-15-1, 133 cm.	17.2	6.04	-	Same as above except density 2.89 g cm ⁻³ .	42
		34.5	6.13	-		
		51.7	6.13	-		
		69.0	6.22	-		
		103.4	6.22	-		
		137.9	6.22	-		
206.8	6.31	-				
33	Basalt, DSDP Leg 34; 319A-1-1, 32-35 cm.	20	6.06	3.32	Leg 34 of Deep Sea Drilling Project (DSDP); density 2.915 g cm ⁻³ ; pulse transmission through water saturated core samples, (pore pressure less than confining pressure); 293-298 K.	31
		40	6.11	3.33		
		60	6.14	3.34		
		80	6.17	3.35		
		100	6.20	3.36		
		200	6.28	3.40		
		400	6.38	3.44		
		600	6.41	3.47		
34	Basalt, DSDP Leg 34; 319A-2-3, 46-48 cm.	20	5.92	3.19	Same as above except density 2.864 g cm ⁻³ .	31
		40	5.94	3.20		
		60	5.95	3.22		
		80	5.98	3.23		
		100	6.00	3.24		
		200	6.06	3.29		
		400	6.19	3.33		
		600	6.32	3.35		

TABLE 2.3. ROOM-TEMPERATURE PRESSURE DEPENDENCE OF COMPRESSIONAL AND SHEAR WAVE VELOCITIES OF BASALT (continued)

Data Set No.	Basalt Type & Location	Confining Pressure, P (MPa)	Compressional Wave Velocity, V_p (km s ⁻¹)	Shear Wave Velocity, V_s (km s ⁻¹)	Remarks	Ref. No.
35	Basalt, DSDP Leg 34; 319A-3-2, 114-117 cm.	20	6.06	3.28	Same as above except density 2.923 g cm ⁻³ .	31
		40	6.09	3.29		
		60	6.12	3.32		
		80	6.15	3.34		
		100	6.17	3.35		
		200	6.27	3.39		
		400	6.38	3.43		
36	Basalt, DSDP Leg 34; 319A-3-4, 85-88 cm.	20	6.14	3.36	Same as above except density 2.939 g cm ⁻³ .	31
		40	6.19	3.37		
		60	6.22	3.37		
		80	6.25	3.38		
		100	6.27	3.39		
		200	6.34	3.41		
		400	6.43	3.45		
37	Basalt, DSDP Leg 34; 319A-4-1, 137-140 cm.	20	6.00	3.30	Same as above except density 2.911 g cm ⁻³ .	31
		40	6.03	3.31		
		60	6.06	3.32		
		80	6.08	3.34		
		100	6.09	3.35		
		200	6.15	3.36		
		400	6.23	3.39		
38	Basalt, DSDP Leg 34; 319A-5-1, 80-83 cm.	20	6.24	3.49	Same as above except density 2.948 g cm ⁻³ .	31
		40	6.28	3.49		
		60	6.30	3.50		
		80	6.32	3.50		
		100	6.34	3.50		
		200	6.40	3.52		
		400	6.46	3.53		
39	Basalt, DSDP Leg 34; 319A-6-1, 145-148 cm.	20	6.11	3.27	Same as above except density 2.882 g cm ⁻³ .	31
		40	6.12	3.29		
		60	6.14	3.31		
		80	6.15	3.32		
		100	6.16	3.33		
		200	6.19	3.35		
		400	6.23	3.35		
40	Basalt, DSDP Leg 34; 319-7-1, 65-68 cm.	20	5.93	3.24	Same as above except density 2.851 g cm ⁻³ .	31
		40	5.97	3.25		
		60	6.00	3.26		
		80	6.01	3.27		
		100	6.03	3.28		
		200	6.07	3.30		
		400	6.13	3.33		
41	Basalt, DSDP Leg 34; 319-13-1, 52-55 cm.	20	6.13	3.26	Same as above except density 2.920 g cm ⁻³ .	31
		40	6.17	3.29		
		60	6.19	3.32		
		80	6.21	3.34		
		100	6.23	3.36		
		200	6.30	3.41		
		400	6.38	3.45		
600	6.46	3.46				

TABLE 2.3. ROOM-TEMPERATURE PRESSURE DEPENDENCE OF COMPRESSIONAL AND SHEAR WAVE VELOCITIES OF BASALT (continued)

Data Set No.	Basalt Type & Location	Confining Pressure, P (MPa)	Compressional Wave Velocity, V_p (km s ⁻¹)	Shear Wave Velocity, V_s (km s ⁻¹)	Remarks	Ref. No.
42	Basalt, DSDP Leg 34; 320B-3-1, 64-67 cm.	20	5.25	2.85	Same as above except density 2.725 g cm ⁻³ .	31
		40	5.27	2.86		
		60	5.28	2.88		
		80	5.29	2.89		
		100	5.31	2.89		
		200	5.37	2.93		
		400	5.48	2.97		
43	Basalt, DSDP Leg 34; 320B-4-1, 144-147 cm.	20	5.62	3.01	Same as above except density 2.837 g cm ⁻³ .	31
		40	5.66	3.03		
		60	5.71	3.06		
		80	5.74	3.08		
		100	5.77	3.10		
		200	5.89	3.16		
		400	6.03	3.20		
44	Basalt, DSDP Leg 34; 320B,5,CC	20	6.01	3.24	Same as above except density 2.832 g cm ⁻³ .	31
		40	6.04	3.27		
		60	6.07	3.28		
		80	6.08	3.30		
		100	6.10	3.31		
		200	6.14	3.38		
		400	6.19	3.44		
45	Basalt, DSDP Leg 34; 321-13-4, 104-107 cm.	20	5.22	2.84	Same as above except density 2.822 g cm ⁻³ .	31
		40	5.26	2.86		
		60	5.29	2.88		
		80	5.32	2.89		
		100	5.35	2.90		
		200	5.44	2.96		
		400	5.57	3.02		
46	Basalt, DSDP Leg 34; 321-14-1, 76-79 cm	20	6.03	3.28	Same as above except density 2.900 g cm ⁻³ .	31
		40	6.05	3.30		
		60	6.06	3.31		
		80	6.07	3.33		
		100	6.08	3.34		
		200	6.12	3.38		
		400	6.19	3.42		
47	Basalt, DSDP Leg 34; 321-14-4, 51-54 cm.	20	5.67	3.09	Same as above except density 2.915 g cm ⁻³ .	31
		40	5.71	3.11		
		60	5.73	3.13		
		80	5.76	3.14		
		100	5.78	3.16		
		200	5.86	3.22		
		400	5.95	3.29		
48	Basalt, DSDP Leg 35; 322-12-1, (piece No. 7).	20	5.50	2.98	Deep Sea Drilling Project (DSDP), water saturated samples at 293 K; density 2.730 g cm ⁻³ .	33
		40	5.52	2.99		
		60	5.53	3.00		
		80	5.54	3.01		
		100	5.56	3.02		
		200	5.61	3.05		
		400	5.69	3.07		
600	5.74	3.09				

TABLE 2.3. ROOM-TEMPERATURE PRESSURE DEPENDENCE OF COMPRESSIONAL AND SHEAR WAVE VELOCITIES OF BASALT (continued)

Data Set No.	Basalt Type & Location	Confining Pressure, P (MPa)	Compressional Wave Velocity, V_p (km s ⁻¹)	Shear Wave Velocity, V_s (km s ⁻¹)	Remarks	Ref. No.
49	Basalt, DSDP Leg 35; 322-18-6, 110-120 cm.	20	4.87	2.58	Same as above, but large open vesicles present, hence low density of 2.553 g cm ⁻³ .	33
		40	4.89	2.60		
		60	4.91	2.61		
		80	4.93	2.63		
		100	4.94	2.64		
		200	5.01	2.69		
		400	5.09	2.74		
50	Basalt, DSDP Leg 35; 323-18-6, 110-120 cm.	20	5.44	2.82	Same as above, except intergranular intersertal textures and contain significant alteration products; calcite veins were avoided in the samples for velocity measurements; density 2.727 g cm ⁻³ .	33
		40	5.45	2.84		
		60	5.47	2.86		
		80	5.48	2.87		
		100	5.49	2.88		
		200	5.55	2.91		
		400	5.62	2.95		
51	Basalt, DSDP Leg 35; 323-20, CC, 104-144 cm.	20	5.30	2.88	Same as above except density 2.727 g cm ⁻³ .	33
		40	5.31	2.90		
		60	5.33	2.91		
		80	5.34	2.92		
		100	5.35	2.92		
		200	5.41	2.95		
		400	5.48	2.97		
52	Basalt, DSDP Leg 39; 354-19-3, 131-134 cm.	20	5.55	3.03	Leg 39 of Deep Sea Drilling Project (DSDP); water saturated samples at 293 K; exact composition unknown except large amount of calcite present; density 2.733 g cm ⁻³ .	32
		40	5.57	3.04		
		60	5.59	3.05		
		80	5.61	3.06		
		100	5.62	3.06		
		200	5.67	3.08		
		400	5.74	3.10		
53	Basalt, DSDP Leg 39; 354-19-5, 93-96 cm.	20	5.63	3.08	Same as above except density 2.753 g cm ⁻³ .	32
		40	5.65	3.09		
		60	5.67	3.09		
		80	5.69	3.10		
		100	5.70	3.11		
		200	5.74	3.12		
		400	5.79	3.14		
54	Basalt, DSDP Leg 39; 355-21-1, 147-150 cm.	20	5.70	2.93	Same as above except density 2.808 g cm ⁻³ .	32
		40	5.71	2.95		
		60	5.72	2.96		
		80	5.73	2.97		
		100	5.74	2.98		
		200	5.75	3.02		
		400	5.80	3.07		
55	Basalt, DSDP Leg 39; 355-22-1, 57-60 cm	20	6.03	3.12	Same as above except density 2.884 g cm ⁻³ .	32
		40	6.05	3.14		
		60	6.07	3.16		
		80	6.08	3.17		
		100	6.10	3.17		
		200	6.15	3.23		
		400	6.22	3.26		
56	Basalt, DSDP Leg 39; 355-22-2, 44-47 cm.	20	5.78	3.20	Same as above except density 2.838 g cm ⁻³ .	32
		40	5.83	3.21		
		60	5.86	3.22		
		80	5.88	3.23		
		100	5.89	3.24		
		200	5.94	3.25		
		400	5.99	3.26		
600	6.07	3.27				

TABLE 2.3. ROOM-TEMPERATURE PRESSURE DEPENDENCE OF COMPRESSIONAL AND SHEAR WAVE VELOCITIES OF BASALT (continued)

Data Set No.	Basalt Type & Location	Confining Pressure, P (MPa)	Compressional Wave Velocity, V_p (km s ⁻¹)	Shear Wave Velocity, V_s (km s ⁻¹)	Remarks	Ref. No.
57	Basalt, DSDP Leg 39; 355-22-4, 69-72 cm.	20	5.35	2.93	Same as above except density 2.757 g cm ⁻³ .	32
		40	5.41	2.94		
		60	5.45	2.95		
		80	5.48	2.96		
		100	5.50	2.96		
		200	5.55	2.96		
		400	5.60	3.02		
600	5.64	3.04				
58	Basalt, DSDP Leg 39; 355-22-5, 119-122 cm.	20	5.54	3.08	Same as above except density 2.798 g cm ⁻³ .	32
		40	5.57	3.09		
		60	5.59	3.09		
		80	5.61	3.10		
		100	5.62	3.10		
		200	5.67	3.12		
		400	5.73	3.15		
		600	5.81	3.17		

results though the added sophistication is hardly necessary.

There are several factors which influence the values obtained over and above purely petrological factors such as mineralogy. These factors include:

- 1) End-effects due to friction between specimen and load platens
- 2) Specimen geometry
- 3) Rate of loading
- 4) Testing environment, e.g., moisture, temperature, etc.

2.4.2. Tensile Strength

Tensile strength of rock is considerably less than the compressive strength. However, since the propagation of tensile cracking leading to tensile failure in rock is not uncommon, it is necessary to assess the tensile strength.

There are basically two methods of determining tensile strength. One is the direct method which implies a direct tensile load on a rock specimen, and the other is the indirect method in which a tensile stress is induced in a specimen rather than directly applied to it.

The direct method is self-explanatory; however, indirect techniques bear some examination. Bending tests and diametral compression of discs give rise to induced tensile stress. In both of these types of test, no direct tensile load is applied. In the case of bending, a certain amount of inaccuracy occurs due to creep which takes place just prior to failure. Disk compression tests (e.g., Brazilian) are somewhat controversial, and conflicting results have been reported. Overall it seems some combination of tensile failure and shear failure occurs making the results questionable unless precautions are taken to prevent the feasibility of shear failure.

2.4.3. Shear Strength

Shear strength lacks an exact definition, but here it will be defined as the shearing force necessary to cause failure divided by the cross-sectional area over which the failure occurs.

Again, there are several tests for determining shear strength. The basic methods are:

The zero normal stress method
 The torsion method
 The oblique shear method
 The triaxial test

The best agreement and best results are given by the torsion and triaxial methods. Shear tests with compression are considerably better than zero normal stress tests since they do not produce bending, plus the usual tensile stress associated with the latter test.

Strength data are presented in tabular form in Table 2.4. Additionally, the ultimate strength of basalt versus stress rate for two different temperatures from ref. [47] is presented in Figure 2.23. Stress rates of 10^{-1} to 10^8 MPa s⁻¹ and two temperatures of 296 K and 77 K are shown. As can be seen from the figure, the lower strength values are associated with the lower temperature.

In Figure 2.24 the effect of confining pressure of the strain rate dependence of the ultimate compressive strength of Dresser Basalt is displayed. Axial strain rates of 10^{-5} to 10^3 s⁻¹ and confining pressures of 0 to 490 MPa were utilized. The temperature was kept constant at 300 K. Testing was accomplished using hydraulic loading equipment for low strain rates and a Hopkinson pressure bar apparatus for higher strain rates.

The effect of temperature and strain rate on the unconfined ultimate strength of Dresser Basalt can be seen in Figure 2.25. Temperatures ranging from 0 to 1400 K and strain rates of approximately 10^3 s⁻¹, 10^{-1} s⁻¹, and 10^{-4} s⁻¹ were used. The testing used the same method indicated in the preceding paragraph.

2.4.4. Creep

Three general approaches are usually adopted to study creep. They are the micromechanistic, phenomenological, and empirical methods. Of the three, the latter is the most popular. In this technique, experiments are conducted to obtain a continuous stress-strain history in terms of parameters like time, stress, and temperature. This information is then used to derive empirical creep equations that describe a particular material's creep behavior. A general equation which defines the performance of a material over its entire range of behavior according to Emery et al. [49] is the following:

TABLE 2.4. ULTIMATE STRENGTH, COMPRESSIVE STRENGTH AND TENSILE STRENGTH OF BASALT

Data Set No.	Basalt Type & Location	Ultimate Strength, σ_{ult} (MPa)	Compressive Strength, σ_c (MPa)	Tensile Strength, σ_t (MPa)	Temp. (K)	Remarks	Ref. No.
Andesite-Basalt -							
1	Bakuviani, Georgia, USSR		88.26			Confining pressure 21.86 MPa.	3
Olivine Basalt -							
2	Blairsden, CA	1540			297	Confining pressure 505 MPa.	13
3	Blairsden, CA	1380			573	Confining pressure 500 MPa.	13
4	Blairsden, CA	1030			773	Confining pressure 505 MPa.	13
5	Blairsden, CA	546			873	Confining pressure 200 MPa.	13
6	Blairsden, CA	531			973	Confining pressure 507 MPa.	13
7	Blairsden, CA	263			1073	Confining pressure 507 MPa.	13
8	Blairsden, CA	131			1073	Confining pressure 507 MPa.	13
9	Eniwetok Atoll		194.4				4
Basalts -							
10	Barra Bonita Dam, Brazil		19.54			Compact; porosity 1.4%.	10
11	Barra Bonita Dam, Brazil		137.4			Same as above.	10
12	Black Canyon Dam, ID		57.9	3.17			7
13	Brooklyn, Vic, Australia		86.2	12.89			11
14	Brooklyn, Vic, Australia		41.8	12.89			11
15	Brooklyn, Vic, Australia		116.9	12.89			11
16	Dresser, WI		292.3				15
17	Green Peters Dam, OR		92.0			Amygdaloidal, porphyritic.	17
18	Howard Prairie Dam, OR		194.0				20
19	Idaho and Washington		118.1				44
20	India		68.3	2.21		Altered, vesicular.	7
21	John Day		355.0	14.5		At 50% of failure, massive.	45
22	Jupia Dam, Brazil		108.7			Compact, porosity 2.1%.	10
23	Jupia Dam, Brazil		104.8				10
24	Jurimirim Dam, Brazil		157.2			Porosity 4.2%.	10
25	Jurimirim Dam, Brazil		133.0				10
26	Knippa, TX		262		297	Confining pressure 0 MPa.	46
27	Knippa, TX		462		297	Confining pressure 69 MPa.	46
28	Knippa, TX		551		297	Confining pressure 103 MPa.	46
29	Little Goose		296.0	11.1		At 50% of failure.	21
30	Lower Granite		228.0	12.9		At 50% of failure.	21

TABLE 2.4. ULTIMATE STRENGTH, COMPRESSIVE STRENGTH AND TENSILE STRENGTH OF BASALT (continued)

Data Set No.	Basalt Type & Location	Ultimate Strength, $\sigma_{ult.}$ (MPa)	Compressive Strength, σ_c (MPa)	Tensile Strength, σ_t (MPa)	Temp. (K)	Remarks	Ref. No.
Basalts - (cont.)							
31	Michigan		344.0	28.4		Heavily altered, amygdaloidal.	22
32	Michigan		232.0			Altered.	22
33	Michigan		81.9			Altered.	22
34	Michigan		12.0	14.6		Altered, amygdaloidal.	22
35	Medford, OR		169.8			Confining pressure 0-41.6 MPa.	22
36	Medford, OR		221.0			Confining pressure 0-41.6 MPa.	22
37	Melhurb Quarry, Brazil		146.0			Porosity 11.6%.	10
38	Mussa Quarry, Brazil		172.1			Porosity 5.7%.	10
39	Mussa Quarry, Brazil		126.8				10
40	South Coulee Dam, WA		171.7				7
41	South Coulee Dam, WA		95.8			Vesicular.	7
42	South Coulee Dam, WA		82.1				7
43	South Coulee Dam, WA		61.4			Vesicular.	7
44	Nevada Test Site (N.T.S.)		144.5	13.10			24
45	Nevada Test Site (N.T.S.)		148.0	18.1		At 50% of failure.	25
46	(a)		255.1	9.65			27
47	(a)		73.77				28

(a) Basalt type and location unknown.

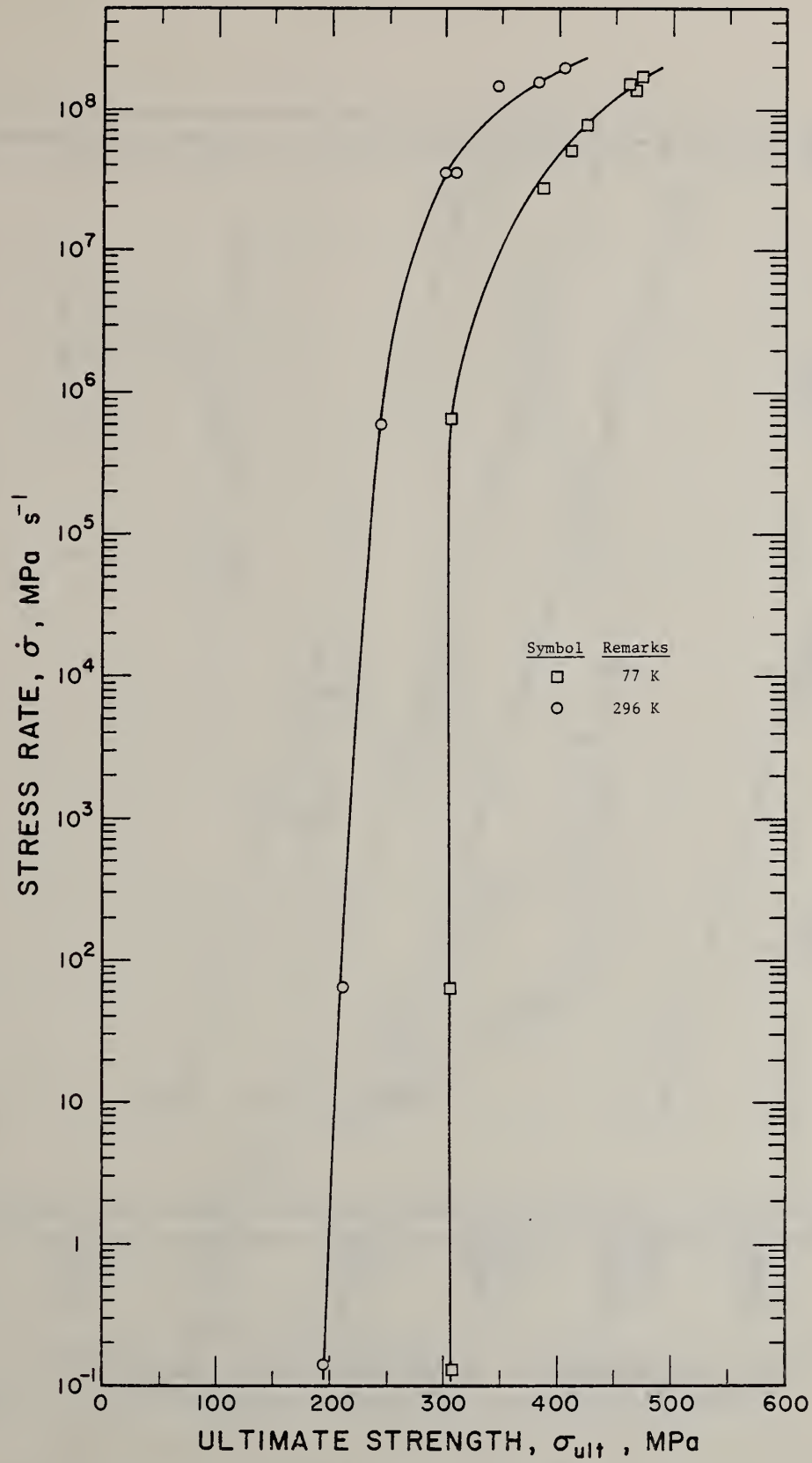


FIGURE 2.23. EFFECT OF STRESS ON THE FRACTURE STRENGTH OF BASALT [47].

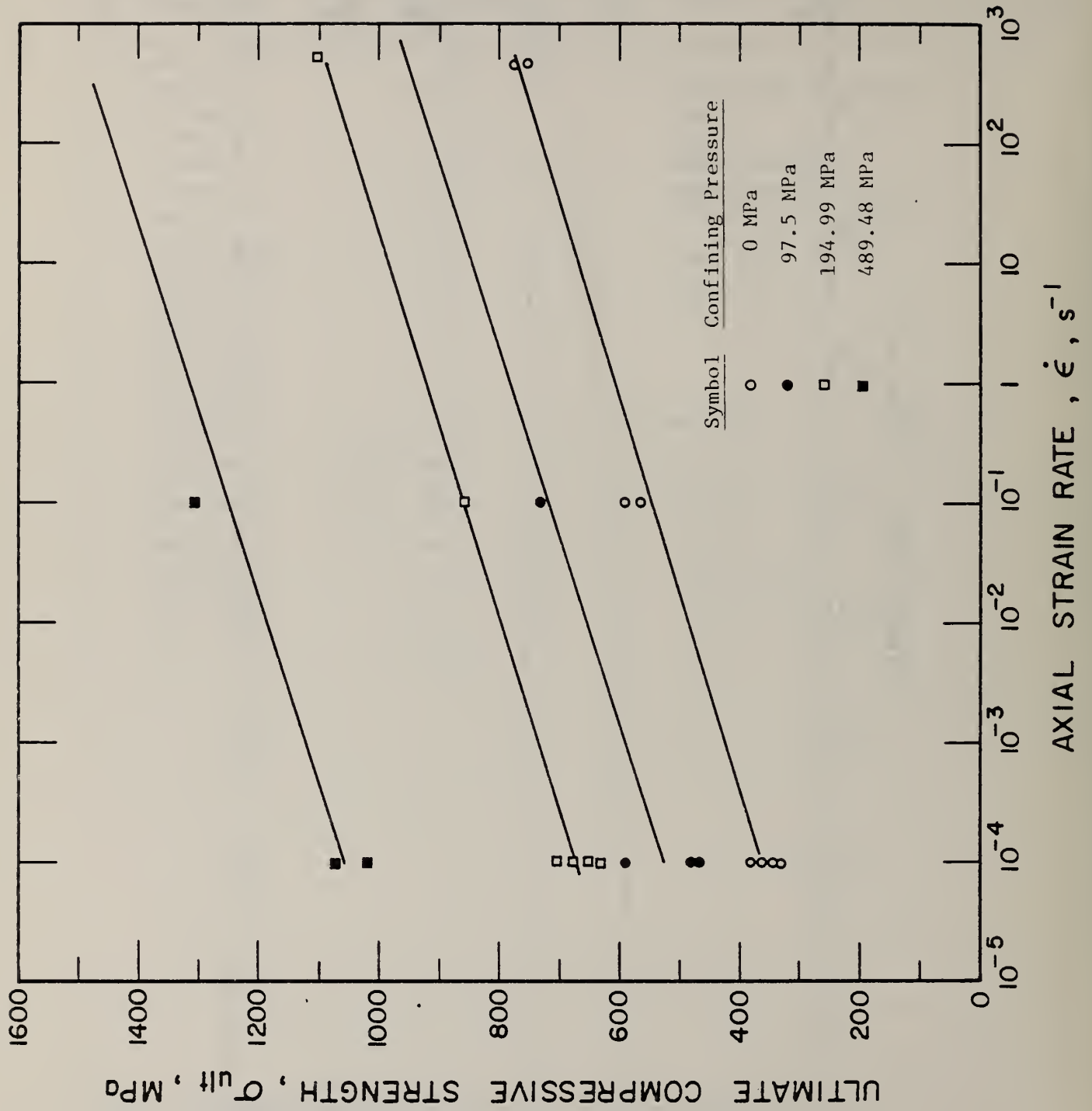


FIGURE 2.24. STRAIN-RATE DEPENDENCE OF ULTIMATE COMPRESSIVE STRENGTH FOR DRESSER BASALT [48].

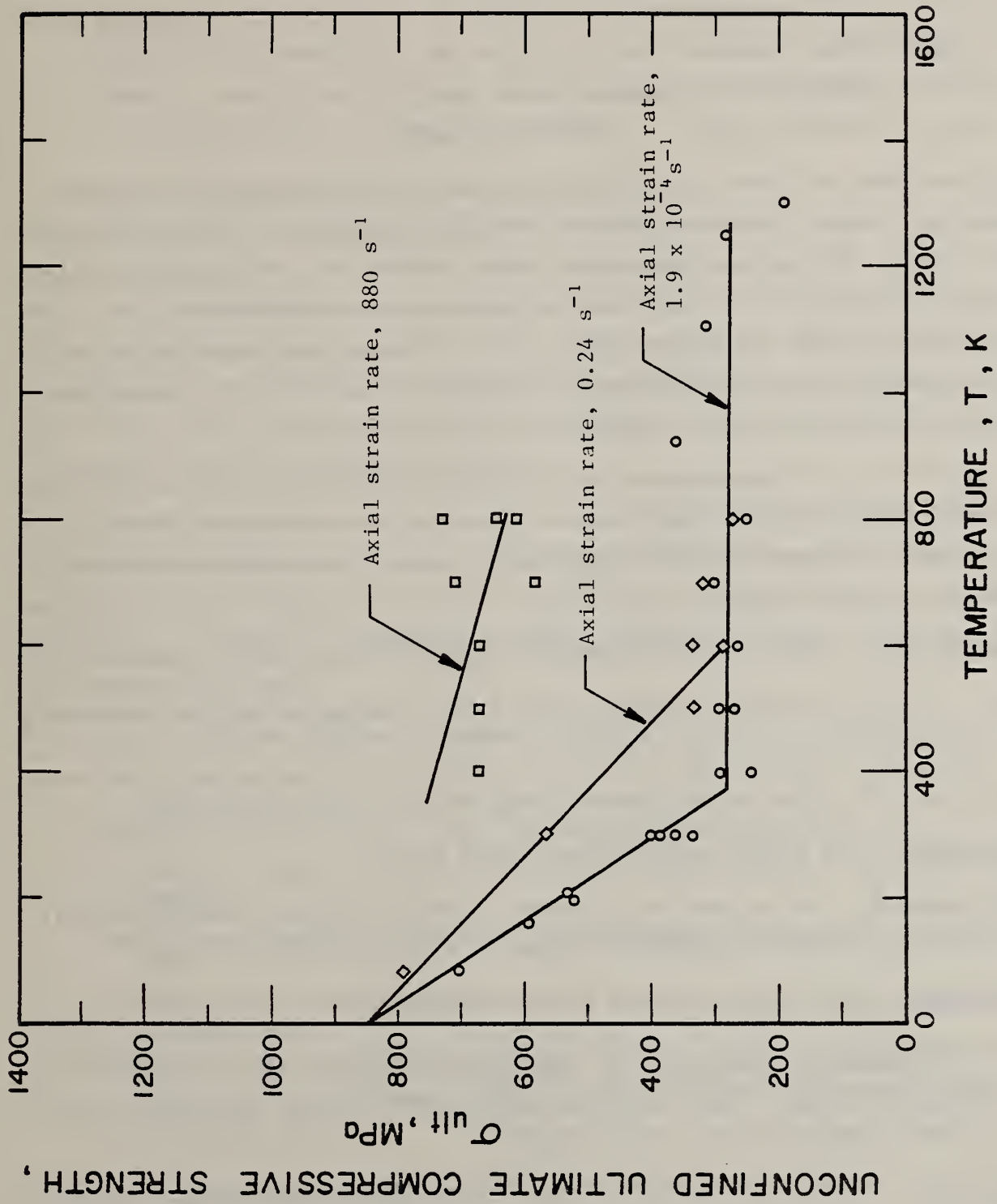


FIGURE 2.25. TEMPERATURE DEPENDENCE OF UNCONFINED ULTIMATE COMPRESSIVE STRENGTH FOR BASALTS [48].

$$\epsilon(t) = \epsilon_0 + \epsilon_p(t) + A(t) + \epsilon_T(t)$$

where

$\epsilon(t)$ = total strain (i.e., elastic + creep)

ϵ_0 = instantaneous strain (elastic)

$\epsilon_p(t)$ = primary creep

$A(t)$ = secondary creep (steady state creep)

$\epsilon_T(t)$ = tertiary creep (See Fig. 2.26)

Since rock is not an ideally elastic material, its behavior is usually complex and often a function of the mineral composition. This complexity gives rise to the problem that it is often difficult to characterize a rock quantitatively without first obtaining stress-strain relationships over the entire range of the conditions anticipated. Theoretical modeling of the stress-strain or time-strain behavior is greatly hindered by the variations in environment possible, e.g., temperature, pressure, etc.

Definitions of characteristics of time-dependent properties are far from universal and controversy still exists. For this reason nomenclature will be defined here and hereafter all references to a particular characteristic will assume these definitions.

Anelastic Creep: creep fully recoverable with time once load is removed.

Creep: plastic deformation under constant load showing an obvious decreasing strain rate.

Creep Rate: the slope of the stress-strain curve in the creep stage.

Creep Strain: the gradual strain observed in creep.

Creep Strength: the stress in a constant stress, constant temperature test that will produce a specified strain in a specified time.

Creep Stress: conventional stress in a creep test.

Plastic Creep Limit: implies below a certain stress all creep is anelastic (= fully recoverable with time once load is removed), whilst above it creep is partly anelastic and partly plastic.

Plasticity: behavior of a solid material once the elastic limit has been exceeded and implies permanent non-recoverable strain.

Ultimate Strength: the maximum stress immediately prior to failure.

Yield Point: some materials show a sudden inhomogeneous extension at constant load in their stress-strain curves as soon as the elastic limit is exceeded.

Yield Strength: to circumvent the problems associated with determining the elastic limit accurately for materials not showing a yield point, one normally chooses an arbitrary plastic strain, usually 0.2%, and quotes the related stress as the yield strength.

Creep is determined from so-called creep tests which are constant stress tests. These tests can be accomplished in several modes: namely, in bending, torsion, compression, or tension. Two approaches are used in these tests. One is to load the specimen and subject it to this load for a long period while measuring deformation with time. The other is to load the specimen incrementally and measure the deformation with time for each increment. In all these cases, steady state creep is required. An idealized curve for rock at constant stress is shown in Figure 2.26.

Primary (transient) and secondary (steady state) creep represent the bulk of the creep work done on rock. Generally, empirical equations have been developed by researchers to fit the time-strain behavior recorded by their experiments. Numerical methods have more recently been used to achieve fits for experimental data.

Several factors influence creep. At this stage it is not our intent to delve into them in any detail other than just to mention them. They are:

- 1) Nature of the stress, i.e., tensional or compressional, etc.
- 2) Level of stress (relationship between creep-stress is not necessarily linear).
- 3) Confining pressure (increase in confining pressure decreases creep rate).
- 4) Temperature (generally an increase in temperature causes an increase in creep rate).
- 5) Moisture and humidity (creep seems to increase with wetting).
- 6) Structural effects (variation in grain size, crystal orientation produce effects).

2.4.4.1. Creep of Rock In-Situ

Most research has been accomplished on rock salt. Several creep

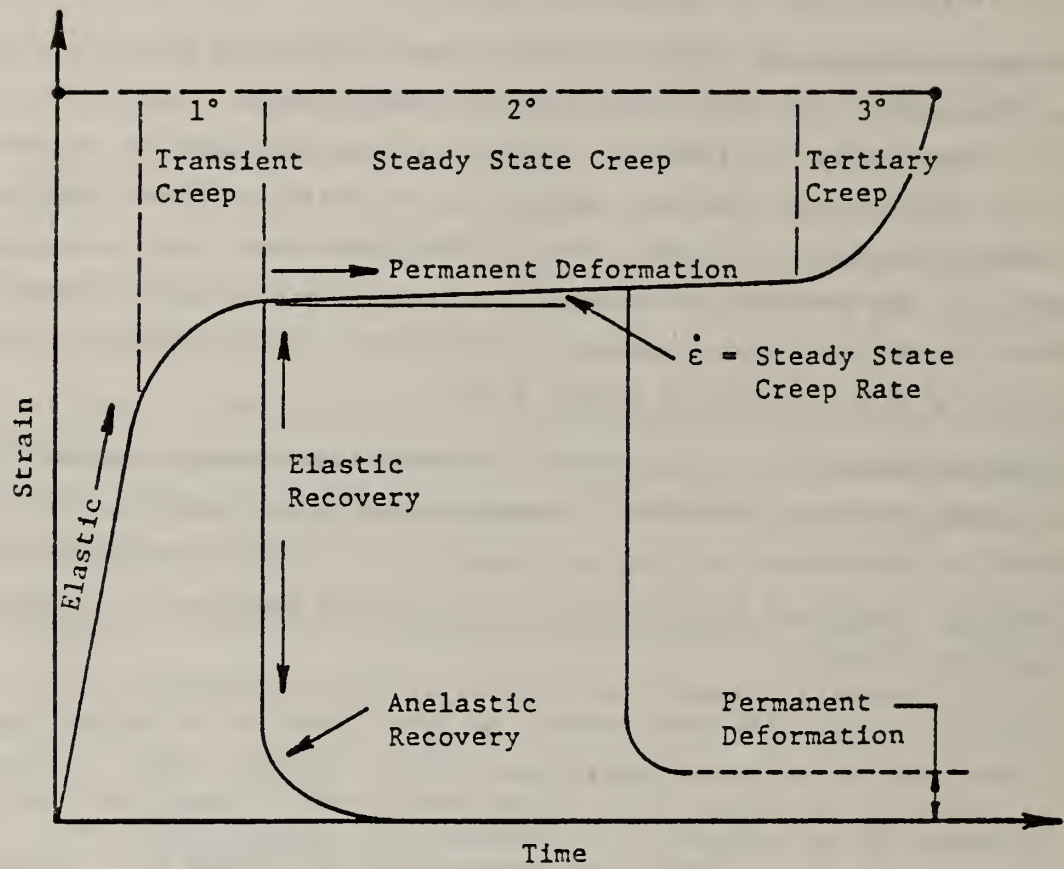


FIGURE 2.26. IDEAL CREEP CURVE [49]

relationships have been developed, generally for underground openings or pillars in rock salt mines. The diversity of relationships developed tends to lead to the conclusion that, as has been indicated earlier, the mechanism of creep is not at all well characterized and so it would seem prototype modeling in the in-situ case is still the best way to go if creep parameters are required.

2.4.4.2. Time Dependent 'Strength'

This, arguably, could be presented under the section entitled 'Strength.' However, as it will be seen later, strength will be defined as time independent for the purposes of this report, although there is a grey area where time effects overlap. For this reason it is probably better to present data as stress-strain or time-strain data and allow the user to select so-called 'strength' values for his particular purpose. Obviously, neither of these two forms are totally independent of time in the former instance and stress in the latter instance, but at least these two parameters have been 'de-emphasized' to some extent due to the nature of the testing being used.

Using the terminology of Price [50], this section deals with 'long term strength.' This 'strength' can be assessed using either direct or indirect methods. The direct method is iterative in nature and is essentially a 'trial and error' method. It required that several creep tests be done at differing loads and the highest load at which no failure takes place enables an assessment of the 'long term strength.' This method is conservative and generally only approximate.

2.4.4.3. Summary of Empirical and Phenomenological Creep Models

A summary of these models is presented in Figure 2.27 and Table 2.5. Empirical models are essentially equations that have been found to fit experimentally obtained creep data. Provided that the conditions and assumptions under which they were obtained are met, they can probably be used to predict creep behavior.

Phenomenological models, on the other hand, seek to express the creep behavior of materials in terms well known mechanical concepts such as the spring representing perfectly elastic behavior, the dashpot representing perfectly viscous behavior, and finally the friction block representing

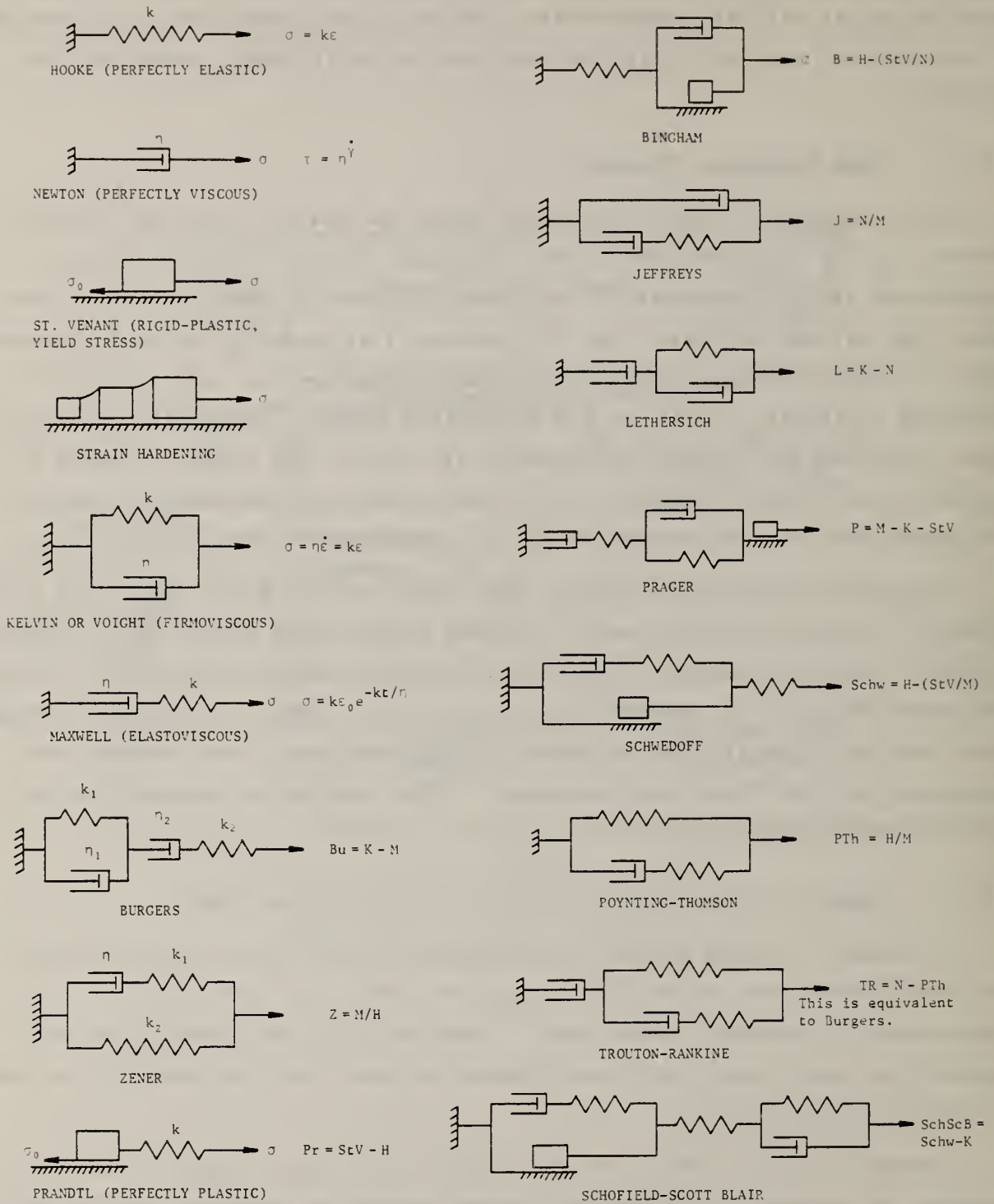


FIGURE 2.27. PHENOMENOLOGICAL MODELS FOR CREEP [51].

TABLE 2.5. EMPIRICAL CREEP RELATIONSHIPS

Creep Equation	Rock Types	Definitions of Variables and Description of Limitations
$\epsilon = 600e^{0.1\sigma} + 20e^{0.3\sigma}(1 - e^{-1.2t}) + 9\sigma^{0.3}t^{0.3} + 11\sigma e^{0.8\sigma}$	Limestone	Michelson [52,53]. This equation was obtained for creep in torsion.
$\epsilon = A - Ae^{\frac{B-Ctn}{t}}$	Marble, Limestone, Sandstone, Slate	Evans [54]. A, B, C are constants and n is approximately 0.4.
$\epsilon = \epsilon_e + B \log t + Dt$		Griggs [55-57]. ϵ_e = elastic strain; $B \log t$ = primary creep; Dt = secondary creep; $D = \sigma/3\eta$ in Maxwell model; B and D are constants depending on σ .
$\gamma(t) = \frac{\tau}{G} [1 + q \ln(1 + \alpha t)]$	Gabbro, Granodiorite	Lomnitz [58]. $\gamma(t)$ = total shear strain in rod. τ = constant shear stress; G = shear modulus; t = time in seconds; q = constant; α = coefficient so that $\alpha t > 1$. Obtained from torsion tests and applicable for small strains only.
$\left(\frac{G}{E}\right)^n = t_K \dot{\epsilon} + B$	Sandstone, Shale	Ruppeneyt [59]. E = Young's modulus; t_K = retardation time; B and n are constants.
$\epsilon = A_0 + A_1 e^{-\alpha_1 t} + A_2 e^{-\alpha_2 t} + A_3 e^{-\alpha_3 t} + B \log t + Ct$	Granite	Matsushima [60]. t = time; $\alpha_1 = 10$; $\alpha_2 = 100$; $\alpha_3 = 10000$ where $1/\alpha_1, 1/\alpha_2,$ and $1/\alpha_3$ are the retardation times in the Kelvin model.
$\epsilon = \epsilon_0 + \alpha \log_e t$	Both equations for limestone, shale, granite, gabbro, rock salt, quartzite	Robertson [61]. t = time in seconds; α = constant; σ = stress; A = rock specific constant. Primary creep only.
$\dot{\epsilon} = A\sigma^n$		
$C = K\sigma^n t^m$	Rock salt and others	Boreis and Deere [62]. K, n, and m are specific for each rock type.

TABLE 2.5. EMPIRICAL CREEP RELATIONSHIPS (Continued)

Creep Equation	Rock Types	Definitions of Variables and Description of Limitations
$\epsilon = \left(\frac{\sigma}{E} \right) \ln t$		Farmer [63]. No secondary creep allowed for. n is stress and modulus dependent.
Generalized Burger's model with 2 Kelvin units included	Limestone, Sandstone, and Granite	Excellent agreement reported.
$\epsilon = 0.4395t^{0.4929} \times 10^{-4}$	Marble	Singh [64]. Equation for primary creep.
$\epsilon = (0.1817t - 0.8022) \times 10^{-4}$	Marble	Equation for secondary creep.
$\epsilon = 0.4205t^{0.5044} \times 10^{-4}$	Marble	Equation for primary and secondary creep combined load of the order of 86 MPa.
$\epsilon_1 = 10^C t^n$	Granite, Marble, and Sandstone	Warversik and Brown [65]. ϵ_1 = primary creep; ϵ_2 = primary creep; C and C' are stress functions and t = time. Marble did not appear to exhibit 2° creep.
$\epsilon_2 = 10^{C'}$		
$\epsilon = A + Bt^C + D(1 - e^{Et})$	Dry soft to medium rocks	Afronz and Harvey [66]. A, B, C, D, E are constants and are stress level dependent.
$\epsilon = A + Bt^C + Dt^E$	Saturated soft rocks	

perfectly plastic behavior. Combinations of these three basic components, however, are required to model the behavior of real materials and here lies a problem. Combinations of these simple models become rather complicated and, therefore, are difficult to handle mathematically. This represents a serious drawback and, hence, the popularity of empirical methods.

It should be stated, however, that there is certainly no universal agreement amongst the models within each model type group nor is there between the two model type groups, i.e., empirical and phenomenological. This is another reason why empirical modeling is popular - it is not subject to constraints imposed by theory provided the final operating environment can be adequately physically modeled.

No data specifically related to basalt has been isolated, although general empirical equations can probably be used with some success provided the equation is selected carefully. Some of these equations are presented in Table 2.5.

2.5. HARDNESS

Several measures of hardness exist, some of them being developed for metallurgical purposes. Certain scales, some of them borrowed from metallurgy, have been utilized to describe the hardness of rocks.

Rock hardness measurements can be divided into two basic groups; namely: indentation and rebound measurements. In the former case scratch hardness and formal indentation are included. Mohs scale is a scratch hardness system in which a suite of standard minerals, each harder than its preceding counterpart, are used to delineate the hardness range in which a given rock or mineral lies. This is a standard technique and, while qualitative, it is simple and probably the most commonly used hardness system for minerals.

Vickers microhardness is an indentation hardness system. Here an inverted diamond pyramid tipped probe falling a specific distance at a specific rate creates a pit the shape of the tip. The size of the pit is measured and compared to a calibration chart to obtain the microhardness.

Rebound hardnesses commonly used are the Schmidt hammer hardness and the Shore scleroscopic hardness. The Shore scleroscope consists of a diamond

tipped hammer that falls a measured distance and rebounds off the surface of the rock. The height of the rebound is measured and used to obtain the hardness. The Schmidt hammer is somewhat similar although more easily used since it is more readily carried around. Rebound readings are converted directly to compressive strength on the hammer which is another advantage. Such conversions from hardness to compressive strength, however, are at best unreliable since they are heavily dependent on the grain size of the rock and the mineral grains in contact with the end of the hammer. Furthermore, grain boundaries do not give the same readings as nongrain boundary contact areas do.

Some difficulty has been encountered in obtaining hardness data. This is probably due to the fact that the previously held belief that hardness could be related to compressive strength has been largely discarded as unreliable. Furthermore, the character of the rock (e.g., vesicular basalt) makes testing difficult due to physical characteristics like friability. Data are presented in Table 2.6.

TABLE 2.6. HARDNESS OF BASALT

Rock Type and Location	Shore Hardness	Reference Number
Dresser	95.0	47
-	93.2	47
-	94.2	47

2.6. POROSITY AND PERMEABILITY

2.6.1. Porosity

Porosity is defined as the ratio of the volume of internal open spaces (pores or voids) to the bulk volume of the rock. It can also be expressed in terms of grain density and the dry density of the rock.

Factors which generally influence the porosity of rocks are:

- 1) Size distribution of grains
- 2) Shape of grains

- 3) Solidity of grains
- 4) Orientation of grains
- 5) Degree of compaction
- 6) Amount of nongranular material in pores or coating of grains

Pores are either interconnected and open to the exterior or closed (isolated) and not connected to the exterior. Different terminology applies to these two cases. When only interconnected open pores are considered, the porosity is known as apparent porosity. When both open and isolated pores are considered, the value obtained is termed total porosity.

If at least two of the three forms of volumes (for example, grain volume, pore volume, and bulk volume) are known, one can calculate porosity. Methods of obtaining these volumes are cited in several sources and will not be discussed here. Porosity has the effect on the mechanical properties of rocks that all strength properties decrease with increase in porosity because:

- 1) Stress concentration caused on the boundary of the pores reduces the strength.
- 2) Decrease in the bearing area of the rock causes decrease in strength.
- 3) Pores may be filled with water or some other liquid which may help in crack propagation by reaction at the points of stress concentration by reducing its surface energy.

2.6.2. Permeability

Permeability is a function of the porosity of rock and can be calculated from the following relationship:

$$k = \eta \frac{q}{A} \frac{L}{(P_i - P_o)} \times 9.7 \times 10^{-4}$$

where:

- k = permeability in cm s^{-1}
- η = viscosity of fluid in centipoise at ambient temperature
- q = volume of fluid in $\text{cm}^3 \text{s}^{-1}$ flowing through specimen
- L = length of specimen, cm
- A = cross-sectional area, cm^2
- P_i = absolute pressure at point of entry
- P_o = absolute pressure at point of exit

Fluid is transmitted throughout a rock by interconnecting pores. The

fact that a rock is porous does not imply that it is permeable since closed pores (not interconnected with the external surface) do not allow the passage of fluids.

Permeability can be a highly anisotropic property; for instance, radial permeability may vary greatly from longitudinal permeability within a rock. Another point to consider is the permeating medium. Permeability is obviously going to vary with fluid viscosity. Generally speaking, laboratory tests are of two basic kinds; namely, either gas permeability tests or liquid permeability tests. Each of these, in turn, can usually be broken down into radial or longitudinal tests.

In-situ tests are generally much better indications of rock mass permeability since they take into account the effects of fractures within the mass. Two conditions exist in-situ, one being the fully saturated case and the other the unsaturated case. Water is pumped from the ground via a borehole in the former case. The reverse is true in the latter since water has to be pumped into the ground.

More recent methods use radioactive isotope tracer techniques. These are introduced into water at one location and their arrival time at another point is noted. Isotopes with very short half lives are chosen so as not to contaminate ground water.

Porosity and permeability data are presented together in Table 2.7 since permeability is a function of porosity.

TABLE 2.7. POROSITY AND PERMEABILITY OF BASALT^a

Basalt Type and Location	Permeability (cm s ⁻¹)	Porosity (%)	Remarks	Ref. No.
Andesite-Basalt				
1. Bakuriani Georgia, USSR		21.86		3
Basalts^a				
1. Armenia, USSR		5.0	Dry	38
2. Armenia, USSR		4.0	Dry	38
3. Armenia, USSR		6.0	Dry	38
4. Barra Bonita Dam, Brazil		1.4	Compact	10
5. Dresser, WI		0.16		67
Dresser, WI		0.15		67
6. Germany		1.49		68
7. Jupia Dam, Brazil		2.1	Compact	10
8. Jurimirim Dam, Brazil		4.2		10
9. Melhurb Quarry, Brazil		11.6		10
10. Mussa Quarry, Brazil		5.7		10
11. -	9.4 x 10 ⁻⁶	17.0		13
12. -		0.047		43
13. -		15.0		44
14. -		4.4-5.6		68
15. -		0.8		68
16. -	1.4 x 10 ⁻⁸	7.7	Moderately dense	69

^aBasalt type and location for basalts 11 through 16 are not given.

2.7. REFERENCES

1. Norman, C.E., 'Behavior of Brittle Rock in Multi Increment Creep Tests,' Geol. Soc. Amer., Eng. Geol. Case Histories Number 11, 17-23, 1977.
2. Lombard, D.P., 'The Hugoniot Equation of State of Rocks,' Lawrence Radiation Lab. Rept. UCRL-6311, 1961.
3. Belikov, B.P., 'Plastic Constants of Rock-Forming Minerals and Their Effect on the Elasticity of Rocks,' in Physical and Mechanical Properties of Rocks (Zalesskii, B.V., Editor), Jerusalem, Israel Program for Scientific Translations, 124-40, 1967.
4. Blair, B.E., 'Physical Properties of Mine Rock, Part IV,' Bureau of Mines Rept. RI-5244, 69 pp., 1956.
5. Iida, K., Wada, T., Iida, Y., and Shichi, R., 'Measurements of Creep in Igneous Rocks,' J. Earth Sci., Nagoya Univ., 8(1), 1-16, 1960.
6. Youash, Y.Y., 'Dynamic Physical Properties of Rocks: Part II, Experimental Results,' Proc. 2nd Cong. Int. Soc. Rock Mech., Belgrade, I, 185-95, 1970.
7. Brandon, T.R., 'Rock Mechanics Properties of Typical Foundation Rock Types,' U.S. Bureau of Reclamation Rept. REC-ERC. 74-10, Denver, Colorado, 1974.
8. Griggs, D.T., Turner, F.J., and Heard, H.C., 'Deformation of Rocks at 500-800°C,' Geol. Soc. Am. Mem., 79, 30-104, 1960.
9. Avila, F.P., 'Some Applications of Seismic Field Tests in Rock Media,' Proc. 1st Cong. Int. Soc. Rock Mech., Lisbon, Vol. I, 3-6, 1966.
10. Ruiz, M.D., 'Some Technological Characteristics of 26 Brazilian Rock Types,' Proc. 1st Cong. Int. Soc. Rock Mech., Lisbon, 1, 115-9, 1966.
11. Bamford, W.E., 'Anisotropy and Natural Variability of Rock Properties,' Proc. Symp. Rock Mech., Univ. Sydney, 1-10, 1969.
12. Windes, S.L., 'Physical Properties of Mine Rock,' Bureau of Mines Rept. RI-4459, Part 1, 79 pp., 1949.
13. Morris, D.A. and Johnson, A.I., 'Summary of Hydrologic and Physical Properties of Rock and Soil Material as Analyzed by the Hydrologic Laboratory of the USGS,' Geol. Surv. Water-Supply Pap. (U.S.), 1839-D, 1948-60,--1967.
14. Krech, W.W., Henderson, F.A., and Hjelmstad, K.E., 'A Standard Rock Suite for Rapid Excavation Research,' Bureau of Mines Rept. BM-RI-7865, 1974.
15. Lehnhoff, T.F., Patel, M.R., and Clark, G.B., 'A Thermal Rock Fragmentation Model,' Proc. 15th Symp. Rock Mech., Rapid City, South Dakota, 523-55, 1973.

16. Somerton, W.H., Ward, S.H., and King, M.S., 'Physical Properties of Mohole Test Site Basalt,' J. Geophys. Res., 68(3), 849-56, 1963.
17. Corns, C.F. and Nesbitt, R.H., 'Sliding Stability of Three Dams on Weak Rock Foundations,' Trans. 9th Cong. Large Dams, Istanbul, I, 463-86, 1967.
18. Wei-Ch'ing, F., 'Dynamic Pulse Method of Determining Elastic Parameters of Rock Samples Under High Multi-axial Pressures,' Bull. (Izv.) Acad. Sci., USSR Geophys. Ser., 10, 1004-8, 1961.
19. Hughes, D.S. and Cross, J.H., 'Elastic Wave Velocities in Rocks at High Pressure and Temperature,' Geophysics, 16(4), 577-93, 1951.
20. Balmer, G.G., 'Physical Properties of Some Typical Foundation Rocks,' U.S. Bureau of Reclamation, Concrete Lab. Rept. SP-59, 150 pp., 1953.
21. Miller, R.P., 'Engineering Classification and Index Properties for Intact Rock,' University of Illinois, Ph.D. Thesis, 1965.
22. Wuerker, R.G., 'Annotated Tables of Strength of Rock,' Trans. AIME, Pet. Paper N-663-G, 12 pp., 1956.
23. Windes, S.L., 'Physical Properties of Mine Rock,' Bureau of Mines Rept. BM-RI-4727, 8-11, 1950.
24. Handin, J.W. and Hager, R.V., 'Experimental Deformation of Sedimentary Rocks Under Confining Pressure,' Am. Assoc. Pet. Geol., 41(1), 1-50, 1957.
25. Handin, J.W. and Hager, R.V., 'Experimental Deformation of Sedimentary Rocks Under Confining Pressure,' Am. Assoc. Pet. Geol., 42(12), 2892-934, 1958.
26. Breyer-Kassel, H., 'Über die Elastizität von Gesteinen,' Zeitschr. Geophysik, 6, 98-111, 1930.
27. Ricketts, T.E. and Goldsmith, W., 'Dynamic Properties of Rocks and Composite Structural Materials,' Int. J. Rock Mech. Min. Sci., 7, 315-35, 1970.
28. Livingston, C.W., 'The Natural Arch, the Fracture Pattern, and the Sequence of Failure in Massive Rocks Surrounding an Underground Opening,' Proc. 4th Symp. Rock Mech., Univ. Park, Penn., 197-204, 1961.
29. Christensen, N.I., 'Compressional and Shear Wave Velocities in Basaltic Rocks, Deep Sea Drilling Project, Leg 16,' Initial Rept. Deep Sea Drill. Proj., 16, U.S. Government Printing Office, 647-9, 1973.
30. Christensen, N.I., 'Compressional and Shear Wave Velocities in Elastic Moduli of Basalts, Deep Sea Drilling Project, Leg 19,' Initial Rept. Deep Sea Drill. Proj., 19, U.S. Government Printing Office, 657-9, 1973.

31. Salisbury, M.H. and Christensen, N.I., 'Sonic Velocities and Densities of Basalts from Nazca Plate, DSDP Leg 34,' Initial Rept. Deep Sea Drill. Proj., 34, U.S. Government Printing Office, 543-6, 1976.
32. Carlson, R.L. and Christensen, N.I., 'Velocities, Densities, and Elastic Constants of Basalt and Trachytic Tuff, DSDP Leg 39,' Initial Rept. Deep Sea Drill. Proj., 39, U.S. Government Printing Office, 493-6, 1977.
33. Christensen, N.I., 'Seismic Velocities, Densities, and Elastic Constants of Basalts from DSDP Leg 35,' Initial Rept. Deep Sea Drill. Proj., 35, U.S. Government Printing Office, 335-7, 1976.
34. Habetha, E., 'Large Scale Shear Tests for the Waldeck-II Pump Fed Storage Station Construction Project,' Proc. 2nd Int. Cong. Int. Assoc. Eng. Geol. Sao Paulo, Vol. I, Paper IV-35, 1974.
35. Adams, L.H. and Williamson, E.D., 'On the Compressibility of Minerals and Rocks at High Pressure,' J. Franklin Inst., 195, 475, 1923.
36. Volarovich, B. and Pavlogradsky, V.A., 'Study of the Compressibility of Igneous Rocks at Pressures Up to 5000 kg cg/cm^2 ,' Bull. (Izv.) Acad. Sci. USSR, Geophys. Ser., 5, 486-92, 1959.
37. Bridgman, P.W., 'The Thermal Conductivity and Compressibility of Several Rocks Under High Pressures,' Am. J. Sci., 7, 81-102, 1924.
38. Aslanyan, A.T., Volarovich, M.P., Levykin, A.I., Beguni, A.T., Artunyan, A.V., and Skvortsova, L.S., 'Elastic Wave Velocities in Armenia Basic and Ultrabasic Rocks at High Pressures,' Izv. Akad. Nauk SSSR, Fiz. Zemli, 12(2), 30-8, 1976.
39. Christensen, N.I., Fountain, D.M., and Stewart, R.J., 'Oceanic Crustal Basement: A Comparison of Seismic Properties of D.S.D.P. Basalts and Consolidated Sediments,' Mar. Geol., 15, 215-26, 1973.
40. Christensen, N.I. and Salisbury, M.H., 'Sea Floor Spreading, Progressive Alteration of Layer 2 Basalts, and Associated Changes in Seismic Velocities,' Earth Planet. Sci. Lett., 15(4), 367-75, 1972.
41. Afanas'yev, N.S., Vavakin, V.V., Volarovich, M.P., Levykin, A.I., and Tarkov, A.P., Izv. Akad. Nauk SSSR, Fiz. Zemli, 6, 59-65, 1975.
42. Hyndman, R.D., 'Seismic Velocities of Basalts from DSDP Leg 26,' Initial Rept. Deep Sea Drill. Proj., 26, U.S. Government Printing Office, 509-11, 1974.
43. Hanley, E.J., DeWitt, D.P., and Roy, R.F., 'The Thermal Diffusivity of Eight Well-Characterized Rocks for the Temperature Range 300-1000 K,' Eng. Geol., 12, 31-47, 1978.
44. Saucier, K.L., 'Tests of Rock Cores, Mountain Home, Idaho, and Fairchild, Washington, Areas,' U.S. Army Engineer Waterways Experiment Station, Misc. Paper C-69-12, 291 pp., 1969.

45. Heard, H.C., Abey, A.E., Bonner, B.P., and Schock, R.N., 'Mechanical Behavior of Dry Westerly Granite at High Pressure,' Lawrence Livermore Lab. Rept. UCRL-5164, 14 pp., 1974.
46. Bredthauer, R.O., 'Strength Characteristics of Rock Samples Under Hydrostatic Pressure,' Trans. ASME, 79, 695, 1957.
47. Kumar, A., 'The Effect of Stress Rate and Temperature on the Strength of Basalt and Granite,' Geophysics, 33(3), 1968.
48. Lindholm, U.s., Yeakley, L.M., and Nagy, A., 'The Dynamic Strength and Fracture Properties of Dresser Basalt,' Int. J. Rock Mech. Min. Sci. Geomech. Abstr., 11, 181-91, 1974.
49. Emery, J.J., Hanafy, E.A., and Franklin, J.A., 'Creep Movements Associated with Excavations in Rock,' Conference on Large Ground Movement and Structures, Institution of Structural Engineers, Cardiff, 26 pp., 1977.
50. Price, N.J., Fault and Joint Development in Brittle and Semi-Brittle Rock, Pergamon Press, Oxford, England, 1966.
51. Singh, M.M., 'Strength of Rock,' Chapt. 5 in Physical Properties of Rocks and Minerals (Touloukian, Y.S., Judd, W.R., and Roy, R.F., Volume Editors), McGraw-Hill Book Co., New York, NY, 83-121, 1981.
52. Michelson, A.A., 'The Laws of Elasto-viscous Flow,' J. Geol., 25, 405-10, 1917.
53. Michelson, A.A., 'The Laws of Elasto-viscous Flow II,' J. Geol., 28, 18-24, 1920.
54. Evans, R.H., 'The Elasticity and Plasticity of Rocks and Artificial Stone,' Proc. Leeds Phil. Het. Soc., 3, 145-58, 1936.
55. Griggs, D.T., 'Deformation of Rocks Under High Confining Pressures, Experiments at Room Temperature,' J. Geol., 44, 541-77, 1936.
56. Griggs, D.T., 'Creep of Rocks,' J. Geol., 47(3), 225-51, 1939.
57. Griggs, D.T., 'Experimental Flow of Rocks Under Conditions Favoring Recrystallization,' Geol. Soc. Am. Bull., 51, 1001-22, 1940.
58. Lomnitz, C., 'Creep Measurements in Igneous Rocks,' J. Geol., 64, 473-9, 1956.
59. Ruppeneyt, K.V., Pressure and Displacement of Rocks in Sloping Lava Beds, Uglelekhezdat, Moscow, 228, 1957.
60. Matsushima, S., Disaster Prevention Res. Inst. Bull., Kyoto Univ., 36, 1-9, 1960.
61. Robertson, E.C., 'Viscoelasticity of Rocks,' Proc. Int. Conf. State of Stress in the Earth's Crust, Santa Monica, CA, 180-224, 1963.

62. Boresi, A.P. and Deere, D.U., 'Creep Closure of a Spherical Cavity in an Infinite Medium,' Holmes Marver Inc., Las Vegas, 1963.
63. Farmer, I.W., Engineering Properties of Rocks, Sporr, London, 1968.
64. Singh, D.P., 'A Study of Creep of Rocks,' Int. J. Rock Mech. Min. Soc. Geomech. Abstr., 12(9), 271-5, 1975.
65. Warversuk, W.R. and Brown, W.S., 'Creep Fracture in Rock in Uniaxial Compression,' Univ. Utah, Salt Lake City, UT, Ref. No. UTEC-ME-71-242, 1971.
66. Afronz, A. and Harvey, J.M., 'Rheology of Rocks Within the Soft to Medium Strength Range,' Int. J. Rock Mech. Min. Sci., 11, 281-90, 1974.
67. Krech, W.W., Henderson, F.A., and Hjelmstad, K.E., 'A Standard Rock Suite for Rapid Excavation Research,' Bureau of Mines Rept. BM-RI-7865, 29 pp., 1974.
68. Schoeller, H., 'A Monographic Compilation of Data on the Occurrence, Migration, and Properties of Ground Waters, the Characteristics of Aquifers and Water Supply Investigations, Exploitations, and Reserves,' in Les eaux Souterraines, Masson, Paris, 642 pp., 1962.
69. Davis, S.N., Flow Through Porous Media, (DeWeist, R.J.M., Editor), Academic Press, New York, NY, 34-89, 1969.

2.8. SYMBOLS AND UNITS, AND CONVERSION FACTORS

2.8.1. Symbols and Units

<u>Symbol</u>	<u>Name</u>	<u>Unit</u>
A	cross-sectional area	cm ²
E	Young's modulus; modulus of elasticity	GPa
G	shear modulus; modulus of rigidity	GPa
H	shore hardness	—
K	bulk modulus	GPa
1/K	compressibility	GPa ⁻¹
k	permeability	cm s ⁻¹
P	confining pressure	GPa
p	porosity	%
V _P	longitudinal wave velocity; compressional wave velocity; P wave velocity	km s ⁻¹
V _S	transverse wave velocity; shear wave velocity; S wave velocity	km s ⁻¹
ε	strain	%, in/in
ε̇	strain rate	s ⁻¹
η	viscosity	centipoise
μ	Poisson's ratio	dimensionless
ρ	density	g cm ⁻³
σ	normal stress	GPa
σ _c	compressive strength	MPa
σ _t	tensile strength	MPa
σ _{ult}	ultimate strength	MPa
σ ₁	major principal stress	GPa
σ ₃	minor principal stress	GPa
τ	shear stress	GPa

2.8.2. Conversion Factors

Pressure

<u>To convert from</u>	<u>to</u>	<u>Multiply by</u>
MPa	lb in ⁻¹ (psi)	1.45138 x 10 ²
MPa	kbar	1 x 10 ⁻²
GPa	lb in ⁻² (psi)	1.45138 x 10 ⁵
GPa	kbar	10
	kbar	10 x 10 ³

Density

<u>To convert from</u>	<u>to</u>	<u>Multiply by</u>
kg · m ⁻³	lb · ft ⁻³	0.06243
kg · m ⁻³	g · cm ⁻³	1 x 10 ⁻³

Temperature

<u>To convert from</u>	<u>to</u>	<u>Subtract</u>
K	°C	273.15

CHAPTER 3

THERMOPHYSICAL PROPERTIES

P. D. Desai*

CONTENTS

	<u>Page</u>
3.1. INTRODUCTION -----	2
3.2. REVIEW OF MEASUREMENT METHODS FOR THERMOPHYSICAL PROPERTIES -----	2
3.2.1. Methods for Thermal Conductivity Measurements -----	2
3.2.1.1. Steady State Methods -----	2
3.2.1.2. Non-Steady State Methods -----	4
3.2.2. Methods for Thermal Linear Expansion Measurements -----	5
3.2.2.1. Interferometer -----	5
3.2.2.2. Dilatometer -----	6
3.2.3. Methods for Specific Heat Measurements -----	7
3.2.3.1. Drop Isothermal Water Calorimeter -----	7
3.2.3.2. Drop Copper Block Calorimeter -----	8
3.2.3.3. Adiabatic Calorimeter -----	8
3.2.4. Methods for Thermal Diffusivity Measurements -----	9
3.2.4.1. Transient Heat Flow Methods -----	9
3.2.4.2. Periodic Heat Flow Methods -----	11
3.3. THERMAL CONDUCTIVITY -----	12
3.4. THERMAL LINEAR EXPANSION -----	35
3.5. SPECIFIC HEAT -----	52
3.6. THERMAL DIFFUSIVITY -----	64
3.7. REFERENCES -----	86
3.8. SYMBOLS AND UNITS, AND CONVERSION FACTORS -----	92

* Center for Information and Numerical Data Analysis and Synthesis (CINDAS),
Purdue University, 2595 Yeager Road, West Lafayette, Indiana 47906.

3.1. INTRODUCTION

The data and information for the thermophysical properties (thermal conductivity, thermal linear expansion, specific heat, and thermal diffusivity) of basalt are presented and discussed. Even though there have been extensive measurements made on basalts from various locations, it is still difficult to generate recommended values in many cases, which arises from the very poorly characterizable nature of rocks and from the large variations in the mineralogical compositions in the basalt samples from various locations. The basalt samples for which the properties were reported, in many cases, were poorly characterized and, as a result, the large variations in these properties could not be adequately explained. Because of these difficulties, experimental data and information for each of the properties are given in graphical and tabular forms in their respective sections. Some attempt has been made to analyze the data wherever possible.

Preceding the presentation and discussion of the data, a brief review of the method for the measurement of the various thermophysical properties is given.

3.2 REVIEW OF MEASUREMENT METHODS FOR THERMOPHYSICAL PROPERTIES

Several experimental methods and their modifications for measuring the thermophysical properties of solids have been developed. Only the methods which are used for measuring thermophysical properties of rocks are briefly described below. For comprehensive reviews of experimental methods, the reader is referred to the reference works on thermal conductivity [1,2], thermal expansion [3-5], specific heat [6,7], and thermal diffusivity [2,9].

3.2.1. Methods for Thermal Conductivity Measurements

The methods for the measurement of the thermal conductivity of rock can be classified into two categories: the steady state and the non-steady state methods.

3.2.1.1. Steady State Methods

In steady state methods, the test specimen is subjected to a steady heat flow and a temperature gradient which is time invariant. The thermal

conductivity is determined by measuring the rate of heat flow per unit area and the temperature gradient across the specimen. Some of the most commonly used steady state methods are described below.

In the 'longitudinal' method the flow of heat is restricted in the axial direction of a rod (or disk) specimen. The radial heat loss or gain is prevented or minimized and evaluated. The thermal conductivity is then determined from the equation

$$k = - \frac{q/A}{\Delta T/\Delta x} = \frac{q\Delta x}{A\Delta T} \quad (3.1)$$

where k is the average thermal conductivity corresponding to the temperature $1/2 (T_1+T_2)$, $\Delta T = T_2-T_1$, q is the rate of heat flow, A is the cross-sectional area of the specimen, and Δx is the distance between points of temperature measurements for T_1 and T_2 .

This method can be further divided into absolute and comparative methods according to the means of measuring the heat flow. In the absolute method, the rate of heat flow is directly determined, while in the comparative method the rate of heat flow is calculated from the temperature gradient over a reference standard sample of known thermal conductivity which is placed in series with the specimen.

Most of the specimens used in the 'radial' method are in the form of a cylinder with a coaxial central hole containing a heater or a heat sink. The thermal conductivity is calculated from the expression

$$k = \frac{q \ln (r_2/r_1)}{2\pi L(T_1-T_2)} \quad (3.2)$$

where L is the length of the central heater and T_1 and T_2 are temperatures measured at radii r_1 and r_2 , respectively.

A variant of this method is the concentric cylinder method, which is used mainly to measure the thermal conductivity of a loose-filled material such as soil. This method can be comparative by using a cylindrical specimen surrounded by a concentric cylindrical reference standard sample of known thermal conductivity.

The essential part of the 'Thermal Comparator' is an insulated probe with a projecting tip. The probe is integral with a thermal reservoir held at a

temperature about 15 to 20 degrees above room temperature. A surface thermocouple is mounted at the tip of the probe and is differentially connected to the thermal reservoir for the measurement of the temperature difference between the reservoir and the tip.

In operation, the probe is gently placed on the surface of the test material. Upon contact of the probe tip of known thermal conductivity k_1 and originally at temperature T_1 with the surface of the test material of thermal conductivity k_2 and at room temperature T_2 , the temperature of the probe tip drops quickly to an intermediate temperature T , given by the expression

$$T_1 - T = (T_1 - T_2) \frac{k_2}{k_1 + k_2} \quad (3.3)$$

This temperature difference is registered by the emf reading of the differential thermocouple after a brief transient period (1 to 2 seconds) has elapsed.

From the emf readings of tests on a series of reference standard samples of known thermal conductivity, a calibration curve is obtained, and the thermal conductivity of an unknown specimen can, thus, be determined from the emf reading through the calibration curve.

3.2.1.2. Non-Steady State Methods

In non-steady state methods, the temperature distribution in the specimen varies with time. The rate of temperature change at certain positions along the specimen is measured in the experiment. Few of the non-steady state methods determine the thermal conductivity directly, and most of them determine the thermal diffusivity, from which the thermal conductivity is calculated with an additional knowledge of the density and specific heat of the test material. In this subsection, only the line heat source and probe methods which determine the thermal conductivity directly are discussed. Those transient heat flow and periodic heat flow methods which determine the thermal diffusivity will be discussed in the next section.

In the 'line heat source' method a long thin heater wire, which serves as a line heat source, is embedded in a large specimen initially at uniform temperature. The heater provides a constant heat, q , per unit time and length, and the temperature at a point in the specimen is recorded as a

function of time. The thermal conductivity is given by the expression

$$k = \frac{q}{4\pi (T_2 - T_1)} \ln \frac{t_2}{t_1} \quad (3.4)$$

where T_1 and T_2 are the temperatures measured at the times t_1 and t_2 , respectively.

The 'probe' method is a more practical line heat source method in which the line heat source is enclosed inside a probe for protection and for easy insertion into a sample. This method can be used for field measurements of the thermal conductivity of rock and soil.

3.2.2. Methods for Thermal Linear Expansion Measurements

The thermal linear expansion, $\Delta L/L$, is the total length change from a reference temperature to a given temperature per length at reference temperature. 293 K is used as the reference temperature. The coefficient of thermal linear expansion, β , is the temperature derivative of the thermal linear expansion. Thus, they are given by the expressions:

$$\frac{\Delta L}{L_0} = \frac{L_T - L_{293}}{L_{293}} \quad (3.5)$$

$$\beta = \frac{d}{dT} \frac{\Delta L}{L_0} = \frac{1}{L_{293}} \frac{dL}{dT} \quad (3.6)$$

A number of different methods for measuring the thermal linear expansion of solids were developed during the last 50 years. A variety of methods and modifications are required for various classes of materials. Among the methods used for rocks, the dilatometric method, which is of intermediate sensitivity, is the most commonly used. The interferometric method is one of the most accurate methods used in research laboratories with small specimens of very low thermal conductivity.

3.2.2.1. Interferometer

The most outstanding early method of any notable precision was due to Fizeau [9,10]. This method was significantly modified in recent years [11-14]. In this method the specimen is placed vertically between two transparent fused quartz plates, each about 4 mm thick and reasonably free from any imperfections. The surfaces of each plate should be flat within one-

fifth of a fringe and inclined to each other at an angle of 20' of arc. This is set in an electric furnace or a cooling chamber. When plates are illuminated normally with monochromatic light, a set of interference fringes is produced by the interference of light reflected between the lower surface of the upper plate and upper surface of lower plate. The fringes are observed by means of a viewing device. Changing the temperature of the specimen brings about a change in length which causes a corresponding movement of the interference fringes past a reference mark on the lower surface of the upper plate. From observed displacement of the fringes, the thermal linear expansion can be determined from the expression:

$$\frac{\Delta L}{L} = \frac{\lambda N}{2L} + \frac{A}{L} \quad (3.7)$$

where L is the initial length of the specimen, ΔL is the change in length, λ is the wavelength of monochromatic light, N is the number of fringes that passed the reference mark, and A is the correction if the specimen is heated or cooled in other than vacuum.

3.2.2.2. Dilatometer

This consists of a quartz tube used to support the specimen and a fused quartz rod to transmit the specimen's dimensional change with temperature to a dial recorder. Quartz is used because of its low thermal expansion. Extensometer is used for measuring length changes over a length of at least 0.05 inches. Dial indicator and linear variable transformer are used the most for measuring length changes, but many other types like optical levers, strain gauge, and optical gratings are also used.

The push-rod dilatometer method for measuring thermal expansion is experimentally simple, reliable, and easy to automate [1]. With this method, the expansion of the specimen is transferred out of the heated zone to an extensometer by means of rods (or tubes) of some stable material. The expansion of the specimen is given by

$$\frac{\Delta L}{L_0} = c_0 \frac{(\Delta L)_a}{L_0} + c_1 \quad (3.8)$$

where $(\Delta L)_a$ is the apparent change in length as calculated from the difference between the extensometer readings at two different temperatures, and c_0 and c_1 are calibration constants for the system. If the reference rod is made the

same length as the push rod and a second specimen placed on the base plate, the dilatometer will measure the difference between the specimens [16]. The difference, or differential expansion, is given by

$$\frac{(\Delta L)_2}{L_0} - \frac{(\Delta L)_1}{L_0} = c_0 \frac{(\Delta L)_a}{L_0} + c_1 \quad (3.9)$$

When used this way the dilatometer can have a very high sensitivity. This technique is also very useful for quality control measurements and for studying phase transitions.

One of the most common sources of error in using dilatometers is the measurement of temperature. All too often the temperature that is measured is not the temperature of the specimen. If a thermocouple is used, care must be taken to ensure that its junctions and specimen are at the same temperature; they can be at different temperatures even if in contact with each other. Another common source of error, especially for flexible materials or materials near their softening temperatures, is deformation under the load of the push rod. Special techniques such as increasing sample diameter, reducing push rod pressure, and using horizontal mounts must be used for these soft materials.

The uncertainty of this method depends on the quality of the push rod used and precision of construction. Results of two or three percent uncertainty may be achieved routinely.

3.2.3. Methods for Specific Heat Measurements

The specific heat, c_p , is the amount of energy required to raise the temperature of one unit of mass by one unit of temperature at constant pressure. There are several methods for the practical and precise determination of the specific heat of solids. Many variants, modifications, and improvements are reported in the literature. The most commonly used methods for rock are as follows.

3.2.3.1. Drop Isothermal Water Calorimeter

In the drop isothermal water calorimeter method the specimen is heated and dropped directly into the calorimeter containing water and enclosed in an isothermal jacket. The top is covered by copper plates. The water is stirred to ensure a uniform temperature. The rise of temperature is measured accurately. The enthalpy change of the specimen is determined from the known

heat capacity of the calorimeter and its temperature rise, and the specific heat is given by the expression

$$c_p = \frac{d(H_T - H_{298.15})}{dT} \quad (3.10)$$

where H is the enthalpy of the specimen.

3.2.3.2. Drop Copper Block Calorimeter

In the drop copper block calorimeter method the sample is heated within a capsule of known heat content in a furnace to a measured temperature and dropped into a copper calorimeter whose heat capacity has been previously determined. The temperature of calorimeter is measured using a special bridge network of copper and manganin resistances. The heat released from the specimen is distributed to the copper calorimeter. The change in enthalpy of the specimen is measured in terms of the amount of heat absorbed by the copper block in changing from its initial to final temperature. Thus,

$$c_p = \frac{d}{dT} (H_T - H_{298.15}) \quad (3.11)$$

3.2.3.3. Adiabatic Calorimeter

The adiabatic calorimeter method is suited for granular materials, fine powders, and materials with low thermal diffusivity and thermal conductivity. The calorimeter consists of a thin-walled, spherical shell made of two copper hemispheres welded together. At the center of this shell a heater element is placed which is made of a hollow copper sphere of 5 mm wall thickness enclosing the electrical heater coil wound onto a ceramic sphere. During the measurement, the gap between the two spheres is filled with test material which is introduced into the gap through a hole at the bottom of the calorimeter. The calorimeter is surrounded by a thermostat made of a thick-walled copper sphere heated electrically and regulated very sensitively to follow the surface temperature of the calorimeter. The thermostat and guard heaters are adjusted to heat up the instrument to a desired temperature. As soon as this is reached, the power input is reduced until it just compensates the heat loss. The calorimeter itself follows the temperature change more slowly. Heater element on the calorimeter is turned on. Enough time is allowed to check that the temperature of all parts of the calorimeter increases at the same rate. The time needed to increase the temperature by a

fixed millivolt increment is measured to get the heat capacity of the calorimeter. The calorimeter is then filled with the specimen and the experiments are repeated. Knowing the heat capacity of the calorimeter, the heat capacity of the specimen can be derived as follows:

$$c_p = \frac{1}{m} \frac{dQ/dt}{dT/dt} - W_c \quad (3.12)$$

where dQ/dt is the heat input per unit time, W_c is the specific heat of the calorimeter, and m is the mass of the specimen.

Additional discussion of the precision and accuracy attainable with adiabatic calorimeters is reported by Schmidt and Leidenfrost [17].

3.2.4. Methods for Thermal Diffusivity Measurements

The method used for the measurement of thermal diffusivity fall into two major categories: the transient heat flow and the periodic heat flow methods. These methods can also be subdivided into longitudinal and radial methods according to the direction of heat flow.

3.2.4.1. Transient Heat Flow Methods

In 'transient heat flow' methods heat is suddenly added to or removed from a specimen initially at a uniform temperature and the thermal diffusivity is determined from a measurement of the temperature as a function of time at one or more points along the specimen.

In the 'longitudinal method' one end of a rod of uniform cross section and initially at a uniform temperature is subjected to a short heating pulse, and the thermal diffusivity, α , is calculated from a measurement of the temperatures as a function of time at properly chosen points along the rod. The one-dimensional heat flow equation

$$\frac{\partial T}{\partial t} = \alpha \frac{d^2 T}{dx^2} \quad (3.13)$$

may be used for the calculation with boundary conditions applying to a finite rod.

In a variant of this method, steady heating is provided at one end of a rod and the temperatures as a function of time at two or more points along the rod are observed.

Although the 'flash' method is a variant of the longitudinal transient heat flow method using a small thin disk specimen geometry, it has a very special feature which makes it a class of its own. In the 'flash' method, a flash of thermal energy is supplied to one of the surfaces of a disk specimen within a time interval that is short compared with the time required for the resulting transient flow of heat to propagate through the specimen.

In the measurement, a heat source such as flash tube or laser, supplies a flash of energy to the front face of a thin disk specimen and the temperature as a function of time at the rear face is automatically recorded. Heat losses are minimized by making the measurement in a time so short that little cooling can occur. The thermal diffusivity is calculated from the expression

$$\alpha = \frac{0.139 L^2}{t_{1/2}} \quad (3.14)$$

where L is the sample thickness and $t_{1/2}$ is the time required for the rear surface to attain half its maximum increase in temperature.

In the 'radial method' a long cylindrical specimen, initially at uniform temperature, is heated either at the axis or at the outer surface and the temperatures as a function of time at different radial distances are measured.

If the outer surface of a long hollow cylindrical specimen of inner radius, r_0 , is heated at a constant rate and the temperatures, T_1 and T_2 , at two radii, r_1 and r_2 , within the specimen are measured, the thermal diffusivity is given by the expression

$$\alpha = \frac{1}{2(T_2 - T_1)} \frac{\partial T}{\partial t} \frac{1}{2} (r_2^2 - r_1^2) - r_0^2 \ln \frac{r_2}{r_1} \quad (3.15)$$

The above equation assumes that the specimen is isotropic and homogeneous, with α independent of T and that $\partial T / \partial t$ is constant and there is no internal loss of heat.

In another variant of this method, a solid cylindrical specimen is placed within a heated enclosure and fitted with end guards to ensure that all heat flows radially inwards. The specimen is heated rapidly by a constant source of power and temperatures are measured at two points at the longitudinal center of the specimen with radii of r_1 and r_2 . For times sufficiently long for a linear rate of temperature increase to be established

$$\alpha = \frac{r_2^2 - r_1^2}{4(t_2 - t_1)} \quad (3.16)$$

where $t_2 - t_1$ is the time interval between the attainment of a specific temperature at r_2 and r_1 .

3.2.4.2. Periodic Heat Flow Methods

In periodic heat flow methods, the heat supplied to the specimen is modulated to have a fixed period. The resulting temperature wave which propagates through the specimen with the same period is attenuated as it moves along. Consequently, the thermal diffusivity can be determined from measurements of the amplitude decrement and/or phase difference of the temperature waves between certain points in the specimen. In most of the periodic heat flow methods, heat flow is in the longitudinal (axial) direction. However, methods with heat flow in the radial direction have also been used.

The 'longitudinal periodic heat flow' method was first developed by Angstrom and is, therefore, called the Angstrom method. In his first experiments, the middle of a long rod was subjected to periodic heating and cooling for equal time periods and the temperatures as a function of time at two points on the same side of the middle of the rod were measured. Angstrom showed that

$$\frac{k}{dc_p} = \frac{\pi L^2}{t \phi \ln \delta} \quad (3.17)$$

where d is density, c_p is the specific heat at constant pressure, L is the distance between the two observation points, t is the period of the temperature wave, ϕ is the phase lag of the temperature fluctuations at the two points, and δ is the amplitude ratio of the temperatures at these points. At that time, the quantity $\alpha \equiv k/dc_p$ had not been defined.

A long rod could equally well be heated and cooled periodically at one end as has been done in most later applications of this method. Angstrom's original method was improved and modified subsequently and several versions of the 'Modified Angstrom Methods' have since been reported.

The Angstrom method which uses a long rod has its limitations. In some cases, specimens in the form of long rods may not be available, and in other

cases, such as in the measurements on poor conductors at high temperatures, heat guarding to prevent lateral heat losses for a long rod may be difficult. Consequently, methods using specimens in the form of small plate or disk have also been developed.

In the 'radial method' the specimen in the form of a cylinder is heated by a heat source capable of producing a periodical temperature variation either at the axis or at the circumference and the radial temperature variations with time are measured. The thermal diffusivity may be calculated from the phase change of the temperature oscillations or from the amplitude variation of the oscillations with frequency.

3.3. THERMAL CONDUCTIVITY

There are over 100 data sets available for the thermal conductivity of basalt [18-41,74] obtained by measurements on a variety of basalts from various locations. Basalt samples used in the above studies range from simulated lunar material to mountains of Washington State (Hanford Site basalts). These can be divided into three major categories: Dresser basalt (data sets 5-9, 30, and 61-66), particulate basalt (data sets 15-29, 31-39, 40-51, 58, and 67-76), and Hanford Site basalts (data sets 77-82, 84-122). Somerton et al. [74] reported the data for augite basalt from Mohole Test Site. For the reasons given in section 3.1, it is rather difficult to generate a set of recommended values which can be applicable to basalts in general. Therefore, a systematic collection of all available data and information is presented in Table 3.1 and shown in Figure 3.1. Since thermal conductivity values for particulate basalts are considerably lower than those for other types, these values are plotted separately in Figure 3.2.

The thermal conductivity of most crystalline rocks above room temperature decreases with increasing temperature. From the data reported in Table 3.1 and Figures 3.1 and 3.2, it is quite clear that this behavior does not always hold true for basalt. Both increasing and decreasing trends with temperature are indicated. This behavior is dependent upon a number of factors, each may affect the thermal conductivity differently. These include porosity, internal

TABLE 1.1. EXPERIMENTAL DATA ON THERMAL CONDUCTIVITY OF BASALT

Data Set No.	Author(s), Year [Ref., No.]	Name and Source	Minerals and/or Chemical Composition		Method Used	Experimental Data		Other Specifications							
			Weight Percent	Volume Percent		T, K	Thermal Conductivity ($\text{W m}^{-1}\text{K}^{-1}$)								
1	Poole, H.H., 1916 [18]				Steady Radial Absolute	364	2.06	Specimen Geometry: Cylinder 3.67 cm dia x 20 cm length.							
						377	2.12								
						406	2.09								
						419	2.04								
						453	2.02								
						463	1.97								
						477	1.97								
						495	1.99								
						538	2.03								
						568	1.93								
						612	1.93								
						651	1.89								
						704	1.85								
						773	1.81								
2	Poole, H.H., 1916 [18]				Steady Radial Absolute	320	1.65	Specimen Geometry: Cylinder 3.6 cm dia x 18.2 cm length.							
						357	1.66								
						383	1.68								
						386	1.59								
						395	1.59								
						402	1.57								
						473	1.72								
						476	1.66								
						520	1.71								
						591	1.65								
						688	1.68								
						678	1.65								
						695	1.66								
						711	1.66								
820	1.65														
871	1.65														
3	Stephens, D.P., 1963 [19]	R.V.S. Basalt, Sample 1, Shot Bo. 12 Hole DR-C and Shot Bo. 11, DR 4 of Project Backboard	Plug Large Iron Mineralite Olivine		Steady Radial Absolute	576	1.75	Density: 2.68 g cm^{-3} . Specimen Geometry: Cylinder (L/D = 5) 45.7 cm length. Texture: Fine grained. Other: Slat grey color; reported circa 15%.							
						595	1.60								
						658	1.78								
						706	1.82								
						751	1.66								
						822	1.86								
						894	1.57								
						964	1.90								
						1041	1.82								
						4	Stephens, D.P., 1963 [19]		Same as above	Plug Large Iron Mineralite Olivine		Steady Radial Absolute	442	1.35	Same as above.
													484	1.46	
													529	1.51	
													585	1.66	
													623	1.78	
712	1.90														
761	1.61														
856	1.61														

TABLE 3.1. EXPERIMENTAL DATA ON THERMAL CONDUCTIVITY OF BASALT (continued)

Data Set No.	Author(s), Year [Ref. No.]	Name and Source	Minerals and/or Chemical Composition		Method Used	Experimental Data		Other Specifications
			Components	Weight Percent		T, K	Thermal Conductivity ($W m^{-1} K^{-1}$)	
5	Marovelli, R.L. and Veith, K.F., 1964 [20]	Dresser Basalt, Dresser, WI	Feldspar (Labradorite) Augite Magnetite	50 40 8	Nonsteady Line Heat Source	298	2.21	Density: 2.97 g cm ⁻³ Specimen Geometry: 12.7-15.2 cm per side. Texture: Mottled grey-green, fine-grained. Other: Block A.
						328	2.12	
						361	2.09	
						374	2.09	
						394	2.09	
6	Marovelli, R.L. and Veith, K.F., 1964 [20]	Same as above	Same as above		Same as above	302	2.34	Same as above except Block C.
						597	2.10	
						855	1.85	
						1074	1.55	
						298	2.21	
7	Marovelli, R.L. and Veith, K.F., 1964 [20]	Same as above	Same as above		Same as above	571	2.11	Same as above except Block D.
						771	1.88	
						1217	1.36	
						294	1.83	
						328	1.83	
8	Marivelli, R.L. and Veith, K.F., 1964 [20]	Same as above	Same as above		Same as above	346	1.75	Same as above except Block B.
						367	1.84	
						383	1.76	
						392	1.81	
						208	3.21	
9	Marovelli, R.L. and Veith, K.F., 1964 [20]	Same as above	Same as above		Same as above	254	3.20	Same as above except Block E.
						298	3.10	
						572	1.50	
						1014	1.38	
						1179	1.21	
10	Murase, T. and McBirney, A.R., 1970 [21]	Columbia River Basalt; Columbia River, OR			Steady Radial Abaxial	1305	1.17	Specimen Geometry: Platinum container, 5 cm dia x 5.5 cm high. Other: Values were corrected to zero porosity; initial measurements were made for molten rock at around 1500 C; cooling cycle.
						1400	0.967	
						1515	1.17	
						1768	2.25	
						300	1.58	
11	Murase, T. and McBirney, A.R., 1970 [21]	Same as above			Same as above	656	1.54	Specimen Geometry: Same as above. Other: Same as above except heating cycle.
						727	1.46	
						878	1.42	
						1077	1.30	
						1277	1.21	
						1383	0.967	
						1480	1.13	
						1578	1.54	
						1679	1.62	

TABLE 3.1. EXPERIMENTAL DATA ON THERMAL CONDUCTIVITY OF BASALT (continued)

Data Set No.	Author(s), Year [Ref. No.]	Name and Source	Minerals and/or Chemical Composition		Method Used	Experimental Data		Other Specifications
			Components	Weight Percent		T, K	Thermal Conductivity ($\text{W m}^{-1}\text{K}^{-1}$)	
12	Murase, T. and McBirney, A.R., 1970 [21]	Synthetic Lunar Sample	Composition of Apollo 11, Sample 22		Steady Radial Absolute	1102	0.962	Porosity: 3%. Specimen Geometry: Platinum container, 5 cm dia x 5.5 cm high. Other: Conductivity values were corrected to zero porosity; initial measurements were for molten rock at 1500 C; cooling cycle.
						1283	0.841	
						1478	0.720	
						1539	0.678	
13	Murase, T. and McBirney, A.R., 1970 [21]	Same as above	Same as above		Same as above	1575	0.598	Same as above except heating cycle.
						1624	0.678	
						1679	0.799	
						1779	1.21	
14	Tadokoro, Y., 1921 [22]	Basalt; Prov. Tamba, Asia	SiO ₂ Al ₂ O ₃ FeO CaO MgO Fe ₂ O ₃ MnO	69.48 11.67 9.43 5.00 2.47 1.00 0.49	Indirect	298	1.44	Density: 2.659 g cm ⁻³ . Texture: Dark grey colored, no vesicular cavities; phenocrysts of plagioclase and olivine both of the order of 0.8 mm in size present very sparingly. Other: Data is obtained from measurements of diffusivity, specific heat and density.
						210	0.137	
						265	0.156	
						319	0.182	
15	Bennett, E.C., Wood, H.L., Jaffe, L.D., and Martens, H.E., 1962 [23]	Olivine Basalt, Pisgah Crater; San Bernardino, CA			Indirect	366	0.180	Density: 1.36 g cm ⁻³ . Other: Particle size 0.30-0.42 mm; reported error ±15%; values obtained from measurements of diffusivity, specific heat, and density.
						210	0.164	
						265	0.188	
						319	0.201	
16	Bennett, E.C., et al., 1962 [23]	Same as above			Indirect	366	0.194	Density: 1.56 g cm ⁻³ . Other: Same as above.
						210	0.164	
						265	0.188	
						319	0.201	
17	Bennett, E.C., et al., 1962 [23]	Same as above			Indirect	320	0.005	Density: 1.56 g cm ⁻³ . Other: Same as above except data measured at 5 x 10 ⁻³ mm Hg pressure.
						365	0.007	
						216	0.004	
						266	0.004	
18	Bennett, E.C., et al., 1962 [23]	Same as above			Indirect	319	0.004	Density: 1.56 g cm ⁻³ . Other: Same as above except values are at 5 x 10 ⁻⁶ mm Hg pressure.
						362	0.005	
						216	0.004	
						266	0.004	

TABLE 3.1. EXPERIMENTAL DATA ON THERMAL CONDUCTIVITY OF BASALT (continued)

Data Set No.	Author(s), Year [Ref. No.]	Name and Source	Minerals and/or Chemical Composition		Method Used	Experimental Data		Other Specifications
			Componenta	Weight Percent		T, K	Thermal Conductivity ($W m^{-1} K^{-1}$)	
19	Bennett, E.C., et al., 1962 [23]	Olivine Basalt, Pisgah Crater; San Bernardino, CA			Indirect	209	0.142	Density: 1.49 g cm ⁻³ . Other: Particle size <0.42 mm; reported error ±15%; values obtained from measurements of diffusivity, specific heat and density.
						250	0.254	
						267	0.165	
						280	0.246	
						338	0.156	
367	0.228							
20	Bennett, E.C., et al., 1962 [23]	Same as above			Indirect	325	0.275	Density: 1.65 g cm ⁻³ . Other: Same as above.
						367	0.303	
21	Bennett, E.C., et al., 1962 [23]	Same as above			Indirect	207	0.223	Density: 1.95 g cm ⁻³ . Other: Same as above except values are at 5×10^{-6} mm Hg; values obtained from measurements of diffusivity, specific heat and density.
						266	0.256	
22	Bennett, E.C., et al., 1962 [23]	Same as above			Indirect	265	0.0017	Density: 1.49 g cm ⁻³ . Other: Same as above.
						320	0.0024	
						362	0.0029	
23	Bennett, E.C., et al., 1962 [23]	Same as above			Indirect	319	0.0041	Density: 1.65 g cm ⁻³ . Other: Same as above.
						321	0.0044	
						360	0.0044	
						367	0.0036	
24	Bennett, E.C., et al., 1962 [23]	Same as above			Indirect	217	0.0015	Density: 1.57 g cm ⁻³ . Other: Same as above.
						266	0.0018	
25	Bennett, E.C., et al., 1962 [23]	Same as above			Indirect	242	0.0017	Density: 1.75 g cm ⁻³ . Other: Same as above.
26	Bennett, E.C., et al., 1962 [23]	Same as above			Indirect	210	0.100	Density: 1.14 g cm ⁻³ . Other: Particle size <0.105 mm; reported error ±15%; values obtained from measurements of diffusivity, specific heat and density.
						266	0.117	
						320	0.118	
						367	0.143	
27	Bennett, E.C., et al., 1962 [23]	Same as above			Indirect	209	0.161	Density: 1.57 g cm ⁻³ . Other: Same as above.
						266	0.183	
						319	0.195	
28	Bennett, E.C., et al., 1962 [23]	Same as above			Indirect	365	0.235	Density: 1.14 g cm ⁻³ . Other: Same as above except values are at 5×10^{-6} mm Hg pressure.
						319	0.0015	
29	Bennett, E.C., et al., 1962 [23]	Same as above			Indirect	363	0.0016	Density: 1.57 g cm ⁻³ . Other: Same as Data Set 28.
						213	0.0027	
						264	0.0026	
						318	0.0031	
						362	0.0031	

TABLE 3.1. EXPERIMENTAL DATA ON THERMAL CONDUCTIVITY OF BASALT (continued)

Data Set No.	Author(s), Year [Ref. No.]	Name and Source	Minerals and/or Chemical Composition		Method Used		Experimental Data		Other Specifications
			Components	Weight Percent	Volume Percent	T, K	Thermal Conductivity ($W m^{-1} K^{-1}$)		
30	Navarro, R.A. and DeWitt, D.P., 1974 [24]	Dresser Basalt; Dresser, WI			Nonsteady Line Heat Source	300	2.72 2.54	Other: Mercury and silicon grease used respectively as contact agents; reported error $\pm 2\%$ and $\pm 5\%$ respectively.	
31	Wechsler, A.E. and Glaser, P.E., 1964 [25,26]	Basalt Powder			Nonsteady Line Heat Source	289	0.0018	Test Environment: Evacuated air, 6.6×10^{-13} atmosphere. Other: Particle size 0.020 mm.	
32	Wechsler, A.E. and Glaser, P.E., 1964 [25,26]	Basalt Powder			Same as above	283	0.0020	Density: $1.27 g cm^{-3}$. Test Environment: Evacuated air, 1.1×10^{-7} atmosphere. Other: Particle size 0.044-0.104 mm.	
33	Wechsler, A.E. and Glaser, P.E., 1964 [25,26]	Basalt Powder			Same as above	331	0.0027	Density: $1.27 g cm^{-3}$. Test Environment: Evacuated air, 5.3×10^{-7} atmosphere. Other: Same as above.	
34	Wechsler, A.E. and Glaser, P.E., 1964 [25,26]	Basalt Powder			Same as above	294 295	0.192 0.165	Test Environment: Air, pressure 1.01 atmosphere. Other: Particle size 0.104-0.150 mm.	
35	Wechsler, A.E. and Glaser, P.E., 1964 [25,26]	Basalt Powder			Same as above	302 303	0.0016 0.0015	Test Environment: Evacuated air, 7.9×10^{-9} atmosphere. Other: Same as above.	
36	Wechsler, A.E. and Glaser, P.E., 1964 [25,26]	Basalt Powder			Same as above	284 341	0.0015 0.0020	Test Environment: Evacuated air, 9.2×10^{-13} atmosphere. Other: Same as above.	
37	Wechsler, A.E. and Glaser, P.E., 1964 [25,26]	Basalt Powder			Same as above	281 282 329 331 334	0.0016 0.0015 0.0029 0.0021 0.0023	Test Environment: Evacuated air, 6.6×10^{-13} atmosphere. Other: Same as above.	
38	Wechsler, A.E. and Glaser, P.E., 1964 [25,26]	Basalt Powder			Same as above	280 300	0.0012 0.0015	Test Environment: Evacuated air, 2.6×10^{-13} atmosphere. Other: Same as above.	
39	Wechsler, A.E. and Simon, I., 1966 [27]	Basalt Powder			Nonsteady Line Heat Source	184 189 229 231 295	0.00075 0.00084 0.00086 0.00092 0.00112	Density: $1.42 g cm^{-3}$. Test Environment: Evacuated air, 7.9×10^{-11} atmosphere. Other: Particle size 0.044-0.074 mm; reported error $\pm 8\%$.	
40	Wechsler, A.E. and Simon, I., 1966 [27]	Basalt Powder			Same as above	298 326	0.00122 0.00165	Density: $1.42 g cm^{-3}$. Test Environment: Evacuated air, 2.0×10^{-9} atmosphere. Other: Same as above.	
41	Wechsler, A.E. and Simon, I., 1966 [27]	Basalt Powder			Same as above	298 299	0.00126 0.00126	Density: $1.42 g cm^{-3}$. Test Environment: Evacuated air, 2.6×10^{-9} atmosphere. Other: Same as above.	

TABLE 3.1. EXPERIMENTAL DATA ON THERMAL CONDUCTIVITY OF BASALT (continued)

Data Set No.	Author(s), Year [Ref. No.]	Name and Source	Minerals and/or Chemical Composition		Experimental Data		Method Used	Other Specifications
			Components	Weight Percent	T, K	Thermal Conductivity ($\text{W m}^{-1} \text{K}^{-1}$)		
42	Wechsler, A.E. and Simon, I., 1966 [27]	Basalt Powder			351	0.00144	Same as above	Density: 1.43 g cm^{-3} . Test Environment: Evacuated air, 1.3×10^{-9} atmosphere. Other: Same as above.
43	Wechsler, A.E. and Simon, I., 1966 [27]	Basalt Powder			231	0.00092	Same as above	Density: 1.43 g cm^{-3} . Test Environment: Evacuated air, 9.2×10^{-11} atmosphere. Other: Same as above.
44	Wechsler, A.E. and Simon, I., 1966 [27]	Basalt Powder			175 177	0.00122 0.00128	Same as above	Density: 1.36 g cm^{-3} . Test Environment: Evacuated air, 2.0×10^{-11} atmosphere. Other: Particle size 0.010-0.037 mm.
45	Wechsler, A.E. and Simon, I., 1966 [27]	Basalt Powder			173	0.00117	Same as above	Density: 1.36 g cm^{-3} . Test Environment: Evacuated air, 2.2×10^{-11} atmosphere. Other: Same as above.
46	Wechsler, A.E. and Simon, I., 1966 [27]	Basalt Powder			296	0.00172	Same as above	Density: 1.36 g cm^{-3} . Test Environment: Evacuated air, 2.4×10^{-11} atmosphere. Other: Same as above.
47	Wechsler, A.E. and Simon, I., 1966 [27]	Basalt Powder			227 229	0.00142 0.00146	Same as above	Density: 1.36 g cm^{-3} . Test Environment: Evacuated air, 2.6×10^{-11} atmosphere. Other: Same as above.
48	Wechsler, A.E. and Simon, I., 1966 [27]	Basalt Powder			296	0.00181	Same as above	Density: 1.36 g cm^{-3} . Test Environment: Evacuated air, 3.9×10^{-11} atmosphere. Other: Same as above.
49	Wechsler, A.E. and Simon, I., 1966 [27]	Basalt Powder			297	0.00186	Same as above	Density: 1.36 g cm^{-3} . Test Environment: Evacuated air, 7.9×10^{-11} atmosphere. Other: Same as above.
50	Wechsler, A.E. and Simon, I., 1966 [27]	Basalt Powder			300	0.00179	Same as above	Density: 1.36 g cm^{-3} . Test Environment: Evacuated air, 1.3×10^{-8} atmosphere. Other: Same as above.
51	Wechsler, A.E. and Simon, I., 1966 [27]	Basalt Powder			356 356	0.00197 0.00208	Same as above	Density: 1.36 g cm^{-3} . Test Environment: Evacuated air, 3.9×10^{-9} atmosphere. Other: Same as above.
52	Johnson, S.A., 1974 [28]	Tholeiitic Basalt; N.E. of Madras, OR			293	1.57	Steady state Longitudinal Comparative	Density: 2.86 g cm^{-3} . Porosity: 2%. Texture: Asphanitic. Other: Dry sample.

TABLE 3.1. EXPERIMENTAL DATA ON THERMAL CONDUCTIVITY OF BASALT (continued)

Data Set No.	Author(s), Year [Ref. No.]	Name and Source	Minerals and/or Chemical Composition Components	Chemical Composition		Method Used	Experimental Data		Other Specifications
				Weight Percent	Volume Percent		T, K	Thermal Conductivity ($\text{W m}^{-1} \text{K}^{-1}$)	
53	Johnson, S.A., 1974 [28]	Same as above			Same as above	293	1.54	Density: 2.84 g cm^{-3} . Porosity: 2%. Texture: Aphanitic. Other: Sample saturated with water.	
54	Sass, J.H., 1964 [29]	Golden Mile Basalt (Amphibolitic); Kalgoorlie, Australia			Steady Longitudinal Comparative	301	4.1	Specimen Geometry: Disk 3.5 cm dia, 6 mm thick. Other: Reported error 13.5%; average of 11 specimens tested.	
55	Sass, J.H., 1964 [29]	Bore Hole No. C-79; Norseman, Australia	Plagioclase, Hornblende, Pyroxene, Epidote, Chlorite, Fe-oxide	major	Same as above	301	2.8	Specimen Geometry: Same as above. Other: Reported error 11.6%; average of 7 specimens tested.	
56	Sass, J.H., 1964 [29]	Golden Mile Basalt (Chloritic); Kalgoorlie, Australia		minor	Same as above	301	4.4	Specimen Geometry: Same as above. Other: Reported error 11.8%; average of 28 specimens tested.	
57	Glaser, P.E., Wechsler, A.E., and Germesles, A.E., 1965 [30]	Basalt Lava			Steady Longitudinal Absolute	223	0.222	Density: 2.08 g cm^{-3} . Other: Measured at 1.32×10^{-5} atm pressure.	
58	Glaser, P.E., et al., 1965 [30]	Olivine Basalt			Non-Steady Line Heat Source	223	0.0017	Density: 1.5 g cm^{-3} . Other: Powdered specimen, particle size 10-200 μ ; measured at 1.32×10^{-5} atm pressure.	
59	Horai, K.I. and Baldrige, S., 1972 [31]	Kalippa Olivine Basalt; Uvalde, TX			Steady Longitudinal Comparative	296	2.29	Density: 3.156 g cm^{-3} . Specimen Geometry: Disk 4.75 cm dia, 6.8-9.3 mm thick. Other: Reported error 15%.	
60	Horai, K.I. and Baldrige, S., 1972 [31]	Same as above			Non-Steady Line Heat Source	296	2.30	Density: 3.158 g cm^{-3} . Porosity: 0.1%. Texture: Pulverized specimen with maximum grain size <0.1 mm. Other: Specimen water saturated; reported error 15%.	
61	Morgan, M.T. and West, G.A., 1980 [32]	Dresser Basalt; Dresser, WI			Cut-Bar Comparator	319 365 411 458 505 540	3.14 3.10 2.97 2.86 2.80 2.72	Density: 3.02 g cm^{-3} . Specimen Geometry: 2 in. dia and 0.75 in. thick prepared from cores (cores were taken from rock cube perpendicular to each of the cube faces). Other: Samples furnished by the Bureau of Mines rough cut 15-20 cm	

TABLE 3.1. EXPERIMENTAL DATA ON THERMAL CONDUCTIVITY OF BASALT (continued)

Data Set No.	Author(s), Year [Ref. No.]	Name and Source	Minerals and/or Chemical Composition		Method Used	Experimental Data		Other Specifications
			Components	Weight Percent		T, K	Thermal Conductivity ($W m^{-1} K^{-1}$)	
61								
cont.								
62	Morgan, M.T. and West, G.A., 1980 [32]	Same as above			Same as above	319 365 411 459 506 540	3.21 3.05 2.93 2.84 2.77 2.72	Density: $3.02 g cm^{-3}$ Specimen Geometry: Same as above. Other: Same as above except cooling cycle; thermal conductivity decreased by 1% after first heating; repeated cyclic heating had no further effects.
63	Morgan, M.T. and West, G.A., 1980 [32]	Same as above			Same as above	319 365 411 459 506 539	3.11 3.04 2.92 2.88 2.76 2.72	Density: $3.02 g cm^{-3}$ Specimen Geometry: Same as above. Other: Same as above except data is for y-core; heating cycle.
64	Morgan, M.T. and West, G.A., 1980 [32]	Same as above			Same as above	319 365 411 458 505 540	3.08 2.99 2.92 2.83 2.75 2.71	Density: $3.02 g cm^{-3}$ Specimen Geometry: Same as above. Other: Same as above except data is for z-core; heating cycle; thermal conductivity decreased 1% for cooling measurements.
65	Morgan, M.T. and West, G.A., 1980 [32]	Same as above			Same as above	319 365 411 458 505 540	3.07 2.98 2.91 2.82 2.75 2.71	Density: $3.02 g cm^{-3}$ Specimen Geometry: Same as above. Other: Same as above except cooling cycle; thermal conductivity decreased 1% after first heating; repeated cyclic heating had no further effects.
66	Hanley, E.J., DeWitt, D.P., and Taylor, R.E., 1977 [33]	Dresser Basalt; Dresser, WI			Indirect	300	2.84	Values calculated from thermal diffusivity and specific heat values.
67	Fountain, J.A. and West, E.A., 1970 [34]	Tholeiitic Particulate Basalt; OR	SiO ₂ Al ₂ O ₃ FeO CaO MgO Na ₂ O Fe ₂ O ₃	51 14 8.8 8.0 4.4 3.4 3.4	Line Heat Source	179 181 183 186 187 188 191	0.00059 0.00056 0.00060 0.00061 0.00064 0.00057 0.00069	Density: $0.79 g cm^{-3}$. Other: Sample baked in vacuum oven at 525 K for 5 days; particle of size 37-62 microns dia; measurements in 10^{-6} torr pressure; the data is approximately represented by $k = 0.509 \times 10^{-3} + 0.169 - 10T^{-1}$.

TABLE 3.1. EXPERIMENTAL DATA ON THERMAL CONDUCTIVITY OF BASALT (continued)

Data Set No.	Author(s), Year [Ref. No.]	Name and Source	Minerals and/or Chemical Composition		Method Used	Experimental Data		Other Specifications	
			Components	Weight Percent		T, K	Thermal Conductivity ($\text{W m}^{-1}\text{K}^{-1}$)		
67 cont.			TiO ₂ K ₂ O P ₂ O ₅ H ₂ O CO ₂ S	2.7 1.7 1.4 0.86 0.03 0.004	Same as above	Same as above	319	0.00110	Density: 0.88 g cm ⁻³ . Other: Same as above except the data is approximately represented by $k = 0.65 \times 10^{-3} + 0.167 \times 10^{-10}T^3$.
							320	0.00106	
							324	0.00106	
							363	0.00132	
							365	0.00128	
							367	0.00133	
							152	0.00079	
							182	0.00081	
							194	0.00074	
							201	0.00082	
68	Fountain, J.A. and West, E.A., 1970 [34]	Same as above	Same as above	Same as above	Same as above	Same as above	208	0.00071	Density: 0.88 g cm ⁻³ . Other: Same as above except the data is approximately represented by $k = 0.65 \times 10^{-3} + 0.167 \times 10^{-10}T^3$.
							214	0.00072	
							222	0.00082	
							228	0.00081	
							233	0.00080	
							237	0.00077	
							241	0.00086	
							248	0.00093	
							257	0.00096	
							262	0.00093	
69	Fountain, J.A. and West, E.A., 1970 [34]	Same as above	Same as above	Same as above	Same as above	Same as above	267	0.00102	Density: 0.98 g cm ⁻³ . Other: Same as above except the data is approximately represented by $k = 0.595 \times 10^{-3} + 0.172 \times 10^{-10}T^3$.
							271	0.00102	
							277	0.00103	
							299	0.00108	
							302	0.00112	
							303	0.00118	
							307	0.00112	
							316	0.00118	
							319	0.00120	
							322	0.00129	
69 cont.			Same as above	Same as above	Same as above	Same as above	334	0.00127	Density: 0.98 g cm ⁻³ . Other: Same as above except the data is approximately represented by $k = 0.595 \times 10^{-3} + 0.172 \times 10^{-10}T^3$.
							354	0.00147	
							356	0.00146	
							359	0.00144	
							362	0.00142	
							362	0.00149	
							363	0.00150	
							363	0.00152	
							159	0.00059	
							159	0.00063	
158	0.00071								
165	0.00066								
167	0.00076								
173	0.00061								
182	0.00070								
194	0.00066								
200	0.00075								
206	0.00074								
212	0.00075								

TABLE 1.1. EXPERIMENTAL DATA ON THERMAL CONDUCTIVITY OF BASALT (cont. lined)

Data Set No.	Author(s), Year [Ref. No.]	Name and Source	Minerals and/or Chemical Components	Mineral and/or Chemical Composition		Method Used	Experimental Data		Other Specifications
				Weight Percent	Volume Percent		T, K	Thermal Conductivity ($W m^{-1} K^{-1}$)	
69 cont.							249	0.00096	
							256	0.00089	
							306	0.00124	
							335	0.00141	
							362	0.00136	
							139	0.00083	
							142	0.00085	
							142	0.00087	
							148	0.00088	
							154	0.00091	
							182	0.00094	
							303	0.00165	
							299	0.00146	
70	Fontaine, J.A. and Weat, E.A., 1970 [34]	Same as above	Same as above			Same as above	101	0.00150	Density: 1.13 g cm ⁻³ . Other: Same as above except the data is approximately represented by $k = 0.007 \times 10^{-3} (0.190 \times 10^{-2} t_0)^2$.
							363	0.00172	
							363	0.00176	
							366	0.00174	
							148	0.00130	
							148	0.00135	
							149	0.00139	
							150	0.00129	
							151	0.00135	
							165	0.00130	
							170	0.00126	
							177	0.00132	
							183	0.00139	
185	0.00135								
186	0.00139								
190	0.00142								
195	0.00139								
197	0.00143								
200	0.00146								
203	0.00141								
207	0.00144								
212	0.00147								
217	0.00150								
217	0.00152								
223	0.00155								
231	0.00153								
235	0.00156								
240	0.00162								
250	0.00172								
254	0.00164								
275	0.00178								
278	0.00176								
289	0.00173								
292	0.00194								
295	0.00191								
295	0.00187								
71	Fontaine, J.A. and Weat, E.A., 1970 [34]	Same as above	Same as above			Same as above	148	0.00130	Density: 1.30 g cm ⁻³ . Other: Same as above except the data is approximately represented by $k = 1.237 \times 10^{-3} (0.243 \times 10^{-2} t_0)^2$.
							148	0.00135	
							149	0.00139	
							150	0.00129	
							151	0.00135	
							165	0.00130	
							170	0.00126	
							177	0.00132	
							183	0.00139	
							185	0.00135	
							186	0.00139	
							190	0.00142	
							195	0.00139	
197	0.00143								
200	0.00146								
203	0.00141								
207	0.00144								
212	0.00147								
217	0.00150								
217	0.00152								
223	0.00155								
231	0.00153								
235	0.00156								
240	0.00162								
250	0.00172								
254	0.00164								
275	0.00178								
278	0.00176								
289	0.00173								
292	0.00194								
295	0.00191								
295	0.00187								

TABLE 3.1. EXPERIMENTAL DATA ON THERMAL CONDUCTIVITY OF BASALT (continued)

Data Set No.	Author(s), Year [Ref. No.]	Name and Source	Minerals and/or Chemical Composition		Method Used	Experimental Data		Other Specifications	
			Weight Percent	Volume Percent		T, K	Thermal Conductivity ($\mu\text{m}^{-2}\text{K}^{-1}$)		
71 cont.						296	0.00190		
						334	0.00206		
						335	0.00220		
						343	0.00216		
						345	0.00217		
						360	0.00246		
						363	0.00247		
						363	0.00256		
						139	0.00169		Same as above
						143	0.00171		
						143	0.00161		
						148	0.00160		
						155	0.00170		
						161	0.00169		
						164	0.00180		
						168	0.00175		
						174	0.00179		
178	0.00185								
185	0.00186								
188	0.00193								
194	0.00192								
198	0.00201								
204	0.00199								
230	0.00222								
234	0.00222								
238	0.00227								
241	0.00227								
243	0.00226								
244	0.00225								
254	0.00242								
257	0.00242								
260	0.00219								
268	0.00260								
270	0.00247								
274	0.00250								
285	0.00262								
288	0.00254								
332	0.00288								
332	0.00294								
331	0.00297								
334	0.00306								
362	0.00311								
361	0.00316								
361	0.00320								
362	0.00326								
360	0.00329								
362	0.00331								

Density: 1.50 g cm^{-3}
 Other: Same as above except the data
 is approximately represented by
 $k = 1.662 \times 10^{-5} + 0.363 \times 10^{-5} T^{0.3}$.

TABLE 3.1. EXPERIMENTAL DATA ON THERMAL CONDUCTIVITY OF BASALT (continued)

Data Set No.	Author(s), Year [Ref. No.]	Name and Source	Minerals and/or Chemical Composition		Method Used	Experimental Data		Other Specifications
			Weight Percent	Volume Percent		T, K	Thermal Conductivity ($W m^{-1} K^{-1}$)	
7)	Fountain, J.A. and West, E.A., 1970 [34]	Same as above	Same as above	Same as above	Same as above	207	0.00118	Density: 0.79 g cm ⁻³ .
						209	0.00114	Other: Same as above except measured in simulated martian environment (5.19-5.25 mm CO ₂).
						214	0.00116	
						216	0.00118	
						218	0.00110	
						219	0.00112	
						221	0.00115	
						223	0.00112	
						226	0.00109	
						228	0.00110	
						230	0.00116	
						231	0.00110	
						233	0.00112	
						233	0.00121	
						236	0.00105	
						237	0.00119	
						239	0.00117	
						241	0.00114	
						242	0.00120	
						243	0.00127	
						245	0.00128	
						245	0.00121	
						247	0.00122	
						249	0.00125	
						251	0.00129	
						252	0.00129	
						251	0.00121	
						252	0.00121	
						254	0.00113	
						255	0.00116	
						256	0.00124	
						258	0.00123	
						259	0.00122	
						262	0.00123	
						265	0.00118	
						265	0.00126	
						267	0.00127	
						271	0.00125	
						273	0.00122	
						277	0.00124	
						277	0.00118	
						288	0.00125	
						292	0.00121	
						292	0.00127	
						296	0.00131	
						296	0.00125	
						298	0.00125	
						316	0.00132	
						318	0.00128	
						318	0.00132	

TABLE 3.1. EXPERIMENTAL DATA ON THERMAL CONDUCTIVITY OF BASALT (continued)

Data Set No.	Author(s), Year [Ref. No.]	Name and Source	Minerals and/or Chemical Composition		Method Used	Experimental Data		Other Specifications
			Componenta	Minerals and/or Chemical Composition Weight Percent Volume Percent		T, K	Thermal Conductivity ($W m^{-1} K^{-1}$)	
74	Fountain, J.A. and West, E.A., 1970 [34]	Same as above	Same as above		Same as above	222	0.00121	Density: 1.13 g cm ⁻³ . Other: Same as above.
						229	0.00114	
						235	0.00113	
						242	0.00115	
						244	0.00120	
						247	0.00128	
						251	0.00117	
						253	0.00115	
						256	0.00132	
						260	0.00117	
						261	0.00131	
						263	0.00119	
						303	0.00136	
						303	0.00124	
						303	0.00130	
						302	0.00134	
						303	0.00134	
75	Fountain, J.A. and West, E.A., 1970 [34]	Same as above	Same as above		Same as above	316	0.00133	Density: 1.30 g cm ⁻³ . Other: Same as above.
						316	0.00131	
						317	0.00133	
76	Fountain, J.A. and West, E.A., 1970 [34]	Same as above	Same as above		Same as above	207	0.00120	Density: 1.50 g cm ⁻³ . Other: Same as above.
						208	0.00117	
						211	0.00127	
						213	0.00114	
						214	0.00123	
						216	0.00116	
						216	0.00122	
						218	0.00125	
						221	0.00139	
						223	0.00135	
						226	0.00130	
						233	0.00135	
						236	0.00125	
						237	0.00124	
						238	0.00126	
						240	0.00125	
242	0.00121							
246	0.00136							
247	0.00133							
247	0.00132							
250	0.00129							
251	0.00135							
252	0.00131							
254	0.00131							
256	0.00142							
257	0.00130							
259	0.00130							

TABLE 3.1. EXPERIMENTAL DATA ON THERMAL CONDUCTIVITY OF BASALT (continued)

Data Set No.	Author(s), Year [Ref. No.]	Name and Source	Minerals and/or Chemical Composition		Experimental Data		Method Used	Other Specifications	
			Components	Weight Percent	T, K	Thermal Conductivity ($W m^{-1} K^{-1}$)			
76 cont.						260	0.00127		
						261	0.00126		
						274	0.00131		
						275	0.00128		
						275	0.00124		
						276	0.00128		
						277	0.00122		
						295	0.00137		
						296	0.00137		
						296	0.00133		
						297	0.00134		
						315	0.00138		
						316	0.00135		
						317	0.00139		
317	0.00135								
77	Martinez-Baez, L.F. and Hal Amick, C., 1978 [35]	Umtanum Basalt, DH-5; Umtanum Basalt Flow Area; WA				328	1.57	Steady State Comparator	Density: 2.78 g cm ⁻³ . Other: Diameter 4.7 cm and 3.20 cm long; measurements were made at constant stress of 500 psi for water saturated (wet) specimens; specimen was obtained by Rockwell-Hanford Operations; recovered from the core of bore hole 2749 ft. deep; cores were diamond drilled longitudinal to the axis to obtain specimens; value at 473 K is estimated.
						396	1.51		
						473	1.44		
78	Martinez-Baez, L.F. and Hal Amick, C., 1978 [35]	Same as above				329	1.49	Same as above	Density: 2.80 g cm ⁻³ . Other: Same as above except specimen recovered from core of hole bore 2808 ft. deep; value at 473 K is estimated.
						396	1.45		
						473	1.41		
79	Martinez-Baez, L.F. and Hal Amick, C., 1978 [35]	Gable Mt. Basalt, (Esquatzel) DB-5; Gable Mt. Flow Area; WA				329	1.62	Same as above	Density: 2.78 g cm ⁻³ . Other: Diameter 5.08 cm and 3.20 cm long; specimen recovered from core of bore hole 521 ft. deep; cores were diamond drilled longitudinal to the axis; measurements were made at constant stress of 500 psi water-saturated (wet); value at 473 K is estimated.
						396	1.57		
						473	1.52		
80	Martinez-Baez, L.F. and Hal Amick, C., 1978 [35]	Same as above				328	1.54	Same as above	Density: 2.82 g cm ⁻³ . Other: Same as above except recovered from the core of bore hole 542 ft. deep.
						396	1.47		
						473	1.42		
81	Martinez-Baez, L.F. and Hal Amick, C., 1978 [35]	Pomona Basalt, DH-5; Pomona Basalt Flow Area; WA				327	1.75	Same as above	Density: 2.87 g cm ⁻³ . Other: Diameter 5.08 cm and 3.20 cm long; specimen supplied by Rockwell-Hanford Operations; recovered from
						396	1.68		
						473	1.63		

TABLE 3.1. EXPERIMENTAL DATA ON THERMAL CONDUCTIVITY OF BASALT (continued)

Data Set No.	Author(s), Year [Ref. No.]	Name and Source	Mineral and/or Chemical Composition		Method Used	Experimental Data		Other Specifications
			Weight Percent	Volume Percent		T, K	Thermal Conductivity ($W m^{-1} K^{-1}$)	
81								
								the core of bore hole 390 ft. deep; cores were diamond drilled longitudinal to the axis to obtain test specimens; measurements were made at constant stress of 500 psi for water saturated (wet) specimens; value at 473 K is estimated.
82	Martinez-Baez, L.F. and Hal Amick, C., 1978 [35]	Same as above			Same as above	329 397 473	1.73 1.68 1.61	Density: $2.88 g cm^{-3}$. Other: Similar to the above except recovered from the core of bore hole 420 ft. deep.
83	West, E.A. and Fountain, J.A., 1975 [36]	Terrestrial Basalt.			Line Heat Source	114 120 131 140 151 160 170 180 191 200 210 219 231 239 250 260 270 278 289 298 308 319 329 337 348 353 357	0.00373 0.00371 0.00369 0.00367 0.00367 0.00367 0.00368 0.00370 0.00372 0.00375 0.00383 0.00386 0.00393 0.00402 0.00411 0.00421 0.00435 0.00447 0.00462 0.00479 0.00495 0.00515 0.00538 0.00559 0.00583 0.00598 0.00612	Density: $1.95 g cm^{-3}$. Other: Specimen provided by Dr. Kl-it-lloral, lunar core tube investigator from Columbia Univ.; the sample size distribution in which the bulk of the particula lie in the range from 53-256 μ ; values taken from smooth curve reported by authors are tabulated.
84	Duvall, V.I., Miller, R.J., and Wang, F.D., 1978 [37]	Pomona Flow Basalt, T11; Drill Hole DC-10; Gable Mountain, WA			Steady State Heat Flow	423 473 523	1.287 1.289 1.268	Density: $2.69 g cm^{-3}$. Other: Test specimens are core sections cut to approximately 5/8 in. length and ground parallel to within 0.003 in.; footage of sample was taken from 143.4-143.55 ft. below drill hole; it is concluded that thermal conductivity is not sensitive to temperature of their measurements.

TABLE 3.1. EXPERIMENTAL DATA ON THERMAL CONDUCTIVITY OF BASALT (continued)

Data Set No.	Author(s), Year [Ref. No.]	Name and Source	Minerals and/or Chemical Composition		Experimental Data			Other Specifications	
			Components	Height Percent	Volume Percent	Method Used	T, K		Thermal Conductivity ($W m^{-1} K^{-1}$)
85	Duvall, W.L., et al., 1978 [37]	Pomona Flow Basalt, TL3; Drill Hole DC-10; Gable Mountain, WA				Same as above	423 473 573	1.481 1.498 1.464	Density: 2.83 g cm ⁻³ . Other: Same as above except footage of sample was taken from 174.9-175.0 ft. below the drill hole.
86	Duvall, W.L., et al., 1978 [37]	Pomona Flow Basalt, TL5; Drill Hole DC-10; Gable Mountain, WA				Same as above	423 473 523	1.607 1.602 1.602	Density: 2.85 g cm ⁻³ . Other: Same as above except footage of sample was taken from 197.6-197.7 ft. below the drill hole.
87	Foundation Sciences, Inc., 1981 [40]	Umtanum Basalt, DC2; Gable Mt., WA				Steady State Axial Comparative	328.8 403.2 525.6	2.33 2.38 2.44	Density: 2.77 g cm ⁻³ (bulk), 2.73 g cm ⁻³ (grain). Texture: Dark grey, aphanitic and massive, moderately fractured and occasionally contains vesicles; fractures usually closed or filled; mineralized fillings are characterized by dark green-black chlorite followed by silica stringers. Other: Umtanum basalt from bore hole DC2; sample no. 4-2-E (depth 3027.0 ft.).
88	Foundation Sciences, Inc., 1981 [40]	Same as above				Same as above	334.4 414.6 550.8	2.40 2.46 2.51	Density: 2.82 g cm ⁻³ (bulk), 2.75 g cm ⁻³ (grain). Texture: Same as above. Other: Same as above except sample no. 4-3-I (depth 3049.3 ft.).
89	Foundation Sciences, Inc., 1981 [40]	Same as above				Same as above	351.9 434.2 577.7	1.82 2.07 2.22	Density: 2.77 g cm ⁻³ (bulk), 2.78 g cm ⁻³ (grain). Texture: Same as above. Other: Same as above except sample no. 4-6-G (depth 3034.7 ft.).
90	Foundation Sciences, Inc., 1981 [40]	Same as above				Same as above	338.0 418.8 556.7	2.13 2.28 2.40	Density: 2.78 g cm ⁻³ (bulk), 2.98 g cm ⁻³ (grain). Texture: Same as above. Other: Same as above except sample no. 4-25-E (depth 3092.4 ft.).
91	Foundation Sciences, Inc., 1980 [39]	Pomona Basalt, (HSTF), Area 1; Gable Mt., WA				Same as above	304.2 403.2 554.2	1.90 2.06 2.36	Other: Sample no. B1-64-B from bore hole IE20 (depth 29.5 ft.); data extracted from ref. [40].
92	Foundation Sciences, Inc., 1980 [39]	Same as above				Same as above	318.2 410.2 561.2	2.05 2.19 2.54	Other: Sample no. B1-77-B from bore hole IE20 (depth 20.2 ft.); data extracted from ref. [40].
93	Foundation Sciences, Inc., 1980 [39]	Same as above				Same as above	310.2 396.2 543.2	1.87 1.91 2.26	Other: Sample no. B1-82-C from bore hole IE20 (depth 10.5 ft.); data extracted from ref. [40].

TABLE 3.1. EXPERIMENTAL DATA ON THERMAL CONDUCTIVITY OF BASALT (continued)

Data Set No.	Author(s), Year [Ref. No.]	Name and Source	Minerals and/or Chemical Composition		Method Used	Experimental Data		Other Specifications
			Components	Weight Percent		T, K	Thermal Conductivity ($W m^{-1} K^{-1}$)	
94	Foundation Sciences, Inc., 1980 [39]	Same as above			Steady State	324.2	1.94	Other: Sample no. Al-95-B from bore hole 1E6 (depth 22.9 ft.); data extracted from ref. [40].
					Axial	464.2	2.03	
					Comparative	573.2	2.18	
95	Foundation Sciences, Inc., 1980 [39]	Same as above			Same as above	308.2	1.91	Other: Sample no. Al-99-B from bore hole 1E6 (depth 17.0 ft.); data extracted from ref. [40].
						440.2	2.19	
						535.2	2.36	
96	Foundation Sciences, Inc., 1980 [39]	Same as above			Same as above	308.2	1.94	Other: Sample no. Al-102-B from bore hole 1E6 (depth 4.4 ft.); data extracted from ref. [40].
						396.2	2.03	
						510.2	2.17	
97	Foundation Sciences, Inc., 1980 [39]	Same as above			Same as above	308.2	1.90	Other: Sample no. Al-102-C from bore hole 1E6 (depth 4.5 ft.); data extracted from ref. [40].
						402.2	2.01	
						538.2	2.35	
98	Foundation Sciences, Inc., 1980 [39]	Same as above			Same as above	308.2	1.80	Other: Sample no. Al-116-D from bore hole 1E6 (depth 8.2 ft.); data extracted from ref. [40].
						403.2	1.97	
						535.2	2.11	
99	Foundation Sciences, Inc., 1980 [38]	Pomona Basalt, (NSIF), Area 2; Gable Mt., WA			Same as above	316.5	2.15	Density: $2.82 g cm^{-3}$ (bulk), $3.12 g cm^{-3}$ (grain). Texture: Porphyritic with lath- or blade-shaped crystals of plagioclase (<5 mm) and less commonly irregular crystals of olivine and clinopyroxene (<5 mm) in a fine-grained groundmass; green to blue-green mineraloid (chlorophaeite) occurs both in irregular interstitial patches in the groundmass and as a vesicle filling or lining; joints commonly lined with chlorophaeite. Other: Basalt from NSIF (Near Surface Test Facility); sample from Full Scale Test No. 2 instrument bore hole (Area 2); sample no. 2-33-B from bore hole 2E8 (depth 27.3 ft.).
						429.6	1.93	
						572.3	2.17	
100	Foundation Sciences, Inc., 1980 [38]	Same as above			Same as above	339.7	1.36	Texture: Same as above. Other: Same as above except sample no. 2-33-H from bore hole 2E8 (depth 27.4 ft.).
						403.8	1.46	
						543.5	1.54	
101	Foundation Sciences, Inc., 1980 [38]	Same as above			Same as above	323.9	1.04	Density: $2.80 g cm^{-3}$ (bulk), $3.10 g cm^{-3}$ (grain). Texture: Same as above. Other: Same as above except sample no. 2-34-E from bore hole 2E8 (depth 28.2 ft.).
						415.9	1.15	
						568.9	1.30	

TABLE 3.1. EXPERIMENTAL DATA ON THERMAL CONDUCTIVITY OF BASALT (continued)

Data Set No.	Author(s), Year [Ref. No.]	Name and Source	Minerals and/or Chemical Composition		Experimental Data		Method Used	Other Specifications
			Components	Weight Percent	T, K	Thermal Conductivity ($W m^{-1} K^{-1}$)		
102	Foundation Sciences, Inc., 1980 [38]	Same as above			Steady State Axial Comparative	314.0 411.8 523.2	1.85 2.01 2.14	Density: 2.79 g cm ⁻³ (bulk), 3.00 g cm ⁻³ (grain). Texture: Same as above. Other: Same as above except sample no. 2-94-B from bore hole 2E14 (depth 4.9 ft.).
103	Foundation Sciences, Inc., 1980 [38]	Same as above			Same as above	324.7 434.6 553.9	2.21 2.31 2.51	Density: 2.81 g cm ⁻³ (bulk), 2.93 g cm ⁻³ (grain). Texture: Same as above. Other: Same as above except sample no. 2-96-B from bore hole 2E14 (depth 18.6 ft.).
104	Foundation Sciences, Inc., 1980 [38]	Same as above			Same as above	328.7 391.8 491.5	1.23 1.31 1.42	Density: 2.81 g cm ⁻³ (bulk), 2.93 g cm ⁻³ (grain). Texture: Same as above. Other: Same as above except sample no. 2-102-C from bore hole 2E22 (depth 12.7 ft.).
105	Foundation Sciences, Inc., 1980 [38]	Same as above			Same as above	334.4 357.7 437.0	1.79 1.80 2.04	Density: 2.83 g cm ⁻³ (bulk). Texture: Same as above. Other: Same as above except sample no. 2-102-D from bore hole 2E22 (depth 12.8 ft.).
106	Foundation Sciences, Inc., 1980 [38]	Same as above			Same as above	319.6 405.6 568.6	1.24 1.35 1.30	Density: 2.84 g cm ⁻³ (bulk), 3.03 g cm ⁻³ (grain). Texture: Same as above. Other: Same as above except sample no. 2-118-C from bore hole 2E4 (depth 21.4 ft.).
107	Colorado School of Mines, 1978 [41]	Umtanum Basalt; Hanford Site, WA			Transient Axial Comparative	378.0 479.1 543.9	1.087 1.453 1.634	Density: 2.60 g cm ⁻³ . Other: Sample no. CP-14 from bore hole D11-5 (depth 2842.7-2842.8 ft.).
108	Colorado School of Mines, 1978 [41]	Same as above			Same as above	372.6 474.4 568.4	0.799 1.047 1.252	Density: 2.27 g cm ⁻³ . Other: Sample no. K-15 from bore hole D11-5 (depth 3295.7-3295.8 ft.).
109	Colorado School of Mines, 1978 [41]	Same as above			Same as above	380.9 467.9 554.3	1.043 1.382 1.728	Density: 2.79 g cm ⁻³ . Other: Sample no. K-16 from bore hole D11-5 (depth 3520.0-3520.1 ft.).
110	Colorado School of Mines, 1978 [41]	Same as above			Same as above	375.1 468.6 548.5	1.142 1.630 1.839	Density: 2.75 g cm ⁻³ . Other: Sample no. K-17 from bore hole D11-5 (depth 4067.3-4067.4 ft.).
111	Colorado School of Mines, 1978 [41]	Same as above			Same as above	379.5 477.9 554.8	1.280 1.787 1.972	Density: 2.80 g cm ⁻³ . Other: Sample no. K-18 from bore hole D11-5 (depth 4824.1-4824.3 ft.).

TABLE 3.1. EXPERIMENTAL DATA ON THERMAL CONDUCTIVITY OF BASALT (continued)

Data Set No.	Author(s), Year [Ref. No.]	Name and Source	Minerals and/or Chemical Composition		Experimental Data		Method Used	Other Specifications
			Components	Weight Percent	T, K	Thermal Conductivity ($W m^{-1} K^{-1}$)		
112	Colorado School of Mines, 1978 [41]	Same as above			395.9	1.154	Transient	Density: 2.73 g cm ⁻³ . Other: Sample no. CP-19 from bore hole DH-5 (depth 4667.7-4667.8 ft.).
113	Colorado School of Mines, 1978 [41]	Same as above			552.3 575.1	1.646 1.701	Axial Comparative	Density: 2.81 g cm ⁻³ . Other: Sample no. K-20 from bore hole DH-5 (depth 4819.5-4819.6 ft.).
114	Colorado School of Mines, 1978 [41]	Same as above			382.4 479.8 575.7	1.228 1.453 1.709	Same as above	Density: 2.74 g cm ⁻³ . Other: Sample no. K-21 from bore hole DC-2 (depth 3051.5-3051.6 ft.).
115	Colorado School of Mines, 1978 [41]	Same as above			383.1 473.4 563.5	1.272 1.646 2.004	Same as above	Density: 2.75 g cm ⁻³ . Other: Sample no. K-22 from bore hole DC-2 (depth 3061.7-3061.8 ft.).
116	Colorado School of Mines, 1978 [41]	Same as above			373.6 469.0 536.8	1.252 2.256 2.484	Same as above	Density: 2.81 g cm ⁻³ . Other: Sample no. K-23 from bore hole DC-2 (depth 2618.5-2618.6 ft.).
117	Colorado School of Mines, 1978 [41]	Same as above			379.9 477.2 557.6	1.114 1.520 1.898	Same as above	Density: 2.73 g cm ⁻³ . Other: Sample no. K-24 from bore hole DC-2 (depth 2479.3-2479.4 ft.).
118	Colorado School of Mines, 1978 [41]	Same as above			374.3 472.6 541.2	1.047 1.409 2.681	Same as above	Density: 2.72 g cm ⁻³ . Other: Sample no. K-25 from bore hole DC-2 (depth 2472.6-2472.7 ft.).
119	Colorado School of Mines, 1978 [41]	Same as above			374.7 472.6 570.6	1.264 1.622 2.173	Same as above	Density: 2.75 g cm ⁻³ . Other: Sample no. K-26 from bore hole DDI-3 (depth 3316.1-3316.2 ft.).
120	Colorado School of Mines, 1978 [41]	Same as above			375.4 468.7 563.8	1.638 2.020 2.500	Same as above	Density: 2.73 g cm ⁻³ . Other: Sample no. K-27 from bore hole DDI-3 (depth 3392.3-3392.4 ft.).
121	Colorado School of Mines, 1978 [41]	Same as above			375.9 474.9 575.4	1.720 2.224 2.992	Same as above	Density: 2.73 g cm ⁻³ . Other: Sample no. K-28 from bore hole DDI-3 (depth 3498.7-3498.8 ft.).
122	Colorado School of Mines, 1978 [41]	Same as above			384.6 470.4 546.8	0.654 0.744 0.783	Same as above	Density: 1.87 g cm ⁻³ . Other: Sample no. CP-29 from bore hole DH-4 (depth 1483.2-1483.3 ft.).
123	Somerton, W.H., Ward, S.H., and King, M.S., 1963 [74]	Augite Basalt, Mohole Test Site			297 302 313 328	1.522 1.464 1.387 1.329	Thermal Comparator	Density: 2.82 g cm ⁻³ . Porosity: 2.06%. Texture: Intracrystalline, normal fine grained; lack of alteration, numerous fractures filled with secondary deposition of carbonate minerals. Other: Measurements on piece no. 36 (EH-5, 355 to 367 cm); [570 to 577 ft below the sea floor at the Guadalupe site (28°58'N, 177°28'W) where depth of the water is 11,760 ft]; oven dried, axial stress 900 psi.

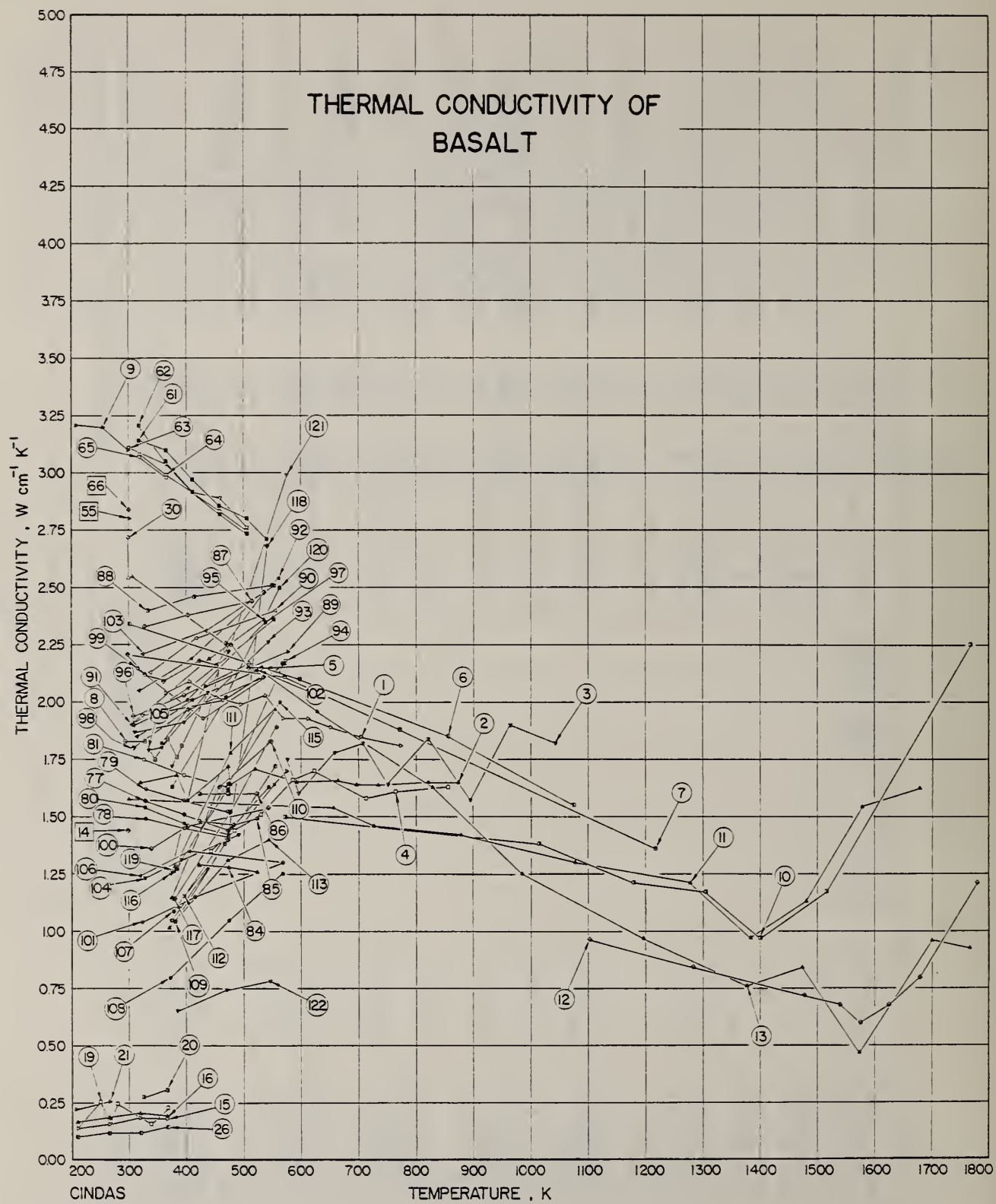


Figure 3.1. Thermal conductivity of basalt.

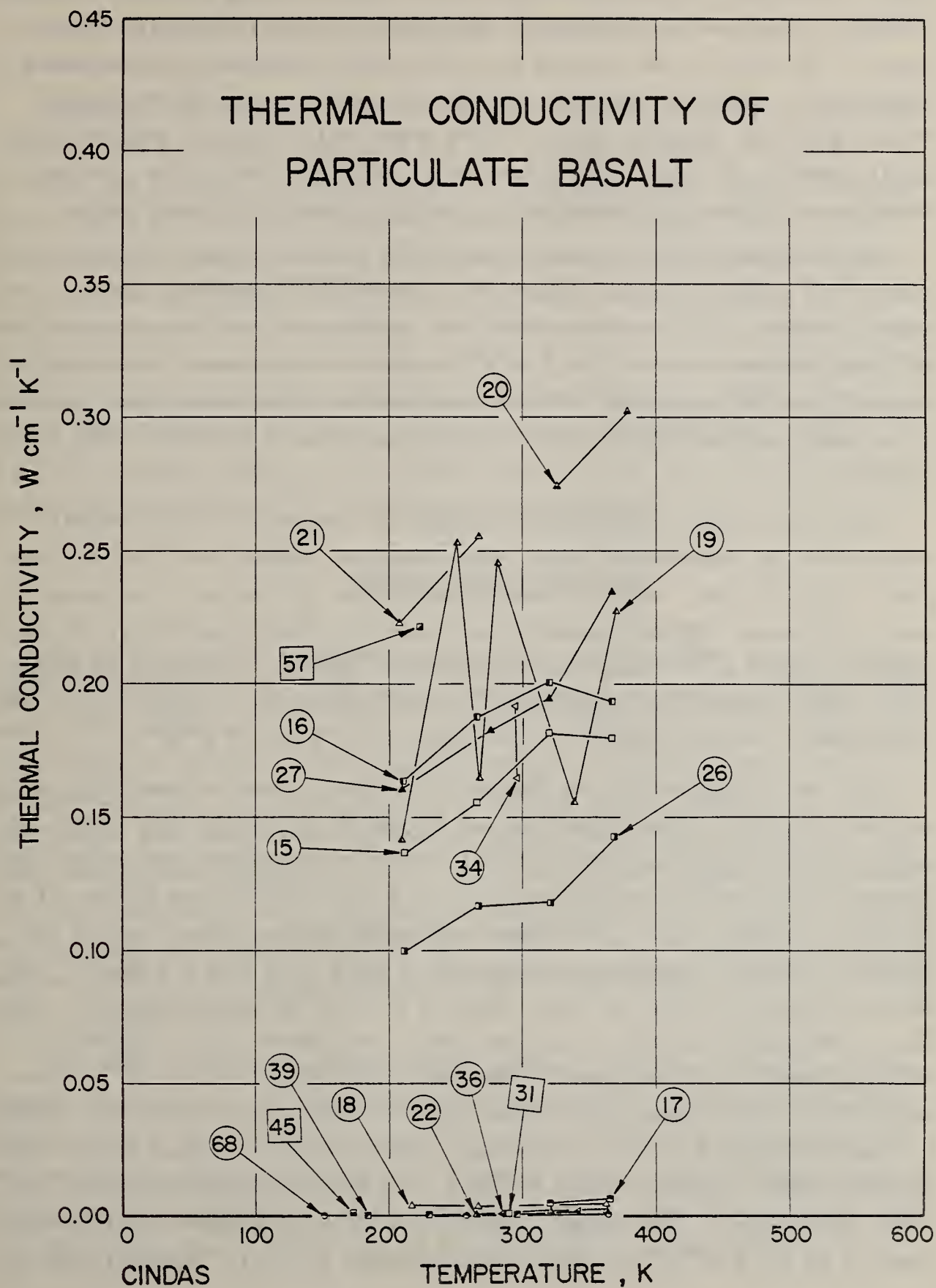


Figure 3.2. Thermal conductivity of particulate basalt.

affect the thermal conductivity differently. These include porosity, internal cracking, structure, water content, and amount of glassy material in the basalt. The data on the Hanford Site basalt show increase with increasing temperature. However, the data for other basalts, including the Dresser basalt, show the opposite trend. It is worth noting that the Hanford Site basalt samples are from a drill hole up to 4800 feet deep. The internal cracking and internally trapped water cannot be ignored for these samples.

The room-temperature thermal conductivity values for most of the basalts studied are within the range from 1.0 to 2.5 $\text{W m}^{-1}\text{K}^{-1}$. However, the data of Morgan and West [32] (data sets 61-65) for the Dresser basalt are much higher and yield a value of about 3.1 $\text{W m}^{-1}\text{K}^{-1}$ near room temperature, decreasing to about 2.7 $\text{W m}^{-1}\text{K}^{-1}$ at 540 K. This is considerably higher than values reported by Marovelli and Veith [20] (data sets 5-9) and Navarro and DeWitt [24] (data set 30).

There has been a considerable amount of work done on the thermal conductivity of particulate basalt with densities ranging from 0.88 to 1.95 g cm^{-3} [23,25,30,34]. Most of these studies were carried out in a vacuum of about 10^{-10} atm. Thermal conductivity values for these basalts are of the order of 0.003 $\text{W m}^{-1}\text{K}^{-1}$ near room temperature. However, the values of Bennett et al. [23], derived from experimental thermal diffusivity, specific heat, and density data, are much higher, of the order of $0.2 \pm 0.05 \text{ W m}^{-1}\text{K}^{-1}$.

The data reported for the Hanford Site basalts can be summarized as follows: the data of Martinez-Baez and Hal Amick [35] (data sets 77-82) for water saturated specimens show a slight decreasing trend with increasing temperature or at most a constant value of $1.6 \pm 0.2 \text{ W m}^{-1}\text{K}^{-1}$ from 329 to 473 K. The data of Duvall et al. [37] (data sets 84-86) indicate that thermal conductivity values at temperatures from 423 to 523 K vary from 1.3 $\text{W m}^{-1}\text{K}^{-1}$ for basalt of density 2.69 g cm^{-3} to a value of 1.6 $\text{W m}^{-1}\text{K}^{-1}$ for 2.85 g cm^{-3} . The data of Foundation Sciences Inc. [40] (data sets 87-90) show a slight increasing trend or, at the most, a constant value of $2.2 \pm 0.4 \text{ W m}^{-1}\text{K}^{-1}$ from 330 to 580 K. The Foundation Sciences Inc. [39] (data sets 91-98) also report a value of $2.0 \pm 0.3 \text{ W m}^{-1}\text{K}^{-1}$ for basalts from Area 1 of the Near Surface Test Facility (NSTF). However, data for Area 2 of NSTF are sample dependant [38] (data sets 99-106). The thermal conductivity values for these basalts range from 1.0 to 2.5 $\text{W m}^{-1}\text{K}^{-1}$ at temperatures from 320 to 570 K. The data from the

Colorado School of Mines [41] (data sets 107-122) for samples from bore holes 14 to 4800 feet deep also exhibit similar variation from 0.8 to $2.5 \text{ W m}^{-1}\text{K}^{-1}$ at temperatures from 375 to 580 K.

Bridgman [42] reported that the thermal conductivity values for diabasic basalt at 348 K increase from $1.73 \text{ W m}^{-1}\text{K}^{-1}$ at zero pressure to $1.78 \text{ W m}^{-1}\text{K}^{-1}$ at 11614 atm pressure. Somerton et al. [74] reported that thermal conductivity at 336 K for sea-water saturated augite basalt increase from $1.8 \text{ W m}^{-1}\text{K}^{-1}$ at 30 atm axial stress to $2.1 \text{ W m}^{-1}\text{K}^{-1}$ at 220 atm axial pressure. Additionally, Hyndman and Drury [43] reported an average value of $1.7 \text{ W m}^{-1}\text{K}^{-1}$ from their measurements on 19 specimens from the Deep Sea Drilling Project (DSDP Leg 37) with an average bulk density of 2.795 g cm^{-3} . Robertson and Peck [44] reported that the thermal conductivity at 308 K of olivine basalt samples from Hawaii with densities varying from 0.049 to 3.06 g cm^{-3} varies from $0.09 \text{ W m}^{-1}\text{K}^{-1}$ (porosity 98%) to $1.8 \text{ W m}^{-1}\text{K}^{-1}$ (porosity 2%) for dry samples and between 0.8 and $2.4 \text{ W m}^{-1}\text{K}^{-1}$ for water-saturated samples.

3.4. THERMAL LINEAR EXPANSION

There are over 60 experimental data sets available for thermal linear expansion of basalt. The temperature range covered by most of these is rather narrow with exception of the data of Griffin and Demou [45] (data sets 1-4), for tholeiitic and for olivine basalt from 136 to 1214 K, and those of Thirumalai et al. [53] (data set 28) for Dresser basalt from 313 to 1337 K. The Hanford Site basalts are studied in detail by Erickson and Krupka [54] (data sets 29,30), Duvall et al. [37] (data sets 31-33), Foundation Sciences Inc. [38] (data sets 34-47), Foundation Sciences Inc. [40] (data sets 48-56), and by Miller and Bishop [55] (data sets 57-63). Some other types of basalts covered in this Chapter are hornblende basalt [46], tephrite basalt [48], and basalt porphyry [50,52].

The data of Griffin and Demou [45] indicate that basalt with low glass content (data set 3) has higher expansion than that with high glass content (data set 4). The 'vesicular basalt olivine no. 1' and 'vesicular basalt olivine no. 2' reported by them have somewhat similar mineralogical compositions, but quite different thermal expansion values. The data of Krupka [51] for 'Los Alamos basalt glass' and of Suleimenov et al. [48] for tephrite

TABLE 3.2. EXPERIMENTAL DATA ON THERMAL LINEAR EXPANSION OF BASALT

Data Set No.	Author(s), Year [Ref. No.]	Name and Source	Minerals and/or Chemical Composition		Method Used	Experimental Data		Other Specifications
			Component	Weight Percent		T, K	Thermal Linear Expansion (%)	
1	Griffin, R.E. and Demou, S.G., 1972 [45]	Tholeiitic Basalt; N.E. of Nadras, OR	Plagioclase	39	Dilatometer	136	-0.071	Density: 2.84 g cm ⁻³ . Porosity: 2%. Powder Density: 1.45 g cm ⁻³ . Magnetic Susceptibility: 1400 x 10 ⁶ cgs units. Dielectric Constant: 3.02 (ratio). Specific Area: 0.8 m ² g ⁻¹ . Other: Zero-point correction 0.007%.
			Olivine	13.5		189	-0.053	
			Plagioclase, Microclites	12		233	-0.035	
			Glass	12		273	-0.011	
			Augite	10.5		311	0.009	
			Magnetite and Ilmenite	8		346	0.033	
			Chlorite	4		383	0.059	
			SiO ₂	51.0		420	0.087	
			Al ₂ O ₃	14.0		458	0.117	
			FeO	8.8		495	0.143	
			CaO	8.0		531	0.163	
			MgO	4.4		568	0.191	
			Fe ₂ O ₃	3.4		604	0.221	
			Na ₂ O	3.4		711	0.337	
			TiO ₂	2.7		746	0.359	
			K ₂ O	1.7		781	0.379	
						817	0.405	
			852	0.437				
			887	0.469				
			922	0.495				
			958	0.511				
			994	0.531				
			1030	0.554				
			1066	0.573				
			1103	0.607				
			1139	0.631				
			1177	0.667				
			1214	0.709				
2	Griffin, R.E. and Demou, S.G., 1972 [45]	Vesicular Basalt No. 1; S. of Bend, OR	Plagioclase	50	Dilatometer	136	-0.022	Density: 2.25 g cm ⁻³ . Porosity: 20%. Powder Density: 1.37 g cm ⁻³ . Magnetic Susceptibility: 340 x 10 ⁶ cgs units. Dielectric Constant: 2.63 (ratio). Specific Area: 0.8 m ² g ⁻¹ . Other: Zero-point correction 0.004%.
			Pyroxene	20		189	-0.020	
			Glass	15		233	-0.010	
			Plagioclase, Microphenocrysts	10		273	-0.005	
			Olivine	<3		311	0.008	
			Magnetite	2		346	0.020	
			Hematite	<1		383	0.036	
			SiO ₂	54.4		420	0.052	
			Al ₂ O ₃	16.8		458	0.064	
			CaO	7.67		493	0.072	
			FeO	5.39		531	0.072	
			MgO	4.94		568	0.072	
			Na ₂ O	2.43		604	0.072	
			TiO ₂	1.13		640	0.076	
			K ₂ O	0.92		711	0.106	
						746	0.124	
						781	0.144	
			817	0.162				
			852	0.180				
			887	0.200				

TABLE 3.2. EXPERIMENTAL DATA ON THERMAL LINEAR EXPANSION OF BASALT (continued)

Data Set No.	Author(s), Year [Ref. No.]	Name and Source	Minerals and/or Chemical Composition		Method Used	Experimental Data		Other Specifications
			Components	Weight Percent Volume Percent		T, K	Linear Expansion (%)	
2						922	0.212	
						958	0.222	
3	Griffin, R.E. and Demou, S.G., 1972 [45]	Vesicular Basalt Olivine No. 2; S. of Bend, OR	Plagioclase Olivine Pyroxene Magnetite Glass Hematite SiO ₂ Al ₂ O ₃ CaO MgO FeO Fe ₂ O ₃ Na ₂ O TiO ₂ K ₂ O	1 25 15 5 5 47.6 17.0 10.99 8.09 6.33 3.56 2.29 1.42 0.92	Dilatometer	136	-0.024	Density: 2.22 g cm ⁻³ . Porosity: 24%. Powder Density: 1.52 g cm ⁻³ . Magnetic Susceptibility: 350 x 10 ⁶ cgs units. Dielectric Constant: 2.83 (ratio). Specific Area: 1.3 m ² g ⁻¹ . Other: Zero-point correction 0.004%.
						189	-0.022	
						233	-0.018	
						273	-0.008	
						311	0.008	
						346	0.024	
						383	0.044	
						420	0.070	
						458	0.098	
						495	0.124	
4	Griffin, R.E. and Demou, S.G., 1972 [45]	Vesicular Basalt Olivine Beds, National Monument, CA	Plagioclase (Labradorite) Olivine (Forsterite) Plagioclase (Bytownite, Microphenocrysts) Glass Magnetite SiO ₂ Al ₂ O ₃	45 20 10 20 5 53.0 16.2		136	-0.033	Density: 1.52 g cm ⁻³ . Porosity: 46%. Powder Density: 1.31 g cm ⁻³ . Magnetic Susceptibility: 260 x 10 ⁶ cgs units. Dielectric Constant: 2.45 (ratio). Specific Area: 0.7 m ² g ⁻¹ . Other: Zero-point correction 0.003%.
						189	-0.031	
						233	-0.025	
						273	-0.011	
						311	0.009	
						346	0.027	
						383	0.049	
						420	0.071	
						458	0.093	
						495	0.113	
						1214	0.836	

TABLE 3.2. EXPERIMENTAL DATA ON THERMAL LINEAR EXPANSION OF BASALT (continued)

Data Set No.	Author(s), Year [Ref. No.]	Name and Source	Minerals and/or Chemical Composition		Experimental Data		Other Specifications	
			Componenta	Weight Percent	Volume Percent	T, K		Thermal Linear Expansion (%)
4 cont.			CaO	8.56		568	0.131	
			MgO	6.73		604	0.135	
			FeO	5.19		640	0.143	
			Fe ₂ O ₃	3.26		676	0.153	
			Na ₂ O	3.01		711	0.167	
			K ₂ O	1.00		746	0.183	
			TiO ₂	0.77		781	0.199	
						817	0.211	
						852	0.227	
						887	0.243	
						922	0.263	
						958	0.285	
						994	0.305	
					1030	0.329		
					1066	0.353		
					1103	0.383		
					1139	0.417		
					1177	0.457		
					1214	0.503		
5	Griffith, J.H., 1937 [46]	Hornblende Basalt; Claiffee County, CO				293	0.000	Porosity: 0.44%.
						373	0.037	
6	Griffith, J.H., 1937 [46]	Olivine Basalt; Jefferson County, CO				293	0.000	Porosity: 0.22%.
						373	0.032	
7	Griffith, J.H., 1937 [46]	Olivine Basalt; Mt. St. Helens, WA				293	0.000	Porosity: 22.06%.
						373	0.048	
8	Griffith, J.H., 1937 [46]	Porphyry Basalt; Lake County, OR				293	0.000	Porosity: 1.76%.
						373	0.037	
9	Mitchell, L.J., 1953 [47]	Basalt Pebble from Gravel; Hungryhorse Dam, MT				263	-0.0123	Other: Average of heating and cooling cycle.
						293	0.0000	
						297	0.0015	
10	Mitchell, L.J., 1953 [47]	Quarried "Table Mountain Basalt"; Golden, CO				263	-0.0120	Other: Average of heating and cooling cycle.
						293	0.0000	
						297	0.0016	
11	Mitchell, L.J., 1953 [47]	Basalt Pebble from Gravel; Republican River Gravel, CO				263	-0.0102	Other: Average of heating and cooling cycle.
						293	0.0000	
						297	0.0014	
12	Suleimenov, S.T., Abduvaliev, T., Sharafiev, M.Sh., and Tropina, L.G., 1966 [48]	Tephrite Basalt; Daubabinsk, Chirchik and Tropina, L.G., 1966 [48]	SiO ₂ Al ₂ O ₃ CaO Fe ₂ O ₃ MgO SO ₂ Ignition loss	45.42 15.68 11.14 9.15 6.67 0.33 6.52		293	0.000	Texture: Fine-grained glassy mass. Other: Specimen melted between 1553-1623 K and 1% Cr ₂ O ₃ added.
						773	0.342	

TABLE 3.2. EXPERIMENTAL DATA ON THERMAL LINEAR EXPANSION OF BASALT (continued)

Data Set No.	Author(s), Year [Ref. No.]	Name and Source	Minerals and/or Chemical Composition		Experimental Data		Other Specifications		
			Components	Weight Percent	Volume Percent	T, K		Thermal Linear Expansion (%)	
13	Suleimenov, S.T. et al., 1966 [48]	Same as above	SiO ₂ Al ₂ O ₃ CaO Fe ₂ O ₃ MgO SO ₂ Ignition loss	45.42		Dilatometer	293	0.000	Texture: Fine-grained glassy mass. Other: The above specimen with 2% waste chrome-magnesite brick.
				15.68			773	0.416	
14	Verbeck, G.J. and Bass, W.E., 1951 [49]	Trap Rock; Dresser, WI				Dilatometer	298	0.0043	Texture: Average grain size 0.62 mm. Test Environment: Water. Other: Specimen water saturated, mean thermal linear expansion calculated from one-third of experimental volumetric expansion. Same as above.
							302	0.0077	
15	Verbeck, G.J. and Bass, W.E., 1951 [49]	Trap Rock, PA				Dilatometer	298	0.0039	Same as above.
							302	0.0070	
16	Hockman, A. and Kessler, D.W., 1950 [50]	Basalt Porphyry; Columbia National Forest, WA	Plagioclase High Fe Glass major			Interferometer	253	-0.024	Texture: Fine Other: Moisture expansion due to immersion in water for 24 hr at 294.7 K is 0.0018%; heating cycle. Texture: Fine. Other: Same as above except cooling cycle.
							273	-0.012	
							293	0.000	
							333	0.024	
							333	0.024	
17	Hockman, A. and Kessler, D.W., 1950 [50]	Same as above	Same as above			Interferometer	293	0.000	Texture: Fine. Other: Same as above except heating cycle.
							273	-0.012	
							250	-0.021	
							262	-0.016	
							273	-0.010	
18	Krupka, M.C., 1974 [51]	Los Alamos Basalt Glass; Los Alamos, MI	SiO ₂ Al ₂ O ₃ Fe ₂ O ₃ FeO MgO CaO Na ₂ O K ₂ O CO ₂ TiO ₂ P ₂ O ₅ MnO H ₂ O (drying only at 180 K)	49.90		Interferometer	284	-0.004	Density: 2.76 g cm ⁻³ . Other: Heating cycle.
				19.00			293	0.000	
				2.78			295	0.001	
				7.40			305	0.006	
				3.98			315	0.013	
				8.90			324	0.017	
				3.82			333	0.022	
				1.08			338	0.026	
				0.04			388	0.033	
				1.54			486	0.096	
				0.36			579	0.174	
				0.16			677	0.250	
				0.10			769	0.326	
		862	0.416						

TABLE 3.2. EXPERIMENTAL DATA ON THERMAL LINEAR EXPANSION OF BASALT (continued)

Data Set No.	Author(s), Year [Ref. No.]	Name and Source	Minerals and/or Chemical Composition Components	Weight Percent	Volume Percent	Method Used	Experimental Data		Other Specifications
							T, K	Thermal Linear Expansion (%)	
20	Krupka, M.C., 1974 [51]	Same as above	Same as above				390 486 577 766 860	0.047 0.115 0.189 0.269 0.350 0.440	Density: 2.76 g cm ⁻³ . Other: Cooling cycle.
21	Krupka, M.C., 1974 [51]	Average or General Basalt	SiO ₂ TiO ₂ Al ₂ O ₃ Fe ₂ O ₃ FeO MnO MgO CaO Na ₂ O K ₂ O P ₂ O ₅ H ₂ O†	49.3 2.0 16.0 3.2 7.8 0.17 6.6 9.9 2.8 1.0 0.32 0.9			273 293 313 333 353 373	-0.0108 0.0000 0.0108 0.0216 0.0324 0.0432	Density: 2.8 g cm ⁻³ .
22	Johnson, W.H. and Parsons, W.H., 1944 [52]	Basalt; Parker Dam, AZ	Labradorite Olivine (3/4 altered to iddingsite) Augite Magnetite Analeite		<3	Interferometer	253 273 293 333	-0.0216 -0.0106 0.0000 0.024	Texture: Fine porphyritic. Specimen Geometry: Disc 0.5-1.5 in. diam. and 0.2-0.4 in. thick. Other: Values calculated from mean coefficient of thermal expansion.
23	Johnson, W.H. and Parsons, W.H., 1944 [52]	Vesicular Basalt; Parker Dam, AZ	Labradorite Olivine (altered to iddingsite) Magnetite Trace Calcite		<3	Interferometer	253 273 293 333	-0.0155 -0.0074 0.0000 0.0197	Same as above.
24	Johnson, W.H. and Parsons, W.H., 1944 [52]	Basalt Porphyry; Shasta Dam, CA	Labradorite Augite Magnetite		<3		253 273 293 333	-0.0242 -0.0120 0.0000 0.0254	Texture: Fine and medium porphyritic. Specimen Geometry: Same as above. Other: Same as above.
25	Johnson, W.H. and Parsons, W.H., 1944 [52]	Same as above	Labradorite Augite Zoisite Magnetite Chlorite Sericite Microcrystalline Quartz		<3	Interferometer	253 273 293 333	-0.0242 -0.0120 0.0000 0.0254	Same as above.
26	Johnson, W.H. and Parsons, W.H., 1944 [52]	Lyon Basalt; Lyon Mt., NY	Pagioclase-laths Augite Chlorite Magnetite		<3	Interferometer	253 273 293 333	-0.0275 -0.0138 0.0000 0.0269	Texture: Very fine. Specimen Geometry: Same as above. Other: Same as above.

TABLE 3.2. EXPERIMENTAL DATA ON THERMAL LINEAR EXPANSION OF BASALT (continued)

Data Set No.	Author(s), Year [Ref. No.]	Name and Source	Minerals and/or Chemical Components	Minerals and/or Chemical Composition		Method Used	Experimental Data		Other Specifications
				Weight Percent	Volume Percent		T, K	Thermal Linear Expansion (%)	
27	Johnson, W.H. and Parsons, W.H., 1944 [52]	Same as above	Same as above			Interferometer	253	-0.0280	Texture: Very fine. Specimen Geometry: Disc 0.5-1.5 in. diam. and 0.2-0.4 in. thick.
							273	-0.0140	
28	Thirumalai, K., Cheung, J.E., Chen, T.S., Bemou, S.G., and Krawza, M.G., 1972 [53]	Dresser Basalt; Dresser, WI	Feldspar Augite Magnetite	50 40 10		Dilatometer	333	0.0000	Texture: Grain size 0.25-0.03 mm. Other: Values calculated by integrating instantaneous coefficient of thermal expansion reported by author.
							313	0.001	
							327	0.002	
							327	0.003	
							345	0.011	
							354	0.017	
							377	0.034	
							390	0.046	
							412	0.066	
							430	0.090	
							462	0.111	
							489	0.137	
525	0.176								
561	0.217								
606	0.271								
629	0.296								
638	0.306								
647	0.315								
682	0.352								
759	0.439								
786	0.471								
818	0.512								
840	0.543								
849	0.557								
908	0.657								
917	0.676								
935	0.712								
962	0.765								
980	0.799								
993	0.820								
1024	0.858								
1042	0.874								
1050	0.882								
1055	0.886								
1064	0.893								
1077	0.902								
1096	0.916								
1114	0.936								
1150	0.985								
1182	1.062								
1187	1.077								
1201	1.122								
1210	1.155								
1214	1.172								
1228	1.217								
1236	1.245								
1245	1.268								

TABLE 3.2. EXPERIMENTAL DATA ON THERMAL LINEAR EXPANSION OF BASALT (continued)

Data Set No.	Author(s), Year [Ref. No.]	Name and Source	Minerals and/or Chemical Composition		Method Used	Experimental Data		Other Specifications
			Componenta	Weight Percent		T, K	Thermal Linear Expansion (%)	
28								
28	cont.							
29	Erikson, R.L. and Krupka, K.M., 1980 [54]	Pomona Basalt, Designated as DB-5-408; Southeastern WA	SiO ₂ Al ₂ O ₃ CaO MgO FeO Fe ₂ O ₃ Na ₂ O TiO ₂ K ₂ O P ₂ O ₅ H ₂ O	52.69 15.03 10.08 6.01 5.88 5.14 2.69 1.60 0.49 0.25 0.17	Dilatometer	293 373 423 473 523 573	0.000 0.097 0.121 0.138 0.148 0.156	Density: 2.88 g cm ⁻³ . Apparent Porosity: 0.60%. Texture: Gray to gray-black on unweathered surfaces, nonvesicular and unfractured. Specimen Geometry: Sample cut perpendicular to the axes of the core, 3.81 cm outside diam. x 1.35 cm inside diam. x 6.51 cm thick. Other: 6.03 cm diam. core supplied by Rockwell Hanford operations from 408 ft. depth; oxide analysis reported here is for cores from 397 ft. depth; minerals identified in X-ray diffractograms of powdered whole rock samples are plagioclase, pyroxene, and magnetite; mineral identified in thin sections in order of decreasing abundance are plagioclase, clinopyroxene, and un-identified clay alteration products, opaques, and olivine; petrographic examination indicate that the Pomona basalt is plagioclase-phyric; authors feel that their data may be in error.
30	Erikson, R.L. and Krupka, K.M., 1980 [54]	Pomona Basalt, Designated as DB-15-308; Southeastern, WA	SiO ₂ Al ₂ O ₃ CaO MgO FeO Fe ₂ O ₃ Na ₂ O TiO ₂ K ₂ O P ₂ O ₅ H ₂ O	53.44 15.01 9.88 5.84 5.57 4.86 2.80 1.60 0.58 0.24 0.16	Dilatometer	293 373 423 473 523 573	0.000 0.077 0.091 0.104 0.112 0.120	Density: 2.86 g cm ⁻³ . Apparent Porosity: 0.50%. Texture: Same as above. Specimen Geometry: Same as above. Other: Same as above except oxide analysis reported here is for core from 310 ft. depth; mineralogy of this sample is same as above except proportion of plagioclase phenocrysts is smaller; authors feel that their data appears to be in error.
31	Duwall, W.I., Miller, R.J., and Wang, F.D., 1978 [37]	Pomona Basalt, Drill Hole DC-10 Designated as XPI; Gable Mt., WA			Dilatometer	293 573	0.000 0.185	Density: 2.86 g cm ⁻³ . Specimen Geometry: 0.25 in. diam. x 1.2 in. length. Other: Sample taken from 143.2 ft. below the drill hole; thermal expansion measured continuously from

TABLE 3.2. EXPERIMENTAL DATA ON THERMAL LINEAR EXPANSION OF BASALT (continued)

Data Set No.	Author(s), Year [Ref. No.]	Name and Source	Minerals and/or Chemical Composition		Method Used	Experimental Data		Other Specifications
			Weight Percent	Volume Percent		T, K	Thermal Linear Expansion (%)	
31 cont.								293-573 K, no significant change in the coefficient of thermal expansion (average value $6.6 \times 10^{-6} \text{K}^{-1}$) was observed.
32	Duvall, W.L., et al., 1978 [37]	Pomona Basalt, Drill hole DC-10 Designated as XP2; Gable Mt.			Dilatometer	293 573	0.000 0.182	Density: 2.84 g cm^{-3} . Specimen Geometry: Same as above. Other: Same as above except sample taken from 175.5 ft. below drill hole; average coefficient of thermal expansion $6.5 \times 10^{-6} \text{K}^{-1}$.
33	Duvall, W.L., et al., 1978 [37]	Pomona Basalt, Drill hole DC-10 Designated as XP3; Gable Mt.				293 573	0.000 0.188	Density: 2.87 g cm^{-3} . Specimen Geometry: Same as above. Other: Same as above except sample taken from 197.3 ft. below the drill hole; average instantaneous coefficient of thermal expansion $6.7 \times 10^{-6} \text{K}^{-1}$.
34	Foundation Sciences, Inc., 1980 [38]	Pomona Basalt (NSTF), Area 2; Gable Mt., WA			Strain Gauge	343 423 573	0.042 0.096 0.224	Density: 2.82 g cm^{-3} (bulk). Texture: Porphyritic with lath- or blade-shaped crystals of plagioclase (<5 mm) and less commonly irregular crystals of olivine and clinopyroxene (<5 mm) in a fine-grained groundmass; green to blue-green mineraloid (chlorophaeite) occurs both in irregular interstitial patches in the groundmass and as a vesicle filling or lining; joints are commonly lined with chlorophaeite. Other: Basalt from NSTF (Near Surface Test Facility); sample taken from Full Scale Heater Test No. 2 in Instrument bore hole (Area 2); sample no. 2-31-B from bore hole 2E8 (depth 5.7-6.5 ft.); measurements are for vertical bore hole; strain gauge axially oriented; values calculated from reported mean coefficients.
35	Foundation Sciences, Inc., 1980 [38]	Same as above			Same as above	343 423 573	0.045 0.107 0.252	Density: 2.87 g cm^{-3} (bulk). Texture: Same as above. Other: Same as above except sample no. 2-35-B from bore hole 2E9 (depth 10.9-11.5 ft.); measurements are for vertical bore hole; strain gauge radially oriented.

TABLE 3.2. EXPERIMENTAL DATA ON THERMAL LINEAR EXPANSION OF BASALT (continued)

Data Set No.	Author(s), Year [Ref. No.]	Name and Source	Minerals and/or Chemical Composition		Experimental Data		Method Used	Other Specifications
			Components	Weight Percent	T, K	Thermal Linear Expansion (%)		
36	Foundation Sciences, Inc., 1980 [38]	Same as above			Same as above	343 423 573	0.042 0.094 0.213	Density: Same as above. Texture: Same as above. Other: Same as above except strain gauge axially oriented.
37	Foundation Sciences, Inc., 1980 [38]	Same as above			Same as above	343 423 573	0.042 0.096 0.216	Density: Same as above. Texture: Same as above. Other: Same as above except sample no. 2-58-B from bore hole 2M3 (depth 28.0-29.0 ft.); measurements for vertical bore hole; strain gauge radially oriented.
38	Foundation Sciences, Inc., 1980 [38]	Same as above			Same as above	343 423 573	0.019 0.086 0.193	Density: Same as above. Texture: Same as above. Other: Same as above except strain gauge axially oriented.
39	Foundation Sciences, Inc., 1980 [38]	Same as above			Same as above	373 423 573	0.063 0.103 0.238	Density: Same as above. Texture: Same as above. Other: Same as above except sample no. 2-80-B from bore hole 2E1 (depth 20.2-20.9 ft.); measurements are for vertical bore hole; strain gauge radially oriented.
40	Foundation Sciences, Inc., 1980 [38]	Same as above			Same as above	373 423 573	0.058 0.091 0.216	Density: Same as above. Texture: Same as above. Other: Same as above except strain gauge axially oriented.
41	Foundation Sciences, Inc., 1980 [38]	Same as above			Same as above	373 423 573	0.062 0.098 0.213	Density: 2.84 g cm ⁻³ (bulk). Texture: Same as above. Other: Same as above except sample no. 2-65-B from bore hole 2E28 (depth 37.6-38.3 ft.); measurements for horizontal bore hole; strain gauge axially oriented.
42	Foundation Sciences, Inc., 1980 [38]	Same as above			Same as above	343 423 573	0.044 0.098 0.216	Density: 2.85 g cm ⁻³ (bulk). Texture: Same as above. Other: Same as above except sample no. 2-72-B from bore hole 2M16 (depth 30.7-31.3 ft.); measurements for horizontal bore hole; strain gauge radially oriented.
43	Foundation Sciences, Inc., 1980 [38]	Same as above			Same as above	343 423 573	0.040 0.088 0.196	Density: Same as above. Texture: Same as above. Other: Same as above except strain gauge axially oriented.

TABLE 3.2. EXPERIMENTAL DATA ON THERMAL LINEAR EXPANSION OF BASALT (continued)

Data Set No.	Author(s), Year [Ref. No.]	Name and Source	Minerals and/or Chemical Components	Chemical Composition		Method Used	Experimental Data		Other Specifications
				Weight Percent	Volume Percent		T, K	Thermal Linear Expansion (%)	
44	Foundation Sciences, Inc., 1980 [38]	Same as above			Same as above	373 423 573	0.060 0.094 0.216	Density: 2.86 g cm ⁻³ (bulk). Texture: Same as above. Other: Same as above except sample no. 2-91-B from bore hole ZM16 (depth 22.3-22.8 ft.); measurements for horizontal bore hole; strain gauge radially oriented.	
45	Foundation Sciences, Inc., 1980 [38]	Same as above			Same as above	373 423 573	0.055 0.085 0.193	Density: Same as above. Texture: Same as above. Other: Same as above except strain gauge axially oriented.	
46	Foundation Sciences, Inc., 1980 [38]	Same as above			Same as above	373 423 573	0.066 0.105 0.246	Density: Same as above. Texture: Same as above. Other: Same as above except sample no. 2-105-B from bore hole 2E26 (depth 18.5-19.0 ft.); measurements for horizontal bore hole; strain gauge radially oriented.	
47	Foundation Sciences, Inc., 1980 [38]	Same as above			Same as above	373 423 573	0.062 0.099 0.235	Density: Same as above. Texture: Same as above. Other: Same as above except strain gauge axially oriented.	
48	Foundation Sciences, Inc., 1981 [40]	Umtanum Basalt, DC2; Cable Mt., WA				346 382 433 515	0.038 0.061 0.098 0.138	Density: 2.80 g cm ⁻³ (bulk). Texture: Dark grey, aphanitic and massive, moderately fractured and occasionally contains vesicles; fractures usually closed or filled; mineralized filling are characterized by dark green-black chlorite followed by silica stringers. Other: Umtanum basalt from bore hole DC2; sample no. 4-6-A (depth 3034.0-3035.4 ft.); strain gauge axially oriented; values calculated from reported mean coefficients.	
49	Foundation Sciences, Inc., 1981 [40]	Same as above				346 382 433 515	0.035 0.058 0.090 0.151	Density: Same as above. Texture: Same as above. Other: Same as above except strain gauge radially oriented.	
50	Foundation Sciences, Inc., 1981 [40]	Same as above				346 382 433 515	0.036 0.058 0.088 0.133	Density: Same as above. Texture: Same as above. Other: Same as above except sample no. 4-7-D (depth 3076.0-3077.4 ft.); strain gauge axially oriented.	

TABLE J.2. EXPERIMENTAL DATA ON THERMAL LINEAR EXPANSION OF BASALT (continued)

Data Set No.	Author(s), Year [Ref. No.]	Name and Source	Minerals and/or Chemical Composition		Method Used	Experimental Data		Other Specifications
			Components	Weight Percent		T, K	Thermal Linear Expansion (%)	
51	Foundation Sciences, Inc., 1981 [40]	Same as above				346 382 433 515	0.033 0.056 0.094 0.144	Density: Same as above. Texture: Same as above. Other: Same as above except strain gauge radially oriented.
52	Foundation Sciences, Inc., 1981 [40]	Same as above				346 382 433	0.037 0.061 0.099	Density: 2.82 g cm ⁻³ (bulk). Texture: Same as above. Other: Same as above except sample no. 4-31-B (depth 3110.2-3110.8 ft.); strain gauge axially oriented.
53	Foundation Sciences, Inc., 1981 [40]	Same as above				346 382 433	0.028 0.041 0.067	Density: Same as above. Texture: Same as above. Other: Same as above except strain gauge radially oriented.
54	Foundation Sciences, Inc., 1981 [40]	Same as above				346 382 433 515	0.038 0.062 0.097 0.133	Density: Same as above. Texture: Same as above. Other: Same as above except sample no. 4-33-B (depth 3118.0-3118.3 ft.); strain gauge axially oriented.
55	Foundation Sciences, Inc., 1981 [40]	Same as above				346 382 433 515	0.035 0.057 0.090 0.144	Density: Same as above. Texture: Same as above. Other: Same as above except strain gauge radially oriented.
56	Foundation Sciences, Inc., 1981 [40]	Same as above				346 382 433 515	0.036 0.059 0.094 0.140	Density: Same as above. Texture: Same as above. Other: Same as above except strain gauge orientation; mean values of the above 8 data sets.
57	Miller, R.J. and Bishop, R.C., 1979 [55]	Umtanum Basalt, Hole DC-6; Hanford Site, WA				845	0.407	Density: 2.63 g cm ⁻³ . Texture: Tight, planar, hairline fracture parallel to core axis sealed with film of montmorillonite. Other: Values calculated from reported mean coefficients; sample no. XP 7 (depth 3148.8 ft.).
58	Miller, R.J. and Bishop, R.C., 1979 [55]	Same as above				666	0.402	Density: 2.79 g cm ⁻³ . Texture: Same as above except scalloped, irregular fracture approximately parallel to core partly filled with montmorillonite. Other: Same as above except sample no. XP 9 (depth 3163.9 ft.).
59	Miller, R.J. and Bishop, R.C., 1979 [55]	Same as above				337-913	0.463	Density: 2.66 g cm ⁻³ . Texture: Tight, planar, hairline fracture parallel to core axis sealed with film of montmorillonite. Other: Same as above except sample no. XP 4 (depth 3182.9 ft.).

TABLE 3.2. EXPERIMENTAL DATA ON THERMAL LINEAR EXPANSION OF BASALT (continued)

Data Set No.	Author(s), Year [Ref. No.]	Name and Source	Minerals and/or Chemical Composition		Method Used	Experimental Data		Other Specifications
			Components	Weight Percent		T, K	Thermal Linear Expansion (%)	
60	Miller, R.J. and Bishop, R.C., 1979 [55]	Same as above				781	0.545	Density: 2.57 g cm^{-3} Texture: Light grey, slightly greenish mottling; mottling is probably patchy secondary, green montmorillonite. Other: Same as above except sample no. XP 5 (depth 3253.0 ft.).
61	Miller, R.J. and Bishop, R.C., 1979 [55]	Same as above				819	0.551	Density: 2.49 g cm^{-3} Texture: Tight, planar, hairline fracture parallel to the core axis sealed with film of montmorillonite, showing wavy discontinuous, slightly greenish mottling approximately perpendicular to core axis and probably representing flow layering; less fractured than previously stated. Other: Same as above except sample no. XP 11 (depth 3256.3 ft.).
62	Miller, R.J. and Bishop, R.C., 1979 [55]	Same as above				849	0.562	Density: Same as above. Texture: Same as above. Other: Same as above except sample no. XP 12 (depth 3256.3 ft.).
63	Miller, R.J. and Bishop, R.C., 1979 [55]	Same as above				821	0.581	Density: Same as above. Texture: Same as above. Other: Same as above except sample saturated.

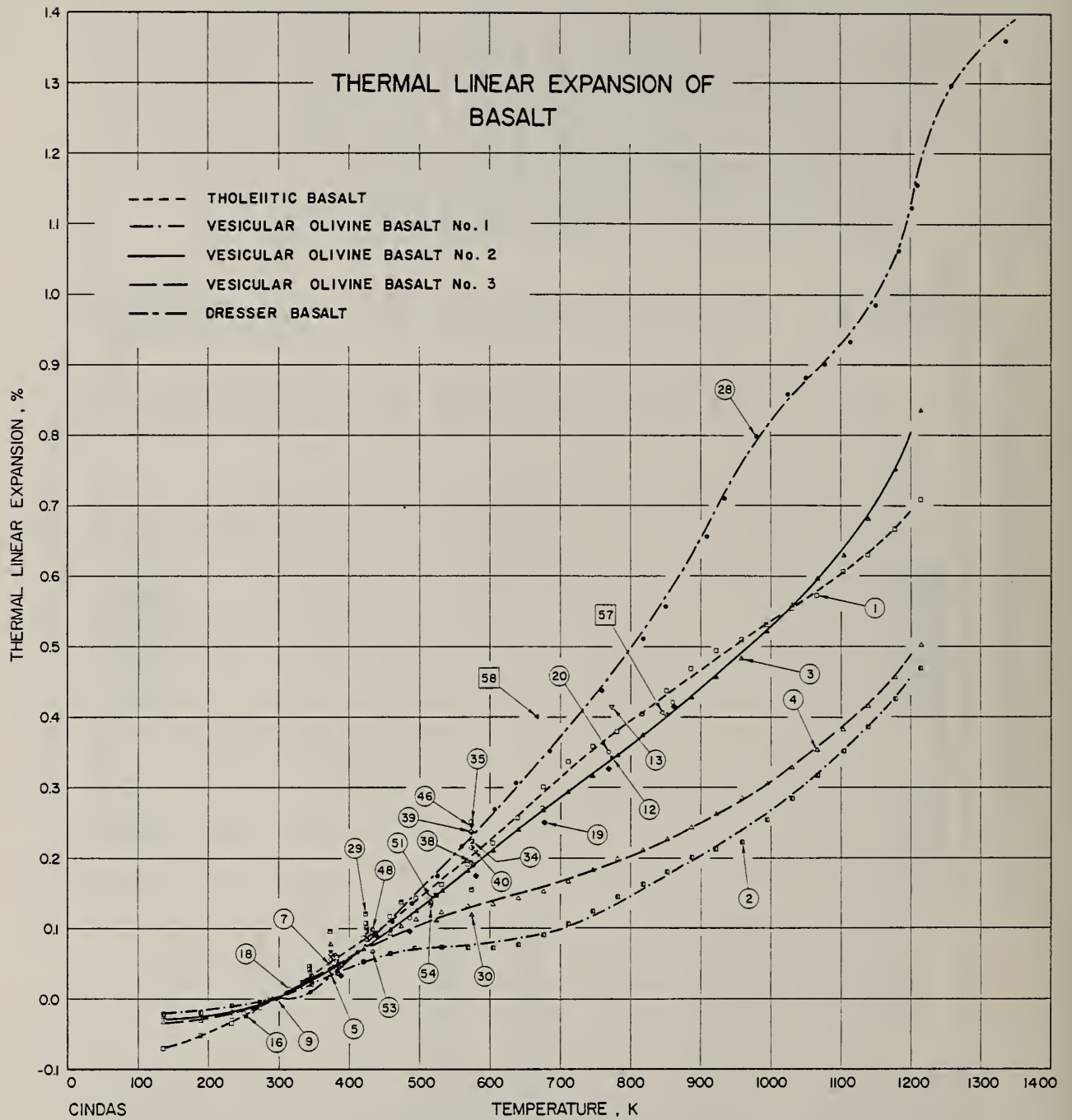


Figure 3.3. Thermal linear expansion of basalt.

basalt with fine-grained, glassy structure fall within the range of the data of Griffin and Demou [45] for basalt with low glass content. Therefore, their [45] results, including three small but distinct anomalies, cannot be explained on the mineralogical composition alone. This anomalous behavior, especially higher thermal expansion values, can be partly attributed to the various degrees of premelting under certain conditions occurring in basalts.

The percent thermal expansion values calculated using instantaneous coefficients of Thirumalai et al. [53] for the Dresser basalt yielded much higher values above 800 K and much lower values below 350 K than those reported for other basalts.

The data of Duvall et al. [37] for Pomona flow basalt from drill hole DC-10 agree well with those for tholeiitic basalt [45] (data set 1). These have similar chemical and physical compositions. Furthermore, they [37] observed no significant change in the instantaneous coefficients from 293 to 573 K. The data of Erikson and Krupka [54] appear to be in error mainly because of their experimental difficulties.

The data of Foundation Sciences Inc. [38] (data sets 34-47) are for Pomona Flow basalt from the Near Surface Test Facility bore hole 5.7 to 38.3 feet deep. Thermal expansion at 573 K varies from 0.196 to 0.252% for various samples of densities 2.82 to 2.85 g cm⁻³. However, the data of Foundation Sciences Inc. [40] (data sets 48-56) are much lower, about 0.14% at 515 K for most of their specimens (density 2.80 g cm⁻³) taken from about a 3100 feet deep bore hole. The data of Miller and Bishop [55] are for another Hanford Site basalt (Umtanum basalt Drill Hole DC-6).

The detailed mineralogical analysis and composition of different basalts, the thermal expansion of each of the minerals, and the effects of each of these minerals on the overall thermal expansion of a given basalt must be known in order to attempt a systematic data analysis and to generate the recommended values. From the above discussion, it is quite clear that a set of recommended values for a basalt from a given location cannot be given. Therefore, the experimental data for each of the individual data sets presently available in the literature are given in Table 3.2 and shown in Figure 3.3 so that the readers will have easy access to this information. At the same time the smooth values taken from the data for basalts from a few selected regions are tabulated in Table 3.3 and shown in Figures 3.3 and 3.4.

TABLE 3.3. THERMAL LINEAR EXPANSION OF BASALTS*

[Temperature, T, K; Thermal Linear Expansion, $\Delta L/L_0$, %]

T	$\Delta L/L_0$				
	Dresser Basalt ^a	Tholeiitic Basalt ^b	Vesicular Olivine Basalt ^c No. 1	Vesicular Olivine Basalt ^d No. 2	Vesicular Olivine Basalt ^e No. 3
150		-0.066	-0.020	-0.027	-0.033
200		-0.047	-0.015	-0.024	-0.027
250		-0.023	-0.009	-0.015	-0.016
273		-0.010	-0.005	-0.008	-0.007
293	0.000	0.000	0.000	0.000	0.000
298	0.001	0.002	0.002	0.002	0.004
300	0.002	0.005	0.004	0.003	0.005
350	0.013	0.036	0.023	0.028	0.032
400	0.056	0.070	0.044	0.058	0.061
450	0.106	0.105	0.061	0.092	0.085
500	0.156	0.144	0.072	0.129	0.105
550	0.207	0.184	0.075	0.169	0.124
600	0.259	0.226	0.080	0.211	0.139
650	0.315	0.270	0.088	0.249	0.152
700	0.372	0.315	0.100	0.287	0.167
750	0.433	0.356	0.120	0.324	0.184
800	0.498	0.395	0.146	0.361	0.203
850	0.570	0.427	0.174	0.400	0.225
900	0.653	0.467	0.203	0.443	0.250
950	0.748	0.503	0.234	0.484	0.278
1000	0.820	0.536	0.268	0.530	0.309
1050	0.878	0.567	0.306	0.579	0.345
1100	0.930	0.604	0.350	0.635	0.385
1150	1.000	0.643	0.398	0.708	0.432
1200	1.120	0.693	0.456	0.804	0.487
1250	1.280				
1300	1.352				
1350					

* The tabulated values are smooth values derived from experimental data. See footnotes below.

^aThe values are from ref. [53] (data set 28).

^bThe values are from ref. [45] (data set 1).

^cThe values are from ref. [45] (data set 2).

^dThe values are from ref. [45] (data set 3).

^eThe values are from ref. [45] (data set 4).

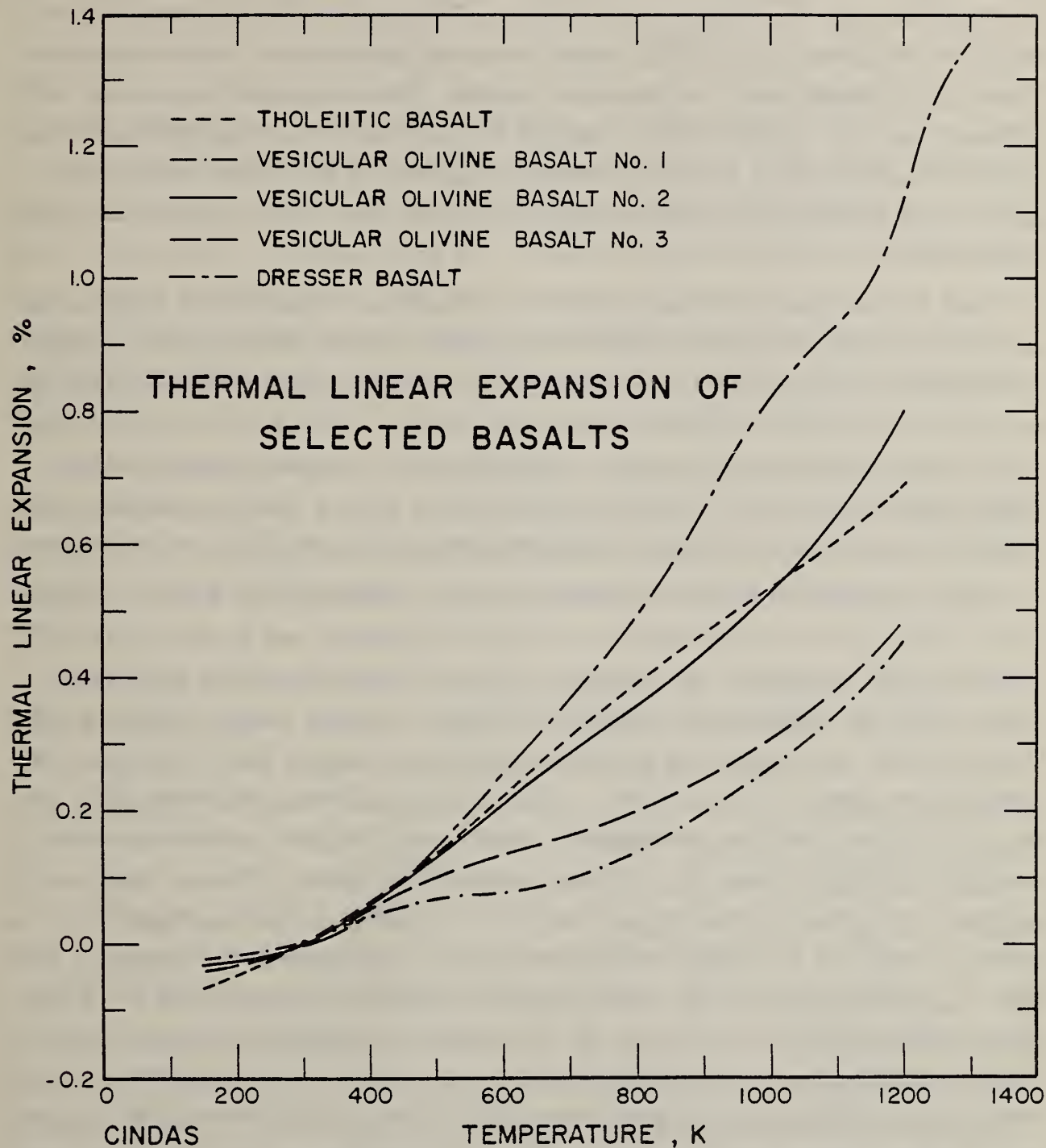


Figure 3.4. Thermal linear expansion of selected basalts.

3.5. SPECIFIC HEAT

There are over 40 data sets available for the specific heat of basalts. Data of Hanley et al. [33], Krupka [51], Thirumalai et al. [53], Lindroth and Krawza [56], and of Stephens and Sinnock [57] are for Dresser basalt. In addition, Dmitriev et al. [58] report the data for andesite basalt and Robie et al. [59] report data for vesicular basalt. The data of Duvall et al. [37] (data sets 12-14), Martinez-Baez and Hal Amick [35] (data sets 16-19), Erikson and Krupka [54] (data set 21), Foundation Sciences Inc. [40] (data sets 23-26), and Foundation Sciences Inc. [38] (data sets 27-42) are for Hanford Site basalts.

Due to the absence of any essential information required for correlating the data with the structural differences among basalts from various regions, it is practically impossible to generate a set of recommended values which can be applied to basalts in general from the specific heat data presently available in the literature. Therefore, specification and data from individual investigators are given in Table 3.4 and Figure 3.5 so that the readers will have easy access to all available information on the specific heat of basalts.

The recommended values for Dresser basalt presented in Table 3.5 are based on the data of Thirumalai et al. [53], Lindroth and Krawza [56], and Leonidov [60] for basalt of somewhat similar composition. The mixing rule calculations of Stephens and Sinnock [57] yield slightly lower values. Krupka [51] reported the specific heat values for Dresser basalt but did not clearly identify the source of his values. The data of Lindroth and Krawza [56] are up to 8% higher than the recommended values, and indicate a distinct anomaly near 848 K which is near the α - β quartz inversion point. This is very surprising since the Dresser basalt which they studied did not contain free quartz. They did not offer any explanation for this anomalous behavior. The data of Leonidov [60] do not show anomalous specific heat near 848 K. Based on the data available so far in the literature, no judgment could be made about the behavior of the specific heat values near 848 K. Therefore, the abrupt drop in the specific heat reported by Lindroth and Krawza [56] is ignored in the present data analysis. It is interesting to note that the data for the Dresser basalt below 300 K join smoothly into the low temperature data

of Robie et al. [59] (data set 8) for Apollo 11 lunar sample and those of Hemingway et al. [62] (data set 22) for Apollo 14 lunar sample. Erikson and Krupka [54] observed anomalous relative enthalpy values for Pomona basalt at 573 K and 623 K. Since basalt does not undergo any phase transition at these temperatures, they attributed this anomalous behavior to the loss of about 1% structural water. Their specific heat values, in general, are about 5% higher than the values recommended for the Dresser basalt. The difference between the CINDAS recommended values for the Dresser basalt and the data of Lindroth and Krawza [56] and of Erikson and Krupka [54] may be partially due to the analytical method which they chose to represent their measured enthalpy data and to derive the c_p values from it. In this type of derivation, uncertainty in c_p values is much higher than that in directly measured ones. The equation representing c_p values based on the data of Allen [64] and Scheller [65] reported by Lehnhoff and Scheller [63] for Dresser basalt yielded extremely high values.

The recommended values for the Dresser basalt tabulated in Table 3.5 are considered accurate to within $\pm 7\%$. The specific heat values for other types of basalts of similar composition and physical structural characteristics are expected to have values similar to those recommended within the limits stated above.

The data of Duvall et al. [37] for basalt from the Pomona flow in the Gable Mountain region for some unknown reason are much higher than those for other basalts. The values of Martinez-Baez and Hal Amick [35] for basalts from Gable Mountain and Umtanum regions are calculated by a method consisting of summation of individual constituents of basalt based on oxide analysis are higher than those reported by Stephens and Sinnock [57] using the simple mixing rule. Foundation Sciences Inc. [40] found that c_p for Umtanum basalt from bore hole DC-2 increases from $950 \text{ J kg}^{-1} \text{ K}^{-1}$ at 343 K to about $1010 \text{ J kg}^{-1} \text{ K}^{-1}$ at 573 K and is constant between 573 K and 623 K and, further, the specific heat data of Umtanum basalt are, in general, in fair agreement with those for Pomona basalt, except that the specific heat of Pomona basalt has a slightly greater temperature dependence. Foundation Sciences Inc. [38] reported that specific heat values for Pomona basalt (NSTF) from Area 2 are quite similar to those from Area 1 [39]. Erikson and Krupka [54] have indicated that the physical and chemical properties of Pomona basalt are similar

TABLE 3.4. EXPERIMENTAL DATA ON SPECIFIC HEAT OF BASALT

Data Set No.	Author(s), Year [Ref. No.]	Name and Source	Minerals and/or Chemical Composition		Experimental Data		Method Used	Other Specifications
			Componenta	Weight Percent	T, K	Specific Heat (J kg ⁻¹ K ⁻¹)		
1	Hanley, E.J., DeKitt, D.P., and Taylor, R.E., 1977 [33]	Dresser Basalt; Dresser, WI	Plagioclase (labradorite)	45	Differential Scanning Calorimeter	300	778	Structure: Massive jointed. Texture: Aphanitic. Specimen Geometry: Solid pieces of 4 mm. Other: Values represent average of 5 sample measurements, variations between measurements and the reported mean are <2%.
			Augite	34		340	833	
			Serpentine	16		380	874	
			Opauques (magnetite and ilmenite)	3		420	916	
			Chlorite	2		460	954	
2	Thirumalai, K., Cheung, J.E., Chen, T.S., Demou, S.G., and Krawza, W.G., 1972 [53]	Dresser Basalt; Dresser, WI	Feldspar	50	Drop Copper Block	380	962	Texture: Fine grained of size 0.25-0.03 mm. Other: No other details are given.
			Augite	40		598	1071	
			Magnetite	10		752	1151	
						854	1205	
						863	1079	
3	Lindroth, D.P. and Krawza, W.G., 1971 [56]	Dresser Basalt; Dresser, WI	Plagioclase	50	Drop Copper Block	372	962	Specific Gravity: 2.97. Texture: Grain size 0.01-0.30 mm. Other: Smooth values calculated from equation: $c_p = 0.216 + 0.123 \times 10^{-3} (T-273)$ for 373<T<848 $c_p = 0.258$ for 848<T<1273; transition near 848 K; reported error $\pm 1.5\%$.
			Pyroxene-Amphibole	45		400	974	
			Magnetite	5		500	1029	
			SiO ₂	48.42		600	1079	
			Al ₂ O ₃	15.23		700	1130	
4	Stephens, H.P. and Simcock, S., 1980 [57]	Dresser Basalt; Dresser, WI	CaO	8.35		800	1184	Other: Values calculated from the specific heat of its components using mixing rule.
			FeO	6.70		848	1205	
			Fe ₂ O ₃	6.60		900	1080	
			MgO	6.14		1000	1080	
			Plagioclase	50		300	736	
5	Krupka, M.C., 1974 [51]	Dresser Basalt; Dresser, WI	Pyroxene	45		380	858	Other: No details given.
			Magnetite	5		500	962	
						800	1092	
						380	966	
						408	982	
		436	994					
		463	1005					
		482	1019					
		510	1031					
		528	1042					
		542	1050					
		556	1054					
		574	1060					
		584	1062					
		602	1068					
		626	1068					
		644	1072					
		667	1076					
		695	1078					
		728	1078					
		774	1078					
		811	1080					

TABLE 3.4. EXPERIMENTAL DATA ON SPECIFIC HEAT OF BASALT (continued)

Data Set No.	Author(s), Year [Ref. No.]	Name and Source	Minerals and/or Chemical Composition		Method Used	Experimental Data		Other Specifications
			Weight Percent	Volume Percent		T, K	Specific Heat ($J kg^{-1} K^{-1}$)	
5	cont.					863	1080	
						904	1078	
						946	1078	
						997	1078	
						1049	1076	
						1114	1077	
						1170	1079	
						1207	1077	
						1258	1075	
						293	799	
6	Dmitriev, A.P., Dukhovskoi, E.A., Novik, G.Ya., and Petrochenkov, R.G., 1972 [58]	Andesite-Basalt			Adiabatic Calorimeter			Specific Gravity: 1.22. Texture: Finely divided powder. Other: Test environment He.
7	Dmitriev, A.P., et al., 1972 [58]	Andesite-Basalt			Adiabatic Calorimeter	293	736	Specific Gravity: 1.14. Texture: Sand size particle. Other: Test environment He.
8	Robie, R.A., Hemingway, B., and Wilson, W.H., 1970 [59]	Vesicular Basalt, Apollo 11 Lunar Sample			Adiabatic Calorimeter	90	238	Specific Gravity: 3.4. Other: Smooth values; reported error $\pm 0.4\%$.
9	Leontidov, V.Ya., 1967 [60]					100	265	Other: Accuracy $\pm 2\%$.
						120	323	
						140	386	
						160	450	
						180	509	
						200	562	
						220	607	
						240	647	
						260	683	
						280	716	
300	747							
320	775							
340	802							
360	830							
374	870							
472	954							
573	1012							
673	1050							
775	1088							
873	1121							
973	1151							
1074	1180							
600	987							
10	Svikits, V.D., 1962 [61]	Canada			Isothermal Water Calorimeter	600	987	Specific Gravity: 3.043. Specimen Geometry: Block 3.8 x 3.8 x 10.2 cm. Texture: Altered rock, irregular banded and fine-grained. Other: Average of 2 runs, mean C_p between 898 K, temp. to which specimen was heated and 300 K, final temp. of bath.
			42					
			23					
			20					
			10					
			5					

TABLE 3.4. EXPERIMENTAL DATA ON SPECIFIC HEAT OF BASALT (continued)

Data Set No.	Author(s), Year [Ref. No.]	Name and Source	Minerals and/or Chemical Composition		Experimental Data		Other Specifications	
			Components	Weight Percent	Method Used	T, K		Specific Heat ($J\ kg^{-1}K^{-1}$)
11	Tadokoro, Y., 1921 [22]	Basalt from Province Tamba (Asia)	SiO ₂ Al ₂ O ₃ FeO CaO MgO Fe ₂ O ₃ MnO	69.48 11.87 9.43 5.00 2.47 1.00 0.49	Isothermal Water Calorimeter	338	787	Specific Gravity: 2.569. Specimen Geometry: Very thin plates 0.1-0.3 mm thick. Texture: Dark grey colored, no vesicular cavities; phenocrysts of plagioclase and olivine both of the order 0.8 mm in size present very sparingly. Other: Average of c_p by dropping specimen at 373 K in water at 303 K.
12	Duwall, W.L., Miller, R.J., and Wang, F.D., 1978 [37]	Pomona Flow of Gable Mt.				373 473 573	1314 1648 1983	Density: 2.69 $g\ cm^{-3}$. Other: Specimen taken from drill hole DC-10; 143.53-144.6 ft. below the drill hole collar.
13	Duwall, W.L., et al., 1978 [37]	Same as above				373 473 573	1485 1925 2448	Density: 2.83 $g\ cm^{-3}$. Other: Specimen taken from drill hole DC-10; 175.0-175.1 ft. below the drill hole collar.
14	Duwall, W.L., et al., 1978 [37]	Same as above				373 473 573	1205 1761 2318	Density: 2.85 $g\ cm^{-3}$. Other: Specimen taken from drill hole DC-10; 197.7-197.8 ft. below the drill hole collar.
15	Bernett, E.C., Wood, H.L., Jaffe, L.D., and Martens, H.E., 1962 [23]	Olivine Basalt, Pisgah Crater; San Bernardino County, CA			ASTM Procedure C351-61	305 332 361	945 975 987	Density: 2.97 $g\ cm^{-3}$. Texture: -35 mesh. Other: Large volcanic bomba crushed to 3 in. size by hydraulic press; passed through Gates jaw crusher and stainless steel hammer-mill type pulverizer to reduce it all to -35 mesh.
16	Martinez-Baez, L.F. and Hal Amick, C., 1978 [35]	Basalt from Gable Mt., Designated as DB-5			Indirect	323 373 423 473 523 573	916 992 1046 1088 1125 1159	Other: c_p calculated by a method consisting of summation of heat capacities of individual constituents of basalt sample based on oxide analysis; c_p values are calculated for "Gable mountain K1005" specimen which are assumed to be the same as those for DB-5.
17	Martinez-Baez, L.F. and Hal Amick, C., 1978 [35]	Same as above			Indirect	323 373 423 473 523 573	979 1059 1117 1163 1201 1238	Other: The above method used to calculate c_p ; c_p values are calculated for "Gable mountain A1266" specimen which are assumed to be the same as those for DB-5.
18	Martinez-Baez, L.F. and Hal Amick, C., 1978 [35]	Umtanum Basalt Flow Designated as DB-5			Indirect	323 373 423 473 523 573	908 983 1033 1075 1112 1151	Other: The above method used to calculate c_p values; the values are applicable to specimen recovered from the core of bore hole 2749 ft. deep.

TABLE 3.4. EXPERIMENTAL DATA ON SPECIFIC HEAT OF BASALT (continued)

Data Set No.	Author(s), Year [Ref. No.]	Name and Source	Minerals and/or Chemical Composition		Method Used	Experimental Data		Other Specifications
			Components	Weight Percent		T, K	Specific Heat (J kg ⁻¹ K ⁻¹)	
19	Martinez-Baez, L.F. and Hal Amick, C., 1978 [35]	Same as above			Indirect	323	925	Other: Similar to the above except the values are applicable to specimens recovered from the core of bore hole 2808 ft. deep.
						373	1000	
						423	1051	
						473	1096	
						523	1134	
						573	1167	
20	West, E.A. and Fountain, J.A., 1975 [36]	Terrestrial Basalt			Indirect	117	298	Density: 1.95 g cm ⁻³ . Texture: 53-256 μ size particles. Other: Values calculated from thermal conductivity and thermal diffusivity measurements.
						120	310	
						140	357	
						160	404	
						180	454	
						200	495	
						220	540	
						240	581	
						260	622	
						280	657	
						300	695	
						320	730	
						340	762	
						360	803	
21	Erikson, R.L. and Krupka, K.M., 1980 [54]	Pomona Basalt, DB-5-408 and DB-15-308; Southeastern, WA	SiO ₂ Al ₂ O ₃ CaO MgO FeO Fe ₂ O ₃ Na ₂ O TiO ₂ K ₂ O P ₂ O ₅ MnO	52.69 15.03 10.08 6.01 5.88 5.14 2.69 1.60 0.49 0.25 0.17	Drop Copper Block	298	707	Density: 2.88 g cm ⁻³ for DB-5-408 and 2.86 g cm ⁻³ for DB-15-308. Apparent Porosity: 0.60% for DB-5-408 and 0.50% for DB-15-308. Texture: Grey to grey-black on unweathered surfaces, nonvesicular and unfractured. Specimen Geometry: 1.54 cm dia x 5.40 cm long cores. Other: 6.03 cm dia cores supplied by Rockwell Hanford operations; cores were extracted from 408 ft. depth (DB-5) and 308 ft. depth (DB-15); oxide analysis reported here is for cores extracted from 397 ft. depth; minerals identified in X-ray diffractograms of powdered, whole rock samples are plagioclase, pyroxene, and magnetite, minerals identified in thin sections, in order of decreasing abundance are plagioclase, clinopyroxene, and unidentified clay alteration product, opaques, and olivine; petrographic examination indicate that the Pomona basalt is plagioclase-phyric; estimated uncertainty in c _p values is ±5-10%.
						300	711	
						310	745	
						323	782	
						348	845	
						373	895	
						398	933	
						423	966	
						448	992	
						473	1017	
						498	1033	
						523	1050	
						573	1071	
						623	1088	

TABLE 3.4. EXPERIMENTAL DATA ON SPECIFIC HEAT OF BASALT (continued)

Data Set No.	Author(s), Year [Ref. No.]	Name and Source	Minerals and/or Chemical Composition		Method Used	Experimental Data		Other Specifications
			Weight Percent	Volume Percent		T, K	Specific Heat ($J kg^{-1} K^{-1}$)	
22	Hemingway, B.S., Robie, R.A., and Wilson, W.H., 1973 [62]	Apollo 14 Lunar Sample			Adiabatic Calorimeter	90	228.9	Other: Sample designated at 1555, 159 (basalt) from Hadley-Apennine landing site; smooth values are tabulated.
						100	292.0	
						120	354.8	
						140	415.1	
						160	472.0	
						180	525.5	
						200	575.7	
						220	623.0	
						240	666.9	
						260	708.4	
						280	746.8	
						300	782.8	
						320	817.1	
340	850.2							
360	886.2							
23	Foundation Sciences, Inc., 1981 [40]	Umtanum Basalt DC2, Gable Mt., WA			ASTM Method C351	348.6	966.5	Density: 2.77 $g cm^{-3}$ (bulk), 2.85 $g cm^{-3}$ (grain). Texture: Dark grey, aphanitic, and massive; moderately fractured and occasionally contains vesicles; fractures usually closed or filled; mineralized fillings are characterized by dark green-black chlorite followed by silica stringers. Other: Umtanum basalt from bore hole DC-2; sample no. 4-4-B (depth 3043.1 ft.).
						465.2	983.2	
617.5	987.4							
24	Foundation Sciences, Inc., 1981 [40]	Same as above			Same as above	347.0	949.8	Density: 2.78 $g cm^{-3}$ (bulk), 2.73 $g cm^{-3}$ (grain). Texture: Same as above. Other: Same as above except sample no. 4-6-II (depth 3034.7 ft.).
						463.2	1016.7	
						618.0	1016.7	
25	Foundation Sciences, Inc., 1981 [40]	Same as above			Same as above	347.9	933.0	Density: 2.80 $g cm^{-3}$ (bulk), 2.61 $g cm^{-3}$ (grain). Texture: Same as above. Other: Same as above except sample no. 4-6-I (depth 3034.7 ft.).
						464.1	1004.2	
						617.2	1012.5	
26	Foundation Sciences, Inc., 1981 [40]	Same as above			Same as above	348.7	916.3	Density: 2.80 $g cm^{-3}$ (bulk), 2.71 $g cm^{-3}$ (grain). Texture: Same as above. Other: Same as above except sample no. 4-6-I (depth 3092.3 ft.).
						464.2	941.4	
						620.0	1008.3	

TABLE 3.4. EXPERIMENTAL DATA ON SPECIFIC HEAT OF BASALT (continued)

Data Set No.	Author(s), Year [Ref. No.]	Name and Source	Minerals and/or Chemical Composition		Method Used	Experimental Data		Other Specifications
			Weight Percent	Volume Percent		T, K	Specific Heat (J kg ⁻¹ K ⁻¹)	
27	Foundation Sciences, Inc., 1980 [38]	Pomona Basalt (NSTF), Area 2; Gable Mt., WA			ASTM Method C351	350.6 460.8 628.4	907.9 962.3 987.4	Density: 2.86 g cm ⁻³ (bulk), 2.97 g cm ⁻³ (grain). Texture: Porphyritic with lath- or blade-shaped crystals of plagioclase (<5 mm) and less commonly, irregular crystals of olivine and clinopyroxene (<5 mm) in a fine-grained groundmass; green to blue-green mineraloid (chlorophaseite) occurs both in irregular interstitial patches in the groundmass and as a vesicles filling or lining; joints are commonly lined with chlorophaseite. Other: Basalt cores from NSTF (Near-Surface Test Facility); samples from Full scale; Heater Test No. 2 Instrument bore holes (Ares 2); sample 2-34-B from bore hole no. 2E8 (depth 28.4 ft.).
28	Foundation Sciences, Inc., 1980 [38]	Same as above			Same as above	347.0 461.0 624.9	962.3 949.8 1012.5	Density: 2.86 g cm ⁻³ (bulk), 2.89 g cm ⁻³ (grain). Texture: Same as above. Other: Same as above except sample no. 2-62-C from bore hole 2E28 (depth 18.7 ft.).
29	Foundation Sciences, Inc., 1980 [38]	Same as above			Same as above	351.3 462.0 626.5	849.4 953.9 987.4	Density: 2.86 g cm ⁻³ (bulk), 3.03 g cm ⁻³ (grain). Texture: Same as above. Other: Same as above except sample no. 2-66-D from bore hole 2E28 (depth 43.2 ft.).
30	Foundation Sciences, Inc., 1980 [38]	Pomona Basalt (NSTF), Area 2, Gable Mt., WA			ASTM Method C351	349.9 465.2 631.2	937.2 966.5 1012.5	Density: 2.86 g cm ⁻³ (bulk), 2.96 g cm ⁻³ (grain). Texture: Same as above. Other: Same as above except sample no. 2-78-B from bore hole 2E1 (depth 11 ft.).
31	Foundation Sciences, Inc., 1980 [38]	Same as above			Same as above	351.0 461.6 624.4	912.1 966.5 1004.2	Density: 2.87 g cm ⁻³ (bulk), 2.97 g cm ⁻³ (grain). Texture: Same as above. Other: Same as above except sample no. 2-92-C from bore hole 2M16 (depth 42.4 ft.).

TABLE 3.4. EXPERIMENTAL DATA ON SPECIFIC HEAT OF BASALT (continued)

Data Set No.	Author(s), Year [Ref. No.]	Name and Source	Minerals and/or Chemical Composition		Method Used	Experimental Data		Other Specifications
			Components	Weight Percent		T, K	Specific Heat (J kg ⁻¹ K ⁻¹)	
32	Foundation Sciences, Inc., 1980 [38]	Same as above			Same as above	351.1 465.4 629.2	924.7 979.1 1012.5	Density: 2.86 g cm ⁻³ (bulk), 2.92 g cm ⁻³ (grain). Texture: Same as above. Other: Same as above except sample no. 2-102-C from bore hole 2E22 (depth 12.7 ft.).
33	Foundation Sciences, Inc., 1980 [38]	Same as above			Same as above	347.0 463.8 629.6	924.7 970.7 1016.7	Density: 2.85 g cm ⁻³ (bulk), 2.95 g cm ⁻³ (grain). Texture: Same as above. Other: Same as above except sample no. 2-112-B from bore hole 2E13 (depth 15.4 ft.).
34	Foundation Sciences, Inc., 1980 [38]	Same as above			Same as above	351.5 461.9 626.9	836.8 937.2 1012.5	Density: 2.86 g cm ⁻³ (bulk), 2.93 g cm ⁻³ (grain). Texture: Same as above. Other: Same as above except sample no. 2-118-E from bore hole 2E4 (depth 21.2 ft.).
35	Foundation Sciences, Inc., 1980 [39]	Pomona Basalt (NSTF), Area 1; Galile Mt., WA			Same as above	346.6 465.7 617.1	849.4 983.2 1020.9	Density: 2.83 g cm ⁻³ (bulk). Other: Sample no. 1-66-E from bore hole 1320 (depth 29.8 ft.); data extracted from Ref. [38].
36	Foundation Sciences, Inc., 1980 [39]	Same as above			Same as above	351.7 467.5 618.0	765.7 941.4 924.7	Density: 2.87 g cm ⁻³ (bulk). Other: Sample no. 1-76-C from bore hole 1E20 (depth 25.7 ft.); data extracted from Ref. [38].
37	Foundation Sciences, Inc., 1980 [39]	Same as above			Same as above	347.8 464.2 626.2	882.8 949.8 1054.4	Density: 2.87 g cm ⁻³ (bulk). Other: Sample no. 1-77-C from bore hole 1E20 (depth 20.2 ft.); data extracted from Ref. [38].
38	Foundation Sciences, Inc., 1980 [39]	Same as above			Same as above	348.4 463.9 605.0	1046.0 903.7 966.5	Density: 2.86 g cm ⁻³ (bulk). Other: Sample no. 1-82-B from bore hole 1E20 (depth 10.6 ft.); data extracted from Ref. [38].
39	Foundation Sciences, Inc., 1980 [39]	Same as above			Same as above	350.8 465.7 629.4	861.9 983.2 1033.4	Density: 2.87 g cm ⁻³ (bulk). Other: Sample no. 1-95-C from bore hole 1E6 (depth 22.9 ft.); data extracted from Ref. [38].
40	Foundation Sciences, Inc., 1980 [39]	Same as above			Same as above	352.2 465.8 628.2	782.4 916.3 1046.0	Density: 2.87 g cm ⁻³ (bulk). Other: Sample no. 1-99-C from bore hole 1E6 (depth 17.1 ft.); data extracted from Ref. [38].

TABLE 3.4. EXPERIMENTAL DATA ON SPECIFIC HEAT OF BASALT (continued)

Data Set No.	Author(s), Year [Ref. No.]	Name and Source	Minerals and/or Chemical Composition		Method Used	Experimental Data		Other Specifications
			Weight Percent	Volume Percent		T, K	Specific Heat ($J kg^{-1}K^{-1}$)	
41	Foundation Sciences, Inc., 1980 [39]	Same as above			Same as above	353.3	882.8	Density: $2.82 g cm^{-3}$ (bulk). Other: Sample no. I-102-D from bore hole IE6 (depth 4.5 ft.); data extracted from Ref. [38].
						469.1	928.8	
						623.0	1058.6	
42	Foundation Sciences, Inc., 1980 [39]	Same as above			Same as above	352.2	795.0	Density: $2.85 g cm^{-3}$ (bulk). Other: Sample no. I-116-B from bore hole IE6 (depth 8.3 ft.); data extracted from Ref. [38].
						462.2	912.1	
						622.5	1020.9	
43	Lehnhoff, T.L. and Scheller, I.D., 1975 [63]	Dresser Basalt				300	954.4	Other: Values based on the data of Allen [64] and Scheller [65]; $c_p = 920.5 \text{ ex } (J kg^{-1}K^{-1})$ $\alpha = 0.11 \times 10^{-2} T + 0.10 \times 10^{-4} T^2$ $\quad - 0.22 \times 10^{-7} T^3 + 0.12 \times 10^{-10} T^4$.
						400	1192.0	
						500	1574.4	
						600	2041.4	
						700	2449.8	

TABLE 3.5. SPECIFIC HEAT OF DRESSER BASALT

[Temperature, T, K; Specific Heat, c_p , J kg⁻¹K⁻¹]

T	c_p	T	c_p
100	260	700	1062
150	426	750	1077
200	557	800	1090
250	678	850	1102
273	772	900	1113
293	756	950	1122
298	765	1000	1131
300	770	1050	1139
350	842	1100	1146
400	898	1150	1152
450	940	1200	1160
500	975	1250	1165
550	1003	1300	1171
600	1026		
650	1045		

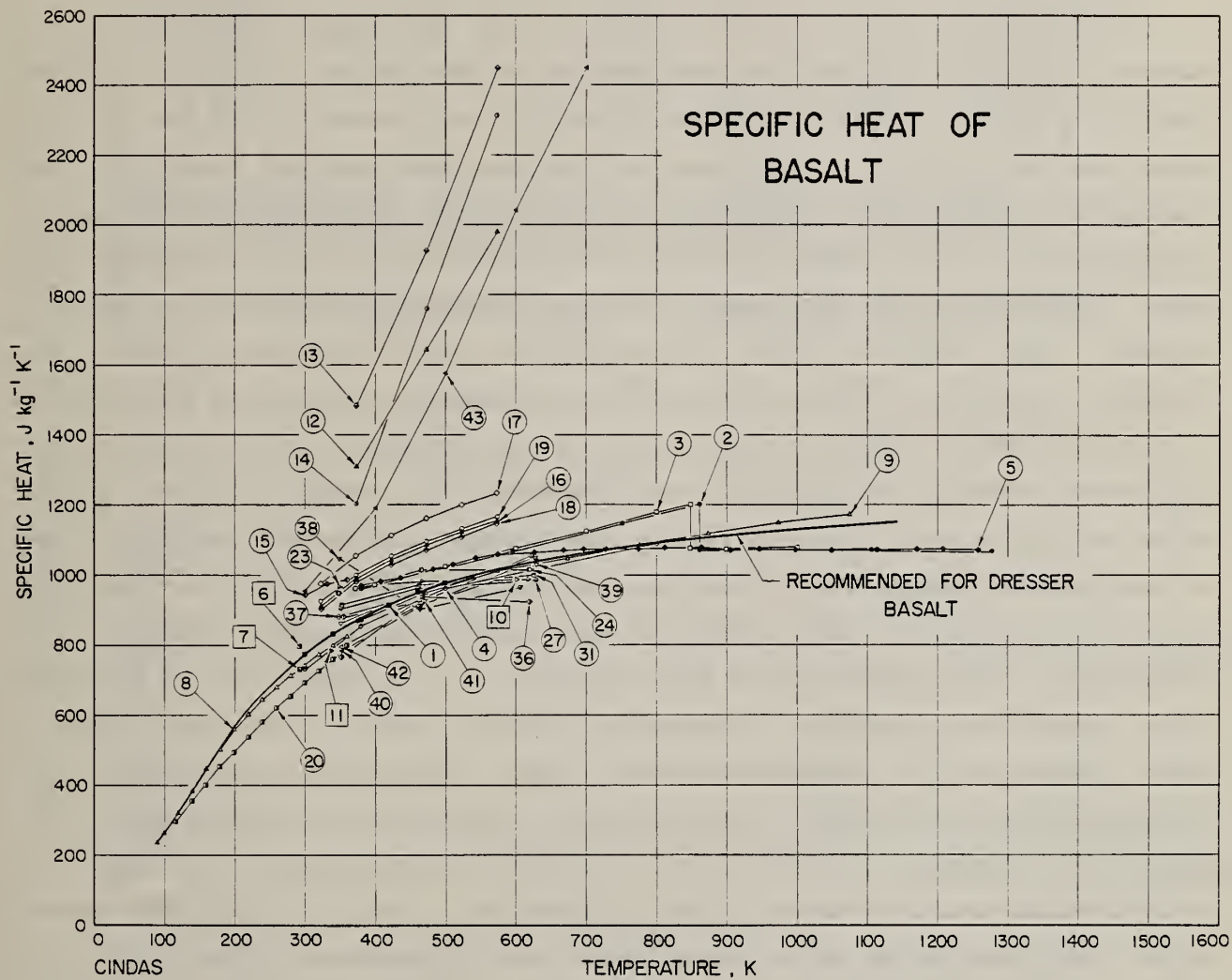


Figure 3.5. Specific heat of basalt.

to those of tholeiitic basalt (density 2.84 g cm^{-3} and porosity 2%), the thermal expansion of which is reported by Griffin and Demou [45]. Specific heat of this basalt is not reported in the literature. However, the above discussion should give guidelines to estimate c_p values for this and other types of basalt.

3.6. THERMAL DIFFUSIVITY

There are over 60 data sets available for the thermal diffusivity of basalt. These include the data for Dresser basalt [33,66] (data sets 1-4,35), tholeiitic basalt [67,71] (data sets 5-8,40), and lunar basalt [70,72,73] (data sets 36-39,41-47). Additionally, Martinez-Baez and Hal Amick [35], and Foundation Sciences Inc. [38-40] report the data on the Hanford Site basalt. Somerton et al. [74] report the data for augite basalt from the Mohole Test Site. Petrunin et al. [69] report the data for basalts from various parts of Armenia. These data sets cover the temperature range from 100 to 1850 K. The problems encountered in the analysis of thermophysical properties is discussed in the sections for other properties. The experimental data for each of the data sets presently available in the literature are given in Table 3.6 and shown in Figure 3.6. The room-temperature thermal diffusivity values for most of the basalts studied fall within the range from $0.0045 \times 10^{-4} \text{ m}^2 \text{ s}^{-1}$ to $0.0075 \times 10^{-4} \text{ m}^2 \text{ s}^{-1}$. Most of these data sets show similar temperature trends. These investigators have demonstrated that structural differences such as mineralogical composition, texture, interstitial fluids, porosity, and others have a larger impact on the thermal diffusivity than temperature dependence. Unusually high thermal diffusivity for Dresser basalt obtained by Hanley et al. [33,75] is accounted partially for relatively low plagioclase content, a mineral which tends to impair thermal diffusion. From the geological viewpoint, the Chinadiyeva and Akhuryan River basalts reported by Petrunin et al. [69], as well as the tholeiitic basalt reported by Lindroth [67], have similar mineralogical composition and structure, but different density and porosity. The data of Petrunin et al. [69] are a representative example of the effect of porosity on the thermal diffusivity of mineralogically similar basalts. Basalt of low porosity has higher thermal diffusivity. However, low thermal diffusivity values reported by Lindroth [67] cannot be adequately explained.

TABLE 3.6. EXPERIMENTAL DATA ON THERMAL DIFFUSIVITY OF BASALT

Data Set No.	Author(s), Year [Ref. No.]	Name and Source	Minerals and/or Chemical Composition		Experimental Data		Method Used	Other Specifications								
			Components	Weight Percent	Volume Percent	T, K			Thermal Diffusivity ($10^{-6} \text{ m}^2 \text{ s}^{-1}$)							
1	Bates, J.L., McNeilly, C.E., and Rasmussen, J.J., 1970 [66]	Basalt; Dresser, MI				299	0.01188	Specimen Geometry: Disk 1 cm dia, 0.076 cm long.								
						445	0.00933									
						566	0.00818									
						664	0.00729									
						791	0.00661									
						923	0.00596									
						962	0.00581									
						1110	0.00478									
						1090	0.00460									
						1194	0.00432									
						407	0.00982		Same as above.							
481	0.00908															
567	0.00804															
679	0.00721															
705	0.00674															
906	0.00589															
1157	0.00490															
1356	0.00414															
1409	0.00415															
1452	0.00378															
3	Bates, J.L., et al., 1970 [66]	Basalt; Dresser, MI				293	0.00554	Same as above except sample fused into sapphire crucible.								
						394	0.00477									
						634	0.00400									
						803	0.00389									
						1025	0.00377									
						1127	0.00321									
						1214	0.00313									
						1313	0.00340									
						1608	0.00335									
						1742	0.00349									
						1846	0.00343									
4	Bates, J.L., et al., 1970 [66]	Basalt; Dresser, MI				534	0.00562	Same as above.								
						904	0.00531									
						1127	0.00431									
						1323	0.00409									
						1531	0.00427									
						5	Lindroth, D.P., 1974 [67]		Tholeiitic Basalt	SiO ₂ Al ₂ O ₃ FeO CaO MgO Fe ₂ O ₃ Na ₂ O TiO ₂ K ₂ O P ₂ O ₅ H ₂ O ⁺ H ₂ O ⁻ CO ₂ S				298	0.00666	Specimen Geometry: Disk 19.05 mm dia, 4 mm thick. Test Environment: Nitrogen at 760 torr pressure. Other: Reported error 15%.
														383	0.00622	
														51.0		
														14.0		
														8.8		
														8.0		
4.4																
3.4																
3.4																
2.7																
1.7																
1.4																
0.76																
0.25																
0.10																
0.03																
0.004																

TABLE 3.6. EXPERIMENTAL DATA ON THERMAL DIFFUSIVITY OF BASALT (continued)

Date Set No.	Author(s), Year [Ref. No.]	Name and Source	Minerals and/or Chemical Composition		Method Used	Experimental Data		Other Specifications
			Components	Weight Percent		T.K Diffusivity ($10^{-4} \text{ m}^2 \text{ s}^{-1}$)	Thermal Diffusivity ($10^{-4} \text{ m}^2 \text{ s}^{-1}$)	
6	Lindroth, D.P., 1974 [67]	Tholeiitic Basalt	Same as above		Flash Method	298 383	0.00654 0.00616	Specimen Geometry: Same as above. Test Environment: Nitrogen at 1.0 x 10 ⁻² torr pressure. Other: Same as above.
7	Lindroth, D.P., 1974 [67]	Tholeiitic Basalt	Same as above		Flash Method	383	0.00623	Specimen Geometry: Same as above. Test Environment: Nitrogen at 7.0 x 10 ⁻⁷ torr pressure. Other: Same as above.
8	Lindroth, D.P., 1974 [67]	Tholeiitic Basalt	Same as above		Flash Method	298	0.00665	Specimen Geometry: Same as above. Test Environment: Nitrogen at 7.0 x 10 ⁻⁹ torr pressure. Other: Same as above.
9	Dmitriev, A.P., Dukhovskoi, E.A., Novik, G.Ya., and Petrochenkov, R.G., 1971 [58]				Periodic Heat Flow	293	0.0064	Density: 1.22 g cm ⁻³ . Texture: Finely divided powder. Specimen Geometry: 1 cm dia, 2 cm high. Test Environment: Air atmosphere.
10	Dmitriev, A.P., et al., 1971 [58]				Same as above	293	0.0098	Density: 1.22 g cm ⁻³ . Texture: Same as above. Specimen Geometry: Same as above. Test Environment: Helium atmosphere.
11	Dmitriev, A.P., et al., 1971 [58]				Same as above	293	0.00072	Density: 1.22 g cm ⁻³ . Specimen Geometry: Same as above. Other: Measurements in 10 ⁻⁶ torr pressure.
12	Dmitriev, A.P., et al., 1971 [58]				Same as above	293	0.00051	Density: 1.14 g cm ⁻³ . Specimen Geometry: Same as above. Other: Same as above.
13	Dmitriev, A.P., et al., 1971 [58]				Same as above	293	0.00445	Density: 1.14 g cm ⁻³ . Specimen Geometry: Same as above. Test Environment: Air atmosphere.
14	Dmitriev, A.P., et al., 1971 [58]				Same as above	293	0.0063	Density: 1.14 g cm ⁻³ . Specimen Geometry: Same as above. Test Environment: Helium atmosphere.
15	Kanamori, H., Mizutani, H., and Fujii, N., 1969 [68]				Angstrom	371 505 538 542 665 668 716 718 779 792	0.00705 0.00586 0.00616 0.00571 0.00530 0.00558 0.00537 0.00506 0.00531 0.00518	Specimen Geometry: Cylinder 2.7 cm long, 1 cm dia.

TABLE 3.6. EXPERIMENTAL DATA ON THERMAL DIFFUSIVITY OF BASALT (continued)

Data Set No.	Author(s), Year [Ref. No.]	Name and Source	Minerals and/or Chemical Composition		Experimental Data		Method Used	Other Specifications							
			Components	Weight Percent	T, K	Thermal Diffusivity ($10^{-4} \text{ m}^2 \text{ s}^{-1}$)									
16	Kanamori, H., et al., 1969 [68]					356	0.00700	Specimen Geometry: Same as above.							
						417	0.00765								
						505	0.00643								
						540	0.00593								
						543	0.00634								
17	Tadokoro, Y., 1921 [22]	Prov. Tamba				666	0.00568	Density: 2.659 g cm ⁻³ . Texture: Dark grey colored, no vesicular cavities, phenocrysts of plagioclase and olivine both of the order of 0.8 mm in size present very sparingly. Specimen Geometry: Cube 60 mm by side.							
						713	0.00577								
						716	0.00560								
						778	0.00513								
						786	0.00490								
18	Petrunin, G.I., Yurchak, R.I., and Ikach, G.F., 1971 [69]	Chinadiyeva (trans-Carpathian Region)				298	0.00677	Density: 2.74 g cm ⁻³ . Porosity: 5.19%. Texture: Porphyric, doleritic matrix; impregnations consisted of plagioclase grains 13%, pyroxene 2%. Specimen Geometry: Disk ~25 mm dia, ~8 mm thick.							
						350	0.00890								
						400	0.00875								
						450	0.00865								
						500	0.00850								
						550	0.00835								
						600	0.00820								
						650	0.00810								
						700	0.00830								
						750	0.00890								
						19	Petrunin, G.I., et al., 1971 [69]		Akhuryan River (South Eastern Armenia)				350	0.00725	Density: 2.67 g cm ⁻³ . Porosity: 8.87%. Texture: Porphyric, doleritic matrix; impregnations consisted of plagioclase 4%, olivine 1%. Specimen Geometry: Same as above.
													400	0.00700	
													450	0.00675	
													500	0.00650	
													550	0.00630	
600	0.00605														
650	0.00580														
700	0.00555														
750	0.00530														
800	0.00505														
850	0.00480														
900	0.00460														
950	0.00440														
1000	0.00445														
1050	0.00480														
1100	0.00505														
1150	0.00525														

TABLE 3.6. EXPERIMENTAL DATA ON THERMAL DIFFUSIVITY OF BASALT (continued)

Data Set No.	Author(s), Year [Ref. No.]	Name and Source	Minerals and/or Chemical Composition		Method Used	Experimental Data		Other Specifications
			Components	Weight Percent		T, K	Thermal Diffusivity ($10^{-4} \text{ m}^2 \text{ s}^{-1}$)	
20	Petruntin, G. I., et al., 1971 [69]	Sikhote-Alin'	Plagioclase	55	Periodic Heat Flow	350	0.00715	Density: 2.72 g cm ⁻³ . Porosity: 7.48%. Texture: Microplitic matrix; aphyric of uniform texture. Specimen Geometry: Same as above.
			Monopyroxene	40		400	0.00685	
						450	0.00650	
						500	0.00625	
						550	0.00605	
						600	0.00590	
						650	0.00575	
						700	0.00565	
						750	0.00555	
						800	0.00545	
						850	0.00535	
						900	0.00510	
						950	0.00500	
		1000	0.00505					
		1050	0.00530					
		1100	0.00560					
		1150	0.00580					
		1200	0.00600					
21	Petruntin, G. I., et al., 1971 [69]	Arzni (Armenia)	SiO ₂	48.53	Same as above	350	0.00700	Density: 6.21 g cm ⁻³ . Porosity: 7.77%. Texture: Aphyric, microdoleritic matrix. Specimen Geometry: Same as above.
			Al ₂ O ₃	18.00		400	0.00670	
			CaO	8.20		450	0.00645	
			Fe ₂ O ₃	6.85		500	0.00615	
			MgO	4.52		550	0.00590	
			Na ₂ O	4.50		600	0.00570	
			FeO	3.20		650	0.00545	
			TiO ₂	0.80		700	0.00530	
			MnO	0.12		750	0.00520	
			Plagioclase	65		800	0.00500	
			Olivine	23		850	0.00470	
			Clinopyroxene	6		900	0.00430	
			Magnetite	4		950	0.00410	
Glass	2	1000	0.00415					
		1050	0.00455					
		1100	0.00485					
		1150	0.00510					
		1200	0.00535					
22	Petruntin, G. I., et al., 1971 [69]	Akhuryan River (Northwestern Armenia)	SiO ₂	58.85	Same as above	350	0.00665	Density 2.50 g cm ⁻³ . Porosity: 15.25%. Texture: Aphyric, somewhat spongy, doleritic matrix. Specimen Geometry: Same as above.
			Al ₂ O ₃	17.31		400	0.00645	
			CaO	8.80		450	0.00630	
			Fe ₂ O ₃	6.69		500	0.00625	
			MgO	5.40		550	0.00620	
			Na ₂ O	4.07		600	0.00620	
			FeO	2.96		650	0.00615	
			K ₂ O	1.25		700	0.00610	
			TiO ₂	0.87		750	0.00595	
			H ₂ O	0.72		800	0.00575	
			P ₂ O ₅	0.30		850	0.00560	
			MnO	0.15		900	0.00535	
			Plagioclase	60		950	0.00510	

TABLE 3.6. EXPERIMENTAL DATA ON THERMAL DIFFUSIVITY OF BASALT (continued)

Data Set No.	Author(s), Year [Ref. No.]	Name and Source	Minerals and/or Chemical Composition		Method Used	Experimental Data		Other Specifications
			Components	Weight Percent		T, K	Thermal Diffusivity ($10^{-6} \text{ m}^2 \text{ s}^{-1}$)	
22	Petrunkin, G.I., et al., 1971 [69]	Yefremovka (South Georgia)	Olivine	18	Periodic Heat Flow	1000	0.00495	Density: 2.44 g cm ⁻³ . Porosity: 14.38%. Texture: Aphyric, doleritic matrix; Impregnations of olivine grains 4%, size 0.6 mm, and plagioclase grains 1%, size 0.5 mm. Specimen Geometry: Same as above.
			Clinopyroxene	15		1050	0.00495	
23	Petrunkin, G.I., et al., 1971 [69]	Yefremovka (South Georgia)	Glass	5	Periodic Heat Flow	1100	0.00510	Density: 2.44 g cm ⁻³ . Porosity: 14.38%. Texture: Aphyric, doleritic matrix; Impregnations of olivine grains 4%, size 0.6 mm, and plagioclase grains 1%, size 0.5 mm. Specimen Geometry: Same as above.
			Magnetite	2		1150	0.00530	
			SiO ₂	51.08		350	0.00630	
			Al ₂ O ₃	16.75		400	0.00625	
			CaO	8.84		450	0.00620	
			MgO	6.34		500	0.00615	
			FeO	6.00		550	0.00610	
			Fe ₂ O ₃	3.80		600	0.00600	
			Na ₂ O	3.48		650	0.00585	
			TiO ₂	1.38		700	0.00565	
			K ₂ O	1.26		750	0.00545	
			MnO	0.14		800	0.00515	
24	Petrunkin, G.I., et al., 1971 [69]	Baranchik (Southeastern Armenia)	Plagioclase	63	Same as above	350	0.00625	Density: 2.60 g cm ⁻³ . Porosity: 8.12%. Texture: Porphyric, pylotoxic matrix. Specimen Geometry: Same as above.
			Olivine	15		400	0.00595	
			Clinopyroxene	13		450	0.00565	
			Magnetite	3		500	0.00540	
			Apatite	1		550	0.00520	
			SiO ₂	52.52		600	0.00500	
			Al ₂ O ₃	18.29		650	0.00485	
			CaO	8.01		700	0.00475	
			Fe ₂ O ₃	6.12		750	0.00470	
			MgO	4.92		800	0.00470	
			Na ₂ O	4.31		850	0.00465	
			FeO	2.69		900	0.00445	
K ₂ O	1.44	950	0.00430					
TiO ₂	0.85	1000	0.00420					
Il ₂ O	0.50	1050	0.00445					
P ₂ O ₅	0.37	1100	0.00475					
MnO	0.11	1150	0.00500					
25	Petrunkin, G.I., et al., 1971 [69]	Akhuryan River (Northwestern Armenia)	Plagioclase	50	Same as above	350	0.00540	Density: 2.51 g cm ⁻³ . Porosity: 11.70%. Texture: Porphyric, pylotoxic matrix. Specimen Geometry: Same as above.
			Rhabdopyroxene	9		400	0.00495	
			Apatite	1		450	0.00460	
			Magnetite	1		500	0.00430	
			Plagioclase	1		550	0.00415	
			Biotite	1		600	0.00525	
			Hornblende	1		650	0.00540	
			SiO ₂	52.68		350	0.00540	
			Al ₂ O ₃	17.07		400	0.00495	
			CaO	7.57		450	0.00460	
			Fe ₂ O ₃	6.86		500	0.00430	
			Na ₂ O	4.83		550	0.00415	
MgO	4.43	600	0.00410					

TABLE 3.6. EXPERIMENTAL DATA ON THERMAL DIFFUSIVITY OF BASALT (continued)

Data Set No.	Author(s), Year [Ref. No.]	Name and Source	Minerals and/or Chemical Composition		Experimental Data		Other Specifications	
			Components	Weight Percent	Volume Percent	T, K		Thermal Diffusivity ($10^{-4} \text{ m}^2 \text{ s}^{-1}$)
25 cont.			K ₂ O	3.31		650	0.00405	
			FeO	1.17		700	0.00400	
			P ₂ O ₅	0.86		750	0.00390	
			TiO ₂	0.80		800	0.00380	
			H ₂ O	0.21		850	0.00370	
			MnO	0.13		900	0.00360	
			Plagioclase		62	950	0.00360	
			Olivine		16	1000	0.00375	
			Pyroxene		16	1050	0.00400	
			Magnetite		6	1100	0.00425	
						1150	0.00450	
						1200	0.00470	
						1250	0.00485	
						350	0.00430	
						400	0.00425	
26	Petruntin, G. I., et al., 1971 [69]	Corlovka (Southern Georgia)	SiO ₂	51.08		Periodic Heat		Density: 2.59 g cm ⁻³ . Porosity: 10.99%. Texture: Aphyric, doleritic matrix. Specimen Geometry: Same as above.
			Al ₂ O ₃	16.75		Flow		
			CaO	8.84				
			MgO	6.34				
			FeO	6.00				
			Fe ₂ O ₃	3.80				
			Na ₂ O	3.48				
			TiO ₂	1.38				
			K ₂ O	1.26				
			MnO	0.14				
			Plagioclase		60			
			Pyroxene		30			
			Olivine		5			
			Magnetite		5			
			27	Petruntin, G. I., et al., 1971 [69]	Akhuryan River (Southeastern Armenia)	SiO ₂	51.68	
Al ₂ O ₃	17.35							
CaO	8.30							
FeO	5.96							
MgO	5.53							
Na ₂ O	4.23							
Fe ₂ O ₃	3.50							
K ₂ O	1.29							
TiO ₂	1.23							
P ₂ O ₅	0.51							
H ₂ O	0.32							
MnO	0.13							
Plagioclase		63						
Olivine		18						
Monoclinic Pyroxene		12						
Secondary Minerals:								
Apatite		1						
Magnetite		1						

TABLE 3.6. EXPERIMENTAL DATA ON THERMAL DIFFUSIVITY OF BASALT (continued)

Data Set No.	Author(s), Year [Ref. No.]	Name and Source	Minerals and/or Chemical Composition		Experimental Data		Other Specifications	
			Components	Weight Percent	Volume Percent	T, K		Thermal Diffusivity ($10^{-4} \text{ m}^2 \text{ s}^{-1}$)
28	Petrmin, G. I., et al., 1971 [69]	Akhuryan River (Northwestern Armenia)	SiO ₂	58.85		Periodic Heat Flow	Density: 2.50 g cm ⁻³ . Porosity: 15.25%. Texture: Aphyric, somewhat spongy, doleritic matrix. Specimen Geometry: Same as above. Other: This specimen was preheated to 1200 K.	
			Al ₂ O ₃	17.31				
			CaO	8.80				
			Fe ₂ O ₃	6.69				
			MgO	5.04				
			Na ₂ O	4.07				
			FeO	2.96				
			K ₂ O	1.25				
			TiO ₂	0.87				
			H ₂ O	0.72				
			P ₂ O ₅	0.30				
			MnO	0.15				
			Plagioclase		60			
			Olivine		18			
Clinochlore		15						
Glass		5						
Magnetite		2						
29	Martinez-Baez, L. F. and Hal Amick, C., 1978 [35]	Umtanum Basalt; Umtanum Flow Bore Hole BH-5, WA	SiO ₂	54		Steady State Comparator	Density: 2.77 g cm ⁻³ . Texture: Dark grey in color with lighter grey vertical band crossing the center about 2 mm thick, several chips missing (about 1 mm long) around edges. Specimen Geometry: 4.7 cm dia and 3.20 cm long. Other: Values calculated for specimen from Rockwell-Hanford Operations, recovered from core of bore hole BH-5, 2749 ft. below the bore hole collar; value at 473 K is estimated; measurements were made at 500 psi and at constant average temperature of 328 and 396 K for water-saturated (wet) samples.	
			Al ₂ O ₃	12.7				
			FeO	12.7				
			CaO	7.0				
			MgO	3.7				
			Na ₂ O	3.1				
			TiO ₂	2.1				
			K ₂ O	1.6				
					328			0.00616
					396			0.00540
		473	0.00483					
30	Martinez-Baez, L. F. and Hal Amick, C., 1978 [35]	Same as above	SiO ₂	55		Same as above	Density: 2.79 g cm ⁻³ . Texture: Light grey in color, very small chips missing around edges. Specimen Geometry: Same as above. Other: Same as above except specimen recovered from 2808 ft.	
			Al ₂ O ₃	12.6				
			FeO	12.5				
			CaO	7.3				
			MgO	3.9				
			Na ₂ O	3.1				
			TiO ₂	2.1				
			K ₂ O	1.6				
					329			0.00570
					396			0.00505
		473	0.00461					
31	Martinez-Baez, L. F. and Hal Amick, C., 1978 [35]	Pomona Basalt; Pomona Flow Bore Hole BH-5, WA	SiO ₂	52.6		Same as above	Density: 2.86 g cm ⁻³ . Texture: Light grey with very small black nodules (about 0.3 mm in dia) distributed in the specimen. Specimen Geometry: 5.08 cm dia and 3.20 cm long; cores were diamond drilled longitudinal to the axis	
			Al ₂ O ₃	14.4				
			FeO	11.0				
			CaO	9.7				
			MgO	7.6				
			Na ₂ O	2.4				
			TiO ₂	1.6				
					327			0.00618
					396			0.00538
					473			0.00490

TABLE 3.6. EXPERIMENTAL DATA ON THERMAL DIFFUSIVITY OF BASALT (continued)

Data Set No.	Author(s), Year [Ref. No.]	Name and Source	Minerals and/or Chemical Composition		Method Used	Experimental Data		Other Specifications
			Components	Weight Percent		T, K	Thermal Diffusivity ($10^{-10} \text{ m}^2 \text{ s}^{-1}$)	
31	cont.							
			K ₂ O	0.7				and then were cut and faced to a height of 3.20 cm keeping parallelism between faces within ± 0.015 cm.
			MnO	0.19				Other: Specimen obtained from Rockwell-Hanford Operations, re-covered from core of bore hole DB-5, 390 ft. below the bore hole collar; measurements were made at 500 psi and at constant average temperature of 327 and 396 K for water-saturated (wet) samples; composition was assumed from oxide analysis for Pomona A1266 basalt.
			SrO	0.016				
32	Martinez-Baez, L.F. and Hal Amick, C., 1978 [35]	Same as above	SiO ₂	52.6	Steady State	329	0.00606	Density: 2.87 g cm ⁻³ .
			Al ₂ O ₃	14.4	Comparator	397	0.00536	Texture: Light grey with the same kind but fewer black nodules than the above specimen.
			FeO	11.0		473	0.00482	Specimen Geometry: Same as above.
			CaO	9.7				Other: Same as above except re-covered from 420 ft.
			MgO	7.6				
			Na ₂ O	2.4				
			TiO ₂	1.6				
			K ₂ O	0.7				
			MnO	0.19				
			SrO	0.016				
33	Martinez-Baez, L.F. and Hal Amick, C., 1978 [35]	Gable Mt. (Esquatzei) Basalt; Bore Hole DB-5, WA	SiO ₂	52.7	Same as above	329	0.00630	Density: 2.77 g cm ⁻³ .
			FeO	14.1		396	0.00542	Texture: Vertically fractured specimen in two pieces with good contact between them; light grey color (much darker grey on the fractured surfaces); shows some small uncommunicated pores on the surfaces and one larger pore (about 4 mm in dia by 5 mm in depth).
			Al ₂ O ₃	13.2		473	0.00504	Specimen Geometry: Same as above.
			CaO	7.0				Other: Same as above except specimen recovered from Gable Mountain DB-5 bore hole 521 ft. deep, and composition was assumed from oxide analysis for Gable Mountain K1005 sample.
			MgO	4.2				
			Na ₂ O	2.9				
			TiO ₂	2.8				
			K ₂ O	1.5				
34	Martinez-Baez, L.F. and Hal Amick, C., 1978 [35]	Same as above	SiO ₂	52.7	Same as above	328	0.00581	Density: 2.81 g cm ⁻³ .
			FeO	14.1		396	0.00513	Texture: Dark grey (almost black) in color; shows pores of about the same size but fewer than above specimen.
			Al ₂ O ₃	13.2		473	0.00465	Specimen Geometry: Same as above.
			CaO	7.0				Other: Same as above except specimen recovered from 542 ft.
			MgO	4.2				
			Na ₂ O	2.9				
			TiO ₂	2.8				
			K ₂ O	1.5				

TABLE 3.6. EXPERIMENTAL DATA ON THERMAL DIFFUSIVITY OF BASALT (continued)

Data Set No.	Author(s), Year [Ref. No.]	Name and Source	Minerals and/or Chemical Components	Chemical Composition		Method Used	Experimental Data		Other Specifications
				Weight Percent	Volume Percent		T, K	Thermal Diffusivity ($10^{-7} \text{ m}^2 \text{ s}^{-1}$)	
35	Hanley, E.J., deHitt, D.P., and Taylor, R.E., 1977 [33,75]	Dresser Basalt; Dresser, WI				Laser "Flash" Method	298 356 441 622 710 792 885 936 1000	0.01223 0.01094 0.00998 0.00896 0.00837 0.00767 0.00713 0.00660 0.00633 0.00606	Density: 2.97 g cm^{-3} . Specimen Geometry: 2.0-4.0 mm thick.
36	Horai, K., Simmons, G., Kanamori, H., and Wones, D., 1970 [70]	Apollo 11 Lunar Material Sample #10020	Pyroxene Plagioclase Ilmenite Olivine Void Troilite Other	45.4 24.6 22.7 3.9 1.8 0.9 0.7		Angstrom (Modified)	171 173 222 315 315 414 415	0.00948 0.01075 0.00899 0.00829 0.00521 0.00426 0.00491	Density: 2.99 g cm^{-3} . Texture: Fine grained vesicular crystalline igneous rock, type A according to the classification of the ISPET (1969). Specimen Geometry: 1 cm x 1 cm x 2 cm.
37	Horai, K., et al., 1970 [70]	Apollo 11 Lunar Material Sample #10057	Approximately same as above			Same as above	149 166 208 304 313 344 345	0.01194 0.01103 0.00906 0.00644 0.00686 0.00606 0.00591	Density: 2.88 g cm^{-3} . Porosity: 0.174%. Texture: Same as above. Specimen Geometry: Same as above.
38	Horai, K., et al., 1970 [70]	Apollo 11 Lunar Material Sample #10046	Matrix (<40 μ) Pyroxene Opaques Plagioclase Unidentified Glass	63.5 16.8 8.6 4.7 3.5 2.9		Same as above	162 176 181 205 313 330 371 430 433	0.00747 0.00659 0.00537 0.00585 0.00575 0.00360 0.00328 0.00326 0.00325	Density: 2.21 g cm^{-3} . Texture: Breccias (type C); the presence of microcracks, larger cracks, and glass is probably the cause of the lower thermal diffusivity. Specimen Geometry: Same as above.
39	Horai, K., et al., 1970 [70]	Apollo 11 Lunar Material Sample #10065	Approximately same as above			Same as above	178 190 191 295 404 414	0.00683 0.00472 0.00465 0.00463 0.00315 0.00269	Density: 2.36 g cm^{-3} . Texture: Same as above. Specimen Geometry: Same as above.
40	Lindroth, D.P., 1974 [71]	Tholeiitic Basalt	SiO ₂ Al ₂ O ₃ FeO CaO MgO Fe ₂ O ₃ Na ₂ O TiO ₂	51.0 14.0 8.8 8.0 4.4 3.4 3.4 2.7		Flash Method	298 298 298 383 383 383 383	0.00666 0.00654 0.00665 0.00622 0.00616 0.00623	Texture: Black color, aphanitic. Specimen Geometry: Disk 19.05 mm dia and 4 mm thick. Other: Disks were cut from cores with a diamond saw and then the surfaces were fine ground and made parallel using a 600 carborundum grit.

TABLE 3.6. EXPERIMENTAL DATA ON THERMAL DIFFUSIVITY OF BASALT (continued)

Data Set No.	Author(s), Year [Ref. No.]	Name and Source	Minerals and/or Chemical Composition		Experimental Data		Other Specifications	
			Components	Weight Percent	Volume Percent	T, K		Thermal Diffusivity ($10^{-4} \text{ m}^2 \text{ s}^{-1}$)
40 cont.			K ₂ O	1.7				
			P ₂ O ₅	1.4				
			Total H ₂ O	0.86				
			H ₂ O ⁺	0.76				
			MnO	0.25				
			H ₂ O ⁻	0.1				
			CO ₂	0.03				
			S	0.004				
			Plagioclase An ₆₇ and An ₅₄		39			
			Olivine		13.5			
			Glass		12			
			Plagioclase microclites		12			
			Augite		10.5			
			Magnetite (titaniferous) and ilmenite		8			
			Chlorite		4			
			Quartz (very small inclusions in plagioclase)		1			
			Apatite		<1			
			Epidote		<1			
41	Fujii, N. and Osaka, M., 1972 [72]	Apollo 11 Lunar Material Sample #10049				100	0.01287	Density: 3.07 g cm ⁻³ (bulk), 3.25 g cm ⁻³ (ideal). Porosity: 5.5%. Texture: Type A, very fine grains. Specimen Geometry: Rectangular prism 3-5 mm long and 6-15 mm ² in cross section. Other: CIPW norms calculated from the data of chemical composition are Or 2.13%, Ab 6.01%, An 21.66%, Wo 13.73%, En 17-51%, Fa 15.40%, Il 21.46%, Cm 0.47%, Qz, 1.55%; measurements at atmospheric pressure.
						200	0.00803	
						300	0.00639	
						400	0.00551	
						500	0.00492	
						600	0.00443	
42	Fujii, N. and Osaka, M., 1972 [72]	Apollo 11 Lunar Material Sample #10049				Same as above	0.00703	Same as above except measurements in vacuum.
						200	0.00505	
						300	0.00441	
						400	0.00412	
						500	0.00400	
						600	0.00398	
43	Fujii, N. and Osaka, M., 1972 [72]	Apollo 11 Lunar Material Sample #10069				100	0.01219	Density: 2.90 g cm ⁻³ (bulk), 3.26 g cm ⁻³ (ideal). Porosity: 11.0%. Texture: Type A, vuggy. Specimen Geometry: Rectangular prism 3-5 mm long and 6-16 mm ² in cross section.
						200	0.00783	
						300	0.00631	
						400	0.00546	
						500	0.00482	
						500	0.00482	

TABLE 3.6. EXPERIMENTAL DATA ON THERMAL DIFFUSIVITY OF BASALT (continued)

Data Set No.	Author(s), Year [Ref. No.]	Name and Source	Minerals and/or Chemical Composition		Method Used	Experimental Data		Other Specifications
			Components	Weight Percent		T, K	Thermal Diffusivity ($10^{-4} \text{ m}^2 \text{ s}^{-1}$)	
44	Fujii, N. and Osaka, N., 1972 [72]	Apollo 11 Lunar Material Sample #10069	Same as above	100	Same as above except measurements in vacuum.	0.00396	Density: 2.71 g cm^{-3} (bulk), 2.85 g cm^{-3} (ideal), 3.05 g cm^{-3} (theoretical). Porosity: 4.9%. Texture: Polymiot fragmental rock. Specimen Geometry: Same as above. Other: CIPW norms calculated from the data of chemical composition are Or 4.79%, Ab 7.19%, An 43.04%, Wo 1.00%, En 19.07%, Fs 14.14%, Fo 3.37%, Pa 2.76%, Il 3.44%, Ap 1.76%; measurements at 1 atmosphere.	
						0.00266		
45	Fujii, N. and Osaka, N., 1972 [72]	Apollo 14 Lunar Material Sample #14311	Same as above	100	Same as above except measurements in vacuum.	0.00230	Density: 2.76 g cm^{-3} (bulk), 2.90 g cm^{-3} (ideal), 2.98 g cm^{-3} (theoretical). Porosity: 4.8%. Specimen Geometry: Same as above. Other: CIPW norms chemical composition are Or 8.86%, Ab 20.54%, An 23.17%, Ne 2.76%, Wo 8.76%, En 6.40%, Fs 1.54%, Fo 13.65%, Mt 5.45%, Il 3.51%, Ap 1.09%; measurements at 1 atmospheric pressure.	
						0.00224		
46	Fujii, N. and Osaka, N., 1972 [72]	Apollo 14 Lunar Material Sample #14311	Same as above	100	Same as above except measurements in vacuum.	0.00237	Density: 2.76 g cm^{-3} (bulk), 2.90 g cm^{-3} (ideal), 2.98 g cm^{-3} (theoretical). Porosity: 4.8%. Specimen Geometry: Same as above. Other: CIPW norms chemical composition are Or 8.86%, Ab 20.54%, An 23.17%, Ne 2.76%, Wo 8.76%, En 6.40%, Fs 1.54%, Fo 13.65%, Mt 5.45%, Il 3.51%, Ap 1.09%; measurements at 1 atmospheric pressure.	
						0.00268		
47	Fujii, N. and Osaka, N., 1972 [72]	Olivine Basalt, Ugal-Zaki S. of Saigo Oki-dogo, Japan	Same as above	100	Same as above except measurements in vacuum.	0.01015	Density: 2.76 g cm^{-3} (bulk), 2.90 g cm^{-3} (ideal), 2.98 g cm^{-3} (theoretical). Porosity: 4.8%. Specimen Geometry: Same as above. Other: CIPW norms chemical composition are Or 8.86%, Ab 20.54%, An 23.17%, Ne 2.76%, Wo 8.76%, En 6.40%, Fs 1.54%, Fo 13.65%, Mt 5.45%, Il 3.51%, Ap 1.09%; measurements at 1 atmospheric pressure.	
						0.00416		
48	Fujii, N. and Osaka, N., 1972 [72]	Olivine Basalt, Ugal-Zaki S. of Saigo Oki-dogo, Japan	Same as above	100	Same as above except measurements in vacuum.	0.02013	Density: 2.76 g cm^{-3} (bulk), 2.90 g cm^{-3} (ideal), 2.98 g cm^{-3} (theoretical). Porosity: 4.8%. Specimen Geometry: Same as above. Other: CIPW norms chemical composition are Or 8.86%, Ab 20.54%, An 23.17%, Ne 2.76%, Wo 8.76%, En 6.40%, Fs 1.54%, Fo 13.65%, Mt 5.45%, Il 3.51%, Ap 1.09%; measurements at 1 atmospheric pressure.	
						0.00620		
49	Fujii, N. and Osaka, N., 1972 [72]	Olivine Basalt, Ugal-Zaki S. of Saigo Oki-dogo, Japan	Same as above	100	Same as above except measurements in vacuum.	0.00572	Density: 2.76 g cm^{-3} (bulk), 2.90 g cm^{-3} (ideal), 2.98 g cm^{-3} (theoretical). Porosity: 4.8%. Specimen Geometry: Same as above. Other: CIPW norms chemical composition are Or 8.86%, Ab 20.54%, An 23.17%, Ne 2.76%, Wo 8.76%, En 6.40%, Fs 1.54%, Fo 13.65%, Mt 5.45%, Il 3.51%, Ap 1.09%; measurements at 1 atmospheric pressure.	
						0.00584		

TABLE 3.6. EXPERIMENTAL DATA ON THERMAL DIFFUSIVITY OF BASALT (continued)

Data Set No.	Author(s), Year {Ref. No.}	Name and Source	Minerals and/or Chemical Composition		Experimental Data		Other Specifications	
			Components	Weight Percent	T, K	Thermal Diffusivity ($10^{-4} \text{ m}^2 \text{ s}^{-1}$)		
50	Horn, K. and Winkler, J., Jr., 1975 [73]	#12002, B5 Basalt, Moon	Plagioclase Olivine Pyroxene Opaque (mostly Ilmenite)	52.2 21.4 19.6 6.8	Angstrom (Modified)	90 100 105 115 119 130 140 150 159 169 179 184 188 200 204 209 214 225 229 235 239 250 255 269 273 280 311 315 320 325 330 334 340 345 349 355 359 364 369 373 380 389 395 400 404 409 415 419 425	0.00673 0.00640 0.00592 0.00552 0.00589 0.00522 0.00501 0.00478 0.00492 0.00511 0.00490 0.00508 0.00520 0.00499 0.00520 0.00448 0.00497 0.00418 0.00469 0.00490 0.00448 0.00427 0.00416 0.00397 0.00337 0.00439 0.00397 0.00379 0.00416 0.00356 0.00307 0.00295 0.00307 0.00319 0.00288 0.00277 0.00277 0.00286 0.00295 0.00295 0.00305 0.00326 0.00337 0.00346 0.00344 0.00356 0.00335 0.00335 0.00335 0.00314	Density: 2.96 g cm^{-3} (bulk), 3.310 g cm^{-3} (intrinsic). Porosity: 10.5%. Texture: Medium grained porphyritic basalt. Specimen Geometry: $0.33 \text{ cm} \times 1.50 \text{ cm} \times 1.60 \text{ cm}$. Other: Measurements taken at 1 atm air.

TABLE 3.6. EXPERIMENTAL DATA ON THERMAL DIFFUSIVITY OF BASALT (continued)

Data Set No.	Author(s), Year [Ref. No.]	Name and Source	Minerals and/or Chemical Composition		Method Used	Experimental Data		Other Specifications
			Weight Percent	Volume Percent		T, K	Thermal Diffusivity ($10^{-4} \text{ m}^2 \text{ s}^{-1}$)	
50								
cont.								
51	Horai, K. and Winkler, J., Jr., 1975 [73]	Same as above	Same as above		Angstrom (modified)	84	0.00894	Same as above except measurements taken at 1 atm helium.
						88	0.00818	
						94	0.00797	
						109	0.00746	
						106	0.00730	
						100	0.00730	
						115	0.00608	
						130	0.00599	
						144	0.00608	
						139	0.00569	
						150	0.00518	
						154	0.00518	
						159	0.00490	
						165	0.00508	
						167	0.00502	
						174	0.00501	
						179	0.00478	
						184	0.00511	
						190	0.00490	
						193	0.00508	
						200	0.00513	
						204	0.00480	
						209	0.00471	
						214	0.00489	
						219	0.00439	
						222	0.00489	
						230	0.00452	
						234	0.00469	
						239	0.00450	
						243	0.00478	
						250	0.00450	
						256	0.00468	
						259	0.00443	
						265	0.00443	
						269	0.00427	
						274	0.00417	
						280	0.00420	
						286	0.00420	
						290	0.00410	
						293	0.00419	
						299	0.00401	
						305	0.00419	
						309	0.00429	
						313	0.00419	
						320	0.00401	

TABLE 3.6. EXPERIMENTAL DATA ON THERMAL DIFFUSIVITY OF BASALT (continued)

Data Set No.	Author(s), Year [Ref. No.]	Name and Source	Minerals and/or Chemical Composition		Method Used	Experimental Data		Other Specifications
			Weight Percent	Volume Percent		T, K	Thermal Diffusivity ($10^{-4} \text{ m}^2 \text{ s}^{-1}$)	
51 cont.						324	0.00398	
						330	0.00389	
						334	0.00407	
						339	0.00389	
						345	0.00389	
						350	0.00380	
						354	0.00387	
						359	0.00380	
						363	0.00389	
						369	0.00379	
						375	0.00379	
						379	0.00368	
						384	0.00375	
						389	0.00370	
						395	0.00370	
						399	0.00361	
						404	0.00370	
						408	0.00361	
						414	0.00365	
						418	0.00360	
						424	0.00349	
						429	0.00349	
434	0.00349							
440	0.00349							
443	0.00360							
450	0.00337							
52	Hori, K. and Winkler, J., Jr., 1975 [73]	Same as above	Same as above		Angstrom (modified)	85	0.00622	Same as above except measurements taken at 1 atm argon.
						90	0.00532	
						96	0.00523	
						100	0.00502	
						104	0.00482	
						115	0.00445	
						120	0.00421	
						144	0.00412	
						151	0.00370	
						155	0.00338	
						159	0.00400	
						165	0.00359	
						170	0.00319	
						179	0.00340	
						186	0.00361	
						188	0.00370	
						196	0.00340	
						199	0.00292	
						205	0.00310	
						208	0.00340	
						215	0.00321	
						219	0.00282	
224	0.00282							
228	0.00330							

TABLE 3.6. EXPERIMENTAL DATA ON THERMAL DIFFUSIVITY OF BASALT (continued)

Data Set No.	Author(s), Year [Ref. No.]	Name and Source	Minerals and/or Chemical Composition		Method Used	Experimental Data		Other Specifications	
			Component	Component		T, K	Thermal Diffusivity ($10^{-6} \text{ m}^2 \text{ s}^{-1}$)		
52 cont.									
						233	0.00250		
						240	0.00321		
						244	0.00259		
						246	0.00330		
						255	0.00309		
						260	0.00330		
						264	0.00261		
						270	0.00222		
						274	0.00261		
						280	0.00210		
						286	0.00249		
						295	0.00258		
						300	0.00249		
						305	0.00251		
						309	0.00258		
						315	0.00249		
						320	0.00230		
						326	0.00230		
						330	0.00221		
						335	0.00202		
						339	0.00232		
						344	0.00202		
						350	0.00223		
						354	0.00211		
						359	0.00232		
						365	0.00221		
						369	0.00271		
						374	0.00211		
						380	0.00225		
						383	0.00225		
						390	0.00241		
						396	0.00229		
						400	0.00250		
						405	0.00234		
						409	0.00250		
						416	0.00245		
						420	0.00243		
						428	0.00243		
						433	0.00231		
						443	0.00229		
						450	0.00222		
	53	West, E.A. and Fountain, I.A., 1975 [16]	Terrestrial Basalt.			Differential	111	0.00638	Density: 1.95 g cm^{-3} (bulk).
						Line Source	117	0.00614	Other: Simulated lunar particulate material supplied by Dr. KI-TI
							136	0.00549	lboral of Columbia University.
							148	0.00507	Thermal diffusivity equation:
							158	0.00480	$\alpha = 1.61 \times 10^{-6} - 1.24 \times 10^{-6} T +$
						169	0.00450	$3.99 \times 10^{-9} T^2 - 4.19 \times 10^{-12} T^3;$	
						179	0.00429	$\sigma = 0.1565 \times 10^{-5}.$	
						190	0.00408		
						198	0.00396		

TABLE 3.6. EXPERIMENTAL DATA ON THERMAL DIFFUSIVITY OF BASALT (continued)

Data Set No.	Author(s), Year [Ref. No.]	Name and Source	Minerals and/or Chemical Composition		Method Used	Experimental Data		Other Specifications
			Componenta	Weight Percent		T, K	Thermal Diffusivity ($10^{-4} \text{ m}^2 \text{ s}^{-1}$)	
54	Foundation Sciences, Inc., 1980 [38]	Pomona Basalt (NSTF), Area 2; Gable NC., WA				210	0.00382	Density: 2.86 g cm^{-3} . Texture: Porphyritic with lath- or blade-shaped crystals of plagioclase (<5 mm) and less commonly, irregular crystals of olivine and clinopyroxene (<5 mm) in a fine-grained groundmass; green to blue-green mineraloid (chlorophaseite) occurs both in irregular interstitial patches in the groundmass and as a vesicles filling or lining; joints are commonly lined with chlorophaseite. Other: Basalt from NSTF (Near Surface Test Facility); sample from Full Scale Heater Test No. 2 instrument bore hole (Area 2); sample no. 2-61-B from bore hole 2-E-28; thickness 0.322 in.; horizontal orientation.
						219	0.00373	
						229	0.00365	
						239	0.00361	
						250	0.00358	
						260	0.00355	
						270	0.00356	
						279	0.00357	
						299	0.00361	
						318	0.00365	
			339	0.00372				
			359	0.00376				
					Heat Pulse Method	296.4	0.00546	
						437.2	0.00714	
						437.4	0.00580	
55	Foundation Sciences, Inc., 1980 [38]	Same as above			Heat Pulse Method	296.2	0.00552	Density: 2.84 g cm^{-3} . Texture: Same as above. Other: Same as above except sample no. 2-61-C from bore hole 2-E-28; thickness 0.351 in.
						296.2	0.00525	
						429.2	0.00788	
						444.2	0.00649	
						593.4	0.00798	
56	Foundation Sciences, Inc., 1980 [38]	Same as above			Heat Pulse Method	296.3	0.00385	Density: 2.85 g cm^{-3} . Texture: Same as above. Other: Same as above except sample no. 2-70-B from bore hole 2-M-16; thickness 0.347 in.
						440.2	0.00539	
57	Foundation Sciences, Inc., 1980 [38]	Same as above			Heat Pulse Method	293.6	0.00472	Density: 2.84 g cm^{-3} . Texture: Same as above. Other: Same as above except sample no. 2-79-B from bore hole 2-E-1; thickness 0.353 in.; vertical orientation.
						296.4	0.00562	
						581.9	0.00715	

53
cont.

TABLE 3.6. EXPERIMENTAL DATA ON THERMAL DIFFUSIVITY OF BASALT (continued)

Data Set No.	Author(s), Year [Ref. No.]	Name and Source	Minerals and/or Chemical Composition	Weight Percent		Method Used	Experimental Data		Other Specifications
				Volume Percent	Volume Percent		T, K	Thermal Diffusivity ($10^{-4} \text{ m}^2 \text{ s}^{-1}$)	
58	Foundation Sciences, Inc., 1980 [38]	Same as above				Heat Pulse Method	296.4 296.4 428.5	0.00527 0.00545 0.00527	Density: Same as above. Texture: Same as above. Other: Same as above except sample no. 2-79-C from bore hole 2-E-1; thickness 0.292 in.
59	Foundation Sciences, Inc., 1980 [38]	Same as above				Heat Pulse Method	433.9	0.00728	Density: 2.79 g cm ⁻³ Texture: Same as above. Other: Same as above except sample no. 2-94-B from bore hole 2-E-14; thickness 0.299 in.; horizontal orientation.
60	Foundation Sciences, Inc., 1980 [38]	Same as above				Heat Pulse Method	295.6 439.8 585.5	0.00518 0.00580 0.00456	Density: 2.81 g cm ⁻³ . Texture: Same as above. Other: Same as above except sample no. 2-96-B from bore hole 2-E-14.
61	Foundation Sciences, Inc., 1980 [38]	Same as above				Heat Pulse Method	296.5 293.2 441.5 591.6	0.00526 0.00556 0.00676 0.00511	Density: 2.85 g cm ⁻³ . Texture: Same as above. Other: Same as above except sample no. 2-103-C from bore hole 2-E-22.
62	Foundation Sciences, Inc., 1980 [38]	Same as above				Heat Pulse Method	296.6 296.5 430.1 592.0	0.00528 0.00528 0.00623 0.00758	Density: 2.81 g cm ⁻³ . Texture: Same as above. Other: Same as above except sample no. 2-107-B from bore hole 2-E-8; thickness 0.312 in.; vertical orientation.
63	Foundation Sciences, Inc., 1980 [38]	Same as above				Heat Pulse Method	295.9 296.0 424.8	0.00516 0.00455 0.00516	Density: 2.83 g cm ⁻³ . Texture: Same as above. Other: Same as above except sample no. 2-113-B from bore hole 2-M-3; thickness 0.294 in.
64	Foundation Sciences, Inc., 1980 [38]	Same as above				Heat Pulse Method	295.8 295.8 433.7	0.00532 0.00487 0.00675	Density: 2.82 g cm ⁻³ . Texture: Same as above. Other: Same as above except sample no. 2-113-C from bore hole 2-M-3; thickness 0.313 in.
65	Foundation Sciences, Inc., 1980 [38]	Same as above				Heat Pulse Method	296.5 427.5 588.2	0.00535 0.00631 0.00519	Density: 2.83 g cm ⁻³ . Texture: Same as above. Other: Same as above except sample no. 2-114-C from bore hole 2-M-3; thickness 0.314 in.
66	Foundation Sciences, Inc., 1981 [40]	Ultatum Basalt, DC2; Gable Mt., WA				Heat Pulse Method	298 298 413 430 576 576	0.00494 0.00423 0.00613 0.00480 0.00329 0.00370	Density: 2.77 g cm ⁻³ (bulk); 2.78 g cm ⁻³ (grain). Texture: Dark grey, aphanitic and massive, moderately fractured and occasionally contains vesicles; fractures usually closed or filled;

TABLE 3.6. EXPERIMENTAL DATA ON THERMAL DIFFUSIVITY OF BASALT (continued)

Data Set No.	Author(s), Year [Ref. No.]	Name and Source	Minerals and/or Chemical Composition		Experimental Data		Method Used	Other Specifications
			Weight Percent	Volume Percent	T, K	Thermal Diffusivity ($10^{-4} \text{ m}^2 \text{ s}^{-1}$)		
66								mineralized fillings are characterized by dark green-black chlorite followed by silice stringers.
67	Foundation Sciences, Inc., 1981 [40]	Same as above			Heat Pulse Method	297 421 425 563	0.00669 0.00796 0.00503 0.00556	Other: Umtanum basalt from bore hole DC-2; sample no. 4-2-E (depth 3027.0 ft.); thickness 0.80 cm. Density: 2.82 g cm ⁻³ (bulk); 2.75 g cm ⁻³ (grain). Texture: Same as above. Other: Same as above except sample no. 4-3-1 (depth 3049.2 ft.); thickness 1.03 cm.
68	Foundation Sciences, Inc., 1981 [40]	Same as above			Heat Pulse Method	297 297 407 419 559 559	0.00558 0.00521 0.00488 0.00625 0.00488 0.00488	Density: 2.77 g cm ⁻³ (bulk); 2.76 g cm ⁻³ (grain). Texture: Same as above. Other: Same as above except sample no. 4-6-F (depth 3034.7 ft.); thickness 0.7 cm.
69	Foundation Sciences, Inc., 1981 [40]	Same as above			Heat Pulse Method	299 424 555 555	0.00623 0.00530 0.00515 0.00386	Density: 2.77 g cm ⁻³ (bulk); 2.78 g cm ⁻³ (grain). Texture: Same as above. Other: Same as above except sample no. 4-6-G (depth 3034.7 ft.); thickness 0.80 mm.
70	Foundation Sciences, Inc., 1981 [40]	Same as above			Heat Pulse Method	299 424 560	0.00466 0.00570 0.00562	Density: 2.77 g cm ⁻³ (bulk); 2.78 g cm ⁻³ (grain). Texture: Same as above. Other: Same as above except sample no. 4-17-E (depth 3033.4 ft.); thickness 1.06 cm.
71	Foundation Sciences, Inc., 1981 [40]	Same as above			Heat Pulse Method	297 299 425 426 564 565	0.00540 0.00433 0.00531 0.00477 0.00558 0.00549	Density: 2.78 g cm ⁻³ (bulk); 2.91 g cm ⁻³ (grain). Texture: Same as above. Other: Same as above except sample no. 4-25-E (depth 3092.3 ft.); thickness 0.77 cm.
72	Somerton, W.H., Ward, S.H., and King, M.S.; 1963 [74]	Augite Basalt; Hobble Test Site			Non-steady State	424 522 646 771 882 993 1091 1197	0.00555 0.00508 0.00413 0.00456 0.00474 0.00452 0.00409 0.00371	Density: 2.82 g cm ⁻³ . Porosity: 2.06%. Texture: Intragranular, normal fine grained, lack of alteration, numerous fractures filled with secondary deposition of carbonate minerals. Other: measurements on piece No. 19 (EM7-5, 160 to 180 cm) [570 to 577 feet below the sea floor at Guadalupe Site (28° 58' N, 177° 28' W) where depth of water is 11,7600 ft; initial run.)

TABLE 3.6. EXPERIMENTAL DATA ON THERMAL DIFFUSIVITY OF BASALT (continued)

Data Set No.	Author(s), Year [Ref. No.]	Name and Source	Minerals and/or Chemical Composition		Method Used	Experimental Data		Other Specifications
			Weight Percent	Volume Percent		T, K	Thermal Diffusivity ($10^{-4} \text{ m}^2 \text{ s}^{-1}$)	
73	Somerton, W.H., Ward, S.H., and King, H.S.; 1963 [74]	Same as above			Same as above	420 495 611 726 837 953 1051 1153	0.00590 0.00469 0.00431 0.00409 0.00435 0.00422 0.00426 0.00426	Same as above except second run.

TABLE 3.7. THERMAL DIFFUSIVITY OF DRESSER BASALT

[Temperature, T, K; Thermal Diffusivity, $10^{-4} \text{ m}^2 \text{ s}^{-1}$]

T	α	T	α
293	0.01200	750	0.00721
300	0.01188	800	0.00692
350	0.01103	850	0.00665
400	0.01023	900	0.00638
450	0.00953	950	0.00612
500	0.00896	1000	0.00586
550	0.00856	1100	0.00536
600	0.00816	1200	0.00487
650	0.00782	1300	0.00440
700	0.00751		

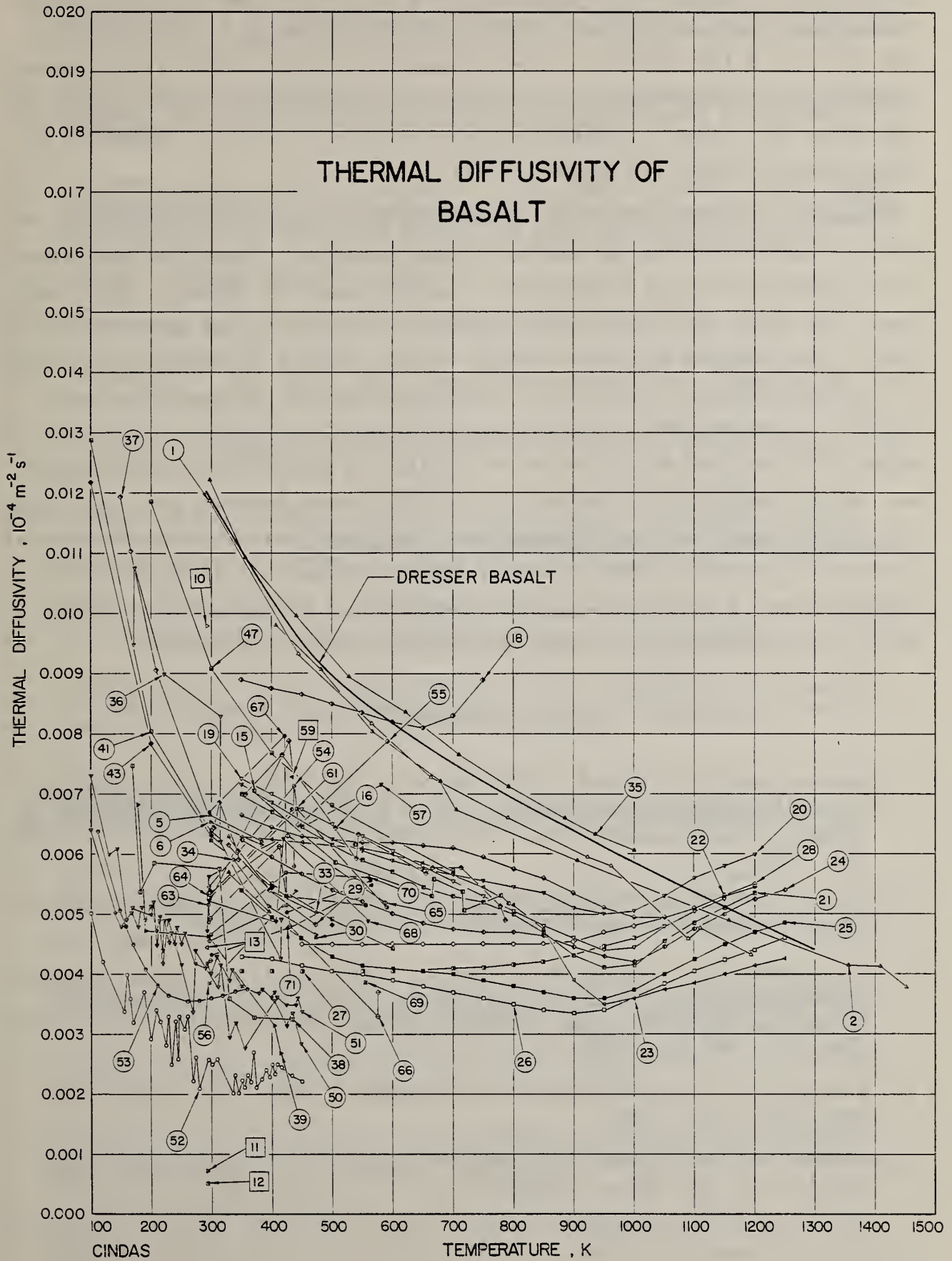


Figure 3.6. Thermal diffusivity of basalt.

Complete petrographic and chemical analyses are the essential part of satisfactory data analysis and only very few have reported this. Hanley et al. [75] observed a 10% increase in room temperature thermal diffusivity of basalt saturated with water. Based on the information available in Refs. [33,66,75], the values for thermal diffusivity given in Table 3.7 can be considered the representative values for Dresser basalt.

Horai et al. [70] (data sets 36-39) and Horai and Winkler [73] (data sets 50-52) reported data for the Apollo 11 lunar material. Their data show significant scatter and vary considerably from one sample to another. Fujii and Osaka [72] (data sets 41-49) reported data for Apollo 11 and Apollo 14 lunar rocks. The porosity of rocks strongly affects thermal diffusivity in vacuum at low temperature. Near 150 K, thermal diffusivity of Apollo 11 basalt (porosity 5.5% and 11%) at one atmosphere is about two to three times that in vacuum. The Hanford Site basalts are studied in greater detail by Martinez-Baez and Hal Amick [35] (data sets 29-34), Foundation Sciences Inc. [38] (data sets 49-60), and Foundation Sciences Inc. [40] (data sets 61-66). The studies reported in [38-40,54] indicated that thermal diffusivity of this group of basalts is not a strong function of temperature. Most of the samples for which thermal diffusivity is reported appeared to have low porosity.

3.7. REFERENCES

1. Touloukian, Y.S., Powell, R.W., Ho, C.Y., and Klemens, P.G., Thermal Conductivity-Nonmetallic Solids, Vol. 2 of Thermophysical Properties of Matter - The TPRC Data Series, IFI/Plenum Data Corp., New York, NY, 1302 pp., 1970.
2. Tye, R.P. (Editor), Thermal Conductivity, Vols. 1 and 2, Academic Press, London, 422 pp. and 353 pp., 1969.
3. Touloukian, Y.S., Kirby, R.K., Taylor, R.E., and Desai, P.D., Thermal Expansion-Metallic Elements and Alloys, Vol. 12 of Thermophysical Properties of Matter - The TPRC Data Series, IFI/Plenum Data Corp., New York, NY, 1348 pp., 1975.
4. Kirby, R.K., 'Thermal Expansion of Ceramics,' Natl. Bur. Stand. Spec. Publ. 303, 41-61, 1969.
5. Hidnert, P. and Souder, W., 'Thermal Expansion of Solids,' Natl. Bur. Stand. Circ. 486, 29 pp., 1950.

6. Touloukian, Y.S. and Buyco, E.H., Specific Heat-Metallic Elements and Alloys, Vol. 5 of Thermophysical Properties of Matter - The TPRC Data Series, IFI/Plenum Data Corp., New York, NY, 1737 pp., 1970.
7. McCullough, J.P. and Scott, D.W. (Editors), Calorimetry of Non-Reacting Systems, Vol. I of Experimental Thermodynamics, Plenum Press, New York, NY, 1968.
8. Touloukian, Y.S., Powell, R.W., Ho, C.Y., and Nicolaou, M.C., Thermal Diffusivity, Vol. 10 of Thermophysical Properties of Matter - The TPRC Data Series, IFI/Plenum Data Corp., New York, NY, 760 pp., 1973.
9. Fizeau, H., Ann. Phys., 2, 1864.
10. Fizeau, H., Ann. Chim. Phys., 8, 1866.
11. Jenkins, F.A. and White, H.E., Fundamentals of Optics, McGraw-Hill Book Co., New York, NY, 637 pp., 1957.
12. Candler, C., Modern Interferometers, The University Press, Glasgow, 502 pp., 1951.
13. Plummer, W.A., 'Thermal Expansion Measurements to 130°C by Laser Interferometry,' in AIP Conference Proceedings No. 3 - Thermal Expansion, American Institute of Physics, New York, NY, 36-43, 1972.
14. ASTM, 'ASTM Method of Test, E289, for Linear Thermal Expansion of Rigid Solids with Interferometry,' ASTM Standards, Part 41, 1974.
15. Clusener, G.R., 'Economy Considerations for Pushrod-Type Dilatometers,' in AIP Conference Proceedings No. 3 - Thermal Expansion, American Institute of Physics, New York, NY, 51-8, 1972.
16. Plummer, W.A., 'Differential Dilatometry, A Powerful Tool,' in AIP Conference Proceedings No. 17 - Thermal Expansion, American Institute of Physics, New York, NY, 147-8, 1974.
17. Schmidt, E.O. and Leidenfrost, W., 'Adiabatic Calorimeter for Measurements of Specific Heats of Powder and Granular Materials at 0 C to 500 C,' in ASME 2nd Symposium on Thermophysical Properties, Princeton, NJ, 178-84, 1962.
18. Poole, H.H., 'On the Thermal Conductivity and Specific Heat of Granite and Basalt at High Temperatures,' Philos. Mag., 27, 58-83, 1914.
19. Stephens, D.R., 'High Temperature Thermal Conductivity of Six Rocks,' USAEC Rept. UCRL-7605, 19 pp., 1963. [N64-15399]
20. Marovelli, R.L. and Veith, K.F., 'Thermal Conductivity of Rock. Measurement by the Transient Line Source Method,' U.S. Bureau of Mines Rept. BM-RI-6604, 19 pp., 1965. [N65-18524]
21. Murase, T. and McBirney, A.R., 'Thermal Conductivity of Lunar and Terrestrial Igneous Rocks in Their Melting Range,' Science, 170, 165-7, 1970.

22. Tadokoro, Y., 'The Determination of the Thermal Conductivity, Specific Heat, Density, and Thermal Expansion of Different Rocks and Refractory Materials,' Sci. Repts., Tohoku Imp. Univ., 10, 339-410, 1921.
23. Bernett, E.C., Wood, H.L., Jaffe, L.D., and Martens, H.E., 'Thermal Properties of Simulated Lunar Material in Air and in Vacuum,' NASA Rept. JPL-TR-32-368, 19 pp., 1962.
24. Navarro, R.A. and DeWitt, D.P., 'Line Heat Source Method and Its Suitability for Measuring Thermal Conductivity of Rocks,' Rept. for NSF-RANN on Project No. 7069 (in course of publication).
25. Wechsler, A.E. and Glaser, P.E., 'Pressure Effects on Postulated Lunar Materials,' in Proceedings of the 4th Conference on Thermal Conductivity, U.S. Naval Radiological Defense Lab., 1-31, 1964.
26. Glaser, P.E., 'Studies of the Physical Characteristics of Probable Lunar Surface Materials. Part II,' U.S. Air Force Rept. AFCRL-64-970 (Pt. 2), 134 pp., 1964. [AD 613 965]
27. Wechsler, A.E. and Simon, I., 'Thermal Conductivity and Dielectric Constant of Silicate Materials,' Progress Rept. April 1965-August 1966, Cambridge, MA, NASA-CR-61495, 133 pp., 1966. [N68-15849]
28. Johnson, S.A., 'Relation Between Thermal Conductivity and Engineering Properties of Six Igneous Rocks,' Purdue Univ., M.S. Thesis, 1974.
29. Sass, J.H., 'Heat-Flow Values from the Precambrian Shield of Western Australia,' J. Geophys. Res., 69(2), 299-308, 1964.
30. Glaser, P.E., Wechsler, A.E., and Germeles, A.E., 'Thermal Properties of Postulated Lunar Surface Materials,' Ann. N.Y. Acad. Sci., 123(2), 856-70, 1965.
31. Horai, K. and Baldrige, S., 'Thermal Conductivity of Nineteen Igneous Rocks. I. Application of the Needle Probe Method to the Measurement of the Thermal Conductivity of Rock,' Phys. Earth Planet. Int., 5(2), 151-6, 1972.
32. Morgan, M.T. and West, G.A., 'Thermal Conductivity of the Rocks in the Bureau of Mines Standard Rock Suite,' Oak Ridge National Lab. Rept. ORNL-TM-7052, 54 pp., 1980.
33. Hanley, E.J., DeWitt, D.P., and Taylor, R.E., 'The Thermal Transport Properties at Normal and Elevated Temperatures of Eight Representative Rocks,' in 7th Symposium on Thermophysical Properties, 386-91, 1977.
34. Fountain, J.A. and West, E.A., 'Thermal Conductivity of Particulate Basalt as a Function of Density in Simulated Lunar and Martian Environments,' J. Geophys. Res., 75(20), 4063-9, 1970.
35. Martinez-Baez, L.F. and Hal Amick, C., 'Thermal Properties of Gable Mt. Basalt Cores Hanford Nuclear Reservation,' Lawrence Berkeley Lab. Rept. LBL-7038, 10 pp., 1978.

36. West, E.A. and Fountain, J.A., 'Thermal Diffusivity Measurements of Particulates Using the Differential Line Source [Applied to Studies of Lunar, Planetary or Asteroid Surfaces],' *Rev. Sci. Instrum.*, 46(5), 543-6, 1975.
37. Duvall, W.I., Miller, R.J., and Wang, F.D., 'Preliminary Report on Physical and Thermal Properties of Basalt: Drill Hole DC-20 Pomona Flow-Gable Mt.,' Rockwell Hanford Operations Rept. RHO-BWI-C-11, 46 pp., 1978.
38. Foundation Sciences Inc., 'Thermal/Mechanical Properties of Pomona Member Basalt--Full-Scale Heater Test #2 (Area 2),' Rockwell Hanford Operations Rept. RHO-BWI-C-85, 154 pp., 1980.
39. Foundation Sciences Inc., 'Thermal/Mechanical Properties of Pomona Member Basalt--Full-Scale Heater Test #1 (Area 1),' Rockwell Hanford Operations Rept. RHO-BWI-C-77, 1980.
40. Foundation Sciences Inc., 'Thermal/Mechanical Properties of Umtanum Basalt--Bore Hole DC-2,' Rockwell Hanford Operations Rept. RHO-BWI-C-92, 130 pp., 1981.
41. Colorado School of Mines, 'Physical and Thermal Properties of Basalt Cores,' Rockwell Hanford Operations Rept. RHO-BWI-C-38, 78 pp., 1978.
42. Bridgman, P.W., 'The Thermal Conductivity and Compressibility of Several Rocks Under High Pressures,' *Am. J. Sci.*, 7(9), 81-102, 1924.
43. Hyndman, R.D. and Drury, M.J., 'The Physical Properties of Oceanic Basement Rocks from Deep Sea Drilling on the Mid-Atlantic Ridge,' *J. Geophys. Res.*, 81(23), 4042-52, 1976.
44. Robertson, E.C. and Peck, D.L., 'Thermal Conductivity of Vesicular Basalt from Hawaii,' *J. Geophys. Res.*, 79(32), 4875-88,
45. Griffin, R.E. and Demou, S.G., 'Thermal Expansion Measurements of Simulated Lunar Rocks,' *AIP Conf. Proc.*, 3, 302-11, 1972.
46. Griffith, J.H., 'Physical Properties of Typical American Rocks,' *Iowa State Coll. Eng. Exp. Sta. Bull.*, 35(36), 56 pp., 1937.
47. Mitchell, L.J., 'Thermal Expansion Tests on Aggregates, Neat Cements, and Concretes,' *Proc. Am. Soc. Testing Mater.*, 53, 963-75, 1953.
48. Suleimenov, S.T., Abduvaliev, T.A., Sharafiev, M.Sh., and Tropina, L.G., 'Investigating Daubabinsk Tephrite Basalts for Making Stone Castings,' *Steklo Keram.*, 23(4), 23-6, 1966; *Engl. transl.: Glass Ceram.*, 23(4), 192-5, 1966.
49. Verbeck, G.J. and Hass, W.E., 'Dilatometer Method for Determination of Thermal Coefficient of Expansion of Fine and Coarse Aggregate,' *Highway Res. Board Proc.*, 30, 187-93, 1951.

50. Hockman, A. and Kessler, D.W., 'Thermal and Moisture Expansion Studies of Some Domestic Granites,' U.S. Natl. Bur. Stand. Res. Papers RP2087, 395, 1950.
51. Krupka, M.C., 'Physicochemical Properties of Balstic Rocks, Liquids, and Glasses,' Los Alamos Scientific Lab. Rept. LA-5540, 11 pp., 1974.
52. Johnson, W.H. and Parsons, W.H., 'Thermal Expansion of Concrete Aggregate Materials,' J. Res. Natl. Bur. Stand., 32, 101-26, 1944.
53. Thirumalai, K., Cheung, J.E., Chen, T.S., Demou, S.G., and Krawza, W.G., 'Thermal Rock Breaker for Hard Rock Crushing - A Feasibility Study,' U.S. Bureau of Mines Rept., 272 pp., 1972. [AD 906 785L]
54. Erikson, R.L. and Krupka, K.M., 'Thermal Property Measurements of Pomona Member Basalt from Core Holes DB-5 and DB-15,' Rockwell Hanford Operations Rept. RHO-BWI-C-76, 1980.
55. Miller, R.J. and Bishop, R.C., 'Determination of Basalt Physical and Thermal Properties at Varying Temperatures, Pressure, and Moisture,' Rockwell Hanford Operations Rept. RHO-BWI-C-50, 83 pp., 1979.
56. Lindroth, D.P. and Krawza, W.G., 'Heat Content and Specific Heat of Six Rock Types at Temperatures to 1000 C,' U.S. Bureau of Mines Rept. BMRI-7503, 28 pp., 1971. [PB-199046]
57. Stephens, H.P. and Sinnock, S., 'Thermophysical Properties of Rocks: A Perspective on Data Needs, Sources, and Accuracy,' Natl. Bur. Stand. Spec. Rept. NBS-SP-590, 27-32, 1980.
58. Dmitriev, A.P., Dukhovskoi, E.A., Novik, G.Ya., and Petrochenkov, R.G., 'Investigation of the Thermal Properties of Lunar Soil and of Its Terrestrial Analogs,' Dokl. Akad. Nauk, SSSR, 199(5), 1036-7, 1971; Engl. transl.: Sov. Phys.-Dokl., 16(8), 611-2, 1972.
59. Robie, R.A., Hemingway, B., and Wilson, W.H., 'Specific Heats of Lunar Surface Materials from 90 to 350 K,' Science, 167, 749-50, 1970.
60. Leonidov, V.Ya., 'Heat Capacities of Rocks at High Temperatures, Geochemistry, USSR, 4, 400-2, 1967.
61. Svikis, V.D., 'Nonmetallic Thermal Storage Media,' Can. Dept. Mines Tech. Surv. Mines Branch Res. Rept. R-96, 42 pp., 1962.
62. Hemingway, B.S., Robie, R.A., and Wilson, W.H., 'Specific Heats of Lunar Soils, Basalts, and Breccias from the Apollo 14, 15, and 16 Landing Sites, Between 90 and 350°K,' Proc. 4th Lunar Sci. Conf., 3, 2481-7, 1973.
63. Lehnhoff, T.L. and Scheller, I.D., 'The Influence of Temperature Dependence Properties on Thermal Rock Fragmentation,' Int. J. Rock Mech. Min. Sci., 12(8), 255-60, 1975.
64. Allen, V., 'Direct and Inverse Conduction in Rock Material Using the Finite Element Method,' Univ. of Rolla, Ph.D. Thesis, 1974.

65. Scheller, J.D., 'Thermal Fragmentation of Rock - The Influence of Temperature Dependent Material Properties,' Univ. of Rolla, M.S. Thesis, 1974.
66. Bates, J.L., McNeilly, C.E., and Rasmussen, J.J., 'Properties of Molten Ceramics,' Battelle-Northwest Lab. Rept. BNWL-SA-3579, 18 pp., 1970. [N71-27426]
67. Lindroth, D.P., 'Thermal Diffusivity of Six Igneous Rocks at Elevated Temperatures and Reduced Pressures,' Private Communication, Bureau of Mines, Twin Cities, MN, 1974.
68. Kanamori, H., Fujii, N., and Mizutani, H., 'Thermal Diffusivity Measurement of Rock-Forming Minerals from 300 to 110 K,' J. Geophys. Res., 73(2), 595-605, 1968.
69. Petrunin, G.I., Yurchak, R.I., and Tkach, G.F., 'Temperature Conductivity of Basalts at Temperatures from 300 to 1200 K,' Izv. Akad. Nauk SSSR, Fiz. Zemli., 2, 65-8, 1971; Engl. transl.: Bull. Acad. Sci., USSR, Earth Phys., 2, 126-7, 1971.
70. Horai, K., Simmons, G., Kanamori, H., and Wones, D., 'Thermal Diffusivity, Conductivity, and Thermal Inertia of Apollo 11 Lunar Material,' Proc. Apollo 11 Lunar Sci. Conf., 3, 2243-9, 1970.
71. Lindroth, D.P., 'Thermal Diffusivity of Six Igneous Rocks at Elevated Temperatures and Pressures,' U.S. Bur. Mines Rept. Invest. BMRI-7954, 38 pp., 1974.
72. Fujii, N. and Osaka, M., 'Thermal Diffusivity of Lunar Rocks Under Atmospheric and Vacuum Conditions,' Earth Planet. Sci. Lett., 18(1), 65-71, 1973.
73. Horai, K. and Winkler, J., Jr., 'Thermal Diffusivity of Lunar Rock Sample 12002,85,' Proc. Lunar Sci. Conf., 6th, 3207-15, 1975.
74. Somerton, W.H., Ward, S.H., and King, M.S., 'Physical Properties of Mohole Test Site Basalt,' J. Geophys. Res., 68(3), 849-56, 1963.
75. Hanley, E.J., DeWitt, D.P., and Roy, R.F., 'The Thermal Diffusivity of Eight Well-Characterized Rocks for the Temperature Range 300-1000 K,' Eng. Geol., 31-47, 1977.

3.8. SYMBOLS AND UNITS AND CONVERSION FACTORS

3.8.1. Symbols and Units

<u>Symbol</u>	<u>Name</u>	<u>Unit</u>
A	Cross-sectional area of the specimen	m ²
A _r	Cross-sectional area of the reference sample	m ²
c ₀ , c ₁	Calibration constants	dimensionless
c _p	Specific heat at constant pressure	J kg K ⁻¹
d	Density	kg m ⁻³
d ₀	Density at room temperature (293 K)	kg m ⁻³
H _T	Enthalpy	J kg ⁻¹
k	Thermal conductivity	W m ⁻¹ K ⁻¹
k _r	Thermal conductivity of the reference sample	W m ⁻¹ K ⁻¹
L	Length at temperature T	m
L _s	Length of the specimen	m
L _r	Length of the reference sample	m
L ₀	Length at room temperature (293 K)	m
ΔL	ΔL = L - L ₀	m
ΔL/L ₀	Thermal linear expansion	%
ℓ	Length of the central heater	m
m	Mass of specimen	kg
N	Order of interference	dimensionless
N ₁ , N ₂ , N ₃	Fringe integers	dimensionless
P	Pressure	atm (use Pa)
q	Rate of heat flow	watt
r ₁ , r ₂	Radii	m
t	Time	sec
T	Temperature	K
T ₁ , T ₂	Temperatures	K
ΔT	ΔT = T ₂ - T ₁	K
W _c	Specific heat of calorimeter	J kg ⁻¹ K ⁻¹
Δx	Distance difference	m

Greek Symbols

α	Thermal diffusivity	m ² s ⁻¹
β	Coefficient of thermal expansion	K ⁻¹

δ	Amplitude ratio	-
ϕ	Phase lag	rad.
λ	Wavelength	m
λ_v	Wavelength of light in vacuum	m

3.8.2. Conversion Factors

Thermal Conductivity

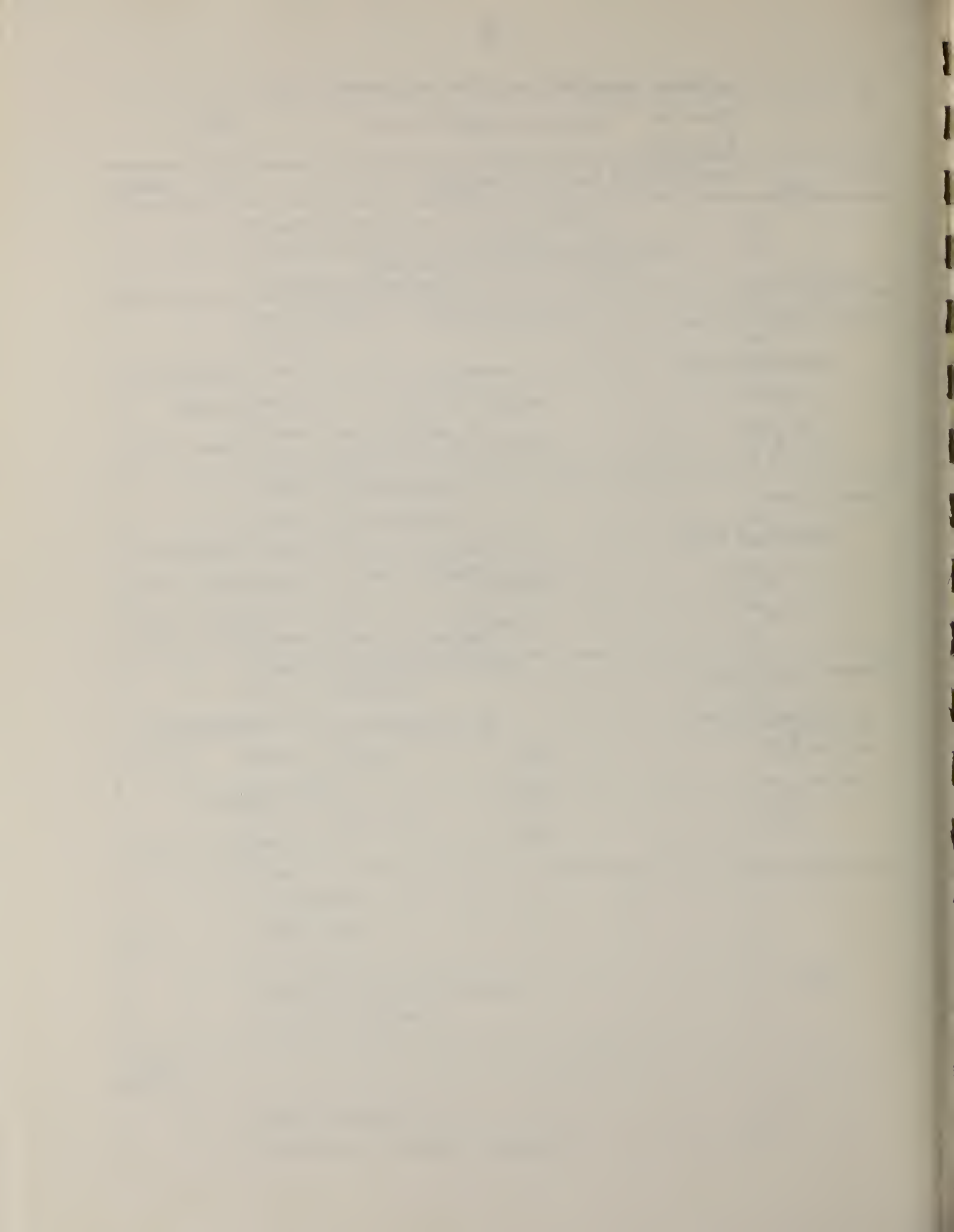
<u>To convert from</u>	<u>to</u>	<u>Multiply by</u>
$W m^{-1} K^{-1}$	$Btu_{IT} h^{-1} ft^{-1} F^{-1}$	0.5777908
$W m^{-1} K^{-1}$	$cal_{IT} s^{-1} cm^{-1} C^{-1}$	2.38846×10^{-3}

Specific Heat

<u>To convert from</u>	<u>to</u>	<u>Multiply by</u>
$J kg^{-1} K^{-1}$	$Btu_{IT} lb^{-1} F^{-1}$	2.3885×10^{-4}
$J kg^{-1} K^{-1}$	$Cal_{IT} g^{-1} K^{-1}$	2.3885×10^{-4}

Thermal Diffusivity

<u>To convert from</u>	<u>to</u>	<u>Multiply by</u>
$m^2 s^{-1}$	$cm^2 s^{-1}$	10^4
$m^2 s^{-1}$	$ft^2 s^{-1}$	10.7639
$m^2 s^{-1}$	$m^2 h^{-1}$	3600



CHAPTER 4

ELECTRICAL PROPERTIES

M. S. Deshpande, P. D. Desai, R. H. Bogaard, and T. C. Chi*

CONTENTS

	<u>Page</u>
4.1. INTRODUCTION -----	2
4.2. METHODS FOR MEASURING ELECTRICAL PROPERTIES -----	3
4.2.1. Methods for Measuring Electrical Conductivity -----	3
4.2.2. Methods for Measuring Dielectric Constants -----	4
4.3. ELECTRICAL CONDUCTIVITY OF BASALTS -----	4
4.3.1. Temperature Dependence of Electrical Conductivity of Basalt -	5
4.3.2. Pressure Dependence of Electrical Conductivity of Basalt ----	53
4.3.3. Other Dependencies of Electrical Conductivity of Basalt ----	63
4.3.4. Conduction Mechanisms and Activation Energy -----	65
4.3.5. Summary -----	72
4.4. DIELECTRIC PROPERTIES OF BASALT -----	73
4.4.1. Relative Dielectric Constant of Basalt -----	73
4.4.2. Tangent of Loss Angle of Basalt -----	98
4.4.3. Summary -----	117
4.5. REFERENCES -----	118
4.6. SYMBOLS AND UNITS, AND CONVERSION FACTORS -----	123

*Center for Information and Numerical Data Analysis and Synthesis (CINDAS),
Purdue University, 2595 Yeager Road, West Lafayette, Indiana 47906.

4.1. INTRODUCTION

Extensive measurements have been reported on the electrical properties of basalt. Although efforts were made here to evaluate these data, it was not possible to generate recommended values. The main difficulties were due to the uncharacterized nature of the samples and the poorly defined experimental conditions. Consequently, this work comprehensively and systematically presents and discusses all the important experimental data and information covering the temperature, pressure, porosity, and density dependences of the electrical conductivity and the frequency dependence of the dielectric constants. An excellent discussion about the considerations necessary to characterize geological samples and details required for physical property measurements are given by Pincus [1] and Olhoeft [2].

According to petrography, basalts are fine-grained in appearance and consist predominantly of plagioclase, pyroxene, and olivine or quartz (or both). There is a wide variation in the mineralogical and chemical composition of basalt dependent on the geographical location of source place. A glassy component is also found in abundance in volcanic rocks and is the principal product of shield volcanoes of Hawaiian type. The general olivine-free or olivine-poor basalt is a special type of calc-alkali basalt and is referred to as tholeiitic basalt. This type is found predominantly among the plateau-building lavas of shield areas of the world. The details of various basalt types, their mineral and chemical compositions and texture, have been reported in an earlier CINDAS report on the thermophysical properties of selected rocks by Desai et al. [3]. In the present study, the sample characterization is reported along with the property data to the extent provided in the source documents.

In the next section, a brief discussion is given on the methods of measurements both for the electrical conductivity (Section 4.2.1) and for the dielectric constant (Section 4.2.2). The purpose is to point out the basic principle of the measurement methods so that the experimental information presented in the tables could be more meaningful to the reader.

4.2. METHODS FOR MEASURING ELECTRICAL PROPERTIES

4.2.1. Methods for Measuring Electrical Conductivity

The electrical conductivity of a solid is determined by measuring the electrical resistance of a slab of material of known dimensions. The resistance is obtained by placing the specimen between metallic electrodes and measuring the electrical current for a given, known electrical potential. To obtain good electrical contacts, material such as Aquadag (a colloidal dispersion of graphite) is sometimes applied to the faces of the sample. The basic discussion on measurements as applied to geologic materials can be found in [4] and [5]. An extended discussion of the details of measuring the electrical conductivity of solids, including the theoretical considerations, is given by Olhoeft [6]. The present review of the measurements on basalt shows that most of the data were obtained using a two-terminal method. A few other data sets obtained with a four-terminal method are discussed in detail by Ucock [7] and Olhoeft [8].

In general, the electrical conductivity of geological materials is dependent on temperature, pressure, void morphology, density, frequency, and water content or aqueous-solution content of the sample. Indeed, it is just these which are being sought in the measurement. However, variations in the electrical conductivity also occur as a result of non-ideal experimental conditions. For example, in the case of dry rock, the largest errors are due to leakage of current around the sample, cable coupling, and capacitance fringing effects. Some of these errors can be reduced by designing a better measurement system. Olhoeft [6] and Von Hippel [9] have accomplished this by using a three-terminal method and Ucock [7] and Olhoeft [8] by using a four-terminal method. In the case of wet samples, errors are due to current leakage around the sample via spurious conduction paths, spurious-coupling between electrode and sample, and chemical reactions between the sample and sample holder. These errors have been reduced to about $\pm 1\%$ in a four-terminal method where the sample holder is shielded with an inert material like Teflon [10]. Generally, the errors in wet-sample measurement are not as well understood as in the case for dry sample.

4.2.2. Methods for Measuring Dielectric Constants

The general concept in determining dielectric constant is the measurement of capacitance. Employment of AC techniques allows one to obtain both the real and imaginary parts of the dielectric constant. This is readily carried out using the same capacitor both with and without the dielectric material present. Different experimental methods are used in different frequency regions. At lower frequencies, typically from 10^2 to 10^7 Hz, 'Bridge' methods are employed. At intermediate frequencies, resonant circuit methods are generally used, while at higher frequencies, above 100 MHz, transmission-line methods are used. The details of these methods are given in refs. [11-14]. The capacitance-meter method appears to be the most popular for measuring the dielectric properties of basalts. Ryu et al. [15] have discussed measurement techniques, contact substitution, and variable air gap in particular. They have also reported data for basalt by an optimum technique, which amounts to a combination of these two techniques. The corresponding accuracies achieved by these methods are also discussed in [15].

4.3. ELECTRICAL CONDUCTIVITY OF BASALTS

A large body of electrical conductivity data on basalts are reported in the literature [6-8, 16-44]. The data as well as specimen specifications are given here in Tables 4.1 and 4.2. Over 150 data sets for the temperature dependence and about 50 data sets for the pressure dependence of basalt are presented. In general, electrical conductivity of geological materials is extremely dependent upon chemical composition, water or aqueous solution content, porosity or density, and void morphology. Therefore, the compilation presented in Tables 4.1 and 4.2 identifies each data set with those parameters for which information is available.

A number of approaches in sample preparation were taken by various researchers to study dry basalts. Some reported measurements on block sample, i.e., as-received, and others on powdered samples. They have also documented details on drying during testing of the samples. Different problems are encountered during measurements on these two textures. For instance, the block samples develop cracks at high temperatures which cause difficulties in electrical measurements. Overall, powdered samples show lower conductivity

values than those for block samples. This difference, which is of the order of ten for a given temperature, is quite significant. However, the relative change in electrical conductivity for the two textures between two given temperatures is approximately the same. This has prompted a few researchers, such as Alvarez et al. [27], to use powdered samples to study the electrical conductivity during partial melting and in the molten state.

In addition to dry basalts, the measurements on rock-fluid mixtures were also of interest. The evaluation of 'rock and aqueous solution mixing' laws was found to be an impossible task because the data were not reported in a unified way and dry-rock properties of such systems are quite sample dependent. Thus, a clear statistical conclusion cannot be drawn and, therefore, only a survey of such measurements for a basalt-water or a basalt-sea water system is attempted. Meaningful comments are made in individual cases and conclusions concerning basalt-fluid mixing laws are reported (see Section 4.3.3).

4.3.1. Temperature Dependence of Electrical Conductivity of Basalt

The majority of studies of the electrical conductivity have been directed toward the temperature dependence [6-8, 16-33]. Data for the electrical conductivity as a function of temperature are given in Table 4.1 and shown in Figure 4.1. This includes basalts from all over the world, and presents the very complicated picture of this property which shows distinct regions for dry, partially molten, and molten basalt. To understand the behavior further, data for basalts from American subcontinents (i.e., from USA, Canada, Mexico, mid-Atlantic region, and Hawaii) are analyzed with an Arrhenius relationship and are plotted in Figure 4.2.

The data sets presented in Figure 4.2 are for the better characterized basalts but do show some anomalous behavior. It is necessary to note that even though very few measurements made are by three or four point methods and are somewhat uncertain, a good qualitative insight may be gained from this figure. It shows several activation-energy regions and thus provides evidence for different conduction mechanisms dominating different temperature regions. Two data sets (data sets 142,143) for wet sea-water saturated basalts are also included in Figure 4.2 for completeness. The electrical conductivity values for these samples are markedly different in character and higher in magnitude than those for dry rocks. These data sets are discussed in connection with the conduction mechanisms and activation energies addressed below in Section 4.3.3.

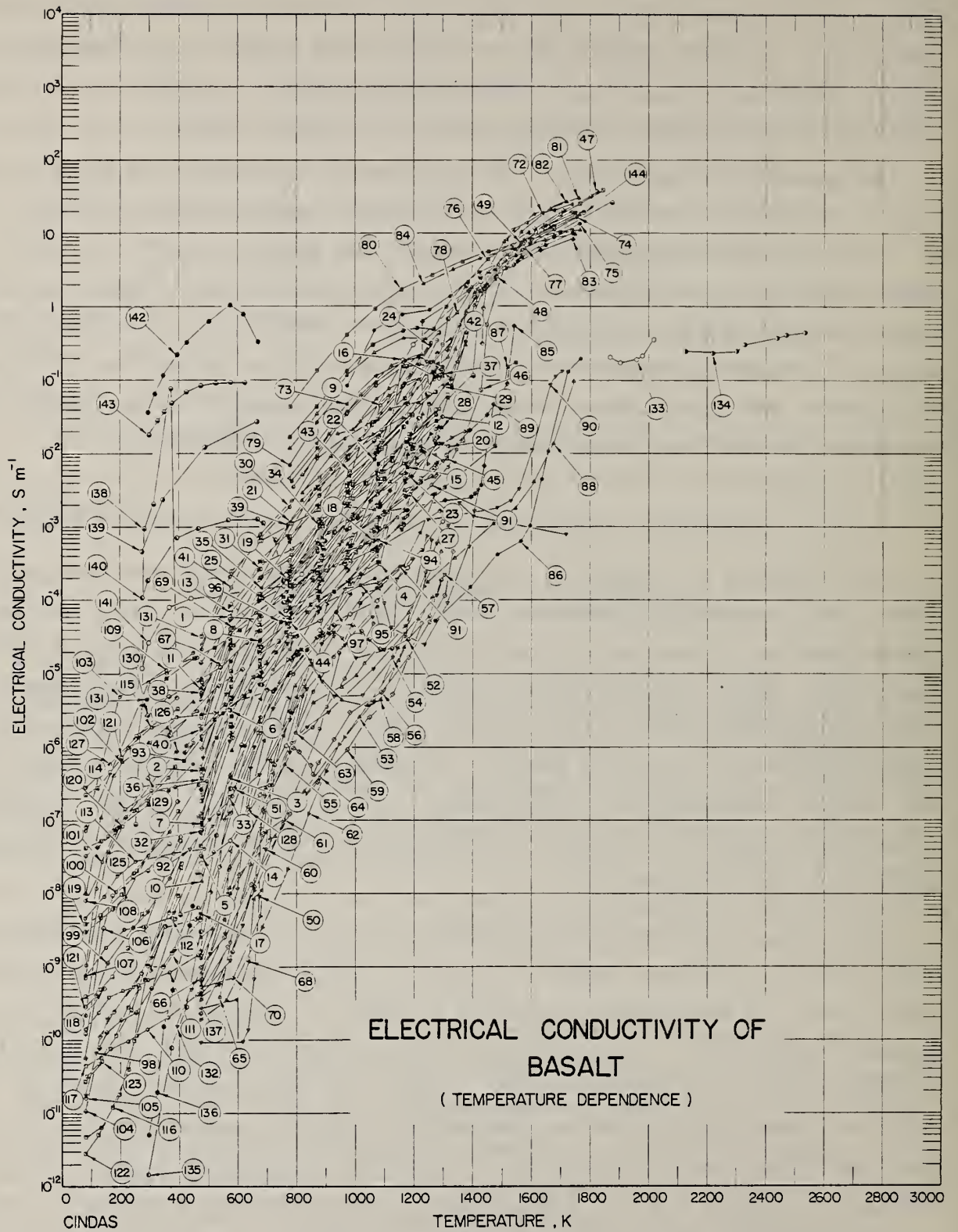


Figure 4.1. Electrical conductivity of basalt (temperature dependence).

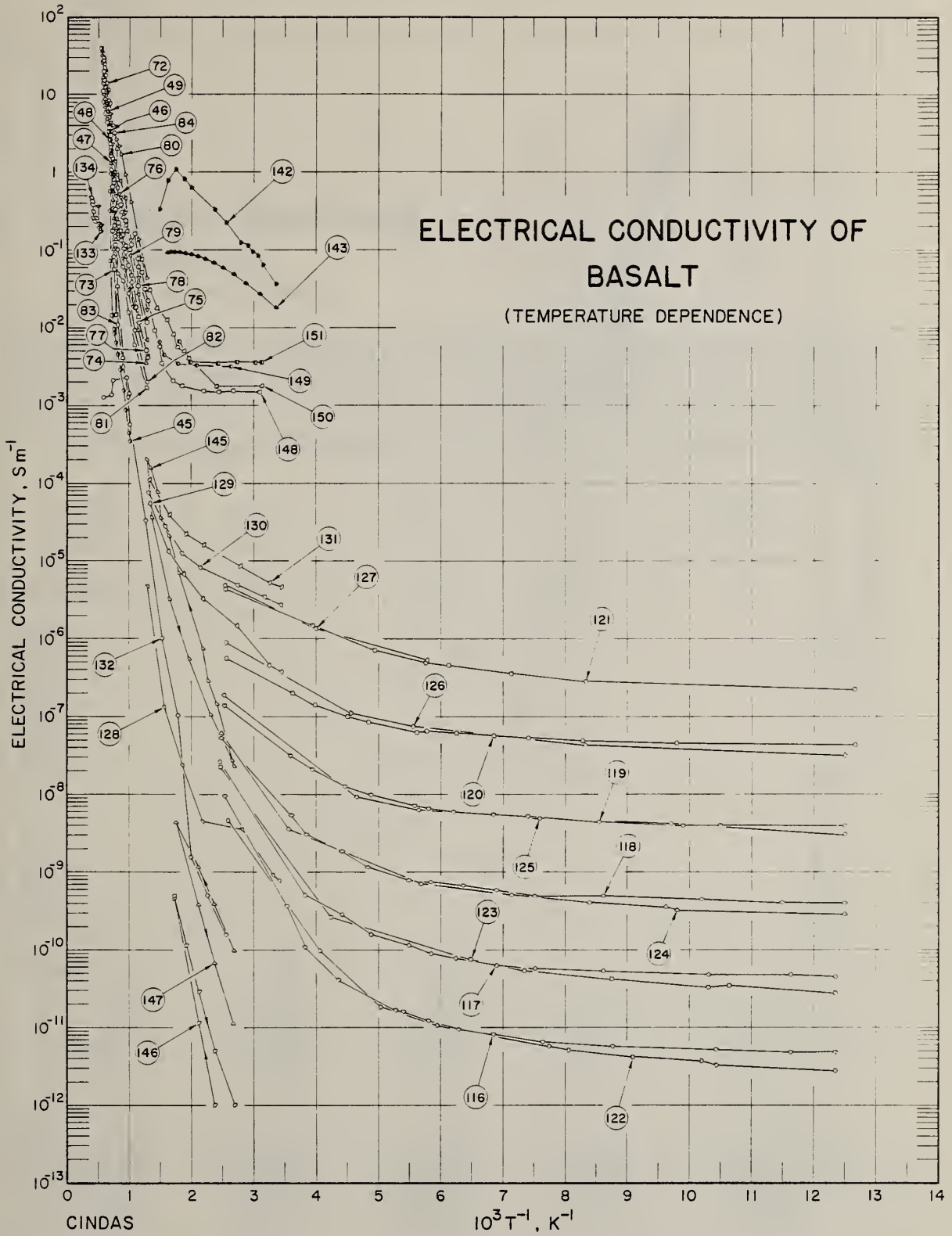


Figure 4.2. Electrical conductivity of basalt (temperature dependence).

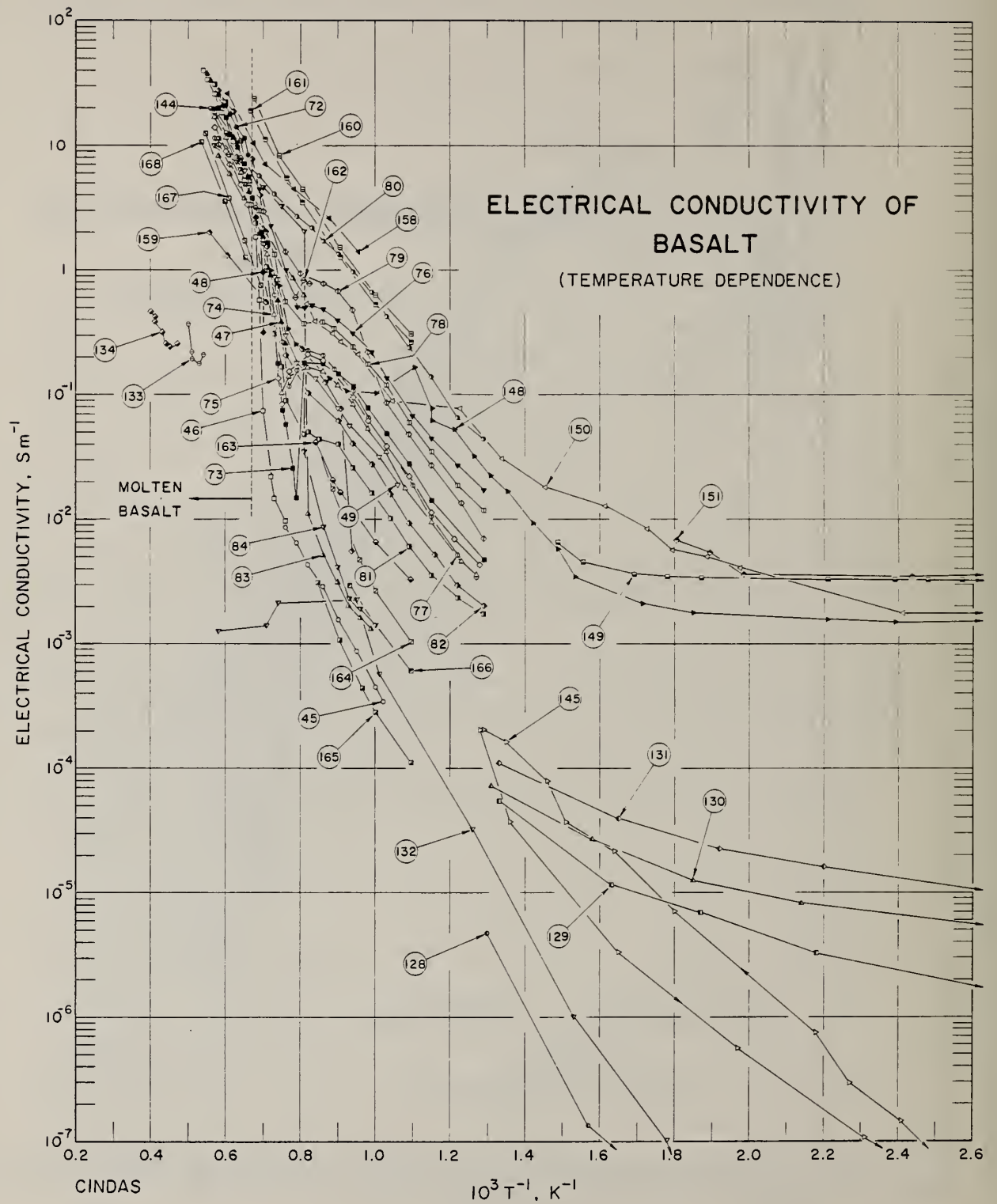


Figure 4.3. Electrical conductivity of basalt (temperature dependence).

TABLE 4.1. EXPERIMENTAL DATA ON ELECTRICAL CONDUCTIVITY OF BASALT (TEMPERATURE DEPENDENCE)

Data Set No.	Author(s), Year [Ref. No.]	Name and Source	Minerals and/or Chemical Composition		Experimental Data		Method Used	Other Specifications
			Components	Weight Percent	T, K	Electrical Conductivity (s m ⁻¹)		
1	Parkhomenko, E. I. and Bondarenko, A. T., 1972 [16]	Basalt (Andesitic) 1373; Russia			474	4.10E-07	Two Terminal Method Assumed	Other: No indication on measurement procedures; assume sample was dried in air and the measurements were at or below 1 kHz in a two-terminal sample holder.
					575	6.13E-05		
					671	5.52E-05		
					775	2.38E-04		
					870	6.75E-04		
2	Parkhomenko, E. I. and Bondarenko, A. T., 1972 [16]	Basalt (Doleritic) 1295 Plagioclase; Russia			971	2.62E-03	Same as above.	
					1076	6.03E-03		
					1174	1.54E-02		
					1272	3.94E-02		
					472	4.61E-07		
3	Parkhomenko, E. I. and Bondarenko, A. T., 1972 [16]	Basalt (Doleritic) 1312 Plagioclase; Russia			575	2.04E-06	Same as above.	
					671	1.54E-05		
					769	9.55E-05		
					870	2.36E-04		
					962	3.15E-04		
4	Parkhomenko, E. I. and Bondarenko, A. T., 1972 [16]	Basalt (Doleritic) 1319; Russia			1058	4.69E-04	Same as above.	
					1161	1.06E-03		
					1250	4.76E-02		
					472	6.74E-08		
					571	3.81E-07		
5	Parkhomenko, E. I. and Bondarenko, A. T., 1972 [16]	Basalt (Gabbroic) 5/166; Russia			676	4.53E-06	Same as above.	
					769	3.22E-05		
					870	8.10E-05		
					971	1.84E-04		
					1076	4.66E-04		
6	Parkhomenko, E. I. and Bondarenko, A. T., 1972 [16]	Basalt (Doleritic) 1319; Russia			1167	1.31E-03	Same as above.	
					1264	2.70E-03		
					474	2.07E-07		
					575	4.11E-06		
					676	1.92E-05		
7	Parkhomenko, E. I. and Bondarenko, A. T., 1972 [16]	Basalt (Gabbroic) 5/166; Russia			775	3.50E-05	Same as above.	
					877	5.28E-05		
					980	1.64E-04		
					1080	3.05E-04		
					1172	1.17E-02		
8	Parkhomenko, E. I. and Bondarenko, A. T., 1972 [16]	Basalt (Gabbroic) 5/166; Russia			1282	4.05E-02	Same as above.	
					474	3.25E-08		
					575	1.10E-05		
					676	1.20E-04		
					775	2.74E-04		
9	Parkhomenko, E. I. and Bondarenko, A. T., 1972 [16]	Basalt (Gabbroic) 5/166; Russia			877	1.17E-03	Same as above.	
					971	3.30E-03		
					1075	2.94E-02		
					1175	1.55E-01		
					1284	4.40E-01		

TABLE 4.1. EXPERIMENTAL DATA ON ELECTRICAL CONDUCTIVITY OF BASALT (TEMPERATURE DEPENDENCE) (Continued)

Data Set No.	Author(s), Year [Ref. No.]	Name and Source	Minerals and/or Chemical Composition		Method Used		Experimental Data		Other Specifications
			Componenta	Weight Percent	Volume Percent	T, K	Electrical Conductivity (s m^{-1})		
6	Parkhomenko, E. I. and Bondarenko, A. T., 1972 [16]	Basalt (Nepheline) 7; Russia				Same as above	474	1.85E-07	Same as above.
						Same as above	571	3.26E-06	
						Same as above	671	4.71E-05	
						Same as above	775	2.99E-04	
						Same as above	877	1.26E-03	
						Same as above	971	3.51E-03	
7	Parkhomenko, E. I. and Bondarenko, A. T., 1972 [16]	Basalt (Olivine Plagio-Porphyrific) 271; Russia				Same as above	1075	1.21E-02	Same as above.
						Same as above	1183	3.38E-02	
						Same as above	1274	6.94E-02	
						Same as above	474	9.08E-08	
						Same as above	575	1.92E-06	
						Same as above	671	1.99E-05	
8	Parkhomenko, E. I. and Bondarenko, A. T., 1972 [16]	Basalt (Olivine) 1104; Russia				Same as above	763	4.92E-05	Same as above.
						Same as above	870	1.10E-04	
						Same as above	962	2.75E-04	
						Same as above	1064	8.44E-04	
						Same as above	1168	3.94E-03	
						Same as above	1256	1.85E-02	
9	Parkhomenko, E. I. and Bondarenko, A. T., 1972 [16]	Basalt (Olivine) 14; Russia				Same as above	474	1.88E-07	Same as above.
						Same as above	578	2.68E-06	
						Same as above	676	2.83E-05	
						Same as above	775	7.84E-05	
						Same as above	877	1.30E-04	
						Same as above	980	5.47E-04	
10	Parkhomenko, E. I. and Bondarenko, A. T., 1972 [16]	Basalt (Olivine) 1843; Russia				Same as above	1078	7.22E-03	Same as above.
						Same as above	1175	1.48E-02	
						Same as above	1264	2.74E-02	
						Same as above	1274	2.74E-02	
						Same as above	474	5.36E-07	
						Same as above	578	9.58E-06	
10	Parkhomenko, E. I. and Bondarenko, A. T., 1972 [16]	Basalt (Olivine) 1843; Russia				Same as above	680	6.11E-05	Same as above.
						Same as above	781	2.87E-04	
						Same as above	885	1.10E-03	
						Same as above	980	2.46E-02	
						Same as above	1083	4.56E-02	
						Same as above	1190	1.28E-01	
10	Parkhomenko, E. I. and Bondarenko, A. T., 1972 [16]	Basalt (Olivine) 1843; Russia				Same as above	1282	4.44E-01	Same as above.
						Same as above	476	1.50E-08	
						Same as above	571	4.20E-07	
						Same as above	671	2.23E-06	
						Same as above	769	9.60E-06	
						Same as above	877	3.35E-05	
10	Parkhomenko, E. I. and Bondarenko, A. T., 1972 [16]	Basalt (Olivine) 1843; Russia				Same as above	971	1.93E-03	Same as above.
						Same as above	1063	1.75E-03	
						Same as above	1167	3.27E-03	
						Same as above	1264	4.96E-03	
						Same as above	476	1.50E-08	
						Same as above	571	4.20E-07	

TABLE 4.1. EXPERIMENTAL DATA ON ELECTRICAL CONDUCTIVITY OF BASALT (TEMPERATURE DEPENDENCE) (Continued)

Data Set No.	Author(s), Year [Ref. No.]	Name and Source	Minerals and/or Chemical Composition		Method Used	Experimental Data		Other Specifications							
			Components	Weight Percent		T, K	Electrical Conductivity ($s\ m^{-1}$)								
11	Parkhomenko, E.I. and Bondarenko, A.T., 1972 [16]	Basalt (Olivine) 3-11; Russia			Same as above	474	6.22E-06	Same as above.							
						671	1.95E-04								
						775	6.84E-04								
						877	2.65E-03								
						1080	1.73E-02								
						1179	4.88E-02								
						1269	2.31E-01								
						1279	2.31E-01								
						12	Parkhomenko, E.I. and Bondarenko, A.T., 1972 [16]		Basalt (Olivine) 625/4; Russia			Same as above	476	4.94E-09	Same as above.
													578	2.13E-07	
													676	2.63E-06	
775	1.03E-05														
885	3.62E-05														
980	1.73E-04														
1085	9.20E-04														
1193	1.24E-02														
1295	3.18E-02														
13	Parkhomenko, E.I. and Bondarenko, A.T., 1972 [16]	Basalt (Olivine) 7-1 Plagioclase; Russia			Same as above			476					7.61E-06	Same as above.	
								578					6.80E-05		
						676	2.14E-04								
						781	4.01E-04								
						885	1.26E-03								
						980	1.92E-03								
						1085	6.03E-03								
						1287	2.11E-02								
						14	Parkhomenko, E.I. and Bondarenko, A.T., 1972 [16]	Basalt (Olivine) 780/lb; Russia			Same as above	474	2.62E-08		Same as above.
												571	5.30E-08		
												671	2.23E-07		
763	1.05E-06														
877	3.94E-05														
980	6.57E-05														
1072	9.89E-05														
1179	2.78E-04														
1299	1.19E-03														
15	Parkhomenko, E.I. and Bondarenko, A.T., 1972 [16]	Basalt (Pyroxene) 651e; Russia			Same as above							476	3.16E-08	Same as above.	
												578	9.01E-07		
						676	9.01E-06								
						775	5.93E-05								
						885	1.87E-04								
						971	5.93E-04								
						1083	2.08E-03								
						1175	6.58E-03								
						1282	2.31E-02								
						16	Parkhomenko, E.I. and Bondarenko, A.T., 1972 [16]	Basalt (Trachyte) 1103; Russia			Same as above	469	1.98E-06		Same as above.
												575	9.11E-05		
676	4.36E-05														
775	8.94E-05														
877	3.43E-04														

TABLE 4.1. EXPERIMENTAL DATA ON ELECTRICAL CONDUCTIVITY OF BASALT (TEMPERATURE DEPENDENCE) (Continued)

Data Set No.	Author(s), Year [Ref. No.]	Name and Source	Minerals and/or Chemical Composition		Experimental Data		Method Used	Other Specifications
			Components	Weight Percent	T, K	Electrical Conductivity ($s \cdot m^{-1}$)		
16					980	9.66E-04		
cont.					1086	4.57E-03		
					1161	1.92E-01		
					1287	1.03E-01		
17	Parkhomenko, E.I. and Bondarenko, A.T., 1972 [16]	Basalt 1109 Plagioclase; Russia			476	5.28E-09	Same as above	Same as above.
					575	1.30E-07		
					676	1.56E-06		
					787	1.00E-05		
					885	3.45E-05		
					980	1.20E-04		
					1085	5.67E-04		
					1176	1.44E-03		
					1274	5.01E-03		
18	Parkhomenko, E.I. and Bondarenko, A.T., 1972 [16]	Basalt 1131; Russia			476	7.57E-08	Same as above	Same as above.
					575	1.44E-06		
					680	7.01E-06		
					781	1.63E-05		
					877	7.89E-05		
					971	2.51E-04		
					1060	6.46E-04		
					1164	1.66E-03		
					1280	1.67E-02		
19	Parkhomenko, E.I. and Bondarenko, A.T., 1972 [16]	Basalt 161; Russia			474	1.41E-05	Same as above	Same as above.
					574	5.58E-05		
					676	1.05E-04		
					769	1.99E-04		
					870	4.61E-04		
					971	3.78E-03		
					1063	1.48E-02		
					1264	1.35E-01		
20	Parkhomenko, E.I. and Bondarenko, A.T., 1972 [16]	Basalt 175-5; Russia			474	1.25E-07	Same as above	Same as above.
					575	1.53E-06		
					671	1.37E-05		
					775	1.69E-04		
					877	5.93E-04		
					971	2.08E-03		
					1075	5.93E-03		
					1166	7.29E-03		
					1314	1.23E-02		
					1282	1.23E-02		
					1283	1.36E-02		
21	Parkhomenko, E.I. and Bondarenko, A.T., 1972 [16]	Basalt 19-3; Russia			474	1.94E-06	Same as above	Same as above.
					575	2.93E-05		
					680	2.12E-04		
					775	1.13E-03		
					877	3.21E-03		
					971	9.11E-03		
					1073	1.70E-02		
					1171	4.84E-02		
					1280	1.70E-01		

TABLE 4.1. EXPERIMENTAL DATA ON ELECTRICAL CONDUCTIVITY OF BASALT (TEMPERATURE DEPENDENCE) (Continued)

Data Set No.	Author(s), Year [Ref. No.]	Name and Source	Minerals and/or Chemical Composition		Method Used	Experimental Data		Other Specifications
			Components	Weight Percent		T, K	Electrical Conductivity (g m^{-1})	
22	Parkhomenko, E.I. and Bondarenko, A.T., 1972 [16]	Basalt 19-5; Russia			Same as above	472	2.70E-06	Same as above.
						575	1.46E-05	
						676	6.26E-05	
						775	2.42E-04	
						870	6.17E-04	
						971	2.94E-03	
23	Parkhomenko, E.I. and Bondarenko, A.T., 1972 [16]	Basalt 211; Russia			Same as above	1064	8.33E-03	Same as above.
						1167	9.15E-02	
						1264	1.25E-01	
						472	2.66E-07	
						575	1.93E-06	
						680	1.02E-05	
24	Parkhomenko, E.I. and Bondarenko, A.T., 1972 [16]	Basalt 3-3; Russia			Same as above	781	6.69E-05	Same as above.
						877	2.11E-04	
						971	9.11E-04	
						1082	1.89E-03	
						1190	4.84E-03	
						1272	1.38E-02	
25	Parkhomenko, E.I. and Bondarenko, A.T., 1972 [16]	Basalt 312; Russia			Same as above	474	5.01E-06	Same as above.
						671	3.33E-04	
						769	7.49E-04	
						870	3.51E-03	
						1068	2.75E-02	
						1166	8.57E-02	
26	Parkhomenko, E.I. and Bondarenko, A.T., 1972 [16]	Basalt 313; Russia			Same as above	1253	2.97E-01	Same as above.
						476	2.08E-07	
						575	4.13E-06	
						671	2.13E-05	
						769	5.92E-05	
						870	1.21E-04	
27	Parkhomenko, E.I. and Bondarenko, A.T., 1972 [16]	Basalt 4/1; Russia			Same as above	971	4.18E-04	Same as above.
						1074	1.98E-03	
						1271	2.16E-02	
						476	3.25E-05	
						578	2.48E-04	
						680	6.52E-04	
28	Parkhomenko, E.I. and Bondarenko, A.T., 1972 [16]	Basalt 4/1; Russia			Same as above	781	1.12E-03	Same as above.
						877	1.73E-03	
						990	2.40E-03	
						1095	5.61E-03	
						1199	1.06E-02	
						1199	1.31E-02	
29	Parkhomenko, E.I. and Bondarenko, A.T., 1972 [16]	Basalt 4/1; Russia			Same as above	1312	6.37E-02	Same as above.
						476	2.46E-07	
						581	1.36E-06	
						676	1.13E-05	
						769	4.47E-05	
						877	1.96E-04	

TABLE 4.1. EXPERIMENTAL DATA ON ELECTRICAL CONDUCTIVITY OF BASALT (TEMPERATURE DEPENDENCE) (Continued)

Data Set No.	Author(s), Year [Ref. No.]	Name and Source	Minerals and/or Chemical Composition		Method Used	Experimental Data		Other Specifications
			Components	Weight Percent		T, K	Electrical Conductivity (s m^{-1})	
27								
cont.								
28	Parkhomenko, E.I. and Bondarenko, A.T., 1972 [16]	Basalt 5/22; Russia			Same as above	990 1098 1183 1274	7.75E-04 1.47E-03 2.76E-03 6.41E-03	Same as above.
29	Parkhomenko, E.I. and Bondarenko, A.T., 1972 [16]	Basalt 506; Russia			Same as above	476 578 676 775 870 980 1073 1179 1290	1.04E-07 8.56E-06 1.07E-04 1.63E-04 3.42E-04 1.34E-03 3.83E-03 1.22E-02 8.02E-02	Same as above.
30	Parkhomenko, E.I. and Bondarenko, A.T., 1972 [16]	Basalt 517; Russia			Same as above	474 571 676 775 870 962 1057 1160 1256	2.15E-05 2.09E-04 7.16E-04 1.81E-03 8.58E-03 1.59E-02 2.67E-02 8.37E-02 3.24E-01	Same as above.
31	Parkhomenko, E.I. and Bondarenko, A.T., 1972 [16]	Basalt 518; Russia			Same as above	474 571 676 775 877 971 1057 1168 1256	1.40E-06 2.49E-05 2.66E-04 7.40E-04 1.86E-03 8.92E-03 2.46E-02 5.62E-02 1.75E-01	Same as above.
32	Parkhomenko, E.I. and Bondarenko, A.T., 1972 [16]	Basalt 520; Russia			Same as above	472 571 676 769 877 980 1076 1294	7.08E-08 1.20E-06 7.17E-06 2.53E-05 9.88E-05 1.86E-04 5.29E-04 1.36E-02	Same as above.

TABLE 4.1. EXPERIMENTAL DATA ON ELECTRICAL CONDUCTIVITY OF BASALT (TEMPERATURE DEPENDENCE) (Continued)

Data Set No.	Author(s), Year [Ref. No.]	Name and Source	Minerals and/or Chemical Components	Minerals and/or Chemical Composition		Method Used	Experimental Data		Other Specifications
				Weight Percent	Volume Percent		T, K	Electrical Conductivity ($s\ m^{-1}$)	
33	Parkhomenko, E.I. and Bondarenko, A.T., 1972 [16]	Basalt 522; Russia			Same as above	472	1.84E-08	Same as above.	
						571	2.10E-07		
						671	1.56E-06		
						769	1.59E-05		
						870	1.30E-04		
						971	1.18E-03		
34	Parkhomenko, E.I. and Bondarenko, A.T., 1972 [16]	Basalt 523 Plagioclase; Russia		Same as above	472	4.53E-08	Same as above.		
					571	1.26E-07			
					676	1.26E-05			
					775	1.72E-04			
					877	1.02E-03			
					980	3.96E-03			
35	Parkhomenko, E.I. and Bondarenko, A.T., 1972 [16]	Basalt 525; Russia		Same as above	474	1.26E-06	Same as above.		
					575	2.54E-05			
					680	1.47E-04			
					775	6.29E-04			
					870	1.97E-03			
					1075	1.03E-02			
36	Parkhomenko, E.I. and Bondarenko, A.T., 1972 [16]	Basalt 528a; Russia		Same as above	1175	2.63E-02	Same as above.		
					1294	3.22E-02			
					476	3.72E-07			
					578	5.84E-06			
					676	2.87E-05			
					775	1.56E-04			
37	Parkhomenko, E.I. and Bondarenko, A.T., 1972 [16]	Basalt 531 Plagioclase; Russia		Same as above	877	2.39E-04	Same as above.		
					990	1.30E-03			
					1074	4.59E-03			
					1189	1.32E-02			
					1269	1.20E-01			
					478	5.18E-07			
38	Parkhomenko, E.I. and Bondarenko, A.T., 1972 [16]	Basalt 54; Russia		Same as above	578	4.77E-06	Same as above.		
					680	2.33E-05			
					781	1.14E-04			
					885	4.05E-04			
					990	1.44E-03			
					1099	4.59E-03			
					1193	1.19E-02			
					1295	1.21E-01			
					472	5.28E-06			
					575	2.64E-05			
					671	1.21E-04			
					769	2.44E-04			

TABLE 4.1. EXPERIMENTAL DATA ON ELECTRICAL CONDUCTIVITY OF BASALT (TEMPERATURE DEPENDENCE) (Continued)

Data Set No.	Author(s), Year [Ref. No.]	Name and Source	Minerals and/or Chemical Composition	Weight Percent		Method Used	Experimental Data		Other Specifications
				Volume	Percent		T, K	Electrical Conductivity (g m^{-1})	
38									
	cont.								
39	Parkhomenko, E.I. and Bondarenko, A.T., 1972 [16]	Basalt 54a; Russia			Same as above	870 962 1070 1183 1274	6.75E-04 2.09E-03 5.83E-03 1.63E-02 3.35E-02	Same as above.	
40	Parkhomenko, E.I. and Bondarenko, A.T., 1972 [16]	Basalt 5d; Russia			Same as above	474 575 676 775 885 990 1088 1188 1277	1.75E-06 2.20E-05 1.07E-04 2.76E-04 7.12E-04 3.44E-03 5.83E-03 1.85E-02 1.50E-01	Same as above.	
41	Parkhomenko, E.I. and Bondarenko, A.T., 1972 [16]	Basalt 5e; Russia			Same as above	476 578 676 781 877 980 1087 1188 1277	2.48E-05 1.48E-04 7.95E-04 2.27E-03 4.74E-03 1.22E-02 2.06E-02 6.53E-02 3.49E-01	Same as above.	
42	Parkhomenko, E.I. and Bondarenko, A.T., 1972 [16]	Basalt 5l; Russia			Same as above	474 575 676 775 885 990 1086 1195 1297	2.52E-06 4.04E-05 2.01E-04 3.47E-04 1.25E-03 4.01E-03 1.16E-02 3.34E-02 3.06E-01	Same as above.	
43	Parkhomenko, E.I. and Bondarenko, A.T., 1972 [16]	Basalt 602; Russia			Same as above	476 575 685 781 885 980 1089 1302	9.61E-07 8.06E-06 3.22E-04 4.98E-04 1.05E-03 5.66E-03 1.46E-02 8.80E-02	Same as above.	

TABLE 4.1. EXPERIMENTAL DATA ON ELECTRICAL CONDUCTIVITY OF BASALT (TEMPERATURE DEPENDENCE) (Cont Inued)

Data Set No.	Author(s), Year [Ref. No.]	Name and Source	Minerals and/or Chemical Composition		Method Used	Experimental Data		Other Specifications
			Componenta	Weight Percent		T, K	Electrical Conductivity ($\Omega^{-1}m^{-1}$)	
44	Parkhomenko, E. I. and Bondarenko, A. T., 1972 [16]	Basalt (Nepheline) 969; Russia			Same as above	474 575 676 775 870 971 1072 1168 1274	1.01E-07 2.05E-06 2.49E-05 5.15E-05 1.18E-04 3.71E-04 1.05E-03 4.50E-03 2.20E-02	Same as above.
45	Presnall, D. C., Simmons, C. L., and Porath, H., 1972 [17]	Synthetic Basalt	SiO ₂ Al ₂ O ₃ CaO Fe ₂ O ₃ MgO Na ₂ O TiO ₂ K ₂ O MnO P ₂ O ₅	48.06 17.21 11.37 10.69 8.62 2.37 1.17 0.25 0.16 0.10	Two Terminal Method	980 1000 1028 1052 1082 1109 1132 1167 1194 1222 1243 1269 1285 1310	3.44E-04 4.49E-04 6.51E-04 8.72E-04 1.20E-03 1.56E-03 2.04E-03 2.88E-03 3.57E-03 4.53E-03 5.46E-03 6.40E-03 7.30E-03 8.56E-03	Other: The basalt was made up to be identical to the composition of the chilled margin of the Skaergaard intrusion; it has a composition very close to much of the basalt on the ocean floor; the sample was completely melted at 1623 K, rapidly cooled in air to form a glass and finally held at 1323 K in air for 2 weeks to produce a completely crystalline material; conductivity measurements were taken in air with decreasing temperature at cooling rate ~ 150 K/hr.
46	Presnall, D. C., et al., 1972 [17]	Same as above	Same as above		Same as above	1310 1339 1366 1391 1427 1447 1464 1466 1477 1488 1503 1531 1545 1569 1594 1612 1626 1644 1666 1697 1721 1730 1763 1785 1808 1824 1841	9.54E-03 1.09E-02 1.46E-02 2.18E-02 7.33E-02 5.68E-01 1.03 1.42 1.81 2.02 2.50 3.3 5.2 5.7 7.3 9.0 10.6 11.8 13.1 15.4 18.1 20.7 23.0 25.6 30.9 33.4 37.2 39.2	Same as above except measurements were taken in air with increasing temperature at heating rate ~ 150 K/hr.

TABLE 4.1. EXPERIMENTAL DATA ON ELECTRICAL CONDUCTIVITY OF BASALT (TEMPERATURE DEPENDENCE) (Continued)

Data Set No.	Author(s), Year [Ref. No.]	Name and Source	Minerals and/or Chemical Composition		Method Used	Experimental Data		Other Specifications							
			Components	Weight Percent		T, K	Electrical Conductivity ($\sigma_{m^{-1}}$)								
47	Presnall, D.C., et al., 1972 [17]	Same as above	Same as above		Same as above	1314	0.258	Same as above except measurements were taken at cooling rate ~ 150 K/hr.							
						1332	0.385								
						1353	0.560								
						1381	0.908								
						1408	1.32								
						1436	1.87								
						1508	4.28								
						1610	11.5								
						1709	20.7								
						1801	32.6								
48	Presnall, D.C., et al., 1972 [17]	Same as above	Same as above		Same as above	1431	0.316	Same as above except measurements were taken on stepwise cooling.							
						1435	0.954								
						1447	1.97								
						1480	2.60								
						49	Presnall, D.C., et al., 1972 [17]		Same as above	Same as above		Same as above	939	1.88E-02	Same as above except measurements were taken on cooling for 1573-939 K at cooling rate 300 K/hr.
													990	3.11E-02	
													1070	5.56E-02	
													1112	7.64E-02	
													1195	1.33E-01	
													1266	1.78E-01	
1318	2.95E-01														
1376	8.61E-01														
1431	1.82														
1508	4.52														
50	Lastovickova, M. and Kropacek, V., 1980 [18]	Nephelinin Basanites (No. 330); Czechoslovakia	Plagioclase Pyroxene Nephelinite Magnetite Olivine	40.12 38.35 8.64 6.35 4.05	Two Terminal Method	472	9.30E-11	Other: Cylindrical sample of dia 21.5 mm; measured in Ar atmosphere; Pt-PtRh thermocouple used; data extracted from the heating curve.							
						617	9.50E-11								
						633	1.39E-10								
						654	6.73E-10								
						671	9.06E-09								
						676	7.66E-08								
						690	2.13E-07								
						709	6.49E-07								
						775	2.39E-06								
						826	6.67E-06								
926	3.25E-05														
1025	1.20E-04														
1080	1.45E-04														
1099	9.10E-05														
1120	4.30E-05														
1235	2.50E-05														
1314	9.17E-05														
1387	5.36E-04														
1403	1.63E-03														
1417	3.12E-03														

TABLE 4.1. EXPERIMENTAL DATA ON ELECTRICAL CONDUCTIVITY OF BASALT (TEMPERATURE DEPENDENCE) (Continued)

Data Set No.	Author(s), Year [Ref. No.]	Name and Source	Minerals and/or Chemical Composition		Method Used	Experimental Data		Other Specifications
			Components	Weight Percent		T, K	Electrical Conductivity ($\Omega^{-1} \text{m}^{-1}$)	
51	Lastovickova, M. and Kropacek, V., 1980 [18]	Same as above	Same as above		Same as above	472	1.65E-09	Same as above except the data was extracted from the cooling curve.
						508	1.06E-08	
						588	2.77E-07	
						700	6.01E-06	
						800	3.22E-05	
						870	6.81E-05	
						1079	4.83E-04	
						1287	1.63E-03	
						1417	3.12E-03	
						52	Lastovickova, M. and Kropacek, V., 1980 [18]	
581	1.62E-09							
657	1.26E-08							
724	5.77E-07							
775	3.09E-06							
800	1.82E-05							
869	3.18E-05							
925	4.62E-05							
990	4.63E-05							
1020	3.85E-05							
53	Lastovickova, M. and Kropacek, V., 1980 [18]	Same as above	Same as above		Same as above	473	2.55E-09	Same as above except cooling curve.
						515	3.39E-09	
						606	1.83E-08	
						724	6.17E-08	
						826	2.51E-07	
						1012	2.58E-06	
						1145	1.52E-05	
						1213	5.61E-05	
						1290	1.88E-04	
						54	Lastovickova, M. and Kropacek, V., 1980 [18]	
556	2.82E-09							
599	1.15E-08							
641	5.19E-07							
719	3.37E-06							
781	1.50E-05							
806	1.81E-05							
813	2.18E-05							
847	1.51E-05							
885	7.91E-06							
926	4.99E-06							
1023	5.04E-06							
1127	1.69E-05							
1240	1.90E-04							
1291	3.65E-04							

TABLE 4.1. EXPERIMENTAL DATA ON ELECTRICAL CONDUCTIVITY OF BASALT (TEMPERATURE DEPENDENCE) (Continued)

Data Set No.	Author(s), Year [Ref. No.]	Name and Source	Minerals and/or Chemical Composition		Method Used	Experimental Data		Other Specifications							
			Components	Weight Percent		T, K	Electrical Conductivity ($s \cdot m^{-1}$)								
55	Lastovickova, M. and Kropacek, V., 1980 [18]	Same as above	Same as above		Same as above	472	8.24E-10	Same as above except cooling curve.							
						571	2.39E-08								
						684	1.43E-07								
						758	5.80E-07								
						854	4.12E-06								
						952	6.61E-06								
						1000	9.62E-06								
						1030	1.40E-05								
						1181	6.84E-05								
						1203	9.92E-05								
						1291	3.65E-04								
						56	Lastovickova, M. and Kropacek, V., 1980 [18]		Pyroxene Plagioclase Magnetite Nephelinite Olivine	35.42 20.20 14.20 3.48 2.81	Same as above	Same as above	476	4.73E-10	Same as above except heating curve.
													568	1.89E-09	
685	6.78E-08														
787	9.70E-07														
806	8.87E-07														
847	5.63E-07														
855	4.28E-07														
870	6.17E-07														
926	1.29E-06														
980	2.94E-06														
1088	5.60E-06														
1180	1.68E-05														
1251	5.05E-05														
1304	1.15E-04														
1330	4.54E-04														
57	Lastovickova, M. and Kropacek, V., 1980 [18]	Same as above	Same as above	Same as above	Same as above	474	3.94E-10	Same as above except cooling curve.							
						537	5.74E-10								
						617	3.61E-09								
						719	6.11E-07								
						833	1.88E-06								
						909	2.93E-06								
						1060	1.16E-05								
						1169	3.50E-05								
						1277	1.15E-04								
						1302	2.19E-04								
						1330	4.54E-04								
						58	Lastovickova, M. and Kropacek, V., 1980 [18]		Plagioclase Magnetite Pyroxene Olivine	19.90 16.50 15.01 13.25	Same as above	Same as above	474	5.76E-10	Same as above except heating curve.
													571	1.21E-08	
694	2.78E-07														
794	6.95E-06														
847	1.33E-05														
877	9.21E-06														
952	4.44E-06														
1040	3.71E-06														
1084	4.46E-06														
1165	2.33E-05														
1261	1.11E-04														

TABLE 4.1. EXPERIMENTAL DATA ON ELECTRICAL CONDUCTIVITY OF BASALT (TEMPERATURE DEPENDENCE) (Continued)

Data Set No.	Author(s), Year [Ref. No.]	Name and Source	Minerals and/or Chemical Composition	Minerals and/or Chemical Composition		Method Used	Experimental Data		Other Specifications
				Weight Percent	Volume Percent		T, K	Electrical Conductivity ($s \cdot m^{-1}$)	
59	Lastovickova, M. and Kropacek, V., 1980 [18]	Same as above	Same as above			Same as above	474	9.99E-10	Same as above except cooling curve.
							552	2.54E-09	
							645	1.34E-08	
							775	1.22E-07	
							870	3.38E-07	
							971	9.33E-07	
							1048	2.57E-06	
							1124	5.37E-06	
							1223	4.87E-05	
							1261	1.11E-04	
60	Lastovickova, M. and Kropacek, V., 1980 [18]	Nephelinic Basanites (No. 360); Czechoslovakia	Olivine Pyroxene Plagioclase Nephelinite Magnetite	31.02 30.63 19.05 8.81 6.55		Same as above	473	4.37E-10	Same as above except heating curve.
							515	4.83E-10	
							543	7.68E-10	
							574	1.22E-09	
							595	2.12E-09	
							645	7.71E-09	
							694	4.04E-08	
							746	2.55E-07	
							775	8.41E-07	
							819	4.83E-06	
							854	1.33E-05	
							884	2.53E-05	
							909	3.33E-05	
							925	3.66E-05	
							952	3.05E-05	
							970	2.11E-05	
							980	1.76E-05	
							1000	1.61E-05	
							1033	1.76E-05	
							1096	2.12E-05	
							1169	4.44E-05	
							1213	9.26E-05	
							1237	2.32E-04	
							1275	5.81E-04	
							1315	1.01E-03	
61	Lastovickova, M. and Kropacek, V., 1980 [18]	Same as above	Same as above			Same as above	476	1.32E-09	Same as above except cooling curve.
							487	1.45E-09	
							505	2.09E-09	
							529	3.03E-09	
							546	5.28E-09	
							571	1.01E-08	
							595	2.10E-08	
							617	3.04E-08	
							653	5.81E-08	
							675	7.00E-08	
							694	7.01E-08	
							729	8.45E-08	
							757	1.02E-07	
							787	1.34E-07	

TABLE 4.1. EXPERIMENTAL DATA ON ELECTRICAL CONDUCTIVITY OF BASALT (TEMPERATURE DEPENDENCE) (Continued)

Data Set No.	Author(a), Year [Ref. No.]	Name and Source	Minerals and/or Chemical Composition		Method Used	Experimental Data		Other Specifications							
			Componenta	Weight Percent		T, K	Electrical Conductivity ($\sigma_{m^{-1}}$)								
61 cont.						813	2.56E-07								
						847	5.85E-07								
						877	1.76E-06								
						900	5.31E-06								
						943	1.92E-05								
						980	5.80E-05								
						1016	9.19E-05								
						1086	1.60E-04								
						1225	4.83E-04								
						1315	1.01E-03								
						473	1.90E-10								
						507	2.26E-10								
						561	3.54E-10								
62	Lastovickova, M. and Kropacek, V., 1980 [18]	Hornblende Basalt (No. 342); Czechoslovakia	Plagioclase Pyroxene Magnetite Olivine Nepheleline	36.07 11.70 11.20 9.30 7.60	Same aa above	625	1.15E-09	Same aa above except heating curve.							
						684	3.44E-09								
						735	7.82E-09								
						769	2.14E-08								
						840	1.22E-07								
						900	4.79E-07								
						943	1.09E-06								
						1062	4.29E-06								
						1141	2.23E-05								
						1233	1.53E-04								
						1259	6.63E-04								
						63	Lastovickova, M. and Kropacek, V., 1980 [18]		Same aa above	Same aa above		Same aa above	471	1.43E-09	Same aa above except cooling curve.
													495	2.96E-09	
529	8.84E-09														
568	2.19E-08														
588	2.63E-08														
609	3.45E-08														
632	5.96E-08														
714	3.08E-07														
793	1.59E-06														
854	5.73E-06														
925	1.71E-05														
1072	8.09E-05														
1259	6.63E-04														
64	Lastovickova, M. and Kropacek, V., 1980 [18]	Nepheleline Basanite (No. 352); Czechoslovakia	Pyroxene Olivine Nepheleline Plagioclase Magnetite	35.72 26.95 16.61 10.58 8.45	Same aa above	473	3.57E-10	Same aa above except heating curve.							
						495	3.89E-10								
						507	3.87E-10								
						537	6.08E-10								
						578	1.65E-09								
						657	1.11E-08								
						714	4.77E-08								
						729	6.27E-08								
						751	9.01E-08								
						800	1.55E-07								
						833	2.23E-07								
						877	3.85E-07								

TABLE 4.1. EXPERIMENTAL DATA ON ELECTRICAL CONDUCTIVITY OF BASALT (TEMPERATURE DEPENDENCE) (Continued)

Data Set No.	Author(s), Year [Ref. No.]	Name and Source	Minerals and/or Chemical Composition		Method Used	Experimental Data		Other Specifications
			Components	Weight Percent		T, K	Electrical Conductivity (g. m. ⁻¹)	
64 cont.	Lastovickova, M. and Kropacek, V., 1980 [18]	Same as above	Same as above		Same as above	961	1.38E-06	Same as above except cooling curve.
						1041	3.42E-06	
						1059	4.10E-06	
						1097	9.32E-06	
						1170	3.34E-05	
						1230	1.58E-04	
						1243	7.47E-04	
						537	3.85E-10	
						552	7.28E-10	
						571	2.17E-09	
						595	4.50E-09	
						641	2.54E-08	
						689	1.31E-07	
						724	3.25E-07	
						751	7.38E-07	
						781	1.16E-06	
						800	1.27E-06	
						840	1.39E-06	
						854	1.83E-06	
900	3.45E-06							
961	8.57E-06							
1060	4.84E-05							
1243	7.47E-04							
66	Lastovickova, M. and Kropacek, V., 1980 [18]	Nephelinitic Basanites (No. 355); Czechoslovakia	Nephelinite Pyroxene Olivine Plagioclase Magnetite	32.01 18.93 14.39 11.23 6.86	Same as above	476	6.93E-10	Same as above except heating curve.
						502	7.59E-10	
						518	7.59E-10	
						529	8.32E-10	
						537	1.00E-09	
						546	1.76E-09	
						555	4.47E-09	
						561	1.14E-08	
						568	2.40E-08	
						574	3.83E-08	
						584	5.56E-08	
						609	8.87E-08	
						632	1.55E-07	
						662	4.33E-07	
						689	1.21E-06	
						704	3.71E-06	
						709	6.50E-06	
						719	1.14E-05	
						746	1.65E-05	
775	2.19E-05							
813	3.83E-05							
877	1.70E-04							
952	6.29E-04							
1053	2.32E-03							
1152	5.38E-03							
1173	9.43E-03							
1196	1.14E-02							

TABLE 4.1. EXPERIMENTAL DATA ON ELECTRICAL CONDUCTIVITY OF BASALT (TEMPERATURE DEPENDENCE) (Continued)

Data Set No.	Author(s), Year [Ref. No.]	Name and Source	Minerals and/or Chemical Components	Minerals and/or Chemical Composition		Method Used	Experimental Data		Other Specifications								
				Weight Percent	Volume Percent		T.K Conductivity (g.m ⁻¹)	Electrical Conductivity									
66 cont.							1221	1.25E-02									
							1270	9.41E-03									
							1297	7.81E-03									
67	Lastovickova, M. and Kropacek, V., 1980 [18]	Same as above	Same as above			Same as above	476	7.23E-06	Same as above except cooling curve.								
							497	8.70E-06									
							531	1.39E-05									
							584	2.42E-05									
							671	6.13E-05									
							763	1.29E-04									
							854	2.48E-04									
							943	5.73E-04									
							1071	1.33E-03									
							1221	4.06E-03									
							1297	7.81E-03									
							68	Lastovickova, M. and Kropacek, V., 1980 [18]		Nephelinitic Basanite (No. 356); Czechoslovakia	Plagioclase Olivine Nephelinite Pyroxene Magnetite	27.69 23.87 19.66 16.49 10.59		Same as above	473	2.72E-10	Same as above except heating curve.
															571	2.97E-10	
595	3.57E-10																
617	5.19E-10																
636	1.20E-09																
645	4.88E-09																
649	7.09E-09																
649	8.55E-98																
653	8.55E-09																
666	9.38E-09																
671	9.38E-09																
680	1.13E-08																
689	1.80E-08																
709	5.53E-08																
719	1.70E-07																
719	4.32E-07																
724	6.28E-07																
729	7.57E-07																
751	1.45E-06																
800	4.90E-06																
909	4.19E-05																
961	1.41E-04																
1018	2.71E-04																
1043	3.59E-04																
1071	3.93E-04																
1070	2.97E-04																
1070	1.70E-04																
1109	2.04E-04																
1162	2.97E-04																
1219	8.29E-04																
1270	2.79E-03																
69	Lastovickova, M. and Kropacek, V., 1980 [18]	Same as above	Same as above			Same as above	476	8.72E-06	Same as above except cooling curve.								
							497	1.26E-05									
							529	2.01E-05									
							584	4.24E-05									

TABLE 4.1. EXPERIMENTAL DATA ON ELECTRICAL CONDUCTIVITY OF BASALT (TEMPERATURE DEPENDENCE) (Continued)

Data Set No.	Author(s), Year [Ref. No.]	Name and Source	Minerals and/or Chemical Composition		Method Used	Experimental Data		Other Specifications
			Components	Weight Percent		T, K	Electrical Conductivity (g m^{-1})	
69								
cont.								
70	Lastovickova, M. and Kropacek, V., 1980 [18]	Nephelinitic Basanite (No. 359); Czechoslovakia	Pyroxene Plagioclase Nephelinite Magnetite Olivine	33.49 24.09 21.61 12.58 5.26	Same as above	474 585 676 709 901 1081 1209 1328 1374	9.79E-05 2.06E-04 8.13 3.28E-04 909 8.34E-04 1071 2.80E-03 1173 5.38E-03 1209 8.58E-03 1233 1.03E-02 1245 7.11E-03	Same as above except heating curve.
71	Lastovickova, M. and Kropacek, V., 1980 [18]	Same as above	Same as above		Same as above	474 574 662 793 900 1017 1100 1141 1259 1314 1342 1374	8.21E-06 3.61E-05 6.88E-05 1.58E-04 2.51E-04 5.27E-04 1.01E-03 1.34E-03 3.73E-03 6.52E-03 1.14E-02 2.00E-02	Same as above except cooling curve.
72	Bacon, J.F., Russell, S., and Carstens, J.P., 1973 [19]	Tholeiitic Basalt			Impedance Bridge	1512 1537 1581 1633 1673 1705 1736	8.35 11.39 13.92 17.90 20.89 21.79 25.06	Molten rock was prepared by heating the rock in a tungsten crucible in an Ar atmosphere; estimated error $\pm 18\%$.
73	Rai, C.S. and Manghani, M.H., 1976 [20]	Tholeiitic Olivine Basalt (C50); Hawaii	SiO ₂ Al ₂ O ₃ MgO FeO CaO TiO ₂ Fe ₂ O ₃ Na ₂ O H ₂ O ⁺ K ₂ O H ₂ O ⁻	46.81 14.50 10.66 8.98 8.96 2.69 2.45 2.21 0.97 0.57 0.45	Two Terminal Loop Method	775 869 917 970 1016 1068 1117 1161 1240 1269 1290	0.0046 0.0139 0.0274 0.0477 0.0767 0.1140 0.1450 0.1760 0.1770 0.0146 0.0254	A.C. electrical conductivity of the rock sample was measured by loop technique; sample was measured in 87.6% CO ₂ and 12.4% H ₂ atmosphere from 773-1823 K; the loop was heated to 1773 K and then cooled slowly to room temperature, the process was repeated twice in order to obtain homogeneous starting samples; the resistance of the sample was measured at 500 Hz; the

TABLE 4.1. EXPERIMENTAL DATA ON ELECTRICAL CONDUCTIVITY OF BASALT (TEMPERATURE DEPENDENCE) (Continued)

Data Set No.	Author(s), Year [Ref. No.]	Name and Source	Minerals and/or Chemical Composition		Method Used	Experimental Data		Other Specifications
			Componenta	Weight Percent		T, K	Electrical Conductivity (s m ⁻¹)	
75								
cont.								
76	Rai, C.S. and Manghanani, M.H., 1976 [20]	Hawaiite Basalt (C42); Hawaii	SiO ₂ Al ₂ O ₃ FeO CaO MgO TiO ₂ Fe ₂ O ₃ Na ₂ O K ₂ O P ₂ O ₅ H ₂ O ⁺ H ₂ O ⁻ MnO	45.88 16.39 10.00 8.90 5.92 3.83 3.39 3.30 1.02 0.59 0.29 0.24 0.18	Same as above	775 819 869 909 970 1013 1059 1109 1160 1209 1236 1264 1287 1310 1347 1381 1422 1451 1589 1647 1748	7.04 8.92 10.9 13.8	Same as above.
77	Rai, C.S. and Manghanani, M.H., 1976 [20]	Alkalic Olivine Basalt (C222); Hawaii	SiO ₂ Al ₂ O ₃ CaO FeO MgO Fe ₂ O ₃ Na ₂ O TiO ₂ K ₂ O H ₂ O ⁺ P ₂ O ₅ H ₂ O ⁻ MnO	46.54 13.95 10.74 9.97 9.40 3.16 2.69 2.25 0.87 0.41 0.29 0.24 0.16	Same as above	787 819 869 909 970 1018 1064 1121 1166 1223 1240 1262 1298 1315 1340 1422 1574 1677 1718 1763	0.0034 0.0051 0.0104 0.0185 0.0389 0.0639 0.1050 0.159 0.204 0.221 0.204 0.153 0.115 0.135 0.262 0.622 1.61 6.28 9.50 10.3 11.2	Same as above.
78	Rai, C.S. and Manghanani, M.H., 1976 [20]	Alkalic Olivine Basalt (C70); Hawaii	SiO ₂ Al ₂ O ₃ CaO	47.48 17.42 8.54	Same as above	775 819 869	0.0117 0.0184 0.0342	Same as above.

TABLE 4.1. EXPERIMENTAL DATA ON ELECTRICAL CONDUCTIVITY OF BASALT (TEMPERATURE DEPENDENCE) (Continued)

Data Set No.	Author(s), Year [Ref. No.]	Name and Source	Minerals and/or Chemical Composition		Method Used		Experimental Data		Other Specifications
			Components	Weight Percent	Volume Percent	T, K	Electrical Conductivity (g m^{-1})		
78 cont.			FeO	8.10			917	0.0586	
			MgO	6.74			970	0.118	
			Fe ₂ O ₃	3.59			1018	0.172	
			Na ₂ O	3.12			1064	0.239	
			TiO ₂	2.63			1119	0.333	
			K ₂ O	1.20			1166	0.378	
			Il ₂ O ⁺	0.40			1218	0.378	
			P ₂ O ₅	0.36			1239	0.363	
			Il ₂ O ⁻	0.22			1297	0.395	
			MnO	0.18			1315	0.549	
							1347	0.830	
							1366	1.31	
							1394	1.82	
							1451	2.99	
							1515	5.11	
							1666	12.2	
							1718	15.6	
				1763	18.4				
79	Raf, C.S. and Nanghanant, N.H., Basalt (C-210); 1976 [20]	Nugearlite Hawaii	SiO ₂	51.80		Same as above	775	0.0069	Same as above.
			Al ₂ O ₃	17.07			819	0.0132	
			FeO	6.93			869	0.0267	
			CaO	6.01			917	0.0475	
			Na ₂ O	5.78			970	0.0845	
			Fe ₂ O ₃	3.12			1017	0.217	
			MgO	3.10			1062	0.475	
			K ₂ O	2.23			1113	0.660	
			TiO ₂	1.95			1158	0.779	
			P ₂ O ₅	1.54			1209	0.847	
			Il ₂ O ⁺	0.48			1230	0.848	
			Il ₂ O ⁻	0.41			1251	0.921	
			MnO	0.22			1269	1.09	
							1298	1.18	
							1322	1.39	
							1408	2.47	
							1422	2.92	
				1499	3.89				
				1547	4.98				
				1592	6.12				
				1647	6.93				
				1697	8.87				
				1739	10.0				
80	Raf, C.S. and Nanghanant, N.H., Basalt (C-128); 1976 [20]	Trachyte Hawaii	SiO ₂	60.85		Same as above	775	0.0433	Same as above.
			Al ₂ O ₃	18.51			819	0.0741	
			Na ₂ O	7.20			869	0.137	
			K ₂ O	3.60			917	0.235	
			Fe ₂ O ₃	3.10			970	0.418	
			FeO	2.08			1009	0.658	
			CaO	1.77			1067	0.953	
			TiO ₂	0.65			1113	1.33	
							775	0.0433	
							819	0.0741	

TABLE 4.1. EXPERIMENTAL DATA ON ELECTRICAL CONDUCTIVITY OF BASALT (TEMPERATURE DEPENDENCE) (Continued)

Data Set No.	Author(s), Year [Ref. No.]	Name and Source	Minerals and/or Chemical Composition		Experimental Data		Other Specifications						
			Components	Weight Percent	Volume Percent	T, K		Electrical Conductivity (g m^{-1})					
80 cont.				MgO	0.58		1158	1.70					
				H ₂ O ⁺	0.47		1209	2.18					
				H ₂ O ⁻	0.42		1230	2.36					
				P ₂ O ₅	0.29		1262	2.68					
				PhO	0.27		1285	3.03					
							1303	3.16					
							1366	4.04					
							1408	4.77					
							1451	5.62					
							1497	6.63					
							1538	7.50					
							1600	8.16					
							1655	9.23					
							1697	10.4					
							1739	11.3					
				81	Ral, C.S. and Maughanau, M.H., 1976 [20]	Nephelinite Basalt (C-95); Hawaii		SiO ₂	38.92		775	0.0017	Same as above.
								CaO	13.21		819	0.0023	
MgO	12.95		869					0.0035					
Al ₂ O ₃	12.25		917					0.0060					
FeO	7.88		961					0.0100					
Fe ₂ O ₃	5.33		1015					0.0158					
Na ₂ O	3.92		1066					0.0252					
TiO ₂	2.62		1117					0.0400					
K ₂ O	1.26		1173					0.0436					
P ₂ O ₅	1.11		1215					0.0495					
H ₂ O ⁻	0.38		1237					0.0475					
H ₂ O ⁺	0.33		1288					0.0612					
MnO	0.20		1312					0.0893					
			1338					0.168					
			1364					0.302					
			1404					1.07					
			1472					2.37					
			1519	5.05									
			1562	10.8									
			1618	17.8									
			1666	22.0									
			1718	27.1									
			1760	30.8									
82	Ral, C.S. and Maughanau, M.H., 1976 [20]	Basaltite Basalt (C-90); Hawaii		SiO ₂	40.66		775	0.0020	Same as above.				
				MgO	15.75		819	0.0029					
				CaO	11.37		862	0.0051					
				Al ₂ O ₃	10.57		917	0.0092					
				FeO	9.74		961	0.0158					
				Fe ₂ O ₃	2.95		1015	0.0274					
				H ₂ O ⁺	2.92		1066	0.0400					
				TiO ₂	2.28		1112	0.0609					
				H ₂ O ⁻	1.65		1164	0.0853					
				Na ₂ O	1.48		1215	0.101					
				K ₂ O	0.69		1259	0.125					
							775	0.0020					
							819	0.0029					
							862	0.0051					
							917	0.0092					
							961	0.0158					
							1015	0.0274					
			1066	0.0400									
			1112	0.0609									
			1164	0.0853									
			1215	0.101									
			1259	0.125									

TABLE 4.1. EXPERIMENTAL DATA ON ELECTRICAL CONDUCTIVITY OF BASALT (TEMPERATURE DEPENDENCE) (Continued)

Data Set No.	Author(s), Year [Ref. No.]	Name and Source	Minerals and/or Chemical Composition		Method Used	Experimental Data		Other Specifications
			Components	Weight Percent		T, K	Electrical Conductivity (s m ⁻¹)	
82 cont.			P ₂ O ₅	0.36	Same as above	1312	0.207	
			MnO	0.19		1364	0.761	
83	Rai, C.S. and Manghanani, M.H., Basalt (C-210); Hawaii 1976 [20]	Mugearite Basalt (C-210); Hawaii	SiO ₂	51.80	Same as above	1006	0.0013	Same as above except held over at 1223 K for 63 hr; cooling curve.
			Al ₂ O ₃	17.07		1044	0.0016	
			FeO	6.93		1070	0.0020	
			CaO	6.01		1117	0.0031	
			Na ₂ O	5.78		1142	0.0041	
			Fe ₂ O ₃	3.12		1168	0.0051	
			MgO	3.10		1196	0.0072	
			K ₂ O	2.23		1223	0.0110	
			TiO ₂	1.95		1228	0.463	
			P ₂ O ₅	1.54		1228	0.628	
			H ₂ O ⁺	0.48		1248	0.733	
			H ₂ O ⁻	0.41		1280	0.855	
			MnO	0.22		1385	1.65	
						1430	2.16	
		1479	2.72					
		1538	3.70					
		1587	4.66					
		1628	5.87					
		1683	6.86					
		1739	8.32					
84	Rai, C.S. and Manghanani, M.H., Basalt (C-128); Hawaii 1976 [20]	Trachyte Basalt (C-128); Hawaii	SiO ₂	60.85	Same as above	1003	0.0014	Same as above.
			Al ₂ O ₃	18.51		1044	0.0019	
			Na ₂ O	7.20		1070	0.0023	
			K ₂ O	3.60		1117	0.0041	
			Fe ₂ O ₃	3.10		1142	0.0056	
			FeO	2.08		1168	0.0086	
			CaO	1.77		1196	0.0148	
			TiO ₂	0.65		1228	0.0345	
			MgO	0.58		1230	2.01	
			H ₂ O ⁺	0.47		1275	2.64	
			H ₂ O ⁻	0.42		1331	3.21	
			P ₂ O ₅	0.29		1381	3.90	
			MnO	0.27		1432	4.56	
						1481	5.33	
		1533	6.22					
		1589	7.27					
		1642	8.17					
		1689	8.84					
		1745	9.94					

TABLE 4.1. EXPERIMENTAL DATA ON ELECTRICAL CONDUCTIVITY OF BASALT (TEMPERATURE DEPENDENCE) (Continued)

Data Set No.	Author(s), Year [Ref. No.]	Name and Source	Minerals and/or Chemical Composition		Method Used	Experimental Data		Other Specifications
			Components	Weight Percent		T, K	Electrical Conductivity (s m^{-1})	
85	Parkhomenko, E.I., 1979 [21]	High-Alumina Tholeiite Basalt; Russia	SiO ₂	48.41	Two Terminal	1170	0.0026	Other: No details given; data extracted from curve.
			Al ₂ O ₃	19.56	Method Assumed	1273	0.0073	
			CaO	15.42		1390	0.0207	
			MgO	8.19		1447	0.0334	
			FeO	4.36		1492	0.0637	
			Na ₂ O	1.36		1512	0.0909	
			Fe ₂ O ₃	1.35		1512	0.142	
			H ₂ O ⁻	0.53		1529	0.552	
			MnO	0.41		1550	3.23	
			TiO ₂	0.23		1557	4.83	
H ₂ O ⁺	0.18		1577	6.37				
			1592	7.52				
86	Parkhomenko, E.I., 1979 [21]	Same as above	Same as above		Same as above	1270	0.00053	Same as above except resistivity was measured at 28×10^8 Pa pressure.
						1390	0.00015	
						1481	0.00032	
						1562	0.00064	
						1592	0.00103	
						1610	0.00180	
						1633	0.00452	
						1655	0.0109	
						1721	0.131	
						1742	0.180	
			1766	0.196				
87	Parkhomenko, E.I., 1979 [21]	Quartz Tholeiite Basalt; Russia	SiO ₂	52.05	Same as above	1157	0.00091	Other: Measured at 2.5×10^8 Pa pressure.
			Al ₂ O ₃	15.16		1303	0.00343	
			MgO	9.49		1475	0.0124	
			CaO	9.29		1517	0.154	
			FeO	5.16		1543	0.174	
			Fe ₂ O ₃	4.48				
			Na ₂ O	2.46				
			K ₂ O	0.89				
			TiO ₂	0.82				
			P ₂ O ₅	0.13				
MnO	0.10							
H ₂ O ⁻	0.06							
H ₂ O ⁺	0.03							
			Same as above		1245	0.000176	Other: Measured at 28×10^8 Pa pressure.	
					1336	0.000378		
					1470	0.00111		
					1543	0.00180		
					1550	0.00195		
					1607	0.00418		
					1655	0.00701		
					1672	0.0139		
					1712	0.0719		
					1742	0.099		

TABLE 4.1. EXPERIMENTAL DATA ON ELECTRICAL CONDUCTIVITY OF BASALT (TEMPERATURE DEPENDENCE) (Continued)

Data Set No.	Author(s), Year [Ref. No.]	Name and Source	Minerals and/or Chemical Composition		Method Used	Experimental Data		Other Specifications							
			Components	Weight Percent		T, K	Electrical Conductivity (s m^{-1})								
89	Parkhomenko, E. I., 1979 [21]	Alkaline Tholeiite Basalt; Russia	SiO ₂	49.58	Same as above	1097	0.00161	Other: Measured at 5×10^6 Pa pressure; no other details given.							
			Al ₂ O ₃	14.62											
			CaO	11.32											
			FeO	7.80											
			MgO	7.34											
			Na ₂ O	3.19											
			Fe ₂ O ₃	3.03											
			TiO ₂	1.71											
			H ₂ O ⁺	0.34											
			H ₂ O ⁻	0.24											
			K ₂ O	0.18											
			MnO	0.16											
			P ₂ O ₅	0.04											
90	Parkhomenko, E. I., 1979 [21]	Same as above	Same as above	Same as above	Same as above	1246	0.00126	Other: Measured at 28×10^6 Pa pressure; no other details given.							
						1481	0.00181								
						1529	0.00229								
						1557	0.00329								
						1600	0.0114								
						1663	0.0877								
						1680	0.112								
						1703	0.131								
						91	Lastovickova, M. and Kropacek, V., 1976 [22]		Leucitite Nephelinite Basalt (230); Bohemian Massif, Czechoslovakia	Ferrimagnetic Minerals	12.7	Two Terminal Method	621	1.04E-06	Other: Measurements were conducted in an argon atmosphere with partial pressure of oxygen of about 8×10^{-6} bar; the rate of heating and cooling was 600 K/hr; Curie temperature 793 K.
													657	1.83E-06	
													671	2.71E-06	
													719	5.67E-06	
													763	1.14E-05	
775	1.35E-05														
781	1.61E-05														
793	1.76E-05														
800	2.00E-05														
819	2.28E-05														
847	2.60E-05														
869	3.09E-05														
884	2.83E-05														
909	3.52E-05														
934	4.57E-05														
952	6.20E-05														
980	7.71E-05														
1074	1.48E-04														
1121	2.29E-04														
1150	2.84E-04														
92	Lastovickova, M. and Kropacek, V., 1976 [22]	Melilitic Olivine Nephelinite Basalt (259); Bohemian Massif, Czechoslovakia	Ferrimagnetic Minerals	5.1	Same as above	434	4.00E-08	Same as above except Curie temperature 493 K.							
						465	6.73E-08								
						469	7.03E-08								
						483	8.36E-08								
						492	9.52E-08								
						502	1.04E-07								
						512	1.08E-07								
						523	1.04E-07								

TABLE 4.1. EXPERIMENTAL DATA ON ELECTRICAL CONDUCTIVITY OF BASALT (TEMPERATURE DEPENDENCE) (Continued)

Data Set No.	Author(s), Year [Ref. No.]	Name and Source	Minerals and/or Chemical Composition		Method Used	Experimental Data		Other Specifications
			Components	Weight Percent		T, K	Electrical Conductivity (g m^{-1})	
92								
cont.								
93	Lastovickova, M. and Kropacek, V., 1976 [22]	Sodalitic Tephrite Basalt (256); Bohemian Massif, Czechoslovakia	Ferrite	7.9	Same as above	416 469 520 574 621 675 719 763 763 781 787 793 800 806 819 847 869 925 970 1024 1075	1.23E-07 1.29E-07 1.18E-07 1.74E-07 4.15E-07 1.08E-06 2.94E-06 6.16E-06 9.95E-06 1.68E-05 2.48E-05 4.01E-05 5.92E-05 6.53E-07 1.42E-06 2.39E-06 3.53E-06 5.00E-06 7.38E-06 1.48E-05 3.24E-05 3.69E-05 3.85E-05 4.21E-05 4.59E-05 4.79E-05 5.46E-05 6.50E-05 8.81E-05 1.05E-04 1.30E-04 1.77E-04 2.29E-04 3.24E-04	Same as above except Curie temperature 793 K.
94	Lastovickova, M. and Kropacek, V., 1976 [22]	Leucitite Basalt (218); Bohemian Massif, Czechoslovakia	Ferrite	10.2	Same as above	480 529 558 574 621 636 662 675 704 724 781 793 813 826 840 854	7.08E-07 2.75E-06 5.29E-06 7.50E-06 1.58E-05 2.24E-05 3.78E-05 4.31E-05 4.92E-05 8.68E-05 1.47E-04 1.67E-04 1.99E-04 2.27E-04 2.48E-04 2.70E-04	Same as above except Curie temperature 813 K.

TABLE 4.1. EXPERIMENTAL DATA ON ELECTRICAL CONDUCTIVITY OF BASALT (TEMPERATURE DEPENDENCE) (Continued)

Data Set No.	Author(s), Year [Ref. No.]	Name and Source	Minerals and/or Chemical Composition		Method Used	Experimental Data		Other Specifications
			Components	Weight Percent		T, K	Electrical Conductivity ($s \cdot m^{-1}$)	
94								
cont.								
95	Lastovickova, M. and Kropacek, V., 1976 [22]	Leucite Bssalt (233); Bohemian Massif, Czechoslovakia	Ferrite	13.4	Same as above	418 471 505 531 537 549 558 564 574 588 606 641 675 729 769 819 833 877 925 1015 1048 1064	2.82E-04 3.08E-04 3.51E-04 4.57E-04 5.44E-04 6.48E-04 8.60E-07 2.07E-06 2.46E-06 2.80E-06 2.80E-06 2.93E-06 2.93E-06 3.20E-06 3.34E-06 3.19E-06 3.34E-06 5.90E-06 8.38E-06 1.93E-05 3.42E-05 6.04E-05 6.89E-05 1.02E-04 1.33E-04 1.59E-04 1.81E-04 1.97E-04	Same as above except Curie temperature 623.5 K.
96	Lastovickova, M. and Kropacek, V., 1976 [22]	Sodalite Nephelinite Basalt (207); Bohemian Massif, Czechoslovakia	Ferrite	11.3	Same as above	529 574 595 617 632 653 675 704 729 746 769 775 806 826 854 877	1.33E-06 2.68E-06 3.49E-06 4.34E-06 4.95E-06 9.16E-06 1.36E-05 2.20E-05 3.42E-05 5.07E-05 6.05E-05 6.90E-05 1.12E-04 1.46E-04 1.89E-04 2.36E-04	Same as above except Curie temperature 553 K.
97	Lastovickova, M. and Kropacek, V., 1976 [22]	Basalt s.s. (231); Bohemian Massif, Czechoslovakia	Ferrite	11.3	Same as above	421 473 497 505	1.05E-06 2.31E-06 2.87E-06 3.27E-06	Same as above except Curie temperature 513 K.

TABLE 4.1. EXPERIMENTAL DATA ON ELECTRICAL CONDUCTIVITY OF BASALT (TEMPERATURE DEPENDENCE) (Continued)

Data Set No.	Author(s), Year [Ref. No.]	Name and Source	Minerals and/or Chemical Composition		Method Used	Experimental Data		Other Specifications							
			Weight Percent	Volume Percent		T, K	Electrical Conductivity (s m ⁻¹)								
97 cont.						515	3.42E-06								
						523	3.57E-06								
						540	3.89E-06								
						555	3.89E-06								
						574	4.07E-06								
						595	4.25E-06								
						621	4.24E-06								
						636	4.06E-06								
						675	4.63E-06								
						724	6.01E-06								
						781	1.21E-05								
						833	2.14E-05								
						884	3.77E-05								
						934	6.96E-05								
						980	1.13E-04								
						1018	2.27E-04								
						1067	4.98E-04								
						1122	1.20E-03								
						1172	1.70E-03								
						98	Chung, D.H., Westphal, W.B., and Simmons, G., 1970 [23]		Lunar Basalt 10020; Moon	Pyroxene Plagioclase Ilmenite Olivine Unidentified Cristobalite Troilite	53 25 15 4 1.4 1 0.6	Two Terminal Method	80.645	1.73E-11	Density: 3.18 Mg m ⁻³ (bulk). Other: Sample was baked at 423 K in vacuum, high temperature run in dry N ₂ from room temperature to 473 K; sample immersed in baths of ice, dry ice, or liquid N ₂ for low temperature run; measurement at 100 Hz.
													90.090	2.78E-11	
													99.010	4.32E-11	
													113.766	6.72E-11	
132.802	1.16E-10														
144.928	1.57E-10														
155.039	1.93E-10														
180.832	2.62E-10														
192.678	3.00E-10														
208.768	3.32E-10														
243.902	5.34E-10														
274.725	8.58E-10														
307.692	1.33E-09														
381.679	5.52E-09														
512.820	8.53E-08														
99	Chung, D.H., et al., 1970 [23]	Same as above	Same as above		Same as above	80.000	5.86E-11	Same as above except measured at 1 KHz.							
						92.593	1.27E-10								
						101.833	2.50E-10								
						116.009	4.29E-10								
						131.752	6.65E-10								
						143.678	9.00E-10								
						156.495	1.14E-09								
						171.821	1.49E-09								
						184.502	1.77E-09								
						192.678	2.02E-09								
206.612	2.31E-09														
243.902	3.47E-09														
270.270	4.55E-09														
293.255	5.76E-09														
367.647	1.64E-08														
465.116	1.16E-07														

TABLE 4.1. EXPERIMENTAL DATA ON ELECTRICAL CONDUCTIVITY OF BASALT (TEMPERATURE DEPENDENCE) (Continued)

Data Set No.	Author(a), Year [Ref. No.]	Name and Source	Minerals and/or Chemical Composition		Method Used	Experimental Data		Other Specifications							
			Componenta	Componenta		T, K	Electrical Conductivity ($s \cdot m^{-1}$)								
100	Chung, D.H., et al., 1970 [23]	Same as above	Same as above	Same as above	Same as above	81	2.11E-10	Same as above except measured at 10 KHz.							
						93	4.15E-10								
						103	1.03E-09								
						116	2.48E-09								
						134	4.72E-09								
						144	5.58E-09								
						157	7.31E-09								
						182	1.06E-08								
						194	1.30E-08								
						206	1.54E-08								
						247	1.94E-08								
						271	3.02E-08								
						293	3.34E-08								
						367	5.73E-08								
						465	3.10E-07								
						101	Chung, D.H., et al., 1970 [23]		Same as above	Same as above	Same as above	Same as above	81	1.05E-09	Same as above except measured at 100 KHz.
87	1.20E-09														
97	1.57E-09														
106	4.63E-09														
119	1.19E-08														
135	2.76E-08														
144	3.74E-08														
158	5.07E-08														
171	6.21E-08														
180	6.87E-08														
192	7.60E-08														
208	8.99E-08														
243	1.35E-07														
265	1.83E-07														
291	1.89E-07														
364	3.83E-07														
448	1.17E-06														
102	Chung, D.H., et al., 1970 [23]	Same as above	Same as above	Same as above	Same as above	81	1.00E-08	Same as above except measured at 1 MHz.							
						122	3.62E-08								
						136	1.10E-07								
						145	1.89E-07								
						158	2.93E-07								
						175	4.10E-07								
						182	4.69E-07								
						194	5.75E-07								
						208	6.36E-07								
						296	1.13E-06								
						357	1.81E-06								
						448	4.20E-06								
						103	Chung, D.H., et al., 1970 [23]		Same as above	Same as above	Same as above	Same as above	81	8.13E-08	Same as above except measured at 10 MHz.
													198	4.97E-06	
													296	7.71E-06	
													357	1.01E-05	
448	1.92E-05														

TABLE 4.1. EXPERIMENTAL DATA ON ELECTRICAL CONDUCTIVITY OF BASALT (TEMPERATURE DEPENDENCE) (Continued)

Data Set No.	Author(s), Year [Ref. No.]	Name and Source	Minerals and/or Chemical Composition		Method Used	Experimental Data		Other Specifications								
			Components	Weight Percent		T, K	Electrical Conductivity (g m^{-1})									
104	Chung, D.H., et al., 1970 [23]	Lunar Basalt 10057; Moon	Pyroxene Plagioclase Ilmenite Glass Unidentified Cristobalite	51	Same as above	Same as above	80	1.08E-11	Density: 2.88 Mg m^{-3} (bulk). Other: Same as above except measured at 100 Hz.							
				20			100	2.52E-11								
				16			109	4.05E-11								
				10			117	4.96E-11								
				2.9			127	7.98E-11								
				<0.1			136	1.01E-10								
							144	1.16E-10								
							152	1.28E-10								
							157	1.38E-10								
							165	1.52E-10								
							172	1.58E-10								
							179	1.63E-10								
							186	1.69E-10								
							204	1.81E-10								
							214	1.87E-10								
							234	2.07E-10								
							251	2.37E-10								
	303	5.17E-10														
	381	1.75E-09														
	515	1.80E-08														
	512	3.79E-08														
105	Chung, D.H., et al., 1970 [23]	Same as above	Same as above		Same as above	Same as above	80	1.68E-11	Same as above except measured at 1 KHz.							
							90	2.69E-11								
							99	4.17E-11								
							112	6.46E-11								
							130	1.11E-10								
							143	1.50E-10								
							153	1.79E-10								
							178	2.49E-10								
							192	2.85E-10								
							206	3.15E-10								
							240	5.23E-10								
							270	8.11E-10								
							297	1.26E-09								
							366	5.56E-09								
							478	8.30E-08								
				106			Chung, D.H., et al., 1970 [23]	Same as above		Same as above		Same as above	Same as above	81	1.23E-10	Same as above except measured at 10 KHz.
														141	3.48E-09	
	155	6.17E-09														
	161	7.56E-09														
	167	8.65E-09														
	173	9.58E-09														
	184	1.10E-08														
	197	1.17E-08														
	214	1.30E-08														
	228	1.48E-08														
	243	1.70E-08														
	270	2.08E-08														
	293	2.08E-08														
	367	4.84E-08														

TABLE 4.1. EXPERIMENTAL DATA ON ELECTRICAL CONDUCTIVITY OF BASALT (TEMPERATURE DEPENDENCE) (Continued)

Data Set No.	Author(s), Year [Ref. No.]	Name and Source	Minerals and/or Chemical Composition		Method Used	Experimental Data		Other Specifications
			Weight Percent	Volume Percent		T, K	Electrical Conductivity (g m^{-1})	
107	Chung, D.H., et al., 1970 [23]	Same as above	Same as above		Same as above	81	7.75E-10	Same as above except measured at 100 Kliz.
						158	3.74E-08	
						166	4.90E-08	
						173	5.80E-08	
						184	7.10E-08	
						196	8.13E-08	
108	Chung, D.H., et al., 1970 [23]	Same as above	Same as above		Same as above	296	1.17E-06	Same as above except measured at 1 Millz.
						364	1.63E-06	
						460	3.10E-06	
						80	7.35E-08	
						296	7.97E-06	
						357	1.12E-05	
109	Chung, D.H., et al., 1970 [23]	Same as above	Same as above		Same as above	460	1.67E-05	Same as above except measured at 10 Millz.
						80	7.35E-08	
						296	7.97E-06	
						357	1.12E-05	
						460	1.67E-05	
						79	3.06E-11	
110	Chung, D.H., et al., 1970 [23]	Lunar Basalt 10046; Moon	Pyroxene Plagioclase Glass Ilmenite	57 20 14 9	Same as above	84	3.28E-11	Density: 2.21 Mg m^{-3} (bulk). Other: Same as above except measured at 100 Hz.
						101	3.90E-11	
						114	4.32E-11	
						126	4.78E-11	
						134	5.47E-11	
						146	6.05E-11	
						159	6.70E-11	
						168	7.66E-11	
						178	7.41E-11	
						210	8.49E-11	
111	Chung, D.H., et al., 1970 [23]	Same as above	Same as above		Same as above	216	9.07E-11	Same as above except measured at 1 Kliz.
						221	9.38E-11	
						227	9.70E-11	
						239	1.11E-10	
						253	1.15E-10	
						277	1.23E-10	
						291	1.40E-10	
						362	2.02E-10	
						467	4.20E-10	
						80	1.41E-10	

TABLE 4.1. EXPERIMENTAL DATA ON ELECTRICAL CONDUCTIVITY OF BASALT (TEMPERATURE DEPENDENCE) (Continued)

Data Set No.	Author(s), Year [Ref. No.]	Name and Source	Minerals and/or Chemical Composition		Method Used	Experimental Data		Other Specifications
			Components	Weight Percent		T, K	Electrical Conductivity (g m^{-1})	
111 cont.						207	4.75E-10	
						223	5.08E-10	
						232	5.26E-10	
						242	5.62E-10	
						252	5.62E-10	
						260	5.63E-10	
						276	5.82E-10	
						294	6.65E-10	
						369	8.40E-10	
						465	1.48E-09	
						80	7.36E-10	
112	Chung, D.H., et al., 1970 [23]	Same as above	Same as above		Same as above	82	7.87E-10	Same as above except measured at 10 KHz.
						107	8.19E-10	
						118	1.18E-09	
						141	1.66E-09	
						150	1.89E-09	
						163	2.32E-09	
						173	2.74E-09	
						183	2.83E-09	
						212	3.24E-09	
						223	3.35E-09	
						232	3.35E-09	
245	3.47E-09							
252	3.59E-09							
263	3.59E-09							
276	3.59E-09							
304	3.84E-09							
375	4.70E-09							
465	6.56E-09							
113	Chung, D.H., et al., 1970 [23]	Same as above	Same as above		Same as above	80	4.61E-09	Same as above except measured at 100 KHz.
						145	9.15E-09	
						152	9.79E-09	
						164	1.24E-08	
						177	1.68E-08	
						186	1.79E-08	
						214	2.35E-08	
						227	2.51E-08	
						236	2.60E-08	
						250	2.78E-08	
						257	2.78E-08	
269	2.97E-08							
277	2.97E-08							
306	3.18E-08							
380	3.52E-08							
483	4.17E-08							
114	Chung, D.H., et al., 1970 [23]	Same as above	Same as above		Same as above	80	3.30E-08	Same as above except measured at 1 MHz.
						156	6.14E-08	
						171	8.04E-08	
						176	1.02E-07	

TABLE 4.1. EXPERIMENTAL DATA ON ELECTRICAL CONDUCTIVITY OF BASALT (TEMPERATURE DEPENDENCE) (Continued)

Data Set No.	Author(s), Year [Ref. No.]	Name and Source	Minerals and/or Chemical Composition		Method Used	Experimental Data		Other Specifications
			Componenta	Weight Percent		T, K	Electrical Conductivity ($s\ m^{-1}$)	
114 cont.								
115	Chung, D.H., et al., 1970 [23]	Same as above	Same as above		Same as above		188 1.12E-07 213 1.42E-07 218 1.52E-07 224 1.57E-07 242 1.99E-07 304 2.52E-07 386 2.89E-07 492 3.42E-07	Same as above except measured at 10 MHz.
116	Chung, D.H., et al., 1970 [23]	Hawaii Basalt; Oahu, Hawaii	Plagioclase Pyroxene Olivine Quartz Unidentified	48 24 21 6 1	Same as above		81 4.81E-12 86 4.80E-12 96 5.11E-12 114 5.62E-12 131 6.41E-12 146 8.10E-12 159 9.58E-12 172 1.21E-11 185 1.59E-11 189 1.64E-11 229 4.08E-11 261 1.09E-10 283 3.67E-10 395 9.44E-09	Density: 2.68 Mg m ⁻³ (bulk). Other: Same as above except measured at 100 Hz.
117	Chung, D.H., et al., 1970 [23]	Same as above	Same as above		Same as above		81 4.50E-11 86 4.80E-11 97 4.78E-11 116 5.25E-11 133 5.79E-11 145 6.39E-11 160 7.81E-11 171 8.93E-11 182 1.17E-10 205 1.58E-10 227 2.81E-10 261 5.16E-10 406 2.61E-08	Same as above except measured at 1 kHz.
118	Chung, D.H., et al., 1970 [23]	Same as above	Same as above		Same as above		80 4.00E-10 87 4.13E-10 98 4.55E-10 116 5.00E-10 133 4.98E-10 145 5.88E-10 157 6.72E-10 171 7.42E-10 182 7.93E-10	Same as above except measured at 10 kHz.

TABLE 4.1. EXPERIMENTAL DATA ON ELECTRICAL CONDUCTIVITY OF BASALT (TEMPERATURE DEPENDENCE) (Continued)

Data Set No.	Author(s), Year [Ref. No.]	Name and Source	Minerals and/or Chemical Composition	Weight Percent		Method Used	Experimental Data		Other Specifications
				Componenta	Volume Percent		T, K	Electrical Conductivity (g m^{-1})	
118 cont.									
119	Chung, D.H., et al., 1970 [23]	Same as above	Same as above			Same as above	207 226 260 277 403 80 91 101 117 135 146 161 172 179 205 224 254 279 395	1.15E-09 1.84E-09 3.04E-09 5.40E-09 5.34E-08 3.98E-09 3.96E-09 3.94E-09 4.49E-09 5.12E-09 5.47E-09 5.83E-09 6.67E-09 7.13E-09 9.96E-09 1.26E-08 2.09E-08 3.13E-08 1.38E-07	Same as above except measured at 100 KHz.
120	Chung, D.H., et al., 1970 [23]	Same as above	Same as above			Same as above	79 102 121 135 146 160 173 178 206 222 251 276 389	4.30E-08 4.55E-08 4.85E-08 5.34E-08 5.70E-08 6.09E-08 6.50E-08 6.28E-08 8.48E-08 1.00E-07 1.40E-07 2.03E-07 5.56E-07	Same as above except measured at 1 MHz.
121	Chung, D.H., et al., 1970 [23]	Same as above	Same as above			Same as above	79 120 140 163 173 202 253 392	2.25E-07 2.80E-07 3.53E-07 4.60E-07 4.93E-07 7.10E-07 1.49E-06 3.32E-06	Same as above except measured at 10 MHz.
122	Chung, D.H., et al., 1970 [23]	Cape Neddick Basalt; Cape Neddick	Plagioclase Pyroxene Olivine Unidentified	55 26 17 2		Same as above	81 96 98 110 124 129 168 198 246 386	2.80E-12 3.29E-12 3.64E-12 4.15E-12 5.07E-12 5.79E-12 1.06E-11 1.81E-11 9.82E-11 4.64E-09	Density: 2.60 Mg m^{-3} (bulk). Other: Same as above except measured at 100 Hz.

TABLE 4.1. EXPERIMENTAL DATA ON ELECTRICAL CONDUCTIVITY OF BASALT (TEMPERATURE DEPENDENCE) (Continued)

Data Set No.	Author(s), Year [Ref. No.]	Name and Source	Minerals and/or Chemical Components	Minerals and/or Chemical Composition		Method Used	Experimental Data		Other Specifications
				Weight Percent	Volume Percent		T, K	Electrical Conductivity (g m^{-1})	
123	Chung, D.H., et al., 1970 [23]	Same as above	Same as above			Same as above	81	2.71E-11	Same as above except measured at 1 KHz.
							94	3.41E-11	
							97	3.29E-11	
							114	4.15E-11	
							136	5.23E-11	
124	Chung, D.H., et al., 1970 [23]	Same as above	Same as above			Same as above	154	7.56E-11	Same as above except measured at 10 KHz.
							236	2.62E-10	
							406	2.28E-08	
							80	2.86E-10	
							102	3.24E-10	
125	Chung, D.H., et al., 1970 [23]	Same as above	Same as above			Same as above	104	3.58E-10	Same as above except measured at 100 KHz.
							119	4.08E-10	
							142	5.14E-10	
							176	7.17E-10	
							281	3.60E-09	
126	Chung, D.H., et al., 1970 [23]	Same as above	Same as above			Same as above	403	6.12E-08	Same as above except measured at 1 MHz.
							80	3.04E-09	
							103	4.22E-09	
							132	4.95E-09	
							177	6.23E-09	
127	Chung, D.H., et al., 1970 [23]	Same as above	Same as above			Same as above	215	9.30E-09	Same as above except measured at 1 MHz.
							396	1.87E-07	
							80	3.18E-08	
							120	4.38E-08	
							180	7.43E-08	
128	Schloessin, H.H. and Dvorak, Z.D., 1977 [24]	Ocean Basalt 332A/16/1/33-36; Mid-Atlantic Ridge				Two Terminal Method	219	1.11E-07	Specimen Geometry: 0.33 cm thick disc. Other: Sample was rinsed and cleaned in water, then washed and dried in acetone; measured at 1900 MPa.
							390	8.91E-07	
							173	5.82E-07	
							250	1.34E-06	
							393	4.81E-06	
129	Schloessin, H.H. and Dvorak, Z.D., 1977 [24]	Same as above				Same as above	293	7.67E-10	Same as above except measured at 2500 MPa.
							302	9.25E-10	
							354	3.60E-09	
							458	4.54E-09	
							537	2.35E-08	
130	Schloessin, H.H. and Dvorak, Z.D., 1977 [24]	Same as above				Same as above	636	1.33E-07	Same as above except measured at 3000 MPa.
							769	4.73E-06	
							291	3.79E-07	
							309	4.57E-07	
							366	1.47E-06	

TABLE 4.1. EXPERIMENTAL DATA ON ELECTRICAL CONDUCTIVITY OF BASALT (TEMPERATURE DEPENDENCE) (Continued)

Data Set No.	Author(s), Year [Ref. No.]	Name and Source	Minerals and/or Chemical Composition		Method Used	Experimental Data		Other Specifications
			Components	Weight Percent		T, K	Electrical Conductivity ($S \cdot m^{-1}$)	
130								
cont.								
131	Schloessin, H.H. and Dvorak, Z.D., 1977 [24]	Same as above			Same as above	290	4.57E-06	Same as above except measured at 3400 MPa.
						307	5.26E-06	
						358	8.79E-06	
						454	1.61E-05	
						520	2.24E-05	
						606	3.93E-05	
						751	1.10E-04	
132	Schloessin, H.H. and Dvorak, Z.D., 1977 [24]	Same as above			Same as above	392	1.54E-10	Same as above except measured at 5000 MPa.
						442	4.99E-10	
						502	1.54E-09	
						561	1.01E-07	
						653	1.00E-06	
						793	3.25E-05	
						990	5.70E-04	
						1055	2.23E-03	
						1362	2.12E-03	
						1400	1.39E-03	
						1715	1.26E-03	
						1715	7.90E-04	
133	Schloessin, H.H. and Dvorak, Z.D., 1977 [24]	Same as above			Same as above	1865	0.209	Same as above except sample in liquid state; measured at 4000 MPa.
						1901	0.174	
						1956	0.191	
						1976	0.219	
						2016	0.364	
134	Schloessin, H.H. and Dvorak, Z.D., 1977 [24]	Same as above			Same as above	2123	0.252	Same as above except measured at 5000 MPa.
						2217	0.240	
						2298	0.252	
						2325	0.317	
						2439	0.382	
						2469	0.419	
						2531	0.459	
135	Olhoeft, G.R., 1979 [6]	Thingvellir Basalt; Iceland			Two Terminal Method Assumed	298	1.46E-12	Density: 2.82 Mg m ⁻³ . Other: Measured in vacuum, D.C.
						323	7.10E-12	
						373	7.87E-11	
						423	2.82E-10	
						474	3.09E-09	
						527	6.31E-08	
						572	2.69E-07	
						929	8.47E-04	
						982	2.31E-03	
						1031	3.83E-03	
						1079	5.25E-03	
						1124	8.15E-03	
						1164	2.36E-02	

TABLE 4.1. EXPERIMENTAL DATA ON ELECTRICAL CONDUCTIVITY OF BASALT (TEMPERATURE DEPENDENCE) (Continued)

Data Set No.	Author(s), Year [Ref. No.]	Name and Source	Minerals and/or Chemical Composition	Method Used	Experimental Data		Other Specifications
					Componenta	Electrical Conductivity (s m ⁻¹)	
			Weight Percent		T, K		
			Volume Percent				
136	Olhoeft, G.R., 1979 [6]	Same as above		Same as above	298	5.08E-12	Same as above except measured in dry air.
					298	8.91E-12	
					322	1.93E-11	
					349	1.55E-10	
					364	2.00E-10	
					374	4.83E-10	
137	Olhoeft, G.R., 1979 [6]	Same as above			436	3.67E-09	Same as above except measured in vacuum at 10 Hz.
					445	6.89E-09	
					298	1.03E-09	
					349	1.01E-09	
					373	1.58E-09	
					400	1.60E-09	
138	Olhoeft, G.R., 1979 [6]	Same as above			474	4.50E-09	Same as above except measurements for water saturated specimen at 0.1 MPa.
					579	3.83E-08	
					252	8.87E-08	
					263	1.41E-06	
					272	3.86E-06	
					276	6.53E-04	
					284	9.57E-04	
					298	1.33E-03	
					311	2.02E-03	
					373	7.80E-02	
					373	4.64E-09	
					403	5.26E-09	
139	Olhoeft, G.R., 1979 [6]	Same as above			460	1.99E-08	Same as above except measured at 30 MPa.
					531	1.27E-07	
					615	1.06E-06	
					890	5.04E-04	
					1124	9.10E-03	
					1406	0.11	
					1425	2.52	
					1873	26.79	
					273	4.63E-04	
					342	2.36E-03	
					488	1.22E-02	
					663	2.79E-02	
140	Olhoeft, G.R., 1979 [6]	Same as above			665	9.73E-06	Same as above except measured at 100 MPa.
					696	1.45E-05	
					736	2.79E-05	
					898	6.55E-04	
					273	1.10E-04	
					291	1.87E-04	
					393	7.18E-04	
					465	9.48E-04	
					569	1.25E-03	
					667	1.27E-03	
					688	1.12E-03	
					727	6.65E-04	
		752	1.81E-04				

TABLE 4.1. EXPERIMENTAL DATA ON ELECTRICAL CONDUCTIVITY OF BASALT (TEMPERATURE DEPENDENCE) (Continued)

Data Set No.	Author(s), Year [Ref. No.]	Name and Source	Minerals and/or Chemical Composition		Method Used	Experimental Data		Other Specifications
			Weight Percent	Volume Percent		T, K	Electrical Conductivity (g m^{-1})	
140 cont.								
141	Olhoeft, G.R., 1979 [6]	Same as above			Same as above	759 772 887 1212 1245 1282 1319 1379	9.40E-05 1.07E-04 5.90E-04 3.00E-02 6.58E-02 0.111 0.690 1.96	Same as above except measured at 300 MPa.
142	Olhoeft, G.R., 1979 [6]	KI-5 Basalt Kilauea-Iki Lava Lake; Hawaii			Same as above	298 317 326 334 343 357 391 421 500 528 571 618 669	3.64E-02 6.50E-02 8.40E-02 9.57E-02 0.116 0.125 0.223 0.330 0.633 0.820 1.06 0.787 0.331	Density: 2.695 Mg m^{-3} (dry bulk density). Porosity: 14.1%. Other: Sample saturated with a 1.7 M (298 K) NaCl aqueous solution; measured at 1119 Pa.
143	Beck, H., 1980 [7]	KI-5 Basalt; Hawaii			Four Terminal Method	298 323 348 373 398 423 448 471 498 521 544 573 623	1.82E-02 2.78E-02 3.79E-02 4.93E-02 5.98E-02 6.94E-02 7.75E-02 8.40E-02 8.93E-02 9.30E-02 9.52E-02 9.52E-02 9.30E-02	Density: 2.695 Mg m^{-3} (dry bulk density). Porosity: 14.1%. Other: Sample saturated with 0.5% NaCl solution, data taken during heating; estimated error 1%.

TABLE 4.1. EXPERIMENTAL DATA ON ELECTRICAL CONDUCTIVITY OF BASALT (TEMPERATURE DEPENDENCE) (Continued)

Data Set No.	Author(s), Year [Ref. No.]	Name and Source	Minerals and/or Chemical Composition Components	Weight Volume		Method Used	Experimental Data		Other Specifications
				Percent	Percent		T, K	Electrical Conductivity ($\Omega^{-1}m^{-1}$)	
144	Waff, H.S., 1974 [25]	Tholeiitic Basalt 70-15; USA				Two Terminal	1473	3.16	Other: Sample in molten state; measured at 1 atm total pressure.
						Method Assumed	1573	7.94	
							1673	12.56	
							1773	19.95	
145	Saint Amant, M. and Strangway, D.W., 1970 [26]	Solid Basalt M; Cape Neddik, MA	Biotite	16			372	0.230E-07	Sample: Solid, dry. Other: Good repeatability is not observed; data extracted during heating and cooling.
							377	0.274E-07	
							415	0.143E-06	
							441	0.290E-06	
							459	0.745E-06	
							556	0.702E-05	
							610	0.215E-04	
							662	0.366E-04	
							685	0.787E-04	
							741	0.160E-03	
							775	0.202E-03	
							372	0.230E-07	
							377	0.274E-07	
							433	0.107E-06	
							508	0.559E-06	
							606	0.329E-05	
	735	0.368E-04							
	781	0.202E-03							
146	Saint Amant, M. and Strangway, D.W., 1970 [26]	Same as above	Biotite	16			370	0.100E-11	Sample: Powdered, dry. Other: Data extracted during heating and cooling.
							420	0.494E-11	
							469	0.290E-10	
							521	0.113E-09	
							578	0.463E-09	
							420	0.101E-11	
							472	0.113E-10	
							578	0.491E-09	
							373	0.977E-10	
							422	0.381E-09	
147	Saint Amant, M. and Strangway, D.W., 1970 [26]	Powdered Basalt AA; Westfield, MA	Biotite	>16			474	0.117E-08	Same as above.
							571	0.431E-08	
							373	0.111E-10	
							422	0.694E-10	
							472	0.384E-09	
							571	0.431E-08	
							321	1.49 E-03	
							349	1.49 E-03	
							373	1.53 E-03	
							389	1.53 E-03	
148	Alvarez, R., Reynoso, J.P., Alvarez, L.J., and Martinez, M.L., 1978 [27]	Mexican Basalts; Zacatecas, Mexico	SiO ₂ Al ₂ O ₃ MgO CaO Fe ₂ O ₃ FeO Na ₂ O K ₂ O TiO ₂ CO ₂	48.82 13.78 9.11 8.33 8.14 4.78 2.89 1.46 1.44 1.02			407	1.49 E-03	Sample: Powdered to 100 mesh size, dry; dehydrated by heating to 105°C and storing in silica desiccator for few hrs. Other: Data extracted during heating; data corresponds to the polarity during measurement.
							418	1.49 E-03	
							443	1.49 E-03	
							452	1.53 E-03	
							541	1.75 E-03	
							569	1.96 E-03	

TABLE 4.1. EXPERIMENTAL DATA ON ELECTRICAL CONDUCTIVITY OF BASALT (TEMPERATURE DEPENDENCE) (Continued)

Data Set No.	Author(s), Year [Ref. No.]	Name and Source	Minerals and/or Chemical Composition		Method Used	Experimental Data		Other Specifications
			Components	Weight Percent		T, K	Electrical Conductivity ($s\ m^{-1}$)	
148 cont.			P ₂ O ₅	0.50		583	2.05 E-03	
			Cr ₂ O ₃	0.41		616	2.40 E-03	
			MnO	0.14		652	3.45 E-03	
						662	4.14 E-03	
						672	5.68 E-03	
						704	9.15 E-03	
						739	16.51 E-03	
						765	22.15 E-03	
						778	26.57 E-03	
						792	31.84 E-03	
						806	3.905E-02	
						821	5.125E-02	
						870	6.148E-02	
						870	7.044E-02	
						870	7.715E-02	
						905	1.63 E-01	
						943	1.24 E-01	
						985	1.108E-01	
						985	1.013E-01	
					1008	1.013E-01		
					1081	1.059E-01		
					1108	1.214E-01		
					1137	1.329E-01		
					1167	1.456E-01		
					1232	1.558E-01		
					1232	2.091E-01		
					1267	2.508E-01		
					1304	3.369E-01		
					1343	7.447E-01		
					1304	7.971E-01		
					1385	9.342E-01		
					1385	9.776E-01		
					319	3.18 E-03		
					346	3.18 E-03		
					369	3.18 E-03		
					389	3.26 E-03		
					403	3.26 E-03		
					418	3.26 E-03		
					443	3.26 E-03		
					452	3.26 E-03		
					534	3.33 E-03		
					561	3.41 E-03		
					591	3.57 E-03		
					607	3.91 E-03		
					643	4.48 E-03		
					662	5.13 E-03		
					672	6.44 E-03		
149	Alvarez, R., et al., 1978 [27]	Same as above	Same as above					Sample: Same as above. Other: Data extracted during heating; data corresponds to negative polarity during cooling.

TABLE 4.1. EXPERIMENTAL DATA ON ELECTRICAL CONDUCTIVITY OF BASALT (TEMPERATURE DEPENDENCE) (Continued)

Data Set No.	Author(s), Year [Ref. No.]	Name and Source	Minerals and/or Chemical Components	Mineral and/or Chemical Composition		Method Used	Experimental Data		Other Specifications	
				Weight Percent	Volume Percent		T, K	Electrical Conductivity (g m ⁻¹)		
150	Alvarez, R., et al., 1978 [27]	Same as above	Same as above					5.285E-01	Sample: Same as above. Other: Data extracted during cooling; data corresponds to positive polarity during cooling.	
								1191		3.845E-01
								1130		3.064E-01
								1102		2.613E-01
								1049		2.081E-01
								1025		1.775E-01
								959		8.769E-02
								816		7.654E-02
								816		5.318E-02
								747		3.014E-02
								688		1.786E-02
								620		1.270E-02
								579		8.25 E-03
								557		5.60 E-03
								530		5.00 E-03
								506		4.07 E-03
								415		1.76 E-03
				366	1.79 E-03					
				330	1.79 E-03					
				318	1.79 E-03					
151	Alvarez, R., et al., 1978 [27]	Same as above	Same as above					6.72 E-03	Sample: Same as above. Other: Data extracted during cooling; data corresponds to negative polarity during cooling.	
								554		5.35 E-03
								528		3.55 E-03
								504		3.55 E-03
								410		3.47 E-03
								366		3.63 E-03
								330		3.55 E-03
								318		3.55 E-03
								313		1.20 E-03
								317		1.47 E-03
								324		1.80 E-03
152	Hyndman, R.D. and Drury, M.J., 1976 [28]	334-18-2-13-14, DSDP Leg 37; Mid Atlantic Ridge	Two Terminal Method Assumed					2.04 E-03	Sample: Seawater saturated; measurements given in Hyndman (1976) and Hyndman and Drury (1976) in volume 37 of Initial Reports of the Deep Sea Drilling Project. Bulk Density: 1.15% or 2.795 ± 0.082 g cm ⁻³ . Grain Density: 0.50 to -0.25% or 3.024 ± 0.020 g cm ⁻³ . Porosity: 7.8 ± 4.1%. Water Content: 2.7 ± 1.5%. Other: Pressure at 0.1 kbar.	
								328		2.35 E-03
								333		2.71 E-03
								339		2.71 E-03
								342		3.06 E-03
								348		3.60 E-03
								353		4.07 E-03
								358		4.41 E-03
								364		4.98 E-03
								368		5.62 E-03
								373		6.25 E-03
								385		7.63 E-03
								303		8.00 E-04
								308		1.06 E-03
								313		1.41 E-03
								318		1.80 E-03
								328		2.82 E-03
				333	3.46 E-03					
				339	4.24 E-03					
				344	5.00 E-03					
153	Hyndman, R.D. and Drury, M.J., 1976 [28]	335-7-2-37-39, Same as above	Same as above					8.00 E-04	Sample: Same as above except pressure is 1 atm.	
								308		1.06 E-03
								313		1.41 E-03

TABLE 4.1. EXPERIMENTAL DATA ON ELECTRICAL CONDUCTIVITY OF BASALT (TEMPERATURE DEPENDENCE) (Continued)

Data Set No.	Author(s), Year [Ref. No.]	Name and Source	Minerals and/or Chemical Composition		Method Used	Experimental Data		Other Specifications
			Components	Weight Percent		T, K	Electrical Conductivity (s m^{-1})	
153								
cont.								
154	Hyndman, R.D. and Drury, M.J., 1976 [28]	335-9-1-11-13, Same as above			Same as above	348 5.99E-03 353 6.76E-03 357 7.52E-03 364 8.47E-03 369 9.35E-03 373 1.06E-02		Same as above except pressure is 0.35 kbar.
155	Hyndman, R.D. and Drury, M.J., 1976 [28]	332A-25-1-83-86, Same as above			Same as above	303 3.30E-03 308 3.65E-03 313 4.12E-03 318 4.29E-03 323 4.65E-03 328 5.15E-03 333 5.59E-03 339 6.06E-03 342 6.41E-03 348 6.94E-03 353 7.41E-03 357 7.87E-03 364 8.55E-03 373 9.62E-03 379 1.04E-02 385 1.08E-02 392 1.18E-02 398 1.25E-02 403 1.36E-02		Same as above except pressure is 0.1 kbar.
156	Hyndman, R.D. and Drury, M.J., 1976 [28]	332B-10-2-125-128, Same as above			Same as above	303 4.03E-03 308 5.26E-03 313 6.58E-03 318 8.70E-03 323 1.02E-03 327 1.25E-02 332 1.47E-02 339 1.77E-02		Same as above.

TABLE 4.1. EXPERIMENTAL DATA ON ELECTRICAL CONDUCTIVITY OF BASALT (TEMPERATURE DEPENDENCE) (Continued)

Data Set No.	Author(s), Year [Ref. No.]	Name and Source	Minerals and/or Chemical Composition		Method Used	Experimental Data		Other Specifications
			Weight Percent	Volume Percent		T, K	Electrical Conductivity (g m^{-1})	
156 cont.								
157	Hyndman, R. D. and Drury, N. J., 1976 [28]	334-16-2-88-91, Same as above			Same as above			Same as above except pressure at 1 atm.
						342	1.95E-02	
						348	2.30E-02	
						353	2.59E-02	
						358	2.92E-02	
						364	3.24E-02	
						369	3.58E-02	
						303	8.70E-03	
						308	1.18E-02	
						313	1.60E-02	
						317	2.04E-02	
						323	2.40E-02	
						327	2.99E-02	
						332	3.58E-02	
						338	4.13E-02	
						342	4.67E-02	
						347	5.26E-02	
						353	5.71E-02	
						358	6.17E-02	
						361	6.33E-02	
158	Murase, T., 1962 [29]	Glassy Basalt				1654	25.177	Other: Measurements at 1 atm; data were used for comparison in work from Presnall et al., 1972.
						1484	10.116	
						1417	6.855	
						1338	5.047	
						1278	4.351	
						1243	3.940	
						1142	2.564	
						1103	1.983	
						1049	1.386	
159	Murase, T., 1962 [29]	Glassy Basalt				1794	1.957	Same as above.
						1658	1.296	
						1419	0.5411	
						1243	0.2257	
						1154	0.1247	
						1106	0.0781	
						1070	0.0054	
160	Nagata, T., 1937 [30]	Glassy Basalt				1478	23.227	Other: Heating curve.
						1418	12.331	
						1384	8.541	
						1359	8.352	
						1347	8.151	
						1318	7.171	
						1241	4.386	
						1157	2.295	
						1104	1.478	
						1034	0.8386	
						996	0.6162	
						913	0.3009	

TABLE 4.1. EXPERIMENTAL DATA ON ELECTRICAL CONDUCTIVITY OF BASALT (TEMPERATURE DEPENDENCE) (Continued)

Data Set No.	Author(a), Year [Ref. No.]	Name and Source	Minerals and/or Chemical Composition		Method Used		Experimental Data		Other Specifications
			Components	Weight Percent	Volume Percent	T, K	Electrical Conductivity (s m ⁻¹)		
161	Nagata, T., 1937 [30]	Glassy Basalt					1495	18,707	Other: Cooling curve.
							1418	11,092	
							1309	5,354	
							1243	3,447	
							1103	1,259	
162	Volarovich, M.P. and Tolstoi, D.M., 1936 [31]	Glassy Basalt					996	5,111E-01	Other: Cooling curve.
							913	2,563E-01	
							1649	8,204	
							1418	2,004	
							1289	6,866E-01	
163	Coster, H.P., 1948 [32]	Glassy Basalt					1274	6,027E-01	Other: Cooling curve.
							1268	5,875E-01	
							1263	6,206E-01	
							1254	7,107E-01	
							1246	7,713E-01	
							1241	7,930E-01	
							1236	8,155E-01	
							1211	7,570E-01	
							1190	4,130E-02	
							1130	2,094E-02	
							1106	1,656E-02	
164	Coster, H.P., 1948 [32]	Crystalline Basalt					998	6,546E-03	Same as above.
							914	3,289E-03	
							1190	4,130E-02	
							1139	1,734E-02	
							1108	1,081E-02	
							1044	4,677E-03	
							999	2,642E-03	
165	Coster, H.P., 1948 [32]	Same as above					951	1,574E-03	Same as above.
							912	1,014E-03	
							1181	3,097E-03	
							1129	1,371E-03	
							1109	1,057E-03	
166	Parkhomenko, E.I., 1967 [21]	Crystalline Basalt Assumed					1038	4,345E-04	Other: Data were extrapolated to 1 atm from high-pressure data; data were used for comparison in work from Presnall et al., 1972.
							998	2,799E-04	
							951	1,622E-04	
							913	1,104E-04	
							1073	2,944E-03	
167	Lundberg, L.B., 1975 [33]	Dresser Basalt					999	1,429E-03	Other: Cooling curve; rock used for measurements had been crushed and heated at 1823 K for 2.5 hr in air in the platinum crucibles used in the viscometer; resistance between the spindle and the cup was a.c. 1 Kilz.
							913	5,943E-04	
							1831	12,023	
							1644	3,658	
							1538	1,683	

TABLE 4.1. EXPERIMENTAL DATA ON ELECTRICAL CONDUCTIVITY OF BASALT (TEMPERATURE DEPENDENCE) (Continued)

Data Set No.	Author(s), Year [Ref. No.]	Name and Source	Minerals and/or Chemical Composition		Experimental Data		Other Specifications	
			Components	Weight Percent	Volume Percent	Method Used		T, K
167			Na ₂ O	2.54				
			TiO ₂	1.45				
			K ₂ O	0.96				
			H ₂ O	0.38				
			P ₂ O ₅	0.16				
			CO ₂	0.048				
168	Lundberg, L.B., 1975 [33]	Jemez Basalt	SiO ₂	50.01			1861	10.328
			Al ₂ O ₃	16.82			1668	3.478
			CaO	9.62			1527	1.235
			FeO	7.60			1435	0.9568
			MgO	6.70				
			Na ₂ O	3.04				
			Fe ₂ O ₃	2.83				
			TiO ₂	1.38				
			K ₂ O	0.97				
			MnO	0.15				
			H ₂ O	0.14				
			CO ₂	0.02				

Same as above.

The overall picture of the melting process can be seen easily from Figure 4.2. The textural changes from crystalline to glassy and then to the molten state and the effect on electrical conductivity are presented in Figure 4.3. These textural changes received considerable attention of several researchers [16-20, 29-33]. Figure 4.3 shows the various zones corresponding to these textures. It also points out the different behavior that occurs during heating and cooling cycles. Solidus-temperature values for the different basalts reported by these researchers vary and are extended from 1400 K to 1750 K. The fact that the electrical conductivity data start merging near 1500 K indicates larger activation energy upon melting along with probable ionic conduction. These conduction mechanisms are discussed in Section 4.3.3.

4.3.2. Pressure Dependence of Electrical Conductivity of Basalt

Over 50 data sets for basalts from various geographical locations are available in the literature. These data sets are given in Table 4.2 and shown in Figure 4.4. Most of the measurements are assumed to be by the two-terminal method. These studies are carried out in the dry and in the partially and fully saturated conditions.

Figure 4.4 shows regions of distinctly different conductivity for these basalts. The first group of high-pressure measurements is due to the work of Schloessin and Dvorak [38] (data sets 21-35) on basalts in the dry condition from 320 K to 570 K from a mid-Atlantic location. Pressure shows hardly any effect as the conductivity is practically constant for a given temperature. The quantification of this result is elaborated in ref. [38].

The electrical conductivity of fully and partially saturated basalt-water or basalt-sea water systems forms another group of experimental results (see, for instance, data sets 3-19). These measurements were carried out at lower pressures from zero to 300 MPa. The electrical conductivities of these systems are much higher than those for dry basalt. This is mainly due to the presence of interstitial water. It has been observed that as the pressure is increased, the electrical conductivity of basalt-water or basalt-sea water system decreases initially and, at about 50 MPa pressure, it stabilizes to a constant conductivity value. This indicates that ionic conduction through the pore-fluid is the dominant mechanism, with the initial decrease being mainly due to closure of pores and cracks.

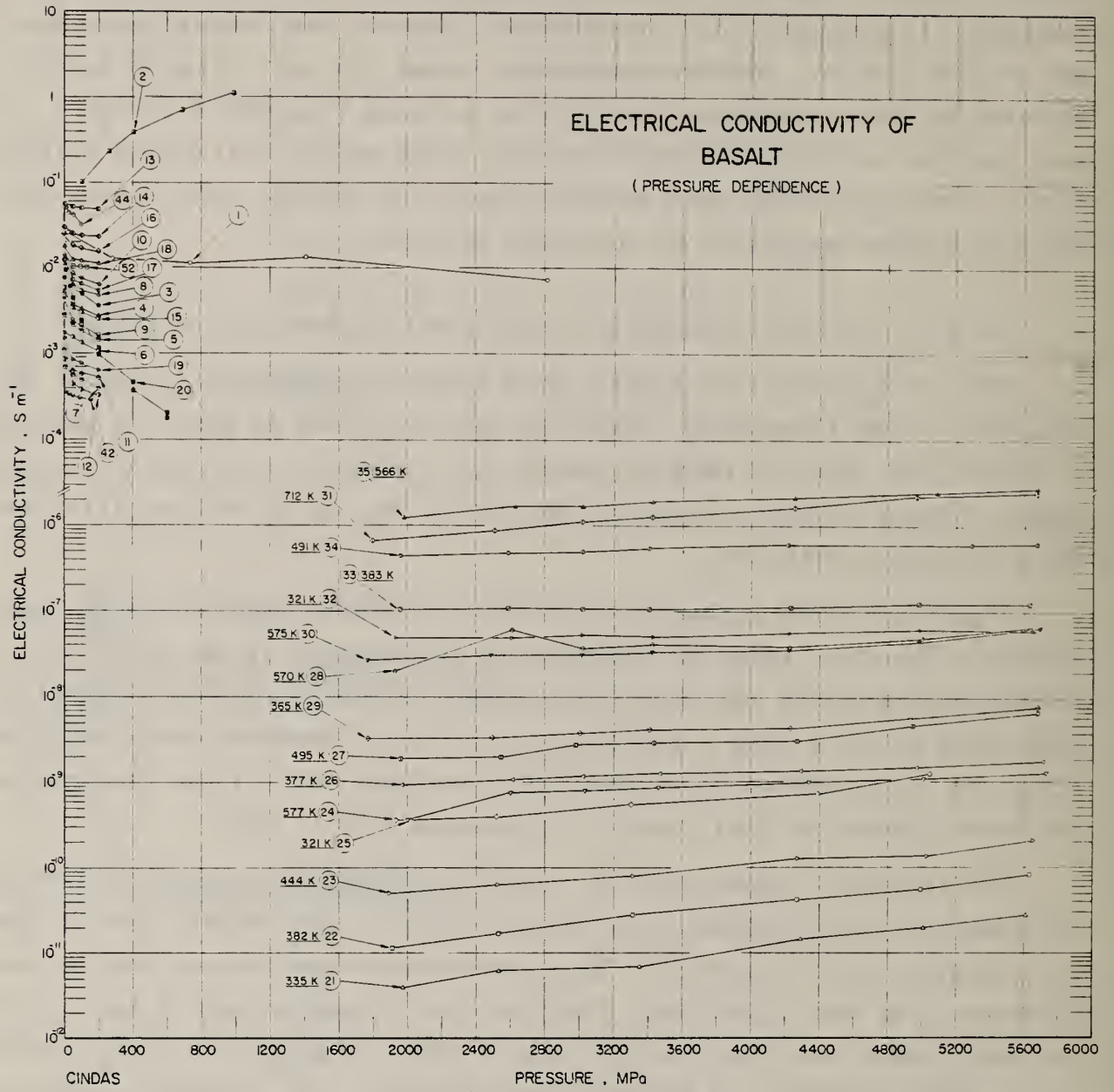


Figure 4.4. Electrical conductivity of basalt (pressure dependence).

TABLE 4.2. EXPERIMENTAL DATA ON ELECTRICAL CONDUCTIVITY OF BASALT (PRESSURE DEPENDENCE)

Data Set No.	Author(s), Year [Ref. No.]	Name and Source	Minerals and/or Chemical Composition		Method Used	Experimental Data		Other Specifications																																																
			Components	Weight Percent		Volume Percent	P, MPa		Electrical Conductivity (g m^{-1})																																															
1	Khitarov, N.I., Lebedev, Ye.B., Slutskim, A.B., Dorfman, A.M., Soldatov, I.A., and Revin, N.I., 1976 [34]	Kirguriich Basalt, Klyucheivka Sopka; Russia	S ₁₀ O ₂ Al ₂ O ₃ MgO CaO FeO Fe ₂ O ₃ Na ₂ O K ₂ O TiO ₂ P ₂ O ₅ MnO H ₂ O ⁺ H ₂ O ⁻	52.05 15.16 9.49 9.29 5.16 4.48 2.46 0.89 0.85 0.13 0.10 0.06 0.03	Two Terminal Method Assumed	20.8 281.6 739.6 1407 2820	0.0261 0.0130 0.0118 0.0133 0.00729	Other: Sample dry melts; measurements at 1673 K.																																																
									2	Khitarov, N.I., et al., 1976 [34]	Same as above	Same as above	Same as above	101 260 404 693 995	0.103 0.233 0.394 0.712 1.109	Other: Sample water saturated melts; measurements at 1673 K.																																								
																	3	Drury, M.J., 1976 [35]	Ocean Basalt, 34-319A-2-1; Nazca Plate in Eastern Pacific	Same as above	Two Terminal Method	0.1 25 50 100 200	0.00787 0.00629 0.00585 0.00508 0.00364	Density: 2.80 Mg m ⁻³ (dry), 2.84 Mg m ⁻³ (saturated). Porosity: 3.75%. Water Content: 1.38 wt.%. Other: Sample sea water saturated; measurements were made at frequency of 10 Hz; measurements at 297 K; author estimated error within 15%.																																
																									4	Drury, M.J., 1976 [35]	Ocean Basalt, 34-321-14-3; Nazca Plate in Eastern Pacific	Same as above	Same as above	0.1 25 50 100 200	0.00524 0.00402 0.00377 0.00340 0.00276	Density: 2.86 Mg m ⁻³ (dry), 2.88 Mg m ⁻³ (saturated). Porosity: 2.30%. Water Content: 0.60 wt.%. Other: Same as above.																								
																																	5	Drury, M.J., 1976 [35]	Ocean Basalt, 34-319A-5-1; Nazca Plate in Eastern Pacific	Same as above	Same as above	0.1 25 50 100 200	0.00287 0.00232 0.00211 0.00186 0.00148	Density: 2.89 Mg m ⁻³ (dry), 2.91 Mg m ⁻³ (saturated). Porosity: 2.40%. Water Content: 0.72 wt.%. Other: Same as above.																
																																									6	Drury, M.J., 1976 [35]	Ocean Basalt, 34-319A-3-4; Nazca Plate in Eastern Pacific	Same as above	Same as above	0.1 25 50 100 200	0.00177 0.00166 0.00156 0.00138 0.00108	Density: Same as above. Porosity: 1.86%. Water Content: 0.51 wt.%. Other: Same as above.								
																																																	7	Drury, M.J., 1976 [35]	Ocean Basalt, 34-319A-7-1; Nazca Plate in Eastern Pacific	Same as above	Same as above	0.1 25 50 100 200	0.00070 0.00061 0.00057 0.00050 0.00039	Density: 2.65 Mg m ⁻³ (dry), 2.67 Mg m ⁻³ (saturated). Porosity: 2.64%. Water Content: 0.82 wt.%. Other: Same as above.

TABLE 4.2. EXPERIMENTAL DATA ON ELECTRICAL CONDUCTIVITY OF BASALT (PRESSURE DEPENDENCE) (Continued)

Data Set No.	Author(s), Year (Ref. No.)	Name and Source	Minerals and/or Chemical Composition		Experimental Data		Method Used	Other Specifications
			Components	Weight Percent	P, MPa	Electrical Conductivity (g m^{-1})		
8	Drury, M.J. and Hyndman, R.D., 1979 [36]	Ocean Basalt, 26-251A-31-2; Indian Ocean			0.1	0.0113	Density: 2.75 Mg m^{-3} (dry), 2.81 Mg m^{-3} (saturated). Porosity: 5.76%. Water Content: 2.07 wt.%. Other: Sample sea water saturated; measurements at 294 K.	
9	Drury, M.J. and Hyndman, R.D., 1979 [36]	Ocean Basalt, 26-251A-31-4; Indian Ocean			0.1	0.00469	Density: 2.89 Mg m^{-3} (dry), 2.93 Mg m^{-3} (saturated). Porosity: 3.51%. Water Content: 1.20 wt.%. Other: Same as above.	
10	Drury, M.J. and Hyndman, R.D., 1979 [36]	Ocean Basalt, 26-254-35-1; Indian Ocean			0.1	0.0142	Density: 2.69 Mg m^{-3} (dry), 2.78 Mg m^{-3} (saturated). Porosity: 8.45%. Water Content: 3.18 wt.%. Other: Same as above.	
11	Drury, M.J. and Hyndman, R.D., 1979 [36]	Ocean Basalt, 26-256-10-3; Indian Ocean			0.1	0.00112	Density: 2.74 Mg m^{-3} (dry), 2.76 Mg m^{-3} (saturated). Porosity: 2.50%. Water Content: 0.73 wt.%. Other: Same as above.	
12	Drury, M.J. and Hyndman, R.D., 1979 [36]	Ocean Basalt, 26-256-11-5; Indian Ocean			0.1	0.000877	Density: 2.92 Mg m^{-3} (dry), 2.94 Mg m^{-3} (saturated). Porosity: 1.71%. Water Content: 0.71 wt.%. Other: Same as above.	
13	Drury, M.J. and Hyndman, R.D., 1979 [36]	Ocean Basalt, 26-257-11-2; Indian Ocean			0.1	0.0575	Density: 2.61 Mg m^{-3} (dry), 2.70 Mg m^{-3} (saturated). Porosity: 9.49%. Water Content: 3.46 wt.%. Other: Same as above.	
14	Drury, M.J. and Hyndman, R.D., 1979 [36]	Ocean Basalt, 26-257-12-2; Indian Ocean			0.1	0.0300	Density: 2.62 Mg m^{-3} (dry), 2.70 Mg m^{-3} (saturated). Porosity: 7.94%. Water Content: 2.82 wt.%. Other: Same as above.	
15	Drury, M.J. and Hyndman, R.D., 1979 [36]	Ocean Basalt, 26-257-13-3; Indian Ocean			0.1	0.00588	Density: 2.68 Mg m^{-3} (dry), 2.72 Mg m^{-3} (saturated). Porosity: 4.27%. Water Content: 1.45 wt.%. Other: Same as above.	
16	Drury, M.J. and Hyndman, R.D., 1979 [36]	Ocean Basalt, 26-257-14-2; Indian Ocean			0.1	0.0258	Density: 2.57 Mg m^{-3} (dry), 2.64 Mg m^{-3} (saturated). Porosity: 7.69%. Water Content: 3.79 wt.%. Other: Same as above.	

TABLE 4.2. EXPERIMENTAL DATA ON ELECTRICAL CONDUCTIVITY OF BASALT (PRESSURE DEPENDENCE) (Continued)

Data Set No.	Author(s), Year [Ref. No.]	Name and Source	Minerals and/or Chemical Composition		Method Used	Experimental Data		Other Specifications
			Weight Percent	Volume Percent		P, MPa	Electrical Conductivity (s m^{-1})	
17	Drury, M.J. and Hyndman, R.D., 1979 [36]	Ocean Basalt, 26-257-17-1, 16; Indian Ocean			Same as above	0.1 25 50 100 200	0.01281 0.00862 0.00740 0.00658 0.00541	Density: 2.81 Mg m^{-3} (dry), 2.85 Mg m^{-3} (saturated). Porosity: 4.21%. Water Content: 1.52 wt.%. Other: Same as above.
18	Drury, M.J. and Hyndman, R.D., 1979 [36]	Ocean Basalt, 26-257-17-1, 100; Indian Ocean			Same as above	0.1 25 50 100 200	0.0182 0.0149 0.0129 0.0123 0.0112	Density: 2.62 Mg m^{-3} (dry), 2.68 Mg m^{-3} (saturated). Porosity: 6.16%. Water Content: 2.31 wt.%. Other: Same as above.
19	Drury, M.J. and Hyndman, R.D., 1979 [36]	Ocean Basalt, 26-257-17-3; Indian Ocean			Same as above	0.1 25 50 100 200	0.00156 0.00102 0.000877 0.000781 0.000641	Density: 2.90 Mg m^{-3} (dry), 2.92 Mg m^{-3} (saturated). Porosity: 2.78%. Water Content: 0.78 wt.%. Other: Same as above.
20	Stesky, R.M. and Brace, W.F., 1973 [37]	Basalt; Indian Ocean Ridge			Two Terminal Method Assumed	10 15 30 50 100 100 200 200 400 400 600 600	0.00964 0.00698 0.00697 0.00453 0.00249 0.00212 0.00117 0.000993 0.000463 0.000374 0.000217 0.000175	Density: 2.79 Mg m^{-3} (dry). Porosity: 2.9-3.9%. Other: Sample saturated with NaCl solution of 0.19 Ωm resistivity; measurement at frequency of 10 Hz and 294 K.
21	Schloessin, H.H. and Dvorak, Z.D., 1977 [38]	Basalt, 332A/07/1/66-69; Mid Atlantic Ridge			Two Terminal Method (DC)	1970 2530 3350 4290 5010 5610	0.393E-11 0.601E-11 0.694E-11 0.148E-10 0.196E-10 0.273E-10	Other: 0.33 cm thick disc sample was thoroughly rinsed and cleaned in water, then washed and dried in acetone; measurements at 335 K.
22	Schloessin, H.H. and Dvorak, Z.D., 1977 [38]	Same as above			Same as above	1910 2530 3310 4270 4990 5630	0.111E-10 0.169E-10 0.271E-10 0.415E-10 0.552E-10 0.805E-10	Same as above except measurements at 382 K.
23	Schloessin, H.H. and Dvorak, Z.D., 1977 [38]	Same as above			Same as above	1890 2520 3310 4270 5030 5650	0.497E-10 0.630E-10 0.799E-10 0.128E-09 0.135E-09 0.206E-09	Same as above except measurements at 444 K.

TABLE 4.2. EXPERIMENTAL DATA ON ELECTRICAL CONDUCTIVITY OF BASALT (PRESSURE DEPENDENCE) (Continued)

Data Set No.	Author (a), Year [Ref. No.]	Name and Source	Minerals and/or Chemical Composition		Method Used	Experimental Data		Other Specifications
			Components	Weight Percent		P, MPa	Electrical Conductivity (g ⁻¹)	
24	Schloessin, H.H. and Dvorak, Z.D., 1977 [38]	Same as above			Same as above	1930 2520 3300 4390 5050	0.358E-09 0.394E-09 0.549E-09 0.730E-09 0.123E-08	Same as above except measurements at 577 K.
25	Schloessin, H.H. and Dvorak, Z.D., 1977 [38]	Basalt, 332A/37/3/54-56; Mid Atlantic Ridge			Same as above	2000 2600 3030 3460 4340 5010 5730	0.352E-09 0.746E-09 0.783E-09 0.861E-09 0.994E-09 0.109E-08 0.126E-08	Same as above except measurements at 321 K.
26	Schloessin, H.H. and Dvorak, Z.D., 1977 [38]	Same as above			Same as above	1970 2610 3020 3470 4290 4970 5710	0.916E-09 0.106E-08 0.116E-08 0.122E-08 0.134E-08 0.148E-08 0.171E-08	Same as above except measurements at 377 K.
27	Schloessin, H.H. and Dvorak, Z.D., 1977 [38]	Same as above			Same as above	1960 2550 2980 3430 4270 4950 5680	0.183E-08 0.192E-08 0.268E-08 0.282E-08 0.297E-08 0.455E-08 0.634E-08	Same as above except measurements at 495 K.
28	Schloessin, H.H. and Dvorak, Z.D., 1977 [38]	Same as above			Same as above	1930 2610 3020 3430 4230 5010 5640	0.199E-07 0.588E-07 0.369E-07 0.407E-07 0.390E-07 0.496E-07 0.660E-07	Same as above except measurements at 570 K.
29	Schloessin, H.H. and Dvorak, Z.D., 1977 [38]	Basalt, 332A/16/1/33-36; Mid Atlantic Ridge			Same as above	1770 2490 3000 3410 4230 4930 5680	0.320E-08 0.322E-08 0.372E-08 0.410E-08 0.412E-08 0.548E-08 0.840E-08	Same as above except measurements at 365 K.
30	Schloessin, H.H. and Dvorak, Z.D., 1977 [38]	Same as above			Same as above	1770 2490 3020 3430 4230 4990 5700	0.264E-07 0.305E-07 0.306E-07 0.337E-07 0.355E-07 0.452E-07 0.661E-07	Same as above except measurements at 575 K.

TABLE 4.2. EXPERIMENTAL DATA ON ELECTRICAL CONDUCTIVITY OF BASALT (PRESSURE DEPENDENCE) (Continued)

Data Set No.	Author(s), Year [Ref. No.]	Name and Source	Minerals and/or Chemical Composition	Weight Percent		Method Used	Experimental Data		Other Specifications
				Volume Percent	Volume Percent		P, Mpa	Electrical Conductivity (s m ⁻¹)	
31	Schloessin, H.H. and Dvorak, Z.D., 1977 [38]	Same as above				Same as above	0.1800	0.659E-06	Same as above except measurements at 712 K.
							0.2510	0.876E-06	
							0.3020	0.111E-05	
							0.3430	0.128E-05	
							0.4260	0.162E-05	
0.4970	0.226E-05								
0.5680	0.249E-05								
32	Schloessin, H.H. and Dvorak, Z.D., 1977 [38]	Basalt, 332B/27/2/93-95; Mid Atlantic Ridge				Same as above	1930	0.486E-07	Same as above except measurements at 321 K.
							2610	0.488E-07	
							3020	0.537E-07	
							3430	0.514E-07	
							4230	0.568E-07	
4990	0.627E-07								
5660	0.601E-07								
33	Schloessin, H.H. and Dvorak, Z.D., 1977 [38]	Same as above				Same as above	1960	0.101E-06	Same as above except measurements at 383 K.
							2590	0.106E-06	
							3020	0.106E-06	
							3410	0.106E-06	
							4240	0.112E-06	
4990	0.123E-06								
5640	0.123E-06								
34	Schloessin, H.H. and Dvorak, Z.D., 1977 [38]	Same as above				Same as above	0.1960	0.432E-06	Same as above except measurements at 491 K.
							0.2590	0.476E-06	
							0.3020	0.500E-06	
							0.3410	0.524E-06	
							0.4220	0.551E-06	
0.5030	0.607E-06								
0.5680	0.638E-06								
35	Schloessin, H.H. and Dvorak, Z.D., 1977 [38]	Same as above				Same as above	1980	0.122E-05	Same as above except measurements at 566 K.
							2630	0.169E-05	
							3020	0.170E-05	
							3430	0.195E-05	
							4260	0.215E-05	
5090	0.249E-05								
5680	0.287E-05								
36	Hyndman, R.D. and Drury, N.J., 1976 [39]	314-16-2, 88-99, DSDP Leg 37; Mid Atlantic Ridge				Two Terminal Method Assumed	2.75	8.77 E-03	Sample: Seawater saturated, measurements given in Hyndman (1976) and Hyndman and Drury (1976) in volume 37 of Initial Reports of the Deep Sea Drilling Project. Bulk Density: 1.15 ± 0.082 g cm ⁻³ . Grain Density: 0.50 to -0.25% or 3.024 ± 0.020 g cm ⁻³ . Porosity: $7.8 \pm 4.1\%$. Water Content: $2.7 \pm 1.5\%$. Other: Measurements at 300 K.
							11.0	6.94 E-03	
							24.7	5.35 E-03	
							50.8	4.44 E-03	
							100	3.72 E-03	
151	3.44 E-03								
200	3.36 E-03								

TABLE 4.2. EXPERIMENTAL DATA ON ELECTRICAL CONDUCTIVITY OF BASALT (PRESSURE DEPENDENCE) (Continued)

Data Set No.	Author(s), Year [Ref. No.]	Name and Source	Minerals and/or Chemical Composition		Experimental Data		Other Specifications	
			Components	Weight Percent	Method Used	Electrical Conductivity (g cm^{-1})		
37	Hyndman, R.D. and Drury, N.J., 1976 [39]	332B-10-2, 125-128, Same as above			Same as above	1.41	6.58E-03	Same as above.
						11.0	5.35E-03	
						26.1	3.91E-03	
38	Hyndman, R.D. and Drury, M.J., 1976 [39]	332A-28-2, 83-86, Same as above			Same as above	1.45	4.12E-03	Same as above.
						11.1	2.85E-03	
						24.8	2.70E-03	
						50.8	2.57E-03	
						98.8	2.38E-03	
39	Hyndman, R.D. and Drury, M.J., 1976 [39]	335-7-2, 37-39, Same as above			Same as above	0.161	1.60E-03	Same as above.
						11.2	1.05E-03	
						26.2	1.03E-03	
						49.5	9.52E-04	
						98.9	7.75E-04	
40	Hyndman, R.D. and Drury, M.J., 1976 [39]	335-9-1, 11-13, Same as above			Same as above	0.195	1.08E-03	Same as above.
						11.2	7.52E-04	
						24.9	6.76E-04	
						50.9	6.58E-04	
						100	5.95E-04	
41	Hyndman, R.D. and Drury, M.J., 1976 [39]	334-23-1, 76-78, Same as above			Same as above	0.205	7.71E-04	Same as above
						8.46	6.76E-04	
						24.9	6.41E-04	
						50.9	6.25E-04	
						100	5.49E-04	
42	Hyndman, R.D. and Drury, M.J., 1976 [39]	334-23-1, 76-78, Same as above			Same as above	0.255	5.46E-04	Same as above.
						0.267	4.81E-04	
						11.3	3.51E-04	
						25.0	3.33E-04	
						51.0	3.25E-04	
43	Chrosten, P.N., Evans, C.J., and Lee, C., 1979 [40]	DSDP Leg 49, 408-38-2			Two Terminal Method Assumed	5.587	0.07174	Sample: Sea water saturated. Density: 2.44 g cm^{-3} .
						11.71	0.06798	
						25.38	0.06729	
						49.44	0.06658	
						199	2.72E-04	

TABLE 4.2. EXPERIMENTAL DATA ON ELECTRICAL CONDUCTIVITY OF BASALT (PRESSURE DEPENDENCE) (Continued)

Data Set No.	Author(s), Year [Ref. No.]	Name and Source	Minerals and/or Chemical Composition		Method Used	Experimental Data		Other Specifications
			Weight Percent	Volume Percent		P, MPa	Electrical Conductivity (S m ⁻¹)	
44	Chrosten, P.N., et al., 1979 [40]	DSDP Leg 49, 407-46-2			Same as above	1.812	0.07112	Sample: Sea water saturated. Density: 2.67 g cm ⁻³ .
						5.532	0.05583	
						10.70	0.05013	
						25.30	0.04496	
45	Chrosten, P.N., et al., 1979 [40]	DSDP Leg 49, 408-37-1			Same as above	49.34	0.04177	Sample: Sea water saturated. Density: 2.59 g cm ⁻³ .
						74.80	0.04023	
						99.33	0.03178	
						5.964	0.04666	
46	Chrosten, P.N., et al., 1979 [40]	DSDP Leg 49, 309-9-3			Same as above	10.68	0.04541	Sample: Sea water saturated. Density: 2.77 g cm ⁻³ .
						25.31	0.04744	
						49.38	0.05086	
						73.92	0.05311	
47	Chrosten, P.N., et al., 1979 [40]	DSDP Leg 49, 408-36-1			Same as above	99.39	0.05348	Sample: Sea water saturated. Density: 2.63 g cm ⁻³ .
						123.9	0.05336	
						148.0	0.05325	
						2.092	0.02983	
48	Chrosten, P.N., et al., 1979 [40]	DSDP Leg 49, 307-38-3			Same as above	6.290	0.02405	Sample: Sea water saturated. Density: 2.91 g cm ⁻³ .
						10.52	0.02378	
						25.60	0.02081	
						50.12	0.01986	
49	Chrosten, P.N., et al., 1979 [40]	DSDP Leg 49, 307-39-2			Same as above	74.64	0.01964	Sample: Sea water saturated. Density: 2.83 g cm ⁻³ .
						100.1	0.01874	
						124.2	0.01821	
						147.7	0.01722	
49	Chrosten, P.N., et al., 1979 [40]	DSDP Leg 49, 307-39-2			Same as above	10.95	0.01888	Sample: Sea water saturated. Density: 2.63 g cm ⁻³ .
						26.03	0.01755	
						50.55	0.01690	
						75.55	0.01656	
49	Chrosten, P.N., et al., 1979 [40]	DSDP Leg 49, 307-39-2			Same as above	100.5	0.01639	Sample: Sea water saturated. Density: 2.63 g cm ⁻³ .
						125.1	0.01621	
						149.1	0.01589	
						2.937	0.01906	
49	Chrosten, P.N., et al., 1979 [40]	DSDP Leg 49, 307-39-2			Same as above	7.644	0.01821	Sample: Sea water saturated. Density: 2.83 g cm ⁻³ .
						11.40	0.01695	
						21.20	0.01053	
						26.82	8.569	
49	Chrosten, P.N., et al., 1979 [40]	DSDP Leg 49, 307-39-2			Same as above	50.48	0.01235	Sample: Sea water saturated. Density: 2.83 g cm ⁻³ .
						75.55	0.01702	
						99.64	0.01960	
						123.7	0.02083	
49	Chrosten, P.N., et al., 1979 [40]	DSDP Leg 49, 307-39-2			Same as above	149.2	0.02135	Sample: Sea water saturated. Density: 2.83 g cm ⁻³ .
						6.649	0.01443	
						11.82	0.01307	
						25.95	0.01215	
49	Chrosten, P.N., et al., 1979 [40]	DSDP Leg 49, 307-39-2			Same as above	50.48	0.01213	Sample: Sea water saturated. Density: 2.83 g cm ⁻³ .
						75.01	0.01211	
						100.0	0.01208	

TABLE 4.2. EXPERIMENTAL DATA ON ELECTRICAL CONDUCTIVITY OF BASALT (PRESSURE DEPENDENCE) (Continued)

Data Set No.	Author(s), Year [Ref. No.]	Name and Source	Minerals and/or Chemical Composition		Method Used	Experimental Data		Other Specifications
			Weight Percent	Volume Percent		P, MPa	Electrical Conductivity (g cm^{-1})	
49 cont.						124.5 148.6	0.01206 0.01193	
50	Chrosten, P.N., et al., 1979 [40]	DSDP Leg 49, 312A-3-2			Same as above	3.033 5.842 11.01 24.67 50.60 75.12 100.1 123.7 147.3	0.01605 0.01391 0.01238 0.01044 9.625 9.268 8.937 8.540 8.006	Sample: Sea water saturated. Density: 2.98 g cm^{-3} .
51	Chrosten, P.N., et al., 1979 [40]	DSDP Leg 49, 407-42-1			Same as above	11.89 25.57 50.56 75.56 149.1	7.782 8.058 7.299 7.418 7.194	Sample: Sea water saturated. Density: 2.90 g cm^{-3} .
52	Chrosten, P.N., et al., 1979 [40]	DSDP Leg 49, 407-36-3			Same as above	11.04 26.56 51.08 75.61 99.66 124.7	0.01493 0.01073 0.01024 0.01032 0.01022 0.01020	Sample: Sea water saturated. Density: 2.86 g cm^{-3} .

Khitarov et al. [34] have reported pressure dependence of the electrical conductivity of molten basalts from USSR (data sets 1 and 2). The data set for the dry basalt melt (data set 1) illustrates that the electrical conductivity is independent of pressure. However, for the melt of a basalt-sea water system (data set 2), an increase in conductivity due to pressure is observed, suggesting the presence of a salt in the system. Further investigations are needed to confirm this finding.

4.3.3. Other Dependencies of Electrical Conductivity of Basalt

Factors which affect the electrical conductivity other than temperature and pressure are porosity and density. Drury [35] and Drury and Hyndman [86] have attempted the evaluation of basalt-water or basalt-sea water system based on mixing laws and have established correlations for electrical conductivity with either porosity or density under ambient conditions. Figure 4.5 illustrates the ambient electrical conductivity as a function of sample density for basalts from various geographical locations. This figure shows very wide variations, which are not considered anomalous. It is important to note that all available data in the density range considered in Figure 4.5 are not plotted because of some very large variations in the data. This also highlights the difficulties encountered in validating or verifying rock-water/rock-sea water mixing laws.

In limited, individual cases the empirical mixing laws can be established and a verification of the generalized Archie's law [45] can be carried out as has been done by Drury [35], Olhoeft [6], and others [36-40]. It is also observed that such an examination is successful for saturated basalt-fluid systems, while partial saturation cases are not yet fully understood. Further, it is noted that the presence of only a few percent of water drastically changes electrical properties of basalt and modifies the temperature dependence significantly, implying that pore-fluid conduction dominates. Figure 4.6 shows schematically the conduction through a pore-water and basalt matrix material. Chemical reactions neglecting pore-water conduction are shown to be dominant. In most cases neglecting chemical reaction is a fair assumption, albeit not a complete one. It turns out that a limiting temperature for this assumption exists which is controlled by variables such as salt concentration, pore morphology, and hydrostatic pressure in the basalt-salt solution system.

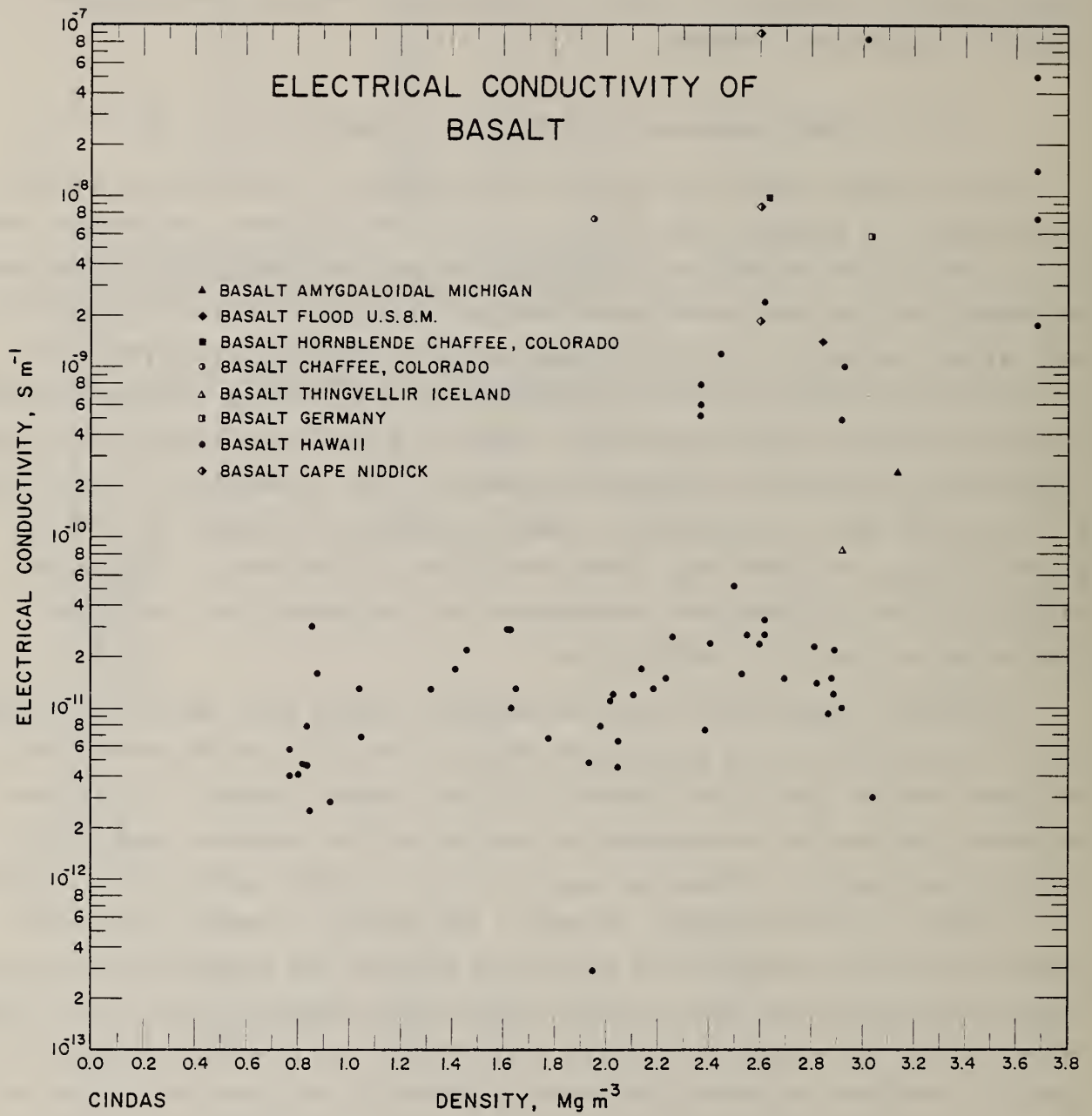


Figure 4.5. Electrical conductivity of basalt as a function of density.

Basalt-salt solution mixtures are studied by Olhoeft [6], UcoK [7], and Drury [46]. Electrical resistivity data on salt solutions and basalt-solution saturated systems are presented in these studies. The data of Olhoeft [6] for electrical resistivity of 1 wt.% NaCl solution versus the solution-saturated KI-5 Hawaiian basalt resistivity, measured at various temperatures under a pressure of 30 MPa and frequency of 10^3 Hz, are shown in Figure 4.7. The data points will follow a straight line of unit slope indicating an agreement with Archie's law if the electrical resistivity of basalt-salt solution systems follow the resistivity of a typical salt solution. Below 353 K the pore-volume conduction dominates, while above 353 K the conduction mechanism along the surface of the pore walls becomes an important and dominant factor. A detailed discussion on electrical conductivity of the rock-sea water saturated system can be found in UcoK [7] and Drury [46]. It has been confirmed experimentally that for a shale and clay-free basalt-salt solution system, Archie's law can predict electrical conductivity provided the brine concentration is high enough to minimize the surface condition along pore walls.

Changes due to frequency cause additional effects on the electrical conductivity. Such effects are mainly due to the presence of moisture or due to the presence of clay-like or oxide materials. Structure and basalt-water chemical reaction are other causes of frequency dependence. Oxides and clay minerals are also considered to be responsible for large frequency dependence. For these reasons, the data available for frequency effects are not considered in this study.

4.3.4. Conduction Mechanisms and Activation Energy

Electrical conductivity in rock specimens can be described by

$$\sigma = \sum_i \sigma_i \quad (1)$$

where σ_i are contributions to the electrical conductivity due to different processes and is given by the Arrhenius relation

$$\sigma_i = \sigma_{oi} \exp(E_i/kT) \quad (2)$$

where E_i is the activation energy, T is temperature, k is Boltzmann constant, and σ_{oi} is carrier density. Thus, the total conductivity may be written as:

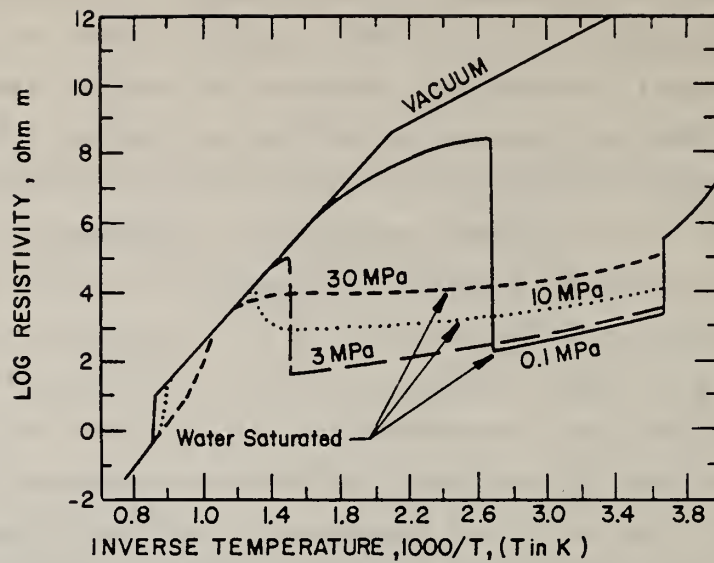


Fig. 4.6. Variation of the electrical resistivity of basalt as a function of temperature and comparison of the effect of pressure on water saturated rock water systems.

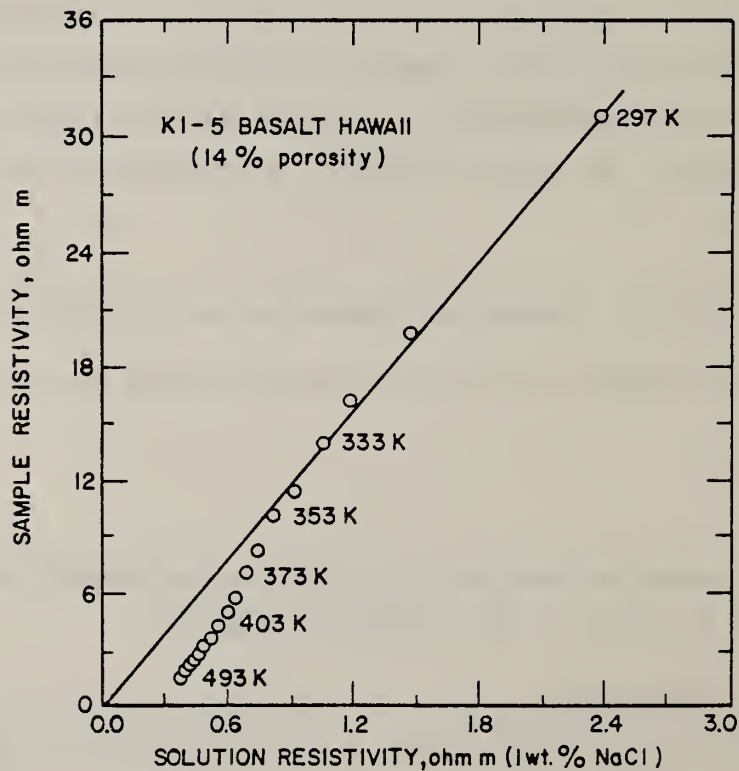


Fig. 4.7. Cross-plot of independently measured electrical resistivity of 1 wt.% NaCl solution-saturated K1-5 basalt resistivity as a function of temperature under 30 MPa hydrostatic pressure at a frequency of measurement of 10^3 Hz.

$$\sigma = \sum_i \sigma_{oi} \exp(E_i/kT) \quad (3)$$

The Arrhenius plots shown in Figures 4.2 and 4.3 allow the determination of the activation energies of the conduction process at various temperature intervals. Table 4.3 summarizes the temperature ranges and corresponding activation energies observed in these figures. Conduction mechanisms which have been identified from time to time as being significant are also given in Table 4.3. A note of caution was introduced by Shankland [47] who pointed out that the comparison of activation energies in a given temperature region could not be made reliably because of its dependence on oxygen fugacity, f_{O_2} . Thus, there is a need for identification of both the carrier species and charge state along with carrier concentration and mobility in order to completely identify the conduction mechanism.

Duba and Nichols [48] and Duba and Ito [49] have shown that the electrical conductivity of olivine melt varies over several decades due to changes in Fe^{2+}/Fe^{3+} and total Fe content. Waff and Weill [50] observed the effects of oxygen fugacity (10^{-7} to $10^{-0.7}$ atmosphere at 1675 K), temperature, and chemical composition on electrical conduction in rock melts and attributed the decrease in the electrical conductivity at relatively high f_{O_2} ($>10^{-3}$ atmosphere) to the high Fe content in the tholeiitic and alkali basalts which they studied.

Rai and Manghnani [20] studied several basalts from Hawaii under known oxygen fugacities of 10^{-6} to 10^{-23} atmosphere which they considered as the stability region for basalt according to the calculations of Nitson [51] and Deinese et al. [52]. They concluded that below 1200 K the alkalic basalts are the most conductive and the naphthalnic basalts are the least. The conductivity values jump 1 to 1 1/2 times during melting over the temperature range of 1200 K to 1475 K. The conduction after melting is ionic in nature for basalt tested in the f_{O_2} stability range. It turns out that stability is controlled by silica, alkali, and femic content. The silica increases the conductivity, whereas the other two tend to decrease the conductivity. Waff and Weill [50] concluded that ionic conduction is Arrhenius type for alkalic basalt but of non-Arrhenius type for tholeiitic and naphthalnic basalts [20] due to polymerization of melts. Furthermore, Rai and Manghnani [20] and Waff and

Table 4.3. Conduction Mechanism and Activation Energies

Author(s), Year, [Ref. No.]	Temperature Range	Activation Energy	Probable Conduction Mechanism	Remarks
CINDAS conclusions	$T \leq 575$ K	0.0 eV to 0.9 eV	Conduction probably by the impurities located near the conduction band.	Cooling values are generally lower than heating values; near 833 K higher conduction is realized possibly due to greater available charge concentration.
	575 K $\leq T < 833$ K	0.9 eV to 1.5 eV	-	-
	833 K $\leq T \leq 1200$ K	1.2 eV to 1.8 eV	Electronic conduction (but as T approaches 1200 K the cations may be also active in partially molten sample).	Crystalline samples; values taken during heating; higher activation energies (1.8 eV) are observed; values during cooling correspond to those for glassy texture resulting in lower values of slope to yield activation energies of 0.8 eV to 1.2 eV; cooling values are time dependent due to devitrification of glass.
Alvarez et al., 1978 [27]	1200 K $\leq T \leq 1475$ K	-	-	The negative slope in Arrhenius plot for majority of data sets indicating melting; if positive slopes for higher heating rates, conductivity values increase by order of magnitude.
	$T \geq 1475$ K	1.65 eV to 3.96 eV predominantly in the neighborhood of 3.00 eV at 1500 K	Ionic conduction (univalent and divalent cations also take part in conduction).	Oxygen fugacity in the stability region of 10^{-6} to $10^{-2.5}$ atmosphere; increase in oxygen fugacity (in stability region) has decreasing effect on electrical conductivity and the decrement is a function of $\Sigma m^{2+}/\Sigma m^{+}$ ratio; conduction is controlled by silica, alkalic, and femic content; cooling values are time dependent due to polymerization.
	$T \leq 575$ K	0.00 eV to 0.002 eV	Conduction by shallow traps or impurities located very close to conduction band	-
Waff and Weill, 1975 [50]	575 K $\leq T \leq 875$ K	0.72 eV to 1.7 eV	-	-
	$T \geq 875$ K	3.08 eV to 3.96 eV	Ionic (probably)	Negative slopes, indicating possible melting at temperatures as low as 875-975 K; cooling values higher than heating values in this temperature region.
	1450 K $< T < 1750$ K	3.00 eV	Ionic	Conduction process is affected by oxygen fugacity, silica, alkalic, and femic content.
Presnell et al., 1972 [17]	$T < 1323$ K	0.72 eV	-	Glassy texture during cooling.
	$T < 1323$ K	1.06 eV	-	Crystalline texture during heating.
	$T \geq 1323$ K	1.46 eV	Ionic (probably)	Test during melting; during melting conductivity jumped two-fold.
Schult and Schober, 1969 [61]	525 K $< T < 875$ K	≈ 0.9 eV	Electronic	-
	875 K $< T < 1225$ K	≈ 1.9 eV	Ionic	-
Khitarov and Slutskiy, 1965 [62]	875 K $< T < 1373$ K	≈ 1 eV	-	-
	1373 K $\leq T \leq 1573$ K	≈ 3 eV	Ionic (probable)	-

Table 4.3. Conduction Mechanism and Activation Energies (continued)

Author(s), Year, [Ref. No.]	Temperature Range	Activation Energy	Probable Conduction Mechanism	Remarks
Runcorn and Tozer, 1955 [60]	T \leq 875 K 875 K < T < 1375 K T < 1375 K	- - -	Controlled by Impurities Intrinsic semiconduction Ionic	-
Coster, 1948 [32]	T < 975 K T > 975 K	- -	Electronic Ionic	-
Nagata, 1937 [30]	T < 1100 K T > 1100 K	-	Electronic Ionic	Negative slope during melting was observed on Arrhenius plot.
Valarovich and Tolstol, 1936 [31]	T < 1275 K T > 1275 K	- -	Electronic Ionic	Negative slope during melting was observed on Arrhenius plot.

Weill [50] pointed out that cooling values are time dependent because of devitrification of glassy components.

Alvarez et al. [27] studied basalts from the Mexican volcanic belt and obtained different activation energies for heating and for cooling cycle in three temperature regions. They interpreted the data suggesting that conduction below 575 K was dominated by shallow impurity traps (i.e., impurities located near conduction band) having such a low concentration that it was immaterial whether the sample was powdered or solid. The change in mechanism above 575 K occurred and conductivity increased more rapidly, probably due to much greater concentrations of available charge carriers (i.e., $\sigma_{0_2} \gg \sigma_{0_1}$) and the corresponding change in activation energy was from 0.7 to 1.7 eV. Conductivity dropped above 875 K for an interval of about 100 degrees. New activation energy was defined for the remainder of the heating interval, ranging from 0.8 to 3.1 eV which was indicative of melting. Alvarez et al. [27] attributed this to the destruction of intergranular contacts and melting in isolated portions. Conductivity values during cooling-interval can be higher or lower than corresponding heating-interval values. These are determined by E_i and σ_{oi} in the preceding interval. Higher activation energies for the heating yield lower conductivity values in spite of the availability of greater carrier concentration or mobility (e.g., $\sigma_{o_{heating}} \gg \sigma_{o_{cooling}}$ for temperatures $> 600^\circ\text{C}$ as observed by Alvarez et al. [27]).

For crystalline basalts, $\ln \sigma$ versus $10^3/T$ behavior below 875 K is initially linear and then it stabilizes to a constant value. This linearity shows an anomaly in a few instances. The possible association of this anomaly with the Curie temperature of ferrimagnetic minerals in their sample was pointed out in [53,54]. Further, Lastovickova and Kropacek [22] studied the temperature and the Curie temperature dependence of saturation magnetization and electrical conductivity. This was examined for magnetite and haemetite to limit the influence of non-ferrimagnetic petrogenetic minerals in basalt (olivine, pyroxenes). They concluded that the electrical conductivity of their basalt was anomalous near the Curie temperature, which was distributed over temperature range. These data sets are not plotted since Figure 4.2 contains data for basalts from American subcontinent, Hawaii, and mid-Atlantic regions only.

The electrical conductivity of partially molten rocks was studied by Shankland and Waff [55] and Waff [56] because of the anomalously high

conductivity values associated with tectonic regions. Partial melting was one of the reasons proposed for such a high level of conductivity. Shankland and Waff [55] analyzed this empirically by modeling the earth's mantle using effective medium theory which considers a basalt-melt fraction within a largely olivine matrix. The effects of pressure, water content, and melt fraction were also discussed in their investigations. Waff [56] used the Hashin-Shtrikman model [57] to establish the bounds based on the consideration of the entropy production and subsequently compared them with his results from geometrical models. The geometrical models gave upper bounds, but the effects of premelting and liquid-path connectivities were similar and were found to be a determining factor for estimating the effective conductivity values.

The data for pressure dependence of electrical conductivity (Table 4.2) have also revealed that the conductivity values for a rock-sea water saturated system decrease rapidly to pressures up to 50 MPa (see, for instance, Drury [35]). Beyond that region the electrical conductivity is essentially insensitive to pressure. The initial decrease is attributed to the closing of microcracks, which were introduced into the sample during drilling. This was not observed for high porosity samples indicating that high vesicular type of porosity dominates over the closure of cracks as shown by Drury [35] and Hyndman and Drury [39]. Lastly, it is noted that the pressure effects on electrical conductivity of dry basalts are very small in magnitude and warrant no further comments.

For the saturated rock system, the conduction is dominant through fluid filled pores, which is explained traditionally by Archie's law

$$\rho_s = A\rho_f\eta^m \quad (4)$$

where ρ_s and ρ_f are rock-fluid system and fluid resistivities, respectively, η is porosity of rock, and A and m are constants. A is frequently taken as unity. If conduction is predominantly through fluid filled pores and cracks, the value of m is unity. According to Brace et al. [58] and Brace and Orange [59], $m = 2$ for randomly connected pore-paths. Most of the rocks exhibit m values in the range of 1 to 2.

In general, three conduction mechanisms are suggested for a rock-fluid system. The first and the dominating one is the pore-fluid conduction, the

second is thermally activated conduction as in salt and clays, and the third is conduction through mineral grains. Although the pore-fluid conduction is the principal conduction, the modification of it takes over in many cases when clay and salt are present in the system. When temperatures above 875 K are considered, the mineral conduction usually dominates.

The conduction through clay or salt is very similar. The role of conduction through salt is decided by brine concentration. Usually, when such conduction is present, it is observed that minerals in clay have strong cation exchange properties and double layers are formed along grain surfaces when they are immersed in an electrolyte solution. These layers consist of a fixed layer of ions of electric charge which are balanced by ions of opposite charge in the mobile layer. Ions on both clay surface and the mobile layer can be exchanged with ions in the electrolyte. Ions entering electrolyte generally have greater mobility in electrolyte than the ions that they have replaced and, thus, create decrease in resistivity.

Temperature dependence of activated conduction has similar form as mineral conduction. Hence, the effective conductivity of saturated rock in which pore spaces are lined with clay or salt may show a thermally activated surface conduction as the predominant mechanism.

However, if clay and salt fill the pores and cracks, the bulk conductivity may decrease particularly at low temperature, because clay acts as a membrane to ion passage. Thus, the overall effect of clay content and salt content is very complicated. A more detailed discussion on these issues is available in the literature, for example, Ucock [7] and Drury [46].

4.3.5. Summary

Electrical conductivity of basalt has been studied to date in great detail. The electrical conductivity at room temperature in dry or air dry state is known. The temperature dependence of basalt has received fairly good attention. The temperature dependence also received attention in the presence of oxygen, water, and salt solutions of different concentrations. The basalt-water system is fairly known, but partial saturation cases are not thoroughly investigated. The pressure dependence is found less important for dry basalts and in the case of wet basalts the changes were only due to crack closures in

basalt. The conduction mechanism discussion in the literature is surveyed for completeness, which shows a gap of knowledge for electrical conductivity of basalts containing altered minerals, zeolites, and organic liquids (e.g., humic acid).

4.4. DIELECTRIC PROPERTIES OF BASALT

4.4.1. Relative Dielectric Constant of Basalt

The dielectric properties are studied on the block and powdered samples in dry as well as partially and fully saturated conditions. The information on the chemical composition or mineralogical characterization of samples is extracted wherever possible, but no attempt is made to correlate the property with mineralogical composition.

Overall, about 140 data sets have been compiled covering frequencies from 10^2 Hz to 10^8 Hz and are presented in Table 4.4. Selected data sets which show typical behavior are shown in Figure 4.8.

In general, room temperature relative dielectric constant of basalt remains fairly constant over frequencies from 10^3 Hz to 10^7 Hz (data sets 1-62, 126, 127, 135-138, 146). Most of the data are for measurements on dry basalts from various geographical locations. The factors affecting the relative dielectric constant (between 10^3 - 10^7 Hz) are temperature, biotite content, and water content (or moisture content). It is also observed that the variations in the relative dielectric constant are larger at lower frequencies.

The temperature dependence of the relative dielectric constant was studied by Chung et al. [23] (data sets 65-94), Saint Amant and Strangway [26] (data sets 95-115), and Griffin and Marovelli [44] (data sets 146,147). The basalts covered in these studies are lunar, from Cape Neddik and Westfield (Massachusetts) and from Minnesota. These data for both powdered and block samples show an increase in relative dielectric constant with temperature over frequency range 10^3 Hz to 10^6 Hz. This behavior was attributed to polarization associated with charge build-up at grain boundaries and grain imperfections.

The comparison of the data for block and powdered samples of different grain size is often found in the literature, for example, by Saint Amant and Strangway [26] and Ryu et al. [15]. A difference of the order of magnitude one

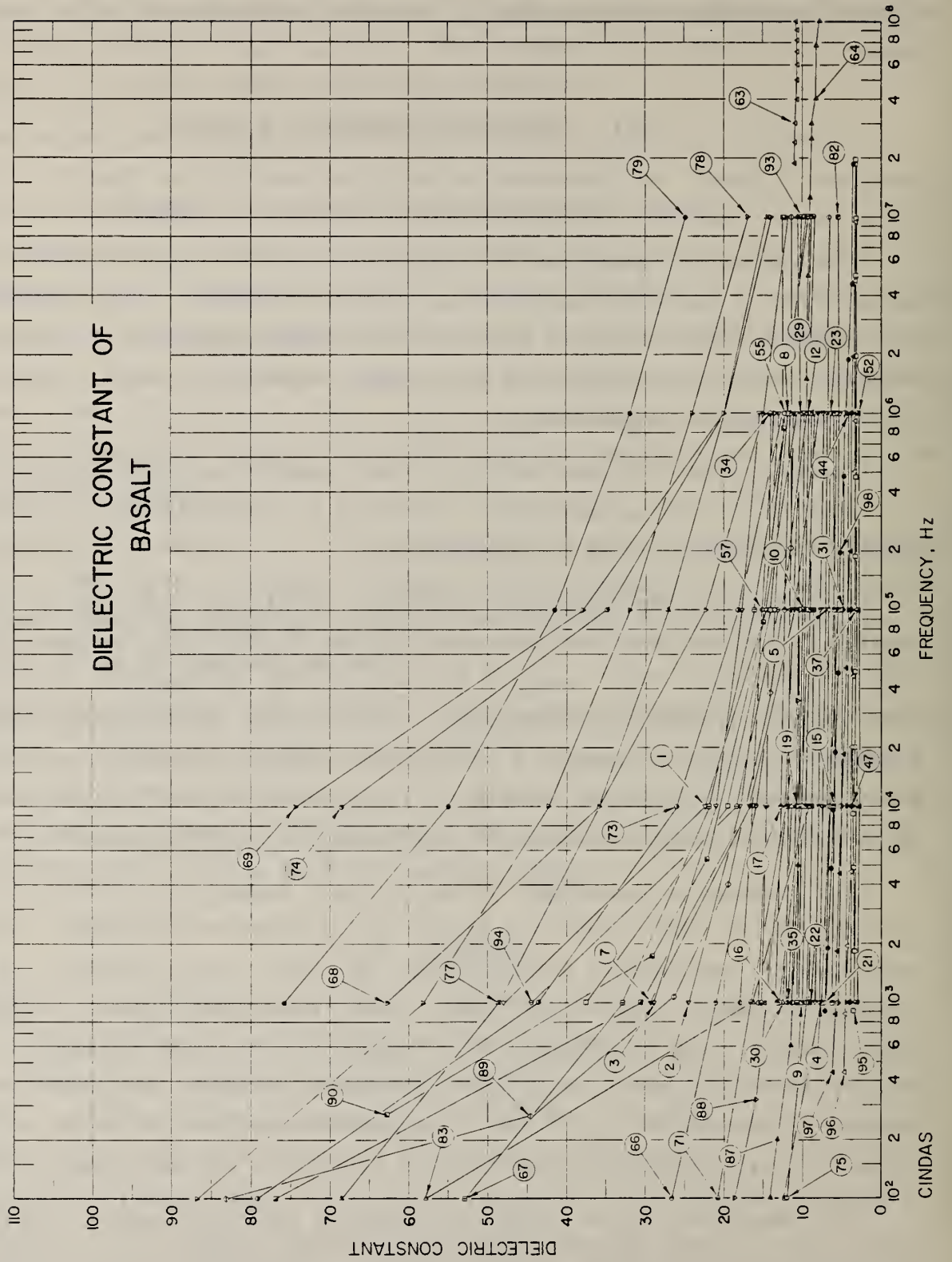


Figure 4.8. Dielectric constant of basalt.

TABLE 4.4. EXPERIMENTAL DATA ON DIELECTRIC CONSTANT OF BASALT (FREQUENCY DEPENDENCE)

Data Set No.	Author(s), Year [Ref. No.]	Name and Source	Minerals and/or Chemical Composition		Method Used		Experimental Data		Other Specifications
			Components	Weight Percent	Volume Percent	Frequency, V, Hz	Dielectric Constant ϵ'		
1	Olhoeft, C.R., 1979 [6]	Basalt Hornblende (7.5); Chaffee, CO			Capacitance Meter	1.0E+03 1.0E+04 1.0E+05 1.0E+06	48.1 22.4 14.6 10.8	Density: 2.635 Mg m ⁻³ (dry). Remarks: Measurement was performed by using a three-terminal sample holder in 8% relative humidity; estimated error $\pm 1\%$; T=293 K.	
2	Olhoeft, G.R., 1979 [6]	Basalt Amygdaloidal (Z46.6); Michigan			Same as above	1.0E+03 1.0E+04 1.0E+05 1.0E+06	24.5 17.9 14.7 13.1	Density: 3.134 Mg m ⁻³ (dry). Remarks: Same as above.	
3	Olhoeft, G.R., 1979 [6]	Basalt Ilcoc (58.5); USBM			Same as above	1.0E+03 1.0E+04 1.0E+05 1.0E+06	29.0 21.1 17.7 15.5	Density: 2.843 Mg m ⁻³ (dry). Remarks: Same as above.	
4	Olhoeft, G.R., 1979 [6]	Basalt (166.6A); Hawaii			Same as above	1.0E+03 1.0E+04 1.0E+05 1.0E+06	8.5 8.0 7.7 7.4	Density: 2.365 Mg m ⁻³ (dry). Remarks: Same as above.	
5	Olhoeft, C.R., 1979 [6]	Basalt (166.6D) Hawaii			Same as above	1.0E+03 1.0E+04 1.0E+05 1.0E+06	7.9 7.5 7.2 6.9	Density: 2.365 Mg m ⁻³ (dry). Remarks: Same as above.	
6	Olhoeft, G.R., 1979 [6]	Basalt (166.6); Hawaii			Same as above	1.0E+03 1.0E+04 1.0E+05 1.0E+06	8.4 7.9 7.5 7.5	Density: 2.365 Mg m ⁻³ (dry). Remarks: Same as above.	
7	Olhoeft, G.R., 1979 [6]	Basalt (5.5); Chaffee, CO			Same as above	1.0E+03 1.0E+04 1.0E+05 1.0E+06	29.3 16.8 11.1 8.0	Density: 1.953 Mg m ⁻³ (dry). Remarks: Same as above.	
8	Olhoeft, C.R., 1979 [6]	Basalt (6.5); Germany			Same as above	1.0E+03 1.0E+04 1.0E+05 1.0E+06	37.6 19.6 14.2 11.8	Density: 3.030 Mg m ⁻³ (dry). Remarks: Same as above.	
9	Olhoeft, C.R., 1979 [6]	Basalt (R604); Hawaii			Same as above	1.0E+03 1.0E+04 1.0E+05 1.0E+06	10.1 9.6 9.2 8.8	Density: 2.136 Mg m ⁻³ (dry). Remarks: Same as above.	
10	Olhoeft, C.R., 1979 [6]	Basalt (F606); Hawaii			Same as above	1.0E+03 1.0E+04 1.0E+05 1.0E+06	10.7 10.4 10.1 9.8	Density: 2.230 Mg m ⁻³ (dry). Remarks: Same as above.	
11	Olhoeft, G.R., 1979 [6]	Basalt (R607); Hawaii			Same as above	1.0E+03 1.0E+04 1.0E+05 1.0E+06	10.3 10.1 9.8 9.5	Density: 2.184 Mg m ⁻³ (dry). Remarks: Same as above.	

TABLE 4.4. EXPERIMENTAL DATA ON DIELECTRIC CONSTANT OF BASALT (FREQUENCY DEPENDENCE) (Continued)

Data Set No.	Author(s), Year [Ref. No.]	Name and Source	Minerals and/or Chemical Composition		Experimental Data		Other Specifications
			Componenta	Weight Percent	Method Used	Frequency, ν , Hz	
12	Olhoeft, G.R., 1979 [6]	Basalt (R608); Hawaii			Same as above	1.0E+03	Density: 2.029 Mg m ⁻³ (dry). Remarks: Same as above.
						1.0E+04	9.5
						1.0E+05	9.3
13	Olhoeft, G.R., 1979 [6]	Basalt (R609); Hawaii			Same as above	1.0E+03	Density: 2.048 Mg m ⁻³ (dry). Remarks: Same as above.
						1.0E+04	8.1
						1.0E+05	7.8
14	Olhoeft, G.R., 1979 [6]	Basalt (R610); Hawaii			Same as above	1.0E+03	Density: 2.043 Mg m ⁻³ (dry). Remarks: Same as above.
						1.0E+04	7.7
						1.0E+05	7.5
15	Olhoeft, G.R., 1979 [6]	Basalt (R611); Hawaii			Same as above	1.0E+03	Density: 1.630 Mg m ⁻³ (dry). Remarks: Same as above.
						1.0E+04	6.3
						1.0E+05	6.1
16	Olhoeft, G.R., 1979 [6]	Basalt (R612); Hawaii			Same as above	1.0E+03	Density: 2.462 Mg m ⁻³ (dry). Remarks: Same as above.
						1.0E+04	12.9
						1.0E+05	10.3
17	Olhoeft, G.R., 1979 [6]	Basalt (R613); Hawaii			Same as above	1.0E+03	Density: 2.617 Mg m ⁻³ (dry). Remarks: Same as above.
						1.0E+04	12.7
						1.0E+05	12.3
18	Olhoeft, G.R., 1979 [6]	Basalt (R614); Hawaii			Same as above	1.0E+03	Density: 2.807 Mg m ⁻³ (dry). Remarks: Same as above.
						1.0E+04	10.7
						1.0E+05	9.8
19	Olhoeft, G.R., 1979 [6]	Basalt (R615); Hawaii			Same as above	1.0E+03	Density: 2.817 Mg m ⁻³ (dry). Remarks: Same as above.
						1.0E+04	11.4
						1.0E+05	10.8
20	Olhoeft, G.R., 1979 [6]	Basalt (R616); Hawaii			Same as above	1.0E+03	Density: 2.882 Mg m ⁻³ (dry). Remarks: Same as above.
						1.0E+04	10.3
						1.0E+05	9.8
21	Olhoeft, G.R., 1979 [6]	Basalt (R617); Hawaii			Same as above	1.0E+03	Density: 2.105 Mg m ⁻³ (dry). Remarks: Same as above.
						1.0E+04	10.9
						1.0E+05	10.6
22	Olhoeft, G.R., 1979 [6]	Basalt (R618); Hawaii			Same as above	1.0E+03	Density: 1.979 Mg m ⁻³ (dry). Remarks: Same as above.
						1.0E+04	7.0
						1.0E+05	6.4

TABLE 4.4. EXPERIMENTAL DATA ON DIELECTRIC CONSTANT OF BASALT (FREQUENCY DEPENDENCE) (Continued)

Data Set No.	Author(a), Year [Ref. No.]	Name and Source	Minerals and/or Chemical Composition		Experimental Data		Other Specifications	
			Components	Weight Percent	Method Used	Frequency, ν , Hz		Dielectric Constant ϵ'
23	Olhoeft, G.R., 1979 [6]	Basalt (R619); Hawaii			Same as above	1.0E+03	7.1	Density: 1.949 Mg m ⁻³ (dry). Remarks: Same as above.
						1.0E+04	6.8	
						1.0E+05	6.7	
24	Olhoeft, G.R., 1979 [6]	Basalt (R620); Hawaii			Same as above	1.0E+03	10.9	Density: 2.402 Mg m ⁻³ (dry). Remarks: Same as above.
						1.0E+04	10.5	
						1.0E+05	10.3	
25	Olhoeft, G.R., 1979 [6]	Basalt (R621); Hawaii			Same as above	1.0E+03	8.0	Density: 2.384 Mg m ⁻³ (dry). Remarks: Same as above.
						1.0E+04	7.5	
						1.0E+05	7.2	
26	Olhoeft, G.R., 1979 [6]	Basalt (R622); Hawaii			Same as above	1.0E+03	12.0	Density: 2.613 Mg m ⁻³ (dry). Remarks: Same as above.
						1.0E+04	10.5	
						1.0E+05	9.6	
27	Olhoeft, G.R., 1979 [6]	Basalt (R623); Hawaii			Same as above	1.0E+03	9.7	Density: 2.498 Mg m ⁻³ (dry). Remarks: Same as above.
						1.0E+04	9.1	
						1.0E+05	8.8	
28	Olhoeft, G.R., 1979 [6]	Basalt (R624); Hawaii			Same as above	1.0E+03	10.0	Density: 2.693 Mg m ⁻³ (dry). Remarks: Same as above.
						1.0E+04	9.5	
						1.0E+05	9.1	
29	Olhoeft, G.R., 1979 [6]	Basalt (R625); Hawaii			Same as above	1.0E+03	15.0	Density: 2.919 Mg m ⁻³ (dry). Remarks: Same as above.
						1.0E+04	12.2	
						1.0E+05	10.9	
30	Olhoeft, G.R., 1979 [6]	Basalt (R626); Hawaii			Same as above	1.0E+03	12.6	Density: 2.886 Mg m ⁻³ (dry). Remarks: Same as above.
						1.0E+04	11.5	
						1.0E+05	10.6	
31	Olhoeft, G.R., 1979 [6]	Basalt (R628); Hawaii			Same as above	1.0E+03	5.5	Density: 1.414 Mg m ⁻³ (dry). Remarks: Same as above.
						1.0E+04	5.1	
						1.0E+05	4.9	
32	Olhoeft, G.R., 1979 [6]	Basalt (R629); Hawaii			Same as above	1.0E+03	7.2	Density: 1.649 Mg m ⁻³ (dry). Remarks: Same as above.
						1.0E+04	7.0	
						1.0E+05	6.8	
33	Olhoeft, G.R., 1979 [6]	Basalt (R630); Hawaii			Same as above	1.0E+03	9.6	Density: 2.012 Mg m ⁻³ (dry). Remarks: Same as above.
						1.0E+04	9.3	
						1.0E+05	9.1	

TABLE 4.4. EXPERIMENTAL DATA ON DIELECTRIC CONSTANT OF BASALT (FREQUENCY DEPENDENCE) (Continued)

Data Set No.	Author(s), Year [Ref. No.]	Name and Source	Minerals and/or Chemical Components	Minerals and/or Chemical Composition		Method Used	Experimental Data		Other Specifications
				Weight Percent	Volume Percent		Frequency, ν , Hz	Dielectric Constant ϵ'	
34	Olhoeft, G.R., 1979 [6]	Basalt (R631); Hawaii				Same as above	1.0E+03	15.1	Density: 2.595 Mg m ⁻³ (dry). Remarks: Same as above.
							1.0E+04	14.7	
							1.0E+05	14.4	
35	Olhoeft, G.R., 1979 [6]	Basalt (R632); Hawaii				Same as above	1.0E+03	12.1	Density: 2.527 Mg m ⁻³ (dry). Remarks: Same as above.
							1.0E+04	11.9	
							1.0E+05	11.6	
36	Olhoeft, G.R., 1979 [6]	Basalt (R802-A); Hawaii				Same as above	1.0E+03	7.0	Density: 1.612 Mg m ⁻³ (dry). Remarks: Same as above.
							1.0E+04	6.7	
							1.0E+05	6.5	
37	Olhoeft, G.R., 1979 [6]	Basalt (R802-B); Hawaii				Same as above	1.0E+03	3.3	Density: 0.767 Mg m ⁻³ (dry). Remarks: Same as above.
							1.0E+04	3.2	
							1.0E+05	3.2	
38	Olhoeft, G.R., 1979 [6]	Basalt (R802-C); Hawaii				Same as above	1.0E+03	3.5	Density: 0.814 Mg m ⁻³ (dry). Remarks: Same as above.
							1.0E+04	3.4	
							1.0E+05	3.4	
39	Olhoeft, G.R., 1979 [6]	Basalt (R802-X-1); Hawaii				Same as above	1.0E+03	7.5	Density: 1.932 Mg m ⁻³ (dry). Remarks: Same as above.
							1.0E+04	7.3	
							1.0E+05	7.1	
40	Olhoeft, G.R., 1979 [6]	Basalt (R802-X-2); Hawaii				Same as above	1.0E+03	6.7	Density: 1.775 Mg m ⁻³ (dry). Remarks: Same as above.
							1.0E+04	6.5	
							1.0E+05	6.4	
41	Olhoeft, G.R., 1979 [6]	Basalt (R802-X-3); Hawaii				Same as above	1.0E+03	5.6	Density: 1.454 Mg m ⁻³ (dry). Remarks: Same as above.
							1.0E+04	5.4	
							1.0E+05	5.3	
42	Olhoeft, G.R., 1979 [6]	Basalt (R803-A-1); Hawaii				Same as above	1.0E+03	6.8	Density: 1.624 Mg m ⁻³ (dry). Remarks: Same as above.
							1.0E+04	6.6	
							1.0E+05	6.4	
43	Olhoeft, G.R., 1979 [6]	Basalt (R803-A-2); Hawaii				Same as above	1.0E+03	5.3	Density: 1.319 Mg m ⁻³ (dry). Remarks: Same as above.
							1.0E+04	5.2	
							1.0E+05	5.0	
44	Olhoeft, G.R., 1979 [6]	Basalt (R803-A-3); Hawaii				Same as above	1.0E+03	4.5	Density: 1.038 Mg m ⁻³ (dry). Remarks: Same as above.
							1.0E+04	4.3	
							1.0E+05	4.2	
							1.0E+06	4.1	

TABLE 4.4. EXPERIMENTAL DATA ON DIELECTRIC CONSTANT OF BASALT (FREQUENCY DEPENDENCE) (Continued)

Data Set No.	Author(s), Year [Ref. No.]	Name and Source	Minerals and/or Chemical Composition		Experimental Data		Other Specifications
			Components	Weight Percent	Method Used	Frequency, ν , Hz	
45	Olhoeft, G.R., 1979 [6]	Basalt (R804-1); Hawaii			Same as above	1.0E+03 1.0E+04 1.0E+05 1.0E+06	Density: 1.048 Mg m ⁻³ (dry). Remarks: Same as above.
46	Olhoeft, G.R., 1979 [6]	Basalt (R804-2); Hawaii			Same as above	1.0E+03 1.0E+04 1.0E+05 1.0E+06	Density: 0.928 Mg m ⁻³ (dry). Remarks: Same as above.
47	Olhoeft, G.R., 1979 [6]	Basalt (R805-1); Hawaii			Same as above	1.0E+03 1.0E+04 1.0E+05 1.0E+06	Density: 0.837 Mg m ⁻³ (dry). Remarks: Same as above.
48	Olhoeft, G.R., 1979 [6]	Basalt (R805-2); Hawaii			Same as above	1.0E+03 1.0E+04 1.0E+05 1.0E+06	Density: 0.876 Mg m ⁻³ (dry). Remarks: Same as above.
49	Olhoeft, G.R., 1979 [6]	Basalt (R806-1); Hawaii			Same as above	1.0E+03 1.0E+04 1.0E+05 1.0E+06	Density: 0.769 Mg m ⁻³ (dry). Remarks: Same as above.
50	Olhoeft, G.R., 1979 [6]	Basalt (R807-A); Hawaii			Same as above	1.0E+03 1.0E+04 1.0E+05 1.0E+06	Density: 0.844 Mg m ⁻³ (dry). Remarks: Same as above.
51	Olhoeft, G.R., 1979 [6]	Basalt (R807-B); Hawaii			Same as above	1.0E+03 1.0E+04 1.0E+05 1.0E+06	Density: 0.853 Mg m ⁻³ (dry). Remarks: Same as above.
52	Olhoeft, G.R., 1979 [6]	Basalt (R808-A); Hawaii			Same as above	1.0E+03 1.0E+04 1.0E+05 1.0E+06	Density: 0.802 Mg m ⁻³ (dry). Remarks: Same as above.
53	Olhoeft, G.R., 1979 [6]	Basalt (R808-B); Hawaii			Same as above	1.0E+03 1.0E+04 1.0E+05 1.0E+06	Density: 0.837 Mg m ⁻³ (dry). Remarks: Same as above.
54	Olhoeft, G.R., 1979 [6]	Basalt (R815); Hawaii			Same as above	1.0E+03 1.0E+04 1.0E+05 1.0E+06	Density: 2.925 Mg m ⁻³ (dry). Remarks: Same as above.
55	Olhoeft, G.R., 1979 [6]	Basalt (R816); Hawaii			Same as above	1.0E+03 1.0E+04 1.0E+05 1.0E+06	Density: 2.874 Mg m ⁻³ (dry). Remarks: Same as above.

TABLE 4.4. EXPERIMENTAL DATA ON DIELECTRIC CONSTANT OF BASALT (FREQUENCY DEPENDENCE) (Continued)

Data Set No.	Author(s), Year [Ref. No.]	Name and Source	Minerals and/or Chemical Composition		Experimental Data		Other Specifications	
			Components	Weight Percent	Method Used	Frequency, ν , Hz		Dielectric Constant ϵ'
56	Olhoeft, G.R., 1979 [6]	Basalt (R818); Hawaii			Same as above	1.0 E+03	9.3	Density: 3.039 Mg m ⁻³ (dry). Remarks: Same as above.
						1.0 E+04	9.0	
						1.0 E+05	8.8	
57	Olhoeft, G.R., 1979 [6]	Basalt (R819); Hawaii			Same as above	1.0 E+06	8.6	Density: 3.019 Mg m ⁻³ (dry). Remarks: Same as above.
						1.0 E+03	18.0	
						1.0 E+04	16.6	
58	Olhoeft, G.R., 1979 [6]	Basalt (R821-A); Hawaii			Same as above	1.0 E+05	15.1	Density: 2.545 Mg m ⁻³ (dry). Remarks: Same as above.
						1.0 E+06	13.7	
						1.0 E+03	10.4	
59	Olhoeft, G.R., 1979 [6]	Basalt (R821-B); Hawaii			Same as above	1.0 E+04	11.6	Density: 2.614 Mg m ⁻³ (dry). Remarks: Same as above.
						1.0 E+05	11.1	
						1.0 E+06	10.6	
60	Olhoeft, G.R., 1979 [6]	Basalt (R822-A); Hawaii			Same as above	1.0 E+03	10.2	Density: 2.914 Mg m ⁻³ (dry). Remarks: Same as above.
						1.0 E+04	10.0	
						1.0 E+05	9.8	
61	Olhoeft, G.R., 1979 [6]	Basalt (R822-B); Hawaii			Same as above	1.0 E+06	9.7	Density: 2.863 Mg m ⁻³ (dry). Remarks: Same as above.
						1.0 E+03	10.2	
						1.0 E+04	10.0	
62	Olhoeft, G.R., 1979 [6]	Basalt (R823-B); Hawaii			Same as above	1.0 E+05	9.8	Density: 2.255 Mg m ⁻³ (dry). Remarks: Same as above.
						1.0 E+06	9.7	
						1.0 E+03	9.1	
63	Griffin, R.E. and Marovelli, R.L., 1967 [41]	Basalt; Dresser, WI	Feldspar (Labradorite), Augite Magnetite	50	Susceptance-Variation Method	1.89E+07	11.0	Density: 2.97 Mg m ⁻³ . Texture: Mottled, gray green, fine-grained. Other: Data were extracted from figure of computer fitted curve; T=293 K.
						2.01E+07	11.0	
						2.40E+07	10.9	
						3.00E+07	10.8	
						4.02E+07	10.6	
						5.01E+07	10.6	
						6.02E+07	10.6	
						7.00E+07	10.6	
						8.00E+07	10.6	
						8.55E+07	10.7	
						9.05E+07	10.7	
1.00E+08	10.8							
1.06E+08	10.9							
64	Bondarenko, A.T., 1971 [42]	Basalt; Russia			Q-Meter Method	1.5 E+06	9.47	Density: 2.55 Mg m ⁻³ . Other: Q-meter method in the meter subband; resonance method in the decimeter subband; short circuit time method in the centimeter
						5.0 E+06	9.25	
						1.25E+07	8.95	
						2.5 E+07	8.82	
						3.0 E+07	8.80	

TABLE 4.4. EXPERIMENTAL DATA ON DIELECTRIC CONSTANT OF BASALT (FREQUENCY DEPENDENCE) (Continued)

Data Set No.	Author(s), Year [Ref. No.]	Name and Source	Minerals and/or Chemical Composition		Experimental Data		Method Used	Frequency, ν , Hz	Dielectric Constant ϵ'	Other Specifications
			Components	Weight Percent	Volume Percent					
64 cont.										
65	Chung, D.H., Westphal, W.B., and Simmons, G., 1970 [23]	Lunar Basalt 10020; Moon	Pyroxene Plagioclase Ilmenite Olivine Unidentified Cristobalite Troilite	53 25 15 4 1.4 1 0.6		Two Terminal Capacitance Substitution Method	3.5 E+07 4.0 E+07 7.5 E+07 1.00E+08 1.30E+08 1.65E+08 1.0 E+02 1.0 E+03 1.0 E+04 1.0 E+05 1.0 E+06 1.0 E+07	8.90 8.20 8.20 7.68 7.84 7.80 8.59 7.99 7.74 7.50 7.57 7.63	subband; in the millimeter subband, the measurements of the dielectric constant were determined by the change of polarization of the wave on reflection; T=293 K. Density: Bulk density 3.18 Mg m ⁻³ . Other: Sample was baked at 423 K in vacuum; high temperature run in dry N ₂ ; constant temperature frequency runs were made with the sample holder immersed in baths of ice, dry ice or liquid N ₂ ; authors estimated accuracy within 13%; T=77 K.	
66	Chung, D.H., et al., 1970 [23]	Same as above	Same as above			Same as above	1.0 E+02 1.0 E+03 1.0 E+04 1.0 E+05 1.0 E+06 1.0 E+07	26.6 21.1 16.0 12.2 9.64 8.97	Same as above except T=196 K.	
67	Chung, D.H., et al., 1970 [23]	Same as above	Same as above			Same as above	1.0 E+02 1.0 E+03 1.0 E+04 1.0 E+05 1.0 E+06 1.0 E+07	52.9 32.9 22.1 16.2 11.8 9.34	Same as above except T=298 K.	
68	Chung, D.H., et al., 1970 [23]	Same as above	Same as above			Same as above	1.0 E+02 1.0 E+03 1.0 E+04 1.0 E+05 1.0 E+06 1.0 E+07	114 62.7 35.9 22.3 15.0 11.9	Same as above except T=373 K.	
69	Chung, D.H., et al., 1970 [23]	Same as above	Same as above			Same as above	1.0 E+02 1.0 E+03 1.0 E+04 1.0 E+05 1.0 E+06 1.0 E+07	432 165 74.4 37.7 20.0 14.0	Same as above except T=474 K.	
70	Chung, D.H., et al., 1970 [23]	Lunar Basalt 10057; Moon	Pyroxene Plagioclase Ilmenite Glass Unidentified Cristobalite	51 20 16 10 2.9 <0.1		Same as above	1.0 E+02 1.0 E+03 1.0 E+04 1.0 E+05 1.0 E+06 1.0 E+07	5.73 5.55 5.17 5.21 5.05 5.10	Density: Bulk density 2.88 Mg m ⁻³ . Other: Same as above except T=77 K.	

TABLE 4.4. EXPERIMENTAL DATA ON DIELECTRIC CONSTANT OF BASALT (FREQUENCY DEPENDENCE) (Continued)

Data Set No.	Author(s), Year [Ref. No.]	Name and Source	Minerals and/or Chemical Composition		Method Used	Experimental Data		Other Specifications
			Components	Weight Percent		Frequency, ν , Hz	Dielectric Constant ϵ'	
71	Chung, D.H., et al., 1970 [23]	Same as above	Same as above		Same as above	1.0E+02 1.0E+03 1.0E+04 1.0E+05 1.0E+06 1.0E+07	20.9 16.5 12.6 9.95 8.89 8.62	Same as above except T=196 K.
72	Chung, D.H., et al., 1970 [23]	Same as above	Same as above		Same as above	1.0E+02 1.0E+03 1.0E+04 1.0E+05 1.0E+06 1.0E+07	45.0 27.9 19.6 14.3 11.3 9.34	Same as above except T=298 K.
73	Chung, D.H., et al., 1970 [23]	Same as above	Same as above		Same as above	1.0E+02 1.0E+03 1.0E+04 1.0E+05 1.0E+06 1.0E+07	79.2 43.6 26.0 18.2 12.8 9.73	Same as above except T=373 K.
74	Chung, D.H., et al., 1970 [23]	Same as above	Same as above		Same as above	1.0E+02 1.0E+03 1.0E+04 1.0E+05 1.0E+06 1.0E+07	339 141 68.6 34.8 20.0 14.0	Same as above except T=473 K.
75	Chung, D.H., et al., 1970 [23]	Lunar Basalt 10046; Moon	Pyroxene Plagioclase Glass Ilmenite	57 20 14 9	Same as above	1.0E+02 1.0E+03 1.0E+04 1.0E+05 1.0E+06 1.0E+07	12.0 9.65 9.62 7.28 6.54 6.52	Density: Bulk density 2.21 Mg m ⁻³ . Other: Same as above except T=72 K.
76	Chung, D.H., et al., 1970 [23]	Same as above	Same as above		Same as above	1.0E+02 1.0E+03 1.0E+04 1.0E+05 1.0E+06 1.0E+07	47.0 29.5 20.0 16.0 13.7 12.9	Same as above except T=196 K.
77	Chung, D.H., et al., 1970 [23]	Same as above	Same as above		Same as above	1.0E+02 1.0E+03 1.0E+04 1.0E+05 1.0E+06 1.0E+07	68.6 48.7 35.9 27.2 20.1 14.5	Same as above except T=298 K.
78	Chung, D.H., et al., 1970 [23]	Same as above	Same as above		Same as above	1.0E+02 1.0E+03 1.0E+04 1.0E+05 1.0E+06 1.0E+07	86.9 58.2 42.3 32.0 24.0 16.9	Same as above except T=373 K.

TABLE 4.4. EXPERIMENTAL DATA ON DIELECTRIC CONSTANT OF BASALT (FREQUENCY DEPENDENCE) (Cont Inued)

Data Set No.	Author (a), Year [Ref. No.]	Name and Source	Minerals and/or Chemical Composition		Method Used	Experimental Data		Other Specifications
			Componenta	Weight Percent		Frequency, V, Hz	Dielectric Constant ϵ'	
79	Chung, D.H., et al., 1970 [23]	Same as above	Same as above		Same as above	1.0E+02 1.0E+03 1.0E+04 1.0E+05 1.0E+06 1.0E+07	125 75.8 55.1 41.5 32.0 24.9	Same as above except T=473 K.
80	Chung, D.H., et al., 1970 [23]	Hawaii Basalt; Oahu, Hawaii	Plagioclase Pyroxene Olivine Quartz Unidentified	48 24 21 6 1	Same as above	1.0E+02 1.0E+03 1.0E+04 1.0E+05 1.0E+06 1.0E+07	5.34 5.18 5.02 4.90 5.14 4.94	Density: Bulk density 2.68 Mg m ⁻³ . Other: Same as above except in vacuum measurements; T=300 K.
81	Chung, D.H., et al., 1970 [23]	Same as above	Same as above		Same as above	1.0E+02 1.0E+03 1.0E+04 1.0E+05 1.0E+06 1.0E+07	6.27 5.83 5.43 5.26 5.10 5.14	Same as above except measurements were in air.
82	Chung, D.H., et al., 1970 [23]	Same as above	Same as above		Same as above	1.0E+02 1.0E+03 1.0E+04 1.0E+05 1.0E+06 1.0E+07	12.3 7.70 6.12 5.48 5.31 5.35	Water Content: 0.1 wt.%. Other: Same as above except T=300 K.
83	Chung, D.H., et al., 1970 [23]	Same as above	Same as above		Same as above	1.0E+02 1.0E+03 1.0E+04 1.0E+05 1.0E+06 1.0E+07	57.9 16.4 9.10 6.68 5.74 5.35	Water Content: 0.8 wt.%. Other: Same as above.
84	Chung, D.H., et al., 1970 [23]	Same as above	Same as above		Same as above	1.0E+02 1.0E+03 1.0E+04 1.0E+05 1.0E+06 1.0E+07	49.4 28.6 11.5 7.52 5.98 5.35	Water Content: 1.5 wt.%. Other: Same as above.
85	Chung, D.H., et al., 1970 [23]	Same as above	Same as above		Same as above	1.0E+02 1.0E+03 1.0E+04 1.0E+05 1.0E+06 1.0E+07	7.96 7.96 7.96 7.96 7.96 7.96	Other: Same as above except dry basalt; T=77 K.
86	Chung, D.H., et al., 1970 [23]	Same as above	Same as above		Same as above	1.0E+02 1.0E+03 1.0E+04 1.0E+05 1.0E+06 1.0E+07	10.6 9.73 9.73 9.80 10.60	Same as above except T=196 K.

TABLE 4.4. EXPERIMENTAL DATA ON DIELECTRIC CONSTANT OF BASALT (FREQUENCY DEPENDENCE) (Continued)

Data Set No.	Author(s), Year [Ref. No.]	Name and Source	Minerals and/or Chemical Composition Components	Minerals and/or Chemical Composition		Method Used	Experimental Data		Other Specifications
				Weight Percent	Volume Percent		Frequency, ν , Hz	Dielectric Constant ϵ'	
87	Chung, D.H., et al., 1970 [23]	Same as above	Same as above			Same as above	1.0 E+02 2.0 E+02 6.0 E+02 5.0 E+03 1.0 E+07	14.2 13.3 11.5 10.6 10.6	Same as above except T=273 K.
88	Chung, D.H., et al., 1970 [23]	Same as above	Same as above			Same as above	1.0 E+02 3.2 E+02 1.58E+03 3.47E+04 1.0 E+07	18.6 15.9 14.2 10.6 10.6	Same as above except T=298 K.
89	Chung, D.H., et al., 1970 [23]	Same as above	Same as above			Same as above	1.0 E+02 2.66E+02 1.08E+03 4.02E+03 3.81E+04 2.06E+05 1.0 E+07	83.2 44.2 26.5 19.5 14.2 11.5 11.5	Same as above except T=373 K.
90	Chung, D.H., et al., 1970 [23]	Same as above	Same as above			Same as above	1.0 E+02 2.7 E+02 1.73E+03 5.33E+03 8.07E+04 8.40E+05 1.0 E+07	17.4 62.8 29.2 22.1 15.0 12.4 12.4	Same as above except T=473 K.
91	Chung, D.H., et al., 1970 [23]	Cape Neddick Basalt; Cape Neddick, MA	Plagioclase Pyroxene Olivine Unidentified	55 26 17 2		Same as above	1.0 E+02 1.0 E+03 1.0 E+04 1.0 E+05 1.0 E+06 1.0 E+07	5.30 5.31 5.35 5.39 5.42 5.46	Density: Bulk density 2.60 Mg m ⁻³ . Other: Same as above except T=77 K.
92	Chung, D.H., et al., 1970 [23]	Same as above	Same as above			Same as above	1.0 E+02 1.0 E+03 1.0 E+04 1.0 E+05 1.0 E+06 1.0 E+07	21.9 14.9 11.5 9.75 9.04 8.95	Same as above except T=298 K.
93	Chung, D.H., et al., 1970 [23]	Same as above	Same as above			Same as above	1.0 E+02 1.0 E+03 1.0 E+04 1.0 E+05 1.0 E+07	76.9 30.6 16.7 11.5 9.08	Same as above except T=373 K.
94	Chung, D.H., et al., 1970 [23]	Same as above	Same as above			Same as above	1.0 E+02 1.0 E+03 1.0 E+04 1.0 E+05 1.0 E+07	15.4 44.6 18.4 13.2 9.15	Same as above except T=473 K.

TABLE 4.4. EXPERIMENTAL DATA ON DIELECTRIC CONSTANT OF BASALT (FREQUENCY DEPENDENCE) (Continued)

Data Set No.	Author(s), Year (Ref. No.)	Name and Source	Minerals and/or Chemical Composition		Method Used	Experimental Data		Other Specifications							
			Components	Weight Percent		Frequency, ν , Hz	Dielectric Constant ϵ'								
95	Saint-Amant, M. and Strangway, D.W., 1970 [26]	Basalt M; Cape Neddick, MA	Biotite	16	Capacitance Method	9.19E+01	3.58	Other: Powdered dry basalt was held in vacuum overnight; data extracted from figure; T=300 K.							
						1.82E+02	3.49								
						4.84E+02	3.49								
						9.14E+02	3.45								
						1.90E+03	3.37								
						4.82E+03	3.33								
						9.55E+03	3.29								
						1.89E+04	3.29								
						4.79E+04	3.25								
						9.50E+04	3.25								
						1.98E+05	3.25								
						5.01E+05	3.17								
						9.93E+05	3.12								
						1.97E+06	3.17								
						96	Saint-Amant, M. and Strangway, D.W., 1970 [26]		Same as above	Same as above	Same as above	Same as above	4.40E+01	4.77	Same as above except T=373 K.
													8.73E+01	4.60	
1.91E+02	4.26														
4.61E+02	3.92														
9.59E+02	3.84														
2.00E+03	3.67														
4.59E+03	3.54														
1.00E+04	3.50														
1.99E+04	3.46														
5.03E+04	3.46														
9.05E+04	3.33														
1.98E+05	3.29														
4.77E+05	3.29														
9.45E+05	3.25														
1.87E+06	3.25														
97	Saint-Amant, M. and Strangway, D.W., 1970 [26]	Same as above	Same as above	Same as above	Same as above			4.39E+01					6.17	Same as above except T=473 K.	
						8.70E+01	5.87								
						1.81E+02	5.66								
						4.59E+02	5.32								
						9.56E+02	5.07								
						1.81E+03	4.82								
						5.05E+03	4.52								
						9.53E+03	4.22								
						1.99E+04	3.97								
						4.79E+04	3.76								
						9.49E+04	3.63								
						1.98E+05	3.50								
						4.77E+05	3.38								
						9.92E+05	3.38								
						1.87E+06	3.42								
						98	Saint-Amant, M. and Strangway, D.W., 1970 [26]	Same as above	Same as above	Same as above	Same as above	9.11E+01	7.28		Same as above except T=573 K.
1.90E+02	6.85														
4.81E+02	6.47														
9.54E+02	6.18														
1.89E+03	5.88														

TABLE 4.4. EXPERIMENTAL DATA ON DIELECTRIC CONSTANT OF BASALT (FREQUENCY DEPENDENCE) (Continued)

Data Set No.	Author(s), Year [Ref. No.]	Name and Source	Minerals and/or Chemical Composition	Weight Percent		Method Used	Experimental Data		Other Specifications
				Percent	Volume Percent		Frequency, ν , Hz	Dielectric Constant ϵ'	
98 cont.									
99	Saint-Amant, M. and Strangway, D.W., 1970 [26]	Basalt AA; Westfield, MA			>16	Same as above	4.79E+03 9.51E+03 1.98E+04 4.78E+04 9.48E+04 1.88E+05 4.53E+05 9.92E+05 1.87E+06	5.50 5.20 5.08 4.74 4.44 4.14 3.80 3.59 3.51	Same as above except T=300 K.
			Biotite				9.42E+01 1.77E+02 4.47E+02 8.82E+02 1.83E+03 4.61E+03 9.11E+03 1.80E+04 4.53E+04 8.96E+04 1.77E+05 4.68E+05 9.24E+05 1.74E+06	3.54 3.49 3.40 3.36 3.27 3.26 3.21 3.12 3.11 3.03 3.11	
100	Saint-Amant, M. and Strangway, D.W., 1970 [26]	Same as above	Same as above			Same as above	4.59E+01 8.63E+01 1.78E+02 4.27E+02 8.86E+02 1.75E+03 4.62E+03 9.12E+03 1.80E+04 4.54E+04 8.96E+04 1.86E+05 4.68E+05 1.02E+06 1.66E+06	5.38 4.99 4.56 4.22 4.00 3.70 3.56 3.48 3.39 3.30 3.29 3.24 3.15 3.24	Same as above except T=373 K.
101	Saint-Amant, M. and Strangway, D.W., 1970 [26]	Same as above	Same as above			Same as above	8.74E+01 1.66E+02 4.33E+02 8.52E+02 1.85E+03 4.43E+03 9.17E+03 1.81E+04 4.55E+04 9.43E+04 1.86E+05	7.21 6.74 6.14 5.71 5.28 4.85 4.41 4.16 3.85 3.63 3.46	Same as above except T=468 K.

TABLE 4.4. EXPERIMENTAL DATA ON DIELECTRIC CONSTANT OF BASALT (FREQUENCY DEPENDENCE) (Continued)

Data Set No.	Author(s), Year [Ref. No.]	Name and Source	Minerals and/or Chemical Composition		Method Used	Experimental Data		Other Specifications
			Weight Percent	Volume Percent		Frequency, ν , Hz	Dielectric Constant ϵ'	
101	Saint-Amant, M. and Strangway, D.W., 1970 [26]	Same as above			Same as above	4.69E+05	3.37	Same as above except T=570 K.
cont.						9.72E+05	3.32	
						1.66E+06	3.32	
						8.87E+01	9.69	
						1.75E+02	8.87	
						4.38E+02	8.06	
						8.62E+02	7.54	
						1.70E+03	7.07	
						4.26E+03	6.47	
						8.82E+03	6.04	
						1.74E+04	5.44	
						4.58E+04	4.96	
						9.49E+04	4.62	
						1.87E+05	4.31	
						4.70E+05	3.93	
	9.28E+05	3.67						
	1.66E+06	3.58						
103	Saint-Amant, M. and Strangway, D.W., 1970 [26]	Basalt M; Cape Meddick, MA		16	Same as above	2.00E+02	14.1	Other: Solid basalt; dry; dried by heating in vacuum until the results were reproducible; sample was heated twice to 423 K and once to 503 K; data obtained after heating to 781 K once; T=300 K.
						5.03E+02	13.7	
						1.04E+03	13.1	
						1.95E+03	12.2	
						5.13E+03	12.0	
						1.01E+04	11.6	
						2.09E+04	11.3	
						5.24E+04	10.9	
						1.03E+05	11.1	
						2.13E+05	10.9	
						5.36E+05	10.9	
						1.01E+06	10.5	
						2.08E+06	10.5	
						2.02E+02	25.1	
						5.22E+02	19.2	
						1.04E+03	17.5	
						2.05E+03	15.8	
						5.39E+03	14.3	
						1.11E+04	13.7	
						2.20E+04	13.0	
						5.25E+04	12.4	
						1.08E+05	12.4	
						2.04E+05	12.2	
						5.36E+05	11.5	
						1.06E+06	11.3	
						2.08E+06	10.9	
105	Saint-Amant, M. and Strangway, D.W., 1970 [26]	Same as above	Same as above		Same as above	1.94E+02	50.1	Same as above except T=439 K.
						4.84E+02	34.6	
						1.05E+03	28.7	
						2.16E+03	23.6	
						5.41E+03	20.0	

TABLE 4.4. EXPERIMENTAL DATA ON DIELECTRIC CONSTANT OF BASALT (FREQUENCY DEPENDENCE) (Continued)

Data Set No.	Author(s), Year [Ref. No.]	Name and Source	Minerals and/or Chemical Composition		Method Used	Experimental Data		Other Specifications
			Components	Weight Percent		Frequency, ν , Hz	Dielectric Constant ϵ'	
105 cont.						1.06E+04	16.8	
						2.20E+04	15.8	
106	Saint-Amant, M. and Strangway, D.W., 1970 [26]	Same as above	Same as above		Same as above	5.14E+02	60.8	Same as above except T=503 K.
						2.08E+03	48.1	
						4.96E+03	39.9	
						1.12E+04	28.0	
						2.10E+04	23.0	
						5.26E+04	18.3	
						1.09E+05	16.4	
						2.04E+05	14.7	
						5.11E+05	13.2	
						1.01E+06	13.0	
107	Saint-Amant, M. and Strangway, D.W., 1970 [26]	Basalt AA; Westfield, MA	Biotite	>16	Same as above	2.97E+02	2.89	Other: Dry sample; no details on drying available for this sample; T=222 K.
						9.38E+02	2.90	
						9.39E+03	2.82	
						9.85E+04	2.83	
						9.39E+05	2.84	
						2.96E+02	3.06	
						9.37E+02	3.07	
						9.38E+03	2.95	
						9.81E+01	3.52	
						2.96E+02	3.48	
108	Saint-Amant, M. and Strangway, D.W., 1970 [26]	Same as above	Same as above		Same as above	5.02E+02	3.32	Same as above except T=258 K.
						9.83E+02	3.23	
						1.92E+03	3.15	
						4.79E+03	3.07	
						9.83E+03	3.08	
						9.84E+04	3.00	
						9.38E+05	2.97	
						2.96E+02	3.23	
						2.96E+03	3.03	
						9.38E+03	3.03	
109	Saint-Amant, M. and Strangway, D.W., 1970 [26]	Same as above	Same as above		Same as above	3.25E+02	3.65	Same as above except T=300 K.
						9.81E+02	3.49	
						3.10E+03	3.37	
						9.82E+03	3.33	
						9.83E+04	3.17	
						9.83E+05	3.09	
						2.96E+02	3.23	
						2.96E+03	3.03	
						9.38E+03	3.03	
						3.25E+02	3.65	
110	Saint-Amant, M. and Strangway, D.W., 1970 [26]	Same as above	Same as above		Same as above	9.81E+02	3.49	Water Content: 0.1%. Other: T=228 K.
						3.10E+03	3.37	
						9.82E+03	3.33	
						9.83E+04	3.17	
						9.83E+05	3.09	
						2.96E+02	3.23	
						2.96E+03	3.03	
						9.38E+03	3.03	
						3.25E+02	3.65	
						9.81E+02	3.49	
111	Saint-Amant, M. and Strangway, D.W., 1970 [26]	Same as above	Same as above		Same as above	3.25E+02	3.65	Same as above except T=258 K.
						9.81E+02	3.49	
						3.10E+03	3.37	
						9.82E+03	3.33	
						9.83E+04	3.17	
						9.83E+05	3.09	
						2.96E+02	3.23	
						2.96E+03	3.03	
						9.38E+03	3.03	
						3.25E+02	3.65	

TABLE 4.4. EXPERIMENTAL DATA ON DIELECTRIC CONSTANT OF BASALT (FREQUENCY DEPENDENCE) (Continued)

Data Set No.	Author(s), Year [Ref. No.]	Name and Source	Minerals and/or Chemical Composition		Experimental Data		Other Specifications
			Components	Weight Percent	Method Used	Frequency, V, Hz	
112	Saint-Amant, M. and Strangway, D.W., 1970 [26]	Same as above	Same as above		Same as above	9.76E+01 3.09E+02 9.78E+02 3.10E+03 9.81E+03 9.82E+04 9.83E+05	4.50 4.20 4.00 3.75 3.58 3.34 3.26 Same as above except T=300 K.
113	Saint-Amant, M. and Strangway, D.W., 1970 [26]	Same as above	Same as above		Same as above	3.48E+02 1.11E+03 3.53E+03 1.07E+04 1.08E+05 3.44E+05 1.04E+06	3.85 3.54 3.32 3.24 3.07 2.94 2.94 Water Content: 0.5%. Other: T=213 K.
114	Saint-Amant, M. and Strangway, D.W., 1970 [26]	Same as above	Same as above		Same as above	3.46E+02 1.10E+03 3.51E+03 1.06E+04 1.13E+05 3.43E+05 1.04E+06	5.04 4.82 4.51 4.25 3.60 3.38 3.12 Same as above except T=243 K.
115	Saint-Amant, M. and Strangway, D.W., 1970 [26]	Same as above	Same as above		Same as above	3.46E+02 1.16E+03 3.33E+03 1.12E+04 1.07E+05 3.42E+05 1.09E+06	5.70 5.35 5.04 4.83 4.35 4.00 3.74 Same as above except T=267 K.
116	Hansen, W., Still, W.R., and Ward, S.H., 1973 [43]	Western Grand Canyon; USA	SiO ₂ Al ₂ O ₃ CaO MgO FeO Ilmenite Na ₂ O TiO ₂ K ₂ O	42.99 13.03 12.31 12.27 10.80 3.8 3.10 2.0 0.73		Contact Substitution Method	7.8 Other: Sample A; measurements were done at room temperature in dry N ₂ atmosphere; measurements done above 1 MHz showed ϵ' as constant at 1 MHz vs. ν ; ilmenite is powdered sand from Melbourne, Florida; Lucite (Dupont trademark) was used as matrix; measurements were done at room temperature and pressure; accuracy $\pm 5\%$.
117	Hansen, W., et al., 1973 [43]	Keweenaw Duluuth Hornfels; MN	SiO ₂ FeO Al ₂ O ₃ CaO TiO ₂ MgO Na ₂ O K ₂ O Ilmenite	41.31 17.72 12.12 11.07 7.04 6.58 2.06 0.16		Same as above	13.0 Same as above except sample B.

11.30

TABLE 4.4. EXPERIMENTAL DATA ON DIELECTRIC CONSTANT OF BASALT (FREQUENCY DEPENDENCE) (Continued)

Data Set No.	Author(s), Year [Ref. No.]	Name and Source	Minerals and/or Chemical Composition		Experimental Data			Other Specifications	
			Components	Weight Percent	Volume Percent	Method Used	Frequency, V, Hz		Dielectric Constant ϵ'
118	Hansen, W., et al., 1973 [43]	Cane Springs Diks; USA	SiO ₂ Al ₂ O ₃ FeO CaO Ilmenite Na ₂ O MgO TiO ₂ K ₂ O	50.08 14.36 13.40 8.33 5.91 3.92 3.54 3.11 2.00		Same as above	1.00E+06	15.0	Same as above except sample C.
119	Hansen, W., et al., 1973 [43]	Hurricane Flow; USA	SiO ₂ Al ₂ O ₃ FeO CaO MgO Na ₂ O Ilmenite TiO ₂ K ₂ O	48.84 15.82 10.39 9.20 7.47 3.36 3.13 1.65 0.95		Same as above	1.00E+06	8.0	Same as above except sample D.
120	Hansen, W., et al., 1973 [43]	St. George; USA	SiO ₂ Al ₂ O ₃ FeO CaO MgO Na ₂ O Ilmenite K ₂ O TiO ₂	54.76 15.87 7.32 6.99 5.80 4.18 2.85 1.90 1.67		Same as above	1.00E+06	9.3	Same as above except sample E.
121	Hansen, W., et al., 1973 [43]	Same as above	SiO ₂ Al ₂ O ₃ FeO CaO MgO Na ₂ O Ilmenite K ₂ O TiO ₂	52.83 16.06 7.46 7.27 5.97 4.18 2.85 1.90 1.50		Same as above	1.00E+06	8.3	Same as above except sample F.
122	Hansen, W., et al., 1973 [43]	Western Grand Canyon; USA	SiO ₂ Al ₂ O ₃ FeO CaO MgO Na ₂ O Ilmenite TiO ₂ K ₂ O	48.13 15.30 12.22 9.79 8.62 2.97 2.53 1.33 0.81		Same as above	1.00E+06	7.5	Same as above except sample G.

TABLE 4.4. EXPERIMENTAL DATA ON DIELECTRIC CONSTANT OF BASALT (FREQUENCY DEPENDENCE) (Continued)

Data Set No.	Author(s), Year [Ref. No.]	Name and Source	Minerals and/or Chemical Composition		Experimental Data			Other Specifications								
			Components	Weight Percent	Volume Percent	Method Used	Frequency, ν , Hz		Dielectric Constant ϵ'							
123	Hansen, W., et al., 1973 [43]	Hinkaret; USA	SiO ₂	46.42		Same as above	1.00 E+06	7.8	Same as above except sample H.							
			Al ₂ O ₃	14.73												
			FeO	12.22												
			MgO	8.12												
			CaO	7.69												
			Ilmenite	5.67												
			Na ₂ O	4.58												
			TiO ₂	2.67												
			K ₂ O	2.29												
			124	Hansen, W., et al., 1973 [43]	Western Grand Canyon; USA					SiO ₂	49.38		Same as above	1.00 E+06	8.0	Texture: Fine grained. Other: Same as above except sample I.
Al ₂ O ₃	16.16															
FeO	10.12															
MgO	8.81															
CaO	8.47															
Na ₂ O	3.47															
Ilmenite	3.27															
TiO ₂	1.72															
K ₂ O	1.00															
125	Hansen, W., et al., 1973 [43]	Same as above				SiO ₂	49.38		Same as above	1.00 E+06	8.0	Texture: Coarse grained. Other: Same as above except sample J.				
			Al ₂ O ₃	16.16												
			FeO	10.12												
			MgO	8.81												
			CaO	8.47												
			Na ₂ O	3.47												
			TiO ₂	1.72												
			K ₂ O	1.00												
			126	Hansen, W., et al., 1973 [43]	Same as above	SiO ₂	49.38						Same as above	0.1042E+03	13.11	Texture: Fine grained. Other: Same as above except sample I.
						Al ₂ O ₃	16.16									
FeO	10.12															
MgO	8.81															
CaO	8.47															
Na ₂ O	3.47															
Ilmenite	3.27															
TiO ₂	1.72															
K ₂ O	1.00															
127	Hansen, W., et al., 1973 [43]	Same as above				SiO ₂	49.38		Same as above	0.1054E+03	10.22	Texture: Coarse grained. Other: Same as above except sample J.				
			Al ₂ O ₃	16.16												
			FeO	10.12												
			MgO	8.81												
			CaO	8.47												
			Na ₂ O	3.47												
			TiO ₂	1.72												
			K ₂ O	1.00												

TABLE 4.4. EXPERIMENTAL DATA ON DIELECTRIC CONSTANT OF BASALT (FREQUENCY DEPENDENCE) (Continued)

Data Set No.	Author(s), Year [Ref. No.]	Name and Source	Minerals and/or Chemical Composition		Method Used	Experimental Data		Other Specifications
			Components	Weight Percent		Frequency, V, Hz	Dielectric Constant ϵ'	
127 cont.								
128	Jisoo, R., Ward, S.H., Nash, W.P., and Buzell, D., 1973 [15]	Duluth Hornfels; NN	Plagioclase Pyroxene Ilmenite Other Olivine	40.6 39.2 11.3 5.6 3.3	Contact Substitution Method (C.S.)	0.1034E+06 0.5700E+06 0.1080E+07 0.5073E+07 0.1076E+03 0.2185E+03 0.5221E+03 0.1109E+04 0.2243E+04 0.5618E+04 0.1072E+05 0.2162E+05 0.5395E+05 0.1027E+06 0.5153E+06 0.9815E+06 0.1074E+03 0.2180E+03 0.5205E+03 0.1108E+04 0.2239E+04 0.5601E+04 0.1071E+05 0.2159E+05 0.5385E+05 0.1026E+06 0.5144E+06 0.1034E+07 0.1070E+03 0.2173E+03 0.5485E+03 0.1106E+04 0.2235E+04 0.5594E+04 0.1070E+05 0.2157E+05 0.5376E+05 0.1025E+06 0.5138E+06 0.1032E+07 0.1971E+07 0.5174E+07 0.1131E+03 0.2394E+03 0.5964E+03 0.1134E+04 0.2276E+04 0.5646E+04	7.725 7.420 7.429 7.290 47.96 38.70 29.91 28.08 24.18 21.05 19.76 17.95 16.68 16.35 14.57 14.12 50.08 40.41 31.57 28.69 24.97 22.22 19.97 18.35 17.23 16.52 15.05 14.59 52.86 42.65 32.27 29.64 25.80 22.70 20.41 18.75 17.80 16.88 15.38 15.07 13.84 13.58 44.32 38.18 29.23 25.73 22.40 20.14	Step 1: At ambient condition.
129	Jisoo, R., et al., 1973 [15]	Same as above	Same as above		Variable Air Gap Method (V.A.)			Same as above.
130	Jisoo, R., et al., 1973 [15]	Same as above	Same as above		Optimum Technique (O.T.), C.S., V.A.			Same as above.
131	Jisoo, R., et al., 1973 [15]	Same as above	Same as above		O.T., V.A., C.S.			Same as above.
132	Jisoo, R., et al., 1973 [15]	Same as above	Same as above		Optimum Technique			Step 2: Sample dried in a vacuum of 3×10^{-3} Torr for 2 days and in the circulating N_2 -gas for 2 days.

TABLE 4.4. EXPERIMENTAL DATA ON DIELECTRIC CONSTANT OF BASALT (FREQUENCY DEPENDENCE) (Continued)

Data Set No.	Author(s), Year [Ref. No.]	Name and Source	Minerals and/or Chemical Composition		Method Used	Experimental Data		Other Specifications
			Components	Weight Percent		Frequency, ν , Hz	Dielectric Constant ϵ'	
132 cont.								
133	Jisoo, R., et al., 1973 [15]	Same as above	Same as above		Variable Gap			Same as above.
						0.1131E+05	18.70	
						0.2389E+05	17.55	
						0.5323E+05	16.47	
						0.1065E+06	16.13	
						0.5280E+06	14.83	
						0.1114E+07	14.53	
						0.1133E+03	41.56	
						0.2155E+03	36.18	
						0.5659E+03	28.31	
						0.1135E+04	24.91	
						0.2277E+04	21.92	
						0.5651E+04	19.50	
						0.1132E+05	18.30	
						0.2148E+05	17.36	
						0.5326E+05	16.12	
						0.1010E+06	15.62	
						0.5572E+06	14.52	
						0.1115E+07	14.07	
134	Jisoo, R., et al., 1973 [15]	Same as above	Same as above		Contact Substitution Method			Same as above.
						0.1134E+03	40.25	
						0.2275E+03	34.67	
						0.5662E+03	27.71	
						0.1136E+04	24.38	
						0.2278E+04	21.46	
						0.5652E+04	19.30	
						0.1132E+05	18.30	
						0.2149E+05	16.99	
						0.5327E+05	15.95	
						0.1066E+06	15.46	
						0.5577E+06	14.06	
						0.1057E+07	14.07	
135	Jisoo, R., et al., 1973 [15]	Same as above	Same as above		O.T., V.A., C.S.			Same as above.
						0.2231E+07	13.63	
						0.5523E+07	13.50	
136	Jisoo, R., et al., 1973 [15]	Same as above	Same as above		Optimum Technique (O.T.)			Step 3: Tin foil was placed on the sample and sample was dried in a vacuum of 3×10^{-3} Torr for 2 days.
						0.9947E+04	19.73	
						0.4708E+06	15.76	
						0.9965E+06	15.59	
						0.1999E+07	15.26	
137	Jisoo, R., et al., 1973 [15]	Same as above	Same as above		Variable Air Gsp (V.A.)			Same as above.
						0.9950E+04	19.10	
						0.4710E+06	15.25	
						0.9449E+06	14.93	
						0.2000E+07	14.78	
138	Jisoo, R., et al., 1973 [15]	Same as above	Same as above		Contact Substitution Method (C.S.)			Same as above.
						0.9950E+04	19.10	
						0.4710E+06	15.09	
						0.9451E+06	14.46	
						0.2000E+07	14.46	
139	Jisoo, R., et al., 1973 [15]	Same as above	Same as above		O.T., V.A., C.S.			Same as above.
						0.1043E+03	42.28	
						0.2094E+03	37.98	
						0.4942E+03	29.98	

TABLE 4.4. EXPERIMENTAL DATA ON DIELECTRIC CONSTANT OF BASALT (FREQUENCY DEPENDENCE) (Continued)

Data Set No.	Author(s), Year [Ref. No.]	Name and Source	Minerals and/or Chemical Composition		Method Used	Experimental Data		Other Specifications	
			Weight Percent	Volume Percent		Frequency, ν , Hz	Dielectric Constant ϵ'		
139 cont.						0.9925E+03	26.07		
						0.2103E+04	22.92		
						0.4957E+04	20.81		
						0.1997E+05	18.30		
						0.4964E+05	17.16		
						0.9960E+05	16.62		
						0.5244E+07	14.47		
						0.9848E+02	52.92		Step 1: At ambient conditions.
						0.2054E+03	42.63		
						0.5182E+03	32.45		
						0.9981E+03	29.28		
						0.2030E+04	25.83		
						0.5142E+04	23.30		
0.1017E+05	20.68								
0.2016E+05	19.30								
0.5113E+05	18.43								
0.1013E+06	17.40								
0.4825E+06	16.05								
0.9569E+06	15.68								
0.1897E+07	15.06								
0.4949E+07	14.71								
141	Jisoo, R., et al., 1973 [15]	Same as above	Same as above		Optimum Technique	0.9545E+02	45.67	Step 2: After the sample was dried in vacuum of 3×10^{-3} Torr for 2 days and in the circulating N_2 -gas for 2 days.	
						0.1994E+03	39.16		
						0.4895E+03	29.64		
						0.1023E+04	25.85		
						0.2023E+04	22.55		
						0.5124E+04	20.23		
						0.1015E+05	19.10		
						0.2012E+05	17.93		
						0.4964E+05	16.83		
						0.1012E+06	16.63		
						0.4821E+06	15.51		
						0.9557E+06	14.90		
						0.1895E+07	14.39		
0.4943E+07	14.06								
142	Jisoo, R., et al., 1973 [15]	Same as above	Same as above		Same as above	0.9797E+02	42.67	Step 3: After tin foil was placed on the sample and sample was dried in a vacuum of 3×10^{-3} Torr for 2 days.	
						0.1993E+03	37.85		
						0.5035E+03	30.66		
						0.1023E+04	26.29		
						0.2025E+04	23.33		
						0.5128E+04	20.81		
						0.1016E+05	19.76		
						0.1959E+05	18.55		
						0.4969E+05	17.51		
						0.1012E+06	16.82		
						0.4822E+06	15.69		
						0.9573E+06	15.95		
						0.1951E+07	15.58		
0.4949E+07	14.79								

TABLE 4.4. EXPERIMENTAL DATA ON DIELECTRIC CONSTANT OF BASALT (FREQUENCY DEPENDENCE) (Continued)

Data Set No.	Author(s), Year [Ref. No.]	Name and Source	Minerals and/or Chemical Composition		Method Used	Experimental Data		Other Specifications							
			Weight Percent	Volume Percent		Frequency, ν , Hz	Dielectric Constant ϵ'								
143	Jisoo, R., et al., 1973 [15]	Same as above	Same as above		Same as above	0.973E+02	32.50	Step 4: After sample was baked at 95°C for 2 days and dried in the circulating N ₂ -gas overnight.							
						0.203E+03	29.33								
						0.5147E+03	24.44								
						0.1019E+04	21.93								
						0.2074E+04	20.24								
						0.5113E+04	18.37								
						0.9862E+04	17.64								
						0.2009E+05	16.94								
						0.4958E+05	15.91								
						0.1010E+06	15.02								
						0.4814E+06	14.66								
						0.9291E+06	14.40								
						0.1947E+07	14.15								
						0.4803E+07	13.51								
						144	Jisoo, R., et al., 1973 [15]		Same as above	Same as above		Same as above	0.1021E+03	23.66	Step 5: After sample was baked at 95°C for 28 more days and dried in circulating N ₂ -gas overnight.
													0.2132E+03	20.29	
													0.5254E+03	18.20	
0.1070E+04	17.29														
0.2009E+04	16.79														
0.5240E+04	16.31														
0.1039E+05	15.75														
0.2061E+05	15.39														
0.5229E+05	14.94														
0.1009E+06	14.60														
0.4809E+06	14.01														
0.9543E+06	14.00														
0.1946E+07	13.91														
0.4943E+07	13.98														
0.1008E+08	13.97														
145	Jisoo, R., et al., 1973 [15]	Same as above	Same as above		Same as above			0.9828E+02					15.30	Step 6: After the sample was baked at 300°C for 7 more days and dried in circulating N ₂ -gas overnight.	
								0.2175E+03					14.94		
						0.5373E+03	14.76								
						0.1037E+04	14.58								
						0.2114E+04	14.41								
						0.5223E+04	14.15								
						0.1036E+05	13.98								
						0.2055E+05	13.82								
						0.5077E+05	13.65								
						0.1007E+06	13.49								
						0.4804E+06	13.31								
						0.9793E+06	13.08								
						0.1944E+07	13.29								
						0.4936E+07	13.13								
						0.1007E+08	13.27								
						146	Griffin, R.E. and Marovelli, R.L., 1967 [44]	Minnesota assumed	Feldspar Augite Magnetite		Susceptance Variation	0.2022E+08	11.87		Sample: Dry basalt. Density: 2.97 g cm ⁻³ . Other: Dried in oven at 150°C for several hours, then stored in desiccator.
												0.2022E+08	11.71		
0.2013E+08	11.50														
0.2004E+08	11.29														

TABLE 4.4. EXPERIMENTAL DATA ON DIELECTRIC CONSTANT OF BASALT (FREQUENCY DEPENDENCE) (Continued)

Data Set No.	Author(s), Year [Ref. No.]	Name and Source	Minerals and/or Chemical Composition		Method Used	Experimental Data		Other Specifications
			Components	Weight Percent		Frequency, ν , Hz	Dielectric Constant ϵ'	
146 cont.						0.2014E+08	10.31	
						0.2985E+08	11.27	
						0.3012E+08	11.37	
						0.3068E+08	11.27	
						0.4019E+08	11.03	
						0.4020E+08	10.59	
						0.4021E+08	10.35	
						0.4986E+08	10.22	
						0.4986E+08	10.41	
						0.5030E+08	10.89	
						0.5055E+08	10.36	
						0.5078E+08	10.22	
						0.6043E+08	10.33	
						0.6014E+08	10.90	
						0.6125E+08	10.90	
						0.6127E+08	10.33	
						0.7061E+08	10.24	
						0.6996E+08	10.43	
						0.8026E+08	10.34	
						0.7989E+08	10.48	
						0.8024E+08	10.92	
						0.8100E+08	10.44	
						0.9082E+08	10.30	
						0.8999E+08	10.49	
						0.8997E+08	10.98	
						0.9037E+08	11.18	
						0.1004E+09	10.98	
0.1004E+09	10.54							
147	Griffin, R.E., et al., 1967 [44]	Same as above	Same as above		Same as above	0.1992E+08	11.43	Sample: Wet basalt. Density: 2.97 g cm ⁻³ . Other: Samples stored in 100% humidity for several days.
						0.2029E+08	11.44	
						0.2029E+08	11.54	
						0.2482E+08	11.42	
						0.2527E+08	11.79	
						0.2529E+08	11.27	
						0.2575E+08	11.37	
						0.3023E+08	11.24	
						0.3022E+08	11.50	
						0.3531E+08	11.53	
						0.3533E+08	11.01	
						0.3580E+08	11.53	
						0.4033E+08	11.34	
						0.4034E+08	11.09	
						0.5025E+08	11.17	
						0.5026E+08	11.02	
						0.5050E+08	10.87	
						0.5029E+08	10.62	
						0.5956E+08	10.80	
						0.5955E+08	10.95	
						0.6006E+08	11.36	
						0.6093E+08	10.95	

TABLE 4.4. EXPERIMENTAL DATA ON DIELECTRIC CONSTANT OF BASALT (FREQUENCY DEPENDENCE) (Continued)

Data Set No.	Author(s), Year [Ref. No.]	Name and Source	Minerals and/or Chemical Composition		Method Used	Experimental Data		Other Specifications
			Weight Percent	Volume Percent		Frequency, ν , Hz	Dielectric Constant ϵ'	
						0.6093E+08	10.85	
						0.7055E+08	10.82	
						0.7053E+08	11.02	
						0.8087E+08	11.41	
						0.8091E+08	11.10	
						0.8093E+08	10.89	
						0.8828E+08	10.96	
						0.9076E+08	10.76	
						0.9073E+08	10.96	
						0.9070E+08	11.22	
						0.9283E+08	10.97	
						0.9902E+08	10.68	
						0.1004E+09	10.68	
						0.1008E+09	10.88	
						0.1008E+09	11.29	

147
cont.

or more is often found for the temperature considered (data sets 95-115). This difference is attributed to biotite and pyroxane present in the sample. It is well known that the presence of biotite modifies low frequency response drastically. The general observation that block samples have a higher dielectric constant than powdered samples is well supported by the studies on powdered samples (see, for instance, data sets 95-102) and on block samples (data sets 108-115).

The frequency dependence of dielectric constant shows a very high value at 10^2 Hz which generally decreases or remains constant in the range 10^2 Hz to 10^3 Hz. The relative dielectric constant behavior is not understood fully in this frequency region. Dielectric constant at higher frequencies is essentially independent of frequencies (see, for example, data sets 63 and 64).

The effect of water (or moisture) content on relative dielectric constant was of concern to Griffin and Marovelli [44] and to Saint Amant and Strangway [26]. It is seen that water or moisture generally increases the relative dielectric constant. However, this increase from 10^2 Hz to 10^7 Hz for low water or moisture content does not depend on frequencies (see, for instance, data sets 110-112). At higher moisture this increase content becomes frequency dependent (see, for instance, data sets 113-115). This frequency dependency suggests an existence of 'critical water (moisture) content' which is known as 'threshold water (moisture) content.' Thus, a 'threshold' or 'critical' water (moisture) content in basalt-water system is defined as the water (moisture) content above which frequency dependence is important. At present, the factors affecting this 'critical amount' are not fully known; however, this critical amount is expected to be somewhere near the amount responsible for ionic conduction.

4.4.2. Tangent of Loss Angle ($\tan \delta$) of Basalt

Overall about 120 data sets have been compiled covering frequencies from 10^2 Hz to 10^8 Hz and are presented in Table 4.5. The selected data sets which show typical behavior are shown in Figure 4.9. As in the case of dielectric constant, the loss factor (i.e., $\tan \delta$) is also studied on the block and powdered samples both in dry as well as partially and fully saturated conditions. The information on chemical composition and mineralogical characterization of samples is also reported wherever possible, but no attempt is made to correlate the property with mineralogical composition.

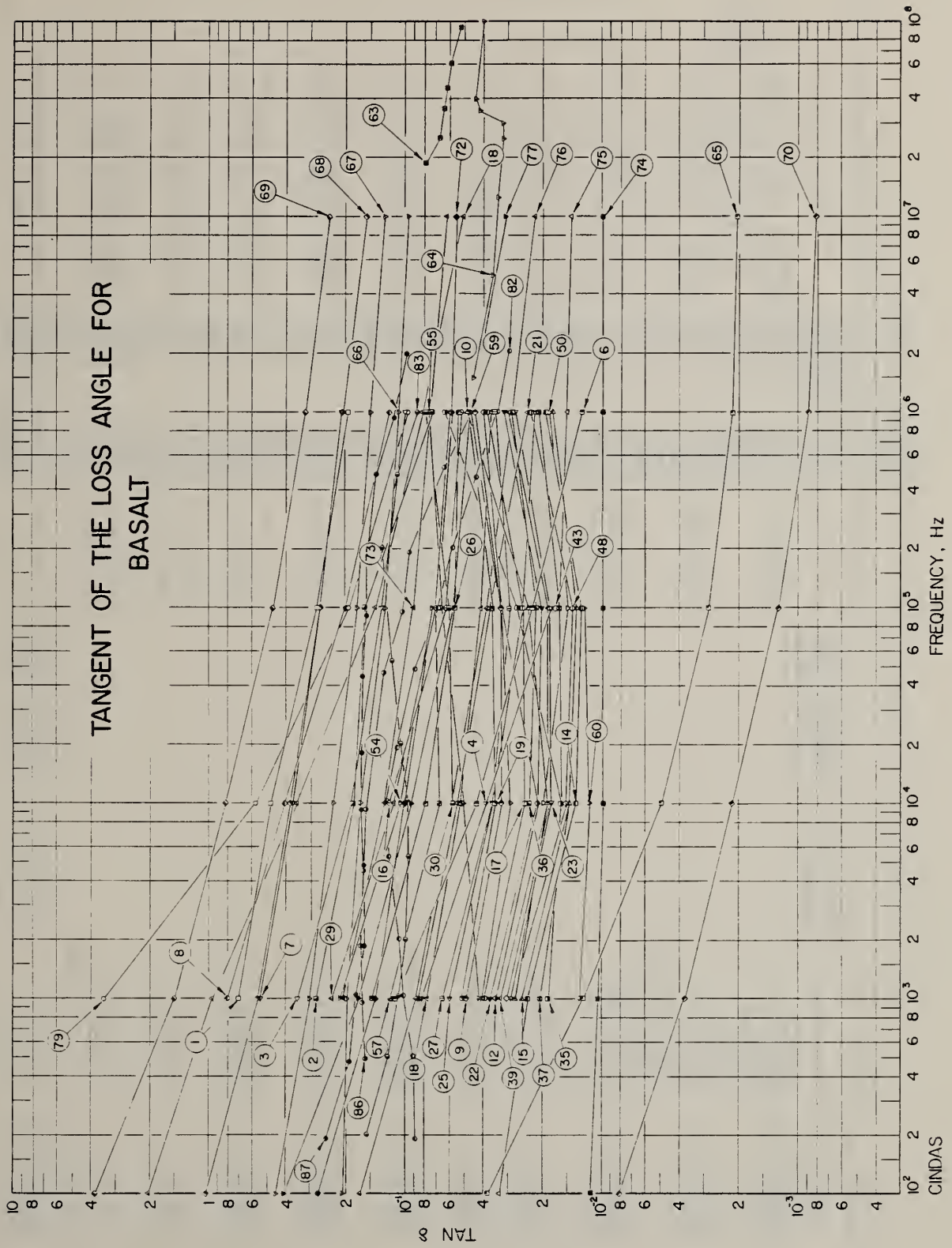


Figure 4.9. Tangent of the loss angle for basalt.

TABLE 4.5. EXPERIMENTAL DATA ON TANGENT OF LOSS ANGLE OF BASALT (FREQUENCY DEPENDENCE)

Data Set No.	Author(s), Year [Ref. No.]	Name and Source	Minerals and/or Chemical Composition		Experimental Data		Other Specifications	
			Component	Weight Percent	Method Used	Frequency, ν , Hz		Tangent of Loss Angle $\tan \delta$
1	Olhoeft, G.R., 1979 [6]	Basalt Hornblende (7.5), Chaffee, CO			Capacitance	1.0E+03	Density: 2.635 Mg m ⁻³ (dry).	
					Meter	1.0E+04	0.4890	Other: Measurement was performed by using a three terminal sample holder in 8% relative humidity; T=293 K.
						1.0E+05	0.2843	
2	Olhoeft, G.R., 1979 [6]	Basalt Smuggalaoidal (246-6); Michigan			Same as above	1.0E+06	0.1973	
						1.0E+03	0.2826	Density: 3.134 Mg m ⁻³ (dry).
						1.0E+04	0.1843	Other: Same as above.
3	Olhoeft, G.R., 1979 [6]	Basalt Ilcoc (58.5); USRM			Same as above	1.0E+06	0.1161	
						1.0E+03	0.0737	
						1.0E+04	0.3533	Density: 2.843 Mg m ⁻³ (dry).
4	Olhoeft, G.R., 1979 [6]	Basalt (166.6A); Hawaii			Same as above	1.0E+03	0.1851	
						1.0E+04	0.1133	Other: Same as above.
						1.0E+05	0.1133	
5	Olhoeft, G.R., 1979 [6]	Basalt (166.6B); Hawaii			Same as above	1.0E+06	0.1004	
						1.0E+03	0.0833	Density: 2.365 Mg m ⁻³ (dry).
						1.0E+04	0.0392	Other: Same as above.
6	Olhoeft, G.R., 1979 [6]	Basalt (166.6C); Hawaii			Same as above	1.0E+05	0.0183	
						1.0E+03	0.0791	Same as above.
						1.0E+04	0.0368	
7	Olhoeft, G.R., 1979 [6]	Basalt (166.6D); Hawaii			Same as above	1.0E+05	0.0185	
						1.0E+03	0.1117	Same as above.
						1.0E+04	0.0438	
8	Olhoeft, G.R., 1979 [6]	Basalt (5.5); Chaffee, CO			Same as above	1.0E+05	0.0229	
						1.0E+03	0.0229	Density: 1.953 Mg m ⁻³ (dry).
						1.0E+04	0.2762	Other: Same as above.
9	Olhoeft, G.R., 1979 [6]	Basalt (6.5); Germany			Same as above	1.0E+06	0.2136	
						1.0E+03	0.5480	Density: 3.030 Mg m ⁻³ (dry).
						1.0E+04	0.3763	Other: Same as above.
10	Olhoeft, G.R., 1979 [6]	Basalt (R604); Hawaii			Same as above	1.0E+05	0.2020	
						1.0E+03	0.8048	Density: 2.136 Mg m ⁻³ (dry).
						1.0E+04	0.4278	Other: Same as above.
11	Olhoeft, G.R., 1979 [6]	Basalt (R606); Hawaii			Same as above	1.0E+06	0.1220	
						1.0E+03	0.0494	Density: 2.230 Mg m ⁻³ (dry).
						1.0E+04	0.0325	Other: Same as above.
12	Olhoeft, G.R., 1979 [6]	Basalt (R607); Hawaii			Same as above	1.0E+05	0.0327	
						1.0E+03	0.0441	Density: 2.184 Mg m ⁻³ (dry).
						1.0E+04	0.0238	Other: Same as above.
13	Olhoeft, G.R., 1979 [6]	Basalt (R608); Hawaii			Same as above	1.0E+06	0.0487	
						1.0E+03	0.0277	Density: 2.029 Mg m ⁻³ (dry).
						1.0E+04	0.0190	Other: Same as above.
14	Olhoeft, G.R., 1979 [6]	Basalt (R609); Hawaii			Same as above	1.0E+05	0.0210	
						1.0E+03	0.0210	Density: 2.184 Mg m ⁻³ (dry).
						1.0E+04	0.0185	Other: Same as above.
15	Olhoeft, G.R., 1979 [6]	Basalt (R610); Hawaii			Same as above	1.0E+06	0.0409	
						1.0E+03	0.0349	Density: 2.029 Mg m ⁻³ (dry).
						1.0E+04	0.0212	Other: Same as above.
16	Olhoeft, G.R., 1979 [6]	Basalt (R611); Hawaii			Same as above	1.0E+05	0.0233	
						1.0E+03	0.0233	Density: 2.029 Mg m ⁻³ (dry).
						1.0E+04	0.0404	Other: Same as above.

TABLE 4.5. EXPERIMENTAL DATA ON TANGENT OF LOSS ANGLE OF BASALT (FREQUENCY DEPENDENCE) (Continued)

Data Set No.	Author(s), Year [Ref. No.]	Name and Source	Minerals and/or Chemical Composition [Ref. No.]	Minerals and/or Chemical Composition		Method Used	Experimental Data		Other Specifications
				Weight Percent	Volume Percent		Frequency, ν , Hz	Tangent of Loss Angle $\tan \delta$	
13	Olhoeft, G.R., 1979 [6]	Basalt (R609); Hawaii			Same as above	1.0E+03 1.0E+04 1.0E+05 1.0E+06	0.0283 0.0196 0.0180 0.0235	Density: 2.048 Mg m ⁻³ (dry). Other: Same as above.	
14	Olhoeft, G.R., 1979 [6]	Basalt (R610); Hawaii			Same as above	1.0E+03 1.0E+04 1.0E+05 1.0E+06	0.0238 0.0137 0.0127 0.0194	Density: 2.043 Mg m ⁻³ (dry). Other: Same as above.	
15	Olhoeft, G.R., 1979 [6]	Basalt (R611); Hawaii			Same as above	1.0E+03 1.0E+04 1.0E+05 1.0E+06	0.0255 0.0146 0.0134 0.0177	Density: 1.630 Mg m ⁻³ (dry). Other: Same as above.	
16	Olhoeft, G.R., 1979 [6]	Basalt (R612); Hawaii			Same as above	1.0E+03 1.0E+04 1.0E+05 1.0E+06	0.2762 0.1208 0.0624 0.0522	Density: 2.462 Mg m ⁻³ (dry). Other: Same as above.	
17	Olhoeft, G.R., 1979 [6]	Basalt (R613); Hawaii			Same as above	1.0E+03 1.0E+04 1.0E+05 1.0E+06	0.0397 0.0246 0.0254 0.0385	Density: 2.617 Mg m ⁻³ (dry). Other: Same as above.	
18	Olhoeft, G.R., 1979 [6]	Basalt (R614); Hawaii			Same as above	1.0E+03 1.0E+04 1.0E+05 1.0E+06	0.0793 0.0532 0.0415 0.0374	Density: 2.807 Mg m ⁻³ (dry). Other: Same as above.	
19	Olhoeft, G.R., 1979 [6]	Basalt (R615); Hawaii			Same as above	1.0E+03 1.0E+04 1.0E+05 1.0E+06	0.0514 0.0350 0.0362 0.0482	Density: 2.817 Mg m ⁻³ (dry). Other: Same as above.	
20	Olhoeft, G.R., 1979 [6]	Basalt (R616); Hawaii			Same as above	1.0E+03 1.0E+04 1.0E+05 1.0E+06	0.0336 0.0224 0.0260 0.0399	Density: 2.882 Mg m ⁻³ (dry). Other: Same as above.	
21	Olhoeft, G.R., 1979 [6]	Basalt (R617); Hawaii			Same as above	1.0E+03 1.0E+04 1.0E+05 1.0E+06	0.0880 0.0545 0.0374 0.0241	Density: 2.105 Mg m ⁻³ (dry). Other: Same as above.	
22	Olhoeft, G.R., 1979 [6]	Basalt (R618); Hawaii			Same as above	1.0E+03 1.0E+04 1.0E+05 1.0E+06	0.0370 0.0215 0.0202 0.0315	Density: 1.979 Mg m ⁻³ (dry). Other: Same as above.	
23	Olhoeft, G.R., 1979 [6]	Basalt (R619); Hawaii			Same as above	1.0E+03 1.0E+04 1.0E+05 1.0E+06	0.0291 0.0180 0.0184 0.0278	Density: 1.949 Mg m ⁻³ (dry). Other: Same as above.	

TABLE 4.5. EXPERIMENTAL DATA ON TANGENT OF LOSS ANGLE OF BASALT (FREQUENCY DEPENDENCE) (Continued)

Data Set No.	Author(s), Year [Ref. No.]	Name and Source	Minerals and/or Chemical Composition		Method Used		Experimental Data		Other Specifications
			Components	Weight Percent	Volume Percent	Frequency, ν , Hz	Tangent of Loss Angle $\tan \delta$		
24	Olhoeft, G.R., 1979 [6]	Basalt (R620); Hawaii			Same as above	1.0E+03 1.0E+04 1.0E+05 1.0E+06	0.0334 0.0212 0.0226 0.0357	Density: 2.402 Mg m ⁻³ (dry). Other: Same as above.	
25	Olhoeft, G.R., 1979 [6]	Basalt (R621); Hawaii			Same as above	1.0E+03 1.0E+04 1.0E+05 1.0E+06	0.0597 0.0354 0.0255 0.0223	Density: 2.384 Mg m ⁻³ (dry). Other: Same as above.	
26	Olhoeft, G.R., 1979 [6]	Basalt (R622); Hawaii			Same as above	1.0E+03 1.0E+04 1.0E+05 1.0E+06	0.1487 0.0796 0.0564 0.0534	Density: 2.613 Mg m ⁻³ (dry). Other: Same as above.	
27	Olhoeft, G.R., 1979 [6]	Basalt (R623); Hawaii			Same as above	1.0E+03 1.0E+04 1.0E+05 1.0E+06	0.0648 0.0349 0.0299 0.0351	Density: 2.498 Mg m ⁻³ (dry). Other: Same as above.	
28	Olhoeft, G.R., 1979 [6]	Basalt (R624); Hawaii			Same as above	1.0E+03 1.0E+04 1.0E+05 1.0E+06	0.0471 0.0350 0.0342 0.0381	Density: 2.693 Mg m ⁻³ (dry). Other: Same as above.	
29	Olhoeft, G.R., 1979 [6]	Basalt (R625); Hawaii			Same as above	1.0E+03 1.0E+04 1.0E+05 1.0E+06	0.2381 0.1164 0.0715 0.0596	Density: 2.919 Mg m ⁻³ (dry). Other: Same as above.	
30	Olhoeft, G.R., 1979 [6]	Basalt (R626); Hawaii			Same as above	1.0E+03 1.0E+04 1.0E+05 1.0E+06	0.0780 0.0574 0.0607 0.0783	Density: 2.886 Mg m ⁻³ (dry). Other: Same as above.	
31	Olhoeft, G.R., 1979 [6]	Basalt (R628); Hawaii			Same as above	1.0E+03 1.0E+04 1.0E+05 1.0E+06	0.0582 0.0387 0.0307 0.0382	Density: 1.414 Mg m ⁻³ (dry). Other: Same as above.	
32	Olhoeft, G.R., 1979 [6]	Basalt (R629); Hawaii			Same as above	1.0E+03 1.0E+04 1.0E+05 1.0E+06	0.0286 0.0187 0.0195 0.0296	Density: 1.649 Mg m ⁻³ (dry). Other: Same as above.	
33	Olhoeft, G.R., 1979 [6]	Basalt (R630); Hawaii			Same as above	1.0E+03 1.0E+04 1.0E+05 1.0E+06	0.0328 0.0181 0.0172 0.0317	Density: 2.012 Mg m ⁻³ (dry). Other: Same as above.	
34	Olhoeft, G.R., 1979 [6]	Basalt (R631); Hawaii			Same as above	1.0E+03 1.0E+04 1.0E+05 1.0E+06	0.0321 0.0186 0.0185 0.0408	Density: 2.595 Mg m ⁻³ (dry). Other: Same as above.	

TABLE 4.5. EXPERIMENTAL DATA ON TANGENT OF LOSS ANGLE OF BASALT (FREQUENCY DEPENDENCE) (Continued)

Data Set No.	Author(s), Year [Ref. No.]	Name and Source	Minerals and/or Chemical Composition		Experimental Data		Other Specifications
			Components	Weight Percent	Method Used	Frequency, V , Hz	
35	Olhoeft, G.R., 1979 [6]	Basalt (R632); Hawaii			Same as above	1.0E+03 1.0E+04 1.0E+05 1.0E+06	0.0188 0.0161 0.0272 0.0629 Density: 2.527 Mg m ⁻³ (dry). Other: Same as above.
36	Olhoeft, G.R., 1979 [6]	Basalt (R802-A); Hawaii			Same as above	1.0E+03 1.0E+04 1.0E+05 1.0E+06	0.0395 0.0236 0.0215 0.0285 Density: 1.612 Mg m ⁻³ (dry). Other: Same as above.
37	Olhoeft, G.R., 1979 [6]	Basalt (R802-B); Hawaii			Same as above	1.0E+03 1.0E+04 1.0E+05 1.0E+06	0.0205 0.0148 0.0165 0.0212 Density: 0.0767 Mg m ⁻³ (dry). Other: Same as above.
38	Olhoeft, G.R., 1979 [6]	Basalt (R802-C); Hawaii			Same as above	1.0E+03 1.0E+04 1.0E+05 1.0E+06	0.0258 0.0140 0.0149 0.0227 Density: 0.814 Mg m ⁻³ (dry). Other: Same as above.
39	Olhoeft, G.R., 1979 [6]	Basalt (R802-X-1); Hawaii			Same as above	1.0E+03 1.0E+04 1.0E+05 1.0E+06	0.0335 0.0192 0.0187 0.0297 Density: 1.932 Mg m ⁻³ (dry). Other: Same as above.
40	Olhoeft, G.R., 1979 [6]	Basalt (R802-X-2); Hawaii			Same as above	1.0E+03 1.0E+04 1.0E+05 1.0E+06	0.0274 0.0179 0.0191 0.0310 Density: 1.775 Mg m ⁻³ (dry). Other: Same as above.
41	Olhoeft, G.R., 1979 [6]	Basalt (R802-X-3); Hawaii			Same as above	1.0E+03 1.0E+04 1.0E+05 1.0E+06	0.0330 0.0179 0.0183 0.0307 Density: 1.454 Mg m ⁻³ (dry). Other: Same as above.
42	Olhoeft, G.R., 1979 [6]	Basalt (R803-A-1); Hawaii			Same as above	1.0E+03 1.0E+04 1.0E+05 1.0E+06	0.0369 0.0241 0.0223 0.0325 Density: 1.624 Mg m ⁻³ (dry). Other: Same as above.
43	Olhoeft, G.R., 1979 [6]	Basalt (R803-A-2); Hawaii			Same as above	1.0E+03 1.0E+04 1.0E+05 1.0E+06	0.0301 0.0187 0.0173 0.0222 Density: 1.319 Mg m ⁻³ (dry). Other: Same as above.
44	Olhoeft, G.R., 1979 [6]	Basalt (R803-A-3); Hawaii			Same as above	1.0E+03 1.0E+04 1.0E+05 1.0E+06	0.0361 0.0192 0.0186 0.0234 Density: 1.038 Mg m ⁻³ (dry). Other: Same as above.
45	Olhoeft, G.R., 1979 [6]	Basalt (R804-1); Hawaii			Same as above	1.0E+03 1.0E+04 1.0E+05 1.0E+06	0.0208 0.0171 0.0181 0.0206 Density: 1.048 Mg m ⁻³ (dry). Other: Same as above.

TABLE 4.5. EXPERIMENTAL DATA ON TANGENT OF LOSS ANGLE OF BASALT (FREQUENCY DEPENDENCE) (Continued)

Data Set No.	Author(s), Year [Ref. No.]	Name and Source	Minerals and/or Chemical Composition		Experimental Data		Method Used	Frequency, ν , Hz	Tangent of Loss Angle $\tan \delta$	Other Specifications
			Componenta	Weight Percent	Volume Percent	Volume Percent				
46	Olhoeft, G.R., 1979 [6]	Basalt (R804-2); Hawaii					Same as above	1.0E+03 1.0E+04 1.0E+05 1.0E+06	0.0135 0.0110 0.0112 0.0127	Density: 0.928 Mg m ⁻³ (dry). Other: Same as above.
47	Olhoeft, G.R., 1979 [6]	Basalt (R805-1); Hawaii					Same as above	1.0E+03 1.0E+04 1.0E+05 1.0E+06	0.0294 0.0163 0.0148 0.0244	Density: 0.837 Mg m ⁻³ (dry). Other: Same as above.
48	Olhoeft, G.R., 1979 [6]	Basalt (R805-2); Hawaii					Same as above	1.0E+03 1.0E+04 1.0E+05 1.0E+06	0.0285 0.0152 0.0143 0.0230	Density: 0.876 Mg m ⁻³ (dry). Other: Same as above.
49	Olhoeft, G.R., 1979 [6]	Basalt (R806-1); Hawaii					Same as above	1.0E+03 1.0E+04 1.0E+05 1.0E+06	0.0135 0.0145 0.0134 0.0121	Density: 0.769 Mg m ⁻³ (dry). Other: Same as above.
50	Olhoeft, G.R., 1979 [6]	Basalt (R807-A); Hawaii					Same as above	1.0E+03 1.0E+04 1.0E+05 1.0E+06	0.0351 0.0194 0.0149 0.0188	Density: 0.844 Mg m ⁻³ (dry). Other: Same as above.
51	Olhoeft, G.R., 1979 [6]	Basalt (R807-B); Hawaii					Same as above	1.0E+03 1.0E+04 1.0E+05 1.0E+06	0.0430 0.0213 0.0166 0.0221	Density: 0.853 Mg m ⁻³ (dry). Other: Same as above.
52	Olhoeft, G.R., 1979 [6]	Basalt (R808-A); Hawaii					Same as above	1.0E+03 1.0E+04 1.0E+05 1.0E+06	0.0292 0.0196 0.0201 0.0214	Density: 0.802 Mg m ⁻³ (dry). Other: Same as above.
53	Olhoeft, G.R., 1979 [6]	Basalt (R808-B); Hawaii					Same as above	1.0E+03 1.0E+04 1.0E+05 1.0E+06	0.0341 0.0198 0.0204 0.0224	Density: 0.837 Mg m ⁻³ (dry). Other: Same as above.
54	Olhoeft, G.R., 1979 [6]	Basalt (R815); Hawaii					Same as above	1.0E+03 1.0E+04 1.0E+05 1.0E+06	0.2114 0.1051 0.0721 0.0631	Density: 2.925 Mg m ⁻³ (dry). Other: Same as above.
55	Olhoeft, G.R., 1979 [6]	Basalt (R816); Hawaii					Same as above	1.0E+03 1.0E+04 1.0E+05 1.0E+06	0.0420 0.0503 0.0642 0.0773	Density: 2.874 Mg m ⁻³ (dry). Other: Same as above.
56	Olhoeft, G.R., 1979 [6]	Basalt (R818); Hawaii					Same as above	1.0E+03 1.0E+04 1.0E+05 1.0E+06	0.0191 0.0189 0.0214 0.0275	Density: 3.039 Mg m ⁻³ (dry). Other: Same as above.

TABLE 4.5. EXPERIMENTAL DATA ON TANGENT OF LOSS ANGLE OF BASALT (FREQUENCY DEPENDENCE) (Continued)

Data Set No.	Author(s), Year [Ref. No.]	Name and Source	Minerals and/or Chemical Composition	Experimental Data			Other Specifications
				Weight Percent	Volume Percent	Method Used	
				ν , Hz	Frequency, Loss Angle	Tangent of Loss Angle	
				Components	$\tan \delta$		
57	Olhoeft, G. R., 1979 [6]	Basalt (R819); Hawaii		Same as above	1.0E+03 1.0E+04 1.0E+05 1.0E+06	0.1196 0.0677 0.0708 0.0738	Density: 3.019 Mg m ⁻³ (dry). Other: Same as above.
58	Olhoeft, G. R., 1979 [6]	Basalt (R821-A); Hawaii		Same as above	1.0E+03 1.0E+04 1.0E+05 1.0E+06	0.0321 0.0224 0.0254 0.0386	Density: 2.545 Mg m ⁻³ (dry). Other: Same as above.
59	Olhoeft, G. R., 1979 [6]	Basalt (R821-B); Hawaii		Same as above	1.0E+03 1.0E+04 1.0E+05 1.0E+06	0.0403 0.0293 0.0324 0.0467	Density: 2.614 Mg m ⁻³ (dry). Other: Same as above.
60	Olhoeft, G. R., 1979 [6]	Basalt (R822-A); Hawaii		Same as above	1.0E+03 1.0E+04 1.0E+05 1.0E+06	0.0131 0.0115 0.0124 0.0187	Density: 2.914 Mg m ⁻³ (dry). Other: Same as above.
61	Olhoeft, G. R., 1979 [6]	Basalt (R822-B); Hawaii		Same as above	1.0E+03 1.0E+04 1.0E+05 1.0E+06	0.0131 0.0116 0.0134 0.0204	Density: 2.863 Mg m ⁻³ (dry). Other: Same as above.
62	Olhoeft, G. R., 1979 [6]	Basalt (R823-B); Hawaii		Same as above	1.0E+03 1.0E+04 1.0E+05 1.0E+06	0.0362 0.0243 0.0264 0.0385	Density: 2.255 Mg m ⁻³ (dry). Other: Same as above.
63	Griffin, R.E. and Marovelli, R.L., 1967 [41]	Basalt; Dresser, WI	Feldspar (Labradorite), Microcline Augite Magnetite	50 40 8	1.88E+07 2.07E+07 2.28E+07 2.54E+07 2.84E+07 3.29E+07 3.58E+07 4.13E+07 5.04E+07 6.19E+07 7.15E+07 8.35E+07 9.69E+07 1.07E+08	0.0793 0.0741 0.0707 0.0677 0.0656 0.0644 0.0637 0.0632 0.0618 0.0589 0.0560 0.0537 0.0526 0.0518	Density: 2.97 Mg m ⁻³ . Texture: Mottled, gray-green; fine-grained. Other: Data were extracted from the figure of computer fitted curve; T=293 K.
64	Bondarenko, A.T., 1971 [42]	Basalt; Russia		Michelson Interferometer	1.50E+06 5.00E+06 1.25E+07 2.50E+07 3.00E+07 3.50E+07 4.00E+07 1.00E+08 1.30E+08 1.65E+08	0.045 0.036 0.034 0.032 0.042 0.044 0.040 0.038 0.038	Density: 2.55 Mg m ⁻³ . Other: T=293 K.

TABLE 4.5. EXPERIMENTAL DATA ON TANGENT OF LOSS ANGLE OF BASALT (FREQUENCY DEPENDENCE) (Continued)

Data Set No.	Author(s), Year [Ref. No.]	Name and Source	Minerals and/or Chemical Composition		Method Used	Experimental Data		Other Specifications
			Components	Weight Percent		Frequency, ν , Hz	Tangent of Loss Angle $\tan \delta$	
65	Chung, D.H., Westphal, W.B., and Simmons, G., 1970 [23]	Lunar Basalt 10020; Moon	Pyroxene Plagioclase Ilmenite Olivine Unidentified Cristobalite Troilite	53	Two Terminal	1.0E+02	0.0382	Density: 3.18 Mg m^{-3} (bulk). Other: High-purity tin foil of 0.025 mm thickness was hard-pressed onto two parallel faces of the rectangular parallelepiped samples; sample was baked at 423 K in vacuum; high temperature runs in dry N_2 ; constant temperature frequency runs were made with the sample holder immersed in baths of ice, dry ice, or liquid N_2 ; authors estimated accuracy within $\pm 3\%$; $T=77 \text{ K}$.
				25	Capacitance	1.0E+03	0.0127	
				15	Substitution	1.0E+04	0.00496	
				4	Method	1.0E+05	0.00285	
				1.4		1.0E+06	0.00216	
				1		1.0E+07	0.00204	
				0.6				
66	Chung, D.H., et al., 1970 [23]	Same as above	Same as above		Same as above	1.0E+02	0.210	Same as above except $T=196 \text{ K}$.
						1.0E+03	0.199	
						1.0E+04	0.168	
						1.0E+05	0.127	
						1.0E+06	0.108	
						1.0E+07	0.0963	
67	Chung, D.H., et al., 1970 [23]	Same as above	Same as above		Same as above	1.0E+02	0.454	Same as above except $T=298 \text{ K}$.
						1.0E+03	0.308	
						1.0E+04	0.234	
						1.0E+05	0.177	
						1.0E+06	0.150	
						1.0E+07	0.127	
68	Chung, D.H., et al., 1970 [23]	Same as above	Same as above		Same as above	1.0E+02	1.04	Same as above except $T=373 \text{ K}$.
						1.0E+03	0.565	
						1.0E+04	0.384	
						1.0E+05	0.275	
						1.0E+06	0.208	
						1.0E+07	0.158	
69	Chung, D.H., et al., 1970 [23]	Same as above	Same as above		Same as above	1.0E+02	3.89	Same as above except $T=473 \text{ K}$.
						1.0E+03	1.52	
						1.0E+04	0.829	
						1.0E+05	0.477	
						1.0E+06	0.324	
						1.0E+07	0.245	
70	Chung, D.H., et al., 1970 [23]	Lunar Basalt 10046; Moon	Pyroxene Plagioclase Glass Ilmenite	57	Same as above	1.0E+02	0.00817	Density: 2.21 Mg m^{-3} (bulk). Other: Same as above except $T=77 \text{ K}$.
				20		1.0E+03	0.00377	
				14		1.0E+04	0.00217	
				9		1.0E+05	0.00125	
						1.0E+06	0.000896	
						1.0E+07	0.000801	
71	Chung, D.H., et al., 1970 [23]	Same as above	Same as above		Same as above	1.0E+02	0.210	Same as above except $T=298 \text{ K}$.
						1.0E+03	0.121	
						1.0E+04	0.0821	
						1.0E+05	0.0658	
						1.0E+06	0.0588	
						1.0E+07	0.0526	

TABLE 4.5. EXPERIMENTAL DATA ON TANGENT OF LOSS ANGLE OF BASALT (FREQUENCY DEPENDENCE) (Continued)

Data Set No.	Author(s), Year [Ref. No.]	Name and Source	Minerals and/or Chemical Components	Minerals and/or Chemical Composition		Method Used	Experimental Data			Other Specifications
				Weight Percent	Volume Percent		Frequency, ν , Hz	Tangent of Loss Angle $\tan \delta$	Loss Angle	
72	Chung, D.H., et al., 1970 [23]	Same as above	Same as above			Same as above	1.0E+02	0.277	Same as above except T=373 K.	
							1.0E+03	0.143		
							1.0E+04	0.102		
							1.0E+05	0.0734		
							1.0E+06	0.0588		
73	Chung, D.H., et al., 1970 [23]	Same as above	Same as above			Same as above	1.0E+02	0.454	Same as above except T=473 K.	
							1.0E+03	0.210		
							1.0E+04	0.128		
							1.0E+05	0.0915		
							1.0E+06	0.0733		
74	Chung, D.H., et al., 1970 [23]	Hawaiian Basalt; Oahu, Hawaii	Plagioclase Pyroxene Olivine Quartz Unidentified	48 24 21 6 1		Same as above	1.0E+02	0.0114	Density: 2.68 Mg m ⁻³ . Other: Same as above except T=78 K.	
							1.0E+03	0.0104		
							1.0E+04	0.00991		
							1.0E+05	0.00991		
							1.0E+06	0.00991		
75	Chung, D.H., et al., 1970 [23]	Same as above	Same as above			Same as above	1.0E+02	0.0334	Same as above except T=188 K.	
							1.0E+03	0.0241		
							1.0E+04	0.0191		
							1.0E+05	0.0166		
							1.0E+06	0.0151		
76	Chung, D.H., et al., 1970 [23]	Same as above	Same as above			Same as above	1.0E+02	0.172	Same as above except T=273 K.	
							1.0E+03	0.0894		
							1.0E+04	0.0534		
							1.0E+05	0.0385		
							1.0E+06	0.0291		
77	Chung, D.H., et al., 1970 [23]	Same as above	Same as above			Same as above	1.0E+02	0.419	Same as above except T=298 K.	
							1.0E+03	0.172		
							1.0E+04	0.0937		
							1.0E+05	0.0560		
							1.0E+06	0.0385		
78	Chung, D.H., et al., 1970 [23]	Same as above	Same as above			Same as above	1.0E+02	2.06	Same as above except T=373 K.	
							1.0E+03	0.972		
							1.0E+04	0.362		
							1.0E+05	0.143		
							1.0E+06	0.0814		
79	Chung, D.H., et al., 1970 [23]	Same as above	Same as above			Same as above	1.0E+02	1.07	Same as above except T=473 K.	
							1.0E+03	3.44		
							1.0E+04	0.581		
							1.0E+05	0.198		
							1.0E+06	0.0981		
							1.0E+07	0.0615		

TABLE 4.5. EXPERIMENTAL DATA ON TANGENT OF LOSS ANGLE OF BASALT (FREQUENCY DEPENDENCE) (Continued)

Data Set No.	Author(s), Year [Ref. No.]	Name and Source	Minerals and/or Chemical Composition		Method Used	Experimental Data		Other Specifications
			Components	Weight Percent		Frequency, ν , Hz	Tangent of Loss Angle $\tan \delta$	
80	Saint-Amant, M. and Strangway, D.W., 1970 [26]	Basalt M; Cape Neddick, MA	Biotite	16	Capacitance	0.105E+03	0.0464	Sample: Powdered dry basalt was held in vacuum overnight. Other: Data extracted from figure; T=300 K.
						0.205E+03	0.0355	
						0.486E+03	0.0296	
						0.105E+04	0.0262	
						0.205E+04	0.0246	
						0.535E+04	0.0238	
						0.998E+04	0.0231	
						0.195E+05	0.0221	
						0.486E+05	0.0221	
						0.952E+05	0.0221	
						0.186E+06	0.0213	
						0.463E+06	0.0222	
						0.907E+06	0.0222	
0.195E+07	0.0231							
81	Saint-Amant, M. and Strangway, D.W., 1970 [26]	Same as above	Biotite	16	Same as above	0.991E+02	0.116	Same as above except T=373 K.
						0.194E+03	0.108	
						0.507E+03	0.0996	
						0.994E+03	0.0828	
						0.204E+04	0.0642	
						0.534E+04	0.0482	
						0.105E+05	0.0406	
						0.205E+05	0.0305	
						0.510E+05	0.0247	
						0.998E+05	0.0247	
						0.195E+06	0.0238	
						0.195E+07	0.0222	
						82	Saint-Amant, M. and Strangway, D.W., 1970 [26]	
0.993E+01	0.0912							
0.194E+02	0.0895							
0.507E+02	0.0912							
0.104E+03	0.101							
0.204E+04	0.106							
0.531E+04	0.120							
0.104E+04	0.123							
0.194E+05	0.108							
0.484E+05	0.0896							
0.995E+05	0.0669							
0.204E+06	0.0576							
0.463E+06	0.0433							
0.997E+05	0.0348							
0.205E+06	0.0298							
83	Saint-Amant, M. and Strangway, D.W., 1970 [26]	Same as above	Biotite	16	Same as above	0.985E+01	0.197	Same as above except T=573 K.
						0.203E+02	0.156	
						0.506E+02	0.123	
						0.104E+03	0.107	
						0.204E+03	0.0988	
						0.532E+03	0.0963	
						0.104E+04	0.0997	
						0.204E+03	0.105	

TABLE 4.5. EXPERIMENTAL DATA ON TANGENT OF LOSS ANGLE OF BASALT (FREQUENCY DEPENDENCE) (Continued)

Data Set No.	Author(s), Year [Ref. No.]	Name and Source	Minerals and/or Chemical Components	Minerals and/or Chemical Composition		Method Used	Experimental Data			Other Specifications
				Weight Percent	Volume Percent		Frequency, ν , Hz	Tangent of Loss Angle $\tan \delta$		
83										
84	Saint-Amant, M. and Strangway, D.W., 1970 [26]	Basalt AA; Westfield, MA	Biotite	>16		Same as above	0.531E+04 0.990E+04 0.203E+05 0.483E+05 0.993E+05 0.195E+06	0.117 0.125 0.131 0.110 0.0880 0.0703		Same as above except T=300 K.
85	Saint-Amant, M. and Strangway, D.W., 1970 [26]	Same as above	Biotite	>16		Same as above	0.101E+03 0.205E+03 0.503E+03 0.102E+04 0.208E+04 0.490E+04 0.952E+04 0.204E+05 0.479E+05 0.977E+05 0.209E+06 0.492E+06 0.100E+07 0.195E+07	0.0774 0.0629 0.0449 0.0372 0.0278 0.0209 0.0192 0.0157 0.0131 0.0131 0.0130 0.0155 0.0138 0.0120		Same as above except T=373 K.
86	Saint-Amant, M. and Strangway, D.W., 1970 [26]	Same as above	Biotite	>16		Same as above	0.974E+02 0.189E+03 0.512E+03 0.104E+04 0.193E+04 0.473E+04 0.962E+04 0.196E+05 0.505E+05 0.103E+06 0.190E+06 0.516E+06 0.100E+07 0.195E+07	0.154 0.149 0.134 0.129 0.116 0.0780 0.0677 0.0523 0.0387 0.0267 0.0215 0.0189 0.0180 0.0154		Same as above except T=468 K.

TABLE 4.5. EXPERIMENTAL DATA ON TANGENT OF LOSS ANGLE OF BASALT (FREQUENCY DEPENDENCE) (Continued)

Data Set No.	Author(s), Year [Ref. No.]	Name and Source	Minerals and/or Chemical Components	Weight Percent		Method Used	Experimental Data		Other Specifications
				Volume Percent	Volume Percent		Frequency, ν , Hz	Tangent of Loss Angle $\tan \delta$	
87	Saint-Amant, M. and Strangway, D.W., 1970 [26]	Same as above	Biotite	>16		Same as above	0.194E+02 0.472E+03 0.105E+03 0.186E+04 0.481E+04 0.937E+04 0.182E+04 0.449E+05 0.915E+05 0.178E+05 0.482E+06 0.931E+06 0.198E+06	0.253 0.193 0.176 0.162 0.161 0.166 0.166 0.165 0.158 0.157 0.141 0.113 0.0954	Same as above except T=570 K.
88	Saint-Amant, M. and Strangway, D.W., 1970 [26]	Basalt M; Cape Neddick, MA	Biotite	16		Same as above	0.961E+02 0.188E+03 0.494E+03 0.924E+03 0.200E+04 0.499E+04 0.980E+04 0.202E+05 0.480E+05 0.943E+05 0.194E+06 0.486E+06 0.954E+06 0.206E+07	0.164 0.122 0.101 0.0880 0.0711 0.0499 0.0498 0.0455 0.0370 0.0327 0.0326 0.0367 0.0366 0.0323	Sample: Solid basalt-dry-dried by heating in vacuum until the results were reproducible; sample was heated twice to 423 K and then to 503 K once; data is obtained after heating to 781 K once; T=300 K.
89	Saint-Amant, M. and Strangway, D.W., 1970 [26]	Same as above	Biotite	16		Same as above	0.968E+02 0.190E+03 0.496E+03 0.973E+03 0.200E+04 0.500E+04 0.981E+04 0.202E+05 0.481E+05 0.990E+05 0.194E+06 0.486E+06 0.954E+06 0.206E+07	0.631 0.497 0.345 0.273 0.210 0.147 0.121 0.100 0.0749 0.0664 0.0663 0.0536 0.0493 0.0492	Same as above except T=373 K.
90	Saint-Amant, M. and Strangway, D.W., 1970 [26]	Same as above	Biotite	16		Same as above	0.201E+03 0.500E+03 0.979E+03 0.201E+04 0.478E+04 0.984E+04 0.202E+05 0.505E+05	1.01 0.842 0.711 0.559 0.391 0.315 0.235 0.163	Same as above except T=439 K.

TABLE 4.5. EXPERIMENTAL DATA ON TANGENT OF LOSS ANGLE OF BASALT (FREQUENCY DEPENDENCE) (Continued)

Data Set No.	Author(s), Year [Ref. No.]	Name and Source	Minerals and/or Chemical Composition		Method Used	Experimental Data		Other Specifications
			Components	Weight Percent		Frequency, ν , Hz	Tangent of Loss Angle $\tan \delta$	
90 cont.								
91	Saint-Amant, M. and Strangway, D.W., 1970 [26]	Same as above	Biotite	16	Same as above	0.991E+05 0.204E+06 0.486E+06 0.954E+06 0.197E+07 0.193E+04 0.505E+04 0.104E+05 0.204E+05 0.508E+05 0.104E+06 0.205E+06 0.511E+06 0.100E+07 0.217E+07	0.125 0.108 0.0830 0.0661 0.0660 1.01 0.863 0.736 0.597 0.454 0.336 0.281 0.188 0.142 0.0997	Same as above except T=503 K.
92	Saint-Amant, M. and Strangway, D.W., 1970 [26]	Basalt AA; Westfield, MA	Biotite	>16	Same as above	0.304E+03 0.922E+03 0.308E+04 0.104E+06 0.100E+07 0.318E+07	0.0110 0.00934 0.00521 0.00535 0.00376 0.00465	Sample: Dry sample; no details on drying available for this sample. Other: T=222 K.
93	Saint-Amant, M. and Strangway, D.W., 1970 [26]	Same as above	Biotite	>16	Same as above	0.304E+03 0.966E+03 0.307E+04 0.978E+04 0.104E+06	0.0210 0.0152 0.0102 0.00860 0.00786	Same as above except T=258 K.
94	Saint-Amant, M. and Strangway, D.W., 1970 [26]	Same as above	Biotite	>16	Same as above	0.992E+02 0.205E+03 0.332E+03 0.566E+03 0.101E+04 0.199E+04 0.307E+04 0.451E+04 0.103E+05 0.104E+06 0.952E+06 0.303E+07	0.0963 0.0746 0.0662 0.0562 0.0445 0.0328 0.0261 0.0203 0.0136 0.0112 0.0113 0.0105	Same as above except T=300 K.
95	Saint-Amant, M. and Strangway, D.W., 1970 [26]	Same as above	Biotite	>16	Same as above	0.319E+03 0.966E+03 0.307E+04 0.977E+04 0.104E+06 0.952E+06 0.303E+07	0.0244 0.0202 0.0161 0.0119 0.00786 0.00878 0.00799	Sample: 0.1% H ₂ O content. Other: T=228 K.

TABLE 4.5. EXPERIMENTAL DATA ON TANGENT OF LOSS ANGLE OF BASALT (FREQUENCY DEPENDENCE) (Continued)

Date Set No.	Author(s), Year (Ref. No.)	Name and Source	Minerals and/or Chemical Components	Minerals and/or Chemical Composition		Method Used	Experimental Data		Other Specifications
				Weight Percent	Volume Percent		Frequency, ν , Hz	Tangent of Loss Angle $\tan \delta$	
96	Saint-Amant, M. and Strangway, D.W., 1970 [26]	Same as above	Biotite	>16		Same as above	0.334E+03 0.101E+04 0.199E+04 0.338E+04 0.102E+05 0.104E+06 0.329E+06 0.105E+07	0.0411 0.0353 0.0328 0.0312 0.0253 0.0221 0.0196 0.0188	Same as above except T=258 K.
97	Saint-Amant, M. and Strangway, D.W., 1970 [26]	Same as above	Biotite	>16		Same as above	0.332E+03 0.106E+04 0.321E+04 0.974E+04 0.103E+06 0.329E+06 0.104E+07	0.0863 0.0663 0.0454 0.0404 0.0371 0.0338 0.0331	Same as above except T=300 K.
98	Saint-Amant, M. and Strangway, D.W., 1970 [26]	Same as above	Biotite	>16		Same as above	0.947E+06 0.340E+03 0.107E+04 0.107E+05 0.956E+05 0.301E+06 0.947E+06	0.0210 0.0777 0.0742 0.0400 0.0296 0.0235 0.0210	Sample: 0.5% H ₂ O content. Other: T=213 K.
99	Saint-Amant, M. and Strangway, D.W., 1970 [26]	Same as above	Biotite	>16		Same as above	0.341E+03 0.102E+04 0.336E+04 0.106E+05 0.100E+06 0.316E+06 0.994E+06	0.0654 0.0742 0.0787 0.0744 0.0464 0.0367 0.0280	Same as above except T=228 K.
100	Saint-Amant, M. and Strangway, D.W., 1970 [26]	Same as above	Biotite	>16		Same as above	0.325E+03 0.321E+04 0.106E+05 0.313E+06 0.104E+07	0.0592 0.0655 0.0691 0.0737 0.0536	Same as above except T=243 K.
101	Saint-Amant, M. and Strangway, D.W., 1970 [26]	Same as above	Biotite	>16		Same as above	0.340E+03 0.107E+04 0.960E+04 0.345E+06 0.103E+07	0.0706 0.0628 0.0621 0.0852 0.0826	Same as above except T=258 K.
102	Saint-Amant, M. and Strangway, D.W., 1970 [26]	Same as above	Biotite	>16		Same as above	0.340E+03 0.107E+04 0.337E+04 0.960E+06 0.329E+06 0.108E+07	0.0812 0.0698 0.0620 0.0603 0.0808 0.0879	Same as above except T=267 K.

TABLE 4.5. EXPERIMENTAL DATA ON TANGENT OF LOSS ANGLE OF BASALT (FREQUENCY DEPENDENCE (Continued))

Data Set No.	Author(s), Year [Ref. No.]	Name and Source	Minerals and/or Chemical Composition		Experimental Data		Other Specifications	
			Components	Weight Percent	Frequency, V, Hz	Tangent of Loss Angle, $\tan \delta$		
103	Hansen, W., Sill, W.R., and Ward, S.H., 1973 [43]	Western Grand Canyon; USA	SiO ₂ Al ₂ O ₃ FeO MgO CaO Na ₂ O Ilmenite TiO ₂ K ₂ O	49.38 16.16 10.12 8.81 8.47 3.47 3.27 1.72 1.00	Contact Substitution Method 0.1257E+03 0.2541E+03 0.6688E+03 0.1544 0.1276E+04 0.1199 0.2433E+04 0.09713 0.5452E+04 0.07387 0.1038E+05 0.06380 0.2192E+05 0.06003 0.5165E+05 0.05080 0.1097E+06	0.3234 0.2118 0.1544 0.1199 0.09713 0.07387 0.06380 0.06003 0.05080 0.03946	Texture: Fine-grained. Other: Sample A; measurements were done at room temperature in dry N ₂ atmosphere; ilmenite is powdered sand from Melbourne, Florida; ilmenite (DuPont trademark) was used as matrix; measurements were done at room temperature and pressure; accuracy $\pm 5\%$.	
104	Hansen, W., et al., 1973 [43]	Same as above	Same as above		Same as above	0.1207E+03 0.2583E+03 0.1141 0.5796E+03 0.08141 0.1163E+04 0.07033 0.2223E+04 0.05232 0.5248E+04 0.04153 0.1110E+05 0.03666 0.2229E+05 0.03167 0.5256E+05 0.02623 0.1005E+06	0.1980 0.1141 0.08141 0.07033 0.05232 0.04153 0.03666 0.03167 0.02623 0.01870	Texture: Coarse-grained. Other: Same as above except Sample J.
105	Jisoo, R., Ward, S.H., Nash, W.P., and Buzzell, D., 1973 [15]	Duluth Hornfels; MN	Plagioclase Pyroxene Ilmenite Other Olivine	40.6 39.2 11.3 5.6 3.3	0.5682E+04 0.2042 0.5771E+05 0.1173 0.1163E+06	0.2042 0.1173 0.09889	Step 1: At ambient conditions.	
106	Jisoo, R., et al., 1973 [15]	Same as above	Same as above		Contact Substitution Method 0.1106E+03 0.2107E+03 0.5558E+03 0.4513 0.1122E+04 0.3565 0.2148E+04 0.2816 0.1145E+05 0.1759 0.2073E+05 0.1483	0.5942 0.5583 0.4513 0.3565 0.2816 0.1759 0.1483	Same as above.	
107	Jisoo, R., et al., 1973 [15]	Same as above	Same as above		Variable Air Gap 0.1164E+03 0.6482 0.2105E+03 0.5831 0.5548E+03 0.4817 0.1122E+04 0.3643 0.2145E+04 0.2941 0.1143E+05 0.1878 0.2070E+05 0.1548	0.6482 0.5831 0.4817 0.3643 0.2941 0.1878 0.1548	Same as above.	
108	Jisoo, R., et al., 1973 [15]	Same as above	Same as above		Optimum Technique Combining V.A. and C.S. 0.1102E+03 0.6769 0.2101E+03 0.6224 0.5535E+03 0.5254 0.1120E+04 0.3889 0.2261E+04 0.3072 0.1141E+05 0.1961 0.2182E+05 0.1618	0.6769 0.6224 0.5254 0.3889 0.3072 0.1961 0.1618	Same as above.	

TABLE 4.5. EXPERIMENTAL DATA ON TANGENT OF LOSS ANGLE OF BASALT (FREQUENCY DEPENDENCE) (Continued)

Data Set No.	Author(s), Year [Ref. No.]	Name and Source	Minerals and/or Chemical Composition Components	Chemical Composition		Method Used	Experimental Data		Other Specifications
				Weight Percent	Volume Percent		Frequency, ν , Hz	Tangent of Loss Angle $\tan \delta$	
109	Jisoo, R., et al., 1973 [15]	Same as above	Same as above			Optimum Technique	0.2203E+03 0.1147E+04 0.2175E+04	0.4893 0.3396 0.2859	Step 2: After sample dried in a vacuum of 3×10^{-3} Torr for 2 days and in the circulating N_2 -gas for 2 days.
110	Jisoo, R., et al., 1973 [15]	Same as above	Same as above			Variable Air Gap	0.2205E+03 0.1149E+04 0.2177E+04	0.4685 0.3182 0.2679	Same as above.
111	Jisoo, R., et al., 1973 [15]	Same as above	Same as above			Contact Substitution Method	0.2205E+03 0.1150E+04 0.2177E+04	0.4584 0.2981 0.2621	Same as above.
112	Jisoo, R., et al., 1973 [15]	Same as above	Same as above			Optimum Technique	0.1294E+03 0.5748E+03 0.5996E+04 0.1137E+05 0.2273E+05 0.5930E+05 0.1124E+06	0.5447 0.3779 0.1897 0.1563 0.1260 0.09732 0.08373	Same as above.
113	Jisoo, R., et al., 1973 [15]	Same as above	Same as above			O.T., C.S., V.A.	0.1077E+03 0.2157E+03 0.5072E+03 0.1071E+04 0.1929E+04 0.5046E+04 0.1011E+05 0.2135E+05 0.5020E+05 0.1005E+06	0.6777 0.5233 0.4041 0.3259 0.2627 0.1943 0.1533 0.1291 0.09758 0.08215	Step 3: After tin foil was placed on the sample and the sample was dried in a vacuum of 3×10^{-3} Torr for 2 days.
114	Jisoo, R., et al., 1973 [15]	Same as above	Same as above			Optimum Technique	0.9554E+02 0.1892E+03 0.4654E+03 0.9434E+03 0.1864E+04 0.4702E+04 0.9302E+04 0.1889E+05 0.4642E+05 0.9431E+05	0.6841 0.6171 0.5030 0.3794 0.3130 0.2281 0.1968 0.1605 0.1251 0.1043	Step 1: At ambient conditions.
115	Jisoo, R., et al., 1973 [15]	Same as above	Same as above			Same as above	0.9772E+02 0.1933E+03 0.4624E+03 0.9413E+03 0.1860E+04 0.4684E+04 0.9774E+04 0.1986E+05 0.4620E+05 0.9397E+05	0.5470 0.4666 0.3719 0.3431 0.2830 0.1907 0.1538 0.1283 0.1000 0.08824	Step 2: After sample was dried in a vacuum of 3×10^{-3} Torr for 2 days and in circulating N_2 -gas for 2 days.

TABLE 4.5. EXPERIMENTAL DATA ON TANGENT OF LOSS ANGLE OF BASALT (FREQUENCY DEPENDENCE) (Continued)

Data Set No.	Author(s), Year [Ref. No.]	Name and Source	Minerals and/or Chemical Composition		Method Used		Experimental Data		Other Specifications
			Components	Weight Percent	Volume Percent	Frequency, ν , Hz	Tangent of Loss Angle $\tan \delta$		
116	Jasio, R., et al., 1973 [15]	Same as above	Same as above			Same as above	0.9801E+02	0.6255	Step 3: After tin foil was placed on the sample and the sample was dried in a vacuum of 3×10^{-3} Torr for 2 days.
							0.1883E+03	0.4990	
							0.4629E+03	0.3933	
							0.9400E+03	0.3208	
							0.1857E+04	0.2617	
							0.4689E+04	0.1995	
							0.9786E+04	0.1627	
							0.1987E+05	0.1312	
							0.4622E+05	0.1023	
							0.9385E+05	0.08344	
117	Jasio, R., et al., 1973 [15]	Same as above	Same as above			Same as above	0.9739E+02	0.4677	Step 4: After the sample was baked at 95°C for 2 days and dried in circulating N ₂ -gas overnight.
							0.1926E+03	0.3946	
							0.4864E+03	0.3075	
							0.9603E+03	0.2426	
							0.1897E+04	0.1957	
							0.4922E+04	0.1491	
							0.9719E+04	0.1190	
							0.1870E+05	0.1004	
							0.4726E+05	0.08089	
							0.9347E+05	0.06900	
118	Jasio, R., et al., 1973 [15]	Same as above	Same as above			Same as above	0.9830E+02	0.2023	Step 5: After the sample was baked at 95°C for 28 more days and dried in circulating N ₂ -gas overnight.
							0.1945E+04	0.1784	
							0.4902E+03	0.1243	
							0.9957E+03	0.1026	
							0.1913E+04	0.08092	
							0.4837E+04	0.06669	
							0.9570E+04	0.05818	
							0.1845E+05	0.05367	
							0.4669E+05	0.04626	
							0.9731E+05	0.03528	
119	Jasio, R., et al., 1973 [15]	Same as above	Same as above			Same as above	0.9874E+02	0.06994	Step 6: After the sample was baked at 300°C for 7 more days and dried in circulating N ₂ -gas overnight.
							0.2058E+03	0.05334	
							0.5057E+03	0.04158	
							0.1000E+04	0.03567	
							0.1979E+04	0.03094	
							0.5010E+04	0.02696	
							0.9920E+04	0.02432	
							0.1913E+05	0.02295	
							0.4987E+05	0.02163	
							0.9H69E+05	0.01908	
120	Griffin, R.E. and Marvelli, R.L., 1967 [44]	Minnocin assumed	Feldspar Augite Nephetine			50 40 8	Susceptance Variation	0.07198	Sample: Dry basalt. Density: 2.97 g cm ⁻³ Other: Dried in oven at 150°C for several hours, then stored in desiccator.
								0.07811	
								0.06311	
								0.06285	
								0.06106	
								0.06108	
								0.06290	
								0.05956	

TABLE 4.5. EXPERIMENTAL DATA ON TANGENT OF LOSS ANGLE OF BASALT (FREQUENCY DEPENDENCE) (Continued)

Data Set No.	Author(s), Year [Ref. No.]	Name and Source	Minerals and/or Chemical Composition		Method Used	Experimental Data		Other Specifications
			Weight Percent	Volume Percent		Frequency, ν , Hz	Tangent of Loss Angle $\tan \delta$	
120								
cont.								
121	Griffin, R.E. and Marovelli, R.L., 1967 [44]	Same as above	Same as above	Same as above	Same as above			Sample: Wet basalt, Density: 2.97 g cm ⁻³ , Other: Stored in 100% humidity.
						0.6153E+08	0.06023	
						0.6077E+08	0.05329	
						0.7092E+08	0.05818	
						0.8109E+08	0.05040	
						0.9201E+08	0.05861	
						0.9139E+08	0.04715	
						1.015 E+09	0.04699	
						1.023 E+09	0.05287	
						1.014 E+09	0.05383	
						0.1991E+08	0.09643	
						0.2489E+08	0.09214	
						0.2947E+08	0.09006	
						0.3001E+08	0.09686	
						0.2987E+08	0.09955	
						0.3504E+08	0.09555	
						0.3999E+08	0.09599	
						0.4036E+08	0.08724	
						0.5000E+08	0.08223	
						0.6028E+08	0.08925	
						0.5946E+08	0.08804	
						0.6111E+08	0.08764	
						0.7007E+08	0.07750	
						0.7136E+08	0.07750	
						0.7039E+08	0.07206	
						0.8108E+08	0.07857	
						0.8071E+08	0.07239	
						0.8182E+08	0.07239	
						0.9087E+08	0.06731	
						1.009 E+09	0.06917	
						1.005 E+09	0.07044	
						1.009 E+09	0.07239	

The room temperature $\tan \delta$ values for dry basalt decrease with frequency. The highest value at 10^2 Hz approaches a constant value at higher frequency (data sets 1-62). The temperature dependence of $\tan \delta$ versus frequency was studied by Chung et al. [23] (data sets 65-79) and by Saint Amant and Strangway [26] (data sets 80-94). The frequency dependence observed at other temperatures is similar to the one at room temperature (data sets 1-62), but $\tan \delta$ values are generally higher at higher temperatures. Sometimes anomalous behavior is observed as in the case of basalts from Cape Neddik and Westfield (Massachusetts) (data sets 82,83,86,87). These data sets show a peak in $\tan \delta$ values before approaching a constant value at higher frequencies. The frequency at which such peak occurs is known as peak absorption frequency. Saint Amant and Strangway [26] attributed this unusual behavior to 16 volume % biotite in their samples. However, they did not observe any peak for their measurements on block samples (see data sets 90,91,93,94).

The effect of 1% water on $\tan \delta$ at 228 K (data set 95), 258 K (data set 96), and 300 K (data set 97) was reported by Saint Amant and Strangway [26]. These results indicated the normal decreasing behavior of $\tan \delta$ with a maximum at 10^2 Hz in the frequency range 10^2 Hz to 10^8 Hz. Their measurements with 0.5% water content for temperature in the range of 213-267 K showed frequency dependent anomalous behavior (see data sets 98-102). The observed peak frequency increased with temperature.

4.4.3. Summary

The compilation of dielectric constants from available literature is presented. The room-temperature behavior of dielectric constants for basalts in dry or air dry state is known for 10^3 Hz to 10^7 Hz. The dielectric behavior below 10^3 Hz to 10^2 Hz is not understood fully. The temperature dependence of dielectric constants on frequency received much attention and it is concluded that temperature tends to increase relative dielectric constant (ϵ') and $\tan \delta$. Both ϵ' and $\tan \delta$ tend to reach constant values at frequencies above 10^6 Hz. The effect of interstitial water in basalt is also evaluated, but is not yet fully quantified. Further, careful experiments should reveal the details. It is also noted that high biotite content in basalt modifies dielectric behavior significantly. The effects of organic liquids and altered minerals on the dielectric constant of basalts are not known.

4.5. REFERENCES

1. Pincus, H.J., 'Constitution of Rocks,' in Physical Properties of Rocks and Minerals (Touloukian, Y.S., Judd, W.R., and Roy, R.F., Eds.), Vol. II-2 of McGraw-Hill/CINDAS Data Series on Material Properties, McGraw-Hill Book Co., New York, NY, 1-20, 1981.
2. Olhoeft, G.R., 'Parametric Considerations,' in Physical Properties of Rocks and Minerals (Touloukian, Y.S., Judd, W.R., and Roy, R.F., Eds.), Vol. II-2 of McGraw-Hill/CINDAS Data Series on Material Properties, McGraw-Hill Book Co., New York, NY, 20-28, 1981.
3. Desai, P.D., Navarro, R.A., Hasan, S.E., Ho, C.Y., DeWitt, D.P., and West, T.R., 'Thermophysical Properties of Selected Rocks,' CINDAS Rept. 23, 255 pp., 1974.
4. Keller, G., in Electrical Properties of Rock (Parkhomenko, E., Ed.), Plenum Publishing Corp., New York, NY, 1967.
5. Keller, G. and Frischknecht, F., Electrical Methods in Geophysical Prospecting, Pergamon Press, Oxford, England, 1966.
6. Olhoeft, G.R., 'Electrical Properties of Rocks,' in Physical Properties of Rocks and Minerals (Touloukian, Y.S., Judd, W.R., and Roy, R.F., Eds.), Vol. II-2 of McGraw-Hill/CINDAS Data Series on Material Properties, McGraw-Hill Book Co., New York, NY, 257-330, 1981.
7. Ucock, H., 'Temperature Dependence of the Electrical Resistivity of Aqueous Salt Solutions and Solution-Saturated Porous Rocks,' Ph.D. Thesis submitted to the Faculty of University of Southern California, Jan. 4, 1980.
8. Olhoeft, G.R., 'Electrical Properties,' in Initial Report of Petrophysics Laboratory, U.S. Geological Survey Circular 789, 1-24, 1979.
9. Von Hippel, A.R., Dielectric Materials and Applications, The Technology Press of MIT and John Wiley and Sons, Inc., New York, NY, 438 pp., 1954.
10. Olhoeft, G.R., 'Initial Report of Petrophysics Laboratory: 1977-1979 Addendum,' U.S. Geological Survey Open File Rept. 80-522, 13 pp., 1980.
11. Scaife, B.K.P., Complex Permittivity: Theory and Measurement, English University Press Ltd., London, England, 170 pp., 1972.
12. Anderson, J.C., Dielectrics, Reinhold Publishing Corp., New York, NY, 171 pp., 1964.
13. Von Hippel, A.R., Dielectrics and Waves, John Wiley and Sons, Inc., New York, NY, 284 pp., 1954.
14. Vaughan, W.E., Smyth, C.P., and Powles, J.C., 'Determination of Dielectric Constant and Loss,' in Physical Methods of Chemistry (Weissberger, A. and Rossiter, B.W., Eds.), Vol. 1, Part IV of Techniques of Chemistry, Wiley Interscience, New York, NY, 351-95, 1972.

15. Ryu, J., Ward, S.H., Nash, W.P., and Buzze, D., 'K and tan δ Spectra of Dry Lunar Analog Measured by Various Techniques,' *Geophysics*, 38(1), 125-34, 1973.
16. Parkhomenko, E.I. and Bordarenko, A.I., 'Electrical Conductivity from 200 to 1000°C for 264 Rocks and Minerals,' U.S. Geological Survey, Open File Rept. 79-846, 159 pp., April 1979.
17. Presnell, D.C., Simmons, C.L., and Porath, H., 'Changes in Electrical Conductivity of Synthetic Basalt During Melting,' *J. Geophys. Res.*, 77(29), 5665-72, 1972.
18. Lastovickova, M. and Kropacek, V., 'Electrical Conductivity of Young Basalt Rocks of Central and Southeast Slovakia,' *Stud. Geophys. Geod. (Cesk. Akad. Ved.)*, 24, 4, 1980.
19. Bacon, J.F., Russell, S., and Casstens, J.P., 'Determination of Rock Thermal Properties,' United Aircraft Research Labs. Rept. UARL-L911397-4, 62 pp., 1973. [AD 755 218]
20. Rai, C.S. and Manghnani, M.H., 'Electrical Conductivity of Basalts to 1550°C,' *Oregon Dept. Geol. Miner. Ind., Bulletin 96*, 219-32, 1977.
21. Parkhomenko, E.I., Electrical Properties of Rocks, Plenum Publishing Corp., New York, NY, 1967.
22. Lastovickova, M. and Kropacek, V., 'Changes of Electrical Conductivity in the Neighborhood of the Curie Temperatures of Basalt,' *Stud. Geophys. Geod.*, 20, 265-72, 1976.
23. Chung, D.H., Westphal, W.B., and Simmons, G., 'Dielectric Properties of Apollo 11 Lunar Samples and Their Comparison with Earth Materials,' *J. Geophys. Res.*, 75(32), 6524-31, 1970.
24. Schloessin, H.H. and Dvorak, Z.D., 'Physical Properties of Samples from the Joides, Leg 37, Deep Sea Drilling Proj. 37, 403-15, 1977.
25. Waff, H.S., 'Electrical Conductivity Measurements on Silicates Melts Using Loop Technique,' *Rev. Sci. Instrum.*, 47, 877-9, 1976.
26. Saint Amant, M. and Strangway, D.W., 'Dielectric Properties of Dry Geologic Materials,' *Geophysics*, 35(4), 624-45, 1970.
27. Alvarez, R., Reynoso, J.P., Alvarez, L.J., and Martinez, M.L., 'Electrical Conductivity of Igneous Rocks: Composition and Temperature Relations,' *Bull. Volcanol.*, 41(4), 317-27, 1978.
28. Hyndmann, R.D. and Drury, M.J., 'The Physical Properties of Oceanetic Basement Rocks from Deep Sea Drilling on Mid-Atlantic Ridge,' *J. Geophys. Res.*, 81(23), 4042-52, 1976.
29. Murase, T., 'Viscosity and Related Properties of Volcanic Rocks at 800°C to 1400°C,' *J. Fac. Sci. Hokkaido Univ. Serial*, 7(1), 487-584, 1962.

30. Nagata, T., 'Some Physical Properties of Lava of Volcanoes, Asama and Mihara,' Bull. Earthquake Res. Inst., Japan, 15, 663-73, 1937.
31. Valarovich, M.P. and Tolstoi, D.M., 'The Simultaneous Measurement of Viscosity and Electrical Conductivity of Some Fused Silicates at Temperatures Up to 1400°C,' Soc. Glass. Tech. J., 20, 54-60, 1936.
32. Coster, H.P., 'The Electrical Conductivity of Rocks at High Temperatures,' Geophys. J. Roy. Astron. Soc., 5, 193-9, 1943.
33. Lundberg, L.B., 'Characterization of Rock Melts and Glasses Formed by Earth-Melting Subterrenes,' Los Alamos Scientific Lab. Rept. LA-5826-MS, 22 pp., Dec. 1974.
34. Khitarov, N.I., Lebedev, Y.B., Slutskiy, A.B., Dorfman, A.M., Soldatov, I.A., and Resin, N.I., 'The Pressure Dependence of the Viscosity of Basalt Melts,' Geokhimiya, 10, 1489-97, 1976.
35. Drury, M.J., 'Electrical Resistivity of Basalts, Leg 34,' Initial Rept. DSDP, 549-52, 1976.
36. Drury, M.J. and Hyndman, R.D., 'Electrical Resistivity of Oceanetic Basalts,' J. Geophys. Res., 89(B9), 4537-45, 1979.
37. Stesky, R.M. and Brace, W.F., 'Electrical Conductivity of Serpentinized Rocks to 6 Kbars,' J. Geophys. Res., 78(32), 7214-21, 1973.
38. Schloessin, H.H. and Dvorak, Z.D., 'Physical Properties of Samples from the Joides, Leg 37, DSDP,' Initial Rept. DSDP, Vol. 37, U.S. Government Printing Office, Washington, DC, 403-15, 1977.
39. Hyndman, R.D. and Drury, M.J., 'Physical Properties of Oceanetic Rocks from Deep Sea Drilling on the Mid Atlantic Ridge,' J. Geophys. Res., 81, 4042-52, 1976.
40. Chorston, C.J., Evans, C.L., and Lee, C., 'Laboratory Measurement of Compressional Wave Velocities and Electrical Resistivity of Basalt DSDP Leg 49,' Initial Rept. DSDP, Vol. 49, 761-3, 1979.
41. Griffin, R.E. and Marovelli, R.L., 'Dielectric Constant and Dissipation Factors for Six Rock Types,'
42. Bordarenko, A.T., 'Study of Temperature Dependence of the Dielectric Constant and of the Tangent of Loss Angle of Dielectric Loss of Rocks at Different Frequencies,' Bull. Acad. Sci., USSR, Geophys. Ser. No. 3, 281-6, 1963.
43. Hansen, W., Sill, R., and Ward, S.H., 'The Dielectric Properties of Selected Basalts,' Geophys., 38(1), 135-9, 1973.
44. Griffin, R.E. and Marovelli, R.L., 'Dielectric Properties and Dissipation Factors for Six Rock Types Between 20 and 100 Megahertz,' Bureau of Mines Rept. BM-RI-6913, 21 pp., 1967.

45. Archie, G.E., 'Electrical Resistivity Log as an Aid in Determining Some Reservoir Characteristics,' *Trans. Am. Inst. Mining Metal. Engr.*, 146, 54-62, 1942.
46. Drury, M.J., 'The Electrical Properties of Ocean Crust and Oceanatic Island Basalts and Gabbros: Results and Implications of a Laboratory Study,' *Dalhousie Univ., Canada, Ph.D. Thesis*, 209 pp., 1977.
47. Shankland, T.J., 'Electrical Conduction in Rocks and Minerals: Parameters for Interpretation,' *Phys. Earth Planet. Interiors*, 10, 209-19, 1975.
48. Duba, A.G. and Nichols, I.A., 'Influence of Oxidation State on the Electrical Conductivity of Olivine,' *Earth Planet. Sci. Lett.*, 18, 59-64, 1973.
49. Duba, A.G. and Ito, J., 'The Effect of Ferric Iron on the Electrical Conductivity of Olivine,' *Earth Planet. Sci. Lett.*, 18, 279-84, 1973.
50. Waff, H.S. and Weill, D.E., 'Electrical Conductivity of Magmatic Liquids: Effect of Temperature, Oxygen Fugacity and Composition,' *Earth Planet. Sci. Lett.*, 28, 254-60, 1975.
51. Nitson, U., 'Stability Field of Olivine with Respect to Oxidation and Reduction,' *J. Geophys. Res.*, 79, 706-11, 1974.
52. Deinese, P., Nafziger, R.H., Ulmer, G.C., and Woerman, E., 'Temperature-Oxygen Fugacity Tables for Selected Gas Mixtures in the System C-H-O at 1 Atm Total Pressure,' *Bull. Earth and Mineral Sciences Experimental Station, Pennsylvania State Univ.*, 1974.
53. Hyndman, R.D. and Ade-Hall, J.M., 'Electrical Conductivity of Basalts from DSDP, Leg 26,' *Trans. AGU*, 1025, 1973.
54. Volger, J., 'Further Experimental Investigations on Some Ferromagnetic Oxidic Compounds of Mn with Petrovskite Structure,' *Physica*, 20, 49, 1954.
55. Shankland, T.J. and Waff, H.S., 'Partial Melting and Electrical Conductivity Anomalies in the Upper Mantle,' *J. Geophys. Res.*, 82(33), 5409-17,
56. Waff, H.S., 'Theoretical Considerations of Electrical Conductivity in a Partially Molten Mantle and Implications for Geothermometry,' *J. Geophys. Res.*, 79(26), 4003-10, 1974.
57. Hashin, Z. and Shtrikman, S., 'A Variational Approach to the Theory of Effective Magnetic Permeability to Multiphase Materials,' *J. Appl. Phys.*, 33, 3125-31, 1962.
58. Brace, W.F., Orange, A.S., and Madden, T.R., 'The Effect of Pressure on the Electrical Resistivity of Water Saturated Crystalline Rocks,' *J. Geophys. Res.*, 70, 5669-78, 1965.
59. Brace, W.F. and Orange, A.S., 'Further Studies of the Effect of Pressure on Electrical Resistivity of Rocks,' *J. Geophys. Res.*, 73, 5407-20, 1968.

60. Runcorn, S.K. and Tozer, D.C., 'The Electrical Conductivity at High Temperatures and High Pressures,' *Ann. Geophys.*, 11, 98-102, 1955.
61. Schult, A. and Schober, M., 'Measurement of Electrical Conductivity of Natural Olivine at Temperatures Up to 950°C and Pressures Up to 42 Kbar,' *Zeits. Geophys.*, 35, 105-12, 1969.
62. Khitarov, N.I. and Slutskiy, A.B., 'The Effect of Pressure on Melting Temperatures of Albite and Basalt (Based on Electroconductivity Measurements),' *Geochem. Int.*, 2, 1034-41, 1965.

4.6. SYMBOLS AND UNITS, AND CONVERSION FACTORS

4.6.1. Symbols and Units

Symbol	Name	Unit
$\tan \delta$	Tangent of the loss angle	dimensionless
T	Temperature	K
ϵ'	Real part of the dielectric constant	dimensionless
	Frequency	Hz
σ	Electrical conductivity	$S\ m^{-1}$
ρ	Electrical resistivity	$\Omega\ m$

4.6.2. Conversion Factors

Temperature

<u>To convert from</u>	<u>To</u>	<u>Use</u>
K	$^{\circ}C$	$K - 273.15$
K	$^{\circ}F$	$(K - 273.15)9/5 + 32$

Electrical Conductivity

<u>To convert from</u>	<u>To</u>	<u>Multiply by</u>
$S\ m^{-1}$	$\Omega^{-1}cm^{-1}$	10^{-2}
$S\ m^{-1}$	$\Omega^{-1}in^{-1}$	2.54×10^{-2}
$S\ m^{-1}$	$\Omega^{-1}ft^{-1}$	3.048×10^{-1}
$S\ m^{-1}$	$\Omega^{-1}cmil^{-1}ft$	1.66243×10^{-9}
$S\ m^{-1}$	$(\mu\Omega\ cm)^{-1}$	1×10^{-8}

THE UNIVERSITY OF CHICAGO
DEPARTMENT OF CHEMISTRY
RESEARCH REPORT NO. 1000
BY
J. H. GOLDSTEIN AND
R. F. FIESHER
PUBLISHED BY THE UNIVERSITY OF CHICAGO PRESS
CHICAGO, ILLINOIS, U.S.A.
1955

1. INTRODUCTION
2. EXPERIMENTAL
3. RESULTS
4. DISCUSSION
5. CONCLUSIONS
6. REFERENCES
7. SUMMARY

U.S. DEPT. OF COMM. BIBLIOGRAPHIC DATA SHEET <i>(See instructions)</i>	1. PUBLICATION OR REPORT NO. NBSIR 82-2587	2. Performing Organ. Report No.	3. Publication Date September 1982
4. TITLE AND SUBTITLE PHYSICAL PROPERTIES DATA FOR BASALT			
5. AUTHOR(S) Lewis H. Gevantman			
6. PERFORMING ORGANIZATION <i>(If joint or other than NBS, see instructions)</i> NATIONAL BUREAU OF STANDARDS DEPARTMENT OF COMMERCE WASHINGTON, D.C. 20234		7. Contract/Grant No. 8. Type of Report & Period Covered	
9. SPONSORING ORGANIZATION NAME AND COMPLETE ADDRESS <i>(Street, City, State, ZIP)</i> Office of Nuclear Waste Isolation Battelle Memorial Institute 505 King Avenue Columbus, OH 43201			
10. SUPPLEMENTARY NOTES <input type="checkbox"/> Document describes a computer program; SF-185, FIPS Software Summary, is attached.			
11. ABSTRACT <i>(A 200-word or less factual summary of most significant information. If document includes a significant bibliography or literature survey, mention it here)</i> This work provides compiled experimental data and associated information on the thermodynamic, mechanical, thermophysical, and electrical properties of basalts from various locations in the United States and abroad. The thermodynamic properties include the chemical characterization of basalts, heat capacity, relative enthalpy, entropy, Gibbs energy, and molar volume. A summing procedure for obtaining values of heat capacity and calorimetric entropy above 298K is introduced.			
12. KEY WORDS <i>(Six to twelve entries; alphabetical order; capitalize only proper names; and separate key words by semicolons)</i> Basalt; chemical characterization; data compilation; dielectric properties; electrical properties; mechanical properties; thermal properties; thermodynamic properties; thermophysical properties.			
13. AVAILABILITY <input checked="" type="checkbox"/> Unlimited <input type="checkbox"/> For Official Distribution. Do Not Release to NTIS <input type="checkbox"/> Order From Superintendent of Documents, U.S. Government Printing Office, Washington, D.C. 20402. <input checked="" type="checkbox"/> Order From National Technical Information Service (NTIS), Springfield, VA. 22161		14. NO. OF PRINTED PAGES 751 15. Price \$49.50	

